



सत्यमेव जयते

INDIAN AGRICULTURAL  
RESEARCH INSTITUTE, NEW DELHI

23154

~!~

I.A.R.I.6.

GIP NLK—H-3 I.A.R.I.—10-5-55—45,000







# Transactions of the Faraday Society

3 MAY 1948

FOUNDED 1903

TO PROMOTE THE STUDY OF ELECTROCHEMISTRY, ELECTROMETALLURGY,  
PHYSICAL CHEMISTRY, METALLOGRAPHY, AND KINDRED SUBJECTS

---

VOL. XLIII, 1947

---

Linlithgow Library.  
Imperial Agricultural Research Institute  
New Delhi.

GURNEY AND JACKSON  
LONDON: 98 GREAT RUSSELL STREET  
EDINBURGH: TWEEDDALE COURT

PRINTED IN GREAT BRITAIN AT  
THE UNIVERSITY PRESS  
Aberdeen

# THE SURFACE LAYER OF COLLOIDAL SOLUTIONS AND THE SIZE OF COLLOIDAL PARTICLES.

BY SERGIUS G. MOKRUSHIN

Received 7th January, 1946

The writer has found <sup>1</sup> that with the ageing of the solutions a very thin invisible film is spontaneously formed on the surface of colloidal solutions of positively charged colloids. The formation of the film is a result of coagulation which occurs on the surface of colloidal solutions. The surface of solutions usually has a negative charge due to the abundance of anions and orientated dipoles of molecules of water in the surface layer.<sup>2, 3</sup>

In preliminary investigations the writer has shown that no films are formed on the surface of solutions with negatively charged colloidal particles. For example, the sol of positively charged colloidal particles of ferric hydroxide, prepared by Krecke, formed a film on the surface of colloidal solutions while the sol of negatively charged particles of ferric hydroxide had no film on its surface. The writer observed also the same phenomenon with sols of silver iodide,<sup>4</sup> the positive sol had, after standing some time, quite a visible film on its surface, but with negative particles of silver iodide no film appeared even after many days. From these and many other observations, the writer concluded that on the surface of positively charged colloidal solutions, surface coagulation with the formation of monomicellar film takes place. More detailed investigations were carried out with positively charged colloidal solutions of ferric hydroxide prepared by Krecke.<sup>5</sup> It has been found that there was formation of a thin, even invisible, film after standing for some days. At first this film was probably only a network which later was transformed into a compact solid film. The calculated "thickness" of the film demonstrates the tendency of the film, on standing for a long time, to obtain quite a definite limit of thickness. This limited thickness of the compact film has been taken for the thickness of the monomicellar layer or for the thickness of a micelle. The determination of the thickness was carried out by the method of Langmuir-Blodgett <sup>6</sup> specially developed for this purpose. Castor oil was used as a piston oil. The layers of surface film were attached to the surface of a polished chromium plate only when the latter was dipped into colloidal solution. On the other hand when taking out the chromium plate from the colloidal solution, the surface film was attached to it only very feebly and could be readily washed off by distilled water.

As many layers were put on the surface of chromium plate as were necessary to ensure that the colour of these multilayers might correspond to the colour of the multilayers of calcium stearate obtained by the Langmuir-Blodgett <sup>6</sup> method. The thickness of the multilayers was determined by the equation  $t = t_0\eta_0/\eta$  where  $t$  and  $t_0$  are the respective thicknesses

<sup>1</sup> Mokrushin, *Bull. Mendeleev Chem. Soc.*, 1941, 7, (N7), 38.

<sup>2</sup> Frumkin, *Kolloid-Z.*, 1926, 40, 9.

<sup>3</sup> Alty, *Proc. Roy. Soc. A*, 1924, 106, 315; Alty and Curie, *Proc. Roy. Soc. A*, 1929, 122, 622.

<sup>4</sup> Mokrushin, (unpublished results).

<sup>5</sup> Ostwald Wo., *Kleines Praktikum der Kolloidchemie*, Dresden, 1920, p. 7.

<sup>6</sup> Blodgett, *J. Amer. Chem. Soc.*, 1935, 57, 1007; Langmuir and Schaefer, *Chem. Rev.*, 1939, 27, 207.

and  $\eta$  and  $\eta_0$  the refractive indices of the multilayer films of ferric hydroxide and calcium stearate respectively. The thickness of monolayer of colloidal ferric hydroxide was determined by division of the thickness of the multilayer by the number of immersions. From these investigations it was found that the thickness of limiting monolayer was equal to 3-4 millimicrons. This value has been taken for the thickness of a micelle.

The data<sup>7</sup> obtained from diffusion and ultra-filtration of ferric hydroxide hydrosol gave the size of these micelles in the neighbourhood of 30-40 millimicrons. It follows from these data that the micelles of ferric hydroxide hydrosol are lamellar in shape. They lie flat on the surface of the hydrosol and form a monomolecular colloidal film on it as a result of coagulation. Therefore, just as the surface layer of ordinary liquids consists of monomolecular films of molecules of liquid,<sup>8</sup> the surface of hydrosols, due to coagulation, is covered with monomolecular film. The method of Langmuir and Blodgett enables us to determine the thickness of a micelle and in an indirect way to judge about its shape.

### Summary.

1. A new phenomenon of spontaneous formation of very thin, invisible surface film as a result of the surface or two-dimensional coagulation in positively charged hydrosol has been found.
2. The Langmuir-Blodgett method was used for the determination of the film thickness of colloidal ferric hydroxide.
3. The thickness of monomolecular film was shown to be about 3-4 millimicrons.
4. It was shown that the investigations of surface films enables us to judge the size and shape of colloidal particles.
5. From these investigations it has been found that the micelles of ferric hydroxide are of a plate-like shape.

### Résumé.

On décrit les couches superficielles, minces et invisibles, comme formées spontanément par une coagulation—dans deux dimensions—d'hydrosols positivement chargés. La méthode de Langmuir-Blodgett établit que l'épaisseur du film monomoléculaire d'hydroxyde ferrique colloïdal est de 3-4 millimicrons et on trouve que les micelles ont la forme plaque.

### Zusammenfassung.

Die spontane Bildung eines dünnen, unsichtbaren Oberflächenfilms durch zwei-dimensionale Koagulation des positiv geladenen Hydrosols wird beschrieben. Messungen nach der Methode von Langmuir und Blodgett ergeben, dass die Dicke eines monomolekularen Films von Ferrihydroxydkolloid  $3-4 \times 10^{-7}$  cm. und die Mizelle tafelförmig ist.

*Colloid Chemical Laboratory,  
Urals Industrial Institute,  
Sverdlovsk, U.S.S.R.*

<sup>7</sup> Duclaux and Amat, *J. Chim. physique*, 1938, **35**, 379; 1939, **36**, 256.

<sup>8</sup> Irany, *J. Amer. Chem. Soc.*, 1939, **61**, 1436; Mokrushin, *J. Physic. Chem.*, 1928, **32**, 879.

# THE SOLUBILITY OF GASES IN ELASTOMERS.

BY R. M. BARRER.

Received 7th January, 1946.

(1) **Introductory.**—Kinetic and statistical methods have led to the progressive interpretation of heterogeneous equilibria. Adsorption of gases in mono-layers,<sup>1</sup> interstitial or zeolitic sorption of a volatile component,<sup>2</sup> multi-layer persorption in gels,<sup>3</sup> and in colloids such as wool,<sup>4</sup> have all proved amenable to fairly precise treatments. The further development of these methods may clarify an increasing range of gas-colloid equilibria, typical among which are gas-elastomer systems. The group of elastic non-polar polymers shows a considerable capacity to sorb non-polar gases, but for these gases above their critical points the sorption isotherm has not so far been calculated in spite of the intrinsic interest and practical importance of the phenomenon. An attempt to calculate the solubility by assuming the gas molecules to enter pre-existing holes in the elastomer gave results not in accord with experiment.<sup>5</sup> The present paper will, however, derive a satisfactory sorption isothermal for permanent gases in elastomers based on the statistical thermodynamics of monomer-polymer mixtures, and will compare experimental with calculated solubilities and isothermals.

(2) **Distinction between the BET and the Present Isothermal.**—For sorption in gel and colloidal sorbents in which two kinds of sorption site co-exist the isotherm often has a characteristic sigmoid form which is well represented by the isotherm first deduced by Brunauer, Emmett and Teller by a kinetic argument.<sup>3</sup> \* The form of the isotherm derives from an entropy of mixing term, in which the sorbate molecules are distributed between the two types of sorption site in such a way as to minimise the energy. In a chemically homogeneous non-polar elastomer such as polyisoprene there is no reason to suppose more than one type of sorption site. Therefore, although the BET isotherm can simulate the gas-rubber isotherm in curving away from the pressure axis (ref. <sup>6</sup>, Fig. 73 and 74), the physical explanation of the form of the gas- or vapour-rubber isotherm cannot be that underlying the BET isothermal.

(3) **Basis of the Present Treatment.**—An alternative explanation of gas-rubber solubilities and isotherms may be based on recent treatments of the statistics of monomer-polymer mixtures. Here the entropy of mixing term is obtained by finding the number of ways of distributing monomer molecules and polymer chains on an array of lattice sites all of one kind, each site having <sup>7</sup> a co-ordination number  $z$ . Each site may be

\* Usually called the BET isotherm.

<sup>1</sup> e.g. Fowler and Guggenheim, *Statistical Thermodynamics*, C.U.P., 1939, Chap. 10.

<sup>2</sup> *Ibid.*,<sup>1</sup> pp. 554 et seq. Lacher, *Proc. Roy. Soc. A*, 1937, 161, 525. Barrer, *Trans. Faraday Soc.*, 1944, 40, 374.

<sup>3</sup> Brunauer, Emmett and Teller, *J. Amer. Chem. Soc.*, 1938, 60, 309. Brunauer, L. S. Deming, W. E. Deming and Teller, *ibid.*, 1940, 62, 1723. Brunauer, *The Adsorption of Gases and Vapours*, O.U.P., 1944, Chap. 6. Foster, *J. Chem. Soc.*, 1945. See also Hill, *J. Chem. Physics*, 1946, 14, 263, for statistical derivation.

<sup>4</sup> Cassie, *Trans. Faraday Soc.*, 1945, 41, 450.

<sup>5</sup> Orr, *private communication*.

<sup>6</sup> Brunauer, *The Adsorption of Gases and Vapours*, O.U.P., 1944.

<sup>7</sup> Meyer, *Helv. Chim. Acta*, 1940, 23, 1063.

occupied by a monomer molecule or by a segment of the polymer chain approximately equal in volume to that molecule. If there are  $n$  of these segments per polymer molecule, and the volume fractions of sorbed molecules and elastomer are  $v_0$  and  $v_r$  respectively, successive treatments have given for the partial molal free energy of mixing of monomer with polymer:

$$\mu = RT/\beta [\ln v_0 + (1 - 1/n)v_r] \quad (\text{Flory})^8 \quad (1)$$

( $\beta$  is the number of sorbed molecules replaceable by one segment of a rubber molecule);

$$\mu = RT [\ln v_0 + g_0(1 - 1/n)v_r] \quad (\text{Huggins})^9 \quad (2)$$

where 
$$g_0 = 1 + \sum_{i=1}^{\infty} \frac{1}{i} \left( \frac{2v_r}{z'} \right)^{i-1} \quad (2a)$$

( $z'$  is very nearly the co-ordination number  $z$ );

$$\mu = RT [\ln v_0 - z/2 \ln \{1 - (1 - 1/n)2v_r/z\}] \quad (\text{Miller})^{10} \quad (3)$$

$$\mu = RT \left[ \ln v_0 - z/2 \ln \{1 - (1 - 1/n)2v_r/z\} + z/2 \ln \frac{(\beta + 1) - 2\alpha}{(1 - \alpha)(\beta + 1)} \right] \quad (\text{Orr})^{11} \quad (4)$$

where 
$$\beta = \{1 + 4\alpha(1 - \alpha)(e^{2w/zkT} - 1)\}^{\frac{1}{2}} \quad (4a)$$

$$\alpha = \frac{\frac{nz + 2n + 2}{nz} \cdot v_r}{\frac{nz + 2n + 2}{nz} \cdot v_r + v_0} \quad (4b)$$

$$w = \frac{z}{2}(2w_{\alpha\beta} - w_{\alpha\alpha} - w_{\beta\beta}) \quad (4c)$$

the energy of interaction between two sorbed molecules being  $w_{\alpha\alpha}$ , between two rubber segments  $w_{\beta\beta}$ , and between a sorbed molecule and a rubber segment  $w_{\alpha\beta}$ ; and finally

$$\mu = RT[v_0/\bar{n} + \ln v_0 + z/2 \ln (1 - 2/z v_r)] \quad (\text{Scott and Magat})^{12} \quad (5)$$

where  $\bar{n}$  is the number of segments in the number average molecular weight polymer molecule.

Orr<sup>11</sup> pointed out that Miller's and Huggins' formulae if expanded term by term are virtually identical; while Flory's equation follows from those of Huggins or Miller on setting  $z = \infty$ . Since  $z$  cannot be  $\infty$ , Flory's equation may for present purposes be omitted.<sup>13</sup> These three equations, and equation (5), all assume random mixing and zero heat of mixing; Orr's equation, however, covers random mixing modified by non-zero energies  $w$  as given in equation (4c). Equation (5) allows for heterogeneity of the polymer in respect of molecular weight. The effect of heterogeneity embodied in the term  $v_0/\bar{n}$  is small, and since  $n$  in equations (2), (3) and (5) is large all three are substantially identical. The equation of Miller will accordingly be used for random mixing with negligible energy  $w$ , and the equation of

<sup>8</sup> Flory, *J. Chem. Physics*, 1941, 9, 660; *ibid.*, 1942, 10, 51.

<sup>9</sup> Huggins, *J. Chem. Physics*, 1941, 9, 440; *Ann. N.Y. Acad. Sci.*, 1942, 43, 1; *J. Phys. Chem.*, 1942, 46, 1; *J. Amer. Chem. Soc.*, 1942, 64, 1712.

<sup>10</sup> Miller, *Proc. Camb. Phil. Soc.*, 1942, 38, 109.

<sup>11</sup> Orr, *Trans. Faraday Soc.*, 1944, 40, 320.

<sup>12</sup> Scott and Magat, *J. Chem. Physics*, 1945, 13, 172. Scott, *J. Chem. Physics*, 1945, 13, 178.

<sup>13</sup> Developments of the statistical theory according to a modified lattice model, in which each molecule of solute occupies several sites have nevertheless shown some approach to the form of Flory's equation, for zero heat of mixing (e.g. Guggenheim, *Proc. Roy. Soc. A*, 1944, 183, 203; Miller, *Nature*, 1946, 157, 842; Gee, *Faraday Soc.*, Discussion on Swelling and Shrinking, (in press).

ORR when random mixing is modified by appreciable values for  $w$ . Even this equation, however, may be inadequate when  $w$  deviates considerably from zero (e.g. for methanol in rubber).<sup>14</sup> \*

(4) Procedure for Determining the Solubility of Gases in Elastomers.

—The following procedure is valid for a gas above its critical temperature, and leads, as a special case, to the vapour-elastomer isotherm.

Consider the isothermal transfer of a mol of gas from the gas phase where there are  $n_1$  molecules per cc. to an infinite amount of gas-elastomer mixture. Then the molar free energy of the gas is

$$A_g = RT \ln n_1 \frac{h^3}{(2\pi mkT)^{3/2}} \cdot \frac{1}{j_\Lambda(T)} \quad (6)$$

where  $h$  = Planck's constant,  $k$  = Boltzmann's constant,  $m$  = mass of the gas molecule, and  $j_\Lambda(T)$  = the partition function for all integral degrees of freedom of the molecule. The Helmholtz free energy of a mol of gas in the gas-elastomer mixture is numerically equal to the chemical potential,  $\mu_s$ , of the gas and is made up of three terms. The first is an energy,  $-\chi$ , where  $\chi$  is the least energy required to remove a mol of gas from the solution to the gas phase.† Then there is a free energy term corresponding to the partition function  $j(T)$  for the internal degrees of freedom of the sorbed molecule and its degrees of freedom relative to its new environment in the mixture. Finally there is the configurational free energy term discussed in section 3, for mixing sorbed molecules and polymer. Adding, one obtains :—

$$\mu_s = -\chi + RT \ln \frac{1}{j(T)} + \mu \quad (7)$$

At equilibrium

$$\Delta A = \mu_s - A_g = 0 \quad (8)$$

so that, substituting equations (6), (7) and (3) (or (4)) in equation (8) one obtains

$$RT \ln n_1 \frac{h^3}{(2\pi mkT)^{3/2}} \frac{1}{j_\Lambda(T)} = -\chi + RT \ln \frac{1}{j(T)} + RT \ln \frac{v_0}{\{1 - (1 - 1/n)2v_r/z\}^{z/2}} \quad (9a)$$

and

$$RT \ln n_1 \frac{h^3}{(2\pi mkT)^{3/2}} \frac{1}{j_\Lambda(T)} = -\chi + RT \ln \frac{1}{j(T)} + RT \ln \frac{v_0}{\{1 - (1 - 1/n)2v_r/z\}^{z/2}} + RT \ln \left\{ \frac{\beta + 1 - 2x}{(1 - x)(\beta + 1)} \right\}^{z/2} \quad (9b)$$

The problem now reduces to the evaluation of  $j(T)$  in equation (9).

\* However, the relation of  $w$  and the experimental heat of mixing is not clear. Equations 20b or 25b of Orr<sup>11</sup> give partial molal heats of mixing of a hypothetical condensed phase of pure monomer in which monomer molecules are distributed on the lattice sites of co-ordination number  $z$  with a lattice of similarly distributed pure polymer (section 3). The relationship such phases bear for example to the actual structure of liquids such as benzene or toluene to be mixed with the rubbers cannot be established with certainty. Moreover  $w$  of equation 4c does not include the heat of condensation of vapour to give the hypothetical condensed phase. It therefore seems best to use  $w$  in Orr's equations as a second adjustable constant (in addition to  $z$ ).

Added in proof.

† For zero values of  $w$ . If  $w$  is not zero,  $-\chi$  is the heat of condensation of a mol of gas to give the hypothetical condensed phase referred to in the previous footnote.

<sup>14</sup> Ferry, Gee and Treloar, *Trans. Faraday Soc.*, 1945, 41, 340.



(5) **Isotherms corresponding to Equation (9).**—First nearly spherical sorbed molecules which may be considered to rotate freely in the mixture as in the gas phase will be considered. These molecules, enmeshed in the polymer, must behave relative to their environment as oscillators. Moreover the weak interactions with neighbouring polymer segments are unlikely to modify internal degrees of freedom, the partition function for which will accordingly still be  $j_A(T)$ . Thus

$$j(T) = j_A(T) \left( \frac{kT}{h\nu} \right)^3 \quad . \quad . \quad . \quad (10)$$

Substitution of equation (10) in equations (9a) and (9b) then gives the isotherms for negligible  $w$  and finite  $w$  respectively. Thus in the former case

$$\frac{v_0}{\{1 - (1 - 1/n)2/z \cdot v_r\}^{z/2} \cdot n_1} = K = \left( \frac{kT}{2\pi m} \right)^{\frac{3}{2}} \cdot \frac{1}{v^3} \cdot e^{\frac{z}{RT}} \quad . \quad (11)$$

whence recalling that  $\frac{\partial \ln K}{\partial T} = \frac{\Delta U}{RT^2}$ , one finds

$$\frac{v_0}{\{1 - (1 - 1/n)2/z \cdot v_r\}^{z/2} \cdot n_1} = \left( \frac{kT}{2\pi m} \right)^{\frac{3}{2}} \cdot \frac{1}{v^3} \cdot e^{\frac{-\Delta U + \frac{1}{2}RT}{RT}} \quad . \quad (12)$$

When permanent gases are sorbed by elastomer at low or moderate pressures the solution is usually very dilute so that  $v_0 \ll 1$  and  $v_r = 1$ . Then equation (12) becomes

$$\frac{v_0}{n_1} = \left( \frac{kT}{2\pi m} \right)^{\frac{3}{2}} \frac{1}{v^3} e^{\frac{-\Delta U + \frac{1}{2}RT}{RT}} [1 - 2/z]^{z/2} \quad . \quad (13)$$

and gas-elastomer systems then obey Henry's law. This low pressure behaviour is common to the Langmuir, the BET, and the present isothermal, and is well substantiated by experiment. Finally one notes that in the case of systems at constant pressure, substitution of  $p = n_1 kT$  in (12) gives

$$\frac{v_0}{\{1 - (1 - 1/n)2/z \cdot v_r\}^{z/2} \cdot p} = \frac{1}{(kT)} \cdot \left( \frac{kT}{2\pi m} \right)^{\frac{3}{2}} \frac{1}{v^3} e^{\frac{-\Delta H + \frac{1}{2}RT}{RT}} \quad . \quad (14)$$

When non-spherical molecules (e.g.  $n$ -paraffins) are sorbed by elastomers, the principal rotations, as well as translational degrees of freedom may be converted to vibrations. Isotherms corresponding to several kinds of mobility of the sorbed molecules in their environment are illustrated for zero  $w$  in Table I (cf. Barrer, ref. 2). The conversion of rotations into vibrations when the gas molecule is sorbed has a much smaller influence upon gas-elastomer equilibria than has conversion of translations.<sup>3</sup>

If a vapour is sorbed by an elastomer, equation (14) simplifies because as  $p \rightarrow p_s$ ,  $v_0 \rightarrow 1$  and  $v_r \rightarrow 0$ , then  $K = 1/p_s$ . Accordingly equation (14) becomes for large  $n$

$$\frac{v_0}{[1 - 2/z \cdot v_r]^{z/2}} = p/p_s \quad . \quad . \quad . \quad (14a)$$

Moreover, for high polymers where  $n$  is very large, unity may replace  $(1 - 1/n)$  in all the equations. Fig. 1 (a), Curves 1, 2 and 3, then show isothermals of  $v_0$  against  $p/p_s$  calculated from (14a) when  $z = \infty$ , 6 and 4. For the physically probable values of  $z = 6$  or 4 the isotherms are strongly concave towards the axis of  $p/p_s$ .

Fig. 1 (b) shows the same isotherms with  $v_0/v_r$  as ordinate since this conforms closely with the usual method of expressing sorption data when using Langmuir or BET isotherms. In Fig. 1 (b) are also given typical Langmuir and BET isotherms.

TABLE I.—SOLUBILITY CONSTANTS FOR GASES IN ELASTOMERS.

Type of Movement Executed in Mixture by Sorbed Molecule.	Solubility Constant $K = \frac{v_0}{[1 - (1 - 1/n)2/s \cdot v_r]^{1/2} p}$	Equation No.
(1) Freely rotating oscillators.	$K = \frac{1}{kT} \left( \frac{kT}{2\pi m} \right)^{\frac{1}{2}} \frac{1}{\bar{v}^3} e^{-\frac{\Delta H + \frac{1}{2}RT}{RT}}$	14
(2) Oscillators with one principal rotation also converted to a vibration.	$K = \frac{1}{kT} \left( \frac{kT}{2\pi m} \right)^{\frac{1}{2}} \frac{1}{\bar{v}^3} \left( \frac{kT}{8\pi^2 I_1} \right)^{\frac{1}{2}} e^{-\frac{\Delta H + RT}{RT}}$	15
(3) Oscillators with two principal rotations also converted to vibrations.	$K = \frac{1}{kT} \left( \frac{kT}{2\pi m} \right)^{\frac{1}{2}} \frac{1}{\bar{v}^3} \frac{kT}{8\pi^2 I_1^{\frac{1}{2}} I_2^{\frac{1}{2}}} e^{-\frac{\Delta H + \frac{1}{2}RT}{RT}}$	16
(4) Oscillators with all three principal rotations converted to vibrations.	$K = \frac{1}{kT} \left( \frac{kT}{2\pi m} \right)^{\frac{1}{2}} \frac{1}{\bar{v}^3} \left( \frac{kT}{8\pi^2 I_1^{\frac{1}{2}} I_2^{\frac{1}{2}} I_3^{\frac{1}{2}}} \right)^{\frac{1}{2}} e^{-\frac{\Delta H + 2RT}{RT}}$	17

(6) Comparison with Experiment : Solubility of Permanent Gases in Rubbers.—Observed solubilities of permanent gases in rubbers are small at normal pressures, and the heats of sorption are of the same order as, or less than, the latent heats of condensation of the gases themselves below

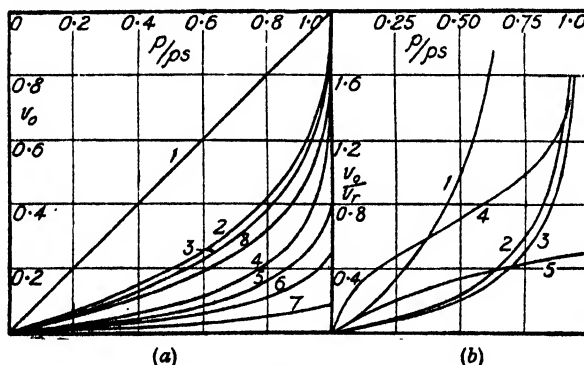


FIG. 1 (a).—Curves 1, 2 and 3: isotherms according to equation 14a, with  $s = \infty$ , 6 and 4 respectively.

Curves 4, 5, 6 and 7: isotherms according to equation 19, with  $s = 4$  and  $w = 0.81 kT$ ,  $1.121 kT$ ,  $1.386 kT$ , and  $2kT$  respectively.

Curve 8: isotherm according to equation 20, with  $\mu = 0.51$ .

FIG. 1 (b).—Curves 1, 2 and 3: isotherms corresponding to curves 1, 2 and 3 of Fig. 1 (a) using as ordinate  $v_0/v_r$  = volume of vapour sorbed per unit volume of elastomer.

Curve 4: BET isotherm with  $C = 5$ .

Curve 5: Langmuir isotherm with same initial slope as curve 1.

their critical temperatures<sup>15</sup> (see Table II). It is therefore probable that  $w$  (eqn. (4c)) is very small so that equation (13) or its constant pressure analogue should be valid. The term  $(1 - 2/s)^{1/2}$  does not vary greatly for probable values of  $s$  ( $6 > s > 4$ ), and the mean frequency  $\bar{v}$  corresponding to weak van der Waals interactions between solute and environment should

<sup>15</sup> Barrer, *Trans. Faraday Soc.*, 1939, 45, 628.

be in the infra-red ( $\sim 10^{12}$  sec.<sup>-1</sup>). Since  $\bar{\nu}$  is not known independently, however, the best test of equation (13) is to determine the values of  $\bar{\nu}$  for which experimental and calculated  $v_0$  agree, (Table II, column 4). The mean frequencies correspond as predicted to thermal vibrations in the infra-red ( $\sim 10-40\mu$ ). The results are consistent among themselves,  $\bar{\nu}$  being greatest for the light molecule  $H_2$ , and least for the heaviest molecule, A; moreover for a given solute  $\bar{\nu}$  does not change much for a series of elastomers. One may conclude that the theory is capable of predicting and interpreting the solubility of permanent gases in elastomers.

TABLE II.—TEST OF THE ISOTHERM FOR PERMANENT GASES IN ELASTOMERS.

Gas.	Elastomer.	Volume Fraction $v_0$ of Gas dissolved at 300° K. and 1 atm. <sup>18</sup>	Value of $\bar{\nu}$ (sec. <sup>-1</sup> ) to give Agreement between Observed and Calculated $v_0$ .	Experimental <sup>18</sup> Sorption Heat $\Delta H$ (cal./mol.) $\pm 400$ .
$H_2$	Vulcanised "Neoprene".	$6.25 \times 10^{-5}$	$3.3 \times 10^{12}$	— 970
	Butadiene - acrylonitrile inter-polymer.	$3.11 \times 10^{-5}$	$3.2 \times 10^{12}$	— 500
$N_2$	Vulcanised "Neoprene".	$7.9 \times 10^{-5}$	$1.0 \times 10^{12}$	— 1400
	Butadiene - acrylonitrile interpolymer.	$8.2 \times 10^{-5}$	$1.1 \times 10^{12}$	— 1700
	Butadiene-styrene inter- polymer.	$1.32 \times 10^{-4}$	$0.77 \times 10^{12}$	— 1000
	Butadiene-methyl meth- acrylate interpolymer.	$1.29 \times 10^{-4}$	$0.98 \times 10^{12}$	— 2000
A	Vulcanised "Neoprene".	$2.08 \times 10^{-4}$	$0.72 \times 10^{12}$	— 1630
	Butadiene-styrene inter- polymer.	$2.75 \times 10^{-4}$	$0.63 \times 10^{12}$	— 1100
	Butadiene-methylmetha- crylate interpolymer.	$1.66 \times 10^{-4}$	$0.69 \times 10^{12}$	— 1450

$v_0$  was obtained from the solubility constant  $\delta$  at  $p = 1$  atm. and  $T = 300^\circ$  K expressed as cc. at N.T.P. per cc. of rubber, by the relation

$$v_0 = \frac{\delta \times \text{mol. vol. of solute}}{22,400}.$$

Assumed molecular volumes were 26.4, 32.8 and 28.1 cc. for  $H_2$ ,  $N_2$  and A respectively.

(7) **Comparison with Experiment: Isotherms of Vapours completely Miscible with Rubber.**—Data with which to test the isotherm of equation (14a) are few in number.\* An outstanding exception is the benzene-rubber system for which complete vapour pressure-composition data are available.†<sup>18</sup>

In the Henry's law region of sorption one sees from equation (14a) that

$$v_0 = p/p_1 (1 - z/z)^{1/2} \quad . \quad . \quad . \quad (18)$$

so that from the limiting slope of the curve of  $v_0$  against  $p/p_1$ ,  $z$  may be found. For benzene in rubber,  $z$  was found in this way to be 3.53 at 25° C. and 4.07 at 100° C. In Fig. 2 (a) are given experimental points for the 100° and 25° isotherms, while the full curves are calculated from equation (14a)

\* There must be complete miscibility of vapour and elastomer, which precludes many of the data of Stamberger<sup>16</sup> and Lens.<sup>17</sup> Complete miscibility is found when solute and elastomer are of nearly equal polarity, e.g. hydrocarbon-rubber systems.

† The experimental sorption heat<sup>14, 18</sup> of liquid benzene in rubber is extremely small so that  $w$  is also likely to be negligible. This is the condition for applicability of equation 14a. See footnote to p. 5, and section 3.

using the above values of  $z$ . Agreement over the whole range of compositions is extremely good.

Less accurate and complete vapour pressure-composition data are available for *n*-heptane,<sup>14</sup> toluene<sup>15</sup> and chloroform-rubber<sup>16, 17</sup> systems

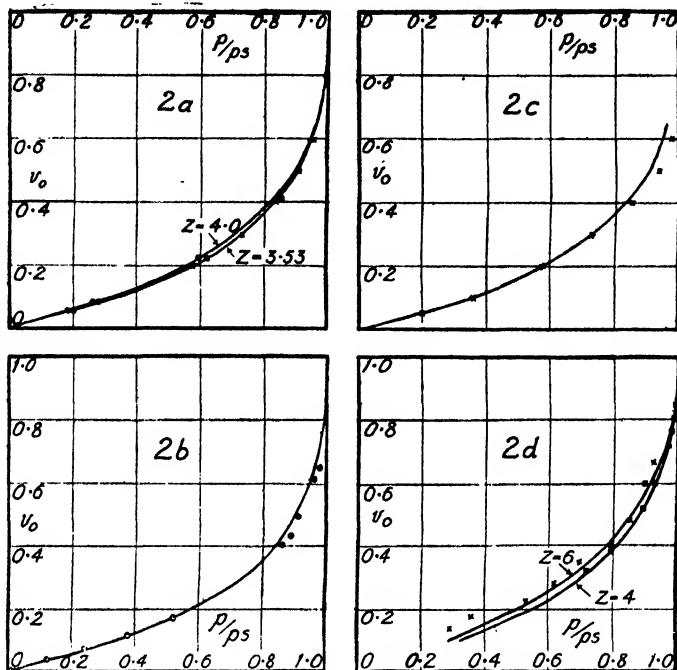


FIG. 2.—The isotherm  $\frac{v_0}{(1 - 2/z v_r)^{1/2}} = p/p_s$  applied to several vapour-rubber equilibria.

(a) Benzene-rubber<sup>18</sup> :

○ = Experimental data at 100° C. } The full curves are calculated isotherms  
 ×, □ = Experimental data at 25° C. } using  $z = 4.0$  and  $3.53$ .

(b) *n*-Heptane-rubber<sup>14</sup> :

○ = Experimental data at 40° C. The full curve is calculated using  $z = 3.5$ .

(c) Toluene-rubber<sup>15</sup> :

× = Experimental data at 30° C. The full curve is calculated using  $z = 3.5$ .

(d) Chloroform-rubber<sup>16, 17</sup> :

× = Experimental data at 35° C. } The full curves are calculated using  
 □ = Experimental data at 25° C. }  $z = 4$  and  $z = 6$ .

for which  $w$  is also small.<sup>14</sup> Fig. 2 (b), 2 (c) and 2 (d) indicate the degree of success obtained with the simple isotherm equation (14a), and it is seen that values of  $z$  of about 4 (chosen by analogy with the benzene-rubber

<sup>18</sup> Stamberger, *J. Chem. Soc.*, 1929, 2318.

<sup>17</sup> Lens, *Rec. Trav. chim.*, 1932, 51, 971.

<sup>16</sup> Gee and Treloar, *Trans. Faraday Soc.*, 1942, 38, 147. Gee and Orr, *Trans. Faraday Soc.* (in press).

<sup>15</sup> Meyer, Wolff and Boissonas, *Helv. Chim. Acta*, 1940, 23, 430.

system) give very reasonable agreement, although small divergencies are noted.\*

(8) **Comparison with Experiment: Isotherms of Vapours partially Miscible with Rubber.**—Partial miscibility of a vapour in an elastomer signifies that  $w$  is no longer negligible, so that Orr's equation (eqn. (4)) must be used to derive the isotherm, giving

$$\frac{v_0(\beta + 1 - 2x)^{z/2}}{\{(1 - 2/z \cdot v_r)(\beta + 1)(1 - x)\}^{z/2}} = p/p_s \quad (19)$$

Fig. 1 (a), Curves 4, 5, 6 and 7, shows characteristic isotherms obtained using equation (19), for  $z = 4$  and various values of  $w$ .

Data for testing equation (19) are seldom complete or very accurate; among the best are those of Lens<sup>17</sup> for the acetone-rubber system. Fig. 3 shows experimental isotherm data and also points calculated from equation (19) with  $z = 4$ ,  $w = 848$  cal., the temperature being  $35^\circ\text{C}$ . The isotherm

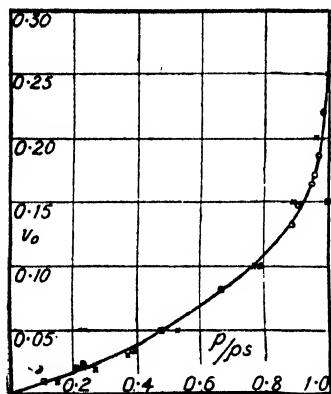


FIG. 3.—Isotherm of acetone in rubber.<sup>17</sup>

- = Experimental points.
- × = Calculated from equation 19 with  $z = 4$ ,  $w = 848$  cal. and  $T = 35^\circ\text{C}$ .
- = Calculated from equation 20, with  $\mu = 1.45$ .

$$\ln v_0 + (1 - v_0) + \mu(1 - v_0)^2 = \ln p/p_s \quad (20)$$

based on an approximate equation of Huggins<sup>9</sup> was also examined. With  $\mu = 1.45$  there is agreement for smaller values of  $v_0$  but marked divergence later.

Orr's equation, however, gives an isotherm which is able to cover the whole composition range reasonably well.

## Summary.

A simple extension of the statistics of liquid-elastomer mixtures gives explicitly the sorption isotherm of gases in elastomers at temperatures above their critical temperatures. This isotherm has been used to compare the experimental and theoretical solubility constants of several permanent gases in various elastomers, with good agreement.

Isotherms of a number of vapours in rubbers were also calculated. In the case of the benzene-rubber system the actual data are very successfully reproduced by the isotherm derived from Miller's equation which assumes random mixing  $\left(\frac{v_0}{(1 - 2/z \cdot v_r)^{z/2}} = p/p_s\right)$ . Other mixtures which

do not deviate greatly from this isotherm were chloroform-rubber, *n*-heptane-rubber and toluene-rubber.

Orr's equation was moderately successful in giving the isotherm for acetone in rubber, a system in which a larger endothermal heat of mixing of liquid and rubber causes departures from random mixing and results eventually in a two-phase system at a critical composition. An equation of Huggins in this case led to a less satisfactory isotherm.

## Résumé.

Une simple généralisation de la statistique des solutions liquide-élastomère donne de façon explicite l'isotherme de sorption des gaz dans

\* The direction of these divergences is compatible with small positive values of  $w$  for the hydrocarbons and with a small negative value for chloroform.

des élastomères à des températures supérieures à leurs températures critiques. Cette isotherme a été utilisée pour comparer les constantes de solubilité théorique et expérimentale de plusieurs gaz permanents dans divers élastomères, constantes qui se sont révélées en bon accord.

Les isothermes de certaines vapeurs dans des caoutchoucs ont aussi été calculées. Dans le cas du système benzène-caoutchouc, les résultats expérimentaux étaient représentés avec succès par l'isotherme établie à partir de l'équation de Miller, qui suppose que la solution ne présente aucun arrangement moléculaire  $\left(\frac{v_0}{(1 - z/2 v_r)^{1/2}} = p/p_s\right)$ . D'autres mélanges qui s'écartaient peu de cette isotherme étaient chloroforme-caoutchouc, *n*-heptane-caoutchouc et toluène-caoutchouc.

L'équation d'Orr ne réussissait à donner qu'imparfaitement l'isotherme pour l'acétone dans le caoutchouc, système dans lequel la dissolution fortement endothermique du liquide dans le caoutchouc provoque un arrangement moléculaire et donne éventuellement un système binaire à une composition critique. Une équation de Huggins conduisait dans ce cas à une isotherme encore moins satisfaisante.

### Zusammenfassung.

Eine einfache Weiterführung der Statistik von Gemischen von Flüssigkeiten mit elastischen hochpolymeren Substanzen („Elastomeren“) führt zu einem Ausdruck für die Absorptionsisotherme von Gasen in Elastomeren bei Temperaturen, die höher als die kritische Temperatur sind. Die mit Hilfe dieser Isotherme für eine Reihe von permanenten Gasen und Elastomeren berechneten Löslichkeitskonstanten stimmen gut mit den experimentellen Werten überein.

Die Isothermen von mehreren Dämpfen in Kautschuk wurden auch berechnet. Für das System Benzol-Kautschuk werden die experimentellen Daten sehr gut von der aus der Miller'schen Gleichung (die auf der Annahme einer statistisch homogenen Mischung beruht) abgeleiteten Isotherme wiedergegeben.  $\left(\frac{v_0}{(1 - z/2 v_r)^{1/2}} = p/p_s\right)$  Binäre Gemische von Kautschuk mit Chloroform, *n*-Heptan und Toluol weichen auch nicht stark von dieser Isotherme ab.

Orr's Gleichung konnte ziemlich gut zur Berechnung der Isotherme von Aceton in Kautschuk angewendet werden, ein System, in dem die grössere endothermische Mischungswärme der Komponenten zu grossen Abweichungen vom Zustand der Strukturlosigkeit und schliesslich, bei einer kritischen Zusammensetzung, zu einem Zweiphasensystem führt. Eine Gleichung von Huggins ergab in diesem Fall eine weniger gute Isotherme.

*The Chemical Laboratories,  
Bedford College (University of London),  
Regent's Park, London.*

# STATISTICAL TREATMENT OF POLYMER SOLUTIONS AT INFINITE DILUTION.

BY THE LATE W. J. C. ORR.

Received 14th January, 1946.

In the current theories<sup>1</sup> of polymer solutions the heats and entropies of mixing are assessed on the basis of a statistical model which treats the solution as a "quasi-crystalline" phase. In this paper a further quantitative extension of this model to the special configurational situation presented by polymer solutions at very high dilutions will be made. In moderate and high concentrations (1 % or more by vol.) of polymer solutions the individual polymer chains so extensively intertwine with each other that the availability of polymer sub-groups is, even on a molecular scale, effectively uniform. At very high dilutions, however, the polymer chains separate out from each other, and at the extreme dilution with which we shall be concerned the statistical problem presented is merely that of determining the average configuration of a set of effectively non-overlapping flexible polymer chains in thermal equilibrium in a solvent phase; that is to say, the problem is ultimately one of determining the average configuration of a single polymer molecule in a given force field environment.

## I. Quasi-Crystalline Description of Highly Dilute Polymer Solutions.

We consider an idealised system in which an average co-ordination number  $z$  applies uniformly for pure solvent and polymer species alike as well as for the solution. For a polymer species having  $n$  sub-groups the number of possible contacting first neighbours is thus  $nz - 2n + 2$ . In the case of a system consisting of  $N_\alpha$   $n$ -group polymer molecules and  $N_\beta$  solvent species, where  $nN_\alpha \ll N_\beta$  the Helmholtz free energy of the mixture may be written<sup>2</sup>

$$F_m = -kT \log [g(N_\alpha, N_\beta) \{G(n, z; w_{\alpha\alpha}, w_{\beta\beta}, w_{\alpha\beta}; T)\}^{N_\alpha} e^{-\frac{1}{2} z N_\beta w_{\beta\beta} / kT} (\phi_\alpha v_\alpha)^{N_\alpha} (\phi_\beta v_\beta)^{N_\beta}]. \quad (1)$$

In this expression  $g(N_\alpha, N_\beta)$  the number of configurations of the system at infinite dilution, will be given by:—

$$[g(N_\alpha, N_\beta)]_{\frac{N_\alpha}{N_\beta} \rightarrow 0} = N_\beta^{N_\alpha} \quad . \quad . \quad . \quad (2)$$

$w_{\alpha\alpha}$ ,  $w_{\beta\beta}$  and  $w_{\alpha\beta}$  are the energies of pairs of polymer-polymer, solvent-solvent and polymer-solvent contacts;  $(\phi_\alpha v_\alpha)$ ,  $(\phi_\beta v_\beta)$  describe the motion and "kinetically effective free volumes" of the polymer and solvent species respectively, and are assumed to be unaltered by configurational changes in the system.

<sup>1</sup> (a) Flory, *J. Chem. Physics*, 1942, **10**, 51.

(b) Huggins, *J. Physical Chem.*, 1942, **46**, 151.

(c) Miller, *Proc. Cambridge Phil. Soc.*, 1943, **39**, 54.

(d) Orr, *Trans. Faraday Soc.*, 1944, **40**, 320.

(e) Guggenheim, *Proc. Roy. Soc., A*, 1944, **183**, 203, 213.

<sup>2</sup> Fowler and Guggenheim, *Statistical Thermodynamics*, Chapter VIII (Camb. Univ. Press, 1939).

The function,  $G$ , describes the contribution to the partition function due to the configurations of the individual polymer molecules which it is postulated are at such high dilution that the interactions of one with another are negligible.

Now, if we write for  $G$  simply

$$G = \frac{1}{2}z(z-2)^{n-2} \quad (3)$$

which is the number of configurations of a  $n$ -group chain arranged on a lattice of co-ordination number  $z$  calculated without excluding self-interfering or "blocking" configurations and without consideration of any "weighting" factors due to the relative proximity of different parts of the chain, we obtain exactly the formulæ given in the earlier treatment<sup>1a</sup> for the limiting case when  $N_\alpha/N_\beta \rightarrow 0$ . However, obviously as a chain is folded on a lattice it will inevitably encounter situations in which it finds lattice sites blocked by sub-groups of the chain already added. Moreover it is in detailed conformity with the level at which the polymer problem is being discussed to include weighting factors of the form  $e^{-w_{\alpha\alpha}/kT}$  for each configuration in which a first neighbour contact between polymer sub-groups occurs. Thus, in place of equation (3) for  $G$  which was used previously, we now write the approximately weighted function

$$G = a e^{-\frac{1}{2}(nz-2n+2)(2w_{\alpha\beta}-w_{\beta\beta})/kT} + b e^{-\frac{1}{2}(nz-2n)(2w_{\alpha\beta}-w_{\beta\beta})/kT + w_{\alpha\alpha}/kT} + c e^{-\frac{1}{2}(nz-2n-2)(2w_{\alpha\beta}-w_{\beta\beta})/kT + 2w_{\alpha\alpha}/kT} + \dots \quad (4)$$

where  $a, b, c \dots$  are the numbers of real (i.e. non-blocking) configurations of a  $n$ -group chain in which are exhibited 0, 1, 2 ... first neighbour contact pairs between polymer sub-groups.

The expressions for the free energies  $F_p$  and  $F_s$  of the pure polymer and solvent species respectively corresponding to equation (1) for the solution are as follows

$$F_p = -kT \log [\{\kappa(n, z)\}^{N_\alpha} e^{-\frac{1}{2}(nz-2n+2)N_\alpha w_{\alpha\alpha}/kT} (\phi_\alpha v_\alpha)^{N_\alpha}] \quad (5)$$

$$F_s = -kT \log [e^{-\frac{1}{2}zN_\beta w_{\beta\beta}/kT} (\phi_\beta v_\beta)^{N_\beta}] \quad (6)$$

where  $\{\kappa(n, z)\}^{N_\alpha}$  is the number of possible configurations exhibited by  $N_\alpha$  polymers close-packed on a lattice of  $nN_\alpha$  sites and co-ordination number  $z$ .

Using the above relations we obtain for the free energy of mixing

$$\Delta F = F_m - F_p - F_s$$

$$\Delta F (\simeq \Delta G) = -N_\alpha kT \log \frac{N_\beta}{\kappa} (a + b\eta + c\eta^2 + \dots) e^{-\frac{1}{2}(nz-2n+2)(2w_{\alpha\beta}-w_{\alpha\alpha}-w_{\beta\beta})/kT} \quad (7)$$

(For a condensed phase  $\Delta F$  may be identified approximately with  $\Delta G$ ). Hence for the partial molal free energy of solution of 1 mole polymer in  $N_\beta$  moles solvent (at infinite dilution since  $N_\beta \gg 1$ ) we obtain

$$(\Delta \mu_\alpha)_0 = N \frac{\partial}{\partial N_\alpha} \Delta G = -RT \log \frac{N_\beta}{\kappa} - RT \log G(\eta) + \frac{nz-2n+2}{z} N w \quad (8)$$

where we have written

$$G(\eta) = a + b\eta + c\eta^2 + \dots \quad (9)$$

$$2w/z = (2w_{\alpha\beta} - w_{\alpha\alpha} - w_{\beta\beta}) \quad (10)$$

and  $\eta = e^{2w_{\alpha\alpha}/kT}$ ;  $N$  is Avogadro's number.

From (8) the following expressions for  $(\Delta H_\alpha)_0$  and  $T(\Delta S_\alpha)_0$

$$(\Delta H_\alpha)_0 = -\frac{\partial}{\partial \frac{1}{T}} R \log G(\eta) + \frac{nz-2n+2}{z} N w \quad (11)$$



$$\text{and} \quad T(\Delta S_a)_0 = RT \log N_\beta / \kappa + RT \log G(\eta) + RT^2 \frac{\partial}{\partial T} \log G(\eta) \quad (12)$$

applying also in the region of infinite dilution, are derived.

As will be understood from the nature of the assumptions involved in the above treatment we obtain from (7) only the first term (that is, the simple osmotic term) in the expansion for  $\Delta\mu_\beta$  as a function of the concentration thus :

$$(\Delta\mu_\beta)_0 = N \frac{\partial}{\partial N_\beta} \Delta G = - RT / N_\beta \quad . \quad . \quad . \quad (13)$$

As a further consequence, we cannot derive an expression for  $\Delta H_\beta$ , since the first term in the expansion of this quantity involves the *square* of the concentration.

In the sequel, sections III and IV, explicit expressions for  $G(\eta)$  will be derived. The most direct comparison of these functions with experiment would be in terms of the entropy equation (12), but so far the necessary experimental data is lacking. Our chief concern will hence be with the application of equation (11) and in particular with its generalised form, (17), derived in the following section.

## II. A Generalisation of the Above Treatment.

In equation (11) the heat of solution at infinite dilution is seen to separate into two distinct terms which we may for convenience refer to as  $\theta$  and  $\phi$  where, on the basis of the above model,

$$\theta = - \frac{\partial}{\partial T} \log G(\eta) \quad \text{and} \quad \phi = \frac{nz - 2n + 2}{z} Nw \quad . \quad (14)$$

It is now important to realise that the separation of  $(\Delta H_a)_0$  in this way is by no means a special feature arising out of the restricted postulates of the "quasi-crystalline" model, but is simply a consequence of the much wider single postulate that no long-range forces are present in the system and that the energy of this solution can be expressed in terms of first neighbour interactions: for, clearly  $\phi$  corresponds to the energy absorbed in evaporating a polymer molecule from the pure polymer species and then dissolving this molecule, in an *uncoiled*\* configuration, in the solvent while  $\theta$  is the energy absorbed as the *uncoiled* polymer coils up making self-contacts to reach its equilibrium configuration. Hence it is evident that, whatever the "structure" of the solution or polymer,  $G(\eta)$  will be expressed formally by a relation similar to (9) in which  $\eta = e^{x/kT}$  say, where  $Nx$  is the increment by which the energy of the solution as a whole changes for every additional polymer-polymer self-contact that occurs within the polymer chain in solution. In a perfectly general case, of course, it may be difficult because of insufficient information about the probable "structure" of the solution or of the forces involved to provide explicit analytical expression for  $\phi$  and  $x$ .

The quasi-crystalline model provides a particularly simple and explicit answer to this problem, namely that given in section I but, as will appear from the discussion in section V, the postulates involved in this model are probably too restrictive ever to give a detailed account of the behaviour of a *liquid phase* polymer-solvent system as exemplified by the rubber-benzene case to be discussed later.

For a specific treatment of the problem of polymer solutions at high dilution which will turn out to be sufficiently general to deal with the experimental data we have to discuss, we may now reconstruct the quasi-crystalline model on the basis of the following postulates. We assume :

\* Here and in the sequel "uncoiled" is consistently used to describe a chain configuration having no first neighbour contacts.

(a) that a definite co-ordination number  $z_\alpha$  can be attributed to the polymer molecule describing its configuration in the pure polymer phase and describing also, in so far as we have to do with polymer self-contacts, its configuration at infinite dilution in a solution; (b) that another co-ordination number  $z_\beta$  can be attributed to the solvent molecules in the pure solvent phase which gives also the number of *solvent-solvent* interactions round a solvent molecule in solution at high dilution. There is then no need, in view of these assumptions, to assume equal volumes for the solvent molecule and polymer sub-group. The customary, less critical assumptions are also made as before, namely, that the  $(\phi_\alpha v_\alpha)$ ,  $(\phi_\beta v_\beta)$  terms in the partition functions are the same in the pure phases as in the solution phase.

It is then easy to see that, in terms of the above postulates, and in view of the foregoing remarks on the nature of the terms involved in  $G(\eta)$  and  $\Phi$ , that we shall obtain by exactly the same steps as detailed above in Section I the result

$$(\Delta\mu_\alpha)_0 = -RT \log N_\beta \{ \kappa(n, z_\alpha) \} - RT \log G(\eta') + \frac{nz_\alpha - 2n + 2}{z_\alpha} Nw' \quad (15)$$

where  $2w'/z_\alpha = (2w'_{\alpha\beta} - w_{\alpha\alpha} - w'_{\beta\beta})$  and  $\eta' = e^{2w'/z_\alpha kT}$ . (16)

and where now  $w'_{\alpha\beta}$  is so chosen that the expression  $(nz_\alpha - 2n + 2)w'_{\alpha\beta}$  is the average energy of interaction of a polymer in an *uncoiled* configuration with its surrounding sheath of solvent molecules in solution, and where  $w'_{\beta\beta}$  is so chosen that  $\frac{1}{2}(nz_\alpha - 2n + 2)w'_{\beta\beta}$  represents the energy required to make a cavity of the appropriate size and shape to accommodate an *uncoiled* polymer molecule. This particular choice of definition of  $w'_{\alpha\beta}$  and  $w'_{\beta\beta}$  is made, of course, in order that an expression of the form  $(nz_\alpha - 2n + r + 2)w'_{\alpha\beta}$  represents correctly the energy appropriate to the solution of a coiled polymer molecule with  $r$  self-contacts. Thus  $w'_{\alpha\beta}$  and  $w'_{\beta\beta}$  will have quite different numerical values from the analogous quantities  $w_{\alpha\beta}$  and  $w_{\beta\beta}$  defined in Section I.  $w_{xx}$  however is, as before, simply the energy of a normal first neighbour polymer-polymer contact.

From equation (15) we obtain in place of (11)

$$(\Delta H_\alpha)_0 = - \frac{\partial}{\partial T} R \log G(\eta') + \frac{nz_\alpha - 2n + 2}{z_\alpha} Nw'. \quad (17)$$

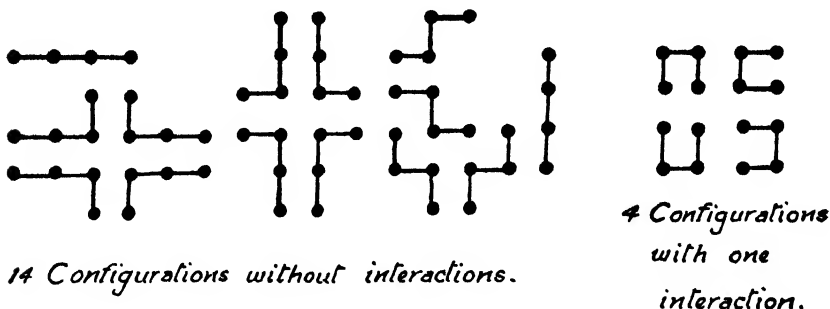
which is of wider applicability than the former result, being subject to less restrictive premises.

In equation (17) the effects of differences in volume of the polymer sub-groups and solvent molecule and the value of the effective polymer-solvent co-ordination number are all, of course, implicitly involved in the function  $Nw'$ , and a formal identity of equations (11) and (17) results at infinite dilution. However, whereas  $Nw$  in the simpler quasi-crystalline model is a constant independent of the relative composition of the solution  $Nw'$  as defined above would vary with composition, and  $z_\beta$  would appear explicitly in any extension of the present treatment to higher concentrations.

### III. The Equilibrium Configuration of Polymer Chains articulated on Simple Lattices. (a) Relatively Short Chains.

In order to amass a volume of statistical data, from which information of a sufficiently general nature on the average configuration and self-energy of polymer molecules might accrue, the actual numbers of configurations exhibited by 4, 5, 6, etc., -group molecules when arranged on simple lattices were counted by direct methods. In the present work arrangements on a planar square array of sites and on a simple cubic lattice have been considered. It is evident first of all that flexible molecules composed of 2 or 3 sub-groups arranged on these lattices exhibit no self-blocking configurations or first neighbour interactions between groups

of the same chain. As an example of the type of counting under discussion all the permitted configurations which compose the molecular partition function  $G(\eta)$  in the case of a 4-group molecule arranged on a square array are shown below.



In this case there are no blocking configurations which only arise when  $n > 5$ . The total number of configurations in this case is thus 18, as given by the general formula  $\frac{1}{2}z(z-1)^{n-2}$ , and the appropriate partition function is

$$G(\eta) = 14 + 4\eta.$$

The complete results as far as this type of analysis was carried are contained in the following tables.\*

TABLE I.  
SQUARE ARRAY ( $z = 4$ ).

$n$ .	$G(\eta) = a + b\eta + c\eta^2 + \dots$	Blocked Configurations.	Total Number $2 \times 3^{n-2}$ .
4	$14 + 4\eta$	0	18
5	$34 + 16\eta$	4	54
6	$82 + 44\eta + 16\eta^2$	20	162
7	$198 + 128\eta + 64\eta^2$	96	486
8	$470 + 368\eta + 172\eta^2 + 76\eta^3$	372	1458
9	$1122 + 1016\eta + 536\eta^2 + 264\eta^3 + 20\eta^4$	1416	4374

Simple Cubic Lattice ( $z = 6$ ).

TABLE II.  
SIMPLE CUBIC LATTICE ( $z = 6$ ).

$n$ .	$G(\eta)$ .	Blocked Configurations.	Total Number $3 \times 5^{n-2}$ .
4	$63 + 12\eta$	0	75
5	$267 + 96\eta$	12	375
6	$1107 + 516\eta + 144\eta^2$	108	1875
7	$4623 + 2688\eta + 1056\eta^2 + 96\eta^3$	912	9375

\* The analysis of this data in terms of the distance between chain endings which was carried out at the same time is given in Appendix I of the present paper.

#### IV. The Equilibrium Configuration of Polymer Chains (*cont.*). (b) Very long Chains.

In order to develop a partition function for very large values of  $n$  it is useful first of all to discuss the behaviour of a function  $p(\eta)$  defining, for a system characterised by a particular value of  $\eta$ , the probability that a given link in the  $n$ -group polymer chain makes a first neighbour contact with another group of the same chain. According to this definition we have

$$p(\eta) = \frac{1}{n} \left( \frac{b\eta + 2c\eta^2 + \dots}{a + b\eta + c\eta^2 + \dots} \right) = \frac{1}{n} \eta \frac{\partial \log G(\eta)}{\partial \eta} \quad (18)$$

Now it will be clear when  $\eta \rightarrow 0$  (indicating infinite repulsion between the polymer sub-groups) that  $p(\eta) \rightarrow 0$  and further when  $\eta \rightarrow \infty$  (indicating infinitely large attractive forces between polymer sub-groups), in which case one is concerned with tightly coiled configurations, that, in the square array case,  $p(\eta) \rightarrow 1$ , while in the case of the cubic lattice  $p(\eta) \rightarrow 2$ . For all intermediate values of  $\eta$  one must expect, on physical grounds, that  $p(\eta)$  will vary in a smooth curve between the limits 0 and 1, in the former, and between 0 and 2 in the latter case.

As a suitable general analytic function for  $G(\eta)$  sufficiently flexible to deal to any required degree of accuracy we may write for a  $n$ -group polymer where  $n$  is sufficiently large

$$G(\eta) = \left\{ \frac{1 + \alpha\eta + \beta\eta^2 + \dots + \kappa\eta^\sigma}{\gamma + \delta\eta + \dots + \eta^{\sigma-\tau}} \right\}^n = \{g(\eta)\}^n \quad \text{say} \quad (19)$$

introducing as many constants  $\alpha, \beta, \gamma, \dots, \kappa; \sigma$  as may be required. It is important to realise, however, that the index of  $\eta$  in the final term in the denominator must, in the case of the square array, be 1 unit less than the index of the final term in the numerator (i.e.  $\tau = 1$ ), whereas, in the cubic lattice case  $\tau = 2$ . In this way one provides for the fact that  $p(\eta)$  derived from (19) must tend to 1 or 2, as the case may be, when  $\eta \rightarrow \infty$ . Further, since  $p(\eta)$  for large values of  $n$  must become independent of  $n$ , it follows that the only way in which  $n$  can appear in  $G(\eta)$  for very long chains is as an index in the way shown in (19).

Referring now to the statistical data obtained for relatively short chains, it seems reasonable in the first place to suppose, for the region  $\eta \rightarrow 0$ , in view of the large number of configurations involved, that a close approach to a statistical limiting law is already being defined even for values of  $n$  as low as 5 or 6.

From Fig. 1(a), where the values of  $\log G(0)$  for the square array cases,  $n = 4$  to 9, and for the cubic lattice cases,  $n = 4$  to 7, are shown plotted as a function of  $n$ , one finds that to be a very good approximation indeed,

$$\begin{aligned} \log G(0) &= n \log (2.39) \dots \text{case of square array} \\ &= n \log (4.13) \dots \text{case of cubic lattice.} \end{aligned}$$

A comparison of these results with the relation

$$\log G(0) = n \log (1/\gamma)$$

given by (19) for  $\eta \rightarrow 0$  provides the value of a first empirical constant  $\gamma$ .

Secondly when  $\eta \rightarrow 0$  we have from (18)

$$\frac{p(\eta)}{\eta} = b/an.$$

From Fig. 1(b), in which again the data on short chains is employed, one obtains the result in both the case of the square array and that of the cubic lattice that for  $n \rightarrow \infty$ ,  $b/an$  is approximately equal to 0.123.

These two deductions from the analysis of short chain data are to be employed in defining the variation of  $G(\eta)$  at small values of  $\eta$ .

Considering now the situation when  $\eta \rightarrow \infty$ , one obtains from (19)

$$\begin{aligned} \log G(\eta) &\rightarrow n(\log \kappa_1 + \log \eta) \quad \text{case of square array} \\ &\rightarrow n(\log \kappa_2 + 2 \log \eta) \quad \text{case of cubic lattice,} \end{aligned}$$

where  $\kappa_1^*$  and  $\kappa_2^*$  are evidently the total numbers of closely coiled configurations for  $n$ -group chains corresponding effectively to  $n$  and  $2n$  contacts per sub-group for the two lattices under consideration. It will now be realised that for  $n \rightarrow \infty$   $\kappa_1$  and  $\kappa_2$  will approximate to the particular values for  $z = 4$  and 6 of the term  $\kappa(n, z)$  appearing in equation (1). A general expression for these numbers has already been given by Miller<sup>2</sup> as follows :

$$\kappa^n = \lim_{n \rightarrow \infty} \left\{ \frac{(z-1)^{n-2} (nz - 2n + 2) \frac{1}{2} (nz - 2n + 2)}{n^{\frac{1}{2}(z-1)} 2^{\frac{1}{2}(nz - 2n + 2)}} \cdot \frac{z}{2} \right\} \quad (20)$$

so that  $\kappa'_1 = 1.5$  and  $\kappa'_2 = 2.22$ .

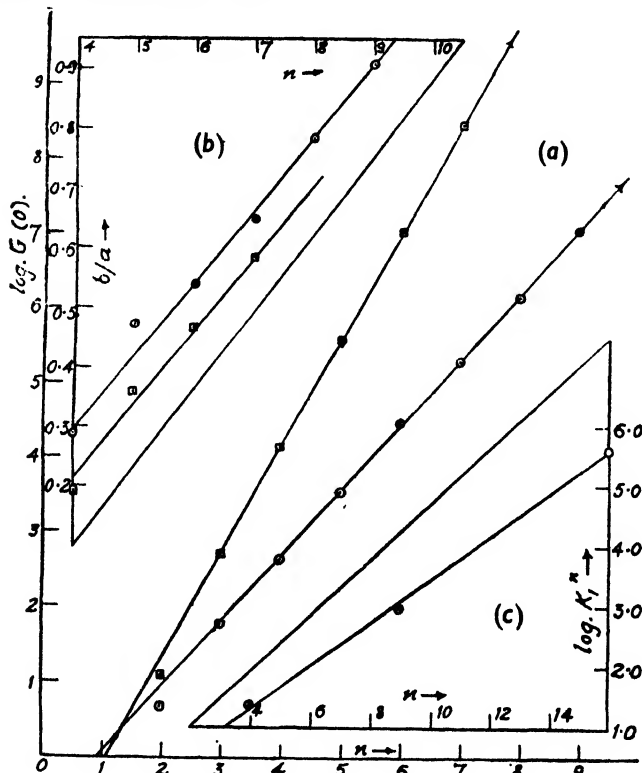


FIG. 1.

These  $\kappa'$  values must be regarded as upper limits to the true values of  $\kappa$  in virtue of the fact that the "flexibility" term  $(z-1)^{n-2}$  in (20) takes no account of blocked configurations, and is hence too large. A lower limit to  $\kappa$ ,  $\kappa''$  say, can, however, be estimated as follows. Chang<sup>4</sup> and Miller<sup>2</sup> have independently obtained the following expression for the number of configurations of a system of  $n/2$  two-group molecules completely filling the  $n$  sites of a lattice of co-ordination number  $z$

$$\left\{ \frac{(z-1)^{\frac{1}{2}(z-1)}}{z^{\frac{1}{2}(z-2)}} \right\}^n \quad (21)$$

Now, it may be seen by taking particular examples of lattices completely filled with "double-molecules" that there is always at least one

<sup>2</sup> Miller, *Proc. Cambridge Phil. Soc.*, 1942, 38, 109.

<sup>4</sup> Chang, *Proc. Roy. Soc. A*, 1939, 167, 512.

way in which such an arrangement of double-molecules can be strung together one after another to form a continuous chain of  $n$  groups. However, as is illustrated in Appendix II, it is sometimes possible to find more than one way of doing this. Thus, using (21), the following lower limits to  $\kappa$  are obtained

$$\kappa_1'' = 1.30 \quad \text{and} \quad \kappa_2'' = 1.55.$$

In the present work the values of  $\kappa_1 = 1.40$  and  $\kappa_2 = 1.9$ , which are the means of the upper and lower limits, i.e.  $\kappa = \frac{1}{2}(\kappa' + \kappa'')$  are used.\* We have thus three constants which can be used to construct *approximate*

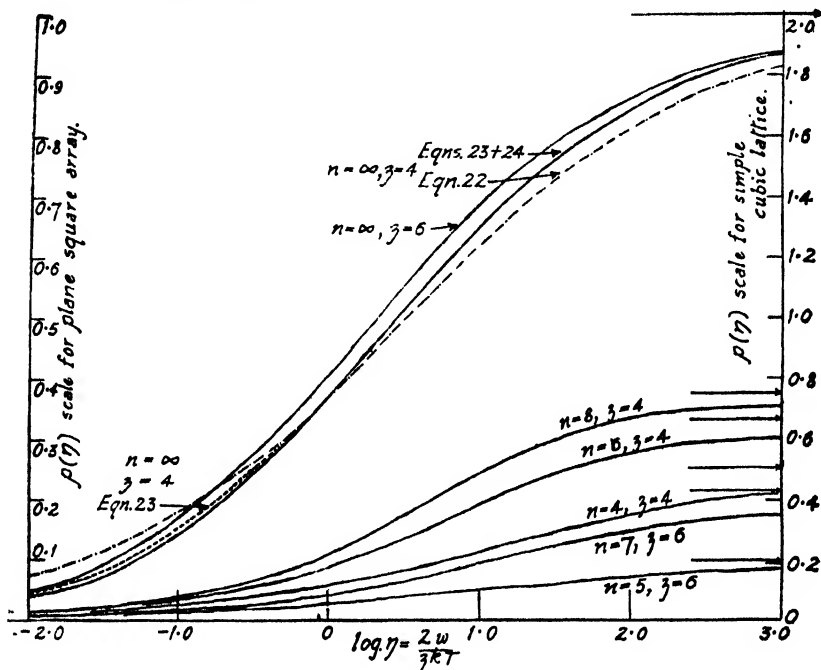


FIG. 2.

functions for  $G(\eta)$  or  $g(\eta)$  and  $p(\eta)$  for very long chains. In the square array case the following formulæ were developed :

$$\left. \begin{aligned} g(\eta) &= 2.39 + 1.4\eta \quad . \quad . \quad . \quad . \quad . \quad (a) \\ p(\eta) &= \frac{1.4\eta}{2.39 + 1.4\eta} \quad . \quad . \quad . \quad . \quad . \quad (b) \end{aligned} \right\} \quad (22)$$

$$\left. \begin{aligned} g(\eta) &= \frac{1 + 2.51\eta + 1.4\eta^2}{0.42 + \eta} \quad . \quad . \quad . \quad . \quad . \quad (a) \\ p(\eta) &= \frac{0.05\eta + 1.17\eta^2 + 1.4\eta^3}{0.42 + 2.05\eta + 3.10\eta^2 + 1.4\eta^3} \quad . \quad . \quad . \quad . \quad . \quad (b) \end{aligned} \right\} \quad (23)$$

$$\left. \begin{aligned} g(\eta) &= \frac{(1 + 1.158\eta)^{3.34}}{(0.524 + \eta)^{1.34}} \quad . \quad . \quad . \quad . \quad . \quad (a) \\ p(\eta) &= \frac{\eta(0.064 + 1.158\eta)}{(1 + 1.158\eta)(0.524 + \eta)} \quad . \quad . \quad . \quad . \quad . \quad (b) \end{aligned} \right\} \quad (24)$$

\* The first value 1.4 for the square array is supported also from direct counting of the number of configurations,  $\kappa_1^n$ , for  $n = 4, 9$  and  $16$  (Fig. 1(c)). When the values of  $\log \kappa_1^n$  are plotted as a function of  $n$  the slope obtained is  $\log(1.42)$ .

In deriving (22) only 2 of the constants are employed. Equation (23) is a simplified form of (19), and (24) is an obvious alternative analytic form of (23). In Fig. 2 the  $p(\eta)$  curves calculated from equations (22), (23) and (24) are compared. Very little difference indeed results from the difference in analytic form of (23) and (24); these curves may, however, be considered slightly more adequate than that given by (22). The effect of employing the upper or lower limiting values of  $\kappa_1$  in (23) instead of the mean value 1.4 affects the  $p(\eta)$  values by about  $\pm 0.02$  units only in the range  $\eta = 1$  to 2, and by smaller amounts at all other values of  $\eta$ .\*

In the case of simple cubic lattice the expressions for  $g(\eta)$  and  $p(\eta)$  were derived in the following analytic form

$$\left. \begin{aligned} g(\eta) &= \frac{(1 + 1.216\eta)^{3.285}}{(0.331 + \eta)^{1.885}} \quad . \quad . \quad . \quad (a) \\ p(\eta) &= \frac{\eta(0.04 + 2.432\eta)}{(1 + 1.216\eta)(0.331 + \eta)} \quad . \quad . \quad . \quad (b) \end{aligned} \right\} \quad (25)$$

The  $p(\eta)$  curve calculated from (25) is shown in Fig. 2. Also included in the same figure are some of the  $p(\eta)$  curves calculated for short chains, using equation (18) and the data of Tables I and II for  $z = 4$  and 6. The latter results are, of course, accurate expressions in terms of the model employed.

## V. Application to Solutions of Polymer Molecules.

In a recent paper<sup>8</sup> the inadequacy of the quasi-crystalline theory of polymer solutions in its present stage of development, to describe *accurately* either the behaviour of the entropy or the heat of mixing curves obtained experimentally for rubber-benzene solutions has been demonstrated, and doubt has thus been thrown on the adequacy of the statistical model employed and in particular on the very restrictive nature of the postulate of a constant co-ordination number. Now as a matter of fact it can easily be deduced (see Appendix III) from a consideration of the geometry of the rubber molecule and the benzene molecule respectively in relation to the densities of their bulk phases that the co-ordination number, in the case of the rubber chain (referred, of course, as is appropriate, to the isoprene sub-groups) is probably only just a little greater than 4, while that of the spheroidal shaped benzene molecule, in the liquid phase, lies probably between 6 and 8 on the average. In view of this fact, then, some discrepancy between the current theory and experiment is to be expected, and for this reason the attempt is made in Section III to enlarge the scope of the present theory in application (for the purposes of the present paper) to the special configurational situation provided by polymer systems at very high dilution. But it is not only in its predictions with regard to polymer solutions that the quasi-crystalline theory model fails, but also in application to the available experimental data on the heats of mixing of relatively simple liquids. In many cases these can be represented reasonably accurately by the simple empirical relation suggested by Hildebrand,<sup>6</sup> namely

$$\Delta H = \alpha v_a v_b V \quad . \quad . \quad . \quad . \quad (26)$$

\* As a test at intermediate values of  $\eta$  of the accuracy of the  $p(\eta)$  curve derived in the above way from the behaviour in the limiting cases of  $\eta = 0$  and  $\infty$ , an independent calculation of  $p(\eta)$ , for the square array case, in the physically important region where  $\eta = 1$  (i.e. where  $w = 0$ ) was made, using a set of random numbers to define the relative direction of successive links. The course of this *average* polymer chain was plotted graphically, blocking configurations being excluded, and first neighbour contacts counted. By continuing the chain eventually to an extent of some 3300 links a limiting value of  $p(1)$  of 0.42 was obtained in fair agreement with the estimate given by equations (23) and (24), namely 0.37.

<sup>8</sup> Gee and Orr, *Trans. Faraday Soc.*, 1946, **42**, 507.

<sup>6</sup> Hildebrand, *Solubility*, Reinhold (1936).

where  $\Delta H$  is the total heat of mixing two components in volume fractions,  $v_a$  and  $v_b$ ,  $V$  being the total volume of the solution and  $\alpha$  a constant independent of composition. In contrast to (26) the current theory (for finite  $z$ )<sup>\*</sup> gives the series of curves shown in Fig. 3 for the "constant"  $\alpha$ . One must strongly suspect that the failure in these cases is due also, at least in part, to the assumption of a fixed co-ordination number, although other factors both geometric and energetic might well be involved.

The only experimental data suitable for comparison with equation (17) for  $(\Delta H_a)_0$  are that published recently<sup>5, 7</sup> on the heats of mixing of benzene with (a) dihydromyrcene, (b) squalene, and (c) rubber, these three polyisoprene compounds providing an excellent example of a series consisting respectively of (a) a 2-group, (b) a 6-group, and (c) an approximately 4000-group multiple molecule, each of which, in the pure state, has nearly the same co-ordination number, approximately 4.

In the case of the dihydromyrcene-benzene system the experimental data can be expressed exactly by (26) with  $\alpha = 5.1$  cal./cc. We now assume that those geometric and energetic factors which result in the dihydromyrcene-benzene system conforming to equation (26) will be

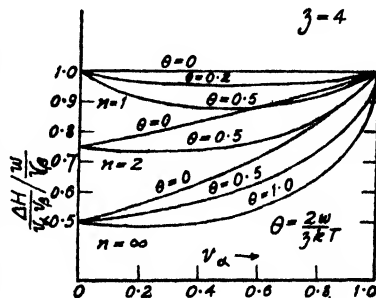


FIG. 3.

equally operative in the cases of the benzene mixtures with the polymeric homologues squalene and rubber, and hence at higher polymeric concentrations,  $v_a \rightarrow 1$ , where the statistical factor arising from the self-coiling of non-overlapping (or incompletely overlapping) polymer chains will not be operative, that a Hildebrand type of relation will apply (this in point of fact being exactly what is observed experimentally, over a considerable concentration range, see Fig. 10, ref. 5). Hence it follows that the contribution to  $(\Delta H_a)_0$  given by a hypothetical uncoiled polymer chain (i.e. the term  $\Phi$  in equations (14) and (17)), will be given by the linear extrapolation of the initial

TABLE III.

	Dihydro- myrcene n = 2.	Squalene n = 6.	Rubber n → ∞.
α cal./cc. . . .	5.1	4.0	3.5
1° cc. . . .	89	79.5	75
$\frac{1}{n} \phi_{\text{ex. cal./mole}}$ sub-group	450	320	260
$\frac{1}{n} \phi_{\text{th.}} . . . .$	450	350	300
α <sub>e</sub> — α . . . .	0	≧ 0.2	0.8
$-\frac{1}{n} \theta_{\text{ex. cal./mole}}$ sub-group	0	≧ 20	60
$-\frac{1}{n} \theta_{\text{th.}} . . . .$	0	21	150

\* The criticism being made here of the non-applicability to actual liquid mixtures of the formulae for the heats of mixing derived from the current quasicrystalline model refers to the present author's formulæ (ref. 1d) which are derived in a consistent way from this model, but which involve only a single explicit finite value of  $z$ . In the following discussion, however, it will be assumed that the Hildebrand relation is not incompatible with the less restrictive geometric assumptions used in Section III.

<sup>7</sup> Ferry, Gee and Treloar, *Trans. Faraday Soc.*, 1945, 41, 340.



portion of the experimental  $\Delta H/v_\alpha v_\beta$  curve from the region  $v_\alpha \approx 1$ , where the self-coiling effect does not affect the heat of mixing to  $v_\alpha = 0$ .

In Table III (page 21) the experimental values of  $\alpha_e$  (given by the extrapolated dotted curves in Fig. 10, ref. 5),  $V_r$  the molar volume per isoprene unit,  $\frac{1}{n}\Phi_{ex.}$  (given by  $\alpha_e V_r$ ) and  $\frac{1}{n}\Phi_{th.}$  are compared,  $\Phi_{th.}$  being given by the relation

$$\frac{1}{n}\Phi_{th.} = \frac{nz_\alpha - 2n + 2}{nz_\alpha} Nw' . \quad (27)$$

with  $z = 4$  and  $Nw'$  taken empirically as 600 cal. to give agreement with the experimental value in the dihydromyrcene case.

It remains now to compare the experimental and calculated values of  $\Theta$ , the term due to molecular self-coiling (equations (14) and (17)). On the basis of the present interpretation of the experimental results  $\frac{1}{n}\Theta_{ex.}$  (in cal. per mol. isoprene sub-group) is given by  $(\alpha - \alpha_e)V_r$  where  $\alpha$  is now the actual observed value of  $\Delta H/v_\alpha v_\beta$  at  $v_\alpha = 0$  (Fig. 10, ref. 5).

From equations (14), (17) and (18) we have

$$\begin{aligned} \frac{1}{n}\Theta &= -\frac{1}{n} \frac{\partial}{\partial T} R \log G(\eta') \\ &= -\frac{1}{n} \left( \frac{b\eta' + 2c\eta'^2 + \dots}{a + b\eta' + c\eta'^2 + \dots} \right) \frac{2Nw'}{z_\alpha} = -\frac{2Nw'}{z_\alpha} p(\eta') \quad (28) \end{aligned}$$

which, on substituting  $Nw' = 600$  cal., gives

$$\frac{1}{n}\Theta_{th.} = -300p\left(\frac{1}{2}\right) \quad \text{for } T = 300^\circ \text{K.}$$

The values of  $\frac{1}{n}\Theta_{th.}$  calculated using the data from the analysis of the square array case, together with the "experimental" values  $\frac{1}{n}\Theta_{ex.}$  are given in the above table.

The agreement of the calculated and experimental values of  $\Phi$  and  $\Theta$  is in all probability not unsatisfactory, considering (a) the quite large possible error of the experimental data itself, and (b) the fact that the use of the plane array  $p(\eta)$  curve to a situation which is approximately tetrahedral will result in an over-estimate\* of the effect of self-coiling.

## VI. Applications to the Configuration of Multiple Molecules in the Gas Phase.

While the analysis of Sections III and IV was primarily undertaken to provide information on the configuration of long chain polymer molecules in *solution*, it will be realised that the function  $-RT \log G(\eta)$ , by itself expresses the configurational contribution to the free energy of a *perfect gas*† of regularly-articulated non-overlapping multiple group molecules (for which the data of Section II on relatively short chains would, of course,

\* This is illustrated by the fact that, in the case of the tetrahedral lattice, polymer-polymer self-contacts are not obtained for polymer chains having less than 6 groups, whereas such contacts begin at the 4 group stage in the case of the square array.

† In the gas phase  $w_{\alpha\beta} = w_{\beta\beta} = 0$ , and hence  $\eta = \exp(-w_{\alpha\alpha}/kT)$ .

be appropriate). The use of the present model, involving the assumption of regular articulation according to a lattice pattern, while exactly appropriate to crystals and to a good approximation appropriate to liquids, no doubt over-emphasises somewhat the effect of steric self-restriction of the movements of a multiple group molecule in the gas phase. However, in view of the very considerable degree of self-coiling that is, in fact, indicated for a value of  $\eta$  appropriate to a hydrocarbon molecule, say 0.8 to 1.0 (compare Fig. 2), it can be judged that such an application would at least provide a useful limiting case.

## APPENDIX I.

In the following tables are collected some additional data, namely the distribution of distances between chain endings, which has resulted from the statistical analysis of the number of configurations of relatively short multiple-group molecules arranged on (a) square arrays, and (b) simple cubic lattices, as described in Section III. This information which, while not primarily required for the present work, is given here in view of its possible application in related problems as, for example, the problem of describing the viscous behaviour of relatively short chain molecules, either in the gas phase or in solution.  $r^2$  is the square of the distance between chain endings,  $n$  is the number of sub-groups of the multiple-molecule concerned, and  $P(\eta)$  is the weighted sum of the permitted (non-blocking) configurations appropriate to each value of  $r$ .

TABLE IV.

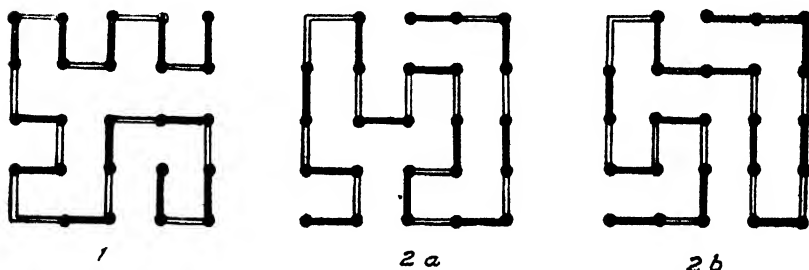
$r^2$ .	$P(\eta)$ .	$r^2$ .	$P(\eta)$ .
(a) Plane Square Arrays.			
$n = 4$		$n = 8$	
9	2	49	2
5	12	37	28
1	$4\eta$	29	84
$n = 5$		25	140
16	2	25	$40 + 20\eta$
10	16	17	$84 + 112\eta + 12\eta^2$
8	12	13	$48 + 136\eta + 36\eta^2$
4	$4 + 8\eta$	9	$20 + 52\eta + 32\eta^2 + 4\eta^3$
2	$8\eta$	5	$24 + 40\eta + 92\eta^2 + 24\eta^3$
$n = 6$		1	$8\eta + 48\eta^2$
25	2	$n = 9$	
17	20	64	2
13	40	50	32
9	$12 + 12\eta$	40	112
5	$8 + 32\eta + 4\eta^2$	36	$60 + 24\eta$
1	$12\eta^2$	34	224
$n = 7$		32	140
36	2	26	$176 + 176\eta + 16\eta^2$
26	24	20	$136 + 272\eta + 64\eta^2$
20	60	18	$48 + 144\eta + 48\eta^2$
18	40	16	$64 + 120\eta + 60\eta^2 + 8\eta^3$
16	$24 + 16\eta$	10	$72 + 152\eta + 188\eta^2 + 56\eta^3$
10	$32 + 64\eta + 8\eta^2$	8	$28 + 56\eta + 96\eta^2 + 40\eta^3 + 4\eta^4$
8	$8 + 32\eta + 8\eta^2$	4	$20 + 32\eta + 64\eta^2 + 64\eta^3 + 8\eta^4$
4	$4 + 16\eta + 20\eta^2$	2	$8 + 40\eta + 96\eta^2 + 8\eta^4$
2	$4 + 28\eta^2$		

TABLE IV.....continued.

$r^2$ .	$P(\eta)$ .	$r^2$ .	$P(\eta)$ .
(b) Simple Cubic Lattices.			
$n = 4$		$n = 6$ (cont.)	
9	3	9	360
5	36	5	$240 + 312\eta + 12\eta^2$
3	24	3	$48 + 144\eta + 24\eta^2$
1	$12\eta$	1	$24\eta + 108\eta^2$
$n = 5$		$n = 7$	
16	3	36	3
10	48	26	72
8	36	20	180
6	144	18	360
4	$12 + 24\eta$	18	120
2	$24 + 72\eta$	16	$72 + 48\eta$
$n = 6$		14	1440
25	3	12	360
17	60	10	$672 + 576\eta + 24\eta^2$
13	120	8	$456 + 384\eta + 24\eta^2$
11	240	6	$624 + 1200\eta + 192\eta^2$
9	$36 + 36\eta$	4	$132 + 192\eta + 228\eta^2$
		2	$132 + 288\eta + 588\eta^2 + 96\eta^3$

## APPENDIX II.

The effect referred to in Section IV, in which an estimate of the number of configurations of a closely coiled polymer is under discussion, may be exemplified by taking the case of a square array of 25 points. This will be "filled" when 12 double-molecules are "adsorbed". Two possible arrangements chosen at random, are shown below where the double-molecules are represented by thickened lines and the links connecting them together to form a polymer chain are indicated by thin double lines.



It will be seen that there is only one possible way (as shown) of stringing the 12 double-molecules together to make a linearly connected polymer chain of 25 sub-groups, in case 1, while the two possibilities, 2a and b, exist for the distribution of double-molecules given in case 2.

## APPENDIX III.

The greater rotational and translational degree of freedom of movement of the individual molecules in a liquid phase compared with that obtaining in the crystal results in a "liquid structure" in which the finer local co-ordination details of the molecules in the crystal are "smeared out". Thus, if we are concerned only to define an average first neighbour co-ordination number for a liquid (or elastic polymer) phase an estimate, useful for the limited purpose of

comparing one liquid with another, can be obtained by applying to the liquid phase the relation

$$\rho = \alpha \frac{M.W.}{r^3} \quad (29)$$

appropriate to the simplest types of crystal lattices, where  $\rho$  is the density (g./cc.)  $M.W.$  the molecular weight, and  $r$ , (A.) the distance between molecular centres, and where, in the particular cases of the tetrahedral, simple cubic, body-centred cubic and face-centred cubic lattices,  $\alpha$  has the values 1.07, 1.65, 2.14 and 2.33 respectively.

In the case of the benzene molecule in the liquid phase, a knowledge of its dimensions from X-rays analysis and an estimate of the extent of its van der Waals' field enables one to conclude that it is roughly an oblate spheroid in shape having two major axes of about 6.0 to 6.3 A., and a minor axis of about 4.0 to 4.3 A. Then, substituting for  $r$  the mean of these three axial distances, namely 5.5 A.

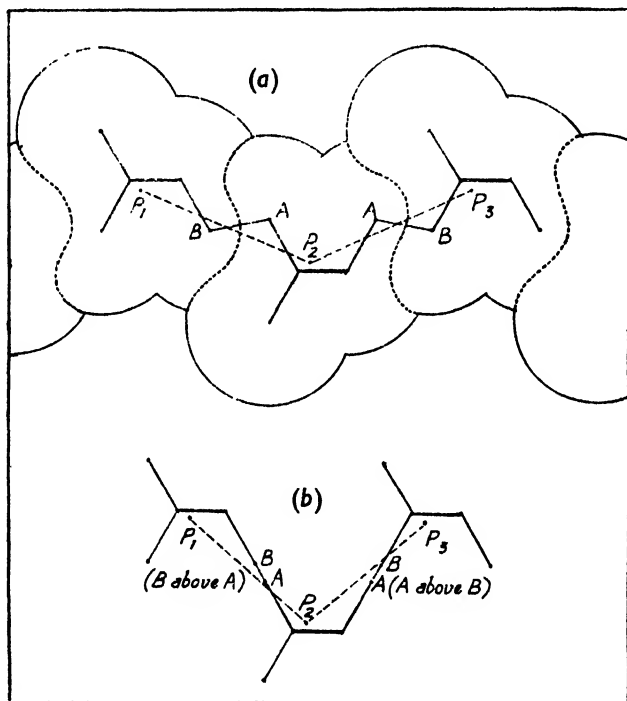


FIG. 4.

together with  $\rho = 0.8734$  (25° C.) in (29) for  $\alpha$ , a value of 1.86 is obtained indicating an average co-ordination of between 6 and 8.

In the case of the rubber polymer molecule the natural unit to take for the sub-group (for the purpose of a quasi-crystalline model) is clearly the isoprene unit, which is able to articulate at the "isoprene-link" with a considerable degree of freedom as may be seen by experimenting with steric molecular models. Diagram (a), Fig. 4, illustrates the general contour of the van der Waals' field round such a molecule (*cis* chain) when in an extended configuration and the kind of division into isoprene sub-groups that is envisaged. The distance between the centres of gravity  $P_1$ ,  $P_2$ ,  $P_3$ , of the sub-groups (which would appear to be the appropriate points to consider as sub-group centres) is in this case 4.84 A., and the angle subtended between two successive "links"  $P_1P_2$  and  $P_2P_3$  is 134°. Using now equation (29), and substituting the experimental density of rubber, namely 0.9094 g./cc. and  $M.W. = 68$  for a sub-group, one obtains the values 4.31 and 4.98 A. for  $r$ , the distance between sub-group centres, in the tetrahedral and simple cubic cases respectively (and larger values of  $r$  for larger  $z$ ). Since,

however, the maximum value of  $r$  is  $< 4.98 \text{ \AA.}$ , a co-ordination number  $< 6$  is indicated. On the other hand, a relative articulation of the links  $P_1P_2$  and  $P_2P_3$  at about  $109^\circ$  is a perfectly feasible and, indeed, probable configuration, combined with a link distance of about  $4.4 \text{ \AA.}$  (A case in point is given in Diagram (b), Fig. 4, where  $P_1\hat{P}_2P_3 = 104^\circ$ , and  $P_1P_2 = P_2P_3 = 4.36 \text{ \AA.}$ ) To complete the tetrahedral configuration two first neighbours are required at point  $P_2$  also at a distance of  $4.4 \text{ \AA.}$  Since, moreover, this distance is just that of the normal van der Waals distance of closest approach, it is concluded that the rubber structure in the unextended state is probably fairly adequately represented by a roughly tetrahedral relative co-ordination of linked sub-groups and neighbouring sub-groups.

The statistical analysis of Section III in the above paper was almost entirely completed while the author was a member of the British Rubber Producers' Research Association, and the general argument of Section V owes much to discussions which the author had while working in collaboration with Dr. Gee on the general problem of polymer solutions. This work was further developed on the theoretical side, and finally completed during the tenure of an I.C.I. Fellowship in the University of Glasgow. In this connection the author's thanks are also due to Professor J. Monteath Robertson, F.R.S., for affording him the privilege of working in his department.

### Summary.

A statistical treatment of the behaviour of polymer solutions at the simplifying limiting case of very high dilution is presented in terms of a generalised quasi-crystalline model in which account is taken of the special configurational situation presented at infinite dilution where the polymer molecules separate out from each other as individual species.

The theoretical formula for the heat of mixing separates into two parts, (a) a term corresponding to the heat of solution of a hypothetical non-self-interacting chain, and (b) a term giving the energy involved in the change from the hypothetical uncoiled state to the equilibrium coiled-up configuration.

To provide information about the average configuration of a coiled-up polymer chain statistical analyses are presented (a) in which the average configurational state of relatively short multiple molecules articulated on two simple types of lattices (taking into account the influence of first neighbour interactions and steric self-blocking effects) is accurately determined, and (b) in which an approximate solution of the same problem is derived for very long polymer molecules.

It is argued that the postulates involved in the current quasi-crystalline theory of polymer solutions are too restrictive for it ever to give an accurate account of a system such as the rubber-benzene case. An application is made of the treatment developed here (for infinitely dilute solutions) to the available experimental data.

### Résumé

On donne ici un traitement statistique des solutions de polymères dans le cas limite d'une très grande dilution pour simplifier ; et ceci, selon un modèle généralisé quasi cristallin, dans lequel on tient compte de la configuration spéciale présentée par une dilution infinie, où les molécules du polymère se séparent les unes des autres en tant qu'individus distincts.

La formule théorique pour la chaleur de dissolution se partage ici en deux termes : l'un correspondant à la chaleur de dissolution d'une chaîne hypothétique n'ayant pas de self-interaction, l'autre donnant l'énergie relative au passage de la forme hypothétique déroulée à la configuration enroulée d'équilibre.

On présente des analyses dans lesquelles (a) on détermine avec précision la configuration moyenne des molécules multiples relativement courtes, qui s'articulent sur deux types simples de réseaux (en tenant

compte des interactions du voisin immédiat et des effets stériques de blocage) et (b) on établit une solution approchée du même problème dans le cas des très longues molécules.

L'auteur démontre que la théorie courante, qui considère les solutions de polymères dans un état quasi cristallin, est basée sur des postulats trop restrictifs pour lui jamais permettre de rendre un compte précis d'un système tel que caoutchouc-benzène. Le traitement développé ici (pour des solutions infiniment diluées) est appliqué à certains résultats expérimentaux connus.

### Zusammenfassung

Eine statistische Erörterung des Verhaltens von Polymerlösungen im vereinfachten Grenzzustand von grosser Verdünnung wurde mit Benützung eines verallgemeinerten quasi-kristallinen Modells unter Berücksichtigung des Konfigurationszustandes, der bei unendlicher Verdünnung besteht, wenn die Polymerelemente als individuelle Moleküle von einander separiert sind, durchgeführt.

Die theoretische Formel für die Mischungswärme zerfällt in zwei Teile, (a) einen Ausdruck, der der Lösungswärme einer hypothetischen Kette entspricht, deren Teile nicht auf einander selbst einwirken, und (b) einen Ausdruck für die Energie, die dem Übergang vom hypothetischen ungeordneten Zustand zu der zusammengewickelten Gleichgewichtslage entspricht.

Zwei statistische Analysen werden durchgeführt. In der ersten wird die Durchschnittskonfiguration von verhältnismässig kurzen Molekülen, die auf zwei einfachen Arten von Gittern (unter Berücksichtigung des gegenseitigen Einflusses unmittelbarer Nachbarstellungen und sterischer Hinderung) arrangiert sind, genau bestimmt; in der zweiten wird eine Näherungslösung des selben Problems für sehr lange Polymerelemente durchgeführt.

Der Verfasser gibt Gründe an, warum die Axiome, auf denen die heutige quasi-kristallinische Theorie der Polymerlösungen aufgebaut ist, zu einschränkend sind, als dass diese Theorie je eine genaue Beschreibung eines wirklichen Systems, wie z.B. Kautschuk—Benzol, erzielen könnte. Die hier (für unendlich verdünnte Lösungen) entwickelte Methode wird auf existierende experimentelle Angaben angewendet.

*Department of Chemistry,  
University of Glasgow.*

---

## BIMOLECULAR QUENCHING PROCESSES IN SOLUTION.

BY E. J. BOWEN, A. W. BARNES, AND P. HOLLIDAY.

*Received 16th January, 1946, as amended 5th February, 1946.*

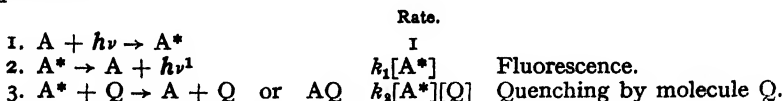
The following paper relates to measurements and calculations made on the quenching of the fluorescence of dilute solutions of anthracene in organic solvents by other added organic molecules. The latter and the solvents, of course, were chosen to have no absorption of the exciting light (3650 Å.) themselves. The solutions were freed from oxygen by a fine current of nitrogen to eliminate oxygen quenching,<sup>1</sup> and the fluorescence intensity was measured with a photocell amplified by an electrometer valve, an Ilford filter 805 being interposed between fluorescence cell and photocell to cut out scattered exciting light. For work at low temperatures the solutions were contained in a small transparent Dewar vessel, and

<sup>1</sup> Bowen and Norton, *Trans. Faraday Soc.*, 1939, **35**, 44.

cooled by the insertion of a metal tube in which liquid air was placed. The fluorescence was observed at right-angles to the exciting beam, and dewing of the vessel walls was avoided by a current of dry air flowing round the apparatus.

Most earlier work (see later references) on fluorescence quenching in solution has been carried out on fluorescent dyes in aqueous solution, and as quenching agent, the iodide ion has often been used. Such systems are complicated by the peculiar polymerisation effects of dyes in water and by the strong ionic forces which the reacting species exert on each other. These difficulties are avoided in the present work by the use of non-polar fluorescent hydrocarbons dissolved in non-aqueous solvents. The aim of the investigation was to discover, if possible, the mechanism of the quenching of the fluorescence of such solutions by adding organic substances.

The collisional quenching of fluorescence may be represented by the equations:



On simple reaction velocity theory

$$(F_0 - F)/F = k_1[Q]/k_1 = k_1\tau[Q] = k[Q],$$

where  $F_0$  = fluorescence intensity without quencher,  $F$  = fluorescence intensity with quencher at concentration  $[Q]$ ,  $\tau$  = mean life of fluorescent molecule.

Since  $\tau$  is of the order of  $10^{-8}$  sec. and  $(F_0 - F)/F$  must be near to unity,  $k_1$  is about  $10^8$  sec. $^{-1}$  mol. $^{-1}$  litre when  $[Q]$  is about molar. We are thus dealing in collisional quenching processes with bimolecular reactions up to a million million times faster than thermal bimolecular reactions ordinarily investigated, and the laws obeyed by the two cases are quite different. Since the number of collisions between quencher and fluorescent molecule in  $10^{-8}$  sec. is small, quenching must occur at a high proportion of the collisions. In a liquid the solvent hems in the solute molecules to give "repeated collisions" between pairs of molecules before they separate,<sup>2</sup> and such groups of collisions are termed "encounters". Because of the high probability of quenching occurring when the two molecules meet, the quenching rate  $k[Q]$  would be expected to be governed by the encounter rate of the molecules. This rate is governed by the diffusion rate of the molecules in the liquid, so that the quenching constant  $k$  is a function of the viscosity of the solvent.

Applying the equation deduced by Smoluchowski<sup>3</sup> for the coagulation of colloidal particles in solution, we have, under *stationary state* conditions

$$\text{Quenching constant } k = 3PV \left( \frac{\tau D}{4R^2} \right),$$

where  $R$  is the radius of fluorescent or quenching molecule (assumed equal), quenching being assumed to occur at ordinary "collisional" distances;  $P$  is the probability of quenching occurring during one encounter;  $V$  is the volume in litres/mole of the "sphere of effective quenching" =  $32\pi R^3 N/3,000$ ; and  $D$  is the diffusional constant of quencher or fluorescent molecules (assumed equal for the molecules used in this work) =  $\frac{1.45 \times 10^{-17}}{R} \times \frac{T}{\eta}$ , assuming Stokes' law where  $T$  = absolute temperature and  $\eta$  = viscosity of solution. Thus  $k$  is a linear function of  $T/\eta$ ; an effect which would be observed in ordinary bimolecular reactions only at viscosities equal to those of the vitreous state.

<sup>3</sup> Franck and Rabinowitch, *Trans. Faraday Soc.*, 1934, 30, 120.

<sup>2</sup> *Z. physikal. Chem.*, 1917, 92, 129.

The derivation of the above, however, assumes *stationary state* conditions, i.e., that the equilibrium diffusion conditions are not disturbed by the actual quenching process. With a high probability of quenching in each encounter this is not justified. Sveshnikoff<sup>4</sup> and Umberger and LaMer<sup>5</sup> have discussed this matter. The mathematical considerations are very complicated and an approximate solution only is possible. For not too large quenching ( $(F_0 - F)/F > 1$ ) these authors show that a corrected expression for  $k$  is

$3PV \left( \frac{\tau D}{4R^2} + \frac{\sqrt{\tau D}}{2R} \right)$ ;  $k$  is now no longer a linear function of  $T/\eta$ . We have applied this equation to our experimental results using molecular constants derived on the following basis.

From values of  $D$  recorded in the literature for organic molecules in solution identical or similar to those used in this work and assuming Stokes' law, it appears that  $R$  must be close to  $3.6 \times 10^{-8}$  cm.  $\tau$  is taken as  $10^{-8}$  sec.

The above table of values then applies.

The relative importance of the second term in comparison with the first is apparent from this table. At high viscosities and low temperatures

TABLE II.—TEMPERATURE RANGE 20 TO 60° C.

Quencher: Carbon Tetrachloride.		Anthracene (Self-quenching).	
Solvent.	P.	Solvent.	P.
Ether . . .	0.16	Cyclohexane . . .	0.46
Alcohol . . .	0.10	Hexane . . .	0.40
Dioxane . . .	0.092	Ether . . .	0.27
Acetone . . .	0.063	Benzene . . .	0.27
Chlorobenzene . . .	0.041	Acetone . . .	0.22
Paraffin (viscous) . . .	0.040	Xylene . . .	0.21
Benzene . . .	0.040	Dioxane . . .	0.16
Xylene . . .	0.037	Chlorobenzene . . .	0.16
Cyclohexane . . .	0.0097		
Hexane . . .	0.005		

TEMPERATURE RANGE — 60 TO + 60° C. SOLVENT TOLUENE.

Quencher.	P.	Quencher.	P.
Oxygen . . .	0.95	Bromoform . . .	0.28
Carbon tetrabromide . . .	0.66	Acetylene tetrabromide . . .	0.16

measurements with perhaps too simplified a treatment of the molecular rotations.

<sup>4</sup> *Acta Physicochimica U.R.S.S.*, 1935, 3, 257; 1936, 4, 452.

<sup>5</sup> *J. Amer. Chem. Soc.*, 1945, 67, 1099.

<sup>6</sup> Gaviola, *Z. Physik*, 1927, 42, 853; W. Szymanowski, *ibid.*, 1936, 95, 440.

<sup>7</sup> *Ann. Physique*, 1929, 12, 169.

TABLE I.

$\frac{T}{\eta}$ .	$\frac{\tau D}{4R^2}$ .	$\frac{\sqrt{\tau D}}{2R}$ .	$\left( \frac{\tau D}{4R^2} + \frac{\sqrt{\tau D}}{2R} \right)$ .
3,000	2.34	1.54	3.88
10,000	7.8	2.8	10.6
18,000	14.0	3.7	17.7
30,000	23.4	4.9	28.3
60,000	46.8	6.9	53.7
90,000	70.0	8.4	78.4
120,000	93.5	9.7	103
150,000	117	10.9	128

$k$  becomes proportional to  $(T/\eta)^{1/2}$ , and at low viscosities and high temperatures to  $T/\eta$ .

The fluorescence lifetime for the dissolved anthracene molecule which we have assumed,  $10^{-8}$  sec., is very close to that found for dyes for direct measurement.<sup>6</sup>

It does not agree with that tentatively put forward by F. Perrin,<sup>7</sup> but the estimation of the latter was based on polarisation



The experiments were made by varying  $T/\eta$  for each solvent containing quencher at a low and anthracene at a very low concentration (or anthracene itself at higher concentration) by changing the temperature, measuring the quenching constant  $k$ , and evaluating  $k/3V\left(\frac{\tau D}{4R^2} + \frac{\sqrt{\tau D}}{2R}\right) = P$  (probability of quenching in each encounter). With the above values of  $\tau$  and  $R$  a reasonably good constancy of  $P$  for each solvent was obtained. These values of  $P$  are shown in Table II.

TABLE III.

Quencher: Bromobenzene.	Values of $k$ ( $T^\circ\text{C}$ ).		
	20.	40.	60.
Solvent.			
Paraffin ( $d = 0.84$ )	1.53	1.43	1.40
Cyclohexane .	1.5	1.4	1.3
Alcohol .	1.53	1.39	1.10
Hexane .	1.38	1.36	1.30
Benzene .	1.34	1.20	1.13
Acetone .	1.04	1.01	1.00
Dioxane .	1.1	1.0	0.98
Xylene .	1.03	0.99	0.87
Chlorobenzene .	0.82	—	0.78

For quenching by  $\text{CCl}_4$  the more polar solvents give the highest values of  $P$ , presumably due to their power of activating the  $\text{CCl}_4$  molecule by polarizing it. For quenching by anthracene, the paraffinic solvents give the highest values of  $P$ , possibly because the aromatic and oxygen-containing solvents protect the anthracene molecules by forming transient combinations through London "dispersion" forces. For the quenchers listed in Table II it seems that the diffusion-controlled bimolecular reaction theory is capable of interpreting the dependence of the quenching constant on temperature and viscosity.

Certain other quenching substances show a totally different behaviour; instead of the quenching constant *increasing* with rise of temperature, it shows a small *decrease*, as in the examples in Tables III and IV.

The simplest explanation of this behaviour is that the quencher molecules  $Q$  form temporary complexes  $AQ$  with the fluorescent molecules  $A$  whose life is longer than  $\tau$ , the mean fluorescent life, i.e., there is the equilibrium in the solution:

$A + Q \rightleftharpoons AQ + H \text{ cal.}$

The molecules  $AQ$  compete with  $A$  for the light absorbed, and are themselves non-fluorescent, or only feebly fluorescent. If  $\epsilon_1$  and  $\epsilon_2$  are the extinction coefficients of  $A$  and  $AQ$ , the quenching constant is given by  $k\epsilon_1/\epsilon_2$  where  $k = [AQ]/[A][Q]$ .

A plot of  $\log k$  against  $1/T$  then gives a value for  $H$ , the heat of association. For the above quenchers  $H$  is less than about 1 kcal./mole. This may be compared with values of 0.6–4.0 kcal./mole. obtained by Briegleb<sup>8</sup> for associations between aromatic hydrocarbons and nitro-compounds. In the stronger associations of nitro-compounds with hydro-

TABLE IV.—QUENCHERS IN TOLUENE SOLUTION.

Quencher.	Values of $k$ ( $T^\circ\text{C}$ ).			$H$ Cal./mole.
	- 30.	0.	30.	
Bromobenzene .	1.53	1.4	1.3	510
Isopropyl bromide .	1.03	0.90	0.79	730
Trimethylene dibromide .	3.5	3.3	2.7	820
<i>p</i> -dibromobenzene .	3.8	4.1	4.0	890
<i>o</i> -bromotoluene .	1.54	1.48	1.44	160
<i>p</i> -bromotoluene .	1.49	1.44	1.45	160
<i>m</i> -bromotoluene .	2.11	2.16	2.14	v. small
$\alpha$ -bromonaphthalene .	4.7	4.6	4.3	990
<i>p</i> -dichlorobenzene .	—	0.23	0.21	1100

<sup>8</sup> *Z. physik. Chem. B.*, 1932, 19, 255; 1934, 26, 63; 1935, 31, 58; 1936, 32, 305.

carbons the absorption spectrum of the solution is markedly changed (i.e.,  $\epsilon_2$  is different from  $\epsilon_1$ ), but the effect of the above quenchers on the absorption spectrum is scarcely discernible. When  $\epsilon_2$  is greater than  $\epsilon_1$  the presence of the compound is obvious and the "quenching" of the fluorescence would be ascribed to the inner-filter effect of the non-fluorescent compound. In the above cases, however, the apparently sharp distinction between collisional quenching and inner-filter simulation of quenching becomes blurred. The distinction appears only in the differences of behaviour of  $k$  with temperature. Even this distinction loses its clarity in intermediate examples. Carbon tetrachloride behaves as a collisional type quencher while chloroform is a weak compound type. One is bound to conclude that probably in all cases of bimolecular quenching in solution transient compounds are involved; the type of variation of  $k$  with  $T$  being determined by the relation of the life time of the compound to  $\tau$ . The nature of the forces holding the molecules together must be specially strong London "dispersion" forces,<sup>9</sup> i.e., not a first order wave-mechanical orbital interaction, but a second order effect arising from the time variation of the wave-functions of the  $\pi$  electrons. For aromatic molecules and polarisable halogen compounds these forces are unusually large because of the simultaneous operation of more than one favourable factor.

### Summary.

The quenching of the fluorescence of solutions of anthracene by organic substances has been examined over a range of temperatures. The variations of the quenching constant are of two types, one explicable in terms of a bimolecular process whose rate is controlled by diffusion, and the other indicating van der Waals' association between quencher and fluorescent molecules. It is concluded that such associations probably always precede quenching; the two types of variation above arising from the relative life-times of complex and fluorescent state.

### Résumé.

L'extinction de la fluorescence des solutions d'anthracène par les substances organiques a été examinée dans un certain domaine de température. Les variations de la constante d'extinction sont de deux types, l'un expliqué par un processus bimoléculaire dont la vitesse est contrôlée par la diffusion, et l'autre indiquant une association de Van der Waals entre les molécules fluorescentes et celles de l'extincteur. On conclut que de telles associations précèdent probablement toujours l'extinction, les deux types de variation mentionnés provenant des durées de vie relatives des états complexe et fluorescent.

### Zusammenfassung.

Die Fluoreszenzauslöschung von Anthracenlösungen durch organische Substanzen wurde bei mehreren Temperaturen bestimmt. Zwei Arten der Veränderung der Geschwindigkeitskonstante der Auslöschung bestehen, von denen eine als bimolekularer Vorgang, dessen Geschwindigkeit durch Diffusion bestimmt ist, erklärt werden kann, während die andere auf Van der Waals Assoziation zwischen Auslöschermolekülen und fluorescenten Molekülen hindeutet. Es wird gefolgert, dass solche Assoziationen wahrscheinlich immer dem Auslöschungsvorgang vorhergehen und dass diese zwei Typen der Veränderung eine Folge der relativen Lebensdauer des Komplex- und des Fluoreszenz zustandes sind.

*University College,  
Oxford.*

<sup>9</sup> London, *Trans. Faraday Soc.*, 1937, **32**, 8.

# THE VAPOUR PRESSURES, LATENT HEATS OF SUBLIMATION AND TRANSITION POINTS OF SOLID HEXACHLOROETHANE.

By K. J. IVIN AND F. S. DAINTON.

*Received 19th February, 1946.*

In the course of another investigation it became necessary to obtain certain thermochemical data concerning hexachloroethane. The data reported in the literature<sup>1</sup> are scanty and unreliable; and as a first step it was decided to make an accurate determination of the vapour pressure curve of solid hexachloroethane. Using the air-saturation method, Nelson<sup>2</sup> obtained vapour pressures in the temperature range 31 to 60° C. leading to a value of  $L_s$  (latent heat of sublimation) of 14 kcal. per mol.<sup>3</sup> Using a static method, van der Lee<sup>4</sup> obtained values of the vapour pressure between 62.1° C. and 239.1° C., and hence  $L_s = 12.0$  kcal. per mol. but the accuracy claimed for each pressure value was only  $\pm 1$  mm. Hg.

## Experimental.

The hexachloroethane was a commercial sample which was crystallised from alcohol and resublimed at atmospheric pressure. On heating the material so obtained *in vacuo* at 200° C. a small amount of decomposition took place with formation of chlorine and probably tetrachloroethylene. After pumping off these decomposition products and reheating the hexachloroethane this phenomenon was not observed again, and it is therefore ascribed to the presence of a trace of a higher chlorohydrocarbon which could be decomposed by heating. The sample of hexachloroethane used for the vapour pressure measurements had been treated in this manner and gave results reproducible to at least 0.1 mm. Hg. or 0.2 %, whichever error was the greater, even after several days interval.

The vapour pressures were measured statically over the temperature range 13 to 174° C. as follows. The hexachloroethane was enclosed in a small tube which could be surrounded by constant temperature baths of melting or boiling pure compounds and was connected to a sensitive Bourdon gauge of the pointer type, mounted on a stone slab, and used as a direct measuring instrument. Deflections of the pointer tip were measured by a travelling microscope, and calibration against a mercury manometer established that the limit of the gauge sensitivity was 0.05 mm. Hg. The spoon of the gauge was sealed into an outer jacket, to which air could be admitted or removed, and the gauge and all connecting tubing electrically heated to 200° C. Before any measurements were made, the whole apparatus was evacuated until a pressure of  $10^{-5}$  mm. Hg. (measured on a McLeod gauge) was obtained with the tube containing the purified hexachloroethane immersed in liquid air. The tube and Bourdon gauge were then sealed off from the pumping system and steady pressures measured whilst the sample tube was immersed in the appropriate bath. Pressure readings were taken for series of ascending and descending temperatures, and the bath temperatures were checked by the use of standard

<sup>1</sup> See, for example, Bichowsky and Rossini, *Thermochemistry of Chemical Substances*, 1936, p. 240.

<sup>2</sup> Nelson, *Ind. Eng. Chem.*, 1930, **22**, 971.

<sup>3</sup> Bichowsky and Rossini, *loc. cit.*<sup>1</sup> give  $L_s = 17$  kcal. from Nelson's data, but we calculate  $L_s = 14$  from the same data.

<sup>4</sup> Van der Lee, *Z. anorg. Chem.*, 1935, **223**, 213.

and calibrated thermometers (making any necessary stem corrections). The temperatures were accurate to  $\pm 0.1^\circ \text{C}$ .

### Results.

The results are presented in the table. The pressure measurements have been reduced to mm. Hg. at  $0^\circ \text{C}$ .

TABLE I.

Constant Temperature Bath.	$T^\circ \text{K}$ .	$P_{\text{obs.}}$ (mm. Hg at $0^\circ \text{C}$ .)	$\log_{10} P_{\text{obs.}}$	$10^3/T^\circ \text{K}$ .	$P_{\text{calc.}}$ (mm. Hg at $0^\circ \text{C}$ .)
Water . . . . .	286.1	0.20	1.3	3.495	0.14
<i>o</i> -Cresol (M) . . . . .	303.6	0.60	1.78	3.294	0.58
<i>p</i> -Cresol (M) . . . . .	307.5	0.80	1.90	3.251	0.77
Phenol (M) . . . . .	313.9	1.25	0.097	3.186	1.22
<i>o</i> -Nitrophenol (M) . . . . .	317.9	1.65	0.217	3.146	1.63
Benzophenone (M) . . . . .	320.5	1.85	0.267	3.120	1.95
<i>p</i> -Dichlorobenzene (M) . . . . .	326.2	2.85	0.455	3.065	2.87
Chloroacetic acid (M) . . . . .	334.9	5.1	0.708	2.986	5.03
Methyl alcohol (B) . . . . .	338.1	6.1	0.785	2.958	6.2
<i>n</i> -Hexane (B) . . . . .	340.8	7.15	0.854	2.934	7.3
Carbontetrachloride (B) . . . . .	349.8	11.7	1.068	2.859	12.0
Naphthalene (M) . . . . .	352.7	13.75	1.138	2.835	13.9
<i>m</i> -Dinitrobenzene (M) . . . . .	363.2	22.6	1.354	2.754	22.9
Water (B) . . . . .	373.1	36.2	1.559	2.680	36.0
Toluene (B) . . . . .	383.5	57.2	1.757	2.607	56.5
Acetic acid (B) . . . . .	390.3	74.8	1.874	2.562	74.7
Chlorobenzene (B) . . . . .	405.5	137.8	2.139	2.466	134.3
Acetic anhydride (B) . . . . .	412.4	175.0	2.243	2.425	173.4
Bromoform (B) . . . . .	423.0	254.7	2.406	2.364	252.3
Cyclohexanol (B) . . . . .	434.6	373.0	2.572	2.301	374.1
<i>p</i> -Dichlorobenzene (B) . . . . .	447.6	559.3	2.748	2.234	563.6

(M) = Melting.

(B) = Boiling.

The curve (Fig. 1) obtained by plotting  $\log_{10} P$  against  $10^3/T^\circ \text{K}$ . consists of two lines, the equations of which were found to be

$$\log_{10} P(\text{mm. Hg}) = \frac{-2677}{T} + 8.731, \text{ above } 72.0^\circ \text{C.},$$

$$\text{and } \log_{10} P(\text{mm. Hg}) = \frac{-3077}{T} + 9.890, \text{ below } 72.0^\circ \text{C.},$$

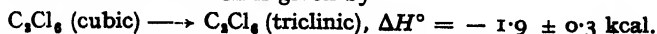
and which intersect at the point,  $T = 72.0^\circ \pm 1.0^\circ \text{C}$ .,  $p = 9.5 \text{ mm.} \pm 0.6 \text{ mm.}$

The validity of these equations may be judged by comparison of column 3 and 6 of the table, the pressures in column 6 have been calculated from these equations;  $72^\circ \text{C}$ . is clearly the transition temperature between the cubic and triclinic forms<sup>5</sup> which has been directly observed by Steinmetz<sup>6</sup> as  $71.3 \pm 0.4^\circ \text{C}$ . and by Wiebanga<sup>7</sup> as  $71.1^\circ \text{C}$ . From these equations we also find that the latent heats of sublimation of the two forms are

$$L_s(\text{cubic}) = 12.2 \pm 0.1 \text{ kcal. per mol.}$$

$$L_s(\text{triclinic}) = 14.1 \pm 0.2 \text{ kcal. per mol.}$$

whence the heat of transition is given by



and the entropy change at the transition point =  $5.5 \pm 0.9 \text{ cal. per degree C. per mol.}$

<sup>5</sup> Schwarz, *Z. Krist.*, 1895, **25**, 614.

<sup>6</sup> Steinmetz, *Z. physik. Chem.*, 1905, **52**, 466.

<sup>7</sup> Wiebanga, *Z. anorg. Chem.*, 1935, **225**, 38.

## 34 VAPOUR PRESSURES OF SOLID HEXACHLOROETHANE

No changes in the slope of the line  $\log_{10} P$  against  $1/T$  could be detected above or below  $72^\circ \text{C.}$ , and it is presumed that the heat changes involved in the transitions which have been recorded ( $43.6^\circ \text{C.}$ , rhombic to triclinic; and  $125^\circ \text{C.}$ ,  $\alpha$  to  $\beta$ )<sup>8</sup> are very small, probably less than 700 cal. per mol.

Van der Lee<sup>4</sup> proposed the equation

$$\log_{10} P(\text{mm. Hg}) = -2636/T + 8.640$$

for the whole of the temperature range  $62^\circ \text{C.}$  to  $186.8^\circ \text{C.}$  (the triple point), which differs considerably from the equations given above. However, we

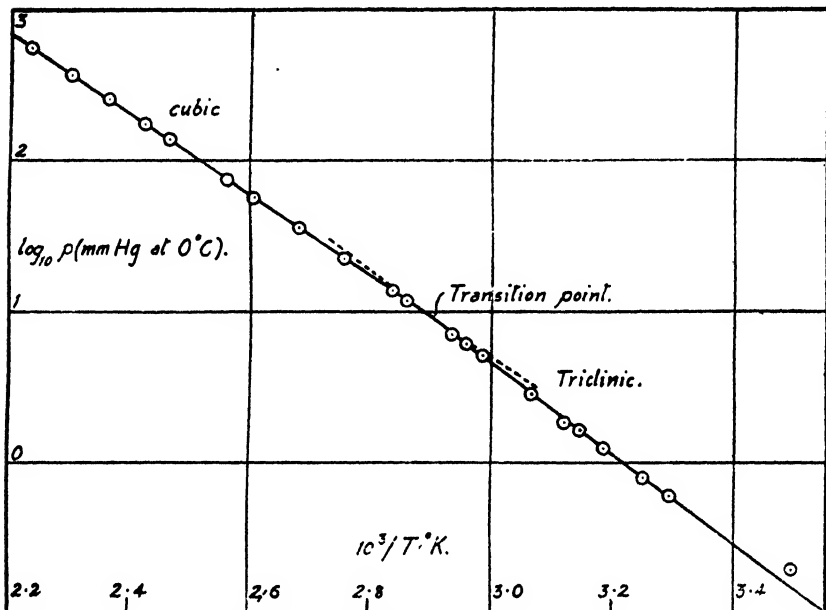


FIG. 1.

consider our equations to be more correct for the following reasons. (1) Van der Lee's pressures were measured to an accuracy of 1 mm. only. Our data are accurate to 0.1 mm. or 0.2 %; (2) his results do not reveal the transition point at  $72^\circ \text{C.}$ ; (3) many of his experimental points lie on, or close to, the line  $\log_{10} P = -2677/T + 8.731$ ; (4) owing to a number of errors in his calculation, his results do not agree as closely as at first appears with the equation proposed in his paper. It is perhaps also significant that Nelson's data<sup>2</sup> support the value 14.1 kcal. for the latent heat of sublimation of the triclinic form, although his vapour pressures are all  $\sim 10\%$  below those given here, a difference which is probably due to his employment of the air saturation method.

### Summary.

The vapour pressures of hexachloroethane have been measured to a greater accuracy than hitherto, over the temperature range  $13^\circ$  to  $174^\circ \text{C.}$  by a static method. The vapour pressure-temperature curve shows a distinct discontinuity at  $72^\circ \text{C.}$  corresponding to the transition between the cubic and triclinic forms. The thermodynamic data appropriate to these forms are:

$$\text{triclinic: } \log_{10} P(\text{mm. Hg}) = -3077/T + 9.890,$$

whence

$$L_s(\text{triclinic}) = 14.1 \pm 0.2 \text{ kcal. per mol.}$$

<sup>8</sup> Pascal, *Comp. Rend.*, 1912, 154, 883.

cubic :  $\log_{10} P(\text{mm. Hg}) = -2,677/T + 8.731$ ,  
 whence  $L_s \text{ cubic} = 12.2 \pm 0.1 \text{ kcal. per mol.}$

and  $\Delta H^\circ$  for the transition triclinic to cubic =  $+1.9 \pm 0.3 \text{ kcal.}$ , and

$$\Delta S^\circ = +5.5 \pm 0.9 \text{ cal. per degree c. per mol.}$$

Reasons are given for regarding these results as better than earlier measurements, and it is concluded that the heat content changes associated with other reported phase changes at  $43.6^\circ \text{ C.}$  and  $125^\circ \text{ C.}$  do not exceed  $700 \text{ cal. per mol.}$

### Résumé.

Les tensions de vapeur de l'hexachloréthane ont été mesurées entre  $13$  et  $174^\circ \text{ C.}$  par une méthode statique avec une précision de  $0.1 \text{ mm.}$  de Hg ou de  $0.2 \%$ , selon que l'une ou l'autre de ces évaluations de la précision est la meilleure. La courbe tension de vapeur-température montre une discontinuité distincte à  $72^\circ \text{ C.}$  correspondant à la transition entre les formes cubique et triclinique. Les résultats thermodynamiques sont les suivants :

$$\begin{aligned} \text{triclinique : } \log P(\text{mm. Hg}) &= -3077/T + 9.890 \\ \text{d'où } L_s(\text{triclin.}) &= 14.1 \pm 0.2 \text{ kcal. par mol.} \end{aligned}$$

$$\begin{aligned} \text{cubique : } \log P(\text{mm. Hg}) &= -2677/T + 8.731 \\ \text{d'où } L_s(\text{cub.}) &= 12.2 \pm 0.1 \text{ kcal. par mol.} \end{aligned}$$

et pour la transition du triclinique en cubique

$$\Delta H = +1.9 \pm 0.3 \text{ kcal.}$$

et  $\Delta S = +5.5 \pm 0.9 \text{ par degré c. par mol.}$

On conclut que les variations d'énergie interne relatives à d'autres changements de phase décrits à  $43.6^\circ \text{ C.}$  et à  $125^\circ \text{ C.}$  ne dépassent pas  $700 \text{ cal. per mol.}$

### Zusammenfassung.

Der Dampfdruck von Hexachloräthan wurde von  $13^\circ$  bis  $174^\circ \text{ C.}$  mit Hilfe einer statischen Methode bestimmt. Die Präzision der Messungen war  $0.1 \text{ mm.}$  oder  $0.2 \%$ , je nachdem welcher dieser Werte der grosseren Genauigkeit entspricht. Die Dampfdruck-Temperatur Kurve zeigt eine deutliche Diskontinuität bei  $72^\circ \text{ C.}$ , die dem Übergang von der kubischen zur triklinen Form entspricht. Die thermodynamischen Daten sind :

$$\begin{aligned} \text{Triklin : } \log_{10} P(\text{mm. Hg}) &= -3077/T + 9.890 \\ \text{und daher } L_s(\text{triklin mm. Hg}) &= 14.1 \pm 0.2 \text{ kcal. per Mol.} \end{aligned}$$

$$\begin{aligned} \text{Kubisch : } \log_{10} P(\text{mm. Hg}) &= -2677/T + 8.731 \\ \text{und daher } L_s(\text{kubisch}) &= 12.2 \pm 0.1 \text{ kcal. per Mol.} \end{aligned}$$

$$\Delta H^\circ \text{ für den Übergang von triklin auf kubisch} = +1.9 \pm 0.3 \text{ kcal.}$$

und  $\Delta S^\circ = +5.5 \pm 0.9 \text{ cal. per Grad. c. per Mol.}$

Es wird gefolgert, dass die Enthalpieänderungen, die den anderen berichteten Phasenübergängen bei  $43.6^\circ \text{ C.}$  und  $125^\circ \text{ C.}$  entsprechen, den Wert  $700 \text{ cal.}$  nicht überschreiten.

*Department of Physical Chem.,  
 Free School Lane,  
 Cambridge.*

# THE EMISSION SPECTRUM OF GLYOXAL.

BY A. G. GAYDON.

Received 28th February, 1946.

The study of the emission spectrum of glyoxal,  $\text{CHO} \cdot \text{CHO}$ , was undertaken with the object of obtaining information about the spectrum of the CHO radical, a radical which is of interest for combustion studies, and which may be the emitter of Vaidya's hydrocarbon flame bands.<sup>1, 2</sup> This object has not so far been achieved, but it has been found that a Tesla coil discharge through flowing glyoxal vapour gives a strong blue-green emission. The spectrum of this discharge shows a close resemblance to the fluorescence spectrum of glyoxal obtained by Thompson,<sup>3</sup> and can safely be attributed to glyoxal itself. There are certain differences between the Tesla spectrum and that obtained in fluorescence and these differences enable the provisional analysis of Thompson's fluorescence spectrum to be checked, and to some extent modified. Additional information about the fundamental modes of vibration of the glyoxal molecule in its normal state is thus obtained.

## Experimental.

The glyoxal was prepared in the usual way by heating the solid polymer with phosphorus pentoxide and fractionating the products by distillation *in vacuo*. The discharge tube was of the simplest, consisting merely of a 10 cm. length of 4 mm. bore capillary tubing, the discharge being viewed end-on through a quartz window. A few turns of copper wire round the outside of this capillary served as external electrode and the discharge was maintained by a small Tesla coil. (A commercial vacuum "leak tester" was used.) A fairly fast flow of glyoxal vapour was maintained at a few mm. pressure.

The spectrum was photographed on a medium size quartz spectrograph (Hilger E. 487) with exposures of from a half to five minutes on plates of various types. The violet absorption spectrum of glyoxal vapour was also photographed, using an electric lamp as source and the discharge tube as absorption cell, the path length between quartz windows being 20 cm. and the pressure of glyoxal vapour of the order 100 mm.

The absorption spectrum of glyoxal in the vacuum ultra-violet has recently been described by Walsh.<sup>4</sup>

## Wave-lengths in Emission, Absorption and Fluorescence.

Thompson<sup>3</sup> studied the violet and ultra-violet absorption spectrum of glyoxal, and also the infra-red absorption and the blue-green fluorescence excited by the Hg lines 4047 and 4358 Å. The violet absorption and blue-green fluorescence bands clearly belong to the same system. Thompson found that all the bands obtained in fluorescence lay to longer wave-lengths than their expected positions, saying "It is peculiar that all the levels in the excited state deduced from the fluorescence data appear to lie about 70-90 cm.<sup>-1</sup> below the corresponding levels deduced from the ultra-violet data. No explanation of this can at present be given." He estimated that his measurements might be in error by  $\pm 10 \text{ cm.}^{-1}$ .

<sup>1</sup> Vaidya, *Proc. Roy. Soc. A*, 1934, 147, 513.

<sup>2</sup> Gaydon, *Spectroscopy and Combustion Theory*, London, 1942.

<sup>3</sup> Thompson, *Trans. Faraday Soc.*, 1940, 36, 988.

<sup>4</sup> Walsh, *Trans. Faraday Soc.*, 1946, 42, 66.







#### DESCRIPTION OF PLATE.

(a) The main strip shows the Tesla emission spectrum of glyoxal taken with a 5-minute exposure on an Ilford Press Ortho 2 plate, with an iron arc comparison spectrum below. The thin upper strip shows a spectrum of carbon monoxide taken on a panchromatic plate; the stronger CO bands are present in the glyoxal spectrum.

(b) The absorption spectrum of glyoxal taken on a Zenith plate. Iron arc below.

(c) Tesla emission spectrum of glyoxal, 1-minute exposure on Zenith plate. Heavily exposed iron arc spectrum below.

(d) Absorption spectrum of glyoxal. Heavily exposed iron arc below.

No such discrepancy occurs in the author's measurements of the absorption and Tesla emission spectrum. The present measurements of the absorption spectrum give slightly longer wave-lengths than Thompson's, the difference is usually around 2 Å., or 10 cm.<sup>-1</sup>, which is only of the order of the experimental error, but in the case of the important band at 4555 Å., which corresponds to transitions between the lowest vibrational levels of the two electronic states, the difference is significant. Thompson gives this band as 4550 Å., but uses a frequency of 21980 cm.<sup>-1</sup>, which should correspond to 4548 Å. The author's plates show that this band has a double maximum, of which the more intense is centred at 4555 Å. and the weaker at 4547 Å.; this is shown in strip (d) of the plate in which the wave-lengths of two iron lines in the comparison spectrum are marked for convenience. The next absorption band lies at about 4532 Å., and is certainly to the red of the strong iron line 4528.6, but Thompson gives 4527 Å. These wave-lengths have been checked on five exposures of the absorption spectrum and no instrumental shift appears possible. The appearance of complex bands of this type does, of course, vary with the dispersion used, but it would hardly seem possible to bring the present observations into line with Thompson's measurements.

The wavelengths of the bands in the Tesla emission spectrum agree with the author's absorption measures. Strip (c) of the plate shows the position of the emission bands 4532, 4547 and 4555 Å. relative to the iron arc comparison. Thompson obtained the corresponding fluorescence bands at 4543 Å. and a broad band at 4564 Å.

The fluorescence spectrum gives a number of bands between 4090 and 4497 Å. which are absent or very weak in the Tesla discharge. Beyond this the Tesla and fluorescence spectra agree closely, apart from an average discrepancy of about 6 Å. between the author's measures and Thompson's. The author's measures are based on

TABLE I.

Gaydon, Tesla Emission.			Thompson Fluorescence.	
ν.	λ.	I.	λ.	I.
			4090	1
			4126	2
			4143	2
			4162	3d
			4203	3
			4221	3
			4243	3
			4275	2
			4295	3d
			4316	3
			4392	4
22700	4404	1	4414	6d
22444	4454	2d		
			4472	5
			4497	2
			4522	4
22057†	4532	7d	4543	5
21950*	4555	10	4564	8d
21816†	4583	5	4582	7
21708*	4605	5	4608	7
21646*	4619	4	4622	6
21520†	4646	2d	4650	2
21407*	4670	7	4675	7
21145*	4728	3	4735	3
21037*	4752	7	4757	6
20969*	4767	3		
20927*	4777	9	4782	10
20897*	4784	6d	} 4794	9
20856*	4793	5d		
20782*	4810	1	4814	2
20727†	4823	2d	4828	2
			4840	2
20627*	4847	4	4853	3
20497†	4877	2	4884	2
20376*	4906	5	4914	6
20328†	4918	1		
20212*	4946	5	4950	5
19837*	5040	2d	5047	4
			5092	1
			5121	1
19415	5149	1	5150	1
19302†	5179	4	5184	2
19193*	5209	7	5212	3
19143*	5222	1		
18836*	5308	2d	5320	2
18634†	5365	2	5376	1
18516*	5399	1	5405	1
17450*	5729	4		

\* Band provisionally assigned to transition from lowest vibrational level of excited state.

† Band assigned to transition from level 110 cm.<sup>-1</sup> above lowest level of excited state.

d Diffuse band.

eight consistent exposures. Should the difference in the wave-lengths of the Tesla emission and fluorescence bands prove real it would be of the greatest interest, but the author is of the opinion that the difference is likely to be due to instrumental causes.

The measurements of the Tesla emission spectrum, with Thompson's fluorescence for comparison, are presented in Table I. Intensities are visual estimates on a scale of 10, without allowance for varying plate sensitivity. Thompson's intensities are based on the line lengths in his diagram. Most of the strong bands, like that at 4555 Å., appear as doublets with the longer wave-length component much stronger than the shorter, from which it is separated by about  $50 \text{ cm}^{-1}$ ; this interval can probably be attributed to the separation between maxima in the rotational structure of these complex bands; only wave-lengths of the stronger (longer wave-length) components are given in Table I.

### The Analysis of the Tesla Emission and Fluorescence Spectrum.

The complete vibrational analysis of the electronic spectrum of a complicated molecule like glyoxal which probably possesses 12 fundamental modes of vibration in each electronic state, will obviously be very difficult and it is not to be expected that a complete and unambiguous solution can be obtained. By combining observations on the absorption, infra-red absorption, and the emission spectrum under different conditions of excitation it should, however, prove possible to build up an energy level scheme for both excited and ground states from which some of the fundamental vibrational frequencies can be deduced.

Thompson used his observations on the fluorescence and violet absorption bands to build up an energy level scheme. This appears, to the author, to give a satisfactory explanation of the absorption spectrum, and there is no reason to doubt the energy level scheme for the excited state. The new observations on the Tesla emission, however, cannot be explained in terms of this scheme without some modification of the ground state energy levels.

The fluorescence spectrum shows a number of bands to the violet of 4555 Å., and these must clearly arise from excited vibrational levels of the upper state. These bands are absent or very weak in the Tesla discharge, and it therefore follows that this source gives a lower population for the excited vibrational levels of the upper state. Now, in general, the relative intensities of all bands arising from the same vibrational energy level will be the same irrespective of the source, while the relative intensities of bands arising from different initial energy levels will vary with conditions of excitation. As far as the present observations are concerned, the only factor likely to affect this generalisation is self-absorption in the glyoxal vapour; in Thompson's work, for which pressures of up to 200 mm. were used, this may be appreciable; for the Tesla discharge the pressure was a good deal lower and self-absorption is unlikely to be important.

The fluorescence band at 4414 Å. is of moderate intensity, despite some possible self-absorption; this band is also observed in absorption and undoubtedly corresponds, as shown by Thompson, to a transition from a level of the excited state about  $750 \text{ cm}^{-1}$  above the lowest level, to the lowest level of the ground state. The weakness of this band in the Tesla discharge shows that the population of the upper level is very small. Now Thompson provisionally assigns several other bands ( $\lambda\lambda$  4622, 4782, 4840, 5405) to transitions from the same upper level; all except the 4840 band are, however, present in the Tesla discharge with intensity comparable with that in fluorescence. The bands 4414 and 4840 therefore probably originate in the level  $750 \text{ cm}^{-1}$  up, as indicated by Thompson, but the bands 4622, 4782 and 5405 must come from some other vibrational level, probably the lowest.

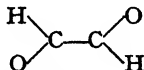
By comparison of the intensities of the emission bands in the two sources in this way it is possible to check the analysis. The accuracy of the comparison is limited by the nature of the experimental data; some variation in the visual estimation of the intensities of bands of different characters must be expected; it also seems that the main band around 4555 Å. was appreciably weakened by self-absorption in the fluorescence work; generally, Thompson's intensities appear to be on a slightly higher scale than the author's, except in the green where the latter probably used photographic plates of higher sensitivity.

Thompson found that the upper state had a vibrational level only about  $110\text{ cm.}^{-1}$  above the lowest, and it seems that the Tesla spectrum can best be explained by assuming that all bands to the red of 4555 Å. arise either from the lowest vibrational level of the excited electronic state or this level  $110\text{ cm.}^{-1}$  higher. The assignment of bands to these two initial levels is indicated by an asterisk or dagger respectively in Table I. The 4752 and 4728 Å. bands could be explained as arising from the higher level, but intensity considerations and the later analysis favour their coming from the lowest level as indicated.

The band at  $\nu = 21950$  is clearly due to the transitions between the lowest vibrational levels of the two electronic states. There are also bands to the red of this by about  $134$  and  $242\text{ cm.}^{-1}$  (at  $\nu = 21816$  and  $21708$ ) in the Tesla discharge, in fluorescence and in absorption \* at high gas pressure. Thompson explained the  $134$  interval as a fundamental ground state vibrational frequency and the  $242$  as the overtone of this frequency. He pointed out, however, that this led to some difficulty in explaining the relative intensities of the bands and required a very high anharmonicity. The author is of opinion that it is best to treat the fundamental frequency as  $242\text{ cm.}^{-1}$  and to assign the  $\nu = 21816$  band to a transition from the level of the excited electronic state  $110\text{ cm.}^{-1}$  up so that the apparent interval of  $134$  comes as the difference of  $242$  and  $110$ .

### The Fundamental Vibrational Frequencies of Glyoxal.

Thompson made some progress with the difficult task of sorting out the fundamental vibrational frequencies of glyoxal and gave as possible fundamentals 135, 550, 800, 985, 1050, 1098, ? 1150, 1315, 1730, ~ 1730 ~ 2700 and 2833. He concluded that the planar "trans" symmetry for glyoxal



was not excluded, but with his assignments some weakening of the selection rules in the infra-red appeared necessary (e.g. the appearance of  $\nu_4$  at  $1315\text{ cm.}^{-1}$ ).

The present observations of the Tesla spectrum give indications of a much greater number of vibrational energy levels of the ground state. These are listed, with the infra-red data, in Table II. It is very difficult, if not impossible to explain these levels using the above fundamentals, and some revision of the choice of fundamentals seems required.

It has already been pointed out that it is best to discard the  $135$  frequency and to adopt  $242$ . There is also good evidence for a level at  $304\text{ cm.}^{-1}$  which cannot readily be explained except as a fundamental. It then seems best to explain the  $543$  level as the sum of  $242$  and  $304$  thus avoiding the necessity of more than two small vibrational frequencies. The use of  $242$  and  $304$  instead of  $135$  and  $550$  then enables us to explain some of the infra-red bands without using so many fundamentals which are active in the infra-red.

\* Owing to the wave-length differences already discussed these intervals are a little higher in Thompson's absorption measurements.

There is reason to believe, from electron diffraction work,<sup>5</sup> that glyoxal does have the "trans" form, and Thompson has listed the vibrational modes and symmetries to be expected for this form. With twelve fundamentals to play with, it is very difficult to obtain a unique solution, but a selection of fundamentals has been made which can lead to all the energy levels required to explain the Tesla and fluorescence spectra and which also gives a reasonable explanation of the infra-red absorption without obvious violation of the selection rules. The interpretation of the bands with these fundamentals is given in Table II. It should be remembered that

TABLE II.—GROUND STATE VIBRATIONAL ENERGY LEVELS OF GLYOXAL.

From Tesla Discharge.	From Infra-red.	From Thompson's Absorption.	Interpretation.
(134 m)		(140)	$\nu_8$ —upper electronic state 110 cm. <sup>-1</sup> .
242 m		250	$\nu_6$
304 m		310	$\nu_6$
543 s		550	$\nu_6 + \nu_8$
?805 w	800 m		$\nu_7$
?913 s			$\nu_8$
981 w	985 m		$\nu_{12}$
1023 vs		1050	$\nu_8$
1053 m			$\nu_6 + \nu_7$
1094 m	1098 m		$\nu_7 + \nu_8$
	1150 w		$\nu_6 + \nu_8$
1323 m	1315 s		$\nu_{11}$ and $\nu_8 + \nu_8$
	?1379 w		$\nu_7 + 2\nu_8$ OR $\nu_8 + \nu_8 + \nu_8$
1574 s			$\nu_8$
	1608 vw		$\nu_8 + \nu_{11}$
1738 m	1730 vs		$\nu_{10}$
	1818 m		$\nu_8 + \nu_8$
	1850 m		$\nu_8 + \nu_8 + \nu_{11}$
	2080 m		$\nu_7 + \nu_8 + \nu_{12}$ , etc.
2113 w			$\nu_8 + \nu_8 + \nu_8$
	2660 m		$\nu_6 + \nu_7 + \nu_{12}$ , etc.
2757 s			$\nu_1$
2807 w			$\nu_7 + \nu_8 + \nu_{10}$
	2833 vs		$\nu_9$
	3077 vw		$\nu_7 + \nu_{11} + \nu_{12}$ , etc.
3114 w			$\nu_8 + \nu_7 + \nu_{12}$ , etc.
3434 w			$\nu_8 + \nu_7 + \nu_8 + \nu_{12}$ , etc.
	3448 m		$\nu_8 + \nu_8 + \nu_{12}$ , etc.
4500 s			$\nu_1 + \nu_7 + \nu_{12}$ , etc.
	4587 m		$\nu_7 + \nu_9 + \nu_{12}$ , etc.
	5525 vw		$\nu_6 + \nu_7 + \nu_9 + \nu_{12}$ , etc.

The strengths of the bands from which the levels are obtained are denoted by vw (very weak), w (weak), m (medium), s (strong) and vs (very strong).

levels due to a combination of vibrations will usually be at slightly lower energies than the values obtained by simple summation of the frequencies because of anharmonic terms and mutual interaction between the vibrations.

The *provisional* assignment of fundamentals with their modes is shown in Table III.

With so many fundamentals it is usually possible to interpret the higher energy levels (above 2000 cm.<sup>-1</sup>) in several ways each; only one is given in each case in Table II. It is not unlikely that the unknown  $\nu_4$  might play a part in some of the observed bands, and this might be invoked perhaps if any infra-red band appeared stronger than might be expected for the explanation given in Table II.

<sup>5</sup> Lu Valle and Schomaker, *J. Amer. Chem. Soc.*, 1939, 61, 3520.

There is a possibility that  $\nu_{11}$  at 1315 might be modified a little. The infra-red gives a double band at 1305, 1326, while the Tesla discharge gives about 1323. We can, with Thompson, take 1315 as the fundamental. Alternatively we could take 1326 and assign the infra-red maximum at

TABLE III.

$\nu_1$	CH valency	2757	$\nu_7$	CHO bending	800*
$\nu_2$	CO valency	1574	$\nu_8$	CHO bending	304
$\nu_3$	CC valency	1023	$\nu_9$	CH valency	2833*
$\nu_4$	CHO deformation	?	$\nu_{10}$	CO valency	1730*
$\nu_5$	CHO rocking	913	$\nu_{11}$	CHO deformation	1315*
$\nu_6$	Torsional	242*	$\nu_{12}$	CHO rocking	985*

\* Fundamentals active in infra-red ; other fundamentals inactive for " trans " form.

1305 to the combination  $\nu_5 + \nu_8$ . It is possible that  $\nu_{11}$  and  $\nu_{12}$  should be interchanged. Similarly,  $\nu_3$  and  $\nu_8$  are interchangeable on present evidence.

### The Flame Spectrum of Glyoxal.

The spectrum of a glyoxal-air mixture burning in air has been photographed. It is of interest briefly to record that it shows strong OH bands at 3064 Å. and the carbon monoxide flame spectrum, but that C, CH and Vaidya's hydrocarbon flame bands are absent.

The author wishes to express his thanks to the Royal Society for the award of a Warren Research Fellowship, and to Sir Alfred Egerton for his interest in this research.

### Summary.

A Tesla discharge through flowing glyoxal vapour gives a spectrum in the blue-green which is related to the fluorescence spectrum and absorption spectrum of this molecule. Differences between the present author's wavelengths of emission and absorption bands and those obtained in fluorescence and absorption by Thompson are discussed. The observations can be explained satisfactorily by assuming that the glyoxal molecule has the planar " trans " form with the following fundamental frequencies.

$\nu_1$	2757	$\nu_4$	?	$\nu_7$	800	$\nu_{10}$	1730
$\nu_2$	1574	$\nu_5$	913	$\nu_8$	304	$\nu_{11}$	1315 or 1326
$\nu_3$	1023	$\nu_6$	242	$\nu_9$	2833	$\nu_{12}$	985

These fundamentals, while adequate to explain the results, do not necessarily constitute the only possible solution. The flame spectrum of glyoxal has been examined.

### Résumé.

Une décharge de Tesla dans un courant de vapeur de glyoxal donne un spectre bleu-vert qui est lié aux spectres de fluorescence et d'absorption de cette molécule. L'auteur discute les différences entre les longueurs, d'onde des bandes d'émission et d'absorption trouvées par lui et celles obtenues par Thompson dans les spectres de fluorescence et d'absorption. On peut expliquer de façon satisfaisante les résultats observés en posant

## 42 VAPOUR PRESSURE OF $\beta\beta'$ -DICHLORETHYL SULPHIDE

que la molécule de glyoxal a la forme plane " trans " avec les fréquences fondamentales suivantes :

$\nu_1$	2757	$\nu_4$	?	$\nu_7$	800	$\nu_{10}$	1730
$\nu_2$	1574	$\nu_5$	913	$\nu_8$	304	$\nu_{11}$	1315 ou 1326
$\nu_3$	1023	$\nu_6$	242	$\nu_9$	2833	$\nu_{12}$	985

Bien que celles-ci soient tout à fait adéquates pour expliquer les résultats, elles ne constituent pas nécessairement la seule solution possible. Le spectre de flamme du glyoxal a été examiné lui aussi.

### Zusammenfassung.

Eine Teslaentladung durch strömenden Glyoxaldampf gibt ein Spektrum im Blau-Grün, das mit dem Fluorescenz- und Absorptions spektrum des Moleküls verwandt ist. Differenzen zwischen den Wellenlängen der Emissions- und Absorptionsbanden des Autors und den von Thompson in Fluorescenz und Absorption erhaltenen werden besprochen. Die Beobachtungen können in befriedigender Weise erklärt werden, wenn angenommen wird, dass Glyoxal die flache „ trans "-Struktur mit den folgenden Fundamentalfrequenzen besitzt.

$\nu_1$	2757	$\nu_4$	?	$\nu_7$	800	$\nu_{10}$	1730
$\nu_2$	1574	$\nu_5$	913	$\nu_8$	304	$\nu_{11}$	1315 oder 1326
$\nu_3$	1023	$\nu_6$	242	$\nu_9$	2833	$\nu_{12}$	985

Obzwar diess Fundamentalfrequenzen genügen, um die Resultate zu erklären, stellen sie nicht die einzig mögliche Lösung dar. Das Flammenspektrum von Glyoxal wurde untersucht.

*Imperial College,  
London, S.W.7.*

## STUDIES IN VAPOUR PRESSURE MEASUREMENT. PART I.—THE VAPOUR PRESSURE OF $\beta\beta'$ -DICHLORETHYL SULPHIDE (MUSTARD GAS).

BY E. W. BALSON, K. G. DENBIGH, AND N. K. ADAM.<sup>1</sup>

*Received 11th March, 1946.*

### Introduction and Summary.

The vapour pressure of pure mustard gas has been determined between the melting-point, 14.35° C., and 80° C., by static and dynamic methods. Between 17° and 40°, a mercury-oil magnifying manometer was used; above 40°, a simple U-tube, for the static determinations. In the dynamic method, the concentration of mustard in a slow stream of air passed over the liquid was determined by estimating the chloride content, by potentiometric titration.

<sup>1</sup> The design of the dynamic apparatus is due to E.W.B., of the static, to K.G.D.

### Experimental.

**Dynamic Method** (Fig. 1).—The mustard was contained in a horizontal coil, B, of 10 mm. bore glass tubing in a compact flat spiral, giving a surface of about 150 sq. cm. for evaporation. Air was driven through this spiral by running water at a steady rate into a 6 litre bottle G; the pressure in this bottle was noted by a water manometer M, and was always within a millimetre or two of atmospheric pressure. The volume of moist air driven out of G was found, after the experiment, by measuring the volume of water run in. The air passed through a calcium chloride drying tube and a charcoal tube J, to remove water vapour and any accidental organic impurities, then through a pre-heating coil A, which was a flat spiral like the saturator but placed vertically. The clean dry air then passed over the mustard in B; after saturation it was mixed with a subsidiary air stream at D, which has been dried and cleaned and warmed to

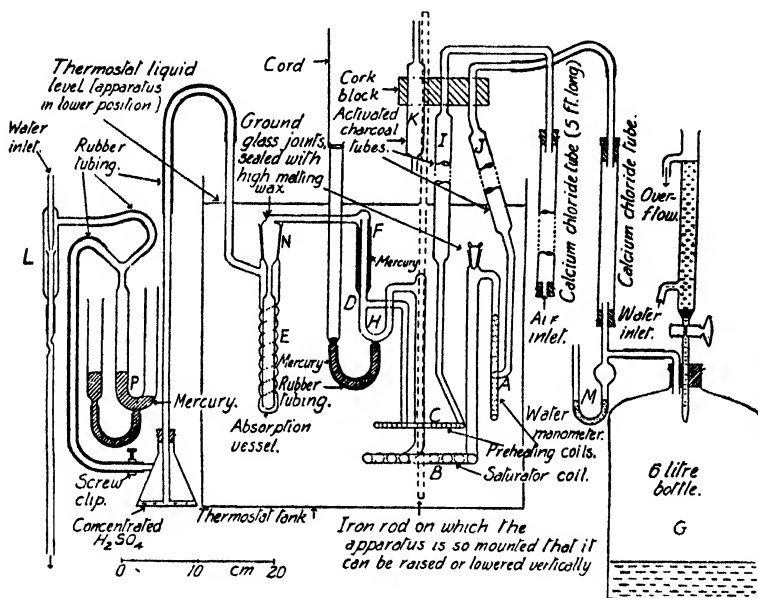


FIG. 1.

thermostat temperature at I and C. The air was sucked through the apparatus, the water pump L, the mercury valve P maintaining an approximately constant suction.

The rate of the subsidiary air stream, whose principal function was to prevent the risk of condensation of liquid mustard, was adjusted to between one and two bubbles per second from a 3 mm. bore tube, a convenient rate for the absorption vessel E. This gave the air a helical path; absorption was in 25 % acetic acid which gave rapid hydrolysis with complete liberation of the chlorine in the mustard. One absorption vessel proved sufficient, no chlorine being ever found in a second. The absorption vessel B was attached to the apparatus by a mercury trap F. After the run was finished, the saturated air stream was cut off by the mercury trap H and the subsidiary air stream continued for a short time to flush out the tubes between D and E. Between runs, a rubber connection was made between the inner tube at F and a charcoal tube K, to keep water out of the apparatus and prevent escape of mustard vapour.



## 44 VAPOUR PRESSURE OF $\beta\beta'$ -DICHLORETHYL SULPHIDE

The contents of the absorption vessel were rinsed, using chloride-free water, into a titration vessel with a silver wire electrode kept well stirred by a stream of hydrogen. The quantity of chloride was determined potentiometrically, using 0.2 or 0.05 N.  $\text{AgNO}_3$ . The accuracy was about 0.01 ml., corresponding to 0.04 mg. mustard with the 0.05 N. solution. The sharpness of the end point was considerably improved by adding about 0.2 g. of chloride-free aluminium sulphate, which helps to coagulate the  $\text{AgCl}$  and expedites the titration.

At each temperature, not less than five, and often many more runs were made, the volumes of air saturated varying from one to twelve litres. The different runs at any one temperature were averaged by plotting the

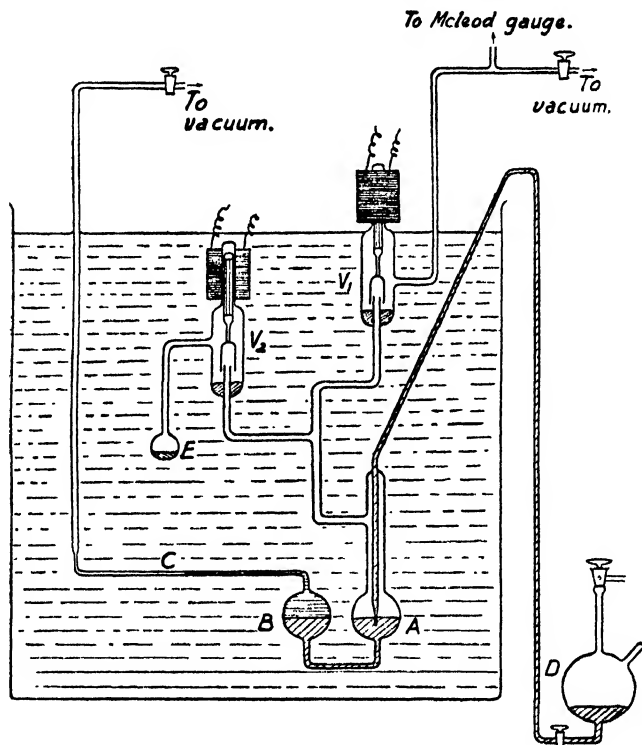


FIG. 2.

volume of  $\text{AgNO}_3$  used in the titration against the volumes of air passed, after correction for moisture present in the measured volume, made from the known vapour pressure of water at the laboratory temperature. All points lay very close to a straight line through zero time and the slope of the best straight line was taken for calculating the quantity of mustard in one litre of saturated dry air at the thermostat temperature.

To test whether the rate of evaporation was sufficient to saturate the air completely, the air-flow was varied between 3 and 8 cc. per minute, at  $47.6^\circ \text{C.}$ , without appreciably affecting the concentration of mustard in the air. Later, the rate was always kept between 5 and 6 cc. per minute.

The vapour pressure was calculated from the formula

$$p = \frac{22.4m(273 + t)760}{159 \times 273},$$

$m$  is the mass of mustard in 1 litre dry air and 159 the molecular weight. This formula neglects the volume occupied by the mustard vapour, which is negligible except perhaps at the highest temperatures. A correction was made for the volume of mustard at  $75.4^{\circ}$  C. only.

Runs at the lower temperatures sometimes took two days, and as successive runs were made occupying many days in all, tests were made to see whether decomposition of the mustard was sufficient to affect the measured vapour pressure. One specimen was kept in the saturator for  $2\frac{1}{2}$  months, including 8 days at  $75^{\circ}$  and 7 days at  $68^{\circ}$ . The m.p. had very slightly fallen ( $13.95^{\circ}$  to  $14.3^{\circ}$  finally, initially  $14.15^{\circ}$  to  $14.3^{\circ}$ ) but no appreciable change in the vapour pressure was found.

Two other methods were tried, and abandoned, for estimating the concentration of mustard vapour in the air. Oxidation by permanganate gave results varying, under different conditions, by some 40 % (usually giving higher results than the chloride titration method and the static method described below). A few attempts to estimate the mustard by absorption in a weighed charcoal tube also gave erratic results.

The potentiometric method was tested against pure mustard; three experiments gave agreement with theory for the chlorine content; expressed in terms of mustard the error was within that estimated, i.e. 0.04 mg. mustard: taken, 14.43, 2.24, 11.05 mg.; theory 14.45, 2.20, 11.06 mg.

**Static Methods** (Fig. 2 and 3).—Fig. 2 shows the two-liquid magnifying manometer used up to  $40^{\circ}$ . There are two bulbs, half filled with mercury, about 65 mm. diameter, A and B. A can be placed in communication with a bulb E containing mustard, via a mercury cut-off  $V_1$ , operated by a solenoid. B communicates with a horizontal capillary C, dibutyl phthalate covers the mercury in B and fills part of the capillary. The precise position of the butyl phthalate meniscus in C was observed with a cathetometer placed horizontally, through a plate glass window; it could be adjusted by means of a mercury reservoir D, communicating with A, outside the thermostat. The manometer was calibrated with known pressures of air measured by a McLeod gauge; 1 mm. travel of the meniscus in the capillary was equivalent to about 0.0025 mm. of mercury change in pressure. Calibration curves at any one temperature were without appreciable hysteresis and were reproducible to about 0.002 mm. mercury pressure. There was, sometimes, a very slow shift of the zero, easily allowed for, by taking frequent readings of the zero, since it was always steady. A Hyvac oil pump and a three-stage mercury diffusion pump were used for evacuation. Thorough de-gassing of both the dibutyl phthalate in the manometer and the mustard was essential; the dibutyl phthalate was boiled in the bulb and tube under vacuum; and the mustard evacuated until it showed no further change in vapour pressure when  $V_1$  was closed and  $V_2$  open, the left-hand side of the manometer being open to vacuum. The liquid mustard touched glass only, the vapour glass and mercury only.

Fig. 3 shows the U-tube used above  $40^{\circ}$ . The mustard was in the

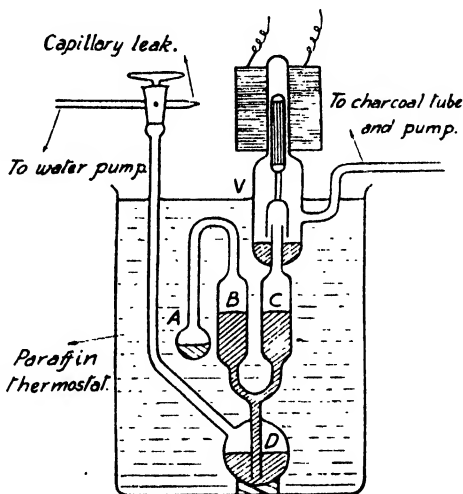


FIG. 3.

bulb A; the mercury could be withdrawn from the limbs B and C of the manometer into the reservoir D, for de-gassing of the mustard. Readings of the height of mercury in the limbs were taken, using a good measuring microscope with vertical screw divided to 0.01 mm. and readable to 0.001 mm. The microscope was supported on a very carefully levelled glass plate; the zero was taken with both limbs open to the atmosphere. Travers' device, a glass plate half white and half black, with a horizontal line of division, placed behind the meniscus, gave a very good light for reading the mercury menisci, when illuminated from the front.

Temperatures were controlled to 0.1 degree, using an N.P.L. standardised thermometer of which the ice-point was re-determined.

**Purification of Mustard.**—The liquid was twice distilled at about 15 mm., using a tall fractionating column. The starting material was from two sources, one made by the ethylene-sulphur chloride process, the other from thiodiglycol. After distillation both samples began to soften at about 13°, were two-thirds melted at 14.0°, and completely melted at 14.3°.

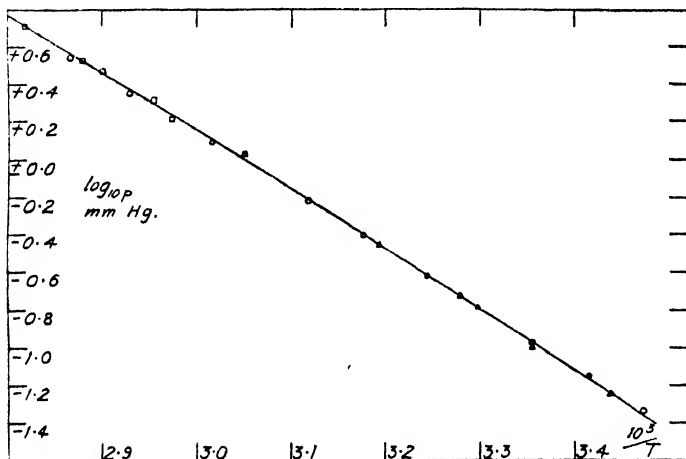


FIG. 4.—Vapour pressure of mustard gas.

Melting points were taken on 2 to 3 cc. samples in a test-tube, heating extremely slowly in a bath never more than 0.5 degree above the temperature of the mustard.

Further purification was done by fractional freezing. In most experiments the liquid mustard was placed in a glass jar surrounded by crushed ice, and the solid scraped off the sides of the jar as fast as formed. After about half had solidified, the mush was filtered through a large sintered glass funnel and well pressed down with a large flat glass stopper, using suction. Four such crystallisations gave a product melting completely between 14.15 and 14.35°.

This procedure is troublesome, and runs the risk that those parts which happen to be near the sides of the jar are completely frozen, and therefore not fractionated. Later the following technique was adopted. About 1½ litres of distilled mustard, boiling within 1 degree at 15 mm., was placed in a glass jar, in a thermostat at 13.3°. A lid covered the jar, provided with holes to admit a thermometer, stirrer, and rod to scrape solid off the sides. After the contents of the jar had cooled to the thermostat temperature, a small crystal of pure mustard was introduced, when immediately the contents began to crystallise slowly. Filtering and pressing

were done as before: this procedure is easier and rather safer than the preceding.

The m.p. of pure mustard is sometimes given as  $14.4^{\circ}$ ; our highest value is  $14.35^{\circ}$  to the nearest  $0.05$  degree.

### Results.

Our figures are given in Table I and Fig. 4. These, together with some unpublished results up to  $140^{\circ}$  c. obtained by a boiling-point method, fit the equation ( $p$  in mm. mercury)

$$\log_{10} p = 38.525 - \frac{4500}{T} - 9.86 \log_{10} T. \quad (1)$$

Over ranges of not more than about  $40^{\circ}$ ,  $\log_{10} p$  was, within experimental error, a linear function of  $1/T$ . From the slope of the complete

TABLE I.—ACTUAL MEASUREMENTS MADE.

Temperature °c.	Vapour Pressure. mm. Hg.	Temperature °c.	Vapour Pressure. mm. Hg.
<b>Dynamic method.</b>		<b>Static methods.</b>	
14.9	0.046	17.8	0.057
19.7	0.070	25.0	0.100
25.0	0.106	25.0	0.099
30.1	0.163	31.9	0.188
35.2	0.239	40.0	0.350
41.8	0.392	54.8	1.07
47.6	0.611	63.2	1.64
68.4	2.26	65.3	2.07
75.8	3.52	71.8	2.97
		74.3	3.39
		81.7	5.12

TABLE IA.

$14.4^{\circ}$	14,420 cal.
54.0	14,300 "
84.0	13,540 "
104.0	13,260 "

$\log_{10} p$  against  $1/T$  curve at various points the values shown in Table IA for the latent heat of evaporation per mole were calculated.

Using Kirchhoff's law, a very rough estimate can be made of the difference between the heat capacity of liquid and vapour; that of the liquid exceeds that of the vapour by roughly 19.5

calories per mole. A very slight error in the vapour pressure would throw this result out by 100 per cent., however.

The consistency was better with the dynamic than with the static measurements. Table II gives the smoothed results, extrapolated down to  $-10^{\circ}$  c. for both solid and liquid mustard: the values for solid being calculated by taking the latent heat of fusion as 4,200 calories per mole (unpublished result).

TABLE II.—SMOOTHED VALUES FOR VAPOUR PRESSURE.

Temperature.	V. P. Solid.	V. P. Liquid.	Temperature.	V. P. Liquid.	Temperature.	V. P. Liquid.
-10	0.0022	0.0042	20	0.072	50	0.716
0	0.0078	0.0112	25	0.108	60	1.39
10	0.0264	0.0295	30	0.162	70	2.56
14.4	0.0437	0.0437	40	0.351	80	4.57

We thank the staff of the Experimental Station, Porton, for advice and assistance with materials; also Drs. A. Lawson and K. R. Webb for help with the purification. The paper describes work done in 1940 and early 1941, and is published by permission of the Chief Scientific Officer, Ministry of Supply.

**Résumé.**

La tension de vapeur du gaz moutarde pur a été déterminée entre 14.35 et 80° c. par des méthodes statique et dynamique. Pour les mesures statiques, on employait entre 17 et 40° un manomètre amplificateur huile-mercure et au-dessus de 40° un simple tube en U. Dans la méthode dynamique, la concentration en gaz moutarde d'un courant d'air passant lentement au-dessus du liquide était déterminée par dosage potentiométrique du chlorure.

**Zusammenfassung.**

Der Dampfdruck von reinem Senfgas wurde zwischen 14.35° c. und 80° c. mittels statischer und dynamischer Methoden bestimmt. Für die statischen Messungen von 17° bis 40° wurde ein vergrößerndes Quecksilber-Öl-Manometer benutzt, über 40° ein einfaches U-Rohr. Bei der dynamischen Methode wurde die Konzentration von Senfgas in einem langsamen, über die Flüssigkeit geleiteten Luftstrom durch potentiometrische Titration des Chloridgehaltes bestimmt.

*University College,  
Southampton.*

## STUDIES IN VAPOUR PRESSURE MEASUREMENT, PART II.—A NEW ALL-GLASS MANOMETER SENSITIVE TO 0.001 mm.

BY E. W. BALSON.

*Received 11th March, 1946.*

Brombenzyl cyanide attacked mercury so rapidly, even in minute vapour concentrations, that the two-liquid manometer described in Part I was unworkable. Oil manometers were useless on account of the solubility of the substance in the oil, and gave very low results. Menzies' method,<sup>1</sup> which measures the pressure of an indifferent gas in contact with the saturated vapour, and is not strictly an equilibrium method, gave varying results, usually about 25 % below those obtained by the two concordant methods given below. Menzies does not give full details of his technique, and his method was abandoned since a prolonged, critical investigation of the conditions required to obtain correct results would clearly have been required.

Rodebush and Coons,<sup>2</sup> Rodebush and Henry,<sup>3</sup> and Deitz<sup>4</sup> have described manometers in which the force required to lift a lid off a seating, a high vacuum being below, and the vapour of the substance above the lid, is measured. After many trials the following design, embodying this principle, was adopted.

**Experimental.**

A light lid, shaped like a bell-jar (B, Fig. 1) rests on the rim of a glass tube C. The substance studied is placed in the small bulb A; its vapour pressure presses the lid on to its seating. The lid was hung by a hook from a silica spring balance G, a closed tube with a little soft iron being suspended just above the lid B. Outside the apparatus and just above the iron, a solenoid was fixed, the current through it being measured by

<sup>1</sup> *J. Amer. Chem. Soc.*, 1920, **42**, 2218.

<sup>2</sup> *Ibid.*, 1927, **49**, 1953.

<sup>3</sup> *Ibid.*, 1930, **52**, 3159.

<sup>4</sup> *J. Chem. Physics*, 1936, **4**, 575.

an accurate milliammeter and controlled by a rheostat. This solenoid was very carefully adjusted to give an accurately vertical pull, using thin copper shims. The seating was observed from outside the instrument by a low power microscope, gradually increasing the current until the lid suddenly leapt off the seating; the current was then read. A small heating coil H, carrying about 0.07 ampere, prevented condensation on the seating; leads to this coil (not shown) passed along the tube IJ. The heating was found necessary to eliminate sticking. A glass fork U, about 2 mm. above the lid, prevented the lid coming off so violently as to jump off its hook.

The flange of the lid is first ground and polished in a lathe; the upper rim of the tube G is ground and polished flat, separately, using the finest flour emery and finally rouge. The fit of the polished surfaces was passed as satisfactory when a vacuum of 0.02 mm. could be maintained in C, with one atmosphere above, using a Hyvac and single stage mercury diffusion pump. No trace of grease was permissible or sticking would have rendered measurements impossible.

Three sizes of instrument were built, with tubes C of bore 26, 10, and 4 mm.; the sensitivities were 0.001, 0.01, and 0.05 mm. and the maximum pressures measurable 0.17, 1, and 5 mm. respectively. In this way the whole range from 0.001 to 5 mm. was covered; each instrument had a sensitivity of about 1 % of the maximum pressure it could measure.

The highest possible vacuum must be maintained below the lid. A mercury diffusion pump M, backed by a rotary oil pump, was used; diffusion of the mercury vapour back, and of the vapour of the substance forward, was minimized by the use of a very long trap DE, the inner tube of which was filled with solid carbon dioxide and acetone. For easy removal this had a flanged joint sealed with vacuum wax at E; three glass studs F prevented the inner tube rubbing against the outer during withdrawal, so that the trap could be cleaned easily, since the whole of the substance which had distilled over from the reservoir A, condensed on the cooled inner tube. It was generally unnecessary to clean any parts of the manometer except this inner tube of the trap D, and the bulb A, between experiments.

To calibrate the manometer, known pressures of air, measured by a McLeod gauge (not shown) were put in contact with the space above the

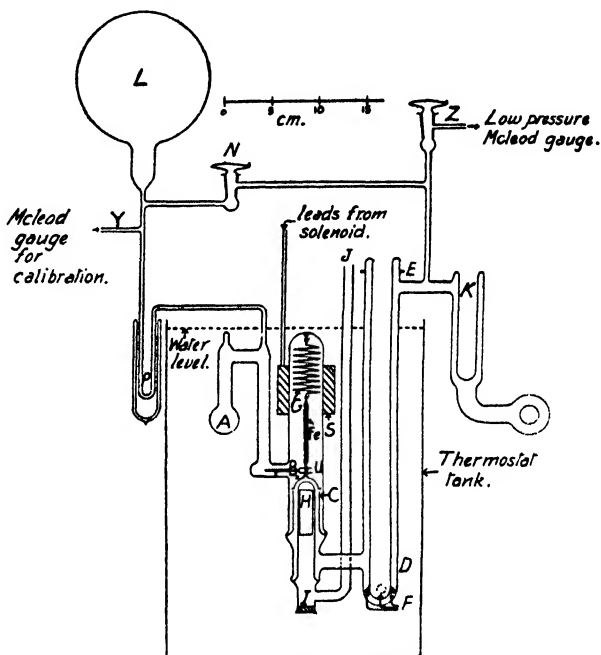


FIG. 1.

lid, and the current through the solenoid needed to unseat the lid measured. The  $\frac{1}{2}$  litre bulb L, was filled with air at a convenient pressure, about the upper limit which could be measured by the apparatus; tap N was closed, the mercury in the McLeod gauge raised to cut the gauge off; the current required to unseat the lid measured, and the measurement of pressure by the McLeod quickly completed. During the short time that the lid was off its seating the air pressure in L fell substantially; the current was reduced immediately after recording the current required to unseat the lid so that the lid returned to its seating. These measurements were repeated several times so that several calibrations were obtained with one filling of L with air. The cooled U-tube P, prevented diffusion of mercury vapour from the MacLeod into the manometer.

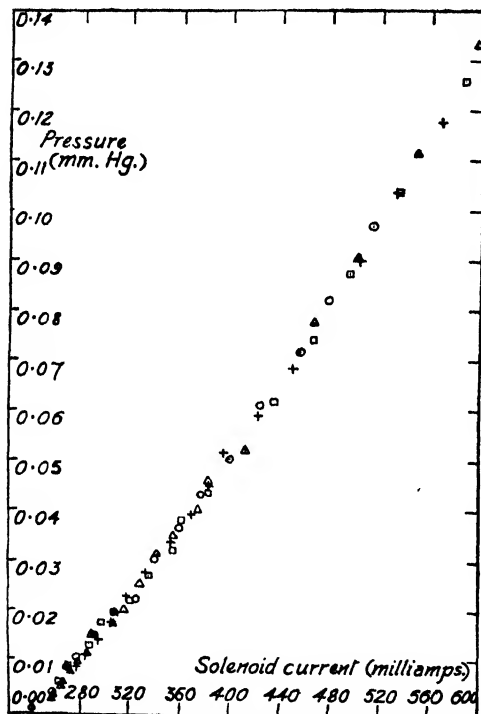


FIG. 2.—Calibration of manometer.

The time elapsing between cutting of the McLeod and reading the solenoid current was small; any leakage past the seating during this time would have to be subtracted from the pressure given by the McLeod. This could be quantitatively allowed for by measuring the rate of loss of pressure in L when the lid was on its seating with a good vacuum below; in almost every case this correction was found to be negligibly small compared with the experimental error. With a little practice, the current required to unseat the lid was reproducible within about 0.5 %, calculated on the maximum pull which could be applied.

When measuring vapour pressures, tap N was closed, and the tube leading to P and L sealed off at a level below the water in the thermostat.

A few cc. of the substance studied were placed in A, which was then sealed. To de-gas, the lid was raised and the pumps started, at first with the  $\text{CO}_2$ -acetone mixture round A. DE and K were filled with  $\text{CO}_2$ -acetone after the moisture introduced during sealing had distilled off. A collar with solid  $\text{CO}_2$  was placed round the neck of A and the substance allowed to distil up completely. It was then melted so as to flow back into the bulb and the distillation repeated. Using liquids, two distillations were sufficient to give a constant vapour pressure in the subsequent measurements; with solids, usually six such sublimations were required to remove air and other very volatile impurities.

The thermostat tank was now put in position without disturbing the apparatus, water run in and a series of measurements taken at various temperatures. The apparatus requires some practice in use, and is liable to give readings one or two thousandths of a millimetre too high at the lower end of its range, possibly because sticking is not entirely eliminated.

If the substance has not been completely de-gassed, the first readings taken are higher than the later readings; this is also a good test for the presence of impurities only slightly more volatile than the substance. Readings can be made every few minutes; and the heat capacity of the manometer being small, readings can be re-commenced about 15 minutes after setting the thermostat to a new temperature. A second calibration was done on completion of a series of vapour pressure measurements; agreement was always very close except when some obvious accident had occurred to the apparatus.

Usually some six successive substances could be measured without dismantling the manometer. Sometimes, however, residual material appeared to collect on the seating causing sticking and erratic values for the unseating current. This could sometimes be removed by substituting a more powerful heating coil for H and pumping out thoroughly; in other cases dismantling and cleaning with chromic acid were required.

Dynamic measurements were also made on brombenzyl cyanide. The apparatus differed from that described in the preceding paper in details

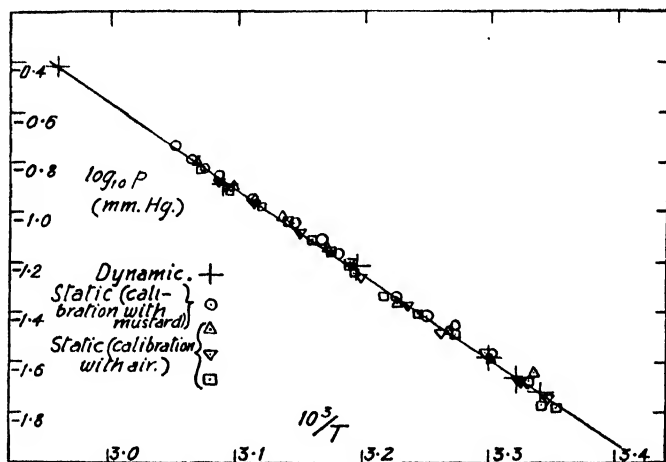


Fig. 3.—Vapour pressure of brombenzyl cyanide.

only; it was found necessary to have an ungreased ground joint at F (preceding paper, Fig. 1) within the mercury seal, and the mercury cut-off at H was removed entirely, since the attack on mercury by the very dilute vapour of brombenzyl cyanide was so rapid as to give results seriously low if any direct contact with mercury was permitted. For absorption, the saturated air passed through a 0.5 % solution of sodium in *iso*-propyl alcohol (ethyl alcohol evaporated too quickly). This hydrolysed the vapour, the amount being determined by potentiometric estimation with  $N/100$  silver nitrate solution, after acidifying with dilute sulphuric acid; the end point could easily be determined with a micro-burette to 0.01 ml. Cyanide might be present in the hydrolysate, but was proved not to affect the end-point in a potentiometric titration of bromide. The rate of passage of air was varied from 4 to 13.8 cc. per minute without affecting the results.

A typical calibration curve for the new manometer is shown in Fig. 2, done with the instrument sensitive to 0.001 mm. Fig. 3 shows the results obtained with brombenzyl cyanide by both static and dynamic methods

The equation

$$\log_{10} p = 9.653 - 3406/T$$

fits the curve between 26° and 65° c. Table I gives smoothed results



extrapolated for liquid brombenzyl cyanide down to 0°, with a probable error of not more than 2 %.

**Purification of material.**—The starting point was technical brombenzyl cyanide (B.B.C.). It was found impossible to distil this, in reasonably large quantities, without decomposition. It was fractionally frozen, drained on a Buchner funnel, and washed with cold alcohol. The pale yellow solid so obtained was recrystallised two or three times from alcohol and twice from light petroleum (40–60°). Recrystallisation from 95 % alcohol sometimes spoiled the product, giving a substance of much higher m.p., lower solubility, and little lachrymatory power; the cause was not

TABLE I.—VAPOUR PRESSURE OF LIQUID BROMBENZYL CYANIDE, mm. Hg.

Temperature.	V.P.	Temperature.	V.P.
0	0·0015	30	0·0262
10	0·0042	40	0·0594
15	0·0068	50	0·130
20	0·0108	60	0·267
25	0·0168		

further studied. The final product was a white crystalline solid, melting at 25·3 to 25·5° C. to a very pale yellowish liquid. The solvent was removed by evacuation in a desiccator, and never gave any trouble in the measurements.

As a further test of the new manometer, the vapour pressure of pure mustard was determined between 31° and 75°, using the least sensitive of the three instruments. Agreement within 3 % was obtained except at the lowest temperatures, when some points about 5 % high were obtained. Fig. 3 shows a few points for brombenzyl cyanide, in which the vapour pressure was calculated using the values of the vapour pressure of mustard from Part I for calibrating the instrument, instead of air; these lie almost on the curve.

**Phenyl dichlorarsine.**—One run was done with the results shown in Table II, which fit the equation

$$\log_{10} p = 9.700 - 3338/T$$

within about 4 %. The phenyl dichlorarsine was prepared by treating magnesium phenyl arsenate with concentrated hydrochloric acid, the crude material converted into the oxide and crystallised several times from a mixture of benzene and light petroleum; the phenyl dichlorarsine was recovered from the purified oxide and distilled with a good column; practically all boiled within 0·3° C.

**Phenol.**—No measurements except at high temperatures appear to have been recorded previously. One run was done on A.R. phenol

TABLE II.

Temperature °C.	V.P. mm. Hg.	Temperature °C.	V.P. mm. Hg.
19·9	0·0180	32·5	0·0580
22·3	0·0275	34·7	0·0705
24·7	0·0317	36·9	0·0807
26·6	0·0375	38·6	0·0992
28·7	0·0445	41·7	0·1280
30·9	0·0525	43·2	0·142

TABLE III.—VAPOUR PRESSURE OF PHENOL.

No.	Temperature °C.	V.P. mm. Hg.	No.	Temperature °C.	V.P. mm. Hg.
3	5·4	0·050	7	12·5	0·107
4	6·6	0·055	8	14·7	0·132
5	7·8	0·065	9	22·2	0·272
2	10·2	0·085	10	28·5	0·48
6	11·4	0·095	11	32·3	0·667
1	12·8	0·107			

(Table III); the first column gives the serial number of the measurement.

Plotted on a log  $p$  against  $1/T$  graph, all points except No. 2 agreed, within 2 %, with the equation

$$\log_{10} p = 11.421 - 3540/T.$$

I thank Professor N. K. Adam for encouragement and advice, Dr. A. Lawson for purifying the phenyldichlorarsine, and Professor Adam and Dr. K. R. Webb for purifying the brombenzyl cyanide, with many tears. The paper is published by permission of the Chief Scientific Officer, Ministry of Supply.

### Summary.

The force required to lift a "lid" off a very accurately fitting seat, when the vapour pressure above is pressing the lid down, is measured. The manometer depends on the attainment of an almost vacuum-tight joint without the use of any grease. The maximum sensitivity was 0.001 mm. and one of the instruments could measure pressures up to 5 mm. Good agreement was obtained with dynamic measurements of vapour pressure, on brombenzyl cyanide. Vapour pressures of phenol and phenyldichlorarsine are also recorded.

### Résumé.

On mesurait la force nécessaire pour soulever un "couvercle" de son siège finement ajusté, pendant que la pression de vapeur régnant au-dessus l'appuyait. Ce manomètre reposait sur la réalisation d'un joint tenant levée presque parfaitement sans l'emploi d'aucune graisse. La sensibilité maximum était de 0.001 mm. et l'un des instruments pouvait mesurer des pressions jusqu'à 5 mm. La tension de vapeur du cyanure de bromobenzyle ainsi obtenue était en bon accord avec les mesures dynamiques. On donne aussi les tensions de vapeur du phénol et de la dichlorarsine.

### Zusammenfassung.

Die Kraft, die nötig ist, um einen „Deckel“ von einer genau passenden Unterlage abzuheben, wenn der Dampfdruck von oben her den Deckel niederhält, wurde gemessen. Das Manometer hängt von der erfolgreichen Herstellung eines fast vakuumdichten Schliffs ohne Gebrauch von Fett ab. Die äusserste Empfindlichkeit war 0.001 mm. und eines der Instrumente konnte Drucke bis zur Höhe von 5 mm. messen. Gute Übereinstimmung wurde mit dynamischen Messungen des Dampfdruckes von Brombenzylchlorid erzielt. Die Dampfdrucke von Phenol und Phenyldichlorarsin werden angegeben.

*University College,  
Southampton.*

# STUDIES IN VAPOUR PRESSURE MEASUREMENT, PART III.—AN EFFUSION MANOMETER SENSITIVE TO $5 \times 10^{-6}$ MILLIMETRES OF MERCURY: VAPOUR PRESSURE OF D.D.T. AND OTHER SLIGHTLY VOLATILE SUBSTANCES.

BY E. W. BALSON.

Received 11th March, 1946.

Effusion through a small hole in a thin wall is a well-known method of determining vapour pressures. Usually the quantity passing the hole in a given time is determined from the loss of weight of the effusion vessel containing the substance, when placed in a high vacuum. This involves breaking the vacuum at intervals, with absorption of air by the substance, unless arrangements are made to weigh *in vacuo*. Volmer,<sup>1</sup> and Deitz<sup>2</sup> have designed balances with beam and knife-edges in an evacuated space; Ubbelohde<sup>3</sup> used the simpler silica spring balance. Volmer,<sup>1</sup> and later Neumann and others,<sup>4</sup> measured the recoil force from the stream of effusing gas, by suspending the effusion vessel from a torsion fibre, so arranged that two streams of effusing gas tended to twist the suspension in the same direction. A modification of the apparatus of Volmer and Neumann has been used here.

Fig. 1 shows the apparatus. The substance is placed in the central tube of the effusion vessel A, which is suspended from a thin Pyrex rod, carrying a mirror M, hung from a quartz fibre. The upper end of the suspension is cemented with fused silver chloride into a cone passing through a ground joint, so that the zero of the suspension could be adjusted from outside. Evacuation was by oil pump and single-stage mercury diffusion pump; a mercury cut-off C, permitted the pressure to be kept at any desired value; a large trap D, cooled by filling with liquid oxygen or CO<sub>2</sub>-acetone mixture ensured rapid passage of vapours away from the holes in A and protected the vacuum train from vapours.

The substance was first distilled in A by means of the heating coil H, so as to distribute it over the inside of the two bulbs, under vacuum. The heating coil was then removed, the opening B being stoppered and the stopper sealed with vacuum wax. The zero of the instrument was then determined. In cases where the substance had a negligible vapour pressure at room temperature this was easily done in a high vacuum. When it was not possible to cool the apparatus far enough for the vapour pressure to be negligible, a pressure of about 10 mm. of air was admitted; at this pressure, the recoil force of vapour effusing from the holes was immeasurably small. At this pressure the zero could be determined to half a millimetre on the scale; at much higher pressures, it was difficult to avoid convection currents which rendered zero determinations at about one atmosphere less accurate. That there was no appreciable recoil force from the effusion, with 10 mm. external pressure, was confirmed by the observation that the same zero was found with, and without cooling

<sup>1</sup> *Z. physikal. Chem.* (Bodenstein Festbd.), 1931, 863.

<sup>2</sup> *J. Amer. Chem. Soc.*, 1933, **55**, 472.

<sup>3</sup> *Trans. Faraday Soc.*, 1938, **34**, 282.

<sup>4</sup> *Z. physikal. Chem. A*, 1932, 161, 33.

liquid in the trap D; with cooling liquid there must have been a slow distillation from the bulbs in A to the trap, without cooling, there should have been equilibrium and no vapour effusing after a time.

The mercury cut-off C was then opened and the vacuum maintained continuously; it was  $10^{-8}$  mm. or better; the trap D was kept cooled. The torsional deflection produced by effusion settled down to a steady value in 15 minutes after setting the thermostat to a given temperature;

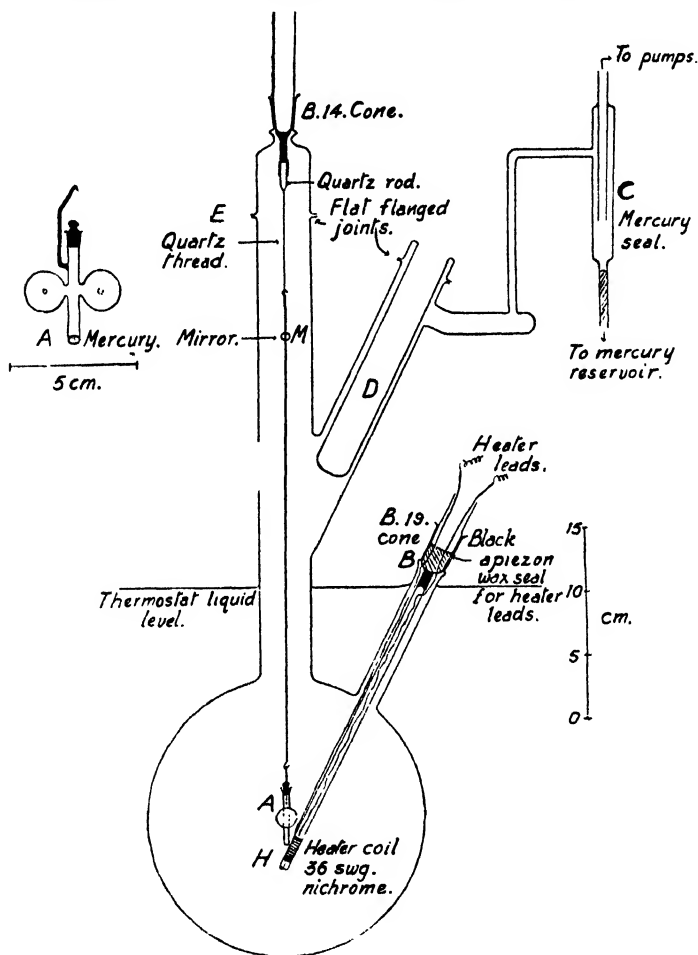


FIG. 1.—Effusion manometer.

scale deflections up to 180 mm. were obtained, and could be read to 0.5 mm. By simple kinetic theory, if the wall thickness at the edges of the holes is negligible compared with their diameter, the recoil force is exactly half the pressure multiplied by the area of the hole. A given angle of twist of the suspension could be converted into pressure, absolutely, from the measured dimensions of the holes and their distances from the axis of suspension, and the torsional rigidity of the suspension. The torsional rigidity was found from the time of swing of each of three brass cylinders, in the usual manner. The holes in the bulbs were bored by a fine tungsten wire fed with carborundum, and the sides of the bulbs round the holes

were then ground to wafer thickness. This produced some irregularity in the shape of the holes, but the area of the holes could be determined by projection on to squared paper by a low power microscope. The distance of the effective centre of each hole, from the axis of suspension, was measured as indicated in Fig. 2. A small weight W was hung from a similar suspension, close by the effusion vessel. The horizontal distance of each hole in the effusion vessel from the second suspension was measured at the

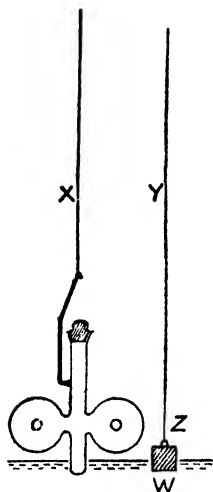


FIG. 2.

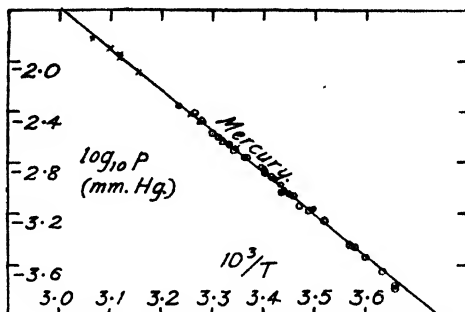


FIG. 3.

Points determined with  
Effusion manometer

1	{	sensitivity	70.6	mm./10 <sup>-3</sup> mm.)	○
2	{	"	19.8	"	×
2a	{	"	24.2	"	+
3a	{	"	6.16	"	△
4	{	"	200.0	"	□
4X	{	"	479.3	"	▽
N	{	"	1.98	"	△

Lid manometers (Part II.)

◇

level Z, and the distance between the two suspending fibres measured at the level XY.

The sensitivity depends on the size and position of the holes and the stiffness of the suspension. Several effusion vessels were made; the dimensions and sensitivities of some are given in Table I.

TABLE I.

No.	First Hole.		Second Hole.		Sensitivity, mm. on scale for 0.001 mm. pressure.
	Area, sq. mm.	Distance from axis, mm.	Area.	Distance from axis.	
1	1.333	12.47	0.9392	11.52	70.3
2	0.3047	11.80	0.3757	11.17	19.8
3	0.2335	8.02	0.177	9.30	9.02
4	2.787	11.12	3.418	11.35	200.0
4X	2.787	11.12	3.418	11.35	479.3
N	0.0727	9.30	hole in one bulb only		1.98

No. 4X was the most sensitive instrument constructed, with a sensitivity about  $5 \times 10^{-6}$  mm. A somewhat greater sensitivity may be obtainable using a lighter effusion vessel and finer suspension, but this has not yet been attempted. No. N, in which one bulb was blind without a hole, worked quite well, and could be used up to several hundredths of a millimetre vapour pressure.

To test the new manometer, the vapour pressure of mercury was determined, using three effusion vessels, between  $0^{\circ}$  and  $53^{\circ}$ . The results are plotted in Fig. 3, the full line being drawn from the values given in International Critical Tables. Except at the lowest temperature, agreement is very good.

Since the effusion vessel must be suspended in a high vacuum, communication of heat from the thermostat to the evaporating substance must be difficult, and there is a risk that the temperature of the evaporating surfaces may be lower than that of the thermostat by an amount which would give low results for the vapour pressure, since the thermostat temperature must be that taken. The following considerations show that the temperature of the evaporating substances was not appreciably lower than that of the thermostat. For every substance, two or more effusion vessels with different sizes of holes were used, and up to the highest temperatures, no difference greater than the random experimental errors was found between the vapour pressure found with large and with small holes. The lowering of temperature should be approximately proportional to the rate at which the substance evaporates and effuses through the holes, and if there had been any lowering of temperature it would have been greater with the large than with the small holes. Further, over a temperature range of about  $40^{\circ}$  to  $50^{\circ}$ , the  $\log p$  against  $1/T$  curves were straight lines within the experimental error. Had there been appreciable cooling in the effusion vessels, this would have been greatest at the highest temperatures, and there would have been a tendency for the points to fall below the straight line at the highest temperatures.

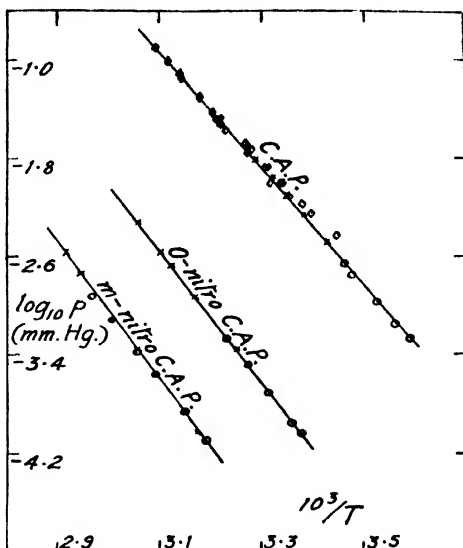


FIG. 4.—Chloracetophenone (C.A.P.); *ortho*-nitrochloracetophenone; *meta*-nitrochloracetophenone.

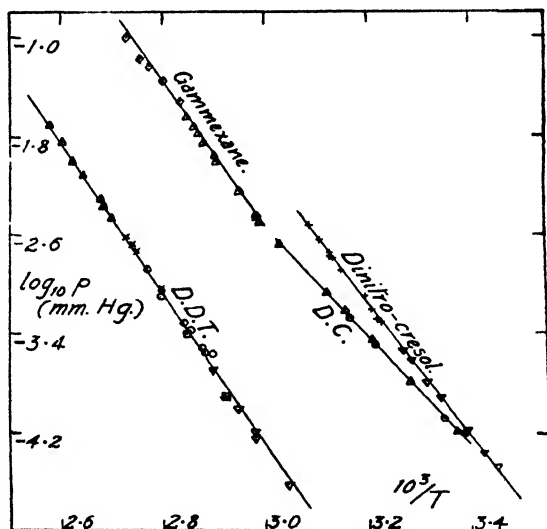


FIG. 5.—1,1-di-*p*-chlorophenyl 2-trichlorethane (D.D.T.); gamma-hexachlorocyclohexane ('gammexane'); diphenyl cyanoarsine (D.C.); 3,5-dinitro-*o*-cresol.

## 58 EFFUSION MANOMETER: VAPOUR PRESSURE OF D.D.T.

The effect of a small residual pressure of air on the recoil force was examined, various air pressures being maintained outside the effusion vessel by the cut-off C. Between  $10^{-5}$  and  $10^{-3}$  mm. air pressure, the recoil force was undiminished. Above  $10^{-3}$  mm. the force gradually diminished, as shown in Table II.

TABLE II.

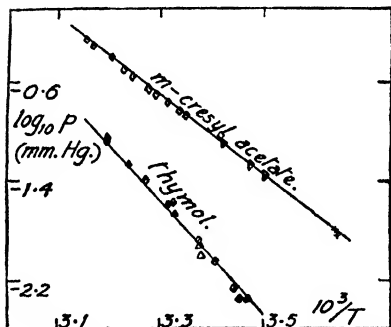
Air pressure, mm. Hg. . . .	< 0.001	0.00435	0.0078	0.0132	0.0226
Recoil force, % of maximum value . . . . .	100	91.9	83.8	71.2	57.3

Since a residual air pressure does not affect the measurements, complete de-gassing of the substance is not quite so important by the effusion method as with strictly static methods for vapour pressure determination. This is useful in dealing with solid substances, some of which are extremely difficult to de-gas completely.

## Results.

The results are summarised in Fig. 4-6.

In every case all the points lie very close to a line obeying an equation  $\log_{10} p = A - B/T$ . In some cases measurements were made with one as the "lid" manometers described in Part II (points marked  $\diamond$ ) as well of with two or more of the effusion manometers. In the case of the liquid *meta*-cresyl acetate agreement was very good between the two manometers. With some of the solids, especially C.A.P., the results obtained with the lid manometer were usually 0.001 or 0.002 mm. high at the lowest temperatures used with this manometer. This was probably due to imperfect de-gassing, possibly to slight sticking at the seating of the "lid".

FIG. 6.—Thymol;  
*meta*-cresyl acetate.

The constants in the equation  $\log_{10} p = A - B/T$  are shown in Table III.

TABLE III.

Substance.*	A.	B.	Range of (Temperature °c.)
C.A.P. . . . .	13.779	4740	5 to 50
<i>ortho</i> -Nitro C.A.P.. . . .	14.239	5413	23 to 54
<i>meta</i> -Nitro C.A.P. . . . .	14.080	5700	26 to 70
D.C. <sup>o</sup> . . . . .	10.724	4420	23 to 53
D.D.T. . . . .	14.191	6160	66 to 100
$\alpha$ -Hexachlorbenzene . . . .	11.950	4850	51 to 71
$\beta$ -Hexachlorbenzene . . . .	11.790	5375	95 to 117
$\gamma$ -Hexachlorbenzene . . . .	15.515	6020	60 to 92
$\delta$ -Hexachlorbenzene . . . .	12.635	5100	55 to 75
3:5-Dinitro- <i>o</i> -cresol . . .	14.140	5400	17 to 51
Thymol . . . . .	14.201	4766	0 to 40
<i>meta</i> -Cresyl acetate . . . .	9.759	3170	2 to 44

\* Notes on Purity: C.A.P. was supplied pure by the Experimental Station, Porton, and several times resublimed before use. The two nitro-C.A.P.'s were supplied by Dr. E. A. Moelwyn-Hughes, from the Research Establishment, Sutton Oak, and resublimed before use once. D.C. and D.D.T. were supplied

The alpha, beta and delta isomers of hexachlorcyclohexane were less carefully done than the gamma, one run only being done with one effusion manometer.

In no case was any appreciable drift of the measured vapour pressure, during a series of measurements at different temperatures, detected, using either the effusion or the "lid" manometers. Had there been any appreciable quantity of an impurity with a vapour pressure substantially different from that of the substance itself, the measured "vapour pressures" would have decreased during the measurements. Measurements were always taken with both rising and falling temperatures, so as to duplicate some of the measurements taken early in the series, with others taken later after much of the material had distilled away.

Table IV gives the "smoothed" results, interpolated or extrapolated (in brackets) by the above equations.

TABLE IV.—SMOOTHED VAPOUR PRESSURES, MM. HG.

°C.	C.A.P.	o-intro-C.A.P.	m-nitro-C.A.P.	D.C.	D.D.T.	di-nitro-o-Cresol.
0	(0.00026)	( $2.6 \times 10^{-6}$ )	( $1.6 \times 10^{-7}$ )	( $3.4 \times 10^{-8}$ )	( $4.4 \times 10^{-9}$ )	( $2.3 \times 10^{-9}$ )
10	0.00107	( $1.31 \times 10^{-5}$ )	( $8.8 \times 10^{-7}$ )	( $1.27 \times 10^{-8}$ )	( $2.7 \times 10^{-9}$ )	( $1.16 \times 10^{-9}$ )
20	0.00406	( $5.9 \times 10^{-6}$ )	( $4.3 \times 10^{-6}$ )	( $4.4 \times 10^{-8}$ )	( $1.5 \times 10^{-7}$ )	$5.2 \times 10^{-8}$
30	0.0137	$2.40 \times 10^{-4}$	$1.88 \times 10^{-5}$	$1.36 \times 10^{-4}$	( $7.2 \times 10^{-7}$ )	$2.12 \times 10^{-4}$
40	0.0434	$8.9 \times 10^{-4}$	$7.5 \times 10^{-5}$	$4.0 \times 10^{-4}$	( $3.2 \times 10^{-6}$ )	$7.8 \times 10^{-4}$
50	0.128	0.00305	$2.75 \times 10^{-4}$	0.00101	( $1.33 \times 10^{-5}$ )	0.00269
60	—	0.0097	$9.3 \times 10^{-4}$	0.00284	( $5.0 \times 10^{-5}$ )	—
70	—	—	0.00293	—	$1.73 \times 10^{-4}$	—
80	—	—	—	—	$5.56 \times 10^{-4}$	—
90	—	—	—	—	0.00168	—
100	—	—	—	—	0.0048	—

## HEXACHLORCYCLOHEXANE.

°C.	alpha	beta	gamma	delta	thymol	m-Cresyl acetate
0	( $1.5 \times 10^{-6}$ )	( $1.3 \times 10^{-6}$ )	( $2.9 \times 10^{-7}$ )	( $9.1 \times 10^{-7}$ )	0.00046	0.0148
10	( $6.5 \times 10^{-6}$ )	( $6.3 \times 10^{-6}$ )	( $1.8 \times 10^{-6}$ )	( $4.1 \times 10^{-6}$ )	0.0023	0.0362
20	( $2.5 \times 10^{-5}$ )	( $2.8 \times 10^{-5}$ )	( $9.4 \times 10^{-6}$ )	( $1.7 \times 10^{-5}$ )	0.0087	0.0875
30	( $8.9 \times 10^{-6}$ )	( $1.15 \times 10^{-5}$ )	( $4.5 \times 10^{-6}$ )	( $6.4 \times 10^{-6}$ )	0.0300	0.200
40	( $2.9 \times 10^{-4}$ )	( $4.2 \times 10^{-6}$ )	( $1.93 \times 10^{-4}$ )	( $2.21 \times 10^{-4}$ )	0.0953	0.431
50	( $8.7 \times 10^{-4}$ )	( $1.43 \times 10^{-5}$ )	( $7.7 \times 10^{-4}$ )	( $7.1 \times 10^{-4}$ )	(0.282)	0.889
60	0.00245	( $4.5 \times 10^{-6}$ )	0.00278	0.0021	—	—
70	0.0065	( $1.32 \times 10^{-4}$ )	0.00925	0.0059	—	—
80	—	( $3.7 \times 10^{-4}$ )	0.0289	—	—	—
90	—	( $9.7 \times 10^{-4}$ )	0.0861	—	—	—
100	—	0.0024	—	—	—	—
110	—	0.00574	—	—	—	—

from Porton. The four hexachlorcyclohexane were purified by Dr. J. Harley Mason at Porton, as follows. The alpha-isomer was purified by steam distillation to remove traces of the beta-isomer, and recrystallised several times from acetic acid. The beta-isomer was recrystallised four times from toluene, the gamma four times from methanol, and the delta four times from 60-80° light petroleum. M.p.s (corr.): alpha, 159.5-160°; beta, 314-5°; gamma, 114-5°; delta, 141.5-142°. All these substances were sublimed at least once in high vacuum before taking their vapour pressures. Thymol was a laboratory "pure" specimen, further recrystallised and distilled once in high vacuum. It melted 50.4 to 50.7° (corr.). Meta-cresyl acetate was a pure specimen supplied by Porton. Dinitro-o-cresol was supplied pure by Porton, after resublimation it melted at 86.5°.



I thank Professor N. K. Adam for advice and encouragement; this paper is published by permission of the Chief Scientific Officer, Ministry of Supply.

### Summary.

An instrument is described in which the recoil force produced by jets of vapour effusing through holes is measured on a torsion balance. Results closely agreeing with accepted values were obtained for mercury; the maximum sensitivity so far attained is  $5 \times 10^{-6}$  mm. The vapour pressures of a number of slightly volatile insecticides and fungicides, and other substances, are given.

### Résumé.

On décrit un instrument dans lequel la force de recul, produite par des jets de vapeur sortant de trous, était mesurée par une balance à torsion. On obtenait ainsi des résultats en excellent accord avec les valeurs généralement acceptées pour Hg; la précision maximum atteinte alors était de  $5 \times 10^{-6}$  mm. On donne les tensions de vapeur d'insecticides et fungicides légèrement volatiles, ainsi que d'autres substances.

### Zusammenfassung.

Ein Instrument wird beschrieben, in dem die Rückstosskraft, die von Strahlen des aus Löchern ausströmenden Gases hervorgerufen wird, auf einer Drehwaage gemessen wird. Für Quecksilber stimmen die so erhaltenen Werte gut mit denen der Literatur überein. Die bisher erzielte Maximalempfindlichkeit beträgt  $5 \times 10^{-6}$  mm. Die Dampfdrucke einer Anzahl von insekten- und pilztötenden und anderen Substanzen werden angeführt.

*University College,  
Southampton.*

---

## REMARKS ON THE STRENGTHS OF BONDS.

By A. D. WALSH.

*Received 1st March, 1946.*

In a recent note,<sup>1</sup> it was shown that the carbonyl bond length increased as the ionization potential of the non-bonding  $p\pi$  electrons on the oxygen atom decreased, *i.e.* as the polarity of the bond increased. Increase of bond length usually means decrease of bond strength. The present notes extend the discussion of this polarity-bond length/bond strength relation to other classes of bonds, and at the same time consider other factors determining bond strength.

The dissociation energy of a bond must in general be dependent upon a number of factors, including the polarity, the extent of resonance involving the bond, the existence of angular strain in the molecule, the extent of valency hybridisation in the orbitals concerned and the amount of "reorganization energy" of the radicals set free on the fission of the bond. Of these, the second, third and fourth have now long been recog-

<sup>1</sup> Walsh, *Trans. Faraday Soc.*, 1946, **42**, 56.

<sup>1a</sup> Walsh, *ibid.* (in press).

nised. The fifth has recently been stressed by Polanyi and his co-workers,<sup>1, 2, 4</sup> who have attributed variations in C—Hal and C—H dissociation energies largely to variation in resonance energy of the radicals produced. In comparison, the first of the above factors has not yet been generally stressed to the extent that, in the writer's opinion, it deserves; though Skinner and Sutton<sup>5</sup> have emphasised its importance in determining the bond lengths of the halogen derivatives of tin, arsenic and nitrogen.

The dissociation energy ( $D$ ) of a bond must, of course, be distinguished from the bond energy ( $E$ ) or bond heat of formation.\* The latter (cf. ref. <sup>1</sup>, p. 651) has a meaning that is clear in the case of, say, the OH bond of water, being just one-half the heat of atomisation. It cannot be the same as the dissociation energy, since it is known that on removing the first H atom from water the strength of the remaining bond changes. For any polyatomic molecule the bond and dissociation energies are not identical, though they are usually so for diatomic molecules. It is important to calculate the heat of atomisation with respect to the atomic states of the atoms concerned that correspond to the states of those atoms in the molecule. For example, the heat of atomisation for methane must be given with respect to the <sup>4</sup>S state of carbon, since this is the lowest tetravalent atomic state.<sup>6</sup> The meaning of bond energy is not so clear in the case of a molecule which, unlike H<sub>2</sub>O and CH<sub>4</sub>, contains different types of bonds. In such a case the bond energies are figures assigned to the various bonds, such that (a) their sum is the heat of atomisation, (b) they will serve as parameters for the inter-conversion of bond properties (force constant, length, ionization potential, etc.), standard points for the relation of bond energy to these properties being provided by molecules where all the bonds are the same. The bond energy is not a quantity whose precision can be pushed over far, for in all molecules the energy involved in atomisation cannot be rigidly divided into parts belonging to the various bonds. Interaction between the bonds must occur to some extent. In molecules such as CH<sub>4</sub> this interaction energy is small; in others, such as CCl<sub>4</sub>, it may be larger. Nevertheless, the concept of bond energy is a useful one, and has at least as much precision as have the traditional bond diagrams of chemists. That the bond energy of a given bond is not constant from molecule to molecule is well established; for example, in the OH radical the bond energy is known to be 100 kcal., whereas in the water molecule it is 110 kcal./mole. The bond energy will depend upon the same factors as the dissociation energy, except for that resulting from the radical reorganization energy. The length and force constants of a bond will presumably depend upon the same factors as the bond energy, though not necessarily to the same relative extent. In what follows, we wish to show how, in many cases, the changes in length and force constant run parallel with changes in polarity. We make no attempt to assert that polarity changes are the *only* factors determining bond length and force constant. In fact, we emphasise the importance of orbital hybridisation. Nor do we maintain that polarity factors are necessarily the most important in determining dissociation energies, but we shall see that in many cases, at least, the dissociation energy changes run qualitatively parallel to polarity changes. The quantitative relative contributions of radical reorganisation energy, polarity and other factors, must await future work.

\* Baughan, Evans and Polanyi<sup>3</sup> use the expression "bond energy term" to correspond with the bond energy or bond heat of formation as here used. The term "bond energy" as used by Baughan *et al.* means dissociation energy.

<sup>1</sup> Baughan, Evans and Polanyi, *ibid.*, 1941, 37, 377.

<sup>2</sup> Butler and Polanyi, *ibid.*, 1943, 39, 19.

<sup>4</sup> Butler, Mandel and Polanyi, *ibid.*, 1945, 41, 298.

<sup>5</sup> Skinner and Sutton, *ibid.*, 1944, 40, 164.

<sup>6</sup> Long and Norrish, *Nature*, 1946, 157, 486; *ibid.*, 1946, 158, 237; *Proc. Roy. Soc. A.*, 1946, 187, 337.

## Carbon-Oxygen Bonds.

Some of the data for carbonyl bonds has already been given,<sup>1</sup> but it is convenient here to summarise and extend it in Table I.

TABLE I.

Molecule.	I.P. (V).	Carbonyl Bond Length (Å.).	Stretching Force Constant (10 <sup>6</sup> dynes/cm.).	Bond Energy (kcal./mole.).
Carbon monoxide	14.55	1.13	18.6 <sup>10</sup>	211
Carbon dioxide	13.73	1.15	$\begin{cases} 15.2^{10} \\ 15.5^{12} \end{cases}$	~ 202
Glyoxal	~ 11.4	1.20	—	~ 186
Formaldehyde	10.83	1.21	$\begin{cases} 11.5^{11} \\ 12.3^{10} \end{cases}$	~ 190
Acetaldehyde	10.18	1.22	—	~ 184

The values in the last column are based upon the values ~ 190 and 125 for the energy changes in the sublimations

$$C_{\text{diamond}} = C(\text{tetravalent})_{\text{gas}}$$

$$C_{\text{diamond}} = C(\text{divalent})_{\text{gas}}$$

respectively.\* In formaldehyde, the C—H distance has been assumed to be 1.102 Å.\* and the C—H bond energy has been obtained by a modification of the method used by Skinner,<sup>7</sup> viz. a curve of energy/length, using as fixed points  $\text{CH}_3\text{OH}_2 = (121 \text{ kcal.},^{13} 1.60\text{Å.})$ ;  $\text{CH}_3\text{OH}_2 = (103, 1.09)$ ;  $\text{CH}_{\text{radical}} = (80, 1.12)$ . The method for  $\text{CH}_3\text{CHO}$  was as used by Skinner except for the revised latent heat value; CH of CHO was assumed to be as in HCHO (~ 96 kcal./mole.),  $\text{CH}_2$  as in  $\text{CH}_4$  and  $E_{(\text{CO})}$  (~ 105 kcal./mole) was obtained from an energy/length graph. In glyoxal, CH was assumed to be as in HCHO and CC (~ 113 kcal./mole.) was obtained from the CC energy/length graph.

Table I shows clearly how the carbonyl bond length increases, and how the carbonyl stretching force constant and bond heat of formation decrease, with increasing polarity of the bond. The only exception lies in the bond energy of glyoxal, which is lower than that of the more polar molecule HCHO; but this is not unexpected, for the well-founded theory of conjugated molecules, as developed by Mulliken, Lennard-Jones, Coulson and others, demands that conjugated multiple bonds be somewhat weaker (cf. cyanogen in the table given below) than would otherwise be the case (other things being equal).

As two examples of the effect of polarity upon single carbon oxygen bonds, we may cite the following.

(1) When dimethyl ether forms its complex with boron trifluoride, the donation of electrons from the oxygen atom towards the boron must clearly result in greater C+O<sup>-</sup> polarisation of the C—O bond electrons of

\* A mean of the values given by Linnett<sup>8</sup> and Stevenson, Lu Valle and Schomaker<sup>9</sup>. No stress should be put upon the exact bond energy figures given in any of the tables of this paper: they are intended only to be rough indications of the true energies.

<sup>7</sup> Skinner, *Trans. Faraday Soc.*, 1945, 41, 645.

<sup>8</sup> Linnett, *ibid.*, 1945, 41, 223.

<sup>9</sup> Stevenson, Lu Valle and Schomaker, *J. Amer. Chem. Soc.*, 1939, 61, 2508.

<sup>10</sup> Thompson and Linnett, *J. Chem. Soc.*, 1937, 1376.

<sup>11</sup> Bailey and Hale, *Nature*, 1937, 139, 1112.

<sup>12</sup> Herzberg, *Infra-red and Raman Spectra*, Van Nostrand, 1945.

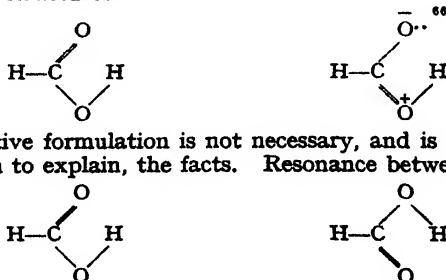
<sup>13</sup> Private information from Dr. L. H. Long; see Cherton, *Bull. Soc. Roy. Sci., Liège*, 1942, 203.

the ether. That the increase of  $C+O^-$  polarity is accompanied by a weakening of the CO bonds is shown by (a) electron diffraction data ( $r_{(CO)}$  in the ether = 1.42 Å.,  $r_{(CO)}$  in the complex = 1.45 Å.<sup>12a</sup>), (b) the chemical facts that  $(CH_3)_2O : BF_3$  is a good methylating agent and that  $BF_3$  is commonly used as a splitting agent for aromatic ethers,<sup>12a</sup> (c) the electrons in the CO bonds become more easily excited when the complex is formed,<sup>12a</sup> i.e. their ionization potential becomes less which, as a result of the relation between ionization potential and "bond order", means the bond strength becomes less.<sup>12b</sup> Also in consequence of the donation of electrons to the boron atom in the complex the  $B^+F^-$  polarity of the BF bonds must be greater in the complex than in  $BF_3$ ; in accord the BF distance increases from 1.30 to 1.41 Å. on formation of the complex,<sup>12c</sup> though in part this increase is due to change of the B atom from the trigonal to the tetrahedral state.

(2) Since the C—O bond has usually a high dipole,  $E_{(C-O)}$  may be expected to show rather considerable variations. The heat of atomisation of dimethyl ether, assuming a value 190 kcal./mole. for the energy change

$$C_{solid} = C(\text{tetravalent})_{gas},$$

can be shown to be 797.7 kcal./mole. (cf.<sup>7</sup>). If the CH bonds are assumed to be as in methane, the C—O link has an energy of  $\sim 86$  kcal./mole.; if the CH bonds are given a strength  $\sim 101$  kcal./mole.  $E_{(C-O)}$  is  $\sim 92$  kcal./mole. In methyl alcohol (for which electron diffraction gives the same CO length as in dimethyl ether), Butler and Polanyi<sup>8</sup> give  $D_{(C-O)}$  as 86.5 kcal./mole. These figures refer, however, to heavily polar C—O bonds. If the polarity were reduced, then, by analogy with carbonyl bonds, we might expect greater bond and dissociation energies. Now in formic acid monomer the competition of the electronegative C=O and OH groups for the electrons of the C—O bond must result in that bond being much less polar than in methyl alcohol or dimethyl ether. From the " % ionicity ",<sup>12</sup> in the C=O group of formic acid monomer (determined from ionization data) we may (from a graph of bond energy/ionicity) estimate the C=O bond energy as  $\sim 194$  kcal. The CH bond energy (cf.  $E_{(CH)}$  in HCHO referred to above) is unlikely to be more than 100 kcal. The OH bond energy is likely to be less than in water (110 kcal./mole.) as a consequence of the expected greater bond polarity. Hence, from thermal data, using the value of the carbon sublimation energy given above and the consequent heat of atomisation of HCOOH (500.7 kcal./mole., based on a heat of formation = 88.65 kcal.<sup>12d</sup>), we find  $E_{(C-O)}$  is probably greater than 97 kcal./mole. While no quantitative stress is to be laid on this figure, we think that the qualitative conclusion—viz. that the C—O bond in formic acid is stronger than in methyl alcohol or dimethyl ether—is strongly indicated and is in accord with polarity expectations. It is also in accord with the force constant value of  $5.4^{12e}$  as against  $4.5 \times 10^6$  dynes/cm. for dimethyl ether. The high strength is expected on the basis of the resonance structures



but this qualitative formulation is not necessary, and is more an attempt to describe, than to explain, the facts. Resonance between the structures

<sup>12</sup> (a) Dunderman and Bauer, *J. Physic. Chem.*, 1946, 50, 32.

(b) Walsh, *Trans. Faraday Soc.* (in press).

(c) Bauer, Finlay and Laubengayer, *J. Amer. Chem. Soc.*, 1943, 65, 889.

(d) Bichowsky and Rossini, *Thermochemistry of Chemical Substances*, 1936.

(e) Bonner and Hofstadter, *J. Chem. Physics*, 1938, 6, 531.

does not occur, since it is known that the H atom concerned is not symmetrically placed.<sup>15</sup> (We may further note that if we took a value for the “% ionicity” determined from the published value of the C=O bond length, we should get a lower figure for  $E_{O-O}$  and a value for  $E_{(C-O)}$  improbably high. This may be used as further evidence for doubting the accuracy of the published electron diffraction conclusions.<sup>1, 16</sup>)

### Carbon-Nitrogen Bonds.

Carbonyl bonds are well suited to the study of polarity effects because, owing to the valency configuration of the carbon atom, they should be almost free from steric effects due to the groups attached to the carbon. C—Hal. and C—H bonds (discussed below) are not so isolated and polarity effects are complicated in them by steric effects. The cyanides would form an excellent series for the study of polarity effects, since the C≡N bond will always be largely unaffected by steric effects from the other group attached to the carbon atom. Unfortunately the data are very scanty. We may, however, note that CH<sub>3</sub>CN has a probable longer CN length (Table II) and smaller CN force constant than has HCN, in accord

TABLE II.

Molecule.	CN Bond Length (Å.).	Stretching Force Constant (10 <sup>8</sup> dynes/cm.).	Bond Energy (kcal./mole).
HCN . .	1.15 <sup>15</sup>	18.1 <sup>10</sup>	~ 176 (~ 204)
CH <sub>3</sub> CN . .	$\begin{cases} 1.172^{16} \\ 1.16 \pm 0.03^{17} \end{cases}$	17.7 <sup>12</sup>	—
ClCN . .	1.13 ± 0.03 <sup>18</sup>	16.7 <sup>10</sup>	~ 165 (~ 192)
BrCN . .	1.13 ± 0.04 <sup>18</sup>	16.8 <sup>10</sup>	—
ICN . .	—	16.8 <sup>10</sup>	—
C <sub>2</sub> N <sub>2</sub> . .	$\begin{cases} \text{CN } 1.16 \pm 0.02^{17} \\ \text{CC } 1.37 \pm 0.02^{17} \end{cases}$	—	$\begin{matrix} \sim 169 (\sim 196) \\ \sim 142 \end{matrix}$

with the fact that CH<sub>3</sub>CN has probably a greater CN polarity than has HCN, just as CH<sub>3</sub>CHO has larger CO polarity than has HCHO. The vacuum ultra-violet spectra of the cyanogen halides<sup>14</sup> indicate that the halogen atoms bear less negative charge than in the alkyl halides. The situation is analogous to that found in the chloro-ethylenes, and we expect a reduced binding of the CN bond electrons in ClCN relative to HCN, either because of repulsion between the negatively charged Cl and the CN bond electrons or else because of conjugation of the Cl non-bonding and the CN  $\pi$  electrons. It is therefore not surprising that the CN force constants (Table II) show a decrease in these molecules relative to HCN, though the electron diffraction length values are not in very satisfactory agreement with this. One would expect the CN polarity to increase and therefore the CN strength of binding to decrease in the order ClCN, BrCN, ICN, but the data give no indication of this. In the table the CN bond

<sup>15</sup> Davies and Sutherland, *ibid.*, 1938, 6, 755.

<sup>16</sup> Price and Walsh, *Trans. Faraday Soc.*, 1945, 41, 381.

<sup>17</sup> Herzberg and Spinks, *Proc. Roy. Soc. A*, 1934, 147, 434.

<sup>18</sup> Quoted by Herzberg, *Molecular Spectra and Molecular Structure*, Prentice Hall, 1939.

<sup>17</sup> Pauling, Springall and Palmer, *J. Amer. Chem. Soc.*, 1939, 61, 927.

<sup>18</sup> Beach and Turkevich, *ibid.*, 1939, 61, 299.

energy of HCN has been obtained by taking the CH energy as  $\sim 120$  from a CH length/strength graph. The CN energy in CNCl results from using the CCl energy of Table III. The CC energy of cyanogen comes from a CC length/strength graph and the CN energy results from this using thermal data. The CN energies in brackets have been obtained by use of the value 225 kcal./mole. for  $D_{(N_2)}$  as recently given by Gaydon<sup>19</sup> and used by Skinner<sup>7</sup>; the figures outside the brackets have been obtained with the old value of 170 as used by Bichowsky and Rossini, Pauling and Herzberg.

### Carbon-Halogen Bonds.

Table III shows the experimental carbon-halogen lengths for a number of compounds. It also records certain data on the ionization potentials of the non-bonding halogen  $p\pi$  electrons. A value for the CCl bond energy in  $\text{CH}_3\text{Cl}$  has been given by taking the CH energy as somewhat greater than 104 (see below).<sup>\*</sup> In vinyl chloride  $E_{(\text{CCl})}$  has been obtained by taking CH as 106 (as in ethylene) and (both in this molecule and in  $\text{C}_2\text{Cl}_4$ )  $\text{C}=\text{C}$  as 140 from a CC length-strength graph.  $E_{(\text{CCl})}$  in CNCl has been found from a graph of CCl length/strength, using as fixed points  $\text{CH}_3\text{Cl}$ ,  $\text{CCl}_4$ ,  $\text{C}_2\text{Cl}_4$  and vinyl chloride.

Replacement of the  $\text{CH}_3$  group in  $\text{CH}_3\text{Cl}$  by the strongly electro-negative  $\text{CH}_2\text{Cl}$ ,  $\text{CHCl}_2$  or  $\text{CCl}_3$  groups must mean that each Cl bears a smaller negative charge in  $\text{CH}_2\text{Cl}_2$ ,  $\text{CHCl}_3$  and  $\text{CCl}_4$  than in the Cl in  $\text{CH}_3\text{Cl}$ . The dipole moments as given by Sutton and Brockway<sup>22</sup> for the C—Cl bonds in  $\text{CH}_2\text{Cl}_2$  (1.35 D.) and  $\text{CHCl}_3$  (1.28 D.) compared with  $\text{CH}_3\text{Cl}$  (1.85 D.) provide evidence of this. The ionization potential of the Cl non-bonding electrons must be greater in  $\text{CCl}_4$  than in  $\text{CH}_3\text{Cl}$ . In accord with this, the CCl distance shows a probable decrease from  $\text{CH}_3\text{Cl}$  ( $1.77 \pm 0.02$  Å.) to  $\text{CCl}_4$  ( $1.755 \pm 0.005$  Å.). The effect should be greater in the corresponding fluorine compounds, as a result of the greater electro-negativity of the fluorine atom. This is indeed the case: methyl fluoride has a C—F length of  $1.42 \pm 0.02$  Å., while  $\text{CH}_3\text{F}_2$  (with an expected higher fluorine ionization potential) has a C—F length of only  $1.36 \pm 0.02$  Å. Similarly,  $\text{FCH}_2\text{Cl}$  and  $\text{F}_2\text{CHCl}$  have C—Cl lengths respectively of  $1.76 \pm 0.02$  and  $1.73 \pm 0.03$  Å. compared with  $1.77 \pm 0.02$  Å. for  $\text{CH}_3\text{Cl}$ .

There is a decrease of C—Cl length from ethyl chloride ( $\sim 1.77$  Å.) to vinyl chloride ( $1.69 \pm 0.02$  Å.). At the same time there is an increase of ionization potential of the non-bonding  $p\pi$  chlorine electrons as shown by the shift in the "D" bands due to excitation of the electrons,<sup>21</sup> i.e. the Cl atom in vinyl chloride bears a positive charge relative to the Cl atom in ethyl chloride. There is also a decrease in CCl length in passing from ethyl to phenyl chloride; with a simultaneous increase of ionization potential of the Cl non-bonding electrons.<sup>22</sup> These cases thus conform to the statement that the CCl distance decreases with decreasing polarity of the CCl bond, but that this is not the only effect at work is shown by the fact that the "D" bands and ionization potentials indicate a lesser CCl polarity in methyl chloride (with approximately the same CCl length as ethyl chloride) than in vinyl or phenyl chlorides. We shall discuss below other causes of the decreased CCl length in vinyl and phenyl chlorides. Vinyl chloride probably has a greater C—Cl force constant than  $\text{CH}_3\text{Cl}$ , since that of  $\text{C}_2\text{Cl}_4$  is probably appreciably greater.<sup>10</sup>  $\text{C}_2\text{Cl}_4$  (C—Cl:  $1.73 \pm 0.02$  Å.)

\* The value given for the CCl bond energy in  $\text{CH}_3\text{Cl}$  ( $\sim 80$ ) is markedly less than the H—Cl dissociation energy (103).  $D_{(\text{CCl})}$  will not be far different to  $E_{(\text{CCl})}$ . It is not therefore surprising that a chlorine atom attacks the methane molecule to give  $\text{HCl} + \text{CH}_3$  rather than  $\text{H} + \text{CH}_3\text{Cl}^{10}$ .

<sup>19</sup> Gaydon, *Nature*, 1944, 153, 407.

<sup>20</sup> Price, *J. Chem. Physics*, 1936, 4, 539, 547.

<sup>21</sup> Walsh, *Trans. Faraday Soc.*, 1945, 41, 35.

<sup>22</sup> Walsh (in course of publication).

<sup>23</sup> Sutton and Brockway, *J. Amer. Chem. Soc.*, 1935, 57, 473.

shows a shortening of C—Cl relative to  $\text{CH}_3\text{Cl}$ , but the C—Cl bonds are not as strong as in vinyl chloride.

The sign of the C—Cl dipole in  $\phi\text{Cl}$  shows that Cl takes charge from the ring. Hence, replacing  $\phi$  by  $\text{C}_6\text{H}_4\text{Cl}$  means that the C—Cl polarity in  $\text{C}_6\text{H}_4\text{Cl}_2$  must be less than in  $\phi\text{Cl}$  (just as in  $\text{CH}_3\text{F}$ , relative to  $\text{CH}_3\text{F}$ ). In full agreement we find a shift of the Cl "D" bands to short wavelengths in passing from  $\phi\text{Cl}$  to  $o\text{-C}_6\text{H}_4\text{Cl}_2$ . An anomaly occurs here,

TABLE III.

Molecule.	Non-bonding I.P. (V).	C—Hal. Bond Length.	C—Hal. Bond Energy.
Methyl chloride . . . . .	{ 11.17 <sup>20</sup> 11.25 <sup>20</sup>	1.77 $\pm$ 0.02 <sup>23</sup>	~ 80
Methylene chloride . . . . .		1.77 $\pm$ 0.02 <sup>23</sup>	
Carbon tetrachloride . . . . .	11.2 <sup>21</sup>	1.755 $\pm$ 0.005 <sup>23</sup>	~ 83
Fluorochloromethane . . . . .		1.76 $\pm$ 0.02 <sup>24</sup>	
Diffuorochloromethane . . . . .		1.713 $\pm$ 0.03 <sup>24</sup>	
Vinyl chloride . . . . .		1.69 $\pm$ 0.02 <sup>25</sup>	
Tetrachloro-ethylene . . . . .		1.73 $\pm$ 0.02 <sup>25</sup>	
Chloro-acetylene . . . . .	> 11.2 <sup>14</sup>	1.68 $\pm$ 0.04 <sup>26</sup>	~ 87.5
Phosgene . . . . .		1.68 $\pm$ 0.02 <sup>25</sup>	
Thiophosgene . . . . .		1.70 $\pm$ 0.02 <sup>25</sup>	
Cyanogen chloride . . . . .		1.67 $\pm$ 0.02 <sup>18</sup>	
Propargyl chloride . . . . .		1.82 $\pm$ 0.02 <sup>27</sup>	
Chlorobenzene . . . . .	11.2 <sup>22</sup>	1.69 $\pm$ 0.02 <sup>28</sup>	~ 103
o-Dichlorobenzene . . . . .		1.71 $\pm$ 0.02 <sup>28</sup>	
Methyl bromide . . . . .	{ 10.19 <sup>20</sup> 10.80 <sup>20</sup>	1.91 $\pm$ 0.02 <sup>29</sup>	
Vinyl bromide . . . . .		{ 2.05 $\pm$ 0.08 <sup>30</sup> 1.86 $\pm$ 0.04 <sup>30</sup>	
Bromo-acetylene . . . . .	> 10.8 <sup>14</sup>	1.80 $\pm$ 0.03 <sup>30</sup>	
Cyanogen bromide . . . . .		1.79 $\pm$ 0.02 <sup>18</sup>	
Propargyl bromide . . . . .		1.95 $\pm$ 0.02 <sup>27</sup>	
Methyl fluoride . . . . .		1.42 $\pm$ 0.02 <sup>34</sup>	
Methylene fluoride . . . . .		1.36 $\pm$ 0.02 <sup>34</sup>	

however, for we should expect a slightly decreased C—Cl distance in  $o\text{-C}_6\text{H}_4\text{Cl}_2$  relative to  $\phi\text{Cl}$ ; but in disagreement Brockway and Palmer<sup>28</sup> find  $1.71 \pm 0.02$  A. for  $o\text{-C}_6\text{H}_4\text{Cl}_2$  as against  $1.69 \pm 0.02$  A. for  $\phi\text{Cl}$  and  $m$ - and  $p\text{-C}_6\text{H}_4\text{Cl}_2$ . The position of the "D" bands must be taken as evidence that the C—Cl polar character is less in  $o\text{-C}_6\text{H}_4\text{Cl}_2$  than in  $\phi\text{Cl}$ ; perhaps in spite of this the C—Cl length is greater in  $o\text{-C}_6\text{H}_4\text{Cl}_2$  because of steric repulsion of the two adjacent Cl atoms,<sup>31</sup> which suggestion accords with the fact that the  $m$ - and  $p$ -compounds do not show the length increase.

The C—Cl distance ( $1.67 \pm 0.02$  A.) in cyanogen chloride is appreciably less than in methyl chloride. This accords with the fact that the spectrum of the non-bonding  $p\pi$  Cl electrons is shifted well to short wavelengths in ClCN (indicating a higher ionization potential) relative to  $\text{CH}_3\text{Cl}$ , which probably means that CCl in ClCN has less polarity than CCl in  $\text{CH}_3\text{Cl}$ . Similarly, the C—Br distance in cyanogen bromide is only  $1.79 \pm 0.02$  A., compared with  $1.91 \pm 0.02$  A. in  $\text{CH}_3\text{Br}$ ; which is in accord with the electronic spectrum.<sup>14</sup> Decreased bond length means increased binding.

<sup>24</sup> Brockway, *J. Physic. Chem.*, 1937, 41, 747.

<sup>25</sup> Brockway, Pauling and Beach, *J. Amer. Chem. Soc.*, 1935; 57, 2693.

<sup>26</sup> Hey, *Ann. Reports*, 1944, 40, 188.

<sup>27</sup> Pauling, Gordy and Saylor, *J. Amer. Chem. Soc.*, 1942, 64, 1753.

<sup>28</sup> Brockway and Palmer, *ibid.*, 1937, 59, 2181.

<sup>29</sup> Brockway and Levy, *ibid.*, 1937, 59, 1662.

<sup>30</sup> Dornet, *J. Chem. Physics*, 1933, 1, 566.

<sup>31</sup> Burawoy, *Trans. Faraday Soc.*, 1944, 40, 537.

Cyanogen chloride and bromide have probably greater C—Hal. stretching force constants than  $\text{CH}_3\text{Cl}$  and  $\text{CH}_3\text{Br}$ .<sup>32</sup> In part, however, the strengthening of C—Hal. in the cyanogen halides probably comes (as in chloro-acetylene) from the "digonal" nature of the carbon atom, as discussed below.

In phosgene, the electronegativity of the carbonyl relative to a methylene group and the "trigonal" nature of the carbon atom (see below) must mean that the polarity of the C—Cl bonds is reduced in phosgene relative to  $\text{CH}_2\text{Cl}_2$ . The C—Cl distance ( $1.68 \pm 0.02$  Å.)<sup>\*</sup> is known to be reduced in phosgene relative to methylene chloride ( $1.77 \pm 0.02$  Å.). The reduced electronegativity of CS relative to CO must mean that the CCl bonds have greater polarity in thiophosgene than in phosgene. Correspondingly, the CCl bond length increases from  $1.68 \pm 0.02$  Å. ( $\text{COCl}_2$ ) to  $1.70 \pm 0.02$  Å. ( $\text{CSCl}_2$ ).

Butler and Polanyi<sup>3</sup> find the dissociation energy of the C—I bond to be less in acetyl iodide than in ethyl iodide. The frequently postulated resonance forms



would lead to a *strengthened* C—I bond. Butler and Polanyi therefore assume that, although the resonance effect occurs, it is offset by some other factor. This factor they identify with withdrawal of electrons from the C—I bond by the electronegative oxygen atom; and they support this identification by reference to the weakened C—I bond that Butler, Mandel and Polanyi<sup>4</sup> observe in  $\text{Cl}_2\text{CHI}$  and  $\text{Br}_2\text{CHI}$ . In contradiction to this it is suggested here that such a process would *strengthen* the C—I bond, not weaken it. The explanation of Butler and Polanyi would lead one to expect a greater weakening of C—I in  $\text{Cl}_2\text{CHI}$  than in  $\text{Br}_2\text{CHI}$  than in  $\text{I}_2\text{CHI}$ , whereas the results of Butler, Mandel and Polanyi show that the opposite is the case. Further, we have given evidence above that the C—Hal. bonds in  $\text{CH}_3\text{F}$  and  $\text{CH}_3\text{Cl}$  are shortened and strengthened by substitution of F or Cl for H. Weakening of C—I bond strength in  $\text{Cl}_2\text{CHI}$  and  $\text{Br}_2\text{CHI}$  must probably be due to steric repulsion of the large halogen atoms, an explanation which accords with the greater weakening of C—I in  $\text{I}_2\text{CHI}$  than in  $\text{Br}_2\text{CHI}$  than in  $\text{Cl}_2\text{CHI}$ . By analogy, the weakening of C—I in acetyl iodide relative to ethyl iodide is probably due to steric repulsion of the negatively charged I and O atoms. We know from infra-red and ultra-violet data that there are very important steric effects in  $\text{C}_2\text{Cl}_4$  and  $o\text{-C}_6\text{H}_4\text{Cl}_2$ ; we know, too, that there are considerable potential barriers hindering internal rotation in the halogenated ethanes; hence we have every reason to expect important steric effects in halogenated methanes (and, by analogy, in acetyl iodide), where the repelling atoms are on the same carbon atom and therefore nearer together. Indeed, X-ray data indicate clearly these steric effects in halogenated methanes since, for example, on passing from  $\text{CCl}_4$  to  $\text{CHCl}_3$ , the Cl atoms move further apart.<sup>33a</sup>

The accuracy of the bond length values is not usually such as to allow great stress to be put upon any one example given above; but, taken together, the discussion may be said to provide strong evidence that as the ionization potential of the non-bonding halogen  $p\pi$  electrons decreases or as the polarity of a carbon-halogen linkage increases, the bond length

\* It has been remarked that the value given by Dornte<sup>33</sup> for the carbonyl distance in phosgene is more in accord with the observations of infra-red and ultra-violet spectroscopy than the value given by Brockway, Pauling and Beach.<sup>26</sup> The value given by Dornte for the CCl distance, however, is  $1.80 \pm 0.04$ , which seems less compatible with the present discussion than the Brockway *et al.* value of  $1.68 \pm 0.02$  Å.

<sup>32</sup> Sutherland, *Ann. Reports*, 1936, 33, 64.

<sup>33</sup> Dornte, *J. Amer. Chem. Soc.*, 1933, 55, 4128.

<sup>33a</sup> (a) Pirene, *Diffraction of X-rays and Electrons*, Cambridge, 1946, p. 142.



usually increases.<sup>34</sup> Further, the shift of bonding electrons from a bond on to one of the atoms concerned means that the orbitals extend further on the side of the atom remote from the bond and therefore have weakened bonding power; slight direct evidence for this has been given in terms of force constants, but all the increases in length may be taken as further evidence. In agreement, Henne and Midgley<sup>35</sup> have pointed out, for example, that the Cl in  $\text{CF}_3\text{Cl}$  is much less reactive than in, say,  $\text{CH}_3\text{Cl}$ , or  $\text{CBr}_3\text{Cl}$ , that  $\text{CH}_2\text{ClF}$  is more stable than  $\text{CH}_2\text{Cl}_2$ , and that  $\text{CH}_2\text{F}_2$  is extremely inert. Similarly, Henne<sup>36</sup> has shown that  $\text{CHF}_3$  is exceptionally inert. In further agreement, Butler and Polanyi<sup>3</sup> have measured the pyrolysis rates of many halides and find, for example, a big reduction in vinyl or phenyl halides relative to the methyl or ethyl halides.

Price<sup>30</sup> has shown that the ionization potential of the non-bonding  $p\pi$  halogen electrons decreases from the methyl to the ethyl halide. Stevenson and Hipple<sup>37</sup> find that further decreases occur in passing to the propyl and thence to the *t*-butyl halides. We may say that the C—Cl link has increased polar character as we pass from methyl to ethyl to *i*-propyl to *t*-butyl chloride. The values of the dipole moments are not in disagreement with this.<sup>3</sup> We may therefore predict that the C—Cl length increases slightly as we pass from methyl to *t*-butyl chloride in the above sequence. Side by side with the increase of bond length goes an expected decrease of force constant and of bond strength. Decrease of bond dissociation energy is just what is found by Butler and Polanyi,<sup>3</sup> and is reflected in the decreasing Raman frequencies.<sup>38</sup>

### Carbon-Hydrogen Bonds.

Table IV lists values of C—H lengths, force constants and bond energies. The latter have been obtained by a combination of thermo chemical data and graphs of length/strength as mentioned above.

Although it has usually been assumed in the past that C—H in  $\text{CH}_3\text{—H}$  has polarity  $\text{C—H}^+$ ,\* it has recently been shown by Coulson<sup>45</sup> to have the reverse sign,<sup>†</sup> i.e., it has the same polarity as the C—Hal. bond in  $\text{CH}_3\text{—Hal}$ . We therefore expect something of the same effects as in the halogen compounds when we replace  $\text{CH}_3$  by other radicals—though differences may occur owing to the small value of  $\mu_{\text{OH}}$  in  $\text{CH}_4$ , e.g. complete reversal of polarity may occur. The changes in bond length will probably be smaller than in the case of C—Hal. because the dipole associated with C—H in  $\text{CH}_4$  is small (0.4 D.) compared with that of C—Cl (1.85 D.) in  $\text{CH}_3\text{—Cl}$ . Similarly C—Br, having a much smaller dipole than C—Cl, shows practically no change in length from  $\text{CH}_3\text{Br}$  to  $\text{CBr}_4$ , although C—Cl does show a small measurable change from  $\text{CH}_3\text{Cl}$  to  $\text{CCl}_4$ .

If CH has polarity  $\text{C}^+\text{H}^-$  we should expect reduction of this polarity on replacing one of the H atoms of, say,  $\text{CH}_4$  by Cl. If other factors (e.g. angular strain) do not offset it, we should therefore expect a slightly

\* Thus Pauling's electronegativity scale places carbon above hydrogen.

† See also Gent, *Nature*, 1946, 158, 27.

<sup>34</sup> A similar statement has already been made by Burawoy,<sup>31</sup> although followed out in less detail.

<sup>35</sup> Henne and Midgley, *J. Amer. Chem. Soc.*, 1936, 58, 882; cf. Henne, *J. Amer. Chem. Soc.*, 1937, 59, 1400, 2434.

<sup>36</sup> Henne, *J. Amer. Chem. Soc.*, 1937, 59, 1200.

<sup>37</sup> Stevenson and Hipple, *J. Amer. Chem. Soc.*, 1942, 64, 2766.

<sup>38</sup> Smyth and McAlpine, *J. Chem. Physics*, 1934, 2, 499.

<sup>39</sup> Jones, *Trans. Faraday Soc.*, 1935, 31, 1036.

<sup>40</sup> Thompson, *Trans. Faraday Soc.*, 1939, 35, 697.

<sup>41</sup> Gallaway and Barker, *J. Chem. Physics*, 1942, 10, 88.

<sup>42</sup> Schomaker and Pauling, *J. Amer. Chem. Soc.*, 1939, 61, 1769.

<sup>43</sup> Linnett, *Trans. Faraday Soc.*, 1945, 41, 223.

<sup>44</sup> Fox and Martin, *Proc. Roy. Soc. A*, 1940, 175, 208.

<sup>45</sup> Coulson, *Trans. Faraday Soc.*, 1942, 38, 433.

increased CH strength in  $\text{CH}_3\text{Cl}$  relative to  $\text{CH}_4$ . That this is probably so is indicated by the following thermochemical argument, which is independent of an assumption concerning the value of the latent heat of sublimation of carbon:

If  $L$  = the latent heat of sublimation of carbon to the tetravalent state, then from data given by Bichowsky and Rossini we may readily calculate

TABLE IV.

Molecule.	C—H Bond Length (Å.).	Stretching Force Constant ( $10^8$ dynes/cm.).	Bond Energy (kcal./mole).
Methane . .	1.094 <sup>13</sup>	$\begin{cases} 4.79^{12} \\ 4.97^{43} \end{cases}$	~ 103
Ethylene . .	$\begin{cases} 1.087^{40} \\ 1.071^{41} \end{cases}$	$\begin{cases} 5.1^{44} \\ 5.0^{10} \end{cases}$	~ 106
Acetylene . .	1.057 $\pm$ 0.002 <sup>12</sup>	$\begin{cases} 5.8^{10} \\ 6.0^{43} \end{cases}$ 5.85 <sup>12</sup>	~ 121 <sup>13</sup>
Benzene . .	1.08 $\pm$ 0.04 <sup>42</sup>	5.1 <sup>43</sup>	~ 106
Formaldehyde .	$\begin{cases} 1.09 \pm 0.01^9 \\ 1.114^{43} \end{cases}$	4.3 <sup>10</sup>	~ 96
Hydrogen cyanide	1.06 <sup>18</sup>	5.67 <sup>10</sup>	~ 120
CH radical . .	1.1201 <sup>16</sup>	4.09 <sup>13</sup>	80.0 <sup>14</sup>

the heats of atomisation of  $\text{CH}_3\text{Cl}$ ,  $\text{CH}_2\text{Cl}_2$ ,  $\text{CCl}_4$ , and  $\text{CH}_4$  as  $L+205.3$ ,  $L+183.9$ ,  $L+142.0$  and  $L+226.1$  respectively. The value for  $\text{CCl}_4$  yields the bond energy in that molecule as  $\frac{1}{4}(L+142.0)$ ; while the energy of a C—H bond in  $\text{CH}_4$  is  $\frac{1}{4}(L+226.1)$  or  $L/4+56.5$ . But we have shown—on the basis of bond lengths—that the bond energy of C—Cl probably increases in the series  $\text{CH}_3\text{Cl}$ ,  $\text{CH}_2\text{Cl}_2$ ,  $\text{CHCl}_3$ ,  $\text{CCl}_4$ . Hence the energy of a C—H bond in  $\text{CH}_3\text{Cl}$  must be greater than  $\frac{1}{4}[L+205.3-\frac{1}{4}(L+142.0)]$ , or than  $L/4+56.6$ ; and the energy of a C—H bond in  $\text{CH}_2\text{Cl}_2$  must be greater than  $\frac{1}{4}[L+183.9-\frac{1}{4}(L+142.0)]$ , or than  $L/4+56.4$ . Hence the C—H bond energies in  $\text{CH}_3\text{Cl}$  and  $\text{CH}_2\text{Cl}_2$  are probably slightly greater than in  $\text{CH}_4$ .† Raman spectra indicate that the CH bond energy in  $\text{CHCl}_3$  is slightly greater than in  $\text{CH}_3\text{Cl}$ .<sup>47</sup>

By analogy with the corresponding halogen compounds, we expect a slight decrease of C—H length in passing from  $\text{CH}_3\text{—H}$  to  $\text{CH}_2\text{Cl—H}$ ; and a slight increase in passing from  $\text{CH}_3\text{—H}$  to  $\text{C}_6\text{H}_5\text{—H}$  to  $n\text{—C}_6\text{H}_7\text{—H}$  to

\* We may note that the raised force constant in benzene relative to methane appears to rule out the value  $1.14 \pm 0.01$  Å.<sup>39</sup> proposed by Jones for the benzene CH length.

† This conclusion is not shown in the force constants given by Linnett,<sup>48</sup> which actually show a slight decrease from  $\text{CH}_4$  to  $\text{CH}_3\text{Cl}$ . In  $\text{CH}_3\text{F}$ , according to Linnett,  $k_{\text{CH}}$  should show a marked decrease. Unfortunately, the thermochemical data for  $\text{CH}_3\text{F}$ , with which to compare this force constant decrease, seem to be lacking. It must, of course, be remembered that F, substituted into  $\text{CH}_4$ , may cause a reversal of CH polarity. In the case of the bromine compounds,  $D_{\text{CH}}$  in  $\text{CH}_3\text{Br}$ ,  $\text{CH}_2\text{Br}_2$  and  $\text{CHBr}_3$  progressively falls, according to Kistiakowsky and Artsdalen.<sup>46</sup> This may be due either to non-equivalence of  $D$  and  $E$  or to offsetting of the polarity reduction by angular strain due to the insertion of the large bromine atom.

<sup>46</sup> Kistiakowsky and Artsdalen, *J. Chem. Physics*, 1944, 12, 469.

<sup>47</sup> Hibben, *Chem. Rev.*, 1936, 18, 14.

$i\text{-C}_2\text{H}_5\text{—H}$  to  $t\text{-C}_4\text{H}_9\text{—H}$ ; but it has not yet been possible to refine the experimental values sufficiently to show these changes. However, just as there is a decrease of C—Hal. length in passing from methyl to vinyl chloride and thence to chloro-acetylene, so there is a decrease of C—H length in passing from  $\text{CH}_3\text{—H}$  to vinyl—H and thence to acetylene. Similarly, the C—H distance in benzene is probably shortened relative to C—H in methane. A tendency towards acidity is evidence of increased positive charge on a hydrogen atom. We can hardly therefore ascribe the CH shortening in  $\text{C}_2\text{H}_2$  and in HCN to low polarity, since these molecules have probably considerable CH polarity in the reverse direction to that of CH in  $\text{CH}_4$ ; as discussed below, we ascribe it largely to change in orbital hybridization of the carbon atom. HCN has greater acidity than  $\text{C}_2\text{H}_2$  because the strong electro-affinity of an acetylenic carbon in a direction away from the triple bond is reinforced in HCN by the dipole in the triple bond.

Since decreased length means increased binding, we expect the C—H stretching force constants of acetylene and HCN to be greater than those of ethylene and methane. Thompson and Linnett<sup>10</sup> have given evidence that this is the case. Linnett<sup>48</sup> finds  $k_{\text{OH}}$  to be greater in ethylene than in methane, as we expect.

Nitro-methane has a high dipole in the  $\text{NO}_2$  group. Assuming that the  $\text{NO}_2$  group behaves like Cl in  $\text{CH}_3\text{Cl}$  (i.e. reduces the  $\text{C}^+ - \text{H}^-$  polarity without reversing it considerably), we expect decreased C—H bond distance and increased C—H force constant. Linnett<sup>48</sup> has given evidence that the force constant increases. Similar ideas and evidence apply to methyl alcohol. In methylamine we expect the reverse to be true—increased  $\text{C}^+\text{H}^-$  polar character, increased C—H bond distance and decreased C—H force constant. Linnett's force constant value is in agreement. If we replace an H in  $\text{CH}_4$  by the relatively electropositive  $\text{CH}_3$  group, we expect increased  $\text{C}^+\text{H}^-$  polarity in ethane relative to methane; and hence increased C—H length and decreased C—H force constant in ethane. Again, Linnett's force constant value is in agreement.\* Similarly, Linnett finds  $k(\text{CH})$  in  $\text{Zn}(\text{CH}_3)_2$  to be low, as we should expect on polarity grounds.

We have already suggested that the low CH force constant of  $\text{CH}_3\text{F}$  may be due to reversal of CH polarity as a result of the powerful electro-affinity of the fluorine atom. A similar suggestion applies to  $\text{HCHO}$ , where Linnett also finds a reduced  $k_{\text{OH}}$ , though proximity to a double bond (as in vinyl-H) might have been expected to increase  $k_{\text{OH}}$ . The interplay of polarity and % CO double bond character may perhaps enable us to explain why  $k_{\text{OH}}$  shows a decrease from  $(\text{HCO})\text{—H}$  to  $(\text{CH}_3\text{CO})\text{—H}$ .

It is now well accepted that CH dissociation energies are not constant from molecule to molecule. Rice<sup>49</sup> finds that secondary CH bonds are about 1.2 kcal. weaker than primary; and tertiary CH bonds about 4 kcal. weaker than primary.† This behaviour is parallel with that of C—Hal. bonds, and accords well with the present discussion. Andersen and Artsdalen,<sup>54</sup> in agreement with Andersen, Kistiakowsky and Artsdalen<sup>55</sup> find the CH dissociation energy in ethane to be about 3 kcal. lower than in methane. Stevenson<sup>56</sup> also finds a decrease in CH dissociation energy in

\* These suggestions largely agree with those of Longuet-Higgins.<sup>48</sup>

† Compare refs. 3, 50, 51, 52, 53, all of which provide evidence that either CH bond energies or dissociation energies decrease in the order  $1^\circ, 2^\circ, 3^\circ$ .

<sup>48</sup> Longuet-Higgins, *Trans. Faraday Soc.*, 1945, **41**, 234.

<sup>49</sup> Rice, *J. Amer. Chem. Soc.*, 1931, **53**, 1959.

<sup>50</sup> Mulliken, Rieke and Brown, *J. Amer. Chem. Soc.*, 1941, **63**, 47.

<sup>51</sup> Kharasch, Hered and Mayo, *J. Org. Chem.*, 1941, **6**, 818.

<sup>52</sup> Kistiakowsky, *J. Physic. Chem.*, 1937, **41**, 180.

<sup>53</sup> Hass, McBee and Weber, *Ind. Eng. Chem.*, 1936, **28**, 333.

<sup>54</sup> Andersen and Artsdalen, *J. Chem. Physics*, 1944, **12**, 479.

<sup>55</sup> Andersen, Kistiakowsky and Artsdalen, *J. Chem. Physics*, 1942, **10**, 305.

<sup>56</sup> Stevenson, *J. Chem. Physics*, 1942, **10**, 291.

ethane relative to methane. This behaviour is also parallel to that of the C—Hal. bonds and accords with the expected increase of  $C^+H^-$  polarity in ethane relative to methane.

On the whole, there seems to be a fair parallelism between C—H al. and C—H bond strengths and lengths. This parallelism may be used as confirmation of Coulson's theoretical conclusions that CH in methane has the same polarity direction as CCl in  $CH_3Cl$ \*. Further, it renders undesirable, exclusive ascription of certain changes in CCl length or strength solely to resonance effects involving the  $p\pi$  lone pair electrons, for H has no such electrons.

Incidentally, we may use polarity considerations to indicate relationships between bond energies and dissociation energies in the following way. If HCHO has  $C-H^+$  polarity, the CH polarity in the radical HCO will be greater than in HCHO. Hence the CH bond energy will be less in HCO than in HCHO and  $D(CH)_{HCO}$  will be  $> E(CH)_{HCHO}$ , which, in turn, will be  $> D(CH)_{HOO}$ . Similarly, in glyoxal, the  $C^+O^-$  polarity will be greater in the radical HCO than in glyoxal. Hence  $E(CO)_{glyoxal}$  will be  $> E(CO)_{HOO}$  and  $D(CC)_{glyoxal}$  will be  $> E(CC)_{glyoxal}$ . In like manner, the OH radical has greater polarity than the  $H_2O$  molecule and

$$D(OH)_{H_2O} > E(OH)_{H_2O} > D(OH)_{OH \text{ radical}}$$

An interesting reflection of CH bond strengths is shown in the facts relating to the course of radical dehydrogenation mechanisms.<sup>57, 58</sup> A particular case of such a mechanism is found in the formation of peroxides by hydrocarbons and similar molecules. Alkyl hydroperoxides form more readily at a tertiary than at a secondary than at a primary CH bond,<sup>59</sup> in agreement with the CH bond strength decreasing in the order  $3^\circ < 2^\circ < 1^\circ$ . Olefines are now known, as a result of the work of Farmer and colleagues, to form hydroperoxides, in many cases at least, at the alpha-carbon atom.† We shall stress below that a reduced C—H bond strength at this carbon atom is expected, just as the allyl—Cl bond shows reduced strength. The fact that aldehydes form peroxides readily at the alpha-carbon atom, and indeed the general reactivity of CH alpha to  $C=O$  or  $C=C$ , can probably be explained in terms of the reduced CH strength. The general statement may be made that peroxides form most readily at the weakest CH bonds in hydrocarbons, aldehydes, ethers, etc. This statement may be utilised to predict that the CH bonds of alpha carbon atoms in ethers will be found to be weaker than the other CH bonds present, since ethers yield hydroperoxides at the alpha-carbon atom. An anomaly seems to occur, however, in the case of chloroform which is usually thought to form a peroxide readily, but yet for which there is evidence that its CH bond energy is slightly greater than in  $CH_3Cl$  (see above).

### Carbon-Carbon Bonds.

Table V tabulates the lengths, force constants and energies of certain carbon-carbon bonds.

\* The fact that the ionization potential of the non-bonding electrons on an atom X is always less in  $CH_3-X$  than in  $H-X$  might also be used to argue that  $CH_3$  gives up negative charge more easily than H and therefore that  $CH_3-H$  will have polarity  $C^+H^-$ .

† Ethyl linoleate, containing the group  $C=C-CH_2-C=C$ , forms a peroxide (at the central,  $CH_2$  group) much more readily than systems containing only one double bond (e.g. ethyl oleate).<sup>60</sup> This agrees with the fact that the central  $CH_2$  group of ethyl linoleate is allyl "twice over" and is therefore expected to have particularly weak bonds.

<sup>57</sup> Waters, *Trans. Faraday Soc.*, 1946, 42, 184.

<sup>58</sup> Walsh, *ibid.*, 1946, 42, 192.

<sup>59</sup> Walsh, *ibid.*, 1946, 42, 269.

<sup>60</sup> Gunstone and Hilditch, *J. Chem. Soc.*, 1945, 836.

The C—C bond of acetic acid dimer will have a high dipole whose positive end will lie in the methyl group. Replacement of the hydrogen of the latter by fluorine will reduce the polarity and accordingly we find the C—C bond is significantly shortened. (The shortening is not to a length characteristic of a single  $sp^3$ - $sp^3$  bond, but to one roughly expected for a nearly non-polar  $sp^3$ - $sp^3$  single bond ( $\frac{1}{2}(1.33 + 1.54) = 1.44$ ). The shortening probably has analogies to that observed by Bateman and Jeffrey <sup>64a</sup> for the central CC bond of a C=C—C—C—C=C group; in this

TABLE V.

Molecule.	CC Length (A.).	Stretching Force Constant (10 <sup>9</sup> dynes/cm.).	Bond Energy (kcal./mole).
Ethane . . . . .	1.55 ± 0.03 <sup>12</sup>	4.5 <sup>64</sup>	89*
Acetic acid dimer . . . .	1.54 ± 0.04 <sup>61</sup>		
Trifluoro acetic acid dimer	1.48 ± 0.03 <sup>61</sup>		
Methyl cyanide . . . . .	1.49 ± 0.03 <sup>17</sup>	5.3 <sup>64</sup>	
Methyl acetylene . . . .	1.46 ± 0.005 <sup>12</sup>	5.5 <sup>64</sup>	116 <sup>13</sup>
Dimethyl acetylene . . . .	1.47 ± 0.02 <sup>17</sup>	5.5 <sup>64</sup>	114 <sup>13</sup>
Acetaldehyde . . . . .	1.50 ± 0.02 <sup>63</sup>		105†
Ketene . . . . .	1.35 ± 0.02 <sup>65</sup>	9.8 <sup>10</sup>	

case also powerfully electronegative groups are attached at either end of the CC bond.

It is known from measurements of the ionization potentials of non-bonding halogen electrons in methyl and ethyl halides <sup>20</sup> that the group C<sub>2</sub>H<sub>5</sub> has a lower electronegativity than CH<sub>3</sub>. Hence, whereas in ethane the CC bond must be non-polar, that in propane must be polar. That the propane CC bond is also weaker is shown by the following facts. (1) Whereas the electrons in the CC bond of ethane only begin to absorb electronic energy at about 1350 Å., those in the CC bonds of propane begin at rather longer wavelengths in a comparable pressure range.<sup>65b</sup> This is a strong indication of a lower ionization potential for the CC bond electrons in propane than in ethane—an expectation which has been confirmed directly by electron impact measurements of the first ionization potentials of these molecules. The values are ethane 11.6 <sup>65a, c</sup>; propane 11.2, <sup>65a</sup> 11.3. <sup>65c</sup> That these values refer to the CC bonding-electrons is expected because in methane the CH ionization potential is known to be 2 v. or higher (13.1, <sup>66f</sup> 14.5 <sup>66g</sup>; also methane starts to absorb at about 1280 Å., that is, to short wavelengths of the ethane onset), and there is much evidence that CH bonds do not differ *greatly* from compound to compound. Now a lowered bond ionization potential means a lowered bond order,<sup>13b</sup> which means a lower CC bond energy for propane than for ethane.

\* Assuming CH as in CH<sub>4</sub>,  $D(CC) = 86 \pm 2$  <sup>62</sup>.

† From CC length/strength graph.

<sup>61</sup> Karle and Brockway, *J. Amer. Chem. Soc.*, 1944, 66, 574.

<sup>62</sup> Artsdalen, *J. Chem. Physics*, 1942, 10, 653.

<sup>63</sup> Stevenson, Burnham and Schomaker, *J. Amer. Chem. Soc.*, 1939, 61, 2922.

<sup>64</sup> Linnett, *Trans. Faraday Soc.*, 1941, 37, 473.

<sup>65</sup> Beach and Stevenson, *J. Chem. Physics*, 1938, 6, 75.

(a) Bateman and Jeffrey, *Nature*, 152, 446; Jeffrey, *Proc. Roy. Soc. A*, 1945, 183, 388.

(b) Price, *Ann. Reports*, 1939, 36, 47.

(c) Hipple, *Physic. Rev.*, 1938, 53, 530.

(d) Stevenson and Hipple, *J. Amer. Chem. Soc.*, 1942, 64, 1588.

(e) Delfosse and Bleakney, *Physic. Rev.*, 1939, 56, 256.

(f) Smith, *ibid.*, 1937, 51, 263.

(g) Mulliken, *J. Chem. Physics*, 1935, 3, 517.

(2) Bonner,<sup>65a</sup> by an approximate but probably significant method, finds the CC stretching force constant for propane to be only  $3.8 \times 10^6$  as against  $4.3 \times 10^6$  dynes/cm. for ethane. (3) Artsdalen<sup>66</sup> finds  $D(C_2H_5-CH_3)$  to be less than  $D(CH_3-CH_3)$ .

Similarly, whereas the ethane CC bond must be non-polar, that in ethyl alcohol must be polar. That the latter is also weaker is indicated by Bonner's force constant calculations.<sup>65a</sup>

In ketene, the presence of the  $C=O$  group must introduce polarity into the  $C=C$  group which in ethylene is non-polar. Accordingly, we find that the CC bond length in ketene appears to be slightly greater than in ethylene. (Ketene also shows a reduced CO length ( $1.17 \text{ \AA}$ ).<sup>66</sup>), and therefore a reduced CO polarity, relative to HCHO. This provides an example of the strong electronegativity of a carbon atom in a multiple bond on the side away from the multiple bond,<sup>66</sup> see below.)

The data are not sufficient to provide other good examples of the effect of polarity upon a given  $C-C$  bond; but we have thought it worth while to include Table V largely to show how the  $C-C$  length is reduced and the force constant and energy increased wherever one of the carbon atoms forms part of a multiple bond. It is probable that this is a general phenomenon for all bonds  $C-X$ , where the C forms part of a multiple bond. We may anticipate that propylene will be found to have a slightly reduced  $C-C$  length relative to ethane, since methyl cyanide, methyl acetylene and acetaldehyde all show such  $C-C$  length reductions. In the analogous case of  $C-C_{\text{arom}}$  an increase of strength is indicated by the facts<sup>67</sup> that (1) hydroperoxides in vapour phase oxidation split at the  $O-O$  bond and then at the weakest bond on the alpha-carbon atom, (2)  $\phi \cdot CH(OOH) \cdot CH_3$  splits at the  $C-CH_3$ , and not at the  $\phi-C$  bond.

### Diatomic Molecules.

It might be thought that the phenomenon of bond weakening with increasing polarity is peculiar to polyatomic molecules. That this is not so may be seen by the following examples. When an HBr molecule is ionized to  $(HBr)^+$  one of the non-bonding Br electrons is removed. The effect of the ionization must therefore be to increase the already existent  $\delta^+ \delta^-$

H Br polarisation of the bond electrons. Accordingly we find the dissociation energy of  $(HBr)^+$  to be less and the bond length to be greater than in HBr.<sup>16</sup> Similarly, the bond length of  $(OH)^+$  is greater than that of OH.<sup>16</sup>

### General Discussion.

We have surveyed several classes of bond. Although lack of data forces the survey to be somewhat cursory, and although further and more accurate information may force revision of some of the details, taken in conjunction with the discussion by Skinner and Sutton<sup>6</sup> of the bond lengths of the halogen derivatives of tin, arsenic and nitrogen, we must conclude that the indications are that polarity changes are among the most important factors determining the energy, length and force constant of bonds.

Several further points emerge from the survey. In the first place, it is clear that, in the examples considered, the energy of a given bond *decreases* with increasing polar character. The energy, bond length and force constant changes are all related and all show that increasing polarity weakens a bond. In recent years, as a result of the suggestions of Pauling,<sup>66</sup>

<sup>65</sup> (h) Bonner, *ibid.*, 1937, 5, 293.

(i) Walsh, *J. Amer. Chem. Soc.*, 1946, 68, 2408.

<sup>66</sup> Pauling, *Nature of the Chemical Bond*, Cornell, 1939.

it has been common to describe polar character as due to resonance between a "normal" covalent bond and a "normal" ionic bond, e.g.

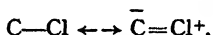


As long as this terminology means only that the actual state is in between the two extremes, no objection arises; but when—following Pauling—we go further and ascribe to the bond a resonance energy, we reach a conclusion (viz. that bond energy increases with polarity), which is in direct contradiction to our survey. The matter is particularly serious because in aldehydes and ketones the "% of ionic character" may be said to approach 50 %, <sup>22</sup> i.e. the resonance energy should be a maximum.

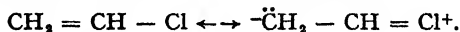
The deduction from this is not that the theory of resonance is wrong, but that it is not here applicable. The hypothesis that a polar bond can be described as resonating between a purely covalent and a purely ionic structure, that in fact the origin of bond dipole moments lies in covalent-ionic resonance, is wrong. The reason is probably simple—the inter-nuclear distance in the purely ionic structure is appreciably greater than in the covalent structure and, therefore one of the essential conditions for the occurrence of resonance is absent. Only if the possible resonance energy were greater than the energy required (a) to stretch the purely covalent bond to its actual length, (b) to compress the purely ionic bond to its actual length, would covalent-ionic resonance in a particular bond occur.

In the second place, contractions in length of carbon-halogen bonds have been attributed either to covalent-ionic resonance or to single bond-double bond resonance. Taking the first of these, we see that it is unsatisfactory because, in the examples cited, the length of a given bond does not decrease but *increases* with increasing polarity. Skinner and Sutton <sup>8</sup> have reached the same conclusion as regards the molecules studied by them. Turning to the second explanation of bond contraction, we find that this too is unsatisfactory, for the following reasons.

(1) The explanation is dependent upon the existence of the  $p\pi$  lone pair electrons in the halogen atoms and supposes



Thus the contraction of C—Cl distance in vinyl or phenyl chloride, relative to  $\text{CH}_3\text{Cl}$ , is supposed to be due to such resonance as



Yet we have seen that not only are vinyl-Hal. bonds shortened and strengthened, but also vinyl-H and phenyl-H bonds and, since H has no  $p\pi$  lone pair electrons, the explanation cannot apply here.

(2) Skinner and Sutton <sup>8</sup> have already pointed out that on this explanation, since successive Cl substitution for H linked to a central atom X leads to successive reduction of the X—Cl length, the surprising conclusion is reached that the more negative charge the central atom has, the more it wants.

There are two related problems: (1) the bond shortening in vinyl or phenyl chloride relative to an alkyl chloride, (2) the spectroscopic shift of the  $\pi$  electronic spectrum to long wavelengths and the decrease of the first  $\pi$  ionization potential in vinyl-Cl and phenyl-Cl relative respectively to vinyl-H and phenyl-H. The shift of the vacuum ultra-violet "D" bands to short wavelengths in passing from ethyl to vinyl or phenyl chloride means that the polar character of the  $\text{C}^+\text{Cl}^-$  bond decreases; and the bond length decrease can probably be attributed in part to this. Another effect is, however, important. In order to discuss this, it is necessary first to ask why it is that such groups as vinyl and phenyl behave with apparent strong electronegativity. Burawoy <sup>21</sup> has discussed this question and pointed out that replacement of two  $\sigma$  bonds of a carbon atom by one  $\sigma$

and one  $\pi$  bond means that strongly bound electrons are replaced by weakly bound ones, i.e. means a decreased electron density at the carbon atom and therefore allows an increased hold (attraction) on the electrons of the other linkages. Atoms belonging to multiple linkages will behave as if they have a smaller atomic radius and the effect should (and does—see Table III) increase in the order  $C_{\text{arom.}} - C_{\text{arom.}}, C = C, C = O, C \equiv C, C \equiv N$ , i.e. with increasing polarisability. There exists a balance between the polarisability, i.e. the strength of binding of the  $\pi$  electrons, and the shortening of the other linkages; the shorter a  $C-X$  bond in  $CH_2 = CH-X$  for instance, the more polarisable must be the double bond  $\pi$  electrons, i.e. the less their ionization potential. In this simple way we can interpret much of the CCl bond shortening in vinyl or phenyl chloride relative to alkyl chlorides. Further, if the CCl electrons of, say, vinyl-Cl are more tightly bound to the C than are the CH bond electrons of vinyl-H, then a  $\pi$  ionization potential decrease in vinyl-Cl will result. Superimposed upon this, there may be also a decrease due to resonance involving non-bonding  $p\pi$  electrons.

In other words, the properties of a bond  $C-X$  depend upon whether the C is in the tetrahedral, trigonal or digonal valency state: i.e. upon the nature of the hybridization of its  $2s$  and  $2p$  electrons.\* The strong electron affinity (due to the presence of weakly bound electrons) of a carbon atom that is part of a vinyl group means that all vinyl  $-X$  bonds will be shortened, whether X is taken to be halogen, H, C, . . . etc. [In some cases (as with vinyl-Hal.) reduction of polarity may cause further shortening.] This means that the electrons in the vinyl-C bond are more tightly bound than in the C-C bond of, say, ethane; i.e. there is (considering only the vinyl-C electrons) an increased electron density at the  $\alpha$  carbon atom, due to the vinyl-C bond. Therefore there must be a repulsion of the electrons in the other bonds attached to the  $\alpha$  carbon atom i.e. a reduced binding of the  $\alpha$  C-H electrons of, say, propylene or toluene † or of the C-Cl electrons of, say, allyl chloride. Reduced CCl dissociation energy in allyl chloride was found by Butler and Polanyi ‡ and was attributed solely to the high resonance energy of the allyl radical. In exactly the same way, we expect a decrease in strength of the C-Hal. bonds of

\* Dr. W. C. Price has pointed out to us the further important point that whereas in ethylene there are two H atoms from which the carbon can draw charge, in acetylene there is only one: we therefore expect a bigger change from  $=C-X$  to  $\equiv C-X$  than the hybridization change would at first sight indicate.

† According to Mayo,<sup>67</sup> CH of  $CH_3$  in toluene is weaker than a 3° CH in paraffins.

It would be possible to describe the butadiene molecule without using the customary resonance language, by saying that each of its  $C=C$  bonds is allyl to a  $C=C$ , and is therefore somewhat weakened, while its  $C-C$  bond is a vinyl bond "twice over", and therefore considerably strengthened. It may be advantageous to use this formulation to supplement the resonance description, for it tells us the important prediction that the terminal CH bonds (being vinyl) will be considerably strengthened relative to paraffins, but that the central CH bonds (being both vinyl and allyl) will be weaker than the terminal ones. Similarly, in glyoxal the CH bonds should not be greatly altered in strength, relative to HCHO, as a result of the conjugation: this is the justification for the assumption made in deriving the glyoxal  $C=O$  energy.

We predict that CH of  $CH_3$  in  $CH_3CN$  and  $CH_3C \equiv CH$  will be found to be abnormally weak. This reinforces the argument of Cherton<sup>13</sup> that in  $CH_3C \equiv CH$ , the weakest bond is CH of  $CH_3$ , and therefore that in the pyrolysis of this compound the first step is the formation of the radical  $-CH_2-C \equiv CH$ .

Rice, on the basis of pyrolysis data (*The Aliphatic Free Radicals*, Johns Hopkins, 1935, p. 75), long ago concluded that vinyl bonds were particularly strong and allyl bonds particularly weak.

<sup>67</sup> Mayo, *J. Amer. Chem. Soc.*, 1943, 65, 2324.

<sup>68</sup> Hugill, Coop and Sutton, *Trans. Faraday Soc.*, 1938, 34, 1518.

<sup>69</sup> Brockway and Coop, *Trans. Faraday Soc.*, 1938, 34, 1429.



the propargyl halides; in accord, these C—Hal. distances show a marked increase relative to those of the  $\text{CH}_3$ —Hal. compounds (see Table III).

Butler and Polanyi<sup>3</sup> and Baughan, Evans and Polanyi<sup>4</sup> recognise the increase of C—Hal. ionic character in the series of halides, methyl, ethyl, *i*-propyl, *t*-butyl; but ascribe the changes of bond dissociation energy mainly to variations in resonance energy of the alkyl radicals produced after fission of the C—Hal. bond. Their whole theory is based upon the idea that increasing polarity means—considering this factor in isolation—increasing homopolar-ionic resonance and therefore increasing bond energy. The dissociation energy is thus the result of two opposing factors—increasing polarity tending to raise the energy and increasing radical-resonance tending to decrease the energy. In the light of the discussion of this paper it is evident that this theory needs extensive revision; increasing polarity and increasing radical-resonance, in the examples considered here, do not usually work in opposite directions but reinforce each other. The changes in C—X strength in passing from methyl to ethyl to . . . *t*-butyl can be interpreted largely as changes due to change in bond polarity. To this may be added effects due to radical-resonance and other causes.

Polanyi and his co-workers assumed the reduction in C—H dissociation energy in passing through the series methyl . . . *t*-butyl to be entirely due to increasing radical-resonance. In this case they neglected all polarity changes. Yet the work of Coulson, showing the ionic contribution to the CH bond in  $\text{CH}_4$  to be larger than usually supposed (and the polarity to be  $\text{C}^+\text{H}^-$  i.e. the opposite of that assumed by Baughan, Evans and Polanyi), and the partial parallel stressed in this paper between C—Hal. and C—H changes again require revision of the postulates used by Polanyi *et al.* We cannot ascribe the whole of the reductions in dissociation energy to increases in radical-resonance, because, as we have shown, the bond energy (as distinct from the dissociation energy) also falls (shown by factors such as  $\nu$ , relating only to the equilibrium part of the energy curve) and this is not affected by radical-resonance.

Finally, we wish to re-emphasise that though we believe polarity to be an important factor determining the length and strength of a bond, we do not believe it to be the only factor. All we wish to assert is that changes in polarity can frequently explain qualitatively the observed changes in length or strength of a given bond.

In conclusion, the author wishes to express his indebtedness to Drs. C. A. Coulson and W. C. Price for much helpful criticism of the first draft of this paper; and to Dr. L. H. Long for many discussions on thermochemical subjects.

### Summary.

A survey of various classes of bonds suggests the importance of polarity changes as one factor determining changes in length and strength. For a given bond (other things being equal), the force constant and energy decrease and the length increases with increasing polarity. Certain explanations of length and strength changes in terms of customary resonance theory are therefore unsatisfactory. The strengthening observed in a C—X bond when the C forms part of a multiple bond occurs also when X is hydrogen and therefore, with the halogens, is not an effect attributable solely to resonance involving the lone pair  $p\pi$  electrons. Instead it is probably due in part to changes in orbital hybridization of the carbon atom. It seems a general rule that all bonds next to a multiple bond are stronger than usual, and that all bonds next-but-one to a multiple bond are weaker than usual.

## Résumé.

Un examen de diverses sortes de liaisons amène à considérer l'importance des changements de polarité comme un facteur déterminant les variations de longueur et de force. Pour une liaison donnée (toutes choses égales d'ailleurs), une polarité croissante fait diminuer la constante de force et l'énergie et augmenter la longueur. Certains changements de longueur et de force sont par conséquent expliqués de façon peu satisfaisante par l'habituelle théorie de résonance. Le renforcement observé dans la liaison C—X quand le C fait partie d'une liaison multiple, se produit aussi lorsque X est l'hydrogène, et par conséquent, dans le cas des halogènes, l'effet de renforcement ne peut être attribué seulement à un phénomène de résonance concernant la seule paire d'électrons  $p\pi$ . Probablement, cet effet est partiellement dû à des changements d'hybridation orbitale dans l'atome de carbone. Que toutes les liaisons voisines d'une liaison multiple soient plus fortes et que toutes les liaisons, séparées d'une liaison multiple par une liaison intermédiaire, soient plus faibles, cela semble une règle générale.

## Zusammenfassung:

Ein Überblick über die verschiedenen Klassen von Bindungen weist darauf hin, dass Polaritätsänderung einer der für Veränderungen an Bindungslänge und -festigkeit verantwortlichen Faktoren ist. Für eine gegebene Bindung (vorausgesetzt, dass alle anderen Faktoren gleich bleiben) ruft ein Zuwachs der Polarität eine Abnahme der elastischen rücktreibenden Kraft und Bindungsenergie und eine Vergrößerung der Bindungslänge hervor. Es folgt daher, dass es unzulässig ist, die Veränderungen von Bindungsfestigkeit und Bindungslänge nur durch die übliche Resonanztheorie zu erklären. Die grössere Stärke der C—X Bindungen, in denen C an einer Mehrfachbindung teilnimmt, wird auch beobachtet, wenn X Wasserstoff ist und ist deshalb im Fall der Halogene nicht nur allein der Resonanz der einsamen  $p\pi$ -Elektronenpaare zuzuschreiben. Hingegen ist dieser Effekt wahrscheinlich teilweise die Folge der Veränderung der Kombination der Elektronenverteilung („orbital hybridization“) des Kohlenstoffatoms. Es scheint eine allgemeine Regel zu sein, dass alle Bindungen, die einer mehrfachen Bindung unmittelbar benachbart sind, stärker und alle Bindungen, die eine Bindung weiter entfernt sind, schwächer als gewöhnlich sind.

*Physical Chemistry Laboratory,  
Cambridge.*

## THE ELECTROSTATIC INFLUENCE OF SUBSTITUENTS ON THE DISSOCIATION CONSTANTS OF ORGANIC ACIDS. A REPLY TO WYNNE-JONES AND RUSHBROOKE.

By F. H. WESTHEIMER AND J. G. KIRKWOOD.

*Received 28th May, 1946.*

### I.

Several years ago the authors of the present paper advanced an electrostatic theory to account approximately for the influence which substituents exercise on the dissociation constants of organic acids.<sup>1</sup> This theory is a modification of the one put forward by Bjerrum.<sup>2</sup> It differs.

<sup>1</sup> Kirkwood and Westheimer, *J. Chem. Physics*, 1938, 6, 506, 513.

<sup>2</sup> Bjerrum, *Z. physik. Chem.*, 1923, 106, 219; Eucken, *Z. Angew. Chem.* 1932, 45, 203.

from his in that an attempt was made to take into account the fact that solute molecules themselves occupy space in the solution. Since the theory does not consider numerous factors (e.g. electrical saturation, electrostriction, the detailed structure of the solute molecules), it is necessarily only approximate and of restricted application. These limitations were carefully pointed out in the original papers.

Two years ago, Wynne-Jones and Rushbrooke<sup>8</sup> published a "Criticism of the Kirkwood-Westheimer Theory" in which they again pointed out its limitations and approximations. They concluded that "the advantages of the more complex theory of Kirkwood and Westheimer, though real, are small compared with the big discrepancy between theory and experiment which remains". A value judgment such as the one just cited is a personal matter, and therefore scarcely a subject for scientific discussion. Furthermore, the reiteration of the known limitations of our theory would not in itself justify a reply. But the criticisms of Wynne-Jones and Rushbrooke fall chiefly into two categories: those related to changes in ionisation constant with change in dielectric constant, and those related to change in ionisation constant with change in temperature. It appears to us that, with respect to the former, they have inadequately reported the data, and with respect to the latter, their most severe criticism is based on a misunderstanding of the field in which our equations are valid. Hence, it seems useful to review the subject.

## II.

A. The application of electrostatic theory to acid strengths is based upon a consideration of the ratio of the ionisation constants of two closely related acids, which differ chiefly in that one contains a charged or highly polar substituent which is absent from the other. In some cases (e.g. in the comparison of symmetrical dibasic acids with their mono-salts) a statistical factor must also be taken into account. The expression  $\Delta pK$  has been defined by the equation

$$\Delta pK = \log_{10} K_1 / \sigma K_2$$

where  $K_1$  and  $K_2$  are the two ionisation constants of the acid in question and  $\sigma$  is the statistical factor. Most of the subsequent discussion deals with  $\Delta pK$ .

From observed values of  $\Delta pK$ , and by means of our theory, reasonable values for  $r$  may be obtained, where  $r$  is the distance between the two ionisable protons in a symmetric dibasic acid, or the distance between the ionisable proton and the centre of the dipole determined by the polar substituent in a monobasic acid. The results of the computations are far from precise. Changes in the assumptions as to the shape of the molecules or as to the distribution of charge within the dipole (where one is present) cause a change of several tenths of an Angstrom unit in the computed value<sup>4</sup> of  $r$ . Because of intramolecular rotations, the average value of  $r$  (to compare with that which we calculate) cannot be calculated merely from tables of bond distances and bond angles. However, such tables do permit the calculation of a maximum and a minimum for  $r$ . In all cases, the new theory gives values of  $r$  which fall between the calculated maximum and minimum. In general, these values lie near a "free rotation" value for  $r$  computed on the assumption that all configurations are equally probable (see, however, footnote 8, ref. 1). The new theory, therefore, represents a distinct advance over the older theory of Bjerrum and over its extension by Eucken, both of which occasionally fail in the respect mentioned. Furthermore, it arranges the calculated values for  $r$  in an order far more plausible than that obtained by the use of any other theory. And lastly, the new theory presents models for solute molecules

<sup>8</sup> Wynne-Jones and Rushbrooke, *Trans. Faraday Soc.*, 1944, 40, 99.

<sup>4</sup> Westheimer and Shookhoff, *J. Amer. Chem. Soc.*, 1939, 61, 555.

which (although still schematic) are more realistic than any hitherto proposed.

B. Our electrostatic theory (as well as that of Bjerrum) predicts that  $\Delta pK$  is a linear function of the reciprocal of the dielectric constant of the solvent. The two theories differ in that the older one predicts that  $\Delta pK$  should vary inversely with the dielectric constant of the solvent,  $D$ , whereas the newer one predicts that  $\Delta pK$  should vary inversely with an "effective dielectric constant",  $D_{\text{eff}}$ . This latter quantity can be computed from the dielectric constant of the solvent,  $D$ , the volume and shape of the molecule, and the "internal dielectric constant",  $D_i$ , a property of the cavity in the solvent occupied by the solute molecules, which "provides a crude means of allowing for the polarisation of a molecule produced by the average charge distribution of polar or ionic substituent groups".<sup>1</sup> For long chain symmetrical dibasic acids (e.g. suberic) the computed value of  $D_{\text{eff}}$  lies close to the dielectric constant of the solvent used; for short, dipole-substituted acids (e.g. chloroacetic), it lies close to  $D_i$ . Shookhoff and one of us pointed out<sup>4</sup> these predictions from our theory and cited the experimental evidence then available showing that (in agreement with the theory) the values of  $\Delta pK$  for the long chain symmetrical dibasic acids increase roughly inversely as the dielectric constant  $D$ , whereas the value of  $\Delta pK$  for the chloroacetic-acetic acid pair is essentially independent of the dielectric constant of the solvent. This evidence, as well as some additional data, is presented in greater detail in Table I and in Fig. 1 of the present paper.

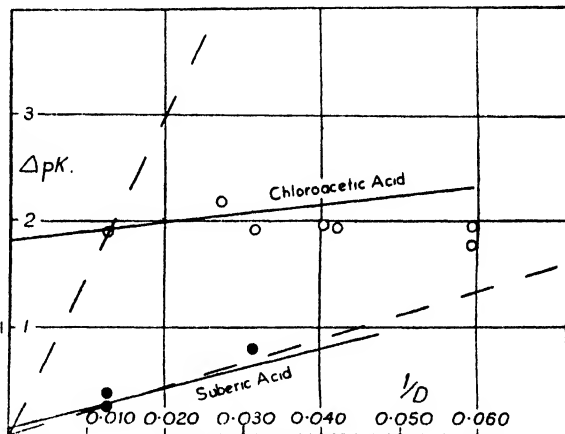


FIG. 1.

Solid line—Kirkwood-Westheimer theory.  
Broken line—Bjerrum theory.

The fact that a single theoretical development takes correctly into account the widely differing behaviour of these extreme cases strongly supports the validity of the theory.

C. In addition to the extreme cases (suberic and chloroacetic acids) cited, there are some others where, according to our theory, the value of the effective dielectric constant,  $D_{\text{eff}}$ , does not approximate to either  $D$  or  $D_i$ , but lies intermediate between them. Here it would be predicted that the values of  $\Delta pK$  should increase with decreasing dielectric constant, but that the increase should be less rapid than if it were inversely proportional to the dielectric constant of the solvent. Such cases are malonic acid, *m*-iodobenzoic acid (Fig. 2), glycine, and *m*-nitrobenzoic acid (Table I). Here the theory is only in qualitative agreement with the experimental facts. Unfortunately, Wynne-Jones and Rushbrooke discussed principally these and similar acids, to the complete exclusion of acids of the chloroacetic type.

As a matter of fact, it is difficult to state with precision the experimental value of  $\Delta pK$  for many symmetrical dibasic acids (including, of course, suberic) in solvents other than water. Malonic acid is a case in

the rates of saponification of the esters of symmetrical dibasic acids.<sup>11</sup> In one particular investigation<sup>12</sup> the rate constants for the saponification of esters of malonic and adipic acids in water and in 80 % alcohol were carefully extrapolated to zero ionic strength. Here also, as with the ionisation constants, the value of  $\Delta p k$  for the adipates varies inversely with the dielectric constant, whereas  $\Delta p k$  for the malonates increases less rapidly. (The symbol  $\Delta p k$  refers to  $k_1/\sigma k_2$ , where  $k_1$  and  $k_2$  are the first and second saponification constants for the ester, and  $\sigma$  the statistical factor.) The results are at best semi-quantitatively in accord with our theory. No claim was made that the agreement was precise; the phrase used was "the agreement [between theory and experiment] is perhaps not unsatisfactory". It is interesting, however, that for the ionisation constants of malonic acid the observed change of  $\Delta p k$  with change in dielectric constant is probably greater than that predicted by our theory, whereas the corresponding change for the saponification constants of the esters is less.<sup>13</sup>

E. Wynne-Jones and Rushbrooke point out that, according to the data of Schwartzbach, and in disagreement with our theory, the graph of  $\Delta p k$  against  $1/D$  is not linear for some acids (e.g. some of the substituted malonic acids) in alcohol-water mixtures. Since these values of  $\Delta p k$  have not been extrapolated to infinite dilution, it is not certain that the observed departure from linearity is significant. In any event, non-linear plots are probably the exception, not the rule. The fact that (in conformity with electrostatic theory) the plot of  $\Delta p k$  against  $1/D$  often is almost linear was long ago suggested by Wynne-Jones.<sup>14</sup>

F. We believe that the following is a fair summary of the success of our admittedly approximate theory in predicting the change in  $\Delta p k$  with change of solvent. The theory is in good quantitative agreement with available experimental data where the effective dielectric constant,  $D_{\text{eff}}$ , is either high or low. Where the effective dielectric constant has intermediate values, the theory is in only qualitative or semi-quantitative agreement with the best data at present known. In such intermediate cases, there may be a general tendency for our theory somewhat to underestimate the effect of the solvent. On the other hand, even for these intermediate cases (e.g. iodobenzoic acid) any theory based on our general assumption will predict the change in ionisation constant with change in solvent more accurately than does any previous theory.

The questions so far treated concern the derivative of the free energy of ionisation with respect to dielectric constant. (Paragraph II E concerns a second derivative.) A general discussion of such derivatives is presented in Section III.

### III.

A. Wynne-Jones and Rushbrooke in commenting on our work state that "There is an explicit admission in the papers that the formulæ do not adequately reproduce the temperature dependence of dissociation constants". Presumably, they refer to the following statement, "Finally, we may mention that, in common with the previous electrostatic theories of dissociation, the temperature coefficients experimentally determined

<sup>11</sup> Ingold, *J. Chem. Soc.*, 1930, 1375; 1931, 2170.

<sup>12</sup> Westheimer, Jones and Lad, *J. Chem. Physics*, 1942, 10, 478.

<sup>13</sup> One of the greatest shortcomings (see ref. 12) of our theory is that it fails to account for the fact that  $\Delta p k$  for the saponification of esters is approximately the same as  $\Delta p k$  for the ionisation of the corresponding acids. Because of the greater molecular volume of the esters, the equations based on our theory predict that  $\Delta p k$  should be greater than  $\Delta p k$ . The difficulty may be more apparent than real, and may arise at least in part from the mathematically convenient but physically unrealistic assumption that in ellipsoidal molecules, all charges are at the foci.

<sup>14</sup> Wynne-Jones, *Proc. Roy. Soc. A.*, 1933, 140, 440.

do not agree with those calculated, on the basis of a constant value of  $\gamma$ . Although a real variation of the average value of  $\gamma$  with temperature is not unlikely, it may be that a more refined theory is necessary before accurate estimates of temperature coefficients can be made. In any case, the temperature coefficients are not large."<sup>1</sup> The significance of this last sentence will be taken up in a later paragraph (III C).

Wynne-Jones and Rushbrooke present in detail the data for some amino-acids. They give a series of graphs in which they plot  $T\Delta pK$  against  $1/D$ , where the dielectric constant chosen was that appropriate to the temperature at which ionisation constants were measured. The graph for alanine (Fig. 7 in their paper) is here reproduced as Fig. 3. They point out that "All these curves are parabolic, or roughly parabolic in form, and it is at once clear that equation 3 [an equation based on our theory] from which  $T\Delta pK$  should be a linear function of  $1/D$ , cannot account for them". Later these authors say that "The most striking discrepancy between experimental data and the predictions of the Kirkwood-Westheimer theory is obviously to be seen in Figs. 5, 6 and 7 . . .". As a matter of fact, however, no equation based on our theory (including equation 3 of Wynne-Jones and Rushbrooke) should ever have been applied to the data in question.

Although our theory (as previously stated) does not accurately predict the temperature coefficient of  $\Delta pK$ , the "striking discrepancy" cited by Wynne-Jones and Rushbrooke is not a case in point. The values of  $T\Delta pK$  given by them can be reproduced by assuming that the  $\Delta pK$  for an amino-acid refers to the ratio of the first to the second ionisation constant of the amino-acid hydrochloride. But this is not the sort of ratio of ionisation constants which the theory was designed to describe, for the first ionisation constant of alanine hydrochloride refers to the loss of a proton from the carboxyl-group, whereas the second refers to the loss of a proton from an ammonium salt group.

Our whole theory is based on the assumption that both the ionisations used in determining  $\Delta pK$  are the ionisations of groups of the same type. That is, both groups must be carboxyl-groups, or both ammonium salt groups, or both thiol-groups, etc. This restriction is clearly implicit in the treatment given.<sup>1</sup> The data for the amino-acids, previously given by Shookhoff and one of us<sup>4, 15</sup> referred to a comparison between the second ionisation constant of an amino-acid hydrochloride and the single ionisation constant of the corresponding amino-ester hydrochloride; in both cases the ionisation was from a positively charged ammonium salt group. (A similar but less attractive comparison is that between the first ionisation constant of an amino-acid hydrochloride and the ionisation constant of the corresponding simple aliphatic acid, e.g. alanine hydrochloride and propionic acid<sup>15</sup>). As can be seen from Fig. 4, a plot of  $T\Delta pK$  against  $1/D$ , where  $D$  is a function of temperature, increases monotonically, with small slope over the small temperature range for which data are available. A similar linear plot with somewhat greater slope is obtained if  $pK$  (propionic acid)  $- pK_1$  (alanine hydrochloride) is set equal to  $\Delta pK$ .

It is worth while to examine in detail the questions related to the<sup>1</sup>

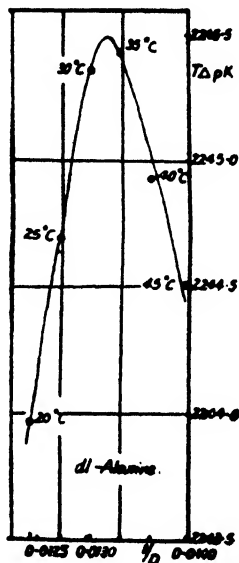
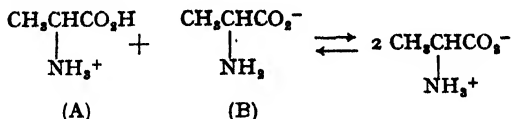


FIG. 3.—Fig. 7 from the article of Wynne-Jones and Rushbrooke.

<sup>15</sup> Neuberger, *Proc. Roy. Soc., A*, 1937, 158, 68.

temperature coefficients of the ratio of the first and second ionisation constants of alanine hydrochloride. This ratio refers to the equilibrium constant for the reaction



The reaction may be described by saying that a proton is removed from the carboxyl group of molecule A, and placed upon the amino group of molecule B, infinitely distant from A in a solvent of dielectric constant  $D$ . The reversible work for this process may be broken up in the following way:

$$\Delta w = \Delta w_1 + \Delta w_{g(\text{el})} + \Delta w_2 + \Delta w_{d(\text{el})}.$$

Here  $\Delta w_1$  is the work, due to the intrinsic structure of the carboxyl-group, of removing the ionising proton from A;  $\Delta w_{g(\text{el})}$  is the electrostatic work gained because of the interaction of the ionising proton with the positive charge of the ammonium salt group in A;  $\Delta w_2$  is the work, due to the intrinsic structure of the amino-group, of attaching the proton to B;  $\Delta w_{d(\text{el})}$  is the electrostatic work gained in this last process because of the interaction of the proton with the negative charge of the carboxylate ion

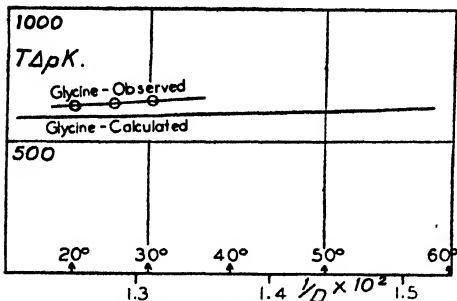


FIG. 4.— $-T\Delta pK$  for glycine as a function of temperature.

group in B. Our theory deals only with such terms as  $\Delta w_{g(\text{el})}$  and  $\Delta w_{d(\text{el})}$ . In the cases considered in our earlier publications, the sum of the terms like  $\Delta w_1$  and  $\Delta w_2$  vanished, at least approximately, because the groups to which the ionisable proton was attached were very similar. In the case of the amino-acids cited by Wynne-Jones and Rushbrooke, the sum of  $\Delta w_1$  and  $\Delta w_2$  does not vanish, since the amino-group and carboxyl-group are in no sense equivalent. Furthermore, the

temperature coefficient of the sum of  $\Delta w_1$  and  $\Delta w_2$  should not be zero because (if for no other reason)  $\Delta w_1$  includes a strong electrostatic interaction, which must be dependent on temperature. Our theory, therefore, makes no prediction concerning the temperature coefficient of the ratio of the first and second ionisation constants of an amino-acid hydrochloride; hence, the "striking discrepancy" of Wynne-Jones and Rushbrooke does not exist.<sup>16</sup>

B. Although Wynne-Jones and Rushbrooke's discussion of amino-acids is not pertinent to our theory, we do not wish to minimise the fact that the temperature coefficients computed by us do not agree well with experiment. The data for the temperature coefficients of a number of

<sup>16</sup> Incidentally, a graph such as Fig. 3 (Fig. 7 of Wynne-Jones and Rushbrooke) may be somewhat misleading. The values for  $\Delta pK$  are all identical within 0.1%. An error of 0.003 log unit in the ionisation constants might completely destroy the indicated parabola. Although the data of Nims and Smith are excellent, it seems more conservative to describe all their values of " $T\Delta pK$ " as identical. The idea (implied in Wynne-Jones' and Rushbrooke's criticism) that our theory should predict changes of the order of magnitude indicated, although flattering, is inconsistent with the avowedly approximate nature of our work.

acids is here presented in Table II. The Bjerrum formulation for electrostatic effects in water solution leads to the equation

$$\frac{d\Delta F(\text{el})}{dT} = -\Delta S = 0.0047 \Delta F(\text{el})$$

where the constant 0.0047 is the value of  $d \ln D/dT$ .<sup>17</sup> All the equations derived by our treatment (and by Sarmousakis' parallel treatment of the oblate ellipsoid) can be and are here treated in similar fashion. In general,  $\frac{d\Delta F(\text{el})}{dT}$  has been set equal to  $c\Delta F(\text{el})$ . The values of  $c$  have been determined from experimental data, and have also been computed by our

TABLE II  
TEMPERATURE COEFFICIENTS

Acid.	Reference.	"c"		"c" Bjerrum.
		Obs. v.	Calc. v.	
Succinic . . . . .	q	0.0062	0.0023	0.0047
Glutaric . . . . .	q	0.0070	0.0034	0.0047
$\beta$ , $\beta$ -Dimethyl glutaric . . . . .	q	0.0025	0.0011	0.0047
Adipic . . . . .	q	0.0070	0.0038	0.0047
cis-Caronic . . . . .	q	0.0027	0.0007	0.0047
trans-Caronic . . . . .	q	0.0051	0.0024	0.0047
Glycine (Me ester) . . . . .	s	0.0026	0.0013	0.0047
Glycine HCl (acetic) . . . . .	t	(0.0046)		
Chloroacetic (acetic) . . . . .	t	0.0020	0.0001	0.0047
Glycollic (acetic) . . . . .	t	0.0041	0.0001	0.0047
m-Nitrobenzoic (benzoic) . . . . .	u	0.0046	0.0004	0.0047
m-Iodobenzoic (benzoic) . . . . .	u	0.0041	0.0003	0.0047
m-Toluic (benzoic) . . . . .	u	0.0000	0.0003	0.0047

The compounds in parentheses are those the ionisation constants of which were used to determine the value of  $\Delta pK$  (observed) and therefore of  $c$  (observed).

(q) Jones and Soper, *J. Chem. Soc.*, 1936, 133.

(s) Edsall and Blanchard, *J. Amer. Chem. Soc.*, 1933, 55, 2337.

(t) Harned and Owen, *Physic. Chem. of Electrolyte Solutions*, Reinhold, New York, 1943.

(u) Schaller, *Z. physik. Chem.*, 1898, 25, 497. Hammett, *J. Chem. Physics*, 1936, 4, 613. Hammett, *Physical Organic Chemistry*, McGraw-Hill, New York, 1940. Sarmousakis, *J. Chem. Physics*, 1944, 12, 277.

(v)  $c$  defined by equation  $\frac{d\Delta F}{dT} = c\Delta F$ .

theory. (The actual temperature coefficients of the ionisation constants of dibasic acids are smaller than would be implied by the values of  $c$  in Table II; the experimental data have been corrected by the statistical factor of four, which is independent of temperature.)

It can be seen from Table II that the older Bjerrum theory gives values of  $c$  which are in better absolute agreement with experiment than those given by our theory. On the other hand, our treatment (as indicated by Wynne-Jones and Rushbrooke) places the acids roughly in the correct order. In point of fact, the values of  $c$  computed by the new theory seem all to be too low by about 0.003 degree<sup>-1</sup>.

C. Wynne-Jones and Rushbrooke used our equations and computed the distance,  $r$ , from the values of the temperature derivative,  $c$ , of the ionisation constants of dibasic acids; the values of  $r$  were, as they pointed

<sup>17</sup> Akerlöf, *J. Amer. Chem. Soc.*, 1932, 54, 4125.



out, unreasonably small. Their computation, however, reflects the ratio of  $c_{\text{obs.}}$  to  $c_{\text{calc.}}$ . In this connection, it is important to point out again (see paragraph A, section III) that the temperature coefficients of  $T\Delta p_K$  are small. The situation for glycine is shown graphically in Fig. 4, where  $\Delta p_K$  is the logarithm of the ratio of the ionisation constant of glycine methylester hydrochloride to the second ionisation constant of glycine hydrochloride. The computed and observed curves do not have the same slope; on the other hand, the slopes themselves are small. The difference between the curves increases by only about 0.25 log unit over a range of  $100^\circ$ —an amount not much larger than the experimental uncertainty in  $\Delta p_K$  (see Tables I and II) and smaller than the uncertainty introduced into the theory by necessary approximations (e.g. choice of a shape for the molecule<sup>4</sup>). When  $c$  is computed from our theory, the expression  $c_{\text{expt.}}/c_{\text{computed}}$  may be large, but  $c_{\text{expt.}} - c_{\text{computed}}$  is small. This sort of situation is typical for approximate theories. Such a theory may reproduce a given function very well, but where the value of the function varies only slightly with change in a given variable  $Y$ , the prediction of the derivative with respect to  $Y$  may be in error by a large factor. For example, the perfect gas equation,  $pv = NRT$ , which can be derived from simplified theoretical considerations, is a useful approximation to the behaviour of real gases. Yet the computed derivative of the pressure-volume product with respect to pressure at constant temperature  $m = \left[ \frac{\partial(pv)}{\partial p} \right]_T$  is zero, whereas in fact this derivative may be either positive or negative. This ratio  $M_{\text{obs.}}/M_{\text{computed}}$  is then infinite, although  $M_{\text{obs.}} - M_{\text{computed}}$  is small. The desirable refinements which might well be introduced into the electrostatic theory of the ionisation of acids might account for the observed temperature coefficients without greatly affecting the general agreement between the experimental and calculated values of  $\Delta p_K$ .

#### IV

Wynne-Jones and Rushbrooke, after a consideration of the data presented in their paper (which, as already explained, are partly insufficient and partly inapplicable) came to the conclusion that "the Kirkwood-Westheimer theory takes insufficient account of the specific interaction between solvent and solute molecules or ions". Although in our first paper<sup>1</sup> we ourselves pointed out this deficiency, we cannot agree with Wynne-Jones and Rushbrooke as to its quantitative importance. Our reasons coincide closely with those given by Baughan.<sup>18</sup> Wynne-Jones and Rushbrooke make their criticism somewhat more specific by speaking of the "'clamping' of the solvent, in the neighbourhood of solute ions". But since they do not prescribe a quantitative method for estimating the influence of the "clamping effect" on the chemical potentials of the ions participating in a dissociation equilibrium, it is difficult to apply their ideas.

There seems to be little doubt that any refinement of the theory dealing with the effect of substituents on dissociation constants and reaction rates must be based upon a model similar to ours, but elaborated to include more details of the local solvent structure. Although there is good reason to believe that short range specific interactions between solvent and ions will cancel when the difference between the free energies of ionisation of two similar substances in the same solvent are considered, nevertheless the longer range interactions remain. In a complete theory, these latter should be taken into account by a suitable description in molecular terms of the solvent structure in the close neighbourhood of the ions. In such a description, electrostatic effects such as electrostriction, electrical saturation, and departures of the local dielectric constant from the macroscopic

<sup>18</sup> Baughan, *J. Chem. Physics.*, 1939, 7, 951.

value in the statistical continuum of the solvent should be taken into account. Formidable difficulties remain to be overcome before such a detailed theory can be adequately formulated. Entropy contributions arising from hindered rotation of solvent molecules in the neighbourhood of the ions would probably account largely for the failure of  $d\Delta p_K/dT$ , as calculated by our theory, to agree with the experimental values.

Until a more refined theory is developed in a form from which quantitative predictions can be made, we see nothing to be gained by objecting that the models on which the newer theory are based are still too simple, and thus minimising the real advantages of the present theory over the less detailed theory of Bjerrum.

### Résumé.

En réponse à l'article de Wynne-Jones et Rushbrooke, critiquant la théorie de Kirkwood-Westheimer, ces derniers auteurs font remarquer que Wynne-Jones et Rushbrooke ont rapporté de façon inexacte les résultats relatifs aux changements de la constante d'ionisation en fonction de la variation de la constante diélectrique et que, en ce qui concerne les changements de la constante d'ionisation avec la température, leur critique est fondée sur une application des équations de Kirkwood-Westheimer dans un domaine où elles ne sont pas valables.

### Zusammenfassung.

Eine Antwort auf den Artikel von Wynne-Jones und Rushbrooke: "Eine Kritik der Theorie von Kirkwood und Westheimer." Die Autoren wenden ein, dass Wynne-Jones und Rushbrooke die Daten bezüglich Änderungen der Dissoziationskonstante durch Änderung der Dielektrizitätskonstante nur mangelhaft berichtet haben und dass ihre Kritik hinsichtlich der Änderungen der Dissoziationskonstante durch Temperaturänderung auf einem Missverständnis des Gültigkeitsbereichs der Kirkwood-Westheimer'schen Gleichungen beruht.

*George Herbert Jones Laboratory,  
University of Chicago.*

*George Fisher Baker Laboratory,  
Cornell University.*

---

## A THEORETICAL INVESTIGATION OF THE DISTRIBUTION OF ELECTRONS IN SOME HETEROCYCLIC MOLECULES CONTAINING NITROGEN.

BY H. C. LONGUET-HIGGINS AND C. A. COULSON.

*Received 26th February, 1946.*

### Introduction.

Many properties of unsaturated organic molecules may be qualitatively correlated with the distribution of electrons in the isolated molecule. Such properties include the ease of cationoid and anionoid substitution at different positions and the relative reactivities of certain groups such as  $\text{CH}_3$ , when substituted at different points in the molecule. In the present paper the electron densities and bond orders are calculated for indole, carbazole, quinoline, isoquinoline, acridine and the hypothetical isoindole

by the method of molecular orbitals.<sup>1, 2</sup> The adjustable parameters which occur in the calculations are as few as possible in number; the same set of values is used for all the molecules investigated; and these values are derived from a similar treatment of pyrrole and pyridine by Wheland and Pauling.<sup>3</sup>

### Description of Method.

The method of calculation is well known. We may conveniently illustrate it here by the example of acridine; the numbering which will be used is given in the appendix.

The fourteen aromatic or  $\pi$ -electrons (one from each CH group and one from the N atom) are assumed to move in orbits covering the whole molecule. We suppose that each of these molecular orbitals  $\phi$  can be represented approximately by a linear combination of fourteen atomic orbitals. That is to say, we write

$$\phi = c_1\psi_1 + c_2\psi_2 + \dots + c_{14}\psi_{14}$$

where  $\psi_1, \psi_2, \dots, \psi_{14}$  are wave functions antisymmetric with respect to the plane of the molecule and having their greatest amplitudes in the neighbourhood of atoms 1, 2,  $\dots$  14 respectively. (The  $\sigma$ -electrons are throughout supposed to be paired in localised bonds between neighbouring atoms, and not to take part in the bond conjugation.) In order that  $\phi$  may be as good a solution as possible of the wave equation, the constants  $c_1, c_2, \dots, c_{14}$  have to satisfy fourteen relations which may be written briefly

$$c_r(\alpha_r - E) + \sum_{s=1}^{14} \beta_{rs}c_s = 0; \quad r = 1, 2, \dots, 14$$

where the prime in  $\Sigma'$  denotes that the term with  $s = r$  is omitted from the sum. In these "secular equations"  $E$  is the energy of a molecular orbital,  $\alpha_r$  is the coulomb integral for the atomic orbital  $\psi_r$ , and  $\beta_{rs}$  is the resonance integral between the atomic orbitals  $\psi_r$  and  $\psi_s$ ; their formal definitions in terms of the Hamiltonian  $H$  are:

$$E = \int \phi H \phi dv, \quad \alpha_r = \int \psi_r H \psi_r dv, \quad \beta_{rs} = \int \psi_r H \psi_s dv.$$

The wave functions  $\psi_r$  and  $\phi$  are normalised and in real form, and overlap\* between different atomic orbitals is neglected, i.e.

$$\int \psi_r^2 dv = 1 = c_1^2 + c_2^2 + \dots + c_{14}^2; \quad \int \psi_r \psi_s dv = 0, \quad r \neq s.$$

In order to solve the secular equations for  $E$  and the coefficients  $c_r$  we need to assume values for the  $\alpha_r$ 's and  $\beta_{rs}$ 's. Following Wheland and Pauling in their calculations for pyrrole we put  $\beta_{rs}$  equal to  $\beta$ , the resonance integral for a C—C bond in benzene, or zero, according as atoms  $r$  and  $s$  are joined by a bond or not; and we put  $\alpha_r$  equal to  $\alpha + 2\beta$ ,  $\alpha + \frac{1}{2}\beta$  or  $\alpha$ , according as  $r$  is a nitrogen atom, a carbon atom bonded to nitrogen, or any other carbon atom,  $\alpha$  being the coulomb integral for a carbon atom in benzene. Apart from its *a posteriori* justification in the case of pyrrole, this choice of values for  $\alpha_r$  is reasonable since N is known to be considerably more electronegative than C, and the C atoms adjacent to the N atom would be expected to share its enhanced electronegativity to a small extent; also, since the difference in energy between the bonds C—C and C=C is nearly

\* Wheland<sup>4</sup> has shown that the quantities  $E$ ,  $\alpha_r$  and  $\beta_{rs}$  may be given a more exact interpretation if overlap between adjacent atomic orbitals is not neglected, but that this does not affect the form of the equations for the coefficients  $c_r$ .

<sup>1</sup> Lennard-Jones and Coulson, *Trans. Faraday Soc.*, 1939, **35**, 811.

<sup>2</sup> Coulson, *Proc. Roy. Soc. A.*, 1933, **169**, 413.

<sup>3</sup> Wheland and Pauling, *J. Amer. Chem. Soc.*, 1939, **57**, 2091.

<sup>4</sup> Wheland, *ibid.*, 1941, **63**, 2025.

equal to that between C—N and C=N, we are justified in taking the resonance integrals to be all equal to  $\beta$ . For the sake of uniformity these values of the parameters are used in the calculations for all the molecules discussed in this paper. The secular equations for acridine may then be written :

$$\begin{array}{ll} c_1(\alpha - E) + \beta(c_2 + c_{13}) = 0, & c_8(\alpha - E) + \beta(c_7 + c_{13}) = 0, \\ c_2(\alpha - E) + \beta(c_1 + c_3) = 0, & c_9(\alpha + 2\beta - E) + \beta(c_{12} + c_{13}) = 0, \\ c_3(\alpha - E) + \beta(c_2 + c_4) = 0, & c_{10}(\alpha - E) + \beta(c_{11} + c_{14}) = 0, \\ c_4(\alpha - E) + \beta(c_3 + c_{14}) = 0, & c_{11}(\alpha - E) + \beta(c_5 + c_{10} + c_{12}) = 0, \\ c_5(\alpha - E) + \beta(c_6 + c_{11}) = 0, & c_{12}(\alpha + \frac{1}{2}\beta - E) + \beta(c_8 + c_9 + c_{11}) = 0, \\ c_6(\alpha - E) + \beta(c_5 + c_7) = 0, & c_{13}(\alpha + \frac{1}{2}\beta - E) + \beta(c_1 + c_9 + c_{14}) = 0, \\ c_7(\alpha - E) + \beta(c_6 + c_8) = 0, & c_{14}(\alpha - E) + \beta(c_4 + c_{10} + c_{13}) = 0. \end{array}$$

It is convenient to put  $(\alpha - E)/\beta = \gamma$ . Then there are fourteen values of  $\gamma$  and fourteen corresponding sets of coefficients  $c$ , which satisfy the last set of equations. Each of these sets gives us a molecular orbital. The fourteen aromatic  $\pi$ -electrons will occupy in pairs the seven molecular orbitals of lowest energy; since  $\beta$  is negative these are the seven orbitals with lowest algebraic values of  $\gamma$ .

Now in acridine the symmetry of the molecule makes it possible to divide the molecular orbitals  $\phi$  into the following classes :

(a) Those symmetric about the plane through atoms 9 and 10 perpendicular to the plane of the molecule; for these  $c_{13} = c_{12}$ ,  $c_8 = c_1$ ,  $c_7 = c_2$ , etc.

(b) Those antisymmetric about that plane; for these  $c_9 = c_{10} = 0$ ,  $c_{13} = -c_{12}$ , etc. This class may be subdivided into ( $b_1$ ) those for which also  $c_{14} = c_1$ ,  $c_4 = c_2$ ; and ( $b_2$ ) those for which  $c_{14} = -c_1$ ,  $c_4 = -c_2$ ,  $c_3 = 0 = c_{13}$ .

Elimination of the  $c$ 's from the secular equations gives for class (a) an eighth order equation in  $\gamma$ , for class ( $b_1$ ) a quartic equation and for class ( $b_2$ ) a quadratic. The seven lowest roots of all these equations are :

$$\left. \begin{array}{l} \gamma = -3.0470 \\ -1.9542 \\ -1.4142 \\ -0.7680 \end{array} \right\} \text{from the octic equation,} \quad \left. \begin{array}{l} \gamma = -2.0472 \\ -1.0840 \end{array} \right\} \text{from the quartic,}$$

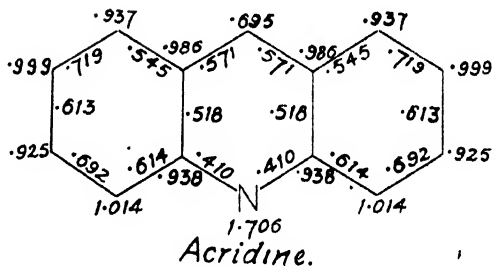
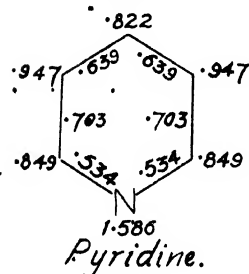
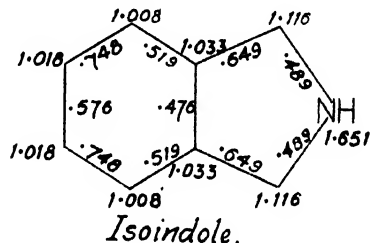
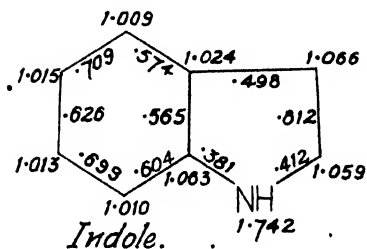
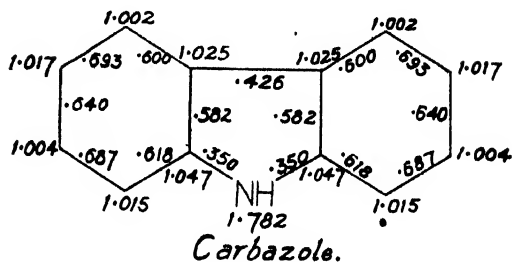
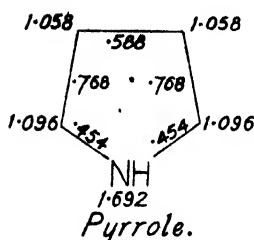
$$\gamma = -1 \text{ from the quadratic.}$$

Hence four of the occupied orbitals are of type (a), two are of type ( $b_1$ ) and one is of type ( $b_2$ ).

We now put each of these values of  $\gamma$  back in turn into the secular equations and find the ratio of the set of coefficients in the corresponding molecular orbital. To get the absolute magnitudes of the coefficients we use the normalisation condition that  $c_1^2 + c_2^2 + \dots + c_{14}^2 = 1$  in each orbital. The total density of  $\pi$ -electrons at, say, atom 5 is then given by  $2\sum c_s^2$  and the mobile order  $s$  of the bond between atoms 5 and 6 by  $2\sum c_5 c_6$ , where the summation is taken over the seven occupied orbitals.

## Results.

The calculated values of the total  $\pi$ -electron densities and mobile bond orders obtained in this way are shown in the diagram. The number at each atom denotes the total mobile charge there, and the number beside each bond indicates the corresponding mobile bond order. The values for benzene are included for comparison. The electron densities in pyrrole agree with those calculated by Wheland and Pauling; and the small differences between their results and ours for pyridine are due to our taking the coulomb integral for the  $\alpha$ -carbon atoms to be  $\alpha + \frac{1}{2}\beta$ , for the sake of uniformity, whereas Wheland and Pauling took  $\alpha + \frac{1}{3}\beta$ .



### Discussion.

At first sight it might seem that the differences in electron density between these molecules and benzene are not very large. However, when it is remembered that in the highly polar HF the dipole moment<sup>6</sup> indicates a charge displacement of only 0.43e, the displacements of charge in these molecules are seen to be considerable; for example, the carbon atom 4 in quinoline has a net charge + 0.23e. Similarly the variations in bond order appear quite large when it is borne in mind that the bond orders in benzene and ethylene differ by only 0.333.

As for the relative magnitudes of the  $\pi$ -electron densities and bond orders, these are much what one would have expected on the basis of experiment. The bond orders in most of the molecules indicate that the uncharged classical structures are the best *single* structures representing the bond orders. The electron densities at the carbon atoms tend to be greater or less than unity according as there are  $n$  or  $n + 1$   $\pi$ -electrons,  $n$  being the number of conjugated atomic orbitals. This is simply explained, as the sum of the densities must add up to the total number of  $\pi$ -electrons, and the density at the N atoms is large owing to their greater electronegativity.

When we come to correlate these results with the facts of organic chemistry, we find that the greater the calculated  $\pi$ -electron density at a position, the greater the ease and rate of cationoid substitution at that point, while anionoid substitution proceeds most easily at those positions where the calculated density is lowest. Those positions at which the calculated density differs considerably from unity are precisely those which are found to have the most marked chemical effect on reagents and substituted groups.

To be specific, the calculated densities in pyrrole and the 5-membered ring in indole are considerably greater than those in benzene or the 6-membered ring of indole; and while the density is greater at the 2- than the 3-position in pyrrole, it is slightly greater at the 3-position in indole. This agrees with the facts that both these molecules are attacked by cationoid reagents much more readily than benzene, and that whereas pyrrole gives 2-derivatives, indole undergoes 3-substitution more easily. In carbazole, on the other hand, the electron densities at the external C atoms hardly exceed those in benzene, being slightly greater at the 1, 3, 6 and 8 positions than the others. Correspondingly we find that carbazole is very stable to cationoid reagents, being attacked by sulphuric acid only at about 300° C., and that when substitution does occur, it gives derivatives in the order 3, 3:6, 1:3:6, 1:3:6:8.

Isoindole, if it existed, would have a  $\pi$ -electron density in its 5-membered ring very close to that of pyrrole. The instability of this compound cannot therefore be explained merely in terms of electron densities.

In quinoline, isoquinoline and acridine the most striking feature of the calculated densities is the very low values that they have at the 2- and 4-positions in quinoline, the 1-position in isoquinoline, and the 10-position in acridine. This is in complete consonance with the characteristic properties of these positions in these molecules: in particular their susceptibility to anionoid attack, the fact that methyl groups at these positions can be ionised and oxidised, and the reactivity of the chloro-derivatives towards ammonia and other anionoid reagents. According to the calculations we should expect quinoline, isoquinoline and acridine to undergo cationoid substitution most readily in the 8-, 5- and 1-positions respectively, the rates of reaction being not very different from those in benzene. Actually, the primary products of nitration in these substances are both 5- and 8-nitro-compounds in both quinoline and isoquinoline, and both 3- and 1-nitro-compounds with acridine; primary nitration does not occur in the heterocyclic rings.

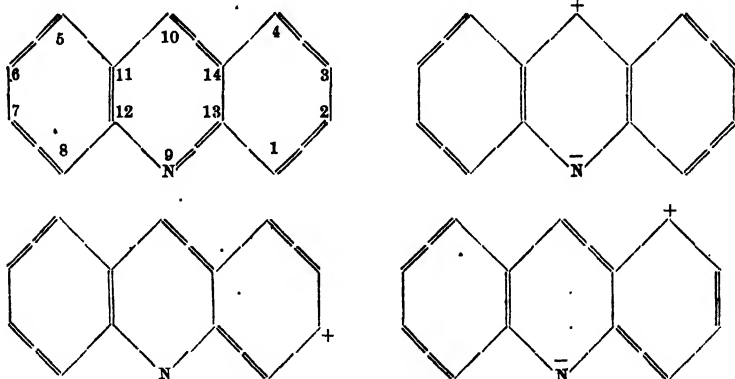
<sup>6</sup> Wheland, *J. Amer. Chem. Soc.*, 1942, 64, 900.

<sup>7</sup> Hannay and Smyth, *J. Amer. Chem. Soc.*, 1946, 68, 171.

At the suggestion of Dr. M. J. S. Dewar we also calculated  $\pi$ -electron densities and bond orders in indolizine. Since it is not yet known which positions in this molecule are attacked in substitution reactions, indolizine affords an instance in which the predictions of the present theory may be verified *a posteriori*. It is interesting that the electron density at position 3 in indolizine is higher than that at the 2-position in pyrrole, and that the electron density at position 1 is much higher. One would therefore expect the molecule to be readily susceptible to cationoid attack, first in position 1, then if this is blocked, in position 3, and if both these are blocked, in positions 2 or 7. Since there are no carbon atoms with abnormally low electron densities in indolizine, one would not expect substituted methyl groups to be easily ionised, or anionoid substitution to occur with any ease.

Thus we see that in all the molecules discussed above the calculated electron densities may be closely correlated with chemical evidence, as far as it is available. If this agreement were confined to pyrrole, it would not be so significant, since the parameters were chosen to give agreement in this molecule; but we find that the same parameters predict correctly the important features of substitution in other molecules also. Now one would not expect the permanent charge distribution in a molecule by itself to determine the relative reactivities of different positions; in fact, when, as in most hydrocarbons, the charge density is the same at each atom, the polarisability of an atom seems to be the most important factor governing substitution. It therefore seems reasonable to suppose that (a) the permanent charge distributions in a pair of molecules are important in orienting them into a suitable configuration for reaction, particularly at fairly large distances apart, when the coulomb forces predominate over the exchange forces, and/or (b) the permanent charge distribution in a molecule reflects the tendencies of the different positions to accept or donate a pair of electrons for bond formation with an anionoid or cationoid reagent. (Reactivities towards radical reagents are not so easily correlated with electron densities; but Wheland<sup>6</sup> has shown that they may be brought into line with heterolytic reactions if polarisation by the attacking groups is considered.)

It is interesting to compare briefly the present semi-quantitative treatment with the qualitative resonance picture of heterocyclic molecules. Acridine will serve again as an example. Important resonance structures will include:



The positions at which lowering of the  $\pi$ -electron density occurs will therefore be the same (2, 4, 5, 7, 10) according to the two approaches. The same applies to the changes in bond order. Qualitatively, therefore, the two methods of approximation give very similar conclusions. However, calculations of the present kind promise to give semi-quantitative results

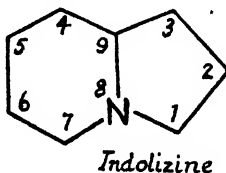
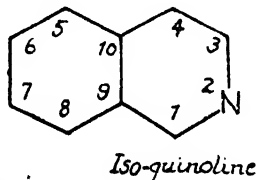
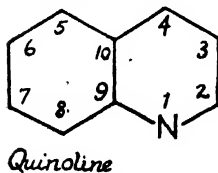
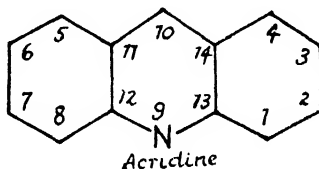
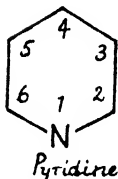
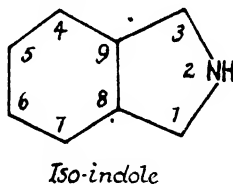
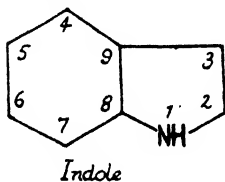
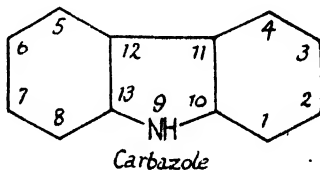
most easily; and since the parameters which predict the facts correctly in one molecule seem to give good results in similar molecules also, it may be possible to build up a semi-empirical set of resonance integrals and electron affinities which will relate a large number of experimental facts in this way.

### Summary.

The charge distributions and bond orders in indole, carbazole, quinoline, *iso*quinoline, acridine, indolizine and the hypothetical *iso*indole are investigated quantitatively by the method of molecular orbitals. The few adjustable parameters used in the calculations have been given values assigned them by Wheland and Pauling in a similar treatment of pyrrole. For indole, carbazole, quinoline, *iso*quinoline and acridine the results are in close correspondence with the chemistries of these molecules; for indolizine, where the chemical data are still incomplete, predictions are made about the relative reactivities of different positions in the molecule.

### APPENDIX.

The numbering used in the discussion is as follows:





## Résumé.

Les distributions de charge et les ordres de liaison dans l'indole, le carbazole, la quinoléine, l'isoquinoléine, l'acridine, l'indolizine et l'hypothétique iso-indole sont étudiés quantitativement par la méthode des fonctions orbitales moléculaires. Les quelques paramètres ajustables employés dans les calculs ont les valeurs que Wheland et Pauling leur attribuent dans une étude comparable du pyrrole. Pour toutes les molécules réelles, les résultats s'accordent étroitement avec les propriétés chimiques de ces molécules; pour l'indolizine, où les données chimiques sont encore incomplètes, on peut prévoir les réactivités relatives des différentes positions dans la molécule.

## Zusammenfassung.

Die Ladungsverteilung und der Gehalt an mobilen  $\pi$ -Elektronen der einzelnen Bindungen („Mobilbindungsordnung“) von Indol, Carbazol, Chinolin, Isochinolin, Acridin, Indolizin und dem in der Praxis unbekannten Isoindol wurden in quantitativer Weise nach der Methode der molekularen Elektronenbahnen ermittelt. Den wenigen Grössen, deren Werte in den Berechnungen willkürlich festzusetzen sind, wurden die ihnen von Wheland und Pauling in ähnlichen Berechnungen für Pyrrol zugewiesenen Werte gegeben. Für alle existierenden Moleküle sind die so gefundenen Ergebnisse in gutem Einklang mit ihrem chemischen Verhalten. Für Indolizin, dessen Chemie teilweise noch unerforscht ist, werden Voraussagen bezüglich der relativen Reaktivität der verschiedenen Stellungen im Molekül gemacht.

*Physical Chemistry Laboratory,  
Oxford.*

## REVIEWS OF BOOKS.

**Actions of Radiations on Living Cells.** By D. E. LEA. (Cambridge University Press, 1946.) Pp. xii + 502. Price 21s. net.

Although X-rays and the radiations from radioactive substances were applied therapeutically within a few years of their discovery, it is only comparatively recently that any detailed knowledge of the origin of their biological effects has been obtained. So far as this country is concerned, at least, the problem has attracted the attention of few chemists or physicists, although there is general agreement that a sequence of physical-chemical changes must occur between the production of an ion-pair during its passage through tissue and the damage to, or destruction of, cells which results. Such detailed physical knowledge as we have has come largely from the biological side, where geneticists and virus pathologists in particular have collaborated with a small group of physicists. Dr. Lea's book is therefore timely, for it collects and collates under one cover an accumulation of physical and chemical information which was previously scattered over a wide field of biological literature. It makes data readily available for any scientists whose interest in radio-chemistry and radio-biology may have been stimulated by discussions on the actions of radiations such as were organised jointly by the Faculty of Radiologists, the British Institute of Radiology, and the Faraday Society in 1941, or by the second of these bodies in 1946.

Dr. Lea is a leading protagonist of the "target" theory, which attributes the biological effects to the production of ionisation in some particular molecules, or to the passage of an ionising particle through some particular structure, in the cell. He believes that "the validity of the target theory is as certain as a scientific theory ever is in a rapidly developing subject, in the case of the inactivation of small viruses by radiation, and the production of certain chromosome aberrations in higher cells". He considers that its validity is highly probable in the killing of larger viruses and bacteria, and the production of gene mutations. Most of the book is devoted to a reasoned exposition of the experimental facts on which these opinions are based.

Nevertheless, Dr. Lea admits that there are other possible theories, and an early chapter is devoted to an excellent account of the known chemical actions of radiations, where the recent experiments of Dale on "indirect" action (i.e. chemical effect on a solute resulting from ionisation of the solvent), and the suggestion by Weiss that the active agents produced by ionisation of water are free hydroxyl or hydrogen radicals, have begun to bring order out of chaos. The chemical approach provides an alternative explanation of some of the biological effects, since the radicals may produce chemical changes at some distance from the initial ionisation. Dr. Lea not only recognises this, but develops a physical mechanism for it. Unfortunately, the data necessary for a quantitative test of the mechanism are not yet available.

The book is lucidly written, and is well illustrated. It contains numerous tables of data, and an excellent bibliography. The production is of the usual C.U.P. standard. Dr. Lea has remembered that such a book will need to be read both by physicists and chemists, and by biologists, and he has therefore prefaced the more technical chapters with explanatory sections, in simple terms, of physics for the biologist and of biology for the physicist. The reviewer strongly recommends it to the attention of physical chemists in the hope that they may be attracted to this very fascinating and rapidly growing field of radiobiology.

C. B. A.

**Industrial Oil and Fat Products.** By ALTON E. BAILEY. (Interscience Publishers, Inc., New York, 1945 and Imperial Book Co., London.) Pp. x + 735. Price 10 dollars (£3).

During the last twenty years considerable advances have been made in our knowledge of the chemical constituents of oils and fats, due largely to the pioneer work of Hilditch. In the same period technological processes for the utilisation of oils and fats have progressed and extended enormously. In general these two advances have been independent of each other and it is difficult to cite anything important in one field which has directly resulted from discoveries in the other; although the greater knowledge of the individual components of oils and fats and their properties has explained in a marked degree certain industrial processes and reactions. A book dealing with industrial oil and fat products must, therefore, be expected to devote only a small part to the purely scientific aspect.

About one-eighth of the present book deals with the composition and character of the fatty oils, and an equal amount is devoted to industrial

raw materials and their availability. The remaining three-quarters is divided, approximately equally, between Industrial Utilisation of Fats and Oils, and Unit Processes in Oil and Fat Technology. The products dealt with cover food (bakery products, butter, margarine), soap (and other surface acting materials), paint and varnishes, and miscellaneous (lubricants, hydraulic oils, illuminants, cosmetic materials and insecticides.) The information fills many gaps in the readily accessible literature and much of the material appears for the first time, particularly with reference to the technology of edible fats and oils. The author has been assisted by other eminent American oil chemists associated with the industry.

This volume will form an important addition to the bookshelves of all fat technologists. Although the relative importance attached to various products is not the same in the United States as in Britain, the raw materials and their treatment are the same; and an up-to-date account of American practice cannot fail to be welcome.

J. R. N.

**Modern Chemistry. Some Sketches of its Historical Development.**

By A. J. BERRY, M.A. (Cambridge: The University Press, 1946.)  
Pp. x + 240. Price 10s. 6d. net.

Mr. Berry states in his preface that he has attempted to consider the development in historical perspective of certain branches of Chemistry in separate chapters, each self-contained and largely independent. The whole is intended to be intelligible to anyone endowed with a moderate stock of chemical knowledge, and is planned in such a way as to make clear the development of some of the important parts of the subject to the position which they occupy to-day. The book is historical in the sense that it traces the progress of the subjects selected, in most cases during the nineteenth and present centuries, but they are presented in modern form, and the book will be a valuable aid to students in getting concise but informative statements of these topics. The author deals in successive chapters with the classical atomic theory; electrochemistry; stereochemistry; radioactivity; elements, isotopes and atomic numbers; some experimental studies on gases; some problems of solutions; some essential features of chemical change; and a retrospect. In all cases the treatment is non-mathematical and should be intelligible and interesting to relatively junior students. The book is a welcome supplement to formal text-books, and the selected references at the ends of the chapters will point the way to those seeking further information, as most readers of the book may be expected to do after their interests have been aroused by its contents. The treatment is well-balanced and unprejudiced, and the book may be most warmly recommended.

J. R. P.

# THE HEATS OF COMBUSTION OF SOME ORGANIC BASES AND THEIR SALTS. THE RESONANCE ENERGIES OF ACRIDINE AND PHENAZINE.

By J. B. WILLIS.

*Received 19th December, 1945.*

The determination of the heat of combustion of the salts of organic acids and bases has seldom been attempted in the past, and the few values recorded in the literature, e.g. those for guanidine nitrate<sup>1</sup> and ammonium urate<sup>2</sup> are, by modern standards, unsatisfactory. Although the combustion of organic acids and bases generally offers no difficulties, the complete combustion of their salts is not easy when the acid or base in question is of low molecular weight and the non-combustible inorganic part of the molecule forms a relatively large proportion of the total weight.

In the case of organic bases, the choice of a suitable salt for combustion is limited by several factors. Firstly, a strong acid must be chosen in order to ensure that the salt is stoichiometric and stable. When a stainless steel bomb is used, halide salts are not permissible, as the liberated halogen would attack it; moreover, difficulties are introduced by the uncertain states of oxidation of the products of combustion. When dealing, as in part of the present work, with di-acid bases, it is advisable to use the salt of a monobasic acid in order to ensure a stoichiometric composition. The salts selected for the present work were all nitrates: the nitric acid formed during the combustion does not attack the bomb, and can be readily estimated in the washings from it. The heats of combustion obtained were completely reproducible. Since the preparation of the nitrates of organic bases in a sufficiently pure condition for this type of work has not previously been described, suitable methods are reported here in some detail.

The selection of the bases was conditioned by the hope of obtaining results from which the extra ionic resonance energy of organic bases could be calculated—in particular, the negative energy<sup>3</sup> of weak bases such as aniline and naphthylamine, and the positive energy, recently discovered by Albert and Goldacre,<sup>4</sup> of the strong bases 2-amino, 5-amino, and 2:8-diaminoacridine. By extra ionic resonance energy is meant that energy due to resonance in the ion over and above that in the base. This change of resonance energy in passing from the base to the ion is probably the most important condition determining the relative stability of the two species and hence the dissociation constant of the base. Although the necessary subsidiary data (e.g. the lattice energies of the salts) for a rigorous calculation are not at present available, it is felt that the results have enough general interest for publication, especially as during the course of the investigation, the heats of combustion, and from them the resonance energies, of acridine and phenazine have been determined. These figures fill an outstanding gap in the data for simple cyclic nuclei.

<sup>1</sup> Matignon, *Ann. Chim. Physique.*, (6), 1893, 28, 70.

<sup>2</sup> Matignon, *Compt. Rend.*, 1890, 110, 1267.

<sup>3</sup> Pauling, *The Nature of the Chemical Bond*, Cornell, 1940, p. 206.

<sup>4</sup> Albert and Goldacre, *J. Chem. Soc.*, 1943, 454.

### Experimental.

**Preparation of Bases.**—The purity required for an accurate determination of heat of combustion is so high that the melting point criterion is of insufficient value. At least two specimens of each substance were obtained and purified, where possible by different methods, and dried *in vacuo* over phosphorus pentoxide for several days. Those which proved to be stable to heat, viz., 3-amino, 5-amino, and 2 : 8-diaminoacridine, were dried in the oven at 110° for an hour. It was considered that the pure condition had been attained when the various specimens gave the same heat of combustion to within the limits of experimental error.

$\beta$ -Naphthylamine was distilled from a good quality reagent sample. Another specimen was obtained by twice recrystallising this product from aqueous alcohol.

Acridine: one sample was obtained from B.D.H. acridine hydrochloride by precipitation of the base with ammonia, followed by two crystallisations from aqueous alcohol. The other sample was prepared from 5-chloroacridine by the method of Albert and Willis,<sup>6</sup> and recrystallised in the same way.

3-Aminoacridine was synthesised by the method of Albert and Ritchie,<sup>6</sup> and repeatedly recrystallised from alcohol.

5-Aminoacridine was obtained from commercial "Monacrin" (base) by repeated recrystallisation from acetone. Another specimen was prepared by the method of Albert and Ritchie<sup>7</sup> and recrystallised in the same way. It was necessary to heat this compound in an oven for two hours, as the acetone of crystallisation was only slowly driven off.

2 : 8-Diaminoacridine was obtained from a good quality commercial proflavine (base) by crystallising from alcohol with a little charcoal, followed by two recrystallisations from the same solvent, without charcoal.

Phenazine was prepared from 22'-dinitrodiphenylamine according to the method of Eckert and Steiner,<sup>8</sup> and purified by distillation with superheated steam.

**Preparation of the Nitrates.**—These were prepared by adding to the solid base N.  $\text{HNO}_3$  (freshly made up from pure analytical grade  $\text{HNO}_3$ , and tested for freedom from  $\text{HNO}_2$  <sup>9</sup>), stirring and warming on the water-bath until the solution was clear, cooling in a freezing mixture, filtering off the crystals and drying them *in vacuo* as above. It was found that the

TABLE I.—ANALYSIS OF THE NITRATES.

Salt.	N (found).	N (calculated for B. $\text{HNO}_3$ ).
	%	%
Aniline nitrate . . . . .	18.00	17.95
$\beta$ -Naphthylamine nitrate . . . . .	13.63	13.60
Acridine nitrate . . . . .	11.50 *	11.57
3-Aminoacridine nitrate . . . . .	16.25	16.34
5-Aminoacridine nitrate . . . . .	16.40	16.34
2 : 8-Diaminoacridine nitrate . . . . .	20.69	20.59

\* If crystallised slowly from water the analysis gives N = 10.02 %. Calculated for  $\text{C}_{11}\text{H}_9\text{N} \cdot \text{HNO}_3 \cdot 2\text{H}_2\text{O}$ : N = 10.07 %.

<sup>5</sup> Albert and Willis, *J. Soc. Chem. Ind.* (in press).

<sup>6</sup> Albert and Ritchie, *J. Soc. Chem. Ind.*, 1941, 60, 120.

<sup>7</sup> Albert and Ritchie, *Organic Syntheses*, 1942, 22, 5.

<sup>8</sup> Eckert and Steiner, *Monatsh.*, 1914, 35, 115.

<sup>9</sup> Scott, *Standard Methods of Chemical Analysis*, 4th Ed., p. 1510.

nitrates of all the acridines used here could be dried at  $110^{\circ}$  for at least an hour without decomposition. Two samples of each nitrate were made, one by using the calculated quantity of nitric acid and the other by using a slight excess. Aniline nitrate was prepared as above, but with 4 N.  $\text{HNO}_3$  and the crystals washed once with a little ice-cold water; the second specimen was slowly crystallised from the calculated quantities of N. nitric acid and aniline.

Since these nitrates, for the most part, have not been described in the literature, a Dumas  $\text{N}_2$  estimation was carried out in each case to determine the formula.

**Apparatus and Procedure.** A Baird and Tatlock instrument was used, with a chromium-plated copper calorimeter can and a stainless steel bomb of 275 ml. volume. The calorimeter water (about 2500 g.) was weighed to 0.1 g. and the specific heat at the temperature of the experiment (about  $20^{\circ}$ ) taken from the values of Callendar and Barnes.<sup>10</sup> The rise of temperature was measured to  $0.001^{\circ}$  with a Beckmann thermometer recently calibrated at the National Physical Laboratory, England. The following corrections were applied to the thermometer readings :

- (1) scale corrections as given by the N.P.L. ;
- (2) emergent stem temperature correction, and
- (3) correction for the changing value of the Beckmann degree with the setting of the thermometer.

The rise of temperature was about  $2.3^{\circ}$ , and the cooling correction was calculated by Dickinson's formula.<sup>11</sup>

The substance was compressed into a pellet. The weighings are given in air, as the densities of few of the substances are known. The bomb was twice filled to 5 atmospheres and emptied before finally charging to 30 atmospheres. Ignition was effected by passing a momentary current from a 4 v. accumulator through a 42 S.W.G. Pt wire from which a loop of cotton was suspended to touch the pellet. Correction was made for the heat of combustion of the cotton. 10 ml. of water were placed in the bomb and the  $\text{HNO}_3$  formed in the combustion was titrated with dilute alkali so that correction could be made for any  $\text{N}_2$  which was oxidised to  $\text{HNO}_3$ . The heat of formation of aqueous  $\text{HNO}_3$  from  $\text{N}_2$ ,  $\text{O}_2$ , and  $\text{H}_2\text{O}(\text{liq.})$  was taken as 14.5 kcal./mole. It might be expected that the nitrate ion of the salts would be entirely converted on combustion to  $\text{HNO}_3$ ; actually it was largely converted to  $\text{N}_2$ , and the total  $\text{HNO}_3$  found in the bomb only accounted for 20-30 % of the nitrate ion. Any small residue of C in the crucible (usually less than 0.5 mg.) was weighed and corrected for.

The combustion of aniline nitrate, unlike that of the other nitrates studied here, was very incomplete, but this was overcome by burning it together with a pellet of naphthalene (Kahlbaum's thermo-chemical naphthalene, heat of combustion 9617 cal.<sub>18</sub>/g. in air). That there is no heat of reaction between these two substances was proved by varying their proportions over a fourfold range: the heat of combustion of the aniline nitrate remained the same.

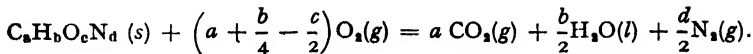
The water equivalent of the system was found by the combustion of B.D.H. thermochemical benzoic acid, its heat of combustion at constant volume being taken as 6324 cal.<sub>18</sub>/g. in air. Using the water equivalent thus found, the heat of combustion of thermochemical sucrose from the Bureau of Standards, Washington, was determined. The value thus found ( $3945.0 \pm 1.6$  cal.<sub>18</sub>/g. in air) was identical with the figure supplied with the standard (3945 cal.<sub>18</sub>/g. in air).

<sup>10</sup> Callendar and Barnes, *Phil. Trans.*, 1902, 199, 149.

<sup>11</sup> Dickinson, *Bur. Stand. Bull.*, 1915, 11, 189.

## Results.

In Table II are given the heats of combustion, corresponding to the reaction :



—  $\Delta U$  is the heat of combustion per mole. at constant volume and —  $\Delta U/m$  the heat of combustion per gram. —  $\Delta H$  is the molar heat of combustion at constant pressure, obtained from  $\Delta U$  in the usual way. The uncertainties quoted are the greatest probable errors in the quantities concerned, calculated from the formula  $\frac{3\Sigma r}{n\sqrt{n}}$ , where  $\Sigma r$  is the sum of the deviations from the mean of all the experimental values, and  $n$  the number of values. In general an accuracy of  $\pm 0.1\%$  was attained.

It will be observed that the differences between the heats of combustion of the weak bases and their corresponding salts are all about the same, and are less than the differences found for the strong bases. This indicates that the salts of the strong bases have lower internal energies relative to their bases than have the salts of the weak bases, and are therefore more stable. However, as mentioned above, lack of subsidiary data, particularly the lattice energies of the salts, prevents a rigorous evaluation of the energy of stabilisation provided by the extra resonance energy in the ions of the strong bases.

TABLE II.

Substance.	No. of Combustions.	— $\frac{\Delta U}{m}$ (cal./g. in air).	— $\Delta U$ (kcal.).	— $\Delta H$ (kcal.).	$\delta\Delta H$ (Base-salt). (kcal.).
Aniline (solid)				810.4*	22.5
Aniline nitrate	8	5051.4 $\pm$ 4.6	788.2	787.9 $\pm$ 0.7	
$\beta$ -Naphthylamine	4	8802.1 $\pm$ 8.1	1259.4	1260.4 $\pm$ 1.1†	19.7
$\beta$ -Naphthylamine nitrate	7	6016.8 $\pm$ 5.3	1240.7	1240.7 $\pm$ 1.1	
Acridine	8	8797.9 $\pm$ 8.9	1576.8	1577.8 $\pm$ 1.6	24.5
Acridine nitrate	7	6412.4 $\pm$ 6.2	1553.3	1553.3 $\pm$ 1.5	
3-Aminoacridine	8	8252.1 $\pm$ 11.4	1602.8	1603.7 $\pm$ 2.2	21.7
3-Aminoacridine nitrate	7	6149.9 $\pm$ 6.5	1582.1	1582.0 $\pm$ 1.7	
5-Aminoacridine	6	8243.0 $\pm$ 8.5	1601.0	1601.9 $\pm$ 1.7	38.2
5-Aminoacridine nitrate	5	6079.1 $\pm$ 5.3	1563.8	1563.7 $\pm$ 1.4	
2 : 8-Diaminoacridine	6	7779.1 $\pm$ 4.3	1627.7	1628.4 $\pm$ 0.9	33.9
2 : 8-Diaminoacridine nitrate	5	5857.8 $\pm$ 5.6	1594.8	1594.5 $\pm$ 1.5	
Phenazine	3	8103.7 $\pm$ 8.0	1460.3	1460.9 $\pm$ 1.4	—

\* This figure is obtained from the heat of combustion of liquid aniline as determined by Anderson and Gilbert<sup>18</sup> correcting this figure from the standard (benzoic acid = 26,419 cal./g. *in vacuo* = 6315.3 cal./g. *in vacuo*) to the present one (benzoic acid = 6319 cal./g. *in vacuo*), subtracting from —  $\Delta H$  so obtained the molar heat of fusion (1.95 kcal.), and finally converting the figure from vacuum to air weighings in order to make it fully comparable with the present values.

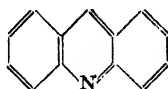
† The value obtained here for  $\beta$ -naphthylamine compares well with that in the literature,<sup>18</sup> viz., —  $\Delta H$  = 1261.0 cal./mole.

<sup>18</sup> Anderson and Gilbert, *J. Amer. Chem. Soc.*, 1942, **64**, 2369.

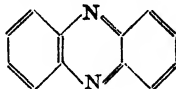
<sup>19</sup> Kharasch, *Bur. Stand. J. Res.*, 1929, **2**, 359.

### The Resonance Energies of Acridine and Phenazine.

In order to calculate the resonance energy of these compounds in the gaseous state, the heats of combustion must be supplemented by the heats of fusion and vaporisation. There are no experimental data available for these quantities, but they can be estimated approximately from the melting and boiling points respectively. By using the rule due to Walden<sup>14</sup> that  $L_f/T = 13.5$  approximately for most organic substances, it is estimated that the molar heats of fusion of acridine (m.p. 111°) and phenazine (m.p. 172°) are 5.2 and 6.0 kcal. respectively. If Trouton's constant is taken as 22, the molar heats of vaporisation are 13.6 and 13.5 kcal. respectively. (Acridine<sup>15</sup> boils at 346°; phenazine<sup>16</sup> at 339°). Thus the heats of combustion of acridine and phenazine in the vapour state are 1596.6 kcal./mole. and 1480.4 kcal./mole. respectively. The heats of formation at constant pressure from the monatomic elements are thus calculated to be -2103.5 kcal. and -1998.4 kcal. respectively. The heats of formation calculated as the sum of the bond energies in the structures



and



respectively

are -1997.1 kcal./mole. and -1893.8 kcal./mole. (The heats of formation of carbon dioxide and water, the heats of dissociation of nitrogen and hydrogen, and the bond energies used in the calculations are those used by Pauling.<sup>17</sup>)

Thus the resonance energies of acridine and phenazine are respectively 106 kcal./mole. and 105 kcal./mole., which, within the limits of experimental error, are identical with the value given by Pauling<sup>18</sup> for anthracene (105 kcal./mole.).

The similarity of the resonance energies of acridine and anthracene suggests that their structures are more closely similar than those of pyridine and benzene or of quinoline and naphthalene.<sup>16</sup>

This work was carried out at the suggestion of Dr. A. Albert, whose interest and encouragement are much appreciated. The author also thanks Dr. D. P. Mellor and Mr. D. P. Craig for their interest and advice, and Miss J. Fildes for the microanalyses.

Thanks are also due to Acting-Professor H. S. H. Wardlaw of the Biochemistry Department of this University for making available the bomb calorimeter and to Bayer Pharma Ltd. for a gift of chemicals.

The author is indebted to the Commonwealth Research Fund for the award of a Scholarship under which the work was carried out.

### Summary.

The heats of combustion of a number of organic bases and their nitrates have been determined, and suitable methods for the preparation and combustion of the latter have been described. From the heats of combustion of acridine and phenazine, the resonance energies of these nuclei are found to be 106 and 105 kcal./mole. respectively, which values are identical with that for anthracene (105 kcal./mole.) to within the accuracy of the experimental technique employed.

<sup>14</sup> Walden, *Z. Elektrochem.*, 1908, 14, 713.

<sup>15</sup> Decker, *Ber.*, 1905, 38, 2493.

<sup>16</sup> Albert and Willis, *Nature* (in press).

<sup>17</sup> Pauling, *ibid.*, p. 54 *et seq.*

<sup>18</sup> Pauling, *ibid.*, p. 136.



## Résumé.

L'auteur détermine les chaleurs de combustion d'un certain nombre de bases organiques et de leurs nitrates et décrit les méthodes appropriées à la préparation et à la combustion de ces derniers. D'après les chaleurs de combustion de l'acridine et de la phénazine, il calcule les énergies de résonance de ces noyaux, qui sont respectivement 105 et 106 kcal./mol., valeurs identiques à celle de l'anthracène (105 kcal./mol.) dans le domaine d'erreur expérimentale de la technique employée.

## Zusammenfassung.

Die Verbrennungswärmen von mehreren organischen Basen und ihren Nitraten wurden bestimmt und für die letzteren geeignete Methoden für ihre Darstellung und Verbrennung beschrieben. Aus den Werten für die Verbrennungswärmen von Acridin und Phenazin folgt, dass die Resonanzenergie dieser Kerne 106, bzw. 105 kcal/Mol beträgt und also mit dem Werte für Anthracen (105 kcal/Mol) identisch ist, soweit dies die Präzision der experimentellen Bestimmungen feststellen lässt.

Chemistry Department,  
University of Sydney,  
Australia.

ELECTROSMOSIS, STREAMING POTENTIALS  
AND SURFACE CONDUCTANCE.

By A. J. RUTGERS AND M. DE SMET.

Received 23rd January, 1946.

1. In this paper we will describe some experiments, which have enabled us to settle a number of questions, which had arisen from former work in this field, described in two earlier communications.<sup>1, 2</sup> In the first of these papers, experiments on streaming potentials were described; capillaries of various diameters were used;  $\zeta$ -values were calculated from these experiments by the original Helmholtz-Smoluchowski formula indicated by  $\zeta_\sigma$

$$\frac{E}{P} = \frac{D\zeta_\sigma}{4\pi\eta\sigma_0}, \text{ or } \zeta_\sigma = \frac{4\pi\eta\sigma_0}{D} \frac{E}{P} \quad (1)$$

( $\sigma_0$  specific conductivity,  $\eta$  viscosity,  $D$  dielectric constant,  $E/P$  measured potential difference per unit of hydrostatic pressure); the  $\zeta$ - $c$ -curves, thus obtained, showed a marked dependence on the radius of the capillary used. From this we inferred that the "true"  $\zeta$ -values could not be obtained in this way, that formula (1) was incomplete, and had to be corrected for the influence of surface-conductivity, i.e.

$$\zeta = \frac{4\pi\eta}{D} \sigma_0 \left( 1 + \frac{2\sigma_w}{r\sigma_0} \right) \frac{E}{P} \quad (2)$$

We could, however, not use this expression in a straightforward way, as we had no means at our disposal for the measurement of  $\sigma_w$ , the specific surface-conductivity. We therefore proceeded in an indirect way, and calculated by extrapolation from our three  $\zeta_\sigma$ -values at every concentration

<sup>1</sup> Rutgers, *Trans. Faraday Soc.*, 1940, 36, 69; see also Rutgers, Verlende and Moorkens. *Proc. Kon. Akad. Wetensch. A'dam*, 1938, 41, 763; and Verlende *ibid.*, 1939, 42, 3.

<sup>2</sup> Rutgers and De Smet, *Trans. Faraday Soc.*, 1941, 41, 758.

a "true  $\zeta$ -value", which we will call  $\zeta_{ex}$ ; in this way  $\zeta_{ex}-c$  curves were obtained for solutions of KCl, HCl and  $\text{CaCl}_2$ , which differed in character from the  $\zeta_{\sigma}-c$  curves in that they showed no maximum.

We were well aware of the uncertainty of this extrapolation.

We therefore decided to measure  $\zeta$ -values in such a way that no questions of surface conductivity could arise. From the derivation of the Helmholtz-Smoluchowski formula for the velocity of electrosmosis

$$\frac{v}{E} = \frac{D\zeta_{E.O.}}{4\pi\eta} \quad . \quad . \quad . \quad . \quad . \quad (3)$$

or

$$\zeta_{E.O.} = \frac{4\pi\eta}{D} \frac{v}{E} \quad . \quad . \quad . \quad . \quad . \quad (4)$$

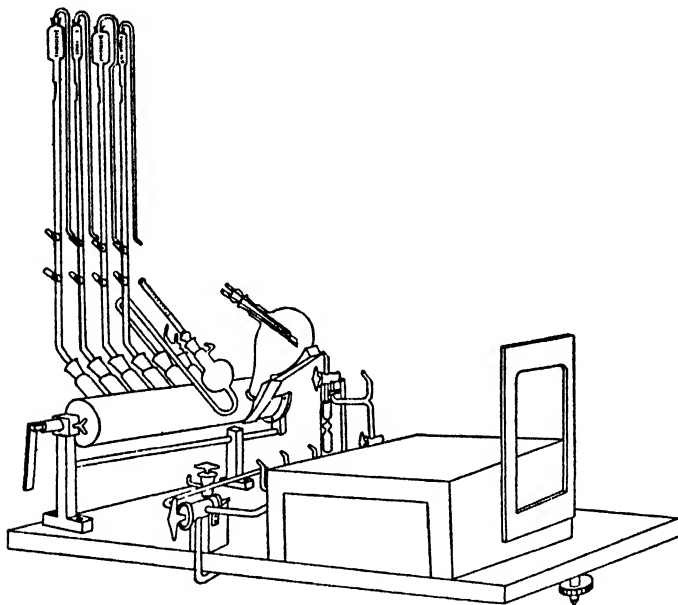


FIG. 1.

it is clear that no such influence can come into play in this phenomenon. We developed, therefore, a method of measurement of the electrosmotic velocity, and investigated a great number of electrolyte solutions between 0 and 10,000  $\mu$  eq./l. The results were published in the second of the papers just mentioned. The  $\zeta_{E.O.}-c$  curves obtained here agreed in character with the  $\zeta_{ex}-c$  curves in so far that they also did not show a maximum; there was however a numerical difference, as we pointed out in this second paper.

The present work was undertaken to remove this discrepancy, and to settle this problem. We decided to construct an apparatus which would allow us to measure in one and the same capillary streaming-potentials, electrosmotic velocity, and the total resistance  $R$  of the liquid in the capillary. For the evaluation of the experimental results we could then use the general formula for the streaming potential

$$\frac{E}{P} = \frac{D\zeta_R R}{4\eta} \frac{r^2}{l}$$

or

$$\zeta_R = \frac{4\eta l}{DRr^2} \frac{E}{P} \quad . \quad . \quad . \quad . \quad . \quad (5)$$

By substituting

$$\frac{1}{R} = \frac{\sigma_0 \pi r^2}{l} \quad . \quad . \quad . \quad (6)$$

or

$$\frac{1}{R} = \frac{\sigma_0 \pi r^2}{l} + \frac{\sigma_w 2 \pi r}{l} \quad . \quad . \quad . \quad (7)$$

eqn. (5) changes into eqn. (1) or eqn. (2).

If eqn. (7) is written in the form

$$\sigma_w = \frac{l}{2 \pi r} \left( \frac{1}{R} - \frac{\sigma_0 \pi r^2}{l} \right) \quad . \quad . \quad . \quad (8)$$

it is seen that our experiments will also give us values of the surface-conductivity.

2. In order to solve the first part of our problem, the measurement of streaming potentials (S.P.) and electrosmotic velocities (E.O.V.) in one and the same capillary, we constructed the apparatus shown in Fig. 1 and Fig. 2. There is almost no difference from our former apparatus for the measurement of E.O.V., nor is there any change in the experimental procedure.

The apparatus differs strongly, however, from our former streaming potential apparatus; for there the liquid flowed through a capillary of a length of about 70 cm. from a large reservoir into another. Owing to the high internal resistance, care had to be taken to prevent electrical leakage from one reservoir to the other. In the present apparatus the liquid flows through a capillary of only 5 cm. length in a vertical direction from the small sphere, containing the electrode  $E_1$ , to the other one, containing  $E_2$ . At the top of the capillary is sealed a reservoir to collect the liquid. Separation from the atmosphere is attained by the auxiliary tube  $T$ . Electrical leakage can only occur along the outer wall of the capillary between  $E_1$  and  $E_2$ , and from  $E_2$  along  $T$ , over the big reservoir to  $E_1$ . By carefully sponging the outer glass parts with benzene, and by coating the inner surface of tube  $T$  with paraffin, these leakage currents could easily be suppressed. Thus a relatively small inner resistance (5 cm. of capillary instead of 70 cm.) and a good outer insulation result automatically from the new construction. The streaming potentials were measured by means of a Cambridge electrometer valve potentiometer as in our previous work.

Special care was taken in the evaluation of the effective hydrostatic pressure. In the first place the applied pressure had to be corrected for the static counter-pressure of the liquid in the vertical system; a calibration was etched on the top reservoir, allowing an accurate reading of the position of the level of the liquid in the reservoir during the measurement of the streaming potential;

secondly, corrections were applied for the loss of pressure accompanying the flow of the liquid through the capillary parts of the system before and behind the measuring capillary.

3. The total resistance  $R$  of the liquid in the capillary was measured

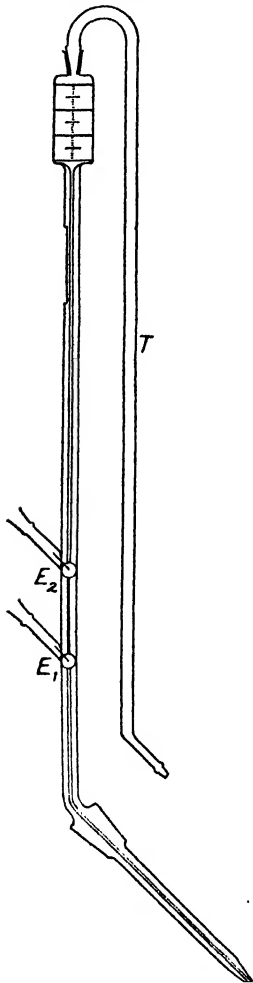


FIG. 2.

in the following way. A special resistance box was constructed, consisting of 10 units of 1  $M\Omega$ , 10 of 10  $M\Omega$ , 10 of 100  $M\Omega$  and 5 of 1000  $M\Omega$  (each unit of the last consisting of 10 resistances of 100  $M\Omega$ ). We express our thanks to Professor Holst, Director of the Natuurkundig Laboratorium der N.V. Philips' Gloeilampenfabrieken at Eindhoven, who put the resistances at our disposal.

A resistance of this box was connected in series with the unknown liquid resistance, a potential difference of about 20 v. applied, and the potential difference at the terminals of the known resistance measured by means of the Cambridge potentiometer; the known resistance was chosen some 15-100 times smaller than the resistance to be measured, so that the potential differences to be measured ranged from 1300-200 millivolts. Beforehand, the exact values of the resistances used had been carefully determined by a similar method, using a General Radio resistance box (up to  $10^6 \Omega$ ) and a Carpentier box (up to  $10^6 \Omega$ ) as a basis for the higher resistances. Every resistance was measured in triplicate, using three different values of the known resistance; concurrent results were obtained, as may be seen from Table I.

TABLE I.—TENSION OF BATTERY: 20.63 v.

Unknown Resistance.	Known Resistance.	Tension Measured.	Tension over Unknown Resistance.	R.
	$\Omega$	volts.	volts.	$\Omega$
Cap. D	1·083 10 <sup>8</sup>	0·2735	20·36	8·061 10 <sup>10</sup>
	3·218 10 <sup>8</sup>	0·794	19·84	8·042 10 <sup>10</sup>
	5·340 10 <sup>8</sup>	1·283	19·35	8·054 10 <sup>10</sup>
Cap. C	5·314 10 <sup>8</sup>	0·461	20·17	2·325 10 <sup>10</sup>
	10·83 10 <sup>8</sup>	0·918	19·71	2·326 10 <sup>10</sup>
	10·14 10 <sup>8</sup>	1·3415	19·29	2·320 10 <sup>10</sup>
Cap. B	3·107 10 <sup>8</sup>	0·5205	20·11	1·200 10 <sup>10</sup>
	5·314 10 <sup>8</sup>	0·8715	19·76	1·205 10 <sup>10</sup>
	7·435 10 <sup>8</sup>	1·1945	19·44	1·210 10 <sup>10</sup>
Cap. A	1·063 10 <sup>8</sup>	0·4485	20·18	4·782 10 <sup>9</sup>
	2·056 10 <sup>8</sup>	0·859	19·77	4·734 10 <sup>9</sup>
	3·107 10 <sup>8</sup>	1·263	19·37	4·766 10 <sup>9</sup>

4. The measurements were carried out on solutions of KCl, KOH, HCl, CaCl<sub>2</sub> and Al(NO<sub>3</sub>)<sub>3</sub> at a number of concentrations between 0 and 200  $\mu$  eq/l. The measurements were performed on 4 Jena 16<sup>III</sup>-capillaries at the same time, length about 5 cm., radius about 0.2, 0.15, 0.1 and 0.05 mm. In Fig. 3 a capillary is represented schematically, while the exact dimensions

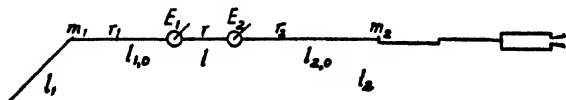


FIG. 3.

(in cm.) of the capillaries A, B, C and D used are given in Table II. (For the meaning of  $r$ ,  $l$ ,  $r_1$ ,  $r_2$ ,  $l_1$ ,  $o$ ,  $l_2$ ,  $o$ , vide <sup>2</sup>;  $l_1$  is the total length of the capillary to the left of  $E_1$ ;  $l_2$  the length to the right of  $E_2$ ; these lengths determine the loss of pressure in the measurement of the streaming potential.)

The last quantity in the table,  $\pi^*/I$ , needs some explanation. Preliminary experiments brought to light the following difficulty. If the values for  $\sigma_0$  and  $R$  were substituted in eqn. (8), then for the higher concentrations

TABLE II.

	A.	B.	C.	D.
$r$	0.0243	0.01502	0.01092	0.00516
$r_1; r_2$	0.05326; 0.05258	0.05116; 0.05057	0.0240; 0.02618	0.02287; 0.02270
$l$	4.64	4.81	5.17	4.72
$l_{1,0}; l_{2,0}$	7.7; 14.7	7.2; 13.5	8.1; 14.1	6.75; 13.4
$l_1; l_2$	23.3; 25.0	22.3; 24.1	23.5; 24.8	22.0; 24.0
$\pi r^2/l$	38.62 $10^{-8}$	14.35 $10^{-8}$	7.185 $10^{-8}$	1.746 $10^{-8}$

and the wider capillaries the values of  $\sigma_w$  decreased, and finally became negative, an unacceptable result. This must be caused by experimental errors, leading to too large a value of  $R$ , or of  $\pi r^2/l$ , or of both.

As for the value of  $R$  our results were influenced by the polarisation accompanying every D.C. measurement; we therefore took measures to reduce this by depolarising by A.C. between two measurements, and by working in such a way that the current in the circuit flowed only for a very short time.

As for the value of  $\pi r^2/l$ , a certain inaccuracy arises from the dimensions of the capillary, as the widening part ran over 1.2 mm. of the total

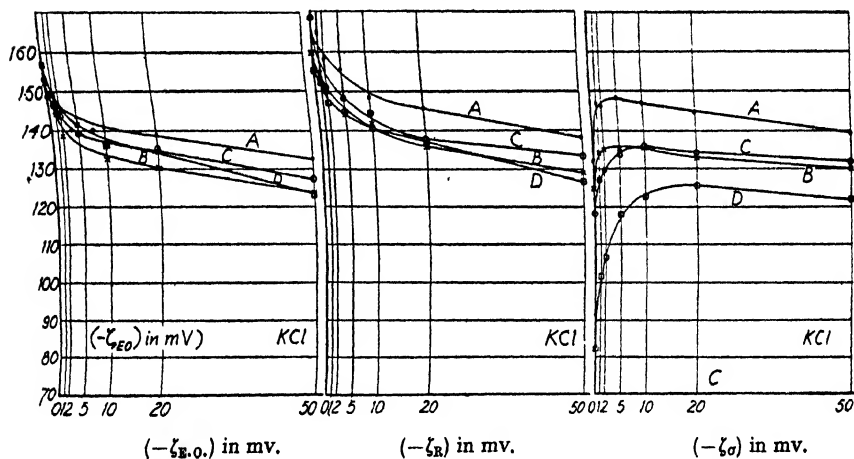


FIG. 4.

length of 50 mm. We therefore decided to take the value of  $\pi r^2/l$  from a measurement of the total resistance when the capillary was filled with a normal solution of KCl, the surface-conductivity being negligible in that case. Only in the case of capillaries A and B was there any appreciable difference between the values of  $\pi r^2/l$  obtained in this way.

The measurements were performed as follows. After the measurement of the specific conductivity  $\sigma_0$  by means of a Kohlrausch bridge, the capillaries were brought into a horizontal position, and the E.O.V. was measured; then  $\sigma_0$  was measured again, the capillaries brought into their vertical position, and liquid passed through under a considerable pressure; the excess pressure was reduced to some 0.5 cm. of water, and  $R$  was measured (in triplicate); then the S.P. was measured under 3 or 4 different pressures; followed by a measurement of  $R$ ; the value obtained should not differ more than a few per cent. from the previous one; all these measurements were

carried out for the four capillaries; they then were emptied by pressure, and  $\sigma_0$  was measured again.

Thus one concentration was finished; some drops of a more concentrated solution of the electrolyte were passed, by pressure of purified nitrogen, into the large reservoir, and the next concentration investigated. In one day one concentration could be finished; the temperature in the room was kept constant at  $22.5^\circ \text{C}$ .

5. The results, obtained with solutions of KCl between 0 and  $200 \mu \text{eq./l.}$  are given in full in Table III and represented graphically in Fig. 4 (a, b, c), and in Fig. 5; the results for the solutions of HCl, KOH,  $\text{CaCl}_2$  and  $\text{Al}(\text{NO}_3)_3$  were quite similar to those obtained for KCl; we therefore communicate only the results for the narrowest capillary D in the form of Fig. 6, 7, 8, and 9.

As for the data, connected with  $\sigma_w$ , given in the second half of Table III,  $R_\sigma$  is an abbreviation for  $l/\pi r^2 \sigma_0$ ; here  $l/\pi r^2$  had been determined by an A.C. measurement of resistance, as described above; nevertheless, at higher concentrations values of  $R_\sigma/R$  less than 1 invariably show themselves, sooner for the wider, later for the narrower capillaries; this is

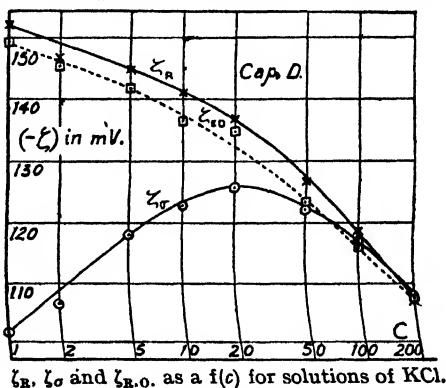


FIG. 5.

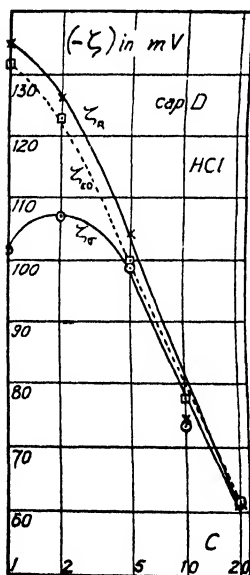


FIG. 6.

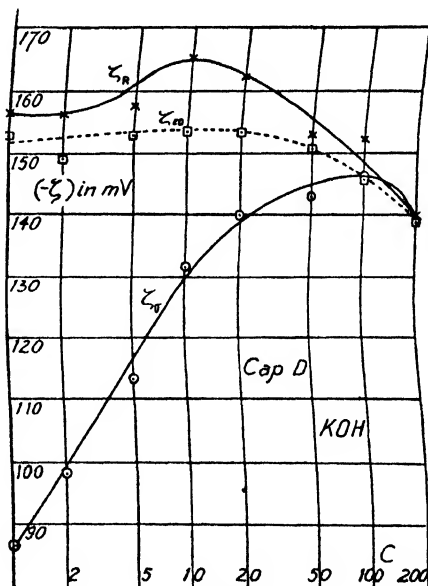


FIG. 7.

caused by the fact, that the D.C. measurement of  $R$ , in which polarisation cannot be avoided, gives too large values for  $R$ ; we consider therefore that only the values of  $\sigma_w$  at the lower concentrations deserve confidence; a new apparatus has been constructed to determine the values of  $\sigma_w$  by means of an A.C. measurement.

TABLE III.—KCl.

c.	A.			B.			C.			D.		
	$-\zeta_{E.O.}$	$-\zeta_R$	$-\zeta_G$	$-\zeta_{E.O.}$	$-\zeta_R$	$-\zeta_G$	$-\zeta_{E.O.}$	$-\zeta_R$	$-\zeta_G$	$-\zeta_{E.O.}$	$-\zeta_R$	$-\zeta_G$
0	149	159	132	152	160	125	153	168	118	156	155	82
1	147	165	147	144	155	134	147	153	127	149	152	101
2	146	158	146	139	150	135	143	151	129	145	147	106
5	144	155	148	139	144	135	139	148	134	142	145	118
10	141	148	147	132	141	135	136	144	136	136	141	123
20	139	145	145	130	136	133	136	138	134	135	137	126
50	133	138	139	124	129	121	127	133	132	123	127	122
100	122	129	132	116	123	125	119	126	126	116	119	117
200	118	130	134	110	113	117	113	120	122	107	107	108

c.	$-\zeta_{E.O.}$				$-\zeta_R$				$-\zeta_G$			
	A.	B.	C.	D.	A.	B.	C.	D.	A.	B.	C.	D.
0	149	152	153	156	159	160	168	155	132	125	118	82
1	147	144	147	149	165	155	153	152	147	134	127	101
2	146	139	143	145	153	150	151	147	146	135	129	106
5	144	139	139	142	155	144	148	145	148	135	134	118
10	141	132	136	136	148	141	144	141	147	135	136	123
20	139	130	136	135	145	136	138	137	145	133	134	126
50	133	124	127	123	138	129	133	127	139	130	132	122
100	122	116	119	116	129	123	126	119	132	125	126	117
200	118	110	113	107	130	113	120	107	134	117	122	108

c.	$\sigma_0 \cdot 10^7$		$R \cdot 10^{-9}$				$R_G \cdot 10^{-9}$			
	A & C.	B & D.	A.	B.	C.	D.	A.	B.	C.	D.
0	2.661	2.817	8.13	19.31	36.6	107.8	9.86	24.7	52.3	203.3
1	5.172	4.958	4.46	12.12	22.3	76.9	5.01	14.05	26.9	115.5
2	6.748	6.711	3.54	9.32	17.7	61.7	3.84	10.38	20.6	85.3
5	12.94	10.94	2.26	5.91	11.48	42.4	2.37	6.37	12.72	52.3
10	17.88	17.79	1.43	3.73	7.31	27.9	1.45	3.91	7.78	32.2
20	31.42	31.39	0.819	2.17	4.28	16.7	0.824	2.22	4.43	18.2
50	71.41	71.45	0.366	0.980	1.927	7.73	0.362	0.975	1.949	8.02
100	136.6	136.0	0.193	0.518	1.017	4.14	0.189	0.512	1.019	4.21
200	205.9	268.7	0.100	0.268	0.528	2.13	0.097	0.259	0.523	2.13

c.	$R_G/R = 1 + \frac{2\sigma_w}{\pi\sigma_0}$				$\sigma_w \cdot 10^{10}$			
	A.	B.	C.	D.	A.	B.	C.	D.
0	1.21	1.28	1.43	1.89	6.92	5.93	6.23	6.44
1	1.12	1.16	1.21	1.50	7.67	5.96	5.87	6.42
2	1.08	1.11	1.17	1.38	7.72	5.75	6.12	6.65
5	1.05	1.08	1.11	1.23	6.38	6.33	6.51	6.63
10	1.01	1.05	1.06	1.15	3.04	6.41	6.35	7.02
20	1.01	1.02	1.03	1.09	2.29	4.95	6.00	7.29
50	0.99	0.99	1.01	1.04	—	—	4.29	6.82
100	0.98	0.99	1.00	1.02	—	—	1.49	5.61
200	0.97	0.97	0.99	1.00	—	—	—	—

## 6. Discussion of Results.

The graphs speak for themselves; we stress the following points.

1.  $\zeta_{R.O.}-c$  curves practically coincide for capillaries of different radii; the same is true for the  $\zeta_R$ -curves; finally the  $\zeta_{R.O.}$  and  $\zeta_R$ -curves coincide with one another; from this we conclude that reliable  $\zeta$ -values can be obtained in either of the following two ways. (a) From the measurement of the electrostatic velocity by means of eqn. (4). (b) From the measurement of streaming potentials, in combination with the measurement of the total resistance, by means of eqn. (5).

2. On the other hand, the  $\zeta_{\sigma}-c$  curves show clearly the dependence on the radius of the capillary, as pointed out by Rutgers, Verlende and Moor-  
kens; they show the maximum, already observed by previous workers, to which Stern has paid attention in his theory of the double layer;<sup>3</sup> we have

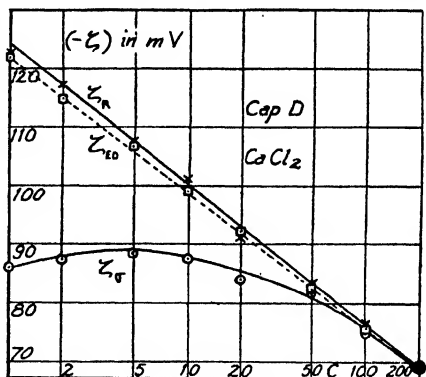


FIG. 8.

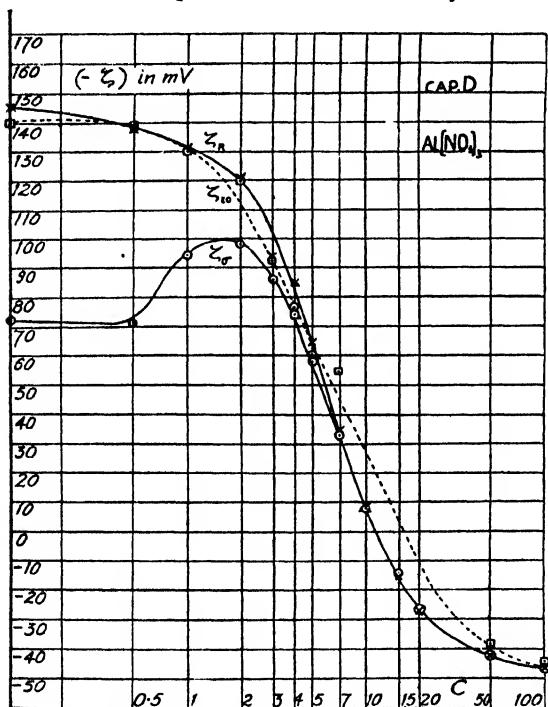


FIG. 9.

now proved that this maximum is caused by the inadequacy of the original Helmholtz-Smoluchowski formula (1); as soon as the more general eqn. (5) is used, the maxima disappear, and in every respect concordant  $\zeta_R$  and  $\zeta_{R.O.}$  curves are obtained.

3. The best experimental results are obtained with the narrowest capillaries.

4. The surface-conductivity can account for 60 % of the total conductivity for the narrowest capillary and the lowest concentration. Our present experiments, although settling the problem of  $\zeta_{R.O.}$ ,  $\zeta_R$  and  $\zeta_{\sigma}$ , give only little information with respect to surface-conductivity; at higher concen-

trations our D.C. measurements become unreliable, especially for the wider

<sup>3</sup> Z. Elektrochem., 1924, 30, 508.



capillaries. We have started work with a special apparatus which will enable us to perform accurate D.C. and A.C. measurements on surface-conductivity.

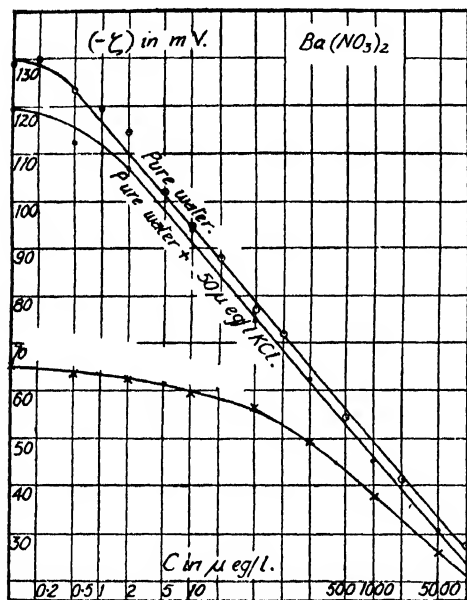
### 7. Electrochemical Interpretation of Elektrokinetic Phenomena.

The present work has proved the correctness of our method of determining  $\zeta$ -potentials from electrophoresis; <sup>2</sup> in that paper <sup>2</sup> a great many results obtained with 1-1, 2-1, 3-1, and 4-1 valent electrolytes were described; we are therefore now faced with the task of giving a theoretical interpretation of these results.

We have already pointed out that a comparison of the results, obtained

with HCl, KOH and KCl, leads to an electrochemical interpretation: the glass-wall, or in any case its surface-layer, acts in the first instance as a H-ion electrode.

If we study the influence of "indifferent" electrolytes, we see, that at 100  $\mu$  eq./l. of a 1-1 valent electrolyte, the role of the H-ions as a potential-determining electrolyte is taken over by the foreign ions added to the solutions, i.e. by the K, Ag and  $\text{NH}_4$  ions; that it is taken over already at 1  $\mu$  eq./l. of a 2-1 valent electrolyte by the Zn, Mg, Ba, Ca ions, etc., and at 0.1  $\mu$  eq./l. of a 3-1 valent electrolyte by the La, Ce, etc. ions. This is most simply explained in this way: the negative potential of the wall causes a concentration of the Zn, Mg, La, or Ce ions at the



Lowest curve refers to pure water +  
50  $\mu$  eq./l. HCl.

FIG. 10.

wall; the factor  $e^{-\frac{e\zeta}{kT}}$  has the same value for H, K, Ag

or  $\text{NH}_4$  ions but a bigger value, however, for 2- or 3-valent cations. If we make the plausible assumption that the intrusion of foreign ions in the glass-wall is determined by their concentration just outside, we see that the ions of higher valency have a great advantage over the monovalent ions and that they act at a much lower concentration as potential-determining ions. This interpretation of our  $\zeta$ -c curves proved to be corroborated by the following experiment. If  $\text{Ba}(\text{NO}_3)_2$  is added to pure water, it destroys the influence of the H-ions as potential-determining electrolyte at 1  $\mu$  eq./l. If our ideas are correct, we will have to add much more  $\text{Ba}(\text{NO}_3)_2$  to a solution of 50  $\mu$  eq./l. HCl in water, in order that it may become potential-determining against this much stronger force of H ions. Experiment proved that this is the case. In order to exclude all ambiguity, we repeated the experiment with  $\text{Ba}(\text{NO}_3)_2$  added to a solution of 50  $\mu$  eq./l. KCl in water. Now there was not much difference with the behaviour in pure water (Fig. 10). We may say that in all these cases an electrochemical explanation of electrokinetic experiments is successful.

### Summary.

Electroosmotic velocity, streaming potential and resistance have been measured for one and the same capillary. The measurements were carried out with four capillaries of various diameters, for solutions of KCl, HCl, KOH,  $\text{CaCl}_2$  and  $\text{Al}(\text{NO}_3)_3$ , at concentrations between 0 and 200  $\mu$  eq./l.

From the experimental data we calculated the values of  $\zeta_{\text{E.O.}}$ ,  $\zeta_\sigma$  and  $\zeta_{\text{R}}$  (definitions see above) as a function of concentration. In all cases a satisfactory agreement between the curves for  $\zeta_{\text{E.O.}}$  and  $\zeta_{\text{R}}$  appeared to exist; this agreement was especially good for the narrowest capillary.

The  $\zeta_\sigma$ - $c$  curves, however, deviate strongly from the curves just mentioned; hence the classical Helmholtz-Smoluchowski formula giving  $\zeta_\sigma$  must be replaced by the expression, giving  $\zeta_{\text{R}}$ .

The well-known maximum in the  $\zeta_\sigma$ - $c$  curves must be ascribed to the inadequacy of the  $\zeta_\sigma$  formula; the concordant  $\zeta_{\text{E.O.}}$ - $c$  and  $\zeta_{\text{R}}$ - $c$  curves do not show such a maximum.

The deviation between the  $\zeta_\sigma$  and the  $\zeta_{\text{R}}$  curves is caused by the surface conductivity  $\sigma_w$ . Values of  $\sigma_w$  have been obtained from our simultaneous measurements of  $\sigma$  and  $R$ .

Finally an electrochemical explanation of the  $\zeta$ - $c$  curves is put forward, in connection with which a few special measurements have been carried out.

### Résumé.

La vitesse électro-osmotique, le potentiel d'écoulement et la résistance ont été mesurés pour le même capillaire avec des solutions (0 à 200 micro-équivalents/litre) de KCl, KOH,  $\text{CaCl}_2$  et  $\text{Al}(\text{NO}_3)_3$ . Les potentiels-zeta,  $\zeta_0$  (de la formule classique de Helmholtz-Smoluchowski),  $\zeta_{\text{E.O.}}$  (de l'équation de Helmholtz-Smoluchowski pour la vitesse électro-osmotique) et  $\zeta_{\text{R}}$  (pour le potentiel d'écoulement) sont calculés comme des fonctions des concentrations. Les courbes en fonction de la concentration de  $\zeta_{\text{E.O.}}$  et  $\zeta_{\text{R}}$  coïncident, mais s'écartent de celle de  $\zeta_0$ ; ceci est attribué à l'imperfection de la formule classique (pour  $\zeta_0$ ), où la conductivité de surface est négligée.

### Zusammenfassung.

Elektroosmosegeschwindigkeit, Strömungspotential und elektrischer Widerstand wurden für dieselbe Capillarröhre mit Lösungen (0-200 Mikrogrammäquivalente/l.) von KCl, HCl, KOH,  $\text{CaCl}_2$  und  $\text{Al}(\text{NO}_3)_3$  gemessen. Die  $\zeta$ -Potentiale,  $\zeta_0$  (aus der klassischen Helmholtz-Smoluchowski Formel),  $\zeta_{\text{E.O.}}$  (aus der Helmholtz-Smoluchowskischen Gleichung für Elektroosmosegeschwindigkeit) und  $\zeta_{\text{R}}$  (aus dem Strömungspotential) wurden als Funktionen der Konzentration berechnet. Die  $\zeta_{\text{E.O.}}$ - $c$  und  $\zeta_{\text{R}}$ - $c$  Kurven sind identisch, aber stimmen nicht mit den  $\zeta_0$ - $c$  Kurven überein, was der Unzulänglichkeit der klassischen Formel (für  $\zeta_0$ ), in der die Oberflächenleitfähigkeit vernachlässigt ist, zugeschrieben wird.

*Laboratory of Physical Chemistry,  
The University of Ghent,  
Belgium.*

# THE CATALYTIC POLYMERISATION OF N-BUTYL VINYL ETHER.

BY D. D. ELEY AND D. C. PEPPER.

Received 22nd January, 1946.

This polymerisation was first investigated by Chalmers,<sup>1</sup> who found that it was catalysed by iodine or Friedel-Crafts catalysts, and that under certain conditions the reaction could proceed with explosive rapidity. In this paper we record data obtained in 1942 on the rates, "chain lengths", and thermal characteristics of the reaction as catalysed by stannic chloride. Although incomplete, these data, we believe, enable us to draw certain interesting conclusions about the mechanism of the reaction, and form a basis for a systematic investigation of the vinyl ethers which is now in hand.

## Experimental.

Apart from a few experiments on undiluted monomer, our procedure was to dissolve the monomer in petrol ether in a boiling tube and bring to temperature equilibrium in the thermostat. At zero time the catalyst solution (usually 2 %  $\text{SnCl}_4$  in petrol ether) was added, vigorously stirred, and the mixture rapidly transferred to an Ostwald viscometer in the thermostat. This transference was facilitated by the presence of an induction period, before reaction. Subsequently the increase in relative viscosity ( $\eta_r$ ) of the solution was followed as a function of time. To convert this to the concentration of polymer-time relation we assumed the Arrhenius equation

$$\log_{10} \eta_r = KC,$$

was applicable (compare Foord<sup>2</sup>), where  $K$  is a constant and  $C$  the concentration of polymer in base moles/litre.

TABLE I.

$\bar{P}$	1.69	2.49	2.85	3.5	4.05	4.6	6.3
$1/K$	1.94	1.48	1.33	1.23	1.09	1.01	0.82

Values of  $1/K$  were determined from the  $\eta_r$  of the final completely polymerised solution where the polymer concentration was known, and are listed in Table I. They show, of course, a dependence on viscosity/molecular weight as measured by  $\bar{P}$  (see Table I). In two cases

where the reaction curve was determined by precipitation of the polymer and weighing, a very good check was obtained with the reaction curve obtained by calculation from  $\eta_r$ . The growth in molecular weight during the course of the reaction recorded later introduces an uncertainty into the reaction curve in the earliest stages of reaction. A main source of inaccuracy in the values of the maximum rates listed lies in the drawing of the tangents, and this is estimated at  $\pm 30\%$ .

The temperature during the course of the reaction was followed by a thin glass-jacketed thermocouple in the lower bulb of the viscometer.

After reaction the mixture was shaken with water to destroy the catalyst, dried over  $\text{CaCl}_2$ , the solvent distilled off and the final traces of

<sup>1</sup> Chalmers, *Can. J. Res.*, 1932, 7, 464.

<sup>2</sup> Foord, *J. Chem. Soc.*, 1940, 48.

monomer and solvent removed by pumping at 15 mm. Hg and 90° c. At the highest catalyst concentrations used it was found necessary to shake with 50 % aqueous alcohol to eliminate the catalyst, otherwise further reaction occurred. As a measure of the average molecular weight or chain length of the product, we employ  $\bar{P}$ , the specific viscosity/concentration ratio in petrol ether solution, taken at a standard  $\eta_{sp}$  value of 0.1. The  $\bar{P}$  values refer to the polymer concentration in base moles/litre.

The *n*-butyl vinyl ether (b.p. 92° c.) was kindly supplied by I.C.I. (Dyestuffs Division), and had been freed from butanol by several distillations off sodium. In some experiments listed the petrol ether used was of A.R. quality. In other experiments the A.R. material was carefully purified by shaking with concentrated  $H_2SO_4$ , washing with water, drying and distilling (b.p. 62-72° c.). Unlike the A.R. solvent, the purified solvent did not decolourise bromine water, or give any gum with  $SnCl_4$  or  $P_2O_5$ . B.D.H. stannic chloride was used without further purification.

Concentration of monomer  $[M]$  is given in moles per litre, and that of catalyst  $[C]$  or inhibitor  $[I]$  in millimoles per litre (m. mol.).

## Results.

(1) **Undiluted Monomer.**—Because of the great viscosity of the undiluted reaction product, only qualitative experiments were made in boiling tubes. In accordance with Chalmers,<sup>1</sup>  $SnCl_4$ ,  $I_2$  and  $SbCl_5$  were found to be active catalysts at a concentration of 1 m. mol.,  $SnCl_4$  being by far the most active. Benzoyl peroxide was without effect, even under extreme conditions (160 m.mol., 92° c.). Accordingly, further investigations were limited to the action of  $SnCl_4$ .

TABLE II.

Initial $T^\circ$ c.	20		60		90	
$[C]$ , m. mol.	0.86	1.71	1.03	3.43	1.03	7.72
$\bar{P}$	3.9	2.4	3.3	1.8	2.7	1.1

In undiluted monomer the reaction has the following general characteristics. There appears to be a threshold catalyst concentration of about 0.6 m. mol., below which reaction occurs only very slowly, e.g. at  $[C] = 0.34$  m. mol. and 25° c. the polymerisation is hardly complete in 1 week. Above this threshold value there is a short induction period (*ca.* 1 min.) followed by a very rapid reaction, the temperature rising by 70-90° c., and then falling back to the thermostat temperature, all within a period of 5-10 minutes. By this time the reaction is apparently complete, but the  $\bar{P}$  values in Table II were determined on products which had stood a subsequent 24 hours before isolation.

The values in Table II are listed for completeness only, since the marked temperature rise precludes any real decision as to whether a true effect of  $[C]$  exists or not. As to the threshold value of  $[C] \sim 0.6$  m. mol., this was found to stay roughly unchanged, over 20-90° c., but to increase on cooling to -80° c. While a marked phenomenon in the polymerisation of undiluted monomer, this threshold may well be an artefact, due to an impurity effect combined with the insensitive method employed. No such effect appeared later for the sensitive viscosity measurements in purified petrol ether, although something similar appears for A.R. petrol ether as solvent, namely an exceedingly long induction period at low values of  $[C]$ .

(2) **Monomer Dissolved in A.R. Petrol Ether.**—While the A.R. petrol ether was shown to contain certain impurities which affected the reaction, the results listed here are of interest when taken in conjunction with those for the purified solvent.

The first observation is quite general for A.R. or purified solvent. Fig. 1 shows the course of a typical experiment from which it can be seen that the maximum rate of polymerisation (maximum slope of  $\log_{10} \eta_r - t$  curve) and the maximum temperature occur simultaneously. The dotted

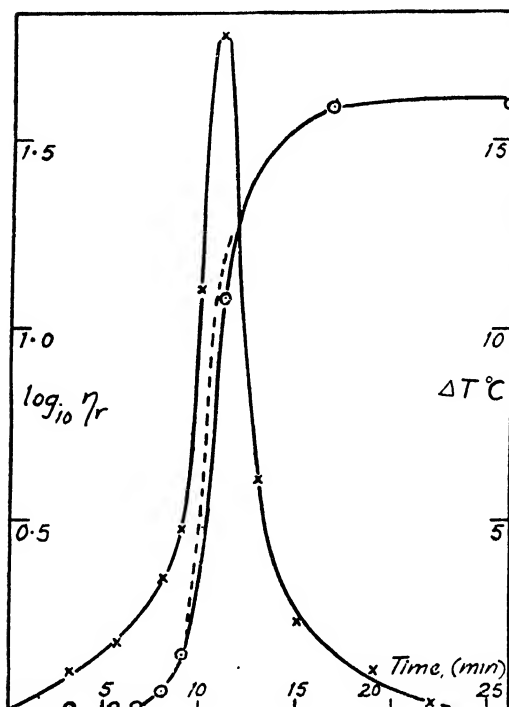


FIG. 1.—Showing the course of polymerisation (circles) and temperature rise. An appreciable exothermic reaction occurs during the induction period. The maximum temperature coincides approximately with the maximum rate.

line shows  $\log_{10} \eta_r$  corrected to 25° c. and in calculating the maximum rate this correction may usually be neglected. From Fig. 1 we see that a rise in temperature is observed before any appreciable increase in  $\eta_r$  occurs. This rise we consider sufficiently large to be accountable only by polymerisation of a part (~ 3%) of the monomer. It is too large to be due to a complex formation  $\text{SnCl}_4$ -monomer, or to a reaction with impurity. If the polymerisation leads to short chains only, in this time, then  $\eta_r$  will be little affected.

Table III summarises our results on the effects of cata-

TABLE III.—EFFECT OF CATALYST CONCENTRATION,  $[\text{M}] = 1.97 \text{ MOL. } 25^\circ \text{ C.}$

Expt.	[C] m. mol.	I.P. min.	Maximum Rate mole/litre/min.	$\bar{P}$ .
26	0.051	> 1000	—	—
27	0.146	32	0.042	4.4
34	0.257	6	0.33	4.5
29	0.471	4.5	0.45	3.4
30	0.772	1.0	0.37	2.9
53	2.36	—	—	1.9

lyst concentration (I.P. signifies induction period). We would draw attention to the large increase in I.P. at the lowest value of [C], and also to the upper limit of the maximum rate observed  $\sim 0.4 \pm 0.1 \text{ moles litre}^{-1} \text{ min.}^{-1}$ . Both these effects arise from the presence of impurity in the solvent, and disappear when these are removed.

(3) **The Effect of Added Inhibitor.**—To see how far the characteristics so far observed arose from impurities, a number of substances were

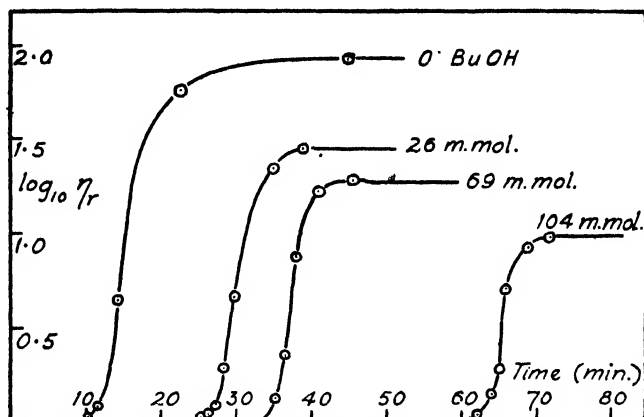


FIG. 2.—Effect of added inhibitor, butyl alcohol.

tried out as inhibitors. Benzene and chloroform had a negligible effect, but the effect of *n*-butyl alcohol was most marked. The results are shown in Fig. 2 and Table IV.

TABLE IV.—EFFECT OF *n*-BUTYL ALCOHOL.  $[M] = 1.97$  MOL.  $[C] = 0.257$  M. MOL.  $25^\circ \text{C}$ .

Expt.	[BuOH] m. mol.	I.P. min.	Maximum Rate mole/litre/min.	$\bar{P}$ .
39	0	8	0.48	5.0
46	26	24	0.53	2.8
49	69	33	0.56	2.5
50	104	61	0.93	1.7

(4) **Monomer Dissolved in Purified Petrol Ether.**—The

reaction was investigated over a range of catalyst concentrations, the results being shown in Fig. 3 and Table V. At the lower catalyst concentrations

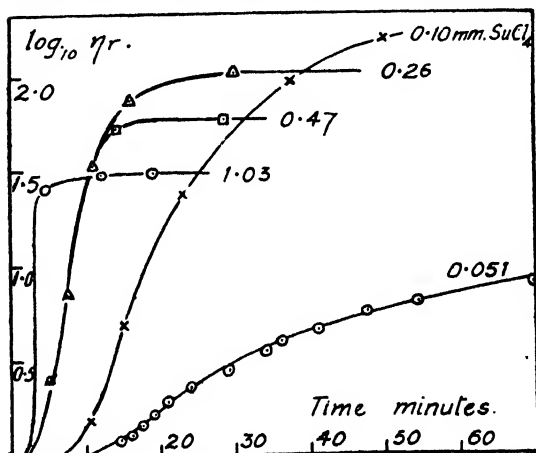


FIG. 3.—Effect of catalyst concentration on polymerisation in purified petrol ether.  $25^\circ \text{C}$ .  $[M] = 1.97$  mol.

where the temperature rise is not too large, the maximum rate increases vary roughly directly with  $[C]$  (Fig. 4), while  $\bar{P}$  is but little affected by  $[C]$ . The anomalously low values of  $\bar{P}$  for  $[C] = 0.051$  is probably associated

with the observed fact that, at this very low catalyst concentration, reaction had only proceeded to 40 % polymer; in all the other cases there

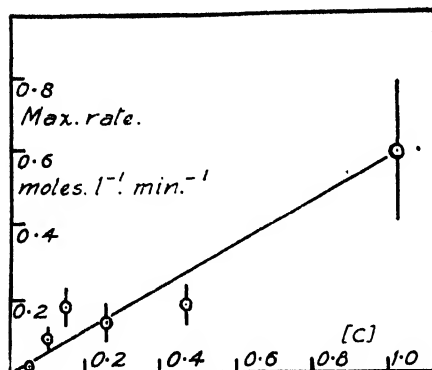


FIG. 4.—The effect of catalyst concentration ( $[C]$  = m. mol. per litre) on maximum rate of polymerisation.

was effectively 100 % polymerisation. At the higher values of  $[C]$ ,  $\bar{P}$  is reduced approximately as  $[C]^{-1}$  (Fig. 5), but the departure from isothermal conditions rules out any discussion of this observation at present.

#### (5) Growth of Molecular Weight in the Reaction.

Samples were withdrawn during a typical reaction (conditions as in Expt. 62-65), and immediately shaken with water to stop the reaction. The products were isolated and percentage polymerisation and  $\bar{P}$  are listed in Table VI. The percentage polymerisation agreed excellently with that

calculated from  $\eta_r$ . The results show that  $\bar{P}$  increases during the course of the reaction.

TABLE V.—EFFECT OF CATALYST CONCENTRATION IN PURIFIED PETROL ETHER.  $[M] = 1.97$  MOL.  $25^\circ\text{C}$ .

Expt.	$[C]$ m. mol.	I.P. min.	Maximum Rate mols./litre/min.	$\Delta T^\circ\text{C}$ (max).	$\bar{P}$ .
66	0.051	10	0.03	0.5	4.1
69	0.051	11	0.02	0.25	4.3
68	0.10	7	0.09	3	6.7
67	0.15	4.5	0.18	6.5	6.3
62-65	0.26	3.5	0.15	8	6.2
70	0.47	$\sim 2$	0.18	17	4.6
71	1.03	$< 2$	0.59	—	3.5
74	2.14	—	—	62	2.7
77	4.28	—	—	62	2.6
78	4.28	—	—	62	2.5

(6) Branching of Chains.—In early experiments using A.R. solvent it was found that if a

reaction mixture containing a high concentration of catalyst ( $[C] = 1.37$  m. mol.) was worked up without destroying the catalyst with water, the final product swelled but did not dissolve in petrol ether. This we consider indicative of cross-linking or chain branching having occurred under the influence of the stannic chloride at  $90^\circ\text{C}$ . In later experiments using purified

TABLE VI.— $[M] = 1.97$  MOL.  $[C] = 0.26$  M. MOL.  $25^\circ\text{C}$ .

Expt.	Time of Reaction min.	% Polymerised.	$\bar{P}$ .
75	8	36	4.3
	10	64	5.96
	14	81	6.16
	$\infty$	85	5.92
76	7	30	4.63
	9	61	6.14
	11	78	6.14

solvent, a similar though less marked effect was observed; e.g. a polymer

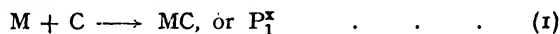
isolated after simple water treatment had  $\bar{P} = 3.7$ , whereas if the catalyst were more thoroughly removed by aqueous alcohol its  $\bar{P}$  value was only 2.7. Even at the low  $[C]$  value of 0.26 m. mol. a water-treated product had  $\bar{P} = 6.0$ , while the polymer from an untreated sample had  $\bar{P} = 6.5$ .

### Discussion.

While Chalmers<sup>1</sup> was of the opinion that these polymers had a ring constitution, it seems more reasonable nowadays to assume that they are long chain molecules similar to the "radical polymerised" vinyl derivatives. At present we can only estimate the Staudinger constant (Kemp and Peters<sup>2</sup>) as  $K_m = 4.8 \times 10^{-4}$ , and so obtain molecular weight values of 5200 for  $\bar{P} = 2.5$  and 14,000 for  $\bar{P} = 6.7$ . With these values one calculates that in Expt. 68 one molecule of  $\text{SnCl}_4$  starts on the average 140 chains, and in Expt. 78, 9 chains. While undoubtedly a possible large error is attached to this estimate of molecular weights, the conclusion that one catalyst molecule may start a number of chains seems clear.

This polymerisation may be supposed to be of the polarised bond,<sup>3,4</sup> rather than the radical type, suggesting certain modifications of the usual scheme of successive reactions. It will be shown that the modifications that one would naturally expect in fact lead to a scheme in general qualitative agreement with the observed facts. More than this cannot be attempted until a body of isothermal rate data is available.

The suggested scheme is



[ $P$  = polymer.  $P^x$  = active polymer.  $M$  = monomer.  $C$  = catalyst.  
 $I$  = inhibitor.]

We may suppose the rate of initiation (1) to be relatively more rapid than in radical reactions, since it is known that complexes between halides and organic molecules are usually formed rapidly. On the other hand, the rate of propagation (2) may be expected to be relatively slower.<sup>5</sup> Unlike "radical" polymerisations, a spontaneous termination process (3a) is more probable than the mutual process often observed with radicals.<sup>6</sup> The catalyst is then liberated to start further chains. Mechanism (3b) operates in the presence of inhibitor. It is essentially a transfer mechanism<sup>7</sup> required to explain the result that inhibitor<sup>\*</sup> reduces the molecular weight of the product while, if anything, raising the maximum rate. This result is quite at variance with Foord's results<sup>8</sup> on the inhibition of the thermal polymerisation of styrene, which probably involves radicals.

A relatively high ratio of initiation to propagation would lead us to expect a number of kinetic features not usually found in typical radical polymerisations. These are, a true induction period (not due to impurity), followed by an accelerating reaction passing through a maximum rate, and a growth of molecular weight during the course of the reaction. In such a case the stationary state method cannot be usefully applied (cf. Ginell

<sup>1</sup> Kemp and Peters, *Ind. Eng. Chem.*, 1942, **34**, 1097.

<sup>2</sup> Hunter and Yohe, *J. Amer. Chem. Soc.*, 1933, **55**, 1248. Whitmore, *Ind. Eng. Chem.*, 1934, **26**, 94.

<sup>3</sup> Price, *Ann. N.Y. Acad. Sci.*, 1943, **54**, 351.

<sup>4</sup> Abere, Goldfinger, Mark and Naidus, *Ann. N.Y. Acad. Sci.*, 1943, **54**, 295.

<sup>5</sup> Flory, *J. Amer. Chem. Soc.*, 1937, **59**, 241.

<sup>6</sup> Whether present as impurity, as in A.R. petrol ether, or deliberately added as butyl alcohol.



and Simha<sup>9</sup>). All these features were, in fact, found. Even in the purified solvent there was an induction period. The accelerating rate was not a thermal effect, since it was found at the lowest catalyst concentrations, where temperature rise was negligible (Fig. 3.  $[C] = 0.051$ ). Further, unlike the methacrylate polymerisation,<sup>9</sup> it was not an effect due to increasing viscosity of the reaction mixture, since this was very low during the period of acceleration. The induction period and acceleration effect would seem to be an effect of a true increase in the number of active centres  $P_n^*$ . The observed growth of molecular weight is a necessary consequence of such a non-stationary mechanism.

The termination mechanism (3a) would lead to a polymer with one double bond per molecule, which might be further activated by  $\text{SnCl}_4$  at

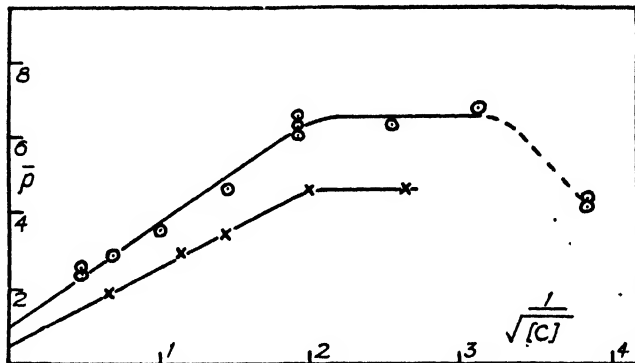


FIG. 5.—Effect of catalyst concentration  $[C]$  on average chain length ( $\bar{P}$ ) of polymer.

$\circ$  Purified solvent.  $\times$  A.R. solvent.

high temperatures. This would explain the "chain branching" observations. We may regard Chalmers'<sup>1</sup> results on unsaturation as directly supporting this conclusion.

A proper discussion of the kinetic results will need the treatment of the non-stationary set of reactions (1-3b). This is scarcely worth while until further data, in very dilute solutions of monomer, and in concentrated solutions under isothermal conditions, are available. The latter case we hope to realise by conducting the reaction in a thin layer of liquid in a Couette viscometer, from which the heat of reaction may be easily withdrawn. A further study of the vinyl ethers is now in hand.

The authors' thanks are due to Professor E. K. Rideal, F.R.S., and Dr. R. Hill (I.C.I. Dyestuffs Division) for their helpful advice. This paper is published by permission of the Chief Scientific Officer, Ministry of Supply.

### Summary.

The polymerisation of *n*-butyl vinyl ether, catalysed by stannic chloride, possesses certain novel features which differentiate it from the usual "radical type" polymerisations. It can proceed with "explosive" vigour at room temperatures, and the rate curve, even in purified solvent, is characterised by a period of induction, followed by an accelerating rate. There is thermal evidence for polymerisation to short chains during the "induction period", and the molecular weight of the polymer grows during the reaction. This and other evidence is in harmony with a set of three successive reactions (1) initiation, (2) propagation, (3) termination, in

<sup>9</sup> Ginell and Simha, *J. Amer. Chem. Soc.*, 1943, 65, 710.

<sup>1</sup> Norrish and Smith, *Nature*, 1942, 150, 336.

which (1) is relatively more rapid, (2) relatively slower than for radical polymerisations. The active intermediate is probably a complex  $\text{SnCl}_4$ -polymer, in which the terminal double bond of the polymer is polarised. On termination the  $\text{SnCl}_4$  is set free to activate further monomer.

### Résumé.

La polymérisation de l'éther *n*-butyl-vinyle, catalysée par le chlorure stannique, possède certains traits nouveaux qui la différencient du type habituel de "polymérisation de radicaux". Elle peut se produire avec une vigueur "explosive" à température ordinaire et la courbe de vitesse, même dans un solvant purifié, est caractérisée par une période d'induction, suivie d'une accélération. Les conditions thermiques mettent en évidence la polymérisation en chaînes courtes pendant la "période d'induction." Le poids moléculaire du polymère croît pendant la réaction. Ces faits, et d'autres, s'accordent avec une suite de réactions : induction, propagation, terminaison, où la première est plus rapide et la seconde plus lente que pour des polymérisations de radicaux. L'intermédiaire actif est probablement un complexe  $\text{SnCl}_4$ -polymère dans lequel la double liaison terminale du polymère est polarisée. À la fin de la réaction,  $\text{SnCl}_4$  est libéré pour activer d'autres molécules du monomère.

### Zusammenfassung.

Die durch Zinnchlorid katalysierte Polymerisation von *n*-Butyl-vinyl-äther besitzt neuartige Züge, welche sie von den gewöhnlichen Polymerisationsreaktionen vom "Radikaltypus" unterscheiden. Sie kann bei Zimmertemperatur mit "explosionsartiger" Heftigkeit vor sich gehen und der Geschwindigkeitsverlauf ist selbst in einem gereinigten Lösungsmittel durch eine Induktionsperiode, der eine anwachsende Geschwindigkeit folgt, gekennzeichnet. Aus dem Temperaturverlauf folgt, dass während der "Induktionsperiode" Polymerisation zu kurzen Ketten stattfindet und dass das Molekulargewicht des Polymers im Laufe der Reaktion zunimmt. Diese und andere Daten stimmen mit der Annahme von drei aufeinanderfolgenden Reaktionen überein, (1) Einleitung, (2) Fortpflanzung, (3) Abschluss, wobei (1) relativ rascher und (2) relativ langsamer als für Radikalpolymerisationen ist. Das reaktive Zwischenprodukt ist wahrscheinlich ein Komplex von  $\text{SnCl}_4$  mit dem Polymer, in dem die End-doppelbindung polarisiert ist. Beim Abschluss wird  $\text{SnCl}_4$  abgestossen und kann ein weiteres Monomermolekül aktivieren.

*Colloid Science Department,  
The University,  
Cambridge.*

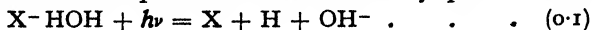
## THE ELECTRON AFFINITY AND SOME REACTIONS OF THE AZIDE ION IN SOLUTION.

BY JOSEPH WEISS.

*Received 14th November, 1945; as amended 20th February, 1946.*

It is well known that the behaviour of the azide ion is in many respects similar to the halogen ions and some of its properties seem to lie between those of  $\text{Br}^-$  and  $\text{I}^-$ .<sup>1, 2</sup>

According to Franck and Haber<sup>3</sup> the light absorption of a halogen ion ( $\text{X}^-$ ) in the near ultraviolet corresponds to an electron affinity spectrum, viz.,



<sup>1</sup> Cf. Philip, *J. Chem. Soc.*, 1908, 93, 918, 925.

<sup>2</sup> Birkenbach and Keller, *Ber.*, B, 1925, 58, 786.

<sup>3</sup> Franck and Haber, *Sitz. Preuss. Akad. Wiss.*, 1931, 250.

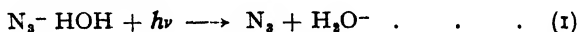
and it is possible to derive from the spectrum a value for the sum of electron affinity + heat of hydration of the ion.

1. In order to obtain the corresponding data for the  $N_3^-$  ion the absorption spectrum of an alkali azide in solution had to be determined as no previous record of this spectrum seems to exist in the literature. The absorption spectrum was determined in the usual way by means of a Hilger quartz spectrograph and a Spekker photometer using a 1 cm. quartz cell and an iron spark as light source. A purified specimen of sodium azide was used and the salt was dissolved in twice distilled water.

The absorption spectrum of a 1 M. solution of  $NaN_3$  is given in Fig. 1 and for comparison the absorption spectrum of a 1.896 M. solution of KI is given, taken from the work of Fromherz and Menschick.<sup>3</sup>

As in the case of the absorption spectra of the alkali halides in solution one may assume that the absorption of the  $NaN_3$  in the near u.v. region is due to the  $N_3^-$  ion and the curve in Fig. 1 actually represents the logarithm of the molar extinction coefficient of this ion plotted against wavelength ( $\lambda$ ).

The photochemical primary process corresponding to the long wave absorption limit can be represented by analogy to the halogen ions as follows:



or

i.e. after the transfer of an electron to one of the  $H_2O$  molecules in the hydration shell of the ion, molecular nitrogen and hydrogen should be produced (eventually) in the ratio 3 : 1.

It has been possible to show that irradiation of solutions of alkali azides in the quartz ultraviolet yields  $N_2$  and some  $H_2$ .<sup>\*</sup> As in most of these photochemical reactions in solution the primary process is somewhat obscured by reverse processes.<sup>\* 4, 5</sup>

Taking for  $N_3^-$ -aq the absorption limit of  $\lambda = 2650 \text{ \AA}$ . (i.e. the energy where the logarithm of the molecular extinction coefficients reaches a value of unity) this corresponds to an energy of 107 kcal. (= 4.65 ev. per g.-mol.).

From equation (1) one obtains, following the modification suggested by Farkas and Farkas:<sup>6</sup>

$$h\nu = 107 \text{ kcal.} = E_{N_2} + H_{N_3^-} - E_{H_2O} \quad (6)$$

where  $E_{N_2}$  and  $H_{N_3^-}$  denote the electron affinity and heat of hydration of the  $N_3^-$  respectively and  $E_{H_2O} \sim 18 \text{ kcal.}$  denotes the electron affinity of the  $H_2O$  molecule.<sup>6</sup>

This leads to a value of:

<sup>3</sup> Fromherz and Menschick, *Z. physikal. Chem.*, 1929, 83, 1.

<sup>\*</sup> Unpublished results. The apparatus was the one employed in previous work on the photochemistry of solutions.

<sup>4</sup> Cf. Weiss, *Trans. Faraday Soc.*, 1940, 36, 356; 1941, 37, 463.

<sup>5</sup> Potterill, Walker and Weiss, *Proc. Roy. Soc., A*, 1936, 156, 561.

<sup>6</sup> Farkas and Farkas, *Trans. Faraday Soc.*, 1938, 34, 1113.

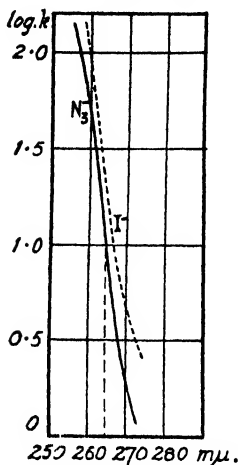
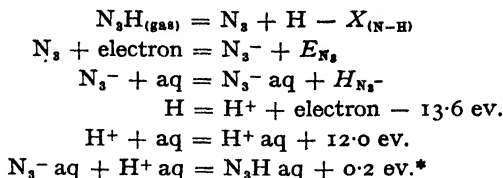


FIG. 1.—Absorption spectra of  $N_3^-$ .

—  $NaN_3$ , 1 M.  
... I' (1.896 M. KI).

$$E_{N_3} + H_{N_3} = 125 \text{ kcal. } (= 5.43 \text{ ev.}) \quad (7)$$

2. Using the value given above one can estimate the bond energy ( $X_{N-H}$ ) of the N—H bond in  $N_3H$  from the following reactions:



$$N_3H_{(gas)} = N_3H aq (-X_{(NH)} + E_{N_3} + H_{N_3^-} - 1.4) \text{ ev. } (8)$$

The heat of solution of hydrazoic acid has been determined directly<sup>7</sup> and was found to be 0.42 ev. per g. mol. This gives (with the value given in eqn. 7)

$$\begin{aligned} -X_{(NH)} + 5.43 - 1.4 &= 0.42 \\ X_{(NH)} &\sim 3.6 \text{ ev.} \quad (9) \end{aligned}$$

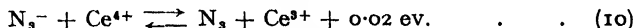
This value is almost identical with the (average) energy given for the N . H bond in  $NH_3$ <sup>8</sup> and actually falls between the bond energies of H . Br (3.8 ev.) and H . I (3.1 ev.) as might be expected on account of a certain similarity between  $N_3H$  and these halogen compounds. Pauling<sup>8</sup> has also pointed out that in  $N_3H$  one has essentially a covalent link and that appreciable resonance in the  $N_3$  radical does not arise until one passes to the ion  $N_3^-$ . In the ion the resonance amounts to approximately 0.87 ev./g.-mol.<sup>8</sup> and is mainly due to the fact that the azide ion can resonate between three structures (on account of the "adjacent charge" rule).

An estimate of the N . H bond in  $N_3H$  based on the calculation of Pauling (op. cit.<sup>8</sup>, p. 53) that the extra ionic energy of the N . H bond in  $NH_3$  amounts to 22.0 kcal./g. mol. and assuming that the actual extra ionic energy in  $H.N_3$  is not higher than that given for H . Br (12.5 kcal./g. mol.) leads to a value of 74.5 kcal. (3.2 ev.) which is within the limits of the above calculation.

This would also indicate that  $E_{N_3}$  in the above equation (7) does not represent the "true" electron affinity but gives a value which is too high by an amount corresponding to this resonance energy (0.87 ev.).

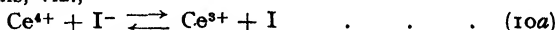
3. On the basis of the energy considerations given above one may attempt to interpret certain simple reactions of the azide ion in solution. It is well known that  $N_3^-$  is oxidised rapidly by ceric salts giving molecular nitrogen in quantitative yields.<sup>9</sup>

It is very likely that a similar simple electron transfer process is involved, viz.,

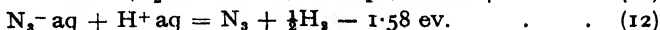
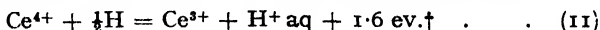


followed by reactions (2) and (3) giving molecular nitrogen.

Reaction (10) is also analogous to the electron transfer process between ceric ions and iodide ions, viz.,



The energy of reaction (10) can be obtained from the equations:



\* Calculated from the heat of neutralisation of hydrazoic acid (cf. Mellor, *Treatise on Inorganic Chemistry*, Vol. VIII, p. 334).

<sup>7</sup> Günther, Meyer and Müller-Skjold, *Z. physikal. Chem.*, A, 1936, **175**, 154.

<sup>8</sup> Pauling, *The Nature of the Chemical Bond* (Cornell University Press, 1944).<sup>\*</sup>

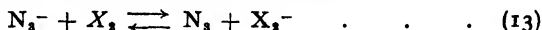
<sup>9</sup> Sommer and Pincas, *Ber.*, 1916, **49**, 259.

<sup>†</sup> From the  $Ce^{4+}/Ce^{3+}$  electrochemical potential (cf. Latimer, *Oxidation Potentials*, New York, 1938).

The azide ion can also be oxidised by  $I_2$  or  $Br_2$ . This reaction is extremely slow but can be catalysed very effectively by thiosulphate and sulphide ions,<sup>10</sup> which are actually used up in the reaction and also by  $CS_2$ , which seems to act as a "true" catalyst.<sup>11</sup>

Raschig,<sup>10</sup> who discovered the first effect, expressed the opinion that active (unstable) intermediates of the type  $Na I S_2 O_3$  or  $Na I S$  are formed in the reaction between  $I_2$  and thiosulphate or sulphides respectively while Feigl<sup>12</sup> assumes the intervention of certain active complexes of an unspecified nature.

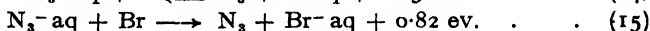
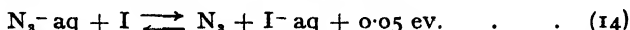
By analogy with the reactions discussed above it is reasonable to suppose that the essential process is an electron transfer, viz.,



where  $X_2$  stands for  $I_2$  (or  $Br_2$ ).

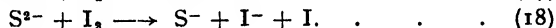
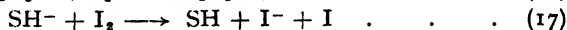
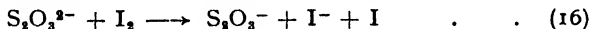
It is clear, however, from the above energy values that the electron affinity of the  $I_2$  and  $Br_2$  molecules is too low to allow a rapid interaction according to equation (13).

This is different in the case of the corresponding atoms, e.g.,



which are both energetically more favourable.\*<sup>13</sup>

It is very likely that, e.g., iodine atoms are formed by the interaction of  $S_2O_3^{2-}$ ,  $S H^-$  or  $S^{2-}$  with molecular iodine (or bromine) according to:



Reaction (16) is supported by the subsequent formation of tetrathionate:



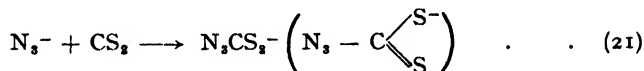
while (17) and (18) should give rise to the formation of free sulphur, e.g., according to:



which has actually been observed in these reactions.

It will be seen also that in these cases the catalyst is actually used up which is also in agreement with experiments.

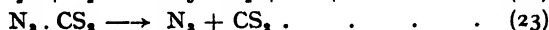
This is different in the case of the carbon disulphide catalysis<sup>11</sup> where there is some support for the following reactions:



viz., the primary formation of azido-dithio-carbonic acid has been observed by Sommer.<sup>14</sup> This is presumably followed by:



and



while the  $I$  atoms formed in equation (22) can bring about further catalysis through reaction (14) and this again is followed by (2) and (3) giving molecular nitrogen.

<sup>10</sup> Raschig, *Ber.*, 1915, 48, 2088.

<sup>11</sup> Feigl and Chargaft, *Z. anal. Chem.*, 1928, 74, 376.

<sup>12</sup> Cf. Feigl, *Qualitative Analyse mit Hilfe von Tüpfelreaktionen* (Leipzig, 1931).

<sup>13</sup> Bernal and Fowler, *J. Chem. Physics*, 1933, 1, 515.

\* The values of the electron affinity and heats of hydration of the halogens are taken from Bernal and Fowler, *loc. cit.*

<sup>14</sup> Sommer, *Ber.*, 1915, 48, 1833.

### Summary.

(i) The absorption spectrum of the  $N_3^-$  ion in aqueous solution has been determined. It is similar to that of the halogen ions and corresponds to an electron affinity spectrum.

(ii) From the above a value of 125 kcal./g. mol. can be deduced for the sum of electron affinity + heat of hydration of the  $N_3^-$  ion.

(iii) The above value leads to an estimate of the N—H bond energy in  $N_3H$  which is found to be  $3.3 \pm 0.3$  ev.

(iv) A simple mechanism, involving electron transfer processes, is suggested for the reaction between  $N_3^-$  and ceric ions and a somewhat similar mechanism is proposed for the reaction with molecular iodine and the catalysis of this reaction by thiosulphate, sulphide and  $CS_2$ .

### Résumé.

(1) Le spectre d'absorption de l'ion  $N_3^-$  en solution aqueuse a été déterminé. Il est semblable à celui des ions halogène et correspond à un spectre d'affinité d'électron.

(2) A partir de ce spectre, on déduit une valeur de 125 kcal./mol.-g. pour la somme : affinité d'électron + chaleur d'hydratation de l'ion  $N_3^-$ .

(3) La valeur ci-dessus permet d'estimer à  $3.3 \pm 0.3$  ev. l'énergie de la liaison N—H dans  $N_3H$ .

(4) On propose pour la réaction entre les ions  $N_3^-$  et cériques, un mécanisme simple comprenant un transport d'électron et un autre assez semblable pour la réaction avec l'iode moléculaire et la catalyse de cette réaction par les thiosulfates, les sulfures et  $CS_2$ .

### Zusammenfassung.

(1) Das Absorptionsspektrum des  $N_3^-$ -Ions in wässriger Lösung wurde bestimmt. Es ist dem der Halogenionen ähnlich und entspricht einem Elektronenaffinitätsspektrum.

(2) Hieraus kann ein Wert von 125 kcal/Mol für die Summe von Elektronenaffinität und Hydratationswärme des  $N_3^-$ -Ions abgeleitet werden.

(3) Dies führt zu einem ungefähren Wert von  $3.3 \pm 0.3$  Volt für die N—H Bindungsenergie in  $N_3H$ .

(4) Es wird vorgeschlagen, dass die Reaktion von  $N_3^-$  mit  $Ce^{4+}$  einen einfachen Mechanismus mit Elektronenübergangsprozessen hat und dass die Reaktion mit molekularem  $I_2$  und ihre Katalyse durch Thiosulfat, Sulfid und  $CS_2$  einen ähnlichen Mechanismus besitzt.

*University of Durham,  
King's College,  
Newcastle-upon-Tyne.*

## A CATHODE RAY OSCILLOGRAPH FOR DETECTION OF LOW VOLTAGE D.C. SIGNALS.

BY R. GUELKE, J. L. N. BESSELING, E. NEWBERY and A. SEMMELINK.

*Received 14th September, 1945, as amended 1st March, 1946.*

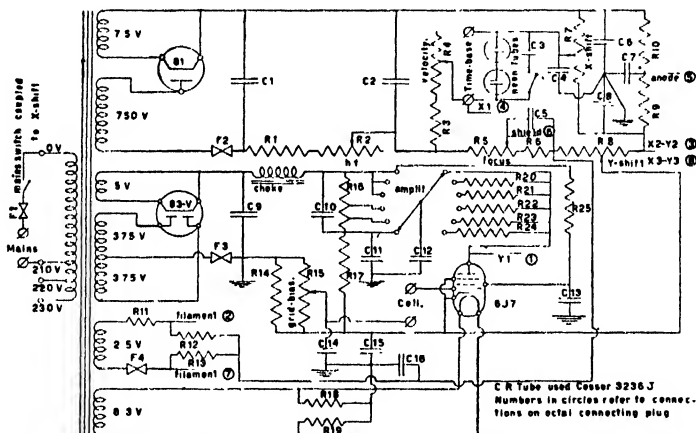
The study of electrode phenomena in aqueous electrolytes has been greatly assisted by the use of the cathode ray oscillograph. An ideal instrument for this purpose should have the following characteristics.

- 

built for A.C. work, it was necessary to design a new circuit fulfilling as nearly as possible the above conditions.

## Experimental.

Fig. 1 refers to the first circuit evolved. As can be seen, the usual cathode-ray oscillograph adjustments are provided viz., h.t., focus, X-shift,



## CATHODE RAY OSCILLOSCOPE CIRCUIT.

FIG. 1.

- |   |   |
|---|---|
| 1 Cossor 3236J (see maker's characteristics). | R5 50,000 ohm., var.                                      |
| 1 R.C.A. 6J7.                                 | R6 20,000 ohm., 1 w.                                      |
| 1 R.C.A. 81.                                  | R7 2 Meg. var. with switch.                               |
| 1 R.C.A. 80 or 83 v.                          | R8 0.5 Meg. var.  |
| 2 neon tubes.                                 | R9, R10 75,000 ohm., 1 w.                                 |
| F1 1 amp. Cartridge.                          | R11 approx. 1.5 ohm., 2 w.                                |
| F2 50 ma Pilot light.                         | R12, R13 100 ohm., $\frac{1}{2}$ w.                       |
| F3 150 ma Pilot light.                        | R14 750 ohm, 2 w.   |
| F4 $1\frac{1}{2}$ amp. Cartridge              | R15 3000 ohm., var. wirewound.                            |
| C1, C2, C3, C'3, C6, C7, 1 mfd., 600 v.       | R16, R17 5000 ohm., 25 w. with adjustable contact straps. |
| C4, C'4, C5, C8, C12, 0.25 mfd., 600 v.       | R18, R19 one 20 ohm. with centre tap.                     |
| C9 8 mfd., 600 v.                             | R20 13,000 ohm., $\frac{1}{2}$ w.                         |
| C10, C11, 16 mfd., 450 v.                     | R21 5000 ohm., $\frac{1}{2}$ w.                           |
| R1 75,000 ohm., 1 w.                          | R22 2200 ohm., $\frac{1}{2}$ w.                           |
| R2 1 Meg. variable.                           | R23 1000 ohm., $\frac{1}{2}$ w.                           |
| R3 1 Meg., 1 w.                               | R24 0.5 Meg., 1 w.  |
| R4 10 Meg. var.                               | R25, R26 5 Meg., 1 w.                                     |

and Y-shift. A simple slow time-base, controlled by  $C_3$  and  $R_4$ , provides a fairly linear X-axis. The necessary tripping of this circuit is performed by an external rotating timing switch P (see Fig. 1 in the following paper on Reversible Overvoltages) or by the neon tubes shown. Thyratrons could be used instead of the neon tubes, which were, however, found to be adequate.

A separate h.t. supply is employed for the direct coupled amplifier (6J7), operated as a pentode. The sensitivity is varied by an adjustable load resistance; the change in plate potential (i.e.  $Y_1$  potential) being compensated for by a change in h.t. supply to the valve and manually by adjustments on the Y-shift and on the grid-bias of the 6J7 valve.

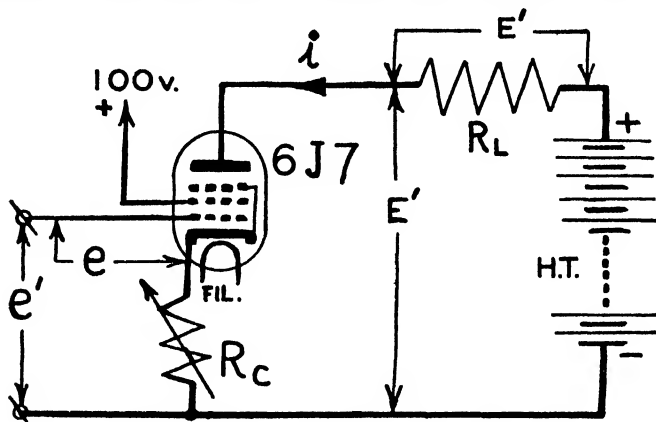


FIG. 2.

The terminology used in Fig. 2 and in text later are :

- $R_c$  Resistance in cathode lead (ohms)  $\ll R_1$  and  $R_a$ ,
- $R_1$  Resistance in anode lead (ohms),
- $R_a$  Anode slope resistance of the valve (ohms),
- $g$  Mutual conductance of the valve (ohms $^{-1}$ ),
- $\mu$  Amplification factor of the valve,
- $e$  A.C. voltage input to amplifier,
- $e'$  A.C. voltage between grid and cathode,
- $E'$  A.C. voltage output from amplifier.
- $i$  A.C. current through the valve (amp.).

Due to the long duration of the pulses (O.o.M. 1 sec.) it was found impossible to decouple the screen sufficiently by means of  $C_{13}$ ; this was shown up by bad distortion of square waves. The screen supply was changed to a tap on the bleeder resistance  $R_{17}$ , with a consequent improvement in the response to square waves. However, on the ranges employing load resistors of values less than 100,000 ohms (i.e. the less sensitive ranges), distortion was again evident due to the regulation of the h.t. supply and the bias from  $R_{14}$ . The latter trouble was remedied by removing  $C_{14}$  and  $C_{18}$ , thus making the change in bias instantaneous and at the same time introducing a slight amount of negative feedback. As the regulation of the h.t. supply could not be improved it meant that the load resistance would have to be high in value (i.e. larger than 100,000 ohms). It was therefore decided to keep this load resistance constant at 500,000 ohms (which was used for the highest gain) and to vary an extra resistance, included in the cathode lead, so as to obtain various amounts of negative feedback as a sensitivity adjustment.

Therefore :

$$e = e' - iR_c \doteq e' - e\mu R_c / (R_a + R_1)$$

i.e. 
$$e = e'(R_a + R_1) / (R_a + R_1 + \mu R_c)$$



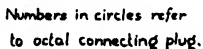
$$E' \doteq e_{\mu} R_1 / (R_0 + R_1)$$

$$\equiv e'(R_s + R_1)\mu R_1 / ((R_s + R_1)(R_s + R_1 + \mu R_c))$$

$$\text{Gain} = E'/e' \doteq \mu R_1 / (R_a + R_1 + \mu R_c)$$
$$R_c \doteq R_1/\text{gain} - (R_s + R_1)/\mu,$$

on  $R_{1,5}$  and the cathode.

(i.e. 3, 4 and 5).



## CATHODE RAY OSCILLOSCOPE CIRCUIT.

FIG. 3.

data on the 3236J Tube.)

due to the shortage of high voltage paper condensers at this time.

### Applications.

cm./volt. As the effective area of the screen is 10 cm.  $\times$  10 cm., the useful

voltage range is approximately 0.01 volt to 7 volts. It should therefore lend itself to many measurements on electrolytic cells.

It could also be used for measurements on higher potentials provided a high resistance potential divider can be connected across the supply concerned without affecting the magnitude of the potential under investigation.

### Résumé.

On résume ici les caractéristiques que devrait posséder un oscillographe à rayon cathodique, idéal pour la détection de signaux à bas voltage en courant continu et on donne les détails complets d'un circuit, dessiné pour remplir ces conditions. L'oscillographe convient à des mesures sur des cellules électrolytiques et aussi à des mesures de potentiels plus élevés, après légère modification.

### Zusammenfassung.

Die Eigenschaften, die ein zum Anzeigen von Gleichstromimpulsen niederer Spannung ideal geeigneter Kathodenstrahloszillograph besitzen soll, werden zusammengefasst. Volle Details eines Gerätes, das entworfen wurde, um diese Bedingungen zu erfüllen, werden beschrieben. Dieser Oszillograph sollte für Messungen an elektrolytischen Ketten und (mit geringen Modifikationen) auch für höhere Spannungen geeignet sein.

## REVERSIBLE OVERVOLTAGE.

BY EDGAR NEWBERY.

*Received 14th September, 1945, as amended 9th March, 1946.*

Since the original investigation of overvoltage phenomena by Caspari, forty-five years ago, the whole subject has been, and still is a centre of keen controversy. Few scientific phenomena have been the source of such a multiplicity of conflicting theories, and the possibility of agreement upon any one of these theories still appears remote.

One of the fundamental reasons for this lies in disagreement as to the correct method of measuring overvoltage, some authors maintaining that the single potential of the experimental electrode must be measured while the current is flowing, whilst others maintain that such a procedure gives fallacious values due to the presence of an electrical resistance at the electrode-electrolyte boundary.

If, during the passage of current, an appreciable resistance exists between the electrode and the electrolyte, the fall of potential across this resistance will be superimposed upon the back E.M.F. of the electrode itself. This fall of potential has no right to the title "Overvoltage" since the term "Voltage" implies an independently active and reversible E.M.F., whereas the potential difference between two ends of a resistance only exists while current is being supplied by an external agency.

It is therefore of fundamental importance to establish once and for all whether such a resistance really exists or not, since it is obvious that no comprehensive theory of overvoltage can receive general recognition until this question is settled.

The total polarisation of an electrolytic cell, i.e., the total opposition to the passage of current through the cell, must be either (a) completely reversible, (b) completely irreversible, or (c) partly reversible and partly irreversible.

Since it is impossible to obtain a cell without *some* resistance between the electrodes, (a) is ruled out.

Since it is well known that, with few rare exceptions, every electrolytic cell gives an active back E.M.F., (b) is also ruled out. The problem therefore resolves itself into one of separating the reversible from the irreversible portions of the total polarisation and in order to do this, it is necessary to trace out accurately the changes of single potential of an electrode when the current is made and broken at known intervals. This must be done without taking any appreciable current from the electrodes, and the apparatus used must be capable of recording changes which occur in times as short as a few micro-seconds. The only instrument fulfilling these conditions is the cathode ray oscillograph.

### Experimental.

The author has previously made use of an early type of cathode ray oscillograph for this purpose,<sup>1</sup> but the great improvements in sensitivity,

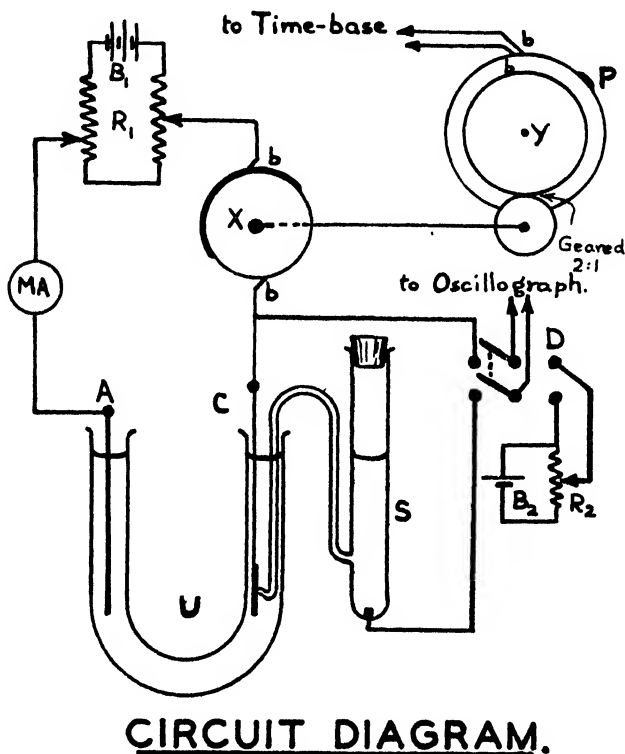


FIG. 1.

flexibility, and range shown by modern valves and oscillographs has not only exposed certain errors in former work, but has also revealed a number of new and interesting features which throw light upon the problem of electrode mechanism.

Since the standard oscillograph circuits are all built for A.C. work, it was necessary to design and build a special apparatus for this work. This was done in the Department of Electrical Engineering of this University and is described in a separate communication.

<sup>1</sup> *Proc. Roy. Soc. A.*, 1925, 107, 486.

The experimental cell and accessories are illustrated in the Circuit Diagram. By means of the tapped rheostat  $R_1$  and battery  $B^1$ , any potential difference from 0 to 6 volts can be applied to the electrodes in the cell U, through a triple range milli-ammeter MA and contact breaker X.

The U-tube type of cell was adopted in order to avoid possible interference of free oxygen with the cathodic potential, and freshly boiled and cooled electrolyte was used, but it was found later that these precautions are quite unnecessary since identical results were obtained when an open beaker replaced the U-tube.

For all the work described in this paper, the cell was filled with  $N. H_2SO_4$  and the standard mercurous sulphate electrode, S, containing the same solution, terminated in a fine jet which could be pressed against the surface of the experimental cathode C.

By means of the double switch D, the two electrodes are first connected to the oscillograph and the variation of potential of C recorded photographically. D is then reversed and voltage lines recorded on the same plate by means of the tapped rheostat  $R_2$ . The time-base is actuated by a platinum bar P, embedded in an ebonite cylinder Y which is rotated by a 2 : 1 gear mounted on the same axle as the contact breaker X. This was rotated by a synchronous motor fitted with worm gear and adjusted to give 2 rev. per sec. Hence the time for one complete traverse across the oscillograph screen was one second.

Two switches (not shown in diagram) were also provided, the one for cutting off the charging current and the other for short-circuiting the contact breaker. For visual observations, a glass plate, ruled in squares, was placed in contact with the oscillograph screen. Photographs were taken through a pair of quartz lenses, using slow "process" plates and allowing two complete traverses for each exposure. Owing to the great variations in speed of the luminous spot, some parts of each photograph are unavoidably under-exposed by this treatment. In order to economise material and printing space, three exposures were made on each plate, using current densities of 1, 10 and 100 milliamperes per sq. cm. This causes overlapping in many cases, but in all the photographs except Plate II (1), the upper curves to the right of each half period are the continuations of the upper curves on the left.

The electrodes were rectangular plates, 1 sq. cm. exposed surface, of the following metals :—

Copper	Zinc	Aluminium	Bismuth	Iron
Silver	Cadmium	Lead	Chromium	Nickel
Gold	Mercury	Antimony	Platinum	Cobalt

Amalgamated electrodes were also used in many cases. Most of the photographs shown were obtained with electrode surfaces finished with "ooo" emery paper.

Results are shown in Plates I to IV. Potentials denoted by the figures on the left of each photograph are referred to the single potential of the hydrogen electrode in  $N. H_2SO_4$  as zero.

### Preliminary Discussion.

Before describing the behaviour of individual electrodes, it is necessary to discuss the general type of curve obtained and to decide upon what part of the curve must be measured in order to separate the reversible portion of the total polarisation from the irreversible.

In previous work by the author (loc. cit.) using an inefficient type of oscillograph, a gap appeared between the upper and lower parts of each curve, and this was taken as evidence of the existence of transfer resistance. The apparatus used in this work, giving a spot approximately 200 times as bright, has shown that this conclusion was undoubtedly incorrect. Most

of the photographs still appear to show a gap, but visual observation indicates that although the change of potential of the electrode on interrupting the charging current is extremely rapid, it is not instantaneous. Ferguson<sup>3</sup> also demonstrated this with the aid of a very elaborate variable-interval commutator, and came to the conclusion that he had thus disproved the existence of Transfer Resistance. Butler<sup>2</sup> and other authors appear to accept this proof as final. The proof, however, breaks down completely when it is realised that a high-capacity condenser is present, and that the steeply falling portion of the oscillograph curve is a typical condenser discharge curve.

This condenser is formed by a film of hydrogen gas acting as the dielectric, whilst electrode and electrolyte respectively form the condenser plates. Langmuir has shown that a gas film of molecular or atomic thickness adheres very firmly to a solid surface, whereas additional layers are easily removed. If the film has a thickness equal to the diameter of a hydrogen atom, approximately  $1.5 \text{ \AA}$ , the capacity of the condenser should be 6 microfarads per sq. cm. Bowden and Rideal<sup>4</sup> immersed certain electrodes in dilute acid which had been very thoroughly saturated with hydrogen, and then found that  $0.6$  micro-coulombs of current were required to change the potential of  $1 \text{ sq. cm.}$  by  $100 \text{ mv.}$  From this they calculated that the above current deposits  $1/3000$  of an atomic layer of hydrogen. It appears fairly obvious that Bowden and Rideal were not depositing hydrogen at all, but merely charging a condenser, the capacity of which was 6 microfarads per sq. cm. Taboury<sup>5</sup> also observed this condenser effect with polished Au or Pt electrodes in dilute  $\text{H}_2\text{SO}_4$ , but ascribed it to the presence of a Beilby layer instead of the more obvious gas film.

Gurney<sup>6</sup> postulates the presence of a "potential barrier" between electrode and electrolyte. This barrier is obviously a gas film, though Gurney attempts to account for it on other grounds, and overlooks the fact that no such barrier exists when metallic ions only are being deposited.

Butler<sup>7</sup> states that "an adsorbed film of atomic hydrogen is formed prior to the liberation of hydrogen at the cathode". It is difficult to understand how he reconciles this statement with his rejection of the theory of transfer resistance. Great confusion at present exists due to the mistaken idea that this gas-film condenser, which we may refer to as X, is identical with the "double layer" of Helmholtz, Gouy, or Stern, which we will call Y.<sup>8</sup>

Y is not really a "condenser" in the usually accepted sense in which this term is used, but is equivalent in its effect to a condenser in *parallel* with a resistance. Its action is due to a certain arrangement of ions at a different concentration near the electrode from that in the bulk of the electrolyte, and this arrangement is capable of acquiring a state of strain, and thus reversibly absorbing electrical energy under the influence of an applied E.M.F. Since the degree of strain induced by an A.C. will depend partly upon the speed with which the ions take up their new positions, the measured capacity will vary with some function of the A.C. frequency.

X on the other hand is a true condenser, with insulating dielectric and conducting plates, and is in *series* and not in *parallel* with the cell circuit. Since the dielectric consists of an uncharged gas film and not of ions, the measured capacity will not vary with the A.C. frequency.

Y permits free passage of D.C., whereas X will completely stop a D.C. unless the applied P.D. is sufficient to break through the dielectric. All D.C. subsequently passing is due to leakage of the dielectric. Finally Y

<sup>3</sup> *Trans. Electrochem. Soc.*, 1939, **76**, 113.

<sup>4</sup> *Electro-capillarity*, p. 131.

<sup>5</sup> *Proc. Roy. Soc. A.*, 1928, **120**, 73.

<sup>6</sup> *Compt. Rend.*, 1937, **204**, 1178; 1938, **206**, 1953.

<sup>7</sup> *Proc. Roy. Soc. A.*, 1931, **134**, 136.

<sup>8</sup> *Trans. Faraday Soc.*, 1938, **34**, 1170.

<sup>8</sup> See, for example, Barclay and Butler, *Trans. Faraday Soc.*, 1940, **36**, 129.

may be produced by any ions, metallic or gaseous, and does not involve the discharge of these ions, whereas X is only found after a gas has been liberated on the electrode surface.

There are two experimental reasons for concluding that the diffuse layer of Gouy or the compound layer of Stern have little effect upon hydrogen overvoltage.

(a) At low current densities, no detectable change can be observed in the oscillograph curves when the Luggin capillary is moved away from its normal position in close contact with the experimental electrode. At higher c.d. the change can be fully accounted for by the fall of potential due to the electrical resistance of the electrolyte. Since the space between the capillary and the electrode surface is of the order of 0.01 mm. or less, this does not leave much room for a "diffuse" layer.

(b) No sudden fall of potential is found close to the electrode surface unless a gas is being liberated. Cu, Ag, or Pb in solutions of their respective nitrates, Hg in  $\text{HgClO}_4$  solution, etc. give continuous horizontal straight line oscillograph records indicating, zero overvoltage. This proves that the double layer, whatever its nature, plays no part in inducing overvoltage when metallic ions only are liberated, and it appears reasonable to conclude therefore that it also plays no part when a gas is being liberated.

Since the gas-film of the condenser is so very thin, small impressed potential differences will produce very large potential gradients, and leakage will occur, increasing rapidly with rising P.D. The usual A.C. methods used for measuring this capacity will therefore tend to give results greatly in excess of the true values, but whatever value is finally assigned to it, it is obvious that the presence of such a condenser *in series* with the electrode must produce *some* resistance (i.e. transfer resistance) at any current density.

Hickling<sup>9</sup> has pointed out some of the absurdities which result from ignoring transfer resistance at high c.d., including the impossibly high single potentials ascribed to electrodes under such conditions, and Glassstone<sup>10</sup> who uses the term "Surface Resistance" appears to be of the same opinion, although both authors assume that the effect is negligible at low c.d. Nevertheless their own results show clearly that transfer resistance *increases* as the c.d. is lowered, and this was also shown by the present author.<sup>11</sup> Finally the work of Bowden and Rideal<sup>4</sup> shows that transfer resistance approaches infinity as the c.d. approaches zero, that is, the gas film becomes an electrical insulator under comparatively low electric strain.

In view of the above evidence, it appears to the author that it is no longer possible to reject the theory of transfer resistance, and no theory of overvoltage can possibly represent the true internal mechanism of electrolytic gas evolution if this is not recognised. We may conclude therefore that true "reversible overvoltage" can only be measured *after* the discharge of the condenser is completed, and may be defined as follows.

Reversible overvoltage (R.O.) is the active back E.M.F. in excess of that of the gas electrode in the same electrolyte, which persists after the gas-film condenser has discharged. The problem of deciding exactly *when* this condenser discharge is completed is a difficult one. Not only is the condenser leaky, but the degree of leakiness varies greatly with the degree of roughness of the electrode surface, and also diminishes rapidly as the condenser discharges. In addition to this, the compound responsible for R.O. may itself be very unstable, giving rise to a falling instead of a horizontal extension of the condenser discharge curve, and this further enhances the difficulty of deciding where one curve ends and the other begins.

Ideal curves obtained with condenser and resistance only, are shown in Plate IV, Fig. 6, 7 and 8, and these show that in the case of a high capacity

<sup>9</sup> *Trans. Faraday Soc.*, 1937, **33**, 1540.

<sup>10</sup> *Trans. Chem. Soc.*, 1923, **123**, 2927; 1924, **124**, 255.

<sup>11</sup> *Proc. Roy. Soc. A.*, 1928, **119**, 687.

in parallel with a high resistance, (upper curve in Fig. 7), the time allowed may not be sufficient for the complete discharge of the condenser.

The higher the degree of polish on the electrode surface, the smaller will be the surface area, and therefore the capacity of the condenser, but the smaller also will be the leak from acute-angled edges and points on that surface.

During charge, a steady potential will be attained when the rate of leak is exactly balanced by the rate of flow of current, and this will occur at the highest potential when the leak is least. This accounts for the well-known fact that overvoltages measured by the so-called "Direct Method" are always higher when the electrode surface is polished.

The discharge curves show a great variety of shapes. In a few cases only, the ideal type with horizontal extremity is found, indicating a fairly stable single potential. This may be due either to the single potential of the metal itself, or to the presence of stable overvoltage-hydrides, and only in the latter case can R.O. be accurately estimated.

In the majority of cases, however, the discharge curves show either a sharp bend, or a kink which later develops into a sharp bend, and here the estimation of the true R.O. is subject to greater errors.

The kinked curves seen in Plate II, 1, and Plate III, 3 are of special interest, as this kink indicates an intermediate stage in the building-up of an overvoltage compound in the electrode surface. Generally the kink only appears for a few seconds, and photographs are difficult to obtain as the curve is in process of changing shape and position, but it is more often seen than would be suggested by the photographs shown. It is very marked with some amalgamated surfaces, and is evidently due to the production of a very small quantity of unstable overvoltage compound which decomposes completely before the next charging period occurs.

The charge curves, which indicate the magnitude of overvoltage when measured by the "direct" method, show far greater variations of position than the discharge curves for any given electrode. Very great changes of position are shown with changes of current density, degree of surface polish, and previous history of the electrode, and the potentials indicated for any given current density are determined by the mechanical nature of the electrode surface, and have little or nothing to do with its chemical nature.

By suitable adjustments of current density and degree of polish, the charge curves for any metal may be made to take up any desired position within wide limits, in sharp contrast to the discharge curves which normally persist in occupying the same position in spite of great variations of current density, etc.

A peculiar feature of many of these charge curves is a sharp bend at the beginning of the curve which may be designated the "Charge Kick" and referred to as positive when pointing upwards and negative when pointing downwards.

The positive charge kick is most marked with highly polished electrodes at low current densities. As the current density is raised, the positive kick diminishes, and at very high c.d. it is frequently reversed. Mercury and freshly amalgamated surfaces show a positive kick at all current densities.

The positive charge kick appears to be due to the delayed breakdown of the dielectric of the condenser, just as in the case of an air gap between two electrodes, when a higher p.d. is required to initiate the discharge than is required to maintain it. This electrolytic condenser, however, differs markedly from a mechanically constructed condenser in that it is self-sealing, since the discharge of an electron through a break in the dielectric leaves a hydrogen atom automatically filling up the break. The horizontal portion of the charge curve therefore represents a dynamic equilibrium where the rate of leak of the condenser is balanced by the inflow of current.

The negative charge kick is characteristic of rough surfaces, and is most often observed at high current densities. Since the application of a high current density is very effective in breaking up a polished surface,<sup>12</sup> the presence of the negative charge kick at high current densities with most metals (and its absence with mercury electrodes which cannot be roughened) is probably due, in part at least, to this roughening action. When the high c.d. is slowly reduced, the strained conditions of the surface is released, and the positive kick may return, though very slowly. If the reduction is more rapid, it is possible to obtain a negative kick even at low c.d., and this is shown in the case of copper, Plate I, 1. Here the three photographs were taken as quickly as possible starting with the highest c.d. A few seconds after the lowest photograph was taken, the direction of the kick had reversed. Lead treated in the same way, sometimes shows a negative kick at low c.d., Plate III, 2, but the phenomenon is still more transient and difficult to reproduce.

### The Behaviour of Individual Electrodes.

**Copper.**—Although only one set of curves is shown, this electrode was studied intensively, the surfaces used being finished as follows: (a) spongy, reduced from basic chloride, (b) rough, No. 1 emery cloth, (c) smooth, No. 000 emery paper, (d) polished, Tripoli mop and rouge paper, (e) burnished, Agate burnisher, (f) amalgamated.

All these electrodes at first show curves completely below the zero line. If the charging current is maintained at 1 ma. per sq. cm., the charge curve rises in a few seconds to the zero line. Then the discharge curve also rises until nearly in line with the charge curve. The E.M.F. necessary to maintain the current now increases rapidly and the whole curve rises to a position as shown in the lowest curve, Plate I, 1, which was obtained with electrode c. Electrodes (d) and (e) showed steeper discharge curves, positive charge kick except at the highest current densities, and much higher charge potentials. Electrode (f) showed the highest charge potentials (over 1 v. at 100 ma.), and the greatest positive charge kick, but the right hand portion of the discharge curve was horizontal at 0.2 v. for all current densities. On cutting off the current, this potential of 0.2 v. persists for two minutes, indicating the presence of an unusually stable overvoltage compound. The rough electrode (b), showed similar preliminary behaviour but required a longer time before steady conditions prevailed. The discharge curves were flatter than those obtained with polished surfaces and the rate of decay slower. At the highest current density, the horizontal portion of the curve was again at 0.2 v., but as the current density was reduced, a kink appeared in the middle of the horizontal portion similar to that shown in the uppermost curve of Plate III, 3. This kink moves to the left, until after a few seconds, the whole discharge curve is steep with no horizontal portion, and the end near the zero line.

The spongy surface of electrode (a) was obtained by dipping in dilute HCl and then leaving exposed to the air for a few days, when it was covered with a uniform layer of basic chloride. This was reduced electrolytically in dilute  $\text{H}_2\text{SO}_4$  and washed free of chloride.

With this electrode at low current densities, the charge and discharge curves formed a nearly straight horizontal line at 0.2 v. Charge kick was negative at all c.d. At higher c.d., the charge curves were at the lowest level observed with any of these surfaces. From these experiments, we may conclude that the R.O. of a copper cathode is 0.2 v.

**Silver.**—The general behaviour of this electrode is very similar to that of copper, but the overvoltage compound is more unstable. Smooth, polished, and burnished electrodes give discharge curves which become

<sup>12</sup> J. Chem. Soc., 1914, 105, 2427.



steeper as the degree of polish is increased. The curves shown in Plate I, 2, were obtained with a smooth electrode.

A sponge surface, obtained by reducing an anodic chloride film, showed a definite reproducible R.O. of 0.19 v. at all current densities. A freshly amalgamated electrode shows two R.O. values, one of 0.3 v. at low c.d., which changes to 0.2 v. at all c.d. after the application of a high c.d. Since the 0.3 v. is only obtained with a freshly amalgamated surface, it is doubtful whether this is a property of silver or of mercury, but there is no doubt that 0.2 v. is *one* value of the R.O. of silver.

**Gold.**—The behaviour of this electrode is again similar to that of Cu and Ag, but the overvoltage compound appears to be still more unstable and it is difficult to induce the electrode to show its true R.O. Normally the discharge curves are very steep, as shown in Plate I, 3, but if a c.d. of 1000 ma./cm.<sup>2</sup> is applied for one minute and then lowered to 100 ma., a kink appears in the discharge curve at 0.2 v., which slowly straightens out to a horizontal line at the same level. Disturbing the electrode by tapping or by lifting out of the solution makes the curves revert at once to the position shown in the photograph.

**Zinc.**—The natural single potential of this metal is so high (0.72 v.) that the discharge curves cannot fall below this value. All the discharge curves obtained with pure metal fell on this same line, and afford no evidence of any R.O. On amalgamating the surface, the single potential is unchanged, but the discharge curves are raised to 0.82 v., and this is probably the R.O. of zinc.

**Cadmium.**—This electrode is similar to zinc in that its natural single potential in the electrolyte used (0.42 v.) determines the position of the discharge curves. In contrast with Zn, however, an amalgamated electrode gives exactly the same discharge curves as the pure metal, and there is no evidence of the formation of any overvoltage compound.

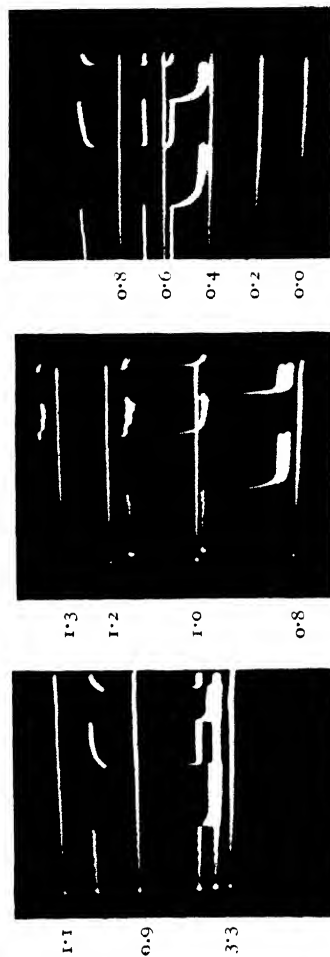
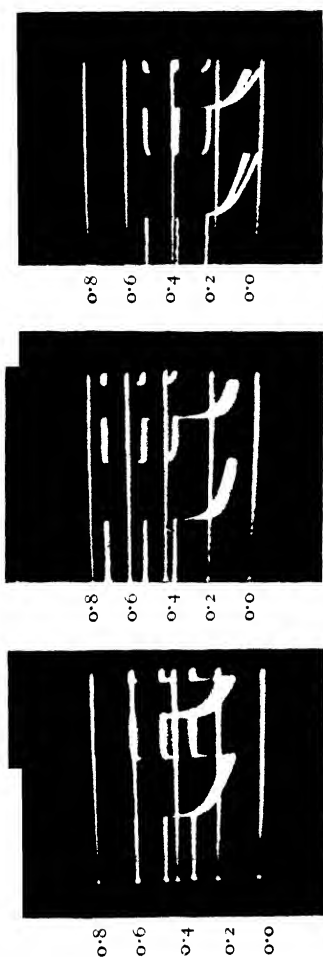
**Mercury.**—This electrode shows many interesting features. Fig. 1, Plate II, was obtained with spectroscopically pure, electrolytic metal. A high E.M.F. (2.7 v.) is required to produce the lowest c.d. of 1 ma./cm.<sup>2</sup> and the discharge curve falls steeply to zero. As the c.d. is increased, this curve is lengthened in *both* directions, the end of the curve now falling below the zero line. When a c.d. of 100 ma. is applied, both ends of the curve are outside the limits of the photograph and this curve has therefore been omitted.

After maintaining the current at 10 ma. for some minutes, a small but quite definite kink appears in the discharge curve at 0.7 v., indicating the presence of a very unstable overvoltage compound. The Hg electrode is very sensitive to traces of impurity. Fig. 2, Plate II, was obtained with a sample known to contain traces of Ni, Cu, and possibly other metals. At the highest c.d., the discharge curves rises to 0.5 v., in marked contrast to that of pure Hg which falls to more than 0.4 v. below the zero line under similar conditions.

**Aluminium.**—Since the affinity of this metal for oxygen is so high, it is not possible to obtain a true metal-electrolyte contact, and the series, electrolyte : hydrogen-film : oxide-film : metal, is unlikely to show any definite single potentials. The curves shown in Plate II, 3, were obtained with a polished surface and show no evidence of R.O. Roughened surfaces frequently give discharge curves closely resembling those obtained with more noble metals, but the potentials indicated vary within wide limits and are not reproducible.

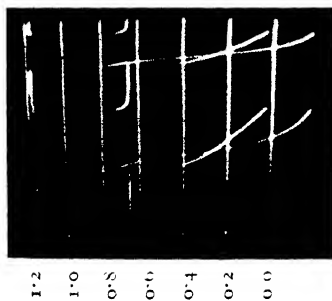
**Antimony and Bismuth.**—These two electrodes are so much alike in their behaviour that curves for Sb alone are given, Plate II, 4, 5. The initial single potentials shown by both electrodes fall below the zero line (Sb — 0.1 v. and Bi — 0.25 v.) and these values are maintained for five minutes with a current of 1 ma. The lowest curve in Fig. 4 shows this condition. The whole curve then rises and the discharge curves for both metals become horizontal at 0.3 v. Fig. 5 shows the position of the curves

PLATE I.



[To face page 134.]

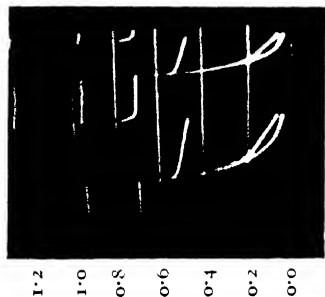
PLATE II.



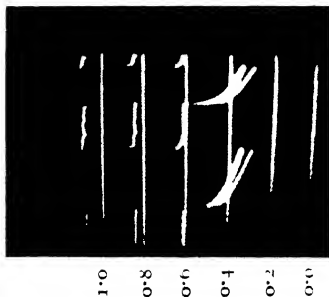
(1) Hg (A)



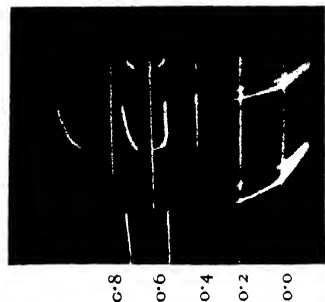
(4) Sb (A)



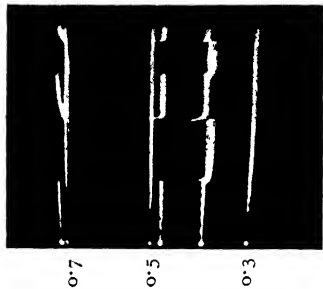
(2) Hg (B)



(5) Sb (B)

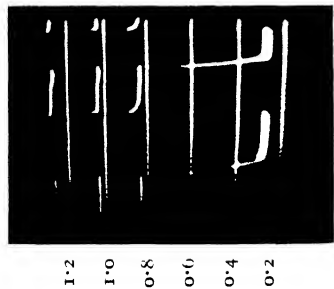


(3) Cr



(6) Cr

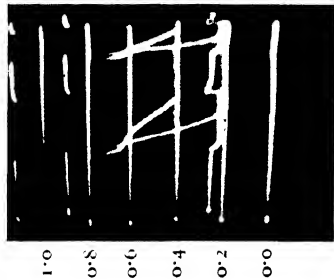
PLATE III.



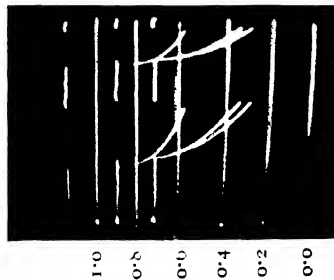
(1) Smooth A



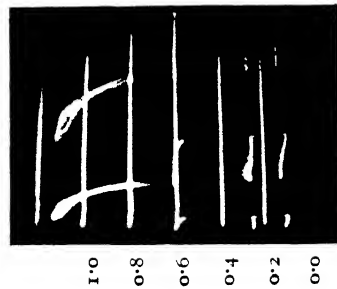
(2) Smooth B



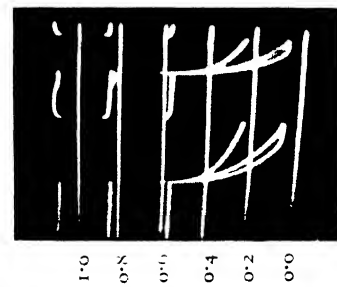
(3) Spongy A



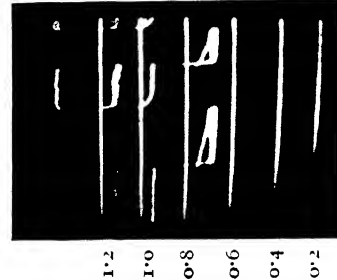
(4) Spongy B



(5) Burnished A



(6) Burnished B



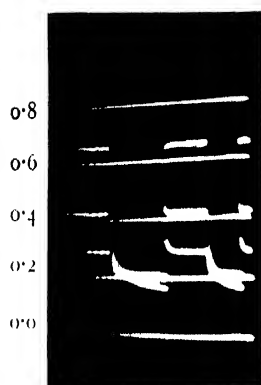
(7) Amalgamated



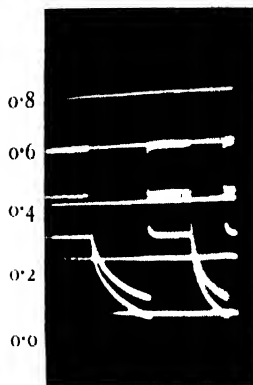
(8) High c.d. after 4

Lead.

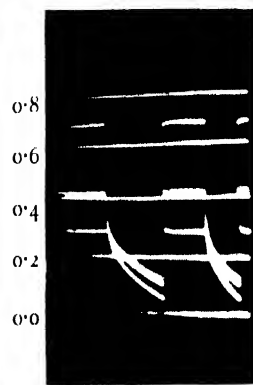
# PLATE IV.



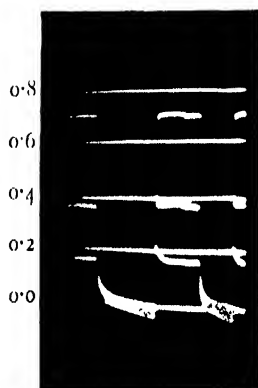
(1) Fe



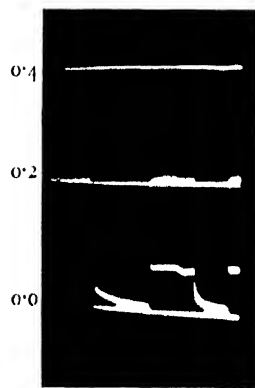
(2) Ni



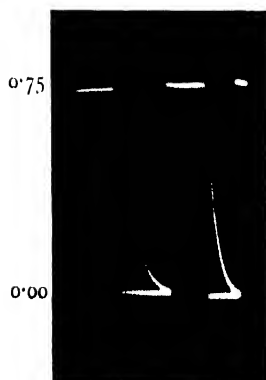
(3) Co



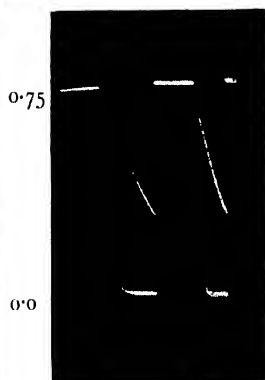
(4) Pt



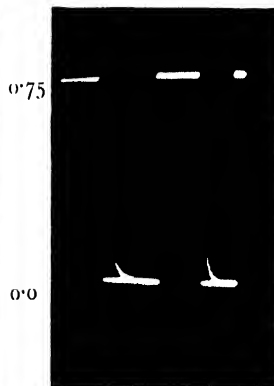
(5) Pt Platinised.



(6)  $10^4 \omega$ ; 0 and  $6 \mu F$ .



(7)  $10^4 \omega$ ; 2 and  $20 \mu F$ .



(8)  $10^3 \omega$ ; 0 and  $20 \mu F$ .

after this rise has occurred. A second R.O. of 0.65 v. is also shown by both electrodes and by Bi amalgamated after prolonged exposure to a c.d. of 10 ma. Both Sb and Bi have therefore two R.O. values of 0.3 and 0.65 v.

**Chromium.**—Pure Cr metal (alumino-thermic) gives very reproducible values for R.O., but the initial single potential in dil.  $\text{H}_2\text{SO}_4$  is somewhat indefinite. An electrode which has been in contact with air for a long period shows a S.P. below the zero line, whereas a freshly abraded surface shows a value of 0.16 v. On applying current, the discharge curve jumps to 0.38 v. and remains there while the c.d. is varied between 0 and 1000 ma. Impure electrodes show quite different behaviour. An electrode containing over 1 % of Fe gave a steeply falling curve at all c.d. with an inflection only at 0.35 v.

**Lead.**—As this electrode is so frequently used for electrolytic reductions, it was studied in great detail. Fig. 1, Plate III, shows the usual figure obtained with rough or smooth surfaces; other surfaces, after long use, tend to show the same features. The horizontal part of the discharge curves at 0.3 v. represents the natural S.P. of Pb in  $\text{N. H}_2\text{SO}_4$ , and is identical with that of the negative plate of a Pb accumulator. Under these conditions therefore, Pb shows no R.O.

After exposure to a high c.d. for some time, the electrode surface is roughened, the charge curves fall by 0.3 to 0.4 v., and the discharge curves acquire a greater slope as shown in Fig. 2, but there is still no indication of R.O.

A spongy surface obtained by alternate oxidation and reduction in dilute  $\text{H}_2\text{SO}_4$  shows the first signs of a genuine R.O. when a kink appears in the curve at about 0.65 v., with a c.d. of 100 ma., as seen in Fig. 3. After a few seconds at this c.d., the discharge curve rises to the position shown in Fig. 4, uppermost curve, which was photographed one minute after Fig. 3. At still higher c.d., 200 and 1000 ma., the discharge curves become nearly horizontal at the same R.O. as shown in Fig. 8.

A spongy surface on a Pb electrode is exceptional in showing high values for the charge curves. Spongy surfaces on other metals (e.g. Cu or Ag) show similar capacity for stabilising the overvoltage compound so that R.O. shows up more clearly, but in all cases except Pb such surfaces show greatly lowered charge curves.

Electrodes burnished with an agate tool, at first show discharge curves falling to nearly zero (Fig. 5) but after a few minutes treatment at high c.d., the surface is roughened and the discharge curves rise to the position shown in Fig. 1. At the same time the charge curves fall to the values shown in Fig. 2. Fig. 6 shows an intermediate stage in this transition. It is remarkable that a surface disintegrated by cathodic treatment only, should show such markedly different properties from one formed by anodic-cathodic treatment.

A freshly amalgamated lead electrode shows the R.O. of 0.65 v. at all c.d. Fig. 7 indicates very clearly why this electrode is chosen when very powerful cathodic reducing action is required (e.g. for the preparation of mannitol and sorbitol from glucose). Even this, however, is not permanent unless sufficient mercury is used to maintain the amalgamated surface. If a thinly amalgamated electrode is kept for two days, the mercury will diffuse into the metal and the curves obtained with such an electrode will again revert to Fig. 1.

**Iron, Nickel, and Cobalt.**—These three metals all behave alike in showing no R.O. under any conditions. The horizontal portion of the discharge curve of iron (Plate IV, Fig. 1) at 0.2 v. shows the natural single potential of the sample of pure iron used, and is not an overvoltage. Amalgams of Ni and Co give similar curves to those obtained with polished electrodes of the pure metals.

**Platinum.**—The tendency of this electrode to show the S.P. of the  $\text{H}_2$  electrode is shown in the length of the horizontal portion of the discharge curves. A well platinised electrode at low c.d. shows a continuous

horizontal line coinciding with the zero line, even with the highest gain on the oscillograph. Fig. 5, Plate IV therefore shows the upper two curves only, with c.d. of 10 and 100 ma. No indication of R.O. could be detected under any conditions.

### Summary and Conclusions.

Experiments with an improved form of cathode ray oscillograph have shown that the total opposition to the passage of current between electrode and electrolyte when a gas is liberated consists of two distinct parts, an irreversible and a reversible.

The irreversible part is due to the electrical resistance of a film of gas of atomic thickness, completely covering the electrode surface and forming the dielectric of a high-capacity condenser. This gas film must not be confused with the electrical double layer of Helmholtz, Gouy, or Stern, which plays little or no part in overvoltage phenomena. The resistance of the gas film is determined (1) by the mechanical nature of the electrode surface, and (2) by the current density. Rough surfaces show lower gas-film resistance than polished surfaces, due to easier escape of gas and easier electrical breakdown of the film. At very low c.d. the resistance approaches infinity, but at current densities of the order of 1000 ma./cm.<sup>2</sup> it may fall below 1 ohm/cm.<sup>2</sup>

The first atomic layer of gas adheres to the electrode surface with great tenacity. Subsequent layers are removed with comparative ease by aggregation to form gas bubbles, and hence offer little obstruction to the passage of the current. It is probable that if a monatomic layer only of H<sub>2</sub> is present, the electrode will not show the true S.P. of the H<sub>2</sub> electrode, since the tendency of this layer to re-ionise will be substantially reduced by the energy of absorption. This appears to be one, at least, of the factors responsible for the unsuitability of polished Pt for H<sub>2</sub> electrode work.

The reversible part of the total polarisation is made up of four factors : (1) concentration polarisation, (2) back ionisation of the deposited gas, (3) back ionisation of the electrode itself, and (4) back ionisation of overvoltage compounds of the gas with the electrode metal.

Of these factors, (1) will obviously form an addition to (2), (3), or (4), since it is in series with any of them, but its magnitude is usually negligible, as may readily be demonstrated by moving the tip of the standard electrode vessel away from contact with the electrode surface. In most cases this will have a barely visible effect on the position of the oscillograph charge curves and none at all upon the discharge curves. Factors (2), (3) and (4) are in parallel, and the observed single potential will therefore be determined by one, only, and that the one showing the greatest solution pressure.

An electrode such as Pt, readily dissolves and dissociates the cathodic gas, which is then electromotively active and tends to show the S.P. of a H<sub>2</sub> electrode, i.e. a R.O. of zero. An electrode such as Hg, in which the solubility of H<sub>2</sub> is very low, fails to retain sufficient gas to maintain the S.P. of a H<sub>2</sub> electrode during the discharge period, and the end of the discharge curve therefore falls below the zero line. An electrode such as Al, the surface of which is covered with an oxide not reducible by the discharged gas, shows similar behaviour, whilst Sb and Bi, whose oxides are reducible, show this property for a short time only.

Zn, Cd, Pb, and Fe electrodes in dilute H<sub>2</sub>SO<sub>4</sub> electrolyte, show single potentials negative to the H<sub>2</sub> electrode in the same liquid when no current is passed (Factor (3)), but these are not overvoltages. Factor (4) is therefore the only one which has any real right to the title "Overvoltage" and this is exhibited by the following metals :

Copper	. 0.2 v.	Zinc	. 0.8 v.	Antimony	. 0.3 and 0.65 v.
Silver	. 0.2 v.	Mercury	. 0.7 v.	Bismuth	. 0.3 and 0.65 v.
Gold	. 0.2 v.	Lead	. 0.65 v.	Chromium	. 0.38 v.

Cd, Al, Fe, Ni, Co, and Pt have so far shown no evidence of R.O. when used as cathodes in dilute  $\text{H}_2\text{SO}_4$  electrolyte.

With regard to the various methods used for measuring overvoltage in the past, it is evident from this work that the "direct" method gives results which are entirely determined by the mechanical condition of the electrode surface and the current density applied, and are independent of the chemical nature of the electrode. The commutator method can only give true R.O. in a few cases, and then only if run very slowly, and an interval of at least 0.1 second allowed for condenser discharge between the instant of cutting-off the charging current and the connecting-up with the potentiometer circuit.

A complete picture of the internal mechanism of cathodic liberation of  $\text{H}_2$  may be briefly summarised as follows.

1. Potential applied; rush of H ions to electrode; first to arrive, discharged and form gas film over surface. This gas tends to re-ionise and exert a back E.M.F. against the applied potential, but at the same time it forms the very thin dielectric of a high-capacity condenser.

2. More ions arrive but their discharge is opposed by the gas film, the electrical resistance of which at this stage is nearly infinite. The condenser is now charged, and great pressure is exerted on the gas film.

3. Potential gradient across gas film increases and leakage begins, but every leak is self-sealing. Consequently, the electrical resistance of the film (transfer resistance) unlike that of a solid dielectric, decreases steadily without any sudden breakdown. At the same time, the pressure on the film becomes so great that gas is forced into the electrode surface, tending to disintegrate it and destroy any polish.

4. Under the influence of the intense pressure, metallic hydrides are formed which tend to ionise with a higher solution-pressure than that of  $\text{H}_2$ . Reversible overvoltage is therefore due to the presence of these "overvoltage compounds".

5. The bulk of the gas is liberated by the passage of electrons through the gas film. Ions discharged outside the gas film by this action will readily aggregate to molecules and then to gas bubbles large enough to overcome surface tension forces and escape.

### Résumé.

Employant un modèle perfectionné d'oscillographe à rayon cathodique, on montre expérimentalement que la résistance à l'interface électrode-électrolyte est constituée par deux parties: l'une réversible, l'autre irréversible. Celle-ci est due au film de gaz d'épaisseur atomique, dont la résistance est déterminée par l'état physique de la surface de l'électrode et par la densité de courant. La partie réversible est formée par une polarisation de concentration et par l'ionisation (1) du gaz déposé, (2) de l'électrode, (3) des composés entre le gaz et l'électrode, associés au survoltage. En fait, il n'y a véritable survoltage que dans cette troisième partie et neuf métaux montrent ce phénomène. Les méthodes directes et "à commutateur" pour mesurer des survoltages réversibles sont critiquées et le mécanisme complet de la libération cathodique de  $\text{H}_2$  est résumé.

### Zusammenfassung.

Unter Benützung eines verbesserten Kathodenstrahloszillographen wird experimentell gezeigt, dass der Widerstand an der Phasengrenzfläche Elektrode-Elektrolyt sich aus einem irreversiblen und einem reversiblen Teil zusammensetzt. Der erstere wird von einem atomdicken Gasfilm hervorgerufen, dessen Widerstand von dem physikalischen Zustand der Elektrodenoberfläche und der Stromdichte bestimmt wird. Der reversible



Teil ist das Ergebnis von Konzentrationspolarisation und der Rückionisation von (a) abgeschiedenem Gas, (b) der Elektrode und (c) den Überspannungsverbindungen des Gases mit der Elektrode. Nur (c) kann korrekterweise als "Überspannung" bezeichnet werden und wird bei neun Metallen vorgefunden. Die "direkte" und die Kommutatormethode zur Bestimmung von reversibler Überspannung werden kritisch besprochen und ein vollständiger Mechanismus der kathodischen Abscheidung von  $H_2$  skizziert.

Department of Physical Chemistry,  
University of Cape Town.

## THE ADAPTATION OF *BACT. LACTIS AEROGENES* TO CRYSTAL VIOLET AND TO SULPHANILAMIDE.

BY D. S. DAVIES, C. N. HINSHELWOOD AND A. M. JAMES.

Received 5th March, 1946.

One of the methods likely to elucidate the mechanism by which bacteria adapt themselves to resist the action of inhibitory drugs is the quantitative investigation of the relation between drug concentration and growth for a complete series of adapted strains. Cells are trained by repeated sub-culture in presence of a given concentration  $\bar{m}$  of the drug, the lags and the mean generation times of the trained strains being then tested at a whole range of concentrations up to values much exceeding  $\bar{m}$  itself. Experimentally the simplest determination is that of the lag-concentration curve, and it is with this that we shall be chiefly concerned.

The most detailed study so far made along these lines is that of the adaptation of *Bact. lactis aerogenes* to proflavine. The principal result is that cells trained at  $\bar{m}$  will, when at the appropriate age, grow without lag up to test concentrations in the neighbourhood of  $\bar{m}$  itself, and that as the test concentration increases beyond  $\bar{m}$  the lag rises rather steeply towards infinite values. This is an important and typical case, but behaviour does not by any means always conform to this pattern. The other extreme of behaviour towards which, as will appear, sulphonamide adaptation of *Bact. lactis aerogenes* tends, is that, instead of developing a resistance precisely graded to  $\bar{m}$ , the cells change over to a new and relatively immune state which is not very dependent upon  $\bar{m}$  (at least so long as this exceeds a necessary minimum). In the first case it is as though an existing cell growth mechanism enlarged itself just enough to perform its normal functions in spite of the drug: in the second case it is as though a qualitatively new mechanism had been called into action.

A quantitative theory of the proflavine adaptation has already been attempted.<sup>1</sup> The essentials of it are as follows. An enzyme I produces an intermediate, M, which is partly lost by diffusion and partly utilised by a second enzyme II, and during growth attains in the cell a steady concentration,  $c$ . By the operation of the drug the concentration  $c$  is lowered to  $c - \phi(m)$ , where  $\phi(m)$  is a function of the drug concentration,  $m$  (and with proflavine a simple linear function). The rate of synthesis of enzyme II is related to  $c$  by an expression of the form, rate =  $kc/(1 + bc)$ . When  $c$  is lowered by the drug the synthesis of II is retarded relatively to that of I, but the division of the cell must await the formation of a standard

<sup>1</sup> Davies, Hinshelwood and Pryce, *Trans. Faraday Soc.*, 1944, 40, 397; 1945, 41, 163.

amount of II. During growth in presence of the drug, I expands relatively to II and  $c$  rises in consequence. It can be shown that finally  $c$  is restored to the value  $c_1$  which it possessed in normal cells in the absence of drug: adaptation is then complete. If the value of  $c$  for cells trained at concentration  $\bar{m}$  and tested at  $m$  is assumed to be approximately

$$c + \phi(\bar{m}) - \phi(m)$$

and if, further, the lag is assumed to be an inverse function of the rate of operation of enzyme II, then the whole family of lag concentration curves can be accounted for.

A corresponding family of curves for sulphanilamide adaptation has not previously been obtained, but from other data a picture of the mechanism rather different from the above has been formed.<sup>2</sup> When *Bact. lactis aerogenes* is grown in presence of sulphanilamide, the curves giving log (number) as a function of time are of a peculiar form, consisting of two roughly linear segments. At a given transition point a slower mode of growth is superseded by a more rapid one. On successive subcultures the transition occurs earlier and earlier, until the whole observable process occurs at the higher rate. This was interpreted as a process whereby the lag of an alternative mechanism, less sensitive to sulphanilamide than the normal one, gradually becomes shorter, until the new type of growth replaces the old. The substitution of this alternative mechanism does not, however, mark the completion of the adaptive process. The growth rate though enhanced is not yet normal, the immunity is readily lost, and it is specific to particular members of the sulphonamide class. On further prolonged subculture, complete, irreversible and non-specific adaptation is attained.

The somewhat different pictures formed of these two drug actions made it desirable on the one hand to obtain further experimental evidence, and on the other to pursue further the theoretical consideration of the problem. In this paper are described the study of the adaptation of *Bact. lactis aerogenes* to Crystal Violet, the determination of the lag concentration relationships for a series of sulphonamide-trained strains and a theoretical exploration of some simple enzyme models of adaptive systems. The latter are compared with the various experimental observations.

### Experimental Data.

(1) **Adaptation to Crystal Violet.**—The action of Crystal Violet was studied by methods similar to those employed for proflavine.

Fig. 1 shows the variation with the dye concentration of the mean generation times (m.g.t.). The ratio of the m.g.t. for a control culture to that observed on addition of the dye falls steeply and almost linearly. Values below 0.2 are not measurable, since at the corresponding concentrations the lag is prolonged indefinitely.

As is also shown in Fig. 1, training reduces the mean generation time considerably, but never restores it to

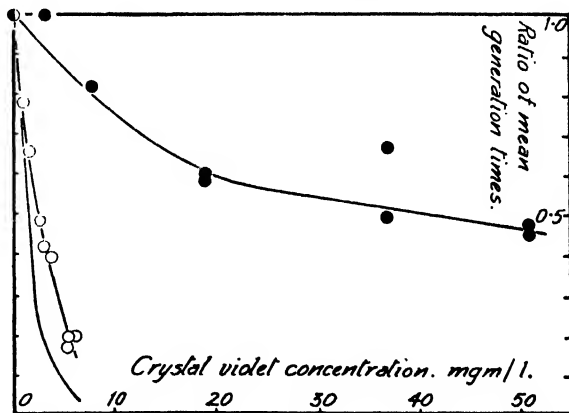


FIG. 1.—●—trained cells.

<sup>2</sup> Davies and Hinshelwood, *Trans. Faraday Soc.*, 1943, 39, 431.

the normal value. Even after 50 subcultures, and long after the lag has fallen to the normal value, the m.g.t. still remains high.

The curves of log (count) against time are not infrequently of the composite form already encountered with sulphanilamide. But there seems to be no regularity about the transition from the slower to the more rapid growth.

Crystal violet has little effect on the total cell population which the given medium will support.

For lags that are minimal with respect to the age of the cells, the lag-concentration relationships are shown by the continuous lines in Fig. 2*b*, where the numbers beside the curves record the dye concentration at which

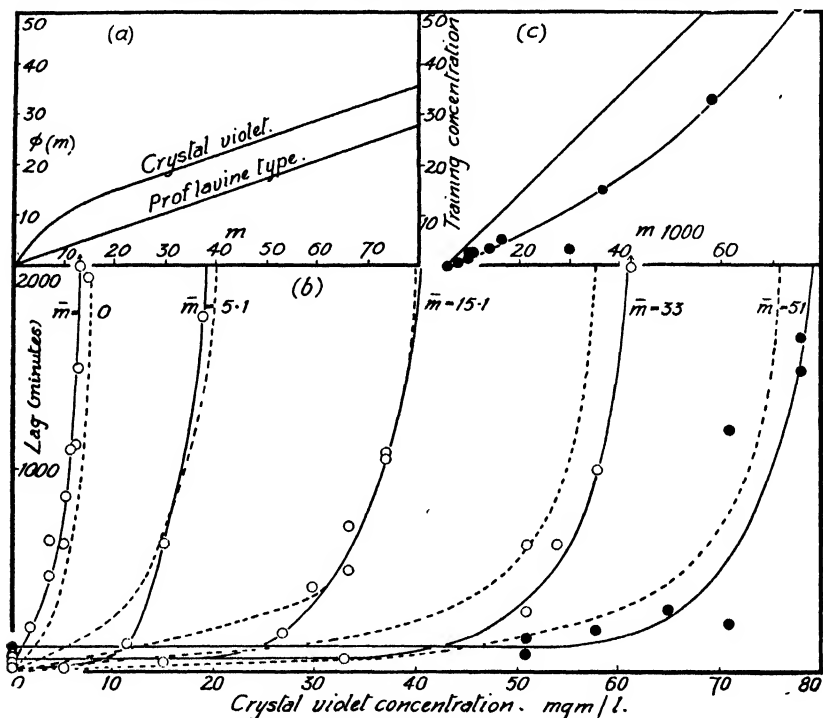


FIG. 2.

the cells have been trained. This family of curves in some respects resembles the corresponding family found for proflavine-trained cells. The shape of the individual lag-concentration curves is very similar, but the spacing is different.

Fig. 2*c* shows the concentration of dye,  $m_{1000}$ , required to cause a lag of 1000 minutes (in a culture at the stage of minimal lag) plotted against the concentration,  $m$ , at which the culture has been trained. With proflavine the result is a straight line of slope  $45^\circ$ . With Crystal Violet, on the other hand, training at the lower concentrations causes a relatively greater shift in  $m_{1000}$ . For example, training at 5.4 mg./l. increases the  $m_{1000}$  value by 11 mg./l. For higher values of  $\bar{m}$ , however, the relationship tends more and more to the proflavine type.

Training to Crystal Violet is not nearly so rapid as with proflavine. In the determination of the curves in Fig. 2*b*, the strains were tested at intervals of about five subcultures until successive tests gave nearly the same result. From twenty to thirty-five subcultures might be necessary for this.

Cells fully trained to concentrations of Crystal Violet up to 51 mg./l. were found to retain their immunity in full when subcultured in the ordinary

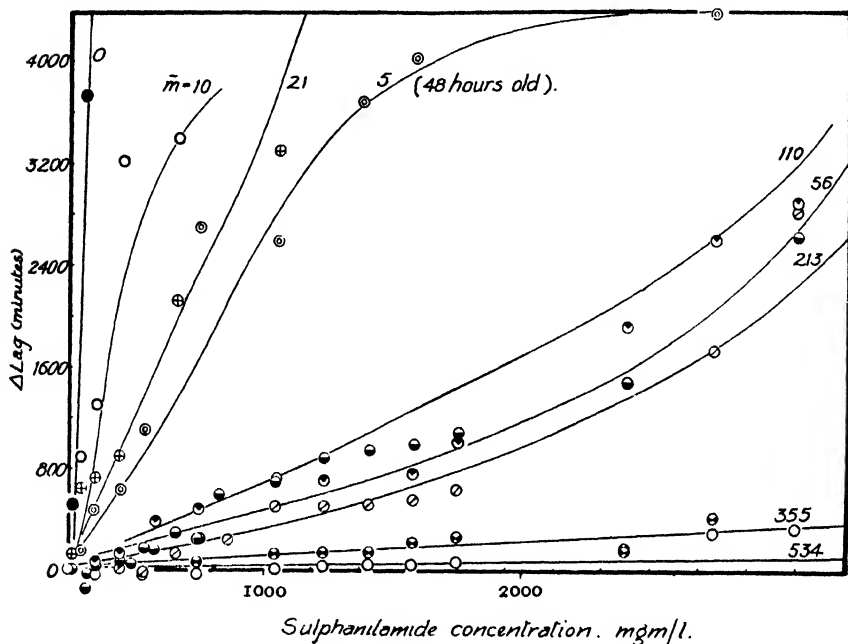


FIG. 3.

medium. Crystal Violet, in contrast with proflavine, did not cause the growth of abnormally long filamentous cells.

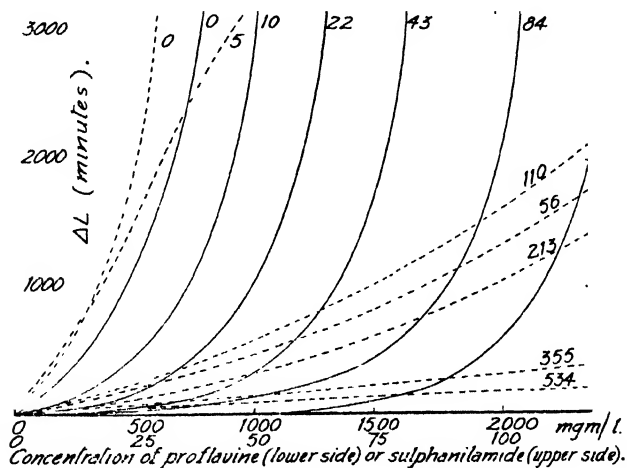


FIG. 4.

It has already been pointed out that the actions of Crystal Violet and of proflavine are in many respects similar.<sup>1</sup> This is shown by the marked effect of both substances on the lag, the reversal of the effect by filtrate from grown cultures, and by the adaptation of the lag on training. The present

evidence confirms this conclusion in so far as the lag-concentration curves are of similar form for both substances, and the variation of immunity with training concentration is the same, at least for higher values of the latter. The previous experiments also revealed differences. The point of attack of the drug in the cell cannot be the same, and the acquired immunity is not reciprocal. The growth rate in Crystal Violet never returns to normal even after training. Adaptation to Crystal Violet is slower. Another important difference now appearing is that a disproportionately large increase of immunity (as measured by lag-concentration curves) occurs on training to the lower Crystal Violet concentrations. We shall seek for an interpretation of these divergences which will not conflict with the idea of their essential similarity.

(2) **Adaptation to Sulphanilamide.**—Experiments were made to observe the variation of the degree of immunity to sulphanilamide of cells trained to various concentrations. The cells were trained in the synthetic medium used for the study of proflavine and Crystal Violet. Complete adaptation to sulphanilamide is rather slow, and thirty to fifty subcultures were usually necessary. In the final state the growth rate is exactly normal.

The determination of the lag-concentration curves presents a certain difficulty. If cells at the stage of minimal lag are inoculated into media containing sulphanilamide there is an initial period of rapid, though quite limited growth, as though the drug required time to exert its inhibitory effect. This effect, (which could not be overcome by devices such as leaving the cells in a medium containing drug but lacking an essential constituent, and starting the experiment by adding the latter), makes it impossible to work at the minimal lag stage. To overcome the difficulty, the parent culture was always allowed to age so that it had a standard lag in the drug-free medium of  $1100 \pm 200$  minutes. The difference between the observed value and the corresponding value for the medium containing the sulphanilamide was taken as the measure of the drug action.

All the trained strains were tested over a wide range of sulphanilamide concentrations. The results are shown in Fig. 3.

The considerable contrast between the action of the sulphanilamide and that of proflavine is shown in Fig. 4.

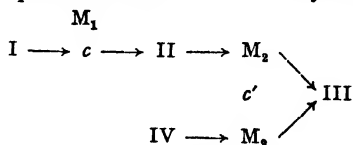
It is apparent that the degree of immunity does not vary linearly with the training concentration. For example, training at 50, 100 and 200 mg./l. leads to almost identical results. The curves in Fig. 3 seem to fall into groups, but these do not depend regularly on the concentration at which the cells are trained, and the difference appears to be more a function of some uncontrolled secondary factor in the tests than of the training concentration. In this connection it may be observed that the sulphonamide sensitivity of untrained cells may vary within fairly wide limits.

### Theoretical.

Independently of the preceding experimental studies, certain theoretical considerations will now be developed. These concern the introduction of alternative cell mechanisms during adaptive processes. Some general observations on alternative mechanisms have been given in two previous papers.\*

The theoretical schemes will be compared with the actual findings for various drug adaptations in a final section.

**Theory I. Development of an Alternative Mechanism.**—The diagram below schematises a possible relation of cell enzymes.



\* Davies and Hinshelwood, *Trans. Faraday Soc.*, 1943, **39**, 431; Lodge and Hinshelwood, *ibid.*, 1944, **40**, 571.



$$K_m(\text{test}) = k'_{1(\text{test})} \left\{ \frac{(x_1)_0}{(x_2)_0} \right\}_{(\text{training})} + k'_4 \gamma \left\{ \frac{(x_1)_0}{(x_2)_0} \right\}_{(\text{training})},$$

$$\text{or} \quad K_m(\text{test}) = \left\{ \frac{(x_1)_0}{(x_2)_0} \right\}_{(\text{training})} \{k'_{1(\text{test})} + k'_4 \gamma\} \quad (6)$$

$k'_{1(\text{test})}$  is the quantity affected by the drug, which immediately depresses it below its normal value. The result is an immediate reduction in initial growth rate, according to (6).  $(x_2)_0/(x_1)_0$ , however, according to (5), gradually adjusts itself to a new value, so that in (6)  $(x_2)_0/(x_1)_0$  then eventually reaches the value, from (5)  $(k'_{1(\text{test})} + k'_4 \gamma)/K$ .  $K_m(\text{test})$  then equals  $K$  once more and complete adaptation has occurred. The essential part of this adaptation is that the small value of  $k'_{1(\text{test})} + k'_4 \gamma$  is exactly compensated by the large value of  $(x_1)_0/(x_2)_0$ . So far the present theory is almost identical with that applied to the proflavine case. But when we now consider the behaviour of the trained cells in still higher concentrations of the drug the difference appears. The more the factor  $(k'_{1(\text{test})} + k'_4 \gamma)$  is reduced, the larger is the relative value of  $k'_4 \gamma$ , since it is  $k'_{1(\text{test})}$  which is changed by the drug. This means that the trained cells become less and less sensitive to further drug, and a larger and larger proportion of the growth is due to the alternative mechanism via enzyme IV.

(5) and (6) may be written in the form

$$\frac{K_m(\text{test})}{K} = \frac{k'_{1(\text{test})} + k'_4 \gamma}{k'_{1(\text{training})} + k'_4 \gamma} = \frac{F(m_{\text{test}}) + B}{F(m_{\text{training}}) + B} \quad (7)$$

As soon as  $F(m_{\text{training}})$  is small compared with  $B$ , the further reduction of  $F(m_{\text{test}})/F(m_{\text{training}})$  is of no consequence and the ratio  $\frac{K_m(\text{test})}{K}$  remains near unity.

To calculate a family of curves for comparison with experiment some simplifying assumptions and approximations are necessary. First, the literal application of equation (7) to the case of cells trained at a concentration,  $\bar{m}$ , and grown at a concentration less than  $\bar{m}$  would suggest that  $\frac{K_m}{K}$  would be greater than unity and the growth rate, under these conditions, greater than normal. This is not observed in fact: trained cells almost always grow in absence of the drug at a normal rate. Equation (7), however, is based on the assumption that the rate of operation of enzyme III is directly proportional to  $c$ . This will in fact cease to be the case just when  $c'$  exceeds the normal value<sup>4</sup>: the enzyme becomes saturated and its growth rate effectively independent of  $c'$ . Accordingly, we superimpose the condition that  $K_m/K$  cannot exceed unity. In the second place, the calculations deal with growth rates, while the most satisfactory experimental determinations deal with lags. (This is unavoidable, since actual multiplication of the cells rapidly brings about some degree of adaptation, and the measurements of generation times therefore apply to partially adapted cells.) We therefore assume that the course of adaptation of the lag will be that of a reciprocal growth rate. This must be at least an approximation to the truth. We cannot, however, simply write  $K_m(\text{test})/K = L_{\text{normal}}/L_m$  since this latter expression becomes indeterminate as  $L$  approaches zero. We shall therefore regard the mean generation time (approx. 30 minutes) as the minimum value of  $L$  (to this small extent modifying the conventional definition of  $L$ ), and write

$$K_m(\text{test})/K = \frac{L_{\text{normal}}/30 + 1}{L_m/30 + 1} \quad (8)$$

Some evidence for this assumption is afforded by the moderate concordance between values for Crystal Violet obtained directly from mean generation times and indirectly by equation (8) from the lags. For small values of the

<sup>4</sup> Davies, Hinshelwood and Pryce, *Trans. Faraday Soc.*, 1945, 41, 163.

lag this expression no longer tends to an indeterminate value, and for large values it is nearly the same as  $L_{\text{normal}}/L_m$ . We now need the form of  $F(m)$  in equation (7). For the original untrained cells

$$F(m_{\text{training}}) = F(0) = 1.$$

For untrained cells the initial growth rate was determined by Davies and Hinshelwood as a function of sulphanilamide concentration. This rate fell steeply with increasing drug concentration to a constant residual value. Here it is reasonable to assume that  $F(m) = 0$ , so that

$$K_{\text{residual}}/K = (0 + B)/(1 + B),$$

whence  $B$  may be obtained. Further, from the curve of rate against drug concentration the form of  $F(m)$  for the intermediate values can easily be calculated. We shall assume that the function so found is the correct one to use in equations (7) and (8), where all the quantities are now known, so that the lags can be calculated at any drug concentration for strains of cells adapted to any other concentration.

The family of curves so computed is shown in Fig. 5. It is evident that, according to this, training to quite small concentrations, e.g. 20 mg./l. would give a high degree of immunity to concentrations up to almost any value.

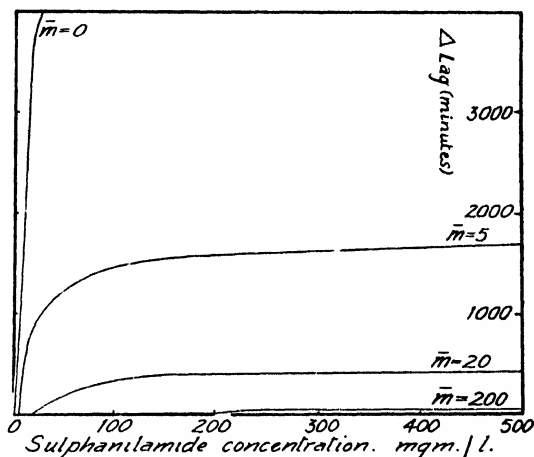


FIG. 5.

**Theory Ia. Adapted Mechanism still Retains some Degree of Drug Sensitivity.**—The above theory can be modified by supposing that the alternative mechanism as a whole is still sensitive to the drug, but only at very much higher concentrations. Enzyme I itself might, for example, suffer inhibition at quite high sulphonamide concentrations. The family of curves in Fig. 5 would then be changed so that each took a rapid upward turn at some appropriately high value of the concentration.

**Theory Ib. Two Adaptable Enzymes.**—As an obvious extension of equation (7) we must consider the case where  $k'_4$  is affected by the drug, but to a smaller extent than  $k'_1$ . We should then have

$$\frac{K_m(\text{test})}{K} = \frac{F(m_{\text{test}}) + BF'(m_{\text{test}})}{F(m_{\text{training}}) + BF'(m_{\text{training}})}.$$

This gives a picture somewhat different from the previous one. As soon as  $F(m)$  becomes negligible compared with  $BF'(m)$ , the behaviour becomes identical with that of the model used to interpret the data for proflavine. Adaptation to small concentrations will involve expansion of enzyme IV to restore the growth rate to normal. The lag-concentration curve will be displaced by an amount well exceeding the drug concentration at which the cells were trained (provided that the drug tolerance of the new mechanism is greater than that of the old). Once sufficient drug is present to reduce  $k'_1$  to very low values, the metabolite  $M_2$  will be furnished only by enzyme IV, which, if attacked by the drug, will itself expand further. The adaptation will from then on be graded to the training concentration, in the manner previously discussed for proflavine.

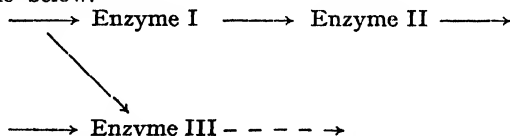
**Theory II. Qualitative Modification of Enzymes.**—An entirely



different mode of introduction of an alternative mechanism is suggested by the work on adaptation to sulphonamides and by certain experiments on adaptation to new media. These various observations have been interpreted in the following way.<sup>5</sup> Alternative growth mechanisms exist, but in normal circumstances one of them has too long a lag to come into play before growth by the competing one is complete. The first mechanism is the more adversely affected by the drug (or change of medium), so that the alternative has a chance to operate, and growth by it may supersede normal growth. In successive subcultures its lag shortens until the new mechanism entirely replaces the old.

Formally this theory gives a good account of the facts, especially of the composite form of the observed growth curves. What requires closer examination, however, is the question how two alternative mechanisms can have independent lags. In a stable culture all the parts of the cell must increase in the same ratio. If the enzymes responsible for the operations which end the lag of the alternative mechanism were not synthesised in normal growth, then they would be eliminated: if, on the other hand, they are built up at the normal rate, then an explanation is needed why the corresponding lag is specially long until after adaptation has occurred. The idea of the two lags is formally so useful that a more detailed development of it is desirable.

To make the behaviour of the system intelligible we need to postulate an enzyme which, during normal growth, loses its power to function with full effect without, however, suffering complete elimination, and which, in changed circumstances can recover its efficiency. This suggests a reversible modification in the qualitative structure, rather than in the mere amount of the enzyme. (It has been found convenient to postulate such modifications in other connections.) The following simple hypothesis accounts for the kind of behaviour envisaged. The normal synthetic route is schematised by the sequence I, II. . . . We suppose the action of the drug to impede the functioning of enzyme (I), thereby causing the intermediate provided by its precursor to accumulate in excess of the normal amount. The changed concentration gradients cause some of the excess to diffuse away to another enzyme (III) the composition of whose substrate is thereby altered. Enzyme (III) is supposed capable of assimilating the changed substrate, though less readily, and to incorporate into its structure somewhat different elements from the usual ones, just as a crystal lattice will accept structural elements differing slightly from its own. With some difficulty enzyme (III) now grows to the accompaniment of an actual modification of its texture. This change becomes easier as it proceeds, since each new layer of substance approximates more completely to the equilibrium configuration. The modified enzyme can now produce with optimal efficiency the substances necessary for the ending of the lag of another sequence of growth reactions. The state of affairs envisaged is illustrated in the scheme below.



When the route indicated by the dotted lines begins to be used the structure of III changes.

With this form of alternative mechanism theory the course of adaptation will appear as shown in Fig. 6.

Relatively to the lag OA of the (retarded) normal mechanism, the lag of the alternative one decreases, e.g. from OC to OB, the growth curves assuming successively the forms OAFH, OAEG, and so on.

<sup>5</sup> Davies and Hinshelwood, *loc. cit.*<sup>3</sup>; Lodge and Hinshelwood, *Trans. Faraday Soc.*, 1944, 40, 571.

**Comparison between the Models and Experiment.**—As has already been shown, the simple model of an expanding enzyme system gives an adequate description of the family of lag concentration curves for various proflavine-trained strains of *Bact. lactis aerogenes*. As explained in the introduction to the present paper, the reduction in concentration of a certain intermediate proves to be a linear function of the drug concentration. A similar theory would give a satisfactory account of the Crystal Violet-trained strains, except that it would not explain: (a) the disproportionately large shift in the curves for the lower training concentrations, and (b) the fact that the growth rate never adapts itself to normal. (a) can be formally accounted for by assuming the appropriate relation between the drug concentration,  $m$ , and the function  $\phi(m)$  expressing its effect on  $c$ . The function required is shown in Fig. 2a. Whether for a single expanding enzyme system, such a  $\phi(m) - m$  relation is plausible is hard to say. This form would, however, be simulated if the simpler theory were falsely applied to a system involving the more complex adaptation represented by the alternative mechanism, as in I (a). (b) could be explained if the drug at lower concentrations was assumed to provoke the training of an alternative mechanism (with a lower inherent growth rate), the further expansion of the enzymes responsible for this second mechanism accounting for the proflavine-like spacing of the family of curves in the higher concentration ranges as in II.

The facts about sulph-anilamide adaptation are, as a whole, most easily interpreted in terms of an alternative mechanism. The behaviour, however, is somewhat complex. Davies and Hinshelwood concluded that there were

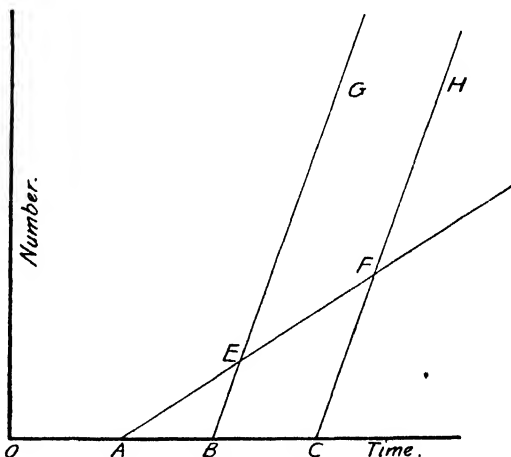


FIG. 6.

two distinct stages in the adaptation. The first stage is characterised by composite growth curves, and is a typical example of the kind of process discussed under the heading of theory II. The second stage involves the complete return of the growth rate to normal. The family of curves in Fig. 3 refers to strains which have completed this second stage. The spacing of them again strongly suggests an alternative mechanism. It is interesting to compare Fig. 3 with Fig. 5 which gives a family of curves calculated from theory 1. The general spacing corresponds fairly well, but the shape of the curves does not agree. The final rise of the experimental curves can be easily accounted for by a modification of the theory such as that introduced under I (a). On the other hand, the calculated curves show an initial rise followed by a horizontal portion, the height of which diminishes with increasing training concentration. This is not in evidence with the experimental curves. Nevertheless, having regard to the uncertainty in our assumptions about the relation between lags and growth rates, we might conclude that there is a reasonable qualitative resemblance between the observed behaviour and that to be expected from a theory of the type of I (a).

One of the authors (D.S.D.) is indebted to I.C.I. (Dyestuffs) Ltd. for the opportunity to undertake this work.

### Summary.

This paper contains :

(a) an experimental study of the adaptation of *Bact. lactis aerogenes* to Crystal Violet and to sulphanilamide, according to the plan followed in previous studies with proflavine;

(b) a theoretical discussion of some possible adaptive mechanisms;

(c) a comparison between the results of (a) and (b).

### Résumé.

Cet article contient :

(1) une étude expérimentale de l'adaptation du *Bact. lactis aerogenes* au Violet Cristallisé et à la sulphanilamide, suivant le même plan que pour les études précédentes sur la proflavine;

(2) une discussion théorique de quelques mécanismes possibles d'adaptation;

(3) une comparaison de (1) et (2).

### Zusammenfassung.

Der Artikel enthält :

(a) Eine experimentelle Untersuchung der Anpassung von *Bact. lactis aerogenes* an Kristallviolett und an Sulfanilamid unter Befolgung des Plans von vorhergegangenen Studien mit Proflavin.

(b) Eine theoretische Erörterung einiger möglicher Anpassungsmechanismen.

(c) Einen Vergleich von (a) und (b).

*Physical Chemistry Laboratory,  
Oxford.*

## THE THERMAL DECOMPOSITION OF MERCURIC OXALATE.

BY E. G. PROUT AND F. C. TOMPKINS.\*

*Received 6th May, 1946.*

The thermal decomposition of mercuric oxalate has not been previously investigated, although it decomposes at a convenient temperature with the production of gaseous products.<sup>1</sup> The reaction has interest because its course is expected to be modified by many factors, as with silver oxalate,<sup>2</sup> and its mode of decomposition might be similar to that of the latter. The mechanism of Macdonald<sup>3</sup> adequately describes his results, but it is not expected to be of general validity, and it is at variance in some respects with the work of Benton and Cunningham.<sup>4</sup> Their interpretation has become of greater significance because of the results obtained by Garner and Maggs,<sup>5</sup> and by Wischin,<sup>6</sup> with BaN<sub>2</sub>, and on account of the theory of Mott<sup>7</sup> in terms of the Wagner-Schottky conception of ionic conductivity<sup>8</sup> and the electron theory of solids. There are, as yet,

\* I.C.I. Research Fellow (University of London).

<sup>1</sup> Kohlschutter, *Ber.*, 1902, **35**, 483.

<sup>2</sup> Macdonald, *J. Chem. Soc.*, 1936, 832; cf. also *ibid.*, 2764, 1925; and *Trans. Faraday Soc.*, 1938, **34**, 589.

<sup>3</sup> Macdonald, *J. Chem. Soc.*, 839, 1936.

<sup>4</sup> Benton and Cunningham, *J. Amer. Chem. Soc.*, 1935, **57**, 2227.

<sup>5</sup> Garner and Maggs, *Proc. Roy. Soc., A*, 1939, **172**, 299.

<sup>6</sup> Wischin, *ibid.*, 1939, **172**, 314.

<sup>7</sup> Mott, *ibid.*, 1939, **172**, 325.

<sup>8</sup> Wagner and Schottky, *Z. physikal. Chem.*, 1930, **11**, 163. Cf. Jost, *Dif-fusion und chemische Reaction in festen Stoffen*, Dresden, 1937.

insufficient data to extend, or modify, this theory to other decompositions which are accelerated by pre-treatment with light and electron bombardment. Mercuric oxalate is sensitive to such stimuli and a study of its decomposition should prove of value. Furthermore, the effect of increasing the area of the metal/oxalate interface can be studied and further information about the nature of the reaction obtained. The investigation reported here is of a preliminary character devised to make a broad survey, and certain general features have now been established.

### Experimental.

Mercuric oxalate was prepared by the dropwise addition of equal volumes (250 ml.) of *M./10* mercuric acetate and *M./10* oxalic acid at equal rates to 100 ml. water at 25° C. with vigorous mechanical stirring. After thorough washing, the precipitate was dried *in vacuo* over  $P_2O_5$ . The salt rapidly darkens in light, consequently all operations were conducted in a dark room using red light. The dried powder detonates on impact. The oxalate content determined volumetrically was 99.8 % theoretical. The apparatus used was similar to that employed previously;<sup>9</sup> in any run, 4 mg. salt was placed in a Pt bucket, exhausted for 16 hours at room temperature, then lowered into the reaction chamber at 180–200° C. Traps of solid  $CO_2$ /alcohol separated the salt from the McLeod gauges; the pressure of gas evolved into a calibrated volume was measured at intervals.

### Results.

Erratic results, obtained initially, were due to the higher rate of production of Hg vapour by the decomposition as compared with that of freezing-out by the traps; when an additional trap was inserted close to the decomposing solid, the reproducibility was good if the samples were taken from the same preparation. Different batches (labelled I, II, etc.), although prepared apparently identically, gave different *p/t* plots, so that throughout each series, the same batch was used.

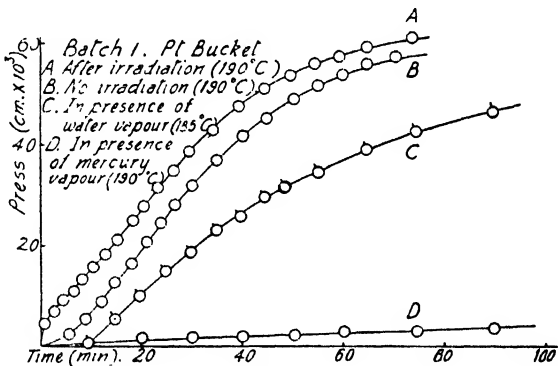
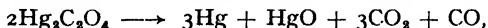


FIG. 1.

Typical plots for various conditions are given in Fig. 1. The chemical nature of the decomposition is best represented by



the volume of gas evolved being 92 % of that calculated theoretically.

Neither the addition of the end products of previous runs, nor allowing the reaction to proceed in presence of its gaseous products, had any effect on the rate. Similarly, interruption of the reaction by sudden cooling caused no change when the decomposition was continued after several hours. Preliminary results showed that water vapour exerted a retarding influence; an appendix was inserted near the reaction chamber, and a constant vapour pressure obtained by maintaining out-gassed water at low temperatures, using solids of suitable melting points.

<sup>9</sup> Prout and Tompkins, *Trans. Faraday Soc.*, 1944, 40, 488.

An induction period of 5-10 min., depending on the pressure, was obtained; afterwards, the rate returned to the normal value (Fig. 1).

In investigating the effect of Hg vapour, an apparatus similar to that used by Garner and Marke<sup>10</sup> was employed, the Pt bucket being provided with a flanged lid to prevent entry of condensed mercury. At 185° c. a marked retardation was found, which, however, was practically unchanged when the temperature was raised to 215° c. This anomaly required examination. In any run, the bucket, at room temperature, was lowered to within 2 cm. of the surface of the boiling mercury, and was heated by radiation and by bombardment with Hg atoms. These latter are in temperature equilibrium with the boiling metal. Since their mean free path *in vacuo* is several centimetres, the bucket would attain in absence of radiation the temperature of the boiling mercury (*viz.*, 155° c., *in vacuo*, or 30° c. below that of the walls). In the present apparatus, the atoms acquired additional energy (partly radiational, partly by collisions with the walls) but because of their approximately unidirectional flow at the low pressures, and because of their continuous production, little of this extra energy was communicated to the bucket.

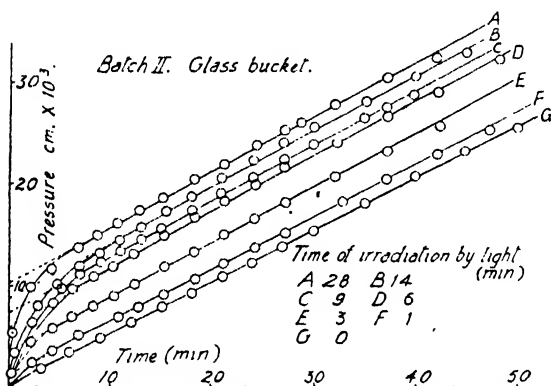


FIG. 2.

When the Pt bucket of high heat capacity was replaced by a light glass one of length four times its diameter (which allowed the use of a narrower reaction chamber), the rate was unchanged in presence of Hg vapour.

When the salt was pre-illuminated with ultra-violet light, the initial rate of decomposition was increased (Fig. 1). Using a quartz-mercury vapour lamp (full arc), running off 200 constant voltage, the rates were erratic due to fluctuations of intensity, although it was "stabilised" for 15-30 min. before use. Concordant rates were obtained when the salt was mechanically stirred in air at room temperature during exposure to sunlight. There was no appreciable decay when the pre-treated salt was stored in the dark *in vacuo* over  $P_2O_5$  at room temperature. Nevertheless, all samples were exposed simultaneously to avoid variations of intensity. No attempt was made to determine the threshold frequency necessary to produce acceleration. The effect of variations in the time of illumination on the rates is given in Fig. 2, using 4 mg. salt (Batch II) at 180° c. in a Pt bucket. The acceleration is clearly confined to the initial stages, the  $p/t$  plots being superimposed (after the first 15 min.) by a shift along the time axis (*cf.* the induction period of  $BaN_3$ ).<sup>8</sup>

Since mercuric oxalate detonates on impact, detonation might be induced by fast electrons (*cf.* Muraour),<sup>11</sup> *e.g.* using cathode rays. Two

The centrally placed container was thus effectively screened from the walls by the upward stream of atoms, whereas the thermometer placed very near, but not touching the walls, correctly recorded the temperature of the chamber. The bucket temperature was thus little changed by increasing that of the walls by 30°, and the slow rate observed was the normal one expected at 155° c.

<sup>10</sup> Garner and Marke, *J. Chem. Soc.*, 1936, 657

<sup>11</sup> Muraour, *Chem. and Ind.*, 1933, 30, 39.

side arms, 20 cm. apart, the lower one ending in a ground joint, were fused into the inner tube of the reaction chamber. A heavy Pt rod was sealed into the upper arm, and welded perpendicular to a stout circular Pt plate to form the cathode. The plate was at right angles to the length of the inner tube, and to one side of the centre, to allow free passage of the suspension wire of the bucket. The anode was similar except that the plate was welded along the length of the Pt rod, which was sealed into the ground joint. Rotation of this allowed sufficient space for the descent of the bucket. The discharge was produced by a potential of 10-30 kilovolts at a pressure of  $1 \times 10^{-3}$  cm., obtained by use of a calibrated micro-gasburette in the main apparatus. At this pressure, the dark space extended over the electrode distance and the green fluorescence of X-ray production was visible at the bottom of the chamber; under these conditions, the discharge was most steady and the effect of bombardment on the subsequent decomposition most marked. During discharge, the pressure increased slightly due to a small heating effect and to desorption of gas from the glass. This could not be eliminated. Since the characteristics of the beam were largely determined by the pressure, the following method was adopted. A thin, slightly compressed layer of salt (4 mg., Batch II) was placed in a flat-bottomed glass bucket, which was lowered to within 1 cm. of the anode; the apparatus was evacuated, after which  $1 \times 10^{-3}$  cm. oxygen was admitted, and the discharge operated for 30 sec. After re-evacuation, the process was repeated until the required period of bombardment was obtained.

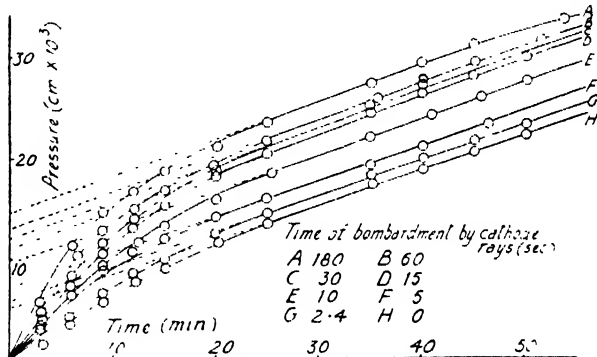


FIG. 3.

Using various pressures, applied voltages, and positions of bucket, no detonation was produced, but the salt darkened after 3-5 min. The oxygen was then evacuated, the bucket lowered, and the decomposition followed as before. The results on the variation of time of pre-bombardment at room temperature on the rates at 180° c. are given in Fig. 3. In contrast to the previous series, the depth of darkening was not related to the magnitude of the initial acceleration, since the increased rate occurred before any visual change was apparent. Furthermore, when the decomposition of pre-bombarded oxalate was interrupted, followed by rebombardment, no new acceleration was obtained. Similarly, a radium needle of 1 mg. contained in a Pt cylinder, placed in contact with the salt during decomposition had no effect on the rate; this, however, could be due to an insufficiently intense electron beam.

A reaction chamber similar to that of Muller and Brous<sup>12</sup> was constructed in order to study the effects of variation of intensity and energy of bombardment. The electron source was a Pt cylinder, coated with alkaline earth oxides and activated in the usual way, and raised to red heat by an inner furnace. No change of colour of the salt was produced even with a beam of 50 milliamp. under an accelerating potential of 50° volts, and no acceleration was produced in the subsequent thermal

<sup>12</sup> Muller and Brous, *J. Chem. Physics*, 1933, 1, 482.

decomposition. During bombardment, however, there was a loss of weight of the salt accompanied by a large evolution of gas. The apparatus proved unsuitable for a quantitative study of this and is being redesigned.

### Discussion.

The variable behaviour of different batches of oxalate is consistent with its semi-colloidal behaviour, which makes an exact control of all variables difficult; the reproducibility of the same batch is probably due to the large number of particles used in a run, and not to the homogeneity of the individual particle. The decomposition is insensitive to end products, both solid and gaseous, and to the presence of Hg vapour. This latter result proves that the decomposition neither proceeds at the metal-oxalate interface (which is largely increased in presence of Hg vapour), nor does the metal catalyse the decomposition. It may be noted that the effect is expected only in the initial period of the decomposition, since in the later stages, other end products, e.g., HgO, covered the surface of the decomposing solid. The retardation produced by water vapour indicates that the decomposition is a surface one since the effect is merely to delay the onset of the reaction but not to alter the subsequent rate. The process is thus not a destruction of centres of reactivity, e.g. by surface crystallisation, but is an adsorption phenomenon, the induction period being due to the desorption of the vapour.

The  $p/t$  plots are similar to those given by silver oxalate, but the equations developed are inapplicable. The present decomposition, it may be noted, is more chemically complex and less quantitative. A mercurous compound has been detected as an intermediate product, suggesting a mechanism involving two consecutive monomolecular reactions, with the second possessing the higher velocity constant.<sup>13</sup> This is disproved by an analysis, similar to that recently developed.<sup>14</sup> Again, from the physical nature of the salt, the surface is probably highly nucleated. After the maximum velocity is reached, the rate should thus be proportional to the surface area and be controlled by the rate of penetration of the interface inwards. The particles are approximately spherical of average radius ( $r$ ),  $1.3 \times 10^{-4}$  cm., as determined by direct measurement under high magnification. The fractional decomposition ( $\alpha$ ) at any time ( $t$ ), calculated from the model of a contracting sphere<sup>15</sup> is given by

$$u/r = (1 - (1 - \alpha)^{1/3})/t \quad . \quad . \quad . \quad (1)$$

but it has been found convenient to transform to the form

$$dp/dt = 3kp_1/r(1 - ut/r)^2 \quad . \quad . \quad . \quad (2)$$

where  $p_1$  is the final pressure in cm.;  $u$ , the linear rate of penetration of the interface in cm./min., and  $k$ , the velocity constant of gas evolution from unit surface in cm. pressure/min., where  $k$  may be a function of  $T$ ,  $\alpha$ , etc. The plot of  $(dp/dt)^{1/2}$  against  $t$  is linear after the inflexion point in the  $p/t$  plot (co-ordinates,  $p_1, t_1$ ) with a slope ( $S$ ) equal to  $-(3p_1k/r)^{1/2}u/r$ , and an intercept ( $I$ ) to  $(3p_1k/r)^{1/2}$  (cf. Fig. 4). Values of  $u = -Sr/I$ , and  $k = I^2r/3p_1$  for various temperatures are given in Table I. From the plots of  $\log u$  and  $\log k$  against  $1/T$ , the activation energy ( $E_u$ ) associated with the linear propagation of the interface, and  $E_k$ , that relating to the gas evolution per unit area of undecomposed reactant, were found to be 37,100 and 46,600 cal. respectively. These should be the same; the difference is due to the divergence from the ideal system assumed in the deduction of (2). Thus, the activation energy calculated from the temperature coefficient of the maximum velocity plots is 40,300 cal. (mean of  $E_u$  and

<sup>13</sup> Cf. Neumann and Kortorowa, *Physik. Z. Sowjetunion*, 1933, 4, 818.

<sup>14</sup> Swain, *J. Amer. Chem. Soc.*, 1 44, 66, 1696.

<sup>15</sup> Hume and Topley, *Proc. Roy. Soc. A*, 1928, 120, 211.

$E_k = 41,700$  cal.). It may be noted, however, that a difference can actually exist, where  $E_k - E_u$  is the energy associated with the break-up of the oxalate radicle and its subsequent escape as  $\text{CO}_2$ , or with a process of activated diffusion or adsorption.

The magnitude of  $u$  ( $3 \times 10^{-8}$  cm.,  $200^\circ \text{C.}$ ) is lower than that found for  $\text{Ag}_2\text{CO}_3$ <sup>16</sup> ( $42 \times 10^{-8}$  cm.,  $180^\circ \text{C.}$ ), as expected from the lower activa-

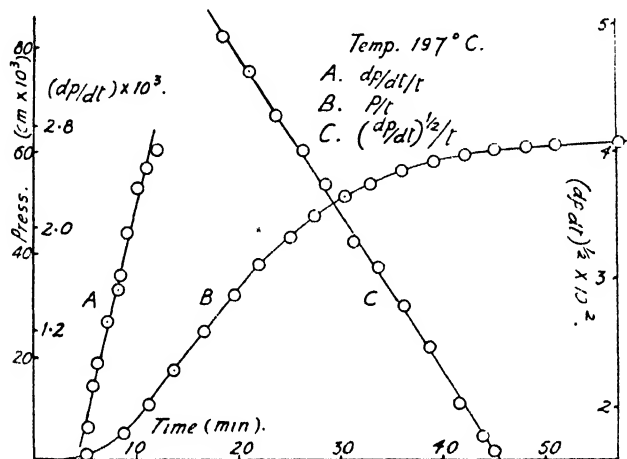


FIG. 4.

tion energy of the carbonate (23,000 cal.). Again, unlike  $\text{Ag}_2\text{CO}_3$ , there is here a difference between the absolute rate of reaction and that calculated from its variation with temperature; thus, if the ionic group vibrates in the interface when its energy exceeds  $E_u$ , the fraction activated

TABLE I

Temp.	$-s \times 10^4$ .	$I \times 10^2$ .	$u \times 10^7$ cm./min.	$h \times 10^4$ cm./min.	$v_{\text{max.}}$ ( $\times 10^6$ ).	$t_1$ min.	$k_1$ ( $\times 10^4$ ).
180	1.15	3.03	4.35	9.17	5.25	48.0	0.75
185	1.87	3.49	6.12	12.20	8.81	27.0	1.00
188	3.71	4.36	9.79	19.04	11.6	21.0	1.40
190	4.37	4.68	10.73	21.88	13.0	17.0	1.60
192	5.39	5.14	12.05	26.45	17.2	16.5	2.50
195	8.59	5.96	16.56	35.56	21.6	13.5	3.13
197	12.27	6.92	20.39	47.89	26.0	11.75	3.58
200	19.57	8.32	27.06	69.16	35.9	9.5	5.53
205	29.0	9.72	34.32	94.48	46.8	8.0	10.94
Activation energy in kcal.			37.1	46.4	40.3	34.5	25.6

at  $200^\circ \text{C.}$  is  $e^{-E_u/RT}$ , or  $1.5 \times 10^{-17}$ , whereas assuming a lattice spacing of  $5 \times 10^{-8}$  cm. and a vibration frequency of  $300 \times 10^{12} \text{ min.}^{-1}$ , then with  $u = 2.7 \times 10^{-8}$  cm./min., the fraction is  $3 \times 10^{-14}$  (cf.  $\text{BaNa}_8$ ,<sup>9</sup> and  $\text{CaCO}_3$ ,  $6\text{H}_2\text{O}$ ).<sup>17</sup>

In the acceleratory period,  $p$  is not an exponential function of the time (ct.  $\text{Ag}_2\text{C}_2\text{O}_4$ ); it is, however, shown in Fig. 4, that the plots of  $dp/dt$  against  $t$  are linear. Now, if the reaction spreads uniformly over the

<sup>16</sup> Spencer and Topley, *J. Amer. Chem. Soc.*, 1929, 2633.

<sup>17</sup> Hume and Topley, *Proc. Leeds Phil. Lit. Soc.*, 1927, 1, 169; and ref. <sup>18</sup>.



surface from  $n_0$  initial centres with an average velocity of  $v$  cm./min. (where  $v$  is large compared with  $u$ ) and if, at time  $t_1$ , the surface is completely covered, then

$$dp/dt = Kn_0 p_1 v / r^2 (v(t - t_0) + r_0) \quad (3)$$

or

$$dp/dt = k_1 t + C. \quad (4)$$

Here,  $K$  is a proportionality constant relating the gas pressure to the surface area and is temperature independent;  $r_0$  is the average radius of the (circular) initial centres, and  $t_0$  is the time which elapses before growth commences (i.e. that to attain the temperature of decomposition, or approximately 1.5 min.). The plot of  $\log k_1$  against  $1/T$  is linear, the slope corresponding to an energy of 51,200 cal. Since  $k_1$  involves  $v^2$ , the activation energy  $E_v$  is 25,600 cal., i.e. appreciably less than  $E_u$ . The low value is confirmed from the magnitudes of  $t_1$  at various temperatures. Ideally,  $v$  should be inversely proportional to  $t_1$ ; thus it is found that the plot of  $\log 1/t_1$  against  $1/T$  is linear, corresponding to an energy of 33,500 cal. This higher value compared with  $E_v$  is expected because the linearity of the  $dp/dt$  against  $t$  plot does not extend to  $t_1$ , and the effect of penetration near  $t_1$  is no longer negligible. The value of

TABLE II

Light.				Cathode Rays.			
Time (min.).	$\gamma$ .	$p_t (\times 10^3)$ cm.	$k_2$ min. <sup>-1</sup>	Time (min.).	$\gamma$ .	$p_t (\times 10^3)$ cm.	$k_2$ min. <sup>-1</sup>
0	0.23	—	—	0	4.49	—	—
1	1.40	1.17	—	0.04	5.71	0.72	—
3	3.85	3.62	0.68	0.083	7.50	2.51	0.21
6	5.70	5.47	0.82	0.17	9.50	4.51	0.21
9	7.25	7.02	0.54	0.25	10.79	5.80	0.22
14	8.73	8.50	0.64	0.50	11.72	6.73	0.19
28	10.25	10.02	0.54	1.0	12.80	7.81	0.41
—	—	—	—	3.0	14.50	9.51	0.32

$v$  cannot be calculated directly from (3); but from the magnitude of  $u$  and the ratio of  $E_u$  to  $E_v$ , it is estimated to be 25 times greater than  $u$ . This is in accord with the accepted ideas of crystal growth in a stepwise manner and also with the assumption made in the derivation of (3). Furthermore, calculations indicate that the number of centres initially present is 20 to 30, if initially their area is assumed to be no greater than corresponding to that of a group of 100 molecules.

Pretreatment with light or by electron bombardment is responsible for higher initial rates in the subsequent thermal decomposition; after a short period, the normal rate is attained and moreover is maintained throughout the subsequent stages. This suggests that the effect is purely a surface one; such a conclusion is consistent with the presence of a saturation value, after which further illumination causes no additional acceleration, and also with the lack of any effect when the partially decomposed oxalate is rebombarded. The change induced is stable at room temperature (cf.  $\text{BaN}_2$ ), i.e. it apparently has the nature of a "latent image formation which is developed subsequently in the thermal treatment." Thus, it is produced without loss of gaseous products, because the final pressure (after complete decomposition) is independent of the time of pretreatment, although the initial gas evolution accounts for as much as 15 % of the total. In contrast to  $\text{Ag}_2\text{C}_2\text{O}_4$ ,<sup>2,4</sup> and  $\text{BaN}_2$ , the initial  $p/t$  plots of illuminated salt are not described by the equation  $p = At^x$  (where  $x > 1$ ), and therefore a mechanism involving the increase in number

of nuclei and their growth with time (cf. Garner,<sup>5</sup> Mott<sup>7</sup>) is not valid. The essential condition of the Mott theory is that the salt should be an ionic conductor at room temperatures. This is unlikely with such a highly polarised molecule as mercuric oxalate, which probably possesses a molecular type structure. Consequently, although the decomposition of  $\text{BaN}_2$  and  $\text{HgC}_2\text{O}_4$  are similar in as far as the effect of pre-treatment is concerned, this analogy does not throw doubt on the theory, as has been done by James<sup>18</sup> from the analogous behaviour of  $\text{Hg}_2\text{Cl}_2$  (molecular type structure) and  $\text{AgCl}$  (ionic conductor) on reduction with hydroxylamine.

The plots (Fig. 2, 3) show that the duration of the initial gas evolution in the thermal decomposition is independent of the time of pretreatment, suggesting that a rapid monomolecular decomposition is superimposed upon the normal one. The presence of two simultaneous, but independent reactions is not improbable because both rates are insensitive to the presence of end-products. The decomposition plots of this "product" of irradiation are thus obtained by subtracting the normal from the measured values of  $p$ . These obey a monomolecular decay law since the plots of  $\log(p_t - p)$  against  $t$  are linear. Velocity constants, calculated from the slopes, are collected in Table II; these are approximately independent of the time of pretreatment, although dependent on whether light or cathode rays are used. The values of  $p_t$ , as can be seen from geometric considerations, are equal to  $(y_t - y_0)$ , where  $y$  refers to the values of the intercepts, which are indicated in Fig. 2, 3, and tabulated in Table II; they are clearly proportional to the mass of the "product" of irradiation.

With  $\text{BaN}_2$ , Garner and Maggs<sup>5</sup> have related the time of irradiation to the induction period in the subsequent thermal decomposition, since the nuclei increased in number and size during this period; here, however, the product is formed *during* pretreatment in an amount ( $y_t$ ) determined by the period of irradiation ( $t'$ ). The results here can be well expressed by the equation:

$$\log(y_{\max} - y_t) = k''t' + C \quad (5)$$

as shown in Fig. 5, where  $y_{\max}$  is the maximum value of  $y$ . Now in photographic work, a definite number of centres (per unit area),  $N_0$ , can be activated by light; assuming this to be true here, and that the energy associated with their formation is the same for all centres, then it follows that

$$dn/dt' = k''(N_0 - n_t) \quad (6)$$

where  $n_t$  is the number formed after the irradiation period,  $t'$ . On integration,

$$n_t = N(1 - e^{-k''t'}) \quad (7)$$

Noting that  $y_{\max}$  is proportional to  $N_0$ , and  $y_t$  to  $n_t$ , equation (5) is obtained. As demanded theoretically, the value of  $N_0$  is approximately

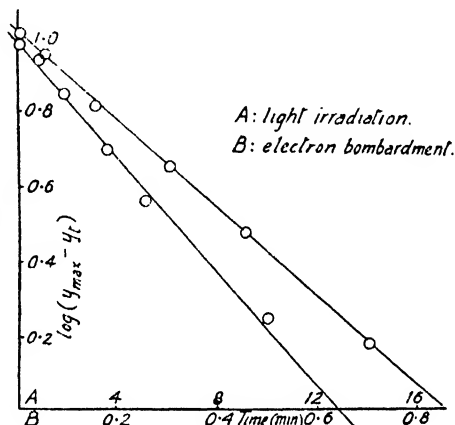
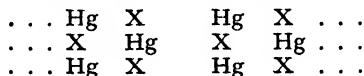


FIG. 5.

<sup>18</sup> James, *J. Amer. Chem. Soc.*, 1941, 63, 1601.

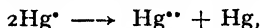
the same and independent of the type of pretreatment. The rate of production of centres is, however, twenty times more rapid for cathode rays on account of the higher intensity as compared with sunlight. Furthermore, the velocity constants ( $k_s$ ) of the decomposition are dependent on the nature of pretreatment. This fact, and the change of colour produced by light, but not cathode rays (except after long bombardment when the constant becomes greater) can mean a difference in structure of the "product," but not in the number of centres.

The nature of the "product" is uncertain, although it is probably associated with the existence of lower-valent Hg compounds. If the radius of the oxalate molecule is  $5 \times 10^{-8}$  cm. (assumed spherical), and if these are arranged in closest pattern to form spherical particles of radius  $1.3 \times 10^{-4}$  cm., then the surface layer of "product" formed at saturation must be 50-100 molecules deep to account for 15 % of the total gas evolution on decomposition. From adsorption data on similar compounds, this figure may be 10-30 too large because of surface irregularities, etc. In addition, there is associated with the formation by precipitation of the salt, a high aggregation, but low orientation velocity,<sup>19</sup> because of its high insolubility and its highly polarised molecule; a highly irregular form of particles is thus produced. It may therefore be concluded with some certainty that pretreatment affects the individual molecule, and the effect penetrates at least two or three molecular layers. The crystal structure of mercuric oxalate has not been determined, but by analogy with similar compounds, such as  $\text{Hg}_2\text{Cl}_2$  and  $\text{HgI}_2$ , it is expected to have a layer structure in which each Hg "atom" is surrounded by four "molecules" of the oxalate group, and vice versa, i.e.



where X is the oxalate group.

The *primary* act of irradiation may be similar to that which is envisaged for  $\text{BaN}_6$ , i.e. to free an electron from a surface oxalate group, which is here subsequently trapped by a Hg "ion" in the second layer. The process thus corresponds to an electron transference, which, when followed by an intramolecular change, can result in the production of "mercurous oxalate". This salt decomposes at a faster rate than does the mercuric salt. The effect of light is normally to cause the reverse transformation, i.e.



but there is an analogous reaction in the photochemical reduction of  $\text{HgCl}_2$  by oxalic acid in aqueous solution. It may be noted that the product of irradiation is formed here without gas evolution, and furthermore, an extension of the process, whereby two electrons are captured by the same mercury ion, leads to the production of the metal; this is the cause of the darkening found experimentally with ultra-violet light, and may well account for the higher velocity constant ( $k_s$ ) in the subsequent decomposition. With a high density electron beam, as produced in the Muller and Brous apparatus used here, groups of molecules may be simultaneously rendered sufficiently unstable<sup>20</sup> as to cause detonation of the surface molecules at room temperature. This would account for the loss of mass and the evolution of gas during bombardment, and for the fact that initial acceleration is found in the subsequent thermal decomposition of the remaining salt.

The authors wish to express thanks to the National Research Council and Board of South Africa for a Research grant for the purchase of apparatus, and one of us (E. G. P.) for a Research Scholarship held during

<sup>19</sup> Haber, *Ber.*, 1922, **55**, 1717.

<sup>20</sup> Kallmann and Schranker, *Naturwiss.*, 1933, **21-23**, 379.

the investigation. We are also indebted to Dr. M. Sacks of Grey's Hospital, and Mr. R. C. Albino for the loan of quartz-mercury vapour lamps, and to the former for providing the radium used in this work.

### Summary.

The present study of the thermal decomposition of mercuric oxalate indicates that the reaction is a surface one, unaffected by end products; it spreads rapidly over the surface from a number of initial centres of reactivity, after which the rate is controlled by the linear propagation of the interface inwards. The activation energies associated with these two processes are 25,600 and 37,100 cal. The initial rate is accelerated by pretreatment with light and cathode rays, which are responsible for the production of mercurous oxalate by electron transference. This decomposes rapidly on heat according to a first-order equation. The Mott theory, valid for ionic conductors at room temperatures, is inapplicable since mercuric oxalate is expected to have a molecular lattice.

### Résumé.

La présente étude de la décomposition thermique de l'oxalate mercurique indique que c'est une réaction de surface, non affectée par les produits finaux; elle s'étend rapidement à la surface, à partir d'un certain nombre de centres actifs initiaux, après quoi la vitesse est contrôlée par la propagation linéaire de l'interface vers l'intérieur. Les énergies d'activation de ces deux processus sont 25.600 et 37.100 cal. La vitesse initiale est accrue par un traitement préalable à la lumière ou aux rayons cathodiques, ce qui produit de l'oxalate mercurieux par transport d'électron; ce dernier oxalate est décomposé rapidement par la chaleur, selon une équation du premier ordre. La théorie de Mott, valable pour des conducteurs ioniques à la température ordinaire, est inapplicable, puisque l'oxalate mercurique doit avoir un réseau moléculaire.

### Zusammenfassung.

Der thermale Zerfall von Merkurioxalat ist eine Oberflächenreaktion, die nicht von den Endprodukten beeinflusst wird. Die Reaktion verbreitet sich zuerst rasch von einer Anzahl von aktiven Ausgangszentren aus über die Oberfläche, wonach die Geschwindigkeit von der linearen Fortpflanzung der Phasengrenzfläche nach innen hin bestimmt wird. Die Aktivierungsenergien dieser zwei Prozesse sind 25.6000, bzw. 37.100 cal. Die Anfangsgeschwindigkeit wird durch vorherige Bestrahlung mit Licht und Kathodenstrahlen, die die Erzeugung von Merkuro-oxalat durch einen Elektronenübergang bewirken, beschleunigt. Dieses zersetzt sich dann rasch in der Hitze unter Befolgung des Gesetzes für eine Reaktion erster Ordnung. Die Mott'sche Theorie, die für Ionenleiter bei Zimmertemperatur gültig ist, ist hier nicht anwendbar, da anzunehmen ist, dass Merkurioxalat ein molekulares Gitter besitzt.

*Natal University College,  
Pietermaritzburg,  
Natal,  
South Africa.*

*King's College,  
Strand,  
W.C. 2.*

# THE DEPENDENCE OF THE PROPERTIES OF CARBONYL COMPOUNDS UPON POLARITY.

BY A. D. WALSH.

Received 7th May, 1946.

In earlier papers <sup>1, 2</sup> we have pointed out that the determination of the ionisation potentials of non-bonding electrons affords direct information on bond dipole moments and thereby permits study of the way in which bond properties change with changing polarity. By such methods we have shown that, as the polarity of a bond increases, so the bond weakens.<sup>2</sup> In particular, we have shown <sup>1, 2</sup> that as the polarity of a carbonyl bond increases so its stretching force constant and bond energy decrease, while its length increases. In this paper we wish to extend our discussion of the dependence of carbonyl properties upon polarity.

Table I shows a list of carbonyl molecules arranged so that as we proceed downwards we follow the probable order of increasing polarity in the CO group. The following notes indicate the experimental foundations on which the table has been built, while on page 160 we suggest a quantitative measure of the polarity.

Carbon monoxide is known from dipole moment and ionisation potential measurements to have a very low polarity. It has been shown <sup>3</sup> that it is fairly included with the carbonyl compounds, since it may be represented approximately by the double bond structure



Carbon dioxide, carbon oxysulphide, formic acid, formaldehyde, acetaldehyde, acetone and acrolein have been placed in the table by reason of their non-bonding oxygen electron ionisation potentials. The order of these molecules is also the probable order of decreasing force constant and increasing C to O distance; though in the case of formic acid an anomaly occurs in that the reported C=O distance is greater and not less than the formaldehyde distance. This anomaly was mentioned in one of the earlier papers.<sup>1</sup> It is relevant to the problem to point out that the infra-red stretching frequency of the carbonyl group in esters of formic acid is greater than in the ketones,<sup>4</sup> so that, in the esters at least, the C=O distance is probably less than in the ketones ( $\sim 1.22$  A.). Further, thioacetic acid, which is expected on the basis of the present discussion to have an appreciably greater C=O distance than formic acid monomer, is reported <sup>5</sup> to have a C=O length of  $1.24 \pm 0.04$  A. The C=O group is less reactive in esters than in aldehydes, because the bond is stronger in esters, e.g. has a higher energy.<sup>5</sup>

Below acetone in the table must come, in order, methyl ethyl ketone, diethyl ketone, methyl *i*-propyl ketone, pinacolin, hexamethyl acetone, since (a) studies of the ionisation potentials of the alkyl halides have shown the electronegativities of alkyl groups to decrease in the order methyl, ethyl, *i*-propyl, *t*-butyl; (b)  $\lambda_{\text{max}}$  for the near ultra-violet spectra of these ketones is known to have this order <sup>6</sup> (see below).

<sup>1</sup> Walsh, *Trans. Faraday Soc.*, 1946, **42**, 56.

<sup>2</sup> Walsh, *ibid.*, 1947, **43**, 60.

<sup>3</sup> Long and Walsh, *ibid.* (in press).

<sup>4</sup> Thompson and Torkington, *J. Chem. Soc.*, 1945, 640.

<sup>5</sup> Sidgwick, *The Covalent Link*, Cornell, 1933, p. 129.

Acetyl chloride shows a shift of its ultra-violet spectrum to short wavelengths relative to acetaldehyde<sup>6</sup>—evidently the Cl atom is more electronegative than the already negatively-charged O atom of an acetyl group. The magnitude of the shift shows that acetyl chloride has a carbonyl polarity probably close to those of formaldehyde and formic acid: its carbonyl bond distance is not known with accuracy. Glyoxal has been inserted in the list by reason of its C=O bond length and of spectroscopic observations which are consistent with an ionisation potential  $\sim 11.4$  v. Diacetyl should be closely similar, though with a slightly greater carbonyl polarity. The benzaldehyde carbonyl electronic spectrum shows<sup>7</sup> a shift to long wavelengths relative to acrolein and benzaldehyde has therefore been placed below acrolein in the table. Urea has been inserted at the bottom of the list on the basis of its high carbonyl distance and low carbonyl stretching force constant. Acetophenone (see<sup>7</sup>) shows a shift of its carbonyl ultra-violet spectrum to short wavelengths relative to benzaldehyde and, on this basis, is thought to have a carbonyl polarity close to that of acetaldehyde.

The ultra-violet spectrum of phenyl isocyanate<sup>8</sup> shows that conjugation between the side chain and benzene ring is hardly appreciable. We may therefore deduce that the electronic condition of the carbonyl group in, say, methyl isocyanate will be much the same as in phenyl isocyanate. The peculiarities of the phenyl isocyanate spectrum and the carbonyl interatomic distance in methyl isocyanate are all consistent with isocyanates being placed as a class between carbon oxysulphide and glyoxal. From considerations of the electronegativity of chlorine atoms we may expect that phosgene lies between carbon oxysulphide and the isocyanates; its carbonyl interatomic distance is in need of a careful re-determination. As one might expect from the conventional bond diagrams, there is a strongly marked parallel between ketene and the isocyanates. The characteristic reactions of both compounds (being, not those of ketones, but additions at the N—C or C=C bond) may be taken as evidence of a much lower carbonyl polarity in ketene and the isocyanates than in the ketones. Further evidence is provided by (1) the carbonyl bond distances; these are nearly the same in ketene and methyl isocyanate, but appreciably less than in formaldehyde; (2) the force constant of the carbonyl group of ketene, which places it between carbon oxysulphide and formaldehyde. Ketene might be expected to have a slightly greater carbonyl polarity than the isocyanates as a consequence of the lower electronegativity of a carbon atom than a nitrogen atom. The lowered carbonyl polarity of ketene relative to, say, formaldehyde affords<sup>9, 10</sup> an example of the high electronegativity of a carbon atom forming part of a multiple bond in a direction away from that bond.

Carbon suboxide has a chemical behaviour rather like that of ketene. It has been placed just below ketene on the basis of its carbonyl bond length, estimates of which vary from 1.18 to 1.20 Å.; but the rather uncertain force constant values would place carbon suboxide above ketene in the table. Nickel carbonyl has been placed just below carbon monoxide on the basis of its carbonyl group length and of the similarity in properties

<sup>6</sup> Walsh (unpublished results).

<sup>7</sup> Walsh, *Trans. Faraday Soc.*, 1946, **42**, 62.

<sup>8</sup> Walsh, *Proc. Roy. Soc. A* (in press).

\* Note added in Proof.

Since this paper was sent for publication, Hannay and Smyth<sup>11</sup> have found ketene to possess a dipole moment (1.45 D.) considerably less than those of aldehydes and ketones and have concluded—in confirmation of the statements made here—that, in ketene, “the oxygen has much less negative charge than the ordinary carbonyl oxygen” of aldehydes and ketones. The same authors also find acrolein to have a moment of 3.04 D. against 2.72 D. for acetaldehyde. Our expected carbonyl group dipole for acrolein is  $\sim 2.78$  D., showing the contribution to the over-all dipole moment made by the  $\text{CH}_2=\text{CH}-$  group.

between its CO groups and the carbon monoxide molecule; we have discussed the matter elsewhere.<sup>8</sup>

In the last column of Table I we have listed values of the "carbonyl % polarity" or " % ionicity " for some of the molecules. This quantity we define<sup>17</sup> as  $100\mu/\epsilon r$ , where  $\mu$  = the carbonyl bond dipole moment,  $\epsilon$  is the electronic charge and  $r$  = the length of the 100 % polar (that is,  $\text{>C}^+-\text{O}^-$ ) bond. The value to take for  $r$  is uncertain because the length of the carbonyl bond varies with polarity and we must estimate  $r$  by

TABLE 1.—LIST OF CARBONYL MOLECULES IN ORDER OF CO POLARITY \*

Molecule.	CO Inter-atomic Distance (A.).	CO Stretching Force Constant dynes/cm. $\times 10^{-5}$ .	First I.P. of Non-bonding O Electrons (v).	CO Bond Energy kcal./mol.	% Polarity.
Carbon monoxide .	1.128	18.6	14.55	211	1
Nickel carbonyl .	1.15 $\pm$ 0.02				
Carbon dioxide .	1.15 $\pm$ 0.02	$\begin{Bmatrix} 15.5 \\ 15.3 \\ 15.2 \end{Bmatrix}$	13.73	$\sim$ 202	9
Carbon oxysulphide .	1.16 $\pm$ 0.02	$\begin{Bmatrix} 15.2^{13} \\ 14.2^{14} \end{Bmatrix}$	$\sim$ 12	$\sim$ 199	13
Phosgene . .	$\begin{Bmatrix} 1.12 \pm 0.02 \\ 1.28 \pm 0.03 \end{Bmatrix}$	—	—	—	—
Isocyanates . .	$\sim 1.18 \pm 0.03^9$	—	—	—	—
Ketene . . .	1.17 $\pm$ 0.02 <sup>10</sup>	$\sim 12.3^{16}$	—	—	—
Carbon suboxide .	1.18-1.20 $\pm$ 0.02 <sup>11</sup>	$\sim 14.2^{16}$	—	—	—
Glyoxal . . .	1.20 $\pm$ 0.02	—	$\sim 11.4$	$\sim$ 186	29
Diacetyl . . .	1.20 $\pm$ 0.02 <sup>12</sup>	—	—	—	—
Formic acid monomer	1.24 $\pm$ 0.03	11.8 <sup>87</sup>	11.3	—	—
Acetyl chloride .	1.14 $\pm$ 0.05	—	—	—	—
Formaldehyde .	1.21 $\pm$ 0.02	$\begin{Bmatrix} 11.5 \\ 12.3 \end{Bmatrix}$	10.83	$\sim$ 190	35
Acetophenone . .	—	—	—	—	—
Acetaldehyde . .	1.22 $\pm$ 0.02	—	10.18	$\sim$ 184	42
Acetone . . . .	—	—	10.2	—	42
Acrolein . . . .	—	—	10.06	—	43
Benzaldehyde . .	—	—	$\sim$ 0.01	—	44
Urea . . . . .	1.25	$\begin{Bmatrix} \sim 10.2^{18} \\ 9.7^{88} \end{Bmatrix}$	—	—	50-60

\* Where references for the experimental figures of this table are not given, they are to be found in our previous papers.<sup>1, 2, 3</sup> The bond energy figures, which are only to be regarded as roughly approximate, have been taken from a previous paper.<sup>2</sup>

extrapolation; <sup>10</sup> a fair estimate might be to take  $r$  as  $\sim 1.40$  A. (see ref.<sup>1</sup>). Fortunately, this doubt as to  $r$  does not mean a big uncertainty in estimates of % polarity, because on a graph of bond dipole-% polarity

<sup>9</sup> Eyster, Gillette and Brockway, *J. Amer. Chem. Soc.*, 1940, **62**, 3236.

<sup>10</sup> Beach and Stevenson, *J. Chem. Physics*, 1938, **6**, 75.

<sup>11</sup> Brockway and Pauling, *Proc. Nat. Acad. Sci.*, 1933, **19**, 860; Boersch, *Monatsch.*, 1935, **65**, 311.

<sup>12</sup> Lu Valle and Schomaker, *J. Amer. Chem. Soc.*, 1939, **61**, 3520.

<sup>13</sup> Glockler and Tung, *J. Chem. Physics*, 1945, **13**, 392.

<sup>14</sup> Branch and Calvin, *Theory of Organic Chemistry*, Prentice Hall, 1941.

<sup>15</sup> Thompson and Linnett, *J. Chem. Soc.*, 1937, 1376.

<sup>16</sup> Bailey and Hale, *Nature*, 1937, **139**, 1112.

<sup>17</sup> Cf. the " % ionic character " used by Pauling<sup>18</sup> and by Hannay and Smyth, *J. Amer. Chem. Soc.*, 1946, **68**, 245.

<sup>18</sup> Pauling, *Nature of the Chemical Bond*, Cornell, 1939.

<sup>19</sup> Pauling<sup>18</sup> neglects change of length with polarity and takes  $r$  as 1.24 A.

the lines joining different choices of point for ( $\epsilon$ , 100) to 0, 0) converge as they approach the origin. Assuming that the observed dipole moments of formaldehyde and acetaldehyde are located wholly in the carbonyl bonds (which is probably nearly true) we can read off from a graph of dipole moment-% polarity the % carbonyl polarity for these molecules and also for carbon monoxide. Using also the expectation that a non-polar carbonyl bond would have an ionisation potential of 14.73 v.<sup>22</sup> we then have four points with which to plot a graph of ionisation potential-ionicity. For these points this is also linear, showing (as we might have suspected) that the ionisation potential is a measure of the ionicity as defined above. From this second graph (that is, from ionisation data) we find the approximate % polarities for carbonyl bonds given in Table I. (The value for urea comes from an estimate of its ionisation potential based on the magnitude of its carbonyl force constant.) These values can be further checked as follows. The electron affinity of an oxygen atom is about 3.1 v.:<sup>20</sup> that is, the ionisation potential of  $O_{\text{gas}}$  is  $\sim 3.1$  v. The ionisation potential of  $O_{\text{gas}}$  is 13.55 v. The negative charge thus results in an ionisation potential decrease of  $\sim 10.5$  v. The expected ionisation potential of the non-bonding O electrons in a purely covalent carbonyl bond is 14.73 v.<sup>22</sup> The ionisation potential of both acetaldehyde and acrolein is close to 10.1 v. We may therefore estimate the % carbonyl polarity in these two molecules as

$$\approx 4.6/10.5 \times 100 \approx 44 \%$$

It is interesting to compare the values of Table I with those deduced theoretically by Coulson<sup>21</sup> for some of the molecules. In another communication<sup>3</sup> we have advocated the writing of the appropriate % polarity value alongside a carbonyl bond in a bond diagram: in this way may be obviated the lack of precision that comes from making a single bond diagram ( $\text{>C=O}$ ) do duty for many carbonyl compounds differing much in their properties.

Mulliken<sup>22</sup> has given the first ionisation potential of a completely non-polar carbonyl bond as 14.73 v. From Table I we may therefore estimate the non-polar bond as having an interatomic distance of  $\sim 1.12$  Å., a stretching force constant of  $19.20 \times 10^8$  dynes/cm. and a bond energy of 213 kcal./mole.

Our main purpose in this paper is to stress the way Table I brings out the unity of all the molecules considered. There is a smooth gradation of properties from the completely non-polar bond through a large number of intermediate molecules all the way to urea. The value of bond polarity knowledge to the understanding of chemistry is widely recognised. Table I should help to explain and predict the related properties of carbonyl compounds. We confine ourselves here to the way the order of Table I is exemplified in the facts relating to the spectroscopy of carbonyl compounds.

### Correlation of Polarity Order with Location of Absorption Bands.

A short table showing the variation of the positions of certain electronic transitions for a number of carbonyl molecules has already been published.<sup>23</sup> This may be expanded. As a particular example, we may take the so-called " $N \rightarrow A$ " transition,<sup>24</sup> consisting of the transfer of an electron

<sup>20</sup> Vier and Mayer, *J. Chem. Physics*, 1944, **12**, 28.

<sup>21</sup> Coulson, *Trans. Faraday Soc.*, 1946, **42**, 106.

<sup>22</sup> Mulliken, *J. Chem. Physics*, 1935, **3**, 564.

<sup>23</sup> Walsh, *Trans. Faraday Soc.*, 1946, **42**, 66.

<sup>24</sup> See McMurtry and Mulliken, *Proc. Nat. Acad. Sci.*, 1940, **26**, 312; Walsh, *Proc. Roy. Soc. A*, 1946, **185**, 176.



from a non-bonding orbital localised on the oxygen atom of a carbonyl group to an anti-bonding orbital of  $\pi$  type in the  $C=O$  bond. The lower the ionisation potential of the non-bonding oxygen electrons, the longer the wavelength of the  $N \rightarrow A$  transition.<sup>25</sup> Table II illustrates this generalisation.

In simple aldehydes and ketones the transition is responsible for the well-known bands in the neighbourhood of 3000-2900 Å. In less polar

molecules the transition lies at shorter wavelengths. Hence  $CO_2$ ,  $HCOOH$  and  $\phi NCO$  all show no "2900 Å." absorption. The evidence is strong that with increasing carbonyl polarity, the transition moves to longer wavelengths, though its spread does not always make this obvious. We may use the generalisation to predict, for example, that (1) formaldehyde will have its (O, O) band at shorter wavelength than acetaldehyde; (2) ketene and carbon suboxide will have the transition origin at shorter wavelengths than formaldehyde. Reversing the

TABLE II

LOCATION OF " $N \rightarrow A$ " TRANSITION  
IN CARBONYL COMPOUNDS

Compound.	Location <sup>26</sup> (Å).
$CO_2$ . . .	$\sim 1600$ <sup>27</sup>
$RCOOR$ . . .	$\sim 2100$ <sup>28</sup>
$CH_3COCl$ . . .	$\sim 2800$
$HCHO$ . . .	$\sim 2900$
$CH_3CHO$ . . .	$\sim 2900$
$(CH_3)_2CO$ . . .	$\sim 3000$ (3330-2940)
$C_6H_5CHO$ . . .	$\sim 3200$

generalisation, we may use it to indicate the extent of the polarity in a molecule: for example, acetyl chloride has bands representing the transition between 2875 and 2725 Å.—it must, therefore, have less polarity in the carbonyl group than has formaldehyde.

The shift of the  $N \rightarrow A$  transition to long wavelengths as the negative charge on the oxygen atom increases is due, partly, to elevation of the ground state of the non-bonding oxygen electrons. This elevation is paralleled by a lessening of binding of the  $\pi$  electrons of the  $C=O$  bond as we proceed downwards in Table I, so that depression of the anti-bonding  $\pi$  level is another cause of the  $N \rightarrow A$  shift. The lessening of binding is known in a few cases directly from the  $\pi^{-1}$  ionisation potentials (carbon dioxide: 17.1 or 18.0; <sup>29</sup> formaldehyde: 11.8; <sup>30</sup> acetaldehyde and acetone: 11.3; <sup>30</sup> acrolein: 11.2<sup>30</sup>) and, more generally, by the fact that the  $C=O$  bond order (shown by the bond length and stretching force constant) falls as we pass downwards and, since bond order can be related to bond ionisation potentials,<sup>31</sup> this means that the  $\pi^{-1}$  ionisation potential falls.

The very high bond strength of  $>C=O$ , relative to  $>C-C<$ , is reflected in the height of the ionisation potentials for both  $\pi$  and  $\sigma$  bonds of  $>C=O$ .

<sup>25</sup> Cf. McMurtry, *J. Chem. Physics*, 1942, **10**, 655.

<sup>26</sup> Figures, except where stated, from Spomer and Teller, *Rev. Mod. Physics*, 1941, **13**, 75.

<sup>27</sup> Price and Simpson, *Proc. Roy. Soc. A*, 1939, **169**, 501.

<sup>28</sup> Price and Evans, *ibid.*, 1937, **162**, 110.

<sup>29</sup> Mulliken, *J. Chem. Physics*, 1935, **3**, 720.

<sup>30</sup> Sugden (in course of publication).

<sup>31</sup> Walsh, *Trans. Faraday Soc.*, 1946, **42**, 779.

<sup>32</sup> Lederle and Rieche, *Ber.*, **B**, 1929, **62**, 2573.

<sup>33</sup> Walsh, *J. Amer. Chem. Soc.*, 1946, **68**, 2408.

<sup>34</sup> Gordy, *J. Chem. Physics*, 1946, **14**, 560.

<sup>35</sup> Hannay and Smyth, *J. Amer. Chem. Soc.*, 1946, **68**, 1357.

<sup>36</sup> Kellner, *Proc. Roy. Soc. A*, 1941, **177**, 456.

<sup>37</sup> Bonner and Hofstadter, *J. Chem. Physics*, 1938, **6**, 531.

### Summary.

A list of molecules containing carbonyl groups is tabulated in such a way that the order is that of increasing carbonyl polarity. This shows the smooth dependence of many carbonyl properties upon polarity and brings out the unity of the molecules considered. The experimental foundations of the table are, fundamentally, spectroscopic measurements, especially of ionisation potentials; but bond lengths and other properties are also used. A definition is given of a quantity called the “% polarity.” By means of this a quantitative measure of the carbonyl polarity of a molecule may be given, using either dipole moment or ionisation potential data. The order of the table is exemplified in the correlation of the locations of absorption bands with carbonyl polarity. The ionisation potential of the  $\pi$  electrons of the  $C=O$  bond, as well as that of the oxygen non-bonding electrons, falls with increasing polarity in the bond.

### Résumé.

On établit un tableau, dans lequel la liste des molécules contenant un groupe carbonyle est ordonnée selon la polarité croissante du carbonyle. Ceci montre que maintes propriétés du carbonyle dépendent régulièrement de la polarité et fait ressortir le caractère d'unité des molécules considérées. Fondamentalement, le tableau a pour bases expérimentales des mesures spectroscopiques (en particulier, de potentiel d'ionisation), mais la longueur des liaisons et d'autres propriétés sont aussi utilisées. On définit une quantité appelée “polarité %.” Celle-ci permet de donner une mesure quantitative de la polarité du carbonyle dans une molécule, employant les valeurs soit du moment dipolaire, soit du potentiel d'ionisation. La position des bandes d'absorption par rapport à la polarité du carbonyle donne un exemple de l'ordre du tableau. Le potentiel d'ionisation des électrons  $\pi$  de la liaison  $C=O$ , de même que celui des électrons qui ne prennent pas part à la liaison de l'oxygène, décroît pour une polarité croissante dans la liaison.

### Zusammenfassung.

Eine Anzahl von Molekülen mit Karbonylgruppen wurde in der Reihenfolge von anwachsender Karbonylpolarität angeordnet. Diese Liste zeigt, dass viele Eigenschaften der Karbonylgruppe in kontinuierlicher Weise von der Polarität abhängen. Die experimentellen Grundlagen der Tabelle sind spektroskopische Messungen, insbesondere von Ionisierungsspannungen, es werden aber auch Kernabstände und andere Eigenschaften benutzt. “%-Polarität,” ein quantitatives Mass der Karbonylpolarität eines Moleküls, wird definiert; sie kann entweder von Dipolmomenten oder Ionisierungsspannungen abgeleitet werden. Die Ionisierungsspannung der  $\pi$ -Elektronen der  $C=O$  Bindung und auch die der nicht-bindenden Elektronen des Sauerstoffs nimmt mit anwachsender Polarität der Bindung ab.

*Laboratory of Physical Chemistry,  
Cambridge.*

## REVIEWS OF BOOKS

**Advances in Colloid Science. Vol. II. Scientific Progress in the Field of Rubber and Synthetic Elastomers.** Edited by H. MARK and G. S. WHITBY. (Published by Interscience Publishers, 1946.) Pp. xl. + 453. Price \$7.00.

The appearance of a comparatively comprehensive book on rubber science is an event of some importance. The last publication of the kind was Davis and Blake's *Chemistry and Technology of Rubber* (1937), and a comparison of this with the volume under review makes one immediately aware not only of the considerable advances which have taken place in almost every aspect of the subject, but even more strikingly of the shift of emphasis away from organic chemistry and towards physics and physical chemistry. This is not due to any reduction in the significance or importance of the organic chemical aspect, but rather to an efflorescence of new concepts and ideas of a somewhat revolutionary character in the physical realm which have combined to make rubber science one of the most fascinating of present-day studies.

In the second volume in the series appearing under the title *Advances in Colloid Science* the editors have succeeded in choosing recognised authorities to write on their particular branches in such a way that the whole subject is fully covered, without introducing any undesirable repetition. Of the nine principal chapters, five deal mainly with physics, two with physical chemistry, and two with organic chemistry. In addition there is an excellent short introductory chapter by G. S. Whitby on the structure of synthetic elastomers, and an appreciative review of the work of the late Elmer O. Kraemer, by whom this series of volumes was initiated.

The rubber-like state, characterised by long-range elasticity, is associated with an amorphous or disordered arrangement of long-chain molecules in a state of micro-Brownian motion. If the regularity of structure along the molecular chain is sufficient the amorphous state may, under suitable conditions, transform to a partially crystalline state, while at low temperatures both crystalline and amorphous states give place to the glass-hard condition. The transition to the glassy state—the so-called second-order transition—is discussed by R. F. Boyer and R. S. Spencer, of the Dow Chemical Company, while the phenomena of crystallisation are treated by L. A. Wood of the U.S. Bureau of Standards. Another aspect of crystallisation, the determination of the exact structure of crystalline polymers by X-ray methods, is dealt with by C. W. Bunn of I.C.I. (Alkali) Ltd., whilst the phenomena of elasticity are interpreted from the theoretical standpoint by E. Guth of the University of Notre Dame, H. M. James of Purdue University, and H. Mark of Brooklyn Polytechnic.

Boyer and Spencer give a careful summary of the existing information on changes in physical properties associated with the second-order transition, including some of their own recent investigations. In a subject bristling with apparent anomalies and difficulties of interpretation, they have made a courageous attempt to produce some sort of order, and

although final agreement on many of the issues cannot be expected, the attempt should provide a welcome stimulus to further work in this hitherto somewhat neglected field.

Wood's chapter on crystallisation is concerned mainly with experimental methods of studying crystallisation, and the principal phenomena observed. From the work of Bekkedahl and others it is shown that crystallisation phenomena in rubbers show certain similarities, but also certain striking differences from crystallisation in ordinary low-molecular systems. In particular the crystalline state does not attain real thermodynamic equilibrium with the amorphous state at any temperature. For example, the temperature of melting depends on the temperature of crystallisation, but not on the time of crystallisation nor on the degree of vulcanisation. It is concluded that none of the theories yet proposed is adequate to explain this, and other remarkable, but well-established observations.

Though very much a specialist's province, the subject of X-ray crystallography is presented by Bunn in a very lucid and readable manner. Exceptional difficulties arise in this particular application, due to the small size and imperfect ordering of the crystallites; it is impossible to obtain a single crystal, hence the usual optical methods for the preliminary examination of crystal symmetry are not available, and the number of measurable reflections is relatively small. But by ingenious arguments of a general character it is often possible to make a plausible estimate of the type of structure; the diffraction pattern of the postulated structure is then calculated and compared with experiment. It is difficult at present to assess the accuracy of this procedure. Some of the structures proposed by the author have been challenged, and may have to be revised.

The section on the theory of rubber elasticity by Guth, James and Mark is based on the conception of vulcanised rubber as a network of long-chain molecules subject to statistical fluctuations of form. The mathematical treatment of the problem leads to quantitative stress-strain relations which show a close agreement with experimental curves, and it is apparent that we are now in possession of a fairly accurate quantitative theory of the mechanical properties of amorphous rubber. The chapter might have been improved by a more general consideration of theories of rubber elasticity other than that of James and Guth. The critical references to the work of Wall, of Flory and Rehner, and of Kuhn hardly do justice to the extensive and stimulating contributions to the subject which these authors have made.

Dealing with reinforcement and the physical effects of compounding ingredients on the properties of vulcanised rubbers, D. Parkinson, of the Dunlop Rubber Company, gives an excellent summary of the effect of various carbons and other fillers on tensile strength and elastic modulus, resistance to abrasion and tearing, rebound resilience, etc. There appears to be no generally accepted criterion of reinforcement, though it is normally taken to include enhancement of tensile strength and abrasion resistance. Most of the effects discussed have not yet received a satisfactory theoretical explanation.

The two sections on physical chemistry are contributed by G. Gee, of the British Rubber Producers' Research Association, who deals with the application of thermodynamics to problems of solution and swelling, and by R. H. Ewart, of the U.S. Rubber Company, who discusses the

significance of viscosity measurements in dilute solutions of high polymers. Gee examines experimental methods of deriving the fundamental thermodynamic properties of solutions, namely the free energy and heat of dilution (or mixing), from which also the entropy of dilution may be deduced. The statistical calculation of the entropy of dilution of a polymer by a low-molecular solvent is a difficult problem, but approximate solutions by Flory and by Huggins agree rather well with experimental data. The phenomena of the swelling and solubility of a rubber in various liquids can be satisfactorily interpreted on the basis of these thermodynamic concepts. It is clear that this type of approach is likely to be of considerable practical as well as theoretical importance.

Ewart considers in some detail the rather closely related topic of the viscosity of dilute polymer solutions, which is of special importance for the measurement of molecular weights, in which connection it has an empirical rather than an absolute significance, and must be applied with caution. Various proposed relations between solution viscosity and polymer concentration are discussed. In general the relation between intrinsic viscosity and molecular weight is a non-linear one, involving the use of two constants, as is shown particularly well by Flory's work on polyisobutylenes. The chapter includes also a consideration of the conclusions which may be drawn from viscosity, light-scattering and other measurements on the form of molecules in solution, and a review of the theoretical background to the subject.

On the organic side E. H. Farmer, of the British Rubber Producers' Research Association, deals with the chemistry of vulcanisation, while the somewhat analogous problem of the formation of photogels and photo-vulcanisates is discussed by H. P. Stevens. Farmer's comprehensive treatment includes a consideration of the various possible reactions of rubber and olefinic systems generally with sulphur and other reagents which are known to produce insolubilisation. Recent investigations have established that sulphur reacts with simple olefins to produce intermolecular linkages containing one or more sulphur atoms. There is little doubt that a similar reaction occurs between polyisoprene rubber and sulphur, but in this case there is the complication of ring-formation by linkages between two points of the same molecule. The chemical evidence for the existence of a cross-linked structure in vulcanised rubber provides a welcome confirmation of a theory which has been extensively postulated in purely physical investigations relating to swelling and elasticity.

Photo-gelation, a form of vulcanisation produced by the action of light on either dry rubber or rubber solutions, is a phenomenon which appears still to be imperfectly understood in terms of detailed reaction mechanisms. From Stevens' review of the subject there is seen to be much conflicting evidence on the effects of illumination, and further work designed with the object of providing more reliable experimental data is clearly called for.

Taken as a whole, this volume provides a much needed co-ordination of recent developments, and will be eagerly studied by all whose work is associated with rubber and polymers, and, it is to be hoped, by others as well.

L. R. G. T.

**An Index of Mathematical Tables.** By A. FLETCHER, J. C. P. MILLER and L. ROSENHEAD. (Scientific Computing Service, Ltd., 23 Bedford Square, W.C.1., London, 1946.) Price 75s.

Modern developments in Theoretical Chemistry and Physics have led to a great use for many old mathematical functions and the introduction of many new ones. Gone are the days when a straightforward "book of logs" and a slide-rule were adequate companions for the theoretician. One thinks almost at once of the people who want tables of the Langevin function for dipole moments, the Planck function for radiation density, the Gaussian function for statistical work, or the Fermi-Dirac function for electron distributions. But a hundred other functions could easily be added to this list, all of them in the "almost-essential" category. To meet the need for numerical values of these and other similar functions there has been a growing publication of tabulated results; witness, for example, the series of British Association Tables and the excellent W.P.A. series issued in America. But not all of these tables are issued in obvious places, and many of them are not likely to be seen in the normal course of a literature survey by a theoretical chemist. Economy and efficiency of time demand that a guide, or index, of mathematical tables should be made available to every worker, as recent and complete as possible. This book, which is an index of mathematical tables of all kinds, published in all kinds of places, sometimes as separate works, sometimes as adjuncts to some specific application, is intended to meet this demand. The book itself will not provide the required numerical values, but it will explain where such tables are to be found, and in many cases it will indicate how reliable these tables are.

Nothing more needs to be said of its relevance. As for its contents, it is divided into two parts. Part 1 (372 pages) lists all the functions under 24 distinct chapters, or sections, each decimally subdivided. And under each subsection it gives the names and dates of publication of the various tables, with information about the number of significant figures in each case. Part 2 (72 pages) gives full details, under authors' names, alphabetically arranged. In addition there is an adequate index.

An example, taken more or less at random, will show how the Index should be used. Suppose, in a diffraction problem, that we want accurate values of  $\sin \pi/x$ . Section 7—headed "Natural Trigonometric Functions"—subsection 63, shows us that there are no less than nine recognised tables of this quantity. But only one of them gives 8 decimals, and this, by Hayashi, was published in 1930, though we shall remember a note in the Introduction warning us that several of Hayashi's tables are especially inaccurate. These particular tables show the values of  $\sin \pi/x$  at intervals of 0.01 from 0 to 10, then by intervals of 0.1 up to 20 and then at unit intervals to 100. But there are no differences shown, so that interpolation, if required, is not easy. On the other hand, fifth differences are available, so the Index informs us, in the 7-figure British Association Tables, vol. 2, 1932.

Two questions inevitably arise in relation to such a work as this. Is it easy to use, and is it complete and reliable? To the first of these questions the answer should have been provided by the example given above: in short, the book is easy to use. The answer to the second question is provided in part by the reputation and experience of the three

authors, all in the Department of Applied Mathematics at Liverpool University, who have spent years in collecting and verifying their material : and in part also by the publishers, from whom the book may be obtained. Under the guidance of Dr. Comrie this organisation has acquired an almost unique knowledge of mathematical computation.

The scientific world ought to be very grateful to these gentlemen for their work. There is no doubt that this Index completely replaces any other Index of Mathematical Tables, and will remain for some time the standard work of its kind. It is no exaggeration to say that every library should have a copy. It is somewhat doubtful whether many private individuals will be willing to afford the extremely high price (75s.). No doubt a book of this kind is expensive to produce, for it is certainly well set-out, with every indication of care and thoroughness in proof reading. But it does seem a pity that the responsibility of publishing such a book could not have been accepted by some organisation willing to bear the anticipated financial loss, and even reduce the price. For there is no doubt that the book performs a public service, and every working scientist ought at very least to know of its existence.

C. A. C.

**Richter's Organic Chemistry. Vol. III. The Aromatic Compounds,** Third English Edition, translated by A. J. MEE. (Elsevier Publishing Co., Inc., New York, 1946.) Pp. xviii+794. Price \$15.00.

The preparation of this volume was interrupted by the outbreak of war in 1939 with the result that, apart from the first fifty pages, the text is a literal translation of the German text of the twelfth edition of 1935. The earlier portion of the volume contains an excellent section on the structure of benzene which has been entirely re-written by Dr. T. W. J. Taylor from the modern standpoint. The greater part of the work, however, has not been revised or brought up-to-date in the light of the very considerable advances which have been made during the past ten or twelve years. In spite of this limitation the publication of this volume will be welcomed, since it provides in a very accessible form a comprehensive summary of the chemistry of the aromatic compounds. The text, which extends to more than 700 pages, contains a vast mass of information, although the attempt to confine the whole of aromatic chemistry within the covers of one volume inevitably means that detailed information is lacking in many cases. Nevertheless, this volume and its predecessors might almost be described as a miniature "Beilstein", and as such they should be of great value as a reliable standard work of reference.

The work is sub-divided into Mononuclear Aromatic Compounds and Multinuclear Aromatic Compounds, and the latter section includes compounds containing separate aromatic nuclei as well as condensed aromatic systems containing four, five and six or more rings. Each main section is sub-divided in a methodical and systematic manner, which makes it easy for the reader to find what he wants. The text contains adequate structural formulæ and references to the literature, and in contrast to the practice in previous editions the reader is referred to the original journals and not to *Chemisches Zentralblatt*. The translation from the German has been carried out with outstanding success.

D. H. H.

27 AUG 1947

# THE CALCULATIONS OF THE LATENT HEAT OF VAPORISATION AND THE VISCOSITY OF CO<sub>2</sub> UNDER PRESSURE ON THE BASIS OF A REVISED EQUATION OF STATE.

By D. B. MACLEOD.

Received 18th June, 1945.

In a previous paper<sup>1</sup> the author proposed a revision of Van der Waals' equation, making  $b$  the volume of the molecules, a function of  $p + a/v^2$ , the total pressure ( $P$ ), where Van der Waals' equation was written

$$P[v - b_0(1 - BP + CP^2)] = RT.$$

It was shown that, contrary to the accepted views, large changes in the value of  $b$  were indicated, as a substance passes from the vapour to the liquid phase. Support, for the physical reality of these changes, was given by the successful calculation<sup>2</sup> of the latent heats of vaporisation of a number of typical substances. In a later paper,<sup>3</sup> the compressible

TABLE I.

Tem. ° K.	M.V.		Press. in Bars.	$p + a/v^2$		$\frac{RT}{v - b}$	
	Liq.	Vap.					
216.4	37.33		5.18	2991		3050	
223	38.10		6.82	2873		2873	
233	39.43		10.05	2686		2662	
243	40.94	1196	14.28	2496	17.2	2461	17.6
253	42.68	845.5	19.68	2304	25.5	2786	26.5
263	44.83	608.7	26.46	2096	37.8	2096	39.2
273	47.57	451.4	34.82	1874	55.2	1894	56.8
283	51.18	332.2	44.97	1633	82.8	1661	83.8
293	56.97	231.6	57.21	1339	134.6	1357	134.5
303	73.56	132.0	72.05	840.5	310.8	840.5	302.4
304.1	94.82	94.82	73.90	536.6	536.6	531.8	531.8

molecule was used as the basis of a new theory of viscosity, and the viscosity of a liquid, both under its own vapour pressure and under external pressures up to 10,000 atmos., was calculated directly from the viscosity of the vapour. Unfortunately, the complete data, required for the calculations, is available for comparatively few substances. However, for CO<sub>2</sub>, satisfactory experimental data are given in the International Critical Tables. CO<sub>2</sub> also differs, markedly, in its constants from the substances discussed in the earlier papers.

An outline of the method of obtaining the necessary constants will be given here (cp. <sup>1, 2, 3</sup>). The constant  $a$  is determined by taking  $b_c = v_c/2$ , so that at the critical temperature  $(p_c + a/v_c^2)v_c/2 = RT_c$ . A discussion of the relation of  $b_c$  to  $v_c$  has been given<sup>1</sup> and CO<sub>2</sub> was discussed there when a value of  $4.266 \times 10^6$  was obtained for  $a$ . A recalculation from the slightly different experimental figures supplied in Table I, gives

<sup>1</sup> Macleod, *Trans. Faraday Soc.*, 1944, 40, 439.

<sup>2</sup> *Ibid.*, 1945, 41, 122.

<sup>3</sup> *Ibid.*, 1945, 41, 771.



$4.160 \times 10^6$ , which is the value taken in all subsequent calculations. In Table I the values of  $p + a/v^2$  are compared with those obtained from  $RT/v - b$ , where  $b$  is calculated from the equation,  $b = b_0(1 - BP + CP^2)$  with  $b_0 = 52.33$ ,  $B = 0.02330$ ,  $C = 0.03326$ .

The agreement between the columns is satisfactory and is similar to that obtained for the substances already published. At the same time, the divergences are greater than could be accounted for by experimental errors. Their systematic nature indicates that the equation of state, as it stands, remains approximate but it has the advantage that a definite physical meaning can be attached to each term. The small change made in the value of  $a$  from that used earlier<sup>1</sup> has made a considerable change in the constants for CO<sub>2</sub>, so that on the present basis CO<sub>2</sub> can be regarded as less compressible than benzene, whereas in the original paper it appeared to be more compressible.

**Latent Heat of Vaporisation.**—The latent heat of vaporisation is next calculated as the sum of three terms,  $\lambda_i$ ,  $\lambda_e$ , and  $\lambda_m$ ;  $\lambda_i$  the internal work, is  $\int_{v_2}^{v_1} a dv$ ;  $\lambda_e$ , the external work, is  $p(v_1 - v_2)$ , and  $\lambda_m$ , the work done against that which has been done on the molecules themselves, is  $\int_{b_2}^{b_1} P db$ . The latter term is obtained by multiplying the change of volume of the molecules themselves, for each interval, by the mean total pressure and converting into calories.

TABLE II.

$$a = 4.160 \times 10^6.$$

Temp.° K.	$P = P_0 + \frac{a}{v^2}$ in Bars.		$b$ .		$\lambda_i$ .	$\lambda_e$ .	$\lambda_m$ .	$\lambda_e$ .	$\lambda_B$ .	$\lambda$ .
216.4	2991		31.43		2663	430	551	3624	3565	
223	2873		31.05		2610	420	535	3565	3454	3670
233	2686		32.15		2520	410	502	3432	3323	
243	2496	17.2	32.73	52.3	2344	392	466	3202	3144	3280
253	2304	25.5	33.48	52.2	2310	378	403	2991	2891	3030
263	2096	37.8	34.40	51.9	2055	356	355	2766	2702	2760
273	1847	55.2	35.59	51.70	1871	337	298	2506	2418	2460
283	1633	82.8	37.05	51.31	1642	302	237	2181	2050	
293	1339	134.6	39.02	50.51	1317	237	144	1698	1546	
303	840.5	310.8	43.60	48.71						
304.1	536.6		46.28		0	0	0	0	0	

Table II shows the latent heat of vaporisation of CO<sub>2</sub>, from 216.4° K. up to the critical temperature calculated in this way. The values of  $b$  used are the same as used in the calculation of  $\frac{RT}{v - b}$  and are obtained from the equation:  $b = 52.33(1 - 0.02330P + 0.03326P^2)$ ;  $\lambda_e$  gives the sum of  $\lambda_i$ ,  $\lambda_e$  and  $\lambda_m$ ; and  $\lambda_B$  gives the values of the latent heat of vaporisation, quoted from the I.C.T., as being due to Bridgman. The last column, also obtained from the I.C.T., gives another set of values, claiming accuracy to within  $\pm 2\%$ . The L.H.s are expressed in cal./g. mole.

The value of  $a$  for CO<sub>2</sub> calculated from the unrevised form of van der Waals' equation is  $2.93 \times 10^6$ . The L.H. of vaporisation at 243° K. calculated from the sum of the terms  $\int_{v_2}^{v_1} \frac{a}{v^2} dv$  and  $p(v_1 - v_2)$ , using this value would be  $1651 + 466 = 2117$  against the correct value between 3100 and 3300; the above calculation of the L.H. is thus very satisfactory.

**Viscosity of CO<sub>2</sub>.**—(Cp. ref.<sup>a</sup>) The viscosity of CO<sub>2</sub> at various pressures and temperatures, is calculated here directly from the value at atmospheric pressure and the corresponding temperature. Satisfactory experimental data is supplied by the I.C.T. from 20° c. to 40° c., i.e. below and above the critical temperature, and the relation between the viscosity and density is also given.

TABLE III.— $a = 4.160 \times 10^6$ .

Press. in Bars.	M.V.	P in Bars.	b.	b <sup>1</sup> .	v - b	φ.	η <sub>calc.</sub>	η <sub>obs.</sub>
TEMP. 30° C.								
111.9	55.35	1469	38.17	38.21	17.18	236.3	0.0 <sub>8</sub> 732	0.0 <sub>8</sub> 770
105.3	56.34	1416	38.56	38.54	17.78	215.5	694	730
97.2	57.90	1338	39.14	39.08	18.76	196.4	655	693
91.1	59.23	1277	39.60	39.51	19.63	182.0	625	643
83.1	61.45	1184	40.33	40.19	21.12	160.5	582	592
81.0	62.33	1152	40.59	40.46	21.74	153.2	566	565
77.0	64.71	1071	41.26	41.20	23.45	135.5	529	529
74.9	66.26	1022	41.69	41.66	24.57	124.7	507	495
73.9	67.39	990	41.97	41.94	25.42	118.0	493	478
72.9	69.30	935.6	42.44	42.42	26.86	107.2	472	458
70.9	153.3	248.0	49.42		103.9	8.5	229	229
60.8	248.3	128.3	50.80		197.5	2.3	193	187
40.5	478.3	58.7	51.6		426.7		171	168
20.3	1242	21.8	52.1		1190		160	159
1.01			52.33				0.0 <sub>8</sub> 153	0.0 <sub>8</sub> 153

Press. in Bars.	M.V.	P in Bars.	b.	v - b.	φ.	η <sub>calc.</sub>	η <sub>obs.</sub>
TEMP. 20° C.							
84.06	52.70	1582	37.40	15.30	263	0.0 <sub>8</sub> 801	0.0 <sub>8</sub> 823
72.91	54.19	1495	37.99	16.20	241	749	771
59.75	57.29	1327	39.21	18.08	200	661	697
56.71	231.6	134.3	50.50	181.1	2.6	190	186
50.63	303.5	95.8	51.00	252.5	1.2	178	177
40.5	440.0	62.0	51.50	388.5	0.4	167	166
20.3	1222	23.0	52.13	1170		155	156
1.01			52.33			0.0 <sub>8</sub> 148	0.0 <sub>8</sub> 148

TEMP. 40° C.							
113.7	62.94	1164	40.43	22.51	155.9	0.0 <sub>8</sub> 562	0.0 <sub>8</sub> 571
109.4	64.51	1108	40.95	23.56	141.8	547	540
101.3	69.18	970	42.14	27.04	112.2	487	483
95.2	75.61	822.8	43.48	32.13	83.5	428	414
86.1	114.3	404.6	47.69	66.60	21.7	282	269
81.0	151.2	263.0	49.24	102.0	9.3	239	218
70.9	215.7	160.3	50.42	165.3	3.4	208	200
60.8	287.6	111.1	50.98	236.6	1.8	193	187
40.5	530.1	55.3	51.66	478.4		176	176
24.1	1078	27.7	52.00	1026		168	169
1.01			52.33			0.0 <sub>8</sub> 159	0.0 <sub>8</sub> 159

In this paper the viscosity of CO<sub>2</sub> at a pressure  $p$  is obtained from the viscosity at atmospheric pressure by the equation,

$$\eta_p = \eta_a \cdot \frac{v_p}{v_p - b_p} \cdot e^{\frac{\phi}{RT}}$$

where  $v$ , and  $b$ , are the molecular volumes of the fluid and the molecules respectively, and  $\phi = \int_{b_1}^{b_2} P db$ . All the quantities required, therefore, in the calculation are obtained directly from the  $p$ ,  $V$ ,  $T$  figures and no artificial constants have been introduced.

The values of  $b$  used throughout, have been obtained from the equation already given, namely,  $b = 52.33(1 - 0.02320P + 0.03326P^2)$ . In the first of the three tables on page 171, a column  $b^1$  has been inserted. These

values of  $b$  have been obtained by first finding  $v - b$  from  $v - b = \frac{RT}{p + a/v^2}$  and subtracting this from  $v$ . Their close agreement with the values obtained from the original equation, developed from the orthobaric densities, is a good vindication of the soundness of the method. The last two columns compare the calculated and observed viscosities.

In view of the fact that the viscosities have increased in the ratio of between five and six times the original value, the excellence of the agreement needs hardly to be emphasised. A systematic error of a few per cent. is, however, evident. The calculated values are lower than the observed values at high pressures and greater at intermediate pressures. This may well be related to the systematic divergences in the original equation of state. The general results, both from the latent heats and viscosities, give strong support to the underlying theory of the fluid state set out previously.<sup>1, 2, 3</sup>

### Summary.

(1) The latent heat of vaporisation of  $\text{CO}_2$ , and the viscosity under pressure, have been calculated on the basis of the author's revised equation of state.

(2) The absolute values of the quantities have been calculated directly from the  $P$ ,  $V$ ,  $T$  data, without the use of any arbitrary constants.

### Résumé.

L'auteur a calculé :

(1) la chaleur latente de vaporisation de  $\text{CO}_2$  et la viscosité sous pression sur la base de l'équation d'état, corrigée par lui.

(2) Les valeurs absolues de ces quantités directement d'après les données numériques de  $P$ ,  $V$ ,  $T$ , sans l'aide d'aucune constante arbitraire.

### Zusammenfassung.

(1) Die Verdampfungswärme von  $\text{CO}_2$  und die Viskosität unter Druck wurden auf Basis der verbesserten Zustandsgleichung des Verfassers berechnet.

(2) Die absoluten Werte dieser Grössen wurden ohne Benützung von willkürlich adjustierbaren Konstanten direkt von den  $P$ ,  $V$ ,  $T$ —Daten berechnet.

*Physics Department,  
Canterbury University College,  
Christchurch, New Zealand.*

# SOME REACTIONS OF HYPOCHLORITES IN SOLUTION.

## PART I. THE ELECTRON AFFINITY OF THE $\text{ClO}^-$ AND $\text{ClO}_2^-$ IONS.

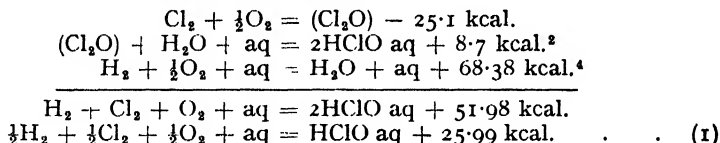
BY JOSEPH WEISS.

Received 14th November, 1945.

It will be shown in subsequent publications that electron transfer processes play an important role in the reactions of the chlorine oxy-acids in aqueous solution. The electron affinity of the  $\text{ClO}^-$  ion or of any of the other ions involved is, therefore, of considerable interest. More recent thermochemical data allow a determination of some of these and related quantities.

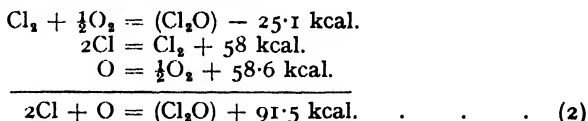
### Heat of Formation of $\text{HClO}$ aq.

The determination of the heat of formation of  $(\text{Cl}_2\text{O})$  by Günther and Wekua <sup>1</sup> allows us to derive a more accurate value for the heat of formation of  $\text{HClO}$  aq, according to the following reactions :

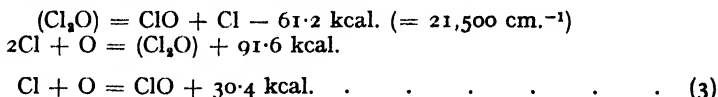


Thus, Latimer's supposition <sup>3</sup> that the value (29.8 kcal.) given by Bichowsky and Rossini <sup>4</sup> is too high seems to be correct.

### Heat of Formation of the $\text{ClO}$ Radical.



Combining this with the dissociation energy of  $(\text{Cl}_2\text{O})$  into  $\text{ClO}$  and  $\text{Cl}$  as determined by Goodeve and Wallace <sup>5</sup>



A similar value (33.5 kcal.) has been obtained by these authors <sup>5</sup> from the optical dissociation of  $\text{ClO}_2$ .

<sup>1</sup> Günther and Wekua, *Z. physikal Chem., A.*, 1931, **154**, 193.

<sup>2</sup> Cf. Neumann and Müller, *Z. anorg. Chem.*, 1929, **182**, 235.

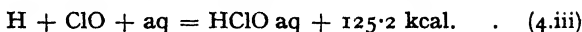
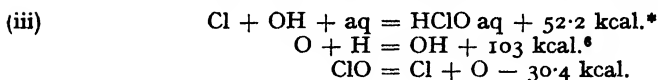
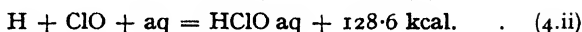
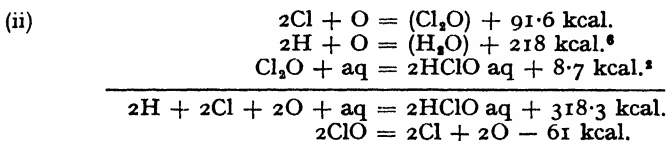
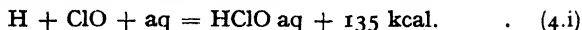
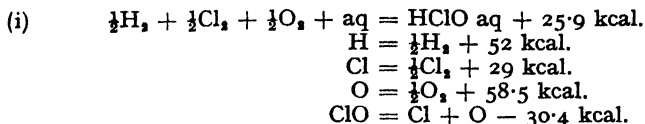
<sup>3</sup> Latimer, *Oxidation Potentials* (Prentice Hall, 1938), p. 48.

<sup>4</sup> Bichowsky and Rossini, *Thermochemistry of the Chemical Substances* (Reinhold, 1936).

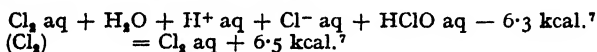
<sup>5</sup> Goodeve and Wallace, *Trans. Faraday Soc.*, 1930, **26**, 255.

**Bond Energy of the H Atom in HClO aq.**

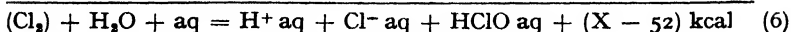
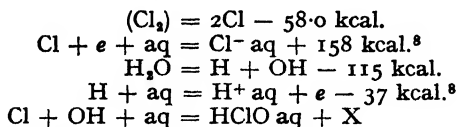
This energy can be calculated now in three different ways :



\* This value is derived from measurements by Roth <sup>7</sup> in conjunction with known thermochemical data, according to :

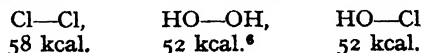


combined with :



from which follows :  $X = 52.2 \text{ kcal.}$

The value for the Cl—OH bond energy appears to be reasonable if one compares this figure with the bond energies of  $Cl_2$  and  $H_2O_2$ , viz. :



although this latter value may be somewhat too low.

**Electron Affinity of the ClO Radical.**

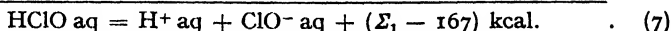
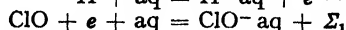
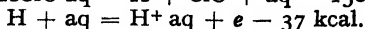
It is possible to calculate now the sum ( $\Sigma_1$ ) of electron affinity ( $E_{ClO}$ ) and heat of hydration ( $S_{ClO^-}$ ) of the  $ClO^-$  ion according to the following cycle processes.

<sup>6</sup> Geib, *Ergeb. exact. Naturwiss.*, 1936, 15, 44.

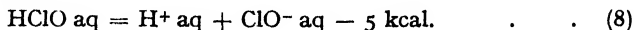
<sup>7</sup> Roth, *Z. physikal. Chem., A.*, 1929, 145, 297.

<sup>8</sup> Bernal and Fowler, *J. Chem. Physics*, 1933, 1, 515.

(i) Starting with the dissociation of HClO aq (equations (4)) and taking 130 kcal./mole. as the most probable value



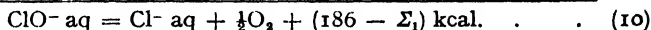
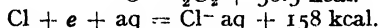
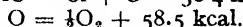
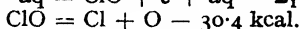
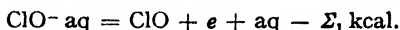
Combining this with the heat of electrolytic dissociation of HClO aq as determined by Roth :<sup>7</sup>



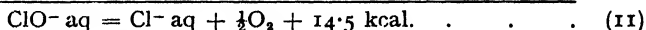
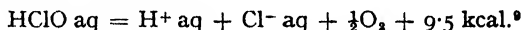
one obtains :

$$\begin{aligned} (\Sigma_1 - 167) &= -5 \\ \Sigma_1 &= 162 \text{ kcal.} \end{aligned} \quad (9)$$

(ii) Another value can be obtained in the following way :



Combining this with the reactions :



$$186 - \Sigma_1 = 14.5$$

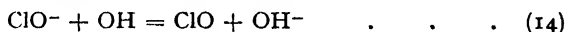
$$\Sigma_1 = 171.5 \text{ kcal.} \quad (12)$$

which is somewhat higher than the value obtained previously.

Therefore the mean value :

$$\Sigma_1 = E_{\text{ClO}} + S_{\text{ClO}^-} = 165 \text{ kcal.} = 7.2 \text{ ev.} \quad (13)$$

This value is approximately the same as the corresponding value for the OH radical where  $E_{\text{OH}} + S_{\text{OH}^-} = 7.0 \text{ ev.}^{10}$  Thus the reaction :



should be practically thermoneutral.

The determination of the electron affinity in the gaseous state requires some knowledge about  $S_{\text{ClO}^-}$ . In absence of any direct data one can take as a first approximation a value somewhat lower than for  $\text{Cl}^-$  ion (as an upper limit), i.e.  $S_{\text{ClO}^-} \sim 60 \text{ kcal.}$

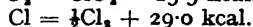
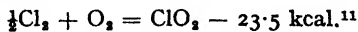
This leaves for the electron affinity in the gaseous state :

$$E_{\text{ClO}} \sim 105 \text{ kcal.} = 4.5 \text{ ev.} \quad (15)$$

### Electron Affinity of $\text{ClO}_2$ .

The sum  $\Sigma_2 (= E_{\text{ClO}_2} + S_{\text{ClO}_2^-})$  can be calculated from a cycle which requires the heat of formation of  $\text{ClO}_2$  from the atoms.

The latter can be calculated from the determination of Booth and Bowen<sup>11</sup> according to :

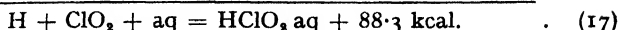
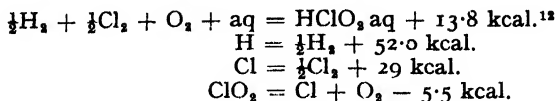


<sup>9</sup> Thomsen, *Thermochem. Untersuch.*, 1882, **2**, 125, 133.

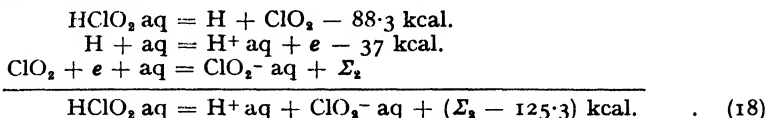
<sup>10</sup> Cf. Weiss, *Trans. Faraday Soc.*, 1935, **31**, 966.

<sup>11</sup> Booth and Bowen, *J. Chem. Soc.*, 1928, **127**, 342.

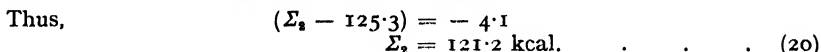
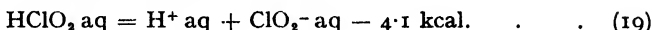
Further :



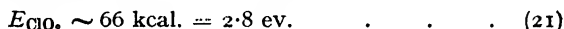
Finally the cycle :



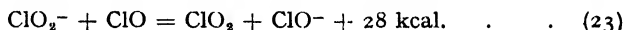
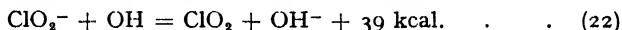
From the work of Barnett it follows that :<sup>13</sup>



Taking again an approximate value for the heat of hydration, i.e.  $\text{Sclo}_2^- \sim 55$  kcal. (somewhat lower than that given for  $\text{ClO}^-$ ), this leaves for the electron affinity of the  $\text{ClO}_2$  molecule the value :



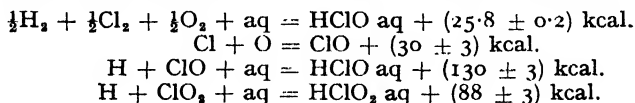
The value  $\mathcal{E}_2$  (for electron affinity + heat of hydration) of  $\text{ClO}_2^-$  given above would make both the electron transfer reactions :



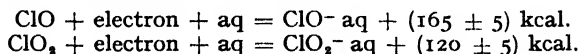
considerably exothermic.

### Summary.

(1) The following thermochemical data have been determined :



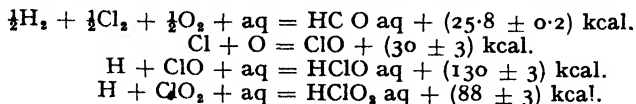
(2) The sums of electron affinity and heat of hydration of the following ions have been determined by cycle processes :



From these values the electron affinities in the gaseous state can be derived from a knowledge of the corresponding heats of hydration of these ions.

### Résumé.

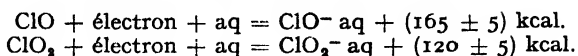
(1) On a établi les données thermodynamiques suivantes :



<sup>12</sup> Latimer, *loc. cit.*<sup>3</sup> p. 48.

<sup>13</sup> Barnett, *Ph.D. Thesis* (University of California, 1935).

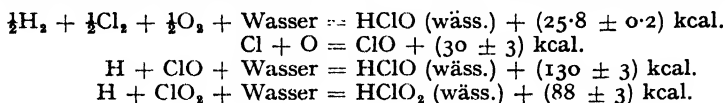
(2) Au moyen de cycles, on a pu déterminer les sommes : affinité d'électron + chaleur d'hydratation des ions suivants :



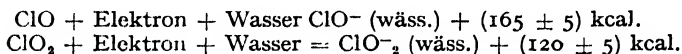
A partir de ces valeurs, on peut établir les chaleurs d'hydratation de ces ions, et de là les affinités d'électrons pour l'état gazeux.

### Zusammenfassung.

(1) Die folgenden thermochemischen Daten sind bestimmt worden :



(2) Die Summe von Elektronenaffinität und Hydratationswärme wurde für die folgenden Ionen durch Kreisprozesse ermittelt :



Bei Kenntnis der entsprechenden Hydratationswärmen können aus diesen Werten die Elektronenaffinitäten dieser Ionen im gasförmigen Zustand berechnet werden.

King's College,  
University of Durham,  
Newcastle-upon-Tyne, 1.

## THE BOND ENERGY, BOND LENGTH AND DISSOCIATION ENERGY DATA FOR CYANOGEN AND THEIR RELATION TO THE HEATS OF ATOMISATION OF CARBON AND NITROGEN.

BY H. D. SPRINGALL.

Received 28th February, 1946.

The heat of formation of cyanogen gas from graphite (the reference state now advocated for solid carbon<sup>1</sup>) and nitrogen gas at 25° C. and 1 atmosphere pressure ( $-\Delta H_{298}^\circ$ ,  $Q_1^\circ$ , is given by thermochemical combustion data as  $-71.9$  kilocalories/gram molecule (k/m). (Bichowsky and Rossini<sup>2</sup> give  $-71.0$  k/m as the heat of formation,  $-\Delta H^\circ$ , of  $\text{C}_2\text{N}_2$  from diamond and  $\text{N}_{2(g)}$  while Rossini and Jessup<sup>1</sup> give  $\Delta H_{298}^\circ = 0.45$  kilocalories/gram atom (k/a) for the change  $C_{\text{graphite}} \rightarrow C_{\text{diamond}}$ .)

The heats of atomisation at 0° K. ( $\Delta H_0$ ) of  $C_{\text{graphite}}$  and  $\frac{1}{2}\text{N}_{2(g)}$ , to ground state atoms, derived from spectroscopic data, especially for CO and  $\text{N}_2$ , are still in some doubt. In each case the uncertainty is not that of a wide range within which the true value must fall but of a choice between two accurately known alternative values, dependent on taking  $D^Z(\text{CO}) = 9.14$  or  $11.11$  ev. ( $210.8$  or  $256.2$  k/m.),  $D^Z(\text{N}_2) = 7.38$  or  $9.76$  ev. ( $170.2$  or

<sup>1</sup> Rossini and Jessup, *J. Res. Nat. Bur. Stand.*, 1938, **21**, 491.

<sup>2</sup> Bichowsky and Rossini, *The Thermochemistry of Chemical Substances* (Reinhold, New York, 1936).



225.1 k/m.), <sup>3, 4, 5, 6</sup>. The derived values for the heats of atomisation, at 0° K.\* are

$$\begin{aligned}(\Delta H_0)_{\text{atom. } C_{\text{graphite}}} & \text{ (to } 3P(C)) \text{ 125.0 or 170.4 k/a.} \\ (\Delta H_0)_{\text{atom. } (\frac{1}{2}N_{2(g)})} & \text{ (to } 4S(N)) \text{ 85.1 or 112.5 k/a.}\end{aligned}$$

From these  $\Delta H_0$  terms the corresponding  $\Delta H_{298}$  terms, needed in thermochemical discussion, may be obtained by the general relation

$H_{298} = H_0 + \int_0^{298} C_p dT$ . The particular values of  $\int_0^{298} C_p dT$  needed are: for  $C_{\text{graphite}}$ , 0.25 k/a.,<sup>1</sup> for  $\frac{1}{2}N_{2(g)}$ , 1.04 k/a.,<sup>†</sup> for  $C_{(g)}$ , 1.48 k/a.,<sup>‡</sup> for  $N_{(g)}$ , 1.48 k/a.<sup>§</sup> The resulting  $\Delta H_{298}$  terms for the heats of atomisation are:

$$\begin{aligned}(\Delta H_{298})_{\text{atom. } C_{\text{graphite}}} & \text{ 126.2 or 171.6 k/a.}^\dagger \\ (\Delta H_{298})_{\text{atom. } \frac{1}{2}N_{2(g)}} & \text{ 85.5 or 112.9 k/a.} \\ \text{(since for } C_{\text{graphite}} \rightarrow C_{\text{diamond}}, \Delta H_{298} & = 0.45 \text{ k/a.,}^1 \\ (\Delta H_{298})_{\text{atom. } C_{\text{diamond}}} & = 125.8 \text{ or 171.2 k/a.)}\end{aligned}$$

This derivation has been given in some detail as the states of solid and gaseous carbon, the temperature, and the assumptions involved as to  $\int C_p dT$ ,  $D^Z(O_2)$  and  $(-\Delta H_0)_I(CO)$  are sometimes unspecified in the literature, with the result that "the latent heat of sublimation of carbon" based on  $D^Z(CO) = 11.11$  ev. has been given values ranging from 168 to 172 k/a.

From the two sets of  $(\Delta H_{298})_{\text{atom.}}$  terms (for  $C_{\text{graphite}}$  and  $\frac{1}{2}N_{2(g)}$ ), each of two possible values, and from the unequivocal  $Q_I^\circ(C_2N_2)$  value, four possible values may be derived for the heat of formation  $(-\Delta H_{298})$  of cyanogen gas from 2C and 2N free atoms, the "atomic heat of formation,"  $AQ_{I(g)}(C_2N_2)$ .|| These are given by the general relation

$$AQ_{I(g)} = \sum (\Delta H_{298})_{\text{atom.}} + Q_I^\circ$$

and have the following numerical values (to the nearest kilocalorie):

$\alpha$ ,	(C, 126.2; N, 85.5), $AQ_{I(g)}(C_2N_2) = 352$ k/m.
$\beta$ ,	(C, 126.2; N, 112.9), " " = 407 "
$\gamma$ ,	(C, 171.6; N, 85.5), " " = 442 "
$\delta$ ,	(C, 171.6; N, 112.9), " " = 497 "

These four possible values for  $AQ_{I(g)}(C_2N_2)$  may be examined in the light of the experimental data on the dissociation of  $C_2N_2$  to free atoms, and of general structural theory, with a view to selecting the "best"  $AQ_{I(g)}$  value and so, indirectly, obtaining evidence towards the selection of the correct values for  $\Delta H_{\text{atom.}}$  for C and for N.

<sup>3</sup> Herzberg, *Chem. Reviews*, 1937, **20**, 145.

<sup>4</sup> Idem., *J. Chem. Physics*, 1942, **10**, 306.

<sup>5</sup> Gaydon, *Nature*, 1944, **153**, 407.

<sup>6</sup> Gaydon and Penney, *Proc. Roy. Soc., A*, 1945, **183**, 374.

<sup>7</sup> Herzberg, *Molecular Spectra and Molecular Structure* (Prentice-Hall, 1939).

<sup>8</sup> Rossini, *J. Res. Nat. Bur. Stand.*, 1939, **22**, 407.

<sup>9</sup> Johnston and Davis, *J. Amer. Chem. Soc.*, 1934, **56**, 271.

\*  $(\Delta H_0)_{\text{atom. } C_{\text{graphite}}} = D^Z(CO) - \frac{1}{2}D^Z(O_2) - (-\Delta H_0)_I(CO)$

where  $D^Z(O_2) = 5.08$  ev. (117.2 k/m) <sup>7</sup>

$(-\Delta H_0)_I(CO) = 27.2$  k/m <sup>8</sup>  
 $(\Delta H_0)_{\text{atom. } \frac{1}{2}N_{2(g)}} = \frac{1}{2}D^Z(N_2)$ .

<sup>†</sup> Treated as a perfect gas consisting of rigid diatomic rotator molecules.<sup>9</sup>

<sup>‡</sup> Treated as perfect gases consisting of monatomic molecules.

<sup>§</sup> Derived independently by Dr. F. D. Rossini—private communication to Dr. L. E. Sutton.

|| The symbol  $AQ$  is used to designate the heat liberated  $(-\Delta H_{298})$  in processes for which the initial state is that of free atoms.

## Review of the Experimental Energy Data on the Stepwise Dissociation of $C_2N_2$ to Free Atoms.

When a cyanogen molecule is disrupted, thermally or photochemically, the first step is the breaking of the C to C linkage, with the production of two CN radicals. The second step is the dissociation of these radicals into C and N atoms. Several experimental values are available for the  $\Delta H_0$  for the reaction  $C_2N_{2(g)} \rightarrow 2CN_{(g)}$ , a term which we may designate by  $D^Z(C_2N_2)$ , and for the dissociation energy of the CN radical,  $D^Z(CN)$ .

### (a) $D^Z(C_2N_2)$ .

Of the several values reported for this  $\Delta H_0$  term, most lie in the range 125 to 146 k/m.<sup>10, 11, 12</sup> but one early value is as low as 77 k/m. There seem to be reasonable grounds for considering that the value of 77 k/m., found spectroscopically by Kistiakowsky and Gershinowitz<sup>13</sup> in 1933, is unduly low. Thus, White,<sup>11</sup> in 1940, gave a treatment indicating that the incomplete resolution and the neglect of pressure broadening effects in the early work could account for the discrepancy between the 1933 results and his own value of 146 k/m. Moreover, the energy necessary to break the C—C bond in ethane has been derived from a combination of kinetic and thermochemical data as 88 k/m.<sup>14</sup> and from direct electron impact experiments as 83 k/m.<sup>15</sup> Since the C to C bond in ethane (bond length, 1.54 Å., bond force constant,  $4.6 \times 10^8$  dynes/cm.<sup>16</sup>) has little or no C=C character, it would indeed be remarkable if the C to C bond breaking energy in ethane were greater than the corresponding energy in  $C_2N_2$ , where the C to C bond is much shorter and more rigid than that in ethane (bond length 1.37 Å.;<sup>17</sup> bond force constant,  $6.7 \times 10^8$  dynes/cm.<sup>18</sup> and has about 50 % C=C character.

The most recent spectroscopic value<sup>11</sup> is  $146 \pm 4$  k/m. with 138 k/m. as an independently estimated lower limit. This value is supported both by the kinetic work of Robertson and Pease<sup>12</sup> on the thermal reaction of  $H_2$  and  $C_2N_2$  and by the earlier work of Hogness and Ts'ai<sup>10</sup> on the photopolymerisation of  $C_2N_2$ , which yield values of 125-130 and 127 k/m. respectively. (This work is reviewed by Evans and Walker.<sup>19</sup>)

In view of all this work, we take 142 k/m. (White's lower limit) the most probable experimental value for  $D^Z(C_2N_2)$ .

### (b) $D^Z(CN)$ .

Mulliken in his review of spectroscopic data<sup>19</sup> gives the most probable value for  $D^Z(CN)$ , obtained by Birge-Sponer extrapolation, as 164 k/m. Bichowsky and Rossini, in their critical compilation in 1936<sup>8</sup> give  $D^Z(CN) = 160$  k/m. Schmid, Gerö and Zemlen<sup>20</sup> have (1938) now obtained by similar methods a value of  $174 \pm 2$  k/m.

Herzberg (1939<sup>7</sup>) gives a value of  $D(CN) = 137$  k/m. but this is not a direct experimental estimation, being derived from the thermochemical  $Q_r^0(C_2N_2) = -71$  k/m. (using  $C_{diamond}$  as standard state for carbon) taken in conjunction with the value 77 k/m. for the  $\Delta H$  for the reaction  $C_2N_2 \rightarrow 2CN$  and the assumptions of  $(\Delta H_0)_{atom}$ ,  $C_{graphite}$  and  $\frac{1}{2}N_{2(g)}$  125 and 85 k/a. respectively ("α" values). This value for  $D(CN)$ , 137 k/m., cannot, therefore, be used as an argument in the matter of selection among

<sup>10</sup> Hogness and Ts'ai, *ibid.*, 1932, **54**, 123.

<sup>11</sup> White, *J. Chem. Physics*, 1940, **8**, 463.

<sup>12</sup> Robertson and Pease, *J. Amer. Chem. Soc.*, 1942, **64**, 1880.

<sup>13</sup> Kistiakowsky and Gershinowitz, *J. Chem. Physics*, 1933, **1**, 432.

<sup>14</sup> Baughan and Polanyi, *Nature*, 1940, **146**, 685.

<sup>15</sup> Stevenson, *J. Chem. Physics*, 1942, **10**, 291.

<sup>16</sup> Linnett and Thompson, *J. Chem. Soc.*, 1937, 1398.

<sup>17</sup> Pauling, Springall and Palmer, *J. Amer. Chem. Soc.*, 1939, **61**, 927.

<sup>18</sup> Evans and Walker, *Trans. Faraday Soc.*, 1944, **40**, 384.

<sup>19</sup> Mulliken, *Rev. Mod. Physics*, 1932, **4**, 81.

<sup>20</sup> Schmid, Gerö, and Zemlen, *Proc. Physic. Soc.*, 1938, **50**, 283.

the hypotheses,  $\alpha$ ,  $\beta$ ,  $\gamma$  and  $\delta$ . Gaydon and Penney<sup>5</sup> point out that a value of  $D(\text{CN})$  as low as 137 k/m. involves a violation of the non-crossing rule, while the value 174 k/m. avoids this difficulty.

It would seem probable that the value 174 k/m. for  $D(\text{CN})$  is the most accurate experimental determination of this quantity.

The spectroscopically estimated dissociation energies  $D^Z(\text{C}_2\text{N}_2)$  and  $D^Z(\text{CN})$  are  $\Delta H_0$  terms but as the correction factors to convert them to the corresponding  $\Delta H_{298}$  terms are within the limits of error of the experimental estimations, the  $D^Z$  terms may be treated as equivalent to  $\Delta H_{298}$  terms for the purposes of rough comparison, without introducing appreciable error.

### The Interrelation of the $\Delta Q_{t(g)}(\text{C}_2\text{N}_2)$ and $D'(\text{C}_2\text{N}_2)$ and $D(\text{CN})$ Terms.

Irrespective of any molecular structural considerations, the following relation must hold

$$D'(\text{C}_2\text{N}_2) + 2D(\text{CN}) = \Delta Q_{t(g)}(\text{C}_2\text{N}_2).$$

Inserting the most probable experimental values for  $D'(\text{C}_2\text{N}_2)$ , 142 k/m., and  $D(\text{CN})$ , 174 k/m., gives  $\Delta Q_{t(g)}(\text{C}_2\text{N}_2) = 490$  k/m., in good agreement with the  $\delta$  value 497 k/m. derived from thermochemical data and taking  $\Delta H_{\text{atom.}}$  (C) and (N) 171.6 and 112.9 k/m. respectively. This agreement between the experimental and the  $\delta$  value for the  $\Delta Q_{t(g)}$  term, pointed out in effect by Gaydon and Penney,<sup>6</sup> and the wide divergence between the experimental and the  $\alpha$ ,  $\beta$ , and  $\gamma$  values, taken together are strong evidence for the  $\delta$  hypothesis.

It is, moreover, necessary that the values, adopted from the review of the experimental data on the dissociations, for  $D'(\text{C}_2\text{N}_2)$  and  $D(\text{CN})$  should be reasonable in terms of general valency theory. Now, the four possible values for  $\Delta Q_{t(g)}(\text{C}_2\text{N}_2)$ , dependent on the hypotheses  $\alpha$ ,  $\beta$ ,  $\gamma$  and  $\delta$ , may be analysed with the help of general bond energy considerations to give four possible sets of energy values for the two bond breaking processes in the stepwise dissociation of  $\text{C}_2\text{N}_2$  to free atoms ( $D'(\text{C}_2\text{N}_2)$  and  $D(\text{CN})$ ). It is found that the values so derived for  $D'(\text{C}_2\text{N}_2)$  and  $D(\text{CN})$  from the  $\delta$  value of  $\Delta Q_{t(g)}(\text{C}_2\text{N}_2)$  are indeed in close agreement with the adopted experimental values.

In the derivation of probable values of  $D'(\text{C}_2\text{N}_2)$  and  $D(\text{CN})$  from bond energy considerations, the bond energy terms ordinarily used for C—C and C $\equiv$ N bonds require modification to allow for the particular character of the cyanogen molecule. The derivation proceeds as follows.

In Table I (A) are listed the general bond energy terms,  $\Delta Q_B$ , for the bond systems C—C and C $\equiv$ N calculated for each of the four possible combinations of the  $(\Delta H_{298})_{\text{atom}}$  values for C and N ( $\alpha$ ,  $\beta$ ,  $\gamma$  and  $\delta$ ). Each bond energy term is the average  $-\Delta H$  contribution appropriate to that bond, such that  $\Sigma \Delta Q_B = \Delta Q_{t(g)}$ , for a covalent molecule exhibiting no valency bond resonance.<sup>21, 22</sup> The  $\alpha$  values are based on those given by Pauling,<sup>23</sup> who used in his evaluation of the energy terms for bonds involving C atoms and N atoms the following  $(\Delta H_{298})_{\text{atom.}}$  values—for C<sub>diamond</sub>, 124.3 (derived from an early estimate of the lower value for  $D^Z(\text{CO})$ ) k/a. and for  $\frac{1}{2}\text{N}_{2(g)}$ , 85.1 k/a. The new conversion factors now give these terms the values 125.8 k/a. and 85.5 k/a. respectively. These changes necessitate the increasing of the bond energy terms given by Pauling by the amounts (125.8-124.3)/4 k/a. (0.4 k/a.) per C atom per

<sup>21</sup> Sidgwick, *Some Physical Properties of the Covalent Link in Chemistry* (Cornell U.P., Ithaca, 1933), Chap. iv.

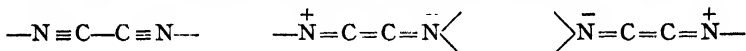
<sup>22</sup> Pauling, *The Nature of the Chemical Bond* (Cornell U.P., Ithaca, 2nd Ed., 1940), Chap. ii, sect. 10.

<sup>23</sup> *Op. cit.*, pp. 53 and 131.

bond and  $(85.5-85.1)/3$  k/a. (0.1 k/a.) per N atom per bond.<sup>24</sup> The Pauling bond energy values, subjected to these minor corrections are given as the  $\alpha$  values in Table I (A). The  $\beta$ ,  $\gamma$  and  $\delta$  values are calculated from the  $\alpha$  values by the addition of the appropriate correcting factors.<sup>24</sup> \*

The C—C bond energy term is that giving the best general agreement for the paraffins.<sup>25</sup> The  $C\equiv N$  term is derived from the alkyl cyanides using the C—C term for the C—C bond in  $C-C\equiv N$ .<sup>25</sup> This assessment of  $\Delta Q_B(C\equiv N)$  includes, therefore, not only the resonance energy due to participation of the excited structure  $C-\overset{+}{C}=\bar{N}$ , but also that due to  $\overset{+}{C}\{C=C=N\}$ . It is known from the dimensions of  $CH_3$ , CN, in which the  $C\leftrightarrow C$  distance is 1.49 Å.<sup>26, 17</sup> that such  $C=C$  double bonding does occur, so that in fact the C to C bond in C. CN systems is strengthened above the single C—C bond energy term value and the use of the C—C single bond term to compute the  $C\equiv N$  term will give a false impression of the strength of the latter.†

In cyanogen itself the C to C distance, 1.37 Å.<sup>27, 17</sup> is considerably shorter even than that in  $CH_3CN$ , indicating resonance among the structures :



(as well as among others such as  $-N=C-\overset{+}{C}=\bar{N}$  etc.)

The dimensions indicate that the C to C bond has about 50 %  $C=C$  character (just as the similar C to C bonds in diacetylene and dimethyl-diacetylene).<sup>17</sup> From an analysis of the thermochemical, spectroscopic and X-ray data, Skinner<sup>28</sup> has prepared curves giving the variation of the bond energy term for a C to C bond, with the bond length for  $(\Delta H_{298})_{\text{atom. } C_{\text{diamond}}} = 125$  and 170 k/a. The combination of the bond energy term for  $C\leftrightarrow C = 1.37$  Å., with the appropriate  $\Delta Q_{t(g)}(C_2N_2)$  term yields a C to N bond energy term,  $\Delta Q_B$  (C to N in  $C_2N_2$ ) by the expression :

$$\Delta Q_B \text{ (C to N in } C_2N_2) = \frac{1}{2}[\Delta Q_{t(g)}(C_2N_2) - \Delta Q_B(C-C, 1.37 \text{ Å.})]$$

<sup>24</sup> Sidgwick, *op. cit.*, 109.

<sup>25</sup> Pauling, *op. cit.*, 131.

<sup>26</sup> Brockway, *J. Amer. Chem. Soc.*, 1936, **58**, 2516.

<sup>27</sup> Idem., *Proc. Nat. Acad. Sci.*, 1933, **19**, 868. See also Wierl, *Ann. Physik*,

1932, **13**, 453.

<sup>28</sup> Skinner, *Trans. Faraday Soc.*, 1945, **41**, 645.

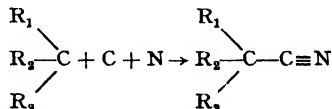
\* The factors are :

For  $\beta$ , O per C atom per bond,  $(112.9-85.5)/3$  k/m. per N atom per bond.

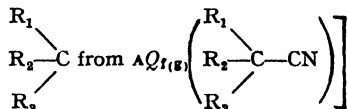
For  $\gamma$ ,  $(171.6-126.2)/4$  k/m. bond, O k/m. per N atom per bond.

For  $\delta$ ,  $(171.6-126.2)/4$  k/m. bond,  $(112.9-85.5)/3$  k/m. per N atom per bond.

† It is found that heat liberated ( $-\Delta H$ ) in the hypothetical gas phase reaction



[computed by subtracting the sum of the energy terms for the bonds and resonance in



is very largely independent of  $R_1, R_2$  or  $R_3$ . This energy term, which may be called the group energy term for the C—CN group, is constant to  $\pm 2$  k/m. (210 k/m. on hypothesis  $\alpha$ , 294 k/m. on hypothesis  $\delta$ ) over a wide range of compounds from acetonitrile to the naphthonitriles. Similar results appear in the nitro-group field. It is hoped to give these subjects separate consideration.

which should be in close agreement with the real state of the C to N linkage in cyanogen. Table I (B) gives the two values for the bond energy term for a C to C bond of length 1.37 Å. (taken from Skinner's curves, corrected for  $(\Delta H_{298})_{\text{atom C}_{\text{diamond}}} = 125.8$  and  $171.2$  k/a.), and the four values derived for the C to N bond energy term in  $\text{C}_2\text{N}_2$ , according to the four combinations,  $\alpha$ ,  $\beta$ ,  $\gamma$  and  $\delta$ , of the permissible  $\Delta H_{\text{atom}}$  values for C and for N.

In the process of stepwise dissociation of a polyatomic molecule into its component atoms, the  $\Delta H$  increment for the breaking of the first bond is greater or less than the thermochemically derived mean bond energy term ( $AQ_B$ ) for that bond, according as the valency systems of the radicals produced by this first bond breaking are less or more stable than the corresponding systems in the parent molecule.<sup>29, 30 \*</sup>

TABLE I

Bond.	Bond Energy Term, $AQ_B$ , (k/m.)			
	$\alpha$ Graphite, 126-2. N, 85.5.	$\beta$ Graphite, 126-2. N, 112.9.	$\gamma$ Graphite, 171.6. N, 85.5.	$\delta$ Graphite, 171.6. N, 112.9.
A. C—C . . .	59.4	59.4	82.0	82.0
C $\equiv$ N (from alkyl cyanides) . . .	151.6	179.0	185.5	212.9
B. C to C bond of length 1.37 Å. . .	85	85	128	128
C to N in $\text{C}_2\text{N}_2$ . .	133	161	157	185
C.	Probable limits for Bond Breaking Energies (k/m.) [ $D'(\text{C}_2\text{N}_2)$ and $D(\text{CN})$ ]			
	$\alpha$	$\beta$	$\gamma$	$\delta$
C to C in $\text{C}_2\text{N}_2$ . .	91-105	91-105	134-148	134-148
C to N in CN radical	130-123	158-151	154-147	182-175

It is likely that the CN radical (ground state  $^2\Sigma^+$ ) is less stable than is the corresponding valency system in  $\text{C}_2\text{N}_2$ . The C $\leftrightarrow$ N distance in the radical is 1.172 Å. and is very accurately known from spectroscopic data.<sup>7</sup> The most probable value for the C $\leftrightarrow$ N distance in  $\text{C}_2\text{N}_2$  is 1.16 Å.,<sup>17</sup> though this electron diffraction determination is not as accurate as the spectroscopic estimation for the radical. The force constant for the C to N linkage in the CN radical is  $16.2 \times 10^5$  dynes/cm., while that for the C to N linkage in  $\text{C}_2\text{N}_2$  is  $17.5 \times 10^5$  dynes/cm.<sup>22</sup> Thus, on the breaking of the C to C linkage in  $\text{C}_2\text{N}_2$ , it appears that in the resulting CN system (a) the bond distance is increased, (b) the bond force constant is decreased, both facts indicating that the stability of the C to N linkage is decreased.

The quantitative assessment of this weakening of the C to N linkage cannot yet be made with any great accuracy, because (a) in the case of valency bond resonance involving a large contribution from a triple-

<sup>29</sup> Pauling, *op. cit.*, p. 52.

<sup>30</sup> Butler and Polanyi, *Trans. Faraday Soc.*, 1943, **39**, 19.

<sup>31</sup> Dwyer and Oldenberg, *J. Chem. Physics*, 1944, **12**, 351.

<sup>32</sup> Linnett and Thompson, *J. Chem. Soc.*, 1937, 1403.

\* Thus the energy needed to break the first H—O bond in  $\text{H}_2\text{O}$  is 118 k/m., and that to break the second is 100 k/m.<sup>31</sup>

bonded structure, small changes in bond length are associated with relatively large changes in bond strength,<sup>18</sup> and (b) the C $\leftrightarrow$ N distance in cyanogen is not yet sufficiently accurately known. It is likely, however, that the C to N linkage in the CN radical is unstable relative to the C to N linkage in C<sub>2</sub>N<sub>2</sub> by about 3 to 10 k/m.

Thus when cyanogen undergoes stepwise disruption, it is to be expected that the energy needed for the first step,  $D'(\text{C}_2\text{N}_2)$ , will be greater than the bond energy term for a C to C bond of length 1.37 Å., by 6 to 20 k/m., while the energy needed for the second step,  $D(\text{CN})$ , will be correspondingly less than the derived bond energy term for the C to N linkage in C<sub>2</sub>N<sub>2</sub>, by 3 to 10 k/m. This gives a means of estimating the probable limits for the energies of the two bond-breaking processes for the cyanogen dissociation. Table I (C) gives the four sets of probable values derived on the four hypotheses  $\alpha$ ,  $\beta$ ,  $\gamma$  and  $\delta$ .

The rough upper limit derived for  $D'(\text{C}_2\text{N}_2)$ , 148 k/m., and the corresponding lower limit derived for  $D(\text{CN})$ , 175 k/m., on the  $\delta$  hypothesis, are in good agreement with the accepted experimental values 142 and 174 k/m. respectively. The values derived on hypotheses  $\alpha$ ,  $\beta$ , and  $\gamma$  diverge widely from the accepted experimental values. These results confirm the correctness of hypothesis  $\delta$ ,  $(\Delta H_{298})_{\text{atom.}} C_{\text{graphite}} = 171.6 \text{ k/a.}; (\Delta H_{298})_{\text{atom.}} \frac{1}{2}\text{N}_{2(\text{g})} = 112.9 \text{ k/a.}$

Herzberg<sup>3</sup> considered the alternatives  $\alpha$  and  $\gamma$ . He pointed out that, on the hypothesis  $\gamma$ , the White value of 146 k/m. for  $D'(\text{C}_2\text{N}_2)$  implied a value of 148 k/m. for  $D(\text{CN})$ . This he considered improbable on the grounds that a C—C single bond, even involving a large amount of C=C double bond character, is not likely to be as strong as a C $\equiv$ N triple bond. Even allowing for the fact that in C<sub>2</sub>N<sub>2</sub> the C to N linkage has a large amount of C=N character, and for the variation of bond breaking energies from the mean bond energy terms, this argument seems most reasonable and is strongly supported by the fact that when C<sub>2</sub>N<sub>2</sub> is disrupted it is the C to C linkage which always breaks first.

Herzberg, therefore, rejected White's 146 k/m. value for  $D'(\text{C}_2\text{N}_2)$ , and the hypothesis  $\gamma$  (Graphite, 171.6; N, 85.5) and accepted the Kistiakowsky-Gershinowitz value of 77 k/m. for  $D'(\text{C}_2\text{N}_2)$  and the hypothesis  $\alpha$  (Graphite, 126.2; N, 85.5). But his argument, from cyanogen data, against hypothesis  $\gamma$  is even better met by the hypothesis  $\delta$  (Graphite, 171.6; N, 112.9), only available since 1944,<sup>5</sup> which has the effects (a) of accommodating the White 146 k/m. value for  $D'(\text{C}_2\text{N}_2)$ , (b) of increasing the expected  $D(\text{CN})$  value well above  $D'(\text{C}_2\text{N}_2)$  and of bringing it into agreement with the latest spectroscopic estimation of  $D(\text{CN})$ , (c) of enabling a reasonable interpretation of the results to be given in terms of general structural theory.

The author wishes to express his thanks to Drs. L. E. Sutton and H. A. Skinner and Mr. L. F. Jones for critical discussions and to Professors E. L. Hirst, F.R.S. and N. V. Sidgwick, F.R.S. for their interest in this work.

### Summary.

The four possible values of the heat of formation of cyanogen gas from free atoms ( $-\Delta H_{298} = A Q_{t(\text{g})}(\text{C}_2\text{N}_2)$ ) have been derived from the two possible values for the heats of atomisation,  $(\Delta H_{298})_{\text{atom.}}$  of graphite (126.2 or 171.6 k/a.) and of nitrogen gas (85.5 or 112.9 k/a.).

Only that value of  $A Q_{t(\text{g})}(\text{C}_2\text{N}_2)$  dependent on taking  $(\Delta H_{298})_{\text{atom.}} C_{\text{graphite}} = 171.6 \text{ k/m.}$  and  $(\Delta H_{298})_{\text{atom.}} \frac{1}{2}\text{N}_{2(\text{g})} = 112.9 \text{ k/a.}$  is in agreement with that obtained from the experimental data on the energies involved in the stepwise dissociation of C<sub>2</sub>N<sub>2</sub> to free atoms,

$[\text{C}_2\text{N}_2 \rightarrow 2\text{CN}, \Delta H_0 = D^Z(\text{C}_2\text{N}_2), 2\text{CN} \rightarrow 2\text{C} + 2\text{N}, \Delta H_0 = 2D^Z(\text{CN})] \quad *$   
by the relation

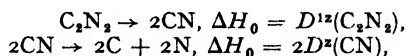
$$A Q_{t(\text{g})}(\text{C}_2\text{N}_2) = D'(\text{C}_2\text{N}_2) + 2D(\text{CN}).$$

The experimental values for  $D'(C_2N_2)$  and for  $D(CN)$  are shown to be reasonable in terms of valency theory if  $(\Delta H_{298})_{\text{atom}} C_{\text{graphite}} = 171.6 \text{ k/m.}$  and  $(\Delta H_{298})_{\text{atom}} \frac{1}{2}N_{2(g)} = 112.9 \text{ k/m.}$  but not on any of the other three available hypotheses as to values of  $(\Delta H_{298})_{\text{atom.}}$  for (C) and (N).

### Résumé.

Les quatre valeurs possibles pour la chaleur de formation du cyanogène gazeux à partir des atomes libres ( $-\Delta H_{298} = \Delta Q_{T(g)}(C_2N_2)$ ) ont été obtenues à partir des deux valeurs possibles des chaleurs d'atomisation  $(\Delta H_{298})_{\text{atom}}$  du graphite (126.2 ou 171.6 kcal. atome) et de l'azote gazeux (85.5 ou 112.9 kcal./atome).

Seulement la valeur de  $\Delta Q_{T(g)}(C_2N_2)$ , obtenue en prenant  $(\Delta H_{298})_{\text{atom.}} C_{\text{graphite}} = 171.6$  et  $(\Delta H_{298})_{\text{atom.}} \frac{1}{2}N_{2(g)} = 112.9$  est en bon accord avec celle obtenue à partir des données expérimentales qui concernent les énergies mises en jeu dans la dissociation de  $C_2N_2$  en atomes libres, dissociation en deux étapes :



les énergies étant reliées par la relation :

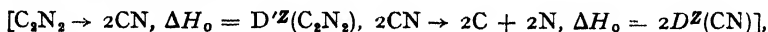
$$\Delta Q_{T(g)}(C_2N_2) = D'(C_2N_2) + 2D(CN).$$

Les valeurs expérimentales de  $D'(C_2N_2)$  et de  $D(CN)$  sont bien fondées d'après la théorie de la valence, si  $(\Delta H_{298})_{\text{atom.}} C_{\text{graphite}} = 171.6 \text{ kcal./atome}$  et  $(\Delta H_{298})_{\text{atom.}} \frac{1}{2}N_{2(g)} = 112.9 \text{ kcal./mol.}$ , mais pas avec toute autre des trois hypothèses possibles pour les valeurs de  $(\Delta H_{298})_{\text{atom.}}$  de (C) et (N).

### Zusammenfassung.

Der Autor berechnet die vier möglichen Werte der Bildungswärme von Dizyngas aus freien Atomen ( $-\Delta H_{298} = \Delta Q_{T(g)}(C_2N_2)$ ) aus den zwei möglichen Werten der Dissoziationsarbeit für die Erzeugung von freien Atomen  $(\Delta H_{298})_{\text{atom.}}$  aus Graphit (126.2 oder 171.6 kcal./Grammatom) und aus Stickstoffgas (85.5 oder 112.9 kcal./Grammatom).

Nur einer dieser vier Werte stimmt mit dem Wert überein, der sich aus den experimentellen Wärmetönungen in der stufenweisen Dissoziation von  $C_2N_2$  in freie Atome



unter Benützung der Beziehung

$$\Delta Q_{T(g)}(C_2N_2) = D'(C_2N_2) + 2D(CN),$$

ergibt. Es wird gezeigt, dass die experimentellen Werte für  $D'(C_2N_2)$  und für  $D(CN)$  nur dann mit der Valenztheorie vernünftig vereinbar sind, wenn

$$(\Delta H_{298})_{\text{atom.}} C_{\text{Graphit}} = 171 \text{ kcal./Mol.}$$

und

$$(\Delta H_{298})_{\text{atom.}} \frac{1}{2}N_{2(g)} = 112.9 \text{ kcal./Mol.}$$

aber nicht, wenn eine andere Kombination der möglichen Dissoziationsarbeiten angenommen wird.

*Department of Chemistry,  
University of Manchester,  
Manchester, 13.*

# SEMI-CONDUCTING PROPERTIES OF STANNOUS SULPHIDE.

## PART II.—THERMOELECTRIC EFFECT.

By J. S. ANDERSON AND (MRS.) M. C. MORTON.

*Received 17th April, 1946.*

In a previous paper<sup>1</sup> we described measurements of the electrical conductivity of stannous sulphide. These were so carried out that the values found for the constants  $A_1$ ,  $E_1$ ,  $A_2$ ,  $E_2$  characterising the conductivity  $\kappa(T)$  in the expression

$$\kappa(T) = A_1 e^{-E_1/2kT} + A_2 e^{-E_2/2kT}$$

could be correlated directly with minute changes in stoichiometric composition brought about by chemical treatment. It was thereby unambiguously shown that (in the low temperature or "structure sensitive" range) changes in the conductivity arose almost entirely from alterations in the excitation energy factor  $E_1$ , the temperature-independent factor  $A_1$ , which involves both the number of potentially-conducting centres and their mobility, remaining almost constant. As we pointed out, the variation in  $E_1$  with concentration of impurity, the invariance of  $A_1$  with concentration of impurity, and the non-specificity of  $E_1$  for different semi-conductors are difficult to harmonise with the accepted theory of semi-conduction unless that theory be modified.

We have now extended our study by measurement of the thermoelectric power of the couple  $\text{Au}|\text{SnS}|\text{Au}$  over a wide range of temperature.<sup>2</sup> Since the early work of Baedeker,<sup>3</sup> relatively few systematic studies have been made of the thermo-electric effect. Theoretical discussions (e.g. by Fowler,<sup>4</sup> Wagner<sup>5</sup> and others) have shown the relation between the direction of the thermoelectric current and the nature of the current carriers within the semiconductor, and the behaviour of several materials has been treated from the standpoint of Wagner's theory (e.g.,  $\text{Cu}_2\text{O}$ ,<sup>6</sup>  $\text{Cu}_2\text{Se}$ ,<sup>7</sup>  $\text{PbS}$ <sup>8</sup>). Quantitatively, however, these treatments are incomplete. The fullest discussion of the subject is that of Mönch,<sup>9</sup> who, with his co-workers, has made an extensive study of the thermoelectric properties of cuprous oxide.<sup>10</sup> With the exception of some measurements by Hochberg and Kvascha, quoted by Joffé,<sup>11</sup> the data for  $\text{Cu}_2\text{O}$  refer to a relatively narrow range of temperature, within which

<sup>1</sup> Anderson and Morton, *Proc. Roy. Soc. A*, 1945, **184**, 83.

<sup>2</sup> Anderson and Morton, *Nature*, 1945, **155**, 112.

<sup>3</sup> Baedeker, *Ann. Physik*, [iv], 1907, **22**, 749.

<sup>4</sup> *Statistical Mechanics*, Cambridge, 1936, § 11.74 et seq.

<sup>5</sup> Wagner, *Z. physikal. Chem. B*, 1933, **22**, 195.

<sup>6</sup> Dünwald and Wagner, *ibid. B*, 1933, **22**, 212.

<sup>7</sup> Reinhold and Mohring, *ibid. B*, 1938, **38**, 221.

<sup>8</sup> Hintenberger, *Z. Physik*, 1942, **119**, 1.

<sup>9</sup> (a) *Z. Physik*, 1933, **83**, 247; (b) *ibid.*, 1933, **84**, 59; (c) *ibid.*, 1934, **91**, 124; (d) *Ann. Physik*, [v], 1936, **26**, 481; (e) *ibid.*, [v], 1939, **34**, 265.

<sup>10</sup> (a) Schweickert, *Ann. Physik*, [v], 1939, **34**, 250; (b) Rohde, *ibid.*, [v], 1939, **34**, 259.

<sup>11</sup> Joffé, *Actualités Scientifiques*, 1935, No. 202; Hochberg and Kvascha, *J. Exp. Theor. Physics. (U.S.S.R.)*, 1935, **5**, 46.



some unexplained anomalies in the conductivity take place.<sup>12</sup> It is therefore of interest to examine the applicability of Mönch's discussion to other semiconductors, and over the widest possible range of temperature.

For this purpose SnS is a suitable material, as the nature of the conduction process at high and low temperatures had been deduced in our previous work. By measuring simultaneously the conductivity and the thermoelectric power of the same specimen it has been possible to correlate the two properties directly with each other and with variations in stoichiometric composition. We agree with Joffé<sup>11</sup> in concluding that the temperature variation of the thermoelectric power is in direct disagreement with the theory. The direction of the thermo-e.m.f. confirmed the occurrence of positive hole conduction at the ordinary temperature, and revealed a change-over from positive hole to electron conduction at higher temperatures; this electron conduction process, as was suggested previously, is presumably the intrinsic conduction of the stannous sulphide lattice. Over an intermediate range of temperature both positive holes in the lower band and electrons in the conductivity band contribute comparably to the conduction process.

### Experimental.

We describe briefly a technique which we have found applicable to a variety of problems involving the properties of semiconductors. The material (SnS, prepared as described previously<sup>13</sup>) is formed into plates, 25 mm.  $\times$  5 mm.  $\times$  1-2 mm. thick, by compression in a hardened steel die, under a pressure of 5 tons/sq. in. or more. Such a plate (A, Fig. 1) is clamped firmly between platinum or gold foil contacts B, which serve as current leads for the potentiometric measurement of conductivity, and as the metal-semiconductor junctions for the thermo-e.m.f. measurements. Probes C, of springy platinum foil, bearing on the edge of the specimen, act as potential leads for the conductivity measurements. Insulation between specimen, clamping blocks, etc., is by thin slips of mica. The upper clamping block D is provided with a heater winding, whereby a temperature difference up to 40° can be maintained between the ends of the plate A. The whole compact assembly is carried on a framework of glass rods, and is enclosed in a demountable glass jacket. The jacket is immersed in an electric furnace or cooling bath, and is connected to vacuum pumps, McLeod gauge, supply of oxygen-free hydrogen, etc. (Fig. 1, B).

By this means it is possible to measure the thermo-e.m.f. corresponding to a small difference of temperature at any desired temperature, rather than an integrated effect as has been measured by a number of previous investigators.<sup>7, 8</sup> Schweickert<sup>10a</sup> made measurements on Cu<sub>2</sub>O between -70° and +60° in a not dissimilar manner, but without that simultaneous correlation with conductivity data that our problem required. The temperature difference between the hot and cold junctions was measured by a Cu-constantan thermocouple (F, Fig. 1a). It proved difficult to ensure that the Cu-constantan junctions took up the true temperature of the ends of the specimen. The most reliable results were obtained with Cu-constantan junctions let into slits in small Cu plates, about 5  $\times$  5 mm., which were clamped (as packing pieces) against the ends of the specimen, and separated from it only by thin cleavage flakes of mica. At the ordinary temperature, the thermo-junctions followed the temperature of the ends of the specimen faithfully, as shown by the fact that the apparent thermoelectric power of the Au | SnS | Au couple was independent of the pressure and thermal conductivity of the ambient

<sup>12</sup> (a) cf. Vogt, *Ann. Physik*, [v], 1930, 7, 46; (b) Engelhard, *ibid.*, 1933, 17, 501.

<sup>13</sup> Ridge and Anderson, *Trans. Faraday Soc.*, 1943, 39, 93.

gas. At elevated temperatures the reliability of the measurements was lower, because of the difficulty of eliminating small local temperature gradients in the furnace. The effect of these was shown in that the apparent thermoelectric power varied with the temperature difference recorded by the Cu-constantan couple. By increasing the temperature difference sufficiently (e.g., to  $10-25^\circ$ ) the thermoelectric power reached a limiting value. If we denote by  $\Delta t_1$  the apparent temperature difference between the Cu-constantan junctions when the heater was not switched on, and by  $\Delta t_2$  the apparent temperature difference with the heater operating, and by  $\theta_1$ ,  $\theta_2$  the respective potentials across the Au | SnS | Au couple, we found that (for  $\Delta t_2 = 10-30^\circ$ )  $\theta_2 - \theta_1 / \Delta t_2 - \Delta t_1$  was practically independent of  $\Delta t_2$ , and close to the limiting slope of the

*Potentiometer Circuits.*

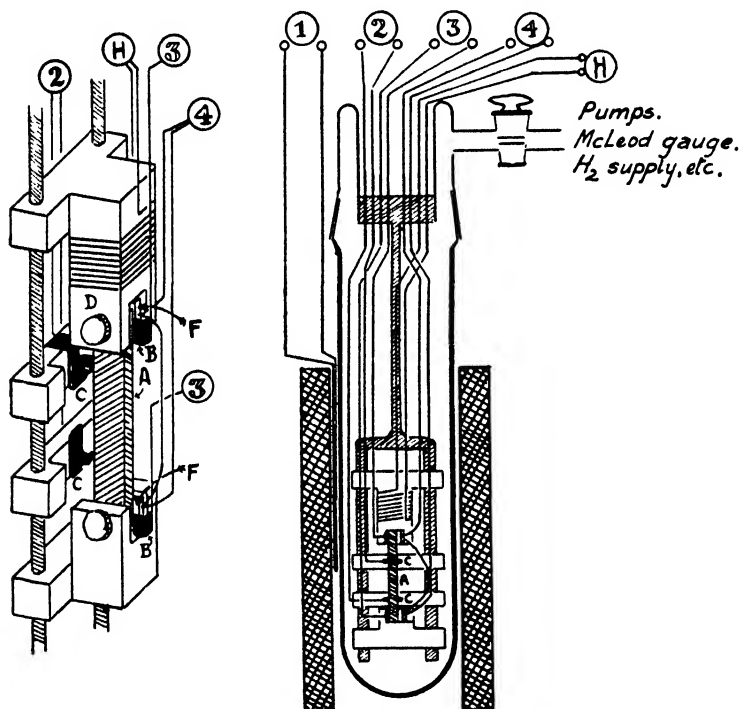


FIG. 1.—Potentiometer circuits: 1. Furnace thermocouple; 2. Probes; 3. Thermo-e.m.f. and current leads; 4. Copper-constantan thermocouple; H: Heater circuit.

$\theta$ - $\Delta t$  curve. This provided an empirical correction for the crude thermoe.m.f. measurements, and obviated the need for a whole series of measurements at each temperature, with different heater currents. Results quoted below have been corrected in this way; the effect of the correction can be judged by comparing Fig. 3 with the curves reproduced in ref.<sup>2</sup> The very high resistance ( $10^6$ - $10^7$  ohms) of some specimens at and below the ordinary temperature adversely limited the accuracy with which the thermoelectric effect could be measured.

Measurements were made on each plate of stannous sulphide during repeated heating runs in vacuum, or after exposure to oxygen, or after heating in hydrogen at  $250-370^\circ$ ; the general procedure was as described in our previous paper.

## Results.

**Conductivity Measurements.**—Measurements of conductivity, made by the technique described above, between room temperature and  $400^{\circ}$  accorded well with those reported previously, and thus showed that the earlier results were not vitiated by contact resistances at the electrodes.<sup>13</sup>

Some measurements were also extended down to  $-78^{\circ}$  (and, in a few cases, to  $-185^{\circ}$ ). In every case, the slope of the  $\log \kappa(T) - 1/T$  curve fell off at lower temperatures; specimens with poor conductivity showed a fairly abrupt change of slope, but with better-conducting material the change of slope was gradual. This behaviour indicates the operation at

TABLE I

Material and Series.	$\kappa(18^{\circ})$ .	$\kappa(-78^{\circ})$ .	$E(18^{\circ})$ .	$E(-78^{\circ})$ .
III. 1	$7.1 \times 10^{-2}$	$1.4 \times 10^{-2}$	0.11	0.03
III. 4	$1.0 \times 10^{-4}$	$2.8 \times 10^{-6}$	0.30	0.13
III. 5	$4.8 \times 10^{-3}$	$2.3 \times 10^{-4}$	0.21	0.12
IX. 1	$1.2 \times 10^{-2}$	$1.7 \times 10^{-3}$	0.14	0.08

low temperatures of another conduction mechanism, involving a relatively small concentration of some type of impurity centre different from the deficit of cations which gives rise to the positive hole conduction at ordinary temperatures. Analogous behaviour, with low temperature conduction mechanisms of very low excitation energy, has been observed for some other semiconductors (e.g.  $\text{ZnO}$ ,<sup>14</sup>  $\text{Cu}_2\text{O}$ ,<sup>12a</sup>  $\text{FeS}$ <sup>15</sup>). Characteristic constants of the low temperature conductivity of a few specimens of stannous sulphide are summarised in Table I.

**Thermoelectric Effect Measurements.**—Results obtained before the experimental technique had reached its final form have (except for some

TABLE II

Experiment.	Treatment.	$\kappa(18^{\circ})$ $\text{ohm}^{-1} \text{ cm}^{-1}$ .	$E$ ev.	$P$ $\text{mv./}^{\circ} \text{ c.}$
VIII. 1	Heated in vacuum : up down	$1.95 \times 10^{-2}$ $1.05 \times 10^{-2}$	0.13 0.16	0.55 0.54
VIII. 2	After hydrogen treatment	$2 \times 10^{-6}$	0.40	0.95
VIII. 4a	After exposure to air	$3.2 \times 10^{-2}$	0.085	0.63
VIII. 4b	After treatment with hydrogen	$1.26 \times 10^{-6}$	0.43	0.80
VIII. 5	Exposed to air ( $p = 10^{-3} \text{ mm.}$ ) and then heated in vacuum	$1.4 \times 10^{-4}$	0.31	0.71
VIII. 6	Similar ; exposure to 1 mm. air Reduced after exposure to oxygen at $113^{\circ}$ . $p_{\text{O}_2} = 0.1 \text{ mm.}$	$3.9 \times 10^{-4}$ $3.5 \times 10^{-6}$	0.28 0.36	0.74 0.86
VIII. 7	Reduced after exposure to 0.2 mm. of oxygen at $170^{\circ}$	$3.9 \times 10^{-3}$	0.18	0.70
VIII. 8	Heated at $275^{\circ}$ in vacuum	$4.5 \times 10^{-5}$	0.33	0.76
IX. 1	Heated in vacuum	$1.2 \times 10^{-2}$	0.14	0.54
IX. 2	" "	$2.1 \times 10^{-3}$	0.19	0.53
IX. 6	" "	$1.4 \times 10^{-3}$	0.19	0.60
IX. 7	" "	$8.1 \times 10^{-5}$	0.26	0.65
IX. 9	After treatment with hydrogen	$2 \times 10^{-5}$	0.33	0.85

measurements at low temperatures—Plate IV, Fig. 3) been discarded. Final results are summarised in Table II. The convention adopted here for the sign of the thermo-e.m.f. is that the flow of current from metal

<sup>14</sup> Miller, *Physic. Rev.*, 1941, 60, 890.<sup>15</sup> Unpublished data.

to semiconductor at the hot junction (i.e., flow of electrons from semiconductor to metal at the hot junction) is denoted as positive. This corresponds to the existence of positively-charged current carriers ("positive holes") within the semiconductor.<sup>18</sup>

From Table II it is evident that the thermoelectric power (like other properties associated with semiconduction) is not a material constant, but is variable from specimen to specimen and dependent upon past history; the same has been found by others, and for other materials. A certain correlation may be noticed, however, with the variations in electrical conductivity, and therefore with variations in the stoichiometric composition of the solid.

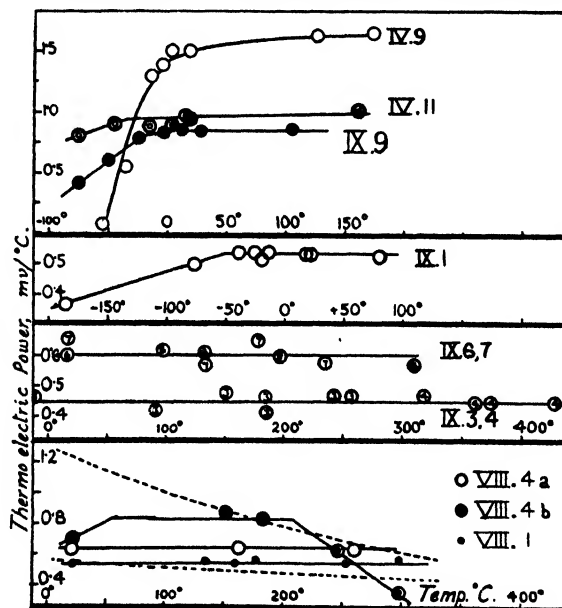
TABLE III

Press. of O <sub>2</sub> , mm.	10 <sup>-6</sup>	0.7 × 10 <sup>-4</sup>	0.9 × 10 <sup>-3</sup>	4 × 10 <sup>-2</sup>	0.1
Resistance, ohms	7.5 × 10 <sup>4</sup>	2.2 × 10 <sup>4</sup>	6.2 × 10 <sup>3</sup>	2.1 × 10 <sup>3</sup>	3.0 × 10 <sup>2</sup>
Thermoelectric power, mv/°	0.85	0.80	0.82	0.78	0.74

Thus, treatment with hydrogen at 250-350°, or heating in vacuum at 350-450°, which lower the electrical conductivity by diminishing the stoichiometric excess of non-metal, bring about an increase in the thermoelectric power  $P \left( = \frac{\theta}{T_2 - T_1} \right)$ . This effect is clearly illustrated by experiments on Plate VIII, summarised in Table III. The SnS was first brought to a state of very low conductivity by reduction with hydrogen; it was then exposed at 113° to progressively increasing low pressures of air, and at each stage the conductivity and thermoelectric power were measured.

**Temperature Dependence of Thermoelectric Power.**—Data for several experimentally reliable series of measurements are summarised graphically

FIG. 2.  
Temperature dependence of thermoelectric power.



in Fig. 2 and 3. The salient points of these results can be summed up as follows.

<sup>18</sup> Fowler, *Statistical Mechanics* (Cambridge, 1936); § 11.81, p. 427.

1. Over a considerable range of temperature—from below room temperature up to  $300^{\circ}$  (experiments VIII. 1, IX. 6, IX. 7, Fig. 2) or even to  $420^{\circ}$  (IX. 4, Fig. 2) the thermoelectric power is quite independent of temperature. Comparison with the conductivity as measured simultaneously (uniformly linear course of the  $\log \kappa(T) - 1/T$  curve) shows that for each of these specimens only one mechanism of conduction appears to be operative over that temperature range for which the thermoelectric power is constant. Hence a satisfactory model for the semiconduction process must yield the result that thermoelectric power is independent of temperature for a single species of current carrier.

2. In all the experiments just considered, the specimens had a high electrical conductivity (cf. Table II). For specimens with a low conductivity, however, the thermoelectric power begins to diminish markedly at temperatures over  $250^{\circ}$  C. (cf. VIII. 4b, Fig. 2) becoming zero and ultimately changing sign at temperatures above  $350^{\circ}$  (cf. VIII. 2, VIII. 3,

Fig. 3). As Fig. 3 shows, the specimens for which this behaviour was found were those for which, because of their relatively small stoichiometric excess of sulphur (small concentration of positive holes), the conductivity curves at high temperatures showed a discontinuity in slope (at point A, Fig. 3, about  $310^{\circ}$ ). The process of higher excitation energy operative above this temperature we attributed in our previous paper to the intrinsic conduction of the stannous sulphide.

The sign of the thermo-e.m.f. is necessarily determined by the sign of the effective current carriers, so that the change of thermoelectric power above  $250^{\circ}$  can be taken as indicative of a progressively developing change in conduction mechanism. We were not able to extend measurements to temperatures where a constant negative value of the thermoelectric power was attained; the largest value recorded was  $-0.66$  mv./ $^{\circ}$  at  $427^{\circ}$ , with no indication of approach to a limiting value.

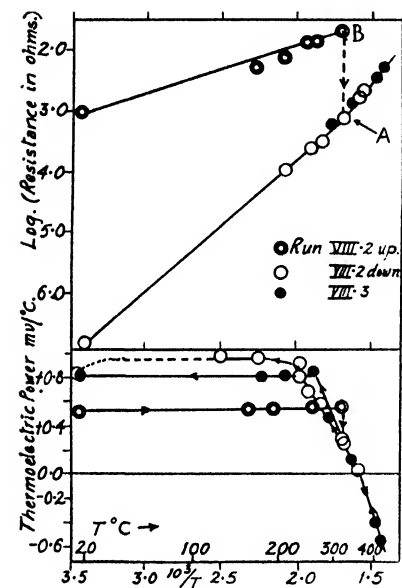


FIG. 3.—Thermoelectric effect on SnS.

That specimens of high conductivity (high concentration of positive holes; relatively large stoichiometric excess of sulphur) do not show a similar decrease in thermoelectric power over the range of temperature studied is quite consistent with their conductivity curves. These would display a discontinuity of slope only at much higher temperatures than were employed; in practice, such specimens cannot be heated to such temperatures in vacuum without change of stoichiometric composition. The influence of a stoichiometric excess of sulphur is particularly clearly shown in experiment VIII. 2 (Fig. 3). The specimen, initially well conducting, gave a very constant value for thermoelectric power  $= +0.56$  mv./ $^{\circ}$  up to  $318^{\circ}$  C., at which temperature hydrogen was admitted (point B, Fig. 3). The resistance rapidly rose from 48 ohms to 1330 ohms, and the thermoelectric power fell simultaneously to  $+0.28$  mv./ $^{\circ}$ , and was (above  $250^{\circ}$ ) strongly dependent upon temperature.

3. At low temperatures there is also a change in thermoelectric properties. "Reduced" specimens, with low conductivity (e.g., IV. 9,

VIII. 2, VIII. 4, Fig. 2) showed a distinct decrease in thermoelectric power at the ordinary temperature; in experiment IV. 9 the thermoelectric power fell practically to zero at  $-78^{\circ}$ . The high resistance of this plate (about 16 megohms at  $-78^{\circ}$ ) made accurate measurement impossible, and the absolute values of thermoelectric power for Plate IV are uncertain, as the final form of copper-constantan thermocouple had not been adopted; nevertheless, the relative values are significant.

With well-conducting specimens, change in thermoelectric power took place only at much lower temperatures (cf. IV. 11, IX. 1). Thus, in experiment IX. 1, a constant value ( $+0.54$  mv./ $^{\circ}$ ) was found down to  $-50^{\circ}$ , but a lower thermo-e.m.f. ( $+0.37$  mv./ $^{\circ}$ ) at liquid air temperature. It has already been stated that the conductivity curves show a discontinuity of slope at low temperatures, and it would appear that the conduction mechanism which then becomes operative is associated with a negative thermo-e.m.f.

### Discussion.

The existing state of the theory of semiconductors is such that, in our view, the most important requirement is to establish properly correlated facts. We may, however, briefly examine the results summarised above in relation to the theoretical treatment of the thermoelectric effect as it at present stands.

**1. The Mechanism of the Conduction Process.**—The sign of the thermoelectric effect up to  $250-400^{\circ}$  confirms the inference drawn previously that the impurity conduction of stannous sulphide was attributable to a stoichiometric excess of non-metal; properly sulphur, but on exposure to air, sulphur  $\rightarrow$  oxygen. The reversal of sign at high temperatures for specimens with small stoichiometric defect shows a transition to an electron conduction process, and it is reasonable to take this as confirming the view that at high temperatures the intrinsic conductivity of stannous sulphide is important. It may be recalled that Schottky and Waibel<sup>17</sup> observed an analogous behaviour with  $\text{Cu}_2\text{O}$ . This, due to a stoichiometric excess of oxygen, is also a positive hole conductor at the ordinary temperature, with positive Hall coefficient. Above  $600^{\circ}$  the sign of the Hall coefficient changes, indicating a change from positive hole to electron conduction.

In terms of the band theory, the number of bound electrons in the full band is so great compared with the number of empty impurity levels that at high temperatures the intrinsic electron conductivity completely outweighs the effect of the positive hole conduction. In the range of temperature actually investigated, we realise experimentally an interesting state envisaged by Fowler,<sup>18</sup> wherein the contributions of free electrons in the conductivity band and of free positive holes in the lower band are comparable, i.e. additive in effect on conductivity, opposed in the thermoelectric effect.

**2. The Magnitude of the Thermoelectric Effect.**—The most complete theoretical treatment of the electromotive force developed by a metal|semiconductor|metal couple is that of Mönch.<sup>9a, 4, \*</sup> He has pointed out that the observed thermo-e.m.f. is the resultant of two effects:  $\theta = V_v + V_b$ .  $V_v$  is a volume effect, determined by the difference in the concentration of free electrons at the two ends of the specimen between which the temperature difference is established.  $V_b$  is a boundary effect, and is itself the resultant of potentials set up at each of the junctions, due to the differences in absolute electron concentrations between metal and semiconductor. The discussion given by Fowler<sup>19</sup> amounts, in effect, to consideration of the volume effect  $V_v$  only. It is true that the dominant

<sup>17</sup> Schottky and Waibel, *Physik. Z.*, 1935, 36, 912.

<sup>18</sup> *Statistical Mechanics*, § 11.81, p. 427, case ii.

<sup>19</sup> *Ibid.*, §§ 11.78, 11.9.

term in Fowler's treatment may be the greatest contribution to the observed thermo-e.m.f., especially if the excitation energy  $E$  of the conduction process is large. Mönch's work has shown, however, that the boundary effect  $V_B$  can make up the larger part of the thermo-e.m.f. Moreover,  $V_V$  and  $V_B$  tend to vary in opposite directions as the concentration of conducting centres alters; the net result is the observed relatively slight dependence of thermoelectric effect upon conductivity (cf. Joffé<sup>11</sup>).

The volume effect in Mönch's treatment agrees with Fowler's expression for the total thermoelectric effect. Inserting values for the natural constants involved, and for junctions at  $T_1$ ,  $T_2$ ,

$$V_V \text{ (in millivolts/}^\circ\text{)} = 0.04 + \frac{2.30E}{T_2 - T_1} \log_{10} \left( \frac{T_2}{T_1} \right).$$

The boundary effect involves the absolute concentrations of electrons,  $n(T_1)$ ,  $n(T_2)$ . According to the Wilson-Fowler model,  $n(T)$  is related to the conductivity  $\kappa(T)$  and the mean free path  $l(T)$  of the electrons, and can be deduced from the Hall coefficient. Summing all the terms involved, and inserting numerical values for the natural constants, Mönch finds

$$\begin{aligned} V_B = & \frac{0.199}{T_2 - T_1} [15.69(T_2 - T_1) + 1.5(T_2 \log T_2 - T_1 \log T_1) \\ & + (T_1 \log 10^{10} \times T_1^{3/2}/3.84 l(T_1) - T_2 \log 10^{10} \times T_2^{3/2}/3.84 l(T_2) \\ & + (T_1 \log \kappa(T_1) - T_2 \log \kappa(T_2))]. \end{aligned}$$

For Mönch's discussion of  $\text{Cu}_2\text{O}$ , the Hall coefficients of certain specimens were available, and (making the assumption that  $l(T)$  was independent

TABLE IV  
 $T_1 = 300^\circ \text{K. } T_2 = 310^\circ \text{K. } l(T) = 10^{-8} \text{ cm.}$

Expt.	$\kappa(300^\circ)$	$E$	$V_V$	$V_B$	$V_V + V_B$	$P$ Obs.
VIII. 4a up	$3.2 \times 10^{-2}$	0.085	0.32	+0.19	0.51	0.63
IX. 1	$1.5 \times 10^{-2}$	0.14	0.50	-0.08	0.42	0.54
VIII. 1	$1.3 \times 10^{-2}$	0.16	0.56	+0.05	0.61	0.54
IX. 2	$2.7 \times 10^{-3}$	0.19	0.67	0.00	0.67	0.53
IX. 7	$1.1 \times 10^{-4}$	0.26	0.90	+0.03	0.93	0.65
VIII. 4b	$2.2 \times 10^{-2}$	0.43	1.47	-0.25	1.22	0.80

of the concentration of impurity centres) rather good agreement was obtained between observed and calculated values of  $V_V + V_B$ . As we pointed out in our previous paper, the conclusion is inescapable that  $l(T)$  does actually vary with the concentration of impurity centres, and the recent work of Maurer<sup>20</sup> on  $\text{CuI}$  has supplied quantitative confirmation of this conclusion. As a 10-fold change in  $l(T)$  makes about 0.2 mv./ $^\circ$  difference to the thermoelectric power, it is still possible to compare the experimental data at least qualitatively with Mönch's theory. The principal contribution to  $V_B$  is made by the last term of the above expression, involving both the conductivity and its temperature coefficient. Because  $E$  is systematically smaller for specimens of high conductivity, the interplay of the several factors concerned is such that (as can readily be verified by numerical calculation from Mönch's data and our own) the importance of  $V_B$  as compared with  $V_V$  increases with the conductivity of the specimen.

Table IV brings a comparison of our results for a few plates of varied conductivities with values calculated according to Mönch's relations; these are approximate in that a constant arbitrary value for  $l(T)$  has been

<sup>20</sup> Maurer, *J. Chem. Physics*, 1945, 13, 321.

used in the calculation ( $l(T) = 10^{-8}$  cm.; this should be of the right order of magnitude). However, the discrepancy between observed and calculated values is evidently not due to the uncertainty in  $l(T)$ , but is systematic, and increases as  $E$  increases. The term which is dominant in the discussions of both Fowler and Mönch for semiconductors of poor conductivity is in disagreement with the experimental facts.

The comparison in Table IV. relates to the thermoelectric power at room temperature. A further decisive test of the theoretical treatment is to be found in the temperature dependence of the thermo-e.m.f. The boundary effect  $V_B$  is but slightly dependent upon temperature, but  $V_V$  decreases with temperature (asymptotic to  $V_V = 0$ ), the slope being proportional to the magnitude of  $E$ ; hence the net effect is a decrease of  $V_V + V_B$  as temperature rises. In Fig. 2, dotted curves represent the calculated thermoelectric power for VIII. 4a and VIII. 4b respectively. It is evident that the observed constancy of thermoelectric power over a wide range of temperature is at variance with the theory. The disagreement is most apparent for semiconductors of low conductivity, for which the excitation energy  $E$  is high. If the results of Hochberg and Kvascha, for  $\text{Cu}_2\text{O}$ , are correct it would seem that the agreement found by Mönch between calculated and experimental values must be fortuitous; we hope shortly to be able to bring further evidence upon this point.

It would seem that the "impurity semiconductor" model requires a critical re-examination. Qualitatively, the model does bring together a number of properties of non-stoichiometric solids, but quantitatively it fails to account for (a) the dependence of the electronic mean free path upon concentration of impurity centres; (b) the dependence of the activation energy of the conduction process upon the concentration of impurity centres; and (c) the magnitude and temperature dependence of the thermoelectric effect.

### Summary.

1. A technique is described for investigating simultaneously the conductivity and the thermoelectric power of semiconductors over a wide range of temperature, under conditions which enable these properties to be correlated with the departure of the material from stoichiometric composition.

2. The thermoelectric effect of the couple  $\text{Au}|\text{SnS}|\text{Au}$  has been measured thereby over the range  $-80^\circ$  to  $+420^\circ$ , and correlated with the conductivity and the chemical history of the material. Decrease of excess of non-metal in the sulphide was associated with increase of thermoelectric power, but the latter is not simply related to the conductivity or to the activation energy of the conduction process.

3. Over the temperature range where a single conduction mechanism operates, the thermoelectric power is independent of temperature. At ordinary temperatures, the sign of the thermo-e.m.f. indicates positive hole conduction. At those temperatures and for those specimens for which intrinsic conduction is important, the thermo-e.m.f. changes its direction.

4. There appears to be a discrepancy between experimental results and predictions of the Fowler-Wilson semiconductor theory as regards both the magnitude and the temperature dependence of the thermoelectric effect.

### Résumé.

(1) On décrit une technique qui permet l'étude simultanée de la conductivité et de la sensibilité thermoélectrique des semi-conducteurs, dans un large domaine de température et dans des conditions telles qu'il est possible de relier ces propriétés à la différence entre la composition de la substance et la composition stoechiométrique.



(2) L'effet thermoélectrique du couple Au/SnS/Au a été ainsi mesuré dans le domaine de  $-80$  à  $+480^{\circ}\text{C.}$ , et relié à la conductivité et au passé chimique du métal. Si l'excès d'élément non métallique décroît, un accroissement de la sensibilité thermoélectrique lui est associé, mais celle-ci n'est pas une fonction simple de la conductivité ou de l'énergie d'activation de la conduction.

(3) Dans le domaine de conduction où un seul mécanisme de conduction opère, la sensibilité thermoélectrique ne dépend pas de la température. A des températures ordinaires, le signe de la force thermoelectromotrice indique une conduction de "trous positifs". Aux températures et avec les échantillons pour lesquels la conduction intrinsèque est importante, la force thermoelectromotrice change de direction.

(4) Il semble y avoir divergence entre les résultats expérimentaux et les prédictions de la théorie de Fowler-Wilson, au sujet des semi-conducteurs, en ce qui concerne l'ordre de grandeur de l'effet thermoélectrique et l'influence de la température sur celui-ci.

### Zusammenfassung.

(1) Eine Methode für die gleichzeitige Messung der Leitfähigkeit und der thermoelektrischen Kraft von Halbleitern, bei der diese Eigenschaften auf die Abweichungen des Materials von der stöchiometrischen Zusammensetzung bezogen werden können und die über ein ausgedehntes Temperaturbereich anwendbar ist, wird beschrieben.

(2) Die thermoelektrische Kraft des Thermoelements Au/SnS/Au wurde von  $-80^{\circ}\text{C.}$  bis  $420^{\circ}\text{C.}$  gemessen und mit der Leitfähigkeit und chemischen Vorgeschichte des Sulfids verglichen. Eine Abnahme des Überschusses an Nichtmetall im Sulfid war mit einer Zunahme der thermoelektrischen Kraft verbunden.

(3) In dem Temperaturbereich, in dem ein einziger Leitungsprozess stattfindet, ist die thermoelektrische Kraft von der Temperatur unabhängig. Bei gewöhnlicher Temperatur deutet das Vorzeichen der thermoelektrischen Kraft auf Leitung durch Wanderung von positiven Löchern hin.

(4) Die experimentellen Ergebnisse scheinen mit der Halbleitertheorie von Fowler und Wilson nicht im Einklang zu stehen.

University of Melbourne  
Carlton, N.3, Victoria.

## SEMI-CONDUCTING PROPERTIES OF LEAD SULPHIDE.

BY MERIAL C. MORTON.

Received 17th April, 1946.

The properties of most semiconductors are conditioned by deviations from stoichiometric composition on one side of the ideal formula, according to the rule of Friederich<sup>1</sup> and Meyer.<sup>2</sup> Stannous sulphide, for instance,<sup>3, 4</sup> normally has semiconducting properties due to the presence of an excess of sulphur. We obtained some evidence, however, that suitable treatment gives rise to a slight metal excess. Hintenberger<sup>5</sup>

<sup>1</sup> Friederich, *Z. Physik*, 1925, **31**, 813.

<sup>2</sup> Meyer, *ibid.*, 1933, **85**, 278.

<sup>3</sup> Anderson and Morton, *Proc. Roy. Soc., A*, 1945, **184**, 83.

<sup>4</sup> Anderson and Morton, *Trans. Faraday Soc.*, 1947 (preceding paper).

<sup>5</sup> Hintenberger, *Z. Physik*, 1942, **119**, 1.

has shown that PbS, which has properties similar to those of SnS, is a semiconductor in which marked deviations occur on both sides of the stoichiometric composition.

Most of the original measurements of the properties of PbS were carried out on natural galena or the fused sulphide, and showed a high conductivity, often with a negative temperature coefficient,<sup>6</sup> while measurements of such properties as the Hall effect<sup>7</sup> and rectifying action<sup>8, 9</sup> showed the current carriers to be positive in some instances and negative in others. Eisenmann<sup>10</sup> and Hintenberger<sup>6</sup> clarified the position with systematic investigations of the relation between the stoichiometric defect and the conductivity, Hall, and thermoelectric effects of synthetic lead sulphide. Hintenberger, using evaporated films, found a minimum conductivity which was increased on heating the film in vacuum (enhanced electron conduction) and also by exposure to increasing pressures of sulphur vapour (enhanced positive hole conduction). The thermoelectric and Hall effect measurements were made at room temperature only, on specimens whose conductivity was known only at that temperature.

In the experiments described in this paper simultaneous measurements of the conductivity and the thermoelectric effect were carried out over a wide range of temperature, on material whose composition was progressively changed. These measurements extend our study of the applicability of the general theory relating to the thermoelectric effect of semiconductors.<sup>4</sup>

It was possible to follow closely the actual change-over process from deficit to excess conduction, and to study the region in which both conduction processes are important.

### Experimental.

Measurements were made between  $-80^{\circ}$  and  $350^{\circ}$  c. using the apparatus designed for the work on SnS and described in the preceding communication.<sup>4</sup> Resistance measurements were by the probe method, and thermoelectric measurements were from the couple Au/PbS/Au.

Compressed powder plates were made from two different samples of PbS. It was first prepared by precipitation with pure  $\text{H}_2\text{S}$  gas, from a solution of A.R. lead acetate. The precipitate was washed many times by decantation, filtered, and dried at  $100^{\circ}$  c. under a reduced pressure of nitrogen. The black powder so obtained was used directly for Plate II. After sixteen runs Plate II developed a crack, was removed from the apparatus, crushed, and the powder pressed again into Plate IIb.

Portion of the original sample was completely sublimed by holding the bottom of a silica test tube containing the powder at  $840^{\circ}$  c. for  $1\frac{1}{2}$  hr. With continual pumping the pressure was kept at or below  $10^{-5}$  mm. Hg. The sublimate, a mass of small crystals adhering to the upper walls of the tube was scraped off and crushed. Plate III was made from this crystalline powder.

To estimate experimentally the amount of excess S held by the respective samples, a scrupulously cleaned Ag wire coil was sealed inside an evacuated tube containing the sulphide powder. It was held out of direct contact with the powder by a constriction in the tube. The quantity of S taken up by the Ag wire, after holding the tube at  $350^{\circ}$  c. for fifteen hours, was determined by weighing the Ag wire on a microbalance before and after the experiment. Results for the original precipitated material show that the Ag wire took up S corresponding to 0.013 g. atom of sulphur per g. atom of lead. Since the conductivity measurements

<sup>6</sup> Frey, *Z. Elektrochem.*, 1930, 36, 511.

<sup>7</sup> Heaps, *Phil. Mag.* [vii], 1928, 6, 1283.

<sup>8</sup> Schleede and Buggische, *Z. anorg. Chem.*, 1927, 161, 85.

<sup>9</sup> Luke, *Physik. Z.*, 1927, 26, 213.

<sup>10</sup> Eisenmann, *Ann. Physik*, [v], 1940, 38, 121.

show that, at 350° c. in vacuum, S is evaporated out, giving a Pb-rich material, we may estimate that the original stoichiometric S excess was of the order of 0.5 atom %.

The sublimed material gave up no S to the wire, even at 450°. This is to be expected, as the sublimate condensed on a surface at 400-500° and was held at that temperature in vacuum for about two hours; this treatment results in the production of a high electronic conductivity, i.e. of a stoichiometric lead excess.

**Procedure.**—After mounting each plate the apparatus was evacuated to  $10^{-6}$  mm. Hg, and conductivity and thermoelectric measurements were made up to that temperature at which a drift in conductivity with time (due to loss of S) could be detected. The S content of the plate was then decreased in steps by heating in vacuum to progressively higher temperatures. Resistance-temperature and thermo-e.m.f.-temperature characteristics were determined at each step from measurements made

below the temperature at which any drift was detectable. Any drift in the thermoelectric effect with change in composition could also be observed.

## Results.

**Conductivity Measurement.**—The results of conductivity measurements are summarised in Table I. On continued heating in vacuum the conductivity of the original material

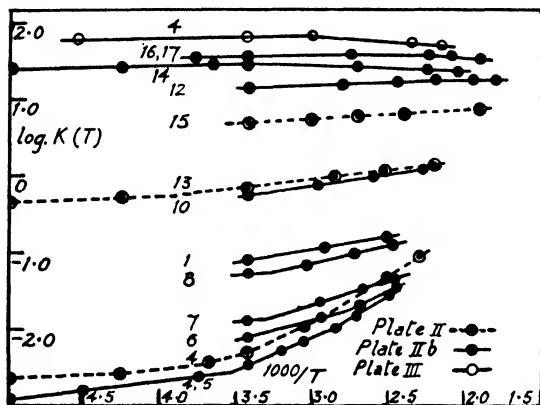


FIG. 1.—Temperature dependence of conductivity.

( $5 \times 10^{-2}$  ohm $^{-1}$  cm. $^{-1}$ ) decreases to a minimum value ( $3$  to  $5 \times 10^{-3}$  ohm $^{-1}$  cm. $^{-1}$ ) and then increases again. The maximum values obtained were 38 ohm $^{-1}$  cm. $^{-1}$  for Plate IIb (which was not increased by heating in oxygen-free hydrogen) and 83 ohm $^{-1}$  cm. $^{-1}$  for Plate III.

The relation  $\kappa(T) = A_1 e^{-E_1/kT}$  expressing the temperature dependence of the conductivity does not hold in every case. As the conductivity approaches the minimum value the slope of the  $\log \kappa - 1/T$  plots (see Fig. 1) falls off towards room temperature. The decrease in slope becomes apparent at progressively lower temperatures as the conductivity is raised by heat treatment. At the highest conductivities the plots are linear down to the lowest temperature measured.

Hintenberger determined the temperature dependence, between 20° and -180° c., of a specimen covering a range of compositions. His  $\log \kappa - 1/T$  plots are more noticeably curved for the higher conductivities.

The values of  $E_1$  and  $A_1$  shown in Table I are calculated from runs

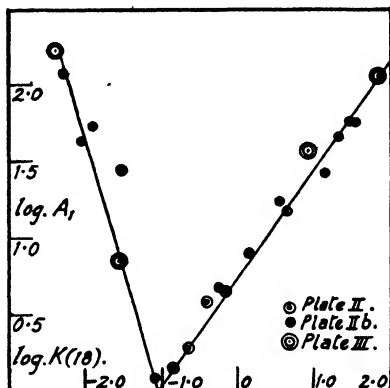


FIG. 2.

which have a linear  $\log \kappa - 1/T$  plot from room temperature up to the highest temperature at which the conductivity remains steady. The activation energy  $E_1$  decreases with increasing conductivity in the same way as is observed for practically all other semiconductors.<sup>11, 3</sup> For very high conductivities ( $\kappa > 10 \text{ ohm}^{-1} \text{ cm.}^{-1}$ ) the temperature coefficient is positive at low temperatures and becomes negative at elevated tem-

TABLE I

CONDUCTIVITY CHARACTERISTICS AND THERMOELECTRIC POWER OF LEAD SULPHIDE

Experiment.	Max. Temp. of Heating.	$\kappa(18^\circ) \text{ ohm}^{-1} \text{ cm.}^{-1}$	$P \text{ mv./}^\circ\text{C.}$	$E_1 \text{ ev.}$	$A_1$
II. 2 up down	185°	$5.2 \times 10^{-2}$ $9 \times 10^{-3}$	+0.42 -0.32	— —	— —
Exposed to atmosphere and re-evacuated.					
II. 3	170°	$3.3 \times 10^{-2}$	+0.38	0.17	29.0
II. 4	180°	$5.0 \times 10^{-3}$	+0.35	Not linear	
II. 5	135°	$2.1 \times 10^{-2}$	-0.27	Not linear	
II. 6	190°	$1.8 \times 10^{-2}$	-0.30	Not linear	
II. 7	135°	0.14	-0.26	0.058	1.4
II. 8	190°	0.105	—	Not linear	
II. 9	140°	0.135	-0.26	Not linear	
II. 10	190°	0.14	—	Not linear	
II. 11	210°	0.22	-0.26	0.063	1.9
II. 12	220°	0.39	-0.25	0.057	3.85
II. 13	235°	0.72	-0.25	0.046	4.5
II. 14	255°	1.4	-0.23	0.044	8.0
II. 15	275°	4.8	-0.22	0.028	14.5
IIb. 1	130°	$8.1 \times 10^{-2}$	+0.33	0.068	1.2
IIb. 2	115°	$1.3 \times 10^{-2}$	+0.48	0.21	52.5
IIb. 3	185°	$8.3 \times 10^{-3}$	+0.50	0.21	41.7
IIb. 4	130°	$3.7 \times 10^{-3}$	-0.15	Not linear : mixed conduction	
IIb. 5	150°	$3.7 \times 10^{-3}$	-0.24		
IIb. 6	180°	$6.3 \times 10^{-3}$	-0.26		
IIb. 7	185°	$1.3 \times 10^{-2}$	-0.27		
IIb. 8	185°	$5.5 \times 10^{-2}$	-0.25	0.08	1.5
IIb. 9	175°	0.10	-0.25	0.08	2.1
IIb. 10	230°	0.60	-0.22	0.052	4.8
IIb. 11	270°	3.5	-0.19	0.04	17.0
IIb. 12	310°	13.8	-0.17	0.016	26.3
IIb. 13	350°	20.4	-0.17	0.019	45.7
IIb. 14	425°	30.2	-0.16	0.016	57.6
IIb. 16	250°	38.0	-0.15	0.010	56.3
Exposed to air, then hydrogen admitted for run 17.					
IIb. 17 up	330°	$5.8 \times 10^{-3}$	+0.32	0.25	120
down	—	38	-0.22	0.01	56
III. 1	100°	$2.7 \times 10^{-3}$	-0.15	0.14	7.1
III. 2	210°	8.7	-0.19	0.036	36.5
III. 3	230°	69	-0.20	0.012	111
III. 4	340°	83	-0.22	Negative	

peratures. (See Fig. 1, runs IIb, 12 to IIb, 17); III, 4). As the conductivity increases the change takes place at successively lower temperatures and the negative temperature coefficient increases. This would occur if there is a mixed conduction process. The highest negative temperature coefficient measured is smaller than that which characterises metallic conduction.

<sup>11</sup> Gudden, *Ergeb. exakt. Naturwiss.*, 1934, 13, 222.

The values of  $A_1$  show a systematic trend. When  $\log A_1$  is plotted against  $\log \kappa$  ( $18^\circ$ ) the values for all plates fall on two intersecting straight lines, which correspond to the positive hole and the electron conduction processes respectively (see Fig. 2). For the S-rich specimens  $A_1$  increases with decreasing conductivity, while the values for the Pb-rich specimens (electron conduction) increase with increasing conductivity. Meyer<sup>12</sup> found a similar relation between  $A$  and  $\kappa$  in measurements carried out on  $\text{TiO}_2$ , a metal excess conductor.

**Thermoelectric Effect Measurements.**—The convention adopted for the sign of the thermo-e.m.f. is that the flow of electrons from semiconductor to metal at the hot junction is denoted as positive. This corresponds to "positive hole" conduction within the semiconductor, brought about by stoichiometric excess of non-metal (S or O), while a negative sign of the thermo-e.m.f. corresponds to electron conduction conditioned by a stoichiometric Pb excess. Temperature differences employed for the measurement of the effect were between  $10^\circ$  and  $30^\circ$  C. All figures presented have an accuracy of  $\pm 5\%$ .

The values of the thermoelectric power ( $P$ ) at room temperature are given in Table I with the conduction characteristics of the specimen. On heating in vacuum the positive thermo-e.m.f. of the original material changes to a negative value, showing how, by progressive evaporation, the original stoichiometric excess of non-metal is lost and a lead excess is produced. There is a certain correlation between the magnitude of the thermoelectric power and the conductivity. With decreasing conductivity the thermoelectric power increases. This is observed for decreasing sulphur excess (IIb, 1, 2, 3) as well as in the case of lead excess. In the region of minimum conductivity where both conduction mechanisms are important the observed effect is small since it is the resultant of two opposed processes.

**Effect of Oxygen.**—On exposing a Pb-rich specimen to air the conductivity decreases and the thermo-e.m.f. becomes positive again. The

TABLE II

Time after exposure (days)	0	$\frac{1}{4}$	4	$6\frac{1}{2}$	7	11	20	31
$P$ mv./°c.	-0.22	-0.25	( $-\frac{1}{2}$ ) ve °C.	+0.04	+0.10	+0.26	+0.35	+0.35
$\kappa$ ( $18^\circ$ ) ohm <sup>-1</sup> cm. <sup>-1</sup> .	38	—	1.7	0.66	0.60	0.48	0.45	0.45

rapidity with which the changes take place depend on the previous history of the specimen. First consider Plate II. At the end of run 2, during which Pb excess was attained for the first time, the thermoelectric power was  $-0.32$  mv./°c. On admission of air at room temperature the conductivity rose immediately; in  $1\frac{1}{2}$  minutes the thermo-e.m.f. was positive, and after four minutes had attained the constant value of  $+0.38$  mv./°c. This rapidity with which O may be built on to the crystal lattice, creating fresh positive holes, is exactly similar to the effect observed with  $\text{SnS}$ .<sup>3, 4</sup> The reaction with  $\text{O}_2$  is very much slower if the material has a large Pb excess due to prolonged vacuum treatment. On admission of air after run IIb, 5, the thermoelectric power remained constant ( $-0.22$  mv./°c) for half an hour. However, the plate was removed, powdered in air and pressed again to form IIb. The material then had a thermopower of  $+0.38$  mv./°c. The changes which took place on exposure of Plate IIb, after run 17 are summarised in Table II.

It will be noticed that all measurements for Plate III indicate electron

<sup>12</sup> Meyer, *Physik. Z.*, 1935, 36, 749.

conduction. The conditions of sublimation were discussed earlier, and it was pointed out that this material had a stoichiometric excess of Pb. Even after grinding in air this material did not take up sufficient O to create an excess of non-metal; but that some O was taken up is indicated by the low thermoelectric power of the original material (run 1) and the rapid increase of conductivity on heating to 180° C.

**Temperature Dependence of Thermoelectric Power.**—Data summarising the results of the thermoelectric measurements are collected in Fig. 3. For the sake of clarity the runs included are a typical selection from all reliable measurements. The corresponding conductivity data may be obtained from Table I and Fig. 1. There are two main features which appear.

1. In those cases where the nature of the conduction process is definite over the range of temperature employed (II. 1, 3, 8, 9, IIb. 17) the thermoelectric power ( $P$ ) is independent of temperature, for both the positive hole and the electron conduction processes.

At low temperatures (0 to  $-75^{\circ}$  C.)  $P$  decreases with decreasing temperature rather more rapidly (II. 1, IIb. 14, III. 3). The results are not sufficient to justify assumption of a change of conduction mechanism, although the conductivity curves also change in slope at sufficiently low temperatures. This behaviour is similar to that of SnS.<sup>4</sup>

2. The temperature variation of the thermoelectric power in the region of minimum conductivity is particularly interesting. The progressive change in composition as the non-metal-rich material is heated in vacuum may be followed—run IIb. 3. Runs 4 and 5 correspond to the minimum conductivity (see Fig. 1). In run 4 the electron mechanism preponderates at room temperature.

At 80° the thermopower is zero and above this temperature is positive. The conductivity curve increases in slope at this temperature. This behaviour would indicate that the energy required to raise electrons from the full band of the crystal to the "deficit" impurity levels is greater than that required for freeing the electrons of the "excess" (Pb) impurity levels. At 80° the opposed thermoelectric powers exactly neutralise each other.

Already in run 5 the number of electron "excess" centres has increased so that a higher temperature is reached before the positive hole mechanism takes over. The progressively increasing importance of the electron process, as non-metal is gradually removed, can be clearly followed in runs IIb. 6, 7, 8.

The mechanism of the conduction process advanced for lead sulphides of differing previous history, as deduced from the sign of the thermoe.m.f., is in agreement with such analytical evidence as is extant. Thus, an analysis of both fused and sublimed material<sup>8</sup> showed an excess of Pb, amounting to 0.3 atom-per cent. in the former case, and to 0.14 atom-per cent. in the latter. Frey<sup>8</sup> also found 0.08 atom-per cent. of excess Pb in a sample which had been fused in an atmosphere of  $H_2S$ . His material

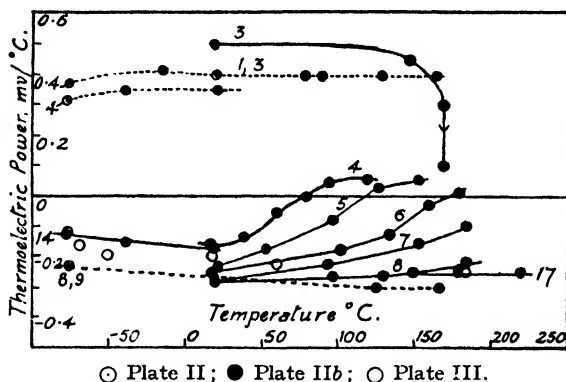


FIG. 3.—Temperature dependence of thermoelectric power.

## 200 SEMI-CONDUCTING PROPERTIES OF LEAD SULPHIDE

(like the Pb-richest specimens in this work) had a negative temperature coefficient of conductivity.

The general conclusions to be drawn from the thermoelectric measurements are similar to those arising from our work on stannous sulphide, as discussed in an accompanying paper.<sup>4</sup> As is pointed out there, the present theory is in disagreement with experiment as regards both the magnitude and—more significantly—the temperature variation of the thermoelectric power.

I am indebted to Dr. J. S. Anderson for much valuable discussion and advice during the course of this work.

### Summary.

1. The electrical conductivity and thermoelectrical power of pressed powder specimens of PbS were measured simultaneously over a wide range of temperature. The composition of the material was progressively changed by heating in vacuum.

2. With progressive change of composition, the conductivity decreased to a minimum value and then increased. The sign of the thermoelectric effect correspondingly changed from positive to negative as the original stoichiometric excess of non-metal was lost, and an excess of metal built up.

3. Thermo-e.m.f. measurements show that both "positive hole" and electron conduction mechanisms are operative in material of minimum conductivity. The temperature dependence of the thermo-e.m.f. in this region shows how, with removal of non-metal, the electron conduction mechanism becomes increasingly important.

4. As long as the conductivity is due to the operation of one predominating mechanism, the thermoelectric power is almost independent of temperature.

5. The activation energy of the conduction process is dependent upon the conductivity, as has been found for other semiconductors. Where conduction is mixed, the normal temperature dependence is not followed. Material of high conductivity has a negative temperature coefficient of conductivity.

6. The thermoelectric measurements do not fit into the present theory of impurity semiconductors.

### Résumé.

(1) On a mesuré simultanément pour des échantillons de poudre de PbS comprimé, la conductivité électrique et la sensibilité thermoélectrique. La composition du corps était modifiée par chauffage dans le vide.

(2) Un changement progressif de composition fait décroître la conductivité jusqu'à une valeur minimum, puis croître. Le signe de l'effet thermoélectrique passait, de façon correspondante, de positif à négatif, au fur et à mesure que l'excès d'élément non métallique par rapport à la composition stoechiométrique disparaissait et qu'un excès de métal apparaissait.

(3) Les mesures des forces thermoélectromotrices montrent que deux mécanismes opèrent dans le cas du minimum de conductivité: une conduction par électron et une par "trous positifs". L'influence de la température sur la force thermoélectromotrice dans cette région montre comment, par départ d'élément non métallique, le mécanisme de conduction par électron devient de plus en plus important.

(4) Tant que la conductivité est due à un mécanisme prédominant, la sensibilité thermoélectrique est presque indépendante de la température.

(5) L'énergie d'activation de conduction dépend de la conductivité, comme précédemment montre pour d'autres semi-conducteurs. Quand la conduction est le fait de deux mécanismes, l'influence de la température sur la sensibilité thermoélectrique n'est pas normale. Une substance de

haute conductivité a un coefficient de température négatif pour la conductivité.

(6) Les mesures thermoélectriques ne s'accordent pas avec la théorie actuelle des semi-conducteurs impurs.

### **Zusammenfassung.**

Die Leitfähigkeit und thermoelektrische Kraft von gepresstem, pulverisiertem PbS wurden gleichzeitig zwischen  $-80^{\circ}\text{C}$ . und  $350^{\circ}\text{C}$ . gemessen. Die Zusammensetzung des Stoffes wurde durch Erhitzen in einem Vakuum allmählich verändert, wobei die Leitfähigkeit bis zu einem Minimum abnahm, aber dann nach Verlust des stöchiometrischen Überschusses an Nichtmetall und bei Bildung eines Metallüberschusses wieder anwuchs. Messungen der thermoelektrischen Kraft zeigen an, dass in der Substanz mit Minimalleitfähigkeit sowohl Leitung durch Wanderung von „positiven Löchern“ als auch Elektronenleitung stattfindet. Die Aktivierungsenergie des Leitungsvorgangs hängt von der Leitfähigkeit ab. Im Bereich der gemischten Leitung wird die normale Temperaturabhängigkeit nicht angetroffen. Material hoher Leitfähigkeit besitzt einen negativen Temperaturkoeffizienten. Die thermoelektrischen Messungen stimmen nicht mit der gegenwärtigen Theorie der Verunreinigungs—Halbleiter überein.

*Chemistry Department,  
University of Melbourne,  
Australia.*

---

## **KINETIC STUDIES IN THE CHEMISTRY OF RUBBER AND RELATED MATERIALS.**

### **IV. THE INHIBITORY EFFECT OF HYDROQUINONE ON THE THERMAL OXIDATION OF ETHYL LINOLEATE.**

By J. L. BOLLAND AND P. TEN HAVE.\*

*Received 2nd May, 1946.*

The manner in which inhibitors interfere with various types of chemical chain reactions, such as oxidation and polymerisation, is a problem which has attracted effort on a scale commensurate with its technical importance. It is, however, fair to say that in no case has the precise chemical mechanism of inhibition yet been determined. Granted that oxidations proceed by chain-type reactions, nearly all of our present understanding of the nature of antioxidant action is due to Bäckström and his collaborators. The salient points established in a series of papers published in 1927-33 were that the inhibitor intervened by providing an alternative and very efficient mode by which the long oxidation chains could be terminated prematurely,<sup>1</sup> and further that in the process the inhibitor molecules themselves underwent oxidation.<sup>2</sup> Bäckström was, however, not in a position to identify the precise nature of the chemical reaction involved, since the chain mechanism of autoxidation (in absence of inhibitor) of the systems with which he was concerned, was then by no means established.

<sup>1</sup> Bäckström, *J. Amer. Chem. Soc.*, 1927, 49, 1460.

<sup>2</sup> Alyea and Bäckström, *J. Amer. Chem. Soc.*, 1929, 51, 90.

\* Seconded by The Netherlands Indies Govt. to the B.R.P.R.A.



Evidence of sufficiently diverse character—chemical,<sup>3</sup> kinetic,<sup>4, 5</sup> spectroscopic,<sup>6</sup> and thermochemical<sup>6</sup>—has been accumulated to establish the mechanism by which certain mono-olefins and 1-4 dienes react with molecular oxygen. As a first step in a programme of work on the mechanism of autoxidation, the effect of inhibitors on such oxidation systems has been investigated. In the present paper we describe in some detail the effect of addition of hydroquinone on the oxidation of ethyl linoleate; a succeeding paper (Part V of the series) considers the characteristics of other representative phenolic inhibitors, and allows us to identify the chemical reactions responsible for the antioxidant properties of this particular type of compound and to assess some of the factors which make for efficient inhibition of olefin oxidation.

### Experimental.

The experimental technique used in determining rates of oxidation was in general that already outlined.<sup>4</sup> It was, however, found convenient to use a flexible spiral constructed from 2 mm. Pyrex quill tubing as connection between reaction vessel and the gas burette system. The spiral could be immersed in the water thermostat heating the reaction vessel, but in practice sufficiently good thermostatic control was achieved by surrounding the spiral with a tissue paper envelope.

The inhibitor was introduced into the reaction vessel as a dilute solution in purified acetone, delivered from a micrometer syringe. The solvent was then evaporated off in a current of nitrogen and the ethyl linoleate and (where required) dibenzoyl peroxide weighed into the reaction vessel. It was in this way possible to introduce accurately amounts of inhibitor of  $10^{-3}$  % and upwards on a 0.2 g. sample of fatty ester.

The ethyl linoleate was obtained as before.<sup>4</sup> Samples which had been subjected to a two-fold molecular distillation at 68° C.,<sup>7</sup> were used in some experiments; in others (indicated by asterisks in Tables I and II) the linoleate used was further purified by chromatographic fractionation on an alumina column. Dibenzoyl peroxide was recrystallised three times from ether; the hydroquinone was a B.D.H. sample recrystallised three times from benzene under nitrogen before use.

When studying the uninhibited oxidation of ethyl linoleate it was found of real diagnostic value to compare the kinetic features of oxidation initiated in the first place by ethyl linoleate hydroperoxide (i.e. autoxidation) and in the second by dibenzoyl peroxide. For similar reasons we have here investigated the effect of addition of hydroquinone on both oxidation systems.

**(A) Effect of Hydroquinone on Dibenzoyl Peroxide Initiated Oxidation of Ethyl Linoleate.**—Suitable standard values of the various experimental variables were chosen: hydroquinone, dibenzoyl peroxide and ethyl linoleate concentrations  $1.4 \times 10^{-4}$ , 0.030 and 1.00 m. ole fatty ester, oxygen pressure 100 mm. and temperature 45° C. These five variables were altered in turn with the results detailed in Table I. The initial rate of oxidation was in each case determined from the smoothed experimental extent of oxidation — time curve by graphical extrapolation of its slope to zero extent of oxidation. Variation of ethyl linoleate concentration was obtained by dilution with carefully purified ethyl stearate.

$(Bz_2O_2)_0$  (Hq)<sub>0</sub> and (RH)<sub>0</sub> represent the initial concentrations (moles/mole fatty ester) of dibenzoyl peroxide, hydroquinone, and ethyl linoleate

<sup>3</sup> Bolland and Koch, *J. Chem. Soc.*, 1945, 445.

<sup>4</sup> Bolland, *Proc. Roy. Soc., A*, 1946, 186, 218.

<sup>5</sup> Bolland and Gee, *Trans. Faraday Soc.*, 1946, 42, 236.

<sup>6</sup> Bolland and Gee, *ibid.*, 1946, 42, 244.

<sup>7</sup> Farmer and Sutton, *J. Soc. Chem. Ind.*, 1946, 65, 164.

respectively and  $p_{O_2}$  the oxygen pressure. The initial rate of oxidation,  $(R_0)_0$  is given in moles  $O_2$ /mole linoleate/min.  $R_u$  represents the corresponding rate of oxidation in absence of inhibitor. The chain length ( $\nu$ ) of oxidation is calculated on the assumption (a) that each molecule

TABLE I

$\frac{[H_2O_2]}{[Bz_2O_2]}$ $\times 10^3$	$\frac{[Bz_2O_2]_0}{[Bz_2O_2]}$ $\times 10^4$	$[RH]_0$	$p_{O_2}$ (mm.)	Temp. (°C.)	$(R_0)_0$	$R_u$	$K$ $\times 10^3$	$K'$ $\times 10^3$	$\nu$
mole/mole ester)					(mole $O_2$ /mole ester/min. $\times 10^4$ )				

## (a) Standard experimental conditions.

1.40	3.0	1.00	100	45	0.059	2.23	1.65	1.65	6.1
nil	3.0	1.00	100	45	—	2.23	—	—	241

## (b) Variation of hydroquinone concentration.

0.154	2.67	1.00	100	45	0.50	2.11	1.73	1.73	63.0
0.286	2.76	1.00	100	45	0.262	2.15	1.63	1.63	31.6
0.776	3.26	1.00	100	45	0.128	2.32	1.84	1.84	13.0
2.97	3.50	1.00	100	45	0.036	2.40	1.95	1.95	3.8
5.46	3.32	1.00	100	45	0.018	2.34	1.80	1.80	1.8
9.05	3.18	1.00	100	45	0.010	2.29	1.72	1.72	1.1

## (c) Variation of dibenzoyl peroxide concentration.

1.53	0.75	1.00	100	45	0.0161	1.19	1.73	1.73	6.2
1.40	1.44	1.00	100	45	0.0324	1.59	1.79	1.79	6.8
1.46	6.18	1.00	100	45	0.110	3.13	1.64	1.64	6.7
2.60	7.30	1.00	100	45	0.074	3.39	1.79	1.79	3.7

## (d) Variation of ethyl linoleate concentration.

*1.30	2.94	0.175	100	45	0.0127	0.392	1.89	0.33	8.3
*1.40	3.28	0.110	100	45	0.0067	0.256	1.58	0.17	6.1

## (e) Variation of oxygen pressure.

1.47	3.02	1.00	30.0	45	0.050	2.24	1.09	5.0	5.6
1.48	3.18	1.00	7.5	45	0.048	2.27	1.40	18.0	5.1
1.67	3.31	1.00	3.5	45	0.045	2.34	1.38	39.4	4.5

## (f) Variation of temperature.

*0.60	2.86	1.00	100	52	0.400	4.06	1.50	1.50	17.0
0.66	1.03	1.00	100	52	0.140	2.52	1.46	1.46	1.7
0.72	2.91	1.00	100	52	0.342	4.09	1.49	1.49	14.2
*1.56	3.10	1.00	100	52	0.166	4.22	1.40	1.40	6.5
*0.60	3.15	1.00	100	38.2	0.0350	1.14	1.78	1.78	12.1
*0.60	3.00	1.00	100	38.2	0.0305	1.21	1.76	1.76	9.2

of dibenzoyl peroxide which decomposes results in the initiation of one oxidation chain and (b) that the unimolecular rate constants for the decomposition at 38, 45, and 52° C. are respectively  $1.10$ ,  $3.0$  and  $8.25 \times 10^{-8}$  min.

(b) Effect of Hydroquinone on the Autoxidation of Ethyl Linoleate. — Samples of ethyl linoleate were allowed to react with molecular oxygen at 45° C. until suitable extents of oxygen uptake were reached; the hydroperoxide content of these oxidised samples was based on volumetric measurements of the oxygen uptake, the final oxidation rate at the conclusion of the preparation, and iodometric determination of the peroxidic oxygen content.<sup>8</sup> These samples, stored *in vacuo* at 0° C., were used to

<sup>8</sup> Dastur and Lea, *Analyst*, 1941, 66, 90.

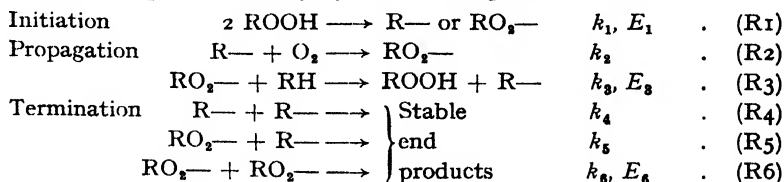
provide material for a series of oxidation runs, in presence of hydroquinone, in which the experimental conditions were systematically varied. Table II summarises the data so obtained.

TABLE II

$[Hq]_0$ $\times 10^4$	$[ROOH]_0$ $\times 10^3$	$[RH]_0$	$p_{O_2}$ (mm.)	Temp. (°C.)	$(R_s)_0$	$R_u$	$K$ $\times 10^3$	$K'$ $\times 10^3$	$\eta$
{(mole/mole ester)}					{(mole $O_2$ /mole ester/min. $\times 10^4$ )}				
nil	18.0	0.82	100	45	—	2.50	—	—	51
<b>(a) Variation of hydroquinone concentration.</b>									
1.22	18.1	0.819	100	45	0.181	2.52	2.84	2.33	3.7
1.40	18.1	0.819	100	45	0.155	2.52	2.80	2.30	3.2
*1.40	17.7	0.823	100	45	0.140	2.32	2.98	2.48	3.0
2.75	18.1	0.819	100	45	0.079	2.58	2.80	2.30	1.6
6.73	18.1	0.819	100	45	0.031	2.52	2.61	2.20	0.6
11.5	18.1	0.819	100	45	0.026	2.52	3.85	3.16	0.5
<b>(b) Variation of ethyl linoleate hydroperoxide concentration.</b>									
*0.28	2.55	0.975	100	55	0.173	1.15	3.56	3.46	5.0
*0.28	4.33	0.957	100	55	0.290	1.44	3.75	3.59	3.0
*2.70	0.9	0.910	100	55	0.106	2.87	3.17	2.88	2.0
*2.98	19.4	0.806	100	55	0.404	5.60	3.08	2.58	2.0
*3.12	27.4	0.726	100	55	0.550	6.9	2.65	1.92	1.5
<b>(c) Variation of ethyl linoleate concentration.</b>									
*0.28	6.3	0.350	100	45	0.052	0.26	2.60	0.91	8.3
*0.256	5.2	0.287	100	45	0.030	0.18	2.47	0.71	7.3
<b>(d) Variation of oxygen pressure.</b>									
1.50	18.1	0.819	725	45	0.150	2.52	2.90	0.33	3.1
1.40	18.1	0.819	100	45	0.157	2.52	2.84	2.32	3.3
1.60	18.1	0.819	11.0	45	0.125	2.52	2.58	19.0	2.6
<b>(e) Variation of temperature.</b>									
3.02	18.1	0.819	100	55	0.290	5.40	2.46	2.01	1.7
13.3	18.1	0.819	100	55	0.063	5.40	2.38	1.95	0.4
2.80	18.1	0.819	100	65	1.150	11.0	2.17	1.78	2.1
12.1	18.1	0.819	100	65	0.250	11.0	2.06	1.69	0.5

### Kinetic Analysis.

**Oxidation Mechanism in Presence of Hydroquinone.**—In absence of hydroquinone the oxidation of ethyl linoleate by molecular oxygen has been shown <sup>4</sup> to proceed mainly by the following chain mechanism :



where R refers to the linoleate residue obtained by removal of an  $\alpha$ -methylenic hydrogen atom, and the radical nature of the chain carriers is indicated by a dash ; the reaction velocity coefficients and activation

energies of the several elementary reactions, (R1)-(R6), are denoted by the symbols  $k$  and  $E$ . Reaction (R1) represents chain initiation by thermal decomposition of ethyl linoleate hydroperoxide, which forms the sole oxidation product; the exact manner in which the initial chain carrier arises cannot as yet be formulated, but it is known that the decomposition is a second order reaction. In addition we may distinguish two additional ways in which oxidation chains may be initiated: the first, which is only of prime importance in the initial stages of autoxidation involves direct interaction between oxygen and ethyl linoleate<sup>5</sup>



the second arises from the presence of traces of free (linoleic) acid which normally contaminate samples of ethyl linoleate prepared as above, even after molecular distillation, and which interact with linoleate hydroperoxide molecules. Removal of this free acid may be accomplished by chromatographing the linoleate through alumina; consistent results are obtained for both chromatographed and unchromatographed samples, when the data are treated as follows.

The rate of autoxidation of ethyl linoleate at high oxygen pressures ( $R_u$ ) may be expressed as follows, if it is assumed that all three types of initiators lead to identical propagation and termination mechanisms:

$$R_u = R_1 \frac{1}{\sqrt{k_6}} \cdot [\text{RH}] \quad . \quad . \quad . \quad (\text{I})$$

where  $R_1$  is the total rate of chain initiation; here

$$R_1 = \alpha_1 k_1 [\text{ROOH}]^2 + \alpha_2 k_2 [\text{O}_2][\text{RH}] + f([\text{acid}][\text{ROOH}])$$

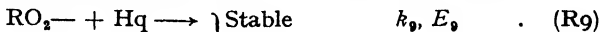
$\alpha_1$  and  $\alpha_2$  represent respectively the number of oxidation chains actually initiated by the decomposition of one molecule of peroxide and the interaction of one molecule of oxygen and RH. Similarly in the case of the oxidation in presence of dibenzoyl peroxide the initiation steps are (R8) and



The appropriate expression for  $R_1$  may be written

$$R_1 = \alpha_7 k_7 [\text{Bz}_2\text{O}_2] + \alpha_8 k_8 [\text{O}_2][\text{RH}].$$

On the basis of Bäckström's work, it is to be anticipated that in the presence of hydroquinone in sufficient quantity the normal chain termination reactions, (R4)-(R6) would be completely replaced by the two reactions, involving hydroquinone and either of the two chain carriers:



Assuming that the initiation and propagation reactions remain as indicated above and that termination occurs exclusively by reactions (R9) and (R10) the precise form of the expressions for the rate of oxidation derived by normal stationary state methods depends on whether the chain carrier produced in the first instance by the initiation process is  $\text{R} \cdot$  or  $\text{RO}_2 \cdot$ . If this is, in fact,  $\text{RO}_2 \cdot$

$$-\frac{d[\text{O}_2]}{dt} = R_s = R_1 \frac{k_2[\text{RH}]}{[\text{Hq}]} \cdot \frac{k_2[\text{O}_2]}{k_2 k_9 [\text{O}_2] + k_3 k_{10} [\text{RH}] + k_3 k_{10} [\text{Hq}]} \quad (2)$$

$$= R_u \frac{k_6}{k_3 [\text{RH}][\text{Hq}]} \cdot \frac{k_2[\text{O}_2]}{k_2 k_9 [\text{O}_2] + k_3 k_{10} [\text{RH}] + k_3 k_{10} [\text{Hq}]} \quad (3)$$

If, however, the initial chain carrier is  $\text{R} \cdot$ , an additional factor

$$(1 + k_9 [\text{Hq}]/k_3 [\text{RH}])$$

must be introduced into (2) and (3). Since (see below)  $k_3 [\text{RH}]/k_9 [\text{Hq}] \sim \nu$ , this difference is only of importance when the inhibitor concentration is

sufficiently high to reduce the chain length to small proportions. In this region measurements of the rate of oxygen uptake are of doubtful significance, since the production of  $\text{CO}_2$  (especially if dibenzoyl peroxide is present) water and other volatile products is certainly comparable with the oxygen absorbed; moreover it is known that high inhibitor concentrations have a marked accelerating influence on the decomposition of ethyl linoleate hydroperoxide, thus introducing uncertainty as to the true value of  $R_1$ . No attempt is made here to examine these aspects of the reaction; since it is therefore not possible to decide between  $\text{R}-$  and  $\text{RO}_2-$  as the initial chain carrier, the latter is chosen for the sake of simplicity.

Two limiting cases of (3) may be noted:

(a) if  $k_9 \gg k_{10}$ , so that the only important termination reaction is  $\text{RO}_2- + \text{Hq}$ ,

$$R_a = R_u^2 \cdot \frac{k_8}{k_9 k_{10}} \cdot \frac{1}{[\text{RH}][\text{Hq}]} \quad (4)$$

(b) if  $k_{10} \gg k_9$ , so that the only important termination reaction is  $\text{R}- + \text{Hq}$ ,

$$R_a = R_u^2 \cdot \frac{k_8 k_2}{k_9^2 k_{10}} \cdot \frac{[\text{O}_2]}{[\text{RH}]^2 [\text{Hq}]} \quad (5)$$

From (4) and (5) constants  $K$  and  $K'$  may be defined:

$$K = \frac{k_8}{k_9 k_{10}} = \frac{R_a}{R_u^2} \cdot [\text{Hq}] \cdot [\text{RH}], \quad (6)$$

and 
$$K' = \frac{k_8 \cdot k_2}{k_9^2 \cdot k_{10}} \cdot [\text{O}_2]_{100 \text{ mm.}} = \frac{R_a}{R_u^2} \cdot \frac{100}{p_{\text{O}_2}} \cdot [\text{Hq}][\text{RH}]^2 \quad (7)$$

where  $(\text{O}_2)_{100 \text{ mm.}}$  is the solubility of  $\text{O}_2$  in ethyl linoleate at 100 mm. pressure. Values of  $K$  and  $K'$  based on data for initial rates of oxidation are included in Tables I and II. The constancy of  $K$  over these ranges of  $[\text{Hq}]_0$ ,  $p_{\text{O}_2}$ ,  $[\text{RH}]_0$  and  $R_u$  shows that equation (4) correctly describes the kinetic characteristics of the oxidation of ethyl linoleate in presence of hydroquinone and initiated by either dibenzoyl peroxide or linoleate hydroperoxide. In contrast, the variation of  $K'$  with change in  $p_{\text{O}_2}$  and  $[\text{RH}]$  is obvious. The conclusion therefore is that hydroquinone interferes in the oxidation in one way only, namely by removing the chain carrier  $\text{RO}_2-$  from the system. The chemical nature of the reaction is considered in a subsequent paper.<sup>9</sup>

**The Energy of Activation of the Termination Reaction.**—It is not possible from the above analysis to determine the energy of activation of the interaction between hydroquinone and the chain carrier,  $\text{RO}_2-$ ; it may, however, be estimated relative to that of the chain propagation reaction ( $R_3$ ). From equation (6)

$$E_k = E_8 - E_9 - E_9$$

where  $E_k$  is the apparent energy of activation corresponding to the temperature coefficient of the constant,  $K$ . Introducing the relation already found to hold for the uninhibited autoxidation of ethyl linoleate, that  $2E_3 = E_8 + 8.4$  kcal./mole.

$$E_k = E_3 - E_9 - 8.4 \text{ kcal./mole.}$$

The values of  $K$  in Table I and Table II agree in indicating a value of 3 kcal./mole. for  $E_k$ . Hence  $E_8 - E_9$  is estimated to be 5.4 kcal./mole.

Introducing the condition, which has now been justified experimentally, that  $k_9 \gg k_{10}$  into equation (2)

$$\nu = k_8[\text{RH}]/k_9[\text{Hq}].$$

Making use of the estimated values of  $\nu$  collected in Table I the mean value

<sup>9</sup> Bolland and ten Have, *Trans. Faraday Soc.* (in press).

of  $k_9/k_8$  at 45° c. is found to be 1,200; the corresponding value from Table II is 1,800. These figures, taken in conjunction with the experimental value for  $E_8 - E_9$ , suggest that the frequency factor of the reaction (R<sub>3</sub>) is 5.6 times greater (at 45° c.) than that of the reaction (R<sub>9</sub>). This calculation is to be interpreted as confirming the reliability of the above estimate for  $E_8 - E_9$ , since it would be expected from the close formal similarity of reactions (R<sub>3</sub>) and (R<sub>9</sub>) that their frequency factors would be of the same order.

### Fate of Inhibitor Molecules.

As oxidation of ethyl linoleate proceeds in presence of hydroquinone, the rate of oxygen uptake increases in the manner shown in Fig. 1, until ultimately it attains an almost constant value. Apparently therefore hydroquinone is removed from the system during oxidation and the supposition that it is converted to benzoquinone is certainly supported by the yellow coloration assumed by samples of ethyl linoleate oxidising in presence of relatively large amounts of hydroquinone. It is apparent from Fig. 1 that the rate of oxidation to which each curve tends, is less than the corresponding uninhibited rate,  $R_u$ , and furthermore that it diminishes with increase in the initial hydroquinone concentration. This behaviour suggests that the product arising from hydroquinone itself possesses weak inhibitory properties, and is therefore not inconsistent with the formation of benzoquinone.<sup>10</sup> This aspect of the oxidation will not, however, be pursued further here; it is, however, our purpose to present two lines of kinetic evidence which point in quantitative fashion to the destruction of hydroquinone during the chain termination process.

If it is supposed that each hydroquinone molecule is capable of terminating  $n$  oxidation chains before being converted to its final product

$$-\frac{d[\text{Hq}]}{dt} = \frac{R_1}{n} \quad (8)$$

Now, from equations (2), (4) and (8)

$$\frac{d[\text{O}_2]}{d[\text{Hq}]} = -\frac{d[\text{ROOH}]}{d[\text{Hq}]} = n \frac{k_8[\text{RH}]}{k_9[\text{Hq}]} \quad (9)$$

Integration of (9) gives

$$\ln [\text{Hq}]_0 - \ln [\text{Hq}] = \frac{k_8}{nk_9} \frac{[\text{ROOH}] - [\text{ROOH}]_0}{[\text{RH}]} \quad (10)^*$$

<sup>10</sup> Calkins and Mattill, *J. Amer. Chem. Soc.*, 1944, 66, 239.

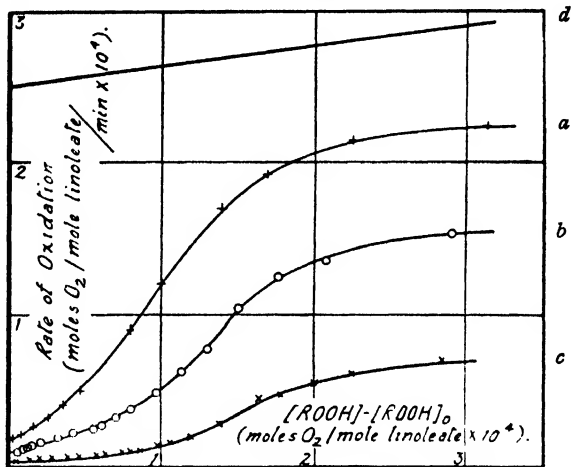


FIG. 1.—Oxidation of ethyl linoleate in presence of hydroquinone.  $[\text{Hq}]_0$  is (a)  $1.22 \times 10^{-4}$ , (b)  $2.75 \times 10^{-4}$ , (c)  $6.73 \times 10^{-4}$  moles/mole linoleate and (d)  $[\text{ROOH}]_0$  is 0.181 moles/mole linoleate.

$$\text{or} \quad \ln R_s = \ln (R_s)_0 + \frac{1}{n} \cdot \frac{k_9}{k_3[RH]} \cdot [\text{ROOH}] - [\text{ROOH}]_0 \quad (11)$$

where  $(R_s)_0$  and  $R_s$  are respectively the initial and current rates of oxidation.

The approximation is made in (10) that  $[RH]$  remains constant and in (11) that the rate of chain initiation remains constant. Both approximations are in fact justified since over the limited extent of oxidation required to remove the small amounts of hydroquinone used in the present experiments the changes in  $[RH]$  and  $R_i$  were always less than 1 % and 10 % respectively.

In Fig. 2 the applicability of equation (11) is tested in the case of three experiments, in which the initial hydroquinone concentration is varied. Certainly in the earlier stages, the linearity of these three curves is satisfactory; deviations occur during the later phases of such runs and are

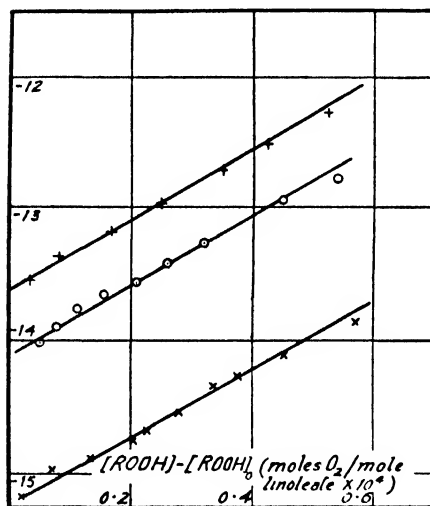


FIG. 2.

to be expected since the equation (11) holds only so long as the termination occurs solely by reaction (R<sub>9</sub>); thus when the rate of oxidation reaches one-third of the uninhibited value at least 10 % of the chains should be terminated by the alternative reaction  $\text{RO}_2^- + \text{RO}_2^-$ , (R<sub>6</sub>). Moreover the additional complication of the antioxidant activity of the final product from hydroquinone has to be reckoned with. A further respect in which these curves conform to the requirements of equation (11) lies in the substantial independence of slope on antioxidant concentration.

The factor  $n$  cannot be evaluated from the slope of curves in Fig. 2. The ratio  $n/\alpha$  may, however, be determined, since at the peroxide concentrations here concerned

$$\text{Slope} = \frac{k_9}{n k_3[RH]} = \frac{\alpha}{n} \cdot \frac{R_D}{(R_s)_0} \cdot \frac{1}{[Hq]} \quad (12)$$

where  $R_D$  is the rate of decomposition of peroxide (as measured *in vacuo*, and equal to  $k_7[\text{Bz}_2\text{O}_2]$  or  $k_1[\text{ROOH}]^2$  according to whether the chain initiator is dibenzoyl peroxide<sup>11</sup> or linoleate hydroperoxide<sup>4</sup>). Values for the slope of a series of  $\ln R_s/[\text{ROOH}] - [\text{ROOH}]_0$  curves are collected in Table III, together with the corresponding figures for  $n/\alpha$ .

In the first place it is apparent that  $\alpha/n$  is unaffected by considerable changes in the experimental conditions of oxidation. This provides strong evidence that the hydroquinone is destroyed in the course of the chain termination process and not by concurrent direct oxidation by peroxide or oxygen.

In these circumstances the divergence between the  $\alpha/n$  values for the dibenzoyl peroxide and linoleate hydroperoxide initiated oxidations must be ascribed to different  $\alpha$  values ( $\alpha_7$  and  $\alpha_1$  respectively) for the decomposition of these two peroxides.  $\alpha_7/\alpha_1$  then becomes 5.0; giving  $n$  its most probable figure of two,  $\alpha_7$  and  $\alpha_1$  assume values of 1.0 and 0.2 re-

<sup>11</sup> McClure, Robertson and Cuthbertson, *Can. J. Research, B*, 1942, **20**, 103.

spectively. The former figure appears eminently reasonable; the latter on the other hand is quite consistent with two features of our earlier results which have at first sight appeared to suggest that the oxidation mechanisms of the oxidations initiated by dibenzoyl peroxide and ethyl linoleate hydroperoxide are not wholly identical. Thus in comparing the rates of oxidation (in absence of inhibitor at 45° c.) of ethyl linoleate when the concentrations of these two peroxides were adjusted to give equal rates of peroxide decomposition, it was found that oxidation in presence of dibenzoyl peroxide was about 2.2 times the faster. The difference may be explained in terms of different  $\alpha$  values for the two peroxides provided  $\alpha_2/\alpha_1 = (2.2)^2 = 4.8$ . Furthermore the numerical values for  $K$  found in Table I and in Table II came to be of the same order, only because the assumption on which they were based was that

TABLE III

[Peroxide] <sub>0</sub>	[Hq] <sub>0</sub>	$p_{O_2}$	Temp.	Slope.	$n/\alpha$
(moles/mole ester) × 10 <sup>4</sup>	× 10 <sup>4</sup>	(mm.)	(°c.)		
<b>(a) Dibenzoyl peroxide initiated oxidation.</b>					
7.30	2.60	100	45	0.69	1.5
6.18	1.46	100	45	0.46	2.1
2.84	1.34	100	45	0.55	2.1
3.26	0.776	100	45	0.46	2.1
2.76	0.286	100	45	0.46	2.8
3.02	1.47	30	45	0.69	1.8
3.18	1.48	7.5	45	0.74	1.8
3.10	0.150	100	52	0.41	2.3
2.86	0.616	100	52	0.46	2.0
1.03	0.660	100	52	0.40	2.1
<b>(b) Ethyl linoleate hydroperoxide initiated oxidation.</b>					
18.1	6.73	100	45	0.27	9.3
18.1	2.75	100	45	0.26	8.7
17.7	1.40	100	45	0.21	11.3
18.1	1.22	100	45	0.26	8.7
18.1	1.50	725	45	0.21	10.1
27.4	3.12	100	55	0.17	12.5
18.1	3.02	100	55	0.19	10.4
4.33	0.280	100	55	0.11	10.9

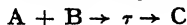
$R_1 = \text{const. } R_u^2$ , where the constant was supposed to be independent of the nature of the initiating peroxide. If, however, conditions under which the decomposition of linoleate hydroperoxide or dibenzoyl peroxide represents the major mode of chain initiation, are considered, and  $R_1$  is equated to the rate of peroxide decomposition,  $K$  becomes on the average about 3.2 times smaller for the ethyl linoleate hydroperoxide initiated oxidation runs, than for the corresponding runs with dibenzoyl peroxide. Again the discrepancy is explicable if  $\alpha_2/\alpha_1 = 3.2$ . The explanation of this variation in  $\alpha$  from peroxide to peroxide must be intimately connected with the question of the precise mechanisms by which the thermal decomposition of peroxides occurs. As yet, insufficient evidence is available to provide a final solution to this problem.

The authors are greatly indebted to Dr. G. Gee for much helpful advice and criticism during the progress of the work, which forms part of the programme of fundamental research undertaken by the Board of the British Rubber Producers' Research Association.





that for the initial state of the reaction system. For association reactions



it has been shown that the configuration of the transition state  $\tau$  is very close to that of the final state C and hence

$$f_\tau = f'(t) \cdot f'(\nu) \cdot \prod_{3N-7} f'(v), \quad f_c = f(t) \cdot f(\nu) \prod_{3N-7} f(v) \\ f'(t) = f(t), \quad f'(\nu) \simeq f(\nu) \quad \text{and} \quad f'(v) \simeq f(v)$$

in which the primed factors refer to the translational, rotational and vibrational contributions to the partition function of the transition state and the unprimed terms to the corresponding terms of the final state of the system.

Equation (1) can be written

$$k = \frac{kT}{h} e^{\frac{\Delta S^*}{R}} \cdot e^{-\frac{\Delta H^*}{RT}}$$

in which the changes in heat content  $\Delta H^*$  and in entropy content  $\Delta S^*$  between the initial and transition state are given by :

$$\Delta H^* = RT^2 \frac{\partial}{\partial T} \log \frac{f_\tau}{f_i} e^{\frac{\epsilon_\tau}{kT}} \\ \Delta S^* = R \log \frac{f_\tau}{f_i} e^{\frac{\epsilon_\tau}{kT}} + RT \frac{\partial}{\partial T} \log \frac{f_\tau}{f_i} e^{-\frac{\epsilon_\tau}{kT}} \\ = R \log \frac{f_\tau}{f_i} + RT \frac{\partial}{\partial T} \log \frac{f_\tau}{f_i}.$$

The fact that, for association reactions, the terms in  $f_\tau$  are closely similar to those of the final state of the system means that an investigation of the entropy changes accompanying the formation of the *final* state of chain propagation and termination reactions will help in understanding the entropy changes accompanying the formation of the corresponding transition states, and hence the temperature independent factors of  $k_p$  and  $k_t$ .

## The Entropy Changes Accompanying the Formation of the Transition States of Polymerisation Steps.

### (a) In Solution.

Many expressions have been developed for the partition functions of long chain molecules in solution.<sup>8</sup> Here we shall use one of the form :

$$F = f_0^{n_0} \cdot f_1^N \cdot \frac{1}{\sigma^{2n_x}} \cdot \frac{(n_0 + N)!}{n_0! \Pi n_x!} \left( \frac{\gamma}{n_0 + N} \right)^{\Sigma(x-1)n_x} \quad (2)$$

in which  $n_0$  is the number of solvent molecules,  $N = \Sigma x n_x$  where  $n_x$  is the number of molecules of chain length  $x$ ,  $\sigma$  is the symmetry number of the units of solute molecules and  $f_0$  and  $f_1$  are the partition functions for the motions of the solvent molecules and of each unit of the polymer chain respectively, in the free volume of the solution and  $\gamma$  is the co-ordination number of the space lattice.  $f_0^{n_0}$  and  $f_1^N$  are important terms because the final results of this treatment depend upon their particular form. The model upon which equation (2) is based is that of an array of centres of both solvent molecules and units of the polymer chain. Every centre, solvent molecule or polymer unit is able to oscillate about its quasi-lattice point in the system. The motion of each centre is described by<sup>9</sup>

<sup>8</sup> Huggins, *J. Physic. Chem.*, 1942, 46, 151; *Ann. N.Y. Acad. Sci.*, 1942, 43, 1; *J. Amer. Chem. Soc.*, 1942, 64, 1712. Flory, *J. Chem. Physics*, 1942, 10, 51; 1944, 12, 425. Tobolsky and Blatz, *ibid.*, 1945, 13, 379.

## 212 VELOCITY CONSTANTS IN POLYMERISATION REACTIONS

the partition function  $f_0$  if it is a solvent molecule, and  $f_1$  if it is a free monomer unit or one in a polymer chain. The whole system of centres can be arranged in

$$\frac{1}{\sigma^{\Sigma n_x}} \cdot \frac{(n_0 + N)!}{n_0! \Pi n_x!} \left( \frac{\gamma}{n_0 + N} \right)^{\Sigma(x-1)n_x}$$

distinguishable configurations.

Equation (2) makes no distinction therefore between the behaviour of a free monomer unit and a monomer unit in a polymer chain. We consider that a monomer unit in a free state will have a different type of motion and hence a different partition function from a monomer unit incorporated in the polymer chain, although as far as occupying lattice sites is concerned, they will both be equivalent. Because of this difference in behaviour we modify equation (2) to

$$F = f_0^{n_0} \cdot f_m^{n - \Sigma' x n_x} \cdot f_p^{\Sigma' x n_x} \cdot \frac{(n_0 + N)!}{n_0! \Pi n_x!} \left( \frac{\gamma}{n_0 + N} \right)^{\Sigma(x-1)n_x} \cdot \frac{1}{\sigma^{\Sigma n_x}} \quad (3)$$

where  $f_m$  is the partition function of free monomer units and  $f_p$  of monomer units in the polymer chain. The summation  $\Sigma'$  is taken over all values of  $x$  except  $x = 1$ , i.e. excluding monomer molecules.

This is clearly a very approximate attempt to differentiate between the behaviour of monomer molecules in a free state and in the polymer, but we believe that it describes the system sufficiently well to enable conclusions to be drawn in the present problem. Strictly separate partition functions should appear in the expression for dimers and trimers, etc., but we single out the free monomer unit because its behaviour will be most different from that of a unit in a long polymer chain.

Equation (3) reduces to the correct form for an ideal solution of monomer molecules and solvent viz.:

$$F = f_0^{n_0} \cdot f_m^{\frac{(n_0 + N)!}{n_0! N!}}$$

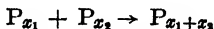
The chemical potential  $\mu_x$  and the molal entropy  $S_x$  of the  $x$ -mer species are given by the equations:

$$\begin{aligned} \mu_x/RT &= 1 - x \log \frac{f_p}{\sigma} - (x-1) \log \gamma \sigma + \log \frac{n_x}{n_0 + \Sigma x n_x} - \frac{x(n_0 + \Sigma n_x)}{n_0 - \Sigma x n_x} \\ - S_x/R &= 1 - x \log \frac{f_p}{\sigma} - (x-1) \log \gamma + \log \frac{n_x}{n_0 + \Sigma x n_x} \\ &\quad - \frac{x(n_0 + \Sigma n_x)}{n_0 + \Sigma x n_x} - T x \frac{\partial \log f_p}{\partial T} \end{aligned}$$

The corresponding terms for monomer molecules are:

$$\begin{aligned} \mu_M/RT &= 1 - \log \frac{f_M}{\sigma} + \log \frac{n_M}{n_0 + \Sigma x n_x} - \frac{n_0 + \Sigma n_x}{n_0 + \Sigma x n_x} \\ - S_M/R &= 1 - \log \frac{f_M}{\sigma} + \log \frac{n_M}{n_0 + \Sigma x n_x} - \frac{n_0 + \Sigma n_x}{n_0 + \Sigma x n_x} - T \frac{\partial \log f_M}{\partial T} \end{aligned}$$

For the reaction



in which two growing polymer chains of lengths  $x_1$  and  $x_2$  respectively combine to give a product of length  $(x_1 + x_2)$ , the change in molal entropy is:

$$\begin{aligned} \Delta S/R &= \frac{S_{x_1+x_2} - S_{x_1} - S_{x_2}}{R} = 1 - \log \gamma \sigma + \log \frac{n_{x_1}}{n_0 + \Sigma x n_x} \\ &\quad + \log \frac{n_{x_2}}{n_0 + \Sigma x n_x} - \log \frac{n_{x_1+x_2}}{n_0 + \Sigma x n_x} \\ &= 1 - \log \gamma \sigma - \log \frac{c_{x_1+x_2}}{c_{x_1} \cdot c_{x_2}} \end{aligned}$$

where  $c_{x_1}$  and  $c_{x_2}$  and  $c_{x_1+x_2}$  are the concentrations of  $x_1$  and  $x_2$  and  $(x_1+x_2)$

species expressed as number of moles/total number of moles of monomer units in the reaction mixture.

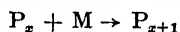
If we set  $c_{x_1+x_2}$  as the number concentration of the transition state then

$$k_t = \frac{kT}{h} \cdot e^{\frac{\Delta S_0^*}{R}} \cdot e^{-\frac{\Delta H^*}{RT}}$$

in which  $\Delta S_0^*$ , the standard entropy change, is equal to  $(1 - \log \sigma \gamma)$  and  $k_t$  is expressed in units of (moles/total number of moles of monomer units) $^{-1}$  sec. $^{-1}$ . Thus the temperature independent factor for the mutual termination  $A_t = \frac{kT}{h} e^{(1 - \log \gamma \sigma)}$  is independent of the chain lengths  $x_1$  and  $x_2$ .

This result will be true not only for mutual termination but for any termination reaction in which the transition state is an associated state involving the two growing chains in an end-to-end configuration.

The chain propagation reaction can be represented :



and the entropy change involved is given by :

$$\Delta S/R = 1 - \log \frac{f_M}{f_P} - \log \gamma \sigma + \log \frac{c_x \cdot c_M}{c_{x+1}}$$

By the same argument as above the temperature independent factor for the propagation is given by :

$$\log A_p = 1 - \log \frac{f_M}{f_P} - \log \gamma \sigma + \log \frac{kT}{h}$$

The two temperature independent factors for the propagation and termination reactions are connected by :

$$A_p/A_t = f_P/f_M$$

### (b) Bulk Polymerisation.

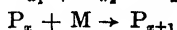
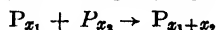
For polymerisation of the monomer in the absence of any solvent equation (3) reduces to

$$F = f_M^{N - \Sigma' x n_x} \cdot f_P^{\Sigma' x n_x} \cdot \frac{1}{\sigma^N} \cdot \frac{N!}{\pi n_x!} \left( \frac{\gamma}{N} \right)^{\Sigma (x-1) n_x}$$

and the chemical potentials and entropies of the monomer and  $x$ -mer become

$$\begin{aligned} \mu_M/RT &= 1 - \log \frac{f_M}{\sigma} + \log \frac{n_M}{\Sigma x n_x} - \frac{\Sigma n_x}{\Sigma x n_x} \\ \mu_x/RT &= 1 - \log \frac{f_P}{\sigma} - (x-1) \log \gamma \sigma + \log \frac{n_x}{\Sigma x n_x} - \frac{x \Sigma n_x}{\Sigma x n_x} \\ - S_M/R &= 1 - \log \frac{f_M}{\sigma} + \log \frac{n_M}{\Sigma x n_x} - \frac{\Sigma n_x}{\Sigma x n_x} - T \frac{\partial}{\partial T} \log f_M \\ - S_x/R &= 1 - \log \frac{f_P}{\sigma} + \log \frac{n_x}{\Sigma x n_x} - (x-1) \log \gamma \sigma - \frac{x \Sigma n_x}{\Sigma x n_x} - xT \frac{\partial \log f_P}{\partial T} \end{aligned}$$

The standard entropy changes accompanying the reactions



are respectively

$$\Delta S_0/R = 1 - \log \gamma \sigma$$

$$\Delta S_0/R = 1 - \log \gamma \sigma - \log f_M/f_P$$

when the standard state is expressed in terms of "molar concentrations"

i.e.,  $c_x = n_x/\Sigma x n_x$  and  $c_M = \frac{n_M}{\Sigma x n_x}$ . Identifying the standard entropy changes with the entropy changes between the initial and transition

states we find the temperature independent factors for chain propagation and termination for bulk polymerisation to be

$$\log A_1 = 1 - \log \gamma \sigma - \log f_m/f_p + \log \frac{kT}{h} \quad (4)$$

$$\log A_t = 1 - \log \gamma \sigma + \log \frac{kT}{h} \quad (5)$$

### The Applications of Equations (4) and (5) to the Experimental Results.

Melville<sup>2</sup> has determined the values of  $k_p$  and  $k_t$  for the photo-initiated polymerisation of vinyl acetate. He finds  $k_p = 1.35 \times 10^8 \exp(-4400/RT)$  moles<sup>-1</sup> litres sec.<sup>-1</sup> and  $k_t = 2.86 \times 10^9$  with no activation energy.  $k_p$  and  $k_t$  are both independent of chain length. The chain termination process is not one involving mutual combination of two growing polymer chains, but although the final state is not an associated state the transition state will involve the association of two active polymer chains.

These experimental results give support to the above treatment of  $A_p$  and  $A_t$  and lead to a value of the ratio  $f_m/f_p$ . Thus setting

$$\log A_t/A_p = \log \frac{2.86 \times 10^9}{1.35 \times 10^8} = \log f_m/f_p$$

$$f_m \sim 10^3 f_p.$$

This relation between the partition functions for monomer units in the liquid and in the polymer chain is understandable on the model that the monomer units in the liquid are free to rotate, whereas in the polymer chain the rotation is greatly restricted and becomes a libration or vibration. On this model we have:

$$f_m/f_p = \frac{8\pi^2(8\pi^3 A \cdot B \cdot C \cdot k^3 T^3)^{1/2}}{h^3} \bigg/ \left(\frac{kT}{h}\right)^3 \prod_{i=1}^3 \left(\frac{1}{\nu_i}\right)$$

where  $A$ ,  $B$  and  $C$  are the moments of inertia of the monomer molecule in the liquid and the  $\nu_i$  are the vibration frequencies of the monomer unit in the polymer chain. Setting  $A = B = 200 \times 10^{-40}$  g./cm.<sup>2</sup> and  $C = 10 \times 10^{-40}$  and  $f_m/f_p = 10^3$ , the value of  $\prod_{i=1}^3 \nu_i = 10^{36}$  is a reasonable value for the frequencies of restricted libration and twisting of the monomer unit in the polymer chain. The absolute value of the temperature independent factor for chain termination is given by:

$$A_t = \frac{kT}{h} \cdot \frac{e}{\sigma \gamma} \text{ in units of (moles/total no. of moles of monomer units)}^{-1} \text{ sec.}^{-1}.$$

Taking a molal volume for monomer of 100 cc. and assuming that only a small change in molal volume accompanies polymerisation:

$$A_t = \frac{1}{10} \cdot \frac{kT}{h} \cdot \frac{e}{\sigma \gamma} \text{ in units of (moles/litre)}^{-1} \cdot \text{sec.}^{-1}$$

The co-ordination number  $\gamma$  of a close-packed structure is 12 and taking  $\sigma$  the symmetry number of the monomer molecule as 2 then

$$A_t = 6 \cdot 10^{10} \text{ (moles/litre)}^{-1} \text{ sec.}^{-1}.$$

This value is larger than that found by Melville by about the factor of 10, a discrepancy probably due to the simplified picture we have developed here and in consequence the approximate form of the partition function.

### Aqueous Phase Polymerisation.

The formulæ obtained above are not applicable to the polymerisation kinetics of reactions in which polymer chains insoluble in the reaction

medium are formed. Under such conditions, in which the heat of solution of the polymer chains is a large negative quantity, the chains will tend to coil up and behave as colloidal spheres. An "active" polymer chain will therefore be terminated by coagulation with other active polymer chains and hence equations applicable to the kinetics of colloidal coagulation must be used in interpreting the reaction rate. The expressions for the velocity constants of coagulation have been developed by Smoluchowski, Fuchs and Derjaguin.<sup>4</sup> The velocity constant for reaction between spheres of radii  $r_1$  and  $r_2$ , in which the diffusion rate is the slow step, has the form

$$k_t = \frac{8RT}{3000\eta} \left\{ \frac{2 + r_1/r_2 + r_2/r_1}{4} \right\} \text{ litres/mole/sec.} \quad (6)$$

If polymer chains of length  $n$  are coiled up into spheres then equation (6) becomes in terms of chain length

$$k_t = \frac{8RT}{3000\eta} \left\{ \frac{2 + (n_1/n_2)^{1/3} + (n_2/n_1)^{1/3}}{4} \right\}.$$

This velocity constant is therefore slightly dependent upon the ratio of the chain length of the combining polymer chain.  $k_t$  is independent of chain length when  $n_1 = n_2$  and is increased by only 15 % when the ratio of the chain lengths is 10:1. It would appear justifiable therefore to consider the above velocity constant as virtually independent of chain length over a very considerable range.

The interpretation of the kinetics of polymerisation of monomers in aqueous solutions reported in a previous publication<sup>1</sup> led to a value of  $k_p/\sqrt{k_t}$  which was found to be independent of chain length but which was dependent upon the concentration of added emulsifying agent. Under these conditions of polymerisation the growing chains are "insoluble" in the aqueous phase and hence equation (6) will be applicable to the chain termination step. The temperature dependence of the overall reaction constant  $k_p/\sqrt{k_t}$  gives  $E_p - \frac{1}{2}E_t = 5000$  cal./mole. But from equation (6)  $E_t$  is given by

$$E_t = -RT^2 \frac{\partial \ln \eta}{\partial T} = 3,500 \text{ cal./mole.}$$

and hence

$$E_p = 6,750 \text{ cal./mole.}$$

The effect of added emulsifying agent upon the value of  $k_p/\sqrt{k_t}$  can now be understood as an effect upon the coagulation constant. An emulsifying agent of the type used, cp. ref.<sup>1</sup> p. 672, will be absorbed on the polymer colloidal particle setting up a Helmholtz layer at the surface. Following Derjaguin it can be shown that the stabilising effect of ionic atmospheres can be expressed

$$k_t'/k_t^0 = 1 / \left\{ \int_0^\infty e^{U(h)/RT} \cdot \frac{(r_1 + r_2)}{(r_1 + r_2 + h)^2} dh \right\} \quad (7)$$

in which  $k_t$  is the velocity constant of coagulation between particles whose energy of interaction is  $U(h)$ , and  $k_t^0$  that between particles for which  $U(h) = 0$  and  $h$  is the distance between the particles. When the particle radius is large compared with the thickness  $d$  of the Debye ionic atmosphere equation (7) can be written

$$k_t'/k_t^0 = 1 / \left\{ 1 + \frac{1}{2\rho} \int_0^\infty [(1 + e^{-z})^2 - 1] dz \right\}$$

<sup>4</sup> Fuchs, *Z. Physik*, 1934, 89, 736. Derjaguin, *Trans. Faraday Soc.*, 1940, 36, 202.

in which  $\rho = \frac{r}{d}$  and  $n = \frac{D + \psi_0^2}{2kT}$  where  $D$  is dielectric constant of the medium and  $\psi$  is the Debye-Hückel potential of the double layer round the particle.

The influence of emulsifying agent on  $k_p/\sqrt{k_t}$  is shown in Table II\*. for the polymerisation of methyl methacrylate in aqueous solution. Assuming that the whole effect is on  $k_t$  we have to account for a 16-fold decrease in  $k_t$ . This can be obtained with a change of  $n$  from 0 to 8 that is with a Debye-Hückel potential rising to about 25 mv. This could be achieved by the adsorption in the polymer particles of about 10 % of the total emulsifying agent present.

### Summary.

This is a discussion of the "temperature independent factors" of the chain propagation and chain termination steps in polymerisation reactions. Experiments<sup>2</sup> have shown that in the case of vinyl acetate  $A_p$  for chain propagation and  $A_t$  for chain termination are independent of chain length and that  $A_p/A_t = 10^{-3}$ . These results are discussed on the basis of the transition state method and the partition functions of long chain molecules in solution.

In the partition function a distinction is made between the behaviour of free monomer units and monomer units incorporated in the polymer chain.

The temperature independent factors for reactions involving insoluble polymer chains are discussed in terms of the coagulation of colloidal particles. The influence of emulsifying agents on the velocity constant for chain termination is described as the effect of emulsifying agents on the charge of colloidal particles and hence on the rate of coagulation. Under these conditions the viscosity and hence the activation energy of viscous flow enter into the reaction constant for the chain termination reaction.

### Résumé.

On discute ici les "facteurs indépendants de la température" pour les étapes de la propagation et de la terminaison de chaîne dans les réactions de polymérisation. L'expérience montre que, dans le cas de l'acétate de vinyle,  $A_p$  pour la propagation de chaîne et  $A_t$  pour la terminaison sont indépendants de la longueur de chaîne et que  $A_p/A_t = 10^{-3}$ . On discute ces résultats en se fondant sur la méthode de l'état de transition et sur les fonctions de partition des molécules à longues chaînes en solution.

Dans la fonction de partition, on distingue entre le comportement des motifs élémentaires du monomère et de ceux incorporés dans la chaîne du polymère.

Les facteurs indépendants de la température pour des réactions qui comportent des chaînes de polymère insoluble, sont discutés d'après la coagulation des particules colloïdales. L'influence d'agents émulsifiants sur la constante de vitesse pour la terminaison de chaîne est décrite comme l'effet de tels agents sur la charge des particules colloïdales, et par conséquent sur la vitesse de coagulation. Dans ces conditions, la viscosité et l'énergie d'activation d'un fluide visqueux entrent dans la constante de réaction pour la réaction de terminaison de chaîne.

### Zusammenfassung.

Der Artikel erörtert die Aktionskonstanten der Kettenfortpflanzungs- und Kettenabbruchsstufen in Polymerisationsreaktionen. Experimente haben gezeigt, dass im Falle von Vinylacetat die Aktionskonstanten der Kettenfortpflanzung ( $A_p$ ) und der Kettenabbruchsreaktion ( $A_t$ ) von der Kettenlänge unabhängig sind und dass  $A_p/A_t = 10^{-3}$ . Diese Resultate

\* *Trans. Faraday Soc.*, 1946, **52**, 672.

werden auf Basis der Übergangszustandstheorie der Reaktionsgeschwindigkeit und der Zustandssummen von langen Kettenmolekülen besprochen.

In der Zustandssumme wird zwischen dem Verhalten von freien Monomereinheiten und von Monomereinheiten, die in Ketten eingebaut sind, unterschieden.

Für Reaktionen, bei denen unlösliche Polymerketten entstehen, werden die Aktionskonstanten auf Basis der Koagulation von Kolloidteilchen erörtert. Der Einfluss von Emulgatoren auf die Geschwindigkeitskonstante des Kettenabbruchs wird als Effekt des Emulgators auf die Ladung der Kolloidteilchen und daher auf die Koagulationsgeschwindigkeit beschrieben. Unter diesen Umständen hängt die Geschwindigkeitskonstante der Kettenabbruchsreaktion explicite von der Viskosität und daher der Aktivierungsenergie des Fließens ab.

*Department of Chemistry,  
The University,  
Leeds.*

---

## REVIEWS OF BOOKS.

**Atomic Theory for Students of Metallurgy** By WILLIAM HUMEROTHY. (The Institute of Metals, London, 1946.) Pp. 286. Price 7s. 6d.

This book is the third of the Monograph and Report Series published by the Institute of Metals; it is written primarily for the more advanced student of metallurgy, but has much that is of interest to the chemist and physicist. The approach has been as non-mathematical as possible and has naturally led in some cases to a somewhat dogmatic presentation particularly of mathematical equations; if, however, this book encourages the reader to study the rigorous treatments in other works, as it is believed it will, it is more than justified. Careful selection of the applications of theories prevents the author from dealing with certain aspects whose interpretation are doubtful, and makes the reading easier and more straightforward.

The book is divided into six parts. The first, the general background, deals briefly with the Bohr-Sommerfeld theory and introduces the basic ideas of wave mechanics as developed by Schrödinger, including a short but clear discussion on potential boundaries. This is followed by three chapters on the structure of the free atom and a good, lucid account of the *s*, *p* and *d* states; only the simpler Schrödinger diagrams are given since, as is stated there, the perturbing forces in metallic combination are much greater than spin effects. In part III an account of the nature of the interatomic forces involved in the formation of solids, liquids and compound molecules and the electronic processes concerned in van der Waals, exchange and resonance forces are discussed in an interesting manner, and the author is to be congratulated on his dexterous avoidance of many obvious pitfalls. The remaining three sections deal with the free-electron theory of metals, the Brillouin-zone theory, and the extension of these to the less ideal, but more real, systems of metals and alloys. As might be expected, the matter here has been well selected and lucidly explained and should prove of real value not only to the metallurgical student but also to the physical chemist, who is so apt to neglect this important branch.



The author throughout has presented his subject <sup>in</sup> ~~matter~~ in a manner calculated to hold the interest of the reader; the book is reasonably self-contained and should form a bridge by means of which the non-mathematical student might be led to an appreciation of the new theories of the structure and properties of metals and alloys. The book is well printed, moderate in price, and can be recommended to all requiring an introduction to the electron theory of metals.

F. C. T.

**Photography by Infra-Red.** By WALTER CLARK. 2nd Ed. (New York : John Wiley & Sons, Inc. London : Chapman & Hall, Ltd.) Pp. 472. Price \$6 or 30s. net.

During the war years, infra-red photography has gone ahead rapidly as regards its applications. Examples are the detection of camouflage, forest surveys from the air, and a host of other things. Luckily, however, marked progress can also be reported concerning basic data for this region of the spectrum, such as the focal properties of lenses, sensitometry and speed designation. Broadly, all these subjects form the raw material out of which Dr. Clark has fashioned the new matter for the second edition of his book.

To confine ourselves mainly to the additions, there are, for example, tables of quantitative information giving the infra-red focal settings for a wide variety of lenses. The difference between these and the "visual" positions is smaller than commonly supposed; in fact 0.5 % as a maximum, and not more than 0.35 % in most cases. Nevertheless, for critical work, parfocal systems are essential; the present reviewer has always used such a lens, focussing through a "dummy" (transparent) filter, before inserting the infra-red screen. The results well justify the trouble and expense of exploring the dispersion specifically.

A recent development has been to establish a kind of photographic thermometry (a parallel to photographic photometry) by infra-red methods. Temperature distributions over a surface between about 250° C. and 500° C. can be studied. Work is in progress with heat-sensitive papers in an attempt to make the process function for lower temperatures. This is most important: many special paints have of course been prepared which change colour on heating, and therefore act as indicators. But in the main the transition points are somewhat high, though a few are lower than the infra-red limit. What is badly needed is a means of charting relatively low-temperature contours.

Towards the end of the book we find some tabular matter giving the properties of a number of common materials in the spectral range accessible to infra-red photography. They are very valuable to know, and such data may well dictate certain aspects of industrial policy in years to come.

In the arts, applications are steadily increasing; they are usually helpful if not spectacular. For paintings, the great advantage is (assuming the method to be feasible at all) the comparative simplicity of the photographic image in contrast to the effects of superposition and imbrication on the X-ray film.

To conclude, Dr. Clark's volume is handsomely produced, attractively illustrated, and well indexed.

F. I. G. R.

**Physical Methods of Organic Chemistry. Volumes I and II.** By ARNOLD WEISSBERGER. (Interscience Publishers, Inc., 215 Fourth Avenue, New York 3, N.Y.) Pp. 1. to 736, and 737 to 1367. Price \$8.50 each volume.

These two volumes contain fairly detailed discussions on twenty-six topics, most of them written by specialists in their particular field. The titles which include electron diffraction, polarography, and radioactivity illustrate the changes in emphasis which have taken place in physical chemistry during the last thirty years. More familiar subjects are also discussed from the modern point of view by experts, e.g., boiling points, by Swietoslawski; conductometry, by Shedslovski; potentiometry, by Michaelis, and many others. These, in general, give an authoritative account of a particular topic which will be valuable not only to the research worker but also to the technical chemist who is seeking for collected information.

The reference in the title to organic chemistry is unduly restrictive. The treatment presumes that the reader has considerable mathematical knowledge and many of the chapters will be of interest to physical chemists and physicists. One reflection after a cursory perusal of these volumes is the frequent references to substances or processes of biological interest. Another impression to an English reader is that a few of the articles have rather a nationalistic bias. Reference to early European work is scanty and inadequate although detailed accounts are given of specialised investigations which are not of general interest.

On the whole, however, the standard of treatment is high and many references are provided. The printing and get-up are excellent. The price is rather high but this is probably one of the penalties of the war. It is a fairly safe prediction that "Weissberger" will soon become an essential work of reference in the chemist's library and that it will serve another useful purpose in the stimulation of new investigations.

S. S.

**An Introduction to Chromatography.** By TREVOR I. WILLIAMS. (Blackie & Son Ltd., 1946.) Pp. 100 and 8 Pl. Price 10s.

Chromatography, discovered in 1906 by the Russian botanist Tswett, lay dormant for a quarter-century, but in recent years has undergone extensive development. "Unfortunately," says Dr. Williams in the preface to his book, "in the majority of university courses chromatography fails to get the attention it deserves, and it is possible that this is due, at least in part, to lack of a suitable book". The large works, by Zechmeister and Chohnoky and by Strain respectively, being intended for the research worker, are too loaded with detail for the student with his crowded syllabus. The present volume is designed to fill this gap and to present the student with a concise and up-to-date account of the subject; at the same time sufficient practical detail has been given to make the book of value to the research worker. The references to original papers have been, restricted to less than fifty, each selected to illustrate some important point in the development of the subject.

The following brief analysis of the nine chapters may serve to indicate the scope of the book. Chapter I gives an historical and general outline of the subject; Dr. Williams makes a plea for wider use of chromatography; in possible scope of application, he points out, the method is comparable with the two everyday tools of the chemist, distillation and crystallisation; the apparatus required is cheap and simple, within the scope of any school laboratory, and no great degree of manipulative skill is required in applying the method.

Chapter II deals with the various adsorbents and solvents employed; in connection with the widely used alumina adsorbent, an account is given of the valuable method due to Brockmann for standardising the activity of the alumina by means of dye solutions; for the benefit of the student desiring to prepare his own adsorbent, there might have been included a description of a suitable method of preparation of the alumina (as is done for silica gel in Chapter VII). Chapter III describes the original apparatus of Tswett and the several refinements and modifications introduced by later workers, including the "disc chromatogram" developed by the author.

Chapter IV gives examples to illustrate the scope of the method, such as the analysis of foods, drugs, urine and dyestuffs. In Chapter V, the application of the method to colourless substances is dealt with and the several artifices for rendering the colourless zones visible are described. (The reference (p. 52) to pigments seems out of place in this section.) The less fully explored subject of chromatography of inorganic substances is considered in Chapter VI.

Chapter VII discusses the so-called "partition chromatography" due to Martin and Synge; as the author points out, this method resembles true chromatography in technique only, the fundamental principles being entirely different in the two cases. Chapter VIII selects for description some striking recent examples of the employment of chromatographic research. The final chapter IX deals first with the mathematical theory of partition chromatography (likewise due to Martin and Synge) and secondly with the little explored subject of the relationship between chemical constitution and adsorption affinity. The volume is completed by the restricted bibliography referred to above and a rather too brief index.

The book is written in an easy and eminently readable style and the proof-reader has done his job thoroughly; the only textual error noted by the reviewer is the reference (p. 95) to J-acid as a "sulphuric" acid. Dr. Williams is to be congratulated on a book which is both stimulating and informative and may be read with pleasure and profit by student and research worker alike.

T. B.

#### CORRIGENDUM.

Vol. XLIII, p. 7. Paper of R. M. Barrer. Curve 1 in Fig. 1 (a) is not, as stated, that for  $z = \infty$ . The latter curve lies between curves 1 and 2 in this figure and close to curve 2.

# MAGNETOCHEMICAL INVESTIGATIONS. PART V.\* THE DIAMAGNETISM OF BINARY LIQUID MIXTURES.

BY W. ROGIE ANGUS AND (THE LATE) DONALD V. TILSTON.

*Received 10th April, 1946.*

## 1. Introduction.

The magnetic behaviour of binary mixtures of liquids was first investigated by Smith and Smith<sup>1</sup> in 1918. They showed that for the mixtures acetone-water, acetone-ethyl alcohol, acetic acid-water, and acetic acid-benzene the specific susceptibility of the mixture was an additive function of the susceptibilities of the two components, and varied linearly with the concentration (wt.-%) of one component. Trifonow, in 1924<sup>2</sup> and 1926,<sup>3</sup> measured the susceptibility of several systems, but found that only in the systems benzene-*m*-xylene and allyl mustard oil-dimethylaniline was strict additivity displayed. The other mixtures studied by him gave susceptibility-composition curves which were either concave (benzene-nitrobenzene, benzene-SnCl<sub>4</sub>) or convex (benzene-CS<sub>2</sub>, acetone-CS<sub>2</sub>) to the composition axis. For two systems, curves possessing maxima were obtained; chloroform-acetone showed a maximum susceptibility at 51.5 mol.-% of chloroform, and stannic chloride-ethyl acetate gave a maximum at a composition corresponding with the compound SnCl<sub>4</sub>.2EtOAc. Trifonow's work, however, appears to have attracted little attention at the time, and it was not until 1931 that further data on such mixtures were published.

In that year Trew and Spencer<sup>4</sup> found wide deviation from additivity in several binary mixtures, and although these results were later shown to be fallacious by the original authors, their publication stimulated an immediate re-investigation of some of the systems by Buchner,<sup>5, 6</sup> Ranganadhan,<sup>7, 8</sup> and Rao and Sivaramakrishnan.<sup>9, 10</sup> Buchner investigated the completely miscible pairs C<sub>2</sub>H<sub>5</sub>OH-CS<sub>2</sub> and acetone-chloroform, and the incompletely miscible pairs phenol-water and methyl alcohol-CS<sub>2</sub>. Each mixture showed only small deviations from additivity, and measurements of the susceptibility at three different field strengths proved that the results of Trew and Spencer could not be due to an extreme dependence of susceptibility on field strength. Ranganadhan investigated

\* The article entitled "Diamagnetism and the Hydrogen Bond," by Angus and Hill, *Trans. Faraday Soc.*, 1940, 36, 923, will henceforth be referred to as Part IV.

<sup>1</sup> Smith and Smith, *J. Amer. Chem. Soc.*, 1918, 40, 1218.

<sup>2</sup> Trifonow, *Mitt. wiss.-techn. Arbeiten Republik (Russ)*, 1924, 13, 10, 11; *Chem. Zentr.*, 1925, II, 386.

<sup>3</sup> Trifonow, *Ann. Inst. Anal. Physico-Chem., Leningrad*, 1926, 3, 434; *Chem. Zentr.*, 1927, I, 2634.

<sup>4</sup> Trew and Spencer, *Proc. Roy. Soc. A*, 1931, 131, 209.

<sup>5</sup> Buchner, *Z. Physik*, 1931, 72, 344.

<sup>6</sup> Buchner, *Nature*, 1931, 128, 301.

<sup>7</sup> Ranganadhan, *Indian J. Physics*, 1931, 6, 421.

<sup>8</sup> Ranganadhan, *Nature*, 1931, 127, 975.

<sup>9</sup> Rao and Sivaramakrishnan, *Indian J. Physics*, 1931, 6, 509.

<sup>10</sup> Rao and Sivaramakrishnan, *Nature*, 1931, 128, 872.

the mixtures benzene- $\text{CCl}_4$ , acetone-chloroform, acetone-water, and  $\text{C}_2\text{H}_5\text{OH}$ -water; each showed small deviations from additivity, but to the least extent in the non-polar mixture. Molecular deformation by dipole-dipole interaction and compound formation were invoked to explain the deviations. It was held, in agreement with Buchner, that the effect of these on the magnetic behaviour could not be large. Rao and Sivaramakrishnan found that the mixture susceptibility was additive for eight pairs of simple non-polar and polar organic substances. van Aubel<sup>11</sup> summarised the position at this time, and pointed to the similarities in the behaviour of the density and the refractive index of mixtures.

Since 1931, numerous papers have appeared on this topic, the majority of which experimentally confirm the existence of small but real deviations from additivity. Agreement is complete, however, neither on the reality of the deviations, nor on their possible causes. A review of previous work, together with graphical data on organic acids, ethers, alcohols, and ketones, and their mixtures has been given recently by von Rautenfeld and Steurer.<sup>12</sup>

The present work was undertaken in the hope of making a quantitative comparison of available data and of providing a more certain basis for the discussion of the experimentally ascertained deviations. An investigation by Angus and Hill<sup>13</sup> of the magnetic behaviour of substances capable of forming hydrogen bonds suggested a method for dealing with the data. Details of this method are given below, and its use in the investigation of the numerical results published by various workers\* is illustrated by selected examples.

## 2. The Calculation of Apparent Susceptibility.

If a mixture contains weight fractions  $w_1$  and  $w_2$  of two components having specific susceptibilities of  $\chi_1$  and  $\chi_2$ , then the susceptibility of the mixture, according to the additivity law is

$$\chi_{\text{add}} = w_1\chi_1 + w_2\chi_2. \quad (1)$$

Where real deviations occur, the mixture susceptibility,  $\chi_{\text{mix}}$ , is the sum of  $\chi_{\text{add}}$  and of the deviations,  $\chi_{\text{dev}}$ ,

$$\chi_{\text{mix}} = \chi_{\text{add}} + \chi_{\text{dev}} \quad (2)$$

$\chi_{\text{app}}$ , the apparent or partial susceptibility of one component, will then be a function of  $w$ , and will have a value, which, substituted in (1) will make  $\chi_{\text{add}} = \chi_{\text{mix}}$ . Hence

$$\chi_{\text{mix}} = w_1\chi_1 + w_2\chi_{\text{app}} \quad (3)$$

and

$$\chi_{\text{app}} = \frac{\chi_{\text{mix}} - w_1\chi_1}{w_2} \quad (4)$$

It will be noted from (2) that, when  $\chi_{\text{dev}} = 0$ , then  $\chi_{\text{mix}} = w_1\chi_1 + w_2\chi_2$  and

$$\chi_{\text{app}} = \frac{w_1\chi_1 + w_2\chi_2 - w_1\chi_1}{w_2} = \chi_2 \quad (5)$$

<sup>11</sup> van Aubel, *Nature*, 1931, 128, 455.

<sup>12</sup> von Rautenfeld and Steurer, *Z. Physik. Chem., B*, 1942, 51, 39.

<sup>13</sup> Angus and Hill, *Trans. Faraday Soc.*, 1940, 36, 923.

\* The published data of Garssen (*Compt. rend.*, 1933, 196, 541), Kido (*Sci. Rep. Tohoku Univ.*, 1932, 21, 385), Rao (*Indian J. Physics*, 1933, 8, 483), Salceanu and Gheorghiu (*Compt. rend.*, 1935, 200, 120), Trew and Spencer (*Trans. Faraday Soc.*, 1936, 32, 701), and Ventkataramiah (*J. Univ. Mysore*, 1942, 3, 19) have been investigated completely although they are not referred to in detail in this paper; they conform to the general trends exhibited by the data presented.

Generally, however, deviations are encountered, and, hence, from (2) and (4),

$$\chi_{2app} = \frac{\chi_{add} + \chi_{dev} - w_1\chi_1}{w_2} = \frac{w_2\chi_2 + \chi_{dev}}{w_2} = \chi_2 + \frac{\chi_{dev}}{w_2} \quad (6)$$

The change of susceptibility, an index of chemical or physical reaction in the mixture, is then given by  $\chi_{2app} - \chi_2 = \Delta\chi_{2app}$ . Therefore,

$$\Delta\chi_{2app} = \chi_{dev}/w_2 \quad (7)$$

Rao and Sriraman<sup>14</sup> and Rao and Aravamudachari<sup>15</sup> subjected their own results on formic acid-water and CS<sub>2</sub>-phosphorus to an equivalent process, calculating the "change of susceptibility per 100 g. of solute." In their notation, this quantity is 100 ( $\chi_2 - \chi_1$ )/*c*, where  $\chi_2$  is the calculated value of  $\chi_{mix} \equiv \chi_{add} = w_1\chi_1 + w_2\chi_2$ ;  $\chi_1$  = observed value  $\equiv \chi_{mix}$ , and *c* = weight percentage of constituent  $\equiv w_2 \times 100$ . Hence

$$\frac{\chi_2 - \chi_1}{c} \times 100 = \frac{\chi_{add} - \chi_{add} - \chi_{dev}}{100w_2} \times 100 = \frac{-\chi_{dev}}{w_2} \quad (8)$$

Rao and Sriraman found that this quantity was constant over a concentration range of 29.79 wt.-% of formic acid, but showed "a tendency to decrease at (the) higher concentrations." This claim of constancy is somewhat illfounded, since the lowest value, 0.020, occurs at 51 %, flanked by values fairly constant at 0.033. Part of Rao and Sriraman's data is reproduced below in Table I, together with the results of the

TABLE I.—THE SYSTEM FORMIC ACID-WATER.

<i>w</i> <sub>2</sub>	$\chi_{mix}$	Rao's Method.		Present Method.	
		$\chi_{add}$	$\frac{(\chi_{add} - \chi_{mix})}{w_2}$	$\chi_{2app}$	$\Delta\chi_{2app}$
0.000	0.7200	—	—	—	—
0.290	0.6292	0.6408	0.039	0.4069	0.0395
0.360	0.6105	0.6217	0.031	0.4159	0.0305
0.490	0.5701	0.5863	0.033	0.4141	0.0323
0.510	0.5705	0.5808	0.020	0.4269	0.0195
(0.575)	0.5434	0.5630	0.034	0.4128	0.0336
(0.575)	0.5414	0.5630	0.037	0.4094	0.0370
0.695	0.5055	0.5303	0.036	0.4113	0.0351
0.710	0.5058	0.5261	0.029	0.4184	0.0280
0.790	0.4834	0.5043	0.026	0.4206	0.0258
1.000	0.4464	—	—	(0.4464)	—

present method of calculation applied to the same data. The similarity of the values of  $(\chi_{add} - \chi_{mix})/w_2$  and  $\Delta\chi_{2app}$  shows the essential equivalence of the two methods.

In the data on the phosphorus-CS<sub>2</sub> system,  $(\chi_{add} - \chi_{mix})/w_2$  increases from 0.06 at 22 wt.-% phosphorus to about 0.15 at 12 %, and then falls rapidly to 0.06 again at 3 %, although the value at 6.5 % is still 0.14. The values are more erratic the lower the concentration. Rao and Aravamudachari<sup>15</sup> again remark on the tendency to decrease at the higher concentrations.

The behaviour of this second mixture is typical of that of the great majority of the 69 sets of available data on which we have carried out our calculations. As an illustration, the results of recalculating the data of Trew and Watkins<sup>16</sup> on *n*-butyl alcohol-*iso*-propyl alcohol

<sup>14</sup> Rao and Sriraman, *J. Annamalai Univ.*, 1938, 7, 187.

<sup>15</sup> Rao and Aravamudachari, *Proc. Indian Acad. Sci., A*, 1940, 12, 361.

<sup>16</sup> Trew and Watkins, *Trans. Faraday Soc.*, 1933, 29, 310.

mixtures after conversion of the published mol.-% into wt.-% are given in Table II.

TABLE II.—RECALCULATION OF TREW AND WATKINS' DATA ON *n*-BUTYL ALCOHOL-*IS*O-PROPYL ALCOHOL, TAKING THE LATTER AS SOLUTE.

Mol.-%.	Wt.-%.	$\chi_{mix}$ .	$\chi_{sapp}$ .	$\Delta\chi_{sapp}$ .
0.0000	0.0000	0.7916	—	—
0.0979	0.0809	0.7944	0.8283	0.034
0.2036	0.1716	0.7969	0.8222	0.028
0.2660	0.2271	0.7975	0.8185	0.024 <sub>s</sub>
0.3998	0.3506	0.7962	0.8046	0.011
0.4914	0.4392	0.7974	0.8048	0.011
0.5955	0.5442	0.7963	0.8004	0.006
0.6980	0.6519	0.7947	0.7966	0.003
0.7988	0.7630	0.7951	0.7964	0.002
0.8974	0.8762	0.7936	0.7939	0.000
1.0000	1.0000	0.7939	(0.7939)	—

The table shows clearly the rapid decrease of  $\Delta\chi_{sapp}$  as the concentration is increased, decreasing by two-thirds between 10 and 40 %.

TABLE III.—RECALCULATION OF DATA RECORDED BY VARIOUS AUTHORS FOR ACETIC ACID-WATER MIXTURES. (CONCENTRATIONS IN 5% RANGES.)

Wt.-% AcOH.	$\Delta\chi_{sapp}$ for acetic acid.			
	Ref. 1.	Ref. 17.	Ref. 18.	Ref. 19.
0-5	—	—	—	—
5-10	—	— 0.018	—	—
10-15	—	— 0.004	—	— 0.020
15-20	—	—	—	—
20-25	0.028	— 0.010	0.000	—
25-30	—	— 0.008 <sub>s</sub>	—	—
30-35	—	— 0.002	—	—
35-40	—	— 0.003	—	—
40-45	0.011	—	— 0.010	—
45-50	—	0.001 <sub>s</sub>	—	—
50-55	—	— 0.005	—	0.000
55-60	—	— 0.002	—	—
60-65	0.000	—	0.001	— 0.012
65-70	—	0.003	—	—
70-75	—	0.003	—	— 0.099
75-80	—	—	— 0.002	—
80-85	0.002	— 0.002 <sub>s</sub>	0.001	— 0.046
85-90	—	0.000	0.003	—
90-95	—	— 0.001	—	— 0.019
$\chi_{AcOH}$	0.520	0.525	0.538	0.580
$\chi_{H_2O}$	0.714	0.720	0.720	0.720

When the data of different authors are compared, after calculating  $\Delta\chi_{sapp}$ , an almost complete inconsistency is immediately revealed as may be seen by reference to Table III in which the results of Smith and

Smith,<sup>1</sup> Rao and Narayanaswamy,<sup>17</sup> Varadachari,<sup>18</sup> and Sibaiya and Venkataramiah<sup>19</sup> on acetic acid-water mixtures are compared. It should be noted that, in the calculations, the value we have used for the susceptibility of water is that given by the individual author; but the absolute numerical value used is of little importance, provided that it is consistent with the measurements on the mixtures. The data of Smith and Smith,<sup>1</sup> and those of Rao and Narayanaswamy<sup>17</sup> show a decrease in the numerical value of  $\Delta\chi_{2app}$  with increasing concentration of acetic acid, but, whereas the first set is large positive at low concentrations, the second is large negative. Varadachari's results<sup>18</sup> change, with the exception of the result for 21.4 %, from large negative at low concentrations to small positive at high concentrations. Sibaiya and Venkataramiah's results<sup>19</sup> are very different, the value increasing numerically to a large negative maximum at 70 %, then falling to lower negative values at 80 and 90 %. Moreover, the experimental curve ( $\chi_{mix}-w_2$ ) based on Sibaiya and Venkataramiah's results differs considerably from those given by the other authors (Fig. 1) in that it shows a deep minimum at approximately 75 % acetic acid, corresponding with a deviation of 12.5 % from the additive value; and, further, it should be noted that they used the falling drop method of measurement,<sup>20</sup> which would be more likely to give erroneous results owing to rapid changes in viscosity, density, and surface tension than the Quincke and Gouy methods used by the other investigators.

That these effects are in no way connected with the ionising power of acetic acid and water is borne out by the data on solutions of acetone in chloroform presented in Table IV (p. 226), in which concentrations have been grouped into 10 % ranges. Here again, the large values of  $\Delta\chi_{2app}$  at the lower concentrations are encountered; in this case, all but the results of Rao and Varadachari<sup>18</sup> are mainly negative. The exceptional case cannot be lightly dismissed, since, although four mixtures only were examined, the examination would appear to be both careful and precise, as evidenced by the constancy of the susceptibility values measured at different temperatures for each mixture.

The explanation of this irregular and uncertain behaviour was puzzling, but examination of the data for mixtures, in which additivity may be expected and for which "additivity" has been established by experiment, suggested a possible explanation. A convenient system is that containing

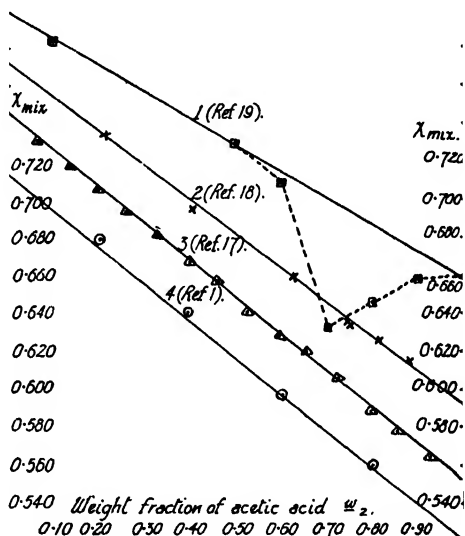


FIG. 1.— $\chi_{mix}-w_2$  curves for acetic acid-water.

The  $\chi_{mix}$  scale, correct for curve 4, must be displaced upwards by 0.027, 0.053 and 0.079 for curves 3, 2 and 1. The continuous lines represent "additivity" values. The broken line joins adjacent experimental points on curve  $\chi_{mix}$ .

<sup>17</sup> Rao and Narayanaswamy, *Proc. Indian Acad. Sci. A*, 1939, 9, 35.

<sup>18</sup> Varadachari, *ibid.*, 1935, 2, 161.

<sup>19</sup> Sibaiya and Venkataramiah, *Indian J. Physics*, 1932, 7, 393.

<sup>20</sup> Abbonnenc, *Compt. rend.*, 1930, 190, 1395.



benzene and carbon tetrachloride, where both molecules, being non-polar, are hence not liable to large mutual polar distortions. The data of Seely<sup>24</sup> on this system are extensive and show little of the large irregularities

TABLE IV.—RECALCULATION OF DATA ON ACETONE-CHLOROFORM MIXTURES.

Wt.-% Acetone.	$\Delta\chi_{\text{app}}$ for acetone.					
	Ref. 21.	Ref. 7.	Ref. 22.	Ref. 9.	Ref. 23.	Ref. 19.
0-10	0.003	— 0.102	—	—	—	—
10-20	— 0.008	—	— 0.009	— 0.001	—	—
20-30	— 0.003	— 0.049	0.000	0.020	0.006	— 0.057
30-40	— 0.002	—	—	—	0.004	— 0.041
40-50	— 0.005 <sub>8</sub>	— 0.007	— 0.003	— 0.010	—	—
50-60	0.001	— 0.005	— 0.002	— 0.005	0.000	—
60-70	— 0.001	0.001	—	— 0.001	—	—
70-80	—	—	0.001	0.006	— 0.001	— 0.010
80-90	0.006	—	—	0.002	—	—
90-100	—	—	0.000	—	—	—
$\chi_{\text{CMe}_2}$	0.5897	0.5971	0.592	0.595	0.5789	0.580
$\chi_{\text{CHCl}_3}$	0.5037	0.4966	0.495	0.494	0.4986	0.505

usually encountered. Seely finds, however, that carbon tetrachloride has a large negative temperature coefficient of susceptibility ( $-0.0005 \times 10^{-6}$  per  $10^\circ\text{C}.$ ), in contrast to Azim, Bhatnagar, and Mathur,<sup>25</sup> who found the susceptibility independent of temperature. Moreover, the

TABLE V.—RECALCULATION OF SEELY'S RESULTS ON  $\text{CCl}_4\text{-C}_6\text{H}_6$  MIXTURES.

Wt. fraction $\text{CCl}_4$ .	$\Delta\chi_{\text{app}}$ for carbon tetrachloride.				
	$10^\circ$ .	$20^\circ$ .	$30^\circ$ .	$40^\circ$ .	$50^\circ\text{C}.$
0.21259	0.0023	0.0033	0.0038	0.0047	0.0057
0.30803	0.0020	0.0028	0.0039	0.0048	0.0056
0.38968	0.0019	0.0027	0.0037	0.0044	0.0052
0.44515	0.0014	0.0023	0.0031	0.0040	0.0047
0.54031	0.0012	0.0020	0.0029	0.0038	0.0046
0.66264	0.0004	0.0012	0.0021	0.0029	0.0037
0.77834	0.0001	0.0008	0.0016	0.0023	0.0031
0.89028	— 0.0001	0.0005	0.0013	0.0020	0.0027
$\chi_{\text{CCl}_4}$	0.4305	0.4300	0.4295	0.4290	0.4285

susceptibilities of all the mixtures varied with temperature. Seely, however, claims that the law of additivity holds good for the system; this, of course, is not incompatible with the unexplained temperature

<sup>21</sup> Cabrera and Madinaveitia, *Ann. Soc. Espanola Fis. Quim.*, 1932, 30, 528

<sup>22</sup> Rao, *Indian J. Physics*, 1933, 8, 483.

<sup>23</sup> Rao and Varadachari, *Proc. Indian Acad. Sci. A*, 1934, I, 77

<sup>24</sup> Seely, *Physic. Rev.*, 1936, 49, 812.

<sup>25</sup> Azim, Bhatnagar and Mathur, *Phil. Mag.*, 1933, 16, 580.

relations. Table V shows the values of  $\Delta\chi_{2app}$  for carbon tetrachloride, at various temperatures and concentrations, calculated from Seely's results.

Here again the behaviour is similar in general to that of the other systems, although differing in some respects. The larger values occur at low concentrations, but the decrease is gradual, leaving, for the results at 50° C., a considerably high value for  $\Delta\chi_{2app}$  at 89 % carbon tetrachloride. The great difference between the five columns of the table may be traced to the fact that, whereas the temperature coefficient is negative for carbon tetrachloride, it is positive for the mixtures (0.0002 per 10° for 44.5-89 %  $\text{CCl}_4$ , 0.0001 for 21.3-39.0 %). If one considers, not the difference between  $\chi_2$  and  $\chi_{2app}$ , but the difference between  $\chi_{2app}$  for 89.0 % carbon tetrachloride and for the other concentrations, then the values of the new quantity,  $\Delta'\chi_{2app}$ , are similar for each temperature, and closely resemble in behaviour the values of  $\Delta\chi_{2app}$  given in Tables I-IV (see Table VI).

TABLE VI.—RECALCULATION OF THE RESULTS IN TABLE V.

Wt. fraction of $\text{CCl}_4$ .	$\Delta'\chi_{2app}$ for carbon tetrachloride.				
	10°.	20°.	30°.	40°.	50° C.
0.21259	0.0024	0.0028	0.0025	0.0027	0.0030
0.30803	0.0021	0.0023	0.0026	0.0028	0.0029
0.38968	0.0020	0.0022	0.0024	0.0024	0.0025
0.44515	0.0015	0.0018	0.0018	0.0020	0.0020
0.54031	0.0013	0.0015	0.0016	0.0018	0.0019
0.66264	0.0005	0.0007	0.0008	0.0009	0.0010
0.77834	0.0002	0.0003	0.0003	0.0003	0.0004
$\chi_{mix}$ for 89 % $\text{CCl}_4$	0.4597	0.4598	0.4600	0.4602	0.4604

From the data in Table VI it will be seen that there still remains a small positive temperature coefficient of  $\Delta'\chi_{2app}$  and that the decrease of  $\Delta'\chi_{2app}$  is more gradual at the lower concentrations than the decrease of the corresponding  $\Delta\chi_{2app}$  of Tables I-IV. But it is of more importance to note that a mixture, reputedly additive, does, in fact, show deviations, that these deviations are of the same progressive type as those shown by mixtures containing at least one polar constituent, and are not small and irregularly positive and negative as might be expected. The possibility that this behaviour was fictitious and resulted from the method of calculation or from minor inaccuracies accentuated by the method of calculation was therefore investigated.

### 3. Errors in Apparent Susceptibility.

The effect of small errors in the variables concerned in its calculation on the value of  $\Delta\chi_{2app}$  can be found mathematically by the following process. Consider a function  $u$  of  $x$ ,  $y$  and  $z$ .

$$u = u(x, y, z).$$

Then,

$$du = \frac{\partial u}{\partial x}dx + \frac{\partial u}{\partial y}dy + \frac{\partial u}{\partial z}dz. \quad (9)$$

If now  $x$ ,  $y$ , and  $z$  are experimentally measured quantities, and any one set of  $x$ ,  $y$ , and  $z$  has errors  $dx$ ,  $dy$ ,  $dz$ , then  $du$  represents the corresponding error in  $u$ . We may make  $dx$ ,  $dy$ , and  $dz$  finite, and write

$$\Delta u = \frac{\partial u}{\partial x} \Delta x + \frac{\partial u}{\partial y} \Delta y + \frac{\partial u}{\partial z} \Delta z \quad . \quad . \quad . \quad (10)$$

In the present instance the function  $u$  is  $\Delta\chi_{2app}$ , a function  $\chi_{mix}$ ,  $w_2$ ,  $x_1$  and  $x_2$ .  $x_1$  and  $x_2$  must be retained as variables since, although they are theoretically "constant," they are as much subject to error as any other experimental measurement.  $w_1$  is not retained since it can be expressed as a function of  $w_2$  alone. Although  $\chi_{mix}$  and  $w_2$  are not independent variables in the general sense, they are independently subject to error and so must both be retained.

$$\begin{aligned} \Delta\chi_{2app} &= \frac{\chi_{mix} - w_1 x_1}{w_2} - x_2 = \frac{\chi_{mix} - (1 - w_2)x_1}{w_2} - x_2 \\ &= \frac{\chi_{mix} - x_1}{w_2} + x_1 - x_2 \quad . \quad . \quad . \quad (11) \end{aligned}$$

Hence,

$$\begin{aligned} \frac{\partial\{\Delta\chi_{2app}\}}{\partial\chi_{mix}} &= \frac{1}{w_2}; \quad \frac{\partial\{\Delta\chi_{2app}\}}{\partial x_1} = 1 - \frac{1}{w_2} \\ \frac{\partial\{\Delta\chi_{2app}\}}{\partial x_2} &= -1; \quad \frac{\partial\{\Delta\chi_{2app}\}}{\partial w_2} = \frac{x_1 - \chi_{mix}}{w_2^2}. \end{aligned}$$

Therefore,

$$\Delta\{\Delta\chi_{2app}\} = \frac{1}{w_2} \Delta\chi_{mix} + \left\{1 - \frac{1}{w_2}\right\} \Delta x_1 - \Delta x_2 + \left\{\frac{x_1 - \chi_{mix}}{w_2^2}\right\} \Delta w_2 \quad (12)$$

The effects of the errors in the four variables on the behaviour of  $\Delta\chi_{2app}$  can now be discussed.

**1. The Effect of Errors in  $x_2$ .**—If only  $x_2$  is subject to error, then

$$\Delta\{\Delta\chi_{2app}\} = -\Delta x_2 \quad . \quad . \quad . \quad (13)$$

The effect of a positive or negative error in  $x_2$  will be to reduce or increase  $\Delta\chi_{2app}$ , respectively, by the same amount. When non-linear deviations are absent,  $\Delta\chi_{2app}$  will be constant and equal, but opposite in sign to, the error in  $x_2$ . This error may be the cause of the change in sign of  $\Delta\chi_{2app}$  often observed at the higher concentrations (80-90 % of component 2), as illustrated by Table III (ref. 18), Table IV (ref. 7, 9 and 22), and the data for 10° C. in Table V. In these examples the effect of  $\Delta x_2$  would be superposed on a variation induced by errors to be described below.

**2. The Effect of Errors in  $x_1$ .**—If only  $x_1$  is subject to error then

$$\Delta\{\Delta\chi_{2app}\} = \left\{1 - \frac{1}{w_2}\right\} \Delta x_1 = \frac{-w_1}{w_2} \Delta x_1 \quad . \quad . \quad (14)$$

The error in  $\Delta\chi_{2app}$  is thus opposite in sign to that in  $x_1$ , for  $w_1$  and  $w_2$  can only be positive. Equation (14) can be re-written

$$w_2[\Delta\{\Delta\chi_{2app}\} - \Delta x_1] = -\Delta x_1 \quad . \quad . \quad . \quad (15)$$

For the results on any one system  $\Delta x_1$  will be constant if the same material was used in making each mixture so that the curve of  $\Delta\{\Delta\chi_{2app}\}-w_2$  will, as equation (15) shows, be a rectangular hyperbola asymptotically approaching the two reference axes,  $w_2 = 0$  and  $\Delta\{\Delta\chi_{2app}\} = 0$ . The behaviour of the experimental values of  $\Delta\chi_{2app}$  closely resembles this in the rise or fall at low concentrations ( $w_2 \rightarrow 0$ ) and the approach at the higher concentrations ( $w_2 \rightarrow 1$ ) to a limiting value of zero. Combining this effect with that of errors in  $x_2$ , a curve is obtained which reflects all the main characteristics of the experimental curves derived from, say, the data of Trew and Watkins on *n*-butyl alcohol-*n*-propyl alcohol and

*n*-butyl alcohol-*iso*-propyl alcohol mixtures. Fig. 2 shows these experimental curves together with the hyperbolæ (assuming  $\Delta\chi_1 = 0$ ) which best fit the data.

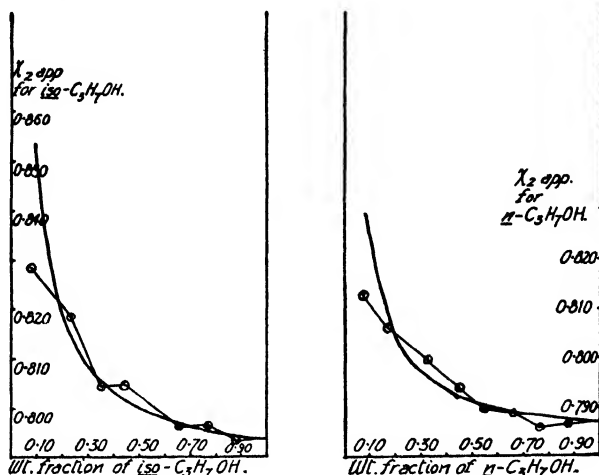


FIG. 2.— $\chi_{2app}$ - $w_2$  curves from the data of Trew and Watkins.<sup>16</sup>

FIG. 2a.—*n*-C<sub>4</sub>H<sub>9</sub>OH-*iso*-C<sub>3</sub>H<sub>7</sub>OH.  
 ○—○—○ = exptl. curves. Hyperbola based on average value of  $\Delta\chi_1$  for *n*-C<sub>4</sub>H<sub>9</sub>OH (—0.0064) derived from the exptl. curves.

FIG. 2b.—*n*-C<sub>4</sub>H<sub>9</sub>OH-*n*-C<sub>3</sub>H<sub>7</sub>OH.  
 ○—○—○ = exptl. curves. Hyperbola based on average value of  $\Delta\chi_1$  for *n*-C<sub>4</sub>H<sub>9</sub>OH (—0.0044) derived from the exptl. curves.

3. The Effect of Errors in  $w_2$ .—If  $w_2$  were the only variable in error, then

$$\Delta\{\Delta\chi_{2app}\} = \frac{\chi_1 - \chi_{mix}}{w_2^2} \cdot \Delta w_2 \quad . \quad . \quad . \quad (16)$$

The sign of the errors in  $\Delta\{\Delta\chi_{2app}\}$  will depend on the sign of  $(\chi_1 - \chi_{mix})$ , as Table VII shows. It will be noticed that if the real deviations from additivity are small or  $|\chi_1 - \chi_2|$  large, then  $\chi_1 \leq \chi_{mix} \leq \chi_2$ , over the range  $0 < w_2 < 1$ . Hence, for most real cases the sign of the error in  $\Delta\chi_{2app}$  will depend in the same way on the sign of  $(\chi_1 - \chi_2)$ . As  $w_2 \rightarrow 0$ , the value of the error  $\Delta\{\Delta\chi_{2app}\}$  corresponding to a given error  $\Delta w_2$  will increase rapidly, and the curve of  $\Delta\{\Delta\chi_{2app}\}$  against  $w_2$  will theoretically approach the axis  $w_2 = 0$  asymptotically. At the higher concentrations the curve should approach  $\Delta\{\Delta\chi_{2app}\} = 0$ . This behaviour, however, only holds for an error in  $w_2$ , constant in both sign and magnitude. Generally this is not true, and the result of the imperfection is to scatter the points on each side of the  $\Delta\{\Delta\chi_{2app}\} = 0$  axis in fairly equal numbers, the scattering covering larger and larger values of  $\Delta\{\Delta\chi_{2app}\}$  as  $w_2 = 0$  is approached. Superposing this effect on the previous two, the curve  $\Delta\chi_{2app}$ - $w_2$  may now be expected to be a rectangular

TABLE VII.—ERRORS IN  $w_2$ .

Sign of Errors in $w_2$ .	Sign of Errors in $\Delta\chi_{2app}$ .	
	$\chi_1 > \chi_{mix}$ .	$\chi_1 < \chi_{mix}$ .
+	+	—
—	—	+

hyperbola approaching  $w_1 = 0$  and  $\Delta\chi_{2app} = -\Delta\chi_2$  asymptotically, and with the experimental points becoming more and more widely scattered about the hyperbola as  $w_2 \rightarrow 0$ . This scattering will not, in general, be symmetrical since evaporation of the more volatile component, which is most likely to produce large errors in  $w_2$ , will be such that  $\Delta w_2$  will have a tendency towards either positive or negative values and will thus both shift and, as the  $\Delta w_2$  variation is not hyperbolic, distort the hyperbola produced by  $\Delta\chi_1$ .

**4. The Effect of Errors in  $\chi_{mix}$ .—**For errors in  $\chi_{mix}$  alone

$$\Delta(\Delta\chi_{2app}) = \frac{1}{w_2} \cdot \Delta\chi_{mix} \quad . \quad . \quad . \quad (17)$$

Here again a hyperbola would be found if  $\Delta\chi_{mix}$  were constant in sign and magnitude but, since neither of these conditions will generally be

TABLE VIII.—BEHAVIOUR OF HYPOTHETICAL  $\chi_{dev}$  CURVES.

Curve.	% of 1 for Max. Dev.	Max. Dev. %.	Lt. $w_2 \rightarrow 0$ $\chi_{dev}/w_2$ .	Behaviour of $\Delta\chi_{2app}-w_2$ curves.
$\chi_{dev} = 0.05$ ( $w_2 - w_2^2$ )	50	2.00	0.05	$\Delta\chi_1 = -0.0063$ ; hyperbola visibly approaches the straight line $\Delta\chi_{2app} = 0.05(1 - w_2)$ at ca. 40 %.
$\chi_{dev} = 0.05$ ( $w_2 - w_2^3$ )	70.7	2.09	0.05	$\Delta\chi_1 = -0.0063$ ; hyperbola visibly approaches the curve $\Delta\chi_{2app} = 0.05(1 - w_2^4)$ at ca. 40 %.
$\chi_{dev} = -0.05$ ( $w_2 - w_2^{\frac{1}{2}}$ )	25	2.29	$\infty$	$\Delta\chi_1 = -0.0063$ ; hyperbola visibly approaches the curve $\Delta\chi_{2app} = -0.05(1 - w_2^{\frac{1}{2}})$ , itself very like a hyperbola, at ca. 40 %.

fulfilled, the effect of  $\Delta\chi_{mix}$  will be to reinforce the scattering due to  $\Delta w_2$ . As the theoretical  $\Delta(\Delta\chi_{2app}) - \Delta\chi_{mix}$  curve is hyperbolic, there will be no distortion of the  $\Delta\chi_1$  hyperbola.

We may now consider the effect produced in systems in which real deviations do occur. Equation (7),  $\Delta\chi_{2app} = \chi_{dev}/w_2$ , will hold only when there are no experimental errors in  $\chi_{mix}$ ,  $w_2$ ,  $\chi_1$  and  $\chi_2$ , but, generally, the effects described above will be superposed on the  $\chi_{dev}/w_2$  curve. It will be immediately obvious that the lower the concentration the more will the hyperbolic effect predominate. The real  $\Delta\chi_{2app}-w_2$  curves will be hyperbolæ, greatly distorted at the higher concentrations, and approximating more and more closely to the ideal hyperbolæ as  $w_2 \rightarrow 0$ .  $\chi_{dev}/w_2$  may itself approach an infinite limit as  $w_2 \rightarrow 0$ , in which case the experimental curve will be almost indistinguishable from a hyperbola—and more particularly so when experimental errors and scattering are large.

Details of three curves, which are very similar to the experimental  $\chi_{mix}-w_2$  curves, for mixtures of two hypothetical substances of susceptibilities 0.500 (component 1) and 0.700 (component 2) are given in Table VIII and in Fig. 3-6. For the first curve of Table VIII both positive and negative deviations are shown, together with the theoretical curves of  $\Delta\chi_{2app}-w_2$ , calculated for an error of  $-0.0063$  in the susceptibility of component 1. This represents an error of about 1 %, not excessively large, nor indeed uncommon, in this type of measurement. Deviations of as much as 2 % are rarely encountered, so that these three  $\Delta\chi_{2app}-w_2$

curves show the effect of real deviations even more strongly than can be expected, or, indeed, is found in the experimental curves. Even so,

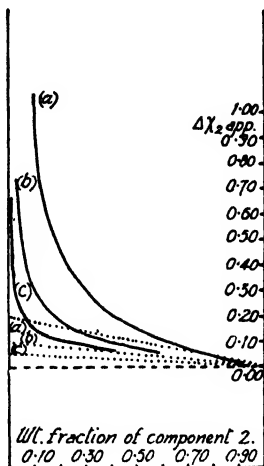


FIG. 3a.—Error hyperbolæ based on the "true"  $\chi_{dev}/w_2$  curve for Fig. 3b (b).—central . . . line.

- (a)  $\Delta\chi_1 = -0.1000$ .
- (b)  $\Delta\chi_1 = -0.0253$ .
- (c)  $\Delta\chi_1 = -0.0063$ .

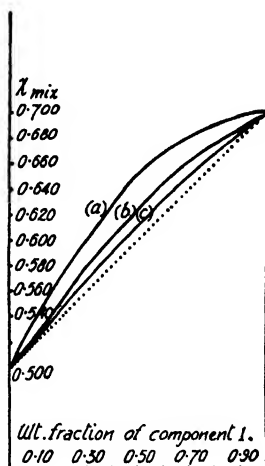


FIG. 3b.—Hypothetical mixture curves for  $\chi_{mix} = \chi_{add} + k(w_2 - w_2^2)$ .

- (a)  $k = 0.20$ .
- (b)  $k = 0.10$ .
- (c)  $k = 0.05$ .

it is clear that the concentration range up to 40 % would have to be excluded from a discussion of the deviations.

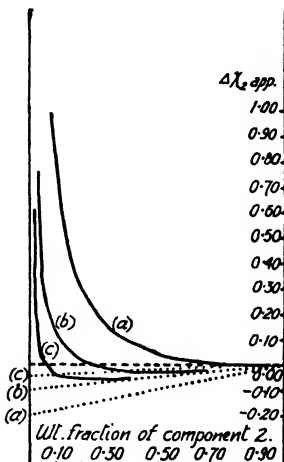


FIG. 4a.—Error hyperbolæ as for Fig. 3a.

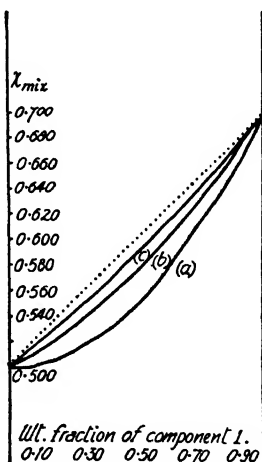


FIG. 4b.—Hypothetical mixture curves for  $\chi_{mix} = \chi_{add} + k(w_2 - w_2^2)$ .

- (a)  $k = -0.20$ .
- (b)  $k = -0.10$ .
- (c)  $k = -0.05$ .

Before discussing the determination of the errors, reference must be made to two other recent applications of this argument.

It has been observed in recent years that the molar polarisation of one component of a binary mixture, calculated by the usual additivity

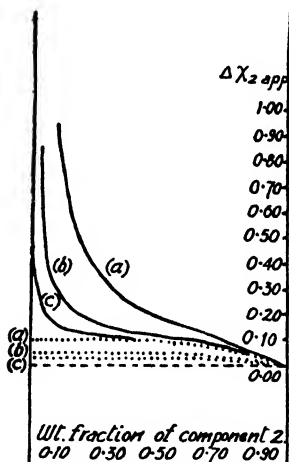


FIG. 5a.—Error hyperbolæ as for Fig. 3a.

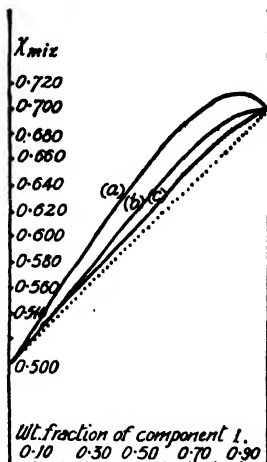


FIG. 5b.—Hypothetical mixture curves for  $\chi_{mix} = \chi_{add} + k(w_2 - w_2^0)^2$ .

- (a)  $k = 0.10$ .
- (b)  $k = 0.05$ .
- (c)  $k = 0.025$ .

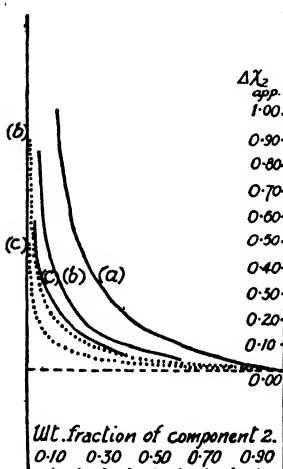


FIG. 6a.—Error hyperbolæ as for Fig. 3a, but the true  $\chi_{dev}/w_2$  for Fig. 3b (a) is not shown.

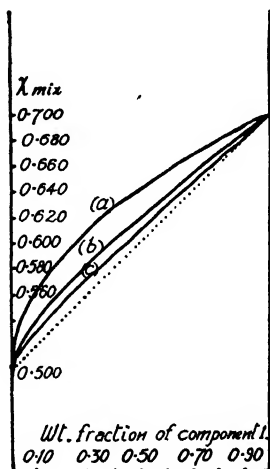


FIG. 6b.—Hypothetical mixture curves for  $\chi_{mix} = \chi_{add} + k(w_2 - w_2^0)^2$ .

- (a)  $k = -0.20$ .
- (b)  $k = -0.10$ .
- (c)  $k = -0.05$ .

relation,  $P_2 = (P_2 - P_1 n_1)/n_2$  (where  $P_1$ ,  $P_2$  and  $P_{12}$  are the molar polarisations of components 1, 2 and solution, and  $n_1$  and  $n_2$  are the mol. fractions of the components), shows anomalous behaviour in very dilute

solutions, less than 0.0005 M.<sup>26,29</sup> Davis, Bridge, and Svirbely<sup>30</sup> and Lander and Svirbely<sup>31</sup> have shown that this anomalous behaviour, which takes the form of a hyperbolic deviation at low values of  $n_1$ , the  $P_1$ - $n_2$  curve approaching the  $n_2 = 0$  axis asymptotically, was due to an error in  $P_1$ , and that the sign of the error determined the sign of the deviation. The error could, in this case, be determined by an extrapolation to  $n_2 = 0$  of the curves of dielectric constant against  $n_1$ . This gave the true value of  $P_1$  for the solvent used in the mixtures, and the value of  $\Delta P_1$ .

Another application is found in the investigation of the molar depression constant of camphor. Meldrum, Saxon and Jones,<sup>32</sup> and Pirsch<sup>33</sup> noticed that the molar depression constant,  $K$ , of camphor and camphor dibromide increased rapidly at low concentrations of solute. They both observed that the curve of  $K$  against molar concentration of solute was independent of the nature of that solute. Pirsch also studied bornylamine as solvent, and it can be seen from his data that, although for small values the calculated and observed molecular weights are very close, the correspondence is not as good with solutes of higher molecular weights, considering solutions of approximately equal weight-per cent. of solute. This behaviour is similar to that of camphor and camphor dibromide since the higher the molecular weight is the lower is the mol. fraction (at constant wt.-%), and hence the greater the deviation. Ricci<sup>34</sup> showed that these hyperbolic anomalies could be explained if it is assumed that  $\Delta T$ , the depression of the melting point, is subject to a small error, constant in sign and magnitude. Thus  $K = \Delta T/m$ , where  $m$  is the molar concentration of solute, and

$$\Delta K = \frac{\Delta\{\Delta T\}}{m} - \frac{\Delta T}{m^2} \cdot \Delta m.$$

The first term represents a hyperbolic deviation, the second a scattering, becoming progressively wider towards the lower concentrations. Ricci suggested that the melting and grinding processes, used in preparing a sample for a melting point determination, decomposed the camphor to a small and fairly constant extent. This explains, of course, why the same  $K/m$  curve is obtained for all solutes, and the sign of such an error is compatible with the observed trend of  $K$  at the lower concentrations. Ricci's diagram, where the first term has been applied as a correction, illustrates well the scattering as lower concentrations are attained. Decomposition to the extent of only 0.005 M. is sufficient to account for Meldrum's results.

#### 4. Determination of the Errors.

The success of Svirbely and Ricci suggested that the constant errors occurring in the present work could be evaluated by some suitable procedure. The value of such a determination lies in the fact that it would enable one to find the  $\Delta\chi_{\text{app}}-w_2$  curve for the real deviations, removing the present hyperbolic concealment. Two methods suggested themselves; one an extrapolation of the experimental  $\chi_{\text{mix}}-w_2$  curves to the  $w_2 = 0$  axis, the other a determination from the calculated  $\Delta\chi_{\text{app}}-w_2$  curves.

**1. Extrapolation of the  $\chi_{\text{mix}}-w_2$  curves.**—This method corresponds to the extrapolation method of Svirbely *et al.*<sup>29</sup> for determining  $\Delta P_1$ .

<sup>26</sup> Halverstadt and Kumler, *J. Amer. Chem. Soc.*, 1942, **64**, 2988.

<sup>27</sup> Hoecker, *J. Chem. Physics*, 1936, **4**, 431.

<sup>28</sup> Maryott, *J. Amer. Chem. Soc.*, 1941, **63**, 3079.

<sup>29</sup> Svirbely, Abland and Warner, *ibid.*, 1935, **57**, 652.

<sup>30</sup> Davis, Bridge and Svirbely, *ibid.*, 1943, **65**, 857.

<sup>31</sup> Lander and Svirbely, *ibid.*, 1944, **66**, 235.

<sup>32</sup> Meldrum, Saxon and Jones, *ibid.*, 1943, **65**, 2023.

<sup>33</sup> Pirsch, *Ber.*, 1932, **69**, 1229.

<sup>34</sup> Ricci, *J. Amer. Chem. Soc.*, 1944, **66**, 658.



However, even a casual inspection of published  $\chi_{mix}-w_2$  curves, or of curves constructed from published data, reveals in the most convincing manner the difficulty of successful extrapolation to  $w_2 = 0$  and  $w_1 = 1$ . When experimental figures are so erratic that it is difficult to decide whether deviations exist or not, none but the simplest extrapolation can be applied. There is, however, little value in a linear extrapolation, since this assumes that the deviations do not exist, and will merely reduce the  $\Delta\chi_{sapp}-w_2$  curves to a symmetric, but scattered, distribution of points about the  $\Delta\chi_{sapp} = 0$  axis. Real deviations will in this way be reduced to errors in the extrapolated values of the susceptibilities of the two components.

**2. Determination from the  $\Delta\chi_{sapp}-w_2$  curves.**—If we neglect the effect of  $\chi_{dev}$  on the hyperbolæ, we can attempt a determination of  $\Delta\chi_1$ . Thus, from (14)

$$\Delta\{\Delta\chi_{sapp}\} = \frac{w_2 - 1}{w_2} \cdot \Delta\chi_1 = \left\{1 - \frac{1}{w_2}\right\} \cdot \Delta\chi_1.$$

If then we plot not  $\Delta\{\Delta\chi_{sapp}\}$ , since  $\Delta\{\Delta\chi_{sapp}\} = \Delta\chi_{sapp} - \frac{\chi_{dev}}{w_2}$  but  $\Delta\chi_{sapp}$  against  $1/w_2$ , then both the slope and the intercept on the axis  $1/w_2 = 0$  will have values equal to  $-\Delta\chi_1$ . This procedure can only be justified when  $\chi_{dev}-w_2$  is small compared with  $\Delta\chi_{sapp}$ , i.e. at low values of  $w_2$ . However, the scattering effect of errors in  $\chi_{mix}$  and  $w_2$  is so large in this region—most  $\Delta\chi_{sapp}-w_2$  curves are wildly zig-zag below  $w_2 = 0.5$ —that an extrapolation is impossible. Extrapolation for large values of  $w_2$  is meaningless, since  $\chi_{dev}/w_2$  is no longer small compared with  $\Delta\chi_{sapp}$ , and the value of  $\Delta\chi_1$  obtained will represent not the hyperbolic region of the curve but the real deviations.

## 5. Conclusions.

The behaviour of the apparent susceptibility of almost every one of the 69 binary organic liquid mixtures studied points to the existence of considerable experimental errors in the published data on the diamagnetism of such mixtures. Although the greater part of the qualitative evidence is in favour of small but real deviations from additivity, no quantitative measure of any accuracy can be derived. The method of calculation, proposed by Angus and Hill,<sup>12</sup> although having considerable possibilities when accurate and self-consistent data become available, cannot be applied with any profit to the data so far recorded, since it tends to accentuate the effect of small errors of measurement. In this connection it is interesting to note that the data of Angus and Hill are strongly hyperbolic, as might be expected from the low concentrations involved.

The work presented above suggests certain important points in connection with an experimental investigation on the subject. The first, somewhat elementary, but to which, apparently, adherence has been by no means invariable, is that the pure components, used in the measurement of "solvent" and "solute" susceptibilities, must be used in preparing the actual mixtures. The absolute values of their susceptibilities are of little importance, but  $\chi_1$  and  $\chi_2$  must accurately represent the susceptibilities of the components. The second point is that the errors in  $\chi_{mix}$  and  $w_2$  should be as small as possible. Accurate values of these variables will allow of an extrapolation of the  $\chi_{mix}-w_2$  curves, and, by decreasing the scattering, of the determination of  $\Delta\chi_1$  from the calculated  $\Delta\chi_{sapp}-w_2$  curves. If this is done, then a correction for  $\Delta\chi_1$  can be applied to the values of  $\Delta\chi_{sapp}$  and the effect of the real deviations freed from the objectionable hyperbolicity observed at present.

If these conditions are fulfilled, then the method will undoubtedly lead to quantitative conclusions regarding chemical and physical changes

in such mixtures and, by a correlation of the magnetic data with those on other physical properties (viscosity, surface tension, refractive index, etc.), will provide a possible test for theories of the structure of liquids and of molecular interaction.

## 6. Summary.

The calculation of the apparent susceptibility ( $\chi_{\text{app}}$ ) of one component of a binary liquid mixture is discussed and a relationship between this value and the magnitude of deviations ( $\chi_{\text{dev}}$ ) from strictly additive behaviour is derived. The change of susceptibility, an index of chemical or physical reaction in the mixture, is given by  $\Delta\chi_{\text{app}} = \chi_{\text{dev}}/w_1$ . Over sixty sets of published data have been examined, but detailed discussion of  $\Delta\chi_{\text{app}}$  values is restricted to the systems formic acid-water, acetic acid-water, *n*-butyl alcohol-*n*-propyl alcohol, acetone-chloroform, and benzene-carbon tetrachloride. The progressive type of deviation shown by all systems, and amply demonstrated by those selected, suggested that the behaviour arose from the method of calculation or minor inaccuracies in certain variables on which  $\Delta\chi_{\text{app}}$  depends. The effect of errors in these variables has been computed and indicate that the real magnitude of observed deviations is not readily ascertainable quantitatively at present owing to the fact that the employed method of calculation can only profitably be applied when self-consistent and accurate data become available.

## Résumé.

On calcule la susceptibilité apparente ( $\chi_{\text{app}}$ ) d'un composant d'un mélange binaire liquide; on discute ce calcul et on établit une relation entre cette valeur et l'importance de l'écart ( $\chi_{\text{dev}}$ ) du comportement strictement additif. L'écart progressif, montré par 69 systèmes examinés, suggère que cela est dû à la méthode de calcul ou à de légères inexactitudes dans certaines variables dont dépend  $\Delta\chi_{\text{app}}$ ; on a calculé l'effet d'erreurs sur ces variables.

## Zusammenfassung.

Der Artikel bespricht die Berechnung der scheinbaren Suszeptibilität ( $\chi_{\text{app}}$ ) einer Komponente in einem binären Flüssigkeitsgemisch. Es wird eine Beziehung zwischen diesem Wert und der Grösse der Abweichung ( $\chi_{\text{dev}}$ ) von streng additivem Verhalten abgeleitet. Der fortschreitende Charakter dieser Abweichung, der in 69 untersuchten Systemen gefunden wird, deutet darauf hin, dass diese auf die Berechnungsmethode zurückzuführen ist oder auf kleine Ungenauigkeiten in bestimmten Variablen, von denen  $\Delta\chi_{\text{app}}$  abhängt; der Effekt solcher Ungenauigkeiten ist berechnet worden.

---

# MAGNETOCHEMICAL INVESTIGATIONS. PART VI. ADDITIONAL NOTES ON STANDARDIZATION AND TECHNIQUE.

By W. ROGIE ANGUS AND (THE LATE) DONALD V. TILSTON.

*Received 10th April, 1946.*

## 1. Introduction.

In Part I of this series<sup>1</sup> the magnet system and general technique of measurement have been described in some detail. Resumption of

<sup>1</sup> Angus and Hill, *Trans. Faraday Soc.*, 1943, 39, 185.

experimental work, after the lapse of some years, made it necessary to recalibrate the apparatus; this paper deals with certain modifications of earlier methods which, it is believed, are more reliable than those formerly used.

The principle of the Gouy method may be fundamentally represented by the simplified equation  $w\chi = c + \alpha F$  . . . (I) in which  $w$  is the weight of an approximately cylindrical specimen of material of specific susceptibility  $\chi$ ;  $c = \kappa l A$  and  $\alpha = 2l/(H_1^2 - H_2^2)$  are constants for a particular tube of cross-sectional area  $A$ , suspended in the pole-gap so that its bottom, at the centre of the gap, is in a field of strength  $H_1$  and the top of the specimen,  $l$  cm. above the centre, is in a field of strength  $H_2$ ;  $\kappa$  is the volume susceptibility of air; and  $F$  is the force in mg. actually experienced by the specimen after applying the necessary correction for the force experienced by the glass tube containing the specimen.

## 2. The Constants $c$ and $\alpha$ .

Since  $c = \kappa l A = \kappa v$  (where  $v$  is the volume of specimen examined)  $c$  may be evaluated precisely if  $v$  or its components  $l$  and  $A$ , can be determined accurately. In the earlier standardisation  $A$  and  $l$  were measured directly, but there are inherent uncertainties in this method, e.g. possible lack of uniformity of bore, non-planarity of the sealed bottom end of the tube, and the need for applying a meniscus correction. The modification now used consists in filling the previously-weighed tube to the graduation mark with conductivity water or (preferably) benzene at a known temperature, weighing it (on the Gouy balance), and calculating  $v$  from density-temperature tables. This yields a value which not only includes the meniscus correction but has the advantage that from a series of values of  $v$  at different temperatures, the average value,  $\bar{v}$ , can be calculated and the deviation,  $\Delta\bar{v}$ , of individual values of  $v$  from  $\bar{v}$  can be derived. The fraction  $\Delta\bar{v}/\bar{v}$ , which can be shown to be equal to  $\Delta\chi/\chi$ , is a measure of the accuracy of filling the tube and also a measure of the errors in  $\chi$  from this cause. It has been found that  $\Delta\bar{v}/\bar{v}$  is of the order of 0.02 % and, since the bore of the tube may be taken as sensibly uniform, this variation in volume corresponds with a variation in length; and, thus, for lengths of the order of 6 cm. amounts to 0.01 mm.

The constant  $\alpha$  cannot be determined with the same precision as  $c$ . Experimental difficulties of determining  $l$ ,  $H_1$ , and  $H_2$  accurately are great and are usually circumvented by the employment of a relative method in which the force exerted on a specimen of material of high purity and accurately known susceptibility is measured and  $\alpha$  is calculated from equation (1). The choice of reference substance is of such great and fundamental importance in respect of subsequent measurements as to merit some general discussion here. Methods of purification are well established for numerous compounds but it is rare to find really concordant magnetic data for common substances.<sup>2, 3</sup> Three choices are available: (1) solid paramagnetic substances, (2) liquid paramagnetic substances, (3) diamagnetic substances.

(1) Solids must be finely ground, and homogeneously and tightly packed, and, since the choice is limited by available magnetic data, to hydrated salts of Ni, Cu, Fe, and Mn, it cannot be ignored that the use of such salts involves other possibilities of error, e.g. efflorescence during grinding, the presence of the metal in different valency states, non-uniform packing, filling "level" to the graduation mark on the tube and thus leaving out of account the meniscus. There is, however, the great advantage that the magnetic effect is large and that errors of weighing are extremely small.

<sup>2</sup> Angus, *Ann. Reports*, 1941, 38, 27.

<sup>3</sup> Sugden, 9th *Liversidge Lecture*, *J. Chem. Soc.*, 1943, 328.

(2) Liquid paramagnetic standards are usually aqueous solutions of strongly paramagnetic salts, the first choice being  $\text{NiCl}_2$ .<sup>4</sup> The solution must fulfil certain requirements: it must obey the additivity law connecting the susceptibilities of solution, solute, and solvent,<sup>5</sup> it must be prepared from solute and solvent of high purity and known susceptibilities, must be relatively concentrated, chemically stable, and subject to precise chemical analysis. It has been noted that the magnetic behaviour of the susceptibility tube is sometimes affected by the use of  $\text{NiCl}_2$  solutions, but this is almost certainly a peculiarity of the particular glass used in making the tube.

(3) The use of diamagnetic substances has the disadvantage that the force experienced by the specimen is very much less (approximately 3 mg. as compared with approximately 100 mg. for solid paramagnetic substances<sup>6</sup>) and, consequently, cannot be measured with the same accuracy. Nevertheless, it has the advantage, particularly if subsequent investigations are contemplated on diamagnetic substances, that the force exerted on the "standard" is of the same type and order as that experienced by the material being measured later.

All three classes of standard have been tested out and it may be succinctly stated (a) that with solid paramagnetic substances the uncertainties attaching to their use outweigh the advantages, and that the mean value of  $\alpha$  derived has a probable error of 0.5 %; (b) that liquid paramagnetic substances involve tedious and frequent analysis; (c) that diamagnetic standards are to be preferred.

Like Selwood,<sup>7</sup> we favour using benzene ( $\chi = -0.702 \times 10^{-6}$ )<sup>1</sup> as standard; using this standard, Mr. G. Stott has carried out an extensive series of determinations of  $\alpha$  and finds that the mean value has a probable error of 0.05 %.

Recently Trew and French<sup>8</sup> have advocated the use of diamagnetic standards, but it is felt necessary to enter a caveat against the use of water as the standard because of the difficulty of ensuring its purity, and also because of the existing uncertainty regarding the temperature coefficient of its susceptibility.

### 3. Calibration of the Magnetic Field.

Repetition of calibration has established that, since the original calibration, no appreciable decrease in field strength has occurred owing to a spreading breakdown of insulation of adjacent coils in the magnet. Periodic checking of the  $\alpha$  values for a particular tube ensures that the field developed by the magnet does remain constant. The recorded values for field strength at different distances from the centre of the pole-gap (see Part I) have been confirmed by the calculated values given in Part VII.

The authors record their thanks to the Department of Scientific and Industrial Research for a maintenance grant to one of them (D. V. T.), and to Professor E. D. Hughes for his interest in the work.

### Summary.

Sources of error in calibration of the Gouy apparatus are critically examined and certain modified procedures are described.

<sup>4</sup> Nettleton and Sugden, *Proc. Roy. Soc. A*, 1939, **173**, 313.

<sup>5</sup> Stoner, *Magnetism and Matter* (Methuen, London, 1934), pp. 325-334.

<sup>6</sup> Ref. <sup>1</sup>, p. 189.

<sup>7</sup> Selwood and collaborators, *J. Amer. Chem. Soc.*, 1939, **61**, 3168; 1940, **62**, 2765, 3055; 1941, **63**, 2509.

<sup>8</sup> Trew and French, *Trans. Faraday Soc.*, 1945, **41**, 439.

## Résumé.

On examine d'un point de vue critique les causes d'erreurs dans l'étalonnage de l'appareil de Gouy et on décrit certaines parties de la technique que l'on a modifiées.

## Zusammenfassung.

Fehlerquellen in der Eichung des Gouy'schen Apparats werden kritisch geprüft und bestimmte Modifikationen der Vorgangsweise beschrieben.

Department of Chemistry,  
University College of North Wales,  
Bangor.

## MAGNETOCHEMICAL INVESTIGATIONS. PART VII. CALCULATIONS ON THE MAGNETIC FIELD.

BY (THE LATE) DONALD V. TILSTON.

Received 10th April, 1946.

In earlier parts the experimental calibration<sup>1, 2</sup> of the magnetic field and its comparison with the calculated curves relating field strength to the distance from the centre of the pole-gap have been discussed. This paper will describe the method of calculation. An expression for the field strength at a point on the vertical line through the centre of the pole-gap is derived and integrated between finite limits related to the extent and shape of the pole-piece. The number of cases capable of solution becomes limited by mathematical difficulties to the following four: (a) magnet with point poles; (b) magnet with line poles; (c) magnet with square poles (vertical line parallel to the side of the square); and (d) magnet with square poles (vertical line parallel to diagonal of the square).

The general technique of integration is similar for all except (a) which requires no integration. Consequently, it is proposed to discuss here only case (d), which, whilst the most complicated of the four cases, does contain all the details of the other integrations.

**Calculation of the Field/distance Curve along the Diagonal of a Square Pole-Piece.**—Consider a unit North pole at the point P (Fig. 1), which is situated on the diagonal  $y = z$ . EFGH is a square pole-piece (North) of a magnet, side  $2b$ , parallel to, and distant  $-a$  from, the  $zOy$  plane; and there is a similar (but South) pole-piece lying parallel at  $x = a$ . Let the magnetisation per unit area of EFGH be  $I$ . The force,  $2dF_z$  in

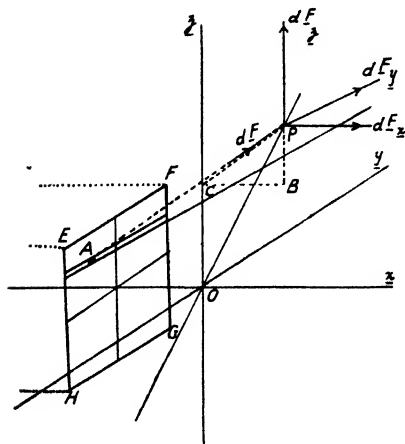


FIG. 1.

the direction parallel to  $Ox$  which is exerted on the unit pole at P by the element of area  $dydz$  at A on the strip MN, width  $dz$ , distance  $z$  from  $yOx$ ,

<sup>1</sup> Angus and Hill, *Trans. Faraday Soc.*, 1943, **39**, 185 (Part I).

<sup>2</sup> Angus and Tilston, *ibid.*, preceding paper.

and by  $A'$  (its image with respect to the  $zOy$  plane) will also be the field strength  $dH_z$  due to  $A$  and  $A'$  and can be expressed as

$$dH_z = \frac{-2aI \cdot dydz}{\{(h-y)^2 + a^2 + (k-z)^2\}^{3/2}} \quad (1)$$

The total field strength at  $P$ ,  $H_z$ , will be the double definite integral of this function, taken between the limits  $y = \pm b$  and  $z = \pm b$ .

$$H_z = \iint_D dH_z = 2 \iint_D dF_z = -2aI \int_{-b}^{+b} dz \int_{-b}^{+b} \frac{dy}{\{(h-y)^2 + a^2 + (k-z)^2\}^{3/2}} \quad (2)$$

It is more convenient to consider the two integrals separately :

$$\int_b^{+b} \frac{dy}{\{(h-y)^2 + a^2 + (k-z)^2\}^{3/2}};$$

Let

$$a^2 + (k-z)^2 = \lambda^2$$

$$(y-h) = \lambda \tan \theta.$$

Then

$$dy = \lambda \sec^2 \theta \cdot d\theta \text{ and}$$

$$\int_{y=-b}^{y=+b} \frac{\lambda \sec^2 \theta \cdot d\theta}{\{\lambda^2 \tan^2 \theta + \lambda^2\}^{3/2}} = -\frac{1}{\lambda^2} \left[ \sin \theta \right]_{y=-b}^{y=+b} \quad (3)$$

But it can be shown that  $\sin \theta = \frac{y-h}{\{(y-h)^2 + \lambda^2\}^{1/2}}$  and hence, from equation (3),

$$\int = -\frac{1}{\lambda^2} \left[ \frac{(b-h)}{\{(b-h)^2 + \lambda^2\}^{1/2}} + \frac{(b+h)}{\{(b+h)^2 + \lambda^2\}^{1/2}} \right].$$

Substituting for  $\lambda$ , and returning to equation (2), we may reconstruct the integral with respect to  $z$ , splitting it into two portions. We then obtain

$$H_z = 2aI(b-h) \int_{-b}^{+b} \frac{dz}{\{a^2 + (k-z)^2\} \{(b-h)^2 + a^2 + (k-z)^2\}^{1/2}} + \quad (4a)$$

$$2aI(b+h) \int_b^{+b} \frac{dz}{\{a^2 + (k-z)^2\} \{(b-h)^2 + a^2 + (k-z)^2\}^{1/2}} \quad (4b)$$

Consider the first of these integrals, (4a); let  $k-z=w$ , then  $-dz=dw$ ; when  $z=b$ ,  $w=k-b$  and when  $z=-b$ ,  $w=k+b$ . On substitution the integral now becomes

$$\int = 2aI(b-h) \int_{k-b}^{k+b} \frac{dw}{\{a^2 + w^2\} \{(b-h)^2 + a^2 + w^2\}^{1/2}}.$$

Now, let  $w = a \tan \phi$ ,  $dw = a \sec^2 \phi \cdot d\phi$ , and  $a^2 + w^2 = a^2 \sec^2 \phi$ . The integral becomes

$$\int = 2aI(b-h) \int_{w=k-b}^{w=k+b} \frac{a \sec^2 \phi \cdot d\phi}{a^2 \sec^2 \phi \{(b-h)^2 + a^2 \sec^2 \phi\}^{1/2}}$$

$$\begin{aligned}
&= 2I(b-h) \int_{w=k-b}^{w=k+b} \frac{\cos \phi \cdot d\phi}{\{(b-h)^2 \cos^2 \phi + a^2\}^{\frac{1}{2}}} \\
&= 2I \int_{w=k-b}^{w=k+b} \frac{\cos \phi \cdot d\phi}{\left\{ \frac{(b-h)^2 + a^2}{(b-h)^2} - \sin^2 \phi \right\}^{\frac{1}{2}}} \\
&= \frac{2I}{\left\{ \frac{(b-h)^2 + a^2}{(b-h)^2} \right\}^{\frac{1}{2}}} \int_{w=k-b}^{w=k+b} \frac{d(\sin \phi)}{\left\{ 1 - \frac{(b-h)^2 + a^2}{(b-h)^2} \sin^2 \phi \right\}^{\frac{1}{2}}} \\
&= 2I \left[ \sin^{-1} \left\{ \frac{(b-h) \sin \phi}{\{(b-h)^2 + a^2\}^{\frac{1}{2}}} \right\} \right]_{w=k-b}^{w=k+b} \quad (5)
\end{aligned}$$

Similarly for (4b)

$$\int = 2I \left[ \sin^{-1} \left\{ \frac{(b+h) \sin \phi}{\{(b+h)^2 + a^2\}^{\frac{1}{2}}} \right\} \right]_{w=k-b}^{w=k+b} \quad (6)$$

Now

$$\frac{(b-h)}{\{(b-h)^2 + a^2\}^{\frac{1}{2}}} = \sin \tan^{-1} \frac{b-h}{a}, \quad \frac{(b+h)}{\{(b+h)^2 + a^2\}^{\frac{1}{2}}} = \sin \tan^{-1} \frac{b+h}{a} \quad (7)$$

and as

$$w = a \tan \phi, \quad \sin \phi = \sin \tan^{-1} w/a \quad (8)$$

Hence from (4), (5), (6), (7) and (8) and substituting the limits of (5) and (6)

$$\begin{aligned}
H_x &= 2I \left[ \sin^{-1} \left\{ \sin \tan^{-1} \left( \frac{b-h}{a} \right) \cdot \sin \tan^{-1} \left( \frac{k+b}{a} \right) \right\} \right. \\
&\quad - \sin^{-1} \left\{ \sin \tan^{-1} \left( \frac{b-h}{a} \right) \cdot \sin \tan^{-1} \left( \frac{k-b}{a} \right) \right\} \\
&\quad + \sin^{-1} \left\{ \sin \tan^{-1} \left( \frac{b+h}{a} \right) \cdot \sin \tan^{-1} \left( \frac{k+b}{a} \right) \right\} \\
&\quad \left. - \sin^{-1} \left\{ \sin \tan^{-1} \left( \frac{b+h}{a} \right) \cdot \sin \tan^{-1} \left( \frac{k-b}{a} \right) \right\} \right] \quad (9)
\end{aligned}$$

Reverting to the original argument it will be seen that, for all such points as P,  $y = z$ , and, hence,  $h = k = \xi$ , where  $\xi = \sqrt{2}OP$  and, since

$$\sin \tan^{-1}(-x) = \sin(-\tan^{-1}x) = -\sin \tan^{-1}x$$

equation (9) becomes

$$\begin{aligned}
H_x &= 2I \left[ \sin^{-1} \left\{ \sin^2 \tan^{-1} \left( \frac{\xi-b}{a} \right) \right\} + \sin^{-1} \left\{ \sin^2 \tan^{-1} \left( \frac{\xi+b}{a} \right) \right\} \right. \\
&\quad \left. - 2 \sin^{-1} \left\{ \sin \tan^{-1} \left( \frac{\xi-b}{a} \right) \cdot \sin \tan^{-1} \left( \frac{\xi+b}{a} \right) \right\} \right] \quad (10)
\end{aligned}$$

Equation (10) relates  $H_x$ , the resultant field strength at P, to  $\xi$ , a linear proportional function of OP, the distance from the centre of the pole-gap. Table I shows the corresponding functions for the other types of pole-pieces studied.

Comparison of these curves with the experimental curve shows good agreement, except at large distances, where the theoretical values approach the distance axis much more rapidly than do the experimental.

TABLE I.—FIELD-DISTANCE CURVES, CASES (a) TO (c).

Type of Pole-Piece.	Distance Variable.	$H_z$ .
(a) $2a$ apart, pole strength = $I$	$y$	$\frac{2aI}{(a^2 + y^2)^{3/2}}$
(b) $2a$ apart, length $2b$ , pole strength per unit length = $I$	$y$	$2I \left[ \sin \tan^{-1} \frac{(y-b)}{a} - \sin \tan^{-1} \frac{(y+b)}{a} \right]$
(c) $2a$ apart, side $2b$ , pole strength per unit area = $I$	$z$	$4I \left[ \sin^{-1} \left\{ \sin \phi \sin \tan^{-1} \left( \frac{z-b}{a} \right) \right\} - \sin^{-1} \left\{ \sin \phi \sin \tan^{-1} \left( \frac{z+b}{a} \right) \right\} \right]^*$

This may be explained by the fact that magnetisation with real pole-pieces is not confined to the area within the pole-gap. Table II gives the values of  $H_z$  calculated for case (b) with various assumptions regarding the variation of the magnetisation with distance along the pole-piece,

TABLE II.—FIELD-DISTANCE CURVES FOR MAGNETISATION OUTSIDE THE POLE-GAP.

Type of Magnetisation.	$H_z$ .
$I_{(a, b)} = I_0$	$H_z = I_0 \left[ \frac{I}{\{a^2 + (y-b)^2\}^{\frac{1}{2}}} + \frac{I}{\{a^2 + (y+b)^2\}^{\frac{1}{2}}} \right]$
$I_{(a, b)} = I_0 \cdot \frac{a}{x}$	$H_z = aI_0 \left[ \frac{I}{(y-b)^2} \cdot \sin \tan^{-1} \left( \frac{y-b}{a} \right) - \frac{2(y^2 + b^2)}{(y^2 - b^2)^{\frac{3}{2}}} + \frac{I}{(y+b)^2} \cdot \sin \tan^{-1} \left( \frac{y+b}{a} \right) \right]$
$I_{(a, b)} = I_0 \cdot \frac{a^2}{x^2}$	$H_z = a^2I_0 \left[ \frac{I}{(y-b)^3} \cdot \text{sh}^{-1} \left( \frac{y-b}{a} \right) + \frac{I}{(y+b)^3} \cdot \text{sh}^{-1} \left( \frac{y+b}{a} \right) - \frac{I}{(y-b)^3} \cdot \text{thsh}^{-1} \left( \frac{y-b}{a} \right) - \frac{I}{(y+b)^3} \cdot \text{thsh}^{-1} \left( \frac{y+b}{a} \right) \right]$

and assuming that magnetisation on the top and bottom of the pole-piece can produce a field within the pole-gap.

$I_{(a, b)}$  = pole strength per unit length at points  $(x, \pm b)$  such that  $x < -a, a < x$ .

$I_0$  = magnetisation at the four points  $(\pm a, \pm b)$ .

$$* \sin \phi = b/(b^2 + a^2)^{\frac{1}{2}}.$$



The graphs (Fig. 2-4) show how closely the theoretical values support the experimental when this last effect is included.

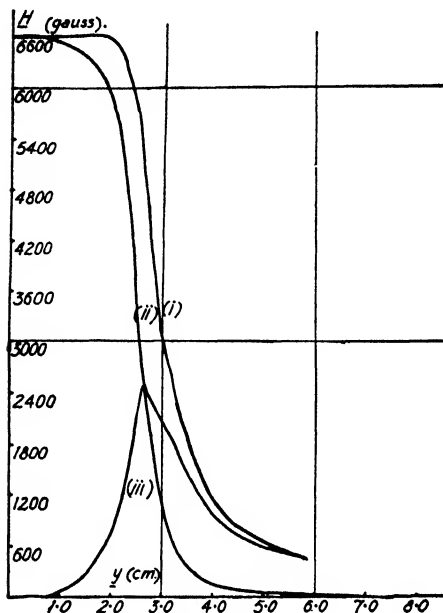


FIG. 2.—Field-distance curves.

- (i) Exptl. curve (ref. 1, Table II).
- (ii) Calc. curve from Table I, case (b), with  $a = 0.05$  cm.,  $b = 2.54$  cm.
- (iii) Difference of curves (i) and (ii).

An extension of this work to disc-shaped pole-pieces was attempted, using the methods of both Cartesian and radial analysis, but the integrals

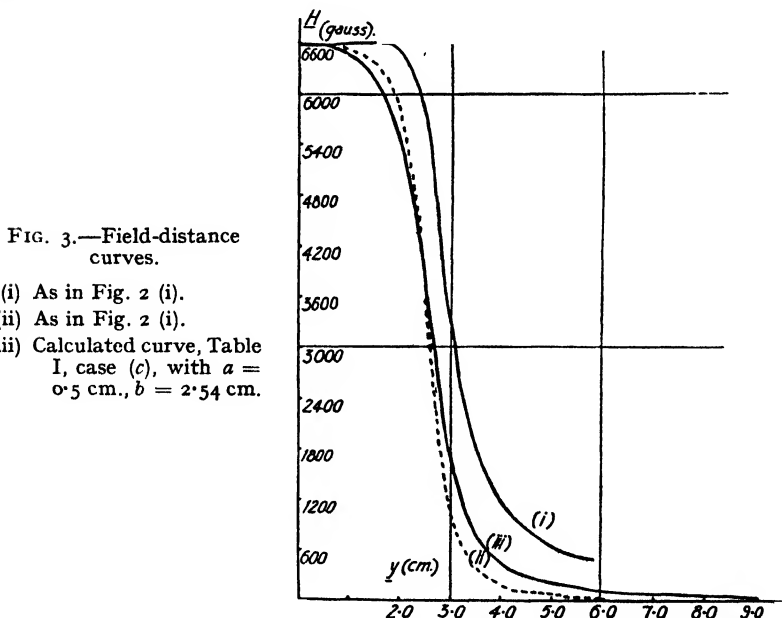


FIG. 3.—Field-distance curves.

- (i) As in Fig. 2 (i).
- (ii) As in Fig. 2 (i).
- (iii) Calculated curve, Table I, case (c), with  $a = 0.5$  cm.,  $b = 2.54$  cm.

proved too complex for solution. An idea of the curve which would be produced by a disc is obtained by comparing the curves for squares

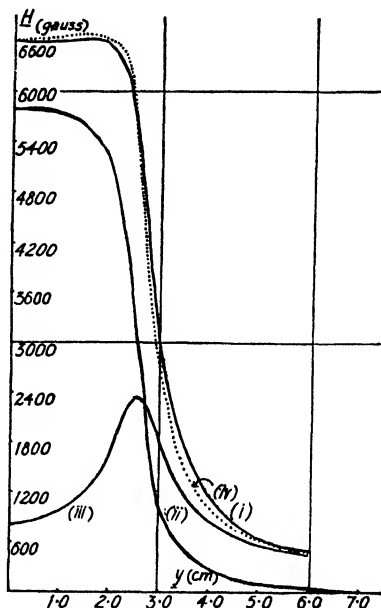
inscribed within (field strength along a line parallel to a diagonal) and outside the circle (field strength along a line parallel to a side). No very great difference exists between these two curves.

Recent papers by Bates and co-workers<sup>3</sup> give an account of a very elegant method of calculating the shape of pole-pieces required to produce

FIG. 4.—Field-distance curves.

- (i) As for (i) in Figs. 2 and 3.
- (ii) Calc. curve, Table I, case (b).
- (iii) Calc. curve Table II,  $I_{(a, b)} = I_0 a/x$ .
- (iv) Calc. curve, being sum of curves (ii) and (iii).

(Curve (iii) was calculated using values of  $I_0$  derived from the  $y = 3.0$  to  $y = 6.0$  region of curve (iii), Fig. 2. The curve (ii) was derived using a value of  $I$  calculated from the field at  $y = 0$  after subtracting that produced by curve (iii) above.



a field with given characteristics but the method has little in common with the present work.

This work was carried out during the tenure of a Department of Scientific and Industrial Research maintenance grant.

### Summary.

The calculation of curves relating field strength to the distance from the centre of the pole-gap is described for four types of pole-piece, viz. point poles, line poles, square poles with the vertical line (a) parallel to the side of the square and (b) parallel to the diagonal of the square.

### Résumé.

On calcule les courbes de l'intensité du champ, en fonction de la distance à partir du centre de l'entrefer, pour quatre types de pièces polaires : pôles points, pôles lignes, pôles carrés avec la verticale parallèle : (1) au côté du carré et (2) à sa diagonale.

### Zusammenfassung.

Die Berechnung der Kurven für die Beziehung zwischen Feldstärke und Entfernung von der Mitte der Lücke zwischen den Polen wird für vier verschiedene Formen von Magnetpolen beschrieben, u.zw. punktförmige, linienförmige, quadratische mit der senkrechten Linie parallel zu einer Seite des Quadrats oder parallel zur Diagonale des Quadrats.

Department of Chemistry,

University College of North Wales,  
Bangor.

<sup>3</sup> Bates, Baker and Meakin, *Proc. Physic. Soc.*, 1940, **52**, 425; Bates and Somekh, *ibid.*, 1944, **56**, 182; Davy, *Phil. Mag.*, 1942, **33**, 575.

# X—X AND X—O BOND ENERGIES OF PHOSPHORUS, ARSENIC AND ANTIMONY AND THEIR IMPORTANCE IN THE KINETICS OF THE OXIDATION OF THESE ELEMENTS.

By F. S. DAINTON.

Received 20th May, 1946.

The similarity in the chemical behaviour of the elements phosphorus, arsenic and antimony is well known. It is the purpose of this paper to compute the X—X and X—O bond energies of these elements (X) and to consider whether these values assist in the interpretation of the reactivity of these elements towards oxygen. The author is very grateful to Dr. H. A. Skinner, whose recent work <sup>1</sup> stimulated the present ideas.

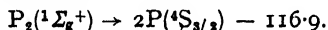
Except where otherwise stated energies are given in kcal.mole.<sup>-1</sup>.

## Bond Energies.

### (a) X—X Bond Energies.

The bond energies of the P—P; As—As; and Sb—Sb bonds are obtained entirely from studies of gaseous equilibria and spectra, both in emission and absorption. The principal source of the equilibria data is Bichowsky and Rossini's <sup>2</sup> book, and the spectral data have been largely drawn from Herzberg's recent book.<sup>3</sup>

(i) **P—P Bond Energy.**—From the detailed analysis of the emission spectrum obtained by an electrical discharge through phosphorus vapour in hydrogen, Herzberg <sup>4</sup> gives:



For the gaseous dissociation  $P_{4(g)} \rightleftharpoons 2P_{2(g)}$ , Bichowsky and Rossini; use Preuner and Brockmüller's results <sup>6</sup> and calculate  $\Delta H = 30$  at 18° C. <sup>5</sup> and as Skinner <sup>1</sup> has shown this leads to an energy of 44 for the P—P bonds in the  $P_4$  molecule. However, the vapour density measurements of Stock, Gibson and Stamm <sup>7</sup> lead to a value of 53.5 for  $\Delta H$  of this reaction at 900° C., which considerably alters the P—P bond energy. Moreover, Stevenson and Yost <sup>8</sup> have been able to evaluate the rotational and vibrational partition functions of the  $P_4$  and  $P_2$  molecules at various temperatures from spectral data, and find these quantities to be consistent with Stock, Gibson and Stamm's results but not with those of Preuner and Brockmüller. We shall therefore take  $\Delta H^{900} = 53.5$  and hence assuming

$$C_P P_4 = 2C_P P_2 + 3 \text{ cal. per } ^\circ\text{C.}, \Delta H^{18} = 50.5$$

whence

$$P_{4(g)} \rightarrow 4P(^4S_{3/2}) - 284.3$$

and the P—P bond energy when  $\angle P P P$  is 60° as in  $P_4$  is 47.5.\*

\* By Skinner's argument when  $\angle P P P = 90^\circ$ , i.e. what he designates as a "normal" bond, the energy is 51.

<sup>1</sup> Skinner, *Trans. Faraday Soc.*, 1945, **41**, 645; 1946, **42** (Oxidation Discussion).

<sup>2</sup> Bichowsky and Rossini, *Thermochemistry of Chemical Substances* (Reinhold, 1936).

<sup>3</sup> Herzberg, *Molecular Structure and Molecular Spectra* (Prentice Hall, 1939).

<sup>4</sup> Ref. 3, p. 491 and *Ann. Physik*, 1932, **15**, 677.

<sup>5</sup> Ref. 2, p. 219.

<sup>6</sup> Preuner and Brockmüller, *Z. physik. Chem.*, 1912, **81**, 129.

<sup>7</sup> Stock, Gibson and Stamm, *Ber.*, 1912, **45**, 3527.

<sup>8</sup> Stevenson and Yost, *J. Chem. Physics*, 1941, **9**, 403.

(ii) **As—As Bond Energy.**—The values  $\text{As}_{4(g)} \rightarrow 2\text{As}_{2(g)} - 21.2$ , and  $\text{As}_{2(g)} \rightarrow 2\text{As} - 91.3^3$ , are well established and lead to a bond energy when  $\angle \text{As As As} = 60^\circ$  of 34.

(iii) **Sb—Sb Bond Energy.**—Bichowsky and Rossini<sup>9</sup> give  $\text{Sb}_{2(g)} \rightarrow 2\text{Sb} - 27$  but do not say how this was estimated. Almy and Schultz<sup>10</sup> have measured the absorption spectrum of antimony vapour in the temperature range  $1350\text{--}1750^\circ\text{C}$ . and conclude that the dissociation energy of  $\text{Sb}_2$  in the ground state is roughly  $3.7\text{ ev.}$  ( $= 85\text{ kcal. mole.}^{-1}$ ). Considerable extrapolation of their measurements was, however, necessary to determine  $D$  and the authors themselves consider this value to be too high. The value of 75 is unlikely to be in error by more than 10 kcal. The vapour density of antimony in the temperature range  $1430\text{--}1650^\circ\text{C}$ . has been measured by V. Meyer and Biltz<sup>11</sup> and if it is assumed that the vapour at this temperature contains only  $\text{Sb}_4$  and  $\text{Sb}_2$  molecules,†  $\Delta H^{1800}$  for this dissociation is 63 kcal. At room temperature this would be lower, and taking  $C_p^{\text{Sb}_4} = 2C_p^{\text{Sb}_2} + 3$ , we have  $\text{Sb}_{4(g)} = 2\text{Sb}_{2(g)} - 58$ . In view of the values from the corresponding dissociations of  $\text{P}_4(50)$ ,  $\text{As}_{(4)}(21)$  this value seems undoubtedly too large and it must be concluded that the vapour of antimony at  $1500^\circ\text{C}$ . contains an appreciable percentage of atoms. The value of  $\Delta H$  for this reaction is not, however, unlikely to be less than 10 kcal. From these data the bond energy  $\text{Sb—Sb}$ , in  $\text{Sb}_4$  lies between 27 and 35, probably closer to the lower than the higher value.

#### (b) X—O Bond Energies.

There are several kinds of X—O bonds in the various oxides of the group V elements. In the structure<sup>12</sup> of the  $\text{X}_4\text{O}_6$  molecules, the X atoms are disposed at the apices of a tetrahedron, each of the six oxygen atoms lying equidistant from the two X atoms on the same edge such that  $\angle \text{XOX} < 180^\circ$ . Each of the 12 X—O bond distances are equivalent in each of the compounds  $\text{P}_4\text{O}_{6(g)}$ ,  $\text{As}_4\text{O}_{6(g)}$ , and  $\text{Sb}_4\text{O}_{6(g)}$  (cubic ‡) and this "bridge" X—O bond energy is thus one-twelfth the heat of the reaction  $4\text{X}_{(g)} + 6\text{O}_{(g)} \rightarrow \text{X}_4\text{O}_{6(g)}$ . Unfortunately this is only known with certainty in the case of  $\text{X} = \text{As}$ . The structure of  $\text{P}_4\text{O}_{10(g)}$  is that of  $\text{P}_4\text{O}_{6(g)}$  with four additional oxygen atoms, each of which is attached to one apical phosphorus atom; and this apical P—O bond distance (1.39 Å.) is shorter than the bridge P—O bond distance (1.62 Å.).§ The structure of  $\text{As}_4\text{O}_{10(g)}$  has not been determined, but it is probable that it would be related to  $\text{As}_4\text{O}_{6(g)}$  in a similar way. Neither  $\text{Sb}_4\text{O}_{6(g)}$  nor  $\text{Sb}_4\text{O}_{10(g)}$  have been studied by electron diffraction methods, but a similar relationship between these two oxides would be reasonable. Since it is generally true that the energy of the bond joining any two atoms decreases as the length increases, it would be expected that the apical X—O bonds would be stronger than the corresponding bridge X—O bonds. Further, provided the bridge X—O distances in  $\text{X}_4\text{O}_{6(g)}$  and  $\text{X}_4\text{O}_{10(g)}$  were identical,§ the apical bond energy would be one-quarter of the heat of the reaction  $\text{X}_4\text{O}_{6(g)} + 4\text{O}_{(g)} \rightarrow \text{X}_4\text{O}_{10(g)}$ . When  $\text{X} = \text{As}$  or  $\text{Sb}$  some thermochemical data are available, but in the case of phosphorus the heat of the reaction  $4\text{P}_{(g)} + 10\text{O}_{(g)} \rightarrow \text{P}_4\text{O}_{10(g)}$  only is known, and the bridge and apical

† Sb vapour must contain  $\text{Sb}_2$ , because the density has a value of 12.31 at  $1437^\circ\text{C}$ . relative to air. The value corresponding to  $\text{Sb}_2$  is 8.45.

‡  $\text{Sb}_4\text{O}_{6(g)}$  has not been investigated.

§ In  $\text{P}_4\text{O}_{6(g)}$  the bridge P—O distance is 1.64 Å.<sup>12</sup> The slightly shorter length (1.62 Å.)<sup>12</sup> of this bond in  $\text{P}_4\text{O}_{10(g)}$ , if real, implies that its energy is slightly greater in  $\text{P}_4\text{O}_{6(g)}$  than in  $\text{P}_4\text{O}_{10(g)}$ .

<sup>9</sup> Ref. 2, pp. 41 and 225.

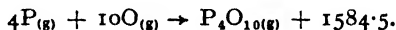
<sup>10</sup> Almy and Schultz, *Physic. Rev.*, 1937, **51**, 62.

<sup>11</sup> Meyer and Biltz, *Ber.*, 1889, **22**, 725; *Z. physik. Chem.*, 1889, **4**, 262.

<sup>12</sup> Hampson and Stosick, *J. Amer. Chem. Soc.*, 1938, **60**, 1814.

bond energies can be calculated only by assuming some definite relation between them. Choice of this relation is facilitated by reference to the relative strengths of the bridge and apical bonds As—O and Sb—O, and from a knowledge of the dissociation energies and interatomic distances which have been determined spectroscopically in  $XO_{(g)}$  molecules.

(i) **P—O Bond Energies.**—From Bichowsky and Rossini's data we have  $4P_{white} + 5O_{2(g)} \rightarrow P_4O_{10(g)} + 700$ , whence using  $P_{4(g)} \rightarrow 4P_{(g)} - 284.3$ , cited in paragraph a(i) and allowing for the heat of sublimation of phosphorus ( $P_4$ ) = 13.2, and  $D_{O_2}$  = 117.1<sup>13</sup> we obtain

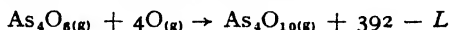


To evaluate the energies of the apical and bridge P—O bonds in  $P_4O_{10(g)}$  some relation between them must be assumed. Now the P—O distance in the bridge bond is 1.64 Å., which is considerably less than the sum of the covalent radii of phosphorus (1.10 Å.) and oxygen (0.74 Å.). Also  $\angle POP$  is  $126 \pm 3^\circ$ , compared with tetrahedral angle of  $109^\circ$  which would have been expected between two oxygen single bonds, and the angle of  $125^\circ 16'$  expected between a single and double bond. Both these facts indicate that the bridge P—O bond has a large amount of double bond character. The apical bond distance of 1.39 Å. suggests an even greater multiplicity for this bond and if bond strength increased with decreasing bond length  $E_{apical P-O} > E_{bridge P-O}$ . Further, Sen Gupta<sup>13</sup> has carried out a rotational analysis of the ultra-violet bands emitted by a carbon arc containing  $P_4O_5$  in the positive crater, and identified the emitter as the molecule PO with an interatomic distance of 1.45 Å. and dissociation energy of  $\sim 6.0$  e.v. = 138 kcal. Hence we can conclude that apical bond energy exceeds 140. This condition is satisfied provided the bridge bond energy does not exceed 85 kcal.; and from the usual length-strength relations which may also hold in the case of the P—O bond the most likely values for these bonds would seem to be

$$\begin{aligned} \text{bridge P—O bond energy } & 80 \pm 2 \\ \text{apical P—O bond energy } & 156 \pm 6. \end{aligned}$$

(ii) **As—O Bond Energies.**—Bichowsky and Rossini<sup>2</sup> quote a value of 154.1 for the heat of formation of arsenious oxide ( $As_2O_3_{(c)}$ ) from metallic arsenic, which is based on E.M.F. measurements. Confirmation of this value has been recently obtained by de Passillé,<sup>14</sup> who obtained 154.7 by calorimetric experiments on burning purified arsenic. Taking the heats of sublimation of metallic arsenic and arsenious oxide as 30.4 and 30\* respectively, together with the result  $As_{4(g)} \rightarrow 4As_{(g)} - 203.6$  used in a(ii) above, we obtain  $4As_{(g)} + 6O_{(g)} \rightarrow As_4O_6_{(g)} + 865$  and hence the "bridge" As—O bond energy is 72.

The heat of formation of  $As_2O_5_{(c)}$  is given by Bichowsky and Rossini as 218. Accepting this as the only value, although insecurely based on old measurements of the heat of solution of  $As_2O_5_{(c)}$  and the heat of formation of arsenic acid ( $H_3AsO_4$ ), we have



where  $L$  is the unknown heat of sublimation of the pentoxide. Assuming that the value is the same as phosphorus pentoxide, the Apical As—O bond energy would be 93. The dissociation energy of the As O molecule

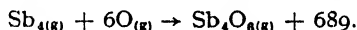
<sup>13</sup> Sen Gupta, *Proc. Phys. Soc.*, 1935, **47**, 247.

<sup>14</sup> de Passillé, *Amer. Chim.*, 1936, **5**, 83.

\* Bichowsky and Rossini take 29 kcal. as  $L_s$  for  $As_2O_6$  (octahedral), but comparison of the vapour pressure data obtained by Rushton and Daniels, *J. Amer. Chem. Soc.*, 1926, **48**, 384, and by Smits and Beljaars, *Proc. K. Akad. Wetensch (Amsterdam)*, 1931, **34**, 1141, indicates that 30 kcal. is the better value.

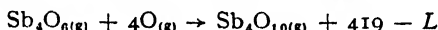
as determined by Jenkins and Strait<sup>15</sup> from the discharge spectrum of the mixed vapour of As and  $\text{As}_2\text{O}_3$  is 113.

(iii) **Sb—O Bond Energies.**—It is fairly certain<sup>16</sup> that the heat of formation of orthorhombic  $\text{Sb}_2\text{O}_3$  from trigonal antimony is 165.4, and that the heat of sublimation of orthorhombic arsenious oxide to  $\text{Sb}_4\text{O}_6$  molecules is 44. The heat of fusion of trigonal antimony is 4.8, and from the vapour pressures of liquid antimony over the range 1070° to 1325° C. Johnston, Fenwick and Leopold<sup>17</sup> calculate the molar heat of vaporisation as 45. Assuming that up to 1325° C. the vapour of antimony contains predominantly  $\text{Sb}_4$  molecules,<sup>18</sup> we have 50 kcal. as the maximum value for the heat of vaporisation of trigonal antimony to  $\text{Sb}_{4(g)}$  molecules. Hence



If the Sb—Sb bond energy in  $\text{Sb}_4$  is 27, then the Sb—O bridge bond energy is 71 but if the former is 35 the latter becomes 75, the more probable value lying nearer 71 than 75.

An estimate of the apical Sb—O bond energy is also possible because the heat of formation of  $\text{Sb}_4\text{O}_{6(c)}$  is known to be 235.7. Whence



where  $L$  is the molar latent heat of sublimation of  $\text{Sb}_4\text{O}_{10}$ . If this molecule is structurally similar to  $\text{P}_4\text{O}_{10}$  and its latent heat of vaporisation is not less than the corresponding quantity for  $\text{P}_4\text{O}_{10}$  then the strength of the apical Sb—O bond  $\nless 99$ . Since  $\text{Sb}_4\text{O}_{10}$  probably has a larger sublimation heat than  $\text{P}_4\text{O}_{10}$  this bond energy may be about 95. The dissociation energy of the Sb—O molecule has been calculated by Mukherjee<sup>19</sup> from the emission spectrum of  $\text{Sb}_2\text{O}_3$  in carbon arc as about 81.

Molecule.	Bond.	Distance (A.).	Energy (kcal.).	
$\text{X}_{2(\text{g})}$	P—P	1.89 <sup>3</sup>	117	
	As—As	?	91.3	
	Sb—Sb	?	(85)	
$\text{X}_{4(\text{R})}$	P—P	2.21 <sup>a</sup>	47.5	
	As—As	?	34	
	Sb—Sb	?	(~28)	
$\text{X}_4\text{O}_{6(\text{R})}$	P—O	} bridge	1.64 <sup>12</sup>	(80)
	As—O		1.80 <sup>12</sup>	72
	Sb—O		?	(71)
$\text{XO}_{(\text{g})}$	P—O	1.45 <sup>13</sup>	(138)	
	As—O	?	<u>(113)</u>	
	Sb—O	?	(81)	
$\text{X}_4\text{O}_{10(\text{g})}$	P—O	} apical	1.39 <sup>12</sup>	(156)
	As—O		?	93
	Sb—O		?	(95)

We may summarise these results in the form shown in the Table. Figures in parenthesis are probable, and about which there is some doubt. The value of 113 for  $D_{\text{AsO}}$  is also underlined as being anomalous in the

<sup>15</sup> Jenkins and Strait, *Physic. Rev.*, 1935, **47**, 136.

<sup>16</sup> See ref. 2, p. 225.

<sup>17</sup> Johnston, Fenwick and Leopold, *International Critical Tables*, Vol. III, p. 205.

<sup>18</sup> Bichowsky and Rossini, ref. 2, p. 225, assume the molecules are largely  $\text{Sb}_2$  but the considerable heat of dissociation of  $\text{Sb}_{4(g)} \rightarrow 2\text{Sb}_{2(g)}$  (see paragraph a(iii)) and Biltz and Meyers vapour density measurements support the view that even at low pressures antimony vapour between 1070° and 1325° C. cannot be regarded as merely diatomic.

<sup>19</sup> Mukherjee, *Z. physik*, 1931, **70**, 552.

<sup>a</sup> Maxwell, Hendricks and Mosley, *J. Chem. Physics*, 1935, **3**, 260.

sense that whereas  $D_{\text{Po}}$  and  $D_{\text{SbO}}$  fall between the values for the energies of the corresponding bridge and apical bonds,  $D_{\text{AsO}} > E_{\text{As},\text{O}}$  apical. It may be that in this case the spectroscopic data are unreliable or have been misinterpreted. It is also evident that a calorimetric determination of the heat of combustion of phosphorus trioxide would remove uncertainty about the values for the P—O bond energies; and that a major improvement in our knowledge of the energies of bonds involving antimony would result from a careful investigation of the vapour density of antimony over a wide range of temperature.

### Kinetics of the Oxidation of Phosphorus, Arsenic and Antimony.

The reactions of phosphorus, arsenic and antimony with oxygen have many features in common. Under suitable conditions all will inflame. Thus Mellor<sup>20</sup> states that antimony heated in air until it boils, burns with a blue-white flame; Emeléus<sup>21</sup> has recorded that arsenic will ignite in air at 400°–450° C.; and the inflammable properties of white phosphorus are well known. In addition, provided the temperature exceeds a certain minimum value and the partial pressure of oxygen lies within certain limits, phosphorus and arsenic will "glow," i.e. they undergo a chemiluminescent vapour phase oxidation. The only mention of a "glow" type of oxidation of antimony found in the literature was that "at a moderate red heat" it burns "with a reddish light," but any luminescence would be difficult to investigate at temperatures where the black body emission is considerable. In the case of phosphorus and arsenic the "glow" reaction is a "cold flame"; only slight rises of temperature occurring, but flame temperatures several hundred degrees higher than the surroundings are attained when these elements ignite. The connection between the glow of phosphorus and the hot flame have been discussed elsewhere<sup>22</sup> and it seems possible that the same relation exists between the corresponding phenomena for arsenic. These and other similarities in behaviour of these elements towards oxygen suggest that the causes of these phenomena might also be similar and that a theory of oxidation which embraced all these elements might be constructed. With this end in view, the bond energy data given in the first part of this paper were computed, and the literature on these reactions carefully considered. It is most convenient to discuss each reaction separately and finally to summarise common conclusions.

(a) **The Oxidation of Phosphorus.**—The kinetics of the glow of phosphorus have been often described<sup>23</sup> and the facts which have to be accommodated in any satisfactory theory of the reaction are: (1) the reaction shows all the characteristics of a branched chain reaction even down to  $-31^{\circ}\text{C}$ . Thus there are pressure limits of oxygen outside which reaction cannot be detected, the upper limit being lowered by addition of non-reactant gases, e.g.  $\text{N}_2$ , A, but is independent of vessel size, the lower limit also being reduced by the addition of these gases or by increase of vessel diameter; (2) the temperature dependence of the limits appears to be determined entirely by the temperature dependence of the vapour pressure of solid white phosphorus when this is present; (3) the products of the reaction are phosphorus pentoxide and traces of ozone; no red phosphorus appears to be found although this is prominent in the products when phosphorus burns or when a hot tungsten filament is used to initiate

<sup>20</sup> Mellor, *Treatise on Inorganic Chemistry*, IX, 378.

<sup>21</sup> Emeléus, *J. Chem. Soc.*, 1927, 783; 1929, 1846; 1934, 974.

<sup>22</sup> Dainton and Bevington, *Trans. Faraday Soc.*, 1946, 42, 377.

<sup>23</sup> Summaries are to be found in Semenov, *Chemical Kinetics and Chain Reactions* (O.U.P., 1935), Chap. VIII, and Yost and Russell, *Systematic Inorganic Chemistry of the Fifth and Sixth Group Elements* (Prentice Hall, 1944), 168.

the reaction chains; <sup>24</sup> (4) the upper limiting pressure is displaced to higher values by traces of ozone and drastically reduced by inhibitors such as aldehydes, hydrocarbons, carbonyls, etc., which are known to be capable of removing oxygen atoms efficiently; <sup>25</sup> (5) the reaction is exothermic, slight temperature rises having been detected when phosphorus glows; <sup>26</sup> (6) the emission spectrum of the glow has been much studied,<sup>27</sup> but no one molecule can be identified as being entirely responsible for the emission. Thus Emeléus and Downey and later Emeléus and Purcell found ultra-violet bands between 3400 and 2500 Å. which also occur in the emission spectrum produced by a silent discharge through  $P_4O_{10}$  vapour at 200° C. Emeléus also found similar bands—one of which at 3270 Å. was very intense—in the flame of phosphine burning in air at low pressures. In addition much of the glow emission lies in the visible region. Emeléus and Downey found a continuous emission extending into the 6000 Å. region, and part of this visible spectrum (6472 to 6771 Å.) has been resolved by Rumpf into a series of bands, the edge frequencies of which he has measured, and fitted into two series which may be superposed by a frequency shift of 530  $cm^{-1}$ . The hot flame (temperature 800° or 125° C.) shows continuous emission in the visible region and bands in the ultra-violet which are identical with those in the glow. Emeléus also showed that  $P_4O_6$  which gives luminous pulses some distance from the solid when this is exposed to air, emits the same spectrum as glowing phosphorus, and he therefore concluded that the emitter was  $P_4O_6$  or a higher oxide. However, Miller <sup>28</sup> has shown that only  $P_4O_6$  contaminated with white phosphorus will glow, and therefore any lower oxide than  $P_4O_6$  may be the emitter. It does seem certain that a molecule of low atomicity is responsible for the glow. That this molecule may be PO is stated by Rumpf, who pointed out that the glow spectrum is identical with the Geissler-tube spectrum of  $P_4O_{10}$  measured by Petricaln.<sup>29</sup> That the frequency shift found in the ground state of the emitter in the glow is  $\sim 1200\text{ }cm^{-1}$  and that Sen Gupta's <sup>13</sup> analysis of the emission spectrum of PO leads to  $\omega_e$  for this molecule of 1230  $cm^{-1}$  is perhaps not without significance in this connection. On the other hand, it has been pointed out by Johnson <sup>27</sup> that below 3200 Å. the bands obtained in the  $P_4O_{10}$  silent discharge (which are also found in the glow) are identical with bands in the emission spectrum of  $O_2^+$  molecule ion. It should also be remembered that illumination of the pentoxide at liquid air temperatures with light from an aluminium spark causes it to phosphoresce in the visible region with strong emission at 4600 Å. The conclusions to be drawn from the results seem to the present author to be: (a) the molecule probably responsible for the emission of many of the bands is PO; (b)  $O_2^+$  may also emit some of the ultra-violet light; (c) part of the visible emission may be due to fluorescent emission of solid pentoxide; and (d) some of the continuous background of the spectrum given out by the hot flame may be due to hot particles of pentoxide. (7) Backström <sup>30</sup> has demonstrated that the full light from a mercury lamp accelerates the glow oxidation. (8) By using a quantum counter, Ouillet <sup>31</sup> has established that between the pressure limits, the intensity of the glow, and hence also the reaction rate, rise to maximum values and then decrease as the pressure of oxygen increases. The properties of the hot flame boundaries <sup>22</sup> afford support for this result.

<sup>24</sup> Melville and Ludlam, *Proc. Roy. Soc., A*, 1932, **135**, 315.

<sup>25</sup> Melville, *Trans. Faraday Soc.*, 1932, **28**, 312.

<sup>26</sup> This may even cause surface melting of the phosphorus, see ref. 22.

<sup>27</sup> See, for example, Emeléus, *et al.*, *J. Chem. Soc.*, 1924, 2491; 1925, 1362; 1928, 628; 1927, 788. Rumpf, *Z. physik. Chem. B*, 1938, **38**, 469; also ref. 13.

<sup>28</sup> Miller, *J. Chem. Soc.*, 1928, 1847.

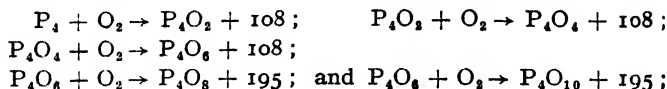
<sup>29</sup> Petricaln, *Z. Physik*, 1924, **22**, 119; 1928, **51**, 395.

<sup>30</sup> Backström, *Medd. Vetenskapsakad. Nobel Inst.*, 1927, **6**, No. 16.

<sup>31</sup> Ouillet, *Trans. Faraday Soc.*, 1933, **29**, 490.

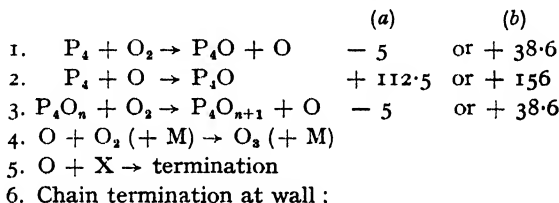


At first sight the bond energy data suggest the possibility of a series of consecutive reactions :



but such a scheme would not account for the pressure limit phenomena, formation of  $\text{O}_3$ , evidence for participation of oxygen atoms, etc., and is therefore rejected.

The kinetic scheme which best accounts for the data is :



in which the heat changes are calculated from the data computed in the first part of this paper, the values in column (a) being based on the assumption that two bridge (P—O) bonds are formed and the values in column (b) derived on the assumption that an apical (P—O) bond is formed. On the basis of the known structures of  $\text{P}_4\text{O}_6$  and  $\text{P}_4\text{O}_{10}$  it would be expected that assumption (a) would be true for values of  $n = 0, 1, 2, 3, 4, 5$ , and assumption (b) correct for values of  $n = 6, 7, 8, 9$ . Reactions 2 and 3 are unusual types of process in oxidation kinetics. It is rare that an oxygen atom attacks a bond symmetrically to form a bridge, e.g. it is more usual to find  $\text{CH}_4 + \text{O} \rightarrow \text{CH}_3 + \text{OH}$  or  $\text{H}_2 + \text{O} \rightarrow \text{H} + \text{OH}$  rather than  $\rightarrow \text{CH}_3\text{OH}$  or  $\rightarrow \text{H}_2\text{O}$ . However, granted that O atoms are present, and the formation and sensitising action of ozone together with Backström's illumination experiment and the action of poisons confirm this, it is difficult to formulate reactions between  $\text{P}_4$  and O which are as plausible as that given and have a sufficiently low energy of activation.\* Reaction 3 is interesting for three reasons. Firstly, like the propagation step in a polymerisation process a new centre is formed of identical reactivity to the centre destroyed but of higher molecular weight. Secondly, if oxygen atoms can start a new chain by reactions of the type of reaction 2 then, unlike the propagation step in a polymerisation chain, reaction 3 involves the formation of two new chains, i.e. the chain is *continuously branched* until the final step when  $\text{P}_4\text{O}_9$  reacts. Thirdly, the initiation reaction 1 is the simplest prototype of step 3 and hence as soon as the experimental conditions are suitable for initiation of chains in the  $\text{P}_{4(\text{g})}/\text{O}_{2(\text{g})}$  system, they are also (leaving out of consideration momentarily the termination process) equally suitable for propagation and branching. In accord with this, outside the pressure limits few chains begin and hence propagate and branch, whilst inside the glow region many chains start and branch almost immediately with high efficiency. Furthermore the bond energies calculated in the earlier part of the paper indicate that both starting and branching-propagation of the chains requires only a low energy of activation, and it is at once clear why such a highly branched chain reaction can proceed below  $0^\circ \text{C}$ .

The appropriate stationary state equations for any reaction outside the limits are :

\*  $\text{P}_4 + \text{O} \rightarrow \text{P}_3 + \text{PO}$  is endothermic and the molecule  $\text{P}_3$  does not *a priori* seem likely.  $\text{P}_4 + \text{O} \rightarrow \text{P}_3 + \text{P}_2\text{O}$  is possible but nothing is known of  $\text{P}_3\text{O}$  and the absence of red phosphorus suggests that no  $\text{P}_3$  molecules are formed.

$$\begin{aligned}
 \text{(i)} \quad \frac{d[\text{O}]}{dt} &= k_1[\text{P}_4][\text{O}_2] - k_2[\text{P}_4][\text{O}] + \sum_{n=1}^{n=\infty} k_3[\text{P}_4\text{O}_n][\text{O}_2] \\
 &\quad - k_4[\text{O}][\text{O}_2][\text{M}] - k_5[\text{X}][\text{O}] - k_6[\text{O}] = 0; \\
 \text{(ii)} \quad \frac{d[\text{P}_4\text{O}]}{dt} &= k_1[\text{P}_4][\text{O}_2] + k_2[\text{P}_4][\text{O}] - k_3[\text{P}_4\text{O}][\text{O}_2] = 0
 \end{aligned}$$

and assuming the rate constant of reaction 3 is independent of the value of  $n$

$$\text{(iii)} \quad \frac{d[\text{P}_4\text{O}_n]}{dt} = k_3[\text{P}_4\text{O}_{n-1}][\text{O}_2] - k_3[\text{P}_4\text{O}_n][\text{O}_2] = 0 \text{ for } n = 2 \dots 9.$$

Since there are nine reactions of type  $\text{P}_4\text{O}_n + \text{O}_2 \rightarrow \text{P}_4\text{O}_{n+1} + \text{O}$ , but when  $n = 9$  the reaction continues to propagate but does not branch, equation (ii) becomes

$$\text{(iv)} \quad \frac{d[\text{P}_4\text{O}]}{dt} = k_1[\text{P}_4][\text{O}_2] + k_2[\text{P}_4][\text{O}] - \frac{1}{9} \sum_{n=1}^{n=9} k_3[\text{P}_4\text{O}_n][\text{O}_2] = 0.$$

Substituting for terms involving  $k_3$  from (iv) into (i)

$$\therefore \frac{d[\text{O}]}{dt} = 10k_1[\text{P}_4][\text{O}_2] + 8k_2[\text{P}_4][\text{O}] - k_4[\text{O}][\text{O}_2][\text{M}] - k_5[\text{X}][\text{O}] - k_6[\text{O}] = 0.$$

The rate of formation of the pentoxide will be given by

$$\begin{aligned}
 \text{(v)} \quad \frac{d[\text{P}_4\text{O}_{10}]}{dt} &= k_3[\text{P}_4\text{O}_9][\text{O}_2] = k_1[\text{P}_4][\text{O}_2] \\
 &\quad + \frac{k_2[\text{P}_4]10k_1[\text{P}_4][\text{O}_2]}{k_4[\text{O}_2][\text{M}] + k_5[\text{X}] + k_6 - 8k_2[\text{P}_4]}
 \end{aligned}$$

Equation (v) can readily be shown to satisfy all the phenomena associated with this reaction listed under items 1, 2, 3, 4, 5, 7 and 8. For example, when it is remembered that  $k_6$  is a diffusion term and therefore proportional to  $D_0/P_d^2$  where  $P$  is total pressure and  $d$  is the vessel diameter, it is clear the rate passes through a maximum value as the pressure is increased and that the lower limit should be proportional to the reciprocal of the square of the vessel diameter and to the reciprocal of the phosphorus vapour pressure. The temperature dependence of the upper limit ( $P_U$ ) should be given by

$$\frac{d \ln P_U}{dT} = \frac{E_2 + L_8 - E_4}{RT^2}$$

where  $L_8$  is the latent heat of sublimation of white phosphorus = 13.2 kcal. mole<sup>-1</sup>. The temperature coefficient of the photochemical formation of ozone from oxygen indicates that  $E_4$  is small.  $E_2$  would also be expected to be small, and hence the observed value of  $E_2 + L - E_4 = 15.5$ , which holds over a wide range of conditions (see ref. 22), represents good agreement. Backström's observations on the sensitising influence of ultra-violet light may be interpreted as due to the photochemical formation of ozone or oxygen atoms. This mechanism also has the advantage of removing the necessity for seeking for a highly excited molecule capable of dissociating an oxygen molecule in a collision of the second kind, which has been proposed previously as the branching mechanism. The glow spectrum does in fact suggest that such excited molecules are present in reacting phosphorus-oxygen mixtures and some branching may occur by this means, but in view of the efficient propagation of the continuously branched chains suggested, it is unlikely that any appreciable amount of branching occurs by any other means.

What at first might appear to be a weakness of this mechanism is that it does not enable a particular molecule to be specified as the emitter of the radiation which characterises the glow; the weakness is shared by all schemes for the oxidation of phosphorus yet proposed. This may not

be so serious an objection, since in such highly exothermic steps as 2 or  $P_4O_7 + O \rightarrow P_4O_8 + 156$  or  $P_4O_n + O_2 \rightarrow P_4O_{n+2} + 108$  or 195 which might occasionally take place, highly excited molecules are produced. Excited  $P_4O_{10}$  itself might well be formed in such a way and remit some of the visible emission round 4600 Å. The origin of excited PO molecules which appear to be responsible for some of the emission is not easy to discover. Rumpf<sup>27</sup> remarks that the light emission process may be entirely secondary and unconnected with the main course of the reaction. He suggests  $P_2 + O_2 \rightarrow [P_2O_2] \rightarrow PO + PO^* \rightarrow 2PO + h\nu$  but there are two objections to this. Firstly, the Table on page 247 indicates that if  $P_2$  and  $O_2$  are in their ground states this reaction is exothermic only to the extent of  $\sim 42$  kcal., i.e.  $\lambda_{\text{emit}} \leq 6900$  Å. Secondly, there is no positive evidence for the presence of an appreciable concentration of  $P_2$  molecules in the glow of phosphorus such as there is in the hot flame where red phosphorus is deposited on the cold surfaces, due, as Melville<sup>22</sup> has shown, to the condensation of  $P_2$  molecules. PO molecules could be formed by occasional depolymerisation of  $P_4O_4 \rightarrow 4PO$  and acquire their excitation energy by collision with the highly excited molecules to which reference was made in the previous paragraph.

(b) **The Oxidation of Arsenic.**—Although many qualitative observations have been made on the glow and flame of arsenic, the only important quantitative data are those obtained by Emeléus, and Emeléus and Damerell.<sup>21</sup> These authors studied the rate of uptake of oxygen, the onset of the glow and the temperature rises which occur when oxygen is admitted to solid sieved arsenic powder in a Pyrex tube. They found that between certain pressure limits of oxygen (e.g. 8 and 290 mm. at 280° C.) the rate of oxygen uptake was rapid, and accompanied by a glow, and that a thermometer embedded in the arsenic registered a temperature rise of  $\sim 7^\circ$  C. above the surroundings. Outside these pressure limits a slow surface reaction took place not characterised by a glow or a temperature rise and of zero order. The upper limit increased with temperature and the lower limit decreased. When a stream of air was passed over 3 g. arsenic in a transparent silica tube heated to 250–300° C., the space above the arsenic was filled with a "feebly luminous white cloud" the spectrum of which was continuous from 4300 to 4900 Å. with a maximum intensity about 4600 Å. No bands were found in the ultra-violet. The spectrum of the hot flame was continuous down to 3200 Å. but no other bands were found. The luminescence of this cloud was inhibited by organic vapours, including benzene, hexane, alcohol, acetone, chloroform, esters and chlorobenzene.

The similarity to the oxidation of white phosphorus is thus very close—the only points of dissimilarity being the absence of bands in the glow spectrum, the existence of the slow zero order surface reaction, and the absence of ozone (which even if formed would decompose at these temperatures). Accordingly Emeléus and Damerell suggested a reaction chain similar to that proposed by Semenov for the phosphorus oxidation involving the steps



If we write the corresponding mechanism to the one adopted in section (a) for phosphorus the steps in the vapour phase glow of arsenic are :

			(a)	(b)
Initiation	$k_1^1$	$As_4 + O_2 \rightarrow As_4O + O$	— 8	— 24·4
Propagation	$k_2^1$	$As_4 + O \rightarrow As_4O$	+ 110	+ 93
Continuous				
Branching	$k_3^1$	$As_4O_n + O_2 \rightarrow As_4O_{n+1} + O$	— 8	— 24·4
Termination	$k_4$	$O + O_2(+M) \rightarrow O_3(+M), (O_3 \text{ destroyed at } 2\text{--}300^\circ \text{ C.})$		
	$k_5$	$O + X(\text{poison}) \rightarrow \text{termination}$		
	$k_6$	$O + \text{wall} \rightarrow \text{termination}$		

<sup>22</sup> Melville and Gray, *Trans. Faraday Soc.*, 1936, **32**, 271.

the major point of difference being that assumption (b) is probably not required since glowing arsenic is not oxidised beyond the  $\text{As}_4\text{O}_6$  stage. The reason for this is probably that apical bond formation from oxygen molecules (reactions 1 and 3) is endothermic to the extent of  $\sim 25$  kcal. mole.<sup>-1</sup> as compared with the exothermicity ( $\sim 39$  kcal. mole.<sup>-1</sup>) of the corresponding reactions for phosphorus. By similar arguments to that used in the case of phosphorus

$$\frac{d[\text{As}_4\text{O}_6]}{dt} = k_1^1[\text{As}_4][\text{O}_2] + \frac{k_2^1[\text{As}_4]\{6k_1^1[\text{As}_4][\text{O}_2]\}}{k_4[\text{O}_2][\text{M}] + k_5[\text{X}] + k_6 - 4k_2^1[\text{As}_4]}$$

and the upper limit ( $P_0^1$ ) should show an exponential dependence on temperature

$$\frac{d \ln P_0^1}{dT} = \frac{E_2^1 + L_8^1 - E_4}{RT^2}$$

where  $L_8^1$  is the latent heat of sublimation of arsenic. Again  $E_2^1$  and  $E_4$  would be expected to be small and hence

$$\ln P_0^1 \simeq \text{constant} - \frac{L_8^1}{RT}$$

In fact Emeléus's data do fit such a relation but suggest that  $L_8^1$  is 21 kcal. mole.<sup>-1</sup>, in apparent disagreement with the known heat of sublimation of metallic or  $\alpha$  modification of arsenic of 30.4 kcal. mole.<sup>-1</sup>. However, Emeléus's method of purification of metallic arsenic involved pumping off the volatile oxide and then subliming the element *in vacuo* at 400° on to a cold surface. The sublimate was scraped off, broken and sieved into small particles before use. The arsenic used was therefore largely in a metastable form, probably consisting of grey amorphous arsenic containing some of the yellow form ( $\gamma$  arsenic). Now the form with the highest vapour pressure, even though present in small quantities will be important because it will determine the vapour concentration of  $\text{As}_4$  molecules; and hence the value of  $L_8^1$  which applies in the equation will refer to the most unstable form present. The heat of transformation of metallic ( $\alpha$ ) to amorphous ( $\beta$ ) arsenic is given<sup>33</sup> as 1 kcal. g. atom.<sup>-1</sup>, and of metallic ( $\alpha$ ) to yellow ( $\gamma$ ) variously as 3.5 kcal. g. atom.<sup>-1</sup> and 1.5 kcal. g. atom.<sup>-1</sup> at 18° C.<sup>34</sup> If the amorphous form was the only unstable form present the value of  $L_8^1$  could not be less than 26.4. The observed value of 21 excludes this possibility and suggests that some of the most unstable form ( $\gamma$  arsenic) was present in the samples used, in which case, taking Latschenko's<sup>34</sup> data the anticipated value of  $L_8^1$  is 24.4, and using Peterson's value<sup>33</sup> (accepted by Bichowsky and Rossini)  $L_8^1$  becomes 16.4; both values which bracket the observed value of  $L_8^1$ .

Some further confirmation for this view is obtained if it is remembered that at the lower limit ( $P_L^1$ ),  $k_6$ , which is a diffusion term, is equal to  $\frac{k_6^1}{P_L^1}$ , and hence

$$\ln P_L^1 = \text{const.} + \frac{E_6 - E_2^1 + L_8^1}{RT}$$

From the kinetics of the phosphorus oxidation  $E_6$  is known to be very small. Moreover,  $E_2^1$  should also be inconsiderable and it would be expected that

$$\ln P_L^1 = + \frac{21 \text{ kcal.}}{RT} + \text{const.}$$

The only available data to test this are four values of the lower limit

<sup>33</sup> Ref. 2, p. 39. Based on Benthelot and Engel's results, *Ann. Chim. Physique*, 1890, 21, 284, and Peterson's data, *Z. physik. Chem.*, 1891, 8, 606.

<sup>34</sup> See Latschenko, *J. Russ. Physic Chem.*, 1916, 48, 279.

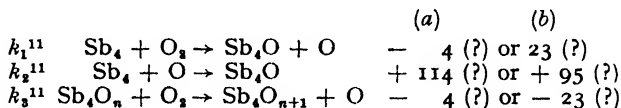
quoted by Damerell and Emeléus and which are integral (10, 8, 5 and 4 mm.), suggesting that they are probably not the observed data but interpolated or approximate values. When  $\ln P_L^1$  is plotted against  $1/T$ , these values lead to points lying alternately on each side of a line of slope  $20 \pm 2$  kcal.

Perhaps the most interesting comparison between the oxidation of these two elements is seen as follows. The tips of the glow peninsulæ, i.e. the lowest temperatures at which the solid arsenic and phosphorus will glow under the most favourable oxygen pressures is given by  $P_v = P_L$  and  $P_v^1 = P_L^1$ , i.e.

$$\frac{k_6}{8k_2[P_4]} = \frac{8k_2[P_4]}{k_4} \quad \text{and} \quad \frac{k_6}{4k_2^1[As_4]} = \frac{4k_2^1[As_4]}{k_4} \quad \text{or} \quad \left( \frac{[P_4]}{[As_4]} \right) \text{ peninsula tip} = \frac{k_2^1}{4k_2}.$$

From Kowalski's work<sup>25</sup> the value of  $[P_4]$  at the tip of the glow peninsula is  $10^{-4}$  mm. Long extrapolation of Emeléus's data indicates a minimum glow temperature of about  $200^\circ$  C. for arsenic, at which temperature the vapour pressure of metallic arsenic is  $10^{-4}$  mm. and the vapour pressure of the more volatile unstable form will be greater than this. We may therefore conclude that the theory of the oxidation of arsenic has much qualitative support, and the quantitative data on vapour pressures, etc., which exist also substantiate this mechanism. It is also clear that a great deal more experimental work requires to be done in this field, e.g. redetermination of the limits and of the effect of temperature, foreign vapours, state of aggregation of the arsenic, etc., on these limits. Further, although it is likely that the transition from glow to hot flame is of the same nature as in the oxidation of phosphorus, this requires testing.

(c) **The Oxidation of Antimony.**—As already mentioned it seems certain that antimony can undergo both "glow" and "hot flame" types of oxidation, but no quantitative measurements have been made. From the bond energy data and the known heats of formation a luminous reaction in the vapour phase, with a light emission lying further into the region of long wavelengths than the arsenic glow would be expected. The "reddish light" which is said to accompany the oxidation at moderate red heat is in accord with this view. The corresponding reaction steps to the phosphorus and arsenic cases are:

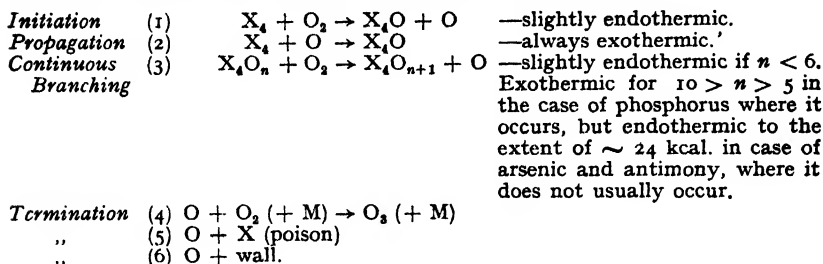


followed by the usual reactions 4, 5 and 6. The same type of limit phenomena would therefore be expected in this case also, with the tip of the explosion peninsula corresponding to a vapour pressure of ca.  $4 \times 10^{-4}$  mm. Vapour pressure data are not available for solid forms of antimony, but if the vapour pressure curve of liquid antimony extended below its melting point ( $630^\circ$  C.) the lowest glow temperature would be ca.  $500^\circ$  C. The vapour pressure of the unstable forms might not be very different from that of the supercooled liquid at this temperature, and hence the observed "moderate red heat" at which antimony burns with a "reddish light" (distinct from the bright bluish-white hot flame) is not at variance with this theory. Glowing antimony does not form  $Sb_4O_{10}$  for the same reason that arsenic does not form  $As_4O_{10}$ , viz. the apical bond is so much weaker than the dissociation energy of oxygen that 1 and 3 are infrequent steps when  $n > 5$ .

<sup>25</sup> Kowalski, *Z. physik. Chem.*, 1929, 48, 288.

### Conclusion.

The similarities between the "glow" oxidations of the solid elements, phosphorus, arsenic and antimony are to be attributed to a vapour phase oxidation of  $X_4$  molecules according to a common scheme which is the following continuously branched luminescent chain reaction :—

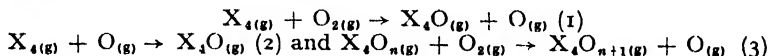


This mechanism, taken with the bond energy data, also accounts for the known differences between the elements in respect of oxidation. Thus the temperature dependence of the glow limits is controlled by the different heats of sublimation of the most unstable solid form present, and the relative minimum glow temperatures can be satisfactorily predicted. Moreover, phosphorus is oxidised to  $P_4O_{10}$  in the glow reaction because reaction (3) is exothermic for values of  $10 > n > 5$ ; whereas in the glow of the other elements the pentoxide is not formed since reaction (3) for  $10 > n > 5$  is endothermic to a considerable degree.

A rigorous test of these views requires further experimental work along the following main lines: (a) determination of vapour pressure data of the unstable forms of arsenic and antimony; (b) determination of the heat of combustion of antimony and  $P_4O_8$ ; (c) a reinvestigation and extension of previous work on the glows of arsenic and antimony. It is hoped that before long this work may become possible.

### Summary.

The X—X and X—O bond energies, where X = P, As, Sb are computed for molecules  $X_2$ ,  $X_4O_6$ , XO and  $X_4O_{10}$  and used to calculate the heat changes involved in the reactions



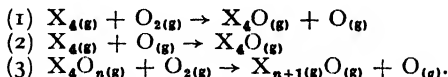
The general conclusion is that the apical X—O bond energies [(156), 93, (95)] are greater than the bonds in XO molecules [(138), (113), (81)] which are larger than the bridge X—O bond energies [(80), 72, (71)] where X = P, As, Sb in that order and is in accord with the increasing bond lengths. Reactions of type (2) are in all cases exothermic to a considerable extent, whereas reactions of types (1) and (3) are slightly endothermic provided  $n < 6$ ; thus for X = P the endothermicity of (1) and (3) is 5 kcal. mole<sup>-1</sup>, X = As = 8, X = Sb = 4. However, where  $10 > n > 5$  reaction (3) is exothermic in the case of phosphorus and endothermic to the extent of 24 and 23 (?) kcal. mole<sup>-1</sup> in the cases of arsenic and antimony respectively; which probably explains why in the glow of phosphorus  $P_4O_{10}$  is formed, but in the glow of arsenic and antimony the final products are  $As_4O_8$  and  $Sb_4O_8$ .

The existing data on the glow type oxidation of these elements is reviewed and it is concluded that they are most satisfactorily explained as continuously branched chain reactions in which the initiation reaction is (1), the propagation reactions are (2) and (3) above, (3) also being the branching reaction provided  $n < 6$  in case of X = As and Sb, and  $< 10$

in the case of  $X = P$ . The chains are terminated by removal of oxygen atoms by poisons, or wall, or by  $O + O_2 (+ M) \rightarrow O_3 (+ M)$  as previously postulated. This scheme also accounts for the observed temperature dependence of the glow limits of arsenic and phosphorus and leads to a relation between the minimum glow temperatures of all these elements in accordance with available experimental data. The shift of the glow spectrum to larger wavelengths in the series  $P-As-Sb$  is expected, but the mode of formation and excitation of the actual emitters is still doubtful.

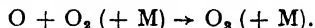
### Résumé.

Les énergies des liaisons  $X-X$  et  $X-O$  (où  $X = P, As, Sb$ ) sont calculées pour les molécules  $X_2$ ,  $X_4O_6$ ,  $XO$  et  $X_4O_{10}$  et employées pour évaluer les variations d'énergie utilisable dans les réactions :



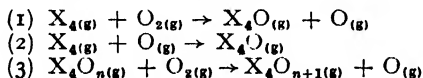
On peut conclure que les énergies de la liaison  $X-O$  du sommet sont supérieures aux énergies de liaison dans les molécules  $XO$ , elles mêmes plus grandes que les énergies de la liaison  $X-O$  du pont, ce qui est en accord avec la longueur croissante de la liaison.

On considère que l'oxydation lente de ces éléments est due à des réactions en chaînes, qui se ramifient continuellement, commencées par (1), propagées par (2) et (3) et terminées par l'élimination des atomes d'oxygène soit par les parois, soit par des poisons, soit par :



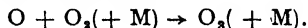
### Zusammenfassung.

Die Energien der Bindungen  $X-X$  und  $X-O$  (wobei  $X = P, As, Sb$ ) wurden für die Moleküle  $X_2$ ,  $X_4O_6$ ,  $XO$  und  $X_4O_{10}$  berechnet und dazu benutzt, die Wärmetönungen der Reaktionen



zu bestimmen. Es kann gefolgert werden, dass die Bindungsenergien der pyramidenspitzenartigen  $X-O$  Bindungen grösser als die der Bindung im  $XO$  Molekül sind, während diese ihrerseits grösser als die Bindungsenergie von brückenförmigen  $X-O$  Bindungen ist, was mit der anwachsenden Länge dieser Bindungen im Einklang steht.

Die langsame Oxydation dieser Elemente wird als Kettenreaktion mit fortwährender Kettenverzweigung betrachtet, wobei (1) die Initialreaktion und (2) und (3) die Kettenfortpflanzungsreaktionen darstellen. Die Entfernung der Sauerstoffatome, entweder durch "Gifte" oder die Gefässwände oder durch die Reaktion



bewirkt den Abbruch der Ketten.

*Laboratory of Physical Chemistry,  
Cambridge.*

# THE EFFECT OF ADAPTATION ON THE ACTIVITY OF THE DEHYDROGENASES OF *BACT. LACTIS AEROGENES*.

By D. S. DAVIES AND C. N. HINSHELWOOD.

Received 23rd May, 1946.

It has been shown, in previous communications, that the behaviour of *Bact. lactis aerogenes* when grown in presence of proflavine, crystal violet, methylene blue or sulphanilamide<sup>1</sup> can be explained by assuming specific inhibition of certain enzymes. The growth of these—upon which cell division waits—is retarded, while other enzymes (not dependent on the former for their growth) continue to expand at the usual rate. The consequent change of the relative amounts of the various enzymes tends to compensate the effects of the inhibitor, and accounts for the adaptation to the drugs.

The question arises whether demonstrable changes in the enzymatic constitution of these bacteria can in fact be detected after adaptation to a new environment. On account chiefly of its simplicity, the Thunberg technique for measuring<sup>2</sup> dehydrogenase activity, as applied to bacterial enzymes by Quastel, was chosen for a first survey.\*

The reactions upon which the method depends are as follows :

substrate + carrier = reduced carrier + oxidised substrate †

reduced carrier + methylene blue = carrier + reduced methylene blue

the carrier being some form of mobile oxidation-reduction system. The first step is rate-determining, the velocity depending on the amount of enzyme (number of cells) and the amount of substrate available for reaction at a given instant. The relation between rate and substrate concentration probably reflects the form of the adsorption isotherm of the substrate on the enzyme. The rate is independent of the methylene blue concentration, the dye acting simply as a redox indicator.

## Experimental.

Since interest centres on the enzyme activity *per cell*, under culture conditions, intact organisms were used, Quastel's method of preparing "washed suspensions" being adopted. Bacteria were grown in a standard synthetic medium,<sup>3</sup> centrifuged and separated. They were then resuspended in 0.85 % NaCl solution, centrifuged, and again separated.

<sup>1</sup> Davies and Hinshelwood, *Trans. Faraday Soc.*, 1943, **39**, 433; Davies, Hinshelwood and Pryce, *ibid.*, 1944, **40**, 397; 1945, **41**, 163; Pryce, Davies and Hinshelwood, *ibid.*, 1945, **41**, 465; Davies, Hinshelwood and James, *ibid.* (in press).

<sup>2</sup> Quastel and Whetham, *Biochem. J.*, 1924, **18**, 519; 1925, **19**, 520, 645.

<sup>3</sup> See ref. 1.

\* It is realised that the Thunberg method measures specifically the dehydrogenating ability in presence of methylene blue and may not give results which necessarily indicate the oxidising powers in other circumstances. This fact, however, does not deprive the test of its value for detecting changes in enzyme balance due to drug-training or other kinds of adaptation. Moreover, *experimentally*, a close correlation of Thunberg test on the suspensions (as actually prepared) and growth rate does in fact appear.

† See p. 264.



This process was repeated three times more. The cells were finally suspended in a suitable volume of NaCl and vigorously aerated for some time

(usually half an hour) to break up clusters. The population of the washed suspension was determined and adjusted to a standard value (usually  $7.50 \times 10^8$  bacteria per cc.).

For determination of the oxidation times Thunberg tubes with hollow stoppers were used. Into the main tube were pipetted 2 cc. of phosphate buffer (usually at  $pH = 7.4$ ),  $x$  cc. of an oxidisable substrate,  $2 - x$  cc. of water, and 0.1 cc. of methylene blue (400 mg./l.). 1 cc. of the enzyme suspension was introduced into the stopper. Series of tubes made up in this way were evacuated with a water pump, filled with nitrogen, and immersed in a thermostat at  $40.0^\circ$  C. After a few minutes the tubes were inverted so as to mix the solutions, and the time for the blue colour in each tube to disappear was measured. With each experiment, a control tube containing no substrate was included; this did not usually turn within 300 minutes. A further control tube containing an easily oxidised

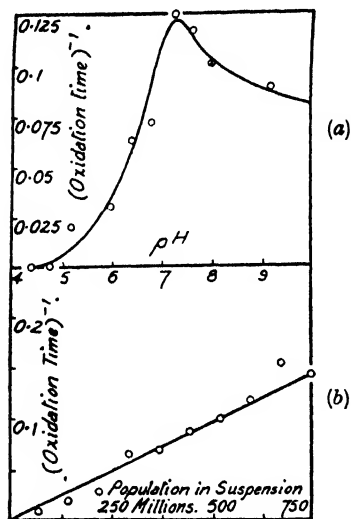


FIG. 1.—Dependence of dehydrogenase activity on  $pH$  and on number of cells in suspension.

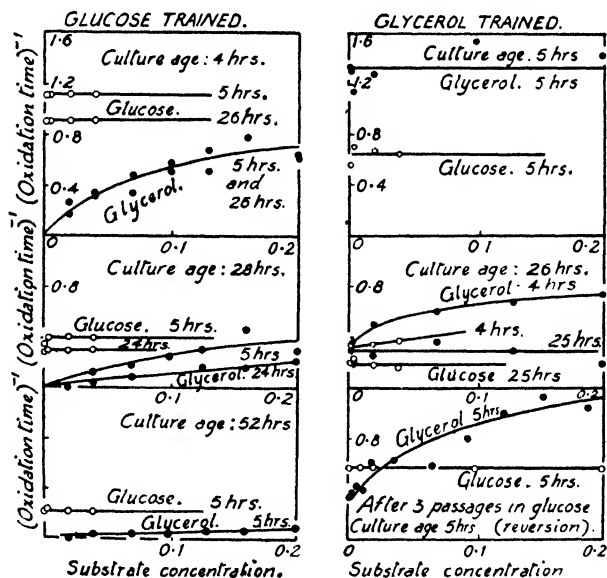


FIG. 2.—Change in oxidation rate with age of culture from which cells are taken (shown on each diagram), age of washed suspension (shown for each separate curve), and state of adaptation of cells.

substrate, but a boiled specimen of the enzyme suspension, was also occasionally included. None of these tubes ever changed colour during the course of an experiment.

Preliminary experiments, made with bacteria adapted to the standard glucose-ammonium sulphate medium confirmed that the rate depends directly upon the number of cells present (Fig. 1*b*), that the oxidation rate of 0.1 M glucose is independent, over a tenfold range, of the methylene blue concentration, and that the colour of the dye fades rather abruptly towards the end of the reaction period. These confirmatory observations bear out the statements made above about the reaction scheme. The dependence upon  $pH$  of the glucose oxidation rate was determined (Fig 1*a*) and guided the selection of the working  $pH$ .

The enzymatic activity of the cells depends to a large extent on the age of the culture from which they are taken, and to a much smaller extent on the time the washed suspension is kept. The second factor was found to be sufficiently controllable by testing the suspension immediately after preparation. The first, however, needed very careful control. Comparison between different strains was always made at a standard age, or preferably, at a series of ages. The influence of the age (measured from the beginning of growth) is evident from Fig. 2.

## Enzyme Changes Accompanying Adaptation.

### (1) Adaptation to Changes in Carbon Source.

Previous work by Stephenson and others has shown that galactozymase activity increases when yeast cells or *Bact. coli* are exposed to galactose,<sup>5</sup> that changes in the formic acid metabolism accompany growth of *Bact. coli* in presence of formate,<sup>6</sup> and that amino-acid metabolism varies after training at different  $pH$  values.<sup>7</sup>

*Bact. lactis aerogenes* undergoes adaptation when certain changes are made in the composition of the growth medium. Cells transferred, for example, from the glucose-ammonium sulphate medium to one containing glycerol in place of glucose grow more slowly at first. After five or six subcultures in presence of glycerol, the growth rate returns to normal. A few further subcultures in presence of glucose partly reverse this adaptation.<sup>8</sup>

This adaptive process is now found to change the ability of the bacteria to oxidise glucose and glycerol. The oxidation rate-substrate concentration curves for glucose-adapted and glycerol-adapted organisms respectively are shown in Fig. 2.

The ability to oxidise glycerol alters on training in two ways. First, the optimum rate which is originally much less than the corresponding rate for glucose now exceeds the value for glucose (which has fallen only slightly). Secondly, this optimum is reached at very much lower concentrations, so that the oxidation rate is now almost independent of the concentration of glycerol over a wide range. Not only the position, but also the actual shape of the curve has changed. With glucose the rate is independent of concentration for all strains. The glycerol-trained bacteria after three subcultures in glucose are still better able to oxidise glycerol than glucose, though the rate-concentration curve for glycerol shows signs of recovering its original shape, the oxidation rate being no longer independent of concentration. These observations were confirmed several times.

The range of experimental substrates was now extended to include five polyhydric alcohols—glycol, glycerol, erythritol, pentaerythritol and sorbitol and four aldoses—arabinose, glucose, lactose and maltose. Tests were all carried out at an age of about five hours, which corresponds to the

<sup>5</sup> Stephenson and Yudkin, *Biochem. J.*, 1936, **30**, 506; Stephenson and Gale, *ibid.*, 1937, **31**, 1311.

<sup>6</sup> Stephenson and Strickland, *ibid.*, 1935, **27**, 1528.

<sup>7</sup> Gale and Epps, *ibid.*, 1942, **36**, 600.

<sup>8</sup> Lodge and Hinshelwood, *Trans. Faraday Soc.*, 1944, **40**, 571.

260 DEHYDROGENASES OF *BACT. LACTIS AEROGENES*

stage of maximum activity. In these experiments, however, less significance can be attached to absolute than to relative rates.

TABLE I.—OXIDATION RATES FOR VARIOUS CARBON COMPOUNDS.

Numbers show relative oxidation rates (100 = 5' oxidation time). Numbers in brackets indicate concentration at which optimum is first reached.

Substrate.	Cells Trained in			
	Glucose.	Glycerol.	Lactose.	Maltose.
Glycol . . .	25(0.1)	0	5(0.2)	0
Glycerol . . .	35(0.2)	100(0.001)	15(0.05)	15(0.1)
Erythritol . . .	20(0.02)	5(0.1)	0	0
Pentaerythritol . . .	15(0.01)	—	0	0
Sorbitol . . .	85(0.001)	100(0.001)	100(0.001)	85(p.001)
d-Arabinose . . .	20(0.1)	0	0	15(0.2)
Glucose . . .	100(0.001)	100(0.001)	100(0.001)	55(0.001)
Lactose . . .	15(0.1)	15(0.2)	100(0.1)	12(0.1)
Maltose . . .	60(0.005)	—	—	62(0.001)

First, normal, glucose-adapted cells were tested in parallel with various concentrations (from 0.001 M. to 0.2 M.) of each substance. The results are shown in Table I. For each substrate, the optimum rate is shown as a percentage of the optimum value in glucose. Some indication of the

TABLE II.—COMPARISON OF MEAN GENERATION TIMES AND OXIDATION RATES IN DISACCHARIDES.

Numbers show relative oxidation rates (100 = 8' oxidation time). Numbers in brackets indicate concentration at which optimum is first reached.

Substrate.	Cells Trained in			
	Glucose.	Maltose.	Lactose.	Sucrose.
Glucose . . .	100(0.001)	73(0.001)	89(0.001)	89(0.001)
Maltose . . .	131(0.01)	84(0.001)	114(0.01)	89(0.01)
Lactose . . .	0	0	100(0.02)	6(0.02)
Sucrose . . .	47(0.2)	32(0.1)	100(0.001)	94(0.001)

## MEAN GENERATION TIMES.

Growth Medium.	Cells Trained in			
	Glucose.	Maltose.	Lactose.	Sucrose.
Glucose . . .	32'	—	32'	—
Maltose . . .	110'	31'	84'	109'
Lactose . . .	100'	77'	32'	97'
Sucrose . . .	60'	42'	46'	33'

shape of the curve is also given by the figure in brackets, which is the smallest concentration at which this optimum is reached. Glucose-trained bacteria are able to bring about the oxidation of all these substances, but only with sorbitol and maltose is the process more than half as efficient as

with glucose. It thus appears that the specificity of action depends not on the *group* to be oxidised (glucose and sorbitol are oxidised with almost equal ease: arabinose only with difficulty) but on the configuration of the *whole substrate molecule*. Tests on organisms adapted to glycerol and lactose bear this out. The improvement in the activity towards the carbon source to which the organisms have become adapted is not paralleled by any other important increase. The activity of maltose-trained cells is generally similar to that of glucose-trained organisms.

At this time, a series of experiments was in progress in the laboratory on the adaptation of *Bact. lactis aerogenes* to growth in various disaccharides.<sup>9</sup> For comparison, the oxidation rates for each of the disaccharides by each of the strains were determined. The results are shown in Table II.

The correspondence between the two sets of results is quite definite. The only anomaly is that cells are always able to oxidise maltose as efficiently as glucose, though they cannot grow optimally in maltose until they have been trained. Apart from this, adaptation to lactose improves the lactose—and to a lesser extent—the sucrose-oxidising power. This is paralleled by a complete training of the growth rate of the cells in lactose, and a partial training of the growth rate in sucrose. Training in sucrose improves growth and oxidation rates in sucrose without affecting either in lactose. Adaptation to glycine (as *nitrogen* source) was without influence on the rate of oxidation of this compound.

## (2) Adaptation to Inhibitors.

(a) **Proflavine** seriously retards the onset of cell growth at concentrations above about 20 mg./l., inhibition being complete at 55 mg./l. At

TABLE III.—OXIDATION TIMES AFTER TRAINING TO PROFLAVINE.

(a) Normal Cells.				(b) Trained to 43 mg./l. proflavine.			
Substrate.	Age of Parent Culture.			Substrate.	Age of Parent Culture.		
	4 Hours.	6 Hours.	24 Hours.		5 Hours.	24 Hours.	
Glucose .	5'	10'	11'	Glucose .	12'	9½'	
Glycerol .	12'	35'	22'	Glycerol .	> 200'	30'	
Lactose .	> 20'	> 50'	56'	Lactose .	> 200'	72'	
Formate .	10'	24'	24'	Formate .	53'	61'	
Glycine .	> 20'	> 50'	54'	Glycine .	> 200'	> 120'	

(c) Trained to 1540 mg./l. Grown in presence of drug.				(d) Trained to 1540 mg./l. of proflavine. Grown several times in absence of drug.			
Substrate.	Age of Parent Culture.			Substrate.	Age of Parent Culture.		
	3 Hours.	10 Hours.	12 Hours.		4 Hours.	6 Hours.	24 Hours.
Glucose .	11'	9½'	8'	Glucose .	14'	18'	25'
Glycerol .	> 200'	24'	9'	Glycerol .	55'	18'	32'
Lactose .	—	> 200'	30'	Lactose .	> 300'	> 100'	> 150'
Formate .	—	11'	9'	Formate .	22'	23'	> 150'
Glycine .	—	> 200'	50'	Glycine .	> 300'	> 100'	> 150'

concentrations up to 100 mg./l. it has, however, little effect either on the ability of glycerol-trained bacteria to oxidise glycerol, or on that of glucose\*

\* Postgate and Hinshelwood, *Trans. Faraday Soc.*, 1946, 42, 45.

262 DEHYDROGENASES OF *BACT. LACTIS AEROGENES*

trained organisms to oxidise glucose, although at still higher concentrations a quite marked effect begins to appear. We may conclude that the operation of the oxidation enzymes is not directly affected by the initial attack of proflavine on untrained cells. This does not, of course, tell us whether the rate of synthesis of these enzymes will be affected during growth in presence of the drug.

Cells were trained to 43 mg./l. of proflavine, and then grown several times in absence of drug. Samples were taken at the conclusion of growth, and 24 hours later. Each was centrifuged as usual and tested in duplicate with a standard concentration (0.05 M.) of each of five substrates—glucose, glycerol, lactose, sodium formate, and glycine. The results, together with the corresponding results for normal cells, are shown in Table III (p. 261).

TABLE IV.—OXIDATION TIMES AFTER TRAINING TO VARIOUS DRUGS

(a) Normal Cells.				(b) Crystal violet trained (after growth in normal medium).				
Substrate.	Age of Parent Culture.			Age of Parent Culture.				
	4 Hours.	6 Hours.	24 Hours.	5.1 mg./l Trained.	51 mg./l Trained.			
				5 Hours.	4 Hours.	5 Hours.	22 Hours.	28 Hours.
Glucose .	5'	10'	11'	10'	4'	7'	9½'	13'
Glycerol .	12'	35'	22'	26'	> 250'	> 200'	> 200'	> 200'
Lactose .	> 20'	> 50'	56'	> 200'	> 250'	> 200'	> 200'	> 200'
Formate .	10'	24'	24'	33'	42'	50'	41'	> 200'
Glycine .	> 20'	> 70'	54'	> 200'	> 250'	> 200'	> 200'	> 200'

(c) Sulphanilamide trained (500 mg./l. after growth in normal medium).

(d) Trained to 190 mg./l. potassium tellurite (after growth in normal medium).

Substrate.	Age of Parent Culture.		Age of Parent Culture.	
	9 Hours.	15 Hours.	5 Hours.	22 Hours.
Glucose . . .	9'	8'	11'	> 300'
Glycerol . . .	31'	20'	20'	> 300'
Lactose . . .	> 200'	> 200'	100'	> 300'
Formate . . .	23'	27'	34'	> 300'
Glycine . . .	> 200'	> 200'	> 200'	> 300'

The differences, if any, due to the training are small. When the trained culture is young, there seems to be no activity towards glycerol, but this disability does not persist, and 20 hours later the behaviour of trained and untrained cells is almost the same.

In the next series of experiments bacteria trained to a very high concentration, 1540 mg./l., of proflavine were tested (1) immediately after culture in presence of the drug and (2) after subsequent equilibration in the normal medium.<sup>10</sup> The results are included in Table III. Certain rather complex changes in activity occur, of which the following may be noted specially. The glycerol and formate oxidation rates vary with the age of the culture, and increase for cells grown in presence of drug to a value almost twice the normal. After the equilibrium of the adapted

<sup>10</sup> Davies, Hinshelwood and Pryce, *Trans. Faraday Soc.*, 1945, 41, 778.

cells, which occurs on growth in normal medium, there is a general reduction in activity (as though the cell size had been reduced). The ratio of the glycerol oxidation rate to that of glucose is still, however, about double the normal.

On the basis of these results (which were confirmed with another trained strain and by further experiments at a series of different glucose, glycerol, and formate concentrations) it might be predicted that proflavine-trained organisms would be somewhat better adapted than normal organisms for growth in glycerol. This was verified. Normal cells have an initial mean generation time in glycerol of 100 minutes; proflavine-trained cells of 50-55 minutes. Nevertheless, the converse is not true. Normal bacteria when trained to glycerol acquire no additional immunity to proflavine, increased ability to oxidise glycerol being therefore only one of the various changes that occur on training to the very high proflavine concentration.

(b) **Sulphanilamide.** No significant change was apparent when bacteria trained to 500 mg./l. of sulphanilamide were tested (Table IV).

(c) **Potassium Tellurite.** Bacteria trained to 190 mg./l. of potassium tellurite and subsequently grown in the normal medium behaved in the same way as untrained organisms when tested at the end of logarithmic growth. A curious anomaly was observed when oxidation rates were determined twenty hours later. Instead of falling off slightly, the values had dropped abruptly to zero. There was, however, no parallel catastrophic change in the ability of these bacteria to grow when subcultured. (It must be borne in mind, however, that the conditions for the Thunberg test do not correspond strictly to those of growth.)

(d) **Crystal Violet.** Training at low crystal violet concentrations (5.1 mg./l.) brought about no considerable change in oxidative activity. However, as with proflavine, there was a more definite effect on training to much higher concentrations (51 mg./l.). The power to oxidise glucose remained unchanged at ages of 4 to 28 hours. On the other hand, the activity towards glycerol vanished, and that toward formate was very seriously impaired.

These crystal violet-trained cells were now adapted to glycerol by repeated subculture, after which process they were found to have recovered completely their ability to oxidise glycerol. They had, however, lost none of their crystal violet immunity which cannot, therefore, be directly dependent on changes in the glycerol oxidising enzyme.

On the other hand, the decrease in glycerol activity of the crystal violet-trained cells affects their ability to grow in glycerol. Curves were plotted showing the lag of these cells in glycerol and glucose media as a function of the age of the inoculum. These were compared with similar curves for normal bacteria. The lags in glycerol of the former were consistently longer. This illustrates further the close correlation between oxidation and growth rates.

## Discussion.

**Adaptation and Dehydrogenase Activity.** The results which have been described show a very definite correlation between the adaptation to utilise a given carbon source in growth and the power to oxidise that compound. Adaptation seems to confer the ability to oxidise molecules of specific form rather than those belonging to a given chemical class. Cells oxidise best those carbohydrates to which they have been adapted, and where changes in the oxidative power towards a particular substrate (glycerol) occur as a secondary result of adaptation to a drug (proflavine, crystal violet), corresponding changes in growth rate are detectable.

The close correlation found here may mean either (a) that oxidation is, an essential step in utilisation, (b) that the two processes have a common initial step (e.g. phosphorylation) or (c) that enzymes can facilitate the

reaction of the same substrate in different ways. There are certain objections to (a). With cells adapted to potassium tellurite, the enzymes concerned in growth and oxidation seem to be capable of independent ageing, while with normal glucose-trained cells, optimum power to oxidise maltose does not seem to be necessarily associated with optimum growth rate in this sugar. (b) and (c) are both possible, but evidence is lacking for more detailed discussion.

No primary correlation is found between the processes of training to various drugs (proflavine, crystal violet, sulphanilamide, potassium tellurite) and changes in the dehydrogenases. Although training to high concentrations of crystal violet greatly impairs the oxidising power towards glycerol, re-training to glycerol does not in its turn impair the crystal violet adaptation. The elimination of the glycerol-oxidation must therefore be a secondary result of the crystal violet adaptation and not essentially linked with it. Moreover, these changes in oxidising power only become evident, if at all, when the cells have been trained to very high drug concentrations. Here we have already had occasion to postulate secondary changes in enzymes other than those directly affected by the drug.<sup>10</sup>

These secondary changes are, however, in themselves of interest in connection with the enzyme model of adaptation which has been discussed in previous papers. According to this model certain enzymes are inhibited while others go on growing, so that changes in relative amount occur. If the inhibited enzymes are essential ones, cell division must await their due increase, and the result of the drug action will be that the amount per cell of the uninhibited enzymes increases. But if the inhibited enzymes are not essential ones they will suffer gradual elimination. The loss of glycerol-oxidation power which accompanies training to crystal violet may very well be an example of this process.

**Changes in Form of the Activity-substrate Concentration Curves.**—Training to glycerol not only raises the optimum oxidation rate, but changes the actual form of the rate-glycerol concentration curve. With the trained cells the optimum is reached at a much lower concentration (Fig. 2). This fact may have some bearing on the nature of the adaptive process. If the rate of oxidation is determined by the first reaction of the scheme on page 257, then the relation between rate and substrate concentrations will be a single characteristic function (probably akin to an adsorption isotherm), the *form* of which is independent of the *amount* of the enzyme. If adaptation to glycerol simply leads to an increase in the amount of an appropriate enzyme then we should expect the *optimum* rate to increase but the *form* of the rate-concentration curve to remain the same. The change in shape suggests that there may have been a more drastic change than a simple increase in the amount of enzyme, namely a change in the actual protein texture of the enzyme, enabling it to accommodate the substrate more easily. We have already been led to suppose that certain adaptive processes involve qualitative changes in the surface of enzymes, as well as changes in amount. The effect now described may be another example of the same type of phenomenon. The reaction in question is, however, somewhat complex, and it might be that an increase in the amount of one of the enzymes involved also changes the rate-determining step of the whole process. If this were so, an alteration in the concentration-dependence would be likely, and would not necessarily imply any qualitative change in any enzyme surface. For the time, therefore, the evidence must simply be noted, until it can take its place in a wider scheme.

The authors wish to express their thanks to Messrs. E. H. Cole, S. Jackson, B. J. Langdon and C. H. Denyer for assistance with this work. They must also record their deep indebtedness to Messrs. Imperial Chemical Industries, Ltd. (Dyestuffs Division) who made it possible for one of them (D. S. D.) to undertake the research.

### Summary.

The Thunberg (methylene blue reduction) method has been used to investigate changes in dehydrogenase activity occurring when *Bact. lactis aerogenes* undergoes various adaptations.

Adaptation to a new carbon source gives specifically increased dehydrogenase activity towards that particular substance. Cells trained to glycerol show no parallel increase in ability to oxidise other polyhydric alcohols: nor do those trained to sucrose give increased oxidation of other disaccharides, though lactose-trained bacteria, besides improved lactose oxidation, show somewhat better sucrose oxidation.

In general, there is a close parallel between the oxidation of the carbon source and its utilisation in growth (though oxidation may not be a necessary preliminary to growth).

Adaptation to glycerol not only increases the optimum rate of glycerol oxidation, but changes the actual form of the curve relating oxidation rate to concentration. This could be explained by the assumption (already suggested on other grounds) that adaptation changes not only the amount but the actual texture of the relevant enzyme, though the present observation does not, in itself, constitute unambiguous independent evidence.

Adaptation to moderate concentrations of crystal violet or proflavine brings about no change in the power to oxidise five representative substances. Adaptation to higher concentrations causes changes in the ability to oxidise glycerol and formate—a decrease with crystal violet and an increase with proflavine. These alterations are shown to be secondary consequences of the main adaptive process. They are reflected in corresponding changes in lag or growth rate. Sulphanilamide training is without effect on the oxidation properties. Bacteria trained to potassium tellurite, though normal in their oxidation properties when young, lose all their dehydrogenase activity long before they lose the power to grow on subculture.

### Résumé.

On a étudié par la réaction de Thunberg (réduction du bleu de méthylène) les variations de l'activité de la deshydrogénase, qui se produisent quand le *Bact. lactis aerogenes* s'adapte à des inhibiteurs ou à des variations de la source de carbone. L'adaptation à ces dernières produit une activité de la deshydrogénase accrue spécifiquement envers la substance particulière et, en général, il y a étroit parallélisme entre l'oxydation de la source de carbone et son utilisation dans la croissance. On a étudié aussi l'adaptation à diverses concentration de proflavine, de violet cristallisé et de tellurite de potassium.

### Zusammenfassung.

Die Thunberg'sche Reaktion (Reduktion von Methylenblau) wurde dazu benützt, um Veränderungen in der Aktivität des Enzyms "Dehydrogenase" zu untersuchen, wenn *Bact. lactis aerogenes* sich an Veränderungen der Kohlenstoffquelle und an wachstumshemmende Substanzen anpasst. Anpassung an eine bestimmte Substanz erzeugt eine spezifische Vergrößerung der Dehydrogenaseaktivität gegenüber dieser Substanz. Im allgemeinen besteht eine enge Beziehung zwischen der Oxydation der Kohlenstoffquelle und deren Verwendung für Wachstum. Die Anpassung an diverse Konzentrationen von Proflavin, Kristallviolett und Kaliumtellurit wird besprochen.



# THE CATALASE ACTIVITY OF *BACT. LACTIS AEROGENES*.

By E. H. COLE AND C. N. HINSHELWOOD.

*Received 23rd May, 1946.*

The determinations of the catalase activity of *Bact. lactis aerogenes* to be described were carried out on cells grown under a variety of conditions, including different temperatures, presence of different substrates and of certain bacteriostatic agents, to which in some cases the cells had been adapted. The object was to investigate what correlation might exist between the changes in the catalase of the cells and the known effects of the applied conditions on the characteristics such as lag, mean generation time, and drug resistance.

## Experimental.

The manner of cultivation of the cells and the experimental technique has been described elsewhere.<sup>1</sup> Unless otherwise stated, the cells were grown at 40.0° C. in a synthetic medium containing the following constituents: glucose (19.15 g./litre), ammonium sulphate (0.958 g./litre), magnesium sulphate (0.0383 g./litre), potassium phosphate—NaOH buffer,  $pH = 7.1$ . This will be referred to as the "normal medium."

The cells were removed by centrifuging from the medium in which they were grown. After removal of the filtrate by decantation the mass of cells was broken up, washed by resuspension in saline and reprecipitated by further centrifuging. This washing process was carried out three times to ensure removal of all traces of the nutrient constituents of the growth medium. The final suspension was stirred for about an hour by a slow stream of sterile air to break up any clumps. The suspension was then counted and diluted with the calculated volume of saline to bring it to a count of 1000 on a Thoma hæmocytometer ( $1250 \times 10^6$  cells per ml.). After dilution it was stored without aeration at 40° C. until required.

For the determination of the catalase activity the suspension of "resting cells" so obtained was allowed to act upon hydrogen peroxide in small flasks in a thermostat at 40.0° C. The flasks contained 20 ml. of potassium phosphate—NaOH buffer,  $pH = 7.4$ , 10 ml. of cell suspension, 2.5–20 ml. of 0.50 N. hydrogen peroxide, and glass-distilled water to make the total volume 50 ml. The reaction was started by the addition of the suspension to the rest of the mixture. Its progress was followed by withdrawal from time to time of 5 ml. samples which were run into about 20 ml. of dilute (*ca.* 2 N.) sulphuric acid. This concentration of acid is known to deactivate catalase completely.<sup>2</sup> The amount of hydrogen peroxide remaining was then determined by titration with N./100 potassium permanganate. Each titration was corrected for the small volume (usually 0.1–0.2 ml.) of permanganate that was reduced in a corresponding blank test with the cell suspension itself. Further control tests were made with hydrogen peroxide and 10 ml. of the suspension which had been previously boiled for 1–2 minutes. These showed no change in hydrogen peroxide concentration during the normal time over which the measurements extended.

<sup>1</sup> Davies, Hinshelwood and Pryce, *Trans. Faraday Soc.*, 1944, **40**, 397.

<sup>2</sup> Morgulis, Beber and Rabkin, *J. Biol. Chem.*, 1926, **68**, 547.



On integration, equation (i) then becomes

$$t = \frac{1}{kg(c_0 - \Delta_\infty)} \ln \frac{(c_0 - \Delta)}{c_0(\Delta_\infty - \Delta)} \quad (ii)$$

where  $c_0$  = initial  $H_2O_2$  concentration (moles/l.),  $\Delta$  = number of moles/l. of  $H_2O_2$  decomposed at time  $t$ , and  $\Delta_\infty$  = total number of moles/l. of  $H_2O_2$  which can be decomposed by the time all reaction stops.

The validity of equation (ii) may be tested by plotting values of

$$\log \frac{(c_0 - \Delta)}{(\Delta_\infty - \Delta)} \text{ against } t.$$

For a set of experiments in which  $c_0$  was varied over the range 0.02 to 0.20 N.

a series of straight lines was obtained (Fig. 3). Furthermore, direct proportionality was found to exist between the slopes of these lines and the corresponding values of  $(c_0 - \Delta_\infty)$  (Fig. 4).

It may be concluded therefore that the reaction is kinetically of the second order, and that the rate of deactivation of the enzyme is in a constant ratio to the rate of the decomposition of the hydrogen peroxide. Comparative tests made at 30.0° C. and 40.0° C. showed the initial rate of reaction to be less and the total amount of decomposition to be greater at the lower temperature. Thus  $g$  increases as the temperature drops.

The results of this brief kinetic study with the resting cells of *Bact. lactis aerogenes* are in complete agreement with those of a previous investigation in which cell free preparations of the enzymes<sup>3</sup> were employed. The activity of the bacterial cells which is measured in the present work is thus identified unequivocally as that of the enzyme catalase of other investigators.

Once the cells have been washed, the catalase activity shows little change over a period of many hours, and there is no difficulty about experimental control. The variation of the catalase activity with the age of the culture from which the cells are taken is a much more serious matter and was investigated by centrifuging samples taken from a culture at various phases of the growth cycle. At any given temperature the value of  $\Delta_\infty$  gives a measure of the amount of enzyme present. Hence reaction mixtures were made up containing excess  $H_2O_2$  and the reaction was allowed to continue for at least 300 minutes, after which the residual amount of substrate was titrated to

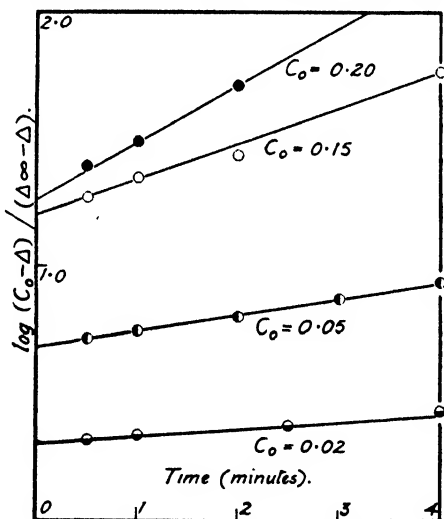


FIG. 3.—Test of kinetic equation.

$c_0$  = initial  $H_2O_2$  concentration.

$\Delta$  = amount decomposed at time  $t$ .

$\Delta_\infty$  = total amount decomposed.

<sup>3</sup> Yamasaki, *Sci. Rep. Tohoku Imp. Univ.*, 1920, 9, 13.

give the amount that had been decomposed. The catalase activity is shown in relation to the growth curve of the culture in Fig. 5. The age of the cells is reckoned arbitrarily from the time when they have a population of  $1.25 \times 10^6$ /ml., which corresponds to a count of unity on a hæmocytometer of area  $1/400$  sq. mm. and depth 0.02 mm. This corresponds to a moment before visible growth has set in.

A maximum activity at an age of about 10 hours was generally observed for cells which grew with a mean generation time of 30-35 minutes, and this maximum value was taken as the characteristic catalase activity for the strain under test. It is expressed as the number of g.-equivalents of hydrogen peroxide decomposed by 1000 ml. of a suspension of the cells with a count of 1000.

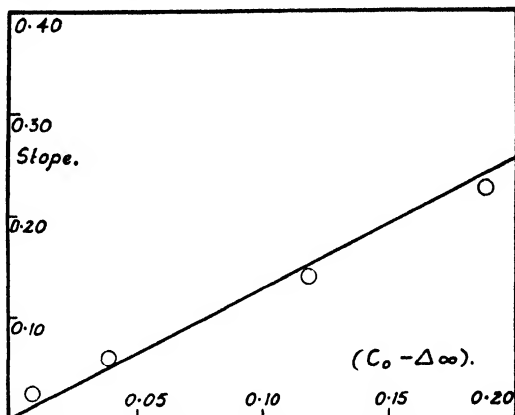


FIG. 4.—Further test of kinetic equation.

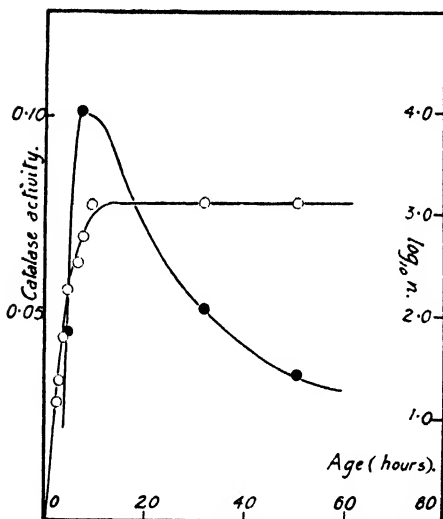


FIG. 5.—Influence of culture age on catalase activity. Black circles—activity; open circles—total count of growing culture at time of sampling (right hand scale). (The activity is measured by  $\Delta \infty$ .)

one of which was added  $2.88 \times 10^{-6}$  g.-ions  $\text{Fe}^{++}$  per litre. Both of the resulting curves were of the usual form, but the presence of the Fe increased the maximum activity from 0.225 to 0.453.

### Growth in the Presence of Iron.

Since catalase consists of protoferrihæm IX<sup>4</sup> linked to a specific protein, the effect on the catalase activity of growth in the presence of ferrous ions was investigated. As a preliminary, ferrous ion concentrations up to  $1.5 \times 10^{-6}$  M. were shown to affect appreciably neither lag nor growth rate. Six media containing amounts of ferrous ammonium sulphate to give a range of ferrous ion concentrations up to  $1.5 \times 10^{-6}$  M. were inoculated, and when fully grown, centrifuged, all in parallel. The catalase activity of the suspensions showed a maximum corresponding to  $2.5 \times 10^{-6}$  g.-ions of ferrous iron per litre (Fig. 6).

Age-activity determinations were carried out simultaneously on two cultures, to

<sup>4</sup> Stern, *J. Biol. Chem.*, 1936, 112, 661.

**Adaptation to Proflavine and to Sulphanilamide.**

It has been observed<sup>1</sup> that growth of sulphanilamide-resistant cells in the presence of proflavine (2:8-diamino-acridine) causes partial re-

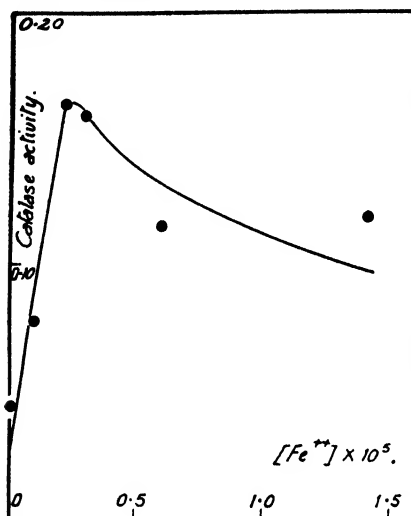


FIG. 6.—Influence of added iron on catalase formation. (Activity measured by  $\Delta_{\infty}$ .)

version of the sulphanilamide adaptation and later work<sup>2</sup> has shown that the extent of the reversion depends on the length of the original training to sulphanilamide and on the proflavine concentration in which the cells are grown. Similar experiments on the development and loss of adaptation have now been made in parallel with catalase determinations, in order to see whether the processes are accompanied by any changes in the amount of this enzyme.

During training to sulphanilamide by repeated sub-culture in a drug concentration of 213 mg./l. the catalase activity increases progressively (Table II). In the Table the total number of subcultures is counted from the transfer of the strain to the normal synthetic medium from bouillon or agar.

This result is of interest in connection with one of the theories which have been postulated to explain the bacteriostatic action of sulphonamides.<sup>3</sup> The drug is considered to become oxidised to hydroxylamine or a substituted hydroxylamine which poisons the catalase of the cells. The bacteriostasis is brought about by the accumulation of hydrogen peroxide within the cells or in their immediate vicinity. According to this view increase in the catalase activity of the cells might well be an integral part of the training process, enabling them to withstand the inhibitory action of the products of the breakdown of the sulphonamides.

TABLE II.

Subcultures in Normal Medium.	Subcultures in Sulphanilamide 213 mg./l.	Total No. of Subcultures.	Activity.	
67	—	67	0.040	} Series I.
58	11	69	0.064	
100	—	100	0.101	} Series II.
58	42	100	0.214	
58	51	109	0.275	

Training to proflavine also leads to changes in the catalase activity, which is here much reduced (Table III).

Proflavine has been shown to exert various actions on untrained cells, including an increase in the lag, decrease in the growth rate, the production

<sup>1</sup> James (unpublished observations).

<sup>2</sup> Main, Shinn and Mellon, *Proc. Soc. Exp. Biol. Med.*, 1938, **39**, 272, 591; 1939, **40**, 640; 1939, **42**, 115; 1940, **43**, 593; 1940, **44**, 596.

of long filaments, and reduction of the total population.<sup>1</sup> Training by repeated subculture in the presence of the drug brings the lag and the growth rate back to their original values with the simultaneous disappearance of abnormal cell-forms. There is, however, no significant return of the total bacterial population to its normal value. It seems, therefore, quite possible that the drug exerts a harmful action upon the mechanisms by which toxic products of cell metabolism are ordinarily countered, and that adaptation is unable to restore them in presence of proflavine. The protective action of catalase in decomposing  $H_2O_2$  may be among such mechanisms.

The effect of one subculture in a medium containing proflavine on cells trained to sulphanilamide is shown in Table IV.

Growth in proflavine causes a considerable decrease in the catalase activity in the cells. It is accompanied by the formation of long filaments and loss of adaptation as indicated by the value of the growth rate in subsequent tests in a medium containing sulphanilamide.

The mean generation time had increased from 35' for the trained cells to 74' for those de-trained by growth in 29.5 mg./l. proflavine.

There is a suggestive relationship between adaptation and change in catalase activity. Training to sulphanilamide increases the latter, while growth in presence of proflavine not only reduces it, but reverses the adaptation. These facts are compatible with the view that production of more catalase plays, with *Bact. luctis aerogenes*, a definite part in the development of resistance to sulphanilamide.

The possibility was, however, explored that the increased catalase activity developed in presence of sulphanilamide might be due merely to extra iron supplied as impurity in the drug. Mr. F. M. Brewer kindly subjected the specimen employed to spectroscopic analysis.

TABLE III.

Subcultures in Proflavine.	Proflavine Conc. Mg./l.	Activity.
37	90	0.017
30	51	0.035

TABLE IV.

Subcultures in Sulphanilamide.	Sulphanilamide Conc. Mg./l.	Subcultures in Proflavine.	Proflavine Conc. Mg./l.	Activity.
17	110	—	—	0.135
22	110	1	30	0.101-0.108
61	110	—	—	0.053
60	110	1	29.5	0.022
60	110	1	51	0.027

A Cu arc was used to obtain a spectrum from: (i) a small amount of the solid sulphanilamide, (ii) the residue from evaporation on to the arc of 0.1 ml. of a saturated solution in glass-distilled water, (iii)-(ix) the residues from evaporation of 0.1 ml. samples of standard ferrous ammonium sulphate solutions containing from 10 to 0.00001 g.  $Fe^{++}$  per litre in steps of tenfold dilution, (x) some of the solid product of evaporating to dryness 50 mg. of Analar  $KIO_3$  and approx. 1 ml. of concentrated  $H_2SO_4$ . (This salt was chosen because it is described as being free from iron). (xi) Some of the solid product of treating 1 g. of solid sulphanilamide, 50 mg. of Analar  $KIO_3$  and approx. 1 ml. of concentrated  $H_2SO_4$  as in (x). (x) and (xi) were repeated using Ag wire electrodes, which give a simpler spectrum.

None of the spectra produced when sulphanilamide or its decomposition products were present gave any lines that could be attributed to iron. From

this it could be calculated that a medium containing 100 mg./l of the drug is not more than  $1.79 \times 10^{-12}$  M. in  $\text{Fe}^{++}$ .

The possibility that the increase in the catalase activity of the cells when repeatedly subcultured in the presence of sulphanilamide is due to iron can be dismissed, as the cells are observed not to respond to an iron concentration of less than about  $5 \times 10^{-7}$  M. (see Fig. 6).

### Change of Temperature of Cultivation.

It has already been mentioned that at lower temperatures a given amount of catalase can decompose a greater amount of the substrate before

TABLE V.

Subcultures.	Grown at.	Activity.	
		Measured at 30°.	Measured at 40°.
67	40°	0.061	0.038
102	30°	0.041	0.029
100	40°	0.149	0.100
193	30°	{ 0.100	0.073
		{ 0.505*	0.387*
64	20°	0.310†	0.146

it is itself deactivated. If the catalase were formed in the cell just to the extent required for dealing with a certain definite amount of  $\text{H}_2\text{O}_2$ , then continued subculture at different temperatures would lead to the establishment of correspondingly different amounts of the enzyme.

To examine this possibility, two strains of cells were derived from the same parent by repeated subcultures at 30° and 40° c. respectively. From time to time catalase determinations were made, the tests on each being carried out at both temperatures. The results are summarised in Table V which also includes a value for the catalase activity of cells grown at 30° c. in the presence of  $3.0 \times 10^{-6}$  M.  $\text{Fe}^{++}$ , and one for cells grown at 20° c. There is no indication of "training" to temperature, as shown by the amount of catalase formed either during growth in the normal medium, or in presence of the optimum concentration of iron. The figures in this Table also illustrate the apparently random changes in the amount of catalase formed in successive subcultures, the fluctuations probably reflecting the variations in the traces of iron provided by the impurities in the medium.

### Decay of the Enzyme.

When a culture ages its enzymes decay, and, at the same time, the lag of inocula transferred to a new medium increases. It is of interest to inquire into the relation between the rate of decay of specific enzymes, and the rate of development of the lag. For this purpose observations on the decline of catalase activity have been made. A culture in the normal medium was allowed to age at 40.0° c. and at intervals determinations were made of (a) the pH, (b) the catalase activity, and (c) the lag of the inocula transferred to fresh normal medium. Once it was fully grown the

TABLE VI.

Age of Cells (Hours).	Catalase Activity.	Lag (Minutes).
12	0.0665	—
14	—	72
36	0.0996	142
109	0.0225	960 $\pm$ 150
123	—	808
157	0.0128	1090 $\pm$ 140
194	—	1610 $\pm$ 150
217	—	2000 $\pm$ 150
229	0.0073	—

\* In the presence of  $3.0 \times 10^{-6}$  M.  $\text{Fe}^{++}$ .

† Measured at 20° c.

culture maintained a  $pH$  of about 4.5. The values of the lag and catalase activity are given in Table VI.

After the maximum value has been reached at the end of the growth phase, the activity of the enzyme decays exponentially. The increase of the lag is very nearly proportional to the age of the cells. The detailed

TABLE VII.

Age of Suspension (Hours).	Catalase Activity.			
	$pH = 7.54.$	$pH = 6.36.$	$pH = 5.40.$	$pH = 4.63.$
4			0.0389 (initial value)	
24	0.0392	0.0369	—	—
32	—	—	0.0432	0.0424
98	0.0345	0.0398	0.0209	0.0226
194	0.0383	0.0208	0.0094	0.0105

discussion of this relation is reserved until results for other enzymes are available. In another series of experiments, cells from a grown culture were centrifuged at a convenient age, and suspended in a series of portions of saline buffered with potassium phosphate-sodium hydroxide mixtures to various known  $pH$  values. The suspensions were maintained at 40.0 c. and gently aerated to prevent the cells from settling out. Samples were taken at intervals over a period of 200 hours, centrifuged and tested for catalase activity in the usual way, the counts and hydrogen-ion concentrations being checked for constancy from time to time.

In the most alkaline buffer the enzyme undergoes no significant change, while it survives unaltered for a considerable period (100 hours) in the slightly acid buffer. In the two more acid ones, however, marked decay occurs which can be represented by a straight line in a plot of  $\log$  (activity) against age. The decay constant for the enzyme of the cells ageing in the parent growth medium of  $pH = 4.5$  differs little from that for the enzyme of the cells ageing in the saline buffered to  $pH = 4.63$  (see Fig. 7). It may be concluded, therefore, that the high hydrogen-ion concentration is the main adverse factor which causes decay of the catalase in cells remaining in a fully grown culture.

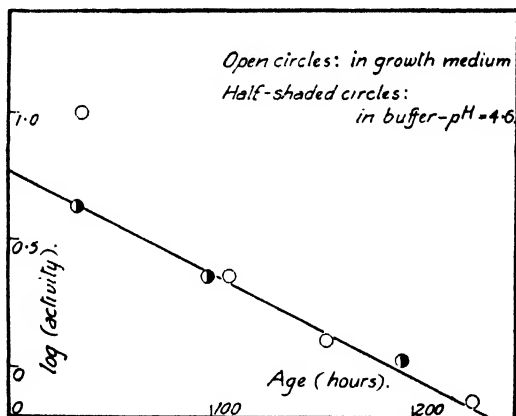


FIG. 7.—Decay of catalase activity in growth medium and in acid buffer. (Activity measured by  $\Delta_{\infty}$ .)

### Summary.

The catalase in washed suspensions of *Bact. lactis aerogenes* possesses the same characteristics (in respect of the kinetics of the catalysed hydrogen peroxide decomposition), as the cell-free preparations of the enzyme obtained from other sources by previous investigators.



The catalase activity is maximal for cells which have been grown in presence of  $\text{Fe}^{++}$  at  $2.5 \times 10^{-6}$  g. ions/l.

Cells adapted to sulphanilamide show an increase and those which have been grown in presence of proflavine a decrease in catalase activity. The loss of sulphanilamide adaptation caused by growth in proflavine is probably connected with this effect.

The decay of the enzyme (from maximum activity) with age is approximately exponential, and a function of  $\text{pH}$ , the adverse  $\text{pH}$  of normal cultures being a principal cause of the observed decline.

### Résumé.

La catalase dans des suspensions lavées de *Bact. lactis aerogenes* possède, par rapport à la cinétique de la décomposition de l'eau oxygénée, les mêmes caractères que les préparations de l'enzyme, exemptes de cellules et obtenues à partir d'autres sources par des auteurs précédents.

L'activité de la catalase est accrue pour des cellules adaptées à la sulphanilamide et diminuée pour des cellules cultivées en présence de proflavine.

La diminution d'activité de l'enzyme avec l'âge est approximativement exponentielle et une fonction du  $\text{pH}$ .

### Zusammenfassung.

Das Enzym "Catalase" in gewaschenen Suspensionen von *Bact. lactis aerogenes* besitzt dieselben Eigenschaften (mit Bezug auf die katalysierte Wasserstoffperoxydzersetzung) wie die zellenfreien Präparate des Enzyms früherer Forscher aus anderen Quellen. An Sulfanilamid gewöhnte Zellen zeigen eine vergrößerte und in der Gegenwart von Proflavin gezüchtete eine verminderte Catalaseaktivität. Die zeitliche Abnahme der Enzymaktivität vom Maximalwert ist ungefähr exponentiell und hängt vom  $\text{pH}$ -Wert ab.

## LOSS OF SULPHANILAMIDE ADAPTATION INDUCED BY GROWTH OF *BACT. LACTIS AEROGENES* IN PRESENCE OF PROFLAVINE.

By A. M. JAMES AND C. N. HINSHELWOOD.

Received 23rd May, 1946.

Previous work <sup>1</sup> has shown that *Bact. lactis aerogenes* trained to resist sulphanilamide by a few passages only through media containing the drug readily loses its partial immunity when passed through the normal drug-free medium. After some 30 sub-cultures in presence of the sulphanilamide, however, this kind of reversion no longer occurs. At this stage a single passage of the sulphanilamide-trained cells through a medium containing about 30 mg./l. proflavine was found to cause marked reversion.<sup>2</sup> The present work was undertaken to investigate how the proflavine-induced reversion depends upon such factors as the age of the cells, the concentration of the drug, the number of preliminary subcultures in the sulphonamide, and any previous adaptation of the bacteria to the proflavine itself. It was also desired to find out whether the presence of proflavine in a medium would prevent or hinder the development of sulphanilamide immunity when training experiments were made with a mixture of the drugs.

The experiments were arranged as follows. Cells were serially sub-

<sup>1</sup> Davies and Hinshelwood, *Trans. Faraday Soc.*, 1943, **39**, 431.

<sup>2</sup> Davies, Hinshelwood and Pryce, *ibid.*, 1944, **40**, 397.

cultured in an artificial medium<sup>1</sup> containing 200 mg./l. sulphanilamide. At various stages after training was complete, namely after 31, 40, 61 and 126 subcultures, identical inocula were made from the trained strain, at an age of about 5 hours, into media containing proflavine at a range of concentrations up to the highest in which growth was possible. Similar inoculations were made with cells at ages of 12, 25 and over 30 hours. When these cultures in the proflavine-containing media had grown they were subcultured once in drug-free medium to remove any proflavine, and then inoculated into media containing 200 mg./l. sulphanilamide. Growth rates were determined in the latter, and served as criteria of the state of adaptation of the cells. The results of these tests are shown in Table I.

TABLE I.

Age of Parent Culture.	Proflavine Concn. Mg./l.	Training to Sulphanilamide.							
		31 Subcultures.		40 Subcultures.		61 Subcultures.		126 Subcultures.	
		$T_{20}^{200†}$	F*	$T_{20}^{200†}$	F*	$T_{20}^{200†}$	F*	$T_{20}^{200†}$	F*
5 hours	22	150						120	
	33	480						165	
	43	120	+					130	
	52	150	+					120	
10-15 hours	22	155		200		165		110	
	33	140		125	+	133	+	150	
	43	120		330	++	143	+	125	
	52							185	
28 hours	22	130	+	150	+	120		120	
	33	220	+	270	++	105	+	130	
	43	180	+	230	++	125	+	170	
	52	165	++			150	+	143	
Over 30 hours	22	180						105	
	33	155						150	
	43	150	+						
	52	140	+						

During the growth of the sulphanilamide-trained cells in the proflavine media there was often abnormal cell division with production of long filaments. Both reversion and filament formation depended upon generally similar conditions of age and of drug concentration, but the two phenomena are not directly connected, and on occasion one occurred without the other. For an inoculum of a standard age the degree of reversion usually increases with the proflavine concentration. The effect of the age of the culture is less definite, though at some stages there is a greater tendency for older cultures to revert. Long continued adaptation of the cells to the sulphanilamide produces a relative stabilisation which makes reversion by the action of proflavine increasingly difficult. Even after 126 passages through the sulphanilamide, however, some loss of adaptation is still caused by proflavine in appropriate circumstances.

Since proflavine induces loss of sulphanilamide adaptation, it seemed possible that the immunity might never be acquired if cells were grown

\* F. indicates the formation of long filamentous cells.

†  $T_{20}^{200}$  is the time taken for the bacterial count to increase from 20 units to 200 units on a standard scale used. It serves as a measure of the state of adaptation, being 110 minutes for a fully adapted culture, and 550 minutes for a completely unadapted one (tested for the first time in sulphanilamide at 200 mg./l.).

in a mixture of the two drugs. Experiments were therefore made in which the bacteria were subcultured in a medium containing 30 mg./l. proflavine and 200 mg./l. sulphanilamide. At intervals tests were made on the growth rate in presence of each drug separately so that the development of the two kinds of immunity could be followed. There proved to be little mutual interference of the two adaptive processes and the resulting strain was fully immune to both drugs at concentrations up to those respectively prevailing in the training medium.

Since proflavine at 30 mg./l. caused reversion of cells adapted to sulphanilamide alone, there seemed a possibility that the cells trained to both drugs might suffer an induced reversion if exposed to the action of proflavine at a concentration greater by 30 mg./l. than that to which they had become adapted. They were therefore subcultured in presence of proflavine at still higher concentrations, up to 80 mg./l. (the highest in which they would grow at all). No reversion occurred, even under the conditions of age which the previous experiments had shown to be most likely to induce it. Correspondingly no filaments were ever formed in these circumstances. It thus appears that adaptation to moderate concentrations of proflavine completely eliminates the reversion of sulphanilamide adaptations even by much higher concentrations.

### Summary.

Adaptation of *Bact. lactis aerogenes* to sulphanilamide may be lost by subculture under appropriate conditions in presence of proflavine. Reversion and filament formation depend upon similar conditions, but the one process may occur without the other.

In presence of a mixture of proflavine and sulphanilamide the adaptation of the cells to each drug is little hindered by the other. Adaptation to a moderate concentration of proflavine renders the cells capable of retaining their sulphanilamide adaptation, even when exposed to much higher concentrations of proflavine.

### Résumé.

L'adaptation du *Bact. lactis aerogenes* à la sulfanilamide peut être perdue par repiquage dans des conditions appropriées en présence de proflavine.

En présence d'un mélange de proflavine et de sulfanilamide, l'adaptation des cellules à chaque produit est légèrement empêchée par l'autre. Une adaptation à une concentration modérée de proflavine rend les cellules capables de conserver leur adaptation à la sulfanilamide.

### Zusammenfassung.

Die Gewöhnung von *Bact. lactis aerogenes* an Sulfanilamid kann unter gewissen Umständen in der Gegenwart von Proflavin verloren werden. In der Gegenwart einer Mischung von Proflavin und Sulfanilamid ist die Anpassung der Zellen an eine der Drogen nur wenig durch die andere behindert. Gewöhnung an eine geringe Konzentration von Proflavin bewirkt auch, dass die Zellen ihre Sulfanilamid Anpassung beibehalten, selbst wenn sie dann viel höheren Proflavinkonzentrationen ausgesetzt werden.

*Physical Chemistry Laboratory,  
Oxford University.*

# THE PHOTO-ELASTIC PROPERTIES OF RUBBER. PART I: THEORY OF THE OPTICAL PROPERTIES OF STRAINED RUBBER.

BY L. R. G. TRELOAR.

*Received 24th May, 1946.*

In this paper the optical properties of vulcanised rubber subjected to the most general type of homogeneous strain will be examined theoretically, on the basis of a molecular-network model essentially similar to that already successfully applied by a number of authors in the determination of the mechanical properties of vulcanised rubber.

The foundations of the optical theory have been laid by Kuhn and Gr $\ddot{u}$ n<sup>1</sup> who considered first the optical properties of a statistically-kinked long-chain molecule, composed of optically anisotropic links. They next examined the problem of a network of such molecules subjected to a simple elongation, obtaining formulæ for the variation of birefringence with elongation. They showed that the stretched rubber could be characterised by two principal refractive indices, corresponding to directions of polarisation respectively parallel and perpendicular to the direction of extension. It is therefore optically equivalent to a uniaxial crystal.

In the more general case of a deformation described by three different extensions in three mutually perpendicular directions (pure homogeneous strain) we may anticipate that the optical properties will correspond to those of a crystal not possessing axial symmetry, i.e. a biaxial crystal. Such a crystal has three principal refractive indices, corresponding to three mutually perpendicular directions of the electric vector of light rays propagated in it. These three principal refractive indices form the principal axes of the index ellipsoid, by which the refractive index for any other direction of electric vector is determined. From general considerations we may expect the principal axes of the index ellipsoid in strained rubber to have the same directions as the principal axes of the strain ellipsoid.

## Optical Properties of Statistically-kinked Molecule.

Before proceeding to the general problem it seems desirable that we should review briefly the treatment of the single molecular chain, as given by Kuhn and Gr $\ddot{u}$ n.

In this treatment the actual chain is replaced by an idealised chain of  $n$  universally-jointed, randomly-oriented links, each of length  $l$ . The links are assumed to be optically anisotropic and characterised by polarisabilities \*  $\alpha_1$  along, and  $\alpha_2$  at right angles to their length.

To determine the principal polarisabilities of the chain, and their dependence on the distance between its ends, we require to know the angular distribution of the individual links corresponding to a given distance between the ends. The solution to this problem has been worked out by Kuhn and Gr $\ddot{u}$ n, and is represented by the formula

$$dn = e^{\alpha} e^{\beta \cos \theta} \cdot \frac{1}{2} \sin \theta d\theta \quad . \quad . \quad . \quad (1)$$

\* Polarisability = ratio of induced dipole moment to electric field strength.

<sup>1</sup> Kuhn and Gr $\ddot{u}$ n, *Koll. Z.*, 1942, 101, 248.

in which  $dn$  represents the number of links making an angle between  $\theta$  and  $\theta + d\theta$  to the line joining the ends of the chain.  $\alpha$  and  $\beta$  are constants whose values depend on the distance  $r$  between the ends of the chain, and are given by the relations

$$\beta = L^{-1}(r/nl) \quad . \quad . \quad . \quad . \quad . \quad (1a)$$

$$\alpha = n\beta/\sinh \beta \quad . \quad . \quad . \quad . \quad . \quad (1b)$$

The function  $L^{-1}$  in (1a) is the inverse Langevin function. Alternatively we may write

$$r/nl = L(\beta) = \coth \beta - 1/\beta \quad . \quad . \quad . \quad (1c)$$

where  $L$  is the Langevin function.

We now consider the polarisability of the whole chain for the directions of the applied field, namely (a) parallel to the line joining the ends of the chain, and (b) at right angles to the line joining the ends of the chain.

Suppose the line joining the ends to coincide with the axis OX of a rectangular co-ordinate system. Let any given link of the chain make an angle  $\theta$  with OX, and suppose that the plane containing the angle  $\theta$  makes an angle  $\phi$  with the plane YOX. The polarisabilities of this link, for fields respectively along OX and OY are then given by the relations

$$\left. \begin{aligned} \alpha_x &= \alpha_1 \cos^2 \theta + \alpha_2 \sin^2 \theta \\ \alpha_y &= (\alpha_1 - \alpha_2) \sin^2 \theta \cos^2 \phi + \alpha_2 \end{aligned} \right\} \quad . \quad . \quad . \quad (2)$$

and the corresponding total polarisabilities of the chain, being the sum of the polarisabilities of the single links will be

$$\begin{aligned} \gamma_1 &= \int \alpha_x dn \\ \gamma_2 &= \int \alpha_y dn \end{aligned} \quad . \quad . \quad . \quad . \quad . \quad (3)$$

The number of links at angles between  $\theta$  and  $\theta + d\theta$  and  $\phi$  and  $\phi + d\phi$  is from (1)

$$dn \, \theta, \phi = e^{\alpha_e \beta \cos \theta} \cdot \frac{1}{2} \sin \theta \cdot d\theta \frac{d\phi}{2\pi} \quad . \quad . \quad . \quad (4)$$

since all values of  $\phi$  are equally probable. Introducing this distribution into (3) gives, for the polarisabilities of the chain respectively parallel and perpendicular to the line joining its ends,

$$\begin{aligned} \gamma_1 &= \iint e^{\alpha_e \beta \cos \theta} \cdot \frac{1}{4\pi} \sin \theta d\theta d\phi (\alpha_1 \cos^2 \theta + \alpha_2 \sin^2 \theta) \\ \gamma_2 &= \iint e^{\alpha_e \beta \cos \theta} \cdot \frac{1}{4\pi} \sin \theta d\theta d\phi [(\alpha_1 - \alpha_2) \sin^2 \theta \cos^2 \phi + \alpha_2] \end{aligned} \quad . \quad (5)$$

which on integration yield the result

$$\left. \begin{aligned} \gamma_1 &= n \left[ \alpha_1 - (\alpha_1 - \alpha_2) \frac{2r/nl}{L^{-1}(r/nl)} \right] \\ \gamma_2 &= n \left[ \alpha_2 + (\alpha_1 - \alpha_2) \frac{r/nl}{L^{-1}(r/nl)} \right] \end{aligned} \right\} \quad . \quad . \quad . \quad (6)$$

and, for the difference of the two principal polarisabilities

$$\gamma_1 - \gamma_2 = n(\alpha_1 - \alpha_2) \left( 1 - \frac{3r/nl}{L^{-1}(r/nl)} \right) \quad . \quad . \quad . \quad (7)$$

Equations (6) and (7) may be written in the expanded form

$$\left. \begin{aligned} \gamma_1 &= \frac{n}{3} (\alpha_1 + 2\alpha_2) + n(\alpha_1 - \alpha_2) \left[ \frac{2}{5} \left( \frac{r}{nl} \right)^2 + \frac{24}{175} \left( \frac{r}{nl} \right)^4 + \frac{72}{875} \left( \frac{r}{nl} \right)^6 + \dots \right] \\ \gamma_2 &= \frac{n}{3} (\alpha_1 + 2\alpha_2) - n(\alpha_1 - \alpha_2) \left[ \frac{1}{5} \left( \frac{r}{nl} \right)^2 + \frac{12}{175} \left( \frac{r}{nl} \right)^4 + \frac{36}{875} \left( \frac{r}{nl} \right)^6 + \dots \right] \end{aligned} \right\} \quad (6a)$$

$$\gamma_1 - \gamma_2 = n(\alpha_1 - \alpha_2) \left[ \frac{3}{5} \left( \frac{r}{nl} \right)^2 + \frac{36}{175} \left( \frac{r}{nl} \right)^4 + \frac{108}{875} \left( \frac{r}{nl} \right)^6 + \dots \right] \quad (7a)$$

From the expanded form (7a) it is seen that if  $r$  is not too large the anisotropy of the chain is proportional to  $r^2$ . Moreover, if the chain is free from external restraint, its average length will be given by  $r^2 = nl^2$ , and hence its average anisotropy is

$$\gamma_1 - \gamma_2 \simeq \frac{2}{3}(\alpha_1 - \alpha_2)$$

i.e.  $\frac{2}{3}$  of the anisotropy of a single link. The complete function (7) is plotted in Fig. 1.

In the following treatment of the network it will be assumed that the strain is not sufficiently large to cause any significant fraction of the total number of chains to assume lengths comparable with their fully-extended length  $nl$ , so that powers of  $r/nl$  above the second, in the above expressions for the polarisabilities, may be neglected. (This assumption is equivalent to that made in the approximate theory of the mechanical properties of the network.<sup>2</sup>) With this approximation, the chain polarisabilities reduce to the form

$$\gamma_1 = C_1 + 2C_2r^2 \quad \gamma_2 = C_1 - C_2r^2 \quad . \quad . \quad . \quad (6b)$$

in which the constants  $C_1$  and  $C_2$  have the values

$$C_1 = \frac{n}{3}(\alpha_1 + 2\alpha_2) \quad C_2 = \frac{\alpha_1 - \alpha_2}{5nl^2} \quad . \quad . \quad . \quad (8)$$

### Optical Properties of the Network.

Starting with a uniform spatial distribution of chain directions, the method employed by Kuhn and Gr $\ddot{u}$  n in calculating the properties of the network involves the derivation of the distribution of length and direction of the chains in the deformed state of the network. The components of polarisability for each chain in directions parallel and perpendicular to the direction of extension are then written down, and the total polarisabilities in these two directions obtained by integration over the whole assembly.

This direct method of approach appears to lead to formidable mathematical difficulties, when applied to the more complex problem of the general homogeneous strain. Fortunately, however, these difficulties may be avoided by means of a somewhat less direct, but physically equivalent method, in which the necessity of integrating over all directions of the chains does not arise. This method will now be explained.

The network will be assumed to contain  $N$  molecular chains, each consisting of  $n$  universally jointed links of length  $l$ . The junction points of the network will be continually fluctuating in position, on account of the random thermal motion of the chains, but for the calculation of the polarisabilities they will be assumed to occupy their average positions. For simplicity, it will be assumed initially that the distances between neighbouring junction points (i.e. the "displacement lengths" of the chains) in the undeformed rubber are all equal. (This restriction will be shown later to be unnecessary.) Finally, it will be assumed that on deformation of the rubber the junction points move as if they were embedded in an elastic continuum. (This assumption is justified by James and Guth's<sup>3</sup> analysis of the mechanical behaviour of a molecular network.)

In the unstrained rubber the "displacement lengths" (referred to

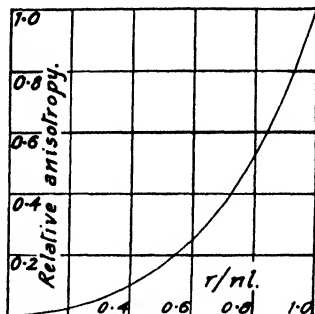


FIG. 1.

<sup>2</sup> Treloar, *Trans. Faraday Soc.*, 1943, **39**, 241.

<sup>3</sup> James and Guth, *J. Chem. Physics*, 1943, **11**, 455.

subsequently simply as "lengths") of the assembly of chains may be represented by a set of vectors, assumed for the present to have equal lengths  $r$ . These vectors are distributed randomly in direction. Let us imagine that a set of three mutually perpendicular vectors is removed from this assembly, then a second set, then a third set, and so on. In this way it is seen that the original assembly of  $N$  vectors may be replaced by  $N/3$  groups of three mutually perpendicular sets, each group being differently oriented with respect to a fixed co-ordinate system XYZ.

Considering for the moment only a single set of three mutually perpendicular chains, let us calculate the polarisabilities in the directions of the co-ordinate axes when the rubber is deformed.

The pure, homogeneous deformation will be defined by stretches along OX, OY and OZ in the ratio  $\lambda_1$ ,  $\lambda_2$  and  $\lambda_3$  respectively. Let  $(l_1, m_1, n_1)$ ,  $(l_2, m_2, n_2)$ ,  $(l_3, m_3, n_3)$  be the direction cosines of the three chains in the unstrained rubber. The direction cosines for the first chain after the deformation will be given by

$$l_1' = \frac{\lambda_1 l_1 r}{r_1}, \quad m_1' = \frac{\lambda_2 m_1 r}{r_1}, \quad n_1' = \frac{\lambda_3 n_1 r}{r_1} \quad . \quad . \quad . \quad (9)$$

and its length  $r_1$  by

$$r_1^2 = (\lambda_1^2 l_1^2 + \lambda_2^2 m_1^2 + \lambda_3^2 n_1^2) r^2 \quad . \quad . \quad . \quad (10)$$

with similar expressions for the other two chains. A chain making an angle  $\theta$  with OX gives rise to a polarisability along OX of amount

$$\beta = \gamma_1 \cos^2 \theta + \gamma_2 \sin^2 \theta$$

where  $\gamma_1$  and  $\gamma_2$  are the polarisabilities of the chain respectively parallel and perpendicular to its length. These polarisabilities are functions of  $r_1$  given by eqn. (6b). We therefore obtain, for the contribution of the first chain to the polarisability along OX

$$\begin{aligned} \beta_{x1} &= (C_1 + 2C_2 r_1^2) l_1'^2 + (C_1 - C_2 r_1^2) (1 - l_1'^2) \\ &= C_1 + C_2 r_1^2 (3l_1'^2 - 1). \end{aligned}$$

From (9)  $l_1'^2 r_1^2 = \lambda_1^2 l_1^2 r^2$  and  $r_1^2$  is given by (10), hence

$$\beta_{x1} = C_1 + C_2 r^2 (2\lambda_1^2 l_1^2 - \lambda_2^2 m_1^2 - \lambda_3^2 n_1^2).$$

Similarly the contributions of the second and third chains to the polarisability along OX are

$$\begin{aligned} \beta_{x2} &= C_1 + C_2 r^2 (2\lambda_1^2 l_2^2 - \lambda_2^2 m_2^2 - \lambda_3^2 n_2^2) \\ \beta_{x3} &= C_1 + C_2 r^2 (2\lambda_1^2 l_3^2 - \lambda_2^2 m_3^2 - \lambda_3^2 n_3^2) \end{aligned}$$

Remembering that  $l_1^2 + l_2^2 + l_3^2 = 1$ , etc., we obtain a total polarisability along OX of amount

$$\beta_x = \beta_{x1} + \beta_{x2} + \beta_{x3} = 3C_1 + C_2 r^2 (2\lambda_1^2 - \lambda_2^2 - \lambda_3^2).$$

The corresponding polarisabilities along OY and OZ are

$$\begin{aligned} \beta_y &= 3C_1 + C_2 r^2 (2\lambda_2^2 - \lambda_3^2 - \lambda_1^2) \\ \beta_z &= 3C_1 + C_2 r^2 (2\lambda_3^2 - \lambda_1^2 - \lambda_2^2) \end{aligned} \quad . \quad . \quad . \quad (11)$$

Eqn. (11) show that the polarisabilities along OX, OY and OZ for a group of 3 mutually perpendicular chains are independent of their directions, since they do not contain the direction cosines. The polarisabilities depend, however, on  $r$ , the initial length of the chains and on the 3 principal extensions  $\lambda_1$ ,  $\lambda_2$  and  $\lambda_3$ .

The advantage of the present method over the more direct method of Kuhn and Gr $\ddot{u}$  n will now be apparent. By choosing a suitable group of 3 chains, we have been able to obtain resultant polarisabilities which are independent of their original direction and thus to avoid the necessity of integrating over all directions. The total polarisabilities are obtained simply by multiplying by the number of groups of three chains in the network.

If instead of all the chains having the same initial length  $r$ , they have a distribution of lengths, such that  $N_a$  have the length  $r_a$ ,  $N_b$  the length  $r_b$ ,  $N_p$  the length  $r_p$ , etc., then, provided that  $N_a, N_b, \dots, N_p, \dots$  are large number, we may assume that the separate groups of vectors  $r_a, r_b, \dots, r_p$  each form a randomly oriented assembly, and may be separately divided into sub-groups of 3 mutually perpendicular vectors for which the results represented by eqn. (11) will apply. For the whole assembly, therefore, the total polarisability per unit volume in the direction OX is

$$P_x = \Sigma \beta_x = \Sigma N_p C_1 + \frac{1}{3} C_2 \Sigma N_p r_p^2 (2\lambda_1^2 - \lambda_2^2 - \lambda_3^2) \Big\} \quad (12)$$

$$= N [C_1 + \frac{1}{3} C_2 \bar{r}^2 (2\lambda_1^2 - \lambda_2^2 - \lambda_3^2)]$$

where  $\bar{r}^2$  is the mean value of  $r^2$ .

If we assume that in the unstrained rubber the chains have the same average length as they would have if they were not attached to the network, we may write  $\bar{r}^2 = nl^2$ . Inserting this value in (12) and expressing the constants  $C_1$  and  $C_2$  in their full forms (8), the resultant polarisabilities per unit volume in the directions OX, OY and OZ (assuming the volume to be unchanged on deformation) become

$$\left. \begin{aligned} P_x &= N \left[ \frac{n}{3} (\alpha_1 + 2\alpha_2) + \frac{1}{15} (\alpha_1 - \alpha_2) (2\lambda_1^2 - \lambda_2^2 - \lambda_3^2) \right] \\ P_y &= N \left[ \frac{n}{3} (\alpha_1 + 2\alpha_2) + \frac{1}{15} (\alpha_1 - \alpha_2) (2\lambda_2^2 - \lambda_3^2 - \lambda_1^2) \right] \\ P_z &= N \left[ \frac{n}{3} (\alpha_1 + 2\alpha_2) + \frac{1}{15} (\alpha_1 - \alpha_2) (2\lambda_3^2 - \lambda_1^2 - \lambda_2^2) \right] \end{aligned} \right\} \quad (13)$$

The principal indices of refraction may be obtained from the polarisabilities by making use of the well-known relation between refractive index ( $n$ ) and polarisability per unit volume,<sup>4</sup> i.e.

$$\frac{n^2 - 1}{n^2 + 2} = \frac{4\pi}{3} \cdot P \quad (14)$$

Equations (13) with (14) provide a complete description of the optical properties of strained rubber, in terms of the three principal extensions. When these extensions are all different, the principal refractive indices are also all different, and the rubber behaves like a biaxial crystal. If, on the other hand, two of the  $\lambda$  are equal as in the case of a unidirectional extension or compression, the equations reduce to the form given by Kuhn and Gr $\ddot{u}$  n, and the system becomes comparable with a uniaxial crystal.

It is of interest to consider the behaviour of light propagated along one of the axes of the index ellipsoid, say OZ. If the refractive indices for light polarised parallel to OX and OY respectively are  $n_1$  and  $n_2$ , then, from (13) and (14)

$$\frac{n_1^2 - 1}{n_1^2 + 2} - \frac{n_2^2 - 1}{n_2^2 + 2} = \frac{4\pi N}{15} (\alpha_1 - \alpha_2) (\lambda_1^2 - \lambda_2^2) \quad (15)$$

If  $n_1$  and  $n_2$  do not differ greatly from the mean index  $\bar{n}$ , the following approximation will be valid :

$$\frac{n_1^2 - 1}{n_1^2 + 2} - \frac{n_2^2 - 1}{n_2^2 + 2} \simeq \frac{6\bar{n}}{(\bar{n}^2 + 2)^2} (n_1 - n_2) \quad (16)$$

and therefore the birefringence for the direction of propagations OZ may be written

$$n_1 - n_2 = \frac{(\bar{n}^2 + 2)^2}{\bar{n}} \cdot \frac{2\pi}{45} N (\alpha_1 - \alpha_2) (\lambda_1^2 - \lambda_2^2) \quad (15a)$$

i.e. the difference between any two of the principal refractive indices is proportional to the difference of the squares of the corresponding extension ratios.

<sup>4</sup> Joos, *Theoretical Physics*, 1934, p. 434.



### The Relation between Birefringence and Stress.

Methods of treating the mechanical properties of a network of molecular chains have been given by a number of authors, among whom may be mentioned in particular James and Guth,<sup>5</sup> Wall<sup>6</sup> and Flory and Rehner.<sup>6</sup> Fundamentally, these different approaches have much in common, and the author has shown<sup>2,7</sup> that the treatments both of Wall and of Flory and Rehner lead to the same expression for the work of deformation in a homogeneous strain of the most general type.

It is a simple matter to confirm that an identical result is obtainable by means of the method used in this paper for the derivation of the optical properties of a network. For this purpose we write the entropy of a randomly-linked chain as a function of its length in the form given by Kuhn

$$s = c - \frac{3k}{2nl^2} \cdot r^2.$$

Taking, as before, a set of 3 mutually perpendicular chains of initial length  $r$  and direction cosines  $(l_1, m_1, n_1)$ , etc., whose lengths after the deformation defined by extension ratios  $\lambda_1, \lambda_2$  and  $\lambda_3$  will be given by equations of the type (10), we find, for the entropy change on deformation

$$\begin{aligned} -\frac{s' - s}{3k/2nl^2} &= (\lambda_1^2 l_1^2 + \lambda_2^2 m_1^2 + \lambda_3^2 n_1^2)r^2 + (\lambda_1^2 l_2^2 + \lambda_2^2 m_2^2 + \lambda_3^2 n_2^2)r^2 \\ &\quad + (\lambda_1^2 l_3^2 + \lambda_2^2 m_3^2 + \lambda_3^2 n_3^2)r^2 - 3r^2 \\ \text{or} \quad -\frac{s' - s}{3k/2nl^2} &= (\lambda_1^2 + \lambda_2^2 + \lambda_3^2 - 3)r^2 \quad . \quad . \quad (17) \end{aligned}$$

Since this expression is independent of the direction cosines of the chains, we may use the same arguments as were employed in the foregoing optical treatment, and write, for the entropy change on deformation for the whole assembly of  $N$  chains, occupying unit volume,

$$\Delta S = -\frac{Nk}{2nl^2}(\lambda_1^2 + \lambda_2^2 + \lambda_3^2 - 3)\bar{r}^2 \quad . \quad . \quad (18)$$

If now we put  $\bar{r}^2$  the mean square length in the unstrained state equal to  $nl^2$ , the work of deformation  $W(= -T\Delta S)$  becomes

$$W = \frac{1}{2}NkT(\lambda_1^2 + \lambda_2^2 + \lambda_3^2 - 3) \quad . \quad . \quad (19)$$

as previously derived by the other methods.

The subsequent calculation of the principal stresses from eqn. (1a) has been dealt with elsewhere.<sup>2</sup> In particular it has been shown that the difference between any two of the 3 principal stresses,  $t_1, t_2$  and  $t_3$  may be expressed in terms of the corresponding strains; thus, for example,

$$t_1 - t_2 = NkT(\lambda_1^2 - \lambda_2^2) \quad . \quad . \quad (20)$$

Comparing this expression with eqn. (15a) we see that the difference between any two of the principal refractive indices is proportional to the difference between the corresponding principal stresses. The proportionality factor is a function only of the anisotropy of the chain link and the mean polarisability (i.e. refractive index) of the medium, and is given by

$$\left(\frac{n_1 - n_2}{t_1 - t_2}\right)_{\lambda_1 \lambda_2 \lambda_3 \text{ const.}} = \frac{(\bar{n}^2 + 2)^2}{\bar{n}} \cdot \frac{2\pi}{45} \cdot \frac{\alpha_1 - \alpha_2}{kT} \quad . \quad . \quad (21)$$

Being independent of the number of links in the chain and the number of chains in the network, this constant should be a specific property of the type of rubber, and independent of the degree of vulcanisation.

<sup>5</sup> Wall, *J. Chem. Physics*, 1942, 10, 485.

<sup>6</sup> Flory and Rehner, *ibid.*, 1943, 11, 512, 521.

<sup>7</sup> Treloar, *Trans. Faraday Soc.*, 1946, 42, 83.

<sup>8</sup> Kuhn, *Koll. Z.*, 1936, 76, 258.

### Strained Swollen Rubber.

In this section the optical and mechanical properties of vulcanised rubber swollen by a low-molecular liquid are considered.

The swelling liquid will be assumed to be optically isotropic. If  $v_r$  is the volume fraction of the rubber in the mixture, the number of chains per unit volume of the swollen rubber will be  $v_r N$ , and their mean square length in the absence of mechanical deformation will be increased from  $nl^2$  to  $nl^2/v_r$ . The contributions to the polarisability per unit volume along the co-ordinate axes due to the network will therefore be given by equations of the form

$$P_{\alpha} = N v_r \left[ \frac{n}{3} (\alpha_1 + 2\alpha_2) + \frac{1}{15} \cdot \frac{\alpha_1 - \alpha_2}{v_r} (2\lambda_1^2 - \lambda_2^2 - \lambda_3^2) \right] \quad (22)$$

in place of (13), and the difference between any two of the principal refractive indices by

$$n_1 - n_2 = \frac{(\bar{n}^2 + 2)^2}{\bar{n}} \cdot \frac{2\pi}{45} \cdot N (\alpha_1 - \alpha_2) v_r (\lambda_1^2 - \lambda_2^2) \quad (23)$$

where  $\bar{n}$  is now the mean refractive index for the mixture of rubber and liquid, and  $N$  is the number of chains per unit volume of the unswollen rubber.

Similarly the work of deformation per unit volume of the swollen rubber will be

$$W = \frac{1}{2} N k T v_r (\lambda_1^2 + \lambda_2^2 + \lambda_3^2 - 3) \quad (24)$$

From this equation it follows that the principal stresses will decrease with swelling, in the ratio  $v_r$ . Since this factor also occurs in the birefringence equation (23) it is clear that the ratio of the birefringence to the difference of the principal stresses will still be given by eqn. (21). The relations between birefringence and stress are therefore unaffected by swelling, except in so far as the swelling liquid may alter the mean refractive index  $\bar{n}$ .

### Conclusion.

The foregoing results bring out certain simple relations between the optical properties and the mechanical properties of a vulcanised rubber. The equations derived are valid only up to moderate strains, and will not apply when the strains begin to approach the limiting deformability of the network.

The treatment given above makes use of the conception of a chain of independently oriented statistical links. Whilst no actual molecular structure conforms exactly to this idealised model, the behaviour of any flexible molecule will approximate to that of the random chain in the region of small or moderate extensions. With this limitation, the theory should therefore be valid for all rubberlike materials.

This work forms part of the programme of fundamental research on rubber undertaken by the Board of the British Rubber Producers' Research Association.

### Summary.

From the consideration of vulcanised rubber as a network of randomly-kinked molecular chains, the optical constants corresponding to the most general type of homogeneous strain are derived. Under such a strain the rubber is shown to acquire the properties of an optically biaxial crystal, characterised by 3 principal refractive indices in the directions of the principal axes of strain. For directions of light propagation parallel

\* Both James and Guth<sup>3</sup> and Flory and Rehner<sup>4</sup> have derived this result for the case of a unidirectional stretch.

to one of the principal axes the birefringence is shown to be a simple function of the principal extensions and is, moreover, proportional to the difference between the two corresponding principal stresses.

If the rubber is swollen with a liquid having the same refractive index as itself, the birefringence for a given state of strain, varies inversely as the cube root of the swelling ratio, as do also the principal stresses.

### Résumé.

On établit théoriquement les propriétés optiques du caoutchouc vulcanisé, soumis au type le plus général de tension homogène, en considérant qu'il a la forme d'un réseau de chaînes moléculaires enroulées au hasard ; on montre que le caoutchouc, sous une telle tension, acquiert les propriétés optiques d'un cristal biaxe, caractérisé par trois indices de réfraction, dans la direction des axes principaux de la tension.

### Zusammenfassung.

Die optischen Konstanten, die der allgemeinsten Art von homogener Deformation von vulkanisiertem Kautschuk entsprechen, wurden unter der Annahme, dass dieser ein aus völlig unregelmässig geknickten Molekülketten gebildetes Netz darstellt, berechnet. Es wird gezeigt, dass Kautschuk unter einer solchen Deformation die Eigenschaften eines optisch zweiachsigen Kristalls, das durch drei Brechungsindizes in den Richtungen der Deformationsachsen charakterisiert ist, erwirbt.

*British Rubber Producers' Research Assoc.,  
48 Tewin Road,  
Welwyn Garden City, Herts.*

## THE PHOTO-ELASTIC PROPERTIES OF RUBBER II. DOUBLE REFRACTION AND CRYSTALLISATION IN STRETCHED VULCANISED RUBBER.

BY L. R. G. TRELOAR.

*Received 24th May, 1946.*

In this paper experimental birefringence data for vulcanised rubber extended at a series of temperatures ranging from  $-50^{\circ}$  to  $+100^{\circ}$  C. are presented. The principal objective was the separation of the birefringence due to crystallisation from the genuine strain-birefringence, with a view to comparing the dependence of strain-birefringence on extension and on stress with the forms predicted by the theory given in the preceding paper. The effects produced by swelling the rubber with solvents before stretching are also examined.

In the case of a simple elongation, defined by the ratio  $\alpha$  of the stretched to the unstretched length, the theoretical variation of the strain-birefringence with  $\alpha$ , obtained by putting  $\lambda_1 = \alpha$ ,  $\lambda_2 = \alpha^{-1/2}$  in eqn. (15a) of the preceding paper, is

$$n_1 - n_2 = \frac{(\bar{n}^2 + 2)^2}{\bar{n}} \cdot \frac{2\pi}{45} \cdot N(\alpha_1 - \alpha_2)(\alpha_1 - 1/\alpha) \quad (1)$$

where  $\alpha_1 - \alpha_2$  represents the optical anisotropy of the equivalent statistical link of the chain molecule, and  $N$  is the number of chains per cc. The tension  $F$  referred to unit area of the unstrained cross-section, has the theoretical form,

$$F = NkT(\alpha - 1/\alpha^2) \quad (2)$$

The stress  $t$  referred to the actual section is  $\alpha F$ , and the ratio of birefringence to stress, for a given value of  $\alpha$  is given by the equation

$$\left(\frac{n_1 - n_2}{t}\right)_\alpha = \frac{(\bar{n}^2 + 2)^2}{\bar{n}} \cdot \frac{2\pi}{45} \cdot \frac{\alpha_1 - \alpha_2}{kT} \quad (3)$$

which is comparable with eqn. (21) of the preceding paper.

### Experimental.

The vulcanised rubber used in these experiments was compounded according to the following formula :

Smoked sheet	.	.	.	100	parts by weight
Sulphur	.	.	.	2	" "
Zinc oxide	.	.	.	2	" "
" MBTS "	.	.	.	1	" "
Stearic acid	.	.	.	0.5	" "
" Nonor "	.	.	.	0.5	" "

The extension was carried out with the apparatus described in an earlier publication,<sup>1</sup> the tension being measured by the deflection of a flat steel spring with attached pointer. The birefringence was measured by using white light polarised in a plane making an angle of  $45^\circ$  with the direction of the extension, in conjunction with a Babinet compensator and analyser at right angles to the polariser. The elongation was measured with a travelling microscope focussed on two fiduciary lines on the test specimen distant 10 mm. apart. At each extension the elongation was measured first, then the birefringence, and finally the tension. The time involved was not controlled, but averaged about 3 minutes for the three measurements. The thickness of the specimen was obtained by weighing. For the experiments at temperatures above room-temperature an air thermostat was employed. For lower temperatures the system was surrounded by a glass tube immersed in a suitable cooling mixture.

Two thicknesses of sheet were used. The thicker sheet (about 0.8 mm. thickness) was used where high extensions were not involved. Dumb-bell test pieces were cut from this sheet. The thinner sheet (about 0.1 mm.) was employed for measurements involving the highest extensions. In these cases parallel test-pieces were used, the effect of non-uniform strain at the clamps being reduced by clamping the rubber in the stretched condition.

In a previous publication<sup>2</sup> the details of the birefringence measurement were discussed in connection with raw rubber. The birefringence  $B$  used in that paper was the path difference per mm. for sodium light. In the present work it is more convenient (for comparison with the theory) to convert this to difference of principal refractive indices by multiplying this quantity by the wavelength, i.e.,  $n_1 - n_2 = B\lambda$ .

### Hysteresis Effects.

A typical birefringence-elongation curve, taken at  $25^\circ$  C. is reproduced in Fig. 1(B), which shows the presence of a marked hysteresis loop on traversing a cycle of extension and retraction. The presence of a hysteresis loop of this kind has been shown by the comparison

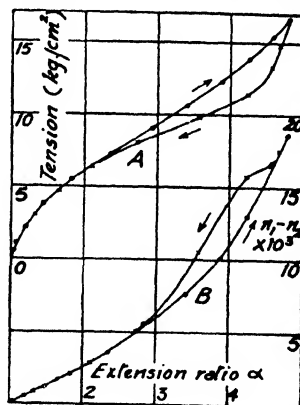


FIG. 1.—Hysteresis phenomena as shown by tension (A) and birefringence (B) in vulcanised rubber at  $25^\circ$  C.

<sup>1</sup> Treloar, *Trans. Faraday Soc.*, 1941, 37, 84.

<sup>2</sup> Treloar, *ibid.*, 1940, 36, 538.

of X-ray and optical observations by Triessin and Wittstadt<sup>3</sup> to be correlated with changes in the state of crystallisation in the rubber. Curve A<sub>1</sub> in Fig. 2, shows a corresponding hysteresis loop in the tension curve. This effect is due to the tendency of the oriented crystalline state to maintain itself when the tension is reduced.

When the birefringence is plotted against the applied stress (Fig. 2) the two hysteresis effects are added together to produce a still larger loop. Raising the temperature successively to 50° and 75° (Fig. 2) leads first to a reduction and then to the complete disappearance of the hysteresis, which must be due to a successive reduction in the amount of crystallisation.

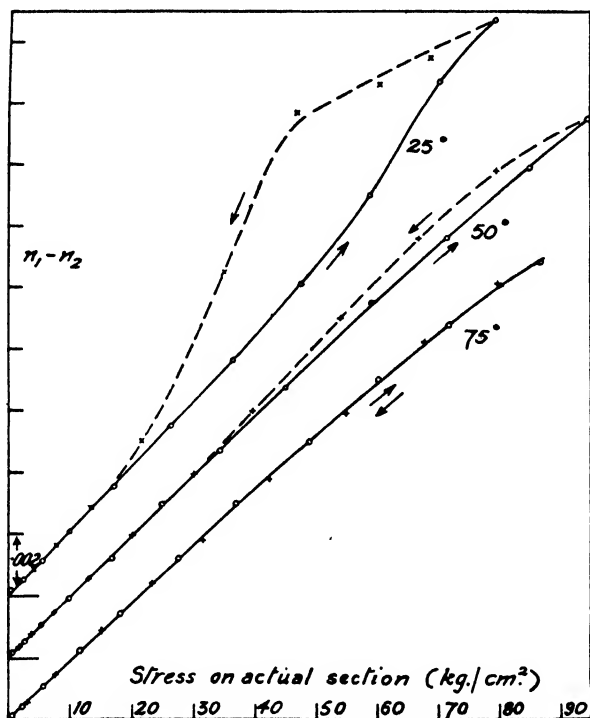


FIG. 2.—Hysteresis phenomena as shown by plot of birefringence against stress. Circles—stress increasing; Crosses—stress decreasing.

At the highest temperature the birefringence-stress relation approximates to the theoretical linear form represented by eqn. (3). The slight curvature is probably due mainly to the departure of the tension curve from the theoretical form (2) at high extensions, as will be apparent later. At the lower temperatures the theoretical relation is followed only at small extensions; thereafter the predominant effects of crystallisation lead to large irreversible departures from this form.

### Temperature Variation of Stress and Birefringence.

In a more extensive examination of the dependence of stress and birefringence on temperature, observations were made from the lowest extensions up to the breaking point at temperatures ranging from - 50 to + 100° C. The birefringence data (Fig. 3 and 4) show a fairly close

<sup>3</sup> Thiessen and Wittstadt, *Z. physik. Chem. B*, 1938, 41, 33.

agreement with the approximate theoretical form of  $n'$  dependence on extension ratio (eqn. 1) at the lower extensions, but diverge from this

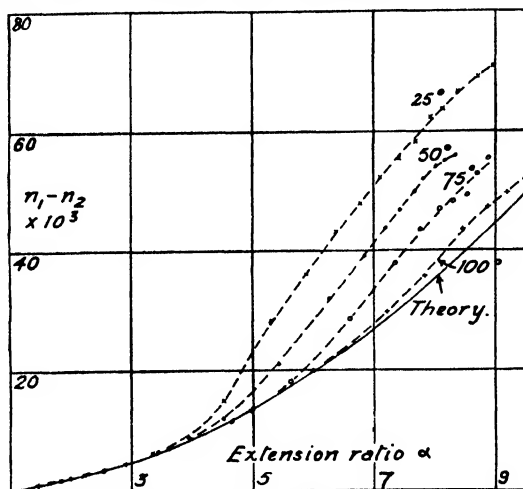


FIG. 3.—Comparison of birefringence-elongation curves at various temperatures with theoretical form (1).

form at higher extensions. Apart from the  $-50^\circ$  curve, which is anomalous, the range over which the experimental data fit the theoretical curve becomes greater with each increase in temperature, indicating a progressive increase in the extension required for the appearance of crystallisation. The  $100^\circ$  curve suggests that even at this temperature some crystallisation may be present at the highest extensions; this is supported by the observation of a strong hysteresis loop when the extension was stopped just short of the breaking point and reversed. The degree of agreement of the birefringence-elongation curves (up to the point where crystallisation begins) with the theoretical relation (eqn. 1) is closer than might have been expected, in view of the approximate nature of the theoretical formula, and must be regarded as somewhat fortuitous.

From the observations of Bekkedahl<sup>4</sup> and others it is known that crystallisation in unstretched rubber takes place most rapidly in the

<sup>4</sup> Bekkedahl, *Bur. Stand. J. Res.*, 1934, 13, 410.

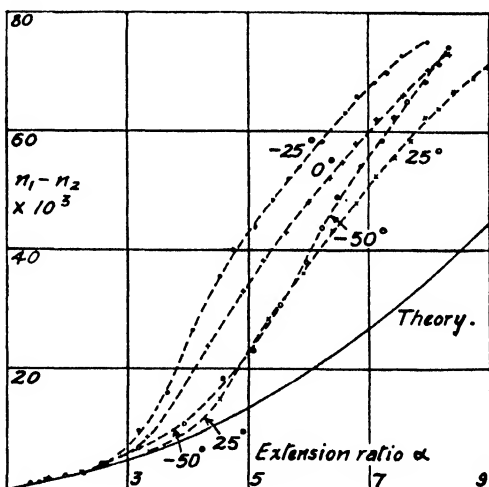


FIG. 4.—Comparison of birefringence-elongation curves at various temperatures with theoretical form (1).

temperature range  $-35$  to  $-15^{\circ}\text{C.}$ , but not at all at a temperature of  $-50^{\circ}\text{C.}$  It is not surprising, therefore, that in the present experiments crystallisation apparently takes place less readily at  $-50^{\circ}\text{C.}$  than at  $-25^{\circ}\text{C.}$  This anomalous behaviour is shown very clearly in Fig. 7, which represents the birefringence-stress relation for selected temperatures; at  $-25^{\circ}\text{C.}$  and  $+25^{\circ}\text{C.}$  crystallisation is revealed by a sudden increase in birefringence at a relatively low stress, but at  $-50^{\circ}\text{C.}$ , as at  $+100^{\circ}\text{C.}$ , no such effect is observed.

A parallel effect of crystallisation is seen in the stress-strain curves (Fig. 5 and 6). As the maximum extensibility of the molecular network is approached, the stress-strain curve shows a strong upward curvature. The extensibility is a function of the length of molecular chain between junction points. In an ideal rubber the only effective junction points are the permanent cross-linkages between molecules produced in vulcanisation. In a real rubber, mechanical entanglements may give rise to

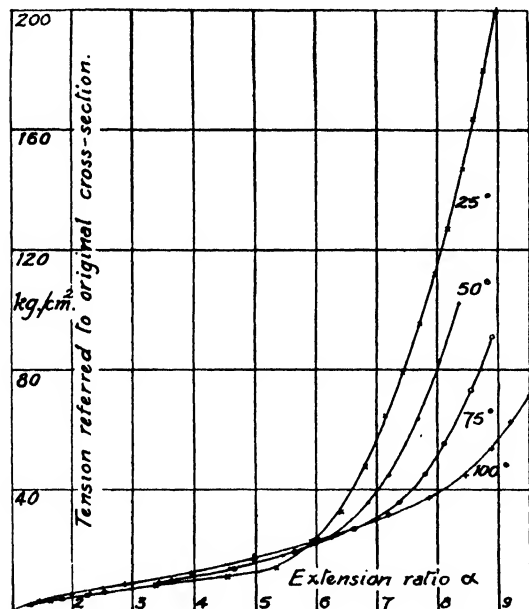


FIG. 5.—Tension-elongation curves at various temperatures.

temporary junction points, which, by reducing the average length of free chain, will reduce the overall extensibility. Crystallisation will act in the same way, since crystallisation has the effect of providing additional cross-linkages between the molecules. As the temperature is lowered, both these effects will normally be increased, and the upward bend of the stress-strain curve will move to a lower extension. This is seen to be true for all the curves from  $+100^{\circ}$  to  $-25^{\circ}\text{C.}$  At  $-50^{\circ}$ , however, the sequence is reversed, and the extensibility again increases, owing to the reduction in crystallisation, which more

than compensates for the increased mechanical cohesion. In connection with the birefringence-stress data, it should be noted that the conditions of the experiment did not give genuine equilibrium stress-strain data, and to this extent are open to criticism. In the present work, however, the object was mainly to obtain a general picture of the phenomena of birefringence, rather than to explore the details in a quantitatively accurate manner.

The downward curvature of the birefringence-stress curves at higher values of  $\alpha$  is connected mainly with the departure of the stress-strain curves from the simple theoretical form, due to the non-Gaussian form of the distribution function for molecular lengths.<sup>5</sup>

### The Maximum Birefringence.

The observations in the preceding paragraph suggest that entanglements may be more numerous at the lower temperatures. It would

<sup>5</sup> Treloar, *Trans. Faraday Soc.*, 1946, 42, 83.

seem to follow from this that if stretching were carried out at a comparatively high temperature, and crystallisation subsequently completed at a lower temperature, a higher proportion of crystalline material might be obtained than by stretching at the lower temperature. This expectation was borne out experimentally, though the effect was not very marked. The maximum birefringence was obtained by stretching to a high extension at room temperature ( $21^\circ \text{C.}$ ), subsequently cooling to  $-25^\circ \text{C.}$ , and then increasing the extension until breaking occurred. In this way a birefringence  $n_1 - n_2$  of 0.0827 at  $\alpha = 9.12$  was obtained, compared with 0.0752 at  $\alpha = 7.99$  for continuous extension at  $-25^\circ \text{C.}$  The corresponding stresses were about the same for both, i.e. 2400 and 2100  $\text{kg./cm.}^2$  respectively (on the actual section). Still higher birefringences were obtained with unvulcanised rubber (crepe film from solution) by a similar process. The highest figure was obtained by stretching at  $0^\circ \text{C.}$ , with subsequent cooling to  $-25^\circ$  and further stretching. This gave  $n_1 - n_2 = 0.0945$  at  $\alpha = 10.1$ , the stress being

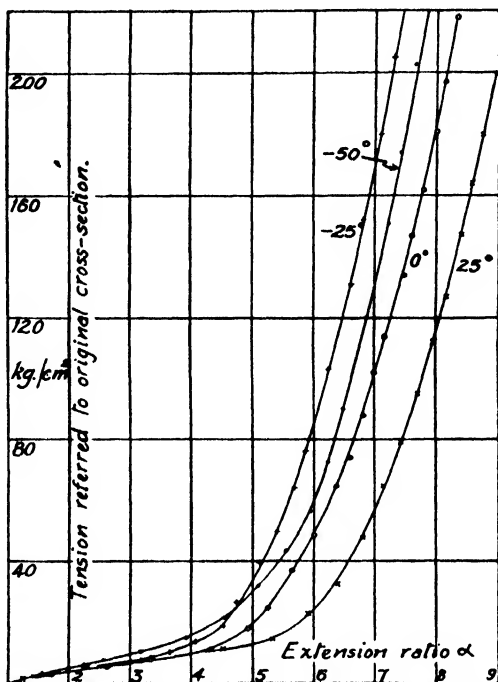


FIG. 6.—Tension-elongation curves at various temperatures.

by stretching at  $0^\circ \text{C.}$ , with subsequent cooling to  $-25^\circ$  and further stretching. This gave  $n_1 - n_2 = 0.0945$  at  $\alpha = 10.1$ , the stress being

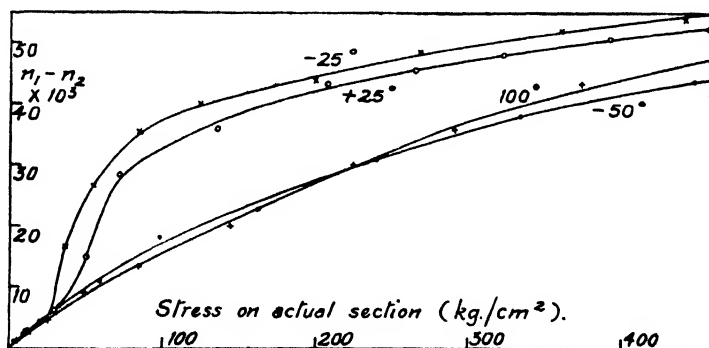


FIG. 7.—Birefringence-stress curves at selected temperatures.

1200  $\text{kg./cm.}^2$ . Unfortunately it is not possible to say how nearly complete crystallisation was approached in these experiments, and it is probable that if held extended for a considerable time at a low temperature, the



samples might have shown further increases in birefringence. They do, however, enable a lower limit to be set up to the birefringence of the rubber crystal.

It is interesting to compare the maximum birefringence obtained experimentally with the maximum theoretical birefringence, that is, the birefringence corresponding to a complete orientation of all the chain links parallel to a fixed direction. This may be estimated from a knowledge of  $\alpha_1 - \alpha_2$ , the anisotropy of the chain link, which is itself determined by the stress-optical coefficient, according to eqn. (3). Experimentally, at 25° C., the plot of birefringence against stress in the region of low elongation gives  $(n_1 - n_2) = 2.33 \cdot 10^{-4}$ . Taking  $\bar{n}$ , the mean refractive index to be 1.525, we obtain, from eqn. (3)

$$\alpha_1 - \alpha_2 = 5.65 \cdot 10^{-24}.$$

The difficulty now arises of interpreting the meaning of the statistical

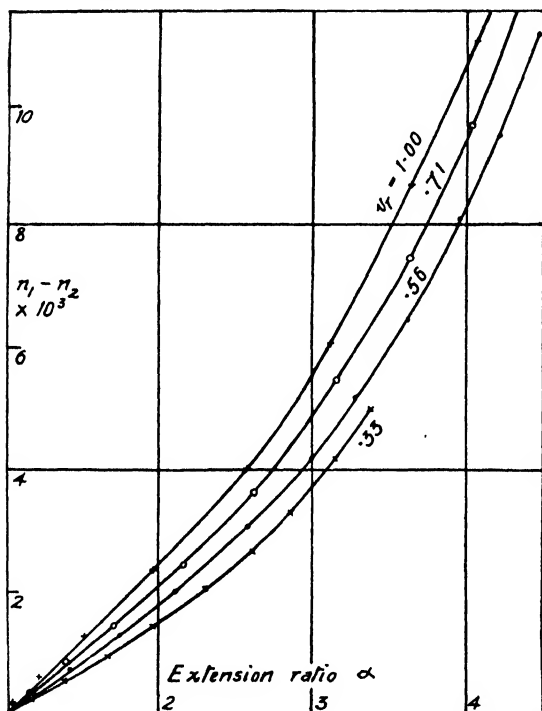


FIG. 8.—Birefringence-elongation curves for rubber swollen with squalene.  $v_r$  = volume fraction of rubber.

are parallel, the resultant difference of polarisability per cc. of rubber will be

$$5.75 \times 10^{21}(\alpha_1 - \alpha_2) = 0.0325 \text{ giving } n_1 - n_2 = \frac{(n^2 + 2)^3}{6n} \cdot \frac{4\pi}{3} \cdot (0.0325) = 0.28.$$

This is about three times the highest experimentally observed birefringence (0.0945). The discrepancy is probably due mainly to the uncertainty in the assignment of the number of effective random links in the polyisoprene chain. However, the general agreement in order of magnitude provides a useful check on the basic correctness of the theory.

chain link. From a theoretical treatment of the isoprene structure, the author<sup>6</sup> has shown that the polyisoprene chain is statistically identical with a random universally-jointed chain in which each link replaces 1.42 isoprene units. This result cannot be accurate, since it assumes perfect freedom of rotation about single bonds and neglects the volume occupied by the atoms. However, we may take it as an approximate basis for calculating the effective number of statistical chain links in the rubber. The number of isoprene units per cc. is  $8.18 \times 10^{21}$ , hence on this basis the number of equivalent random links per cc. is  $8.18 \times 10^{21}/1.42 = 5.75 \times 10^{21}$ . If all these links

**Birefringence in Swollen Rubber.**

For the experiments with swollen rubbers the sample was surrounded with a tube dipping into a cup of mercury to prevent escape of vapour.

TABLE I

$v_r$	$n_1 - n_2$ at $\alpha = 2$	$v_r^{\frac{1}{3}}$	$\frac{n_1 - n_2}{v_r^{\frac{1}{3}}}$	$\frac{n_1 - n_2}{\ell}$
1.00	$2.45 \cdot 10^{-3}$	1.00	$2.45 \cdot 10^{-3}$	$2.33 \cdot 10^{-4}$
0.71	2.05	0.893	2.29	2.30
0.56	1.74	0.825	2.11	2.22
0.33	1.48	0.690	2.14	2.14

The upper clamp was connected to the tension-measuring spring by means of a wire passing through a short length of capillary tubing. Diffusion of vapour through this aperture was not fast enough to be noticeable in the course of an experiment. The amount of swelling liquid present was calculated from the change in length of the unstretched sample.

The relation between birefringence and extension for rubber swollen with squalene ( $C_{30}H_{60}$ ) up to about three times its original volume is shown in Fig. 8. Neglecting the effect of the very small difference in refractive index of squalene and rubber (1.497 against 1.525) on the mean refractive index of the mixture, the birefringence should fall with swelling in proportion to  $v_r^{\frac{1}{3}}$  (eqn. (23) of preceding paper). Table I. gives the observed values of  $n_1 - n_2$  at  $\alpha = 2.0$  and the corresponding values of the ratio  $(n_1 - n_2)/v_r^{\frac{1}{3}}$ . Evidently the birefringence falls rather more rapidly with swelling than is to be expected theoretically. From the curves for birefringence against stress (Fig. 9) the ratio of birefringence to stress at low extensions was obtained. Theoretically this should be independent of the amount of swelling. The actual values are given in Table I. Birefringence stress data for rubber swollen with toluene, shown in Fig. 10, yield very similar results.

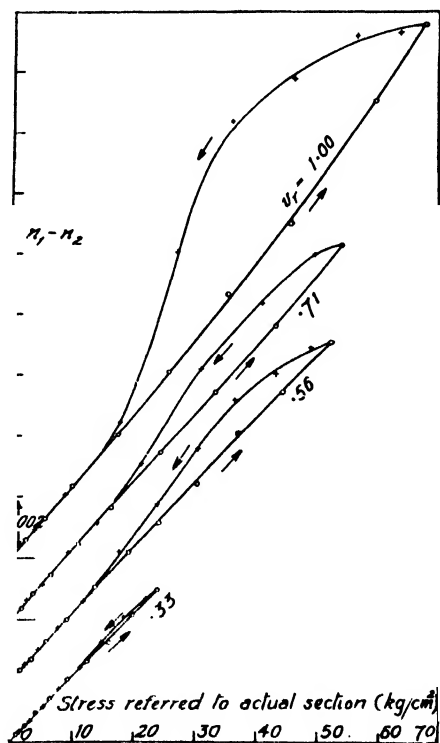


FIG. 9.—Birefringence-stress curves for rubber swollen with squalene.  $v_r$  = volume fraction of rubber.

There is, however, an interesting difference in the magnitude of the hysteresis loops for the two liquids. It appears that crystallisation (or, at least, irreversible orientation) persists

to higher degrees of swelling with squalene than with toluene. Presumably the similarity of the squalene molecule to rubber enables it to

conform to some extent with the local alignments of the rubber chains.

### General Conclusion.

From the experiments described in this paper, it is concluded that the molecular network theory gives a reasonably accurate description of the optical properties of stretched rubber in the dry and in the swollen state, so long as crystallisation is avoided.

When crystallisation is present, the departures from the theoretical form of the birefringence-elongation and birefringence-stress curves are apparent, and variations in birefringence give qualitative information about the variations in amount of crystallisation. It does not seem possible, however, to obtain reliable quantitative estimates of the amount of crystallisation corresponding to a given birefringence, firstly because the birefringence corresponding to 100 % crystallisation is not known,

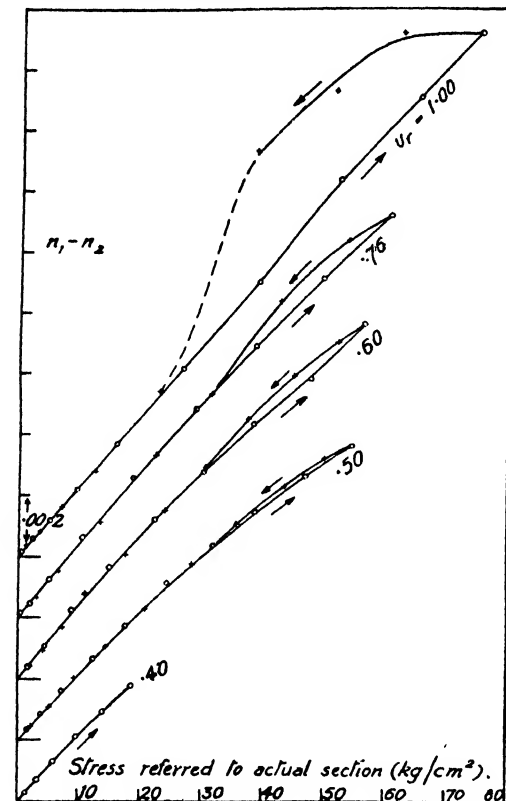


FIG. 10.—Birefringence-stress curves for rubber swollen with toluene.  $v_r$  = volume fraction of rubber.

and secondly, because the presence of crystallites, by altering the effective number of cross-links between molecules will alter the contribution of the strain-birefringence to the whole.

This work forms part of the programme of fundamental research on rubber undertaken by the Board of the British Rubber Producers' Research Association.

### Summary.

From an investigation of the variation of birefringence, with elongation in vulcanised rubber extended at temperatures ranging from  $-50^\circ$  to  $+100^\circ$  C., it is possible to distinguish the effects of crystallisation from the true strain-birefringence. The latter agrees closely with theoretical expectations, in its dependence on stress and on elongation. The data do not permit of a quantitative estimation of the relative amounts of crystalline material present under various conditions.

Experiments with stretched swollen rubber further confirm the theory and yield further evidence on the effects of crystallisation.

### Résumé.

Une étude de la variation de la biréfringence avec l'allongement du caoutchouc vulcanisé à des températures allant de  $-50$  à  $100^{\circ}\text{C}$ . permet de distinguer entre les effets de la cristallisation et une véritable biréfringence de tension. Cette dernière dépend de la tension et de l'allongement, comme prévu par la théorie. A partir des données expérimentales, il n'est pas possible d'évaluer de façon précise les quantités relatives de matière cristalline présente dans diverses conditions.

### Zusammenfassung.

Die Untersuchung der Doppelbrechung durch vulkanisierten Kautschuk, der bei Temperaturen zwischen  $-50^{\circ}$  und  $+100^{\circ}\text{C}$  ausgedehnt wurde, und ihrer Abhängigkeit vom Dehnungsbetrag ermöglicht, zwischen der durch Kristallisation bedingten Eigendoppelbrechung und der durch Zug verursachten Zwangsdoppelbrechung zu unterscheiden. Die letztere stimmt gut mit theoretischen Erwartungen überein, was ihre Abhängigkeit von Zugkraft und Ausdehnung anbelangt. Die Daten gestatten nicht, eine quantitative Berechnung der relativen Mengen von kristallinischem Material unter verschiedenen Bedingungen zu machen.

*British Rubber Producers' Research Assoc.,  
48 Tewin Road,  
Welwyn Garden City, Herts.*

---

### REVIEWS OF BOOKS.

**Organic Preparations.** By CONRAD WEYGAND. (Interscience Publishers: New York, 1946.) Pp. 534. Price 6.00 dollars.

This text on preparative organic chemistry has been translated from the German, and is up to date to the year 1938. It seems to be designed for the advanced undergraduate student, being a stage more exhaustive than "Cohen." Looked at from the viewpoint of the physical chemist, it may prove a useful addition to the library of a department working on such topics as the kinetics of organic reactions. It often happens in such work that the substances are not purchasable and just have to be made. In these circumstances the physical chemist hopes to find clear instructions for his preparation, and he may well find them here. The index occupies 35 pp., of two columns each, the number of preparations given being sufficiently large to discourage a count by the reviewer. Where substances are treated in "Organic Syntheses" a reference only is given. As to quality, many of the recipes are quoted directly from the original literature. They do not seem to have been independently checked, and in this respect a method from "Organic Syntheses" is definitely to be preferred, wherever possible.

The preparations are classified into thirteen chapters, on the basis of the type of bond formed or broken, e.g. carbon-hydrogen, carbon-halogen, etc. Each topic is introduced by general conclusions of an empirical nature, followed by one or two specific recipes. The author states in the Introduction that he is treating the subject as an experimental art, and there is no theoretical discussion. Readers of these *Transactions* taking the utilitarian viewpoint mentioned above may find this no disadvantage. The reviewer is not competent to judge its effect on the undergraduate

organic chemist. If he were attempting to relearn his organic chemistry he thinks he would still prefer the enthralling mixture of theory and practice provided by "Gattermann."

It is, of course, impossible to include everything in a work of this kind. A chapter on deuterocarbon compounds is promised but unaccountably fails to materialise. The peroxide effect in the addition of hydrogen halides to double bonds is not mentioned. Aluminium bromide is not mentioned as a Friedel-Crafts catalyst. It would, however, be impossible to compress all the details one might like in one's own specialised fields of interest into a volume of this size. One can definitely advise the physical chemist embarking on a spell of preparative organic chemistry to turn to "Weygand," if his copies of "Gattermann" or "Cohen," hunted out from the remote corner of his library, fail him. The book should find a place on the departmental shelves beside the works of Fieser, Hickinbottom and Houben-Weyl.

D. D. E.

**The Measurement of Colour.** By W. D. WRIGHT. (London, Adam Hilger, Ltd.) Pp. vii + 223. Price 30s.

This is a useful little book and deserves to be widely read. Dr. Wright has set out to give a comprehensive but concise account, in language which the uninitiated can understand, of the principles and methods of colour measurement and colour specification, with particular emphasis on the trichromatic system. Although he has clearly found the task difficult in places, he has, on the whole, succeeded, and both he and the publishers are to be congratulated on producing a book which should fill a real gap in the literature of chemical optics.

The science of colour measurement is still so young that its achievements are unknown to, and its potentialities unrealised by, many workers who should know better. British industry has grown up on and has accumulated a mass of empirical knowledge which is of tremendous value; but is that enough? Must we expect the traditional skill and insight of the British workman, valuable as they have been in the past, to be sufficient of themselves to meet the growing competition of the future? Ought they not to be reinforced with every device and aid which the skill and insight of the scientist can provide? Here is a case in point. Colour measurement and colour specification already have vital applications in dyeing, in lighting, in agriculture, in medicine, in engineering, in analysis, and in many other fascinating fields. How many senior chemists engaged in industry could specify them?

Dr. Wright describes some of them in a very instructive last chapter. The earlier sections include accounts of the physiology of colour reception, of the trichromatic system, of colorimeters and spectrophotometers (including the most recent photo-electric types), and of the colour atlas. They are full of information, which is enhanced by technical appendices. Once the reader has mastered these chapters, he should be quite at home with original papers in the literature, which may possibly convey knowledge to the expert, but usually conceal it from those (like the reviewer) whose contact with the subject is not quite so intimate.

The book is well produced, especially for a war-time publication.

The reviewer noticed very few errors, and none was important. It is illustrated with many well-drawn diagrams, and with a number of colour plates. These, no doubt, account for the book's chief drawback—the price ; but a book on colour needs pictures in colour, and the advantage gained outweighs the disadvantage. The book is to be recommended.

**Electronic Theory of Acids and Bases.** By W. F. LUDER and SAVERIO ZUFFANTI. (John Wiley & Sons, Inc., New York, 1946.) Pp. viii + 165. Price 16s. net.

The exact definition of scientific terms is concerned chiefly with questions of convenience and consistency. Occasionally, however, new definitions have had a stimulating effect on theory and experiment, and this was notably the case for the Brönsted-Lowry definition of acids and bases as proton donors and proton acceptors. More recently G. N. Lewis (to whom this book is dedicated) has proposed an extension of the acid-base definition in two directions. Empirically, all substances which exhibit "typical" acid-base reactions (neutralisation, titration with indicators, displacement reactions, catalysis) are regarded as acids or bases, independent of whether their reactions involve proton transfer. Theoretically, the behaviour of acids and bases is referred to their ability to accept or donate electron-pairs rather than protons. The book under review advocates in the strongest terms that the terms acid and base should be employed universally in this extended sense.

There are valid arguments on both sides of this question, and any decision should clearly be made on a balanced judgment of which definition is the more convenient in practice. Unfortunately, Professors Luder and Zuffanti have an exaggerated view of the status of the Lewis definition, which they regard as a chemical "theory" comparable in importance with the theory of relativity in physics (see Preface and Chap. 13). Arguments against its use are omitted or dismissed as wilful conservatism. Thus it is significant that less than two pages of the present book (pp. 105-106) are devoted to the quantitative aspect of acid-base equilibria, which occupies such an important place in both the classical and the Brönsted-Lowry treatments. The authors admit that on the Lewis definition it is not possible to construct a consistent scale of acid-base strengths, but do not regard this as a material disadvantage. Similarly, there are a number of qualitative anomalies which are passed over without comment. For example, both  $\text{BF}_3$  and  $\text{SO}_2$  are regarded as primary acids, because they can expand their electron shells. On the other hand,  $\text{HCl}$  can only be regarded as an electron acceptor after separation of the proton or in virtue of hydrogen bond formation, and  $\text{CO}_2$  has to be written in the "activated state"

$\text{O} = \overset{+}{\text{C}} - \overset{-}{\text{O}}$ ; hence both of these substances are ranked as secondary acids.

The most interesting aspect of the Lewis definition lies in the correlation of the behaviour of different molecules as catalysts and reagents, especially in benzene substitution and reactions with indicators. However, much of the space devoted to this topic contributes little that is new: for example, Chapter 5 is essentially a re-statement of the familiar electronic theories of substitution in which the terms electrophilic (or cationoid) and nucleophilic (or anionoid) are replaced throughout by acidic and basic respectively.

The 165 pages of text are only achieved by a good deal of repetition and the extensive use of structural formulæ written out in full. This serves to obscure the real contributions made by G. N. Lewis and his school, to which the book does less than justice.

R. P. B.

**The Theory and Methods of Investigation of Metallic Corrosion.**

By G. V. AKIMOV. (Academy of Sciences Publishing House, Moscow, 1945.) (In Russian.)

This is a comprehensive work of some 400 closely filled pages with numerous diagrams, tables and photographs, and deals with the subject clearly and thoroughly. Literature references are given at the end of individual chapters only and there is no general index, though a very full list of contents enables the reader to find his way about fairly well.

The scope of the work extends almost into what would be called technology, but there is the fullest discussion of all the relevant fundamental principles and the treatment is strictly scientific and, in places, mathematical. There is, for example, a chapter of about 40 pages devoted to the theory of electrode potentials: and elsewhere a discussion, illustrated with seven photographs, of corrosional fatigue of metals. The various phenomena are submitted to detailed and fundamental analysis in physico-chemical terms, and the book as a whole will be of value primarily to experts, though selected sections can be read with profit by all serious students of physical chemistry.

The increasing production of valuable monographs of this kind in the Russian language is going to present an interesting problem to the chemists of English-speaking countries. If it is solved in the obvious way the results may well be beneficial in a larger sphere than the purely professional.

C. N. H.

**The Mechanism of Contact Catalysis (2nd Edn.).** By R. H. GRIFFITH. (Oxford University Press, 1946.) Pp. xii + 273. Price 21s.

In this edition, the author has preserved the general style and arrangement of the earlier (1936) one; certain sections have now been omitted or shortened, and this process might have been performed more extensively with advantage; others have been re-written in order to bring the subject-matter up-to-date. The logical development of the material presented could have been clearer, and the treatment still tends to be unduly descriptive and more superficial than even this subject demands. It provides, however, a very useful summary of a large mass of experimental facts, together with a guide, if at times a somewhat uncertain one, to the theoretical aspects. The subject does not lend itself well, or easily, to interpretations in terms of broad principles, but one feels that the author might be apologising too readily for these shortcomings. The comments are sound, if on occasion not highly illuminating, and the writing, although not lacking in clarity, would have gained force by greater exactness and precision. For those whose interest in the subject is a general one, this informative book will be welcomed. The printing, paper and binding are in keeping with the high standards of the Oxford University Press.

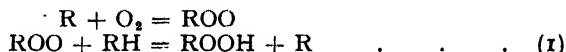
F. C. T.

# PROCESSES IN THE OXIDATION OF HYDROCARBON FUELS—II.

BY A. D. WALSH.

Received 23rd January, 1946.

The first paper of this series<sup>1</sup> suggested the outline of a scheme of oxidative degradation of paraffinic fuels. The outline was limited to "low temperature" oxidation, i.e. to that mode of oxidation which is associated with cool flames, two-stage ignition and the existence of a peninsula in the pressure-temperature ignition curve. It was based upon certain simple ideas, notably (1) the formation of alkyl hydroperoxides as the initial molecular products of oxidation, (2) the formation of these peroxides at a tertiary C—H in preference to a secondary and at a secondary in slighter preference to a primary C—H bond, (3) the formation of these peroxides according to the formal scheme:



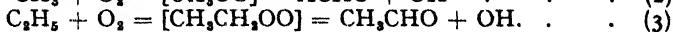
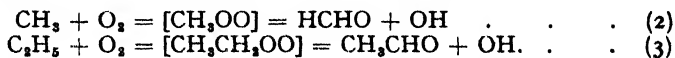
(4) the decomposition of peroxides into radicals by fission first at the O—O bond and subsequently at the weakest bond attached to the  $\alpha$ -carbon atom. The present paper briefly considers the formation of carbon monoxide and excited formaldehyde, both well-known products of "low temperature" combustion.

## Section V.—The Formation of Carbon Monoxide and Excited Formaldehyde.

### (A) Carbon Monoxide.

A complication of the simple degradation scheme of the previous paper has already been suggested, in that any of the alkyl radicals functioning as intermediates may decompose according to the schemes proposed by Rice, so accounting for the production of olefines. A further complication obviously exists in that the peroxide radicals may also decompose.

We have a certain amount of evidence as to the way in which this decomposition of peroxide radicals may occur. In the first place, evidence has been given by Bates and co-workers<sup>2</sup> that the combustion of methyl and ethyl radicals occurs according to the following reactions:



In the second place, reactions such as (2) and (3) are very strongly exothermic (see below) and the C—O distance shortens considerably from ROO to RCHO: therefore, especially at higher temperature, the issuing aldehydes are likely to be endowed with such vibrational activation energy that the process



(i.e. the well-established thermal pyrolysis reaction of aldehydes) will

<sup>1</sup> Walsh, *Trans. Faraday Soc.*, 1946, **42**, 269.

<sup>2</sup> Bates and Spence, *J. Amer. Chem. Soc.*, 1931, **53**, 1689; Jones and Bates, *ibid.*, 1934, **56**, 2285.

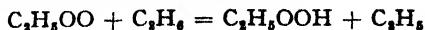




$$\begin{array}{c} \text{CH}_3 \\ \diagup \quad \diagdown \\ \text{CH}_3\text{CH}_2\text{CH}_2\text{CH}_2\text{CH}_2\text{CH}_2\text{CH}_2\text{CHO} \end{array}$$
$$\begin{array}{c} (\text{CH}_3)_3\text{C} \cdot \text{CH}_2 \rightarrow (\text{CH}_3)_3\text{C} \cdot \text{CH}_2\text{OO} \cdot \rightarrow (\text{CH}_3)_3\text{C} \cdot \text{CHO} + \text{OH} \cdot \\ \downarrow \\ (\text{CH}_3)_3\text{CH} + \text{CO} \end{array}$$
$$\begin{array}{rcl} \text{CH}_3 + \text{O}_2 & \rightarrow & \text{HCHO} + \text{OH} \\ \text{HCHO} & \rightarrow & \text{H}_2 + \text{CO} \\ \text{OH} + \text{CH}_4 & \rightarrow & \text{CH}_3 + \text{H}_2\text{O}. \end{array}$$

<sup>7</sup> Damkohler and Eggerglüss, *Z. physik. Chem. B*, 1942, 51, 157.

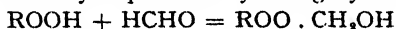
methane is thus understandable. With ethane, the radical  $C_2H_5OO\cdot$ , will be rather more stable \* and the reaction



will compete with the decomposition reaction (3). With higher paraffins, the peroxide radicals formed will usually be secondary or tertiary and therefore stable enough at "low" temperatures for some of them to produce peroxide molecules. Two modes of degradation occur—that via peroxide molecule decomposition as described in Paper I and that via peroxide radical decomposition as described here. At temperatures  $\sim 300$ – $400^\circ\text{C}$ . the first of these predominates. As the temperature rises, the peroxide molecule decomposition will become less important, since peroxide radicals will decompose instead of forming peroxide molecules. Since the peroxide molecule decomposition is essentially a *branching* process and the radical decomposition is not, we have a simple explanation of the negative temperature coefficient of oxidation rate, so often observed in the approximate range  $400$ – $450^\circ\text{C}$ .<sup>8</sup> At still higher temperatures the rate of the radical decomposition process increases so much that thermal explosion may ensue. The existence of two types of ignition—"low" and "high" temperature ignition, only the first being associated with peroxides, and forming an ignition peninsula<sup>9</sup>—is thus in natural accord with the present schemes. The simple ability of the schemes to explain the further fact that only "low" temperature ignition is of a two-stage type will be shown in the succeeding paper.

### Catalytic Peroxide Decomposition.

It may be objected that in many of the "low temperature" schemes, ROO has been supposed stable when ROOH has been supposed to decompose readily. This is because ROOH is thought to be decomposed catalytically by aldehydes according to the following process. We may take catalysis by formaldehyde as an example. Formaldehyde is well known to condense with hydroperoxides yielding hydroxy peroxides:



Hydroxy peroxides probably have a lowered O—O bond strength as a result of the withdrawal of electrons from the O—O link by the OH group.<sup>6</sup> They therefore decompose more readily than the corresponding simple hydroperoxides. Applying the usual rules of peroxide decomposition to a hydroxy peroxide, we have first of all fission at the O—O bond, producing

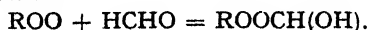


and then fission at the weakest bond on the  $\alpha$  carbon atom, producing  $HCHO + OH$ . This means that the products of decomposition of  $ROOCH_2OH$  are those of ROOH, save for the addition of HCHO; and the process



is really a *catalytic* decomposition of ROOH according to the schemes already formulated.<sup>1</sup>

Lewis and von Elbe<sup>22</sup> suppose that it is the condensation not of peroxide molecules but of peroxide radicals with aldehydes that is important in hydrocarbon oxidation:



This reaction is unlikely for it means an attack by an electrophilic entity (ROO) at the electron-deficient carbon atom of an aldehyde (cf. ref.<sup>1</sup> which deals with the point of attack of molecules by peroxide radicals).

\* Bates and co-workers<sup>3</sup> find that in their experiments on the combustion of methyl and ethyl radicals,  $C_2H_5OO\cdot$ , unlike  $CH_3OO\cdot$ , has a separate existence.

<sup>8</sup> See, e.g., Pease, *Equilibrium and Kinetics of Gas Reactions* (Princeton, 1942).

<sup>9</sup> Townend, *Chem. Rev.*, 1937, **21**, 259.

Further, the experiments of Wirtz and Bonhoeffer,<sup>10</sup> using heavy hydrogen peroxide, show that the hydrogen atoms of a formaldehyde molecule condensing with a peroxide molecule remain attached to the original carbon atom of the formaldehyde.

## B. The Formation of Excited Formaldehyde.

A peculiar feature of "low temperature" hydrocarbon combustion is the appearance of cool flames. These flames<sup>10</sup> have usually a pale blue colour; travel slowly; give only a small pressure rise; reveal on analysis considerable formation of substances intermediate to complete combustion, such as peroxides and aldehydes; do not deposit carbon; and are associated with a pressure pulse. Normal flames are usually fast travelling; give rise to a whitish emission and high pressure development; show only traces of intermediate compounds; frequently deposit carbon; and show a much higher temperature rise than cool flames. Further, the two types of flame have quite different spectra.

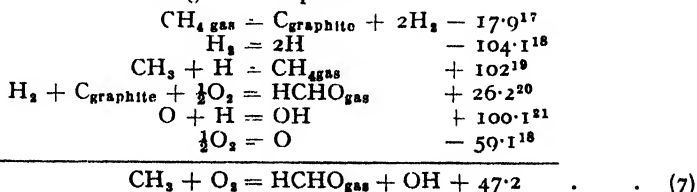
That cool flames can be propagated through cold mixtures has been shown by many beautiful experiments due to Townend and his co-workers.<sup>16</sup> The propagation of cool flames evidently does not depend upon the pre-formation of peroxidic material ahead of the flame.

Cool flames occur with all the paraffins from propane upwards and with all the simple aldehydes from acetaldehyde upwards. Methane, ethane, formaldehyde and glyoxal have not been observed to give a cool flame. Diethyl ether gives a cool flame very readily, di-isopropyl ether with more difficulty.<sup>11</sup> Acetone gives weak cool flames.<sup>10</sup> Olefines from propylene upwards give weak cool flames.<sup>12</sup> Benzene does not give a cool flame, but its mono alkyl derivatives, from *n*-propyl benzene upwards, do.<sup>12</sup>

The pressure-temperature regions of occurrence of cool flames have been systematically plotted by Townend and his co-workers (see, e.g.,<sup>8, 10</sup>). They occur at pressures usually of several atmospheres and, no matter what the fuel, at temperatures lying roughly between 150° C. and 410° C. (280-410° C. for hydrocarbons). Emelëus<sup>13</sup> succeeded in recording the spectra of the cool flames of diethyl ether, acetaldehyde, propaldehyde and hexane; and found the important result that these were all *identical*. For some time the emitter of the bands was unknown, but it has now been firmly established as formaldehyde.<sup>14</sup> The cool flame spectra are identical with the fluorescence spectrum of formaldehyde.

Any theory of hydrocarbon combustion must explain the appearance of cool flames with so many fuels, their associated phenomena (e.g. the periodicity) and their absence with certain fuels such as methane, formaldehyde and benzene.

The reaction of methyl radicals with oxygen is known to produce formaldehyde<sup>9</sup> and it has been suggested that this may be responsible for the observed chemiluminescence. That this is not so can be seen quite definitely from the following set of equations.



<sup>10</sup> McCormac and Townend, *J. Chem. Soc.*, 1938, 238.

<sup>11</sup> Neumann, *Acta Physicochim.*, 1938, 9, 327.

<sup>12</sup> Burgoyne, *Proc. Roy. Soc. A*, 1940, 174, 394; 175, 539. Burgoyne, Tang and Newitt, *ibid.*, 1940, 174, 379.

<sup>13</sup> Emelëus, *J. Chem. Soc.*, 1926, 2948; 1929, 1733.

<sup>14</sup> Gaydon, *Spectroscopy and Combustion Theory* (Chapman and Hall, 1942).

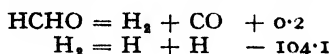
[Footnotes <sup>15</sup> to <sup>21</sup> on following page.]

Since at least 77 kcal. are required to account for the excitation of the formaldehyde, we conclude that the above reaction of methyl radicals with oxygen is not the source of the observed chemiluminescence. This conclusion is independent of assumptions concerning the twin uncertainties in thermochemical calculations, namely the latent heat of sublimation of carbon and the energy difference of the  $^1S$  and  $^3P$  states of carbon.

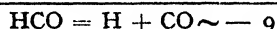
Lewis and von Elbe<sup>22</sup> have suggested that the reaction



is exothermic to the extent of 110 kcal. and so may be responsible for the production of excited formaldehyde. It is doubtful, however, if the reaction is in fact exothermic to anything like this extent. Lewis and von Elbe<sup>22</sup> themselves suggest that the decomposition of the formyl radical is almost thermoneutral. They base their suggestion on an assumption concerning the energy difference of the  $^1S$  and  $^3P$  states of carbon, but the same result follows without such an assumption. We have



Now the CH bond strength in formaldehyde probably lies between 90 and 100 kcal.<sup>24</sup> and the energy to remove the first H atom is probably not far different from this. Hence



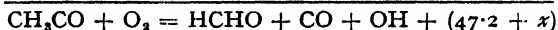
Now if we add the equations



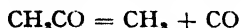
and



we get



and  $x$  would have to be 62.8 in order for the Lewis and von Elbe figure of 110 kcal. to be correct; i.e. the dissociation energy of the C—C bond in  $\text{CH}_3\text{CO}$  would have to be  $\sim 72$  kcal. weaker than that of the CH bond in HCO—a conclusion which seems most unlikely. More probably the dissociation of  $\text{CH}_3\text{CO}$  is not widely different to thermoneutral and the energy evolved in (8) is not so very different to that evolved in (7). Rice<sup>20</sup> finds the activation energy for the decomposition



to be 10 kcal., this figure affording an upper limit for the dissociation energy. The energy evolved by (8) can also be estimated as follows. A predissociation limit gives 93 kcal. as an upper limit for the energy required to dissociate the aldehydic H from the acetaldehyde molecule.

<sup>18</sup> Kane, *Proc. Roy. Soc. A*, 1938, 167, 62.

<sup>19</sup> See, e.g. Maccormac and Townend, *J. Chem. Soc.*, 1940, 143.

<sup>17</sup> Rossini, *Chem. Rev.*, 1940, 27, 1.

<sup>18</sup> Herzberg, *Molecular Spectra and Molecular Structure*, (Prentice Hall, 1939).

<sup>19</sup> Anderson, Kistiakowsky and Artsdalen, *J. Chem. Physics*, 1942, 10, 305; Kistiakowsky and Artsdalen, *ibid.*, 1944, 12, 469; Stevenson, *ibid.*, 1942, 10, 291; Artsdalen, *ibid.*, 1942, 10, 653.

<sup>20</sup> Long, private communication, from consideration of the values given by Delépine and Badoche, *Compt. rend.*, 1942, 214, 777; and von Wartenberg and Lerner-Steinberg, *Z. angew. Chem.*, 1925, 38, 591.

<sup>21</sup> Dwyer and Oldenberg, *J. Chem. Physics*, 1944, 12, 351.

<sup>22</sup> Lewis and von Elbe, *Combustion, Flames and Explosions in Gases*, (Cambridge, 1938).

<sup>23</sup> *Ibid.*, p. 387.

<sup>24</sup> Skinner, *Trans. Faraday Soc.*, 1945, 41, 645; Walsh, *ibid.*, 1947, 43, 60.

A figure of 93 kcal. for this dissociation energy is unlikely to be in error by more than 10 kcal. : it is not expected to differ greatly from estimates of the CH bond strength in the similar molecule, formaldehyde.<sup>24</sup> Adding the equations (8) and



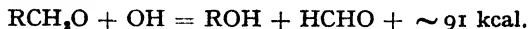
and using the known heats of formation of  $\text{CH}_3\text{CHO}$ ,  $\text{HCHO}$ ,  $\text{H}$ ,  $\text{OH}$  and  $\text{CO}$ , we find (8) to evolve  $\sim (39 \pm 10)$  kcal./mole. A further objection to the reaction (8) for the production of excited formaldehyde is the instability of  $\text{CH}_2\text{CO}$  above  $60^\circ \text{C}$ .<sup>1</sup>

The above calculations are an example of the fact, recognised by Damkohler and Eggerglüss,<sup>7</sup> that it is very difficult to find a radical-molecule reaction producing formaldehyde which is sufficiently exothermic to account for the excitation. On energetic grounds one is inclined to conclude that the observed chemiluminescence is due to a radical-radical reaction.

This conclusion receives support from a completely independent line of reasoning. Radical-radical reactions will be rare compared with radical-molecule or molecule-molecule reactions. Day and Pease<sup>25</sup> found that only some two quanta of radiation from formaldehyde fluorescence were emitted for each  $10^{16}$  fuel and oxygen molecules reacting. Topps and Townend<sup>26</sup> find the ratio of the number of quanta emitted to the number of fuel molecules reacting to be  $\sim 10^{-6}$ . This ratio is enormously greater than that suggested by Day and Pease, but it is still far too low for the excited formaldehyde molecules to be produced in the main chains. On grounds of quantity of light emission it therefore seems probable that the reaction giving rise to excited formaldehyde is of rare occurrence compared with those by which the main oxidation occurs.

The two lines of evidence are thus in accord and the tentative conclusion is that the excited formaldehyde is formed by a reaction starting as a radical combination.

In a wealth of papers of the Russian school (e.g.<sup>11</sup>), much evidence has been provided to show that the main reactions in cool flames are the alternate formation and decomposition of hydroperoxides. The precise radical reaction responsible for excited formaldehyde production must at present be very speculative. The most important clue we have is the fact that methane has not been observed to give the formaldehyde fluorescence. The radicals concerned in "low temperature" hydrocarbon oxidation are believed to include  $\text{OH}$ ,  $\text{R}$ ,  $\text{ROO}$ ,  $\text{RO}$ ,  $\text{CHO}$  and  $\text{HO}_2$ . With methane,  $\text{OH}$ ,  $\text{CH}_3$ ,  $\text{CHO}$  and  $\text{HO}_2$  are believed to play a part (see other papers of this series). It is possible, therefore, that excited formaldehyde is produced when a radical  $\text{RO}$  or  $\text{ROO}$  collides with another radical. An example would be

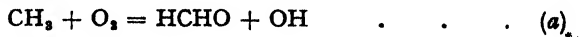


but we do not wish to specify any particular reaction until more evidence is forthcoming.

We note, however, that the production of excited formaldehyde is not in disagreement with the scheme of oxidation we have put forward : that is to say, it plausibly arises in the process of hydroperoxide formation and decomposition which we identify with cool flames.

### Exothermicity of Reactions.

We may conclude this paper by considering the exothermicity of some of the main reactions postulated to occur in hydrocarbon oxidation. We have seen that the reaction



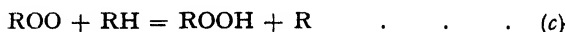
<sup>25</sup> Day and Pease, *J. Amer. Chem. Soc.*, 1940, **62**, 2234.

<sup>26</sup> Topps and Townend, *Trans. Faraday Soc.*, 1946, **42**, 345.

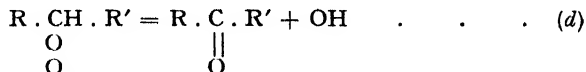
is exothermic to the extent of *ca.* 47 kcal. This very considerable exothermicity renders it highly probable that the explosion of methane-oxygen mixtures is, at least in part, chain-thermal—a conclusion in favour of which Norrish and Foord<sup>27</sup> have given strong evidence. Now, with higher alkyl radicals, the reaction may take either of two courses, viz.,



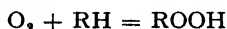
followed either by



or by, for example,

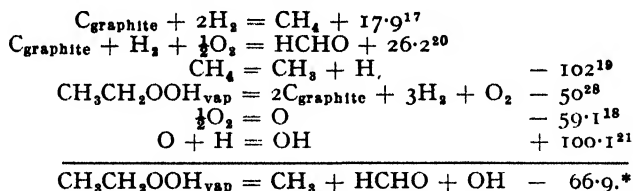


(b) followed by (d) will liberate, very roughly, the same energy as (a) viz. ~50 kcal. The over-all energy liberated by (b), followed by (c), i.e. the energy liberated in the reaction



is readily calculated from the heats of formation of ROOH<sup>28</sup> and RH as ~35 kcal. The conclusion is therefore that the reaction (d), whereby a peroxide radical decomposes to an aldehyde or ketone or CO, is considerably more exothermic than the reaction whereby a peroxide radical gives rise to a peroxide molecule. The strong exothermicity of the peroxide radical decomposition degradation renders it entirely plausible to suppose, as we did above, that "high temperature" hydrocarbon-oxygen explosions are chain-thermal.

On the other hand, though cool flames involve peroxide formation with considerable (but less) exothermicity they also involve peroxide breakdown with considerable absorption of energy, so that little heating occurs. In the particular case of ethyl hydroperoxide, we can calculate the energy of break-down into radicals by the following equations:



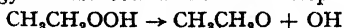
If peroxide breakdown is nearly as frequent as peroxide formation, little heating will therefore occur.

We shall find these conclusions of use in the following paper.

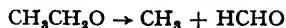
### Summary.

The scheme of hydrocarbon oxidation put forward in an earlier paper has been extended to include the possible decomposition of one of the radicals concerned. This decomposition gives a ready explanation of the formation of carbon monoxide during oxidation and of the existence of a negative temperature coefficient of oxidation rate within a certain

\* Most of this energy is absorbed in the initial step



the subsequent step



being close to thermoneutral.

<sup>27</sup> Norrish and Foord, *Proc. Roy. Soc. A*, 1936, **157**, 503.

<sup>28</sup> Stathis and Egerton, *Trans. Faraday Soc.*, 1940, **36**, 606.

<sup>29</sup> Wirtz and Bonhoeffer, *Z. physik. Chem. B*, 1936, **32**, 108.

<sup>30</sup> Rice, *The Aliphatic Free Radicals* (Johns Hopkins, 1935).

temperature range. The question of the production of excited formaldehyde is also considered and the tentative conclusion drawn that it arises from a reaction of a radical with a radical.

### Résumé.

Le schéma de l'oxydation des hydrocarbures, présenté dans un article précédent, a été étendu pour inclure la décomposition possible de l'un des radicaux concernés. Cette décomposition donne une explication facile de la formation d'oxyde de carbone au cours de l'oxydation et du coefficient de température négatif de la vitesse d'oxydation dans un certain domaine de température. On considère aussi la formation de formaldéhyde excitée et on tend à conclure qu'elle est formée dans une réaction de radicaux.

### Zusammenfassung.

Das in einer früheren Mitteilung vorgeschlagene Schema der Kohlenwasserstoffoxydation ist erweitert worden, sodass es die Möglichkeit des Zerfalls eines der Radikale mit einschliesst. Dieser Zerfall erklärt die Kohlenmonoxydbildung in der Oxydation und den negativen Temperaturkoeffizienten der Oxydationsgeschwindigkeit innerhalb eines bestimmten Temperaturbereichs. Die Frage der Erzeugung von angeregten Formaldehydmolekülen wird erwogen und es wird geschlossen, dass diese möglicherweise die Folge einer Reaktion zwischen zwei Radikalen ist.

*Laboratory of Physical Chemistry,  
Cambridge.*

## PROCESSES IN THE OXIDATION OF HYDRO-CARBON FUELS—III.

BY A. D. WALSH.

*Received 23rd January, 1946.*

In the two previous papers of this series <sup>1, 2</sup> the following hypotheses were proposed to describe the "low temperature" \* combustion of paraffins: (1) that the probability of oxygen attack at a CH bond increases in the order  $1^\circ < 2^\circ < 3^\circ$ ; (2) that alkyl hydroperoxides are the first molecular products of oxidation; (3) that these may break down by fission first at the O—O bond and then at the weakest bond on the  $\alpha$  carbon atom, and that peroxide formation and decomposition constitute the main reactions in cool flames; (4) that alkyl radicals may decompose to yield olefines as a side product; (5) that peroxide radicals (especially primary) may decompose to yield carbonyl compounds or carbon monoxide and that this reaction occurs in the "high temperature" \* oxidation, as with methane. It was then pointed out that (a) the suggested rules of peroxide decomposition led to the expectation that this decomposition is catalysed by aldehydes; (b) process (5) was very exothermic, so that "high temperature" explosion was probably chain-thermal; (c) the exothermicity of hydroperoxide formation was offset by the absorption of heat in peroxide breakdown; but that since peroxide formation and decomposition—in contrast to process (5)—was a strongly branching process, cool flames could be attributed to a form of isothermal branched chain explosion; (d) the negative temperature coefficient of oxidation

\* For the meaning of these terms, see previous papers.

<sup>1</sup> Walsh, *Trans. Faraday Soc.*, 1946, **42**, 269.

<sup>2</sup> Walsh, *ibid.*, 1947, **42**, preceding paper.



rate in the range 400-500° C. could be attributed to increase of process (5) with increase of temperature, causing consequent decrease of process (3).

We have shown that the above hypotheses are able to explain a considerable number of experimental facts. So far, however, the evidence has been mostly analytical. In this paper we wish further to extend the scheme and to show how it explains some of the kinetic facts of combustion.

## Section VI.—(A). The Two-Stage Nature of "Low Temperature" Combustion.

Passage of a cool flame predisposes a charge to give the "hot" flame of true ignition.<sup>3,4</sup> Indeed, at ordinary pressures "low temperature" explosion has been shown usually to involve a cool flame. It is a two-stage process, being characterised by two ignition lags,  $t_1$  and  $t_2$ ;  $t_1$  is the time that elapses before the formation of a cool flame,  $t_2$  is the time that elapses after the appearance of a cool flame before the hot flame appears. These facts have been established by Townend and Mandlekar<sup>5</sup> working with butane and pentane; Townend, Cohen and Mandlekar<sup>6</sup> working with hexane and isobutane; Aivazov and Neumann<sup>7</sup> working with pentane; Andreev<sup>8</sup> using butane; Kane<sup>9</sup> using propane and propylene; Blat, Gerber and Neumann<sup>10</sup> using butane; Burgoyne<sup>11</sup> using mono alkyl derivatives of benzene; and other workers. Both  $t_1$  and  $t_2$  decrease with increase of pressure, but  $t_2$  is much more sensitive to pressure than  $t_1$ .<sup>4,12,13,14</sup> Thus at high pressures the cool flame gives rise at once to the hot flame;  $t_2$  is too small to be measured and the ignition appears as a one-stage process.<sup>9,15</sup>

The apparent change from two-stage to one-stage ignition with increasing pressure made Neumann<sup>12</sup> and Kane<sup>9</sup> suppose that the two-stage pressure-temperature explosion region was closed, a single-stage "degenerate" explosion alone being possible at high pressures; and consequently to suppose knock in internal combustion engines was essentially a single-stage ignition. Sokolik and Jantovsky<sup>13</sup> have recently shown, however, that there is no discontinuity in the variation of the induction period  $t_1$  with pressure; the apparent disappearance of transition from cool to hot flame is only a consequence of the decrease of  $t_2$  below the limits of measurement; and the two-stage, cool flame, process of ignition may be retained, at high pressures, even within the apparent single-stage region. The two-stage process of explosion at low temperatures is far from vanishing at high pressures: it even persists at high temperatures (> 500° C.) if the pressure is sufficiently high.

There is evidence that  $t_1$  measures the time for a critical concentration of alkyl hydrogen peroxides to be attained. Neumann<sup>12</sup> and Neumann and Tutakin<sup>16</sup> show that it is possible to deduce the correct dependence of  $t_1$  on various experimental factors (pressure, temperature, inert gas addition, vessel dimensions and particularly on the quantity of peroxide added), if it is assumed that a critical concentration of alkyl hydrogen

<sup>3</sup> Sokolik, *Acta Physicochim.*, 1938, 9, 593.

<sup>4</sup> Hsieh and Townend, *J. Chem. Soc.*, 1939, 332, 337, 341.

<sup>5</sup> Townend and Mandlekar, *Proc. Roy. Soc. A*, 1933, 141, 484; 143, 168.

<sup>6</sup> Townend, Cohen and Mandlekar, *ibid.*, 1934, 146, 113.

<sup>7</sup> Aivazov and Neumann, *Acta Physicochim.*, 1936, 4, 575.

<sup>8</sup> Andreev, *ibid.*, 1937, 6, 57.

<sup>9</sup> Kane, *Proc. Roy. Soc. A*, 1938, 167, 62.

<sup>10</sup> Blat, Gerber and Neumann, *Acta Physicochim.*, 1939, 10, 273.

<sup>11</sup> Burgoyne, *Proc. Roy. Soc. A*, 1940, 174, 394; 175, 539. Burgoyne, Tang and Newitt, *ibid.*, 1940, 174, 379.

<sup>12</sup> Neumann, *Acta Physicochim.*, 1938, 9, 527.

<sup>13</sup> Sokolik and Jantovsky, *ibid.*, 1944, 19, 329.

<sup>14</sup> Maccormac and Townend, *J. Chem. Soc.*, 1940, 143, 151.

<sup>15</sup> Belov and Neumann, *Compt. rend.*, U.S.S.R., 1938, 18, 333.

<sup>16</sup> Neumann and Tutakin, *Compt. rend.*, 1937, 46, 205, 278.

peroxides has to accumulate before rapid decomposition to give the cool flame occurs. Unpublished experiments by Kogarko, Poliak and Stern, quoted by Sokolik and Jantovsky,<sup>18</sup> are said to support the idea of  $t_1$  representing the time for accumulation of a critical concentration of peroxides. Maccormac and Townend<sup>14</sup> find the initiation of "blue" flames to depend upon the attainment of a critical concentration of certain materials, probably peroxides. One may mention also that studies of the decomposition of alkyl peroxides have shown that they explode above a critical partial pressure.<sup>10, 16, 17, 18</sup> Neumann and Tutakin<sup>16</sup> found that butane-oxygen mixtures containing diethyl peroxide ignite and give rise to cool flames at the same limiting partial pressure of peroxide as would lead to explosion of the latter alone. Harris and Egerton<sup>17</sup> do not find this behaviour in the case of mixtures of diethyl peroxide with propane, but they, too, ascribe cool flames to the accumulation of substances behaving like alkyl peroxides—i.e. needing a critical partial pressure for explosive decomposition. Frank-Kamenetzki,<sup>19</sup> in a theory to be described below, has shown that many of the features of "low temperature" oxidation can be explained with the idea of a critical concentration of some intermediate being attained and has tentatively identified this intermediate with alkyl hydrogen peroxides. Altogether, we may conclude that there is strong evidence of a critical concentration of peroxides being necessary for the appearance of a cool flame: \* the mere formation of peroxides is not enough.

Experimentally, the course of the "low temperature" ignition process of hydrocarbon-oxygen mixtures at moderate pressures is as follows. First there is a period in which nothing appears to be happening. Then, after a time  $t_1$ , peroxides begin to be detectable, followed by formaldehyde; simultaneously, the pressure begins to rise rapidly and a cool flame appears. In the cool flame, peroxides and excited formaldehyde molecules are produced together. After the cool flame, the pressure drops somewhat, no doubt because of slight cooling after the flame passage. After a further time  $t_2$ , the pressure again increases and culminates in explosion. It is clear that two processes are involved, the first—culminating in the cool flame—functioning as the initiation process for the chains involved in  $t_2$ . One or more products are formed in the cool flame which are able to start a further oxidation of the original molecules and, under appropriate conditions, lead to explosion.

Any branching chain process is characterised by the equation

$$dn/dt = \theta + \phi n + \Delta n^2$$

where  $n$  = the number of centres at time  $t$ ;  $\theta$  = the rate of initiation of centres;  $\phi$  = the net linear branching factor;  $\Delta$  = the net quadratic branching factor. The variation of the rate of the reaction with time is proportional to  $dn/dt$ . It seems probable that the  $t_2$  chains are similar to those that also occur at "high" temperatures. The  $t_1$  chains represent a potent mode of initiation of basic chains that is only appreciable between 200 and 400° C. at moderate pressures. All the facts relating to the  $t_1$  chains relate to a somewhat complicated initiation process for the  $t_2$  chains. Now, if the above equation relates to the  $t_2$  process, in the absence of the  $t_1$  chains, the area of the "low temperature" peninsula must be characterised by negative values of  $\phi$  since explosion does not

\* The evidence cited by Sokolik<sup>3</sup> however, viz. the curves of Egerton, Smith and Ubbelohde (ref. 20, p. 457), is not valid. In the first place the curves refer to nitrogen peroxide and not to organic peroxides alone, and in the second place the maxima are due, not to a critical concentration being attained, but to the complicating effects of  $SO_2$ , as fully explained in the paper.

<sup>17</sup> Harris and Egerton, *Proc. Roy. Soc. A*, 1938, 168, 1.

<sup>18</sup> Harris, *ibid.*, 1939, 173, 126.

<sup>19</sup> Frank-Kamenetzki, *J. Russ. Physic. Chem.*, 1940, 14, 30.

<sup>20</sup> Egerton, Smith and Ubbelohde, *Phil. Trans. Roy. Soc. A*, 1935, 234, 433.

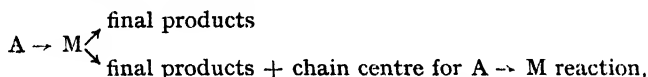
then occur (neglecting the effect of  $\Delta$ ). The  $t_1$  chains only affect  $\theta$  of the  $t_2$  chains. If  $\phi$  is negative, neglecting quadratic interaction of centres, explosion cannot occur by chain branching: it can only do so by the rate of initiation,  $\theta$ , being so high that lack of thermal equilibrium results. The idea of  $t_1$  representing a mode of initiation of the  $t_2$  chains therefore carries with it the chain thermal (as opposed to chain isothermal) nature of the explosion.

In summary of this survey, we may say (1) "low temperature" paraffin combustion is two-stage, (2)  $t_1$  ends and the cool flame arises when a critical concentration of hydroperoxides has been reached, (3) the cool flame functions as an initiation process for the  $t_2$  chains which may proceed to a chain thermal explosion.

### (B) The $t_2$ Chains.

In common with most other authors we shall suppose that the  $t_2$  chains include reactions similar to those occurring in the "high temperature" oxidation of paraffins. We can, in part, therefore, exemplify their nature by considering the combustion of methane.

We have already proposed a scheme of methane combustion, which is a special case of the wider outline of hydrocarbon combustion being described in these papers. It is well known that the length of the induction periods in hydrocarbon oxidation may be much greater than that of those in the  $H_2-O_2$  or  $CO-O_2$  reactions; and that therefore Semenov<sup>11</sup> proposed the hypothesis of "degenerate branching" in order to explain this. The number of  $H_2-O_2$  or  $CO-O_2$  chain centres grows rapidly because of branching as normally understood. We must still suppose branching to occur in hydrocarbon-oxygen mixtures because the reaction rate increases before self-heating becomes apparent. This branching must, however, be of such a nature that it occurs comparatively infrequently. Semenov supposes that a primary chain process forms a certain product which may either remain (or proceed to become) inert or sometimes undergo a reaction that gives rise to reaction centres of the primary chain. We may symbolise the idea in the equations



where  $A$  = molecule of original hydrocarbon,  $M$  = molecule of intermediate product. This is, of course, a form of chain branching, but since  $M$  is supposed to be stable relative to the chain carriers, the branching can take place long after the primary chain has ceased. If this is the only form of branching that occurs in the system and if  $M$  only occasionally undergoes the reaction that leads to further centres for the  $A \rightarrow M$  reaction, we have a satisfactory explanation for the slow growth of the number of chains with time.  $H_2-O_2$  and  $CO-O_2$  mixtures show true explosions due to branching chains: under active isothermal conditions the velocity becomes infinite. With hydrocarbons, however—if the degenerate branching hypothesis be true—the reaction rate grows so slowly with time that before it can reach infinite proportions by branching alone, the consumption of reactants begins to make itself felt, slowing down the rate. We never get, therefore, a true isothermal explosion but only a *degenerate explosion* in which the reaction velocity may become high, but remains finite. Where degenerate branching is the only form of branching present, it becomes necessary to suppose that explosions are due to self-heating of the mixture.

Our belief that the "high temperature" explosion of paraffins, including methane, is chain thermal enables us to adopt Semenov's hypoth-

<sup>11</sup> Semenov, *Chain Reactions*, (Oxford, 1935).

esis. In the case of methane, Norrish and Foord<sup>21a</sup> have shown that the kinetics of oxidation fit very well with the idea of degenerate branching if the intermediate product M is identified with formaldehyde. The combustion of methane can be regarded as the formation and oxidation of formaldehyde, the latter process giving rise (sometimes after a considerable interval from the ending of the primary chains) to new chain centres for the first.

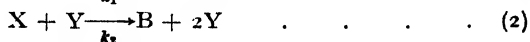
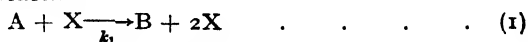
In accordance with this we shall therefore suppose the  $t_2$  chains to be as described in Paper II, for the "high temperature" process, but with the addition of degenerate branching via aldehydes, particularly formaldehyde.\*

### (C) The Periodicity of Cool Flames.

A remarkable feature of the cool flame process is its periodicity. Experimentally, the occurrence of a cool flame can be recognised by manometer observations: a pressure pulse occurs. Under some conditions—as observed by Beatty and Edgar<sup>22</sup> and others—one cool flame may succeed another at regular intervals. As many as five such successive cool flames may be observed.<sup>23</sup>

Pease<sup>24</sup> has attributed the oscillations to rise of temperature in the cool flame carrying the system into the range of negative temperature coefficient, i.e. bringing about reduced rate until the temperature drops and the process begins over again. While Pease's suggestion may be a contributory cause of the oscillations, Herwart and Frank-Kamenetzki,<sup>25</sup> studying the factors on which the frequency of cool flame pulsations depends, adduce strong evidence that the oscillations have their origin at least partly in the peculiar combination of chemical equations governing the oxidation.

Frank-Kamenetzki<sup>19†</sup> has put forward a system of formal equations that explains very well the pulsations, the two-stage nature of "low temperature" combustion and the necessary critical concentration of peroxides. Consider the reactions



where A is a molecule of original hydrocarbon, X is a product formed auto-catalytically from A, Y is a product formed auto-catalytically from X and B represents inert final products. These equations, for the moment, are to be taken as symbolic only. They may represent complicated processes or simple reactions, chain-reactions or non-chain reactions. We then obtain for the rate of growth of the concentration of X

$$dx/dt = k_1ax - k_2xy \quad . \quad . \quad . \quad . \quad (4)$$

and for the rate of growth of the concentration of Y

$$dy/dt = k_2xy - k_3ay \quad . \quad . \quad . \quad . \quad (5)$$

where the symbols have obvious meanings.

\* It should be noted that the formation of peroxides and their occasional decomposition to give new chain centres for further peroxide formation is also an example of degenerate branching and explains the possible great length of the time interval  $t_1$ .

† I am indebted to the Shell Petroleum Co. for a translation of this paper. A fairly full description of it is given here since no adequate English account has yet appeared.

<sup>21a</sup> *Proc. Roy. Soc. A*, 1936, **157**, 503.

<sup>22</sup> Beatty and Edgar, *J. Amer. Chem. Soc.*, 1934, **56**, 112.

<sup>23</sup> Newitt and Thornes, *J. Chem. Soc.*, 1937, 1656, 1669; Walsh and Chamberlain (to be published).

<sup>24</sup> Pease, *Equilibrium and Kinetics of Gas Reactions*, (Princeton, 1942).

<sup>25</sup> Herwart and Frank-Kamenetzki, *Bull. Acad. Sci., U.S.S.R., Cl. Sci. Chim.*, 1942, 210.

These two differential equations form a system already well known.<sup>26</sup> Their particular property is that they lead to a periodic dependence upon time of the concentrations  $x$  and  $y$ , of X and Y respectively. This may, be seen as follows. Starting with a mixture of hydrocarbon (A) and oxygen, suppose by some means a little of X is formed. Then, in the absence of Y, the concentration of X increases according to (1):

$$dx/dt = k_1ax$$

and

$$x = x_0 \exp. (k_1at).$$

An exponential increase with time thus takes place. Suppose, then, that a little Y is formed. While  $x$  remains small, by (5)  $dy/dt$  will be negative. The concentration of Y will not begin to increase until  $x$  becomes greater than the value  $x_k$  given by

$$\begin{aligned} k_1xy - k_2ay &= 0 \\ x_k &= k_2a/k_1 \end{aligned} \quad (6)$$

Y then begins to grow in its turn. If we assume that reaction (1) is only slightly exothermic, whereas reaction (3) is considerably so, then the growth of Y may lead to (3) becoming explosive and we have a system showing two-stage ignition. First, an induction period occurs, during which only reaction (1) takes place. The concentration of X rises until, when a critical concentration given by (6) is attained, an abrupt change takes place. Y now begins to increase exponentially (more rapidly than X, since X itself is also increasing). Simultaneously much self-heating occurs and explosion may result.

If the pressure-temperature conditions are not suitable, then the self-heating may not result in explosion before  $y$  reaches such a value that  $dx/dt$  becomes negative and  $x$  decreases to  $x_k$  again.  $dx/dt$  changes from positive to negative at the critical value of  $y$  given by

$$\begin{aligned} k_1ax - k_2xy &= 0 \\ y_k &= k_1a/k_2 \end{aligned} \quad (7)$$

$y$  increases beyond this value while  $x$  is falling to  $x_k$ . When  $x$  reaches  $x_k$ ,  $y$  ceases to increase and thenceforward decreases. As soon as  $y$  becomes less than  $y_k$ , then  $dx/dt$  again becomes positive and  $x$  begins to increase again. If no explosion takes place as a result of the formation of the maximum value of Y, then the concentrations of X and Y will change periodically about the values  $x_k$  and  $y_k$ .

While admittedly drastically over-simplified, the system gives a very good representation of many of the facts of two-stage ignition. Most of the ideas of the sections previous to the last were developed independently of Frank-Kamenetzki. When the latter's work became available, we were struck at once with the remarkable way his symbolic equations fitted the conclusions we had arrived at on quite other grounds. It is true that Frank-Kamenetzki tentatively interprets his formal equations usually in ways quite different to those we shall give below, but like us he identifies X and Y as alkyl hydroperoxides and aldehydes respectively. The agreement between the analytical-chemical and kinetic-mathematical approaches is so striking as to strengthen our confidence in each.

To identify X as alkyl hydroperoxides, means that Frank-Kamenetzki's theory then explains very well the need for a critical concentration of peroxide to be reached before the cool flame appears. The time required for  $x$  first to reach  $x_k$  is what we have been calling  $t_1$ . The theory agrees with the fact that peroxides are formed both prior to the cool flame and during the cool flame.

We identify Y particularly as formaldehyde. Explosion cannot occur until Y begins to grow rapidly. This in turn cannot happen until  $x$  reaches  $x_k$ . Equation (4) shows that the larger the initial value of  $y$ ,

<sup>26</sup> Frank-Kamenetzki and Salnikoff, *J. Physic. Chem. Russ.*, 1943, 17, 79.

the slower will be the increase of  $x$  and the higher the time taken to reach  $x_k$ . Addition of Y should therefore result in an anti-knock effect. This is a striking consequence of the theory, not pointed out by Frank-Kamenetzki. By its means we explain the remarkable *anti-knock* effect of formaldehyde.<sup>27</sup> Higher aldehydes have zero or slightly pro-knock effect as engine dopes, presumably because in their case removal of peroxide is offset by ease of oxidation producing peroxide. Under conditions where peroxide formation is difficult (i.e.  $t_1$  is long) their ease of oxidation to peroxides may be all important and their accelerating effect great. Like us, Frank-Kamenetzki includes the formation of peroxides during oxidation of higher aldehydes:  $A + Y \rightarrow X$ . This complicates, but does not necessarily alter, the general properties of equations (4) and (5).

Frank-Kamenetzki suggests (1)—the auto-catalytic production of peroxides—may occur by the simple auto-catalytic reaction



We have already suggested the scheme of section IV (Paper I) and prefer this because (a) it accords with our knowledge of the decomposition modes of peroxides, (b) it affords a simple interpretation of the production of a little aldehyde from the peroxides ( $X \rightarrow Y$ ), (c) it accords with the action of fuel additives to be described later.

We identify the auto-catalytic production of aldehyde from peroxide (equation (2)) with the catalytic decomposition of peroxides as described in section V (Paper II). It produces the cool flame.

Finally we identify the reaction  $A + Y \rightarrow B$  with the  $t_2$  chains described in this and the preceding paper and involving degenerate branching by formaldehyde; and we note the agreement with our own suggestion of Frank-Kamenetzki's supposition that explosion occurs by a *thermal* mechanism. Little or no self-heating is observed prior to the appearance of the cool flame, but marked self-heating in the production of the hot flame. The scheme agrees with the fact that knock in engines occurs when the formaldehyde concentration is rising steeply.<sup>27</sup> Reactions (1) and (2) represent chain-branching processes, but their peculiarity is that this branching is controlled and does not lead *directly* to explosion. Explosion occurs by (3) and is thermal. Reactions (1) and (2) may be thought of as a process of initiation for the process (3).

The fact that methane does not show the cool flame oscillations receives a simple explanation: no peroxides are present and therefore (2) cannot occur.

The upper temperature limit of cool flame is accounted for in the same way as we have explained the negative temperature coefficient of oxidation observed within a certain temperature range: viz. by the assumption of instability, with rising temperature, of one of the essential intermediates in the scheme. There is only one such intermediate which can well be chosen viz. peroxide radicals. Peroxides themselves cannot be chosen since their function is in any case to decompose and since they are preceded by peroxide radicals which will probably be unstable if peroxides are unstable. It is entirely plausible to suppose that as the temperature rises the lifetime of ROO radicals becomes less: <sup>28</sup> the first order decomposition of ROO overtakes the second order reaction of ROO with RH. In consequence peroxides cannot be formed and no peroxide-aldehyde condensation, with its concomitant production of cool flames, can occur. Higher pressure will compensate for a decreased lifetime of ROO (due

<sup>27</sup> Walsh, results obtained in collaboration with Mr. Ricardo.

<sup>28</sup> Cf. Lewis and von Elbe, *Combustion, Flames and Explosions in Gases* (Cambridge, 1938)

to temperature rise), so that ROOH may still be strongly produced. Hence the boundary of "low temperature" ignition on the pressure-temperature graph shows a positive slope—as Sokolik and Jantovsky<sup>18</sup> have shown.

It is not difficult to explain why richness of mixture strength favours oxidation: the greater the hydrocarbon concentration, the greater the likelihood of the unstable intermediate ROO forming ROOH and not

TABLE I

<i>Symbolic Representation.</i>	<i>Interpretation.</i>
(i) $A \rightarrow X$	Production of hydroperoxide from fuel according to $R + O_2 = ROO$ $ROO + RH = ROOH + R$ where R especially represents a 2° or 3° alkyl radical.
(ii) $A + X \rightarrow 2X$	The auto-catalysis of the production of hydroperoxide, due to occasional peroxide decomposition forming an OH radical and thence an alkyl radical.
(iii) $x_k$	The critical concentration of peroxides, the reaching of which brings to an end the first time interval $t_1$ .
(iv) $X \rightarrow Y$	The formation of a little aldehyde from peroxide, by peroxide decomposition.*
(v) $X + Y \rightarrow 2Y$	Auto-catalytic decomposition of peroxides, due to condensation with aldehydes and subsequent decomposition of the resulting hydroxy peroxides to more aldehydes. Begins as soon as $x$ has reached $x_k$ . The cool flame appears during this stage. Little over-all heating.
(vi) $A + Y \rightarrow B$	The $t_2$ chains, involving $R + O_2 \rightarrow (ROO) \rightarrow$ decomposition, liberating (OH), where R represents especially a 1° radical. Degenerate branching by aldehydes occurs and much heat is evolved. The chains are given a high rate of initiation by process (v). The mode of initiation includes the injection of alkyl (including 1° alkyl) and OH radicals. These lead to repetition of (i) and (ii) and simultaneous operation of (vi); the high initiation rate may cause (vi) to produce thermal instability,† with consequent thermal explosion after time $t_2$ ; if not, the whole process repeats.
(vii) $A + Y \rightarrow X$	The formation of peroxides during the combustion of higher aldehydes.

decomposing. The luminescence on ignition of alkyl hydrogen peroxides is now explained as identical with that of a cool flame. If peroxides are added to a hydrocarbon-oxygen mixture in a concentration greater than  $x_k$ , then the maximum concentration of Y, and with it the probability of explosion, will increase. The results of Neumann and Tutakin<sup>16</sup> concerning the effect of added peroxides on the hot flame thus receive a simple explanation.  $t_1$  continues until peroxides begin to be rapidly removed by HCHO. Little or no CO is produced during  $t_1$  (i.e. while reaction (1) almost alone is occurring), but as soon as (2) begins to occur

\* The surface reaction  $RCH_2OOH \rightarrow RCHO + H_2O$  may occur if 1° peroxides are formed, but in general the peroxides concerned are 2° or 3° and these cannot produce aldehyde in this way.

† As the temperature rises, (vi) increases relative to (i) both directly and indirectly because the probability of "end attack" by OH, forming a 1° radical, increases.

rapidly (i.e. the cool flame appears) much CO is formed: the work of Pope, Dykstra and Edgar<sup>22</sup> shows the very close association of CO formation with the cool flame. The periodic nature of the whole process need not always be apparent since the initial substance may of course be consumed during a period shorter than the period of pulsation and since explosion may cut short the process.

Solution of equations (4) and (5)<sup>19</sup> gives expressions of the form

$$\begin{aligned}\zeta &= \zeta_0 \sin (k_1 k_2)^{\frac{1}{2}} a t \\ \eta &= -\eta_0 \cos (k_1 k_2)^{\frac{1}{2}} a t\end{aligned}$$

where  $\zeta$  and  $\eta$  represent the fluctuations of concentrations  $x$  and  $y$  respectively about their critical values. The frequency of oscillation is

$$\nu = \frac{(k_1 k_2)^{\frac{1}{2}} a}{2\pi}$$

$k_1$  and  $k_2$  are both expected to be exponential functions of temperature.  $(k_1 k_2)^{\frac{1}{2}}$  will therefore also be an exponential function of temperature.

Herwart and Frank-Kamenetzki<sup>25</sup> have shown that a plot of  $\log \nu / T$  is linear. " $a$ " must be a function of the hydrocarbon and oxygen concentrations. Herwart and Frank-Kamenetzki<sup>25</sup> have shown in fact that  $\nu$  is almost independent of hydrocarbon concentration, though it depends markedly on the oxygen concentration.

We summarise in Table I the symbolic equations of Frank-Kamenetzki and the interpretation given to them in our papers thus far.

The author desires to acknowledge his indebtedness to the Shell Petroleum Co. for financial and other help.

### Summary.

The two-stage and periodic nature of "low temperature" paraffin combustion is reviewed and it is shown that a formal scheme proposed by Frank-Kamenetzki to explain these kinetic facts accords very well with the oxidation outline described by the author.

### Résumé.

L'auteur critique la combustion des hydrocarbures saturés à "basse température," considérée comme un processus périodique et à deux étapes et il montre que le schéma formel, proposé par Frank Kamenetzki pour expliquer ces faits cinétiques, s'accorde très bien avec sa propre description de l'oxydation.

### Zusammenfassung.

Der Zweistufencharakter und Periodizität der "Paraffinverbrennung bei niedrigen Temperaturen" werden besprochen und es wird gezeigt, dass ein formales Schema, das von Frank-Kamenetzki zur Erklärung der kinetischen Tatsachen vorgeschlagen wurde, gut mit der Oxydationstheorie des Verfassers übereinstimmt.

Laboratory of Physical Chemistry,  
Cambridge.

<sup>22</sup> Pope, Dykstra and Edgar, *J. Amer. Chem. Soc.*, 1929, **51**, 1875, 2203, 2213.



# SOME ASPECTS OF THE CHEMICAL AND BIOLOGICAL ACTION OF RADIATIONS.

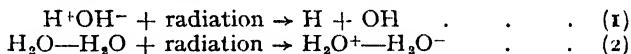
By JOSEPH WEISS.

Received 28th January, 1946.

Some of the general principles involved in the chemical action of radiation (X-rays,  $\gamma$ -rays,  $\alpha$ -particles, neutrons) have been outlined in a previous communication.<sup>1</sup> In that paper a very simple hypothesis was put forward which seems capable of bringing into line radiation chemistry with the general chemical behaviour of, e.g., aqueous solutions.

Although there exists a certain parallelism between radiation chemistry and photochemistry there is the important difference that in the case of penetrating radiations the absorption of radiation energy is not specific and is approximately proportional to the mass but practically independent of the chemical linkage. Consequently, particularly in dilute solutions, most of the energy is absorbed by the solvent medium where, therefore, most of the primary changes must take place. It has been indicated previously that in many simple cases in solutions, direct and indirect action of the radiation often lead to the same *qualitative* result. For aqueous solutions, in particular, the theory outlined gives a quantitative agreement with experiment. Aqueous systems are of considerable importance in many biological objects and it is the purpose of this paper to show how the chemical theory can be applied to some of the problems in the biological action of radiations.

It is well known that the absorption of penetrating radiations generally results in excitation and ionisation. With water as solvent the following electron transfer processes are likely to be of importance : <sup>1, 2</sup>



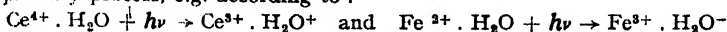
followed by \*



All the above processes are energetically possible under the influence of radiations. Thus one obtains eventually H atoms and OH radicals.

It has been suggested \* that the initial distribution of OH and H is the same as the initial distribution of positive and negative ions, i.e., the H atoms thus are produced at some distance from the path of the ionising particles. The new hypothesis thus embodies two features. (i) Single electron transfer processes. These might have been anticipated from the physical process but now they receive a definite chemical meaning. (ii) The formation of atoms and free radicals (partly as a consequence of (i)).

\* The behaviour of these molecular ions is known also from the photochemistry of certain simple ions in aqueous solution, where they are formed in the primary process, e.g. according to :

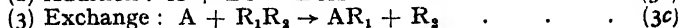
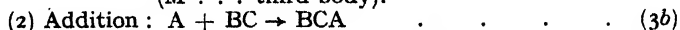
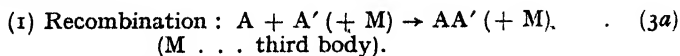


(cf. Weiss, *Trans. Faraday Soc.*, 1941, **37**, 463).

<sup>1</sup> Weiss, *Nature*, 1944, **153**, 748 ; 1946, **157**, 584.

<sup>2</sup> Cf. Lea, *Actions of Radiations on Living Cells* (Cambridge, 1946).

In general, radicals and atoms can undergo three different types of elementary processes.



The latter reaction is of considerable interest as new radicals are formed and this provides the possibility of a chain reaction.

The chemical behaviour of a number of radicals and atoms is well known and some of the reactions of OH radicals and of H atoms have been discussed previously in connection with the radiation chemistry of aqueous solutions.<sup>1</sup> In these cases the primarily formed H and OH are subject to recombination according to the back reaction :



although—under certain conditions—a small amount of molecular hydrogen and oxygen may be formed resulting from the interaction of the primary fission products.<sup>1</sup> However, in the presence of other substances in the aqueous medium these will react with the chemically reactive radicals and atoms.<sup>1</sup> In the chemical and related biological action of radiations it is useful to distinguish between two cases, namely, if (a) the back reaction (4) can be neglected, (b) the back reaction (4) must be taken into account.

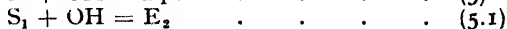
The known biological effects can be classified also into two groups, namely where the action of the radiation—i.e., the mean ( $D_m$ ) or half lethal dose ( $D_1$ )

(a) is independent of the nature and wave-length of the radiation.

(b) is dependent on these factors.

In the latter case the simple hypothesis of one quantum = one (biologically) active hit, which has been put forward would lead to the relation  $D_m \propto \frac{1}{\lambda}$  ( $\lambda$ , wave-length). Actually the experimental evidence mostly obeys different relationships as, for instance, in some cases Glocker's formula :<sup>3</sup>  $D_m \propto \frac{1}{\lambda} \cdot \frac{a}{R + a}$ , seems to hold, where according to this author's interpretation  $R$  denotes the range of the secondary electrons and  $a$ , their mean path in the biological structure.

**CASE A. Recombination of the Primary Radicals can be Neglected.** Interaction with the acceptors is fast compared with their recombination. This case, as will be come apparent, coincides with Class (A) of the biological effects. In biological systems a number of acceptor molecules are generally present which can react with the strongly oxidising OH radicals (and/or H atoms).<sup>\*</sup> In general the different acceptor molecules ( $S, S_1, S_2, \dots$ ) present will react with the OH radicals according to :



The different substrates need not be entirely unrelated and may be partly identical with one or more of the previously formed reaction products ( $E_1, E_2, \dots E_{n-1}$ ). In ordinary chemical action in solution the case of

<sup>\*</sup> There is some evidence, for instance, that a strongly oxidising substance is produced in cells under the action of X-rays which counteracts the formation of desoxyribose nucleic acid which is normally formed from ribose nucleic acid and a reducing agent.

<sup>3</sup> Glocker, *Z. Physik*, 1932, **77**, 653.

two substrates leads to a mutual "protection effect"<sup>1</sup> and the case ( $S_1 = E_1$ ) to an inhibition by the reaction product itself.<sup>5</sup>

Most of the biological phenomena belonging to Class A have been explained previously by the "single hit" hypothesis which was introduced very early into the biological action of radiation.<sup>4</sup> In general, the "hit theory" is concerned with the number of "hits" which are necessary to "kill" (or damage) an active region and this can be deduced by means of Poisson's formula. In these cases the independence of the dose on the nature of the radiation follows from the experimental fact that the same number of ions are formed for equal doses, nearly independent of the nature of the radiation.

From the view point of the "hit" theory the chemical reaction (5) corresponds to a single "hit" while if, e.g.,

$$E_1 = S_1, E_2 = S_2, \dots, E_{n-1} = S_{n-1} \dots \dots \dots (6)$$

one gets a successive change of the starting substrate (S) by 1, 2, 3, . . .  $n$  hits, i.e.,  $n$  reactions with the OH radicals.

Actually, there exists a complete formal analogy between Poisson's "hit" formula and the mathematical expression of the system (5, 5.1, . . . 5. $n$ ) of successive chemical reactions if relation (6) holds and all the rate constants ( $k_s, k_{s,1}, \dots k_{s,n}$ ) are equal. This corresponds to the assumption of the same "sensitive volume" throughout in the "hit" theory.

Assuming that the biological important structure (e.g., giant molecule) is represented by the acceptor S occurring in reaction (5) one obtains for the stationary state from the eqn. (1) (5) . . . (5. $n$ ) :

$$\frac{d[OH]}{dt} = \epsilon I_{abs} - k_s[S][OH] - k_{s,1}[S_1][OH] \dots - k_{s,n}[S_{n-1}][OH] = 0 \quad (7)$$

$$\text{and} \quad -\frac{d[S]}{dt} = k_s[S][OH] \dots \dots \dots (8)$$

(Square brackets denote concentrations, e.g., molecules per unit of volume.)  $I_{abs}$  denotes the total radiation energy absorbed per unit of volume per sec. As the total number of active radicals formed (through the ions) is only dependent on  $I_{abs}$  one has :

$$N_{OH} = \epsilon I_{abs} \dots \dots \dots (9)$$

$\epsilon$  is a proportionality factor and  $N_{OH}$  represents the mean number of OH radicals generated per sec. per unit of volume and is defined by the integral :

$$N_{OH} = \frac{1}{V} \int_0^V n_{OH} dv \dots \dots \dots (10)$$

where  $n_{OH}$  denotes the differential concentration, i.e., number of radicals per volume element  $dv$  (of, e.g., the ionisation tracks where the radicals are primarily formed) and the integration is performed over the total volume  $V$ .

From eqn. (7) and (9) one obtains :

$$[OH] = \frac{N_{OH}}{\sum_n k_{s,n}[S_{n-1}] + k_s[S]} \dots \dots \dots (11)$$

In order to satisfy the experimental requirements it is necessary to put :

$$k_s[S] \ll \sum_n k_{s,n}[S_{n-1}] \dots \dots \dots (12)$$

which means that a considerable fraction of the OH radicals reacts with some other acceptor molecules present which, however, are not essential for the (biological) active structure (S) itself. This assumption is almost

<sup>4</sup> Cf. Mayneord, *Proc. Roy. Soc. A*, 1934, 146, 867.

<sup>5</sup> Cf. Dale, Meredith and Tweedie, *Nature*, 1943, 151, 280.

certainly fulfilled. Biologically, eqn. (12) expresses a "protection effect" of non-essential substrates molecules towards the active substance S. In the "hit" theory this corresponds to the fact that the observed "sensitive volume" is very much smaller than the actual physical "target" volume.

From equations (8) to (12) one obtains :

$$-\frac{d[S]}{dt} = \frac{k_s N_{OH}[S]}{\sum_n k_{s,n}[S_{n-1}]} = \frac{k_s N_{OH}[S]}{k_{sm}[S_m]} \quad (13)$$

if, for reasons of simplicity, one replaces all the biologically non-essential acceptors by the mean "concentration"  $[S_m]$  of one substance  $S_m$ , with a rate constant  $k_{sm}$ . As the actual number of active radicals formed, even with the highest doses employed, is relatively small,  $[S_m]$  can be considered as practically constant during the course of an experiment.

Integration of equation (13) then yields :

$$S = S_0 \exp \left( -\frac{k_s N_{OH} t}{k_{sm}[S_m]} \right) = S_0 \exp (-KD) \quad (14)$$

where concentrations are replaced by number of molecules and  $S_0$  represents the number of biologically active units at  $t = 0$ , where

$$N_{OH} \cdot t = D \quad (15)$$

represents the (total) dose applied in  $t$  seconds per unit volume, and  $K$  (eqn. 14), has the dimensions of a volume per molecule.

A bimolecular rate constant can be expressed by the kinetic cross-section ( $q$ ) for the particular interaction and the relative velocity ( $\tilde{v}$ ) as :

$$k_{bi} \propto q \cdot \tilde{v} \quad (16)$$

In the case of free radical reactions the Boltzmann factors can be neglected practically (on account of the low heats of activation) and, therefore,  $K$  can be represented formally by :

$$K = q_s \left( \frac{1}{q_{sm}[S_m]} \right) \quad (17)$$

where  $q_s$  represents the kinetic cross-section of the biological structure S and the term in the bracket can be interpreted as the "mean linear region" available per one molecule of  $S_m$ .

From equation (14) the half or mean lethal doses are given by :

$$D_{\frac{1}{2}} = \ln 2 \cdot D_m = \ln 2 / K \quad (18)$$

In this case, therefore,  $K$  and the  $D$ 's are independent of the nature and wave-length of the radiation.

From equation (14) one also obtains for the number of S structures destroyed at time  $t$  :

$$(S_0 - S) = S_0(1 - e^{-KD}) \sim S_0 KD \quad (19)$$

Without taking into account the biologically nonessential molecules  $S_1, \dots, S_{n-1}$  one obtains instead of eqn. (13) the equation :<sup>1</sup>

$$-\frac{d[S]}{dt} = N_{OH} \quad (20)$$

In this case the number of S molecules destroyed depends only on the dose. This state of affairs actually exists, e.g., in aqueous solutions containing one substrate.<sup>1</sup>

In order to compare the above results with the "hit" theory one starts from Poisson's formula which gives the probability ( $P_r$ ) that a number of objects ( $E_r$ ) out of a total number ( $S_0$ ) have received  $r$  "hits", viz. :

$$P_r = \frac{E_r}{S_0} = \frac{1}{r!} (KD)^r e^{-KD} \quad (21)$$

where  $D(= I_{\text{abs}}.t)$  again represents the total number of "hitting" particles per unit volume during time  $t$  and  $k$  (probability factor) is assumed to be the same for any "hit".

The number of structures ( $S$ ) which have not received a "hit" in time  $t$  is given for  $r = 0$  from (19) by an expression identical with equation (14) if  $k \equiv K$ .

This formal identity of the two theories can be proved for any arbitrary number of "hits". For instance, the number of objects ( $E_1$ ) having received just one hit ( $r = 1$ ) can be deduced from the reactions (5) and (5.1) for  $S_1 = E_1$ , and is expressed by the differential equations (8) and :

$$\frac{d[E_1]}{dt} = k_s[\text{OH}]\{S\} - [E_1] \quad . \quad . \quad . \quad (22)$$

assuming the same rate constant ( $k_s$ ) throughout the whole process and putting :

$$k_s[\text{OH}] = kI_{\text{abs}} = \text{const.} \quad . \quad . \quad . \quad (23)$$

which in the chemical theory is equivalent to a constant (stationary) concentration of the OH radicals.

**CASE B. Recombination of the Radicals taken into Account.** This, in general, coincides with Class B of the biological effects.

The discussion in this case will be confined to a single solute which is identified with the biologically active (giant) molecule  $S$ . The reverse reaction (4) must be of importance in all cases where either (i) the acceptors are chemically relatively non-reactive or (ii) are present in too low concentrations.

The recombination of the active radicals which are formed in the tracks of the ionising particles depends on their *local* concentration and distribution. This is fundamentally different from Case A where only their *average* concentrations are of importance.

The course of the total reaction is determined again by the differential eqn. (8) and :

$$\frac{d[\text{OH}]}{dt} = N_{\text{OH}} - k_4[\text{OH}][\text{H}] - k_5[\text{S}][\text{OH}] \quad . \quad . \quad . \quad (24)$$

Solving (24) for the stationary state ( $\frac{d[\text{OH}]}{dt} = 0$ ), one obtains :<sup>1</sup>

$$-\frac{d[\text{S}]}{dt} = \frac{k_5 N_{\text{OH}}[\text{S}]}{k_4[\text{H}]_t + k_5[\text{S}]} \quad \left( \sim \frac{k_5 N_{\text{OH}}[\text{S}]}{k_4[\text{H}]_t} \right) \quad . \quad . \quad . \quad (25)$$

$[\text{H}]_t$ , now represents the *local* (differential) concentration of the active radicals in the spaces where the actual reaction takes place.

The formation of the active radicals follows the ionisation (and sometimes excitation) by the fast particles (electrons,  $\alpha$ -particles, recoil protons). The radicals are thus initially localised in the ionisation tracks and very probably their initial distribution follows closely that of their ionic precursors. The radius ( $P_0$ ) of these tracks is originally only of the order of  $10^{-6}$  cm. (in a medium of density 1).<sup>6, 7</sup> However, once the radicals are formed they begin to diffuse away relatively rapidly. The average square of their mean displacement ( $\bar{x}^2$ ) can be estimated directly from Einstein's equation :  $\bar{x}^2 = 2Dt$ , where  $D$  is the diffusion coefficient of the radicals. Therefore the mean radius of the columns after time  $t$  is given by :

$$\bar{P}_t = (P_0^2 + 4Dt)^{\frac{1}{2}}.$$

This must be taken into account in the calculation of the local concentration of the radicals. Therefore  $(\text{H})_t$  in eqn. (25) should be calculated from a differential equation of the type :

$$\frac{d[\text{OH}]}{dt} = n'_{\text{OH}} - k_2\{\text{H}\}\{\text{OH}\} - \dots \text{etc.} \quad . \quad . \quad . \quad (26)$$

<sup>6</sup> Jaffé, *Ann. Physik*, 1913, 42, 303 ; *Physik. Z.*, 1929, 30, 849.

<sup>7</sup> Lea, *Proc. Cambridge Phil. Soc.*, 1934, 30, 80 ; *Brit. J. Radiol.*, 1943, 16, 338.

where the differential (*local*) concentrations ( $\{\}$ ) enter and  $n_{\text{OH}}^1$  for the initial stages\* is given by:

$$n_{\text{OH}}^1 \sim \frac{n_{\text{OH}}}{\pi(P_0^2 + 4Dt)} \quad (27)$$

The initial distribution of the OH radicals and H atoms is probably identical with the initial distribution of positive and negative ions the effects of the H atoms will be found at some distance from the path of the ionising particles. Generally, some further spread of the radicals and of their effects can be brought about by (i) diffusion (as indicated by eqn. 27), (ii) by the initiation and propagation of a chain reaction mechanism (as indicated on p. 315). Considerably greater distances may be covered in this way than by any of the other effects.

The extension into space of such reaction chains can assume significant proportions and may be of considerable importance in the biological effects. It can be determined, e.g., from the life time of the radicals, i.e., the duration of the actual chain process. This has been measured in some cases<sup>7a</sup> and was found to be of the order of a few 0.01 sec. to 0.1 sec. from which the distance covered can be calculated, using Einstein's equation.

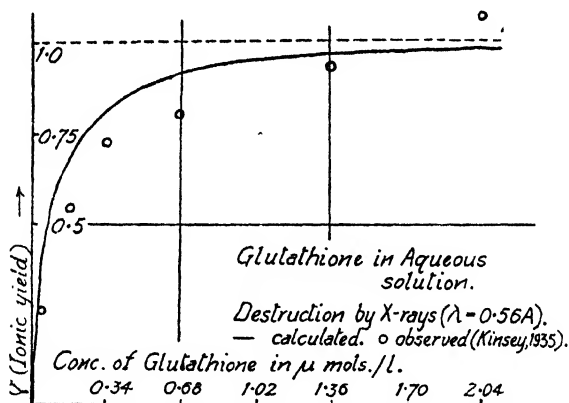


FIG. 1.—Destruction of glutathione by X-rays in aqueous solution. Ionic yield: observed values according to Kinsey;<sup>9</sup> calculated values from the equation:  $\gamma = 1 / \left\{ 1 + \frac{a \times 10^{-6}}{c} \right\}$  ( $c$ , mean concentration of the glutathione).

Taking  $D \sim 10^{-5}$  cm.<sup>2</sup> sec.<sup>-1</sup> for an average diffusion coefficient at room temperature in the aqueous medium one finds for this distance:  $\Delta x = \sqrt{2Dt} \sim 10^{-3}$  cm. In certain cases the difficult integration of the above equations may be avoided by adopting a simple (semi-quantitative) method which brings out the main features of the process.

This method will be illustrated by applying it to some of the reactions in solution which have been investigated experimentally. Eqn. (25) can be used to calculate the ionic yield ( $\gamma$ ) as:

$$\gamma = \frac{\text{number of molecules destroyed}}{\text{number of ions produced}} = \frac{1}{N_{\text{OH}}} \cdot \frac{dS}{dt} = \frac{dS}{dD} = \frac{k_5[S]}{k_4[H] + k_5[S]} \quad (28)$$

\* i.e. before intermingling of the different columns and dissipation of the original tracks has occurred.

<sup>7a</sup> Weigert and Kellermann, *Z. physik. Chem.*, 1923, **107**, 1; Briers, Chapman and Walters, *J. Chem. Soc.*, 1926, 562.

### 320 CHEMICAL AND BIOLOGICAL ACTION OF RADIATIONS

Thus, for otherwise similar conditions  $\gamma$  increases with increasing concentration of the substrate. This is illustrated by the experiments of Kinsey<sup>9</sup> on the destruction of glutathione by X-rays in aqueous solution. In Fig. 1 the points (o) have been deduced from the experimental data while the theoretical curve is calculated from an expression similar to eqn. (28).

Generally, some knowledge of the value of  $(H)_i$  (the local concentration of the active radicals) is essential.

As a first approximation one may assume that the concentration of these active radicals in the ionisation tracks is given by :

$$(H)_i \sim \text{prop. number of ion pairs per unit length of track} \quad (29)$$

This assumption is closely related to Lind's principle of ionic chemical equivalence.<sup>10</sup>

Stenstrom and Lohmann<sup>11</sup> determined the ionic yield for the destruction of tyrosine by X-rays (of 200 kev.) in aqueous solution. They found  $\gamma_x = 1/6$  (for 1.0 mg./cc.);  $= 1/12$  (for 0.02 mg./cc.). Nürnberger<sup>12</sup>

found a considerably lower yield for  $\alpha$ -rays :  $\gamma_\alpha = \frac{1}{350}$  (for 0.04 mg./cc.).

The ratio of the ionic yields can be calculated on the basis of assumption (29) as the ionic densities are known experimentally (cf. Table I).

TABLE I.—AVERAGE NUMBER OF PAIRS OF IONS PER MICRON OF TRACK (IN TISSUE).<sup>7, 8</sup>

$\gamma$ -rays.	X-rays.		Recoil Protons from 2.7 Mev. (neutrons).	$\alpha$ -particles.
	$\lambda=0.15 \text{ \AA.}$ (200 kev.).	$\lambda=4 \text{ \AA.}$		
15	60	270	1200	4000

$$\frac{\gamma_x}{\gamma_\alpha} = \begin{cases} \text{observed : } 350/12 \sim 29 \\ \text{calculated : } \frac{0.02}{60} / \frac{0.04}{4000} \sim 33. \end{cases}$$

The agreement is better than expected considering the very rough approximation used and also that the radicals are obviously not uniformly distributed along the tracks. Actually they appear in small clusters in the case of X-rays and it is known that the ion (radical) density increases considerably towards the end of the tracks. However, one can draw the general conclusion that lower yields are to be expected from these radiations where the local ion (radical) concentration is high and vice versa, which is in agreement with the experimental results.

For all radiations the total number of ions produced by the same dose (e.g., 1r) is approximately the same while their local distributions may differ widely. It is known<sup>13, 14, 15</sup> in the case of  $\gamma$ -rays and X-rays, where fast electrons are the ionising particles, that the total number of ions (radicals),  $T$ , per one fast electron i.e., per one quantum  $h\nu$ , or per one track) is proportional to the energy ( $V$ ) of the electrons, viz. :

$$N_i \propto V \quad . \quad . \quad . \quad . \quad . \quad (30)$$

<sup>8</sup> Cf. Gray and Read, *Brit. J. Radiol.*, 1942, 15, 72.

<sup>9</sup> Kinsey, *J. Biol. Chem.*, 1935, 110, 551.

<sup>10</sup> Cf. Lind, *The Chemical Effects of Alpha Particles and Electrons* (New York, 1928).

<sup>11</sup> Stenström and Lohmann, *J. Biol. Chem.*, 1928, 79, 763.

<sup>12</sup> Nürnberger, *Proc. Nat. Acad. Sci.*, 1937, 23, 189.

<sup>13</sup> Cf. Rutherford, Chadwick and Ellis, *Radiations from Radioactive Substances* (Cambridge, 1930).

<sup>14</sup> Livingston and Bethe, *Rev. Mod. Physics*, 1937, 9, 245.

<sup>15</sup> Cf. Bagge, *Ann. Physik*, 1937, 30, 72.

The total range of a fast electron ( $R_e$ ) is given by

$$R_e \propto V^2 \quad (31)$$

Consequently the number ( $n_e$ ) of ions (radicals) per unit length of track is:

$$n_e \propto V^{-1} \quad (32)$$

Eqn. (30) holds for  $\alpha$ -particles as well but as their range ( $R_\alpha$ ) is given by:<sup>13, 14</sup>

$$R_\alpha \propto V^{\frac{3}{2}} \quad (33)$$

the number of radicals ( $n_\alpha$ ) per unit length of track is given by:

$$n_\alpha \propto V^{-\frac{1}{2}} \quad (34)$$

In order to analyse those cases of biological action which depend on the nature and wave-length of the radiation it is often sufficient (as a first approximation) to start from the simplified form of eqn. (25) which on integration yields:

$$S = S_0 \exp \left( -\frac{k_5 N_{OH} t}{k_4 [H]_i} \right) = S_0 \exp \left( -\frac{k_5 D}{k_4 [H]_i} \right) \quad (35)$$

then:

$$D_{\frac{1}{2}} = \ln 2 \cdot D_m = \ln 2 / \alpha \quad (36a)$$

and

$$\alpha = \frac{k_5}{k_4 [H]_i} \quad (36b)$$

Similar to the previous case,  $\alpha$ , has the dimensions of a volume per molecule and can be expressed by:

$$\alpha = q_s \left( \frac{1}{q_H [H]_i} \right) \quad (37)$$

where  $q_s$  denotes the (kinetic) cross-section of the molecules S and  $(q_H [H]_i)^{-1}$  can be interpreted as the mean length of the track available per one radical (H or OH).

The ultimate evaluation of  $D_{\frac{1}{2}}$  depends on the value of  $[H]_i$  in (eqn. 37). It is clear that  $[H]_i$  cannot generally be taken as constant throughout the whole course of the reaction. As a first approximation one may confine oneself to the consideration of two essential periods where one may work with different (approximately) constant values of  $[H]_i$ .

(i) **The Initial Stages** i.e., before any appreciable amount of diffusion has set in, where, one may assume that eqn. (29) is approximately fulfilled. This gives (from eqn. 32 and 34):

$$[H]_{i(1)} \propto V^{-1}, \text{ (for X-rays)} \quad (38)$$

$$[H]_{i(1)} \propto V^{-\frac{1}{2}}, \text{ (for } \alpha\text{-rays)} \quad (38a)$$

(ii) **The Advanced Stages** of the reaction when diffusion processes assert themselves increasingly and a broadening and (finally) a dissipation of the initial tracks occurs which eventually leads to an intermingling of the different tracks.\*

In the earlier stages, i.e., before an appreciable intermixing of the tracks has occurred, one can assume that according to eqn. (30):

$$[H]_{i(11)} \propto V \quad (39)$$

while in the later stages, after attainment of a more or less homogenous distribution, a better approximation is obviously:

$$[H]_{i(11)} \sim \text{const} (\propto D) \quad (40)$$

This last stage is probably only important for the "tail" of the reaction and can be neglected in the majority of cases.

The relative importance of the different stages must depend on the rate of diffusion of the radicals compared with their rate of chemical interaction.

\* This intermingling of the tracks must also depend on their (mean) initial distance, which is given by their density (i.e. number of  $h\nu$  or  $\alpha$ -particles per unit of volume).



## 322 CHEMICAL AND BIOLOGICAL ACTION OF RADIATIONS

In the case of X-rays one obtains, taking into account the different regions with their appropriate weights :

$$\alpha_{(1)} \propto \frac{k_5}{k_4 V^{-1}} = \frac{k_5}{k_4} \beta_1 V \quad . \quad . \quad . \quad (41a)$$

$$\alpha_{(11)} \propto \frac{k_5}{k_4 V} = \frac{k_5}{k_4} \frac{\beta_2}{V} \quad . \quad . \quad . \quad (41b)$$

$$\alpha_{(11)}^1 \propto \frac{k_5}{k_4} = \frac{k_5}{k_4} \beta_2^1 \quad . \quad . \quad . \quad (41c)$$

where the proportionality factors ( $\beta_1$ ,  $\beta_2$ ,  $\beta_2^1$ ) are meant to include the weight factors. Whereas in general :

$$\alpha = \alpha_{(1)} + \alpha_{(11)} + \alpha_{(11)}^1 \quad . \quad . \quad . \quad (42)$$

In special cases one or two regions may be sufficient to describe the essential part of the reaction.

If for the present purpose we take :

$$\alpha = \alpha_{(1)} + \alpha_{(11)} = \frac{k_5}{k_4} \frac{\beta_2}{V} \left( \frac{V^2}{\beta_2/\beta_1} + 1 \right) \quad . \quad . \quad . \quad (43)$$

Putting  $(\beta_2/\beta_1) = a$ , and making use of eqn. (31) and of the fact that from energy considerations :

$$V^{-1} \propto (\hbar\nu)^{-1} \propto \lambda \quad . \quad . \quad . \quad (44)$$

one obtains :

$$\alpha \propto \lambda \left( \frac{R_e + a}{a} \right) \quad . \quad . \quad . \quad (45)$$

which with eqn. (36a) gives an expression which is formally identical with Glocker's formula.

It is possible to calculate  $[H_2]$  more accurately by making use of eqn. (27). However, at present the experimental material is not sufficient to warrant any elaborate calculations.

Glocker's derivation of this equation is open to criticism which has been amplified recently by Jordan.<sup>16</sup> On the other hand, the chemical theory, as outlined above, provides a new physico-chemical basis for this relation, which is free from the previous difficulties.

It is now possible to predict that if  $\gamma$ -rays or sufficiently hard X-rays are used that the dependence of, e.g., the mean lethal dose on the wave-lengths should gradually diminish and finally disappear. This can be demonstrated by Wykoff's own figures<sup>17</sup> for *B. coli*, where the mean lethal dose decreases in the series of decreasing wave-length as: 8.4, 6.67, 4.33, 4.65,  $4.20 \times 10^3$  r. and in order to achieve the same effect with  $\alpha$ -rays  $24 \times 10^3$  r. are required.<sup>18</sup> On the other hand, while it is known, that the doses of radiation for the production of mutations are independent of the wave-length in the case of  $\gamma$ - and X-rays it has been found recently that a higher dose of neutrons is required to produce the same effect.<sup>19, 20</sup> This is to be expected on the basis of the chemical theory as the recoil protons produce a much higher local ion (radical) density (cf. Table I) leading to increased recombination.

### Temperature Effects.

As has been pointed out previously, all the important chemical elementary processes involved, should possess only low heats of activation because of the participation of free radicals (or atoms).

<sup>16</sup> Cf. Jordan, *Radiologica*, 1938, 2, 16.

<sup>17</sup> Wykoff, *J. exp. Med.*, 1930, 51, 921; 1930, 52, 435, 769.

<sup>18</sup> Lea, Haines and Coulson, *Proc. Roy. Soc. B*, 1936, 120, 147.

<sup>19</sup> Timoféeff-Ressovsky and Zimmer, *Naturwiss.*, 1938, 26, 362.

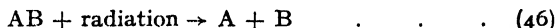
<sup>20</sup> Lea, *J. Genetics*, 1940, 39, 181. Lea, Haines and Bretscher, *J. Hygiene*, 1941, 41, 1.

On the other hand, the local concentrations of the radicals (possibly also some of the other substances) must be greatly affected by diffusion. This effect is important whenever the rate of reaction is comparable with the rate of diffusion. Generally a lowering of the temperature will result in a greater "persistence" of the original tracks\* and thus the recombination reaction will be enhanced and a general "immobilisation" of the radicals will result. Both effects may *lessen* the attack on the biological structures. The present experimental evidence which seems to support this conclusion<sup>21, 22</sup> is somewhat obscured by biological factors.

**Direct Action of Radiation.** Apart from the indirect action of radiation discussed above where the radicals produced from the medium react with the acceptor molecules, there is also the possibility of a direct absorption of the radiation followed by some chemical change.

This has been discussed previously for the case of simple substances in solution where the direct and indirect effect often lead to the same *qualitative* result.<sup>1</sup>

In the case of direct action of radiation by, e.g., a biologically active giant molecule (AB) direct absorption of radiation will lead to ionisation followed, in general, by dissociation (e.g., formation of the radicals A and B) according to:



There is again the possibility of either, recombination:



or first order reactions of the fission products according to the schemes:



(X, Y, acceptors).

The above reactions can be treated as before.

If one neglects the recombination (reaction 47) the rate of disappearance of the AB units (for the stationary state) is given by:

$$-\frac{d[AB]}{dt} = E_{abs}^{(AB)} \quad . \quad . \quad . \quad (49)$$

Where  $E_{abs}^{(AB)}$  denotes the total energy of radiation absorbed by the AB units per unit of time. If (as a first approximation) one may put:

$$E_{abs}^{(AB)} \propto [AB] \quad . \quad . \quad . \quad (50)$$

this leads again to an exponential law.

If, on the other hand, recombination is taken into account one obtains:

$$-\frac{d[AB]}{dt} = \frac{k_{48} E_{abs} [X]}{k_{47} [B]_l + k_{48} [X]} \sim \frac{k_{48} E_{abs}}{k_{47} [B]_l} \quad . \quad . \quad (51)$$

where  $[B]_l$  stands for the local concentration of the primary fission product which enters into the recombinations process and which is directly dependent on the *local* ion density in the tracks.

It is apparent, that, while the target theory in its classical or modern form<sup>2</sup> is fully maintained as it enters into the computation of the radiation absorbed by the biologically active structure (eqn. 49) this need no longer be true in the case of the more densely ionising radiations when the recombination must be taken into account (eqn. 51). In the latter case the local ion (radical) density and the rate constant of the recombination process tend to change the simple geometrical aspects.

\* One finds easily that  $n_{OH}^1 \propto D^{-1} \propto T^{-1} e^{b/T}$  which follows from equation (27) with Einstein's formula for the diffusion constant and from the known temperature dependence of the viscosity of liquids (cf. Ewell, *J. Appl. Physics*, 1938, 9, 252).

<sup>21</sup> Hevesy, *Rev. Mod. Physics*, 1945, 17, 102.

<sup>22</sup> Lacassagne, *Compt. rend.*, 1942, 215, 231.

All the above considerations correspond to "one hit" cases, which is expressed chemically by the destruction of the biologically vital unit (e.g., giant molecule) by *one* active radical (OH or H).

This is in full agreement with the "quantum" concepts expressed by Delbrück and Schrödinger<sup>23, 24</sup> in the case of mutations and also with Jordan's views.<sup>16</sup> On the basis of the present discussion this can be extended to those cases where the mean dose is not independent of the nature and wave-length of the radiation, e.g., to the lethal effects on unicellular organisms, etc.

In the case of more highly organised biological structures the lethal effects most probably depend on the simultaneous destruction of more than one important unit. In these cases "multiple hit effects" are probably important and it is conceivable that neutrons or  $\alpha$ -rays are more effective than  $\gamma$ - or hard X-rays.<sup>2</sup>

I would like to thank Dr. D. E. Lea and Dr. W. M. Dale for valuable discussions.

### Summary.

The simple hypothesis put forward by the author in 1944 to explain the chemical action of ionising radiations in solution has been developed further and has been applied to some biological effects of radiations in aqueous media.

In connection with this the direct and indirect action of radiations, the formation, action and the implications of free radicals and the relation to the physical "hit" theory have been discussed in detail.

It is found that the recombination process following the primary formation of the radicals, is of considerable importance. If recombination can be neglected the effects are approximately independent of the nature and wave-length of the radiation, and depend only on the total dose while this is no longer the case if the recombination process plays a part.

### Résumé.

La théorie précédemment exposée, concernant l'action chimique de radiations ionisantes, a été développée, puis appliquée à quelques effets biologiques en milieu aqueux. On discute ici l'action directe et indirecte des radiations, la formation et l'action de radicaux libres et la relation avec la théorie physique de "choc". Si l'on néglige la recombinaison de H et OH, les effets ne dépendent à peu près pas de la dose totale; ceci n'est plus vrai dans les cas où la recombinaison est un facteur important.

### Zusammenfassung.

Die früher vom Verfasser entwickelte Theorie der chemischen Wirkung von ionisierenden Strahlungen wurde erweitert und auf einige biologische Effekte angewendet. Die direkte und indirekte Wirkung, die Bildung, Wirkung und Bedeutung von freien Radikalen und die Beziehung zur physikalischen "Treffer"-Theorie werden erörtert. Wenn die Wiedervereinigung von H und OH ausseracht gelassen wird, ist die Wirkung fast unabhängig von der Art und Wellenlänge der Strahlung, aber dies stimmt nicht, sobald diese Wiedervereinigung ein wichtiger Faktor ist.

*University of Durham,  
King's College,  
Newcastle-upon-Tyne, 1.*

<sup>23</sup> Timoféeff-Ressovsky, Delbrück and Zimmer, *Göttinger Nachr.*, 1935 (VI), 1, 189.

<sup>24</sup> Schrödinger, *What is Life?* (Cambridge, 1944).

# THE ABSORPTION OF DYESTUFFS BY CELLULOSE—PART VIII.

## THE ANALYSIS OF IONIC DISTRIBUTION BY MEANS OF DIFFUSION POTENTIALS.

BY S. M. NEALE.

*Received 28th February, 1946.*

The application of thermodynamic methods to the further elucidation of the phenomena of dyeing has been attempted during the last decade by several workers. In Part VI of the present series of papers, Hanson, Neale and Stringfellow<sup>1</sup> attempted to apply such methods to the problem of dyeing, making an arbitrary division of the system into two phases: (a) fibre with adsorbed dye anions plus imbibed water, and (b) solution in bulk.

Phase (a) was regarded as an equipotential region and the Donnan equilibrium was invoked to calculate the distribution of ions between it and the external solution. By assigning an arbitrary, but quite plausible value for the amount of imbibed water, they were able to deduce equations which were in agreement with experimental data for the variation of adsorption with dye concentration and with amount of added salt. Gilbert and Rideal<sup>2</sup> have more recently approached the problem in a somewhat different way, which avoids the necessity for assuming a specified volume for the equipotential region within the fibre. Their method of treatment when applied to the dyeing of cellulose leads to conclusions<sup>3</sup> regarding the effect of dye concentration and salt concentration upon the absorption, and upon the electrical potential of the dyed fibre, very similar to those deduced for the model visualised by Hanson, Neale and Stringfellow.<sup>1</sup> Still more recently, Willis, Warwicker, Standing and Urquhart<sup>4</sup> have put forward a further thermodynamic treatment of the dyeing equilibrium, which again leads to generally similar conclusions as to the effects of dye and salt concentration on the amount of dye absorbed. They also present new data for the absorption of Chrysophenine G by cellulose, which are in fair agreement with their equations.

Usher and Wahbi<sup>5</sup> attempted to throw light on the problem from a new angle, which provides a crucial test of the common fundamental hypothesis that only the colour anion is absorbed by cellulose, whilst the corresponding local concentration of cations is maintained by electrostatic attraction. They attempt to show, by direct analytical determination of the ammonium and chloride ions in a dyed cellulose sheet immersed in ammonium chloride solution, that the depression of chloride ion concentration in the cellophane below that in the external solution is not in quantitative agreement with the assumptions made by Hanson, Neale and Stringfellow.<sup>1</sup> They reach the surprising conclusion that "a Donnan equilibrium exists in 0.1 N., but not in 0.5 N. ammonium chloride solution". It can hardly be doubted that the model assumed by Gilbert and Rideal, which assumes that the adsorbed ions are in an equipotential region, and even more that of Hanson, Neale and Stringfellow, which

<sup>1</sup> *Trans. Faraday Soc.*, 1935, **31**, 1718.

<sup>2</sup> Gilbert and Rideal, *Proc. Roy. Soc. A*, 1944, **182**, 335.

<sup>3</sup> G. A. Gilbert, *private communication*.

<sup>4</sup> Willis, Warwicker, Standing and Urquhart, *Trans. Faraday Soc.*, 1945, **41**, 506.

<sup>5</sup> Usher and Wahbi, *J. Soc. Dyers Col.*, 1942, **58**, 221.

assigns a definite volume to this equipotential region, are simplified pictures of actuality. The possibility of a more precise analysis is foreshadowed by Neale,<sup>6</sup> Neale and Peters,<sup>7</sup> who assume the adsorbing surface to be equipotential and attempt to analyse both by theory and by experiment, the composition of its ionic atmosphere, in which there is a steady fall of potential away from the adsorbing surface. The first model of Hanson, Neale and Stringfellow<sup>1</sup> makes an arbitrary division between imbibed water (equipotential) and external solution (also equipotential) with a sharp potential difference (the Donnan potential) at the plane of division. The model of Gilbert and Rideal<sup>2</sup> whilst avoiding such arbitrary division, fails to give any information concerning the composition of the diffuse ionic atmosphere.

The first model, assuming an equipotential enclosed region, is a plausible one provided the region (imbibed water), is enclosed partly by equipotential surfaces (dyed cellulose), and partly by surfaces across which the potential gradient is sensibly zero (width of opening small relative to thickness of diffuse ionic atmosphere), for the potential in such a region is constant.<sup>8</sup>

The validity of such a model is subjected to a critical check by the method of Usher and Wahbi<sup>6</sup> in which the concentrations of the salt ions in the wet dyed cellulose sheet are determined by direct analysis. Unfortunately, however, the depression below unity of the concentration ratio anion/cation ( $C^-/C^+$ ) will be greatest in dilute solutions, and the experimental difficulties of carrying out a sufficiently accurate analysis by direct chemical methods are great, as is shown by irregularities in the results of Wahbi and Usher. It is possible, however, by the use of an electrochemical method such as that devised by Meyer and Sievers,<sup>9</sup> accurately to determine the anion/cation ratio for mobile ions, and the effective concentration of immobile ions in the small quantity of dilute solution which is contained in the pores of a membrane. Their technique is not directly applicable to cellulose membranes and a method independently developed will be described. It will be shown that the results obtained by applying this analytical method to dyed cellophane are in good agreement with the theory of Hanson, Neale and Stringfellow<sup>1</sup> in which the dyed cellulose with its imbibed water is treated as a single phase containing immobile anions or negatively charged centres.

### Theoretical Basis for Experimental Technique using a Mono-Monovalent Electrolyte.\*

This has already been worked out by Meyer and Sievers, but the results may be recapitulated in a form better suited to the interpretation of the present experiments.

#### \* Notation :

$E$  = electromotive force of concentration cell.

$R$  = gas constant.

$F$  = Faraday constant.

$f$  = activity coefficient.

$V$  = mobility of anion.

$U$  = mobility of cation.

$a$  = activity of electrolyte.

$C^+ : C^-$  = concentrations of diffusible cation : anion in pores of membrane.

$A$  = sum of equivalent concentrations of immobile anions in cellulose phase.

$C = \sqrt{C_1 C_2}$  = mean concentration of external solutions.

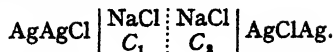
$\lambda = \frac{C^-}{C} = \frac{C}{C^+}$

$\psi$  = mean electric potential of diffusion space relative to bulk solution.

$C_1, C_2$  = concentrations of electrolyte in bulk solutions.

$\tau$  = cationic transport number in solution.

Let a concentration cell be set up thus :



The E.M.F. of such a combination is

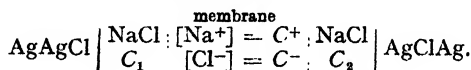
$$E = \frac{2RT}{F} \int_1^2 \tau(d \ln c + d \ln f) \quad (i)$$

when account is taken of the variation of the cation transport number with concentration. Provided the difference between  $C_1$  and  $C_2$  is not large, this reduces to

$$E = \frac{2\tau RT}{F} \ln a_1/a_2 \quad (ii)$$

since  $\tau$  and  $f$  do not vary rapidly with  $C$  and, as is well known<sup>10</sup> the E.M.F. of such a cell affords one of the most accurate means available for determining the transport number  $\tau$ .

Now instead of a liquid-liquid junction  $C_1$ — $C_2$  let the solutions be separated by a membrane whose pores are large compared with the diameters of the ions, so that the velocities of ionic migration bear the same ratio to each other as in water.



Let the resistance of the membrane be much greater than that of the solution, so that the gradient of concentration is localised within the membrane. The observed potential difference  $E$  then consists of two terms, the electrode potential difference ( $E_{\text{Ag}}$ ) plus the potential difference across the membrane ( $E_m$ )

$$E = E_{\text{Ag}} + E_m$$

where

$$E_{\text{Ag}} = \frac{RT}{F} \ln a_1/a_2.$$

The potential difference ( $E_m$ ) across the membrane may then be divided into three parts (see Fig. 1) as follows :

$E_1$ ;  $E_2$  = the Donnan potentials between solutions (1); (2) cellulose.

$E_d$  = the diffusion potential across the membrane.

$$E_m = E_2 - E_1 + E_d.$$

$$E_1 = \frac{RT}{F} \ln \frac{(C^+)_1}{C_1}$$

$$= \frac{RT}{F} \ln \frac{A + \sqrt{A^2 + 4C_1^2}}{2C_1}$$

$$(\text{since } (C^+)_1 = (C^-)_1 + A \text{ and } (C^+)_1 (C^-)_1 = C_1^2).$$

$$E_1 = \frac{RT}{F} \sinh^{-1} \frac{A}{2C_1} \quad (iii)$$

similarly

$$E_2 = \frac{RT}{F} \sinh^{-1} \frac{A}{2C_2}$$

and

$$E_d = \frac{RT}{F} U \ln \frac{x_2 + AU}{x_1 + AU} \quad (\text{see Meyer and Sievers } ^9) \quad (v)$$

<sup>8</sup> *Trans. Faraday Soc.*, 1946, 42, 473.

<sup>7</sup> *Ibid.*, 1946, 42, 478.

<sup>6</sup> Rutherford, *Vector Methods* (London, 1939), p. 102.

<sup>5</sup> Meyer and Sievers, *Helv. Chim. Acta.*, 1936, 19, 649. Meyer, *Trans. Faraday Soc.*, 1937, 33, 1073.

<sup>10</sup> McKenna, *Theoretical Electrochemistry* (London, 1939).

where

$$U = \frac{U - V}{U + V} \text{ and } x = \sqrt{A^2 + 4C^2},$$

whence

$$E_m = \frac{RT}{F} \left\{ \sinh^{-1} \frac{A}{2C_2} - \sinh^{-1} \frac{A}{2C_1} + U \ln \frac{x_2/A + U}{x_1/A + U} \right\}.$$

$E_m$  therefore depends on  $U$ , on  $C_1/A$ , and on  $C_2/A$ .

Now if concentrations  $C_1 : C_2$  are in a constant ratio (say  $\sqrt{10}$ )  $E_m$  is a function of only two parameters,  $U$  and  $C_1/A$ . If the experimental values of  $E_m$  are then plotted against  $\log C_1$  (or  $\log C_2$ ), it is possible to

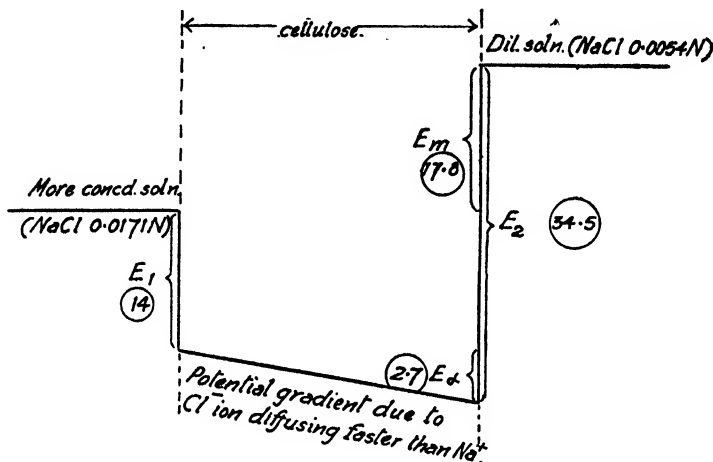


FIG. 1.—Electrical potential diagram NaCl 0.0171 N.—cellophane—NaCl 0.0054 N (The interphase potential changes appear as abrupt, although they are probably diffused over a distance of  $10^{-7}$  to  $10^{-6}$  c.m.).

determine by a comparison with a set of standard curves (see Meyer and Sievers<sup>9</sup>) both  $U$  and  $A$ . The value of  $U$  is obtained from the limiting value of the membrane potential at high concentration thus:

$$\lim_{C \rightarrow \infty} E_m = \frac{RT}{F} U \ln C_2/C_1$$

and for both dyed and undyed cellophane membranes is found to be much the same as in water, substantiating the assumption that the relative velocities of migration of the two ions are not much affected by the "sieve" action of the cellulose structure.

### Experimental.

The most simple apparatus suffices. Solutions of NaCl or other electrolyte, conveniently in a concentration ratio of  $1 : \sqrt{10}$  and at precisely the same temperature, are placed in 50 cc. beakers standing close together on a block of paraffin wax, and containing chloride-coated silver electrodes connected to an electrometer valve potentiometer. A bridge is established between the two beakers by means of a strip of filter paper or a strand of cotton yarn drawn through an inverted glass U-tube, when the E.M.F. corresponding to the accepted values of  $\tau$  and  $f$  should be at once obtained, as the "pores" in the paper or yarn bridge are so much larger than the effective thickness of the diffuse ionic atmosphere<sup>6,7</sup> that the conduction of current proceeds chiefly by ionic transport through the water held by capillary action. This bridge is now removed, and replaced by a strip of dyed or undyed cellophane sheet about 5 mm. wide,

which has been soaked in a mixture of the two cell liquids, and then carefully pressed between dry filter paper to remove surface liquid.

The E.M.F. then obtained gives, on subtracting  $E_{Ag}$ ,  $E_m$  the total potential difference across the cellulose sheet. It is essential to make a long conducting path through the cellophane so that the resistance is high. This can be done by clamping twenty or more sheets of cellophane as a transverse separator between the two solutions, which must be constantly stirred, but the use of a strip is more convenient and gives stable E.M.F. more quickly. A single cellulose membrane must not, as was done by Prideaux,<sup>11</sup> be clamped between the two solutions so that conduction takes place across it, for, on account of the extreme thinness and high permeability of wet cellophane, most of the gradient of concentration will then be localised in the solution, whereupon the E.M.F. becomes unstable and is much affected by shaking the vessel. Prideaux, using single transverse membranes, found that various chlorides appeared to show the same transport members across a cellophane membrane as they do at a normal water junction. He concluded that cellophane behaved as a neutral sieve, which, as will now appear, is by no means the case.

### Results.

**1. Undyed Cellophane.**—(Temperature 18° c. Concentration ratio of  $C_1/C_2$  of electrode solutions =  $\sqrt{10}$ ). The values of  $\tau$  calculated from the E.M.F. readings obtained with the liquid bridge (wet cotton) are in good agreement with the most recent data, as collected by McKenna.<sup>10</sup> The values from undyed cellophane are given in Table I and plotted in Fig. 2.

TABLE I.—UNDYED CELLOPHANE.

Electro-lyte.	$C_1$ moles/ litre.	E.M.F. mv. cotton bridge.	$\tau$	E.M.F. mv. cello- phane bridge.	$E_{Ag}$ calc. mv.	$E_m$ obs. mv.	$E_1$ calc. mv.	$E_2$ calc. mv.	$E_d$ calc. mv.	$E_m$ calc. mv.
NaCl	1·71	21·3	0·37	21·3	28·5	— 7·2	0·14	0·46	— 7·5	— 7·2
	0·54	20·2	0·361	20·8	28·0	— 7·2	0·46	1·46	— 7·5	— 6·5
	0·171	21·3	0·384	24·0	27·8	— 3·8	1·46	4·6	— 6·7	— 3·6
	0·054	21·8	0·387	32·3	28·1	+ 4·7	4·6	14·0	— 5·3	+ 4·1
	0·0171	22·0	0·390	41·6	28·3	+ 13·3	14·0	34·5	— 2·7	+ 17·8
	0·0054	22·5	0·394	42·0	28·2	+ 14·0	34·5	62·0	— 1·5	+ 26·0
KCl	1·0	27·5	0·484	27·5	28·4	— 0·9	0·3	0·9	— 0·7	— 0·1
	0·316	26·6	0·482	26·8	27·6	— 0·7	0·9	2·5	— 0·7	+ 0·9
	0·1	25·9	0·47	29·0	27·8	+ 1·2	2·5	7·8	— 0·6	+ 4·7
	0·0316	27·7	0·492	38·5	28·2	+ 10·3	7·8	22·3	— 0·5	+ 14·0
HCl	0·0316	46·4	0·831	5·0	27·9	+ 22·1	7·8	22·3	+ 11·5	+ 26·0
BaCl <sub>2</sub>	0·48	15·4	0·405	13·7						
	0·152	15·0	0·40	13·3						
	0·048	15·4	0·433	14·9						
	0·0152	17·0	0·44	22·1						
	0·0048	17·8	0·455	28·0						

The calculated values of  $E_1$ ,  $E_2$ , and  $E_d$  have been obtained from eqn. (iii), (iv) and (v) on the assumption that  $A$ , the concentration of immobile anions in the cellophane phase, is 0·02 N. It will be seen that this assumption provides a variation of  $E_m$  with concentration of salt, which is in fair agreement with experiment. The experimental values of  $E_m$ , however, fail to approach the theoretical maximum of 29 mv. at infinite dilution (where  $E_d = 0$ ).

<sup>11</sup> Prideaux, *Trans. Faraday Soc.*, 1942, 38, 121.



It might be supposed that as  $E_1$  and  $E_2$  increase rapidly with decreasing concentration, that is to say as the negative potential of the cellulose increases, the liberation of protons from acidic groups will be reduced, so that  $A$ , the "acidity" of the cellulose, instead of remaining constant

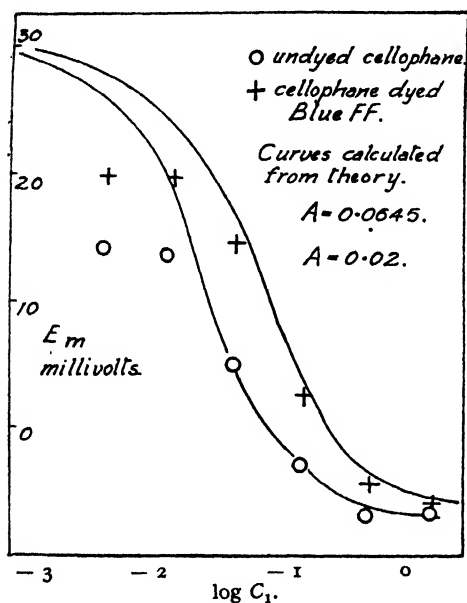


FIG. 2.

as is assumed, actually falls rapidly at very low concentrations of electrolyte. This decrease of dissociation will prevent  $E_m$  from increasing in dilute solution to the value calculated on the assumption that  $A$  is constant.

The proportion of carboxylic acid groups in the cellophane used is 5 milliequiv./100 g. by the method of direct titration<sup>12</sup> and 100 g. take up about 100 g. of water, so that if all the groups dissociate  $A$  would become 0.05, and two-fifths dissociation, the order one would expect for a carboxylic acid, would account for the origin of the value  $A = 0.02$ . It is not to be supposed, however, that such dissociation of acid groups is the only source of the negative charge shown by cellulose in water, for Neale and Peters<sup>7</sup> have shown by

electrokinetic measurements that cotton free from carboxylic acid groups shows a strong negative charge.

The results obtained with  $\text{BaCl}_2$  are of special interest. A comparison of the experimental E.M.F.'s shown in the third and fifth columns of the table, shows that, above 0.03 N.,  $\text{BaCl}_2$  reverses the charge on cellophane. This could only be due to a selective adsorption of  $\text{Ba}$  ions, and if this occurs it would also explain the abnormally high effect of  $\text{BaCl}_2$  as an "assistant" in dyeing.<sup>13</sup>

## 2. Dyed Cellophane.

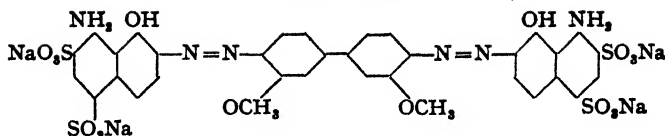
TABLE II.—DYED CELLOPHANE (WITH  $\text{NaCl}$  SOLUTIONS).

$C_1$ moles/ litre.	$E_m$ Undyed.	$E_m$ dyed Blue FF.	Calculated values for $A = 6.45 \times 10^{-2}$ . (Blue dyed cello.)				$E_m$ (dyed Janus Red).	$E_d$ for $\text{H}_2\text{O}$ .
			$E_1$	$E_2$	$E_d$	$E_m$		
1.71	-7.2	-6.4	0.5	1.5	-6.7	-5.7		
0.54	-7.2	-4.4	1.5	4.8	-6.7	-3.4		
0.17	-3.8	+2.5	4.8	14.3	-6.5	+3.0	-6.5	-6.5
0.054	+4.7	+14.4	14.3	35.1	-2.5	+18.3	-6.0	-6.3
0.017	+13.3	+19.7	35.1	62.8	-1.0	+26.7	-5.3	-6.3
0.0054	+14.0	+19.8	62.8	91.2	-0.3	+28.1	-5.3	-6.3

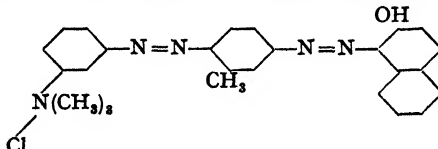
Chlorazol Sky Blue FF (mol. wt. 992) Type ( $\text{Na}^+$ ), R.... 1.6 % on cellophane ( $\rightarrow A = 0.0645$ ) (dyed 4 hr. at 100° C. dye 0.05 g/l  $\text{NaCl}$  20 g/l, analysed by pyridine stripping.)

<sup>12</sup> Neale and Stringfellow, *Trans. Faraday Soc.*, 1937, **33**, 881.

<sup>13</sup> Neale and Patel, *ibid.*, 1934, **30**, 905.



Janus Red B. (mol. wt. 460) Type R<sup>+</sup>Cl<sup>-</sup> 6 % on cellophane (dyed at 70° c.)



The observed and calculated values of the membrane potentials for dyed cellophane given in Table II are also plotted in Fig. 2.

It will be seen that, again with the exception of the very dilute solutions, the results for the blue dyed cellophane are in good agreement with the theory of dyeing put forward by Hanson, Neale and Stringfellow, and it is suggested that they provide conclusive proof of the validity of the application of the principles of the Donnan membrane equilibrium to the treatment of the system dyed cellulose-salt solution. The presence of 6 % of the red basic dye appears entirely to neutralise the intrinsic negative charge of cellulose, so that a membrane so dyed behaves as a neutral sieve and the observed E.M.F.'s are the same as at a liquid-liquid junction.

The author is much indebted to Dr. G. A. Gilbert of the University of Birmingham for most helpful suggestions on the theoretical aspect of this work.

### Résumé.

On a établi, d'un point de vue théorique, une méthode pour déterminer le rapport anion/cation d'ions mobiles et la concentration effective d'ions immobiles, en solution dans des pores de cellophane au cours de l'adsorption de colorants. On a employé, pour obtenir des résultats qui viennent appuyer la théorie, le fait que la cellulose teinte imbibée d'eau peut être regardée comme une seule phase contenant des anions immobiles et des centres négativement chargés.

### Zusammenfassung.

Eine elektrochemische Methode zur Bestimmung des Verhältnisses von beweglichen Anionen zu beweglichen Kationen und der wirksamen Konzentration von unbeweglichen Ionen in der Lösung in den Poren von Zellophan während Farbstoffadsorption wurde theoretisch ausgearbeitet. Die damit erhaltenen Resultate unterstützen die Theorie, dass gefärbte Zellulose nach Imbibition von Wasser als ein Einphasensystem, das unbewegliche Anionen oder negative Zentren enthält, behandelt werden darf.

*College of Technology,  
Manchester, 1.*

## THE ABSORPTION OF DYES BY CELLULOSE— PART IX.

### MEASUREMENTS OF THE ABSORPTION OF SKY BLUE FF BY COTTON.

By C. E. F. FISHWICK AND S. M. NEALE.

*Received 28th February, 1946.*

In the preceding papers of this series,<sup>1-8</sup> and in the recent work of Willis, Warwicker, Standing and Urquhart,<sup>9</sup> measurements of the absorption of various purified dyes on regenerated cellulose sheet (Cellophane) have been described. The use of this material as the absorbent is advantageous where the time rate of dyeing is being studied, as the smoothness and small extent of its outer surface (compared with natural cellulose fibres) makes it possible by mechanical agitation to ensure that the rate of take-up of dye is dependent wholly on its diffusion from the surface into the interior of the sheet. Furthermore, the geometrically simple shape confines the diffusion to the direction normal to the surface, so that the mathematical analysis of experimental kinetic data is simplified. As was pointed out by Hanson, Neale and Stringfellow,<sup>6</sup> however, in their thermodynamic treatment of the dyeing of cellulose as a process involving the specific adsorption of the anion, Cellophane is by no means an ideal form of cellulose for the provision of equilibrium absorption data which are to be used to check any quantitative hypothesis which purports to predict the variation of absorption with dye or with salt concentration. It contains ionisable carboxylic acid groups which interfere with the ionic equilibrium and by electrostatic influence depress the absorption of colour anions and alter the shape of the absorption isotherms. The material is not constant in thickness nor in optical anisotropy. The experimenter has, furthermore, no control over the uniformity of other physical and chemical characteristics such as molecular weight and reactivity, which are dependent on conditions of manufacture. Natural cotton cellulose, on the other hand, after the usual technical scour with dilute caustic alkali under pressure followed by a properly controlled hypochlorite bleach, is a reasonably reproducible material much better suited for equilibrium absorption measurements, for its chemical and physical properties do not vary appreciably from one variety of cotton to another, nor are they appreciably dependent on the normal variations of technical bleaching. Any slight variation in the molecular weight can be checked by the sensitive measurement of fluidity in cuprammonium hydroxide. The complications which its irregular cross-section raised in kinetic measurements are of no account when dyeing is continued to equilibrium. It was therefore thought desirable to extend the rather scanty data for the absorption of dye by cotton, which were included in the earlier work of Hanson, Neale and Stringfellow,<sup>6</sup> by more

<sup>1</sup> Neale and Stringfellow, *Trans. Faraday Soc.*, 1933, **29**, 1167.

<sup>2</sup> Garvie, Griffiths and Neale, *ibid.*, 1934, **30**, 271.

<sup>3</sup> Hanson and Neale, *ibid.*, 1934, **30**, 386.

<sup>4</sup> Griffiths and Neale, *ibid.*, 1934, **30**, 395.

<sup>5</sup> Neale and Patel, *ibid.*, 1934, **30**, 905.

<sup>6</sup> Hanson, Neale and Stringfellow, *ibid.*, 1935, **31**, 1718.

<sup>7</sup> Neale, *J. Soc. Dyers Col.*, 1936, **52**, 252.

<sup>8</sup> Garvie and Neale, *Trans. Faraday Soc.*, 1938, **34**, 335.

<sup>9</sup> Willis, Warwicker, Standing and Urquhart, *ibid.*, 1945, **41**, 506.

precise and extensive measurements. The technique and results of some such measurements are described in the present paper.

Sky Blue FF (Colour Index No. 518) \* was used as the dye to provide continuity with previous work, and because its colour is very well suited to visual determination, showing its maximum light absorption at about 6,200 Å. It undergoes slow decomposition losing up to one-fifth of its colour intensity on heating overnight with cotton in a dye bath at 90° C., but is not more unstable under such conditions than the majority of direct cotton colours.

### Experimental.

**Materials.**—The cotton used was a standardised bleached Egyptian cotton cloth made by Messrs. Tootal, Broadhurst, Lee & Co. Ltd. Its characteristics were—warp: 50's Sakel 98 ends per inch; weft: 50's Uppers, 100 picks per inch; copper number 0.04; fluidity (0.5 % soln.) 4.4; the low values of copper number and fluidity indicate freedom from depolymerisation by chemical attack.

The dye was obtained from various sources—highly purified samples were supplied by I.C.I. (Dyestuffs) Ltd. and I.G. Farbenindustrie, and a concentrated sample supplied by Sandoz Chemical Co. Ltd. was purified in the laboratory by the usual process of repeated precipitation with sodium acetate and alcohol,

followed by thorough washing with cold alcohol to remove sodium acetate. Boiling or refluxing with the laboratory alcohol caused the dye to be partly reduced to a reddish substance. The various purified samples were compared in the spectrophotometer.

The optical densities of 20 mg./l. solution of the sample showing the highest colour intensity at 6,200 Å. were as shown in Table I.

**Measurement of Dye Concentration.**—The optical density of solutions in water at 6200 Å. was taken as a measure of the dye content of aqueous solutions in subsequent tests, that at 6300 Å. in 25 % aqueous pyridine as a measure of the dye content of "strip solutions" obtained by extraction of dyed cotton. The optical measurements were made visually in a Koenig Martens spectrophotometer, made by Schmidt and Haensch. This instrument has a circular field of view and errors due to inequality of intensity of the two beams of light or to reflection at the cell surface are compensated by an arrangement whereby layers of the solution differing in thickness by 1 cm. are brought alternately into the paths of the two beams. The error of estimation of density is about 0.01, about one-half per cent. of the measured quantity when the concentration is near the optimum of about 20 mg./l.

TABLE I

Wave-length Å.	$\text{Log}_{10} I_0/I.$		
	In water.	In 6.25 % Pyridine.	In 25 % Pyridine.
4600	0.16	0.171	0.174
4800	0.225	0.215	0.206
5000	0.327	0.311	0.300
5200	0.461	0.448	0.420
5400	0.699	0.703	0.650
5600	1.030	0.997	0.938
5800	1.467	1.442	1.374
6000	1.806	1.752	1.685
6200	1.998	1.986	1.918
6300	—	2.058	2.034
6400	1.780	1.922	1.98
6600	1.135	1.187	1.28
6800	0.503	0.40	0.39
7000	0.181	0.11	0.10

\* See Part VIII.

**Conditions of Dyeing.**—The dye solutions were made up by dilution from standard concentrated solutions of dye, A.R. NaCl and distilled water. For the experiments above 25° c. they were contained in Jena G glass tubes of 250 ml. capacity having ground-in water-cooled hollow stoppers to prevent evaporation, immersed in thermostats maintained at the temperature found necessary to give a fixed temperature in the dye solution (e.g. thermostat at 91.3°, dye bath 90° c.). In the hollow stopper was incorporated a long central glass tube through which passed a silver wire connected at its upper end to a solenoid device by means of which the wire was made to rise and fall about 2 cm. about once every second. On the lower end of the wire, immersed in the dye solution, a carefully weighed and "fringed" piece or pieces of cloth were threaded and, in this way, agitated in the dye solution for the time found necessary for the attainment of equilibrium. They were then removed, quickly rinsed in ice-cold water and squeezed between dry filter papers.

TABLE II  
(Showing reproducibility of results.)

<i>(a) Four samples in one bath.</i>				
Temperature of dye bath 90° c.				
NaCl 20 g./l.				
Time (min.) . . . . .	120	180	240	310
Wt. of cotton air-dry (mg.) . . . . .	51.26	50.4	53.2	52.45
ML. pyridine . . . . .	24.94			
Opt. density of strip . . . . .	1.727	1.714	1.830	1.805
Opt. density bath ( $\times 2/5$ ) . . . . .				1.440
End concn. of bath mg./l. . . . .				41.5
% dye on cotton (g./100 g.) . . . . .	0.893	0.888	0.896	0.887
<i>(b) Five separate baths.</i>				
Temperature of baths 70° c.				
NaCl 10 g./l. . . . .				
Time (min.) . . . . .	540			
Air-dry wt. of cotton (mg.) . . . . .	51.1	50.75	51.25	51.5
ML. pyridine . . . . .	35	35	35	35
Opt. density of strip . . . . .	1.540	1.540	1.554	1.572
Opt. density of bath ( $\times 1/5$ ) . . . . .			1.741	1.741
End concn. of bath mg./l. . . . .			92	92
% dye on cotton . . . . .	1.10	1.11	1.11	1.12
				1.11

To allow for decomposition of the dye, the residual dye solutions were, after dilution if necessary, analysed by comparison in the spectrophotometer with the unheated dye bath solution of the same salt content.

It was found that when the dye bath contained 20 g./l. NaCl, as much as 20 % of the blue dye was decomposed on heating at 90° c. for 24 hours, giving rise to a less intensely coloured reddish compound. The decomposition was dependent upon, and increased with the salt content of the bath. The residual dye baths were thereupon all analysed in this way, and their recorded dye contents have been determined by a comparison with a standard solution of the same salt content, at the wave length of maximum absorption. At 25° c., where there was apparently no decomposition, the dye absorptions calculated from the degree of exhaustion of the bath agreed with those determined by stripping the dyed cotton.

**Analysis of the Dyed Cotton.**—The dye was removed by extracting the cotton in a sealed tube at 40° to 60° c. with a volume of 25% aqueous pyridine calculated to give a solution whose optical density would be of the optimum order (1.5 to 2.0). The solution was poured through a sintered glass filter into the spectrophotometer cell, after cracking the sealed tube, and its optical density at 6300 Å. was carefully measured.

Control experiments showed that the shape of the absorption spectrum curve for the stripped dye was the same as that of a pyridine solution of the "pure" solid dye, thus affording some proof of the purity of the latter. From the optical density at 6300 Å. the concentration of dye in the strip solution was calculated by Beer's Law, which was obeyed within less than 1 % over the range 0.01-0.02 g./l. The amount of dye on the cotton was then calculated as weight percentage, grams dye per 100 g. dry cotton. The dye, as originally weighed out, was assumed to retain 2 % of moisture after overnight drying in an air oven at 110° C. and the cotton equilibrium with the atmosphere 6 % of its weight of moisture.

### Results.

In this way the values given in the following tables were obtained; each value is the mean of at least four closely agreeing determinations. A detailed account of two typical experiments is given in Table II.

### Discussion.

The mean values given in Table III are believed to be self-consistent within about one part in a hundred. There is a somewhat larger uncertainty as to their absolute value, on account of the fact that it was impossible to prepare purified samples of the dye showing identical optical properties. The values for absorption and for dye bath concentration have been calculated on the assumption that the optical density of a 20 mg./l. solution in 25 % pyridine is 2.03 at 6300 Å. and in pure water 2.00 at 6200 Å., being somewhat lower in solutions containing salt.

The somewhat lower degree of purity and consequently lower optical density of the dye used by Hanson, Neale and Stringfellow,<sup>6</sup> as well as a temperature error of about 1° due to condensation of vapour on the water-cooled stoppers of the dyeing tubes, not detected in this earlier work, accounts for the fact that the earlier absorption data are consistently higher than those now presented.

The data have been plotted in the forms of graphs (a)  $\log D$  against  $\log c$  at constant salt concentration, and (b) of  $\log D$  against  $\log s$  at constant dye concentration. Good straight lines were thus obtained whose slopes are recorded in Table III.

The theory of Willis, Warwicker, Standing and Urquhart<sup>9</sup> predicts a slope of not more than 0.80 for the  $\log D - \log s$  plot for a tetravalent dye and of not less than 0.2 for the  $\log D - \log c$  plot. The theory of Hanson, Neale and Stringfellow<sup>6</sup> leads to a similar conclusion, i.e. slope  $\log D - \log s \gtrsim 0.80$  approaching 0.80 when  $W$  (the effective water take-up) is assumed small; slope  $\log D - \log c \lesssim 0.20$  approaching 0.20 when  $W$  (the effective water take-up) is assumed small.

In agreement with this, the value of the  $\log D - \log s$  slope ranges between 0.51 and 0.62 and that of the  $\log D - \log c$  slope ranges between 0.19 and 0.33 at 70° and 90° C. At the lower temperatures, however, the latter slope falls to 0.14. As it does not appear that this can be accounted for by either of the quantitative theories, their precise applicability to the present data will not be further considered in this paper.

It is clear from the recent experiments of Neale,<sup>10, 11</sup> Neale and Peters<sup>12</sup> that cellulose carries in aqueous solutions a negative electric charge, which must influence the absorption of dye anions in some way which is not yet fully determined.

**The Heat of Dyeing.**—Although the present data are not ideally suited to the calculation of this quantity, this has been attempted, by the use of the equation

$$\frac{d \log c}{dT} = \frac{Q}{RT^2}.$$

<sup>10</sup> Neale, *Trans. Faraday Soc.*, 1946, 42, 473.

<sup>11</sup> Neale, *ibid.* (in course of publication).

<sup>12</sup> Neale and Peters, *ibid.*, 1946, 42, 478.

TABLE III.—SUMMARY OF ABSORPTION DATA, MOST OF WHICH ARE THE MEANS OF SIX INDEPENDENT MEASUREMENTS IN CLOSE AGREEMENT.

Dye. mg./l. (c).	NaCl. g/l. (s).	Abs. % (D.).	Dye. mg./l. (c).	NaCl. g/l. (s).	Abs. % (D.).
<b>25° C. (Time of dyeing 27 to 37 days.)</b>			<b>70° C. (Time of dyeing 7 to 9 hours.)</b>		
18.0	1	0.470	23.8	2	0.303
16.7	2	0.726	20.9	7.5	0.652
16.9	4	1.12	20.8	10	0.779
12.8	5	1.23	21.4	20	1.15
11.8	6	1.32			
10.2	8	1.52	45.3	1	0.228
			44.5	2	0.363
41	0.5	0.380	43.7	5	0.635
41.5	1	0.567	42.0	7.5	0.810
40.5	2	0.845	42.4	10	0.968
39.6	3	1.10	42.1	15	1.18
38.2	4	1.32	44.3	15	1.18
36.6	6	1.62			
			89.2	2	0.424
86.3	0.5	0.430	87.5	5	0.758
86.5	1	0.623	91.7	5	0.758
90	1.5	0.775	88.1	7.5	0.935
92	2	0.966	92	10	1.11
94	3	1.22	87.5	15	1.40
94	4	1.42			
			176	2	0.505
181	0.5	0.470	174	5	0.867
183	1	0.71	176	7.5	1.11
183	1.5	0.895	177	10	1.315
184	2	1.06	Plot of log <i>D</i> vs. log <i>c</i> gives straight lines of slope 0.19 to 0.25.		
183	3	1.33	Plot of log <i>D</i> vs. log <i>s</i> gives straight lines of slope 0.59 to 0.605.		
			<b>90° C. (Time of dyeing 3 to 20 hours.)</b>		
365	0.125	0.319	41	1	0.141
369	0.25	0.405	41.7	2	0.233
368	0.50	0.567	42	5	0.402
371	1.0	0.822	42	10	0.600
362	2.0	1.15	41.5	20	0.893
			43	20	0.900
Plot of log <i>D</i> vs. log <i>c</i> gives straight lines of slope 0.14 to 0.19.			46	20	0.930
Plot of log <i>D</i> vs. log <i>s</i> gives straight lines of slope 0.51 to 0.60.			50	20	0.970
<b>51.6° C. (Time of dyeing 36 to 48 hours.)</b>			92	1	0.185
20.5	5	0.812	92	2	0.285
20	7.5	1.04	87	5	0.505
20.2	10	1.19	87	10	0.756
			86	20	1.132
44.5	0.5	0.216	183	1	0.234
45	1	0.351	183	2	0.367
44.9	2	0.542	194	5	0.644
42.5	4	0.820	190	10	0.923
44.0	5	0.938	180	20	1.43
43.0	7.5	1.18			
			366	0.5	0.202
64.6	5	0.953	363	1	0.303
			358	2	0.447
			365	5	0.763
			359	10	1.12
Plot of log <i>D</i> vs. log <i>c</i> gives a straight line of slope 0.14.			Plot of log <i>D</i> vs. log <i>c</i> give straight lines of slope 0.27 to 0.33.		
Plot of log <i>D</i> vs. log <i>s</i> gives a straight line of slope 0.62.			Plot of log <i>D</i> vs. log <i>s</i> gives straight lines of slope 0.57 to 0.615.		

The values (Table V) of the dye concentration ( $c$ ) in solutions of fixed salt content ( $s$ ) in equilibrium at the various temperatures with cotton containing a fixed amount of dye ( $D$ ), were obtained by interpolation or extrapolation—(extrapolated values bracketed), from the data of Table III.

TABLE IV

Absorption data at room temperature ( $18^{\circ}\text{C}$ . approx.). Time of dyeing 60 to 90 days. Dye 400 mg./l.

NaCl mg./l.	0	10	20	40	80	160
Absorption %	0.209	0.230	0.254	0.268	0.309	0.402

TABLE V

Temp. $^{\circ}\text{C}$ .			25.	50.6	70.2.	90.
(i) $s = 1.0\text{ g./l.}$	$D = 0.36$	$c\text{ mg./l.}$	(4)	46	180	(520)
(ii) $s = 2.0\text{ g./l.}$	$D = 0.54$	$c\text{ mg./l.}$	(2)	45	230	(676)
(iii) $s = 5\text{ g./l.}$	$D = 0.94$	$c\text{ mg./l.}$	(3.8)	44	266	(76)
(iv) $s = 10\text{ g./l.}$	$D = 1.45$	$c\text{ mg./l.}$	(4.5)	45	250	(930)

The values of  $\log c$  plotted against  $1/T$  should then give a series of straight lines if the activity coefficient of the dye and the heat of absorption are not temperature dependent, and if the device of keeping the dye absorption and salt concentration constant is effective in keeping the fibre potential constant. Actually the series (iv) values give a very good straight line, but the other lines are all slightly curved showing a steeper slope at the lower temperatures. The heats of dyeing calculated from these slopes are as in Table VI.

As would be anticipated from the hypothesis that the effect of salt upon the absorption is merely due to its effect

on the electrostatic forces, the heat of absorption is found to be independent of the salt concentration, within the experimental error, which on account of the necessity for extrapolation in some cases, is magnified in this method of calculating  $Q$  from data not ideally suited for the purpose.

TABLE VI

(i) $s = 1\text{ g./l.}$	$Q = 10.6\text{ kcal. evolved.}$
(ii) $s = 2\text{ g./l.}$	$Q = 19.2\text{ kcal. evolved.}$
(iii) $s = 5\text{ g./l.}$	$Q = 17.8\text{ kcal. evolved.}$
(iv) $s = 10\text{ g./l.}$	$Q = 18.2\text{ kcal. evolved.}$

### Résumé.

Des mesures plus précises de l'adsorption de colorants par la cellulose ont été faites sur du coton naturel avec la Diamin FF.

On indique la technique employée et les résultats obtenus; on compare les pentes des droites:  $\log$  de la concentration du colorant en fonction du  $\log$  de l'adsorption ou du  $\log$  de la concentration en sel neutre, avec celles prévues selon deux théories précédentes.

### Zusammenfassung.

Die existierenden Daten <sup>8</sup> über die Farbstoffabsorption durch Baumwolle sind durch Messungen mit Diaminreinblau FF und natürlicher Baumwollzellulose erweitert worden. Messmethode und Resultate werden angegeben. Die Steigungen der Kurven für die Beziehung zwischen dem Logarithmus der Farbstoffkonzentration einerseits und dem Logarithmus der Absorption und dem Logarithmus der Neutralsalzkonzentration andererseits werden mit den in zwei theoretischen Abhandlungen berechneten verglichen.<sup>9, 9</sup>

College of Technology,  
Manchester, 1.



# THE ABSORPTION OF DYES BY CELLULOSE— PART X.

## THE ABSORPTION OF CATIONIC DYES.

BY S. M. NEALE.

*Received 2nd May, 1946.*

It has been shown by various workers<sup>1-4</sup> that cellulose oxidised under alkaline conditions contains carboxylic acid groups, and that such an "oxycellulose" shows an enhanced absorption of cationic dyes such as Methylene Blue, Malachite Green and Crystal Violet. The absorption of Methylene Blue under standardised conditions has been used as an empirical test<sup>5</sup> for the quantitative characterisation of such acidic "oxycelluloses". It may be presumed that these dyes, which have little or no specific affinity for pure cellulose, are attached by salt linkages, i.e. by electrostatic attraction, to the acid groups in oxycellulose, which dissociate and so produce negatively charged centres which attract the cations of the dye.

The majority of the known dyes which have specific affinity for pure unoxidised cellulose are of the anionic type, their molecules having been made soluble in water by di-, tri-, or tetra-sulphonation. The absorption of some of these anionic dyes by cellulose has been closely studied by several workers.<sup>6-11</sup>

It seems probable that the anions of these dyes are held on to the cellulose by bonds of the resonance type, whose range of action is very short. Their adsorption increases the natural negative electric potential of the fibre and is therefore opposed by the electrostatic forces. It is facilitated by the addition of any electrolyte to the solution, because the ions of this electrolyte serve to reduce the thickness of the ionic atmosphere, and so decrease the negative potential of the fibre.<sup>12, 13</sup> The absorption of such anionic "direct" dyes by cellulose is therefore increased in amount when a neutral electrolyte is added to the bath<sup>11</sup> ("positive salt effect"). The first stages of absorption of any cationic dyes with specific affinity for cellulose should on the other hand, be assisted by the electrostatic forces and decreased by addition of salt ("negative salt effect"), for it is well known, see e.g. <sup>12, 13</sup> that undyed cellulose carries, in water or in dilute salt solutions, a strong negative charge. The existence or otherwise of such a negative salt effect for basic or cationic dyes on cellulose,

<sup>1</sup> Neale and Stringfellow, *Trans. Faraday Soc.*, 1937, **33**, 881.

<sup>2</sup> Schmidt and others, *Ber.*, 1934, **67**, 2037.

<sup>3</sup> Ludtke, *Angew. Chem.*, 1935, **48**, 650.

<sup>4</sup> Hess, *Cellulose Chemie*, 1922, **3**, 61. Henser and Stockigt, *Papier Fabrik*, 1925, **23**, 126.

<sup>5</sup> Clibbens and Geake, *Shirley Inst. Mem.*, 1926, v, 19.

<sup>6</sup> Boulton, Delph, Fothergill and Morton, *J. Text. Inst.*, 1933, **24**, 113P.

<sup>7</sup> Hanson, Neale and Stringfellow, *Trans. Faraday Soc.*, 1935, **31**, 1718.

<sup>8</sup> Neale, *J. Soc. Dyers Col.*, 1936, **52**, 252.

<sup>9</sup> Neale and co-workers, *Trans. Faraday Soc.*, 1933, **29**, 1167; 1934, **30**, 271, 386, 395, 905; 1938, **34**, 335.

<sup>10</sup> Willis, Warwicker, Standing and Urquhart, *ibid.*, 1945, **41**, 506.

<sup>11</sup> Neale and Fishwick, *ibid.*, in course of publication.

<sup>12</sup> Neale, *ibid.*, 1946, **42**, 473.

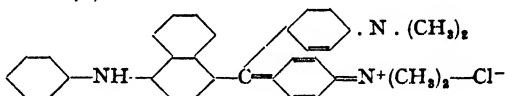
<sup>13</sup> Neale and Peters, *ibid.*, 1946, **42**, 478.

therefore affords a crucial test between those theories of dyeing, which ascribe the salt effect to the reduction of the electrostatic forces between dye ion and fibre, and the rather ill-defined hypothesis of "aggregation of the dyestuff". If the former is the determining factor the cationic dyes should show a negative salt effect, if the latter is predominant both classes of dye should show "positive salt effect" since both classes may be "salted out" of solution by the addition of a sufficient excess of common salt.

Only a very small number of basic dyes with specific affinity for cellulose are known, but the study of two typical ones, which will be described, is clearly in favour of the electrostatic theory of the "salt effect," for their absorption shows the predicted "negative salt sensitivity".

### Experimental.

**Dyes Used.**—The cationic dyes used in this work were Janus Red B. (Colour Index No. 266, mol. wt. 460),\* and Victoria Blue B. (Colour Index No. 729, mol. wt. 648).



Both these dyes have a strong affinity for bleached cotton, dyeing it heavily even from a neutral solution containing no added electrolyte. They were purified as far as possible by repeated precipitation from hot aqueous solution, by adding alcohol and cooling, but they did not crystallise. The dyes, as used, had the absorption spectra shown in Table I.

TABLE I

$\lambda(\mu\mu)$	470	480	500	520	540	560	580	600	620	640	660	680	700
Optical density of 1 cm. layer.													
Janus Red in H <sub>2</sub> O 40 mg./l.	1.23	1.55	2.00	1.84	1.34	0.96	0.53	0.242	0.071	0.060	0.02	0.03	0.02
Janus Red in 25 % Py. 25 mg./l.	0.68	0.92	1.35	1.73	1.69	1.33	0.42	0.090	0.067	0.052	0.03	0.03	0.02
Victoria Blue in H <sub>2</sub> O 20 mg./l.	0.06	0.09	0.17	0.34	0.58	0.90	1.07	1.21	1.27	0.72	0.28	0.09	0.03
Victoria Blue in 25 % Py. 20 mg./l.	0.07	0.10	0.15	0.29	0.48	0.76	1.11	1.44	1.67	1.30	0.57	0.27	0.09

The following absorption values at the peak of each curve were employed in the analysing of the dye baths and of the pyridine strippings: Janus Red 25 mg./l. in 25 % pyridine,  $\log I_0/I$  for 1 cm. layer at 5300 Å. = 1.75. Victoria Blue 20 mg./l. in 25 % pyridine,  $\log I_0/I$  for 1 cm. layer at 6200 Å. = 1.67.

**Conditions of Dyeing.**—The absorption experiments were carried out by the methods described in detail in the earlier papers<sup>9, 11</sup> of this series. The samples of cotton or of cellophane were agitated in the thermostatically controlled solution and the amount of dye absorbed was estimated by spectrophotometric analysis of the extract obtained by "stripping" the dyed material with 25 % aqueous pyridine in a sealed tube at 40-60° C.

\* See Part VIII; *J. Colloid Sci.*, 1946, 1, 371.

## Results.

TABLE II

Dye concn. mg./l.	NaCl g./l.	Per cent. dye on cotton.	Per cent. dye on cellophane.
(a) <i>Janus Red</i> : equilibrium dyeings (20 hours at 70° c.)—salt effect.			
88	0	0.638	2.57
83	1	1.00	3.1
73	2	1.13	4.16
70	5	1.35	—
85	10	0.985*	—
90	20	0.66*	—

(b) *Janus Red*: lighter equilibrium dyeings  
(20 hours at 70° c.)—salt effect.

(pH of baths 5.2-5.9)	0	0.461	2.86
	0.05	0.466	2.86
	0.1	0.481	2.62
	0.2	0.475	2.56
20 mg./l.	0.4	0.51	2.36
	0.8	0.413	1.72

(c) *Victoria Blue*: equilibrium dyeings (20  
hours at 70° c.)—salt effect.

	0	1.78	5.90
20 mg./l.	0.05	1.56	4.00
	0.1	1.50	3.76
	0.2	1.25	2.00
	0.4	0.93	1.99
	0.8	1.37	5.10

\* Dye bath cloudy.

TABLE III

RATE OF DYEING (CELLULOSE DIFFUSION  
CO-EFFICIENT) OF JANUS RED B. IN CELLO-  
PHANE AT 70° C. (Weight of cellophane 2.15  
mg./cm. (air-dry)).

Time (min.).	Per cent. dye on cellulose (dry wt.).
(a) Dye concn. 100 mg./l.; NaCl-zero.	
1	1.97
2	2.76
5	2.99
7.5	3.13
10	3.14
20	3.09
60	3.11

$D_{\infty}$  taken as 3.2 %; diffusion co-efficient  
( $k$ ) =  $53.4 \times 10^{-8}$  cm.<sup>2</sup>/min.

(b) Dye concn. 100 mg./l.; NaCl-1 g./l.

$\frac{1}{2}$	0.74
1	0.86
$1\frac{1}{2}$	1.55
2	1.75
3	2.25
840	4.51

$D_{\infty}$  taken as 4.5 %; diffusion co-efficient  
( $k$ ) =  $9.4 \times 10^{-8}$  cm.<sup>2</sup>/min.

(c) Dye concn. 100 mg./l.; NaCl 2 g./l.

$\frac{1}{2}$	0.56
1	0.97
$1\frac{1}{2}$	1.07
2	1.40
3	1.60
4	2.01
10	2.69
30	4.52
960	6.59

$D_{\infty}$  taken as 6.59 %; diffusion co-efficient  
( $k$ ) =  $2.8 \times 10^{-8}$  cm.<sup>2</sup>/min.

The equilibrium absorption of the two dyes on cotton and on cellophane are plotted against the salt concentration in Fig. 1 and 2 and their

TABLE IV.—RATES OF DYEING. (Cellulose  
diffusion coefficient, see ref. 9) OF JANUS  
RED B (summarised) AND OF VICTORIA  
BLUE IN CELLOPHANE AT 70° C. COMPARED  
WITH SKY BLUE FF AT 101° C.\*

NaCl g./l.	Janus Red.	Vict. Blue.	Sky Blue FF.
(Dye concn. 100 mg./l.).			
0	53.4	36.4	—
1	9.4	28.4	7.5
2	2.8	19.5	11.4

It is not easy to see how this behaviour can be reconciled with what may be called the "aggregation theory" of the salt effect, since both

diffusion coefficients are plotted in Fig. 3. Whereas it has already been shown that the addition of salt increases the absorption, and also the cellulose diffusion coefficient of the anionic direct cotton dyes, it is clearly capable of having exactly the opposite effect upon the basic or cationic dyes, causing both their absorption and their diffusion rates to decrease.

cationic and anionic dyes are coagulated by a sufficient addition of salt. On the other hand it finds a ready explanation in terms of the electric charge on the fibres. For, as Neale and Peters,<sup>12</sup> and many other workers have shown, cellulose carries an "intrinsic" negative charge in water, whilst the potential difference between fibre surface and solution is reduced by addition of a neutral salt, which decreases the thickness of the ionic atmosphere.<sup>13</sup> Consequently, the cationic dyes are absorbed partly by specific short range forces, and partly by long range electrostatic forces both acting in the same sense, so that addition of salt, by reducing the latter, reduces the absorption, except in the more concentrated solution

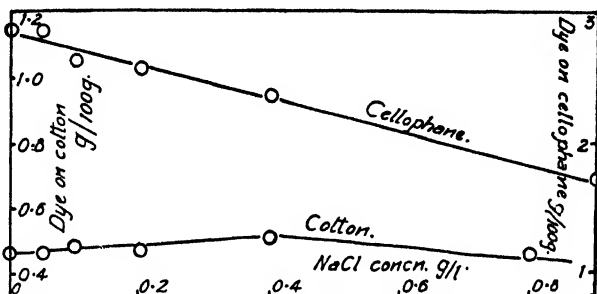


FIG. 1.—Absorption of Janus Red on cellulose.

of Janus Red, which showed a positive salt effect. This is readily explained by the electrostatic theory, for if sufficient cationic dye be absorbed the sign of charge of cellulose is reversed; we then have a positive dye cation absorbed on a positive substrate, the electrostatic forces oppose dyeing, and addition of salt then assists it, as in the usual dyeing of anionic dyes on cellulose.

The behaviour of acid dyes on wool also emphasises the importance of the electrostatic forces. Wool in mineral acid solutions is positively

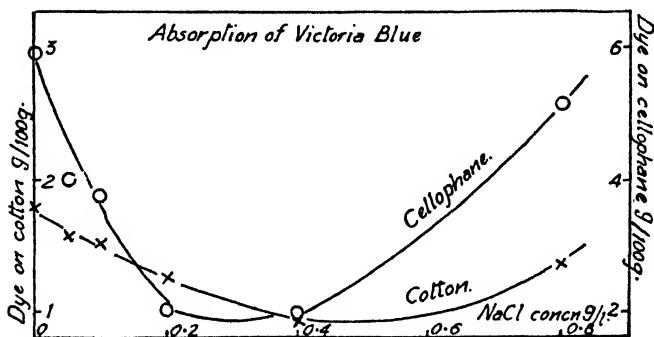


FIG. 2.

charged,<sup>12</sup> and the absorption of the negative dye anions then shows "negative salt effect". Fig. 3 shows that the effect of salt is even more marked in reducing the rate of diffusion, than in reducing the equilibrium absorption. This is to be expected, for the rate of diffusion depends upon the entry of dye ions into undyed cellulose, whereas the absorption at equilibrium is concerned with interchange of ions between solution and a substrate

whose negative charge has been more or less neutralised by adsorption of dye cations.

The absorption curves for Victoria Blue (Fig. 2) show a well marked

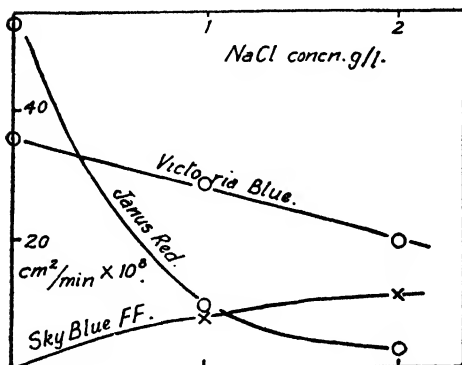


FIG. 3.—Diffusion coefficient of basic and acid dyes in cellophane.

minimum with a steep rise in absorption when the salt concentration exceeds 0.4 g./l. The rise may be due to adsorption of dye in multi-molecular layers, i.e. the adsorption of further dye ions upon centres whose natural negative charge has already been neutralised by the previous adsorption of a cation.

Such a process could be regarded as "aggregation on the fibre", and is plausible for these two dyes, which, at 70° C., are salted out at quite low concentrations of sodium chloride.

The author wishes to thank Mr. C. E. F. Fishwick, who assisted in this work.

### Résumé.

On trouve que la première étape dans l'adsorption de colorants "cationiques"—"Janus Red B" et "Victoria Blue B"—par la cellulose, est diminuée par l'addition de sel neutre; ceci est attribué à la diminution des forces électrostatiques entre la cellulose et l'ion colorant et s'oppose à la théorie "d'agrégation du colorant", qui prédit un effet de sel positif.

### Zusammenfassung.

Es wird gefunden, dass die erste Stufe in der Absorption der Kationenfarbstoffe "Janusrot B" und "Victoriablau B" durch Zellulose durch die Hinzufügung von Neutralsalz verringert wird, was einer Reduktion der elektrostatischen Kräfte zwischen dem Farbstoffion und der Zellulose zugeschrieben wird und nicht mit der "Farbstoffaggregation"-Theorie, die einen positiven Salzeffekt voraussagt, übereinstimmt.

College of Technology,  
Manchester.

## REMARKS ON THE STRUCTURE OF CARBON MONOXIDE.

BY L. H. LONG AND A. D. WALSH.

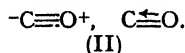
Received 8th April, 1946.

Earlier chemists<sup>1</sup> were content to regard carbon monoxide as an example of a substance containing divalent carbon and consequently to suppose the molecule to be satisfactorily represented by the "double bond" formula

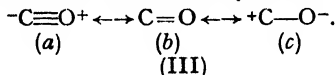


<sup>1</sup> e.g. *J. Amer. Chem. Soc.*, 1904, **26**, 1549.

During the last two decades, however, the formula (I) has been generally abandoned in favour of one of two other representations. In the first of these the molecule is regarded as formed from the ions  $C^-$  and  $O^+$  and consequently to be written in either of the two equivalent "triple bond" formulæ



The "semi-polar" or "co-ordinate" link of (II) offsets the natural polarity of the other bonds, so that the well-known low dipole moment is explained. In the second of the representations that have come to replace (I), the CO molecule is regarded as a resonance hybrid <sup>2</sup> of the forms



The central one of these forms is regarded as non-polar so that the opposite polarities of the first and third forms result in the almost zero dipole of the hybrid. Taken together, (b) and (c) amount to a description of the "natural" polarity of the carbonyl group. It is our purpose to show that neither of the representations (II) or (III) is satisfactory: the double bond structure still remains the best simple diagram for the carbon monoxide molecule. We deal first with the "triple bond" structure (II).

### The "Triple Bond" Structure.

The "triple bond" structure (II) has been suggested on the basis of (1) comparison of the interatomic distances, force constants and energies of the CO bond in aldehydes and in carbon monoxide; <sup>3</sup>

(2) the isoelectronic principle and the similarities of nitrogen and carbon monoxide; <sup>4</sup>

(3) the molecular orbital theory.<sup>5</sup>

As regards CO interatomic distances, force constants and bond energies, one of us has already pointed out <sup>6, 7, 8</sup> that these vary sensitively with the quantitative polarity of the CO bond. The greater the polarity the weaker the bond, i.e. the greater the interatomic distance and the less the force constant and bond energy. It is entirely arbitrary to take the CO bond in aldehydes as a standard and to do so obscures the important relation between polarity and strength of binding. The only satisfactory comparison is that between carbon monoxide and a *non-polar* carbonyl bond. When this is carried out we find that the bond distance, force constant and energy of carbon monoxide are closely similar to those we should expect for a non-polar carbonyl bond. There is thus no argument from these properties for a triple bond in carbon monoxide, but considerable indication of an approximate double bond.

According to the empirical isoelectronic principle, molecules containing the same number of electrons are best represented by essentially similar chemical diagrams. We should therefore expect carbon monoxide to be best represented by a triple bond structure, since the molecule has the same number of electrons as that of nitrogen where there is no doubt of the triple bond. This conclusion is supported by a comparison of the physical properties of carbon monoxide and nitrogen <sup>4</sup>—notably the boiling point, critical constants, interatomic distance, solubility, viscosity, etc.

<sup>3</sup> Pauling, *The Nature of the Chemical Bond* (Cornell, 1939).

<sup>4</sup> Palmer, *Valency* (Cambridge, 1944).

<sup>5</sup> Langmuir, *J. Amer. Chem. Soc.*, 1919, **41**, 1543; Kronig, *Optical Basis of the Theory of Valency* (Cambridge, 1935).

<sup>6</sup> Mulliken, *Rev. Mod. Physics*, 1932, **4**, 1.

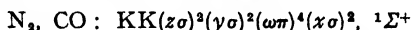
<sup>7</sup> Walsh, *Trans. Faraday Soc.*, 1946, **42**, 56.

<sup>8</sup> Walsh, *ibid.*, 1947, **43**, 60.

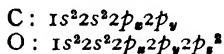
<sup>9</sup> Walsh, *ibid.* (in press).

On closer examination, however, it is apparent that the support is hardly logical, for the properties cited argue rather similar molecular volumes, molecular weights and external force fields than similar internal electronic arrangements. That CO and N<sub>2</sub> should have similar molecular volumes is expected from the positions of the C, N and O atoms in the Periodic Table. That they should have similar external force fields is also expected because at distances large compared with the internuclear distance both molecules can be considered as approximately single nuclei of positive charge 14 screened by 14 electrons. Further, both molecules are without appreciable dipole moments. The similar molecular volume means a similar *b* factor in the van der Waals equation of state. The similar external force field means a similar *a* factor in that equation. Experimentally *a* and *b* are closely similar for the two molecules. The correspondence of all the above properties follows from these similarities. One cannot use the comparison of physical properties as compelling evidence of similar internal structure.\* As for the iso-electronic principle itself, in spite of its usefulness on occasions, it can hardly be that it is always to be applied rigidly: one would expect electronic arrangements to depend not only on the *number* of electrons but also on the nature of the nuclei.

It is usually said that the molecular orbital theory indicates a triple bonded structure for carbon monoxide. Thus Mulliken<sup>5</sup> formulates the electronic structures of both CO and N<sub>2</sub> as



where *zσ*, *ωπ* (doubly degenerate), and *xσ* represent 4 bonding orbitals and *yσ* an anti-bonding orbital, so that the net structure is roughly a triple bond. It is quite possible, however, to give a molecular orbital description of the carbon monoxide molecule that amounts to an approximate *double* bond. Let us imagine † the two atoms brought together without allowing the electrons of one atom to interact with those of the other. The interaction may then gradually be allowed to take place, forming molecular orbitals out of the atomic ones. We start with



the carbon atom being in the state in which it is produced on dissociation of CO, viz. the <sup>3</sup>P and not the <sup>5</sup>S state. Taking the *x* axis along the CO line and starting to form molecular orbitals, the central 1s and 2s electrons of the two atoms will remain nearly unaffected,‡ while the 2*p<sub>x</sub>* electron of carbon interacts with the 2*p<sub>x</sub>* electron of oxygen to form a basic single

bond of type 2*pσ*. The basic single bond will be polar with sign C<sup>+</sup>O<sup>-</sup>, but as shown later, interaction of the subsequent electrons will probably reduce its polarity. The carbon 2*p<sub>y</sub>* and oxygen 2*p<sub>y</sub>* electrons may now interact to form a π bond. Two 2*p<sub>z</sub>* oxygen electrons remain. These will show a small drift towards the carbon 2*p<sub>z</sub>* atomic orbital by occupying a molecular orbital of form *aψ*(C : 2*p<sub>z</sub>*) + *bψ*(O : 2*p<sub>z</sub>*). The co-ordinate link formula (II) implies that *a* is of the same order of magnitude as *b*. There is nothing in the molecular orbital theory, however, to indicate this: in fact, there is direct evidence, referred to later, that the ratio *a/b* is small, indicating that the 2*p<sub>z</sub>* electrons are pulled only a little towards

\* Similarly, the close similarity in physical properties of CO<sub>2</sub> and N<sub>2</sub>O is not necessarily evidence of a similar internal electronic arrangement in the two molecules.

† We are greatly indebted for this description to Dr. C. A. Coulson.

‡ The four 2s electrons can be regarded as filling a bonding and an anti-bonding pair of orbitals which more or less cancel out as regards bonding function. It is also true that interchange of the *y* and *z* axes may give rise to a species of resonance. This will mean a stabilisation of the molecule, but will not alter the electron densities as described here.

the carbon nucleus and remain effectively on the oxygen atom. It is therefore not justifiable to speak of this third occupied orbital as forming a bond: the total carbon monoxide bond, according to this description, is still approximately double. This is not to say, of course, that on the approach of a reagent to the carbon monoxide molecule, or under other conditions, there may not be appreciable change in the ratio  $a/b$ .

### The Resonance Description.

Turning now to the resonance description (III) of the carbon monoxide molecule, we note that, since the first and third forms are supposed to contribute almost equally to the hybrid (so that the dipole moment may be close to zero), the description amounts in essence to a doubly bonded structure that is nearly non-polar. Apart from its cumbersome nature, however, the description includes the resonance (III)  $b \longleftrightarrow c$  and, as already shown,<sup>7</sup> this is not a desirable way of describing the polarity of the carbonyl bond. It implies that increasing polarity would be associated with increasing strength of bonding, which is in direct contradiction to the facts. It has been further pointed out<sup>7</sup> that the reason for the unsatisfactory nature of the resonance description of the bond dipole moment is doubtless the difference between the lengths of the purely homopolar and ionic links in  $b$  and  $c$ , and that the resonance concept is not here applicable.

In addition, there is no experimental indication of a resonance energy (such as (III) implies) in the carbon monoxide molecule relative to a non-polar carbonyl group: the stretching force constant and the inter-atomic distance are just about what we should expect for such a non-polar doubly bonded, carbon-oxygen group. Further, accepting Herzberg's value for  $D(\text{CO})^9$  and a value of 190 kcal. for the heat of atomisation of carbon into the  $^3\text{S}$  state,<sup>10</sup> the bond energy is also just about that to be expected for a non-polar bond.

### The "Double Bond" Structure.

Having shown how many of the arguments put forward in favour of the triple bond structure are not valid, we wish now to cite what evidence exists in favour of the double bond structure (I).

In the first place this evidence comes from a closer study of the comparison between CO and  $\text{N}_2$ . We have seen that the physical similarity between the two substances is no argument for a similarity of internal

TABLE I

	$\text{N}_2$	$\text{N}_2^+$	CO	$(\text{CO})^+$
Vibrational frequency ( $\text{cm}^{-1}$ ) .	2360	2207	2168	2211
Interatomic distance (A.) .	1.095	1.117	1.128	1.115

electron arrangement. More detailed examination in fact reveals a very significant way in which the two molecules differ. When the  $\text{N}_2$  molecule is ionised to give  $\text{N}_2^+$ , the bond between the atoms weakens, as shown by the vibrational frequency and by the interatomic distance. When, however, the CO molecule is ionised, to give  $(\text{CO})^+$ , the interatomic binding *increases*, as shown by the vibrational frequency and interatomic distance.\* Table I shows the relevant values of these quantities, taken from the

\*  $r(\text{N}_2)$  and  $r(\text{CO})$  are not actually very close: but the increase of the former and the decrease of the latter on ionisation make  $r(\text{N}_2)^+$  and  $r(\text{CO})^+$  almost identical.

<sup>9</sup> Herzberg, *Molecular Spectra and Molecular Structure* (Prentice Hall, 1939); *Infra-red and Raman Spectra* (Van Nostrand, 1945).

<sup>10</sup> Long and Norrish, *Proc. Roy. Soc. A*, 1946, **187**, 337.



compilation by Herzberg.<sup>9</sup> This striking difference between the  $N_2$  and CO molecules is understandable if, unlike  $N_2$ , CO is taken to contain a double bond and to form, on ionisation, something of a triple bond: but it is not so easy to explain on any other basis. Mulliken's formulation of the CO and  $N_2$  structures expects the lowest ionisation potential to correspond to the removal of a similar bonding electron in each. The weakening of the N—N bond in  $N_2^+$  is understandable as due to the removal of such a bonding electron. If CO has a double bond structure, then we expect the first ionisation potential to result in the removal of one of the oxygen almost non-bonding  $2p_z$  electrons just as in the carbonyl compounds.<sup>11</sup> We shall give below strong evidence in support of this interpretation of the CO ionisation potential. Here we may note that further evidence is provided by the ability of the interpretation to explain the strengthening of the carbon-oxygen bond on ionisation of the molecule. Removal of a non-bonding oxygen electron will result in the odd electron interacting with the lone pair of electrons on the carbon atom to exercise a ("three electron") bonding function.\* On ionisation of  $N_2$ , a triple bond weakens but on ionisation of CO a double bond strengthens, so that the remarkable similarity of  $N_2^+$  and  $(CO)^+$  (see Table I) receives some explanation.

TABLE II.—TERM VALUES OF RYDBERG SERIES

CO <sup>12</sup> .	CO <sub>2</sub> <sup>12</sup> .	HCHO <sup>14</sup> .	CH <sub>3</sub> CHO <sup>14</sup> .	Acrolein. <sup>15</sup> .
—	22450	23440	22335	20931
—	10650	10040	10147	10021
6100	6200	5960	5912	5858
4150	4100	3900	3884	3876
2770	obscured	2760	2742	2744
2090	2090	2060	2025	2063
—	1610	1590	1569	1586

In the second place, comparison of the absorption Rydberg Series for CO,<sup>12</sup> CO<sub>2</sub>,<sup>13</sup> and carbonyl molecules generally,<sup>14, 15, 16</sup> indicates a very close similarity between the term values in series found for all these molecules (Table II). In the case of CO and CO<sub>2</sub> for example, the similarity can be seen in the Rydberg series formulæ given respectively by Anand<sup>12</sup> and by Price and Simpson:<sup>13</sup>

$$CO: \nu_0^n = 117,500 - \frac{R}{(n + 0.27)^2}$$

$$CO_2: \nu_0^n = 111,250 - \frac{R}{(n + 0.21)^2}$$

We regard this close correspondence as strong evidence that the electron being excited has the same characteristics in both molecules. Since in CO<sub>2</sub> it is known<sup>13</sup> that the electron concerned is one of the oxygen non-bonding  $2p\pi$  electrons, it follows that the CO molecule must contain a similar lone pair (that is, the ratio  $a/b$  in the molecular orbital  $a\psi(C: 2p_z) + b\psi(O: 2p_z)$  must be small), and therefore that the CO molecule has the approximately doubly bonded structure (I). If it had the triply-bonded

\* It is relevant to note that the process  $CO \rightarrow (CO)^+$  contrasts with that of  $CO_2 \rightarrow (CO_2)^+$ . In the latter case the CO distance lengthens.<sup>9</sup>

<sup>11</sup> See Mulliken, *J. Chem. Physics*, 1935, 3, 564.

<sup>12</sup> Anand, *Science and Culture*, 1942, 8, 278.

<sup>13</sup> Price and Simpson, *Proc. Roy. Soc., A*, 1939, 169, 501.

<sup>14</sup> Price, *J. Chem. Physics*, 1935, 3, 256.

<sup>15</sup> Walsh, *Trans. Faraday Soc.*, 1945, 41, 498.

<sup>16</sup> Walsh, *Proc. Roy. Soc. A*, 1946, 185, 176.

structure (II), where the originally  $2p\pi$  oxygen electrons possessing the lowest ionisation potential had been drawn into the bond, we should not expect similarity of term values between the Rydberg series found for these electrons in  $\text{CO}_2$  and  $\text{CO}$ .

The ionisation potential of  $\text{CO}$  (14.55 v.) is in good agreement with what we should expect (if  $\text{CO}$  is  $\text{C}=\text{O}$ ) from the low dipole moment and Mulliken's estimate<sup>11</sup> (14.73 v.) for the non-bonding  $\text{O} : 2p$ , ionisation potential of a non-polar carbonyl group.

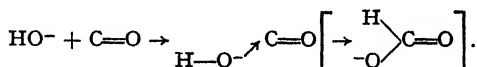
We therefore consider that the balance of the evidence is in favour of the structure (I) rather than (II). It remains to anticipate objections to (I) and to suggest a way in which the diagram might be made a more precise representation of the molecule.

The fact that carbon monoxide is so stable, whereas substances such as  $\text{CH}_2$  or  $\text{CCl}_2$  cannot be isolated, has been put forward as evidence against carbon monoxide containing divalent carbon. We do not consider this argument sound, since, apart from the evidence that the bonds in (say)  $\text{CH}_2$  may be strongly polar, and this together with the strain resulting from the repulsion of the similarly charged H atoms may make  $\text{CH}_2$  much more reactive than the almost non-polar molecule  $\text{CO}$ , energetic considerations would lead us to expect precisely the differences in behaviour between  $\text{CO}$  and  $\text{CH}_2$  which are in fact observed. In reactions involving either of these two substances, as, for example, polymerisation, energy is absorbed in raising the carbon atom from the divalent to the tetra-valent state, and this energy must be offset against that liberated by the change in the total energy of linkage before and after the reaction.

In the case of carbon monoxide, energy will be absorbed by the change in strength of the  $\text{C}=\text{O}$  link since this link is invariably weaker when the carbon is in the tetravalent state. It has been demonstrated recently by Long and Norrish<sup>10</sup> that there is strong chemical evidence for regarding the excitation energy of the  $^4\text{S}$  state of carbon (the lowest atomic state corresponding to tetravalence) to be about 65 kcal., and that the mean bond energy in  $\text{CO}_2$  is some 10 kcal. less than in  $\text{CO}$ , it being still weaker in other carbonyl compounds.\* A possible reason is, therefore, apparent why  $\text{CO}$  does not polymerise to  $\text{O}=\text{C}=\text{C}=\text{O}$ . To raise the  $\text{CO}$  molecule to a radical with two free valencies would require an expected excitation energy of more than 75 kcal. and the energy required to excite two molecules in this manner is greater than the energy normally associated with a  $\text{C}=\text{C}$  bond. That all attempts to prepare  $\text{C}_4\text{O}_4$  have failed may be explained on the basis that it is thermodynamically unstable with respect to carbon monoxide.

On the other hand, we would expect the energy of the  $\text{C}-\text{H}$  bonds in the  $\text{CH}_2$  molecule to be roughly the same as that in the  $\text{CH}$  radical where the carbon is also in the divalent state, that is, about 80 kcal. The  $\text{C}-\text{H}$  bonds in ethylene are known to be about 25 kcal. stronger than this figure,<sup>7</sup> so that, in contrast to  $\text{CO}$ , energy is liberated by the bonds when  $\text{CH}_2$  is promoted to a radical structure. The net energy required by this promotion is in consequence only 15 kcal., and the polymerisation to ethylene a very exothermic process.

A further problem of the reactivity of  $\text{CO}$  lies in the common statement that the molecule has no electron acceptor properties such as would be expected for structure (I) in which the carbon has an incomplete octet. We do not think this statement is completely in accordance with fact. Thus  $\text{CO}$  reacts with alkalis to give formate ions, a reaction which is presumably to be formulated



\* In carbon suboxide, which resembles  $\text{O}=\text{C}=\text{C}=\text{O}$  in structure, the  $\text{CO}$  bond strength is probably some 20 kcal. weaker than in  $\text{CO}^*$ .

It is true that this reaction occurs only under conditions which imply that the acceptor properties of carbon in CO are not large, but this is to be expected since, if a co-ordinate link from the O to the C hardly occurs in CO itself, appreciable acceptor properties will only be exhibited to the extent that the donor is stronger than the O atom in CO.

The electron donor properties which are usually assumed for CO (as in the formation of  $\text{BH}_3 \cdot \text{CO}$ ) presumably mean that any structure written for CO must contain a lone pair situated on the C atom. The metallic carbonyls have often been cited as further examples of such donor properties. While this may in part be true, there is evidence that some of the electrons of the metal atom are employed in the bonds formed. The reason for this can be regarded as the existence of acceptor properties in the carbon atom of CO, as well as in the metal atom. Pauling<sup>8</sup> has already pointed out objections to the view in which, for example, the NiC bonds in  $\text{Ni(CO)}_4$  are regarded solely as co-ordinate links from the carbon atoms to the nickel atom. In the first place, the Ni atom in  $\text{Ni(CO)}_4$  shows in its reactions an electropositive and not an electronegative character. Four co-ordinate links to the nickel atom would give it a strong negative charge. In the second place, the NiC bond is so short as to necessitate the supposition of a stronger form of binding. Pauling supposes a considerable amount of double bond character in the NiC binding. The postulation of resonance structures other than the double bond form may in this case be unnecessary. The structure

$\text{Ni}=\text{C}=\text{O}$  makes it clear why the Ni, C and O atoms are collinear.

Furthermore, it will have a resemblance to ketene. In ketene, one of us<sup>9</sup> has reasoned (a) the presence of the oxygen atom results in the  $\text{C}=\text{C}$  bond being polar with consequent reduction in strength, and (b) the carbonyl C atom being part of a  $\text{C}=\text{C}$  bond means that the  $\text{C}=\text{O}$  group has a much reduced polarity relative to that in formaldehyde, and approaches in bond strength that in carbon dioxide. We therefore expect the

$\text{Ni}=\text{C}=\text{O}$  structure to show (i) a definite Ni C bond polarity, and

therefore a weakening relative to a non-polar NiC bond, (ii) a  $\text{C}=\text{O}$  bond of low polarity and therefore high strength. The latter fact explains at once why the CO groups in  $\text{Ni(CO)}_4$  resemble the carbon monoxide molecule so closely in their properties.<sup>17</sup> The polarity of the NiC bond will be small because there are four CO groups competing for the one Ni atom. Hence the CO bonds will probably be less polar than in ketene. In accord with this, the CO length in  $\text{Ni(CO)}_4$  is 1.15 Å.,<sup>18</sup> that is, slightly less than that found for ketene (1.17 Å.).<sup>19</sup> To grant that the NiC bond in  $\text{Ni(CO)}_4$  is to be represented  $\text{Ni}=\text{C}$ , means that the CO bond in  $\text{Ni(CO)}_4$  must be represented  $\text{C}=\text{O}$ ; and since the CO of  $\text{Ni(CO)}_4$  closely resembles in properties the CO molecule itself, this in turn means that CO must be represented approximately as  $\text{C}=\text{O}$ . We have already implied a similar argument from the similarity in bond properties of CO and  $\text{CO}_2$ .

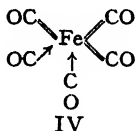
Related compounds also supply evidence that metals employ their electrons in bond formation with the carbon of CO groups. The formulæ for the nitrosyl carbonyls are such that we must suppose each N atom contributes three electrons to the metal-N bond, the metal atom presumably contributing a fourth electron to each such bond. The formulæ  $\text{Ni(CO)}_4$  and  $\text{Co(CO)}_3\text{NO}$  suggest that the metal uses all its outer (3d, 4s and 4p) electrons but two in bond formation. The production of  $\text{Fe(CO)}_5(\text{NH}_3)_2$  from  $\text{Fe(CO)}_5$  indicates that the same is true of the iron

<sup>17</sup> Anderson, *Nature*, 1932, 130, 1002.

<sup>18</sup> Brockway and Cross, *J. Chem. Physics*, 1935, 3, 828.

<sup>19</sup> Beach and Stevenson, *ibid.*, 1938, 6, 75.

atom in these compounds, the latter probably being a resonance hybrid of structures such as IV



The very low dipole moment of CO presents a problem in all formulations of the molecule. It may be that the oxygen  $2p_z$  electrons, situated, as they will be, somewhat on the C side of the O atom, screen the oxygen nucleus from the bond, that is, reduce the effective electronegativity of the O atom and result in the  $2p\sigma$  and  $2p\pi$  bonds being nearly non-polar. Such an explanation avoids any necessity to suppose the  $2p_z$  electrons move so far into the bond that they set up a moment equal and opposite to a large "natural" polarity in the first two bonds. However, other factors probably play a part, some of these possibly being related to the surprising fact that the double bond strength in CO and  $\text{CO}_2$  is greater than twice the single C—O bond strength in ethers and alcohols ( $\sim 87$  kcal./mol.). In part this may be due to the C—O bonds in ethers and alcohols being weakened by polarity, but the double bonds in  $\text{CO}_2$  and CO still seem rather stronger than one would expect on the basis of a  $\sigma$  bond (closely similar in strength to that of  $\text{>C—O—}$ ) plus a  $\pi$  bond. With C=C bonds, the  $\pi$  bond is weaker than the  $\sigma$  bond.<sup>20</sup> An explanation may possibly be forthcoming in terms of the important effects of orbital hybridisation on bond strength. It is certainly remarkable that CO should have properties so closely similar to those expected for the non-polar extreme of the carbonyl series, if in the latter the carbon valency basis is  $p +$  hybridised  $sp^3$  (as in ethylene), but in the former is  $p + p$ .\*

According to Samuel,<sup>21</sup> the increase of C—O bond dipole on passing from  $\text{:C=O}$  to  $\text{>C=O}$  is understandable in terms of the replacement of a lone pair by more distant (shared) electrons with consequent reduction of screening effect. But this would probably result in a dipole CO in  $\delta-\delta+$   $\text{>C=O}$  relative to  $\text{:C=O}$ , that is, the reverse of that observed. We are tentatively inclined to attribute the dipole increase to the fact that in  $\text{>C=O}$  there is no longer an available carbon  $2p_z$  atomic orbital. In CO, as we have already indicated, this atomic orbital results in the O :  $2p_z$  electrons occupying a molecular orbital on the carbon side of the O atom. In  $\text{>CO}$ , this molecular orbital must shift back towards the side of the O atom away from the C: the electronegativity of the O atom on the C side therefore increases, and polarity C  $\delta+\delta-$  O results.

The difficulty of the representation (I) for the CO molecule is that it does not distinguish sufficiently between the carbon-oxygen double bond found in CO and that found in, say, the aldehydes. The carbon-oxygen bonds of CO,  $\text{CO}_2$ , aldehydes, ketones and urea have markedly different properties, but yet they are all represented by the single chemical bond diagram  $\text{C=O}$ . The suggestion of Lowry<sup>22</sup> that the aldehydes and ketones should be

written  $\begin{array}{c} \text{R}_1 \\ \diagup \\ \text{C}^+ \text{—O}^- \\ \diagdown \\ \text{R}_2 \end{array}$  rather than  $\begin{array}{c} \text{R}_1 \\ \diagup \\ \text{C}=\text{O} \\ \diagdown \\ \text{R}_2 \end{array}$ ; and the attempt at a resonance

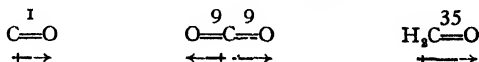
\* See note added in proof.

<sup>20</sup> Walsh, *Trans. Faraday Soc.*, 1946, **42**, 779.

<sup>21</sup> Samuel, *J. Chem. Physics*, 1944, **12**, 193.

<sup>22</sup> Lowry, *J. Chem. Soc.*, 1932, 822.

formulation, have indeed arisen from dissatisfaction with a single bond diagram being made to do service for all the various carbonyl compounds. Since, however, we have shown<sup>8</sup> that the variation in properties is correlated with a variation in degree of polarity, the simplest solution of the problem of representation would seem to retain the diagram  $C=O$  but to write alongside the bond a figure expressing the quantitative polarity. We have indicated<sup>8</sup> a definition and methods of evaluating the “% polarity” in carbonyl bonds. We suggest therefore that the  $CO$ ,  $CO_2$ , and  $HCHO$  molecules should be written respectively



where the figures 1,\* 9 and 35 represent percentage polarities and the arrows give the polarity directions.

In another sense also the argument of this paper is fundamentally concerned with a language difficulty. Just as the diagram  $\text{>C=O}$  cannot do duty *with precision* for such diverse molecules as  $CO$ ,  $CO_2$ ,  $HCHO$ , so the symbol  $\longleftrightarrow$  or  $\overset{+}{-}$  cannot be expected to do duty with precision for all co-ordinate links. In  $CO$  the bond that has been so often represented as a co-ordinate link is hardly a bond at all, but yet we think that the electrons that might compose it do lie somewhat on the carbon side of the oxygen atom. The change we propose in  $CO$  representation may therefore be described as a change from a full co-ordinate link to an “incipient co-ordinate link.”

We wish to express our indebtedness to Dr. C. A. Coulson for kindly criticism and for permission to use notes contributed by him.

### Summary.

It is shown that arguments for a “triple bond” structure of carbon monoxide are not valid. An alternative resonance description is criticised. Evidence mainly from (a) the dependence of carbonyl properties on bond polarity, (b) Rydberg series, (c) comparison of the processes  $CO \rightarrow (CO)^+$  and  $N_2 \rightarrow N_2^+$  is then given in favour of a “double bond” structure for  $CO$ . Some objections are briefly discussed and a simple way of improving the representation of carbonyl compounds suggested.

### Résumé.

On montre que les arguments en faveur d'une structure à “triple liaison” pour l'oxyde de carbone ne sont pas valables. On critique aussi une autre description possible: celle d'un hybride de résonance. Au contraire, on apporte, en faveur de la structure à “double liaison” pour  $CO$ , des preuves principalement puisées dans (1) la relation entre les propriétés du carbonyle et la polarité de liaison, (2) les séries de Rydberg, (3) la comparaison des processus  $CO \rightarrow (CO)^+$  et  $N_2 \rightarrow N_2^+$ . On discute brièvement quelques objections et on suggère une manière simple d'améliorer la représentation des composés du carbonyle.

### Zusammenfassung.

Es wird gezeigt, dass die Argumente, auf denen die dreifache Bindung in Kohlenmonoxyd beruht, nicht zulässig sind. Eine alternative Resonanzformulierung wird kritisiert. Hingegen werden Gründe für eine Zweifach-

\* Some discussion has taken place as to the reality of the very small dipole moment of  $CO$ . Ionisation data<sup>8</sup> indicate quite definitely that  $CO$  has a dipole moment of sign  $\overset{+}{-}CO$ , albeit a very small one.

bindungsformel für CO angegeben; insbesondere können diese in (a) der Abhängigkeit der Karbonyleigenschaften von der Polarität der Bindung, (b) Rydbergserien und (c) einem Vergleich der Prozesse  $\text{CO} \rightarrow \text{CO}^+$  und  $\text{N}_2 \rightarrow \text{N}_2^+$  gefunden werden. Einige Einwände dazu werden kurz erörtert und es wird eine einfache Verbesserung in der Formulierung von Karbonylverbindungen vorgeschlagen.

*Note added in proof.* If the carbon orbital involved in the  $\sigma$  bond of the CO molecule has considerable  $s$  character through hybridization with the orbital occupied by the unshared electron pair on the C atom, we can then explain (a) the continuity of carbon monoxide with other carbonyl molecules, (b) the fact that the bond energy is more than twice as great as for a  $\sigma$  bond from  $sp^3$  C to O (since bond strength increases with electronegativity, and C valency electronegativity increases with  $s$  character,<sup>23</sup> and (c) *a fortiori*, the resemblance to the CO group in  $\text{Ni(CO)}_4$  (for the C atom in carbon monoxide is then nearer the acetylenic state of the C atoms in  $\text{Ni(CO)}_4$ ). This would also help to explain the low dipole moment, since the C atom would then have a greater electronegativity towards the O atom. The "driving force" for this hybridization can be regarded as the resulting reduction of polarity with consequent increase of bond strength. The same "driving force" may operate in  $\text{CH}_2$ . This would make the CH bonds in  $\text{CH}_2$  appreciably stronger than 80 kcal., but would probably not upset the argument that the process  $2\text{CH}_2 \rightarrow \text{C}_2\text{H}_4$  is exothermic in contrast to the process  $2\text{CO} \rightarrow \text{C}_2\text{O}_2$ .

<sup>23</sup> Walsh, *J. Chem. Soc.* (in press).

Laboratory of Physical Chemistry,  
Cambridge.

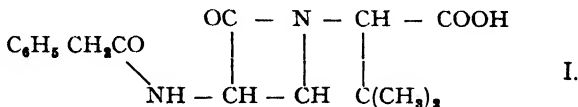
## INACTIVATION OF PENICILLIN G BY ACIDS— A REACTION-KINETIC INVESTIGATION.

BY ROLF BRODERSEN.

Received 29th May, 1946.

### Theory.

According to investigations carried out by the Committee on Medical Research (Washington) and the Medical Research Council (London),<sup>1</sup> and to subsequent reports from Chain, penicillin G (in U.S.A. named penicillin II) as a free acid must be supposed to have the constitution shown in I.



This formula we shall term HPn.

In neutral solution the carboxyl group gives up a hydrogen ion, forming the negatively charged penicillin ion ( $\text{Pn}^-$ ), the form in which penicillin is found at neutral reaction.

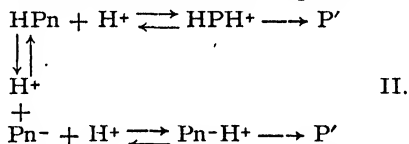
The acid dissociation constant of the carboxyl group is stated to be  $10^{-2.6}$ . This is a strikingly high value for a carboxyl group, when no strong, electronegative substituents are found in the molecule. It appears, however, from the following statements that penicillin actually has an acid group of a strength corresponding to this value.

<sup>1</sup> Committee on Medical Research and the Medical Research Council, *Nature*, 1945, 156, 766.

The tertiary nitrogen atom in the ring can presumably combine with a hydrogen ion in acid solution; the basic properties must, however, be very weak, as in the case of other amides. This accords with the fact that no basic group can be demonstrated in the penicillin molecule by electrometric titration. If the uncharged penicillin molecule combines with a hydrogen ion we get the positive ion  $\text{HPnH}^+$ , while the negative penicillin ion when combining with a hydrogen ion at this tertiary nitrogen atom becomes the amphi-ion  $\text{Pn-H}^+$ .

The nitrogen atom in the lateral chain may also give rise to protolysis. This amide group must even be supposed to have both acidic and basic properties. Since, however, the degree of dissociation it produces must in any event be very small, and since, unlike the ring nitrogen atom, it has no effect on the rate of the process of inactivation, it will be left out of account in this paper. In other words we must provide an equilibrium between four species of molecules in acid and neutral penicillin solutions:  $\text{Pn}^-$ ,  $\text{HPn}$ ,  $\text{Pn-H}^+$ , and  $\text{HPnH}^+$ .

$\text{Pn}^-$  is relatively stable, as appears from the fact that penicillin solutions are fairly stable at neutral reaction. As the penicillin is decomposed in acid media, at least one of the other molecular species must be labile. The difference between  $\text{Pn}^-$  and the other forms is partly the hydrogen ion in the carboxyl group and partly the hydrogen ion combined with the tertiary nitrogen atom. The lability must depend on one or both of these differences. Since the inactivation is due to opening of the four-membered ring it seems reasonable to presume that the lability is due to the presence of the hydrogen ion combined with the tertiary nitrogen atom, whereas it seems less likely that the state of dissociation of the carboxyl group should be of any great importance for the stability or lability of the molecule. The state of the carboxyl group may, on the other hand, very well influence to some extent the rate of the inactivation. We therefore take the forms  $\text{Pn}^-$  and  $\text{HPn}$  to be stable and the ions  $\text{Pn-H}^+$  and  $\text{HPnH}^+$  to be labile. This means that we presume the mechanism shown in II for the inactivation of penicillin by acids, where



$\text{P}'$  is an inactive decomposition product which may possibly, through successive reactions, be transformed into other inactive substances. The reactions indicated by a single arrow are taken to be irreversible and rate-determining, whereas the equilibrium reactions, which are purely protolytic processes, must be supposed to proceed at rates which are very high in comparison with those of the irreversible processes. The following calculation can be made from this hypothesis as to the rate of the inactivation.

If  $h^+$  is the rate of decomposition of the positive ion and  $h_{\pm}$  that of the amphi-ion, and  $c_+$  and  $c_{\pm}$  the concentrations of these ions, we obtain

$$h_+ = k_+ \cdot c_+; \quad h_{\pm} = k_{\pm} \cdot c_{\pm}; \quad (1)$$

where  $k_+$  and  $k_{\pm}$  indicate the velocity constants of the two processes. The total rate,  $h$ , of the inactivation equals the sum of these two rates:

$$h = h_+ + h_{\pm} = k_+ c_+ + k_{\pm} c_{\pm}. \quad (2)$$

At constant concentrations of hydrogen ion and salts  $c_+$  and  $c_{\pm}$  are proportional to the total penicillin concentration. Accordingly, the total rate is proportional to the total penicillin concentration,  $c$ :

$$h = k \cdot c. \quad (3)$$

This means that, according to this hypothesis, the inactivation must proceed as a first-order reaction with a velocity constant,  $k$ , which depends

on the concentrations of hydrogen ion and salts. The relation between the rate of decomposition and the hydrogen ion concentration at a constant salt concentration can be deduced in the following manner.

If  $K_+$  and  $K_{\pm}$  indicate the acid dissociation constants for the positive ion and the amphoteric ion, and  $K_0$  the dissociation constant for the carboxyl group, while  $c_0$  and  $c_-$  indicate the concentrations of the uncharged acid and the negative penicillin ion, respectively, and  $c_{H^+}$  the hydrogen ion concentration, we obtain

$$c_{H^+} \cdot c_0 / c_+ = K_+; \quad c_{H^+} \cdot c_- / c_{\pm} = K_{\pm}; \quad c_{H^+} \cdot c_- / c_0 = K_0; \quad (4)$$

$$c = c_0 + c_- + c_+ + c_{\pm}. \quad (5)$$

Since  $c_+$  and  $c_{\pm}$  are very small in comparison with  $c$ , if the hydrogen ion concentrations are not extremely high, as the tertiary nitrogen atom has only weakly basic properties, we can with good approximation put

$$c = c_0 + c_-. \quad (6)$$

$c_0$  and  $c_-$  are eliminated from eqn. (4) and (6), and  $c_+$  and  $c_{\pm}$  expressed by means of the other symbols.

$$c_+ = \frac{c}{K_+(K_0 + c_{H^+})} \cdot (c_{H^+})^2 \quad (7)$$

$$c_{\pm} = \frac{K_0 \cdot c}{K_{\pm}(K_0 + c_{H^+})} \cdot c_{H^+} \quad (8)$$

These two expressions give together with eqn. (2) and (3)

$$k = \left( \frac{k_+}{K_+} \cdot c_{H^+} + \frac{k_{\pm}}{K_{\pm}} \cdot K_0 \right) \frac{c_{H^+}}{K_0 + c_{H^+}} \quad (9)$$

If  $c_{H^+}$  is small as compared with  $K_0$  we obtain, assuming that  $\frac{k_+}{K_+}$  and  $\frac{k_{\pm}}{K_{\pm}}$  are of the same order of magnitude,

$$k = \frac{k_{\pm}}{K_{\pm}} \cdot c_{H^+} \text{ for } c_{H^+} \ll K_0. \quad (10)$$

If, on the other hand,  $c_{H^+}$  is high as compared with  $K_0$  we get

$$k = \frac{k_+}{K_+} \cdot c_{H^+} \text{ for } c_{H^+} \gg K_0. \quad (11)$$

Thus hydrogen ion concentrations which are very low and very high give a linear relation between  $k$  and  $c_{H^+}$ , whereas hydrogen ion concentrations of the same order of magnitude as  $K_0$  give a curvilinear relation.

### Experimental.

The penicillin used was an American commercial preparation (Abott) of the sodium salt of penicillin G. The buffers used were mixtures of Sørensen's glycine-HCl, citrate-HCl, and acetic acid-acetate, to which was added NaCl to a total ionic strength of 0.5 M. The experiments were carried out at a temperature of 30° C.

Experiments were made with hydrogen ion concentrations up to 1 M. In such determinations the ionic strength can obviously not be kept at 0.5 M. Besides, at these hydrogen ion concentrations the decomposition rates become so high that it is difficult to determine them with accuracy. The experiments in which the hydrogen ion concentration exceeded 0.1 M. were therefore carried out at 0.1° C. in mixtures of HCl and NaCl with a total ionic strength of 1 M. At hydrogen ion concentrations of 0.1 M. determinations were made partly at 30° C. and an ionic strength of 0.5 M., and partly at 0.1° C. and an ionic strength of 1 M., the ratio between these rates of decomposition being 13.8. Thus, the values obtained at an ionic



strength of 1 M. and 0.1° c. were multiplied by 13.8. The figures found in this manner must be supposed to indicate the rates at which the process would have proceeded, if it had been possible to carry out the experiment at 30° c. and with an ionic strength of 0.5 M.

The initial concentrations of the penicillin were about 5 o.u./ml. A sample of the mixture was taken immediately after the addition of penicillin; later samples were taken three times at such intervals that the penicillin concentration had decreased to about 50% between each interval. The process of inactivation was stopped immediately after removal of the sample by neutralisation to a pH value of about 7. Next, the penicillin concentrations were determined turbidimetrically, as described by Vesterdal.<sup>2</sup> The penicillin concentration of each sample was determined at two different dilutions, each of which was measured in duplicate, and the average of these four values was deduced. The logarithms of the concentrations thus found for each sample were plotted against time, and the velocity constant was determined graphically by means of the expression

$$k = \frac{\ln c_1/c_2}{t_1 - t_2}$$

Assuming the standard deviation of a single turbidimetric determination to be 10%, the standard deviation of the velocity constant must be 5 to 10%, which means that the standard deviation of the logarithm of the velocity constant is 0.02 to 0.04.

The hydrogen ion concentrations were determined electrometrically by means of a glass electrode. The relation between the pH values read from the apparatus and the hydrogen ion concentrations was determined by measuring the pH of solutions of HCl in different concentrations of NaCl with a total ionic strength of 0.5 M. The hydrogen ion concentrations of these solutions being equal to the molarity of the HCl, the following relation was found to hold within less than 0.01 pH unit:

$$-\log c_{H^+} = pH - 0.05,$$

where pH indicates the value read from the potentiometer.

### Results.

The inactivation proceeds as a first-order reaction, as has been shown also by Benedict, Schmidt, Coghill and Olesen,<sup>3</sup> since, in all experiments,

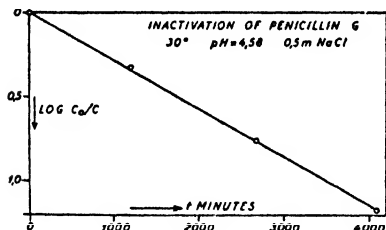


FIG. 1.

the relation between the logarithm of the penicillin concentration and time in good approximation proved to be linear. Fig. 1 illustrates this fact. This accords with the hypothesis advanced above and shows that the penicillin preparation used does not contain measurable amounts of other penicillins. In experiments with some other preparations considerable deviations from the linear relation have been found on account of the presence of several penicillins.<sup>4</sup>

In Fig. 2 the negative logarithm of the velocity constant in min.<sup>-1</sup> is plotted against the negative logarithm of the hydrogen ion concentration. The curve has been calculated from formula (9), as

$$\frac{k_+}{K_+} = 5.5 \quad \frac{k_{\pm}}{K_{\pm}} = 22.5 \quad K_0 = 10^{-2.8} = 0.0016. \quad (12)$$

<sup>2</sup> Vesterdal, Diss. (Copenhagen, 1947).

<sup>3</sup> Benedict, Schmidt, Coghill and Olesen, *J. Bact.*, 1945, 49, 85.

<sup>4</sup> Brodersen, *Acta pharmacol.*, 1946, 2, 1.

These values have been chosen so that the best possible coincidence is obtained between the curve calculated from the formula and the experimental points. The value used for  $K_0$  is the one stated by British and American investigators.

The accordance between the calculated curve and the experimental points seems to be in favour of our hypothesis concerning the mechanism of the inactivation. As, however, there will always be a constant relation between the concentrations of the amphi-ion  $H^+Pn^-$  and the isomeric form HPn, when the salt concentration is constant, we cannot, on the basis of these experiments, distinguish between decomposition of one or the other of these two forms. The possibility that the molecule HPn may undergo inactivation without previous transformation to the amphi-ion will therefore have to be left open, although, as stated above, this possibility seems less likely.

The experiments reported in this paper were made with financial support from "Foreningen af Medicinalfabriker af 1933". The penicillin applied was kindly placed at my disposal by Professor

K. A. Jensen. I am greatly indebted to Professor J. N. Brønsted for his perusal and kind criticism of the manuscript.

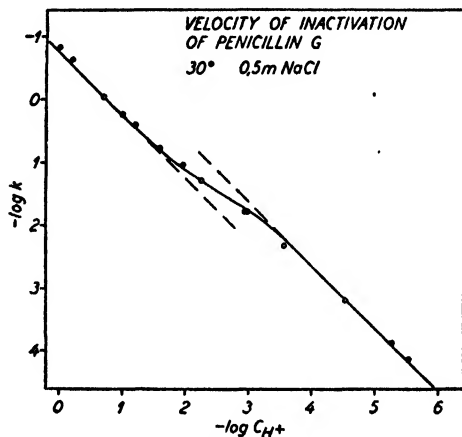


FIG. 2.

### Summary.

The hypothesis is made that the inactivation of penicillin in acid medium depends on the taking up of a hydrogen ion by the ring nitrogen atom, by which either a positive ion or an amphi-ion (depending on the hydrogen ion concentration) is formed, which is subsequently transformed into an inactive substance. This latter process is supposed to be rate-determining. The experimentally determined relation between the rate of the process and the hydrogen ion concentration accords with this hypothesis.

### Résumé.

L'inactivation de la pénicilline en milieu acide dépend de l'addition d'un ion H sur l'atome d'azote du noyau pour former un ion positif ou un amphi-ion, qui est ensuite transformé en une substance active par un processus qui détermine la vitesse de réaction.

### Zusammenfassung.

Der Verlust der Aktivität von Penicillin in Säuren ist darauf zurückzuführen, dass das N-Atom im Ring ein Proton anlagert und dadurch ein positives Ion oder Zwitterion gebildet wird, das dann in eine inaktive Substanz umgewandelt wird; diese Umwandlung ist die geschwindigkeitsbestimmende Reaktion.

*The University Institute for General Pathology,  
Juliane Mariesvej 22,  
Copenhagen, Denmark.*

# THE DIAMAGNETIC SUSCEPTIBILITY OF SOME ALIPHATIC ACIDS AND ESTERS.

By C. M. FRENCH.

*Received 1st July, 1946.*

The series of measurements, of which the results are now presented, was designed in order that comparisons might be made between the various acids, and their corresponding esters both in the mono- and di-carboxylic acid series. The results obtained include magnetic susceptibility values of compounds which have either not previously been measured, or for which there are only very few previously recorded values. Furthermore, where several values are already available for any one compound, they often differ quite appreciably, although measurements on a series of compounds by any one group of investigators are generally sufficiently self-consistent, suggesting that the actual overall experimental error in recorded values, inherent in the use of different types of apparatus and by different workers, is larger than that generally assumed in a single set of experiments. Hence, until a greater degree of co-ordination is achieved between the various methods, further measurements of the magnetic susceptibility of extensive series of compounds by different investigators would seem desirable. This is especially the case where comparisons are to be made between the members of a series, as in the evaluation of the contribution to the diamagnetic susceptibility made by the  $\text{CH}_3$  group, since such comparisons should be made only between the results of the same author—a precaution already noted by Angus.<sup>1</sup>

Of the aliphatic acids and esters, the subject of the present paper, few extensive series of determinations have been made by any one author, the most notable recent exception being the contribution of Angus and Hill<sup>1</sup> who record the values of some 23 such compounds together with those of other related compounds. Bhatnagar, Mitra and Tuli<sup>2</sup> have also presented a series of 12 aliphatic acids and esters, but the number of compounds in this series measured by any one other author, is considerably fewer.

## Experimental.

The substances used were carefully purified by drying and redistillation in all-glass apparatus, or by recrystallisation, until a high standard of purity was attained, as evidenced by reference to accepted standards of boiling point or melting-point, density, and refractive index. Refractive index determinations were carried out using a Pulfrich refractometer (sodium D line at 20° c.). Details are given in Table I, columns 2-7, and include a value for the refractive index of dipropyl oxalate which has apparently not previously been recorded.

The Gouy balance and method previously described<sup>3</sup> with the modification introduced for the case of liquids,<sup>4</sup> was used for determinations of magnetic susceptibility. D.C. mains current of 220 v. was employed, giving a current strength of 3.1-3.2 amp., which, although not quite sufficient to give the maximum diamagnetic thrust possible on the specimen, was nevertheless, the maximum obtainable owing to the

<sup>1</sup> Angus and Hill, *Trans. Faraday Soc.*, 1943, **39**, 185.

<sup>2</sup> Bhatnagar, Mitra and Tuli, *Phil. Mag.*, 1934, **18**, 449.

<sup>3</sup> Trew and Watkins, *Trans. Faraday Soc.*, 1933, **29**, 1310.

<sup>4</sup> French and Trew, *ibid.*, 1945, **41**, 439.

resistance of the coils of the electromagnet, and provided a thrust of satisfactory magnitude. The tubes were filled to a length of 7 cm., and under these conditions, using a pole gap of 1.2 cm., a field of 7,430 gauss was obtained.

The susceptibility of the solids was calculated from the equation :

$$10^6 \chi_A = \frac{F_A \alpha + 10^6 K_{\text{air}} V}{W_A}$$

where  $\chi_A$  is the susceptibility of the substance under investigation,  $F_A$  is the thrust on the specimen in mg.,  $V$  and  $W_A$  its volume in cc., and weight

TABLE I \*

Substance.	Density ( $d_4^{20}$ ).		Boiling Point ( $^{\circ}\text{C}$ ).		Refractive Index ( $n_D^{20}$ ).	
	Obs. Val.	Lit. Val.	Obs. Val.	Lit. Val.	Obs. Val.	Lit. Val.
Acetic acid .	1.050	1.051 H	118	118 H	1.37303	1.37182 H
Propionic acid .	0.9956	0.992 I	141	141.35 H	1.38703	1.3868 I
Butyric acid .	0.9596	0.9587 H	161.6	162 H	1.39853	1.39906 H
Methyl formate .	0.9705	0.97421 P	31.5	31.5 H	1.344	1.344 I
Methyl acetate .	0.9330	{ 0.9280 H 0.9338 P	56.9	{ 56.95 P 57.5 H	1.36146	1.36143 P
Methyl propionate .	0.9165	0.9151 H	80	79.7 H	1.37743	1.3779 I
Methyl butyrate .	0.8981	0.8982 II	102.5	102.3 H	1.38775	1.3879 I
Ethyl formate .	0.9210	{ 0.91678 H 0.9225 P	54.3	54.3 II	1.35994	1.35975 H
Ethyl acetate .	0.9008	0.9005 P	77.1	77.1 H	1.37280	1.37257 P
Ethyl propionate .	0.8901	0.8904 P	99.1	99.1 H	1.38403	1.38385 H
Ethyl butyrate .	0.8791	0.8788 H	120	119.9 H	1.39192	1.40002 H
Propyl formate .	0.9000	0.9006 P	81.0	80.89 P	1.37781	1.37789 P
Propyl acetate .	0.8868	0.8869 P	101.6	101.67 P	1.38457	1.38422 P
Propyl butyrate .	0.8737	0.879 I	143	143 I	1.40095	1.4005 I
Oxalic acid ( $2\text{H}_2\text{O}$ )	—	—	101	101 I	—	—
Oxalic acid (anh.) .	—	—	189	189 I	—	—
Malonic acid .	—	—	135.6	135.6 I	—	—
Succinic acid .	—	—	186.2	185 I	—	—
Dimethyl succinate	1.120	1.1202 H	192.8	195.2 H	1.41964	1.41976 H
Diethyl oxalate .	1.0875	1.0785 H	185	185.4 H	1.41011	1.41011 H
Diethyl malonate	1.0560	1.0550 P	199	198.9 H	1.41426	1.41428 H
Diethyl succinate	1.041	1.0402 H	216.5	217.7 II	1.42048	1.42007 H
Dipropyl oxalate .	1.015	1.018 B	213	209-215 B	1.4147	—

\* "H" refers to Heilbron's Dictionary, "P" to Proskauer and Weissberger's "Organic Solvents", "I" to the International Critical Tables, and "B" to Beilstein's Handbuch.

in grams respectively, and  $K_{\text{air}}$  the specific susceptibility of air =  $0.094 \times 10^{-6}$ ;  $\alpha$  is the balance constant,

$$\alpha = \frac{2l \times 10^6 \times 981}{H^2 \times 1000}$$

where  $l$  is the length of the specimen filling the tube, and  $H$  is the field strength. The balance constant was determined using benzene as the standard, for each set of measurements, in order to exclude errors due to slight daily variations in the current supplied.

For liquids the modified formula \* was used :

$$10^6 \chi_A = \left( 10^6 \chi_B - \frac{0.0294}{d_B} \right) \frac{F_A d_B}{F_B d_A} + \frac{0.0294}{d_A}$$

where the subscript B refers to the standard liquid, in this case benzene ( $\chi_B = -0.702 \times 10^{-6}$ ) and  $d_A$  and  $d_B$  are the densities of the liquid under investigation, and benzene respectively.

## Results.

The results of the magnetic susceptibility measurements (a mean of six closely agreeing determinations in each case), are given in Table II,

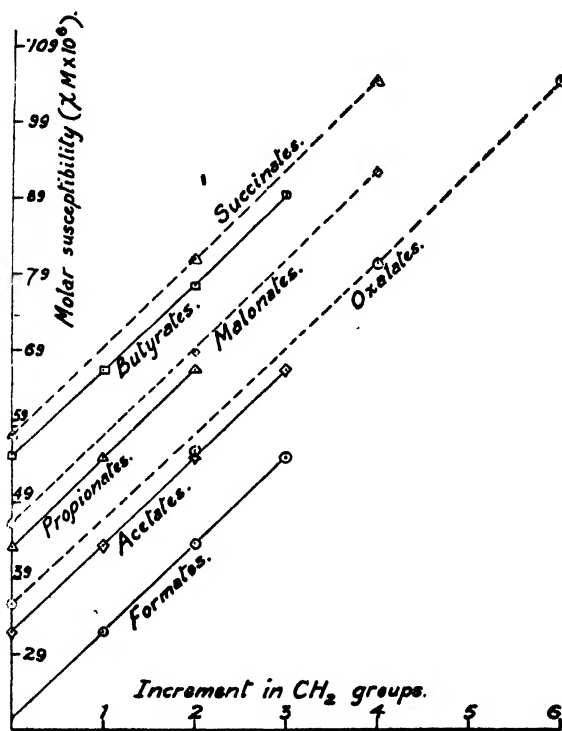


FIG. 1.

columns 2 and 4, whilst in column 7 are noted values for the same compounds obtained by other investigators. The maximum experimental error in the specific susceptibility in the present series of determinations

<sup>6</sup> Pascal, *Ann. Chim. Physique*, 1912, **25**, 289.

<sup>6</sup> Selwood, *J. Amer. Chem. Soc.*, 1933, **55**, 3161.

<sup>7</sup> Woodbridge, *Physic. Rev.*, 1935, **48**, 672.

<sup>8</sup> Rao, *Ind. J. Physics*, 1934, **8**, 483.

<sup>9</sup> Henrichson, *Ann. Physik*, 1888, **34**, 180.

<sup>10</sup> Rao and Narayanaswamy, *Proc. Ind. Acad. Sci. A*, 1939, **9**, 35.

<sup>11</sup> Varadachari, *Proc. Ind. Acad. Sci. A*, 1935, **2**, 161.

<sup>12</sup> Nevgi, *J. Univ. Bombay*, 1938, **7**, Part 3, 74.

<sup>13</sup> Rao and Govindarajan, *Proc. Ind. Acad. Sci. A*, 1942, **15**, 35.

<sup>14</sup> Kido, *Sci. Rep. Tohoku Univ.*, 1932, **21**, 385.

<sup>15</sup> Cabrera and Fahlenbrach, *Z. Physik*, 1933, **85**, 568.

<sup>16</sup> Smith and Smith, *J. Amer. Chem. Soc.*, 1918, **40**, 1218.

<sup>17</sup> Bhatnagar and Mathur, *Phil. Mag.*, 1928, **6**, 217.

<sup>18</sup> Farquharson and Sastri, *Trans. Faraday Soc.*, 1937, **33**, 1472.

<sup>19</sup> Mathur, *Ind. J. Physics*, 1931, **6**, 207.

<sup>20</sup> Kido, *Rep. Yokohama Tech. Coll.*, 1934, **2**, 203.

<sup>21</sup> Vaidyanathan, *Ind. J. Physics*, 1928, **2**, 135.

<sup>22</sup> Takagi and Ishiware, *Sci. Rep. Tohoku Imp. Univ.*, 1914, **3**, 127.

<sup>23</sup> Isnadi and Gans, *Ann. Physik*, 1920, **61**, 585.

<sup>24</sup> Gray and Birse, *J. Chem. Soc.*, 1914, **105**, 2707.

<sup>25</sup> Hadfield, Cheneveau and Geneau, *Proc. Roy. Soc., A*, 1917, **94**, 65.

<sup>26</sup> Rao and Sriraman, *Phil. Mag.*, 1937, **24**, 1025.

TABLE II

Substance.	Specific Suscept. $\chi_g \times 10^6$ .	$\Delta\chi_g$ .	Molar Mass Suscept. $\chi_M \times 10^6$ .	Estimated Values of		Previously Recorded Values of Molar Susceptibility.
				$\chi_g \times 10^6$ .	$\chi_M \times 10^6$ .	
Formic acid	—	—	—	0.4474	20.59	$19.87^8$ ; $19.93^{10}$ ; $19.97^{16}$ ; $20.53^{16}$ ;
Acetic acid	0.5332	—	32.01	0.5339	32.06	$30.56^7$ ; $31.22^8$ ; $31.4^8$ ; $31.52^{10}$ ; $31.58^8$ ; $31.63^8$ ; $31.70^1$ ; $31.8^{11}$ ; $31.9^{12}$ ; $31.82^{13}$ ; $32.06^{14}$ ; $32.1^{15}$ , $16$
Propionic acid	0.5890	0.0558	43.62	0.5877	43.53	$42.93^4$ ; $43.36^1$ ; $43.49^5$ ; $43.8^{12}$ ; $43.83^{17}$ ;
Butyric acid	0.6265	0.0375	55.18	0.6243	54.99	$55.07^{18}$ ; $55.20^1$ ; $55.43^8$ ; $55.48^{17}$ ; $55.39^{18}$ ; $55.68^8$ ; $55.70^{20}$ ; $55.9^{12}$ ;
Methyl formate	0.5327	0.0548	31.98	0.5339	32.06	$31.11^5$ ; $38^{21}$
Methyl acetate	0.5875	0.0365	43.51	0.5877	43.53	$39.78^{17}$ ; $42.23^7$ ; $42.37^1$ ; $43.39^2$ ; $43.68^5$
Methyl propionate	0.6240	0.0258	54.96	0.6243	54.99	$54.06^1$ ; $54.66^2$ ; $55.30^5$
Methyl butyrate	0.6498	0.0375	66.35	0.6509	66.46	$65.83^1$ ; $65.99^2$ ;
Ethyl formate	0.5880	0.0375	43.55	0.5877	43.53	$42.88^{14}$ ; $43.01^5$ ; $43.43^8$ ; $51.18^{22}$ ; $53.47^{23}$ ; $53.98^7$ ;
Ethyl acetate	0.6255	0.0259	55.10	0.6243	54.99	$54.00^1$ ; $54.66^2$ ; $55.20^5$ ; $54.5^8$ ; $59.70^{17}$
Ethyl propionate	0.6514	0.0179	66.51	0.6509	66.46	$65.75^1$ ; $66.02^2$
Ethyl butyrate	0.6693	0.0258	77.73	0.6711	77.93	$77.43^1$ ; $77.54^2$
Propyl formate	0.6248	0.0258	55.03	0.6243	54.99	—
Propyl acetate	0.6506	—	66.43	0.6509	66.46	$65.74^1$ ; $65.91^1$ ; $65.94^2$
Propyl propionate	—	0.0361	—	0.6711	77.93	$77.31^2$
Propyl butyrate	0.6867	—	89.37	0.6869	89.40	—
Oxalic acid (2H <sub>2</sub> O)	0.4874	—	61.44	—	—	$75.63^8$
Oxalic acid (anh.)	0.3954	0.0499	35.60	0.3910	35.20	—
Malonic acid	0.4453	0.0449	46.33	0.4486	46.68	—
Succinic acid	0.4902	—	57.88	0.4925	58.15	$54.45^{24, 25}$
Dimethyl oxalate	—	—	—	0.4925	58.15	$55.78^5$
Dimethyl malonate	—	—	—	0.5270	69.61	$68.74^5$
Dimethyl succinate	0.5547	—	81.05	0.5550	81.09	—
Diethyl oxalate	0.5519	0.0263	80.52	0.5550	81.09	$81.12^5$
Diethyl malonate	0.5782	0.0217	92.59	0.5780	92.56	$93.60^5$
Diethyl succinate	0.5999	—	104.48	0.5974	104.04	$105.23^5$
Dipropyl oxalate	0.5997	—	104.44	0.5974	104.04	—

is  $\pm 0.0010$  in the case of liquids, and  $\pm 0.0035$  in the case of solids, resulting, of course, in a considerably larger possible error in the molar susceptibility. In Fig. 1 are plotted the molar susceptibilities against

## 360 DIAMAGNETIC SUSCEPTIBILITY OF ACIDS AND ESTERS

the  $\text{CH}_2$  increment (similar curves are, of course, obtained by plotting against molecular weight instead of the  $\text{CH}_2$  increment), the only previously recorded values for dimethyl oxalate and dimethyl malonate, due to Pascal,<sup>5</sup> being included.

### Discussion of Results.

Values somewhat higher than those of Angus and Hill<sup>1</sup> for the magnetic susceptibility of the monocarboxylic acids and their esters, are shown in the present investigation, but they are, at the same time, lower in some cases, than those of other authors, and in general, no significant difference is observable. In the case of the dicarboxylic acids and their esters, however, whereas the present values for the diethyl esters accord fairly well with those of Pascal,<sup>5</sup> the value for succinic acid and its isomer, dimethyl oxalate, are both higher than the previously recorded values; but it is to be noticed that the latter are definitely low in comparison with other members of the series. The only previously recorded value for oxalic acid is that of Selwood<sup>6</sup> who finds the specific susceptibility of the hydrated crystals to be  $0.6 \times 10^{-6}$  to within  $0.1 \times 10^{-6}$ , giving the extraordinarily high figure of 75.6 for the molar susceptibility as compared with 61.4 in the present investigation. This latter figure, assuming the validity of the additivity rule for such compounds, gives a value for the molar susceptibility of the anhydrous acid of 35.5, which agrees well with the value 35.6 obtained from measurements on the anhydrous acid.

The series of compounds whose magnetic susceptibility has been measured in the present investigation is, however, incomplete, the most serious omission being that of the first member of the monocarboxylic acid series, formic acid. In this case, although the specific susceptibility of a small specimen whose refractive index agreed with the previously recorded value (1.37008 as compared with 1.3714), was determined and found to be 0.4705, giving a molar susceptibility of 21.65, the boiling point and the density indicated that the specimen was considerably contaminated. The impurity was almost certainly entirely water, since formic acid decomposes readily into carbon monoxide and water on standing. The true susceptibility of this compound is therefore undoubtedly lower than this figure, the general shape of the graphs also supporting this view. From Fig. 1 and 2 a value of 0.4476 for the specific susceptibility, with a corresponding value of 20.60 for the molar susceptibility would appear to be more nearly correct.

Three other compounds for which it has not been possible to obtain experimental values in the present investigation, are propyl propionate, dimethyl oxalate, and dimethyl malonate, and for these compounds the general shape of the graphs would suggest the values shown in Table III.

TABLE III

Propyl propionate	.	.	.	$\chi_s$ 0.6699 ; $\chi_M$ 77.8
Dimethyl oxalate	.	.	.	$\chi_s$ 0.4904 ; $\chi_M$ 57.9
Dimethyl malonate	.	.	.	$\chi_s$ 0.5254 ; $\chi_M$ 69.4

Interest in the results of magnetic susceptibility determinations in a series such as the aliphatic acids, centres largely round the contribution to the magnitude of this property, made by the addition of a  $\text{CH}_2$  group to each succeeding member of the series, and we now consider whether, particularly in the earlier members of such a series, a constant increment is to be expected. Farquharson and Sastri<sup>18</sup> have observed that in the first few members of a series, the effects of the end group may be such as to influence the result. In the present series, the difference in the molar susceptibility between oxalic and malonic acid is 10.73, whereas the difference between malonic and succinic acids, where the effect of the

end groups might be expected to be smaller, is 11.55. Again, however, paucity of data prevents, at the present time, confirmation of the effect of the end groups on the magnitude of the magnetic susceptibility.

Angus and Hill<sup>1</sup> found experimentally that the increment in the change acid to methyl ester, was one susceptibility unit lower than in subsequent changes, a phenomenon explained by them, and by Anantakrishnan and Varadachari<sup>27</sup> as due to H bonding in the acid molecules. The magnitude of this effect has not been confirmed in other cases where an extensive series has been investigated, notably by Pascal,<sup>5</sup> Woodbridge,<sup>7</sup> and Bhatnagar, Mitra and Tuli<sup>3</sup>—the latter authors actually finding a tendency for the acid-methyl ester change to have a higher magnetic susceptibility increment—and the differences observed in the

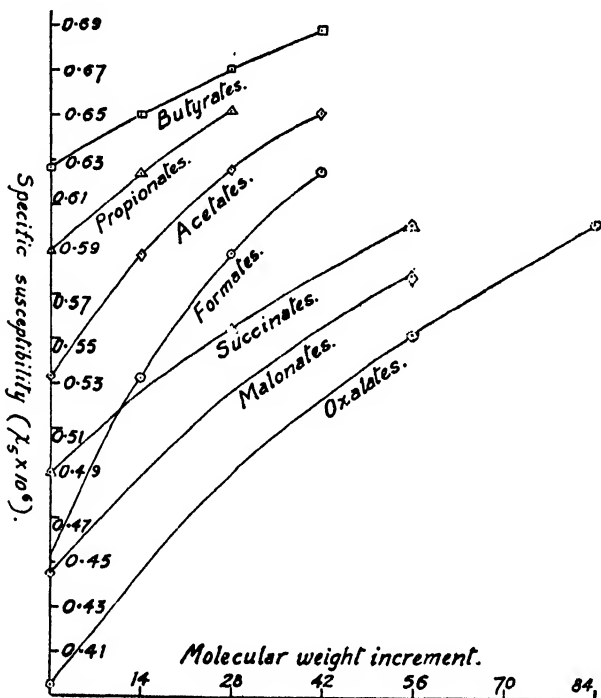


FIG. 2.

present investigation are scarcely large enough to be significant. It is to be noted, however, that the linkages involved in the first change ( $-\text{O}-\text{H}$  to  $-\text{O}-\text{C}\equiv\text{H}_2$ ) are different from those involved in subsequent methylations ( $-\text{C}-\text{H}$  to  $-\text{C}-\text{C}\equiv\text{H}_2$ ), and this alone may account for any difference in magnetic susceptibility. Indeed, theoretical calculations of magnetic susceptibility based on Gray and Cruickshank's method,<sup>28</sup> indicate that the difference in bond depressions resulting from the acid to methyl ester change is 0.2 susceptibility units less than that resulting from subsequent changes in the series.

Similar considerations apply to the dicarboxylic acid series, but almost the only available data are those now presented, and although the oxalic acid-dimethyl oxalate increment is slightly less than either the dimethyl-diethyl or the diethyl-dipropyl oxalate increment, the experimental uncertainty renders this small difference of no significance. The change

<sup>27</sup> Anantakrishnan and Varadachari, *Proc. Ind. Acad. Sci. A*, 1941, 20, 128.



in bond depressions calculated on Gray and Cruickshank's method<sup>22</sup> would, however, be 0.4 susceptibility units less for the acid-methyl ester change than for subsequent changes.

Apart from the effects mentioned, the molar susceptibility increment might be expected to be the same for successive methylations in such series, but in order to eliminate such effects due to the end group, it would be necessary to examine longer chain acids and esters. Whereas, however, the experimental uncertainty in the specific susceptibility is generally of the order  $\pm 0.001$  for liquids, it is  $\pm 0.0035$  for solids, of which many of the higher members of such a series would consist. Furthermore, since the uncertainty in the molar susceptibility is equal to the product of the molecular weight and the uncertainty in the specific susceptibility, the differences between the molar susceptibilities of the higher members of a series will be even less reliable. Thus whereas the uncertainty in the difference between the molar susceptibilities of formic and acetic acids is only  $\pm 0.11$ , the uncertainty in the same difference even between malonic and succinic acids is  $\pm 0.78$ . It is doubtful therefore, whether the effect of such factors as have been noted in this paper will be detectable by these methods, and in any case, attempts to evaluate the  $\text{CH}_3$  increment to four significant figures in this way, as is frequently the case, can have but doubtful value. The following method would, however, obviate these difficulties.

If the molar susceptibility of the first member of a series is denoted by  $A$ , and its molecular weight by  $M_1$ , the molar increment between successive members of the series by  $\delta$ , and the molecular weight of a given member by  $M$ , then the molar susceptibility of this member can be expressed by the equation :

$$\chi_s \times M = A + \frac{\delta}{k}(M - M_1) \quad (1)$$

where  $\chi_s$  is the measured specific susceptibility of the member, and  $k$  is the constant increment in molecular weight between two successive members of the series.

$$\text{or} \quad \chi_s = \frac{\delta}{k} + \frac{Ak - \delta M_1}{kM} \quad (2)$$

Now if  $\delta$ , the molar increment, is a constant, this reduces to

$$\chi_s = K + K'/M \quad (3)$$

where  $K$  and  $K'$  are constants.

Hence as the molecular weight increases (i.e. with higher members of the series) the specific susceptibility  $\chi_s$  should tend towards a constant value  $K$ .

Using the results obtained in the present investigation, an estimate by the method of least squares, of the constants involved gives for the monocarboxylic acids and esters the equation :—

$$\chi_s = 0.8179 - 17.05/M \quad (4)$$

and for the dicarboxylic acids and esters :

$$\chi_s = 0.8182 - 38.46/M \quad (5)$$

indicating that in both series the specific susceptibility tends towards the limiting value of 0.818 for compounds of very high molecular weight.

A more accurate estimate is likely to be obtained for the susceptibility of compounds for which an experimental determination is not practicable, from a mathematical analysis of this nature of the general results for the series, than by the graphical method already indicated. In this way the values finally suggested for the four compounds whose susceptibilities were not measured in the present investigation, are shown in Table II, columns 5 and 6, where the specific and molar susceptibilities estimated from equations (4) and (5) above, are recorded.

<sup>22</sup> Gray and Cruickshank, *Trans. Faraday Soc.*, 1935, 31, 1491.

Furthermore, by expressing the results in this form, the standard deviation can be calculated, and in consequence any significant deviations of the experimental from the calculated results will be more easily detected. The standard deviations are 0.0011 and 0.0031 for the monocarboxylic and dicarboxylic acid series respectively, and the differences between the experimental and estimated results in the present investigation would not therefore appear to be significant. Finally, it may be noted that a mean value of 11.47 for the  $\text{CH}_2$  increment is now obtained by this method.

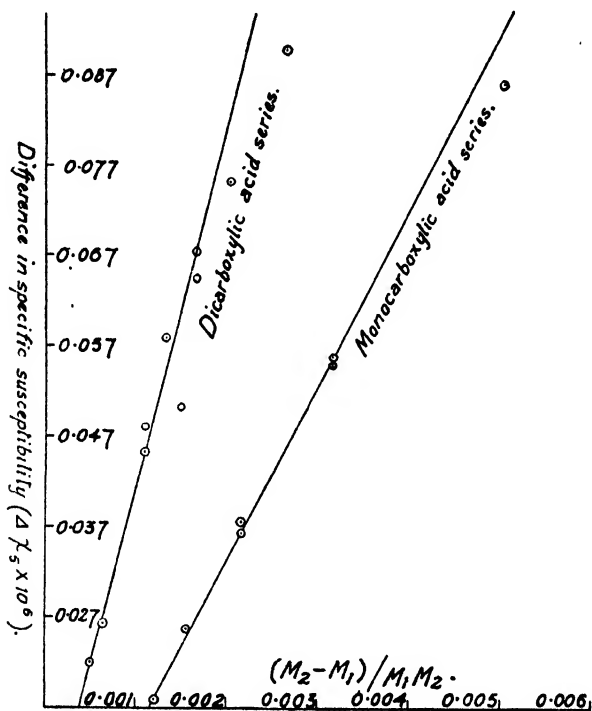


FIG. 3.

A graph of the specific susceptibility against the molecular weight increment should have the form of a curve, approaching the value of  $K'$  asymptotically as the molecular weight increases (Fig. 2 shows such curves for the present series of measurements). The experimentally determined points should all lie within the same distance from the curve, in contrast to the graph obtained by plotting molar susceptibility against molecular weight, where, owing to the increasing uncertainty in the molar susceptibility of the higher members of a series, the experimental points may be expected to diverge from the curve increasingly on both sides, as the molecular weight increases, and hence any significant variation in the values for the higher members of the series may be missed.

Such a curve as shown in Fig. 2 is, however, somewhat difficult to construct accurately, and an alternative method is clearly available. If subscripts 1 and 2 denote any pair of compounds in the series, then from equation (3):

$$\chi_{s2} - \chi_{s1} = \Delta \chi_s = (K + K'/M_2) - (K + K'/M_1) = K' \left( \frac{M_1 - M_2}{M_1 M_2} \right)$$

or

$$\Delta \chi_s = -K' \left( \frac{M_2 - M_1}{M_1 M_2} \right).$$

Hence, if by plotting the difference in specific susceptibility against  $(M_2 - M_1)/M_1M_2$ , a straight line is obtained, it may be assumed that  $\delta$ , the molar increment is sensibly constant. The experimentally determined points for all members of the series should lie within the same

TABLE IV

Substance.	$x_g$	$(M_2 - M_1)/M_1M_2$
Oxalic acid	0.0893	0.00264
Dimethyl oxalate	0.0672	0.00163
Diethyl oxalate	0.0478	0.00110
Dipropyl oxalate	0.0751	0.00204
Malonic acid	0.0578	0.00133
Dimethyl malonate	0.0645	0.00163
Diethyl malonate	0.0452	0.00110
Succinic acid		
Dimethyl succinate		
Diethyl succinate		

distance, represented by twice the experimental error, of the straight line, and any feature disturbing the constancy of the increment will be far more easily detectable.

The value for the molar increment (assuming this is constant) can, of course, be obtained from the slope of the graph (slope  $= K' = (AK - \delta M_1)/k$ ), since  $A$ ,  $M_1$  and  $k$  are known or can be measured.

Figure 3 shows the result of plotting these differences in specific susceptibility given in

Table II, column 3, and in Table IV, column 2, in this manner, and it is interesting to note that the points fall on an appreciably straight line for both the mono- and di-carboxylic acid series, as might be expected. Much more extensive series need to be investigated, however, before it is possible to determine whether the lower members of a series diverge from the overall direction of the curve to any significant extent.

### Summary.

(1) The diamagnetic susceptibilities of 24 mono- and di-carboxylic acids and esters have been measured and are recorded.

(2) An examination is made of various possible causes of variation in the molar susceptibility increment, and the theoretically calculated magnitude of certain of these effects is noted.

(3) Finally, the magnitude of the possible error in the molar susceptibility, and hence the accuracy of the evaluation of the  $\text{CH}_2$  increment in the higher members of the series is discussed, and an alternative method of examination of results is suggested.

### Résumé.

On a mesuré les susceptibilités diamagnétiques de 24 acides et esters mono- et di-carboxyliques et on examine diverses causes possibles de la variation dans l'augmentation de la susceptibilité molaire. On discute finalement la précision de cette augmentation en fonction des  $\text{CH}_2$  dans les membres supérieurs de la série et on suggère une autre méthode pour examiner les résultats.

### Zusammenfassung.

Neue Messungen der diamagnetischen Suszeptibilität von 24 Mono- und Dikarboxylsäuren werden berichtet und die möglichen Gründe für die Veränderungen im Zuwachs der Molsuszeptibilität per  $\text{CH}_2$ -Gruppe untersucht. Die Genauigkeit der Auswertung dieser  $\text{CH}_2$ -Kontribution für die höheren Mitglieder der Reihe wird besprochen und eine andere Methode für die Untersuchung der Resultate vorgeschlagen.

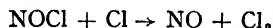
Laboratory for Physical Chemistry,  
Bedford College,  
Regent's Park, N.W. 1.

# THE INHIBITION OF THE PHOTOCHEMICAL FORMATION OF PHOSGENE BY NITROSYL CHLORIDE—I

By F. S. DAINTON.

Received 13th June, 1946.

The atomic reaction



has been postulated as a stage in the photolysis of nitrosyl chloride,<sup>1</sup> and has also been used in the interpretation of the kinetics of the sensitisation of the explosion of hydrogen and oxygen by nitrosyl chloride.<sup>2</sup> The reaction is exothermic to the extent of 19.5 kcal., and the dissociation energy of the N—Cl bond is 38 kcal.\* If it is permissible to apply the empirical rule<sup>3</sup> which states that the activation energy of an atomic reaction of the type



rarely exceeds 5% of the YZ bond strength and to regard NO as a mono-valent atom for this purpose it would be expected that the reaction  $\text{Cl} + \text{NOCl}$ , which is the special case of  $\text{X} + \text{YZ}$  when  $\text{X} = \text{Z}$ , would be very rapid at room temperature.

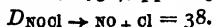
The existence of this rapid reaction would be proved if it could be shown that nitrosyl chloride inhibited chain reactions in which the chain propagation involved chlorine atoms. Of the many chain reactions in which Cl atoms play a part, the photosynthesis of phosgene from carbon monoxide and chlorine, was chosen for the initial investigation, because it can be followed manometrically. At temperatures below 160°C. and pressures greater than 30 mm. the rate of formation of phosgene from the pure gases was found by Bodenstein<sup>4</sup> to be given by the equation (1)

$$\frac{d(\text{COCl}_2)}{dt} = K \cdot I_{\text{abs}}^{\frac{1}{2}} [\text{CO}]^{\frac{1}{2}} [\text{Cl}_2] \quad (1)$$

where  $I_{\text{abs}}$  is the intensity of the absorbed light and  $K$  a constant. The quantum yield is of the order  $10^3$ .

There has been considerable discussion about the mechanism<sup>5</sup> but all the postulated reaction schemes have the following features in common: (a) the chains are initiated by chlorine atoms produced by optical dissociation of chlorine molecules, (b) the chains are unbranched, (c) the chain

\* The dissociation energy  $\text{NOCl} \rightarrow \text{NO}(^2\pi) + \text{Cl}(^2P_{3/2})$  is given by Bailey and Cassie (*Proc. Roy. Soc. A*, 1934, **145**, 336) and by Goodeve and Katz (*ibid.*, 1939, **172**, 432) as 38, and this value is confirmed by  $2\text{NO}_{(g)} + \text{Cl}_{2(g)} \rightarrow 2\text{NOCl}_{(g)} + 18$  and  $\text{Cl}_{1(g)} \rightarrow 2\text{Cl}(^2P_{3/2}) - 58$  (Bichowsky and Rossini, *Thermochemistry of Chemical Substances* (Reinhold, 1936), pp. 215 and 22, whence



<sup>1</sup> See for example Rollefson and Burton, *Photochemistry*, p. 165, and Natanson, *Acta Physicochim.*, 1939, **11**, 521.

<sup>2</sup> Dainton and Norrish, *Proc. Roy. Soc. A*, 1941, **177**, 421.

<sup>3</sup> Eyring, Glasstone and Laidler, *Theory of Rate Processes* (McGraw Hill, 1941), p. 151.

<sup>4</sup> Bodenstein *et al.*, *Z. physik. Chem.*, 1927, **130**, 422; **131**, 153.

<sup>5</sup> Rollefson and Burton, *Photochemistry*, pp. 313-319. Leighton and Noyes, *Photochemistry of Gases*, pp. 277-283. Semenov, *Chemical Kinetics and Chain Reactions*, pp. 127-138.

centres are Cl atoms and COCl radicals, and (d) the mode of chain termination which preponderates over all others is self neutralisation of pairs of chains by recombination of centres. Adopting a convention used elsewhere<sup>6</sup> this type of chain development may be summarised by

$$\frac{dn}{dt} = KI_{abs} - \delta n^2 \therefore n_e = \left(\frac{K}{\delta}\right)^{\frac{1}{2}} \cdot I_{abs}^{\frac{1}{2}}$$

where  $K$  and  $\delta$  are constants and  $n$  is the concentration of centres. In an unbranched chain reaction  $n$  attains an equilibrium value  $n_e$ , and since the steady reaction rate is proportional to  $n_e$ , the rate will depend on the square root of the incident light intensity.

In the presence of nitrosyl chloride the recombination (d) is likely to be superseded as a chain ending process by reactions of the type:  $\text{NOCl} + \text{Cl} \rightarrow \text{NO} + \text{Cl}_2$ , and  $\text{NOCl} + \text{COCl} \rightarrow \text{NO} + \text{Cl}_2 + \text{CO}$  or  $\text{NO} + \text{COCl}_2$ . The chains will now be terminated singly at a rate proportional to the first power of the concentration of the centres and the appropriate equation will be

$$\frac{dn}{dt} = KI_{abs} = k'[\text{NOCl}]n \therefore n_e = \frac{k I_{abs}}{k'[\text{NOCl}]}$$

The reaction rate of the  $\text{CO}-\text{Cl}_2-\text{NOCl}$  system should therefore be inversely proportioned to the nitrosyl chloride concentration and directly proportional to the first power of the intensity of absorbed light, i.e.

$$\frac{d[\text{COCl}_2]}{dt} = \frac{A I_{abs}[\text{CO}][\text{Cl}_2]}{[\text{NOCl}]}$$

where  $A$  is a constant.

The preliminary investigations described\* in the following pages demonstrates that these predictions are almost entirely fulfilled.

### Experimental.

**Apparatus**—The apparatus is shown diagrammatically in Fig. 1. It consisted of a cylindrical reaction vessel A made of clear fused quartz, 2 cm. deep, 3.5 cm. radius and with optically plane ends. This vessel

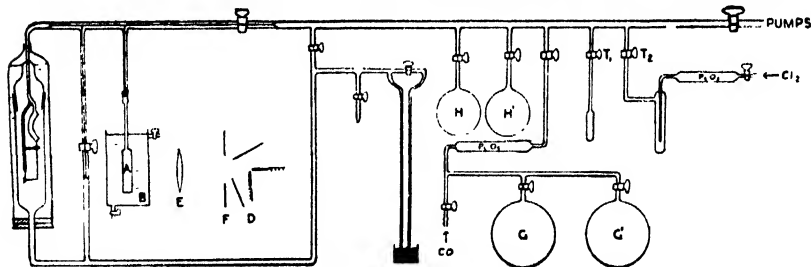


FIG. 1.—Apparatus.

was connected to a glass Bourdon gauge of the mirror type described by Foord,<sup>7</sup> through capillary tubing and a quartz-soda ground joint, and

\* It was not until after the MS. of this paper had been typed that the discovery by Chapman and Gee (*Trans. Chem. Soc.*, 1911, 1726) that 0.3% nitric oxide by volume prevented the combination of equimolar amounts of CO and  $\text{Cl}_2$  in sunlight at atmospheric pressure, came to the present author's notice. These workers correctly ascribed the inhibition to NOCl, and showed that sufficiently intense illumination could cause slow combination, but they did not pursue the investigation further.

<sup>6</sup> Dainton, *Trans. Faraday Soc.*, 1942, 38, 230.

<sup>7</sup> Foord, *J. Sci. Instr.*, 1934, 11, 126.

was clamped vertically in a water bath B fitted with glass windows and mounted on an optical bench. The light from a Zeiss automatic 220 v. D.C. carbon arc D mounted on the optical bench 18.0 cm. from A was condensed by a lens E (focal length 10 cm. and aperture 10 cm.) placed 8.5 cm. from A, so that a circular patch of light covered the front face of A. The intensity of the strong emission of the arc, i.e. visible and 2478 Å. line, was constant. A quick acting pneumatically operated shutter F was mounted on the optical bench 4.5 cm. from the arc. G and G' were 2-litre vessels for storage of carbon monoxide, H and H' smaller vessels used for making up dilute mixtures of NOCl in chlorine. The taps T<sub>1</sub> and T<sub>2</sub> led off to small glass bulbs immersed in liquid air and in which pure samples of nitrosyl chloride and chlorine were frozen until required. The whole apparatus could be evacuated rapidly by a 2-stage mercury diffusion pump backed by a Hyvac pump.

**Preparation of Gases** :—Nitrosyl chloride was made by the action of nitrosyl bisulphate on warm dry sodium chloride as described by Dainton and Norrish<sup>8</sup> and distilled *in vacuo* twice before use. Carbon monoxide was obtained by the action of concentrated sulphuric acid on dry sodium formate in a previously evacuated bulb at 140° C., and after washing by alkali was collected over water in a 10 l. aspirator. A sample from this aspirator was analysed by Miss D. McKay Ohm and contained 0.7 % N<sub>2</sub>, 0.10 % H<sub>2</sub>, 0.4 % O<sub>2</sub> and 98.8 % CO. This gas was dried by passage over phosphorus pentoxide and then passed over platinised asbestos heated electrically in a Pyrex tube, and finally through a liquid air trap, from which it was allowed to evaporate into the storage bulbs G and G'. It is unlikely that the gas used was less than 99.3 % CO, the remainder being N<sub>2</sub>. Chlorine was generated by dropping pure concentrated hydrochloric acid on to Analar potassium permanganate. It was dried over phosphorus pentoxide and fractionated *in vacuo* twice before use.

**Procedure** :—Owing to the corrosive action of chlorine and nitrosyl chloride on mercury, all pressure measurements were made using the Bourdon gauge which gave 20.1 mm. scale deflections for each 10.0 mm. Hg. The preparation of mixtures of gases containing accurately known small amounts of nitrosyl chloride between 1 and 10<sup>-2</sup> mm. Hg partial pressure, mixtures of chlorine with 1 % and 0.1 % nitrosyl chloride were made up in subsidiary mixing vessels H and H' and allowed to attain uniform composition for a period of at least 15 hours. All concentrations of gases were measured as the pressures they would exert at 18° C.

In each experiment the appropriate CO—Cl<sub>2</sub>—NOCl mixture was allowed to mix in the reaction vessel for a minimum time of 30 min. The arc was then started and the times and pressures recorded from the moment of opening the shutter F.

## Results.

The incident light intensity ( $I_0$ ) was constant throughout all the experiments and the temperature of the water bath controlled at 20° C.  $\pm$  0.5° C.

(a) **Pressure-Time Curves** : The form of the  $p$ - $t$  curves for the inhibited reaction was similar to that of the uninhibited reaction. Fig. 2 is a typical record. No induction periods were found although these have been recorded;<sup>9</sup> and their absence may be taken as evidence of the purity of the reactant gases. The decrease in pressure associated with the formation of phosgene was always preceded by an initial temporary pressure increase which was probably due to a combination of Budde and Draper effects. This effect was the larger the faster the reaction, and though it always occurred, was smaller the more nitrosyl chloride was present. The rate was taken as the initial slope in mm.

<sup>8</sup> Ref. 1, p. 412.

<sup>9</sup> Semenov, p. 129.

### 368 FORMATION OF PHOSGENE BY NITROSYL CHLORIDE

Hg/min. of the pressure time curve, which was straight over the first 15 mm. change. The rates recorded below were the average of several determinations.

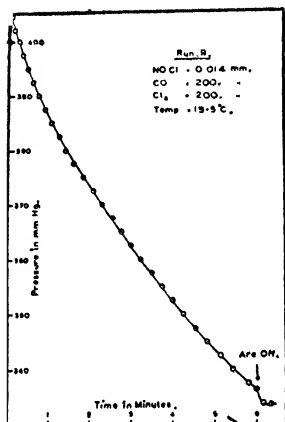


FIG. 2.—A typical pressure-time curve.

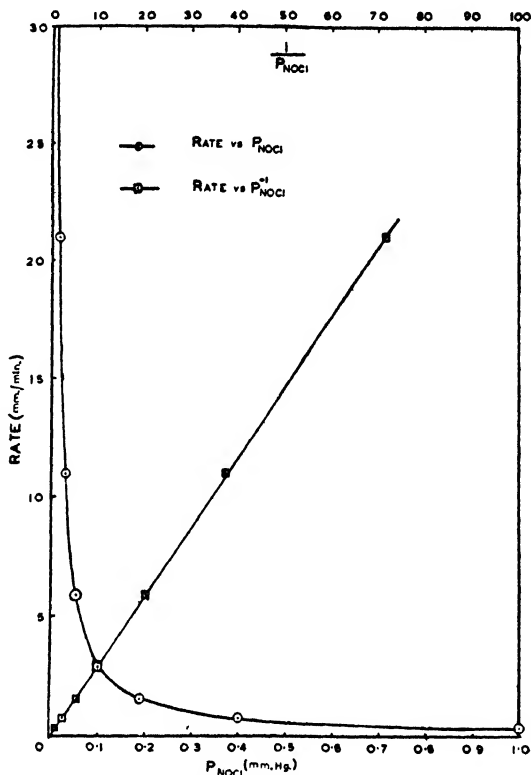


FIG. 3.—The dependence of rate on  $[\text{NOCl}]$ .

(b) **Dependence of the Rate on  $[\text{NOCl}]$ :** Nitrosyl chloride inhibits the formation of phosgene; 0.0035 % by volume reduces the rate to at least 1/rooth the uninhibited value. The effect of amounts of nitrosyl chloride ranging from 0.25 % to 0.003 % of the total gas present on the rate of combination of 200 mm. CO and 200 mm.  $\text{Cl}_2$  is shown in Table I

TABLE I

$[\text{NOCl}]$ mm. Hg	0	0.014	0.027	0.05	0.10	0.19	0.40	1.0
Initial Rate (mm. Hg/min.)	$100 \pm 5$	21.0	11.0	5.90	2.85	1.52	0.72	0.30
$[\text{NOCl}] \times \text{Rate}$	—	0.294	0.297	0.295	0.285	0.289	0.288	0.30

and Fig. 3, from which it is clear that the rate is inversely proportional to the nitrosyl chloride concentration.

(c) **Dependence of the Rate on  $[\text{Cl}_2]$ :** Maintaining the pressures of nitrosyl chloride and carbon monoxide constant at 0.1 mm. and 200 mm. respectively, the chlorine pressure was varied from 50 to 500 mm. The results are given in Table II and Fig. 4 and which show that the rate is

proportional to a power of the  $[Cl_2]$  approaching 2 but falling off at higher pressures.

TABLE II

$[Cl_2]$ in mm. Hg	50	100	200	300	400	500
Initial Rate (mm. Hg/min.)	0.22	0.82	2.85	6.0	8.35	11.0

(d) **Dependence of the Rate on  $[CO]$ :** With the pressures of chlorine and nitrosyl chloride kept constant at 200 mm. and 0.1 mm. respectively,

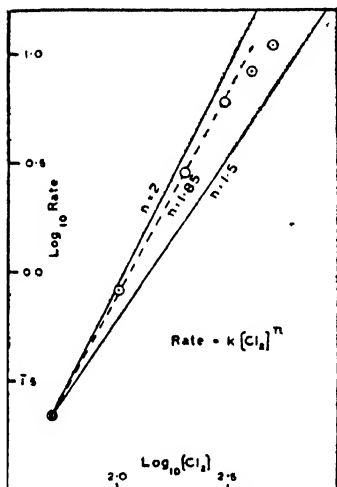


FIG. 4.—Dependence of rate on  $[Cl_2]$  at constant incident light intensity.

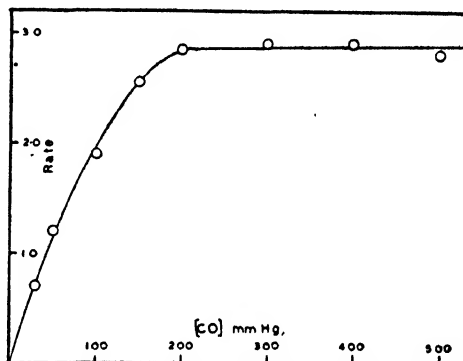


FIG. 5.—Dependence of rate on  $[CO]$ .

the carbon monoxide pressure was varied from 30 to 500 mm. The results are shown in Table III and Fig. 5. Below 150 mm. CO the rate

TABLE III

$[CO]$ in mm. Hg	30	50	100	150	200	300	400	500
Initial Rate (mm. Hg/min.)	0.70	1.20	1.90	2.55	2.85	2.90	2.90	2.80

is roughly proportional to  $[CO]$  whereas at pressures  $> 200$  mm. the rate is independent of  $[CO]$ .

### Discussion.

(a) **Mechanism of the Inhibition.**—The experimental results for the dependence of the rate of phosgene formation on reactant and inhibitor concentrations at constant incident light intensity are summarised in equation (2),

$$\frac{d[COCl_2]}{dt} = \frac{A[CO][Cl_2]^n}{[NOCl]\{B[CO] + C\}} \quad (2)$$

where  $A$ ,  $B$  and  $C$  are constants and  $n$  is about 1.85 for chlorine pressures up to 300 mm. and decreases at higher pressures.



## 370 FORMATION OF PHOSGENE BY NITROSYL CHLORIDE

The absence of half integral powers, and the inverse dependence of the rate on  $[\text{NOCl}]$ , is clear evidence that chain termination occurs by interaction of single chain centres with nitrosyl chloride, unlike the uninhibited reaction where the centres recombine in pairs. Chain termination steps involving nitric oxide and which would lead to a similar inverse relation between the rate and  $[\text{NOCl}]$  provided the equilibrium  $2\text{NO} + \text{Cl}_2 \rightleftharpoons 2\text{NOCl}$  was maintained are also feasible, e.g.  $\text{NO} + \text{Cl} = \text{NOCl}$  and  $\text{NO} + \text{COCl} = \text{NOCl} + \text{CO}$ . In view of the large excess of chlorine present which would ensure  $[\text{NOCl}] \gg [\text{NO}]$ , and because the former process might well require a third body it is considered justifiable to neglect such reactions in comparison with those involving nitrosyl chloride.

The mechanism of the uninhibited (i.e.  $\text{NOCl}$  free) reaction favoured by the Bodenstein school is

1.  $\text{Cl}_2 + h\nu \rightarrow \text{Cl} + \text{Cl}$ .
2.  $\text{Cl} + \text{CO} \rightarrow \text{COCl}$ .
- 2'.  $\text{COCl} \rightarrow \text{CO} + \text{Cl}$ .
3.  $\text{Cl}_2 + \text{COCl} \rightarrow \text{COCl}_2 + \text{Cl}$ .
4.  $\text{COCl} + \text{Cl} \rightarrow \text{CO} + \text{Cl}_2$ .

in which it is assumed that reactions 2 and 2' are in equilibrium. The kinetic form of this assumption is  $k_2 \cdot \frac{1}{2} \gg k_3[\text{Cl}_2] + k_4[\text{Cl}]$ , and combining this with the appropriate stationary state equations we obtain

$$\frac{d[\text{COCl}_2]}{dt} = k_3 \left[ \frac{k_1 k_2}{2k_4 k_2^1} \right]^{\frac{1}{2}} \cdot I_{\text{abs}}^{\frac{1}{2}} \cdot [\text{CO}]^{\frac{1}{2}} \cdot [\text{Cl}_2] \quad (3)$$

where  $k_2$ ,  $k_2^1$  and  $k_3$  and  $k_4$  are the appropriate rate constants and  $k_1$  is the quantum efficiency of the primary process. A feature of this scheme is the unusual termination step (4) which involves both centres, whereas it might have been expected that either the process  $\text{Cl} + \text{Cl} \rightarrow \text{Cl}_2(4^1)$  or the reaction  $\text{COCl} + \text{COCl} \rightarrow 2\text{CO} + \text{Cl}_2(4'')$  would have been responsible for stopping the chains. If reaction 4' was operating exclusively, the rate expression would be

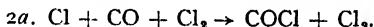
$$\frac{d[\text{COCl}_2]}{dt} = \frac{k_3 k_2}{k_2^1} \cdot \left( \frac{k_1}{2k_4^1} \right)^{\frac{1}{2}} \cdot I_{\text{abs}}^{\frac{1}{2}} [\text{CO}] [\text{Cl}_2] \quad (3')$$

which does not express the dependence of the rate on the carbon monoxide concentration correctly (cf. equation (1)) unless reaction 4' requires a third body which must be CO, i.e. is really  $\text{CO} + \text{Cl} + \text{Cl} \rightarrow \text{CO} + \text{Cl}_2(4')$ , when we must substitute  $k_4^1[\text{CO}]$  for  $k_4^1$  in equation (3'). If the recombination of  $\text{COCl}$  radicals was the only chain termination reaction the expression for the rate would become

$$\frac{d[\text{COCl}_2]}{dt} = k_3 \cdot \left( \frac{k_1}{2k_4^1} \right)^{\frac{1}{2}} \cdot I_{\text{abs}}^{\frac{1}{2}} [\text{Cl}_2] \quad (3'')$$

which also differs from equation (1). It is interesting that the expression (3'') would hold whether the equilibrium  $\text{COCl} \rightleftharpoons \text{CO} + \text{Cl}$  was, or was not, maintained.

It may therefore be concluded that, unless the reaction (4') is specifically catalysed by carbon monoxide, the termination reaction must be (4), viz.:  $\text{COCl} + \text{Cl} \rightarrow \text{CO} + \text{Cl}_2$ . This fact was also realised by Lenher and Rollefson,<sup>10</sup> who pointed out that the experimental rate equation could also be deduced from a reaction scheme involving the same reaction centres ( $\text{COCl}$  and  $\text{Cl}$ ), the same initiation (1) and termination (4) reactions as those postulated by Bodenstein, Lenher and Wagner;<sup>11</sup> but avoiding their condition that  $k_2[\text{CO}][\text{Cl}] = k_2^1[\text{COCl}]$ . Lenher and Rollefson omit reaction 2' and substitute 2a for reaction 2.



<sup>10</sup> Lenher and Rollefson, *J. Amer. Chem. Soc.*, 1930, **52**, 500.

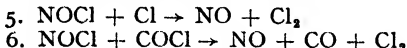
<sup>11</sup> Bodenstein, Lenher and Wagner, *Z. physik. Chem.*, B, 1929, **3**, 459.

Provided the chains are long, i.e.  $4k_3k_2[\text{CO}][\text{Cl}_2]^2 \gg k_4$ , this scheme leads to equation (4),

$$\frac{d[\text{COCl}_2]}{dt} = \left( \frac{k_1k_2k_3}{k_4} \right)^{\frac{1}{2}} \cdot I_{\text{abs}}^{\frac{1}{2}} \cdot [\text{CO}]^{\frac{1}{2}}[\text{Cl}_2] \quad (4)$$

The necessity of using the chain termination reaction (4) is readily demonstrated.<sup>12</sup> A weakness of Rollefson's scheme is that it implies that chlorine is a specific third body for the formation of the COCl radical, although this objection is somewhat weakened by the existence of theoretical evidence for strong interaction between a chlorine atom and a chlorine molecule.<sup>13</sup> This fact, combined with the conclusion that for the rate to decrease with temperature we have the unlikely inequality  $E_4 > E_{2a} + E_3$  lead us to prefer the Bodenstein scheme.

In the presence of nitrosyl chloride it is likely that reactions 5 and 6



will replace reaction 4 as the chain ending process, and accepting the Bodenstein propagation reactions, the rate of formation of phosgene will now be given by

$$\frac{d[\text{COCl}_2]}{dt} = \frac{k_1k_3I_{\text{abs}}[\text{CO}][\text{Cl}_2]}{[\text{NOCl}]\{k_2k_2'/k_2 + k_6[\text{CO}]\}} \quad (5)$$

so long as the  $\text{CO} + \text{Cl} \rightleftharpoons \text{COCl}$  equilibrium is maintained, i.e.

$$k_2^1 > k_3[\text{Cl}_2] + k_6[\text{NOCl}].^{14}$$

This equation has several points of interest in relation to equation (2) which summarises the experimental findings. It expresses the same kind of dependence of the rate on nitrosyl chloride and carbon monoxide concentration; and it is important that if either reaction 5 or 6 is omitted, then the observed variation of rate with  $[\text{CO}]$  cannot be accounted for. Equation (5) also provides an explanation of the decrease of  $n$  in equation (2) as the chlorine pressure is increased. The high extinction coefficient of chlorine gas in the region  $\lambda\lambda$  3000-4000  $\text{\AA}$ ., together with the path length employed (2 cm.) imply that only at very low chlorine pressures can  $k_1I_{\text{abs}}$  be set equal to  $k'I_0[\text{Cl}_2]$ ,  $I_0$  being the incident light intensity; and as the chlorine pressure is raised  $k_1I_{\text{abs}}$  may cease to be a function of the chlorine concentration. Hence, for a constant incident light intensity equation (5) indicates that at very low chlorine concentrations the order of reaction with respect to this substance would approach two, falling off to a limiting value of unity as the pressure of chlorine is raised. It is hoped to test this view at a later date by measurement of quantum yields.

### (b) Estimation of the Relative Rate Constants of Reactions 5 and 6 at 20° C.

The experimental results here presented establish the existence of facile reactions between nitrosyl chloride and either chlorine atoms or COCl radicals. By comparing the rates of the inhibited and uninhibited reactions, estimates may be made of the rate constants of reactions 5 and 6 in terms of the constants  $k_1/k_2'$ ,  $k_3$  and  $k_4$ . Thus in mixtures containing the same concentration of nitrosyl chloride and chlorine the ratio

<sup>12</sup> If 4' is the chain stopping reaction, the rate is  $k_2(k_1/2k_4')^{\frac{1}{2}} \cdot I_{\text{abs}} [\text{CO}][\text{Cl}_2]$ , which does not represent the results unless carbon monoxide is a specific third body. If 4'' is concerned, the rate is  $k_2(k_1/2k_4'')^{\frac{1}{2}} \cdot I_{\text{abs}}^{\frac{1}{2}} [\text{Cl}_2]$ , an equally unsatisfactory expression.

<sup>13</sup> Rollefson and Eyring, *J. Amer. Chem. Soc.*, 1932, **54**, 170.

<sup>14</sup> The Lenher-Rollefson propagation scheme leads to an equation of similar form to 5 (the differences being solely in the constants) and subject to the same limitation, i.e. that both reaction 5 and 6 must be included.

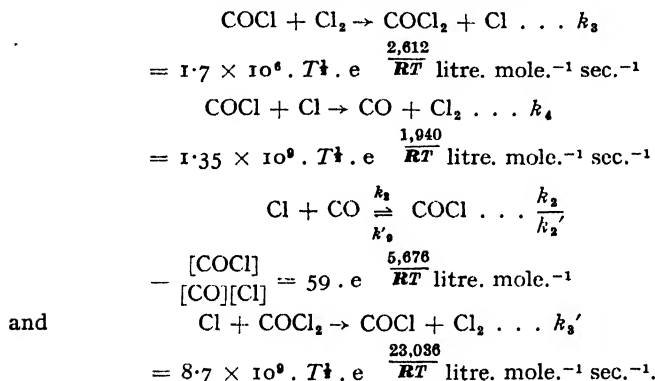
## 372 FORMATION OF PHOSGENE BY NITROSYL CHLORIDE

of the limiting rate at high concentrations of carbon monoxide to the dependence of the rate on carbon monoxide concentration in the region where the reaction is first order with respect to CO is  $k_3 k_3' / k_4 k_3$ . Further, the square of the rate of the uninhibited reaction divided by the rate of the inhibited reaction, where this is still dependent on carbon monoxide concentration, for the same pressures of chlorine and carbon monoxide, is  $k_3 k_3' [\text{NOCl}] [\text{Cl}_2] / 2k_4$ . Accurate values of these quantities must await more refined experiments, but examination of the present measurements in this way leads to the tentative values

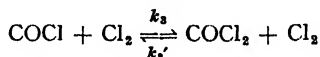
$$(k_3/k_4)^{20^\circ\text{C.}} = \text{ca. } 8 \times 10^{-3} (k_3/k_3')^{20^\circ\text{C.}}$$

$$\text{and } k_3^{20^\circ\text{C.}} = 8 \times 10^4 \cdot (k_4/k_3)^{20^\circ\text{C.}}$$

Bodenstein and Brenschede<sup>15</sup> have published the following values of the rate constants of the uninhibited reaction which they regard as being in best accord with their experimental data:—



In principle, by using these values, it is possible to calculate the velocity constants of reactions 5 and 6 in equal detail. In fact, closer inspection of these elaborate expressions, the details of the deduction of which have not been published, reveals them to be not entirely satisfactory. Firstly, if the radical COCl is supposed to have the triangular structure  $r_{\text{O-Cl}} = 1.70^*$  (cf. in COCl<sub>2</sub> where  $r_{\text{O-Cl}} = 1.68$ ),  $r_{\text{C-O}} = 1.30$  (cf. COCl<sub>2</sub> where  $r_{\text{C-O}} = 1.28$ ),  $\angle \text{O C Cl} = 120^\circ$  (cf.  $117^\circ$  in COCl<sub>2</sub>)<sup>17</sup> and vibration frequencies similar to the corresponding frequencies in phosgene,<sup>18</sup> and to exist in a doublet ground state; assumptions which are probably not grossly in error; approximate values of the vibrational, rotational<sup>19</sup> and translational partition functions at 20° C. may be computed. The corresponding functions for CO ( $g_{\text{vib.}} = 1$ ,  $\sigma = 1$ ,  $r = 1.13$ ,  $\nu = 2168 \text{ cm.}^{-1}$ ) and the chlorine atom ( $g_{\text{vib.}} = 4 + 2 \cdot e^{-ch \cdot 881/kT}$ ) can also be evaluated. Following established methods the approximate value of the non-exponential term in the equilibrium constant  $k_3/k_3'$  at 27° C. may be computed to be about  $1.5 \times 10^{-3} \text{ litre. mole.}^{-1}$  in marked contrast to Bodenstein's value of 59. Secondly, using the same model for the COCl radical the non-exponential term in the equilibrium constant ( $= k_3/k_3'$ ) in the reaction



\* All internuclear distances are in Å.

<sup>15</sup> Bodenstein and Brenschede, *Z. physik. Chem. B*, 1938, **40**, 121; **41**, 254.

<sup>16</sup>  $k_3'$  refers to the reverse of reaction 3. It does not take place to any appreciable extent in the photosynthesis of phosgene, and is included for completeness and later discussion.

<sup>17</sup> See Brockway, Beach and Pauling, *J. Amer. Chem. Soc.*, 1935, **57**, 2693.

<sup>18</sup> Thompson, *Trans. Faraday Soc.*, 1941, **37**, 257.

<sup>19</sup> The symmetry number is taken as unity.

may be similarly computed. At 27° c. the computed value is  $2 \times 10^{-3}$  whereas Bodenstein's expressions for  $k_3$  and  $k_3'$  indicate  $2 \times 10^{-4}$  for this quantity. Thirdly, there are theoretical reasons<sup>20</sup> for believing that a reaction between a radical and an atom (COCl and Cl), which are under the influence of attractive polarisation forces at all ranges, is not characterised by a precisely defined energy of activation, contrary to the expression adduced by Bodenstein for  $k_4$ . The values of  $k_3/k_3'$  advanced

by Bodenstein, or the values of  $k_3/k_3' \cdot e^{\frac{-(E_3-E_3')}{RT}}$  calculated above,

taken in conjunction with the experimental results render it probable that  $k_3 \ll k_3'$  at 20° c. This difference may lie entirely in the difference between  $E_3$  and  $E_3'$  and be entirely unconnected with the non-exponential terms; but preliminary calculations based on conjectural activated complexes of plausible configuration indicate the possibility of the non-exponential term in  $k_3$  being considerably greater than the corresponding term in  $k_3'$ . This effect is due partly to the higher moments of inertia of the activated complex of reaction 6, partly to the possibility of internal rotation in this complex and partly to its generally "looser" structure<sup>21</sup> compared with the complex for reaction 5. Such large differences in these terms would not be predicted by the classical collision theory applied to these reactions.

We wish to thank Dr. B. A. Kilby for assistance in recording some of the more rapid reactions, and Messrs. N. Sheppard and D. A. Ramsay for calculating moments of inertia of unsymmetrical molecules. We are also grateful to Professors Norrish and Melville for helpful criticism.

### Summary.

The photosynthesis of phosgene from carbon monoxide and chlorine has been shown to be retarded very strongly by traces of nitrosyl chloride. The pressure-time curves for the inhibited and uninhibited reactions are of similar shape. At constant incident light intensity the rate of the inhibited reaction is summarised by

$$\frac{d[\text{COCl}_2]}{dt} = \frac{A[\text{CO}][\text{Cl}_2]^n}{[\text{NOCl}]\{B[\text{CO}] + C\}}$$

where  $A$ ,  $B$  and  $C$  are constants and  $n$  decreases with pressure of chlorine from a value of about unity at high pressure to a value of 2 at low pressures.

A chain mechanism for the inhibited reaction is suggested which is:—

- (1)  $\text{Cl}_2 + h\nu \rightarrow \text{Cl} + \text{Cl}$ ; (2)  $\text{Cl} + \text{CO} \rightarrow \text{COCl}$ ; (2')  $\text{COCl} \rightarrow \text{CO} + \text{Cl}$ ; (3)  $\text{COCl} + \text{Cl}_2 \rightarrow \text{COCl}_2 + \text{Cl}$ ; (5)  $\text{Cl} + \text{NOCl} \rightarrow \text{NO} + \text{Cl}_2$ ; (6)  $\text{COCl} + \text{NOCl} \rightarrow \text{NO} + \text{CO} + \text{Cl}_2$ ; and which differs from the scheme suggested by Bodenstein for the uninhibited process in that (5) and (6) replace (4)  $\text{Cl} + \text{COCl} \rightarrow \text{CO} + \text{Cl}_2$ , as the chain termination mechanism.

The values proposed by Bodenstein for  $k_3/k_3'$ ,  $k_3/k_3'$  and  $k_4$ , together with reactions (5) and (6), are discussed in terms of the transition state theory.

<sup>20</sup> See for example the discussion of the association of two methyl radicals given on p. 220 *et seq.* of ref. 3. Following the argument there advanced, taking the ionisation potential and polarisability of the chlorine atom to be 13.01 ev. and  $3.6 \times 10^{-24}$  cc. molecule<sup>-1</sup> respectively; and assuming the ionisation potential of COCl to be 8 ev. (cf. the value of 8.4 ev. calculated by Mulliken, *J. Chem. Physics*, 1933, 1, 492, for  $\text{CH}_3$ ) and its polarisability to be  $4 \times 10^{-24}$  cc. molecule<sup>-1</sup> ( $= \alpha_{\text{C}=\text{O}} + \alpha_{\text{C}-\text{Cl}}$ ),  $k_4^{27^\circ\text{C.}}$  is computed to be  $2.4 \times 10^{11}$  litre. mole<sup>-1</sup> sec<sup>-1</sup>. The Bodenstein expression gives  $1.6 \times 10^{10}$ .

<sup>21</sup> This "loose" structure might be expected for the complex of a reaction in which two triatomic units form three diatomic molecules.

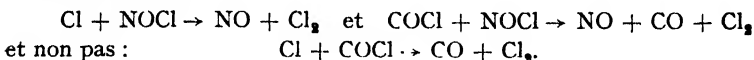
## Résumé.

La photosynthèse du phosgène, à partir de l'oxyde de carbone et du chlore, est fortement retardée par des traces de chlorure de nitrosyle. A une intensité constante de lumière incidente, la vitesse de la réaction inhibée est donnée par

$$\frac{d[\text{COCl}_2]}{dt} = \frac{A[\text{CO}][\text{Cl}_2]^n}{[\text{NOCl}]\{B[\text{CO}] + C\}}$$

où  $A$ ,  $B$ ,  $C$  sont des constantes et où  $n$  décroît pour des pressions croissantes de chlore, depuis une valeur de 2 à basse pression jusqu'à environ l'unité à haute pression.

Un mécanisme en chaîne pour la réaction inhibée diffère de celui suggéré par Bodenstein pour le processus non inhibé, par le mécanisme de terminaison de chaîne :

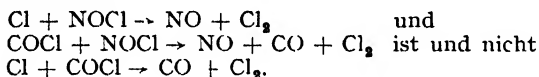


## Zusammenfassung.

Die Photosynthese von Phosgen wird durch Spuren von Nitrosylchlorid stark verzögert. Bei konstanter Belichtungsintensität kann die Geschwindigkeit der verzögerten Reaktion durch

$$\frac{d[\text{COCl}_2]}{dt} = \frac{A[\text{CO}][\text{Cl}_2]^n}{[\text{NOCl}]\{B[\text{CO}] + C\}}$$

ausgedrückt werden, wobei  $A$ ,  $B$ ,  $C$  Konstanten sind und  $n$  bei Druckerhöhung von 2 bis auf ungefähr 1 fällt. Ein Kettenreaktionsmechanismus für die verzögerte Reaktion unterscheidet sich von dem von Bodenstein für die gewöhnliche Reaktion vorgeschlagenen dadurch, dass der Kettenabbruchmechanismus.



Laboratory of Physical Chemistry,  
Cambridge University.

## THE DEPENDENCE ON STATE OF THE APPARENT DIPOLE MOMENTS OF AMMONIA, METHYLAMINE, DIMETHYLAMINE, AND TRIMETHYLAMINE.

By R. J. W. LE FÈVRE\* AND P. RUSSELL.

Received 1st July, 1946.

At the time when this work was started it had already become clear that whilst the majority of molecular species, examined by conventional methods,<sup>1</sup> gave apparent dipole moments varying with the state in the gradation :

$$\mu_{\text{gas}} > \mu_{\text{dissolved}} > \mu_{\text{liquid}}$$

there exists a minority for which these quantities are nearly equal or even

\* Present Address : Chemistry Dept., University of Sydney, Australia.

<sup>1</sup> Debye, *Polar Molecules*.

for which the order is reversed.<sup>1-10</sup> Recorded experimental data<sup>8</sup> displaying the less common relationships were, however, sparse and often old or uncertain.

Several workers<sup>7-10</sup> had indicated how molecular geometrical or derived factors could be used to forecast *a priori* the ratios of the differently determined moments and it therefore seemed that a useful contribution to the problem would be to take a series of structurally related simple molecules, which might be expected to exhibit the less usual behaviour, and study the dielectric polarisations of each in the gaseous, dissolved, and liquid conditions. Ammonia and its three methylated derivatives were selected for this purpose.

Accordingly, we constructed apparatus of a convenient type for the measurement of the dielectric constants of gases and liquids. The details of design and standardisation of these, together with their use in the present work, are described in the following three Sections of this paper. The results are summarised and discussed in Section 4.

## Section I. The Dielectric Polarisation of Ammonia, Methylamine, Dimethylamine, and Trimethylamine as Vapours.

The majority of reliable measurements of the dielectric coefficients of gases and vapours have been made by the heterodyne null beat method. This can be extremely sensitive, but in the opinion of the authors possesses, in operation under laboratory conditions, some disadvantages due to its complexity. On the other hand, owing to the difficulty of constructing circuits with a decrement of less than 1 %, the simple resonance method with a parallel condenser (as employed for measurements with liquids and solutions) cannot be made sufficiently delicate. Groves and Sugden<sup>11</sup> therefore utilised a variation in which all capacity readings were referred to a point on *one* side of the resonance curve and in which a *series* method of measuring changes of capacity was used. In view of criticisms by Watson,<sup>12</sup> it seemed likely that such an arrangement would be liable to errors arising from either frequency drift or amplitude changes, or both, in the oscillator.

It appeared, therefore, that to retain the advantages of the resonance method it would be necessary to devise some modification in this technique which would allow readings to be taken *on each side* of a current-capacity curve not more than a few  $\mu\text{F.}$  wide.

**Present Method.**—The last requirement has been satisfied by utilising the properties of a resonance circuit in parallel with a small condenser whose dielectric is a section of a quartz crystal. If this circuit (e.g.,  $L_2C_2$  in the diagrams below) is approximately tuned to the natural frequency ( $f_0$ ) of the quartz section and is coupled to a generator ( $L_1C_1$ ) of variable frequency a response curve is obtained in the voltmeter circuit  $V_2$ ,  $G$ , etc.) containing a sharp crevasse (cf. Fig. 1). The decrement of this circuit is determined principally by the quartz. A calculation from the sharpness of the crevasses gives values *ca.* 0.05 % for the equivalent decrement. The response frequency ( $f_0$ ) of a wavemeter of this type will depend on (1) the size of the air gaps between the crystal and its holder, and (2) the closeness to resonance of the tuned circuit in which the quartz condenser is contained.

<sup>1</sup> Müller, *Physik. Z.*, 1933, **34**, 689.

<sup>3</sup> Jenkins, *Nature*, 1934, **133**, 106.

<sup>4</sup> Sugden, *ibid.*, 415.

<sup>5</sup> Le Fèvre, *J. Chem. Soc.*, 1935, 773.

<sup>6</sup> Henriquez, *Rec. Trav. Chim.*, 1935, **54**, 574.

<sup>7</sup> Le Fèvre, *Nature*, 1935, **136**, 181.

<sup>8</sup> Le Fèvre, and Le Fèvre, *J. Chem. Soc.*, 1935, 1747.

<sup>9</sup> Higasi, *Sci. Pap. I.P.C.R.*, 1936, **28**, 284.

<sup>10</sup> Frank, *Proc. Roy. Soc. A*, 1935, **152**, 171.

<sup>11</sup> Groves and Sugden, *J. Chem. Soc.*, 1934, 1094.

<sup>12</sup> Watson, Rao and Ramaswamy, *Proc. Roy. Soc. A*, 1933-34, **143**, 558.

Dye<sup>13</sup> has, however, shown that the chief effect of detuning is to blunt the crevasse, the *displacement* being negligible. By altering  $C_p$  in the oscillator until maximum absorption occurs it is possible to adjust the frequency with an accuracy of 1 part in 50,000. To obtain the precision desired for the present work it is necessary to set the frequency to 1 part in 10<sup>6</sup>; measurements have therefore always been made in pairs, one on each side of the crevasse. All readings were taken at the same value of the anode current of the valve voltmeter in the wavemeter.

In our final apparatus the condenser system (gas cell,  $C_g$ , standard variable condenser,  $C_p$ , etc. in parallel) was placed in the anode circuit of a dynatron oscillator (A). With such an arrangement, comparisons of

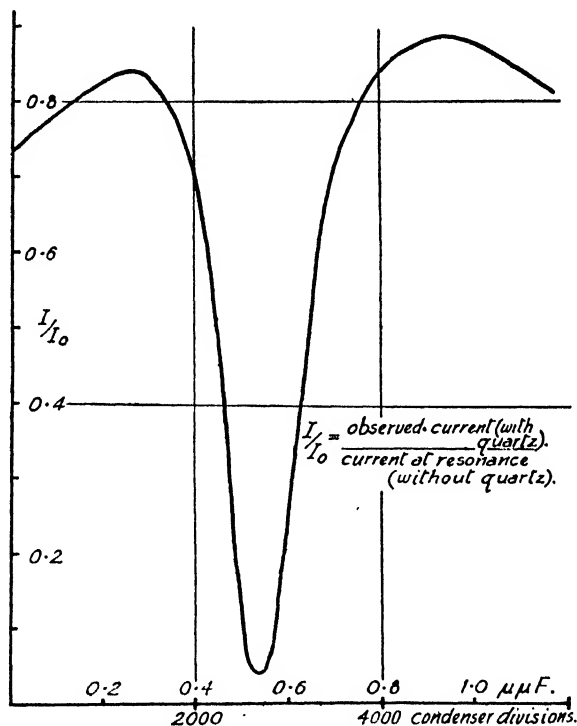


FIG. 1.

capacities are possible because the *total capacity* in the anode circuit of the generator is capable of adjustments such that the frequency of oscillation, indicated by the response of the quartz, is the same. If the inductance remains unaltered the constancy of total capacity for a fixed frequency provides a means of estimating any increases in the capacity of the condenser, by making compensating decreases in the parallel measuring condenser.

It is believed that this apparatus gives the sensitivity of the heterodyne method without losing the essential simplicity and consequent reliability of the resonance methods.

**Constructional Details.**—A diagram of the apparatus employed is shown in Fig. 2. The oscillatory circuit (A) consisted of an inductance  $L_1$  in parallel with three condensers,  $C_1$ ,  $C_p$  and  $C_g$  driven by a Mullard PM12 valve ( $V_1$ ) with 36 v. and 74 v. on the anode and screen grid respectively. The wavemeter (B) consisted of an inductance  $L_2$  in parallel with a 500  $\mu F$ .

<sup>13</sup> Dye, *Proc. Physic. Soc.*, 1926, 38, 399.

condenser  $C_s$ , and a suitably mounted quartz crystal  $Q$  which had a natural frequency of 837 kc./sec. The potential developed across the quartz was observed with a thermionic voltmeter.  $V_s$  was a Mullard PM4DX valve.  $R_1$  was a potentiometer used for biasing the grid of the valve, a value of ca. 1 v. being used. The galvanometer  $G$  in the anode circuit was used as a null instrument, the steady anode current being balanced out by an accumulator in series with the variable resistance  $R_2$ . The values of the various components were:  $C_1$ , 100  $\mu\text{F}$ .;  $C_2$ , 500  $\mu\text{F}$ .;  $C_3$ ,  $C_4$ , 2.  $\mu\text{F}$ .;  $C_5$ , 1  $\mu\text{F}$ .;  $R_1$ , 20  $\omega$ ;  $R_2$ , 40,000  $\omega$ ;  $R_3 \approx 0.5 \text{ M}\omega$ .  $L_3$  was a choke, 250,000  $\mu\text{H}$ .

The two inductances  $L_1$  and  $L_2$  were coils of 4 in.-diam. consisting of 28 and 35 turns respectively of no. 26 d.c.c. wire wound on ebonite formers. They were placed with their axes parallel to each other and separated by a distance of 40 cm. The total anode current in the wave-meter circuit did not exceed 5  $\mu\text{a}$ . and a change of current of  $2 \times 10^{-8}$  amp. was detectable. This corresponded to a change of 0.0002  $\mu\text{F}$ . in the measuring condenser  $C_p$ .

The gas condenser  $C_g$  consisted of three rhodium plated brass tubes 10 cm. long. These were mounted concentrically, the central cylinder being insulated from the other two by Pyrex spacers. The inner and outer tubes were held together, in a press fit, by accurately machined

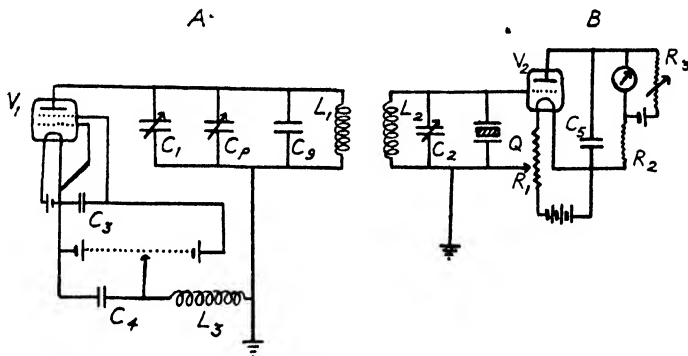


FIG. 2.

annular end caps through which the insulated lead was led by a Pyrex bush. The condenser was sealed into a hollow cylindrical Pyrex glass vessel; the leads were platinum and were taken through the walls to mercury contacts in tubes just above the container. The capacity of the condenser was about 220  $\mu\text{F}$ . The only mixed dielectric in the cell is the capacity between the insulated lead and earth. (Calculation showed that this would not affect the observable linearity between capacity and dielectric constant).

Changes in the capacity of this condenser caused by the introduction of a gas were measured by the precision condenser,  $C_p$ , in parallel. This was of the stepped rod type, and was similar to that described by Watson, Rao, and Ramaswamy.<sup>13</sup> It had a total capacity of 27  $\mu\text{F}$ . and a capacity range of 1.2  $\mu\text{F}$ . The condenser could be set with an accuracy of 0.0002  $\mu\text{F}$ .  $C_1$  was a short wave radio condenser used to tune the oscillator to the frequency of the quartz. It remained unaltered during a series of measurements.

The gas cell was placed in an electrically heated oil bath, surrounded by two air jackets to minimise thermal conduction to the rest of the apparatus. The temperature of the bath did not vary by more than 0.5° during a series of measurements which usually took two hours, and was obtained from mercury thermometers in the bath with an accuracy of 0.3°. The pressure of the gas in the cell was read from a mercury manometer.



**Operation.**—Before making measurements the apparatus was allowed to run for several hours with the oscillator tuned to the frequency of the quartz. The cell which was filled with gas while the apparatus was reaching thermal equilibrium was washed out with the vapour several times and then evacuated. The precision condenser was adjusted until zero current flowed through the galvanometer and a second reading then taken on the other side of the crevasse. The vapour was allowed to enter the cell, its pressure was recorded and the procedure repeated. A second vacuum reading was then made. A single determination involving six readings usually took eight minutes. All readings were made in the same direction

TABLE I  
Example : Dimethylamine at 93.0° c.

$p$ (cm.).	$C_1$ .	$C_2$ .	$\bar{C}$ .	$C$ .
67.35	4082	4872	4477	3291.5
	795	1582	1188.5	
	4088	4876	4482	
25.15	2873	3659	3266	1216.5
	4090	4876	4483	
68.15	761	1550	1155.5	3327.2
	4096	4875	4482.5	
24.60	2900	3680	3290	1190
	4086	4870	4478	
47.70	1761	2547	2154	2325
	4086	4073	4479.5	
39.65	4155	4936	4545.5	1930
	2225	3005	2615	
	4155	4934	4544.5	
40.10	2210	2982	2596	1949.5
	4158	4835	4546.5	
	4162	4941	4551.5	
19.70	3218	3987	3602.5	950.2
	4165	4942	4553.5	
22.65	3069	3842	3455.5	1098.5
	4167	4942	4554.5	
50.80	1687	2465	2076	2477.5
	4164	4941	4552.5	
49.75	1739	2522	2130.5	2423.3
	4165	4945	4555	
30.70	2677	3458	3067.5	1488.8
	4167	4948	4557.5	
31.70	2633	3415	3024	1533.8
	4168	4948	4558	
60.50	1220	2000	1610	2947.7
	4167	4948	4557.5	

to avoid errors due to backlash in the precision condenser, and any set of measurements during which there was a large change in frequency were discarded; observations were taken alternately at high and low pressures. The number of readings obtained was too great to be shown in full. A typical set is shown in Table I, in which the five columns contain respectively 1, the pressures at which readings were taken, 2, and 3, the settings on the precision condenser, 4, the arithmetic means of these, and 5, the differences between the  $\bar{C}$  values when the cell was evacuated and filled to the stated pressure.

The crevasse was symmetrical and any slight variations of amplitude during a series of measurements did not affect the mean value of a pair of readings. The part of the crevasse at which readings were made varied slightly for each series of determinations; the extreme limits of amplitude

were between 600 and 1000 scale divisions of the precision condenser (Fig. 1). The replaceable capacity of the gas cell at  $25^\circ$  was equivalent to  $1.124 \times 10^6$  scale divisions of the precision condenser. A series of experiments was made with carbon dioxide in which the apparatus was adjusted so that readings of the condenser when the cell was evacuated fell on different parts of the scale. The value of  $\delta C$  for any particular pressure of gas was independent of the part of the scale at which the readings were taken, showing that the precision condenser followed a linear capacity law.

**Limitations of the Apparatus.**—Before summarising the remainder of our observations and discussing calculations based upon them, an examination of the present use of the apparatus will be given. For this it is necessary to consider in further detail the dependence of the frequency of oscillation upon the components of the circuit and their relative positions in that circuit. The dynatron circuit may be represented as shown in Fig. 3; it consists of a driving impedance —  $Z_a$  coupled to a circuit of

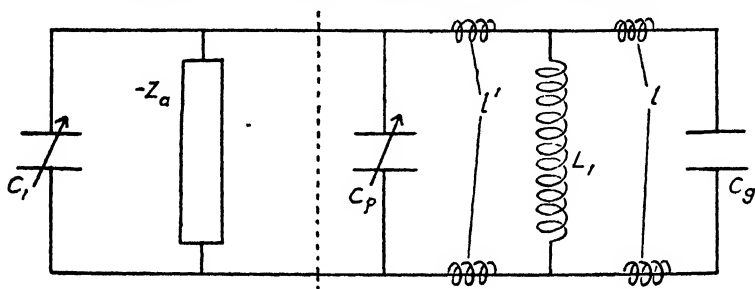


FIG. 3.

total impedance  $Z$ . For the maintenance of oscillations of constant amplitude

$$-Z_a + Z = 0.$$

Let  $l' + l$  be the inductances of the leads between the two condensers  $C_p$  and  $C_g$  and the inductance  $L_1$ . The conditions of the experiment are that the introduction of gas into the condenser  $C_g$  causes it to increase its capacity by  $\delta C_g$  which is compensated by reducing the capacity of the precision condenser  $C_p$  by  $-\delta C_p$  so that the total impedance of the circuit, and the frequency of oscillation, remain unvaried. Since  $C_1$  stands unaltered during an experiment and the resistance of the circuit is unaffected by change in  $C_p$  and  $C_g$ , it is sufficient to consider the conditions under which the reactance  $X$  of the components on the right of the dotted line remain constant. This is the case when

$$\frac{1}{X} = \frac{1}{X_p} + \frac{1}{X_{l'} + \left[ \frac{1}{X_L} + \frac{1}{X_g + X_l} \right]^{-1}} = \text{a constant}$$

whence

$$C = C_p + \left[ C_g(1 + \omega^2 l C_g) - \frac{1}{\omega^2 L} \right] \left[ 1 - \frac{l'}{L} + \omega^2 l' C_g(1 + \omega^2 l C_g) \right]$$

$$C_p + C_g(1 + \omega^2 \cdot \overline{l + l'} C_g) - \frac{2l'}{L} C_g(1 + \omega^2 l C_g) = \text{const.} \quad (i)$$

Considering small changes in  $C_p$  and  $C_g$

$$\delta C_p = \delta C_g \left[ 1 + 2\omega^2 \cdot \overline{l + l'} \cdot C_g - \frac{2l'}{L}(1 + 2\omega^2 l C_g) \right] \quad (ii)$$

In the final apparatus the inductance was placed between the two condensers for reasons of constructional convenience although its more logical

position would be between  $-Z_s$  and  $C_p$ . It is important to notice that this alteration in position is entirely responsible for the introduction of the term

$$\frac{2l'}{L} C_s (1 + \omega^2/C_s) \text{ in equation (i).}$$

Measurements made relative to a gas of known dielectric constant only require proportionality between  $\delta C_p$  and  $\delta C_s$ . Equation (ii) shows (since the quantity within the square brackets is a constant) that this condition will be satisfied if all determinations are made at one frequency.

In the present work carbon dioxide was used as the standard gas. Air was considered unsuitable for this purpose, being a mixture, having a small dielectric constant, and the published values not being so concordant as those for carbon dioxide.

**The Dielectric Constant of Carbon Dioxide.**—Thirteen absolute

determinations of the dielectric constant of  $\text{CO}_2$  have been made. These are listed in Table II. The various values have been corrected to  $25^\circ$  and 760 mm. Other determinations at high pressures have been made by Keyes and Kirkwood<sup>26</sup>,<sup>27</sup> and John.<sup>28</sup> Of the tabulated results, those due to Stuart, McAlpine and Smyth, and Watson are probably the most accurate. From these measurements after correcting for the compressibility, the polarisation of carbon dioxide, which was assumed to be temperature invariant, was taken as 7.341 cc. Measurements have been made with carbon dioxide at six tem-

TABLE II

Reference.	$(s - 1) \times 10^6$ .	Author.
14	867	Boltzmann
15	902	Klemencie
16	911	Pohrt
17	919	Reigger
18	1013	Jona
19	869	Fritts
20	891	Zahn
21	920	Braunmühl
22	904	Stuart
23	882	Forro
24	906	McAlpine and Smyth
12	906	Watson
25	905	Kubo

peratures, No deviation from proportionality between  $\delta C$  and  $p$  was observed. The actual values obtained are given in Table III.

TABLE III

$T(^{\circ}\text{A})$ .	$\left(\frac{\delta C}{p}\right)$ .	$\left(\frac{\delta C}{p}\right)$ calc.	$p$ Range in Cm. of Hg.	Number of Observations.
297.4	13.33	13.37	50-90	10
319.4	12.45	12.43	20-80	16
342.7	11.65	11.57	53-90	13
374.4	10.57	10.56	46-92	10
398.3	9.83	9.91	50-96	10
439.6	8.97	9.95	60-96	10

<sup>14</sup> Boltzmann, *Pogg. Ann.*, 1875, **155**, 403.

<sup>15</sup> Klemencie, *Wien. Ber.*, 1885, **91**, 712.

<sup>16</sup> Pohrt, *Ann. Physik*, 1913, **42**, 569.

<sup>17</sup> Reigger, *ibid.*, 1919, **59**, 753.

<sup>18</sup> Jona, *Physik. Z.*, 1919, **20**, 14.

<sup>19</sup> Fritts, *Physic. Rev.*, 1924, **23**, 345.

<sup>20</sup> Zahn, *ibid.*, 1926, **27**, 455.

<sup>21</sup> Braunmühl, *Physik. Z.*, 1927, **28**, 141.

<sup>22</sup> Stuart, *Z. Physik*, 1928, **47**, 457.

<sup>23</sup> Forro, *ibid.*, 430.

<sup>24</sup> McAlpine and Smyth, *J. Amer. Chem. Soc.*, 1933, **55**, 453.

<sup>25</sup> Kubo, *Sci. Pap. I.P.C.R.*, 1935, **26**, 242.

<sup>26</sup> Keyes and Kirkwood, *Physic. Rev.*, 1930, **36**, 754.

<sup>27</sup> Uhlig, Kirkwood and Keyes, *J. Chem. Physics*, 1933, **1**, 155.

<sup>28</sup> John, *Phil. Mag.*, 1936 (7), **22**, 274.



TABLE IV

$T(^{\circ}\text{A.})$	$\left(\frac{\delta C}{P}\right)_{P \rightarrow 0}$	$P$	$P_{\text{calc.}}$	$\rho$ Range in cm. of Hg.	No. of Observations.
<b>Ammonia.</b>					
293.8	92.76	50.22	50.25	15.40	9
318.0	(80.30)	(47.20)	(46.87)	17.44	10
346.8	(68.51)	(44.00)	(43.46)	24.48	13
375.4	58.30	40.65	40.61	23.56	10
419.4	47.23	36.93	36.96	30.60	10

$$P = 5.90 + 13030/P.$$

**Methylamine.**

292.6	84.31	45.48	45.54	21.38	9
294.5	83.30	45.23	45.32	17.45	8
300.8	80.34	44.61	44.58	13.41	10
321.8	(70.13)	(41.72)	(42.37)	19.44	6
347.4	62.42	40.19	40.02	26.50	7
352.1	(60.09)	(39.21)	(39.63)	19.52	10
379.1	53.63	37.75	37.57	23.61	10
420.0	44.36	34.72	34.94	28.56	8

$$P = 10.58 + 10230/T.$$

**Dimethylamine.**

292.4	68.77	37.09	37.00	19.50	8
321.3	58.59	34.80	35.02	24.48	12
343.9	52.92	33.70	33.71	21.55	17
366.1	48.23	32.78	32.57	19.68	14
437.1	36.54	29.80	29.71	40.61	6
439.5	35.94	29.48	29.63	29.60	8

$$P = 14.96 + 6447/T.$$

**Trimethylamine.**

294.1	52.63	28.56	28.66	28.63	14
295.4	52.46	28.59	28.62	27.61	8
319.9	47.28	27.97	27.96	22.70	10
343.9	43.25	27.56	27.40	27.69	12
372.0	39.04	26.96	26.84	37.62	5
403.1	35.08	26.30	26.31	39.81	11
404.1	34.91	26.26	26.30	47.80	6
440.8	31.19	25.67	25.77	49.81	7

$$P = 20.01 + 2553/T.$$

observations on ammonia and the three methylamines. Column 3 shows the polarisation calculated by equation (v) and column 4 the calculated values when represented by equation (vi). Table V shows the dipole moments, distortion polarisations (electronic plus atomic polarisations =  $A$ ) and the total polarisations at  $25^{\circ}$  c. calculated from the present work: while Table VI compares our results with those of previous observers. The values in brackets (Table IV) show the results of

TABLE V

	$\mu$ .	$P_D$ .	$^{25}P_T$ .
$\text{NH}_3$	1.45	5.90	49.60
$\text{MeNH}_2$	1.28	10.58	44.90
$\text{Me}_2\text{NH}$	1.02	14.96	36.59
$\text{Me}_3\text{N}$	0.64	20.01	28.57

experiments in which the compressibility correction was uncertain: these figures have not been used for calculating the relation between  $P$  and  $T$ .

TABLE VI

Previous Measurements.		NH <sub>3</sub> .	MeNH <sub>2</sub> .	Me <sub>2</sub> NH.	Me <sub>3</sub> N.
18	Jona . . . . .	1.53	—	—	—
20	Zahn . . . . .	1.44	—	—	—
30	Watson . . . . .	1.48	—	—	—
31	Hojendahl . . . . .	—	1.31	1.05	—
32	Steiger . . . . .	1.47	1.23	0.96	0.60
33	Ghosh and Chatterjee . . . . .	—	0.99	0.90	0.82
26	Keyes and Kirkwood . . . . .	1.44	—	—	—
27	Uhlig, Keyes and Kirkwood . . . . .	1.48	—	—	—
34	Smyth and de Bruyne . . . . .	1.47	—	—	—
35	Ramaswamy . . . . .	—	1.25	—	—
36	Groves and Sugden . . . . .	—	1.32	1.02	0.65
	Present work . . . . .	1.45	1.28	1.02	0.64

## Materials.

**Carbon Dioxide** was taken from a cylinder; dried with P<sub>2</sub>O<sub>5</sub> and distilled several times. Some earlier measurements were made with CO<sub>2</sub> from a Kipp washed with NaHCO<sub>3</sub> and dried with H<sub>2</sub>SO<sub>4</sub> and P<sub>2</sub>O<sub>5</sub>. However, the gas had a larger dielectric constant/temperature coefficient than that from the cylinder and the results are not recorded.

**Ammonia** was taken from a cylinder of anhydrous ammonia; dried over soda lime and distilled repeatedly through a soda lime tower. The use of metallic sodium as a drying agent as employed by Kirkwood and Keyes<sup>26</sup> and Uhlig, Kirkwood and Keyes<sup>27</sup> was unsafe.

**Methylamine.** A 33 % aqueous solution was distilled; dried with soda lime and distilled repeatedly over soda lime.

**Dimethylamine.** B.D.H. "anhydrous" Me<sub>2</sub>NH was allowed to stand over soda lime and fractionally redistilled before use.

**Trimethylamine** was prepared as follows. Ammonium chloride (500 g.) was heated with paraformaldehyde (1330 g.) at 85°. The temperature was gradually raised to 160° as the reaction proceeded. Caustic soda (1100 g.) in water (2 litres) was slowly added to the trimethylamine hydrochloride, and the free amine after passing through a soda lime tower condensed. Several distillations over soda lime followed. The material used had a vapour pressure of 658 mm. at 0° and 96.1 mm. at 11°, corresponding with a b.p. 3.9°/760 mm. (Hofmann 3.4 — 3.8°).<sup>37</sup>

## Section (2). The Dielectric Polarisation of Ammonia, Methylamine, Dimethylamine, and Trimethylamine as Dilute Solutions in Benzene.

The measurements recorded in this section involved the obvious experimental difficulties associated with gaseous solutes. When this work was planned three previous investigations of this type were described in the literature—namely those of Fairbrother on the halogen hydrides,<sup>38, 39</sup> of Le Fèvre and Le Fèvre on phosgene, carbon suboxide, etc.<sup>40</sup> and of Kumler on ammonia<sup>41</sup>—and these suggested that it would be possible

<sup>30</sup> Watson, *Proc. Roy. Soc. A*, 1927, **117**, 43.

<sup>31</sup> Hojendahl, *Dipole Moments*, (Copenhagen 1928).

<sup>32</sup> Steiger, *Helv. Phys. Acta.*, 1930, **3**, 161.

<sup>33</sup> Ghosh and Chatterjee, *Physic. Rev.*, 1931, **37**, 427.

<sup>34</sup> Smyth and de Bruyne, *J. Amer. Chem. Soc.*, 1935, **57**, 1203.

<sup>35</sup> Ramaswamy, *Proc. Ind. Acad. Sci., A*, 1936, **4**, 108.

<sup>36</sup> Groves and Sugden, *J. Chem. Soc.*, 1937, 1779.

<sup>37</sup> Hofmann, *Ber.*, 1889, **22**, 703.

<sup>38</sup> Fairbrother, *J. Chem. Soc.*, 1932, 43.

<sup>39</sup> Fairbrother, *ibid.*, 1933, 1541.

<sup>40</sup> Le Fèvre and Le Fèvre, *ibid.*, 1935, 1696.

<sup>41</sup> Kumler, *J. Amer. Chem. Soc.*, 1936, **58**, 1049.

fairly easily to avoid errors due to the escape of dissolved substance during the course of observations.

**Apparatus and Method**—The data required were the dielectric constants and densities of a graded series of solutions of known concentrations. The preparation of the latter is described later; the densities have been measured relatively to pure benzene in a Sprengel-Perkin pyknometer of *ca.* 10 cc. capacity with capillary side arms (to facilitate accurate adjustment) and require no further comment.

The dielectric constants were found using a resonance circuit, which having the merit of simplicity—and being the apparatus upon which most of the various dipole moment measurements published from this department have been made\* will now be described. Its lay-out is indicated in Fig. 4.

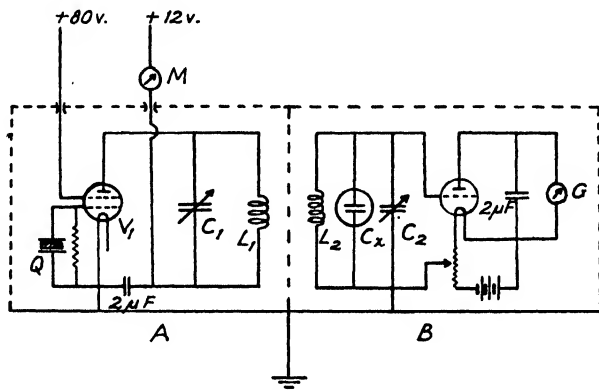


FIG. 4.

The oscillator (A) consists of a Mullard, PM12, 2 v., screened-grid valve between the grid and filament of which is connected a quartz crystal section in a suitable holder shunted by a grid leak high resistance. The anode circuit is a  $0.0005 \mu\text{F}$ . variable radio air condenser in parallel with an inductance of approximately  $280 \mu\text{H}$ . wound on a Bakelite former of 3 in.-diameter. The applied voltages are as shown in Fig. 4. The circuit is brought into oscillation by adjusting  $C_1$  until the natural frequency of  $L_1C_1$  equals that of the quartz (1200 kc. per sec.), this point being clearly indicated by a sharp drop in the current registered in the milliammeter M.

The pick-up circuit stands 2-3 ft. away with its inductance co-axial with  $L_1$ .  $L_2$  was constructed to ensure least temperature dependence by using a "Keramot" former, cut longitudinally into three sections, and mounted on Bakelite end pieces; the windings were so placed that the coil had a length-diameter ratio of 1 : 1.37, and a diameter of just under 3 in.  $L_2$  is in parallel with the glass cell ( $C_x$ ) and a (Sullivan) variable air condenser of maximum capacity  $250 \mu\text{F}$ . The slow motion worm drive of the latter has been refitted by us with a toothed wheel and divided drum by which 0.01 of a revolution can easily be read. This condenser has a rectilinear relationship between scale reading and capacity for the middle three-quarters of its motion so that for the present purposes it is possible to make readings in "turns of the adjusting arm" and not in degrees or capacity units. Resonance is detected by a valve voltmeter and a Moll galvanometer, the components involved being shown in Fig. 4 ( $V_2$  is an ordinary triode such as a Mullard PM 4DX or PM252). The cell ( $C_x$ ) is immersed in a small earthed copper thermostat containing water and the whole assembly built into a perforated zinc case having openings to permit the necessary observations; the drum of the revolution counter projects beyond the screen at a spot just below the scale of the galvanometer. The setting

of  $C_1$  requisite for resonance is found by taking a series of readings through the maximum, the drum head being always rotated clockwise to avoid backlash, and the actual maximum obtained by calculation.

The cell ( $C_x$ ) is of the type recommended by Sayce and Briscoe<sup>42</sup> modified in the small particulars that its entrance and exit tubes are fitted with standard ground glass cone ends and extended over the sides of the thermostat (so that it can easily be filled and emptied by pressure or suction), and that its main body has a 3-in. glass collar at the top (so that all the dielectric material is immersed in the thermostat water). The opposing faces of  $C_x$  are heavily silvered by the recipe of Sugden<sup>43</sup> for about two-thirds of their lengths, thus giving capacities of the order 30-50  $\mu\mu\text{F}$ .

This type of cell has the advantage that practically no solid dielectric intervenes between its plates, that the separation of the latter is small compared with their length and area, and that the outer surface, if earthed, makes almost a complete screen. Nevertheless, a small "end effect" arises from the capacity of the upper end of the inner silver layer to earthed objects other than the outer film. If the thickness of the outer glass wall is  $l_g$  and  $\epsilon_g$  is its dielectric constant and  $l$  and  $\epsilon$  are corresponding quantities for the material in the cell, the end effect varies as  $1/(l_g/\epsilon_g + l/\epsilon)$ —i.e., the end effect is neither proportional to the dielectric constant of the cell contents nor independent of it. Clearly, however, so long as dielectrics of approximately the same dielectric constant are being compared the cell can be regarded as an absolute condenser, the capacity of which is proportional to the dielectric constant of the medium between the plates.

Dielectric constants are determined from the following observations: the capacity ( $C_A$ ) required in the Sullivan condenser for resonance when  $C_x$  is filled with dry air, that ( $C_B$ ) with benzene, and that ( $C_S$ ) with a solution; then (if the required dielectric constant be  $\epsilon_B$  and that of benzene be  $\epsilon_B$ ):

$$\epsilon_B = 1 - \frac{(\epsilon_B - 1)(C_A - C_S)}{(C_A - C_B)}.$$

The value ( $C_A - C_B$ ) for a given cell remained practically constant for months provided the silvering was not visibly blemished. The dielectric constant of benzene was taken as 2.2725 at 25° (Hartshorne and Oliver<sup>44</sup>).

**Limitations of the Apparatus.**—The resonance points could be determined to 1/100 of a rotation,  $C_A - C_B$  was commonly about 80 turns, i.e., 8000 divisions, so that the fourth decimal places in the dielectric constant values given below should be significant. This type of apparatus has limitations, however, the chief of which arise from the effects of lead inductance and conductivity of the liquid in  $C_x$ . If the leads from the standard variable condenser  $C_s$  have inductance  $L_L$  and capacitance  $C_L$  and terminate in the cell  $C_x$  of capacitance  $C$  and equivalent shunt resistance  $R$ , then for a pulsance  $\omega$  the effective capacitance  $C_{\text{eff}}$  of the arrangement is given by:

$$C_{\text{eff}} = \frac{(C + C_L)(1 - \omega^2 L_L C) - \frac{L_L}{R^2}}{(1 - \omega^2 L_L C)^2 + \frac{\omega^2 L_L^2}{R^2}}.$$

Now the present dielectric constant measurements of benzene solutions involved the examination successively of three dielectrics, similar in that  $R$  is uniformly high and the capacities under comparison are of the same order so that

$$C_{\text{eff}} = (C + C_L)/(1 + \omega^2 L_L C).$$

<sup>42</sup> Sayce and Briscoe, *J. Chem. Soc.*, 1925, 127, 315.

<sup>43</sup> Sugden, *ibid.*, 1933, 770.

<sup>44</sup> Hartshorne and Oliver, *Proc. Roy. Soc. A*, 1929, 123, 664.



With the components now used, assuming  $L_{\text{L}}$  to be about  $5 \times 10^{-7}$  H. and  $C$  about  $50 \mu\mu\text{F.}$ , the denominator of this expression will not be different from unity (to four places), when media of dielectric constant 1.3 fill  $C_{\text{x}}$ . Hence, for the dissolved amines, ratios of differences of effective (i.e., measured) capacities as found are not notably unequal from those ratios of differences of true capacities required for the accurate evaluation of the dielectric constants sought.

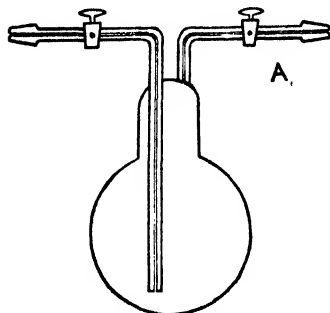


FIG. 5.

The solutions were made up by weight, preliminary experiments having showed that the concentrations of solutions could not satisfactorily be found by titration with standard acid (although this method was used by Kumler in the case of ammonia). A small Pyrex bottle

TABLE VII

Results :  $\epsilon_{25}^{\circ} = 2.2725$ ,  $d_{4}^{25^{\circ}} = 0.87378$ , whence  $p_2 = 0.34086$  and  $C = 0.18809$ .

$w_1 \times 10^5$	$\epsilon$	$d$	$\alpha\epsilon_2$	$\beta d_2$
<b>Monomethylamine (Mol. Wt. = 31)</b>				
444	2.2995	0.87250	6.1	-0.29
826	2.3338	0.87109	7.4	-0.33
1229	2.3547	0.86946	6.7	-0.35
1975	2.4052	0.86730	6.7	-0.33
2507	2.4588	0.86476	7.4	-0.36
2695	2.4514	0.86461	6.6	-0.34

Whence  $\frac{\Sigma\Delta\epsilon}{\Sigma w_1} = 6.91$  and  $\frac{\Sigma\Delta d}{\Sigma w_1} = -0.341$ .

Therefore mean  $\beta = -0.390$ ,  $p_{\infty} = 1.772$  cc. and  $P_{\infty} = 54.9$  cc.

**Dimethylamine (Mol. Wt. = 45).**

289	2.2812	0.87304	3.0	-0.26
1082	2.3002	0.87077	2.6	-0.28
1881	2.3229	0.86848	2.7	-0.28
1946	—	0.86820	—	-0.29
4962	2.4092	0.85962	2.8	-0.28

Whence  $\frac{\Sigma\Delta\epsilon}{\Sigma w_1} = 2.72$  and  $\frac{\Sigma\Delta d}{\Sigma w_1} = -0.283$ .

Therefore mean  $\beta = -0.324$ ,  $p_{\infty} = 0.9630$  cc. and  $P_{\infty} = 43.3$  cc.

**Trimethylamine (Mol. Wt. = 59).**

354	2.2751	0.87276	0.74	-0.29
440	2.2762	0.87250	0.82	-0.29
1181	2.2832	0.87028	0.91	-0.30
1801	2.2856	0.86851	0.74	-0.30
2045	2.2873	0.86779	0.72	-0.29
2075	2.2883	0.86777	0.76	-0.29

Whence  $\frac{\Sigma\Delta\epsilon}{\Sigma w_1} = 0.769$  and  $\frac{\Sigma\Delta d}{\Sigma w_1} = -0.292$ .

Therefore mean  $\beta = -0.334$ ,  $p_{\infty} = 0.5994$  cc. and  $P_{\infty} = 35.4$  cc.

(Fig. 5) having capillary lead in and out tubes with stopcocks and standard ground glass cone ends was found convenient for this purpose. A weighed amount of benzene was first introduced and the bulb placed in ice water. If A were now joined to a supply of the amine under examination the latter would slowly enter when stopcock A was opened. Absorption required  $\frac{1}{2}$ -1 hour, after which the vessel was dried and reweighed, thus giving the weight of dissolved amine directly. The solutions were always transferred from this bottle to the condenser or the pyknometer by pressure of dry  $\text{CO}_2$ -free air and not by suction, since this led to loss of gas.

**Results.**—The data tabulated (p. 386) are: the weight fractions ( $\omega_1$ ) of the solutes in the solutions, the dielectric constants ( $\epsilon$ ) of the solutions, and their densities ( $d$ ) compared with water at  $4^\circ$ ; specific polarisations of the solute, solvent, and the former at infinite dilution are indicated by  $p_1$ ,  $p_2$  and  $p_\infty$  respectively, and the corresponding molecular quantities by capitals. A graphical examination of the data shows that both dielectric constants and densities vary rectilinearly with concentration, so that:

$$\epsilon_{\text{solution}} = \epsilon_2(1 + \alpha\omega_1) \text{ and } d_{\text{solution}} = d_2(1 + \beta\omega_1).$$

The specific polarisation of the solute at infinite dilution is then calculable by the expression

$$p_\infty = (\epsilon_2 - 1)/(\epsilon_2 + 2) \cdot 1/d_2 \cdot (1 - \beta) + 3\alpha\epsilon_2/d_2(\epsilon_2 + 2)^2$$

or more briefly:  $p_\infty = p_2(1 - \beta) + C\alpha\epsilon_2$  (Le Fèvre and Vine).<sup>46</sup> The coefficients  $\alpha\epsilon_2$  and  $\beta d_2$  are given in the tables for each solution, but the mean values, used in the final results, have been obtained by summing the differences between solutions and solvent and dividing by the total  $\omega_1$ .

### Section (3). The Dielectric Polarisation of Ammonia, Methylamine, Dimethylamine, and Trimethylamine as Pure Liquids.

Reliable values for the dielectric constants and densities of some of the substances named above are not on record in the literature. The dielectric constant of liquid ammonia has been examined on several occasions (see references <sup>46-49</sup> inclusive), whilst numerous data for its density have been reported. The latter are reviewed and supplemented in a valuable paper by Cragoe and Harper.<sup>50</sup> Dielectric constants of mono- and tri-methyl amines, apparently the only measurements previous to the present work, have been given by Schlundt<sup>51</sup> as  $\epsilon = < 10.5$  for  $\text{MeNH}_2$  at  $21^\circ$  and  $\epsilon = 2.95$  for  $\text{Me}_3\text{N}$  at  $4^\circ$ , while the densities of the three amines have been described by Hofmann<sup>52</sup> and Jaeger.<sup>53</sup>

**Experimental Methods.** As indicated previously, the procedure of Section II is dependable only with liquids whose dielectric constants are such that  $(1 - \omega^2 L_C C)$  is not significantly different from unity, and whose resistances are sufficiently high to be neglected. The liquid amines satisfy neither of these conditions fully.

The effect of higher dielectric constants is to increase the capacitance  $C$  and thus lower  $(1 - \omega^2 L_C C)$  by varying amounts respectively when the resonance points for air, standard liquid, and experimental liquid are being determined. Accordingly the simple ratio of observed capacity changes (p. 385) will not be the ratio of true capacity changes, nor can the capacity of the leads  $C_L$  be taken as constant, and therefore disappearing in the

<sup>46</sup> Le Fèvre and Vine, *J. Chem. Soc.*, 1937, 1805.

<sup>47</sup> Palmer and Schlundt, *J. Physical Chem.*, 1911, 15, 381.

<sup>48</sup> Schlundt and Schaefer, *ibid.*, 1912, 16, 253.

<sup>49</sup> Smyth and Hitchcock, *J. Amer. Chem. Soc.*, 1934, 56, 1084.

<sup>50</sup> Grubb, Chittum and Hunt, *ibid.*, 1936, 58, 776.

<sup>51</sup> Cragoe and Harper, *Scientific Papers Bureau Stand.*, No. 420.

<sup>52</sup> Schlundt, *J. Physical Chem.*, 1901, 5, 503.

<sup>53</sup> Hofman, *Ber.*, 1889, 22, 701.

<sup>54</sup> Jaeger, *Z. anorg. Chem.*, 1917, 101, 86.

subtractions. However, calculations based on the circuit used shows that, although comparisons of liquids of  $\epsilon$  order 10 with standards of  $\epsilon$  order 2 will produce errors in the  $\epsilon$  found of about 0.5 %, this effect can be extinguished in the third decimal place by selecting standards with dielectric constants as close as possible to the expected values for the liquids under test. In this respect we have used the data tabulated by Le Fèvre.<sup>54</sup>

Conductivity of the dielectric may cause further difficulties. The first of these is obvious experimentally. A condenser of capacitance  $C$  (farads) containing a dielectric of  $\epsilon$  and conductivity  $k$  (ohms<sup>-1</sup> cm.<sup>-1</sup>) has an equivalent shunt resistance given by  $R = \frac{8.84 \times 10^{-14} \epsilon}{kC}$  ohms. This may

considerably diminish the "sharpness" of tuning, expressed by the narrowness of the peaked curve between galvanometer deflection and capacity in  $C_s$ . For example, if  $R_c$  is the resistance of the coil  $L_s$ , the widths ( $P$ ) of the curves at half heights when a liquid of resistance  $R$  and air ( $R = \infty$ ) respectively fill  $C_x$  are given by :

$$P_{114}/P_{air} = 1 + \frac{R_c^2 + \omega^2 L_s^2}{RR_c},$$

i.e., the higher the conductivity the flatter will be the tuning and the greater the chance of inaccuracy.

With our components, this ratio is around unity for liquids with  $k$  values from  $< 10^{-18} \Omega^{-1} \text{ cm.}^{-1}$  down to *ca.*  $10^{-10} \Omega^{-1} \text{ cm.}^{-1}$ , but afterwards

increases rapidly, reaching several thousands for  $k$ 's greater than  $10^{-7} \Omega^{-1} \text{ cm.}^{-1}$ . Benzene, carbon tetrachloride, etc., are high in this range and give very sharp resonance curves. The alkylamines are less satisfactory the fewer the alkyl groups per molecule. Ammonia (conductivity around  $10^{-7} \Omega^{-1} \text{ cm.}^{-1}$ ) is the worst case. For the latter substances we have therefore checked our dielectric constants with apparatus described by Le Fèvre<sup>54</sup> and Le Fèvre and Rayner,<sup>55</sup> in which the

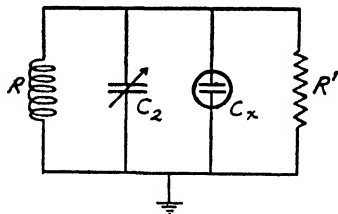


FIG. 6.

threshold of oscillation of a quartz crystal—used as the "reference" point—can still be easily displayed even when damping is considerable. It may be objected, however, that conductivity can cause "false" capacitance readings, Jazewski<sup>56</sup> having shown that, with a condenser having finite resistance in the circuit of Fig. 6, the total capacity,  $C_m$ , necessary for maximum current (i.e., resonance capacity) depends, for a given pulsance,  $\omega$ , on the circuit constants as follows :

$$C_m = \frac{1}{2} C_0 \left( 1 + \frac{2R}{R'} \right) \left( 1 + \sqrt{1 + \frac{4\omega^2 L_s^2}{(2R + R')^2}} \right).$$

$C_0 (= C_s + C_x$ , see B, Fig. 4) is the Kelvin resonant capacitance when  $R' = \infty$ , this occurs with the pure solvents, for which  $R'$  is effectively infinite. Unfortunately reliable conductance data for liquid amines do not appear to be on record, but all figures quoted (e.g., in Landolt Bornstein's *Tabellen*) are smaller than that for "equilibrium" water namely  $0.8 \times 10^{-8} \Omega^{-1} \text{ cm.}^{-1}$ . If this value, in conjunction with the appropriate dimensions and other features of our components, is applied to the above equation,  $C_m/C_0$  is about 1.0002. Errors from this will cause therefore be less with the compounds now under examination.

For the above reasons we feel justified in reporting our dielectric constant measurements to the same number of significant figures as the standards employed.

<sup>54</sup> Le Fèvre, *Trans. Faraday Soc.*, 1938, **34**, 1127.

<sup>55</sup> Le Fèvre and Rayner, *J. Chem. Soc.*, 1938, 1921.

<sup>56</sup> Jazewski, *Z. Physik*, 1927, **43**, 442.

**Present Measurements**—Density and dielectric constant determinations have been made in sealed apparatus. For the former, pyknometers were constructed from thick Pyrex capillary tubing of about 1 mm. internal diameter, selected for uniformity. Lengths of about 8 in. were expanded to a bulb of approximately 10 cc. capacity at one end and a regular and arbitrary scale etched for a few inches above the bulb. After cleaning and drying etc. the other end was sealed to a doubly stopcocked bulb joined in turn to a supply train containing the materials described on page 383. The contents of the reservoir bulb were then frozen in liquid air and the apparatus evacuated. With the tap to the supply train closed the liquid air bath was placed around the pyknometer and liquid distilled until sufficient had collected to reach the lowest mark. The pyknometer was then sealed off and weighed. Observations of the height of the liquid were then made in a number of baths at different temperatures. Finally the seal was broken as cleanly as possible, the pyknometer emptied and its weight determined. The

volumes represented by the graduations were then ascertained directly by filling at different temperatures with determinable weights of purified water, and applying the data tabulated by Landolt-Bornstein (*Physikalisch-chemische Tabellen*, 1923, Vol. I, p. 78).

Dielectric constants were measured in small Sayce-Briscoe cells, specially constructed in thick Pyrex glass to hold only about 5 cc. These were sealed to the supply train, etc., and filled with the experimental materials by distillation as above.

The cells were fixed in a rigid cradle surrounded by a small earthed thermostat. Contact was made with the electrical circuit via mercury cups mounted on a bridge across the thermostat. The cells could be repeatedly removed and replaced without change in the point of resonance. By unsealing, the contents could be cleared, the cells swept clean by a current of dry air and a resonant point in this condition determined. Lastly the cells were filled with a number of standard, purified liquids and appropriate resonance points recorded. The dielectric constant values were then obtained by interpolation.

TABLE VIII

Temperature. °C.	Density $t_0^\circ$	Dielectric Constant.	Total Polarisation. cc.
<b>Ammonia.</b>			
5	0.6317*	18.94†	23.10
15	0.6175	17.82	23.29
25	0.6028	16.90	23.77
35	0.5875	16.26	24.23
<b>Methylamine.</b>			
-10.0	0.6952	—	—
0	0.6839	11.3	35.1
13.6	0.6676	—	—
25.0	0.6539	9.4	34.9
<b>Dimethylamine.</b>			
0	0.6683	6.32	43.1
25.0	0.6386	5.26	41.3
<b>Trimethylamine.</b>			
-10.5	0.6667	—	—
0	0.6557	2.57	30.9
14.4	0.6395	—	(30.8)
16.0	—	2.496	
25.0	0.6267	2.44	

## Results.

These follow in Table VIII. Total polarisations shown are calculated by the Clausius-Mossotti formula.

\* From Cragoe and Harper, ref. 50.

† From Grubb, Chittum and Hunt, ref. 49.

## Section (4). Conclusions and Discussion.

The values now found for the distortion polarisations (see Table V) in the gaseous condition agree well with the molar refractions calculated by the data of Brühl.<sup>57, 58</sup> The comparison shows that in none of these compounds does atomic polarisation make an unusual contribution to the total polarisation. For the

	NH <sub>3</sub> .	MeNH <sub>2</sub> .	Me <sub>2</sub> NH.	Me <sub>3</sub> N.
$P_D$ found .	5.9	10.6	15.0	20.0
$(R_L)_D$ calc. .	5.8	10.4	15.2	20.2

purpose of Table IX, therefore, apparent moments have been calculated as  $0.22 \times (\tau P_{25} - P_D)$ †.

TABLE IX.—DEPENDENCE OF APPARENT MOMENT AND POLARISATION AT 25° C. ON STATE.\*

Substance.	State.					
	Liquid.		Benzene Solution.		Gaseous.	
	$\mu$	$\tau P$	$\mu$	$\tau P$	$\mu$	$\tau P$
Ammonia .	0.93D ;	23.8 cc.	1.40D ;	46.2 cc.†	1.45D ;	49.6 cc.
Methylamine .	1.08 ;	34.9	1.46 ;	54.9	1.28 ;	44.9 <sub>0</sub>
Dimethylamine	1.13 ;	41.3	1.17 ;	43.3	1.02 ;	36.5 <sub>0</sub>
Trimethylamine	0.72 ;	30.6	0.86 ;	35.4	0.64 ;	28.5 <sub>7</sub>

To make easier the application of the various empirical or theoretical relationships between polarisation and state, our results are shown also as  $\mu_1^2/\mu_2^2$  ratios ( $= {}_0P_1/{}_0P_2$ ), and as  $\Delta\mu/\mu_{\text{gas}}$  fractions :—

TABLE X ‡

	Liquid-Gas.		Solution-Gas.	
	$\mu_{\text{liq}}^2/\mu_{\text{gas}}^2$ .	$\Delta\mu/\mu_{\text{gas}}$ .	$\mu_{\text{soln.}}^2/\mu_{\text{gas}}^2$ .	$\Delta\mu/\mu_{\text{gas}}$ .
Ammonia .	0.41	+ 0.36	0.93	+ 0.03
Methylamine .	0.71	+ 0.16	1.30	— 0.14
Dimethylamine .	1.22	— 0.11	1.32	— 0.15
Trimethylamine .	1.27	— 0.12	1.80	— 0.34

Ammonia and trimethylamine are thus shown as the extreme cases, with the mono- and di-methyl-derivatives occupying intermediate positions. The first named substance exemplifies the behaviour of the majority of compounds—behaviour which is, at least qualitatively, represented by the formulae of Müller,<sup>2</sup> Jenkins,<sup>3</sup> Sugden,<sup>4</sup> Arkel and Snoek,<sup>60</sup> etc., all of which require that  $\mu_{\text{gas}}$  should be greater than  $\mu_{\text{liquid}}$  or  $\mu_{\text{solution}}$ , since

\* N.B.—The data recorded by Le Fèvre and Russell<sup>59</sup> contained some errors which are here corrected.

† Kumler, ref. 41.

‡  $\Delta\mu = \mu_{\text{gas}}$  minus  $\mu_{\text{liquid}}$  or  $\mu_{\text{solution}}$ .

<sup>57</sup> Brühl, *Z. physikal Chem.*, 1895, **16**, 193, 226, 497, 512.

<sup>58</sup> Brühl, *ibid.*, 1897, **22**, 373.

<sup>59</sup> Le Fèvre and Russell, *Nature*, 1938, **142**, 617.

<sup>60</sup> Arkel and Snoek, *Trans. Faraday Soc.*, 1934, **30**, 707.

they consider only the medium or solvent and imply that its effect is proportionately the same for all polar solutes.

Di- and tri-methylamines illustrate the necessity of including factors for the solute as well. Our measurements display the relative magnitudes forecast by such treatments as those due to Weigle,<sup>61</sup> Higasi,<sup>9</sup> Frank,<sup>10</sup> or Le Fèvre and Le Fèvre.<sup>8</sup> In these, the simultaneous effects of geometrical factors and the anisotropy of polarisability of solvent and solute molecules are recognised. When a polarisable assemblage of molecules contains one which is polar, the latter will set up an induced polarisation in the former, which, being fixed relatively to the primary dipole and being independent of any motion of the medium, must be vectorially combined with the primary moment. Thus the apparent moment in the liquid or dissolved state  $= \mu_{\text{liquid}} = \mu_{\text{gas}} + \Sigma \mu_{\text{induced}}$ . Only for the minority of organic substances is  $\Sigma \mu_{\text{induced}}$  algebraically positive; its *a priori* calculation is always rather speculative. Weigle, Higasi and Frank in different ways use the shapes and dimensions of the molecules concerned to lead to correct predictions. Le Fèvre and Le Fèvre, noting that for a given substance only the orientation polarisation seems to be affected by the nature of the medium, proposed the following:—

$${}_0P_{\text{liquid}}/{}_0P_{\text{gas}} = 1 + 3 \Theta(\epsilon - 1)/(\epsilon + 2)4\pi\mu^2$$

$\Theta$  having the significance given by Raman and Krishnan<sup>63</sup> and  $\epsilon$  being the D.C. of the pure liquid, or—if the ratio  ${}_0P_{\text{solution}}/{}_0P_{\text{gas}}$  is sought—that of the solvent. This expression is related easily<sup>64</sup> to that of Higasi. The sign of  $\Theta$  is opposite to that of the Kerr constant which for the majority of compounds is positive. The Kerr constant of ammonia is positive<sup>65</sup> and—consistently— $\mu^2_{\text{liq}}/\mu^2_{\text{gas}}$  is less than unity. Requisite data for the methylated ammonias are lacking, but elementary considerations suggest that di- and tri-methylamines should show negative electric double refraction, and therefore, in the present work,  ${}_0P_{\text{liq}}/{}_0P_{\text{gas}}$  ratios greater than unity. It is notable that for chloroform and ethyl ether these ratios are 1.04 and 1.19—i.e., of the order now observed for  $\text{Me}_2\text{Nl}$  and  $\text{Me}_3\text{N}$ —and the corresponding Kerr  $B$ 's are ca.  $-3.10^{-7}$  and  $-0.7 \cdot 10^{-7}$  respectively.

Finally it is of interest to apply the formula of Onsager<sup>66</sup> to our results, since this author utilises for the internal field an expression alternative to that of Clausius-Mossotti. His equation:

$$\frac{4\pi N\mu^2}{9kT} = \frac{(\epsilon - n^2)(2\epsilon + n^2)}{(n^2 + 2)^2}$$

should allow the calculation of  $\mu$  from observations of  $\epsilon$  and  $n$  on pure liquids at  $T^\circ$ . Böttcher<sup>67</sup> has reviewed an extensive range of examples and has demonstrated that dipole moments thus evaluated often agree well with those obtained by D.C. methods on gases. This is not the case with ammonia and the methyl-amines, as the last two columns of Table XI show. (Figures for nitrobenzene are included as an instance where the agreement is good.)

Disagreement between Onsager's theory and experiment is not surprising in view of the basic assumptions made. No account is taken of the optical anisotropy of the polar molecule, which is regarded as a sphere, containing a central dipole, surrounded by a homogeneous continuum. It is difficult to foresee either the signs or the magnitudes of errors due to an over simple

<sup>61</sup> Henriquez, *Rec. Trav. Chim.*, 1935, **54**, 574.

<sup>62</sup> Weigle, *Helv. Phys. Acta.*, 1933, **6**, 681.

<sup>63</sup> Raman and Krishnan, *Proc. Roy. Soc. A*, 1927, **117**, 589.

<sup>64</sup> Le Fèvre, *Dipole Moments* (Methuen, 1938), p. 51.

<sup>65</sup> Breazeale, *Physical Rev.*, 1935, **48**, 237.

<sup>66</sup> Onsager, *J. Amer. Chem. Soc.*, 1936, **58**, 1486.

<sup>67</sup> Böttcher, *Physica*, 1939, **6**, 59.

model. It might be expected that ammonia, with the most nearly spherical molecule, would show best agreement, but this is not so.

Wilson<sup>68</sup> has repeated Onsager's calculations using  $\alpha_1$ , as the polarisability along the dipole axis, and  $\alpha$ , the average polarisability, as that in

TABLE XI

Substance.	$\epsilon_{25^\circ}$ .	$n_D^{25^\circ}$ .	$d_{40}^{25^\circ}$ .	$\mu_{\text{Onsager}}$ .	$\mu_{\text{gas}}$ .
NH <sub>3</sub> . . .	16.90	1.7350	0.6028	1.77	1.45
MeNH <sub>2</sub> . . .	9.4	1.8265	0.6539	1.62	1.28
Me <sub>2</sub> NH . . .	5.26	1.8140	0.6386	1.38	1.02
Me <sub>3</sub> N . . .	2.44	1.8087	0.6267	0.74	0.64
C <sub>6</sub> H <sub>5</sub> NO <sub>2</sub> . .	34.89	1.5501	1.1986	4.18	4.23

the direction of the applied field. The two polarisabilities are related to corresponding refractive indices,  $n_1$  and  $n$ . The orientation polarisation then becomes:—

$${}_0P = \left[ \frac{\epsilon - 1}{\epsilon} - \frac{3(n^2 - 1)}{2\epsilon + n^2} \right] \left[ \frac{(2\epsilon + n_1^2)^2}{(2\epsilon + 1)(n_1^2 + 2)^2} \right].$$

Inspection shows this to be qualitatively an improvement in that, due to the effect of the multiplying factor  $(2\epsilon + 1)$ , which occurs in the denominator only, the magnitudes of  ${}_0P$  and  $n_1$  will change oppositely. Two substances may therefore have similar  $\epsilon$  and  $n$  values, but if their Kerr constants are positive and negative respectively,  $n_1$  will be greater or less than  $n$ , and accordingly the first orientation polarisation smaller than the second. A test is difficult to make owing to the inaccessibility of  $n_1$  values. However, in view of the unpredictable types and degrees of association possible there seems little reason to suppose that a general relation between  $\mu_{\text{liquid}}$  and  $\mu_{\text{gas}}$  should exist. Clearly trimethylamine will, of the present cases, be most likely to associate co-linearly—a process whose effect *should* raise the apparent moment considerably. Thosar<sup>69</sup> has recorded X-ray evidence which is explicable if the molecules of the lower aliphatic amines are flat pyramids which, in the liquid state, aggregate to cybotactic groups containing these pyramids piled on top of each other. However, although our experiments show  $\mu_{\text{liquid}} > \mu_{\text{gas}}$  for trimethylamine, the excess is so small that evidently no such simple association pattern as the above can be alone occurring. More information is required concerning the structure of liquids as well as data such as molecular shape, dimensions, anisotropy of polarisability,<sup>7</sup> polarisation, etc. The collection of these at the present stage will be useful for an eventual discussion of the problem of apparent moment and state.

This investigation was started in 1937 but had to be suspended at the end of 1939. The present paper covers the first part of a programme in which the polarisations of ammonia and its alkylated and arylated derivatives were to be compared in the liquid, dissolved and gaseous conditions. Its publication has been delayed until the opportunity to resume experimental work could be foreseen.

The authors wish to acknowledge the help and advice they have received from Professor H. E. Watson; they are also grateful for financial assistance from the Department of Scientific and Industrial Research, the Chemical Society and the Dixon Fund of the University of London.

<sup>68</sup> Wilson, *Chem. Rev.*, 1939, **25**, 377.

<sup>69</sup> Thosar, *J. Chem. Physics*, 1938, **6**, 654.

### Summary.

The dielectric polarisations of the substances named in the title have been measured as gases, as solutes in benzene, and as pure liquids.

Suitable apparatus is described. For the gaseous dielectrics the replaceable capacity is placed in the anode circuit of a dynatron oscillator which is tuned to a fixed frequency, determined by the response of a quartz section in a loosely coupled wave-meter circuit. For the liquid dielectrics a simple resonance method is satisfactory. The apparent moments found, in D. units, for the liquid, dissolved ( $C_6H_6$ ), and gaseous states, are respectively:  $NH_3$ , 0.93, 1.40, 1.45;  $MeNH_2$ , 1.08, 1.46, 1.28;  $Me_2NH$ , 1.13, 1.17, 1.02;  $Me_3N$ , 0.72, 0.86, 0.64. These results illustrate behaviour forecast by a number of theories for molecules specifiable in some cases by elongation or extension along, and in others across, their dipole axes.

### Résumé.

Les moments dipolaires apparents de  $NH_3$ ,  $MeNH_2$ ,  $Me_2NH$  et  $Me_3N$  ont été mesurés pour ces substances à l'état gazeux, en solution dans le benzène et à l'état de liquides purs et sont respectivement : 0.93, 1.40, 1.45 pour  $NH_3$ ; 1.08, 1.46, 1.28 pour  $MeNH_2$ ; 1.13, 1.17, 1.02 pour  $Me_2NH$ ; 0.72, 0.86, 0.64 pour  $Me_3N$ . On indique en détail les méthodes de mesure employées et on discute les résultats d'après un certain nombre de théories.

### Zusammenfassung.

Die scheinbaren Dipolmomente von  $NH_3$ ,  $MeNH_2$ ,  $Me_2NH$  und  $Me_3N$  als Gase, in Benzollösung und als reine Flüssigkeiten sind bestimmt worden, u.zw.  $NH_3$ : 0.93, 1.40, 1.45;  $MeNH_2$ : 1.08, 1.46, 1.28;  $Me_2NH$ : 1.13, 1.17, 1.02;  $Me_3N$ : 0.72, 0.86, 0.64. Die Messmethoden werden im Detail beschrieben und die Resultate auf Basis von verschiedenen Theorien besprochen.

*The Sir William Ramsay and Ralph Forster Laboratories,  
University College,  
London.*

## REVIEWS OF BOOKS.

**The Chemical Link and the Structure of Molecules.** By Y. K. SYRKIN and M. E. DYATKINA. (Moscow, Leningrad, 1946.) (In Russian.)

This is an advanced text-book of nearly 600 pages, and is by far the best which the reviewer has seen on the subject. It begins at the beginning, explains the quantum mechanical foundations, and discusses the periodic law, the hydrogen atom, homopolar links, the saturability and directed nature of valency, resonance, heteropolar forms, and molecular orbitals. It then deals with what is learnt from spectral data, and frequencies, from dipole moments, and bond energies, and proceeds to treat the theory of intermolecular forces and of the crystalline state. Chapters on special structures follow, including complex compounds and the boron hydrides. Finally the three- and many-electron problems are dealt with, and the calculation of activation energy discussed.

The treatment is admirably balanced: theoretical derivations of important relations are given fully, and in general as simply as the subject



permits. Much less use than usual is made of the formula, "Quantum mechanics shows" (or worse still, "Pauling says"). On the other hand, the qualitatively interesting chemical facts receive their due prominence, and the book never becomes an abstract or formal mathematical treatise.

A translation would be welcome.

C. N. H.

**The Chemical Kinetics of the Bacterial Cell.** By C. N. HINSHELWOOD.  
(Clarendon Press, Oxford, 1946.) Pp. x + 284. Price 20s.

Much of Prof. Hinshelwood's study of bacterial growth and adaptation will already be familiar to readers of the *Transactions*. Here he seeks to find the extent to which the co-ordinated processes of growth and metabolism observed in living organisms can be understood in terms of chemical kinetics, and it is a measure of his contribution to the subject that so large a part of this book consists of work from his own laboratory, placed now in a wider setting and in logical sequence.

The subject of bacterial growth is approached through a preliminary discussion of some chemical and physical topics which are of importance in considering the activities of all living organisms: the resolving of complex reactions to stages; the properties of surfaces as seats of adsorption and of chemical reactions, the formation of crystals and macromolecules and the effects of temperature changes on cell processes. Throughout the book it is emphasized that processes of the bacterial cell are closely integrated and take place within narrow limits of space and time. Loss of materials from the cell by diffusion, and the decay of enzymes in the absence of cell-growth, are therefore to be taken into account.

A major part of the book studies problems of the relative growth of systems which form part of growing bacterial cultures. Changes in bacteria, which permit them to utilise new foodstuffs or to grow in the presence of drugs, are ascribed in part to changes in the enzyme balance of the cells. Such adaptation requires growth in the presence of the compound concerned, and as a working hypothesis the rate of growth of enzyme species in a growing bacterial population is considered to be dependent on their initial concentrations, and on the concentrations of their substrates. Deductions can then be made concerning the rate and extent of adaptation, and these deductions are consistent with many experimental findings. Moreover, reaction sequences, in which the product of one enzyme is the substrate for others, can be treated on this basis. Deductions can then be made with respect not only to the steady state attained in the concentrations of intermediate substrates, but also with respect to that attained in the relative abundance of enzymes in the bacterial population, and how this will change under changed conditions of growth. Experimental observation shows that the original hypothesis contains a large measure of truth.

Perhaps this hypothesis seems most challenging when it is expressed in the form:

enzyme + substrate = more enzyme + product,

and the enzyme is described as autotrophic. One then realises the extent to which other processes of the cell must be involved in providing

the environment for such behaviour, and the magnitude of the gap which separates our ordinary knowledge of enzymes, from our knowledge of their formation or of their behaviour during cell growth. Prof. Hinshelwood's use of the term enzyme is not the same as that of the biochemist, but involves also much of the biologist's conception of the plasmagene. It is important to recognise both the existence of this difference, and also the fact that in most cases we do not know which conception of enzymes carries the larger measure of truth; whether the intracellular enzymes are entirely the products of other systems, and that we can ignore the question of their origin when studying them as catalysts, or whether their origin is as closely bound up with their functioning as is suggested by the behaviour of adaptive enzymes. To such problems the present book is a major contribution.

Discrimination between selection and adaptation in changing bacterial populations is also discussed. Here, and in the description of phases of the growth cycle, Prof. Hinshelwood draws largely from the investigations of his own laboratory which illustrate well the value of propounding hypotheses which are susceptible to mathematical expression. The book throughout is carefully prepared and well produced.

H. M.

**Characterisation of Organic Compounds.** By F. WILD, M.A., Ph.D., F.R.I.C. (Cambridge University Press, 1947.) Pp. viii + 306  
Price 18s.

The author has attempted to make this book suitable for use both by Honours students during their laboratory course and by experienced research workers. It is doubtful whether it is possible to achieve this aim since qualitative organic analysis is included in a degree course to help to teach chemistry, while the need of the research worker is entirely different.

The main difficulty encountered by the student when identifying an unknown substance is to relate it to the class to which it belongs: this is difficult since it requires thought, judgment and application of facts learned in the lecture room. The preparation of a suitable derivative is comparatively straight-forward. In this book the section on the classification of compounds and the separation of mixtures occupies but eight pages and is inadequate. There is no mention, for instance, of such essential reagent solutions as Fehling's, Schiff's, ferric chloride, bromine and potassium permanganate. While details are given of the method and apparatus required for determining melting-points, no mention is made of how to carry out Lassaigne's test: indeed, identification of the elements present is not considered to be of primary importance.

That part of the book devoted to the choice and preparation of suitable derivatives is very full and occupies about 250 pages. It is claimed that every important general method published before 1944 is summarised. To the average student this will probably be a bewildering richness: the research worker, however, will welcome such a complete review which will save him much time searching the literature. An excellent feature is the presence of compact tables of melting-points of the derivatives mentioned in the text. Many of the reagents described are expensive and difficult to obtain commercially but references are given to their preparation. This, again, will be of use mainly to the research worker since many of the preparations are unsuitable for teaching purposes.

J. H.

**The Diffraction of X-Rays and Electrons by Free Molecules.** By M. H. PIRENNE—with a Foreword by P. DEBYE. (The Cambridge Series of Physical Chemistry.) (Cambridge: At the University Press, 1946.) Pp. xii + 160. Price 12s. 6d. net.

"The Cambridge Series of Physical Chemistry" is a phrase which brings to mind examples of specialist literature dealing with borderland subjects; subjects which are not exactly traditional physics, and assuredly not within the scope of the older chemistry. In a sense, the theme is chemical physics. Dr. Pirenne's book is a most acceptable addition to the family. It is written with exceptional clarity, it leads up always to actual evaluations, and yet is a monograph about principles, with not too rigid an insistence upon results. Naturally perhaps there is more about X-ray diffraction than there is about electron diffraction: certain types of molecules offer scope for the use of both methods, as the author indicates. Throughout, molecular structure is the prime object of investigation, and it is here that chemists will experience a strong appeal. Moreover, the limits of validity of the various theories are very well defined. A considerable amount of tabular data is included: for example, atomic scattering factors ( $f$ ) calculated by interpolation, by the Hartree distribution, by the Thomas model and by the hydrogen wave function in the ground state. The format and printing are of the high quality one associates with the University Press.

F. I. G. R.

**Mechanism of Reactions of Carbon-Carbon Double Bonds.** By C. C. PRICE. (Interscience Publishers Inc., New York.) Pp. 120. Price 15s.

In 120 brief pages, Professor C. C. Price has succeeded in giving a lucid account of the reactions of olefines, and leaves the reader with a clear picture of the trends and import of recent scientific work in this field. After summarising, and distinguishing clearly between, the ionic and the free radical reactions of olefines he considers polymerisation processes in some detail, and discusses carefully the mechanisms of the reactions concerned, picking out the crucial experimental evidence without going into mathematical or technical detail.

As a summary of the essential organic chemistry of chain polymerisation, this effort deserves high praise, for, unlike so many monographs on polymerisation, it does show us the subject as a whole growing wood, and not as individual trees of detail. Unfortunately, American price levels and English dollar scarcity will make many chemists think twice before expending fifteen shillings on so small a book.

W. A. W.

# THE EFFECT OF STEAM ON SOME ALUMINA TRANSITIONS.

By P. W. COOKE AND J. N. HARENAPE.

*Received 29th March, 1946.*

No definite transition temperature has been established above which  $\alpha$ -alumina, and below which  $\gamma$ -alumina is the stable modification. Laubengayer and Weisz<sup>1</sup> suggest that  $\gamma$ -alumina is unstable to  $\alpha$ -alumina at all temperatures, and they have determined transition points between many of the modifications of alumina for the case where water is in large excess (liquid water present up to the critical temperature, and water vapour pressure about 700 atmospheres at 450° c.). In these conditions, they find that  $\alpha$ -alumina is formed from all the other modifications at temperatures in excess of 450°  $\pm$  5° c. with diasporic existing as the stable modification from this temperature down to 280° c. and Boehmite apparently the stable modification between 280° and 155° c. Seeding is essential to produce diasporic, and in its absence there exists a metastable transition point of 415°  $\pm$  10° c. above which  $\alpha$ -alumina and below which Boehmite is the favoured modification.

However, the temperature at which the transition from  $\gamma$ - to  $\alpha$ -alumina takes place at a measurable rate in normal use in catalytic processes, or in the atmosphere, is in the region of 900°-1,100° c. Since steam is used in many catalytic processes, it is of interest to investigate how this transition temperature varies with the steam pressure between these extremes. It is well known that steam at temperatures in the region of 600°-800° c. and at atmospheric pressure will cause rapid decrease of surface area,<sup>2</sup> but whether this is due merely to crystal growth of the  $\gamma$ -alumina, or to the formation of the highly crystalline,  $\alpha$ -alumina does not appear to have been established.

In this laboratory, the transformation of Boehmite to  $\alpha$ -alumina in the presence of steam at a pressure considerably below that used by Laubengayer and Weisz and at a similar temperature, has been noticed, and this paper describes experiments designed to clarify the position and to increase, to some extent, knowledge of the behaviour of the system at intermediate steam pressures.

## Experimental.

(a) **Preparation of Alumina Samples.**—Samples of Boehmite and  $\gamma$ -alumina with varying amounts of water were heated at temperatures between 400 and 500° c. With one exception, namely, experiment (3) below, the experiments were performed in a small stainless steel bomb of 30 ml. capacity. Seven experiments were performed as follows.

(1) 12 g. Boehmite heated with 0.5 g. of water (Boehmite to water = 24 to 1) for 14 hours at a temperature of 425°-440° c.\* The X-ray pattern of the resultant material is shown in (a) of Fig. 1.

(2) 12 g. Boehmite heated with 0.5 g. water (Boehmite to water = 24 to 1)

<sup>1</sup> Laubengayer and Weisz, *J. Amer. Chem. Soc.*, 1943, **65**, 247.

<sup>2</sup> Turkevich, *J. Chem. Physics*, 1945, **13**, 237.

for 14 hours at a temperature of 500° c. The X-ray pattern of the resultant product is shown in (b) of Fig. 1.

(3) Boehmite was roasted in an open silica dish for 14 hours at 500° c., to produce  $\gamma$ -alumina. The X-ray pattern of the  $\gamma$ -alumina is shown in (c) of Fig. 2.

(The Boehmite referred to in experiments (1), (2) and (3) was an "Alorco" activated alumina, grade D, manufactured by the Aluminium Ore Company of U.S.A.)

(4) 5.6 g. of  $\gamma$ -alumina (from experiment (3)) was heated with 0.2 g. of water ( $\gamma$ -alumina to water = 28 to 1) for 14 hours at 425°-440° c.\* The X-ray pattern of the resultant product is shown in (d) of Fig. 3.

(5) 14 g. of  $\gamma$ -alumina (from experiment (3)) was heated with 0.5 g. of water ( $\gamma$ -alumina to water = 28 to 1) for 14 hours at 500° c. The X-ray pattern of the resultant product is shown in (e) of Fig. 3.

(6) 12 g. of  $\gamma$ -alumina (from experiment (3)) was heated with 2.5 g. of water ( $\gamma$ -alumina to water = 4.8 to 1) for 14 hours at 430°-450° c.\* The X-ray pattern of the resultant product is shown in (f) of Fig. 4.

(7) 12 g. of  $\gamma$ -alumina (from experiment (3)) was heated with 2.5 g. of water ( $\gamma$ -alumina to water = 4.8 to 1) for 14 hours at 460° c. The X-ray pattern of the resultant product is shown in (g) of Fig. 4.

(b) **X-Ray Analysis.**—A small amount of the material from each experiment was mixed to a paste with a collodion-ether solution and extruded from a fine-bore capillary tube (0.33 mm. diameter). The rod-like specimens formed were cut to a standard length of 2.0 mm. and mounted in a 9 cm. powder diffraction camera. Rotation of the specimens was unnecessary, due to the small crystal size. Hence broadening of diffraction lines due to specimen wobble or eccentricity was eliminated. Exposures of  $\frac{1}{2}$  hour were necessary at 50 kv. and 20 ma. using copper  $K_{\alpha}$  radiation and a 0.0007 in. thick nickel foil to remove the  $\beta$  component. Each film before development had an intensity wedge imprinted. Standard specimens of Boehmite,  $\gamma$ -alumina and  $\alpha$ -alumina, were prepared and X-ray patterns taken to give standards for comparison with the products obtained in the series of experiments outlined above. Fig. 5 shows the patterns of the standards at  $h$ ,  $i$ ,  $j$ , respectively.

(c) **Crystal Size Determination.**—For crystal size determination, the method employed by Jellinek and Fankuchen<sup>3</sup> was used. The 440 band of the  $\gamma$ -pattern of  $d = 1.396$  Å. and  $\theta$  (Bragg angle) = 33° 24' was photometered. The band width was corrected for specimen diameter and absorption effects, by taking the mean width of the two lines of the  $\alpha$ -alumina pattern straddling the 440 band of the  $\gamma$ -pattern. The spacings of the  $\alpha$ -alumina lines photometered were

$$d_{401} = 1.370 \text{ Å. at } \theta \text{ (Bragg angle)} = 34^{\circ} 05'$$

$$d_{300} = 1.402 \text{ Å. at } \theta \text{ (Bragg angle)} = 33^{\circ} 14'.$$

The crystal size determinations were carried out on samples (3), (4), and (5). The values obtained were: samples (3) and (4) 50 Å.; sample (5) 90 Å., all  $\pm 5$  Å.

Close inspection of the pattern (g) of Fig. 4 shows that the lines of the diffraction pattern are not wholly continuous, but consist of spots very close together. This indicates that the crystals of the material are large enough to produce incomplete diffraction haloes corresponding to a crystal size in the region of 0.002 cm.

### Discussion.

1. From Fig. 1 (a) it is seen that sample (1) is Boehmite, together with a small amount of  $\gamma$ -alumina, and Fig. 1 (b) shows sample (2) to be mainly  $\alpha$ -alumina, together with a small amount of Boehmite.

2. From Fig. 2 (c) it is seen that sample (3) is  $\gamma$ -alumina.

3. From Fig. 3 (d) and 3 (e) it is seen that both samples (4) and (5) are  $\gamma$ -alumina, together with a trace of Boehmite, but that the lines of sample (5) are considerably sharper than those of sample (4), indicating an increase in crystal size. The average crystal sizes deduced for samples (3), (4), and (5) are respectively 50, 50 and 90 Å.

4. From Fig. 4 (f) it is seen that sample (6) is mainly Boehmite, but with a small amount of  $\gamma$ -alumina still present, and sample (7) (Fig. 4 (g)) is mainly  $\alpha$ -alumina, together with an amount of Boehmite, estimated

\* Two extremes of temperature range.

<sup>3</sup> Jellinek and Fankuchen, *Ind. Eng. Chem.*, 1945, 37, 158.



FIG. 1.—Boehmite to  $\alpha$ - $\text{Al}_2\text{O}_3$  transition in presence of steam.



FIG. 2.—Boehmite to  $\gamma$ - $\text{Al}_2\text{O}_3$  transition.



FIG. 3.— $\gamma$ - $\text{Al}_2\text{O}_3$  crystal growth in presence of steam.



FIG. 4.— $\gamma$ - $\text{Al}_2\text{O}_3$  to  $\alpha$ - $\text{Al}_2\text{O}_3$  transition in presence of steam.

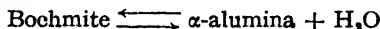


FIG. 5.—Standard alumina patterns, 9 cm. powder camera  $\text{CuK}_\alpha$  radiation.  
(h) Boehmite. (i)  $\gamma$ -Alumina. (j)  $\alpha$ -Alumina.



at 10 %. The crystal size of sample (7) may be deduced as being in the region of 0.002 cm.

The data of Laubengayer and Weisz suggest that  $\gamma$ -alumina is metastable under all conditions of temperature and steam pressure. Moreover, they make it plain that in presence of water (and absence of diaspore) Boehmite is unstable to  $\alpha$ -alumina above  $415^{\circ}\text{C.} \pm 10^{\circ}\text{C.}$  at a steam pressure of *ca.* 500 atmospheres. Now by the phase rule the system Boehmite— $\alpha$ -alumina—steam ( $P = 3$ ,  $C = 2$ ,  $F = C - P + 2$ ) has one degree of freedom so long as there is only one aqueous phase, which must be the case above the critical point of water ( $374^{\circ}\text{C.}$ ). Thus the transition point is only fixed after either the temperature or the steam pressure is fixed and the transformation—



will take place reversibly at that temperature for which the vapour pressure of Boehmite is just equal to the external steam pressure. This vapour pressure of Boehmite must be *ca.* 500 atmospheres at  $415^{\circ}\text{C.}$ , and will, of course, be lower the lower the temperature. Thus the eventual formation of  $\alpha$ -alumina (unless diaspore intervenes) in low-pressure alumina-steam systems may be expected at any temperature exceeding  $415^{\circ}\text{C.}$  The fact that the transformation of Boehmite to  $\alpha$ -alumina is not observed when Boehmite is heated for long periods in atmospheric air and at temperatures up to  $700^{\circ}\text{C.}$  shows that water has an important effect on the rate of production of  $\alpha$ -alumina. The removal of water from the system so reduces the rate of the reaction that the alternative dehydration to metastable  $\gamma$ -alumina is the only one observed. Thus steam appears to behave as a catalyst for the transformation of Boehmite to  $\alpha$ -alumina and possibly acts by providing a medium in which the two phases can dissolve and transform.

The present experiments enable a first estimate to be made of the relationship between the rate of the transformation and the water content of the system.

In a tube of 30 ml. capacity, containing 12 g. of  $\gamma$ -alumina and 2.5 g. of water, the formation of highly crystalline (0.002 cm.)  $\alpha$ -alumina is extensive after 14 hours at  $460^{\circ}\text{C.}$  (experiment 7), but is inappreciable after 14 hours at  $440^{\circ}\text{C.}$  (experiment 6). A similar difference in behaviour, between two temperatures, at a very similar composition, but with the alumina initially in the form of Boehmite is noted in experiments (1) and (2). Thus this transformation to  $\alpha$ -alumina is rapid at  $460^{\circ}\text{C.}$  at a water vapour pressure very much lower than that used by Laubengayer and Weisz; they estimated the pressure to be 10,000 lb./in.<sup>2</sup>, and if it is assumed that the alumina produces no lowering of the vapour pressure, it is possible to calculate from tables<sup>4</sup> that the pressure in experiments (1), (2), (6), and (7) is *ca.* 2,000 lb./in.<sup>2</sup>.

In a tube of 30 ml. capacity containing 14 g. of  $\gamma$ -alumina, and only 0.5 g. of water, the conversion to  $\alpha$ -alumina is inappreciable in 14 hours at  $500^{\circ}\text{C.}$  (experiment 5). The estimated water vapour pressure here, making the same assumption as above, is *ca.* 600 lb./in.<sup>2</sup>. However, from the fact that the crystal size has almost doubled at  $500^{\circ}\text{C.}$  in experiment (5), it is evident that rapid loss of activity of an alumina base catalyst is to be expected even under these conditions.

In a tube of 30 ml. capacity containing 6 g. of  $\gamma$ -alumina and 0.2 g. of water, neither formation of  $\alpha$ -alumina nor crystal growth of  $\gamma$ -alumina is appreciable in 14 hours at  $440^{\circ}\text{C.}$  (experiment 4). This corresponds to an estimated water vapour pressure of 240 lb./in.<sup>2</sup>, again assuming no lowering of water vapour pressure by alumina under these conditions.

In experiment (7) the formation of the very highly crystalline  $\alpha$ -alumina with an average crystal diameter of 0.002 cm., from a  $\gamma$ -alumina of average

<sup>4</sup> Perry, *Chemical Engineering Handbook* (McGraw Hill, 1941), p. 2441.



## 398 EFFECT OF STEAM ON ALUMINA TRANSITIONS

crystal diameter 50 A. or 0.000002 cm. (in other words, an increase in crystal size of approximately 1,000 diameters) is remarkable.\*

The authors wish to acknowledge the work done in the preparation of the samples by Mr. J. O. Clarke and Miss K. Rowland, and also to express their thanks to the Chairman of the Anglo-Iranian Oil Company for permission to publish this paper.

### Conclusion.

The rates of transformation of  $\gamma$ -alumina and of Boehmite to  $\alpha$ -alumina, and the rate of crystal growth of  $\gamma$ -alumina are all increased on increasing the water vapour pressure at a fixed temperature. At temperatures below 450° C. and water vapour pressures below 240 lb./in.<sup>2</sup>, none of these reactions is appreciable after 14 hours. After 14 hours at 500° C. at a water vapour pressure of 600 lb./in.<sup>2</sup>, crystal growth of  $\gamma$ -alumina is extensive, but formation of  $\alpha$ -alumina is inappreciable. After 14 hours at 460° C. at a water vapour pressure not exceeding 2,000 lb./in.<sup>2</sup>, formation of an extremely highly crystalline  $\alpha$ -alumina is extensive. Thus, there is evidence that steam behaves as a catalyst with regard to these transformations. It possibly acts by providing a medium in which the phases can dissolve and transform.

### Résumé.

Les vitesses de transformation de l'alumine  $\gamma$  et de la boehmite en alumine  $\alpha$  et la vitesse de croissance des cristaux d'alumine  $\gamma$  sont accrues, à température fixe, par un accroissement de la pression de vapeur d'eau. Celle-ci se comporte comme un catalyseur pour ces transformations, probablement en procurant un milieu où les phases peuvent se dissoudre et se transformer.

### Zusammenfassung.

Die Umwandlungen von  $\gamma$ -Aluminiumoxyd und Boehmit in  $\alpha$ -Aluminiumoxyd und der Kristallwuchs von  $\gamma$ -Aluminiumoxyd werden bei konstanter Temperatur durch Erhöhung des Wasserdampfdruckes beschleunigt. Es bestehen Hinweise dafür, dass Dampf auf diese Umwandlungen als Katalysator einwirkt, möglicherweise dadurch, dass es ein Lösungsmittel in dem sich die verschiedenen Formen auflösen und umwandeln können, beistellt.

Research Laboratories,

The Anglo-Iranian Oil Company, Ltd.,

Sunbury-on-Thames,

Middlesex.

\* Since the above paper was submitted for publication, two further experiments have been conducted. It has been suggested:

- (a) that the increased rate of transition from  $\gamma$ -alumina to the  $\alpha$ -alumina modification may have been due to traces of impurity in the  $\gamma$  variety, notably the presence of fluorides, and
- (b) that the lowering of the transition temperature might be attributable to pressure *per se*.

Suggestion (a) was checked by the following experiment on pure Gibbsite supplied by the British Aluminium Company, and stated by them to be very low in fluoride. Sufficient Gibbsite  $\text{Al}_2\text{O}_3 \cdot \text{H}_2\text{O}$  was placed in the 30 ml. bomb to give a water vapour pressure of 2,000 lb. per sq. in. at 460° C. (as a repeat of experiment (7)) and the bomb was heated for fourteen hours at this temperature. The resulting product was found to be almost pure  $\alpha$ -alumina, with about 5 % of Boehmite.

(b) The possible effect of high pressure in the absence of steam was examined by heating  $\gamma$ -alumina in the bomb for fourteen hours at 500° C. under a dry nitrogen pressure of 2,000 lb. per sq. in. The resulting product was found to be unchanged  $\gamma$ -alumina and no trace of  $\alpha$ -alumina could be detected.

# CHEMICAL SIMILARITY IN HETEROGENEOUS CATALYSIS

By R. C. L. BOSWORTH.

*Received 6th May, 1946.*

In the development on the industrial scale of a chemical process founded on any known reaction a number of steps each involving a limited increase in the size of the equipment are usually considered to be necessary. The reaction is first studied in small scale glass equipment in the laboratory and later is repeated in larger equipment referred to as of the semi-pilot scale. In terms of the optimum reaction conditions thus found, a larger or pilot scale equipment is designed, the performance of which will in turn decide the design of the factory scale equipment. In general with each change in scale there is an apparent change in the optimum working conditions. This state of affairs is, however, not peculiar to chemical engineering equipment. The performance, for example, of a full scale yacht cannot be estimated directly from that of a small model. It is necessary to set up a condition of dynamical similarity between the model and the large scale or prototype and to record the relationships between the observational variables in terms of dimensionless products. We might infer by analogy that we could obtain from small scale chemical equipment information of more direct use in the design of large scale equipment could we set up the conditions for chemical similarity between the two.

The author has already pointed out that the quantities now used to express the results of a physico-chemical investigation are seldom dimensionless in character,<sup>1</sup> and that an essential preliminary step towards the organisation of a small scale chemical investigation with a view to its most effective utilisation on the larger scale, is the arrangement of the experimental parameters in dimensionless groups.

## (1) The Method of Damköhler.

An attack on this problem was made by Damköhler.<sup>2</sup> The arguments he advanced have been discussed and extended by Edgeworth-Johnstone.<sup>3</sup> Damköhler's method consisted in writing down the fundamental equations for the conservation of mass, energy and momentum in the system in which the chemical reaction occurs. Dimensional homogeneity required that all the terms in any one equation should have the same physical dimensions, and the ratio of any pair of terms in any equation should be a dimensionless quantity. Damköhler deduced from such considerations that two different reactors of different sizes could act as model and prototype provided the following five conditions are satisfied; namely that the ratios

$$\frac{\text{Rate of generation of each substance by chemical reaction}}{\text{Rate of removal of such substance by convection}} \quad . \quad \text{(I)}$$

$$\frac{\text{Rate of generation of each substance by chemical reaction}}{\text{Rate of removal of such substance by diffusion}} \quad . \quad \text{(II)}$$

$$\frac{\text{Inertial force acting per unit volume}}{\text{Viscous force acting per unit volume}} \quad (\text{Reynolds number}) \quad . \quad \text{(III)}$$

<sup>1</sup> Bosworth, *J. Sci. Inst.*, 1943, **29**, 142.

<sup>2</sup> Damköhler, *Z. Elektrochem.*, 1936, **42**, 846.

<sup>3</sup> Edgeworth-Johnstone, *Trans. Inst. Chem. Eng.*, 1939, **17**, 129.

$$\frac{\text{Rate of generation of heat per unit volume by chemical reaction}}{\text{Rate of removal of heat per unit volume by convection}} \quad (\text{IV})$$

and

$$\frac{\text{Rate of generation of heat per unit volume by chemical reaction}}{\text{Rate of removal of heat per unit volume by conduction}} \quad (\text{V})$$

are the same in both model and prototype.

If the industrial chemist is considering the one chemical system in reactors of two different sizes he has in general only four independent experimental variables, namely, size of vessel, temperature, pressure, and flow rate. In general, therefore, it is not possible to satisfy five conditions, so that a given reaction taking place in a continuous manner in a large scale reactor cannot exhibit complete chemical similarity to the same chemical system in a smaller reactor.

Edgeworth-Johnstone<sup>2</sup> has claimed that Damköhler has overestimated the number of degrees of freedom of a molecular assembly in a continuous reactor by ignoring the Arrhenius relationship between the reaction velocity  $U$  and the absolute temperature  $T$ , namely

$$U = U_0 e^{-E/RT},$$

where  $E$  is the activation energy for the system concerned. The implied relationship between  $U$  and the temperature-excess controlling the rates of heat convection and conduction reduces by one the number of independent conditions of the Damköhler type, but at the same time introduces another dimensionless parameter, namely  $E/RT$ , equality of which in model and prototype has to be satisfied before complete chemical similarity is attained. In an ordinary chemical assembly  $E$  is a property of the reaction concerned and may not be varied independently of it. We therefore still have one experimental variable too few for satisfaction of all the conditions of chemical similarity. In catalysed systems, however, the magnitude of  $E$  varies with the activity of the catalyst, and by using different catalysts in model and prototype we have at least a sufficient number of variables to satisfy the conditions of similarity, provided, of course, that we can arrange that no two of the conditions are mutually inconsistent.

## (2) The Physical Variables in Cylindrical Reactors involving Heterogeneous Catalysis.

A system involving heterogeneous catalysis has a larger number of degrees of freedom than one involving homogeneous catalysis, so that the possibility of attaining complete similarity is more promising in the former case. The usual type of heterogeneous catalyst employed industrially takes the form of a granular solid. For a given chemical reaction taking place on a granular mass packed in a cylindrical reactor we have the following experimental variables.

- (a) The length  $L$  of the reactor—dimension  $l$ .
- (b) The diameter  $D$  of the reactor—dimension  $l$ .
- (c) The mean diameter ( $d$ ) of the pores between the catalyst granules—dimension  $l$ .
- (d) The space velocity ( $S$ ) expressed in litres of reagent per litre of catalyst per second—dimension  $t^{-1}$ .
- (e) The temperature ( $T$ ) at any standard point in the reactor (say at the walls)—dimension  $\theta$ .
- (f) The excess temperature ( $\theta$ ) between the centre of the catalyst mass and the walls (the overtemperature of Damköhler)—dimension  $\theta$ .
- (g) The concentration  $C_j$  of the  $j^{\text{th}}$  component of the reaction mixture expressed in grams per litre—dimension  $m l^{-3}$ . The  $j^{\text{th}}$  component may conveniently be taken as the dominant reagent.

- (h) The reaction rate controlled by the catalyst activity (and the temperature) and expressed as the rate of change of the concentration  $C_j$ , namely as  $\dot{C}_j$ —dimensions  $m\ l^{-3}\ t^{-1}$ .

In addition the following physical and chemical properties are involved in setting up the conditions of chemical similarity :

- (i) The density ( $\rho$ ) of the reagent stream—dimensions  $m\ l^{-3}$ .  
 (j) The kinematic viscosity ( $\nu$ ) of the reagent stream—dimensions  $l^2\ t^{-1}$ .  
 (k) The thermal conductivity ( $k$ ) of the reagent stream—dimensions  $m\ l\ t^{-3}\ \theta^{-1}$ .  
 (l) The heat capacity (at constant pressure) ( $c_p$ ) of the reagent stream—dimensions  $l^2\ t^{-2}\ \theta^{-1}$ .  
 (m) The diffusion coefficient of the  $j^{\text{th}}$  component  $\Delta_j$ —dimensions  $l^2\ t^{-1}$ , and  
 (n) The heat of reaction ( $Q$ ) per unit mass—dimensions  $l^2\ t^{-2}$ .

The physical and chemical properties,  $\rho$ ,  $\nu$ ,  $k$ ,  $c_p$ ,  $\Delta_j$  and  $Q$  will in general all vary with the temperature in a way which will not be specified until the chemical composition is known. It would therefore seem advisable, in obtaining a general solution, to make the wall temperature  $T$  the same in both model and prototype, leaving the overtemperature ( $\theta$ ) as the only temperature variable. Solutions to specific problems in similarity other than that given below could possibly be found in which the wall temperature is different in model and prototype. Such specific problems demanding a knowledge of the rate at which  $\rho$ ,  $\nu$ ,  $k$ ,  $c_p$ ,  $\Delta_j$  and  $Q$  vary with the temperature will not further be considered in this paper.

The diffusivity  $\Delta_j$  effective in transporting molecular species across the flowing stream will clearly be identifiable with the ordinary molecular diffusivity if the flow through the packed catalyst is laminar in nature. If the flow is turbulent  $\Delta_j$  will be the turbulent diffusivity of the type studied by Richardson<sup>4</sup> and will be dependent on the Reynolds number and independent of the temperature. Since under condition III the Reynolds number must be the same in model and prototype,  $\Delta_j$  must also be the same in both.

In a similar way  $k$ , the thermal conductivity effective in transporting heat across the reagent stream will only be identifiable with the ordinary molecular conductivity under conditions of laminar flow. In turbulent flow the effective thermal conductivity may be taken, in terms of the Reynolds analogy, as dependent only on the Reynolds number and will thus be made the same in model and prototype under condition III.

At the higher temperatures, conduction (molecular or turbulent) and convection of heat are supplemented by radiation. Radiation may be treated as a diffusion (or effusion) process in which photons act as additional carriers of heat energy travelling with the velocity of light and moving through relatively long mean free paths.<sup>5</sup> Since the catalyst grains consist of extremely porous solids they may be regarded as effectively black bodies and the mean free path of the photons is thus the average distance between granule surfaces, namely, the pore diameter  $d$ . The diffusion coefficient for a photon is thus proportional to  $d$ . The effective thermal conductivity for the transport of heat by the two mechanisms of conduction and radiation in parallel may therefore be put in the form :

$$k(1 + \alpha d),$$

where  $k$  is the contribution due to molecular or turbulent conduction and  $\alpha kd$  the contribution due to radiative transfer ;  $\alpha$  is thus a proportionality factor of dimensions  $l^{-1}$  describing the relative intensity of the radiative and other radial means of transporting heat. Under conditions of complete similarity  $\alpha$  must have the same value in model and prototype.

<sup>4</sup> Richardson, *Proc. Physic. Soc.*, 1937, **49**, 479.

<sup>5</sup> Bosworth, *Proc. Roy. Soc. (N.S.W.)*, 1945, **79**, 63.

## (3) Similarity Conditions.

In terms of the variables given above the five similarity conditions may be written in the form :

$$I = \frac{\dot{C}_j}{SC_j} \quad . \quad . \quad . \quad . \quad . \quad (1)$$

$$II = \frac{\dot{C}_j d^2}{\Delta_j C_j} \quad . \quad . \quad . \quad . \quad . \quad (2)$$

$$III = Re = \frac{SdI}{\nu} \quad . \quad . \quad . \quad . \quad . \quad (3)$$

$$IV = \frac{Q\dot{C}_j}{\rho c_p \theta S} \quad . \quad . \quad . \quad . \quad . \quad (4)$$

$$V = \frac{Q\dot{C}_j D^2}{h(1 + \alpha d)\theta} \quad . \quad . \quad . \quad . \quad . \quad (5)$$

In the expressions above  $\dot{C}_j$  represents the rate of change in the mass of component  $j$  per unit volume due to chemical reaction and  $SC_j$  the rate of change of the mass of component  $j$  per unit volume due to forced convection. The equality of expression I in two vessels ensures that the average time spent by the molecules in contact with the catalyst mass in either vessel is the same fraction of the mean life of molecules under the conditions obtaining in the vessel concerned. If this condition is not satisfied it is quite clear that the chemical reaction will proceed further in one vessel than in the other.

All molecules in the assembly constituted by the reagent stream do not travel at the same rate through the reaction zone. If two systems in different sized vessels are to be similar each must exhibit not only the same mean time for reaction (expressed in terms of the speed of the reaction) but also must give identical functions representing the departure of definite fractions of the stream from the mean time of transit through the reaction zone. These functions, as shown by the author,<sup>6</sup> are controlled by the diffusivity of the reagents. Condition II above appears to be an interpretation of this requirement. The rate of change per unit volume due to diffusion is equal to

$$\text{div } \Delta_j \text{ grad } C_j.$$

The mean distance through which this diffusion takes place is governed by the diameter  $d$  of the pores between the catalyst grains. The rate of change of mass of component  $j$  per unit volume due to diffusion is therefore proportional to

$$\Delta_j C_j / d^2,$$

from which the expression for condition II given in equation (2) follows.

Expression III is the modified Reynolds number for flow through porous spaces of average diameter  $d$ . The space velocity multiplied by the length is equal to the linear flow velocity through the reaction zone. Equality of the Reynolds numbers in two vessels ensures the same hydrodynamical flow pattern and in addition equality of the coefficients for the turbulent transfer of heat and of molecular species.

The heat loss ratios IV and V follow from arguments analogous to those used in the discussion of mass changes.  $D^2$  instead of  $d^2$ , however, occurs in V because the mean distance over which heat is transported is not the distance from grain to grain but the distance from wall to wall.

The heat of reaction  $Q\dot{C}_j$  and the overtemperature  $\theta$  may be eliminated from equations (4) and (5) and the requirement for similarity put in the form,

$$\frac{IV}{V} = \frac{h(1 + \alpha d)}{\rho c_p S D^2} \quad . \quad . \quad . \quad . \quad . \quad (6)$$

which has to be the same in all vessels exhibiting complete similarity.

<sup>6</sup> Bosworth, *Phil. Mag.*, 1947 (in press).

## (4) Comparison of Model with Prototype:

The dimensional problem which usually arises in chemical industry may be illustrated by the following generalised example. Suppose that we have found a satisfactory method of operating the required chemical reaction in a vessel of a certain size and we require to transform the operation to a larger scale. Let  $D$  be the diameter of the experimental reactor and let the diameter of the larger scale vessel to which transfer is to be made be  $D'$ , where

$$D' = mD. \quad (7)$$

$m$  is thus the scale factor associated with the transference.

In view of what has been written above we will make the temperature  $T$  of the walls of both vessels the same. The properties  $k$ ,  $\alpha$ ,  $\rho$ ,  $c_p$ ,  $\nu$  and  $\Delta_f$  are therefore the same in both vessels.\* We will denote the variables referring to the former or model vessel by the symbols used above in section (3). The corresponding variables referred to the new or prototype vessel will be denoted by the same symbols written with a prime. Thus from conditions IV and V (equation 6) we obtain:

$$\frac{1 + \alpha d}{SD^2} = \frac{1 + \alpha d'}{S'D'^2}$$

which on inserting the scale factor defined by equation (7) becomes:

$$\frac{1 + \alpha d}{S} = \frac{1 + \alpha d'}{m^2 S'}$$

or

$$S' = \frac{1}{m^2} \frac{1 + \alpha d'}{1 + \alpha d} S. \quad (8)$$

This means that in the larger vessel the space velocity should be reduced.

Applying condition I (equation (1)) we obtain:

$$\frac{d}{dt} \left( \frac{\log C_f}{S} \right) = \frac{d}{dt} \left( \frac{\log C'_f}{S'} \right),$$

which on substitution in equation (8) gives:

$$\frac{d}{dt} (\log C'_f) = \frac{1}{m^2} \frac{1 + \alpha d'}{1 + \alpha d} \frac{d}{dt} (\log C_f). \quad (9)$$

This means that in the larger vessel the reaction rate and therefore the catalyst activity should be reduced. Large scale equipment can satisfactorily use a less active heterogeneous catalyst than can small scale equipment.

On account of the constancy of the diffusivity condition, II may be expressed as:

$$d^2 \frac{d}{dt} (\log C_f) = d'^2 \frac{d}{dt} (\log C'_f),$$

and this on substitution in equation (9) becomes:

$$d^2 = \frac{d'^2}{m^2} \frac{1 + \alpha d'}{1 + \alpha d}$$

or

$$m^2 (d^2 + \alpha d^3) = d'^2 + \alpha d'^3.$$

If we take  $a$  as the scale factor for the grain pore diameters, i.e.

$$d' = ad \quad (10)$$

we have for the relation between  $a$  and  $m$

$$a^2 + \alpha a^3 d = m^2 (1 + \alpha d). \quad (11)$$

\* This is strictly correct only if in addition the excess temperature  $\theta$  is the same at corresponding points in the similar reactors. In general, however, effective variation with  $\theta$  at fixed  $T$  is small.

Condition III, the constancy of the Reynold's number finally requires that :

$$SdL = S'd'L'$$

$$\text{or} \quad L' = \frac{m^2}{a} \frac{1 + \alpha d}{1 + a\alpha d} L. \quad (12)$$

Thus if we solve for  $a$  we may express equations (8), (9), (10) and (12) explicitly in terms of  $m$ , the scale factor for the diameter of the reactors. The solution of the cubic equation (11) in general leads to a complicated expression but in two special cases very simple solutions are obtained. The two special cases arise when (1) radiative heat loss is negligible in comparison with conduction, and (2) when conduction is negligible in comparison with radiation.

**(4.1) Conductive Heat Transfer Dominating.**—In this case  $\alpha d$  is a small quantity and we may express equation (11) as :

$$a = m\{1 + \frac{1}{2}\alpha d(1 - m)\} \quad (13)$$

The conditions for similarity then become :

$$d' = m\{1 - \frac{1}{2}\alpha d(m - 1)\}d \quad (14)$$

$$S' = m^{-2}\{1 + \alpha d(m - 1)\}S \quad (15)$$

$$\frac{d}{dt}(\log C_i') = m^{-2}\{1 + \alpha d(m - 1)\} \frac{d}{dt}(\log C_i) \quad (16)$$

$$\text{and} \quad L' = m\{1 - \frac{1}{2}\alpha d(m - 1)\}L \quad (17)$$

If we neglect the small quantities in  $\alpha d$  these expressions become :

$$d' = md \quad (14a)$$

$$S' = m^{-2}S \quad (15a)$$

$$\frac{d}{dt}(\log C_i') = m^{-2} \frac{d}{dt}(\log C_i) \quad (16a)$$

$$\text{and} \quad L' = mL \quad (17a)$$

In this simple case geometrical similarity between the shapes of model and prototype reactors is maintained and the grain size is directly proportional to the diameter of the reactor. The reaction velocity constant and space velocity are both to be maintained inversely proportional to the square of the diameter of the reactor. When the effect of radiation is taken into account the geometrical similarity between length and diameter and between grain diameter and reactor diameter no longer obtains.

**(4.2) Radiative Heat Losses Dominating.**—In this case  $1/\alpha d$  becomes a negligibly small quantity and equation (11) may be written :

$$a^3 + \frac{a^2}{\alpha d} = m^2\left(\frac{1}{\alpha d} + 1\right)$$

from which

$$a = m^{2/3}\left\{1 + \frac{1}{3\alpha d}(1 - m^{-2/3})\right\} \quad (18)$$

The conditions for similarity then become :

$$d' = m^{2/3}\left\{1 + \frac{1}{3\alpha d}(1 - m^{-2/3})\right\}d \quad (19)$$

$$S' = m^{-4/3}\left\{1 - \frac{2}{3\alpha d}(1 - m^{-2/3})\right\}S \quad (20)$$

$$\frac{d}{dt}(\log C_i') = m^{-4/3}\left\{1 - \frac{2}{3\alpha d}(1 - m^{-2/3})\right\} \frac{d}{dt}(\log C_i) \quad (21)$$

$$\text{and} \quad L' = m^{2/3}\left\{1 + \frac{1}{3\alpha d}(1 - m^{-2/3})\right\}L \quad (22)$$

When the small contribution due to conduction (or turbulent conduction) is neglected these expressions become :

$$d' = m^{2/3}d \quad . \quad . \quad . \quad . \quad (19a)$$

$$S' = m^{-4/3}S \quad . \quad . \quad . \quad . \quad (20a)$$

$$\frac{d}{dt}(\log C_i') = m^{-4/3} \frac{d}{dt}(\log C_i) \quad . \quad . \quad . \quad (21a)$$

and

$$L' = m^{2/3}L \quad . \quad . \quad . \quad . \quad (22a)$$

In this case the conditions for geometrical similarity either between the length and diameter of the reactors or between the diameters of reactors and of catalyst grains are not maintained. The large scale reactor is relatively shorter than the small scale one.

### (5) The Output.

The output ( $O$ ) of the reactor expressed in volume of reactant per unit time is, for a given reaction efficiency, proportional to the product of the space velocity by the bulk volume of the catalyst. Thus we have

$$O = \frac{\pi}{4} D^2 L S \quad . \quad . \quad . \quad . \quad (23)$$

In the case of a system in which conductive heat transfer is dominating, i.e. at relatively low temperatures or under conditions of high Reynolds number so that the turbulent conduction is large, the output  $O'$  of the prototype is related to the output of the model  $O$  by :

$$\begin{aligned} O' &= [m^3 \cdot m\{1 - \frac{1}{2}\alpha d(m-1)\} \cdot \frac{1}{m^2}\{1 + \alpha d(m-1)\}]O \\ &= m\{1 + \frac{1}{2}\alpha d(m-1)\}O \quad . \quad . \quad . \quad . \quad (24) \end{aligned}$$

which is obtained by combining equations (7), (15), (17) and (23).

When radiative heat transfer dominates we may similarly find the output of the prototype in terms of the output of the model by substituting equations (7), (20) and (22) in (23), i.e.

$$\begin{aligned} O' &= m^2 m^{2/3} \left\{ 1 + \frac{1}{3\alpha d} (1 - m^{-2/3}) \right\} m^{-4/3} \left\{ 1 - \frac{2}{3\alpha d} (1 - m^{-2/3}) \right\} O \\ &= m^{4/3} \left\{ 1 - \frac{1}{3\alpha d} (1 - m^{-2/3}) \right\} O \quad . \quad . \quad . \quad . \quad (25) \end{aligned}$$

It will be seen in either case that the output from chemically similar reactors varies much less rapidly than the cube of the linear dimensions. This result arises from the fact that the conditions of chemical similarity require that the smaller vessel be operated at a more rapid rate than the large vessel.

This particular result sets a limit to the usefulness of the model method of studying large scale chemical systems. If the catalyst used on the large scale is relatively efficient it will in general simply not be possible to find a catalyst with the very much higher efficiency required in order to attain conditions of similarity on any appreciable smaller scale. Conversely if a catalyst of accessible activity is used on the smaller scale, chemical similarity would demand the use on the large scale of a catalyst of such inferior activity that its employment could not be tolerated on economic grounds. It must be admitted therefore that although variation in the activity of the catalyst permits Damköhler's five conditions for chemical similarity all to be satisfied, the necessary variation in the catalyst activity is so large that only vessels of approximately the same geometrical size may be compared by this means.



### Summary.

The five conditions for similarity in chemical systems as given by Damköhler may all be satisfied in systems involving heterogeneous catalysis if both the grain size and the catalyst activity are allowed to vary. When the reaction mixture passes over the catalyst mass, heat and each particular molecular species produced (or destroyed) by chemical reaction, are carried along by the stream or are carried to the walls by diffusion or turbulent diffusion in the case of molecular species, or by conduction, turbulent conduction or radiation in the case of heat.

When conduction (or turbulent conduction) provides the dominant mode of heat transfer the length of the reaction tube and the size of the catalyst grains are directly proportional to the diameter of the reaction tube. The space velocity and the catalyst activity are to be adjusted inversely proportional to the square of the diameter of the reactor. The output, under conditions of chemical similarity, is proportional to the diameter of the reactor or proportional to the cube root of the catalyst volume.

When radiation dominates the heat transfer similarity requires that the grain diameter and length of the reaction zone be both proportional to the two-thirds power of the diameter of the reactor, while the catalyst activity and the space velocity are both proportional to the inverse four-thirds power of the reactor diameter. The output in this case is proportional to the four-thirds power of the reactor diameter or to the square root of the volume of catalyst.

### Résumé.

Les cinq conditions de similarité chimique, définies par Damköhler, peuvent être satisfaites dans la catalyse hétérogène, si l'on fait varier et la taille du grain et l'activité du catalyseur. Quand la conduction est le facteur dominant dans le transport de chaleur, la longueur de la zone de réaction et la taille du grain varient directement comme le diamètre du tube à réaction, tandis que la "vitesse" (litre de réactif par litre de catalyseur par seconde) et l'activité du catalyseur varient comme le carré du diamètre; le rendement est donc proportionnel au diamètre du tube ou à la racine cubique du volume du catalyseur. De la même façon, des relations sont établies dans le cas où la radiation domine le transport de chaleur.

### Zusammenfassung.

Die Bedingungen von Damköhler angegebenen der chemischen Ähnlichkeit in heterogener Katalyse können erfüllt bleiben, auch wenn die Korngrösse und Aktivität des Katalysators verändert werden. Wenn Wärmeübertragung hauptsächlich durch Leitung erfolgt, sind die Länge der Reaktionszone und die Korngrösse proportional zum Durchmesser der Röhre und die Raumgeschwindigkeit und Katalysatoraktivität müssen proportional zum reziproken Quadrat des Durchmessers des Reaktionsgefässes adjustiert werden. Die Ausbeute ist dann zum Durchmesser des Reaktionsgefässes oder zu der Kubikwurzel des Katalysatorvolumens proportional. Ähnliche Beziehungen werden für den Fall, wenn die Wärmeübertragung hauptsächlich durch Strahlung erfolgt, ausgearbeitet.

41 *Spencer Road,*  
*Killara, N.S.W.,*  
*Australia.*

# ELECTROPHORETIC DEPOSITION OF POWDERED MATERIALS FROM NON-AQUEOUS SUSPENSIONS.

BY C. G. A. HILL, P. E. LOVERING AND A. L. G. REES.\*

Received, 15th May, 1946.

There have been several publications concerning qualitative observations on the deposition of layers of powdered substances by means of electrophoresis.<sup>1-5</sup> On the basis of certain quantitative investigations, Hamaker<sup>6</sup> has built up an expression relating the yield,  $Y$  in grams, in terms of several variables, upon which it was found to depend. Hamaker's expression is :

$$Y = \sigma C \int \frac{dV}{dn} \cdot dS \cdot dt,$$

where  $C$  is the concentration,  $dV/dn$  the electric field perpendicular to the surface  $S$ ,  $t$  the time of application of the field, and  $\sigma$  a coefficient which depends on the chemical constitution of the suspension and has the dimensions of  $v. cm.^{-1}/cm. sec.^{-1}$ . Hamaker identified this constant with the electrophoretic velocity in the case where every particle reaching the electrode is deposited. Benjamin and Osborn<sup>4</sup> quote experiments in which some of the particles possessed negative and others positive  $\zeta$ -potentials, migration taking place to the anode and cathode simultaneously. The addition of high molecular weight polymers to these suspensions tended to suppress one direction of migration and enhance the other. This behaviour is consistent with the results of certain quantitative experiments reported here.

## Theoretical.

It will be as well to define at the outset the conditions under which our equations are derived. The assumptions regarding the behaviour of a particle in the suspension are those normally made in the treatment of electrokinetic problems, namely, that the particles are substantially spherical, that the electrical double layer is spherically symmetric and that Stokes's hydrodynamic equations apply. The electrolyte responsible for double-layer formation is chosen to be symmetric,<sup>†</sup> since in the experiments conducted by us this is certainly the case, so that Hermans's correction terms<sup>7</sup> for the double-layer distortion under the influence of the applied field may be neglected, and Henry's theory of electrophoresis employed. Our experimental conditions corresponded to  $\kappa a \gg 1$ , in which case Henry's function  $f(\kappa a) \approx 1$  and  $\mu/\mu' \ll 10^{-3}$ , where  $a$  is the particle radius,  $1/\kappa$  the effective thickness of the double layer on the Debye-Hückel theory,  $\mu$  the conductivity of the disperse phase and  $\mu'$

\* Present address, Council for Scientific and Industrial Research, Melbourne Australia.

† A symmetric electrolyte is one in which  $\sum n_k e_k = 0$ , where  $n_k$  is the concentration of ions of charge  $e_k$  in the bulk of the liquid. See ref.<sup>7</sup>, p. 137.

<sup>1</sup> de Boer, Hamaker and Verwey, *Rec. trav. chim.*, 1939, **58**, 662.

<sup>2</sup> Patai and Tomaschek, *Kolloid Z.*, 1936, **74**, 253; **75**, 80.

<sup>3</sup> Brit. Pat. No. 444,723.

<sup>4</sup> Benjamin and Osborn, *Trans. Faraday Soc.*, 1940, **36**, 287.

<sup>5</sup> Hamaker and Verwey, *ibid.*, 180.

<sup>6</sup> Hamaker, *ibid.*, 279.

<sup>7</sup> Hermans, *ibid.*, 133.

that of the medium. We can then employ the original Smoluchowski expression for the electrophoretic velocity<sup>8</sup>

$$u = \frac{\epsilon \zeta dV/dn}{4\pi\eta},$$

where  $\zeta$  is the electrokinetic potential of the double layer,  $\epsilon$  the dielectric constant of the medium, and  $\eta$  the viscosity of the medium in which the particle is moving.

For convenience in experimental technique we have carried out our investigations with a concentric cylindrical electrode arrangement, in which the deposition always occurred on the inner electrode. The subsequent theoretical developments apply to such an electrode assembly, although the general case is easily derived from this discussion.

Putting the initial concentration of the suspension at  $C_0$  g. cm.<sup>-3</sup>, the radius of the inner electrode  $r_1$  and that of the outer electrode  $r_2$ , we have:

$$u = \frac{\epsilon \zeta V}{4\pi\eta \log_e r_2/r_1} \cdot \frac{1}{r'},$$

as

$$dV/dn = \frac{V}{r \cdot \log_e r_2/r_1},$$

where  $V$  is the potential drop across the electrodes and  $r$  the normal distance of the particles under consideration from the symmetry axis of

the electrode assembly ( $r_1 < r < r_2$ ). Writing  $\lambda = \frac{\epsilon \zeta V}{4\pi\eta \log_e r_2/r_1}$ , we

have  $u = \lambda/r = -dr/dt$  or  $\int_0^t \lambda \cdot dt = - \int_{r'}^r r \cdot dr$ , where  $r = r'$  at  $t = 0$ .

In the case in which  $\lambda$  is a function of the time owing to polarisation phenomena, the integration cannot be made, as the function is not known. However, our experimental case did not exhibit a dependence of the potential drop across the cell with time and for our purposes at least we can integrate to obtain

$$r = \sqrt{r'^2 - 2\lambda t}. \quad (1)$$

The concentration  $C_r$  at  $r$  after time  $t$ , due to particles arriving from  $r'$  is  $C_0 r'/r$ , so that

$$C_r = C_0 \sqrt{r'^2 + 2\lambda t}/r. \quad (2)$$

We have not as yet considered the limiting packing of the particles nor the interactions of their double layers at short distances. Denoting the maximum possible concentration representing a coherent layer of particles on the electrode by  $C_m$ , we know that a fraction  $\alpha$  of the particles within a distance  $r' = \sqrt{r_1^2 + 2\lambda t}$  will be packed around the electrode with concentration  $C_m$ . The factor  $\alpha$  can be identified with the probability of a particle entering the deposited layer from the region of suspension within the distance  $r'$ . The radius  $r_a$  of this deposited layer will then be such that

$$r_a = \sqrt{r_1^2 + \alpha \cdot C_0/C_m \cdot 2\lambda t}. \quad (3)$$

Combining equations (2) and (3) we can obtain concentration-distance curves for various values of  $t$ . These are essentially the same as those represented by Hamaker and Verwey.<sup>5</sup> In terms of weight deposited on length  $h$  cm. of the electrode, we have

$$Y = 2\pi \cdot \alpha \lambda C_0 h t. \quad (4)$$

The derivation of this equation, however, ignores the mutual interaction of the particles, an effect which must be taken into account for the explanation of certain phenomena. An extension of the arguments of Hamaker and Verwey leads us to the belief that there will be a region of concentration, more or less sharply defined, much higher than the

<sup>8</sup> Smoluchowski, *Graetz' Handbuch Elec. Mag.*, 1914, 2, 366.

original suspension concentration and yet still fluid. Hamaker<sup>\*</sup> has derived expressions for the energy of interaction between two particles as a function of the distance between them, and it appears likely that the potential energy curve applying to most cases with which we are concerned can be represented as in Fig. 1 (i),  $\rho$  being here the shortest distance between the particles and *not* the distance between centres. The potential energy due to the applied potential field, of a single particle moving towards a layer of particles already on the surface can be represented by a straight line over the small distance involved (ii), the slope depending on the applied

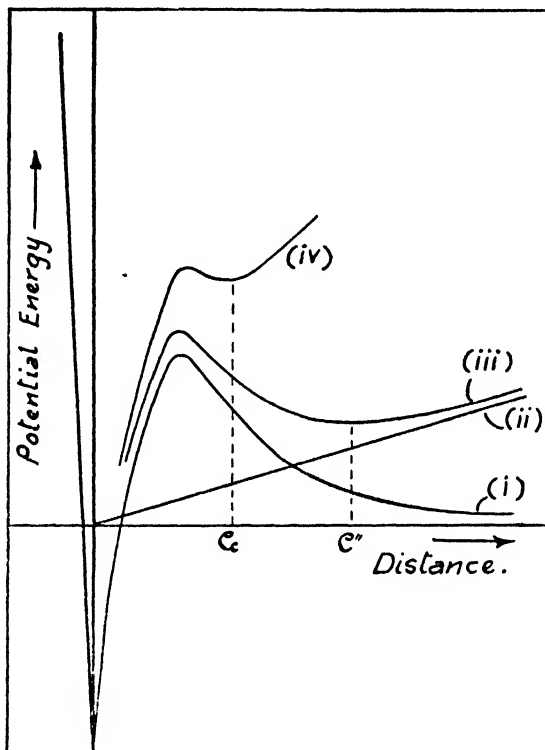


FIG. 1.—The interaction between two particles : (i) before and (iii) after application of the electric field (ii). Curve (iv) indicates the potential energy function when deposition begins.

potential. From the sum, curve (iii), it is apparent that, independently of any other influences, the particles will take up an equilibrium separation  $\rho''$ . Unless the slope of curve (ii) is sufficiently great to eliminate the potential minimum in (iii) at  $\rho''$ , the first layer of particles will remain at such a separation. However, the second layer of particles will take up a position at a distance  $\rho''$  from the first layer and the pressure exerted by this layer on the first layer will increase the slope of (ii) with the subsequent displacement of the minimum to a smaller separation,  $\rho'''$ , say. This process is repeated in time until finally the layer of particles closest to the cathode have a separation,  $\rho_e$  (iv), where the energy derived from Brownian movement takes them over the potential barrier into the minimum at  $\rho = 0$ . The distribution of the suspended phase at a time  $t$  is then represented as in Fig. 2, for the case where convection currents

\* Hamaker, *Rec. trav. chim.*, 1937, 56, 3; 727.

in the suspension are ignored. The existence of a point of inflexion at  $C_{\rho''}$  is a direct result of the mutual interaction of the particles.

From  $t = 0$  to some critical time  $t^*$ , there will be no deposition at concentration  $C_m$ , but only a steady increase in the radius  $r_b$  of the layer of concentration  $C_{\rho''} \sim C_{\rho_c}$ . Not until the radius  $r_b$  has reached a value such that force exerted by all the particles on the innermost layer is sufficient to push the particles over the potential barrier will the layer of concentration  $C_m$  begin to appear. Now the force due to the potential field acting on a single particle and directed towards the axis of the electrode system is  $e\zeta a \cdot dV/dn$ , where  $a$  is the radius of the particle. The number of particles in a ring of radius  $r$ , thickness  $dr$  and of unit length is  $\frac{2\pi r \cdot dr \cdot C_s(r)}{m}$ , where  $m$  is the mass of a single particle. Therefore, the total force acting on the particles closest to the cathode surface, i.e. is

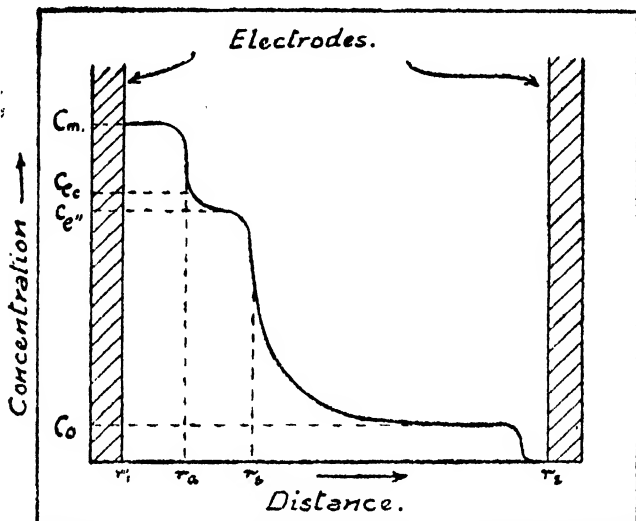


FIG. 2.—Distribution of suspended phase about a cylindrical electrode during deposition.

at  $r_1$ , due to the layer of particles of concentration  $C_s(r)$  between  $r_1$  and  $r_b$

$$\begin{aligned} & \frac{2\pi a e \zeta V}{m \cdot \log_e r_2/r_1} \int_{r_1}^{r_b} C_s(r) dr \\ &= \frac{8\pi^2 \lambda a \eta}{m} \int_{r_1}^{r_b} C_s(r) dr \end{aligned}$$

The force acting on a single particle at  $r_1$ , of projected area  $\pi a^2$ , is therefore

$$\frac{3\pi \lambda \eta}{r_1 d} \int_{r_1}^{r_b} C_s(r) dr,$$

where  $d$  is the particle density in g. cm.<sup>-3</sup>.

In order that the potential barrier might be surmounted this force must be  $> f\left(\frac{\phi}{(\rho'' - \rho_c)}\right) = q$ , where  $\phi$  is the energy of the barrier at  $\rho_c$  (i.e. the difference in the ordinates of curves (iv) and (iii) at  $\rho_c$  and  $\rho''$  respectively). We may then equate this expression to the preceding one if  $r_b$  is replaced by a critical value  $r_b^*$ , obtaining

$$q = \frac{\eta 3\pi \lambda}{r_1 d} \int_{r_1}^{r_b^*} C_s(r) dr.$$

For our purposes an average value of  $C_s(r)$ , say  $C_s$ , can be employed, when the above equation reduces to

$$r_b^* = r_1 + \frac{r_1 q d}{C_s 3 \pi \lambda \eta}.$$

We know also that  $r_b^* = \sqrt{r_1^2 + 2 \frac{C_0}{C_s} \cdot \lambda t^*}$ , where  $t^*$  is the time at which the critical radius  $r_b^*$  is reached, so that

$$t^* = \frac{r_1^2 q d}{3 \pi \lambda^2 C_0 \eta} \left( \frac{q d}{6 \pi \lambda C_s \eta} + 1 \right) \quad (5)$$

The complete equation for deposition is then  $Y = 2 \pi \alpha \lambda C_0 h (t - t^*)$  where  $Y = 0$  for  $t < t^*$ .

The corresponding equation for the yield and critical time for plane parallel electrodes can be established readily along similar lines.

We can make certain assumptions about the values of the parameters in the equations for  $t^*$  and  $r_b^*$ , so that some idea of their order of magnitude may be obtained. Strictly speaking,  $q$  is the maximum slope of the locus of the minima in the family of curves between (iii) and (iv) of Fig. 1.

For the present purpose we may take this as linear and write  $q = \left( \frac{\phi}{\rho'' - \rho_c} \right)$ .

$\phi$  will be of the order of  $10^{-12}$  erg (see Hamaker<sup>9</sup>),  $C_s$  will be close to  $C_m$ , that is, about  $1.2 \text{ g. cm.}^{-3}$  and  $(\rho'' - \rho_c)$  must be of the order of the double layer thickness,  $\sim 10^{-6} \text{ cm.}$  For the conditions of our experiments,  $t^*$  is then of the order  $10^{-3} - 10 \text{ sec.}$  and  $r_b^* > 10^{-3} \text{ cm.}$  It is also noticed that the term in parenthesis in equation (5) is close to unity. This calculation gives some indication of the possibility of observing these critical phenomena experimentally. An observation of the critical time, under conditions chosen to be the most favourable for large  $t^*$ , can be made, but observations of the critical radius are clearly impossible.

The formation of a layer of high concentration close to the deposit described above is due to the interaction of the particles approaching the deposit itself and will occur at both plane and cylindrical electrodes. For the cylindrical case, however, the possibility of a further complication arises. We have seen (equation (2)) that during the deposition a concentration gradient is set up in the cell owing to the fact that all the particles are moving towards the central electrode. It is possible, therefore, that concentrations considerably higher than  $C_0$  will be found at distances greater than  $r_b^*$ . Should the concentration in this region approach  $C_s$ , then again the interaction between the particles will become significant. It can be seen that this interaction will increase in importance as the ratio  $C_0/C_s \rightarrow 1$ . In our experiments this ratio was never greater, than 0.1, so that this interaction may be justifiably neglected. However, with suspensions of higher initial concentration approaching pastes, the equations for the yield will break down owing to this interaction.

### Experimental.

The experiments were carried out with a barium strontium carbonate (molar proportions 1 : 1), precipitated from a solution of the mixed nitrates by  $\text{Na}_2\text{CO}_3$ . The impurity ions are then expected to be  $\text{Na}^+$  and  $\text{NO}_3^-$ ; this was confirmed by analysis. Suspensions were prepared from freshly dried carbonate (at  $120^\circ \text{C. in vacuo}$ ) in a disperse medium of composition—methyl alcohol 80 %, amyl acetate 20 % by volume—by ball-milling with steatite balls in a porcelain mill under standard conditions for 12 hours. Where suspensions containing high molecular weight polymers were required, polyvinyl acetate resins were dispersed in the methyl alcohol-amyl acetate and the suspensions prepared as before. The mean molecular weights of these resins had been previously determined by Staudinger's method.

(i) **Particle Size.**—The particle size distribution was determined both before and after milling the suspensions by a modified Sven Odén sedimentation

<sup>10</sup> Hamaker, *Trans. Faraday Soc.*, 1940 36, 187.

method<sup>11</sup> and by microscopic analysis. The two methods gave results which closely agreed; it was found that the distribution was not appreciably altered during ball-milling, which appeared to break down loosely bound aggregates only and bring the suspension into equilibrium as far as the distribution of ions was concerned. The mean radius for the weight distribution was  $2.50\mu$  and the variance of  $\log_e a = 0.132$ .

(ii) **Viscosity**.—Viscosity measurements were carried out on all disperse media at  $25^\circ\text{C}$ . using an Ostwald viscometer. The values obtained have been tabulated along with other data in Tables I and II.

(iii) **Electrophoretic Mobility**.—Mobility determinations were carried out by a moving-boundary technique similar to that of Sen Gupta.<sup>12</sup> By using disperse medium obtained by centrifuging a quantity of the suspension under investigation, it was ensured that the supernatant medium was in ionic equilibrium with the suspension with which it formed the boundary. No attempt was made to derive the  $\zeta$ -potentials as such, since measurements of the dielectric constants of the methyl alcohol-amy acetate mixture and polyvinyl acetate solutions would have been necessary. As the dielectric constant occurs in the mobility and yield equations in the same way, these were not carried out. The  $\epsilon\zeta$ -values were calculated by means of the Smoluchowski relation, which, as we have

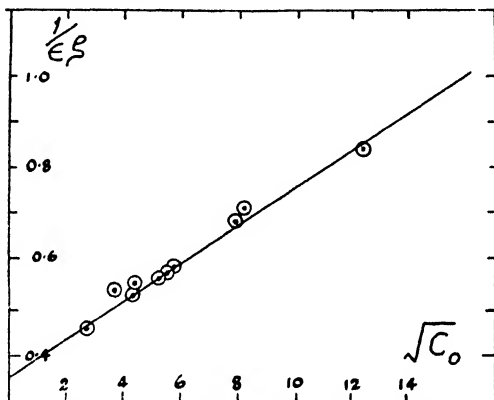


FIG. 3.

shown earlier, is applicable here. The results for suspensions in methyl alcohol-amy acetate without resin occur in Table I and are shown graphically in Fig. 3 as a linear plot of  $1/\epsilon\zeta$  against  $\sqrt{C_0}$ , from which it is inferred that the empirical law describing the behaviour is  $\zeta/\zeta_0$

$$1 + k \cdot \sqrt{C_0}$$

where  $\zeta_0$  is the electrokinetic potential at infinite dilution and  $k$  is a constant. This dependence of the  $\zeta$ -potential on suspension concentration appears to be related to

the partition of ions from the solid and water from the liquid between the double layer and the disperse medium. The addition of polyvinyl acetate resins caused a marked reduction in the mobility of the particles. As this reduction is more than can be accounted for by the increased viscosity of the medium, it must be due to a drop in the value of  $\epsilon\zeta$ . The presence of 2.2 g. resin of molecular weight 21,000/litre in a suspension of concentration 0 g. barium strontium carbonate/litre gave an  $\epsilon\zeta$ -value of 0.85, whereas the corresponding suspension without resin gave  $\epsilon\zeta = 1.58$ . It seems unlikely that the dielectric constant should be reduced by a factor of two by the addition of this small quantity of resin; we conclude, therefore, that some of the resin molecules have entered the electrical double layer and modified the  $\zeta$ -potential.

(iv) **Electrophoretic Yields**.—The experimental technique was similar to that of Hamaker.<sup>6</sup> The cathode, a Ni tube, 0.8 mm. in diameter, was held rigidly and symmetrically in the electrode assembly in an insulating mount, its position with respect to the anode, a Ni cylinder, 2.5 cm. in diameter, could be reproduced accurately. The average length of coating was 3 cm. Coating thicknesses were measured to within  $\pm 3\mu$  by means of a profile projector and the coating times to within 0.2 sec. on a stop watch. The circuit was made and broken by means of a bell-push. Density determinations were carried out on a large number of coatings, formed under a variety of conditions. We did not find any dependence of the coating density on the conditions of deposition as was reported by Hamaker. All the determinations lay within the range  $\pm 0.03$  of the mean value, 1.30 g. cm.<sup>-3</sup>. The yield of coating, expressed as

<sup>11</sup> Sven Odén, *Trans. Faraday Soc.*, 1922, 17, 327.

<sup>12</sup> Sen Gupta, *J. Indian Chem. Soc.*, 1938, 15, 483.

TABLE I.—DATA FOR SUSPENSIONS OF BARIUM STRONTIUM CARBONATE IN 80 % METHYL ALCOHOL—20 % AMYL ACETATE MIXTURES. VISCOSITY OF DISPERSE MEDIUM  $5.57 \times 10^{-3}$  POISE. TEMPERATURE  $25^{\circ}\text{C}$ .

$C_0$ (g l. <sup>-1</sup> )	$\xi$ ( $\xi$ in Volts)	$V$ (Volts)	$Y/h$ ( $10^{-6}$ g cm <sup>-1</sup> sec <sup>-1</sup> )	$\frac{d(Y/h)}{dV}$ ( $10^{-6}$ g cm <sup>-1</sup> sec <sup>-1</sup> volt <sup>-1</sup> )	$\alpha$
25	1.52	10	24	3.64	0.27
		25	81		
		50	182		
		100	364		
		150	680		
50	1.58	25	224	11.5	0.50
		5	618		
		100	1000		
		150	1840		
100	1.32	10	140	33.0	0.85
		25	620		
		50	1720		
		100	2960		
		150	5600		
150	1.20	10	390	46.0	0.92
		20	900		
		50	2500		
		100	5250		

TABLE II—DATA FOR SUSPENSIONS OF BARIUM STRONTIUM CARBONATE IN 80 % METHYL ALCOHOL—20 % AMYL ACETATE MIXTURES CONTAINING POLY-VINYL ACETATE RESINS. TEMPERATURE  $25^{\circ}\text{C}$ 

Mol Wt of Resin	$\eta$ ( $10^{-3}$ Poise)	$C_{lim}$ (g l. <sup>-1</sup> )	$C_0$ (g l. <sup>-1</sup> )	$\frac{d(Y/h)}{dV}$ ( $10^{-6}$ g cm <sup>-1</sup> sec <sup>-1</sup> volt <sup>-1</sup> )	Critical Voltage (Volts)
2,500	6.25	9.0	25	1.0	40
				2.5	
			50	3.5	
				9.6	22
			100	2.5	
2,500	6.07	20.7		29.5	12
			50	3.2	
				7.7	40
			100	5.0	
2,800	9.43	53.4		25.7	18
			50	0.4	—
			100	2.6	
				15.7	55
21,000	6.72	2.2	50	1.9	
				8.9	65
			100	3.5	
				22.2	~10
21,000	8.85	6.5	50	0.5	—
			100	1.0	
				20.2	25



grams per cm. length of cathode per second, was determined for various concentrations of suspension, applied potential differences and, in the case of suspensions containing resins, for different concentrations of two resins of

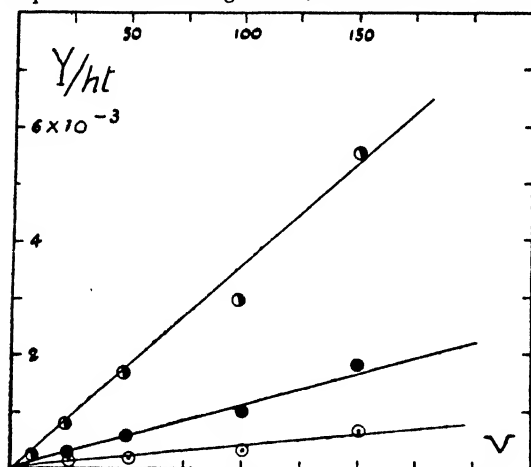


FIG. 4.—Dependence of yield, in g. cm.<sup>-1</sup> sec.<sup>-1</sup>, on voltage for suspensions without resin. Initial concentration of suspension: ○ 0.1 g. cm.<sup>-3</sup>, ● 0.05 g. cm.<sup>-3</sup>, ○ 0.025 g. cm.<sup>-3</sup>.

the previous section would be expected to demonstrate the existence of a critical time, as the voltages employed are too high and the cathode radius too small. Careful experiments were therefore carried out at several concentrations of suspension for a number of cathode radii and a number of voltages below 10 v. Representative curves are given in Fig. 6 and the dependence of the critical times derived from these curves on applied voltage and cathode radius is demonstrated in Fig. 7 and 8 respectively.

### Discussion.

The probability factors,  $\alpha$ , have been calculated from the observed results and plotted against concentration in Fig. 9. As Hamaker and Verwey<sup>5</sup> have pointed out, values of  $\alpha$  less than unity are due to electro-decantation. The dependence of  $\alpha$  on the concentration of the suspension can be explained qualitatively on this basis. The greater the suspension concentration the less the difference in density between the bulk of the suspension and the layer of average concentration  $C_c$  about the cathode. Increased viscosity of suspensions at higher con-

widely different molecular weight. These values have been tabulated in Tables I and II and representative plots have been made in Fig. 4 and 5. It will be noted from the results of Table II and Fig. 5 that suspensions containing resins show a sharp change in the rate of deposition per volt at a point, which we choose to call a "critical voltage," and which depends on both the concentration of resin and powder in the suspension and on the molecular weight of the resin. The reason for the existence of this critical voltage will be discussed later.

### (v) The Critical Time, $t^*$ .

—None of the experiments recorded in

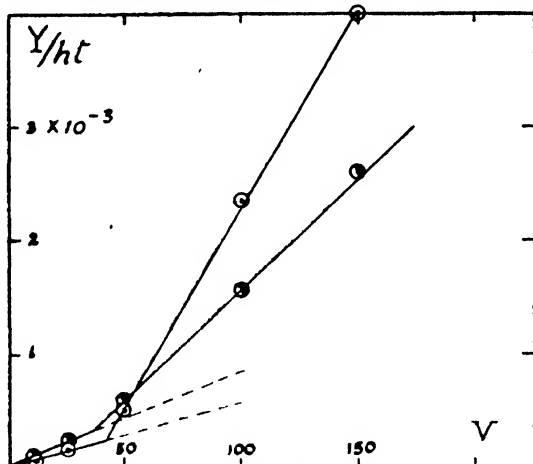


FIG. 5.—Dependence of yield, in g. cm.<sup>-1</sup> sec.<sup>-1</sup>, on voltage for suspensions containing polyvinyl acetate. Suspended phase: 0.05 g. cm.<sup>-3</sup>; resin: ○  $C_r = 2.2$  g. l.<sup>-1</sup>; mol. wt. 21,000, ●  $C_r = 9.0$  g. l.<sup>-1</sup>, mol. wt. 2,800.

centrations will also tend to decrease the extent of electro-decantation. The presence of this fluid layer of high concentration near the cathode is obviously of considerable significance in determining the hydrodynamic conditions in any continuous deposition process such as that described by Benjamin and Osborn<sup>4</sup> for the coating of wires or thin strips.

The existence of a critical time in the deposition process as predicted by equation (5) is confirmed by experiment. The correct dependence of this time on the applied potential and the cathode radius was also obtained (see Fig. 7 and 8). The plots of yield against time, however, do not show the yield to be zero for  $t < t^*$  as expected. This is because the first layer of particles to be deposited has a unique place in the deposition. Here the interaction forces are not between two particles, but between

a particle and the cathode wall, for which a dependence of the potential energy on distance of separation different from that represented in Fig. 1 will

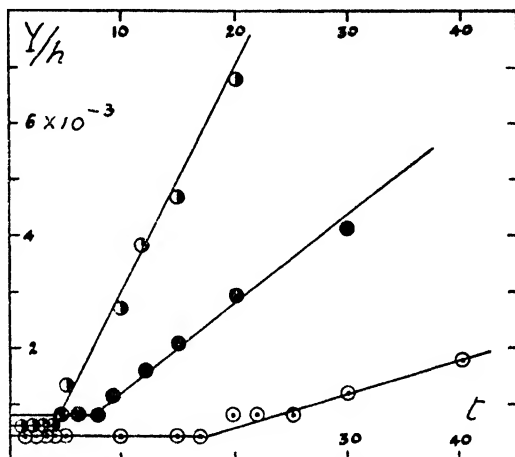


FIG. 6.—Dependence of yield, in g. cm.<sup>-1</sup>, on time for various voltages and cathode radii.

●  $v = 10$  volts.  $r_1 = 1.66$  mm.  
● 7.5 2.0  
○ 2.5 1.0.

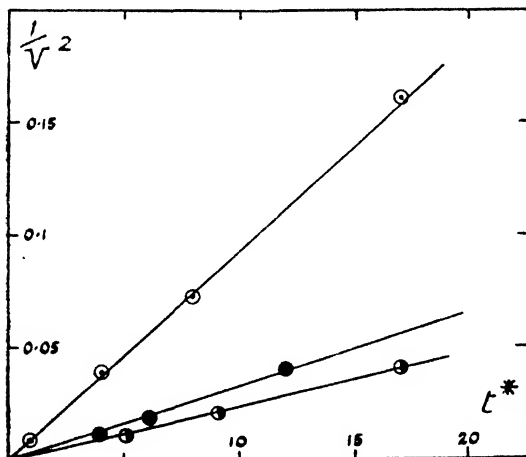


FIG. 7.—Dependence of the critical time on  $1/v^2$ .

○  $r_1 = 1.0$  mm.; ●  $r_1 = 1.66$  mm.; ●  $r_1 = 2.0$  mm.

obtain. This potential energy relation arises from the interaction of the double layer present on the cathode wall and that on the particle. It would be expected to have a similar form to that obtained for the interaction of two particles, but from the results appears to have a much smaller  $\phi_{pe}$  value. This potential energy-distance relation is presumably the factor determining whether or not a layer adheres to the cathode surface.

The existence of a critical voltage in suspensions containing polymeric sub-

stances is evidently connected with an abrupt change in the electrokinetic behaviour of the particles. Below this voltage, deposition occurs at a slow rate, indicating a low mobility, which we have shown can only be due to a small  $\zeta$ -potential. Above the critical voltage, deposition occurs

at a rate only slightly slower than that of a suspension with no polymer, the difference between the two values in this case being readily accounted for by the slight changes in dielectric constant and viscosity caused by the presence of the polymer. The presence of the resin considerably modifies the structure of the double layer and this may be due either to adsorption of

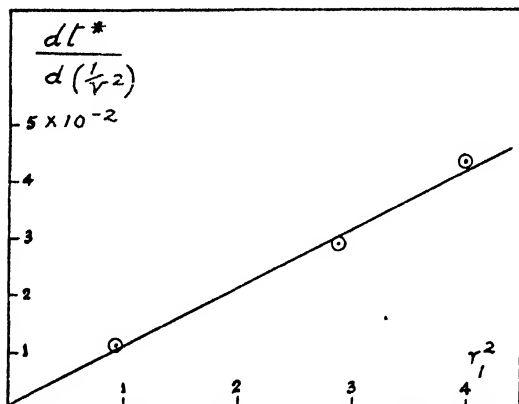
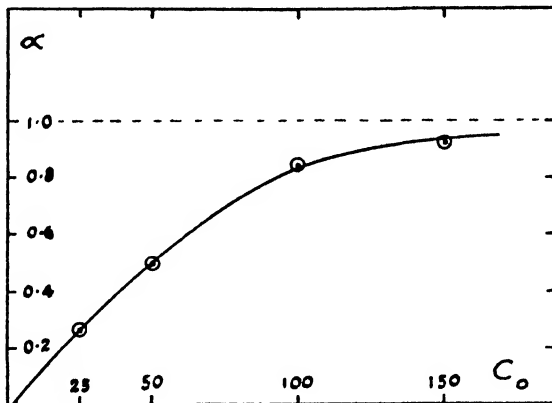


FIG. 8.

resin dipoles on the surface of the particle itself or to the presence of charged resin micelles in the diffuse part of the double layer. Such conditions would account for a reduction or even a reversal of the electrophoretic migration. At the same time, owing to the large size of the resin molecules, the relaxation time of the double layer is much increased and it is possible that at high field strengths the particle would be pulled out of its atmosphere of resin molecules, to migrate with a velocity comparable with that attained in the absence of resin.

Such an effect would be analogous to the Wien effect in electrolyte solutions. Further study of the phenomenon is necessary before a more definite mechanism can be proposed, but additional confirmatory evidence appears in the results of Benjamin and Osborn<sup>4</sup> and in work of our own on the electrokinetic behaviour of suspensions of zirconia in the same media. In the course of these experiments it was found that deposition invariably occurred at the anode and there was no evidence of a critical voltage in the presence of polymers. In fact, the mobility and the yield were only very slightly lowered by the presence of resins. Benjamin and Osborn reported that the introduction of nitrocellulose into suspensions of barium strontium carbonate in acetone reversed the direction of migration of the particles from cathodic to anodic, while there was no reversal when similar additions were made to alumina suspensions, which always migrated to the anode. Both these examples indicate some interaction between resin micelles and powder particles when their  $\zeta$ -potentials are of opposite sign, and no interaction when both are of the same sign.

FIG. 9.—Dependence of the probability factor  $\alpha$  in equation (4) on the initial suspension concentration.

One further point deserves some comment. In none of our experiments, with either carbonates or zirconia, did we observe any drop in current during deposition unless there was sufficient water in the suspensions to

cause an obvious evolution of gas at the electrodes. We therefore agree with Hamaker's conclusion that such a drop is due to polarisation and attribute Benjamin and Osborn's results with carbonates to the fact that their suspensions still contained excessive moisture, originating either from the solvent or the powder.

The authors wish to record their thanks to Mr. J. A. M. van Moll and the Directors of Philips' Lamps Ltd., for permission to publish this paper.

### Summary.

A theoretical approach to the problem of the formation of a deposit by electrophoresis of an inorganic powder suspended in a non-conducting liquid has been made, taking into account the mutual interaction of the particles. Quantitative experiments have been carried out and lend support to the theoretical predictions. The effect of high polymers dissolved in the liquid medium on the electrophoresis of the particles is described and a possible explanation of this effect suggested.

### Résumé.

La formation d'un dépôt, par électroforèse d'une poudre minérale en suspension dans un liquide non conducteur, est considérée d'un point de vue théorique, tenant compte de l'interaction des particules. Les expériences quantitatives effectuées viennent confirmer les prévisions de la théorie. L'effet de hauts polymères—dissous dans le liquide—sur l'électroforèse des particules est décrit, et une explication du phénomène est suggérée.

### Zusammenfassung.

Das Problem der elektrophoretischen Abscheidung eines anorganischen Pulvers, das in einer nicht-leitenden Flüssigkeit suspendiert ist, wurde theoretisch angegriffen, wobei die gegenseitige Einwirkung der Teilchen berücksichtigt wurde. Die theoretischen Voraussagen werden durch quantitative Messungen unterstützt. Der Einfluss von in der Flüssigkeit gelösten hochpolymeren Substanzen auf die Elektrophorese der Teilchen wird beschrieben und eine mögliche Erklärung des Effekts vorgeschlagen.

*Material Research Laboratory,  
Philips' Lamps Ltd.,  
Mitcham Junction,  
Surrey.*

## ELECTROLYTIC POLARISATION—I. THE OVER-POTENTIAL OF HYDROGEN ON SOME LESS COMMON METALS AT HIGH CURRENT DENSITIES.

### INFLUENCE OF CURRENT DENSITY AND TIME.

By J. O'M. BOCKRIS.

*Received 15th May, 1946.*

The dependence of the hydrogen overpotential upon current density has been reported frequently in the literature: a large proportion of the work, however, has been carried out at low current densities and of the work at high current densities, none, until recently, has been free from serious objection. Thus, numerical values recorded by Tafel<sup>1</sup> contain

<sup>1</sup> Tafel, *Z. physik. Chem.*, 1905, **50**, 641.

an uncertain contribution from the resistance error, or ohmic overpotential, the existence of which was not fully realised at the time. Newbery<sup>3</sup> used an early form of the commutator method in which errors due to the rapid decay of overpotential after interrupting the polarising current have been shown to be very considerable. Kabanov<sup>4</sup> more recently reported results of measurements up to c.d.'s of 100 amp./sq. cm. but his calculations of the resistance errors inherent at very high c.d.'s in the method which he used are open to the strongest criticism.

Some important new aspects of the measurement of hydrogen overpotential at high c.d.'s were described by Hickling and Salt<sup>5</sup> in 1940. These workers pointed out that one of the main sources of divergence in previous determinations was the lack of uniformity among various authors of the treatment of the variation of overpotential with time. This is a very considerable factor for a number of metals; the difference between values at the steady value attained before polarisation (the so-called static potential) and that at a few seconds after commencement of polarisation may be several hundred per cent. of the latter value. Some authors make no mention of the time variation; others have suggested arbitrary times of polarisation which appear to have little rational basis. Hickling and Salt<sup>5</sup> suggested that a steady state, or at least a polarisation maximum must be attained before the overpotential of various metals at a given c.d. could be comparable. They further pointed out that another error attaches to the usual procedure of progressively increasing the polarising current in steps during determinations of the dependence of overpotential on c.d. This causes values at one c.d. to be affected by polarisation at a previous c.d. and as the duration of this may vary for different metals and even for different experiments on the same metal, the results obtained are not comparable. It was therefore proposed by Hickling and Salt that the polarisation should be discontinued after measurements at one c.d. had been completed and the electrode potential be allowed to come to a steady value before polarisation was resumed at another c.d.

These contributions to the method of measuring hydrogen overpotential seem to be essential improvements which lessen the usual lack of reproducibility of such measurements. Hickling and Salt reported a reproducibility of about 2-3 centivolts and this was also obtained by the present author using the two modifications of the method of measurement discussed above.

The measuring circuit used by Hickling and Salt was an improved form of the commutator method which utilises an electrical interrupter free from moving parts, whereby polarisation can be interrupted at any desired frequency, the potential being measured by a special potentiometer left in permanent connection with the electrode. The results obtained by these authors for the effect of variation of overpotential with c.d. were somewhat controversial. Firstly, negative deviations from the Tafel equation<sup>\*</sup> was reported for most of the metals examined over the c.d. range  $10^{-3}$  — 1 amp./sq. cm., only electrodeposited gold, tungsten, nickel, iron and bismuth showing a linear dependence of overpotential on the logarithm of the c.d. Secondly, the slopes of the overpotential-log c.d. relation observed were characteristic of the metal and not a constant as expected from some recent theories. Thirdly, a decrease of overpotential with increase in c.d. was observed at the highest c.d.'s for

<sup>3</sup> Newbery, *J. Chem. Soc.*, 1914, 2422.

<sup>4</sup> Kabanov, *Acta Physiochim.*, 1936, 5, 193.

<sup>5</sup> Hickling and Salt, *Trans. Faraday Soc.*, 1940, 36, 1226.

<sup>\*</sup> Namely, the logarithmic relation between overpotential ( $\eta$ ) and the logarithm of the current density ( $d_0$ ) discovered by Tafel, i.e.  $\eta = a + b \log d_0$ , where  $a$  and  $b$  are constants. Negative deviations are taken to signify values of the overpotential less than those expected from this linear relation.

lead and platinum cathodes. These results, especially the reported deviations from the logarithmic relation, have been criticised by Frumkin,<sup>5</sup> it being asserted that they are due to there being an error in the commutator method of determination.

On account of the theoretical interest and importance which attaches to Hickling and Salt's results, it seemed of some interest to carry out determinations of hydrogen overpotential at high c.d.'s with a technique analogous to that of Hickling and Salt as regards to general procedure but utilising the direct method of measurement, carefully carried out with attention to the avoidance of resistance errors. The possible source of error in Hickling and Salt's method is thereby removed and because any possible errors arising from the present method would tend to give too high results, whereas commutator experiments tend to give too low results, agreement with the general influence of c.d. upon overpotential found by these workers would doubly confirm their results. Further, Hickling and Salt's determinations were carried out on well-known metals, whereas it is desirable, both from the general advantages gained by extending the examination of overpotential as a function of the cathode material and also from the viewpoint of some observations which it was wished to make upon the relation between overpotential, atomic number and work function to examine especially cathodes of the less common metals beryllium, niobium, molybdenum, indium, tantalum and thallium.

### Experimental.

**(1) The Direct Method.**—Criticism of Hickling's commutator method of measuring hydrogen overpotential is of two kinds. Firstly, there may still be a significant error made in the extrapolation of overpotential to zero time after cessation of the polarising current. Secondly, a more serious objection, overpotential measured under conditions in which the polarising current is continuously interrupted may not be comparable with that observed under conditions of continuous polarisation. Both these errors are avoided by use of the direct method of measurement, but this of course involves the inclusion of an ohmic overpotential in the measured overpotential. Justification of use of the direct method depends on the magnitude of this extraneous component.

Hickling quotes some measurements which tend to show that above c.d.'s of  $10^{-1}$  amp./sq. cm. results obtained by the direct method are much greater than those obtained by the new commutator method. Experimental details of the direct method used in these comparison experiments are not recorded and the author seems to base his criticism of the direct method upon the supposition of a gas film very near to the cathode surface, which follows from his theoretical views. Contrary to Hickling's conclusions, Glasstone<sup>6</sup> earlier found agreement between commutator and direct methods could be obtained to within a few centivolts by the use of an appropriate modification of the former. It must be conceded that above c.d.'s of about  $10^{-1}$  amp./sq. cm. and in N. aqueous solutions of strong acids even at electrodes where there is no evidence of a poorly conducting solid film at the electrode surface, the ohmic overpotential may become appreciable, just as at this and higher c.d.'s under the same conditions the commutator methods tend to become less reliable owing to an increasing error in extrapolation to zero time. For this reason measurements in the present work have not usually been made at c.d.'s above about  $10^{-1}$  amp./sq. cm.

**(2) Apparatus.**—The apparatus consisted essentially of an electrolytic cell containing an anode and cathode compartment of equal volume (see Fig. 1). These were comparatively large (about 400 cc.) because

<sup>5</sup> Frumkin, *Acta Physicochim.*, 1943, **23**, 18.

<sup>6</sup> Glasstone, *Introduction to Electrochemistry* (1944), p. 464.

preliminary experiments in smaller cells showed undesirable heating effects at  $10^{-1}$  amp./sq. cm. Cleaning and manipulation were facilitated by connection of the anode compartment to the rest of the apparatus by means of a ground glass joint. Some 30 cm. of glass tubing, of diameter 1 cm. connected the anode to the cathode compartment and a sintered glass disc of porosity 1 was inserted in the anode side of the connecting tube. Stoppers were made of rubber. Through that in the cathode compartment was inserted a large diameter glass tube down which the limb of the bridge to the hydrogen electrode passed, and the end of the cathode limb, 1 mm. in diameter was pressed fairly tightly against the cathode. The limb was held in the large diameter glass tube by means

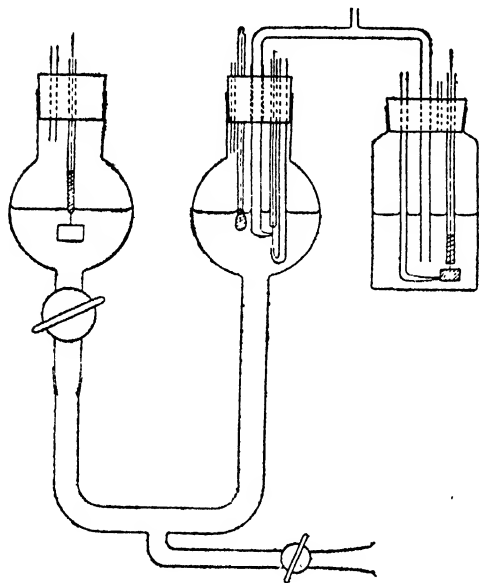


FIG. 1.—Electrolytic Cell.

of a piece of thin rubber tubing so that a certain degree of freedom of movement was allowed by which the cathode tip could be adjusted to the correct position. The anode was of platinum foil and of area about 1 sq. cm. The hydrogen and chlorine evolved during electrolysis were allowed to escape freely and the P.D. between the working cathode and the hydrogen electrode was measured by means of a Cambridge potentiometer with an established accuracy of 2 mv. A Cambridge-Paul unipivot milliammeter, fitted with multi-range current shunt, was used to measure the current.

Cylinder hydrogen was passed through two bubblers charged with alkaline pyrogallol, each containing sintered glass diffusion discs

and then through a solution of N. HCl, which was the electrolyte used. The gas was passed to a reservoir vessel and from here led through separate lines of glass tubing to the hydrogen electrode, and cathode and anode compartments of the cell, the pressure to each line being separately adjusted. (The line to the anode compartment, the purpose of which was to maintain saturation with hydrogen, was later abandoned as it did not seem to affect results.) In the cathode compartment a stream of  $H_2$  was directed on to the cathode, the resulting agitation of the electrolyte minimising concentration polarisation.

**(3) Preparation of the Cathodes.**—It was difficult to obtain specimens of the rarer metals both in a suitable form and a good state of purity. The specimens used were more than 99.8 % pure except in the case of Be, which contained about 0.5 % impurities, principally Si and Mg. The cathodes were in the form of wires for In, Mo, Tl and Ta, in the form of a rectangular strip for Be and a disc for Nb. Attachment to the glass rods used as cathode holders was made with Faraday's cement. For the disc-shaped cathode of Nb, attachment was made by cementing the cathode to the end of a glass tube, the tube being bent at right angles so that when supported vertically the disc was in a vertical plane. The general method of preparing the cathodes was that due to Hickling and Salt,<sup>4</sup> namely washing with distilled water and wiping with filter paper. Preliminary

scraping with a sharp knife was also used in the cases of the soft metals, In and Tl.

(4) **General Procedure.**—A saturated aqueous solution of HCl was prepared by the dissolution of HCl gas, prepared by the action of concentrated  $\text{H}_2\text{SO}_4$  on a sludge composed of a mixture of HCl with  $\text{NH}_4\text{Cl}$  in distilled water. The solution was diluted to normal strength, boiled for five minutes, and cooled during vigorous passage of  $\text{H}_2$  for about thirty minutes. A slow stream of  $\text{H}_2$  was kept circulating through the electrolytic cell (which was cleaned between experiments by standing for twelve hours in chromic-sulphuric cleaning mixture) and continued during introduction of the solution and attachment of the cathode and of the bridge between the hydrogen cell and the cathode compartment.

The potential of the electrode was observed as it gradually changed towards a steady value, which process generally completed itself in less than  $1\frac{1}{2}$  hours. Polarisation at the lowest c.d. ( $10^{-3}$  amp./sq. cm.) was then commenced and the overpotential read at intervals of fifteen or thirty minutes until it became substantially constant. A rate of variation of 0.01 v. in thirty minutes was considered to indicate relative constancy. During polarisation, qualitative tests were made of the effect, of varying the rate of bubbling of  $\text{H}_2$  in the cell, i.e. the rate of stirring and this was always regulated till it was greater than the critical value at which increase of bubbling rate did not affect the overpotential, i.e., presumably the effect of concentration polarisation had been reduced to negligible proportions. The effect of slightly moving the cathode out of close contact with the electrode was frequently examined and should this have caused any significant variation in the measured total overpotential between cathode and hydrogen electrode, the presence of a large resistance error would have been suspected.

During its decay after the cessation of polarising current, the potential of the cathode was measured every few minutes and when it had become constant to within 1.2 mv., polarisation at the next highest c.d. was commenced. It was found in most cases that static potentials were reached in less than  $1\frac{1}{2}$  hours; these were, however, not always the same as those attained before commencement of polarisation.

Measurements were made in the above manner at c.d.'s of  $10^{-3}$ ,  $10^{-2}$ ,  $5 \cdot 10^{-2}$ ,  $10^{-1}$  and in some cases 1 amp./sq. cm. A small increase of temperature in the cathode compartment takes place for the highest c.d.'s; assuming a temperature coefficient of about  $2 \times 10^{-3}$  volts/ $^{\circ}\text{C}$ . for hydrogen overpotential in aqueous solutions, this temperature increase was always insignificant for the results.

## Results.

The reproducibility of the results was in general about  $\pm 0.01$  v. For the soft metals, In, and Tl, it was considerably better, being  $\pm 0.004$  and  $\pm 0.003$  v. respectively. Conversely for Be the reproducibility was less good—partly owing to the tendency of the metal to dissolve at the lowest c.d.'s, even in the N./10 HCl used in this case.

### (i) Variation with Time.

There appear to be two well-defined types of variation of overpotential with time, the former of which comprises some sub-types.

**Type 1.**—The general character of the variation was an increase with time towards a maximum value, after which the overpotential either remained approximately constant or decreased with time. The shape of the overpotential-time curves was variable but it seems that three main sub-types are discernible.

a. The overpotential increases relatively slowly from a low value and attains a steady state in one to two hours. The rate of increase with



time during the earlier period of polarisation is approximately linear. This behaviour occurs during polarisation at c.d.'s of less than  $10^{-2}$  amp./sq. cm. and is shown by Ta, Ti and Mo (see Fig. 2).

b. The overpotential rises rapidly at first and then more slowly to a maximum. The initial change in potential from the steady value attained in the absence of a polarising current is too rapid to be examined without the aid of more complex measuring circuits. This type of time variation is observable at some c.d.'s for all the metals studied and for Nb and In over the whole c.d. range examined in the present work. It is the most usual type of variation at c.d.'s greater than  $10^{-2}$  amp./sq. cm.

c. A type of behaviour qualitatively similar to type (b) was also occasionally observed at high c.d.'s when the maximum value of the overpotential was reached before measurements could be made so that a steady potential is observed for some minutes and then a decrease with time. In such a case the initial steady value of the overpotential has been taken to be the representative value. This type of behaviour was observed

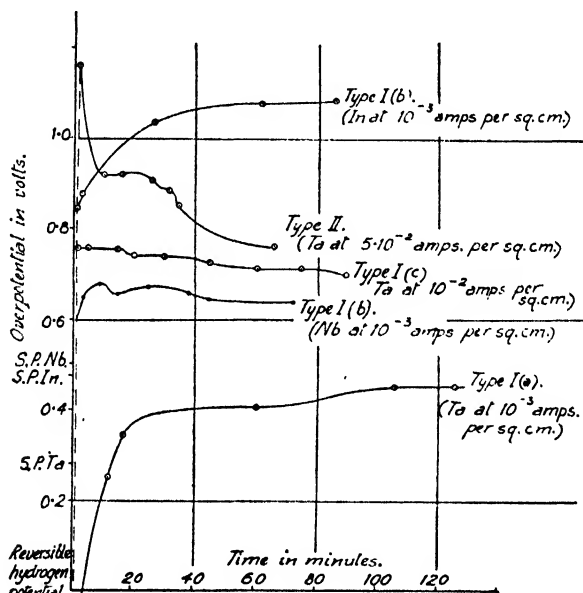


FIG. 2.—Types of Variation of Hydrogen Overpotential with Time.

for Ta at a c.d. of  $10^{-2}$  amp./sq. cm. and for Mo at c.d. greater than  $5 \cdot 10^{-2}$  amp./sq. cm.

**Type 2.**—There is an initial decrease of overpotential with time and then a steady value is reached which is maintained constant to within 3-4 mv. for some period, usually about half an hour. This is followed by an indefinite decrease. In such a case, e.g., for the polarisation of Ta at c.d.'s greater than  $10^{-2}$  amp./sq. cm. the overpotential at the steady rate attained after the initial fall has been taken to be the appropriate result.

The steady state is reached more rapidly at high c.d.'s than at low for all the metals examined and the mode of variation with time at high c.d. for a given cathode is not necessarily the same as that at lower c.d.'s. Thus, for the overpotential on Ta, the rate of increase with time is different in degree for polarisation at c.d.'s of  $10^{-2}$  and  $10^{-3}$  amp./sq. cm. respectively

and another type of variation, namely, a decrease, is found at c.d.'s greater than the latter.

The "long time" decay of overpotential was observed for Ta, Mo and Nb cathodes, the potential of which continue to change slowly for more than one hour after cessation of the polarising current. The general form of the  $V/t$  relation observed (see Fig. 3) was the same for these three cathodes, i.e. a rapid fall, roughly linear with  $\log t$ , towards or below the reversible hydrogen potential and then a sharp fall followed by a slow change towards a steady potential. The potential of the cathodes Be, In and Tl decayed too quickly to be measured by the means available.

Two further observations on the time variation of overpotential are of interest. It was observed that for some cathodes a kind of "breathing" phenomenon took place, i.e. a regular periodic variation of the overpotential with time with an amplitude of about 2-3 mv.\* This occurred more markedly in later stages of the polarisation when the potential was approaching a steady value. The other is the variation of the hydrogen overpotential on Ni during polarisation lasting eighteen hours. The potential was observed to increase for about six hours and then to decrease initially at about the same rate for approximately six hours. A slow

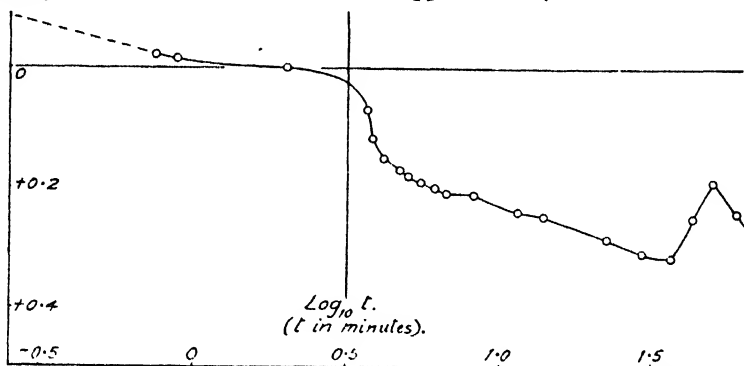


FIG. 3.—Decay of Hydrogen Overpotential on a Molybdenum Cathode after Polarisation at  $10^{-3}$  amps. per sq. cm.

increase of potential then occurred, lasting some one and a half hours and then an equally slow decrease for one and a half hours, when the polarisation was terminated.

## (ii) Overpotential as a Function of Current Density.

Tabulated results are shown in Table I, those for Cu, Ni and Pb cathodes being given for comparison with Hickling and Salt's values obtained by use of the commutator method; Fig. 4 shows the results as a function of log current density.

The general order of the results is as expected from work on the related elements. The easily fusible metals have high and those of high m.p., low overpotentials. It is well known that smooth Pt is an exception to this rule, especially at high c.d. Another interesting anomaly now appears in Ta, which melts at  $2850^{\circ}\text{C}$ . and has an overpotential greater than that of Be at a c.d. of  $10^{-1}$  amp./sq. cm.

The general shape of the overpotential-log c.d. relation is mainly similar to the types of behaviour found by Hickling and Salt's commutator method, i.e. either (a) the Tafel equation is applicable over the whole c.d. range, or (b) there are negative deviations from the Tafel equation, or (c) the cathode potential reaches a specific constant value at high c.d. characteristic

\* Cf. Williams, *Thesis* (London, 1928).

TABLE I

c.d. (amp./ sq. cm.).	$10^{-3}$ .	$10^{-2}$ .	$5 \cdot 10^{-2}$ .	$10^{-1}$ .	1.	Mean deviation from mean. Volts.
Ni	0.32	0.43	0.54	0.57		0.01
Ni*	0.33	0.42	0.49†	0.51		
Cu	0.57	0.77	0.79	0.81	0.84	0.03
Cu*	0.60	0.75	0.80†	0.82	0.84	
Pb	0.85	1.11	1.15	1.15		0.01
Pb*	0.67	0.97	1.11†	1.12		
Mo	0.30	0.44	0.55	0.57		0.02
Ta	0.41	0.75	0.90	0.90		0.02
Nb	0.65	0.74	0.77	0.82		0.01
Be	0.63	0.73	0.85	—		0.01
In	0.80	1.05	1.18	1.19		0.01
Tl	1.05	1.13	1.15	1.15		0.01

\* Hickling and Salt.

† Interpolated.

of each metal (Fig. 4). No cases were observed here of the decrease of overpotential with increasing c.d., in which aspect the results reported here for Pb cathodes differ from those reported by Hickling and Salt.\*

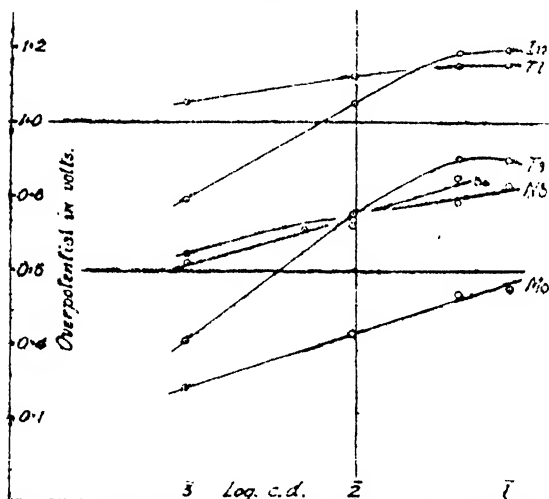


FIG. 4.—Hydrogen Overpotential on less common Metals in Aqueous Solution.

Thus, the results for Be and Mo are best represented by a linear dependence of overpotential on log c.d. Owing to the ready solubility of Be in N. HCl, experiments were carried out in N./10 solution, in which the metal is still slightly soluble at a c.d. of  $10^{-3}$  amp./sq. cm. Further results at a c.d. of  $10^{-1}$  amp./sq. cm. could not be reproduced for Be and the metal surface became darkened so that four values at c.d.'s below  $10^{-1}$  amp./sq. cm. were

obtained. For Nb the results at  $5 \times 10^{-2}$  and  $10^{-1}$  amp./sq. cm. are definitely lower than would have been expected had the Tafel equation accurately applied and for In, Th and Ta there is a clear approach to a constant value, specific to each metal, at c.d.'s of less than  $10^{-1}$  amp./sq. cm.

### Discussion.

Experimental results on the variation of overpotential with time have been the subject of particularly contrary opinions. Most workers,<sup>7, 8, 9</sup>

<sup>7</sup> Bowden and Rideal, *Proc. Roy. Soc. A*, 1928, 59, 120.

<sup>8</sup> Knobel, Caplan and Eisemann, *Trans. Amer. Electrochem. Soc.*, 1923, 43, 55.

<sup>9</sup> See Harkins and Adams, *J. Physic. Chem.*, 1925, 29, 205; Massing and Laue, *Z. physik. Chem.*, 1926, 178, 1.

\* The present author has, however, observed this type of behaviour in certain non-aqueous systems, to be reported in a later paper.

agree that there is a variation with time but there has been a marked tendency to ascribe this to some secondary effect, for example, the deposition of dissolved metal. Baars<sup>10</sup> found considerable variations with time and that at lower c.d. on some cathodes the overpotential continued to vary for days. Hickling and Salt<sup>6</sup> found that, except for Hg, platinumised Pt and W cathodes, a time of two hours or more was often necessary for a steady overpotential to be attained.

The results of the present work entirely support the contention of Hickling and Salt that the variation of hydrogen overpotential with time is a fundamental characteristic of this phenomenon. As is well known, the theories of hydrogen overpotential divide themselves roughly into two classes: (a) those postulating the formation of H atoms from ions as the slow stage ("Slow Discharge Theories") and (b) those postulating combination of H atoms as the slow stage ("Atomic Hydrogen Combination Theories"). Without as yet postulating any of the detailed mechanisms advocated by exponents of either view it seems more easy to explain the variations with time in terms of a gradual inactivation of the active centres on the metal surface thus causing a deceleration of the combination of atomic H on the metal surface. Thus there is a greater variation with time at lower than higher c.d.'s (e.g. compare Ta at  $10^{-3}$  and  $5 \cdot 10^{-2}$  amp./sq. cm.) and this agrees with a heterogeneous catalytic view for the rate of inactivation of active centres would clearly tend to be greater at the commencement of polarisation than at higher c.d., when there may be a tendency towards saturation of the surface. For some metals definite steps are found in the overpotential-time curves and this is in harmony with a catalytic phenomenon. Layer planes of the metal lattice may be removed from the surface thus exposing fresh surfaces upon which to deposit hydrogen. The breathing phenomenon also reported above may be of similar origin, and/or possibly connected with the effect of the diffusion of hydrogen into the metal.

A particularly interesting time variation is that of Ta, which in one observed case showed an initial potential more *positive* than the hydrogen electrode. An underpotential does not appear to have been recorded before in the literature of measurements of hydrogen overpotential at notable c.d.'s. Cohen, however, measuring the minimum overpotential on palladium found a value of +0.26 v. It is noteworthy that the properties of Ta for the adsorption of hydrogen are similar to those of Pd. It is difficult to understand the evolution of H<sub>2</sub> at a potential more positive than the reversible potential of hydrogen and it seems probable that in such instances hydrogen is not evolved on deposition, but absorbed into the cathode surface. Kobosew and Nekrassow<sup>11</sup> have discussed in a different way the possible existence of an underpotential in a paper on a version of the atomic H combination theory; they deduce that underpotentials are to be expected if the energy of adsorption of atomic H on the electrode surface is greater than half the heat of dissociation of hydrogen.

Results observed by the present author for Ni cathodes at high c.d. on polarisation for eighteen hours are puzzling. It is possible that a general increase in the surface area of the electrode takes place and that the apparent decrease of overpotential is due simply to a change in the effective area. This would have to increase by about five times in six hours to explain the fall in overpotential observed and does not clearly indicate why the overpotential again begins to increase after fifteen hours. This phenomenon seems to show the same kind of periodicity as that mentioned above. The "long time decay" observations are also in a general way in accordance with the atomic H combination theories. Explanation of the variation with time reported by Baars, Hickling and Salt and the present worker do not seem to be within the scope of the neutralisation theories.

<sup>10</sup> Baars, *Sitzungsber. Ges. Beförd. Naturwiss., Marburg*, 1928, 63, 213.

<sup>11</sup> Kobosew and Nekrassow, *Z. Elektrochem.*, 1930, 36, 529.

The negative deviations from linearity of the overpotential-log c.d. relation and the approach to constant values specific to the cathodes In, Tl and Ta observed in the present investigation compare well with the behaviour reported by Hickling and Salt of the majority of their cathodes. Confirmation of the lack of applicability of the Tafel equation at high c.d. by the direct method, which, as already remarked, would tend to lead to positive errors, appears to be strong evidence against the claim of Kabanov to have verified the equation up to very high c.d.

Considerable theoretical interest attaches to the constant  $b$  of the Tafel equation and the present work enables a more complete set of experimental values of this coefficient to be given. In Table II are collected

TABLE II

Metal.	$b$ .	Metal.	$b$ .	Metal.	$b$ .	Metal.	$b$ .
Be <sup>12</sup>	0.11	Nb <sup>12</sup>	0.11	W <sup>14</sup>	0.09	Hg <sup>4</sup>	0.15
C <sup>10</sup>	0.84	Mo <sup>12</sup>	0.13	Pt* <sup>12</sup>	0.02	Hg <sup>17</sup>	0.12
Al <sup>14</sup>	0.12	Rh <sup>4</sup>	0.14	Pt* <sup>15</sup>	0.08	Tl <sup>13</sup>	0.08
Fe <sup>4</sup>	0.12	Ag <sup>14</sup>	0.12	Pt <sup>4</sup>	0.3	Pb <sup>4</sup>	0.3
Ni <sup>4</sup>	0.12	Cd <sup>4</sup>	0.25	Pt <sup>15</sup>	0.10	Pb <sup>16</sup>	0.23
Ni <sup>3</sup>	0.11	In <sup>12</sup>	0.25	Au <sup>4</sup>	0.08 <sup>14</sup>	Bi <sup>4</sup>	0.10
Cu <sup>4</sup>	0.16	Sn <sup>4</sup>	0.2	Au <sup>15</sup>	0.12	—	—
Cu <sup>13</sup>	0.12	Ta <sup>12</sup>	0.34	—	—	—	—

Pt\* = platinised platinum.

what seem to be the most reliable values in the literature. Where more than one recent value is available, both are given.

The mean of these values is 0.15 and it may be seen that for many metals there is little evidence to support the contention of the neutralisation theory<sup>17</sup> that the  $b$  value should be about 0.1 for all metals. This point is now emphasised by the high values observed on Ta and In which are of the same order as those obtained by other workers on lead and cadmium. The value of 0.09 obtained for the  $b$  value of a Tl cathode, which is similar to the values of 0.09 and 0.03 recently reported for W and Pt, is even more difficult to interpret on the neutralisation view, according to certain modifications of which values greater than 0.1 might follow. It is possibly important to note that for metals having small values of  $b$  (e.g. W, Au, Tl) there is a particularly quick attainment to the polarisation maximum.

The value of the slope and shape of the overpotential-log c.d. relation for Ta is of special interest in connection with the ability of the element to take up large quantities of hydrogen.<sup>18</sup> Since the shape of the overpotential/log  $d_0$  curve for Ta closely resembles that for smooth Pt, which is also a good adsorbent for hydrogen, the similarity between these two metals may be evidence for the view that the heat of adsorption of hydrogen on the electrode is of critical importance to the magnitude of the overpotential.<sup>11</sup> Conversely it should be noted that the overpotential-log c.d. relation for Pb, which has a low power of adsorption for hydrogen, has a slope similar to that for Ta and Pt.

The present results of the hydrogen overpotentials on metals closely related in the periodic table such as In and Tl draw attention to the fact that elements of similar properties possess similar orders of the hydrogen

<sup>12</sup> The present work.

<sup>13</sup> Wirtz, *Z. physik. Chem. B*, 1937, **36**, 435.

<sup>14</sup> Bowden and Stout, quoted by Bowden and Agar, *Ann. Reports*, 1938, 99.

<sup>15</sup> Volmer and Wick, *Z. physik. Chem.*, 1935, **172**, 429.

<sup>16</sup> Erdy, Gruz and Wick, *ibid.*, 1932, **162**, 53.

<sup>17</sup> Gurney, *Proc. Roy. Soc. A*, 1931, **134**, 137.

<sup>18</sup> von Bolton, *Z. Elektrochem.*, 1905, **11**, 50.

overpotential and a closer examination of this has been made in the next section.

### Overpotential as a Function of Atomic Number.

Observations on the relation of the hydrogen overpotential of the metals to their position in the Periodic Table seem first to have been made by Newbery<sup>19</sup> who allotted to each group in the Periodic Table a "characteristic overpotential". His classification is of little interest to modern work owing to the erroneous overpotential values used. It was Ellingham and Allmand<sup>20</sup> who pointed out the general consequences of the relation referred to above between melting point and overpotential, namely that the parallelism noted must, owing to a periodic relation between m.p. and atomic number, indicate that hydrogen overpotential is a periodic function of the latter. Weeks<sup>21</sup> and Partington<sup>22</sup> have also commented upon the relation between m.p. and overpotential.

Another regularity between overpotential and the Periodic Table is shown by the variation in a given period. For example, considering period VI, we have :

Metal.	Au.	Hg.	Tl.	Pb.	Bi.	Pt.
Overpotential at c.d. of $10^{-3}$ amp./sq. cm. (volts) . . .	0.17	1.04	1.05	0.85	0.69	0.25

A similar variation of overpotential with atomic number occurs in other periods and it may be significant that the atomicity of the hydrides of the elements of a given period passes through a similar maximum.

The overpotential-atomic number relation is periodic in a way similar to those for atomic vibration frequencies, melting points, atomic volumes, and so on (cp. Fig. 5). In a general way the lowest troughs tend to be occupied by elements of Group VIII to the right of the Periodic Table, and the heights to the middle and left of the table, Ag and Au being exceptions.

Tentative theoretical conclusions based upon the periodic variation of overpotential with atomic number may be briefly made. In Fig. 5 the overpotential on various metals at an arbitrary c.d. and the work function of the metals are represented as a function of the atomic number. The possibility of a relation between the work function and overpotential has already been referred to by Adam,<sup>23</sup> who concluded that there was no connection. When the work function is plotted as a function of atomic number it can be seen, however, that there is a definite correlation between it and the overpotential at a given c.d., namely that an increase in the work function from one metal to another leads to a decrease of the overpotential. There is only one exception to this in the available results plotted in the figure, namely in the transition from In to Sn, where both overpotential and work function increase.

The work function is an important quantity in Gurney's theory of overpotential<sup>17</sup> but its influence upon the overpotential is somewhat obscure. It would appear from this theory that the opposite results to that recorded might be expected; increased difficulty of removal of an electron might be expected to lead to a larger overpotential. This expected relation may be vitiated, however, because although electrons

<sup>19</sup> Newbery, *J. Chem. Soc.*, 1916, 1107.

<sup>20</sup> Ellingham and Allmand, *Trans. Faraday Soc.*, 1924, 19, 748.

<sup>21</sup> Weeks, *Chem. News*, 1924, 129, 17.

<sup>22</sup> Partington, *ibid.*, 1924, 129, 77.

<sup>23</sup> Adam, *Physics and Chemistry of Surfaces*, (1938), p. 332.

have to be extracted from the metal, they do also in a reversible electrode and in either case the work function might be expected to cancel out through a second contact potential elsewhere in the circuit. In either case, conclusions made from the theory are in opposition to the described results.

If a different view be taken and the slow stage in the evolution of hydrogen be ascribed as predominantly due to the slow combination of hydrogen atoms on, or in, a catalytic surface, the correlation between the work function and overpotential is comprehensible. Increased electron affinity would indicate an increased power of adsorption of hydrogen

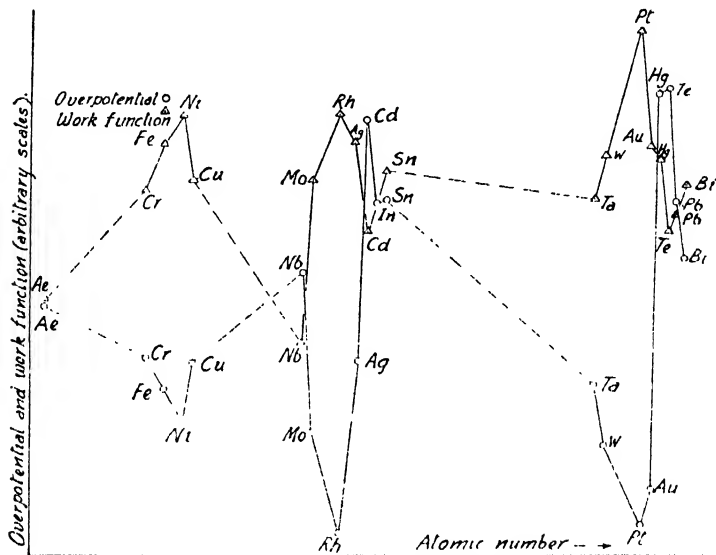


FIG. 5.—Overpotential as a Function of Atomic Number.

atoms, presumably in a deformed state on the metal surface. This would be expected to induce an easier combination and therefore a decreased overpotential in accordance with the indications of Fig. 5.

### Summary.

1. The hydrogen overpotential of Ni, Cu, Pb, Mo, Ta, Nb, Be, In, and Ti cathodes has been measured in aqueous solution at c.d.'s between  $10^{-3}$  and  $10^{-1}$  amp./sq. cm. by the direct method using the same general method with regard to resting the cathode between polarisation at different c.d.'s as that used by Hickling and Salt.

2. Negative deviations from the Tafel equation have been observed for Cu, Pb, Ta, Nb, In and Ti. The overpotential on Pb, Ta, In and Ti tends towards a limiting value at the highest c.d.'s which is specific to each material. Comparable results agree closely with those of Hickling and Salt, obtained by the indirect method.

3. Two main types of increase of overpotential with time have been distinguished and the results are shown to support the contention that the increase with time is a fundamental phenomenon of hydrogen overpotential.

4. The average value of the constant  $b$  of Tafel's equation from reliable values in the literature is 0.15.

5. Experimental values of hydrogen overpotential at a given c.d. on various cathodes plotted against the atomic number of the cathode material show that overpotential is a periodic function related to the work function of the metal. Hydrogen overpotential increases when the work function decreases.

6. Qualitative interpretations of the reported results are afforded more readily by the atomic hydrogen theories of hydrogen overpotential.

## Résumé.

La surtension d'hydrogène aux cathodes de Ni, Cu, Pb, Mo, Ta, Nb, Be, In et Tl a été mesurée en solution aqueuse à des densités de courant de  $10^{-3}$  à  $10^{-1}$  amp./cm.<sup>2</sup> par la méthode directe. Les résultats sont discutés d'après l'équation de Tafel. L'accroissement de la surtension avec le temps est un phénomène fondamental dans la surtension d'hydrogène et celle-ci est une fonction périodique, reliée à la "fonction travail" du métal. Les résultats sont plus faciles à interpréter d'après les théories de l'hydrogène atomique.

## Zusammenfassung.

Die Wasserstoffüberspannungen an Kathoden aus Ni, Cu, Pb, Mo, Ta, Nb, Be, In und Tl sind in wässrigen Lösungen bei Stromdichten zwischen  $10^{-3}$  und  $10^{-1}$  A/cm.<sup>2</sup> durch die direkte Methode gemessen worden. Die Resultate werden auf Grundlage von Tafel's Gleichung besprochen. Zeitliches Anwachsen ist eine fundamentale Erscheinung der Wasserstoffüberspannung; die Überspannung ist eine periodische Funktion, die eine Beziehung zur Elektronenaustrittsarbeit des Metalls besitzt. Die Resultate können am besten durch die Atomarwasserstofftheorie erörtert werden.

Imperial College,  
London, S.W.7.

## THE THEORY OF THE FORMATION OF PROTECTIVE OXIDE FILMS ON METALS.—III.

By N. F. MOTT.

Received 28th May, 1946. Revised August, 1946.

### 1. Introduction.

On many metals, if they are exposed to air, a compact oxide film is formed. At sufficiently high temperatures the rate of growth usually conforms to the parabolic law

$$x^2 = Kt$$

where  $x$  is the thickness of film at a time  $t$  after exposure to air. This law may easily be deduced theoretically, either on the assumption that metal atoms diffuse through the film to react with oxygen at the interface between oxide and air, or on the less probable assumption that it is the oxygen which diffuses through the oxide layer. Many cases are, however, known where a logarithmic law of the type

$$x = a \log (1 + bt)$$

gives a better representation of the growth; zinc below <sup>1</sup> 225° C., iron and copper under certain conditions <sup>2</sup> are examples. For this logarithmic law an explanation based on a mechanism involving repeated cracking and healing has been given by Evans.<sup>3</sup> Finally, for metals such as aluminium and chromium, a protective film grows up to a certain thickness of the order 50 Å., beyond which further growth hardly occurs unless the film cracks.

In two recent papers <sup>4</sup> the present author has put forward one possible explanation of the formation of protective films. This explanation is based on the following assumptions.

(a) Positive metal ions at the temperature considered can leave the metal and diffuse through the oxide; at the surface between the oxide

<sup>1</sup> Vernon, Akeroyd and Stroud, *J. Inst. Metals*, 1939, **65**, 301.

<sup>2</sup> Lustman, *Trans. Electrochem. Soc.*, 1942, **81**, 359.

<sup>3</sup> Evans, *Nature*, 1946, **157**, 732.

<sup>4</sup> *Trans. Faraday Soc.*, 1939, **35**, 1175; 1940, **39**, 472.



and air they will combine with oxygen to form new layers of oxide if electrons too can get through the layer from the metal to the free surface.

(b) Electrons can in principle get through the oxide layer by two mechanisms; either by thermionic emission from the metal into the conduction levels of the oxide, or by quantum mechanical tunnel effect. The former process will be impossible at room temperature if the corresponding work function  $\phi$  is greater than about 1 ev. Quantum mechanical tunnel effect is then the only possible mechanism, and this is only possible if the thickness of the oxide film is less than about 40 Å.

If the film growth is limited by this mechanism we should expect the ultimate thickness of the oxide film formed after exposure to air to be independent of temperature over a certain range, though at sufficiently high temperatures thermionic emission from the metal into the conduction band of the oxide would begin, and hence the parabolic law is to be expected, while at low temperatures the positive ions would lose their mobility and growth would be impossible.

It is the purpose of this paper to put forward another hypothesis to explain the formation of protective films, which seems to the author more probable, though the experimental evidence does not yet exist to provide a decision between them. This is based on the following hypotheses.

(a) The work function  $\phi$  is small enough to allow the thermionic emission of electrons from the metal into the conduction levels of the oxide. If, then, oxygen is adsorbed on to the surface of the oxide and oxide ions are formed, a strong electric field will be set up in the oxide.

(b) The solubility of metal ions in the oxide is at the temperatures considered too small for any passage of metal by diffusion. It can, however, be shown that under these very strong fields, migration of ions can take place.

We shall show that a theory based on these assumptions gives a limiting thickness which increases rapidly with temperature up to a certain critical temperature, which should be about 600° K. for aluminium, above which the parabolic law should hold.

## 2. Electrolytic Formation of Films.

In order to understand the formation of oxide films in air, it will be instructive first to consider their formation electrolytically in solutions, for instance, of ammonium carbonate or borate. In this case oxygen ions are brought up to the free surface of the oxide, and so there is no passage of electrons through it.

Whether an oxide film is being formed electrolytically or in air, we must consider the metal ions as passing through it as shown in Fig. 1; each layer of atoms must be stripped off atom by atom and pass through the oxide. In Fig. 2, therefore, we show the potential energy of an ion at the end of a layer as it leaves the metal and passes into the oxide; the point marked A represents the position of an ion in the metal and the points marked, B' represent interstitial positions in the oxide. The energy  $W$  is the difference between the energy of the ion in the two positions;  $U$  is the additional activation energy which must be surmounted to move the ion in either direction.

In the absence of a field a rough application of the principle of detailed balancing may be made as follows: let  $p$  be the probability that the position B is occupied ( $p$  is proportional to the solubility). Then the probability per unit time that an ion jumps from A to B is  $\nu e^{-(W+U)/kT}$ ; here  $\nu$  is the frequency of atomic vibrations, assumed the same at B as at A. The probability per unit time that an atom jumps from B to A is  $\nu p e^{-U/kT}$ . Equating these two, we find

$$p = e^{-W/kT}. \quad (1)$$

\* Not to be confused with the work function of a clean metal surface.

This quantity  $p$  gives the probability that a site is occupied in the immediate neighbourhood of the metal surface; in materials which in bulk do not show ionic conductivity, the concentration of occupied interstitial sites will drop off as we go away from the surface; owing to the space charge set up. The distance in which this fall-off occurs is of the order  $(\kappa kT/2\pi p N_0 e^2)^{\frac{1}{2}}$ , as may be shown<sup>5</sup> by an analysis similar to that employed by Debye and Hückel in their theory of strong electrolytes.

We shall assume in this paper that the thicknesses of the films are small compared with this distance, so that no appreciable space charges are set up by the dissolved ions.

If a field  $F$  is applied through the oxide a current will flow; this for small fields will be equal to

$$N_0 e p v F \quad (2)$$

where  $N_0$  is the number of interstitial positions per unit volume in the oxide and  $v$  the mobility of an ion.

Now the most conspicuous fact about the electrolytic formation of oxide films on aluminium and similar metals is that the ionic current and rate of growth are exponential functions of the field strength;<sup>6</sup> thus

$$dx/dt \propto \alpha e^{\beta F} \quad (3)$$

and that for small fields ( $\beta F \sim 1$ ) the rate of growth is negligibly small; Verwey<sup>7</sup> has attempted to explain this in the following way: for very strong fields the rate of drift of an ion should be equal to<sup>8</sup>

$$2vc e^{-U/kT} \approx \sinh(eF/kT)$$

where  $2c$  is the distance between interstitial positions. Only if  $ecF \ll kT$ , and thus for fields much less than  $10^6$  volt/cm., is this proportional to the

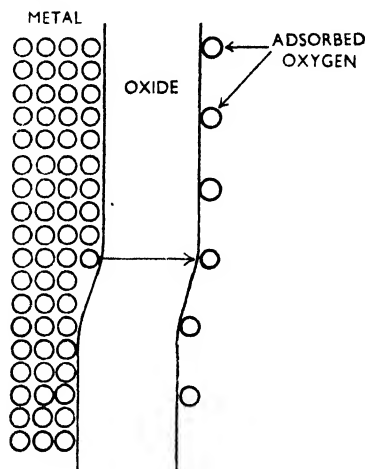


FIG. 1.—Showing the mechanisms by which ions leave a metal and pass through the oxide layer.

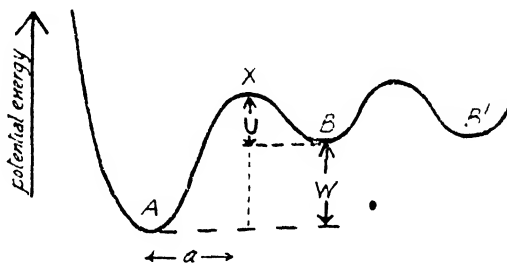


FIG. 2.—Potential energy of an ion in a metal in contact with oxide.

field  $F$ ; for strong fields the  $\sinh$  can be replaced by an exponential and, from (2), the current is

$$N_0 e p c v e^{-U/kT} e^{ecF/kT}.$$

This assumes that  $p$  is unaltered by the field; this may not be correct, and we therefore prefer the following derivation.

<sup>5</sup> Cf. Mott and Gurney, *Electronic Processes in Ionic Crystals*, p. 170.

<sup>6</sup> Gunter-schultze and Betz, *Z. Physik*, 1934, **91**, 70; 1934, **92**, 36.

<sup>7</sup> Verwey, *Physica*, 1935, **2**, 1059.

<sup>8</sup> Mott and Gurney, *loc. cit.*<sup>5</sup>, p. 43.

Suppose that at the temperature concerned  $W/kT$  is so large that  $p$ , the concentration of interstitial ions, is negligibly small. The presence of the field depresses the barrier between A and B in Fig. 2 by  $aeF$ , where  $a$  is the distance shown in the figure. Thus the probability per second that an ion will jump from A to B is

$$v e^{-(W+U+eaF)/kT}.$$

The chance that it will jump back before it jumps on is negligible. Thus the number of ions crossing unit area per unit time is

$$n v e^{-(W+U)/kT} e^{eaF/kT} \quad (4)$$

where  $n$  is the number of ions at the ends of layers (Fig. 1) per unit area.

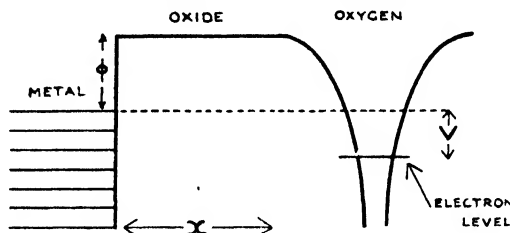


FIG. 3a.

Experimental values of  $\alpha$ ,  $\beta$  in formula (3) are, for aluminium at room temperature,  $\beta = 4.2 \times 10^{-6}$ ;  $\alpha = 4 \times 10^{-17} \mu\text{A./cm.}^2$ . Verwey deduces from this that  $a \sim 10^{-7} \text{ cm.}$ , a rather larger value than one would expect and that  $U + W \sim 1.8 \text{ ev.}$

Thus finally we have for the two extreme cases :

For high temperature and weak fields

$$\text{current} = \frac{N_0 e^2 c^2 F v}{kT} e^{-(W+U)/kT}.$$

For low temperatures and strong fields

$$\text{current} = e a n v e^{-(W+U)/kT} e^{eaF/kT}.$$

$n$  will be smaller than  $N_0 c$ , by a factor difficult to estimate, say,  $10^2$  or  $10^3$ .

### 3. Oxidation in Air.

We assume that oxygen atoms are adsorbed to the surface of the oxide film as in Fig. 1; these will produce vacant energy levels for electrons, as

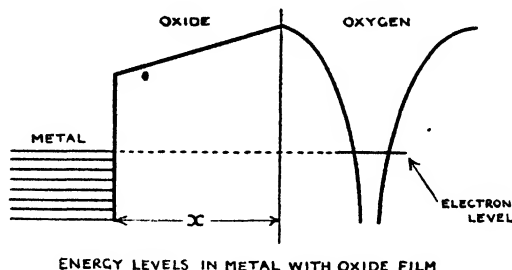


FIG. 3b.

shown in Fig. 3a. Since electrons can pass through the oxide film, they will fill these levels, forming negative ions and setting up a field in the oxide layer, which will increase until their level is raised to that of the Fermi distribution in the metal, as shown in Fig. 3b. A constant potential

difference  $V$ , of the order of perhaps a volt or two, is thus set up across the layer. The field  $F$  in the layer will thus be given by

$$F = V/x.$$

For thick films and high temperatures, the ionic current is, as we have seen, proportional to the field, say

$$j = \gamma e F.$$

If  $\Omega$  is the volume of oxide per metal ion, the growth law is thus

$$\frac{dx}{dt} = \frac{\Omega \gamma v}{x}$$

which gives the parabolic law. For thin films and low temperatures, on the other hand, we obtain

$$\frac{dx}{dt} = n v e^{-\frac{W+U}{kT}} \frac{a e V}{k T x}$$

which gives a rapid initial growth followed by a faster fall-off than according to the parabolic law.

We can estimate the thickness at which the growth rate becomes insignificant. We do not know  $n$  exactly; let us assume that one surface atom in a hundred is in a position to jump from the metal into the oxide. Then the number of layers of metal atoms which pass through the oxide per unit time is

$$0.01 v e^{-\frac{W}{kT}} \frac{a x_0}{x}$$

where

$$W' = W + U \sim 1.8 \text{ ev. for Al}$$

and

$$x_0 = a e V / k T \sim 10^{-6} - 10^{-5} \text{ cm.}$$

Taking  $v$  to be  $10^{12}$ , and defining an insignificant growth rate as one where one layer of atoms passes in  $10^8$  sec., this gives for the thickness  $x$  at which growth stops

$$\exp \left\{ \left( W' - \frac{e a V}{x} \right) / k T \right\} \sim 10^{18}$$

so

$$x = \frac{e a V}{W' - 45 k T}.$$

Thus for temperatures below  $T_0 = W'/45k$ , a stable film is formed; for temperatures above this, growth continues indefinitely.

For aluminium with  $W' \sim 1.8$  ev. and  $a \sim 10^{-7}$  cm., we have

$$x = (eV/W') 10^{-7} (1 - T/600^\circ)^{-1}.$$

The first factor should be of the order unity. Thus at room temperature the thickness of the film formed should be *ca.*  $2 \times 10^{-7}$  cm., at  $200^\circ$  C. it should be  $6 \times 10^{-7}$  cm., and above *ca.*  $300^\circ$  C. no limiting film will be formed and growth will proceed according to the parabolic law.

The theory thus gives the right order of magnitude for the film formed at room temperature; experiments on the temperature dependence of the film thickness would be of great interest.

#### 4. The Value of the Work Function $\phi$ .

The fact that thick films of  $\text{Al}_2\text{O}_3$  on aluminium give good insulation suggests that the  $\phi$  is too great for thermionic emission into the oxide; on the other hand in electrolytic condensers electrons pass from aluminium into the oxide under the influence of not very strong fields. We have attempted to estimate  $\phi$  from the work of Mohr<sup>9</sup> on the rectifying action of a layer of oxide on aluminium formed electrolytically, the other electrode being still the electrolyte. We assumed that the current from metal to oxide was given by the usual formula for strong field emission

$$A F^2 e^{-BF}$$

<sup>9</sup> Mohr, *Z. Physik*, 1933, **85**, 679.

where

$$A = 6.2 \times 10^{-6} \mu^{1/2} / (\phi + \mu) \phi^{1/2}$$

$$B = 6.8 \times 10^7 \phi^{3/2}.$$

The best fit with experiment gave

$$\phi \sim 1.3 \text{ ev.}$$

We do not therefore feel quite certain which of the two mechanisms proposed for limiting the film growth is valid; possibly both are operative in different temperature ranges.

Cabrera<sup>10</sup> has pointed out recently that according to the mechanism of the author's previous papers, irradiation with light of frequency  $\nu$  such that  $h\nu > \phi$  would produce a considerable increase of film thickness. Recent experiments of aluminium<sup>11</sup> suggest that the effect of ultra-violet light is too small for the mechanism to be tenable. On the other hand, some results on the temperature dependence of the rate of growth of thickness of oxide seem to be in accord with the theory of this paper. The limiting thickness, in a dry atmosphere, is at 10° C. about  $3.5 \times 10^{-7}$  cm.; at 100° C. this thickness is greater by a factor of about 2; above 300° C. the rate of growth is very rapid and seems to continue without any limit.

### Summary.

A new mechanism is proposed to account for the formation on metals of oxide films which grow to a limiting thickness. According to this, electrons can pass the film easily, but ions can only penetrate it in the presence of a very strong field. This mechanism is compared with the author's previous theory based on tunnel effect; further experimental work is required to determine which is correct.

### Résumé.

Pour rendre compte de la formation, sur des métaux, de films d'oxyde, qui n'atteignent qu'une épaisseur limite, on propose un nouveau mécanisme, selon lequel les électrons peuvent traverser le film facilement, tandis que les ions n'en sont capables qu'en présence d'un champ très fort. On compare ce mécanisme avec un autre, précédemment exposé par l'auteur et basé sur l'effet tunnel; seul, un travail expérimental ultérieur permettra de déterminer lequel des deux est correct.

### Zusammenfassung.

Zur Erklärung der Bildung an Metallen von Oxydfilmen, deren Dicke bis zu einem Grenzwert anwächst, wird ein neuer Mechanismus vorgeschlagen, demzufolge Elektronen den Film leicht durchdringen können, wogegen Ionen dies nur in Gegenwart eines sehr starken Feldes vermögen. Es wird ein Vergleich dieses Mechanismus mit der früheren Theorie des Verfassers, die auf dem Tunneleffekt beruht, angestellt; weitere Experimente sind nötig um zu entscheiden, welche Theorie richtig ist.

H. H. Wills Physical Laboratory,  
University of Bristol.

<sup>10</sup> Cabrera, *Compt. Rend.*, 1945, **220**, 111.

<sup>11</sup> Cabrera, Terrien, Hamon, *ibid.*, 1947, **224**, 1558.

# ADSORPTION AND LUBRICATION AT CRYSTAL SURFACES. PART I. ON THE BOUNDARY LUBRICATION OF SODIUM NITRATE.

By E. HUTCHINSON AND E. K. RIDEAL.

*Received 14th June, 1946.*

The phenomenon of boundary lubrication is now well established. Hardy<sup>1</sup> and Langmuir<sup>2</sup> showed that the deposition of monomolecular films of materials such as long chain fatty acids on metal and glass surfaces, resulted in a marked lowering of static friction. Similar effects are obtained in the case of sliding friction although, due to the wear and tear of the film during sliding, considerably more film material than that required to produce the same effects as in static friction may be required to maintain a low coefficient of friction. The work of Hardy<sup>3</sup> and Bowden<sup>4</sup> on the lubricant effect of vapours has shown that adsorbed films, presumably monomolecular, also give rise to effects exactly similar to those produced by mechanically deposited monolayers.

In normal lubrication practice, boundary lubricants such as the long chain fatty acids are used in the presence of a medium such as hydrocarbon oil. It is generally assumed that a monomolecular film is adsorbed from solution and that the effects produced are identical with those produced by deposited films. This is a reasonable assumption but no work directly verifies this hypothesis. A good deal of indirect evidence has been produced, particularly from experiments on the phenomenon of "stick-slip" transition.<sup>5, 6</sup> Indeed in a recent paper Frewing<sup>7</sup> attempts to define a close correlation between the "stick-slip" transition temperature and the degree of saturation of the adsorbed boundary film.

It is well established that both inorganic ions and organic compounds can be adsorbed on crystal facets from solution. The adsorption of suitable organic compounds should effect a lowering of the coefficient of friction of the crystal surface. The experiments described here and in the succeeding paper are an attempt to verify directly for crystal surfaces that lubrication by solutions of boundary lubricants is achieved through the adsorption of a monomolecular film.

## Experimental.

In order to study the lubrication of crystal surfaces such as sodium nitrate, most of the standard methods of measuring friction were unsuitable (due to the relatively fragile nature of the crystals).

The first apparatus used is shown diagrammatically in Fig. 1. It is similar to a friction pendulum built by Kyropoulos.<sup>8</sup> It consists of a thin brass rod 50 cm. long provided with a moveable weight of 200 g. and screwed at right angles to the axis of a duralumin cylinder 5 cm. long and 1 cm. in diameter.

<sup>1</sup> Hardy, *Phil. Mag.*, 1910, **37**, 32.

<sup>2</sup> Langmuir, *Trans. Faraday Soc.*, 1920, **15**, 68.

<sup>3</sup> Hardy and Doubleday, *Proc. Roy. Soc. A*, 1922, **100**, 550.

<sup>4</sup> Bowden and Hughes, *ibid.*, 1939, **172**, 263.

<sup>5</sup> Hughes and Whittingham, *Trans. Faraday Soc.*, 1942, **37**, 9.

<sup>6</sup> Frewing, *Proc. Roy. Soc. A*, 1942, **181**, 23.

<sup>7</sup> Frewing, *ibid.*, 1944, **182**, 270.

<sup>8</sup> Kyropoulos, *Rev. Sci. Inst.*, 1937, **8**, 151.

Long flat crystals of ammonium nitrate were bent round the circumference of the cylinder, one at each end, and each of these crystals rested on two flat crystals on opposite sides of an L-shaped angle-rod. The angle-rod was provided with a hole to permit free swinging of the pendulum.

If deflected to one side and then released the pendulum swings with decreasing amplitude. The coefficient of friction may be readily calculated from the decrease in amplitude. Considerable difficulty was experienced with this apparatus notably in attaching the crystals. Adhesives fouled the crystals and could not be used in the presence of organic solvents. The dry crystals could be attached by touching with a hot wire but this method was not satisfactory in the presence of solvents. It is important to record, however, that a number of measurements of the coefficient of friction between dry ammonium nitrate crystals were made. Fairly consistent results were obtained giving a value  $0.50 \pm 0.05$  for clean dry crystals.

The final design of apparatus is shown diagrammatically in Fig. 2. A crystal firmly clamped in an aluminium holder moves in a circular track over a steel disc. The friction between the crystal and the disc is transmitted as a couple to a central pillar and is balanced by a couple due to a weight placed in a scale pan, attached by a thread to a pulley on the pillar. The central pillar is supported in a ball-bearing housing which is practically frictionless. The steel disc can be rotated at any desired speed by means of a motor and gears.

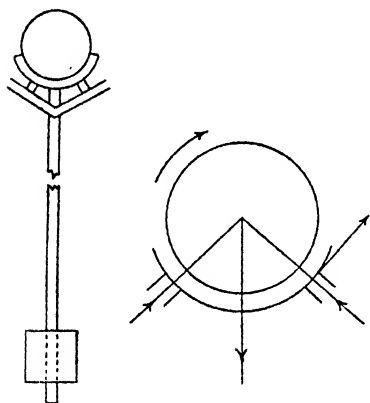


FIG. 1.

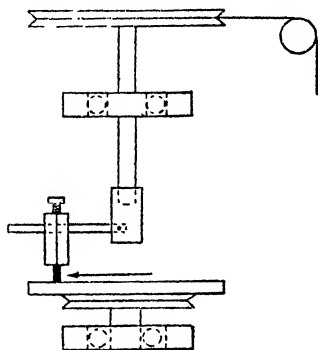


FIG. 2.

The disc was turned on the lathe from a piece of mild steel and finished by rubbing with "O" Emery cloth, but was not polished.

It would at first sight appear that this apparatus would record the value of the coefficient of friction between crystal and steel, but it is believed that this is not so, and that crystal-crystal friction is in fact measured. There is considerable evidence to support this hypothesis. The coefficient of friction as measured for a dry crystal on the disc was 0.55, almost the same as with the original pendulum apparatus. Moreover, although it was not possible to fuse ammonium nitrate or sodium nitrate into smooth discs to replace the steel discs, due to the invariable appearance of cracks, a visible film of ammonium nitrate was formed on the disc by rotating at high speed in the lathe and holding a large crystal firmly against the rotating disc. The coefficient of friction was in no way altered by this treatment. Finally, after one revolution of the clean steel disc under a crystal of ammonium nitrate a layer of deposited crystals on the disc was clearly shown on microscopic examination. A photograph of the surface ( $\times 1400$ ) is given in Fig. 3 in which the deposited crystal layer is clearly visible. The width of the deposited track corresponds closely to the width of the crystal used and so far as can be judged the thickness of the track appears to be about  $0.02-0.05$  mm. The phenomenon is clearly very similar to that of "pick-up" such as occurs in the case of a hard and a soft metal contact, but appears to differ in that "pick-up" by metals is a gradual process.

The apparatus was used to examine the frictional behaviour of sodium nitrate and ammonium nitrate in the presence of solutions of various surface active



FIG. 3.

[To face p. 436.]





materials in nitrobenzene at linear sliding speeds of 2-12 cm. per min. and under loads of 50-400 g. In this region Amonton's law was found to hold both for lubricated and unlubricated surfaces. The crystals were grown by slow evaporation from solution in surface clean water and were dried on filter paper before storing in sealed bottles. It is difficult to ensure that the crystals are perfectly clean but the procedure adopted was to dip the crystals into surface-clean alcohol just before use to dissolve any surface impurity. After such treatment the crystal produced no lowering of the surface tension of water when dissolved. At first the disc was cleaned by washing with 20 % caustic soda, distilled water and acetone but as no difference could be detected between a disc cleaned in this way and one cleaned merely by washing with acetone, the latter was more generally used.

### Results.

It may be stated at the outset that there was no observable difference in the behaviour of ammonium and sodium nitrates; it should, however, be borne in mind that the results are only accurate to some 5-10 % and it may be that there are differences which are too small to be observed by this method. While it is reasonable to expect similarity in behaviour in the presence of solutions of lubricant it is, at first sight, surprising to find the friction of the dry crystals to be the same. Experiments using other materials such as potassium nitrate, and sodium chloride also gave values of the coefficient of friction of about 0.5 however.

Results for various solutions of surface active compounds in nitro-benzene, are given in Fig. 4 and 5. It will be seen that at low concentrations the coefficient of friction is markedly dependent on the concentration of lubricant.

In sufficiently concentrated solutions, however, all straight chain paraffin derivatives give more or less the same coefficient of friction 0.12. That the same final value should be obtained for different materials is to be expected on the hypothesis that in the final state a saturated monolayer is adsorbed on the crystals. (The materials were all of sufficiently high chain length for the Hardy-Doubleday rule<sup>8</sup> not to apply.) Below the limiting concentrations the coefficient of friction is dependent on the concentration and the friction-concentration curves are not identical for different materials. There are considerable differences between the limiting concentrations for different materials and this provides one means of deciding the suitability or efficiency of a given material as a boundary lubricant since it is generally desirable to use the minimum possible amount of lubricant in solution.

A number of compounds are exceptions to the rule that a final lowering of friction to a value of about 0.12 occurs. These exceptions are polymeric in nature. One such compound is shown in Fig. 5 (a low molecular weight polymer prepared by the condensation of adipic acid and glycol). The final value of the coefficient of friction with these polymeric compounds

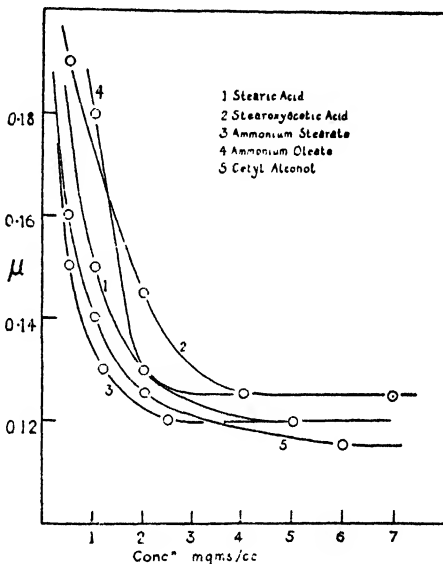


FIG. 4.

is about 0.16, which is considerably higher than that found with compounds like stearic acid. On the other hand the persistence, or wearability, of polymeric compounds is much higher than that of paraffin chain derivatives, in that on removal of all excess solution and with continued running of the apparatus the coefficient of friction remained at a low value ( $< 0.3$ ) much longer. It seems probable that whereas a fatty acid might be attached to the crystal surface only at the polar head with the hydrocarbon chain projecting away from the surface, the polymeric lubricants lie flat on the crystal, and are attached at a large number of points of adsorption, corresponding to the polar groups along the chain. The protective layer will therefore be of the order of the width of a hydrocarbon chain, i.e., much less than that provided by a vertically oriented fatty acid layer. This is

reflected in the higher final value of the coefficient of friction. It is noteworthy, however, that although the lubricant film is so much thinner the lowering of friction is some 80 % of that produced by the fatty acid film.

The effect of increased concentration of lubricant on the lowering of the coefficient of friction, suggests that the concept of the formation of an adsorbed monolayer on the solid surfaces in solutions of boundary lubricant is true, and the individuality of the curves for different lubricants suggests that the ease of formation and completion of the boundary film is specific for any one lubricant. It is clear that the adsorption of the lubricant into the boundary film is one factor which determines the efficiency of a lubricant in practice. As regards the efficiency of a lubricant in repeated use, however, it is important

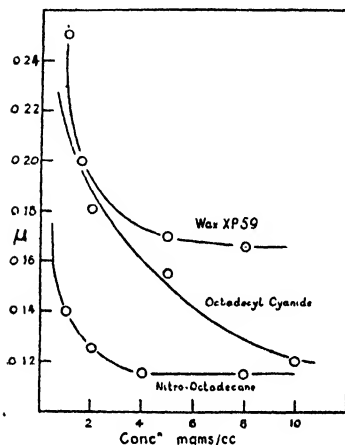


FIG. 5.

that the adhesion of the film to the surface be high and it would appear that this may be effected by the use of polymeric materials containing a large number of adsorbable polar groups.

The authors are grateful to the Director-General, Scientific Research and Development, Ministry of Supply, for permission to publish this work.

### Résumé.

On a tenté de vérifier directement, pour des surfaces de cristaux, que la lubrification par des solutions de "boundary lubrifiants" est réalisée par un film monomoléculaire adsorbé. L'efficacité du lubrifiant pour des usages répétés exige une très bonne adhésion du film sur la surface.

### Zusammenfassung.

Es wird versucht, für eine Kristalloberfläche direkt zu beweisen, dass Schmierung durch Lösungen von Grenzflächenschmiermitteln durch die Adsorption eines monomolekularen Films wirkt. Die Wirksamkeit des Schmiermittels bei wiederholter Benützung erfordert ausserdem eine hohe Adhäsion des Films an der Oberfläche.

# ON ADSORPTION AND LUBRICATION AT CRYSTAL SURFACES. PART II. ON THE ADSORPTION OF PARAFFIN CHAIN COMPOUNDS ON SODIUM NITRATE.

BY E. HUTCHINSON.

(Communicated by Professor E. K. Rideal.)

Received 14th June, 1946.

The method of studying the adsorption from solution of materials such as long chain acids adopted here is widely applicable to long chain paraffin compounds. The analysis is carried out by spreading a known volume of the solution on a Langmuir trough and estimating the concentration of the solution from a determination of the force-area characteristics of the monomolecular film formed on the trough.\*

## Experimental.

To make a measurement of the adsorption of a surface agent on the powder, some 2.5 g. of the powder were placed in a stoppered tube, 5 cc. of solution added, and the mixture shaken for about an hour to attain equilibrium (experiment showed that one hour was more than adequate for the attainment of equilibrium). By spreading the same volume of solution before and after adsorption on a Langmuir trough a direct comparison of the original and final equilibrium concentrations was obtained, and from the difference between the two the amount adsorbed on the powder was readily calculable.

Fine-grained powders with an area of some 5000 cm.<sup>2</sup> per g. were required in order that the uptake should produce a measurable change in the concentration of the solution. Sodium nitrate was prepared as large crystals from solutions in surface clean water and dried by dipping into clean acetone before bottling. For a measurement about 10 g. of these crystals were rapidly ground in a clean mortar, transferred to stoppered tubes, weighed and the solution added. Grinding was carried out as quickly as possible so as to minimise contamination; such contamination became serious if the powder was exposed for more than 10-15 minutes. This grinding of small quantities of powder sufficient only for the points of one isotherm resulted in small variations of particle size from one isotherm to another. As judged by the maximum uptake by the powders, these variations were in general less than 20 % but in order to make comparison between various surface agents easier the results are expressed as fractional surface covering ( $\theta$ )-concentration curves. These results are given in Fig. 1 and 2. The effect of the nature of the solvent on the adsorption was investigated by using solutions in benzene, CCl<sub>4</sub> and petro-ether. From Fig. 2

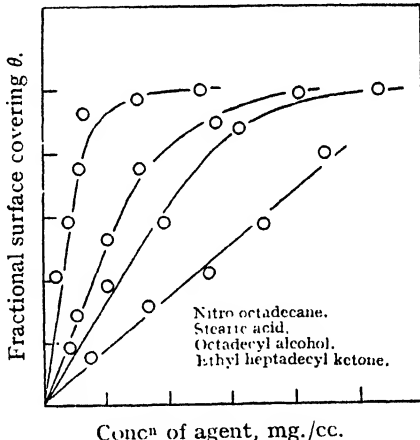


FIG. 1.

\* The method has been used with success by Dr. Crisp of this department in a study of adsorption phenomena on very large alumina surfaces.

it will be seen that there is very little difference between  $\text{CCl}_4$  and benzene but that, at the same concentrations, surface covering is more complete from petro-ether solutions. Adsorption from nitrobenzene solutions is not expected to be markedly different from that in benzene or  $\text{CCl}_4$  solutions.

Making this latter assumption it is interesting to compare directly, the variations of the surface covering and of the coefficient of friction as determined in Part I with the variation of the concentration of the solution. In Fig. 3 the fractional surface covering  $\theta$  is plotted against the lowering of friction  $\mu$  and it is clear that the order of efficiency as lubricants is the same as the order of ease of adsorption in agreement with the hypothesis that adsorption is a precursor to boundary lubrication. Closer inspection, however, reveals that the specific differences between various agents is more marked in the case of the friction experiments. The reason for this appears to be that the effect of

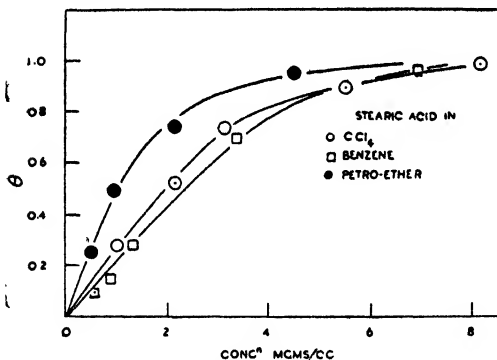


FIG. 2.

the adsorbed molecules on the surface is not uniform throughout the whole isotherm, in that the relative lubricant effect at low surface covering is greater than at higher surface covering. For example, in Fig. 3, at a surface covering of only 0.1 the lowering of the coefficient of friction is about 60 % of that with a complete monolayer. This phenomenon can be interpreted on the weld theory of Bowden.

Calculations can be made of the free energy change for the adsorption process. The change in free energy is given by the equation :

$$\Delta G = -RT \ln c_s/c_L \quad (1)$$

where  $c_s$  = the concentration of the agent in the adsorbed film, and  $c_L$  = the concentration of the agent in the bulk solution. In order to apply

TABLE I

Solvent.	Surface agent.	$\Delta G$ in kcal. per g. mol.
Carbon tetrachloride	1-Nitro-octadecane	4.50
"	Stearoxyacetic acid	4.09
"	Methyl heptadecyl ketone	3.45
"	Octadecyl alcohol	3.63
"	Stearic acid	3.83
Benzene	Stearic acid	3.49
"	Octadecyl alcohol	3.55
"	Stearoxyacetic acid	3.68
"	1-Nitro-octadecane	4.15
Petro-ether 100°-120° C.	Stearic acid	4.03

equation (1) it is necessary to make certain assumptions about the state of packing in the adsorbed film. It seems legitimate to assume that a molecule is adsorbed on the crystal by virtue of its possessing a polar head, and that in the film the molecule is orientated with the polar head attached to the surface and the hydrocarbon chain projecting away from the surface. Examination of the nature of the polar heads suggests that with the possible exception of an alcohol the adsorbed molecule is sited above a positive ion.

From studies at air-water interfaces the area per molecule of long chain

paraffin derivatives is not less than about 18 to 20 Å.<sup>2</sup>, and it therefore follows that it is not possible to pack molecules of this size above each sodium ion in the surface, since the separation of neighbouring ions is of the order of 4 Å. Hence the closest possible packing of molecules having an area lying between 18 and 30 Å.<sup>2</sup> is that shown in Fig. 4. This packing, in which only one-half of the total sodium ions are sites for adsorption, will be the same for all molecules with areas in the above limits. The concentrations of the molecules in the film at surface covering  $\theta = 1$  will be one molecule per  $2a^2$  cm.<sup>2</sup> where  $a$  is the lattice constant of the crystal. For intermediate surface covering  $\theta$  the concentration will be  $\theta$  molecules  $2a^2$  cm.<sup>2</sup> or,  $\theta/2 Na^2$  g. moles per cm.<sup>2</sup>. In order to convert this concentration, expressed as g. moles per cm.<sup>2</sup> to a concentration expressed as g. moles per cc., it is necessary to postulate a thickness for the film. In these calculations a thickness of 5 Å. has been assumed. Since the thickness term is incorporated in the logarithmic part of equation (1) even large

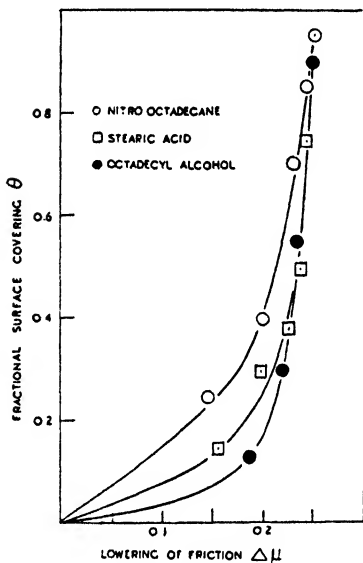


FIG. 3.

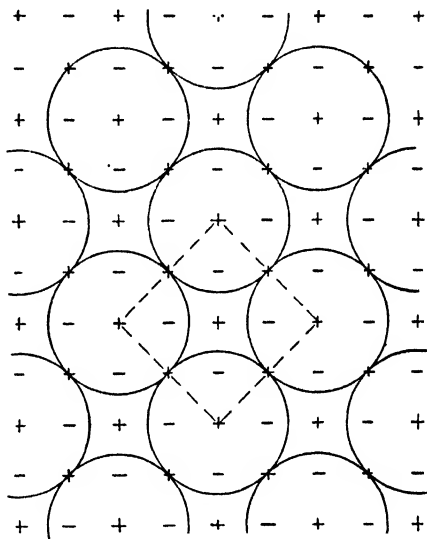


FIG. 4.

differences in the value of the assumed thickness make only a small modification in the value of  $\Delta G$ .

At low concentrations the plot of  $\theta$  against concentration is approximately linear, and it is possible to calculate the free energy change for the initial adsorption from the slope of the  $\theta$ -concentration curve.

At surface covering  $\theta$

$$\begin{aligned} c_s &= \theta/2 Na^2 c_L \\ \text{and } \Delta G &= -RT \ln \theta/2 Na^2 c_L \quad . \quad . \quad . \quad (2) \\ &= -RT \ln \theta/c_L + \text{constant} \quad . \quad . \quad . \quad (3) \\ &= \text{constant} - RT \ln (\text{initial slope}) \quad . \quad . \quad . \quad (4) \end{aligned}$$

The standard states to which these calculations refer are an infinitely dilute solution and an infinitely expanded adsorbed film. The calculated values of the free energy change are given in Table I.

A plot of  $1/\theta$  against  $1/c_L$  does not give a linear graph indicating that the adsorption does not follow a simple Langmuir isotherm

$$\theta = Kc_L/(1 + Kc_L) \quad . \quad . \quad . \quad (5)$$

In view of the possible association of the polar molecules in solution it is unlikely that, except in dilute solution,  $c_L$  represents the concentration of the monomeric form of the adsorbed molecule. Data are unfortunately not available to investigate whether the Langmuir equation holds for the monomer in equilibrium with the adsorbed film.

Table I shows that the free energy change is greater for the more readily absorbed molecules, but the function is not very satisfactory for the comparison for different molecules, due to the relative insensitivity of equation (4) to even large changes in the initial slope of the isotherm. It proved difficult to examine the temperature dependence of  $\Delta G$  by the methods described here since the possible errors in these experiments were so large that value of  $\Delta H$  and  $\Delta S$  derived from the temperature coefficient of  $\Delta G$  would be subject to large errors of the order of 100 %. Thus, although it is not possible from the results of this work to deduce much as to the nature of the adsorbed film, these experiments do demonstrate directly, however, that boundary lubrication is closely associated with the phenomenon of adsorption. This is important since it now becomes clear what direction a search for more efficient boundary lubricants to be used in solution, should take. For, no matter how firmly the film is held when once formed, or how efficient it may be in lowering the coefficient of friction, unless it be readily adsorbed it will not, in general practice, be an economical lubricant.

The author is grateful to the Director-General, Scientific Research and Development, Ministry of Supply, for permission to publish this work.

### Summary.

It has been shown, by a study of boundary lubrication in the presence of solutions of surface active compounds, and by a study of the adsorption phenomena occurring at the crystal surface, that boundary lubrication of sodium nitrate crystals is achieved through the adsorption of a boundary film. The degree of saturation of this boundary film, and hence the coefficient of friction, is markedly dependent on the concentration of the lubricant solution. From a study of the friction and adsorption curves it is possible to compare the relative lubricant efficiency of a series of film-forming materials.

### Résumé.

Une étude des "boundary lubrifiants" en présence de solutions de composés à activité de surface et une étude de l'adsorption à la surface du cristal ont montré que la lubrification de cristaux de nitrate de sodium est effectuée par l'adsorption d'un film. Le coefficient de friction dépend de la concentration du lubrifiant dans la solution et, à partir des courbes de friction et d'adsorption, il est possible de comparer les efficacités relatives de lubrification de plusieurs substances, capables de former des films.

### Zusammenfassung.

Die Untersuchung der Grenzflächenschmierung in der Gegenwart oberflächenaktiver Substanzen und der Adsorption von einer Kristalloberfläche zeigt, dass Schmierung von Natriumnitratkristallen durch die Adsorption eines Grenzflächenfilms bewirkt wird. Der Reibungskoeffizient hängt von der Konzentration der Schmiermittellösung ab und Vergleiche der relativen Schmierwirksamkeit von einer Reihe von filmbildenden Stoffen können aus den Reibungs- und Adsorptionskurven abgeleitet werden.

# ADSORPTION AND LUBRICATION AT CRYSTAL SURFACES. PART III. ON HEATS OF WETTING AND ADSORPTION ON IONIC CRYSTALS.

BY E. HUTCHINSON.

(Communicated by Professor E. K. Rideal.)

Received 14th June, 1946.

A large number of experimental results on the heats of wetting of various systems have been obtained by different investigators, but few of these are of any fundamental value due to the lack of information as to the state and purity of solid surfaces and the wetting liquids. The experiments of Harkins<sup>1</sup> are probably the most carefully carried out, and these show clearly the need for great care in the preparation of the materials used.

The measurement of heats of wetting involves the accurate determination of temperature changes of the order of 0.01 to 0.1° C. Earlier workers have used Beckmann thermometers for this purpose but these have a great disadvantage of large thermal capacity and fairly slow response to small temperature changes. Harkins<sup>1</sup> overcame these difficulties by using a multiple thermocouple an arrangement which, while it is accurate and responsive, requires considerable precautions to prevent the pick-up of stray E.M.F.'s. In the experiments described below, a new method of accurate thermometry was used which fulfils all the requirements of accuracy and response and which is in addition very compact and easy to operate.

## Experimental.\*

The apparatus is shown in Fig. 1. It consists of a stout-walled transparent Dewar vessel of about 300 cc. capacity provided with a well-fitting cork, and small heating coil of 0.90 ohms resistance wound round a glass tube. A glass rod which lies squarely along the axis of the Dewar vessel is provided with a brass sleeve to which is attached a tube containing the powder to be wetted. The tube containing the powder carries a set of removable paddles which serve to stir the liquid and distribute the heat evolved. The thermometer is a "thermistor" or resistance thermometer composed of a mixture of fused oxides, principally uranium oxide, sealed by means of two thin platinum wires, into a protective glass sleeve.

Like all electrical semi-conductors, its electrical resistance decreases exponentially with increased temperature,

$$\text{i.e.} \quad R = R_0 e^{-b/T} \quad . \quad . \quad . \quad . \quad . \quad (1)$$

$$\text{or} \quad T = -b \ln (R/R_0) \quad . \quad . \quad . \quad . \quad . \quad (2)$$

Thermistors have been subject of considerable research<sup>2</sup> but this appears to be the first occasion on which they have been used in the accurate determination of small temperature rises.

The particular thermistor† used throughout this experiment had a

<sup>1</sup> Harkins, *Ind. Eng. Chem.*, 1930, **22**, 897.

<sup>2</sup> Sillars, *J. Sci. Instr.*, 1942, **19**, 81.

\* This method of calorimetry was evolved in collaboration with Mr. Hugh Campbell of this department.

† The author is grateful to Messrs. Standard Telephones and Cables, Limited, for supplies of thermistors used in these experiments.



resistance of about  $4,500\ \Omega$  at room temperature, and a temperature coefficient of about  $150\ \Omega$  per degree in this region. The thermistor was made one arm of a Wheatstones bridge circuit, in which differences of  $0.1\ \Omega$  were readily measurable, so that temperature changes of  $0.001^\circ\text{C.}$  were measurable. This accuracy is considerably better than that obtainable with a Beckmann thermometer. The response to small temperature changes was less than one second and this, together with the negligible thermal capacity and good reproducibility of the instrument, renders it very suitable for this kind of work. The wetting liquids were prepared according to directions given in Weissberger's *Organic Solvents*.<sup>3</sup>

In order to have results of real significance it is necessary to know the surface area of the powder, so that in order to avoid numerous determinations of surface area it is necessary to have a large number of uniform samples of the powder to be wetted. For these experiments a finely divided and uniform sample of sodium fluoride was used. By washing this powder in clean benzene and spreading the washings on a Langmuir trough it was found that there was no surface active impurity on the powder, and it was concluded that surface contamination would consist mainly of water vapour. To remove this, thin bulbs were blown on the end of pieces of 6 mm. glass tube, being made sufficiently thin to break readily on gentle tapping. About 3 g. of powder were introduced into

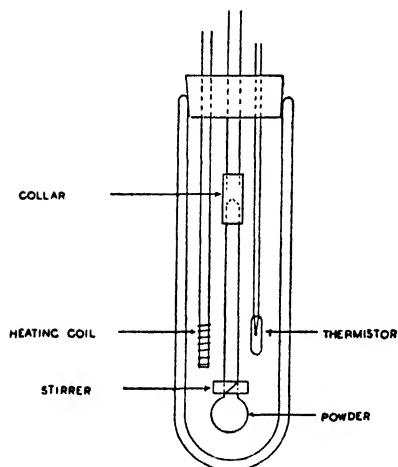


FIG. 1.

each bulb and the tube sealed on to a vacuum line and evacuated. The time of evacuation did not appear to affect the results provided that it was greater than 5 hours and it may be assumed that all adsorbed moisture was removed by this means. The bulbs were sealed off under vacuum and stored before use.

In carrying out an experiment the tube containing the powder is weighed and fitted to the stirrer by means of the brass sleeve. About 60 cc. of the wetting liquid are placed in the Dewar vessel and the stirrer connected to the electric motor. The system is left to attain temperature equilibrium for 3-4 hours and stirring is then commenced. Since the stirring causes a rise in temperature a time-temperature curve is followed for 5-10 minutes at half-minute intervals. When a steady rise in temperature has been observed for about 5 minutes, stirring is stopped and the bulb is broken under the liquid, the time being noted. Stirring

is recommenced for another 5 minutes in which time all the heat of wetting is generally evolved. A known current is then passed through the heating coil for a measured time and the time-temperature curve followed for a further 5 minutes. In this way final curves similar to that shown in Fig. 2 are obtained. The two sharp changes in resistance are due respectively to the breaking of the bulb and to the heating current. The measured heat input from the coil serves to calibrate the apparatus so that it is not necessary to know the thermal equivalent of the system. At the end of the experiment the tube which contained the powder is removed, dried, and weighed, so that weight of powder wetted is obtained from the difference between the initial and final weight of the tube. A small error is introduced here since the final weight of the tube does not include that of the thin glass bulb blown on the end, this having been broken and fallen into the liquid. A number of experiments showed that the weight of these bulb fragments invariably lies in the region of 20-30 mg. and a standard correction of 25 mg. has been made. (It was not possible to assume that the weight of powder introduced into the bulb originally is the same as that finally broken under the liquid as appreciable quantities are sucked off in the initial stages of the evacuation.)

In the determination of a heat of adsorption instead of a heat of wetting the procedure is identical except that a known solution of the chosen compound is substituted for the pure liquid. Four determinations were made for

<sup>3</sup> Weissberger and Proskauer, *Organic Solvents* (Oxford Univ. Press).

each system, reproducibility being usually better than 3 % and never worse than 6 %.

The surface area of the powder was determined for several random samples by measurement of the maximum adsorption of stearic acid, agreement to within 5 % being obtained. The maximum uptake of stearic acid by the powder was 11.2 mg. per g. so that in order to convert the heats of wetting and adsorption to the heat of wetting per gram mole. of liquid, it is necessary to multiply the measured heats per gram of powder by factor  $285/11.2 \times 10^{-3}$ .

### Results.

In Table I are listed values for the heat of wetting per g. of sodium fluoride and per g. mole of liquid, and in Table II heats of adsorption on sodium fluoride.

The heat of wetting is not identical with the heat of adsorption; as will be seen the largest discrepancy between the two is in the case of octyl alcohol, but in nearly all cases there is a slight difference. Heats measured in this way are the overall effect of at least two processes, viz., (1) removal of the adsorbate molecule from its surroundings in the bulk liquid involving a term  $\Delta H_1$ , (2) adsorption on the solid surface involving a term  $\Delta H_2$ . Hence  $\Delta H_{obs} = \Delta H_1 + \Delta H_2$ .

The term  $\Delta H_1$  is different according to whether the bulk liquid is pure wetting liquid or a solution of the adsorbate. In some cases there appears to be only a small difference, but in the case of octyl alcohol there is a marked difference. The term  $\Delta H_1$  is, in fact, largely responsible for the occurrence of adsorption in this case because the surface-dipole interaction, which is measured by the heat of wetting, is less than the Van der Waals attraction between the surface and the solvent, so that in the absence of a large repulsive action between the solvent and the solute molecules the powder would be preferentially wetted by the solvent. This is clearly brought out by the observation that a solution of ethyl alcohol in benzene gives the same heat as pure benzene. Here the term  $\Delta H_1$  is not very great and it is only when it is increased by the addition of a long chain, as with octyl alcohol, so that the sum of  $\Delta H_1 + \Delta H_2$  is greater than the heat of wetting by the solvent, that adsorption occurs. The difference between the heat of adsorption and the heat of wetting by the solvent is quite small in the case of both alcohols and ketones which explains why these compounds are relatively poorly adsorbed and are inefficient lubricants.

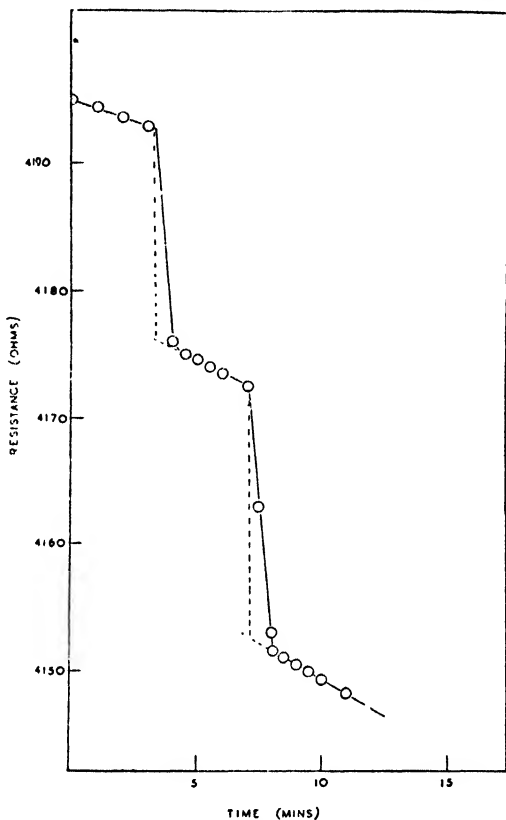


FIG. 2.

In Table III are given values for heat of mixing of several liquids with benzene, and the heat of solution of methyl heptadecyl ketone. These are quoted in a rather arbitrary manner, viz., the heat of mixing of 2 cc. of liquid and 60 cc. of benzene. This is an unsatisfactory way to define the heat of mixing but there appears to be no well-defined thermodynamic quantity to characterise heats of mixing. The actual quantities used were

TABLE I

Wetting liquid.	Heat per gram of powder (cal.).	Heat per gram-mole. of liquid (kcal.).
Carbon tetrachloride .	0.96	24.7
Chlorobenzene . . .	0.48	12.3
Petro-ether 60°-80° C.	0.31	8.1
Benzene . . . . .	0.54	14.0
Octyl alcohol . . .	0.42	10.9
Nitrobenzene . . .	0.84	21.7
Amyl acetate . . .	0.92	23.7
Acetone . . . . .	0.33	8.6
Acetophenone . . .	0.33	8.6
Benzaldehyde . . .	0.64	16.6
Oleic acid . . . . .	0.92	23.3
Caprylic acid . . .	0.94	24.3

dictated by the dimensions of the apparatus. The results serve as a comparison of the relative effects with different materials however. These values were obtained by an analogous method to heats of wetting by breaking a bulb of the liquid under benzene.

The results show that the term  $\Delta H_1$ , which is a measure of repulsive fields between the solute and the solvent, is affected both by the polar nature and the chain length of the

solute molecule. It will be seen from Tables II and III that if to the heat of wetting by octyl alcohol a term equal to 0.2 cal. is added, corresponding to the heat evolved in withdrawing about 10 mg. of alcohol from solution to cover a gram of powder, a total heat change of some 0.6 cal. is obtained in reasonable agreement with the observed value for the heat of adsorption of octyl alcohol. Experiments were carried out to test the applicability of Hess' Law to the two-stage

TABLE II

Solvent.	Adsorbate.	Concn. (vol.).	Heat per gram of powder (cal.).	Heat per gram-mole. adsorbate (kcal.).
Benzene	Carbon tetrachloride	10%	0.92	23.7
"	"	20%	1.01	26.2
"	Oleic acid	10%	0.97	25.0
"	"	20%	1.03	26.7
Nitrobenzene	"	10%	1.05	27.2
Carbon tetrachloride	"	10%	1.03	26.7
Benzene	Lauric acid	12%	1.07	28.6
"	"	18%	1.10	29.2
"	Amyl acetate	20%	0.90	23.3
"	Acetone	10%	0.62	16.1
"	Octyl alcohol	10%	0.68	17.8

wetting of a powder by the following method. The heat  $\Delta H_B$  evolved in breaking the powder under benzene was measured. A known amount of carbon tetrachloride was then added to the benzene with a heat evolution  $\Delta H_1$ . This term  $\Delta H_1$  includes the heat of mixing  $\Delta H_2$  of benzene and  $\text{CCl}_4$  and the heat of substitution  $\Delta H_3$  of  $\text{CCl}_4$  displacing the benzene on the surface of the powder.

i.e.,

$$\Delta H_1 = \Delta H_2 + \Delta H_3.$$

2.5 g. of powder were broken under benzene and 2 cc. of  $\text{CCl}_4$  added.

TABLE III.—(SOLVENT: BENZENE)

Solute.	Heat of mixing (cal.).
Carbon tetrachloride . . . . .	— 2.12
Nitrobenzene . . . . .	— 7.12
Octyl alcohol . . . . .	— 21.7
Acetone . . . . .	— 28.4
Methyl heptadecylketone . . . . .	— 47.2
n-Decane . . . . .	— 8.4

$\Delta H_1$  was observed to be  $-0.91$  cal. From Table III  $\Delta H_2 = -2.12$  cal. Hence  $\Delta H_3 = \Delta H_1 - \Delta H_2 = 1.21$  cal. per 2.50 g. powder = 0.48 cal. per g. of powder. If Hess' Law holds for the process then:  $\Delta H_3 = \Delta H_{\text{CCl}_4} - \Delta H_B$  where  $\Delta H_{\text{CCl}_4}$  heat of wetting per g. by  $\text{CCl}_4$  and  $\Delta H_B$  heat of wetting per g. by benzene. From Table I  $\Delta H_{\text{CCl}_4} = 0.97$  cal. and  $\Delta H_B = 0.54$  cal., therefore  $\Delta H_{3(\text{calc.})} = 0.43$  cal. The

agreement between observed and calculated values is good considering the possible accumulative error.

### Summary.

The heats of wetting and adsorption on sodium fluoride of a number of liquids have been measured. These heats are greater for highly polar than for non-polar liquids. The heat of adsorption may be considerably influenced by the heat of mixing of the adsorbate and the solvent.

### Résumé.

Les chaleurs de mouillage et les chaleurs d'adsorption sur le fluorure de sodium pour un certain nombre de liquides ont été mesurées. Elles sont plus grandes pour des liquides fortement polaires que pour des liquides non-polaires. La chaleur d'adsorption peut être considérablement influencée par la chaleur de mélange du solvant et du corps adsorbé.

### Zusammenfassung.

Die Nässungs- und Flüssigkeitsadsorptionswärmen von Natriumfluorid sind für eine Reihe von Flüssigkeiten gemessen worden; sie sind für stark polare Flüssigkeiten grösser als für nicht-polare. Die Adsorptionswärme kann durch die Mischungswärme des Adsorbats und Lösungsmittels stark beeinflusst werden.

## THE MECHANICAL PROPERTIES OF HIGH POLYMERS.

A Lecture given by PROFESSOR H. MARK, Director of the Polymer Res. Inst., the Polytechnic Institute of Brooklyn, N.Y., before the Faraday Society at the Royal Institution in London, on 26th June, 1946.

### 1. Introduction.

High polymeric materials have received much attention by scientists and technologists during the past fifteen or twenty years. The scientific interest centres around three problems.

(1) What kind of structure must a simple organic molecule possess in order to be capable of easy polymerisation and what are the mechanisms of the various types of polycondensation and polymerisation reactions? Studies of this kind require close co-operation between organic chemists and physical chemists; they begin with the preparation of new monomers and culminate in a thorough analysis of the various steps of a polymerisation reaction.

(2) What is the adequate statistical and thermodynamical treatment of macromolecules in solution and in bulk; how do the mechanical, electrical and thermal properties of a polymer depend upon the chemical

nature of the material? Progress in this field has mainly been led by physicists and physical chemists and the fundamental outline of a statistical thermodynamics for polymers has been worked out.

(3) What are the implications of polymer behaviour for the treatment of biological problems, particularly for the properties of protein molecules? This is a highly interesting approach and it seems that a thorough analysis of the typical behaviour of long flexible chain molecules and of their mutual interaction may be capable of contributing valuable aspects to questions such as the contraction and relaxation of muscles, the permeability of animal and plant membranes and the existence of forces which act over comparatively long distances (100 Å. and more).

The great technical interest of polymer chemistry is caused by the vast number of valuable building and constructional materials of all kinds which have been produced during recent years and will, in increasing degree, be developed in the near future. Almost any branch of mechanical, electrical and aeronautical engineering depends to-day essentially upon the availability of new and improved types of rubbers, plastics and fibres, which permit the construction of better functioning elements for the various composite engines and devices. This practical industrial application of polymeric materials is being piloted by the fundamental work as mentioned under (1) and (2) and it is the purpose of this brief article to report on recent progress in this specific direction. It will, however, be attempted, at least, to mention briefly those points where a successful application of recent results of polymer research on biological problems appears to be indicated.

The two main sources for new and improved types of polymers in the last few years have mainly been the use of *new chemical systems* and the capability of producing polymeric materials possessing a better *phase texture* than before. It may therefore be appropriate to discuss these two points one after the other.

## 2. The Use of New Chemical Systems in Preparing High polymers.

Organic chemical synthesis has principally contributed to this progress, which is not at all confined to preparing a new monomer, but preparing it in a high degree of purity and at low cost. Rather spectacular progress has been achieved in this direction during the last few years.

(a) **Hydrocarbon Monomers.**—A series of new vinyl derivatives with comparatively heavy aromatic substituents, have been prepared; their polymerisation characteristics and the properties of the polymers have been studied. In general they appear to be all of the *polystyrene type*: colourless, non-crystalline (disordered), transparent resins of high softening point (in some instances up to 150° C.) with low density (around 1.1), excellent electrical properties (dielectric constants between 2.6 and 2.9; power factors around and below 0.0002) and a high resistance against acids and alkalis. It would lead too far in this comprehensive article to enumerate them all and to give a detailed account of their properties, but it seems to be worth while to give a few references about some of them. There have been investigated recently:  $\alpha$ -methylstyrene,<sup>1</sup> four isomeric di-methylstyrenes,<sup>2</sup> several other alkylated styrenes,<sup>3</sup> *as*-diphenyl-ethylene,<sup>4</sup> 2-vinylnaphthalene,<sup>5</sup> 5-vinylfluorene<sup>4</sup> and vinylanthracene.<sup>4</sup> From the point of view of co-polymerisation, these materials represent

<sup>1</sup> Hershberger *et al.*, *Ind. Eng. Chem.*, 1945, **37**, 1073.

<sup>2</sup> Marvel, Saunders and Overberger, *J. Amer. Chem. Soc.*, 1946, **68**, 1085.

<sup>3</sup> Marvel, Overberger *et al.*, *ibid.*, 1946, **68**, 736, 1088.

<sup>4</sup> Unpublished experiments in progress at the Institute of Polymer Research, Polytechnic Institute of Brooklyn, New York.

<sup>5</sup> Grimm *et al.*, lecture given at the A.C.S. Meeting in Atlantic City, 10th April, 1946.

hardening and flowpoint elevating components; they can all be activated by radical type initiating systems; most of them also seem to be susceptible to the carbonium-ion type catalysis.

A series of new dienes and trienes have been prepared and their utility in the synthetic rubber field has been studied very systematically. Whether their incorporation into three or four component co-polymers at the side of butadiene and its simple derivatives brings enough advantages to balance their relatively high cost, is a question which cannot yet be answered unambiguously.

Perhaps the most interesting new hydrocarbon monomers are the *cyclo*-polyolefines, which have been recently prepared by Reppe and his co-workers<sup>6</sup> by simple polymerisation of acetylene under moderate pressure.\* Outstanding among them is *cyclo*-octatetraene, which was prepared by Willstätter and his co-workers a long time ago<sup>7,8</sup> and which seems to be capable of polymerising in various ways to give hard transparent resins of almost saturated character or soft, rubbery products which still contain a certain degree of unsaturation.<sup>9</sup>

**(b) Monomers of the Ether, Ketone and Ester Type.**—A long series of vinyl ethers<sup>9</sup> has been prepared and the polymers have been studied; they range from soft rubbers with low brittle points (polyvinyl-*isobutyl* ether) over waxy materials (polyvinylstearyl ether) to relatively hard, colourless resins (polyvinylmethyl ether) and may well prove to be rather interesting components for many types of co-polymers.

Similarly a number of vinyl ketones have been prepared, the polymers of which are mostly resins with general characteristics similar to polymethacrylates.

Many new ester monomers have been prepared in the vinyl- and acrylic ester series. They all polymerise and co-polymerise easily and represent a very valuable arsenal of components for various types of co-polymers, which, in one extreme, are sticky adhesives, whereas, in the other extreme, they represent completely colourless plastics of high transparency and remarkable surface hardness, which are extremely interesting materials for optical uses.

An interesting sideline may be mentioned here. For many purposes it is important to impart to a polymer in its final state, as film, coating, or moulded article, a high resistance against solvents and swelling agents and a considerable degree of surface hardness. This is best achieved by a process of controlled cross-linking, in the sense that in the first phase of polymerisation, long linear (un-crosslinked) chain molecules are being produced, which are soluble, plasticisable and thermoplastic. The cross-linking reaction is supposed to set in only *after* the main form-giving process is completed. Obviously such a separation of the formation of the polymer molecules themselves and their interlocking by a cross-linking reaction can be in principle achieved, if the monomer contains two (or more) reactive (functional) groups, which react under different conditions. For instance, if a monomer contains *two double bonds*, one of which polymerises already at low temperatures, whereas the other requires higher temperatures to become activated, it is possible to build up first (under mild conditions) independent long chain molecules, which can be spun, cast, extruded or moulded and to produce later (at higher temperatures)

<sup>6</sup> Kline, *Modern Plastics*, 1946, **23**, January, February, March and April issues.

<sup>7</sup> Willstätter and Waser, *Ber.*, 1910, **43**, 1176; 1911, **44**, 3423.

<sup>8</sup> Willstätter and Heidelberger, *ibid.*, 1913, **46**, 517.

<sup>9</sup> McKinley *et al.*, lecture given at the A.C.S. Meeting in Atlantic City, 11th April 1946.

\* The method of preparation is only briefly described in a few reports issued by W. Reppe in 1944 and 1945. There existed some doubt as to whether Reppe's description actually does lead to such cyclic compounds. Recently, however, several laboratories in England and the United States succeeded in preparing *cyclo*-octatetraene under the conditions as disclosed in Dr. Reppe's reports.

a system of cross-links between them, which results in an insoluble and infusible three-dimensional network. An example for such a monomer is vinyl-allyl-ketone where the vinyl-double bond is much more reactive than the allyl-double bond. Upon co-polymerising vinylpropyl-ketone (90 %) with vinylallyl-ketone (10 %) one first obtains a linear chain vinyl polymer which can be easily handled but contains a (small) number of not yet reacted allyl-double bonds, which, however, can be activated at higher temperatures and produce the desired thermosetting resin. Other cases of similar character are vinyl-isocrotonate and allyl-methacrylate. The success of such a *double reactivity monomer* depends clearly upon the sufficient differentiation in the activation energy of the two double bonds or upon their different sensitivity against various types of activating systems. It seems that a thorough study of the reactivity of a double bond and its dependence upon its substituents should reveal how the effects of *induction* and *polarisation* are being balanced by steric hindrances and should provide a basic understanding as to how the ethylene bond can be activated or deactivated by certain substituents or by a combination of them. Quite generally, it has been found that the vinyl- and acrylic-double bonds are highly reactive, whereas the allyl-, crotyl- and cyclohexenyl-double bonds are much more difficult to activate.

**(c) Halogenated and Nitrilic Monomers.**—Rather interesting monomers have been obtained by introducing halogens and nitrile groups into various ethylenic compounds. Chloro-acrylo-nitrile and chloro-acrylic-esters give mouldable plastics of improved abrasion resistance mono-, di- and polychlorostyrenes have been rather thoroughly investigated by several workers in the field<sup>10-12</sup> and are yielding plastics of high density, high refractive index, excellent electrical properties and high heat distortion point. Chlorinated polythene (halothene<sup>13</sup> polyisobutylene<sup>14</sup> and polybutadiene<sup>14</sup> seem to be of interest for the production of water vapour impermeable, incombustible and tough films and coatings, although their ageing characteristics are still calling for substantial improvement. Other monomers, which have been prepared and the polymerisation of which is now being investigated are  $\alpha$ - and  $p$ -cyanostyrene<sup>14</sup> and cyanoacrylic esters.<sup>14</sup> In general the cyano group seems to produce strong intermolecular forces, based on polar interaction and on hydrogen bridges and therefore, favours crystallisation and lateral order.

A most spectacular polymer has been found in polytetrafluoroethylene<sup>15</sup> a material which is resistant against acids, alkalis and solvents of all kinds and has electrical properties even superior to those of polythene. It is usually obtained in films sheets or test samples, has a very smooth, fatty touch, is strongly water-repellent, and can be heated for long periods to temperatures above 300° C. without decomposing. All of these properties make it a remarkably high-temperature insulating material which is attracting great interest on the part of the electrical engineers particularly in the ultra high frequency field.

**(d) Polyesters, Polyamides and other Polycondensation Products.**—

A large number of new bi-functional and multi-functional alcohols, mercaptans, amines and carboxylic acids have been prepared and have been converted into polycondensation products. They cover the range from rather soft and tacky rubbers, such as Paracon, Paraplex, and the more recent Thiokol types, over thermoplastic and thermosetting resins, such

<sup>10</sup> Michalek and Clark, *Ind. Eng. Chem. (News Ed.)*, 25th September, 1944.

<sup>11</sup> Marvel, Overberger *et al.*, *J. Amer. Chem. Soc.*, 1946, **68**, 861.

<sup>12</sup> Styramic HT of the Monsanto Chemical Company has been disclosed to be a polydichlorostyrene.

<sup>13</sup> Cf. Thompson and Torkington, *Trans. Faraday Soc.*, 1945, **51**, 281.

<sup>14</sup> Unpublished experiments in progress at the Institute of Polymer Research, Polytechnic Institute of Brooklyn, New York.

<sup>15</sup> Renfrew and Lewis, lecture given at the A.C.S. Meeting in Atlantic City, 11th April, 1946.

as the novel soluble glyptal and alkydal modifications, the various Columbia resins and the newer types of Bakelite to certain new types of Nylon, the strength and recovery of which is even superior to that of the commercial 6-6-Nylon (polyhexamethylene-diamine-adipamate). A particularly interesting effect has been achieved by replacing a certain fraction

of the amide-bonds  $\left( \begin{array}{c} \text{H} \\ | \\ -\text{C}-\text{N}- \\ || \\ \text{O} \end{array} \right)$  in normal polyamides, by methylated amide-bonds  $\left( \begin{array}{c} \text{CH}_3 \\ | \\ -\text{C}-\text{N}- \\ || \\ \text{O} \end{array} \right)$ , which have the same strength as far as the

individual chain is concerned but which eliminate the possibility for the establishment of a hydrogen bond and, therefore, reduce very substantially the tendency for lateral chain attraction. In such a polyamide the mutual forces between the parallelised chains in the extended state of a fibre or a film are not strong enough to keep the individual chains in their ordered crystal-like state, but are liable to succumb to the random thermal motion of the chain segments. This has the consequence that a sample, if stretched and oriented, cannot maintain the extended state of low entropy after the external forces ceases to act, but relaxes into a contracted state of higher entropy against the action of the intermolecular forces, which are too weak to enforce the ordered state on the system. In this way it has been possible to produce elastic Nylons, which combine in a most remarkable way the properties of a strong and tough fibre with those of an extensible and snappy rubber.<sup>16</sup> In this connection it deserves to be mentioned that fibres exhibiting high elasticity have also been produced from vinylchloride co-polymers (Vinyon E) and from certain polyesters.

It seems that the elasticity of proteins which is so essential for many biological processes, such as muscle contraction, respiration, etc., can be reasonably well understood on the basis of limited lateral chain attraction and can be very successfully influenced by carrying out certain chemical adjustments at the various substituents along the length of a protein chain.<sup>17-19</sup> By assisting the establishment of strong lateral bonds by stretching under appropriate conditions, it has been possible to produce strong fibres out of globular proteins, which exhibit a surprising degree of crystallinity<sup>20</sup> and, therefore, a comparatively good wet strength.

**(e) Polymeric Silicon Compounds.**—An extremely interesting group of new polymers is based on monomeric silicon compounds, such as alkyl- or aryl-siliconhalides or esters. Silicon is tetravalent and may be expected to enter into many structures analogous to those encountered in carbon chemistry. The simplest is that corresponding to methane ( $\text{CH}_4$ ), namely, silane ( $\text{SiH}_4$ ). The hydrogens of silane are readily replaced by halogens, forming the various halosilanes. Virtually all of these compounds have been investigated and their properties reported in the literature. Technologically, the most important is silicon tetrachloride ( $\text{SiCl}_4$ ), produced in large quantities from ferrosilicon and chlorine, or from free silicon and chlorine. Silicon tetrachloride is highly reactive. It hydrolyses readily to the unstable orthosilicic acid,  $\text{Si}(\text{OH})_4$ , which quickly loses two moles of water to form the oxide, silica,  $\text{SiO}_2$ .

If, however, one or more of the halogens is first replaced by an organic

<sup>16</sup> Wittbecker *et al.*, lecture given at the A.C.S. Meeting in Atlantic City, 10th April, 1946.

<sup>17</sup> Croston, Evans and Smith, *Ind. Eng. Chem.*, 1945, **37**, 1194.

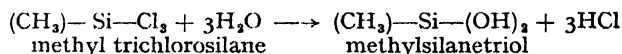
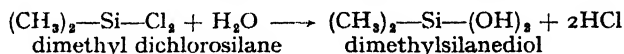
<sup>18</sup> Peterson *et al.*, *ibid.*, 1945, **37**, 492.

<sup>19</sup> Cf. also Alexander, *Colloid Chemistry*, Vol. VI (Reinhold Publishing Company, New York, 1946), pp. 1129 and 1140.

<sup>20</sup> Lundgren and O'Connell, *Ind. Eng. Chem.*, 1944, **36**, 370.



group such as the methyl radical, and then hydrolysis occurs, there results a series of compounds called silanols. For example :

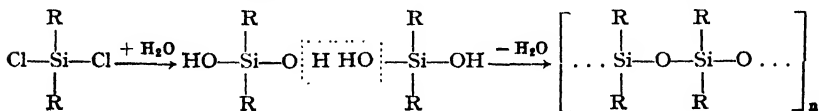


Kipping sought to isolate and to study the silicols and their reaction products.<sup>21</sup> After extracting crystalline products from the reaction mixture, attempts to determine melting points often caused changes in solubility, in physical form, and in the melting point itself. It is common to read in his work of a "lower melting" material readily converted to a "higher melting" substance, or even to an oil or gelatinous mass, merely by the heat of the melting point bath. Nevertheless, Kipping was able to prepare and characterise a considerable variety of organo-silicon compounds during forty years of research.

Beginning in 1935 in the United States, several investigators embarked upon a study of organosilicon compounds from a different point of view. They were willing to admit the difficulties of classical chemical research in this field. But their impetus was not academic; it was highly practical. Rather than aiming at isolating pure, crystalline products, they attempted to make use of the oily and gelatinous masses which had interfered so frequently with Kipping's efforts. It seemed reasonable to assume that these complex substances were condensation polymers of the silanols, which had united to form siloxane (Si—O—Si) linkages, with the loss of water. These products were termed "silicones," a classification that now includes all compounds containing the siloxane linkage, in which organic groups are bonded to the silicon by means of the C—Si bond.

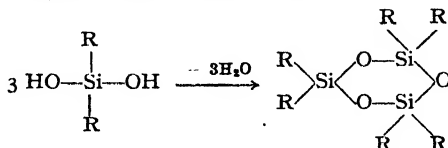
During the last few years, a large number of very able investigators<sup>22-25</sup> have developed a host of commercially valuable polymers for use as insulators, saturants, varnishes, greases, oils and elastomers, and have contributed to the chemistry as well as to the technology of these compounds.

Simple condensation of a silanediol, resulting from the hydrolysis of the corresponding dihalide, yields a linear system of siloxane linkages :



where R is a simple organic group, such as CH<sub>3</sub>, C<sub>6</sub>H<sub>5</sub> etc.

Cyclic polymers can also be formed by simple condensation of a silanediol, e.g., the cyclic trimer shown below :



<sup>21</sup> Cf. Kipping, *Proc. Roy. Soc. A*, 1938, **159**, 139.

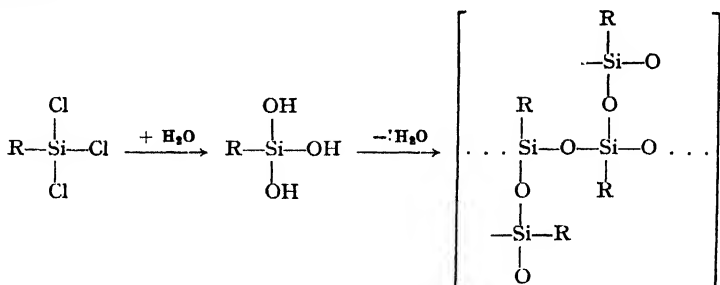
<sup>22</sup> Andrianov, *Org. Chem. Ind., U.S.S.R.*, 1941, **6**, 203.

<sup>23</sup> Hyde and de Long, *J. Amer. Chem. Soc.*, 1941, **63**, 1194.

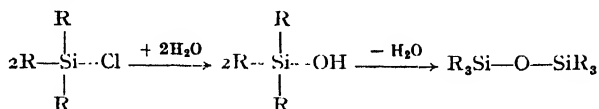
<sup>24</sup> Rochow and Gilliam, *ibid.*, 1941, **63**, 798.

<sup>25</sup> Norton, *General Electric Rev.*, 1944, **47**, 6.

Simple condensation of a silanetriol yields a highly branched siloxane network :



On the other hand, condensation of silanols can result only in the formation of the dimeric ether :



Carothers, Hill and others,<sup>26, 27</sup> have discussed the necessary conditions for the production of a linear carbon chain polymer of high molecular weight by polycondensation of bifunctional monomers. In the first place, purity is of very great importance. In the case of Nylon, for example, this demand for purity can fortunately be met by successive recrystallisation of the proper aminocarboxylic acid salts. A second factor lies in the competition between cyclisation and chain condensation. In the case of carbon compounds, only five-, six-, and seven-membered rings are formed to any appreciable extent. In the silicones, however, the formation of larger rings seems to take place much more readily than among the carbon compounds, and hence cyclisation is a more serious competitor of chain formation.

For the preparation of a linear polymer of high molecular weight, dichlorosilanes are the obvious starting materials. Traces of monohalide will decrease the attainable molecular weight. For example, the presence of 1 % (on a molar basis) of monohalide would limit the polymerisation degree to 200, even if condensation could go absolutely to completion. The "practically attainable" polymerisation degree, of course, will be much lower than 200 if 1 % of monohalide is present in the dihalide.

Presence of traces of trihalide in the dihalide will lead to branched structures and eventually to gelation. If both monohalide and trihalide are present in appreciable amounts in the dihalide, polymer structures will be obtained which are characterised by frequent cross-links between short chains.

The above considerations emphasise the important role of "monomer purity" in the production of useful polymers of this type. The high mechanical strength of rubber, cellulose, silk, and Nylon results from the long, linear, threadlike molecular chains which compose most of their total mass. A moderate number of cross-links between chains reinforces the structure and increases the mechanical strength of a given material.

At the beginning it was difficult to obtain sufficiently pure monomers to build up very long linear chain molecules, but recently both the investigators in the General Electric and in the Dow-Corning group have succeeded in producing silicones of very high molecular weight. Considering the structure of a linear methyl-, ethyl- or phenyl-silicone it

<sup>26</sup> Carothers, *Collected Papers* (Interscience Publishers, Inc., New York, 1941).

<sup>27</sup> Cf. also Alfrey, Honn and Mark, *J. Polymer Sci.*, 1946, 1, 102.

appears that each individual molecule represents a thin thread of quartz ( $\text{—Si—O—Si—O—Si—}$ ) wrapped into a molecular layer of paraffin. This combination accounts, in fact, for the two most spectacular properties of the silicones: high stability against elevated temperatures and considerable repellency against water. These two qualities together cause the silicones to be among the most interesting modern insulating materials, which allow motors, generators and transformers to run at much higher working temperatures ( $200^{\circ}\text{C.}$  and more) than is possible with the conventional resins or fabrics. Higher current densities can be used and as a consequence the efficiency of the system is very much increased. The remarkable water repellency as such suggests interesting uses in the coating of paper, fabrics and leather. Using the above-mentioned principle of cross-linking with the aid of small amounts of trichloroalkylsilanes one has succeeded in producing elastomers on the silicon basis, which excel because of the fact that they possess a very wide range of rubberiness. Silicone rubbers maintain their elasticity and flexibility down to temperatures of  $-80^{\circ}\text{C.}$  and are still resistant to permanent deformation and chemical deterioration at  $250^{\circ}\text{C.}$  and more. The presence of long chains with rather limited internal flexibility and with very small mutual interaction creates rheological conditions, which are most unusual for normal organic polymers, but have already been observed with swollen silica gels and have been called *dilatancy*,<sup>28-30</sup> A particularly spectacular case for this behaviour is a moderately cross-linked dimethylsilicone which contains an inorganic filler and is known as "bouncing puddy". This material yields easily, so long as the deformation can take place slowly, but reacts like a rigid elastic body towards rapid and sudden impacts or shocks. Considering the relatively limited period (about ten years) during which silicones have been prepared and investigated, it seems entirely probable that many interesting and useful materials will emerge from further studies of these peculiar polymers.

### 3. Phase Changes in Polymeric Systems.

Let us now suppose that for some good reasons a chemist or a company has decided to use a given chemical material, such as cellulose acetate or Nylon. Is there still a chance left to vary the mechanical properties of fibres, films or moulded pieces of such a given material, thereby making it possible, at least to a certain degree, to adjust the properties of the final samples to some given specifications? Experience has, in fact, shown for a long time that, out of the same polymer, samples with very different mechanical properties can be made depending upon the *state of order* in which the polymer is brought in the course of the various processing steps, such as spinning, casting, drawing, extruding, moulding, etc. We are faced here with an *organic chemical metallurgy and metallography* in which the characteristic features of the *condensed state* are *superimposed* over the *fundamental chemical properties*. Therefore, the question arises: do we know what connections exist between the principal structural features of a given polymer and the mechanical properties of samples made from it? Such knowledge, if it exists, obviously would be of great value in designing polymers for special purposes and in improving their properties. A fair answer to this question seems to be that we have no well-developed mathematical theory which connects *quantitatively* the structure of a given polymer with its properties, but we do know a number of general rules and principles which correlate properties and structures and which have been helpful in many cases in obtaining materials with superior properties.

<sup>28</sup> Reynolds, *Phil. Mag.*, 1885, 20, 469.

<sup>29</sup> Cf. Fischer and Gans in J. Alexander, *Colloid Chemistry*, Vol. VI, p. 287.

<sup>30</sup> See also Green and Weltman in *ibid.*, Vol. VI, p. 332.

There are, as already mentioned, two main factors that influence the ultimate behaviour of a polymer: (i) the structural configuration of the long chain molecules themselves; and (ii) the way in which these molecules are arranged in the sample of the polymer. The same distinction can also be expressed in a somewhat briefer form in terms of (i) the chemical structure of the molecules and (ii) the physical texture of the macroscopic sample. We shall now attempt to discuss these two factors in order.

### Details of Chain Structure and Mechanical Properties of Polymers.

Let us first enumerate the most important structural details of high polymer molecules and briefly report our present knowledge on their significance for the mechanical properties of polymers. There are, first of all, the average molecular weight and the average D.P.\* of the substance, which according to Table I, vary from 20,000 to 1,000,000 and from 100 to 5000, respectively. There is the molecular weight distribution, which describes the heterogeneity of the material and is comparatively narrow in some cases and fairly wide in others, and there is the internal flexibility of the individual chains, which is a consequence of the chemical nature of the bonds between the monomers.

The connection between mechanical properties and average D.P. has been frequently investigated.<sup>31, 32</sup> The general result is that, in order to obtain mechanical strength at all, a certain minimum D.P. which ranges between 40 and 80 is necessary. As soon as this critical value is exceeded, the material starts to exhibit mechanical strength and its ultimate tensile strength increases from now on continually with the average D.P. It was found that up to a D.P. between 40 and 80 the tensile strength of a film cast from this material is negligible and that it then increases about in proportion to the chain length. The proportionality between mechanical strength and D.P. holds up to a D.P. of about 250. Then the curve bends, and after a D.P. of about 600 is reached, the mechanical properties depend but moderately upon D.P.

While the influence of the average D.P. on the mechanical strength is fairly well established, the significance of the molecular weight distribution is still an unsolved problem. Promising attempts have been made recently to establish a connection between the distribution curve and the mechanical properties of high polymers; it is found that relatively small amounts (between 10 and 15 % by weight) of constituents having a D.P. below 150 are detrimental for such mechanical properties as tensile strength, resistance to flexing, fatigue performance, and so forth. Removal of such constituents of low molecular weight improves the material considerably.<sup>33</sup>

Let us next consider the internal flexibility of the individual molecules. It is a well-established fact that each atom in a small molecule carries out rapid vibrations, the energy of which represents the main part of the heat content of a solid (crystallised) material and can be studied by the molecular spectrum (ultraviolet, infra-red, Raman) and the temperature dependence of the thermal capacity. In larger molecules, such as the polymers listed in Table I, there exist, in addition to these rapid vibrations of the individual atoms, comparatively slow vibrational and rotational movements of certain parts or segments of a large molecule. This does not imply that the rotation about the single C—C bond is actually free. In fact, recent investigations have shown that, owing to the mutual interaction of the substituents, subsequent CH<sub>2</sub> groups in a long chain paraffin

<sup>31</sup> Sookne and Harris, *Ind. Eng. Chem.*, 1945, **37**, 475.

<sup>32</sup> Mark in E. Ott, *Chemistry of Cellulose and Its Derivatives* (Interscience Publishers, Inc., New York, 1944), p. 990.

<sup>33</sup> Mark, *Paper Trade J.* 1941, **113**, 34.

\* D.P.: Degree of polymerisation.

molecule cannot rotate freely about the connecting bond. However, vibrational movements within angles of about  $10^\circ$  are much less inhibited, and as a consequence a chain of many  $\text{CH}_2$  groups—say a thousand or more—will exhibit as a whole a considerable degree of internal flexibility. There are no sharp bends to be expected within the range of a few  $\text{CH}_2$  groups but the chain as a whole will be capable of assuming a large number of slightly curved or coiled geometric configurations, and the probability of finding such a large molecule in its most extended state is extremely small. If an isolated long chain molecule is brought into this state of extreme elongation by external forces (mechanical stretching), it has the tendency, under the influence of its random thermal motions, to return to the most probable configuration, which is characterised by a certain degree of folding and curling. This represents a tendency of the long chain to contract if it is once extended.

The *rate* at which it contracts, however, will not depend upon how much more probable the final (contracted) configuration is than the

TABLE I.—MOLECULAR WEIGHTS AND DEGREE OF POLYMERISATION OF SOME REPRESENTATIVE POLYMERS.

Material.	Elements.	Molecular Weight.	Degree of Polymerisation.
Cellulose in native cotton	C, H, O	<i>ca.</i> 1,600,000	<i>ca.</i> 10,000
Cellulose in wood pulp .	C, H, O	<i>ca.</i> 500,000	<i>ca.</i> 3000
Cellulose in rayon .	C, H, O	80,000-160,000	500-1000
Cellulose acetate in rayon	C, H, O	80,000-140,000	300-500
Cellulose acetate in film .	C, H, O	100,000-160,000	400-600
Native rubber . . .	C, H	200,000-400,000	3000-6000
Buna-S . . .	C, H	100,000-150,000	1500-2000
Polyvinyl chloride (Geon)	C, H, Cl	100,000-200,000	1500-3000
Polyvinylidene chloride			
(Saran) . . .	C, H, Cl	100,000-300,000	1000-3000
Polyvinyl chloride acetate	C, H, O, Cl	100,000-200,000	1500-3000
(Vinylite) . . .			
Polystyrene . . .	C, H	100,000-300,000	1000-3000
Polymethylmethacrylate	C, H, O	100,000-200,000	800-1600
(Lucite) . . .			
Protein in native silk .	C, H, O, N	<i>ca.</i> 150,000	2500
Polyamides (Nylon) .	C, H, O, N	<i>ca.</i> 25,000	250

original (extended), but upon how fast the chain-like molecule can pass from the extended into the curled-up state, which in turn will depend upon how quickly the individual segments of the molecule can swing from one geometric position to another that is separated from the first by a certain energy barrier. Thus, the rate of contraction of a polymer is a matter of the rate of chain segment diffusion in the face of energy barriers that separate the possible positions of the individual chain segments from one another. In an isolated long-chain molecule these barriers depend upon how much the free rotation about the consecutive bonds in the chain is hindered, either by the intrinsic rigidity of the bond or by the mutual interaction of substituents. It must be added that in an actual piece of rubber there are no *isolated* chain molecules, but a condensed multitude of them in a state of irregular entanglement, attracting each other with intermolecular (van der Waals) forces. This mutual interaction also contributes to the hindrance of the free mobility of the individual molecules and their segments and hence affects the rate of contraction of the material.

There is another aspect of the hindered internal flexibility of the molecules in a polymer. The reason for this hindrance is the existence

of energy barriers which have to be overcome as the segments move into less and less geometrically biased positions. Each elementary step of recovery, therefore, requires a certain activation energy, which is responsible for the influence of temperature on the rate of segment diffusion and hence on the rate of recovery. If the energy barriers over which the segments have to go are high, it will, at low temperature, become more and more difficult for an individual segment to acquire this energy and the rate of recovery will be considerably reduced. This means that the material will be slow in adapting itself (by segment movement) to the external stress, and hence it may develop brittleness.

Thus we may conclude that the intrinsic flexibility of the individual chains is of great importance for the mechanical characteristics of elastomers and affects mainly the rate of recovery from the extended state and its temperature dependence, particularly the point at which the material begins to exhibit brittleness.

It may be added here that the chemical nature of a given polymer is of great importance for its chemical reactivity, swelling, and solubility. Thus polyhydrocarbons, such as natural rubber, polystyrene, polyisobutylene, and so forth, are very resistant to acids and alkalis, and do not absorb water, but eventually swell and dissolve in hydrocarbons and other typically organic solvents. Polymers containing many hydroxyl groups, such as cellulose or polyvinyl alcohol, are in turn very resistant to the action of organic solvents but absorb moisture and eventually even dissolve in water or in weak alkali. It seems, however, that the mechanical properties of polymers depend not so much upon whether the monomer is a hydrocarbon, an ester, a sugar, or an alcohol, but rather upon the chemical characteristics as embodied in the molecular chain structure and expressed by average D.P., D.P. distribution and internal flexibility of the chain molecules. In fact, Table I shows that fairly strong fibres can be made from materials that are very different chemically.

After having now briefly discussed how the structural details of the individual chains affect the mechanical properties of a polymer, let us pass to the importance of the mutual arrangements of the chain molecules in a sample.

### **Arrangement of the Chain Molecules and Mechanical Properties of Polymers.**

It may be worth while to consider very briefly the behaviour of an ordinary organic substance. At the freezing temperature a liquid of low molecular weight, such as benzene, toluene or isoprene, undergoes a very distinct change in mechanical properties within a narrow temperature range. Below the freezing temperature ordinary substances are crystalline solids; they respond to shearing stress by undergoing small (1 % or less) predominantly reversible deformations and exhibit the long range order (100 Å. or more) of a three-dimensional crystal lattice. Each molecule is held by attractive and repulsive forces of all surrounding particles in a relatively well-defined equilibrium position, about which it performs rapid, quasi-harmonic vibrations. Transition of an individual molecule from one equilibrium position to another (self-diffusion) is extremely infrequent, the average amplitude of the vibrations amounting only to about 5 % of the distance between adjacent equilibrium positions. Such systems appear to us as rigid, hard substances, having a definite shape and all other characteristics of a solid body.

As the temperature is increased, the vibrations of the individual particles become more and more vigorous until, at the melting temperature, the forces between the constituents of the lattice can no longer maintain the long range order of the crystal, and the whole structure breaks down. The result is a liquid, characterised by the absence of any far-reaching geometric order. The nearest neighbours of any individual molecule,

it is true, are arranged about the latter in much the same manner as in the crystalline state, but molecules a few Angstroms farther away are distributed practically at random. Each single particle, again, carries out rapid quasi-elastic vibrations about an equilibrium position; but this equilibrium position itself (being a position of minimum potential energy) is not fixed in its location and the molecule undergoes, in addition to vibrations, an irregular translational Brownian movement, which makes it change its place rather frequently—self-diffusion is rapid. The lack of long range order prevents a liquid from sustaining shear or stress and from assuming a definite shape; it flows. Eyring, Lennard-Jones and their co-workers have succeeded in giving a very satisfactory explanation of many important properties of liquids on the basis of this picture.

A liquid can be undercooled below its equilibrium melting temperature, thus retaining the characteristics of its disordered (amorphous) geometric structure. The coefficient of viscosity  $\eta$  decreases with increasing temperature, roughly following an exponential relationship,

$$\eta = A e^{B/T}$$

where  $A$  and  $B$  are constants and  $T$  is the temperature, and at a sufficiently low temperature the material becomes hard and brittle; it is then called a glass. The transition from rigid glass to viscous liquid frequently occurs in a relatively narrow temperature range (the softening point) with no sudden change in structure and with no discontinuity in the primary thermodynamic variables, such as heat content, free energy and specific volume. Thus in the case of ordinary (low molecular weight) organic substances, the relationship between the crystalline, glassy and liquid states can be represented by the scheme of Table II.

TABLE II.—COMPARISON OF THE VARIOUS STATES IN WHICH ORDINARY ORGANIC SUBSTANCES CAN EXIST.

State.	Extent of Geometric Order.	Viscosity.
Crystalline . .	Long range (more than 1000 Å.)	High
Glassy . .	Short range (only a few Å.)	High
Liquid . .	Short range (only a few Å.)	Local viscosity low

High polymers consisting of long chain molecules exhibit a more complicated behaviour. The strong chemical bonds inside the individual chains are seldom, if ever, severed during the normal mechanical deformation of the polymer, such as stretching of rubber or spinning of Nylon, or during the various thermal treatments, such as annealing or moulding. The changes in shape which take place during these processes occur at the expense of opened (and reclosed) bonds between the individual chains, which are not due to chemical forces, but to the various types of intermolecular interaction, such as hydrogen bridges and van der Waals forces.

Let us, from this point of view, compare the crystal lattice of isoprene with that of stretched (or frozen) rubber and consider what happens if the temperature of both systems is increased. In frozen isoprene, each individual molecule ( $C_5H_8$ ) is located in a definite equilibrium position, about which it undergoes irregular, quasi-harmonic vibrations. The distance between any one molecule and its next neighbour is about 4 to 5 Å., while the interatomic distances within the molecule are only 1.0 to 1.5 Å. This elucidates the fact that the  $C_5H_8$  molecule is held together by strong chemical bonds, having dissociation energies of 70 kcal./mole, or more, so that it forms a well-defined unit in the lattice, while the forces

between the molecules are of the much weaker, van der Waals type (about 5 to 8 kcal./mole.). Nevertheless, below the melting temperature, the bonds between molecules suffice to maintain the long range order of a crystal lattice, and frozen isoprene is a hard, rigid substance. Above the melting temperature; however, all long range connections between the molecules disappear and the result is a liquid with rapid self-diffusion of the individual molecule and small coefficient of viscosity (about  $10^{-2}$  poise).

In frozen rubber, each individual isoprene residue ( $C_5H_8$ ) as well as each C and H atom within it, vibrates about a definite equilibrium position; but a thorough investigation of the lattice shows that each isoprene residue is particularly close to two other residues, indicating that long linear chains of residues exist, within which all next-neighbour distances correspond to strong chemical bonds. The main valence chains of isoprene extend parallel to the direction of the stress have a length of several thousand monomers and represent the backbone of the whole structure. In all directions perpendicular to the axes of the chains the distances between adjacent molecules are determined by normal van der Waals forces. This lattice therefore is highly anisotropic with strong forces along the parallelised chains and weak forces perpendicular to them. As the temperature is increased the weak intermolecular bonds gradually are severed and thus the lateral arrangement of the chains is disturbed and eventually destroyed. The chains start rotating about their axes, changing their mutual distances and eventually curling and coiling up in an irregular way. However, while the weak bonds between the individual chain molecules are opened the strong (chemical) linkages within them remain unaffected. The molecules are not degraded at temperatures at which the lattice structure has already broken down. This has the important consequence that although the long range geometric order of the lattice disappears upon raising the temperature to the softening point a long range entanglement due to the unaltered existence of the long chain molecules is maintained. This long range entanglement is responsible for the fact that at the softening point of a polymer, we get not a liquid, but a rubbery solid.

An individual isoprene residue in (amorphous) unstretched rubber vibrates with about the same intensity as does an isoprene molecule at the same temperature in liquid isoprene, and it will also carry out about the same short range Brownian movement; but, owing to its position in the chain molecule, it will not be able to diffuse farther away from its original positions without affecting other parts of the chain to which it belongs. This geometric restriction of the various segments of the flexible linear macromolecules due to the strong bonds between them produces a long range entanglement, which enables the material to sustain moderate stresses of shears, hence to maintain a certain definite volume and shape and resist elastically any attempt of deformation. In this sense rubbers have a state between the solid and liquid, just as glasses do, and one may say that glasses are liquids with high viscosity, whereas rubbers are liquids with long-range entanglements (see Table III). The self-diffusion of chain segments is not essentially affected by the long range entanglement and, therefore, is rapid, whereas any displacement of the large linear molecules as a whole, is impeded by their mutual interaction over long ranges and therefore is very slow. The irregular motion of portions of the chains under the influence of the temperature has been termed, by Kuhn<sup>24</sup> internal, or micro-Brownian movement; the displacement of the macromolecules as a whole is referred to as external, or macro-Brownian movement.<sup>25</sup>

Using these terms, we can say briefly (and with a certain degree of oversimplification) that rubbers are materials that have rapid internal,

<sup>24</sup> Kuhn, *Kolloid Z.*, 1936, 76, 258.

<sup>25</sup> Cf. also, Mark, *Amer. J. Physics*, 1945, 13, 207.



TABLE III.—TRANSITION POINTS FOR ORDINARY SUBSTANCES AND HIGH POLYMERS.

**(a) Behaviour of Ordinary Substances :***Melting Point.*

Long range molecular order No Brownian motion Sustains external forces ; exhibits short range, high modulus elasticity	Short range molecular order Rapid Brownian motion Does not sustain external forces flows and has low viscosity
--	--

**(b) Behaviour of Polymers :***Brittle Point.**Flow Point.*

Solid State.	Rubbery State.	Liquid State.
Long range molecular order	Short range molecular order, but long range entanglement	Short range molecular order
Both Brownian movements are frozen in	Internal Brownian motion rapid ; external Brownian motion still frozen in	Both Brownian motions are activated
Sustains external forces ; exhibits short range, high modulus elasticity	Sustains external forces ; exhibits long range, low modulus elasticity	Does not sustain external forces ; flows and has medium viscosity

but slow external Brownian movement. It is this combination that characterises the rubbery state.

**Significance of the Two Different Brownian Movements.**

Let us first consider for which essential feature of rubberiness the two types of Brownian or molecular motion are responsible. If we start stretching a rubber, we expect it to begin deforming at comparatively low stresses ; it is supposed to be a soft, extensible material, having a small initial Young's modulus. For typical elastics (soft rubbers or gum stocks), Young's modulus is between  $10^6$  and  $10^7$  dyne/cm.<sup>2</sup> (15 to 150 lb./in.<sup>2</sup>). If a material is to extend appreciably under the influence of such small stresses, it needs a considerable degree of internal mobility, much like a normal liquid. In fact, rubbers have many properties in common with ordinary liquids. They possess a compressibility very similar to that of liquids. Poisson's ratio for all "soft" elastics is in the neighbourhood of 0.50 ; the thermal expansivity of rubber is of the same order of magnitude as that of ordinary liquids, and (perhaps most surprising) the solubility of gases (hydrogen, oxygen, etc.) and solids (sulphur, selenium, etc.) in rubbers resembles rather closely the solubility of the same materials in ordinary liquids. The "local" fluidity of elastics produced by the fast internal Brownian motion is also responsible for this rapid contraction. In a stretched rubber certain segments of the individual chains assume configurations the free energy of which is larger than in the unstretched condition. Therefore, as soon as the external force ceases to act, these portions will start to diffuse back into their unstrained (equilibrium) positions, which correspond to a minimum free energy and represent the relaxed state of the sample. How quickly this contraction takes place depends upon the rate of segment diffusion, which determines the "local" fluidity of the material.

Certain materials "snap" back into their original shape, because segment motion is fast ; others "creep" back, because the local mutual

interaction of the chain segments is strong and prevents them from assuming their unstrained positions with a short time. Natural rubber, Neoprene, Butyl-rubber and the Buna types are examples of the first case; polystyrene above  $80^{\circ}\text{C.}$ , Vinylites and moist polyvinyl alcohol, of the other. In order to get a good, snappy elastic, one has to keep the internal Brownian motion as rapid as possible, which means that one has to accentuate the local liquid character of the system.

On the other hand, if we provide in an elastomer for *nothing* but this high local fluidity and keep a macroscopic sample of the material under stress for a certain length of time, the material will *flow*. It will not sustain the imposed stress or shear, but, with the very aid of the rapid internal Brownian motion, will relax into the extended state instead of into the contracted. Hence it will behave like a viscous liquid or plastic rather than like a rubber. To prevent this permanent loss of shape, one has to provide for *strong long-range entanglement*, which makes the external Brownian movement (slipping of whole chains along one another) so slow that it cannot produce any appreciable permanent set within the time the sample is in its extended state. In general, the mutual attraction of the chain by van der Waals forces alone does not provide for a sufficiently stable long-range entanglement to conform with practical requirements. Therefore, one usually produces a system of irregularly distributed, widely spaced fix points. They provide a stable, but highly deformable network throughout the sample, which can be stretched several hundred per cent. and will return to its original shape, because its individual knots are connected with one another by flexible chain molecules. Such fix points can be made in different ways. One way is to produce strictly localised, strong chemical bonds between the individual chains, such as sulphur, oxygen, or methylene bridges, as is presumably done during the various processes of curing and vulcanising. Another way is to have groups of particularly strong molecular interaction (hydrogen bonds, strong dipoles, highly polarisable groups) or of great bulkiness (phenyl, benzyl or naphthyl groups) randomly and in large distances distributed along the chains, thus producing an irregular network of areas with high molecular cohesion. Still another method is to distribute very small particles with high adsorption power (active fillers) in the polymer, which provide for fix points by adsorbing parts of the mobile chains irreversibly on their active surfaces. If a rubber crystallises upon stretching, the areas of crystallisation themselves act like strong cross-links between the individual chains.

In all these cases, the localized and infrequent strong links between the individual flexible chains suppress the external Brownian movement sufficiently to prevent permanent flow of the sample as a whole, while they leave the internal Brownian movement sufficiently unaffected to allow rapid extension and contraction to be possible.

This discussion shows that a polymer can exist not in two but in *three condensed states*: the *solid*, the *rubbery* and the *liquid*. In the solid state (crystal or glass) *both* Brownian movements are *frozen in*; in the *rubbery* state the *internal* Brownian motion is *activated* while the *external* Brownian movement is still *frozen in*; and finally, in the *liquid* state of a polymer (in the melt or in a highly swollen sample) *both* Brownian movements are *activated*. Under the influence of an external force the solid state exhibits only short range, high modulus elasticity, the rubbery state possesses long range, low modulus elasticity, whereas the liquid state provides for flow. An ordinary organic substance has only two condensed states, the solid and the liquid; there exists only one type of Brownian motion, which is activated in the latter and frozen in the former state. These two phases, solid and liquid, are in equilibrium with each other at the freezing (or melting) temperature. In the case of polymers there are two characteristic temperatures (or temperature ranges): the *brittle temperature*, which separates the solid from the rubbery state, and the *flow*

*temperature*, which separates the latter from the liquid. Table III attempts to give a schematic picture of this situation.

Considering the facts as discussed in the preceding section, it becomes clear that, in order to produce a polymer for practical purposes, one has to synthesise chain molecules with a D.P. around or above 1000, having a certain degree of internal flexibility. This material has then to be brought into the proper physical state or mixture of states. And here we realise that we have at our disposal three different phases: the *solid*, the *rubbery* and the *liquid*. The task of bringing the polymer into the best physical state is similar to that of a metallurgist, who attempts to find the best properties of his alloy in the phase diagram of his system, with the difference that this organic chemical "metallurgy" puts one more state at his disposal, namely, the rubbery. This is because of the presence of the long chain molecules.

It is now obvious that, if the desire is to produce a strong and resilient fibre, one will have to accentuate the solid crystalline state in order to get stiffness and tenacity and will have to provide for only as much rubberiness as will give a sufficient resiliency. Any liquid constituent in such a fibre would be unwelcome because of the permanent set to which it leads under prolonged external stress. If one aims at the production of a typical rubber, it will be necessary to have the bulk of the material in the rubbery state, with perhaps some crystalline domains in order to provide for a sufficiently strong fix-point system. Finally, in producing a plastic, one will have to provide for an appropriate mixture of solid and liquid material with as little rubberiness as possible in order to guarantee smooth extruding, casting or moulding without recovery after the desired shape has been obtained.

In this sense it can be said that fibres, plastics and rubbers are not intrinsically different materials: they are merely different combinations of three fundamental states in which organic high polymers can appear; and there exists, obviously, a continuous range of systems, starting with extreme fibre properties and ending with extreme rubber qualities, depending essentially upon the degree to which the solid, rubbery and liquid state are represented in the sample.

Hence, there are two independent ways to arrive at new polymers with novel and interesting mechanical properties: (i) to prepare chemically new monomers and produce long chain molecules of them with a high D.P. and a favourable molecular weight distribution, and (ii) to bring these substances into the proper physical state by adjusting the proportions of these solid, rubbery and liquid constituents such that they incorporate to the best degree the desired properties. Along both lines a large number of research chemists and physicists are active, and there can be little doubt that their work will lead to an ever-increasing number of new materials with valuable and surprising properties.

### Résumé.

Les différents systèmes chimiques employés dans la préparation des hauts polymères—dérivés du silicium inclus—sont ici classés et brièvement passés en revue. L'influence de la structure chimique des molécules et de la texture physique de l'échantillon macroscopique sur le comportement ultime du polymère est discutée sous l'angle de la configuration des molécules, de leur arrangement dans la chaîne et des mouvements browniens interne et externe.

### Zusammenfassung.

Die verschiedenen chemischen Systeme, die zur Darstellung hochpolymerer Substanzen Verwendung finden, darunter Siliziumverbindungen, werden klassifiziert und kurz besprochen. Die Beziehung zwischen der chemischen Struktur und makroskopischen physikalischen Textur einerseits und dem allgemeinen Verhalten der polymeren Substanz andererseits wird auf Basis der Kettenstruktur, Anordnung der Kettenmoleküle und der internen und externen Brownschen Bewegung erörtert.

## REVIEWS OF BOOKS

**A First Course in Mathematical Statistics.** By C. E. WEATHERBURN.  
(Cambridge University Press, 1946.) Pp. xii + 271. Price 15s.

Here is a book that provides the explanations, and proofs, of the fundamental laws of mathematical statistics. It is called first course, and it certainly requires very little preliminary mathematical knowledge other than simple calculus. But it differs from most of the "first courses" known to the reviewer in that it really is up-to-date. The discussion does not keep centred, almost exclusively, on the so-called normal distribution—which is neither so normal nor so interesting as many of the older text-books would have us believe—thus, for example, beta and gamma variates are introduced quite early, and the moment generating function is used almost from the start. In this way we obtain a general perspective in the subject.

Nothing could make the up-to-date character of the book clearer than to say that, after dealing with individual distributions of various types, the discussion covers the theory of correlation, rank correlation, the chi-squared test, and finally leads to an introduction to the very important theory of the analysis of variance. These latter topics are now so rooted in the daily experience of statisticians that it is good to see them expounded so clearly.

Prof. Weatherburn has already shown in other books that he can write simply and intelligibly. The present book is no exception, and might be termed a really good text-book at a very moderate price. That is to say, a person would not look here to find what particular technique he should adopt in dealing with some particular problem that has arisen (he would find that sort of thing in the works of Fisher to which reference is often made); but he would find the explanation of the technique, and the reason why it gives correct conclusions.

The book is excellently printed, as befits the Cambridge University Press, and each chapter has a bunch of interesting and relevant examples.  
C. A. C.

**Calculating Machines.** By HARTREE. (Cambridge University Press.)  
Pp. 40. Price 2s. net.

It is a significant sign of the changed emphasis of modern applied mathematics that when Professor Hartree delivers his inaugural lecture, following the late R. H. Fowler in the Plummer Chair at Cambridge, he should give it the title, "Calculating Machines, recent and prospective developments". But here, in this little book of 40 pages, are the reactions of an experienced mathematician (or theoretical physicist, or theoretical chemist: choose whichever you will) to the astonishing new machines which have been developed in America for numerical computation. It is singularly fitting that Hartree should describe these new tools, for he alone in Britain has actually used the magnificent ENIAC machine (Electronic Numerical Integrator and Computer) which was built at Pennsylvania during the war, and can speak with authority of the changed

outlook in applied mathematics that must inevitably result from its use. It is thrilling to read his account of this machine which employs 18,000 valves to perform a million separate multiplications in an hour, and which, because it is 1000 times as fast as any other kind of calculating machine, can compress 16 hours of work into 4 minutes. But perhaps more interesting still are his reflections concerning the back-reaction of this potentiality on the development of the very processes that it uses. For this is not a case where a man, or a theory suggests a machine; rather is it a case where the machine itself dictates in what form certain problems must be cast, and drives the theoretician into detailed study of certain techniques. Professor Hartree supports this thesis with several apt illustrations. For example, if he is right, then when we are confronted with the need to solve a set of simultaneous linear equations, our minds will in future instinctively turn from the conventional method of solution by determinants to the equivalent minimisation of an associated quadratic form. Those who read this lecture (and there will be many) will wonder somewhat fearfully whether scientific man is being driven by the Frankenstein, or "electronic brain", that he has created. If they do so, let them take courage from these words culled from the lecture itself—"use of a machine is no substitute for the thought of organizing the computations, only for the labour of carrying them out". There is still hope for most of us!

C. A. C.

**Achievements in Optics.** By A. BOUWERS. (Monographs on the Progress of Research in Holland.) (Elsevier Publishing Co. Inc., New York and Amsterdam, 1946.) Pp. 135, with 64 illustrations. Price 26s.

Scientists in the Netherlands have always contributed generously to the world's knowledge. During the war years, their activity must indeed have been remarkable: the series of manuals—of which this is the first—now appearing in this country are a testimony alike to exceptional analytical and experimental ability combined with doggedness of purpose. Preparation for publication went on in spite of such international activities being very much *verboden* during the German occupation.

Broadly, these "achievements" fall into four classes—(1) new optical systems, (2) new optical instruments, (3) geometrical optics, (4) physical optics. In every case, there are some noteworthy improvements. Perhaps the most outstanding features are the construction of a microscope using mirrors in place of lenses for the objective, and the establishment of a practical means of obtaining phase contrast in optical systems. In the latter case particularly, long and detailed research was involved before the necessary instrumentation was complete. The outcome is a Reichert 0.65 objective fitted with a phase plate and a Koristka 1.30 apochromat containing a phase ring in the cement layer of the third component. Illustrations, using both positive and negative phase contrast, show vapourised shellac at a magnification of  $\times 370$ , and chromosomes at  $\times 2200$ . The power of structure-differentiation is immediately apparent. Combined with the interest in phase contrast for opaque substances now being stimulated in England, these advances are likely to become of considerable

power. In general, such researches are yet another example of the capacity of classical physics to produce new results which are both elegant and useful. A final point concerns the phraseology: here and there are sentences which are slightly obscure, or which only convey their intended meaning after a second attempt on the reader's part. This might be rectified in any future edition: considering the difficulties of language, the authors have done their work well.

F. I. G. R.

**Piezoelectricity. An Introduction to the Theory and Applications of Electromechanical Phenomena in Crystals.** By WALTER GUYTON CADY. (International Series in Pure and Applied Physics. McGraw-Hill Book Co., Inc., New York and London, 1946.) Pp. 806 + 168 Fig. Price \$9.00.

The electrical polarisation of crystals brought about by thermal or mechanical means has been known for a long time. Many centuries ago oriental merchants were familiar with the peculiarity of tourmaline, "the Ceylon magnet," which, when heated, exerted forces of interaction on other bodies. Aepinus explained this in 1750, when he showed that opposite charges of electricity are developed at the two ends of a heated tourmaline crystal; the so-called pyroelectric effect. The discovery of electrical polarisation produced by mechanical pressure we owe to the brothers Curie in 1880. They observed the piezoelectric effect in a number of crystals including those which subsequently found most practical use, quartz and Rochelle salt. Several million quartz oscillator plates were used during the war for radio frequency stabilisation, and the peacetime uses of quartz and other piezoelectric crystals are firmly established. Thus it is evident that the subject of piezoelectricity is of great practical as well as fundamental interest.

In his book Prof. Cady wisely begins with a recapitulation of crystal symmetry applied to elastic and electrical properties. Voigt's theory of piezoelectricity is stated for the twenty crystal classes which can show the effect, and also for certain specific crystals. Account is taken of the variation of crystal properties with rotation of the orthogonal axes of reference, and considerations affecting the choice of crystal cut for practical measurements are discussed. Alternative formulations of piezoelectric theory and secondary effects are given due prominence. Then follows a full treatment of the piezoelectric resonator and oscillator including their equivalent electrical circuits, and special attention is paid to the technology of quartz. The latter half of the book deals with a fascinating aspect of piezoelectricity: Rochelle salt and related materials have abnormally high dielectric constants, with correspondingly large piezoelectric effects, in certain temperature regions. The polarisation-field characteristics are non-linear and show dielectric hysteresis, so that by analogy with ferromagnetism these materials are called ferroelectrics. Their study and the theories which have been advanced to explain their behaviour are rightly given much emphasis. The book concludes with miscellaneous applications of piezoelectricity, pyroelectric and piezo-optic theories, piezoelectricity and atomic theory, and a useful appendix on ferromagnetism.

There are comprehensible bibliographies and the practical-minded will appreciate the numerous tables and charts. The specialist will remember Prof. Cady's distinguished pioneer work on piezoelectricity and will acknowledge his competence to give a critical account of a subject which is not free from controversy. The reader interested in the explanation of piezoelectricity in terms of atomic theory may be disappointed that Prof. Cady has had to treat this aspect rather sparingly; it is apparent that herein lies scope for future research.

The binding and presentation of the book are of the high standard characteristic of the International Series, and there appear to be few misprints. There are so few books on crystal physics that any new addition is very welcome, and there is no doubt that Prof. Cady has given us a valuable book.

L. A. T.

**Thermodynamics for Chemists.** By SAMUEL GLASSTONE. (D. van Nostrand Co. Inc., New York, 1947). Pp. viii + 522. Price 28s.

Bacon in his "Of Studies" wrote: "Some books are to be tasted, others to be swallowed and some few to be chewed and digested; that is, some books are to be read in parts; others to be read but not curiously; and some few to be read wholly and with diligence and attention." *Thermodynamics for Chemists* should be placed in the first, rather than in the last, of these categories. It has many features that many of its readers will welcome in an introductory treatise on this subject; thus more than 100 numerical problems are worked out in the text and nearly 400 more appear as exercises for the student (who will regret the absence of answers!); many of these have been taken straight from the literature. In keeping, there is an emphasis on the practical value of the subject and its use in yielding results: this provides an air of reality and utility which is often missing in many treatments. Regretfully, and perhaps of necessity, the development of principles has suffered; the purist will condemn, where the utilitarian will praise. It has been recently stated that there is a surprisingly small number of chemists and physicists who have a thorough grasp of thermodynamics; it is predicted that there will be few new members to this group if the emphasis, as in this book, is more associated with the ability to juggle with symbols in accordance with certain rules than with concept and principle.

There is, we believe, no need of a detailed picture of the contents since most prospective readers will no doubt be acquainted with at least one of the author's publications—the present volume follows the general pattern and much of the ground has been covered less fully in his monumental work. One may note that the symbols and nomenclature are those adopted by the *J. Amer. Chem. Soc.*; the Gibbs' symbol  $\mu$  and the name "chemical potential" return once more to replace "partial molar free energy"; statistical methods are employed fairly generally.

The student will not regret the purchase of this book; the lecturer can recommend it; but they must be both certain that the lecture-course insists that true appreciation of the fundamentals before this volume has been too well-thumbed.

F. C. T.

# COLLOIDAL CRYSTALLITES AND MICELLES.

## PART I.—THE MICELLE IN SOLUTION.

### APPARENT ANOMALIES IN THE SURFACE- AND INTERFACIAL - TENSION - CONCENTRATION CURVES OF AQUEOUS SOLUTIONS OF PARAFFIN-CHAIN SALTS.

BY D. REICHENBERG.

(Communicated by ERIC K. RIDEAL, F.R.S.)

Received 17th January, 1946, as revised 7th August, 1946.

In recent years considerable attention has been paid to certain apparent anomalies in the surface tension-concentration and interfacial tension-concentration curves of aqueous solutions of paraffin-chain salts. Most striking among these anomalies is the occurrence of a minimum in these curves. McBain and Mills<sup>1</sup> have pointed out that, according to Gibbs' adsorption equation, this would imply that, at the concentration corresponding to the minimum, the Gibbs' "Surface Excess" is zero, while above this concentration, the salt becomes *negatively* adsorbed. This negative adsorption co-exists with a considerable decrease in the surface- or interfacial-tension as compared with that of pure water. Also the numerical value of the negative adsorption demands that even if the surface layer is supposed to be pure water, it must be assumed that this surface layer is several hundred or several thousand Angstroms thick, which is contrary to the view generally accepted nowadays that adsorbed molecules on the surfaces of solutions form a layer only one (or, at most, a few) molecules thick. In any case, microtome measurements<sup>2</sup> show that the adsorption of the salt is positive over the whole range of concentration in which the minimum occurs. Therefore, thermodynamics would seem to imply that no minimum should occur.

A number of theories have been put forward with the object of resolving the anomaly. These have been carefully reviewed by Alexander<sup>3</sup> and have all been shown to be incorrect or inadequate to explain the anomaly. They may be summarised as follows.

(1) It has been suggested<sup>2, 4</sup> that Gibbs' equation is only a limiting law (resembling the ideal gas law), and fails to take account of such factors as the effect of orientation, of submerged double layer and of free electric charge (if any) on the surface.

Gibbs' treatment, however, being thermodynamically rigorous, is independent of any particular molecular interpretation of the surface layer. Also, since both the surfaces and the systems as a whole, are electrically neutral, no term to allow for the effect of free electrical charge is necessary. Dickinson<sup>5</sup> demonstrates this point very elegantly.

(2) Long and Nutting<sup>6</sup> assume a surface layer of solute (giving positive adsorption at the interface) above a diffuse double layer of considerable depth, the concentrations in this diffuse layer determining the value of the Gibbsian surface excess.

<sup>1</sup> McBain and Mills, *Rep. Progress Physics*, 1938, **5**, 30.

<sup>2</sup> McBain and Wood, *Proc. Roy. Soc. A*, 1940, **174**, 286.

<sup>3</sup> Alexander, *Trans. Faraday Soc.*, 1942, **38**, 248.

<sup>4</sup> Gibby and Addison, *J. Chem. Soc.*, 1936, 119.

<sup>5</sup> Dickinson, *Trans. Faraday Soc.*, 1944, **40**, 48.

<sup>6</sup> Long and Nutting, *J. Amer. Chem. Soc.*, 1941, **63**, 625.



However, microtome<sup>1</sup> and interferometer measurements and the study of froth formation show that the total surface adsorption is invariably positive.<sup>1, 2</sup>

(3) Several authors<sup>7, 8</sup> have suggested that solutions of soap are not really two component systems and that Gibbs' equation should include terms for extra components. Thus with fatty acid soaps, considerable hydrolysis occurs at the very low concentrations employed and such solutions are very sensitive to carbon dioxide and to traces of heavy metals. However, the same anomalies are found with other paraffin-chain salts where hydrolysis cannot occur.<sup>1, 2</sup>

Alexander points out that the minimum always occurs at or about the same concentrations as that at which the paraffin-chain salt ions are known to aggregate to micelles. This concentration is known as the *critical micelle concentration*. He suggests that, in writing down the appropriate form of the Gibbs' equation, the unaggregated salt and the micelles must be treated as separate components. Thus he derives the equation

$$\Gamma_s^{(w)} + \Gamma_M^{(w)} = -d\gamma/RTd \ln c_s f_s \quad (13)$$

for the dilute solutions under consideration, where  $\Gamma_s^{(w)}$  and  $\Gamma_M^{(w)}$  are the Gibbsian surface excesses of unaggregated salt and micelles, respectively, the surface excess of water being taken as zero,  $\gamma$  is the surface or interfacial tension of the solution,  $c_s$  is the concentration of unaggregated salt, and  $f_s$  is its activity coefficient.

For concentrations above the critical,

$$c = c_s + c_m \quad (14)$$

where  $c_s$  and  $c_m$  are expressed in equivalents and  $c$  is the stoichiometric concentration of solute

"If now  $d\gamma/dc = 0$  as at the minimum of surface tension, either  $\Gamma_s^{(w)} + \Gamma_M^{(w)} = 0$ ", (which is disproved by microtome measurements) or

$$dc_s f_s / dc = 0 \quad (17)$$

Alexander goes on to suggest that, at the critical concentration,  $dc_s f_s / dc$  does actually become zero and that this is the explanation of the minimum in surface- or interfacial-tension.

That this suggestion is incorrect may be demonstrated in two ways.

(1) Alexander himself points out that " $dc_{\text{soap}} f_{\text{soap}}$  must have the same sign as  $dc_{\text{soap}}$  for stable solutions".

In other words, for stable solutions  $d\mu_{\text{soap}}/dc_{\text{soap}}$  must be positive and cannot be zero or negative. ( $\mu$  is the thermodynamic potential or Gibbs' free energy per gram-mole.)

If  $\mu_s = \mu_m$  (Alexander's equation (10)), both must be equal to  $\mu_{\text{soap}}$ , where  $\mu_{\text{soap}}$  is the quantity which determines, for example, the solubility of the soap at a given temperature, the lowering of vapour pressure, depression of freezing-point, etc. If, then,  $d\mu_{\text{soap}}/dc_{\text{soap}}$  cannot be zero or negative, neither can  $d\mu_s/dc_{\text{soap}}$  or  $d\mu_m/dc_{\text{soap}}$ . Hence Alexander's equation (17) cannot be true for any stable solution.

(2) In (13), it is obvious that  $\Gamma_s^{(w)} + \Gamma_M^{(w)} = \Gamma_{\text{soap}}^{(w)}$ , provided that  $\Gamma_s^{(w)}$ ,  $\Gamma_M^{(w)}$  and  $\Gamma_{\text{soap}}^{(w)}$  are all expressed in g. equivalents per unit area. Therefore,  $-d\gamma = \Gamma_{\text{soap}}^{(w)} \cdot d\mu_s$  which is Gibbs' equation in its usual form for a 2-component system with  $d\mu_s$  substituted for  $d\mu_{\text{soap}}$  (and we know that the two are identically equal). Hence the original paradox remains once more.

### Preliminary Treatment.

The suggestion put forward in the present paper is, as is implied above, that a solution containing only pure water and the pure soap can show no minimum in the surface- or interfacial-tension concentration curves.

<sup>7</sup> Nickerson, *J. Physic. Chem.*, 1936, 40, 298.

<sup>8</sup> Adam, *Physics and Chemistry of Surfaces*, p. 408.

(For the sake of brevity, throughout the present paper, the word "curve" will, unless otherwise stated, be understood to mean "the curve of surface- or interfacial-tension plotted against the natural logarithm of the soap concentration". Also the word "soap" will be used for all long paraffin-chain salts, whether carboxylate, sulphonate, pyridinium bromide, etc.) Robinson<sup>9, 10</sup> found, in agreement with this suggestion, that when ordinary distilled water was used for preparing the soap solutions, the usual minimum was shown, but with specially purified water (specific conductivity  $0.2 \times 10^{-6}$  ohms<sup>-1</sup> cm.<sup>-1</sup>), no minimum was shown.

This conclusion will now be examined in the light of thermodynamics and it will be shown that it is capable of resolving the anomaly and explaining the known experimental results better than any theory put forward hitherto. It must be pointed out, however, that the more detailed speculations lack any extensive experimental confirmation at present (and the word "probably" will, of necessity, be used several times).

We must consider, then, that there are in the solution three independent components: water, soap, and the salt or salts of a polyvalent ion of opposite charge to the long-chain ion of the soap. The Gibbs' equation now becomes

$$-dy = \Gamma_{\text{water}} \cdot d\mu_{\text{water}} + \Gamma_{\text{soap}} \cdot d\mu_{\text{soap}} + \Gamma_{\text{salt}} \cdot d\mu_{\text{salt}} \quad (1)$$

We may, in accordance with Gibbs' convention, place the mathematical surface so that  $\Gamma_{\text{water}}$  becomes zero. Since, in the range we are considering, the concentration of soap and salt are very small, the "surface excesses" of these components will not differ appreciably from the physical concept of surface excess (Guggenheim and Adam's  $\Gamma^{(v)}$ ).

We may dispense, therefore, with the usual superfixes. We now have

$$-dy = \Gamma_{\text{soap}} \cdot d\mu_{\text{soap}} + \Gamma_{\text{salt}} \cdot d\mu_{\text{salt}}$$

$$\therefore \frac{-dy}{d \log_e c_{\text{soap}}} = \Gamma_{\text{soap}} \cdot \frac{d\mu_{\text{soap}}}{d \log_e c_{\text{soap}}} + \Gamma_{\text{salt}} \cdot \frac{d\mu_{\text{salt}}}{d \log_e c_{\text{soap}}} \quad (2)$$

The first term on the R.H.S. of (2) will always be positive, since  $\Gamma_{\text{soap}}$  is positive throughout the range and  $d\mu_{\text{soap}}/d \ln c_{\text{soap}}$  must be positive for stable solutions.

Now simple salts of the type NaCl, CuSO<sub>4</sub>, CuCl<sub>2</sub>, CaCl<sub>2</sub>, etc., are negatively adsorbed in pure water.<sup>12</sup> However, in the presence of the soap with the surface of the solution already covered with a monolayer of soap, it is most probable that the ion (of the salt) with the opposite charge to the paraffin-chain ion will be strongly adsorbed, and will tend to displace from the surface the corresponding ion of the soap itself.

For example, with cetyl pyridinium bromide and CuSO<sub>4</sub>, sulphate ions will tend to displace bromide ions from the surface. With sodium dodecyl sulphate and CuSO<sub>4</sub>, Cu ions will displace, wholly or partially, Na ions from the surface.

This view is supported by two lines of evidence.

(1) The precipitation of Ca or Cu soaps when small quantities of salts of these ions are added to soap solutions,<sup>13</sup> insolubility and surface activity usually going hand in hand.

(2) Cassie and Palmer<sup>14</sup> have succeeded in explaining semi-quantitatively the effect of added salts in lowering the surface- or interfacial-tension of soap solutions. Their analysis is based on the distribution of ions in the vicinity of the surface, and their influence on this potential. It is shown, in accordance with experiment,<sup>10</sup> that the effect is due almost entirely to the ions of opposite charge to the long-chain ions, and that the

<sup>9</sup> Robinson, *Symposium on Wetting and Detergency*, 1937 (Harvey, London), p. 137. <sup>10</sup> Robinson, *Nature*, 1937, 139, 626.

<sup>11</sup> Guggenheim and Adam, *Proc. Roy. Soc. A*, 1932, 139, 218.

<sup>12</sup> Harkins and McLaughlin, *J. Amer. Chem. Soc.*, 1925, 47, 2083; 1926, 48, 604.

<sup>13</sup> Powney and Addison, *Trans. Faraday Soc.*, 1937, 31, 1243.

<sup>14</sup> Cassie and Palmer, *ibid.*, 1941, 37, 156.

effect increases greatly with the valency of these ions. To produce this effect, it must be postulated that these ions are strongly adsorbed under the influence of the electric field at the surface.

Thus we may assume provisionally that  $\Gamma$  salt will be positive. This means that the composition of *both* the surface and bulk of the solution can no longer be represented by only three independent components, since the two kinds of ions of the salt will be adsorbed unequally. Four components at least will be required, although the simplest procedure is to allow a term in the Gibbs' equation for each of the separate kinds of ion. Hence equation (2) can no longer be regarded as adequate. However, we will use it first to obtain an approximate result and give a more rigorous treatment later.

The concentration of salt is assumed constant with varying soap concentrations since it is the amount of salt in the distilled water used. Hence

$$\begin{aligned} d\mu_{\text{salt}}/d \ln c_{\text{soap}} &= d[RT \ln c_{\text{salt}} f_{\text{salt}}]/d \ln c_{\text{soap}} \\ &= RT d \ln f_{\text{salt}}/d \ln c_{\text{soap}}. \end{aligned}$$

Now  $d \ln f_{\text{salt}}/d \ln c_{\text{soap}}$  will normally be negative in dilute solutions, in accordance with the "ionic-strength principle". Hence of the two terms on the R.H.S. of (2), the first will be positive and the second negative.

If, therefore, the first term becomes sufficiently small numerically and the second sufficiently large numerically,  $d\gamma/d \ln c_{\text{soap}}$  will pass through zero and become positive.

Let us now examine the possibility of this happening. In the extreme case, when the appropriate polyvalent ion of the salt has completely displaced from the surface the soap ion of the same charge sign,  $\Gamma_{\text{salt}}$  will be approximately equal to  $\Gamma_{\text{soap}}/Z$  where  $Z$  is the valency of the adsorbed polyvalent ion.

$$\text{Therefore} \quad - \frac{d\gamma}{d \ln c_{\text{soap}}} = \Gamma_{\text{soap}} \left[ \frac{d\mu_{\text{soap}}}{d \ln c_{\text{soap}}} + \frac{1}{Z} \cdot \frac{d\mu_{\text{salt}}}{d \ln c_{\text{soap}}} \right] \quad (3)$$

Now as the soap concentration is increased from zero, it is known<sup>15, 16</sup> that  $\mu_{\text{soap}}$  at first increased steadily with concentration in accordance with the relation

$$\begin{aligned} d\mu_{\text{soap}} &= RT d \ln a_{\text{soap}} \\ &= 2RT d \ln c_{\text{soap}} + 2RT d \ln f_{\pm \text{soap}} \end{aligned}$$

where  $f_{\pm \text{soap}}$  does not differ much from unity.

When, however, the critical concentration is reached, aggregation occurs and is reflected in a sharp decrease in  $f_{\pm \text{soap}}$ . Hence  $d\mu_{\text{soap}}/d \ln c_{\text{soap}}$  falls sharply to a fraction of its original value, but will, as stated before, remain positive. (Herein lies the truth and also the fallacy in Alexander's argument:  $da_{\text{soap}}/dc_{\text{soap}}$  does, it is true, decrease very considerably when aggregation occurs, but it can never become zero or negative for a stable solution).

It is under the circumstances of micelle formation, therefore, that the first term on the R.H.S. of equation (2) becomes sufficiently small as to permit the expression as a whole to become zero or negative. It is for this reason that the minimum in the curves is manifested at or about the critical concentration.

We now make a comparison of the numerical values of the quantities involved. McBain, Dye and Johnston<sup>17</sup> have measured freezing-points of dodecyl-sulphonic acid solutions over a wide range of concentrations. They worked out the results in terms of the osmotic coefficient of the soap. For the present purpose, however, it is necessary to obtain  $d\mu_{\text{soap}}/d \ln c_{\text{soap}}$  over a range of concentrations. This may be done as follows:—

Let  $\theta$  be depression of freezing-point of the solution from that of pure water,  $L_f$  = latent heat of fusion per g. mole of solvent,  $T_0$  = freezing-point

<sup>15</sup> Johnston and McBain, *Proc. Roy. Soc.*, 1942, 181, 119.

<sup>16</sup> Robinson, Smith and Smith, *Trans. Faraday Soc.*, 1942, 38, 70.

<sup>17</sup> M. E. L. McBain, Dye and Johnston, *J. Amer. Chem. Soc.*, 1939, 61, 3210.

of solvent,  $M$  = molecular weight of solvent,  $c$  = concentration of solution in g. moles solute to 1000 g. solvent.

$$\text{Then} \quad d\mu_{\text{soap}} = \frac{1000L_f}{T_0M} \cdot \frac{d\theta}{c}.$$

Inserting the actual values of the quantities, i.e.,  $L_f = 1438$  cal. per g. mole,  $M = 18$ ,  $T = 273$ , we have  $d\mu_{\text{soap}} = 292.3 d\theta/c$ .

We may also replace the molality by the concentration in g. moles per litre solution without appreciable error in these dilute solutions.

$$\text{Therefore} \quad \frac{d\mu_{\text{soap}}}{d \ln c_{\text{soap}}} = 292.3 \frac{d\theta}{dc_{\text{soap}}}.$$

In Fig. 1, the values of  $d\mu_{\text{soap}}/d \ln c_{\text{soap}}$  have been plotted against soap concentration for dodecyl-sulphonic acid solutions. The values of  $d\theta/dc_{\text{soap}}$  were calculated from McBain, Dye and Johnston's data by choosing suitably spaced points and evaluating  $\Delta\theta/\Delta c_{\text{soap}}$ . It will be observed that in the most dilute solutions  $d\mu_{\text{soap}}/d \ln c_{\text{soap}}$  has a value approximating closely to the theoretical value of  $2RT$  for a completely dissociated 1:1 electrolyte. At a concentration of 0.01 molar, it falls very sharply to a value of about 60 cal. per g. mole.

Now from (3), we have seen that  $d\gamma/d \ln c_{\text{soap}}$  may attain a value of zero if  $\frac{d\mu_{\text{soap}}}{d \ln c_{\text{soap}}} = -\frac{1}{Z} \cdot \frac{\mu d_{\text{soap}}}{d \ln c_{\text{soap}}}$ . But  $\frac{d\mu_{\text{salt}}}{d \ln c_{\text{soap}}} = RT \frac{d \ln f_{\text{salt}}}{d \ln c_{\text{soap}}}$ , and by the Debye-Hückel approximation,  $-\log_{10} f = 0.5Z^2\sqrt{I}$ , where  $I$  is the ionic-strength of the solution. Owing to the extremely minute concentration of the salt, then while the soap remains unaggregated,

$$I = \frac{1}{2}c \cdot I^2 + \frac{1}{2}c \cdot I^2 = c_{\text{soap}}.$$

$$\text{Therefore} \quad -\log_{10} f_{\text{salt}} = 0.5Z^2\sqrt{c_{\text{soap}}}.$$

$$\text{Therefore} \quad \frac{d\mu_{\text{salt}}}{d \ln c_{\text{soap}}} = -2.303RT \frac{d(0.5Z^2\sqrt{c})}{d \ln c_{\text{soap}}} = -2.303RT \cdot \frac{1}{2}Z^2\sqrt{c_{\text{soap}}}.$$

$$\text{Therefore, when } d\gamma/dc = 0, \quad \frac{d\mu_{\text{soap}}}{d \ln c_{\text{soap}}} = \frac{2.303}{Z} \cdot RT \cdot \frac{1}{2}Z^2\sqrt{c_{\text{soap}}} \\ = \frac{2.303}{4} RTZ\sqrt{c_{\text{soap}}}.$$

In Fig. 1, the values of  $\frac{2.303}{4}RT(2)\sqrt{c}$  and  $\frac{2.303}{4}RT(3)\sqrt{c}$  have also been plotted against  $c$ . It will be seen that  $d\mu_{\text{soap}}/d \ln c_{\text{soap}}$  become equal to  $-\frac{1}{2}d\mu_{\text{salt}_2}/d \ln c_{\text{soap}}$  at a concentration of about 0.0125 molar and  $d\mu_{\text{soap}}/d \ln c_{\text{soap}}$  becomes equal to  $-\frac{1}{3}d\mu_{\text{salt}_3}/d \ln c_{\text{soap}}$  at a concentration of about 0.0115 (where the suffixes of 2 and 3 refer to the valency of the appropriate ion of the salt).

Thus it is seen that the conditions for the occurrence of a minimum in surface- or interfacial-tension are adequately satisfied in the case of dodecyl-sulphonic acid solutions, and in actual fact a minimum occurs at a concentration of about 0.006 molar.<sup>1</sup> In a later section, it will be shown by a more rigorous treatment that the minimum should occur at a lower concentration than that indicated by the above treatment and may occur even if  $d\mu_{\text{soap}}/d \ln c_{\text{soap}}$  does not fall to a value equal to  $-\frac{1}{Z}d\mu_{\text{salt}}/d \ln c_{\text{soap}}$ .

When aggregation occurs, the ionic strength of the solution is no longer equal to  $c_{\text{soap}}$ . Indeed, it is doubtful if the ionic strength principle will hold at all. However, it will be shown later that the value of

$$-d \ln f_{\text{salt}}/d \ln c_{\text{soap}}$$

will probably be greater than calculated on this principle, so that the conclusions arrived at above will still hold good.

\* Cf. Glasstone.<sup>18</sup>

It should also be observed that in equation (3), the value of the expression on the R.H.S. will be independent of the value of  $c_{\text{salt}}$ , provided only that this is sufficient to enable the appropriate ion to be adsorbed to the extent that  $\Gamma_{\text{salt}}$  will approximate to  $\frac{1}{2} \cdot \Gamma_{\text{soap}}$ . This accounts for the extremely small amounts of salt which enable the minimum to be manifested.

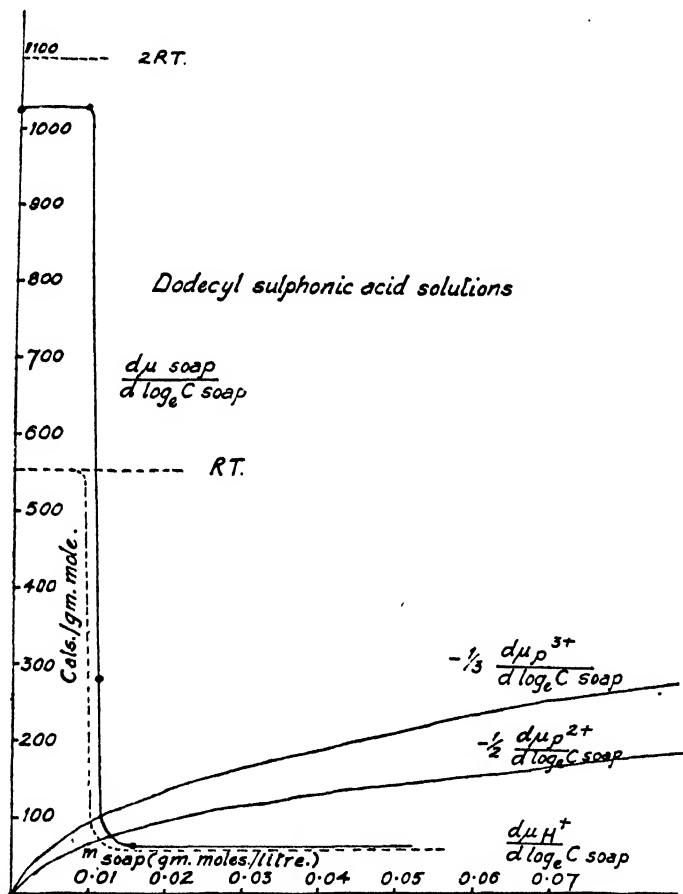


FIG. 1.

### More Rigorous Treatment.

This involves the separate consideration of each ion.

**Salt with a Common Ion.**—The following notation will be used.

The soap is called  $G^+S^-$  where  $S^-$  denotes the long-chain soap ion and  $G^+$  the gegenion. (The argument that follows applies equally if the soap is "cationic", i.e.,  $G-S^+$ .) The salt is  $G^+A^-$ , where  $A^-$  is the auxiliary ion. We have

$$-d\gamma = \Gamma_G + d\mu_G + \Gamma_S - d\mu_S + \Gamma_A - d\mu_A \quad (5)$$

By the condition of electro-neutrality at the interface  $\Gamma_G + \Gamma_S = \Gamma_A$ . Also we make the reasonable assumption that  $\Gamma_A$  is negligible,

therefore

$$\Gamma_G + \Gamma_S = \Gamma_A;$$

therefore

$$-d\gamma = \Gamma_S - (d\mu_G + d\mu_S)$$

therefore

$$-d\gamma/d \ln c_{\text{soap}} = \Gamma_{\text{soap}} \cdot d\mu_{\text{soap}}/d \ln c_{\text{soap}} \quad (6)$$

The expression on the R.H.S. must be positive throughout, therefore no minimum can occur in this case.

It would appear at first sight that this expectation is contradicted by Powney and Addison's curves for sodium dodecyl-sulphate solutions with added sodium chloride where the usual minimum is shown.<sup>18</sup> But it must be remembered that it was postulated that the distilled water used contained dissolved salts with polyvalent ions. These will still manifest their effect, unless completely "swamped" by the salt with a common ion. This view receives confirmation from Powney and Addison's curves for sodium octadecyl sulphate solutions with added sodium chloride. With no added NaCl or 0.025 % NaCl, the interfacial tension against xylene at 60° C. showed a minimum, but with 0.05 % or 0.1 % NaCl, no minimum was shown.

It is clear that in these systems, there is a competition between the Na<sup>+</sup> ions (G<sup>+</sup>) and polyvalent ions of the salt (Pz<sup>+</sup>) for possession of the surface. This case will be worked out more fully later.

Equation (6) is identical with that for a pure soap in pure distilled water. However, the  $\gamma - \ln c_{\text{soap}}$  curves will not be identical since the presence of the salt modifies the values of  $\mu_{\text{soap}}$ ,<sup>19</sup> and also, in the more dilute solutions, of  $\Gamma_{\text{soap}}$ .<sup>14</sup>

**Salt with no Common Ion.** We have, in solution, the soap G<sup>+</sup>S<sup>-</sup> and a salt Pz<sup>+</sup>A<sup>-</sup> with no common ion (where Pz<sup>+</sup> denotes the polyvalent ion of opposite charge to the long-chain ion). This is the case that has been discussed already, but the present treatment is more rigorous and a somewhat different result is obtained.

We have

$$-d\gamma = \Gamma_{\text{S}^-} \cdot d\mu_{\text{S}^-} + \Gamma_{\text{G}^+} \cdot d\mu_{\text{G}^+} + \Gamma_{\text{Pz}^+} \cdot d\mu_{\text{Pz}^+} + \Gamma_{\text{A}^-} \cdot d\mu_{\text{A}^-} \quad (7)$$

Now  $\Gamma_{\text{S}^-} + \Gamma_{\text{A}^-} = \Gamma_{\text{G}^+} + Z\Gamma_{\text{Pz}^+}$  and if  $\Gamma_{\text{A}^-}$  is assumed negligible,

$$\Gamma_{\text{S}^-} = \Gamma_{\text{G}^+} + Z\Gamma_{\text{Pz}^+} \quad (8)$$

Neglecting the term  $\Gamma_{\text{A}^-} \cdot d\mu_{\text{A}^-}$  in (7), and eliminating  $\Gamma_{\text{G}^+}$  between (7) and (8),

$$-d\gamma = \Gamma_{\text{Pz}^+}(d\mu_{\text{Pz}^+} - Zd\mu_{\text{G}^+}) + \Gamma_{\text{S}^-}(d\mu_{\text{S}^-} + d\mu_{\text{G}^+}) \quad (9)$$

$$-\frac{d\gamma}{d \ln c_{\text{soap}}} = \Gamma_{\text{S}^-} \cdot \frac{d\mu_{\text{G}^+\text{S}^-}}{d \ln c_{\text{soap}}} + \Gamma_{\text{Pz}^+} \left( \frac{d\mu_{\text{Pz}^+}}{d \ln c_{\text{soap}}} - Z \frac{d\mu_{\text{G}^+}}{d \ln c_{\text{soap}}} \right) \quad (10)$$

Again, the first term on the R.H.S. must be positive.  $\Gamma_{\text{Pz}^+}$  is positive.  $d\mu_{\text{Pz}^+}/d \ln c_{\text{soap}}$  will probably (as before) be negative, and  $d\mu_{\text{G}^+}/d \ln c_{\text{soap}}$  will most probably be positive throughout the range since increase of soap concentration increases the concentration of G<sup>+</sup>, though not to the same extent above the critical concentration. Hence, the second term on the R.H.S. of (10) will be negative.

Let us now again take the extreme case where Pz<sup>+</sup> ions have completely displaced G<sup>+</sup> ions from the surface. Then

$$\Gamma_{\text{S}^-} = Z\Gamma_{\text{Pz}^+}$$

$$\text{and} \quad -\frac{d\gamma}{d \ln c_{\text{soap}}} = \Gamma_{\text{S}^-} \left[ \frac{d\mu_{\text{G}^+\text{S}^-}}{d \ln c_{\text{soap}}} - \frac{d\mu_{\text{G}^+}}{d \ln c_{\text{soap}}} + \frac{1}{Z} \cdot \frac{d\mu_{\text{Pz}^+}}{d \ln c_{\text{soap}}} \right] \quad (11)$$

$$\text{or} \quad -\frac{d\gamma}{d \ln c_{\text{soap}}} = \Gamma_{\text{S}^-} \left[ \frac{d\mu_{\text{S}^-}}{d \ln c_{\text{soap}}} + \frac{1}{Z} \frac{d\mu_{\text{Pz}^+}}{d \ln c_{\text{soap}}} \right] \quad (12)$$

This equation (12) should be compared with equation (3) obtained by the approximate method. It is seen that the term  $d\mu_{\text{soap}}/d \ln c_{\text{soap}}$  in (3) is replaced by  $d\mu_{\text{S}^-}/d \ln c_{\text{soap}}$  in (12). Since  $d\mu_{\text{S}^-}/d \ln c_{\text{soap}}$  is less than  $d\mu_{\text{soap}}/d \ln c_{\text{soap}}$  (being half as much in the most dilute solutions and considerably less than this above the critical concentration), it will be seen that the minimum in the curves will be manifested at a lower concentration

<sup>18</sup> Glasstone, *Textbook of Physical Chemistry* (1940), 680.

<sup>19</sup> Hartley, *Aqueous Solutions of Paraffin-chain Salt* (Paris, 1936).

than previously indicated. In fact, it may be manifested even if  $d\mu_{\text{soap}}/d \ln c_{\text{soap}}$  never falls to the value of  $-\frac{1}{Z}d\mu_{p^{2+}}/d \ln c_{\text{soap}}$  at any concentration, since it is only necessary that  $d\mu_{p^{2+}}/d \ln c_{\text{soap}}$  should fall to the value of  $-\frac{1}{Z}d\mu_{p^{2+}}/d \ln c_{\text{soap}}$ .

An example of this is shown in Fig. 2. The values of  $d\mu_{\text{soap}}/d \ln c_{\text{soap}}$  have been calculated for sodium deoxycholate solutions from the data of

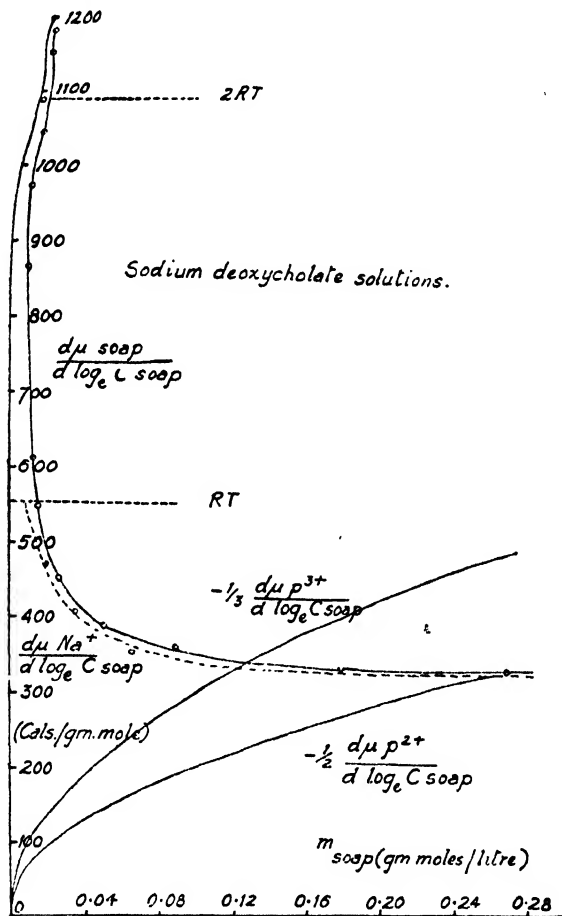


FIG. 2.

Johnston and McBain,<sup>16</sup> and plotted against soap concentration. It will be observed that, as before, at low concentrations  $d\mu_{\text{soap}}/d \ln c_{\text{soap}}$  approximates to the theoretical value of  $2RT$  for a 1:1 electrolyte. At a concentration of about 0.1 M, it reaches a fairly steady value of about 330 cal. per g. mole. On the same graph, are plotted the values of

$$-\frac{1}{2}d\mu_{p^{2+}}/d \ln c_{\text{soap}} \text{ and } -\frac{1}{3}d\mu_{p^{3+}}/d \ln c_{\text{soap}}$$

against soap concentration. It will be observed that at no point in the

measured range does  $d\mu_{\text{soap}}/d \ln c_{\text{soap}}$  become equal to  $-\frac{1}{2}d\mu_{\text{Pz}^+}/d \ln c_{\text{soap}}$ , and it becomes equal to  $-\frac{1}{3}d\mu_{\text{Pz}^+}/d \ln c_{\text{soap}}$  at a concentration of 0.126 molar.

Hence by the approximate treatment a minimum might not be expected, unless the adsorbed ion is trivalent. The more rigorous treatment indicates that the values of  $d\mu_{\text{Pz}^+}/d \ln c_{\text{soap}}$  must be known before this point can be settled.

It is impossible to evaluate this quantity from the experimental data. One can only guess at its probable value and the result is the dotted line in Fig. 2. Thus it is assumed that at very low concentrations  $d\mu_{\text{Pz}^+}/d \ln c_{\text{soap}}$  has the theoretical value of  $RT$ . When aggregation occurs, it falls fairly sharply but the final value it assumes is nearly equal to that of  $d\mu_{\text{soap}}/d \ln c_{\text{soap}}$ . (In other words, above the critical concentration, nearly all the increased activity with increasing soap concentration is due to free gegenions.)

If this surmise is correct, then  $(d\mu_{\text{soap}}/d \ln c_{\text{soap}} - d\mu_{\text{Pz}^+}/d \ln c_{\text{soap}})$  will become equal to  $-1/2 d\mu_{\text{Pz}^+}/d \ln c_{\text{soap}}$  at quite a low value, i.e., soon after aggregation has commenced. Aggregation commences at about 0.005 molar and a minimum in the surface tension-concentration curve at 25° C. occurs at 0.25 %, i.e., at 0.006 molar (Bruce, cf. McBain<sup>20</sup>) since the molecular weight of sodium deoxycholate is 414.

In Fig. 1, too, the probable values of  $d\mu_{\text{Pz}^+}/d \ln c_{\text{soap}}$  for dodecylsulphonic acid solutions, has been indicated by a dotted line. As a result the more accurate equation (12) would lead to the conclusion that the minimum should occur at a somewhat lower concentration than 0.0125 or 0.0115 M. In actual fact it occurs at 0.006 M, which is in very good agreement with the critical concentration as indicated by the osmotic measurements.

Thus the two examples quoted lend strong support to the theory outlined before. We may now consider more closely the effect of colloidal aggregation of the soap upon the value of  $d\mu_{\text{Pz}^+}/d \ln c_{\text{soap}}$ .

When the soap is unaggregated,  $d\mu_{\text{Pz}^+}/d \ln c_{\text{soap}}$  will have a negative value, which is given at least approximately, by the Debye-Hückel equation.  $\Gamma_{\text{Pz}^+}$  will be positive, and if the concentration of  $\text{Pz}^+$  ions is sufficient (which appears to be the case in many of the experiments hitherto recorded), the  $\text{Pz}^+$  ions will displace almost completely the  $\text{G}^+$  ions from the surface. Now Cassie and Palmer<sup>14</sup> have shown that the electrical forces at the surface of micelles (if these are as postulated by Hartley)<sup>15</sup> are not very different quantitatively from those at the oil-water or air-water interface. Thus, as aggregation begins and develops,  $\text{Pz}^+$  ions will be adsorbed on the surfaces of the micelles, and will occupy a fraction of their surface approximately equal to that which they occupy in the macroscopic surface or interface. This will result in a decrease in  $d\mu_{\text{Pz}^+}/d \ln c_{\text{soap}}$  (i.e., an increase in its numerical value) since the solution becomes more stable to  $\text{Pz}^+$  ions. It may also result in a much greater decrease in  $\Gamma_{\text{Pz}^+}$  provided the concentration of  $\text{Pz}^+$  ions in the solution is not too high.

If this condition is satisfied, then there will probably be a net decrease in the value of the second term on the R.H.S. of equation (10). Thus  $dy/d \ln c_{\text{soap}}$  may again pass through zero and become negative once more, i.e., the minimum in the curve will be followed by a maximum.

This actually occurs sometimes (Powney and Addison,<sup>18</sup> McBain<sup>20</sup>). Let us therefore consider more closely the conditions under which we should expect the minimum and maximum to be manifested separately (i.e., at different concentrations) and the different conditions under which the two effects may largely neutralise one another and produce a smooth curve. If the paraffin-chain is sufficiently long, e.g., about 16 C atoms, aggregation will occur fairly sharply over a narrow range of concentration. Hence, as soon as aggregation begins, the value of  $d\mu_{\text{soap}}/d \ln c_{\text{soap}}$  drops sharply to its new value and then remains fairly constant (cf. Fig. 1). Hence, in equation

<sup>20</sup> McBain, article in *Advances in Colloid Science* (New York, 1942), 99.



(10), the first term falls sharply in value. The value of  $d\mu_{Pz+}/d \ln c_{\text{soap}}$ , as implied above, depends on two factors

- (1) The total concentration of  $Pz^+$  ions.
- (2) The ratio of  $\frac{\text{Area of surface of micelles}}{\text{Area of macroscopic interface}}$ .

As explained above, the  $Pz^+$  ions will occupy approximately equal fractions of the two kinds of interface (macroscopic and micellar). For a minimum to be manifested, it is probably necessary that the concentration of  $Pz^+$  be sufficient to cause it to displace completely or nearly completely the  $G^+$  ions from the macroscopic surface when the soap is unaggregated. If the concentration is little more than sufficient to satisfy this, then clearly  $\Gamma_{Pz+}$  will begin to decrease at a soap concentration slightly higher than the critical. Hence, both a minimum and maximum will be manifested.

If, on the other hand, the concentration of  $Pz^+$  is considerably more than sufficient to satisfy the condition for a minimum, then there will be a "reserve" of  $Pz^+$  ions to provide for the increased area of the surface of micelles with increased soap concentrations. Hence the value of  $\Gamma_{Pz+}$  may not decrease appreciably until a much higher soap concentration is reached and the saturation-solubility of the soap (or of the  $Pz^+Sx^-$  soap) may be reached before the maximum is manifested. Hence high concentrations of  $Pz^+$  will tend to inhibit the appearance of a maximum.

This is in accordance with the results of Powney and Addison.<sup>13</sup> The interfacial tensions of sodium dodecyl sulphate solutions at 20° c. were measured with increasing amounts of added  $\text{CaCl}_2$ . An increase of  $\text{CaCl}_2$  concentration from zero to 0.001 % decreased the concentration at which the minimum was manifested from 0.0065 M to 0.0057 M (since it decreased the critical concentration) while it also increased the concentration at which the maximum was shown from 0.008 molar to 0.01 M.

When the paraffin-chain is fairly short, e.g., 8 C atoms, aggregation will be more gradual and the two effects may well "swamp" one another, giving rise to smooth curves without maxima or minima. There does not at present appear to be available any reliable experimental data on which this expectation can be tested.

**Salt with Common Ion Plus Salt with no Common Ion.** This case often occurs when the salt with the common ion  $G^+A^-$  is added deliberately, and the salt with no common ion  $Pz^+B^-$  is present (sometimes unsuspected) in the distilled water used. We have

$$-d\gamma = \Gamma_{G+} \cdot d\mu_{G+} + \Gamma_{S-} \cdot d\mu_{S-} + \Gamma_{Pz+} \cdot d\mu_{Pz+} + \Gamma_{A-} \cdot d\mu_{A-} + \Gamma_{B-} \cdot d\mu_{B-} \quad (13)$$

Since  $\Gamma_{A-}$  and  $\Gamma_{B-}$  are negligible, we may leave out the last two terms in (12).

$$\text{Then,} \quad -d\gamma = \Gamma_{G+} \cdot d\mu_{G+} + \Gamma_{S-} \cdot d\mu_{S-} + \Gamma_{Pz+} \cdot d\mu_{Pz+}$$

$$\text{and since} \quad \Gamma_{S-} = \Gamma_{G+} + Z\Gamma_{Pz+},$$

$$\text{therefore} \quad -d\gamma = \Gamma_{S-}(d\mu_{S-} + d\mu_{G+}) + \Gamma_{Pz+}(d\mu_{Pz+} - Zd\mu_{G+}) \quad (14)$$

This is identical with equation (9) which refers to the case of the soap and the salt with no common ion. All the terms in the equations will have the same signs as before, but different values. In particular, at a given soap concentration, we may expect lower values of  $\Gamma_{Pz+}$  since the higher concentration of  $G^+$  ions will tend to displace  $Pz^+$  ions from the surface to a greater extent. If the concentration of salt with a common ion is sufficiently high, the second term on the R.H.S. of equation (10) will be sufficiently small numerically that  $d\gamma/d \ln c_{\text{soap}}$  will not change sign as the soap concentration is varied, i.e., no minimum will occur.

An example of this has been given already in the section dealing with the effect of a salt with a common ion. This effect of the addition of a salt with an ion common with the soap in decreasing  $\Gamma_{Pz+}$  is also shown, by

the results of Powney and Addison on the addition of sodium chloride to sodium dodecyl sulphate solutions at 20° C. The effect on the interfacial tension against xylene was, initially at any rate, to decrease the soap concentration where the maximum occurred from 0.008 molar with no added NaCl to 0.0065 molar with 0.025 % added NaCl.

### Phase Separation.

Consider once more the case of added salt with no common ion with the soap. In the extreme case, when all the  $G^+$  ions have been displaced from the surface, we have (equation 12),

$$\frac{-dy}{d \ln c_{\text{soap}}} = \Gamma_s - \left[ \frac{d\mu_{s-}}{d \ln c_{\text{soap}}} + \frac{1}{Z} \frac{d\mu_{pz+}}{d \ln c_{\text{soap}}} \right] = \frac{\Gamma_s - \left[ \frac{d\mu_{pz+} + s_{s-}}{d \ln c_{\text{soap}}} \right]}{Z} \quad (15)$$

$\mu_{pz+} + s_{s-}$  is the hypothetical chemical potential of the soap  $P_{pz+} + s_{s-}$ . We have seen that  $\gamma$  passes through a minimum with increasing soap concentration. Hence  $\mu_{pz+} + s_{s-}$  will pass through a maximum.

It is known that if the chemical potential of a component of a mixture passes through a maximum with varying composition, this sometimes results in phase separation. For the sake of clarity, it is considered desirable to re-state the exact conditions under which this may occur:—

In a liquid mixture of several components, a, b, c . . . , let the relative amounts of b, c . . . be kept constant and let the amount of -a- be varied. Then

- (1) If the chemical potential of "a" passes through a maximum, phase separation will occur into two liquid phases, one rich and the other poor in the component "a".
- (2) If the chemical potential of "b" passes through a maximum, phase separation may not necessarily occur.
- (3) If the chemical potential of "b" in the mixture increases above the value of the chemical potential of "b" in another phase, which can be formed chemically from the components of the mixture and is stable at that temperature and pressure (e.g., the solid phase "b"), then this phase will separate.
- (4) If in (3) the chemical potential of "b" passes through a maximum, then the phase which has separated will begin to re-dissolve, and if the chemical potential of "b" becomes less than in the external phase again, the external phase will be completely re-dissolved.

If we apply these principles to the example considered above, we see that if the soap  $P^{+}S^{-}_z$  is to be considered as a component, it must be treated as component "b" and not component "a", i.e., the relative amounts of  $P^{+}S^{-}_z$  and water are kept constant while the amount of the soap  $G^{+}S^{-}$  is varied. Hence, it does not follow that the solution will separate into two liquid phases merely because  $\mu_{pz+} + s_{s-}$  passes through a maximum, but if  $\mu_{pz+} + s_{s-}$  exceeds the value for the solid soap  $P^{+}S^{-}_z$  (or a hydrated form) then this solid soap must separate. Again, since the value of  $\mu_{pz+} + s_{s-}$  passes through a maximum, the solid soap will be partly, and may be completely, re-dissolved.

Support for these conclusions is obtained from the experiments of Powney and Addison.<sup>13</sup> These authors found that if sodium dodecyl sulphate was added to  $CaCl_2$  solutions in water, the solution became turbid through the separation of the Ca soap at a soap concentration slightly below that at which the minimum in interfacial tension is manifested, i.e., slightly below the critical concentration. At a concentration slightly above the critical concentration, the solution became clear again, i.e., the calcium salt was completely re-dissolved. As is to be expected, the higher the concentration of  $CaCl_2$  present initially, the lower will be the soap concentration at which the solution becomes turbid, and the higher the soap concentration at which it becomes clear again. Similar results were found with salts of other polyvalent ions.

### Other Factors which may Cause a Minimum.

Miles and Shedlovsky<sup>21</sup> have shown experimentally some of the conditions under which a minimum can occur. They find in agreement with Robinson<sup>9</sup> and with the conclusions of the present paper, that pure sodium dodecyl sulphate or pure sodium tridecane-2-sulphate dissolved in pure distilled water, show no minimum in the curves. When 0.1 % or 0.5 % dodecanol of the amount of soap was added with the sodium dodecyl sulphate, a minimum in surface tension was shown at a soap concentration of 0.007 M. It will be observed that this is the same concentration at which minima occur in Powney and Addison's curves. It suggests strongly that here, too, micelle formation is an essential factor in producing the minimum.

The following explanation is offered:—

The appropriate form of the Gibbs' equation is

$$-d\gamma = \Gamma_{\text{soap}} \cdot d\mu_{\text{soap}} + \Gamma_{\text{dodecanol}} \cdot d\mu_{\text{dodecanol}} \quad (16)$$

$\Gamma_{\text{dodecanol}}$  will certainly be positive and of appreciable magnitude.  $d\mu_{\text{dodecanol}}/d \ln c_{\text{soap}}$  might be expected to be positive, since dodecanol is being added with the soap (1/1000 or 1/200 of the amount of soap). This will certainly be the case while the soap is unaggregated.

Soap micelles are known, however, to have a strong power for dissolving organic compounds.<sup>10, 15</sup> This will tend to make  $d\mu_{\text{dodecanol}}/d \ln c_{\text{soap}}$  negative. It is most probable, therefore, that when aggregation occurs,  $d\mu_{\text{dodecanol}}/d \ln c_{\text{soap}}$  becomes negative, thus causing a minimum in the curves.

McBain and Perry<sup>22</sup> have found that dodecyl sulphonic acid when dissolved in some organic solvents shows a minimum in surface tension, whereas in other organic solvents, no minimum is shown. Alexander<sup>3</sup> suggests that this may be due to aggregation of the soap when dissolved in organic solvents. Though very little is known of these solutions of soaps in organic solvents, it is quite possible that aggregation of the soap does occur. It must be pointed out, however, that as shown earlier in this paper, this in itself is insufficient to cause a minimum, if the materials used are pure.

A brief examination of McBain and Perry's data does, indeed, indicate that minima are shown with those solvents least likely to be pure (e.g., Nujol, Mineral Oil, Tetra-isobutylene, Hydrogenated Isobutylene), and are not shown with solvents readily purified (e.g., Benzene, Hexane).

It is clear that further knowledge of these very interesting systems is required before any definite conclusion can be drawn.

The author desires to express his indebtedness to Professor E. K. Rideal, F.R.S., for his never-failing advice and encouragement during the development of the ideas embodied in this paper and to Dr. A. E. Alexander for many helpful discussions.

### Summary.

A discussion is given of the surface- and interfacial-tension-concentration curves of soap solutions. It is shown that minima in these curves are not to be expected if the materials used are pure, and that therefore the minima found experimentally must be due to impurities. Assuming the impurities to be salts of polyvalent ions present in the water used, the theory explains why the minimum occurs at the critical concentration of the soap, and why a maximum is also shown sometimes. Such experimental data as are available appear to support the theory put forward.

### Résumé.

Les courbes de la tension superficielle et de la tension à l'interface en fonction de la concentration sont discutées pour des solutions de savon. Les minima obtenus sont dûs à des impuretés et, quand celles-ci sont des sels d'ions polyvalents, la théorie rend compte du minimum observé à la concentration critique de savon et aussi de l'existence d'un maximum dans certains cas.

<sup>21</sup> Miles and Shedlovsky, *J. Physic. Chem.*, 1944, 48, 51.

<sup>22</sup> M. E. L. McBain and Perry, *J. Amer. Chem. Soc.*, 1940, 62, 989.

**Zusammenfassung.**

Die Kurven für die Beziehung zwischen der Oberflächen- und Phasengrenzflächenspannung einerseits und der Konzentration von Seifenlösungen andererseits werden besprochen. Die beobachteten Minima werden von Verunreinigungen verursacht. Für den Fall, wenn diese Verunreinigungen Salze mehrwertiger Ionen sind, wird eine Theorie vorgeschlagen, die das Minimum bei einer kritischen Seifenkonzentration und das Auftreten eines Maximums in manchen Fällen zu erklären vermag.

*Note added in Proof.*

As regards the effect of polyvalent ions, the treatment given above is based on the idea that these are present as impurity in (constant proportion to) the water. It is, of course, possible that they may be present as an impurity in the soap. This may also give rise to a minima in the curves, and in this case the appropriate treatment will be analogous to that given above for the dodecanol case. If polyvalent ions are present *both* in the soap and the water, the treatment is, of course, much more complicated.

*Laboratory of Colloid Science,  
Cambridge.*

---

**PENETRATION OF SODIUM CETYL SULPHATE  
INTO CETYL ALCOHOL. EFFECT OF SALT  
ON THE TIME-PENETRATION CURVES.**

By R. MATALON AND J. H. SCHULMAN.

*Received 20th August, 1946.*

The penetration of sodium cetyl sulphate into a monolayer of cetyl alcohol was first investigated by Schulman and Hughes.<sup>1</sup> Using 5 mg./l. of the cetyl sulphate, the surface pressure of the alcohol film increased from 16 to 40 dynes in 2 min. at  $pH$  2, while the surface pressure at the free surface of cetyl sulphate was very small, between 5 and 6 dynes. Schulman and Rideal<sup>2</sup> showed that the 10 dynes surface pressure of the cetyl alcohol film is changed to 58 dynes within 10 min. when 1 mg. of cetyl sulphate is injected into 300 cc. of buffer underneath the alcohol film at  $pH$  7.2.

Schulman and Stenhagen<sup>3</sup> operating with phosphate buffer at  $pH$  8 described the compression curve of the mixed film and deduced the existence of three stoichiometric complexes. This conclusion was supported by the existence of three kinks at the respective areas of 78, 58 and 38 Å.<sup>2</sup> corresponding to complexes where the ratio of the alcohol to the cetyl sulphate is 1 : 3, 1 : 2, 1 : 1, assuming that during the whole range of compression from 26 to 48 dynes (where the film is solid), the area occupied per molecule of alcohol and cetyl sulphate is the same, and equal to 19 Å.<sup>2</sup>. In other words, during compression of the mixed film, it was supposed that the cetyl sulphate molecules were ejected from the surface in number corresponding to the decrease in area during compression, and that the remaining cetyl sulphate and cetyl alcohol molecules in the surface occupied 19 Å.<sup>2</sup> each. Further evidence<sup>3</sup> for the existence of complexes 1 : 3 and 1 : 1 was obtained from the ejection curve under the constant pressure of 23 dynes; the 1 : 2 complex was characterised as being unstable and in a transitory state.

<sup>1</sup> Schulman and Hughes, *Biochem. J.*, 1935, **29**, (5), 1251.

<sup>2</sup> Schulman and Rideal, *Proc. Roy. Soc. B*, 1937, **122**, 38.

<sup>3</sup> Schulman and Stenhagen, *ibid.*, 1938, **126**, 364.

More recently Joly<sup>4</sup> used the piston-oil technique permitting him to find the area at which a mixed film attains equilibrium under definite pressures. The piston-oil used was triricinoleine which has a pressure of 23 dynes on distilled water. This author found that if the film was allowed to stand 3 hr. after the injection and if the piston-oil pressure was established after this period, the film rests at an area of 80 A.<sup>2</sup> or 40 A.<sup>2</sup> depending on the initial area of the film. If this area is greater than 80 A.<sup>2</sup> the film will come to rest at 80 A.<sup>2</sup>, but if the initial area is smaller than 80 A.<sup>2</sup> the film will always rest at 40 A.<sup>2</sup> In the same work the 1 : 2 complex was characterised by the change in slope at 60 A.<sup>2</sup> of the curve determined under rapid compression. The quantity of cetyl sulphate used by this author was 10 mg./l. and m./300 phosphate was present in the bath maintaining a constant pH of 8.

Whilst all the previous work on this particular problem has been carried out on the Langmuir trough and mainly by compression of the film, from which the existence of stoichiometric complexes was first deduced, Harkins, Florence and Copeland<sup>5</sup> used the Wilhelmy plate method for measuring equilibrium surface pressures, a principle previously used by Schulman and Stenhagen<sup>3</sup> in their study of cholesterol-cetyl sulphate mixed films. Harkins and his co-workers spread the alcohol film on the solution of cetyl sulphate after having swept the surface. They measured the values of the equilibrium pressures (attained after several hours) for films maintained at different areas on distilled water in which varying amounts of cetyl sulphate had previously been dissolved. With the above modifications in technique, for the same concentration of cetyl sulphate and for the same area of the alcohol film, the pressures obtained by Schulman and Stenhagen are much greater than those of Harkins and his co-workers, but Harkins did not take into account the solidification of the mixed film at pressures above 25 dynes.

The following is an attempt to determine the reasons for the large discrepancies in the values of the pressure of the mixed film given by the different authors. It was thought that the most likely explanation would be found in the conditions and techniques used, e.g. composition of the bath, the presence of salt, or nature of the process to which the film was subjected, i.e. a dynamic process in the compression curve and a static process in the penetration curve.

### Experimental.

The Langmuir trough used was enclosed in a box so as to avoid impurities from the air. The quantity of cetyl sulphate used throughout was 1 mg./300 cc., the volume of the bath being 900 cc. and the total area of the trough  $17 \times 21$  cm.<sup>2</sup>. The temperature of the bath was 20-23° C. Cetyl sulphate (3 mg.) was dissolved in 2 cc. distilled water, heated to 60° C., diluted with 10 cc. liquid from the bath and injected immediately afterwards. The solution was injected from behind the glass slide confining the film, and the tip of the pipette used was large enough for performing the injection rapidly and allowed stirring of a large volume of the bath. The injection lasted 3 min. after which readings of the pressures were taken. Before every reading, the area behind the boom was swept several times by waxed slides so as to remove the adsorbed film of cetyl sulphate, this process being stopped when the movement of the slide towards the boom did not alter the position of the latter as shown by the light image on the scale. Cleaning must be carried out with great care and minimum vibration of the surface, as the film becomes very sensitive to mechanical disturbances, especially at pressures above 30 dynes, where

<sup>4</sup> Joly, *Nature*, 1946, 158, 26.

<sup>5</sup> Harkins, *Amer. Ass. Adv. Sci.*, 1943, No. 21, pp. 79-80; Alexander, *Colloid Chemistry*, Vol. V, p. 67.

the mixed film is in a very strong solid state, and where the tendency to break and collapse is very high. Furthermore, when pressures above 30 dynes are reached the rigidity of the film becomes abnormally high, and a certain time to establish an even pressure in the film is needed.

To obtain the pressure of a strong solid film, the torsion head must be turned very slowly. If it is turned quickly a much higher pressure is found necessary to bring the light image to its zero position. It is evident that this value is not the true pressure of the film, as shown by the slow and continuous movement of the light image with time below the reference point of the scale. This very high rigidity of the film above 30 dynes renders the determination of the pressure values difficult and great care must be taken in the experimental procedure.

### Results and Discussion.

In Fig. 1 are represented time-penetration curves on  $M./500$  phosphate buffers at  $pH$  8. Every curve refers to an alcohol film maintained at constant area throughout the experiment; the curve of adsorption of cetyl

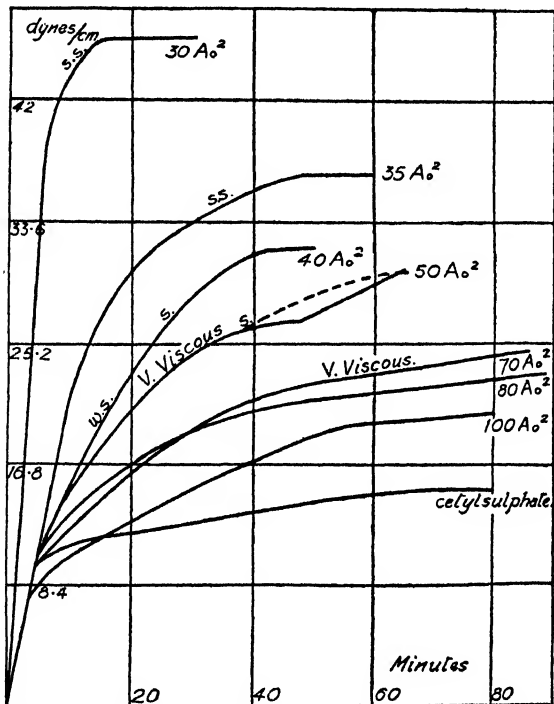


FIG. 1.—Time-penetration curves.  $M./500$  phosphate  $pH$  8.  $t = 20-23^\circ C$ .  
s.s. = strong. s. = solid. w.s. = weak solid or very viscous.

sulphate alone is also given so as to be able to compare the pressure of the adsorbed film with that of the mixed film. Changes in the physical state observed by the talc method showed that solidification occurred with mixed films when the pressure exceeded 26 dynes, irrespective of the initial area of the alcohol film, whilst a very viscous state was observed at 23 dynes pressure. It is seen from these curves that the pressure attained at 80 min. or less after injection increases as the initial area of the alcohol film decreases, i.e. as the number of alcohol molecules covering the

surface is increased. The penetration is already noticeable at 100 A.<sup>2</sup>, where the pressure is 5 dynes higher than with cetyl sulphate alone.

At areas of 30 A.<sup>2</sup> and 35 A.<sup>2</sup> the pressure is increased very markedly 10 min. after the injection, whereas the adsorption of cetyl sulphate alone is only commencing after this length of time. This is due to the fact that at areas of 30 A.<sup>2</sup> and 35 A.<sup>2</sup> per alcohol molecule, very few cetyl sulphate molecules are needed to condense the film. When the amount of alcohol decreases, the increase of pressure with time proceeds at a much slower rate as shown by the curves corresponding to initial areas greater than 40 A.<sup>2</sup>. To demonstrate the effect of the initial area of alcohol on the number of penetrating molecules after injection had proceeded for a given time a film of 30 A.<sup>2</sup> was decompressed to 35 A.<sup>2</sup> (Fig. 2), the pressure

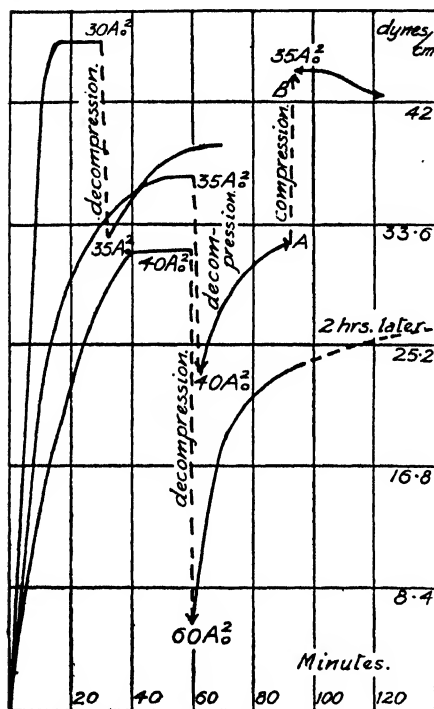


FIG. 2.—Compression and decompression of penetrated cetyl alcohol films by Na cetyl sulphate.

obtained being only 1 dyne smaller than that measured on the 35 A.<sup>2</sup> film at the same time (32 min.). If a film at 35 A.<sup>2</sup> is decompressed to 40 A.<sup>2</sup>, however, a corresponding difference of 13 dynes is found, showing that many less molecules have been penetrating the film at 35 A.<sup>2</sup> than at 40 A.<sup>2</sup>. In the same manner if a 40 A.<sup>2</sup> film is decompressed to 60 A.<sup>2</sup> a very low pressure is obtained. These experiments show the importance of the steric factors in the penetration phenomena. As would be expected, the penetration is facilitated when the surface becomes less covered with the alcohol molecules. If, after decompression, the film is allowed to stand at constant area, its pressure rises with time, and reaches a value which is, within experimental error, the same as that shown in the time-penetration curve for the same area.

Fig. 2 also shows that when a film which has come to equilibrium is compressed from, say 40 A.<sup>2</sup> to 35 A.<sup>2</sup> the pressure obtained is higher than that given by the spontaneous process represented in the time-penetration curve, showing that the compressed film contains more molecules, or a different surface arrangement of molecules. If the time-penetration curves of Fig. 1 are considered for periods greater than 80 min., it is observed that the pressure continues to rise very slowly. For example, an alcohol film of 100 A.<sup>2</sup> which reached a pressure of 20 dynes, 80 min. after the injection, had a pressure of 24.5 dynes after a period of 3 hr. 35 min. This shows that more and more cetyl sulphate molecules accumulate in the surface with time. Several examples not given in the figure have shown that if the experiments were carried on for a period of 24 hr., pressures up to 46 or 50 dynes were reached. It is considered by the authors that results on mixed films must be treated with particular caution when the experiments last for such a long period. Not only is the film liable to pick up impurities, but the paraffin wax used

to coat the glass slides and the edge of the trough may be solubilised when one of the components of the film is a detergent. Furthermore, cetyl sulphate would have a tendency to hydrolyse<sup>6</sup> after a time, especially in distilled water. For these reasons time-penetration curves in Fig. 1 are only shown for periods up to 80 min. This is just sufficient time to obtain a steady pressure value in the adsorption curve of pure cetyl sulphate in  $M./500$  phosphate buffer.

The effect of the concentration of phosphate has also been studied. Increasing the concentration of phosphate from  $M./500$  to  $M./25$  increases the pressure by a very small amount, i.e. a maximum of 2 dynes (at initial cetyl alcohol areas of  $100 \text{ A.}^2$  and  $40 \text{ A.}^2$ ). Schulman and Stenhagen used phosphate buffers in order to prevent hydrolysis of the cetyl sulphate during penetration. The presence of salts<sup>7</sup> is known to reduce the surface tension of many detergent solutions and to decrease the critical concentration for micelles. The following experiments carried out on distilled water show by comparison the part played by phosphate buffer on the rate of penetration of cetyl alcohol films by cetyl sulphate and on the final value of the pressure obtained. In Fig. 3 the time-penetration curves on distilled water at areas of  $100 \text{ A.}^2$ ,  $50 \text{ A.}^2$  and  $40 \text{ A.}^2$  are shown; it is seen that the penetration proceeds at a much lower speed than when phosphate is present, and that the pressure attained several hours after injection is lower than that attained 60 min. after injection in the presence of phosphate buffer. A direct demonstration of the effect of phosphate buffer is also shown in Fig. 3 curve II, where a quantity of phosphate sufficient to bring the bath to  $pH 8$  and to a concentration of  $M./500$  phosphate, is injected under a film of  $50 \text{ A.}^2$  2 hr. 22 min. after the cetyl sulphate injection. A sudden increase of pressure of 9 dynes is observed within the first 10 min.

At pressures greater than 26 dynes, when the mixed film is in the solid state, phase boundary potentials of 260 to 285 mv. are obtained in all cases whether the solid state is obtained by spontaneous penetration or by compression of the film and irrespective of whether phosphate is present or not. The effect of the phosphate is, apparently, to increase the thermodynamic activity of the cetyl sulphate and not to affect the electric charge; this would conform with the lowering of the critical concentration for micelles in the presence of salts which have been observed by different authors.<sup>7</sup> Whilst phase boundary potentials obtained for the solid films formed either by compression or by penetration are in agreement, the values of the pressure differ markedly as shown in Fig. 4. In this figure the curve obtained by Harkins on distilled water and the compression curve of the mixed film of Schulman and Stenhagen are both shown.

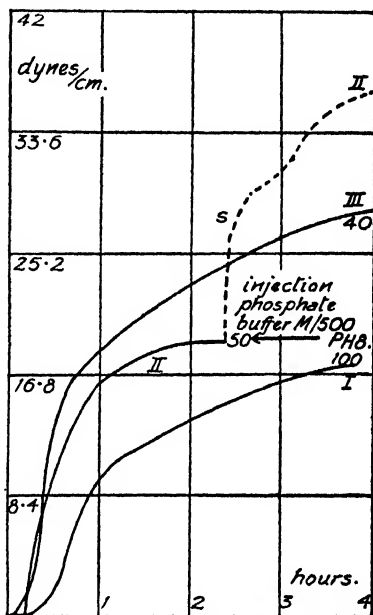


FIG. 3.—Time penetration curves in distilled water 1 mg./300 cc. Effect of phosphate buffer injections.

<sup>6</sup> Desseigne, *Bull. des Services Chim. de l'Etat*, 1944, Tome 31, 347-78.

<sup>7</sup> Powney and Addison, *Trans. Faraday Soc.*, 1937, 33, 1253; Long, Nutting and Harkins, *J. Amer. Chem. Soc.*, 1937, 59, 2197.



Between these two curves are plotted the values of the pressures obtained (80 min. or less after injection of the cetyl sulphate) using  $M./500$  phosphate buffer, these values being taken from the curves given in Fig. 1. It is seen that the pressures are above those of Harkins and agree fairly well with those of Schulman and Stenhagen only when the mixed film is liquid or viscous (initial area greater than  $75 \text{ A.}^2$ ); a marked difference is noted when the film is solid, confirming the fact that during the compression of a solid film, a closer state of packing is obtained than with spontaneous penetration. This very marked difference between compression values and penetration values is not due to the fact that Schulman and Stenhagen allowed only 2 min. intervals between readings for, by taking 15 and 20 min. intervals, we still find pressures much higher than those in the penetration curves of Harkins and the present authors.

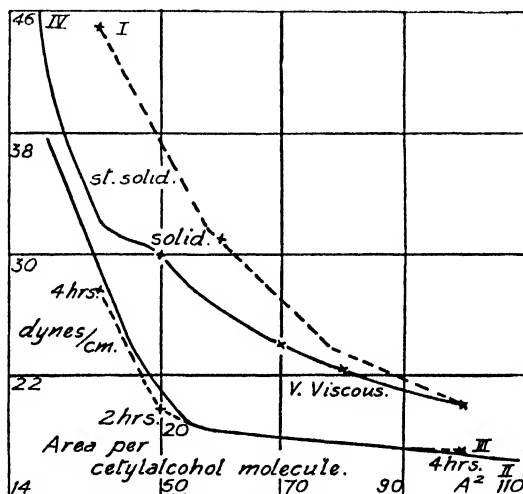


FIG. 4.—Comparison between penetrated and compressed mixed films of cetyl alcohol and sodium cetyl sulphate.

- I Compression curves by Schulman and Stenhagen on phosphate  $pH$  8.
- II Equilibrium values of Harkins and co-workers on distilled water.
- III Equilibrium values obtained by us on distilled water.
- IV Pressures attained 80 min. or less after injection on phosphate  $M./50$  and  $pH$  8.

The agreement between our surface pressures obtained by the penetration technique and those of Schulman and Stenhagen in the liquid region of the mixed film is explicable if, during compression of the liquid film, ejection of cetyl sulphate proceeds easily, thus allowing the same surface packing to be obtained as in the penetration process.

The fact that our pressure values using phosphate buffers are above those of Harkins is due to this author having carried out his experiments on distilled water. When no phosphate was used by us (curve 3) very good agreement with Harkins's data was obtained. It will be noted also that at high concentrations of alcohol, e.g.  $40 \text{ A.}^2$ ,  $35 \text{ A.}^2$  and  $30 \text{ A.}^2$  per molecule, our curve using phosphate buffer approaches more closely that of Harkins, as a very slight error in the area affects the pressure markedly in this region. This is because a very small number of cetyl sulphate molecules are needed, at these areas, to raise the pressure considerably (as shown previously) and thus the effect of the phosphate is much less noticeable.

Our thanks are due to Prof. E. K. Rideal for much helpful criticism; also to the French Centre of Research and the "Relations Culturelles" for a grant given to one of us (R. M.).

### Summary.

A study of the penetration of cetyl sulphate into cetyl alcohol films has been made. It is shown that the presence of phosphate in the underlying solution and the nature of the process to which the film is subjected, i.e. penetration at constant area or compression of a preformed mixed film, are two factors influencing strongly the results obtained. These factors would account for the discrepancies found in the values of the pressure of the mixed film by Schulman and Stenhagen, and Harkins, Florence and Copeland. During compression, the mixed film is presumably in a metastable state where the packing of the molecules is different from that resulting from spontaneous penetration owing to the high rigidity and the strong solid character of the mixed film. Rigidity and hysteresis effects make the study of this particular system difficult. It is preferable to refer to liquid or less rigid films, e.g. elaidyl alcohol-cetyl sulphate, cholesterol-cetyl sulphate, oleyl alcohol-cetyl sulphate<sup>3</sup> when conclusions about stoichiometric complexes are to be deduced from compression curves. The changes of slope in the penetration curve Fig. 4 denoting complexes between cetyl alcohol and sodium cetyl sulphate will be the subject of another paper on the general field of complexes in monolayers.

### Résumé.

On a étudié la pénétration du sulfate de cétyle dans des films d'alcool cétylique. On a montré que deux facteurs influencent fortement les résultats obtenus : ce sont la présence de phosphate dans la solution sous-jacente et la nature du traitement auquel le film est soumis—c'est-à-dire pénétration à surface constante ou compression d'un film mixte préformé. Ces facteurs rendraient compte des divergences trouvées par Schulman et Stenhagen d'une part et Harkins, Florence et Copeland d'autre part, dans les valeurs de la pression du film mixte. Pendant la compression, le film mixte est probablement dans un état métastable, où l'empilement des molécules est différent de celui résultant d'une pénétration spontanée, à cause de la grande rigidité et du caractère solide marqué du film mixte. Des effets de rigidité et d'hystérésis ont rendu difficile l'étude de ce système particulier. Lorsque l'on veut, à partir des courbes de compression, tirer certaines conclusions en ce qui concerne les complexes stoechiométriques, il est préférable de s'en rapporter à des films liquides ou moins rigides, tels que sulfate de cétyle et d'élaidyle, sulfate de cétyle et de cholestérol, enfin sulfate de cétyle et d'oléyle.

### Zusammenfassung.

Das Eindringen von Cetylsulfat in Cetylalkohol-filme ist untersucht worden, wobei gezeigt wurde, dass die Anwesenheit von Phosphat in der Lösung und die Art des Prozesses, dem der Film unterworfen wird (z.B. Eindringen bei konstanter Oberfläche oder Zusammenpressen eines vorhergebildeten gemischten Films), zwei Faktoren sind, die die Resultate stark beeinflussen. Diese Faktoren könnten die Widersprüche erklären, die zwischen den Werten von Schulmann und Stenhagen und denen von Harkins, Florence und Copeland für den Druck des gemischten Films bestehen. Bei Zusammenpressen ist der gemischte Film wahrscheinlich in einem metastabilen Zustand, in dem das Arrangement der Moleküle wegen der grossen Starrheit und Festigkeit des gemischten Films verschieden von dem ist, das bei spontanem Eindringen eintritt. Starrheit und Hystereseeffekte erschweren die Untersuchung dieses speziellen Systems. Es wäre vorzuziehen, Resultate für flüssige oder weniger starre Systeme zu verwenden (wie z.B. Elaidylalkohol-Cetylsulfat, Cholesterol-Cetylsulfat, Olein-alkohol-Cetylsulfat), wenn Folgerungen über stoichiometrische Komplexe aus den Kompressionskurven gezogen werden sollen.

*Department of Colloid Science,  
The University,  
Cambridge.*

# THE AGGREGATION OF CYANINE DYES IN AQUEOUS SOLUTION.

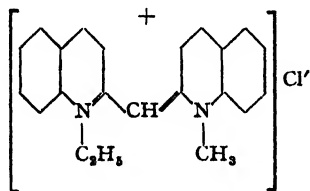
By H. O. DICKINSON.

Received 18th November, 1946.

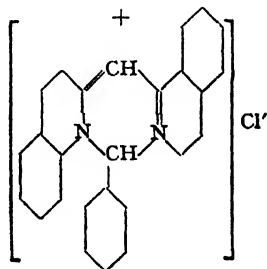
The aggregation of certain photographic sensitising dyes in aqueous solution has been established by the work of Scheibe,<sup>1</sup> Sheppard,<sup>2</sup> Jelley<sup>3</sup> and others. This aggregation is apparent from the anomalous spectral absorption of aqueous solutions of these dyes and the degree of aggregation has been calculated using data obtained from the absorption curves and from measurements of the partition coefficients of the dye between water and an immiscible solvent. The absorption curve of a typical dye such as 2 : 2'-diethyl pseudocyanine chloride exhibits  $\alpha$ - and  $\beta$ -bands in dilute aqueous solution and a third very intense  $\gamma$ - or "polymer" band in more concentrated solutions. In the case of pinacyanol the  $\beta$ -band has been attributed to reversible dimerisation and the  $\gamma$ -band is accepted as indicating a higher degree of polymerisation.<sup>4</sup>

The photographic sensitising properties of cyanine dyes are closely connected with their behaviour in aqueous solution. The spectral sensitivity curve of an emulsion sensitised with 2 : 2'-diethyl pseudocyanine chloride shows a pronounced peak at 5740 Å. whereas other types of cyanine dyes produce only a broad sensitivity band with no sharp maximum. This "peak" sensitivity is due to the polymerisation of the dye on the surface of the silver bromide grains and with panchromatic dyes it is possible to distinguish several sensitising bands corresponding to various dye aggregates. It seems probable that the difference between good and bad sensitisers may, in part, be accounted for by the inability of the latter to form aggregates either in solution or when adsorbed to silver bromide.

The present paper deals with two dyes,



2-ethyl-2'-methyl pseudocyanine chloride referred to as dye A.



isoquinoline red chloride referred to as dye B.

rather similar in structure but possessing markedly different sensitising and absorption properties. The degree of aggregation in dilute aqueous solution has been determined by osmotic pressure and electrical conductance measurements.

## Experimental.

(a) **Purification of Dyes.**—Samples of dye free from electrolyte were obtained by recrystallisation from ethyl alcohol followed by dialysis in a

<sup>1</sup> Scheibe, *Z. angew. Chem.*, 1937, 50, 51 and 212.

<sup>2</sup> Sheppard, *Science*, 1941, 93, 42.

<sup>3</sup> Jelley, *Nature*, 1936, 138, 1009.

<sup>4</sup> Scheibe, *Kolloid. Z.*, 1938, 82, 1.





FIG. 3



FIG. 4

U. S. GEOLOGICAL SURVEY

parchment membrane and further recrystallisation from a mixture of acetone and ethyl alcohol.

(b) **Absorption Measurements.**—The absorption curves of aqueous solutions of the dyes at various concentrations, measured on a Hilger-Nutting spectrophotometer, are shown in Fig. 1 and 2. These curves are plotted as density against wavelength. No attempt has been made to calculate the molar extinction coefficients but the relative heights of the three absorption bands can be readily seen at each concentration. At high concentrations dye A exhibits the characteristic narrow polymer band at 5730 Å., the  $\alpha$ - and  $\beta$ -bands are just apparent. In more dilute solution ( $2.5 \times 10^{-3}$ ) the  $\beta$ -band is stronger than the  $\alpha$ -band but the latter becomes more pronounced as dilution is continued. Dye B shows no change in absorption properties over the range of concentrations studied.

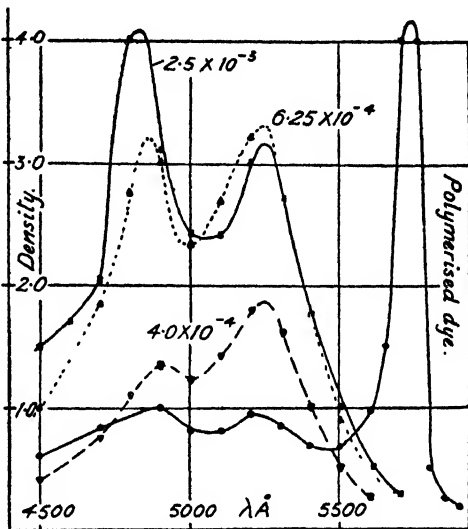


FIG. 1.

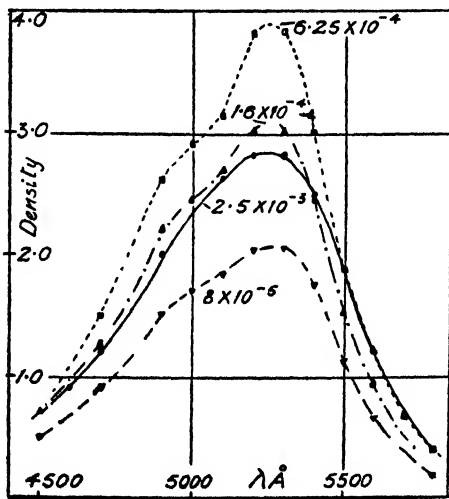


FIG. 2.

(c) **Sensitising Properties.**—

The spectrograms of an emulsion sensitised with the two dyes are shown in Fig. 3 and 4. Each unit in the ordinate scale corresponds to a threefold increase in sensitivity.

(d) **Osmotic Pressure Measurements.**—If the osmotic pressure is to be a true measure of the concentration of non-diffusible ions, the back pressure caused by unequal distribution of diffusible ions must be eliminated or calculated. The osmotic pressure of a dye chloride measured against KCl solution is given by the expression

$$\pi = RT(K_i + D + Cl_i - K_o - Cl_o)$$

where the subscripts  $i$  and  $o$  denote solution inside and outside

side the membrane.  $K$ ,  $Cl$  and  $D$  represent the concentrations of potassium, chloride and dye ions respectively. It can be shown, by applying Donnan's equations for membrane equilibria, that, if the concentration of electrolyte outside the membrane is progressively increased, the concentrations of diffusible ions inside and outside the membrane approach equality and the back pressure is nearly eliminated. By measuring the osmotic

pressure of a dye solution against a series of salt solutions a limiting value of the pressure can be obtained which is that due solely to the non-diffusible ions. This procedure has been adopted for the two dyes, each being measured against a series of KCl solutions.

**Preparation of Colloidion Membranes.**<sup>5</sup>—A test-tube with a small hole in the bottom was mounted horizontally on the spindle of an electric motor fitted with a reduction gear. A 4% colloidion solution in ether-alcohol mixture containing 1 cc. of ethylene glycol per g. of pyroxylin was poured on to the tube rotating at 5 rev./min. A second coat was poured when the first had dried for 10 min., excess solvent being removed with blotting paper. After the second coating the tube was rotated for 30 min. and then removed and dried in a vertical position. Membranes used too soon after coating proved to be too permeable and at least 12 hr. drying was necessary. When dry the membranes can be slipped off the test-tube after soaking in water for 1 hr. The permeability was checked by placing an osmometer containing water in water; the pressures equalised in a time considerably less than that required by the experimental solutions to reach equilibrium. A simple water manometer proved satisfactory. A short glass tube of the same diameter as the membrane but slightly tapered was sealed to the manometer tube (4 mm. bore). The membrane was then  $\frac{3}{4}$  filled with dye solution, slipped over the tapered end of the glass tube, wired on and sealed with colloidion solution. The osmometer was then filled to the required height by means of a small pipette. Preliminary experiments indicated the order of pressures to be expected and the osmometers were filled so that the rise or fall was as small as possible thus minimising error due to concentration changes.

In every experiment, equilibrium was reached after 48 hr. and the permeability of the membranes to chloride was checked by measuring the chloride ion concentration inside and outside the membrane with an Ag—AgCl electrode. With strong (N./100) KCl solutions outside the membrane, the chloride ion concentrations were identical when equilibrium pressure had been attained. Both dyes were fairly strongly adsorbed by the membranes and consequently the concentration of dye inside the membrane at equilibrium had to be determined. This was done by diluting a sample of the solution with ethyl alcohol and comparing it with a standard solution using a spectrophotometer.

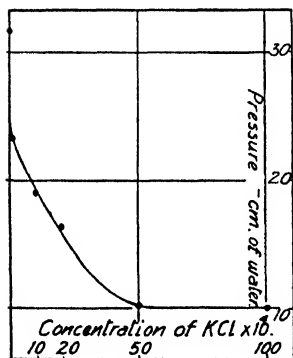


FIG. 5.

## Results.

**Dye A.**—The results are summarised in Fig. 5. The limiting pressure was taken as 10.0 cm. at a dye concentration of  $2.4 \times 10^{-3}$ . The ratio theoretical pressure/observed pressure = 5.7 where the theoretical pressure is calculated as the pressure developed by a monomeric solution of the dye.

**Dye B.**—The adsorption of this dye by the membrane was not constant and a limiting value of the osmotic pressure could therefore not be obtained. The ratio theoretical pressure/observed pressure is given for each determination. In the last two determinations the ratio of KCl: dye is sufficiently large to render the back pressure

negligible compared with the pressure due to the non-diffusible ions.

(e) **Conductivity Measurements.**—A Pyrex glass conductivity cell (cell constant = 0.263) was used; the conductivity water used had a

<sup>5</sup> Adair, *Cambridge Univ. Colloid Sci. Course*, 1945.

conductivity of  $2.3 \times 10^{-8}$  mhos. All measurements were made in a thermostat at  $25^\circ \text{C}$ . The results are plotted in Fig. 6. Both dyes show a linear relationship between  $\sqrt{C}$  and  $\Lambda$  and there is no indication of a maximum value of  $\Lambda$ , indicating that the degree of aggregation appears

TABLE I.

Solution Outside Membrane.	Height of Water Manometer (cm.).	Dye Concentration Inside Membrane (M.).	Theoretical Pressure Observed Pressure *
$1 \times 10^{-3}$ N. KCl	16.2	$6.2 \times 10^{-4}$	0.93
$2.5 \times 10^{-3}$ N. "	14.5	$6.8 \times 10^{-4}$	1.1
$5 \times 10^{-3}$ N. "	12.3	$4.3 \times 10^{-4}$	0.85
$1 \times 10^{-2}$ N. "	13.7	$7.1 \times 10^{-4}$	1.26

to be fairly constant over the range of concentrations studied. Some additional experiments with dye A showed that at higher concentrations the equivalent conductivity drops. This drop appears to be related to the increase in viscosity of the dye solution.

The method described by Holmes and Standing <sup>6</sup> has been used to calculate the degree of aggregation from the conductivity data. By equating the electrostatic driving force on the micelle to the frictional resistance and assuming that no anions are included in the dye aggregate, the aggregation number  $G$  is given by the expression,

$$G = 0.852 (M/\rho)^{1/2} (\eta)^{3/2} (\Lambda - u)$$

where  $M$  = molecular weight of dye cation,  $\rho$  = density of micelle,

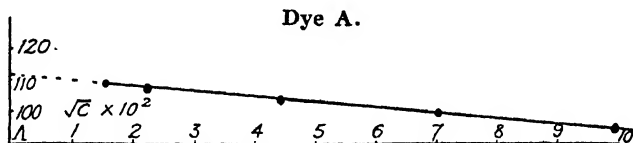


FIG. 6.

$\eta$  = viscosity of solvent,  $u$  = equivalent conductivity of anion. To obtain an approximate value of  $\Lambda$ , the  $\Lambda - \sqrt{C}$  curve is extrapolated to infinite dilution thus obtaining a value of the equivalent conductance of the micelle free from interionic effects.

The value of the micellar density is not known but Robinson <sup>7</sup> assumes it to lie between the density of the solution and that of the solid dye. The density of the solution is in each case nearly 1 and the densities of the solid dyes have been measured by the specific gravity bottle method using benzene as the non-solvent liquid. Values of  $G$  for the two dyes using both values of  $\rho$  are given in Table IV.

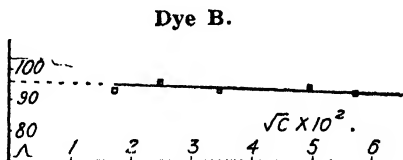


FIG. 6.

<sup>6</sup> Holmes and Standing, *Trans. Faraday Soc.*, 1945, 41, 506.

<sup>7</sup> Robinson and Garrett, *ibid.*, 1939, 35, 771.



## Discussion.

Both methods of measurement indicate that dye *B* exists in solution in the monomeric form whereas dye *A* is aggregated even at low concentrations ( $2 \times 10^{-3}$ ). The absorption properties of the two dyes support this conclusion.

The difference between the two values of *G* for dye *A* could be explained by the inclusion of anions in the cationic micelle thus decreasing the value of *G* calculated from the conductance data. A more likely explanation, however, is the presence of electrolyte in the osmotic pressure experiments. It was found, from light absorption measurements that electrolyte added to an aqueous solution of dye *A* affected the degree of aggregation. Also, the sample of dye *A* gelled at lower concentrations in KCl solution than in distilled water. It seems reasonable to assume that the higher value of *G* obtained from the osmotic measurements is due to the aggregating influence of the KCl and that the figure obtained from the conductance measurements is a fair indication of the size of aggregate under electrolyte-free conditions. The figure of 2.3 is in fair agreement with that of 2 obtained by Sheppard and Geddes<sup>8</sup> from measurements of conductance, transport number and diffusion properties of aqueous solutions of cyanine dyes. The aggregation number can only be regarded as a mean value as several aggregates of different sizes may exist in solution.

The emulsion spectrograms of the two dyes show that *A* produces a peak at 5720 Å. with a sharp cut-off on the longer wavelength side. *B* produces a rather feeble broad band of sensitivity with no pronounced

TABLE II.

Dye.	<i>A.</i>	<i>u.</i>	<i>p.</i>	<i>G.</i>
<i>A</i> . .	112	75.5	1.26	2.5
<i>A</i> . .	112	75.5	1.0	2.8
<i>B</i> . .	96	75.5	1.26	1.4
<i>B</i> . .	96	75.5	1.0	1.2

maximum. Peaks similar to the one produced by dye *A* have been observed with other cyanine and carbocyanine dyes and are usually attributed to an aggregated form of the dye adsorbed to the surface of the AgBr. The results of the aggregation measurements with dyes

*A* and *B* confirm the belief that the presence of "peak" sensitising is an indication of dye polymerisation as it is unlikely that a dye which cannot aggregate even to a limited extent in solution will do so when adsorbed on AgBr. The sensitising maximum of dye *A* is closely related to the absorption band of the polymerised dye in aqueous solution and this peak sensitising is undoubtedly due to an aggregated form of the dye. The fact that high aggregates of dye *A* do not exist in dilute aqueous solution is further evidence in favour of the theory that polymerisation on AgBr proceeds by adsorption of dimeric ions from solution. If a dye such as *B* can exist only in the monomeric form then its sensitising band will show no pronounced peak.

Scheibe's work on the polymerisation of cyanine dyes when adsorbed to mica,<sup>9</sup> together with the observations of Sheppard, Lambert and Walker<sup>10</sup> suggests that, in the polymeric state the distance between adjacent dye molecules is approximately 3.5-4.0 Å. If the polymer is built up from dimer units the distance between dye molecules (or cations) in the dimer must have the same value.

The different properties of the two dyes can possibly be accounted for by steric factors. Dye *B* contains a benzyl group which will project beyond the plane of the molecule whereas *A* possesses a planar structure.

<sup>8</sup> Sheppard and Geddes, *J. Amer. Chem. Soc.*, 1944, **66**, 2007.

<sup>9</sup> Scheibe, *Z. angew. Chem.*, 1939, **52**, 631.

<sup>10</sup> Sheppard, Lambert, and Walker, *J. Chem. Physics*, 1939, **7**, 265.

The non-planarity of the dye *B* cations will prevent the close approach necessary for dimer formation. The importance of planarity of dye molecules as a factor influencing the sensitising properties of dyes has been stressed by Sheppard and co-workers<sup>11</sup> who found that non-planar isomers were feeble sensitisers compared with the planar dyes although both forms of dye were adsorbed to AgBr. Planarity has been considered essential for maximum resonance in the dye molecule but may also play an important part in determining the aggregation properties of the dye. A study of a related series of merocyanine dyes has shown that small structural changes which have little effect upon the molar extinction coefficient or the position of the absorption band can produce complete loss of sensitising power. These structural changes, however, are sufficient to prevent the approach of two dye molecules to within 4 Å. (as determined by calculations of the dimensions of the substituent groups), hence dimerisation is inhibited and possible polymer formation prevented.

The author's thanks are due to the Directors of Ilford Limited for permission to publish this paper.

### Summary.

The absorption and photographic sensitising properties of 2-ethyl-2'-methyl pseudocyanine chloride and *isoquinoline* red have been examined. The degree of aggregation of both dyes in aqueous solution has been determined by osmotic pressure and electrical conductance measurements, and the absorption and sensitising properties of the two dyes have been related to their degree of aggregation.

### Résumé.

On a examiné les produits d'absorption et de sensibilisation photographique du chlorure d'éthyl-2 méthyl-2' pseudocyanine et du chlorure du rouge d'*isoquinoléine*. On a déterminé, par des mesures de pression osmotique et de conductance électrique, le degré d'aggrégation des deux colorants en solution aqueuse et on a relié celui-ci aux propriétés d'absorption et de sensibilisation.

### Zusammenfassung.

Die Absorption und photographischen Sensibilisierereigenschaften von 2-Äthyl-2-Methyl-pseudocyaninchlorid und "Isoquinoline Red" sind untersucht worden. Der Aggregationsgrad der beiden Farbstoffe in wässriger Lösung ist durch Messungen des osmotischen Drucks und der elektrischen Leitfähigkeit bestimmt worden und mit den Absorptions- und Sensibilisierereigenschaften in Zusammenhang gebracht worden.

*Research Laboratory,  
Ilford Ltd.,  
Essex.*

---

## THE AGGREGATION OF DIRECT DYES AND OF METHYLENE BLUE 2B IN AQUEOUS SOLUTION.

BY D. R. LEMIN AND T. VICKERSTAFF.

*Received 14th January, 1946. As amended, 29th March, 1946.*

The aggregation of dyes in aqueous solution has already been the subject of much study in view of the importance it may have in determining dyeing behaviour especially in the case of direct dyes on cellulosic fibres. A full evaluation of the importance of aggregation in dyeing is not possible at the present time, owing to the absence of adequate data

<sup>11</sup> Sheppard, Lambert, and Walker, *Nature*, 1940, 145, 386.

on a sufficient number of dyes under a variety of dyeing conditions. This lack of information is due, not to any lack of interest in the subject, but to the tedious and difficult experimental methods available for the determination of aggregation and the ambiguous nature of the results when obtained. The method of measurement in most general use involves measuring the speed of diffusion of a dye from aqueous solution into pure water or into a dilute solution of an inorganic electrolyte. Difficulties arise owing to the fact that the dye itself is an electrolyte so that great precautions must be taken to avoid accelerated diffusion due to the potential gradient existing across the diffusing boundary. Even if these difficulties are surmounted, however, the interpretation of results is difficult for if the dye solution contains aggregates of varying size in dynamic equilibrium, then at the diffusing boundary it may be expected that the smaller particles will diffuse more rapidly, thus upsetting the equilibrium and leading to break-down of higher aggregates, giving a fictitiously low degree of aggregation.

Other methods of measuring particles size are open to similar objections and clearly there would be considerable advantage in some way of measuring particle size which would involve no disturbance of the state of the solution. A method which relies upon changes in absorption spectra on aggregation might well satisfy these requirements, and the present paper records a study of the possibilities of this approach.

The subject has been investigated previously by Kortum<sup>1</sup> and by Rabinowitch and Epstein.<sup>2</sup> The latter workers obtained the most outstanding results with the basic dyestuffs, Methylene Blue and Thionine. They found that the absorption peak of aqueous Methylene Blue solution moved towards longer wave-lengths on dilution, and this they ascribed to the existence in solution of monomeric and dimeric forms of the dye, the proportions of which varied with concentration. From the experimental results they were able to calculate the proportion of monomer and dimer in any solution of Methylene Blue and to follow the change in the equilibrium distribution with temperature.

Kortum<sup>1</sup> investigated a much wider range of dyes including Methylene Blue together with many acid and direct dyes and showed that in nearly all cases the value of the extinction coefficient changed with concentration, although the changes with all the direct dyes were very much smaller than with Methylene Blue.

From these results it appears that aggregation does produce changes in the absorption spectra of dyes which might be used as a measure of that aggregation, and accordingly some preliminary experiments were carried out to test the feasibility of the approach

### Experimental.

The method employed was to prepare solutions of dyes covering a wide range of concentrations and to measure the absorption spectra of these in a spectrophotometer over the range 4400-7000 Å. In order to do this accurately it was necessary to vary the thickness of solution examined and a number of glass cells were used giving optical paths through the solution ranging from 200-1 mm. In addition, a micrometer cell was employed which gave thickness from 0 to 5 mm. in steps of 0.01 mm. Some of the cells were jacketed for measurements at elevated temperatures. Much work was done with a 1 cm. cell fitted with inlet and outlet tubes through which dye solution at temperatures up to 80° C. could be circulated from a thermostated reservoir by means of a diaphragm pump.

The direct dyes used were purified by a repeated precipitation from

<sup>1</sup> Kortum, *Z. physik. Chem.*, 1936, **B 33**, 255.

<sup>2</sup> Rabinowitch and Epstein, *J. Amer. Chem. Soc.*, 1941, **63**, 69.

aqueous solution by sodium acetate, followed by boiling with alcohol to remove sodium acetate and finally were crystallised from water. The Methylene Blue 2B was purified by repeated crystallisation from alcohol followed by three crystallisations from water. When examined chromatographically it appeared homogeneous and titration with titanous sulphate indicated a purity of 97 % calculated on the weight after drying at 110° C. to constant weight.

**Measurements on Single Direct Dyes.**—As a preliminary step, measurements were made on three commercial unpurified direct dyes and in all cases deviation from Beers' Law was observed. The results are shown in Table I.

TABLE I.—VARIATION OF OPTICAL DENSITY WITH CONCENTRATION.

Chlorazol Sky Blue FFS (Colour Index 518).			Durazol Fast Yellow G 400 (Colour Index 814).			Durazol Fast Rubine B 150.		
Wavelength 6250 Å.			Wavelength 4500 Å.			Wavelength 5300 Å.		
Conc. g./l.	Cell Length, mm.	Observed Density.	Conc. g./l.	Cell Length, mm.	Observed Density.	Conc. g./l.	Cell Length, mm.	Observed Density.
16.0	0.1	1.96	4.0	0.2	0.85	4.0	0.2	1.80
3.2	0.5	2.14	0.8	1.0	0.97	0.8	1.0	2.10
1.6	1.0	2.17	0.2	4.0	1.04	0.2	4.0	2.13
0.8	2.0	2.24	0.02	40.0	1.04	0.02	40.0	2.14
0.4	4.0	2.25	0.01	80.0	1.02	0.01	80.0	2.20
0.04	40.0	2.33						
0.02	80.0	2.41						

These results suggest that the extinction coefficients of the direct dyes decrease with increasing aggregation and this is supported by experiments in which the addition of electrolyte decreased optical densities while an increase of temperature increased optical densities. Since these changes are known to increase and decrease aggregation respectively, there can be little doubt as to the origin of the effect. The decrease in aggregation caused by an increase in temperature was readily reversible, the density returning to its original value on cooling.

When an attempt was made to place the method on a quantitative basis, however, the inherent difficulties quickly became apparent. The problem was approached along the lines used by Rabinowitch and Epstein in which an oversimplified model of the aggregation process is employed. In this model, aggregation is supposed to proceed to the dimeric stage only, with the dimer in dynamic equilibrium with monomer according to the equation :



In actual practice it is certain that higher polymers are formed. Thus Valko<sup>3</sup> reports an aggregation number of 14 for Chlorazol Sky Blue FF and this is supported by experiments which will be described later. It is, however, possible that in a relatively dilute solution the monomer and dimer do form the bulk of the solute so that it may be justifiable to work with this simplified model under certain conditions.

At infinite dilution with this simple system, the dye is wholly in the monomeric form and at infinite concentration in the dimeric form, so that by plotting the observed extinction coefficient against concentration and extrapolating to zero and infinite concentration, it is possible to estimate the extinction coefficients,  $\epsilon_m$  and  $\epsilon_d$  of the monomer and dimer respectively. If the extinction coefficient of any solution containing a

<sup>3</sup> Valko, *Trans. Faraday Soc.*, 1935, **31**, 237.

mixture of the two forms is  $\epsilon_d$  then the degree of association  $\alpha$  which is the fraction of the total dye present in the dimeric form, will be

$$\epsilon_d = (1 - 2\alpha)\epsilon_m + \alpha\epsilon_d$$

or

$$\alpha = \frac{\epsilon_d - \epsilon_m}{\epsilon_d - 2\epsilon_m}$$

The accuracy with which the degree of association  $\alpha$  can be determined is therefore dependent on the accuracy with which a difference in optical densities can be measured, and in particular it can be shown on statistical grounds that the standard error in  $\alpha$  will be very great unless the magnitude of the denominator is more than 4 times the standard error in determining the extinction coefficients,  $\epsilon_d$  and  $\epsilon_m$ . Since both these values are determined by extrapolation, a reasonable degree of accuracy in  $\alpha$  can be obtained only if the values of  $\epsilon_m$  and  $\epsilon_d$  are widely different and if the optical densities of the solution are determined with great precision. In the present experiments, the limitations of the apparatus available precluded any very great degree of precision in the optical measurements, but by taking the average value of a large number of estimations (usually 20), the error in the density measurements was reduced to about  $\pm 1\%$ . Even so the error in the extrapolated extinction coefficient is probably at least  $\pm 5\%$  and in the most favourable case of Chlorazol Sky Blue FF (Table I) this leads to an error in  $\alpha$  of 20% or more, depending upon the actual value of  $\epsilon_d$ . Results of such accuracy are of little practical value and the use of this method for measuring the aggregation of direct dyes must therefore be abandoned until some method of measuring optical densities with a minimum accuracy of  $\pm 0.1\%$  is developed.

This disappointing conclusion does not apply to all dye systems, for if the optical differences between monomer and polymer are great, then the degree of association may be determined with sufficient accuracy with a more reasonable standard of precision in the optical measurements. The most interesting example of such a system appears from the work of both Kortum and Rabinowitch to be Methylene Blue 2B but another system offering some promise occurs in binary mixtures of direct dyes in aqueous solution, and such mixtures were examined in some detail.

**Mixtures of Direct Dyes.**—It has been shown by Neale and Stringfellow<sup>4</sup> that the absorption spectra of direct dyes are not always additive in mixtures. Thus the optical density of a mixture of two dyes, at a particular wavelength, was not equal to the sum of the densities of the components. This behaviour must be attributed to the formation of complexes between the dyes, a view which is supported by the fact that the addition of pyridine renders the spectra additive by preventing complex formation. The differences between the observed absorption spectra of such mixtures and the calculated spectra are often quite large and it seemed possible that the optical method might yield satisfactory results in this case.

In the first place a number of dye mixtures were examined in aqueous solutions and non-additivity was observed with binary mixtures of Chrysophenine G (Colour Index 365) and Chlorazol Blue B (Colour Index 406), Chlorazol Fast Scarlet 4B and Chlorazol Sky Blue FF (Colour Index 518), Benzopurpurine 4B (Colour Index 448), and Chlorazol Sky Blue FF and Durazol Red 2B (Colour Index 278) and Chlorazol Sky Blue FF. A mixture of Durazol Fast Rubine B and Durazol Fast Blue 2GN appeared to behave additively while a mixture of Durazol Fast Yellow 6G and Chlorazol Blue B showed only slight deviation. In all cases, the deviation consisted of an increased absorption at the shorter wavelength peak and a decreased absorption at the longer wavelength peak. At the same time the absorption maxima were shifted towards longer wavelengths. From the examination of these combinations, the mixture of Chlorazol Sky Blue FF and Durazol Red 2B was selected as being most suitable for further

<sup>4</sup> Neale and Stringfellow, *J. Soc. Dyers. Col.*, 1943, **59**, 241.

examination. The complete absorption curves of these dyes and of their mixture are shown in Fig. 1. Experiments were first carried out to determine whether the complex between the two dyes was bimolecular or of a higher order. For this purpose, measurements were made of mixtures

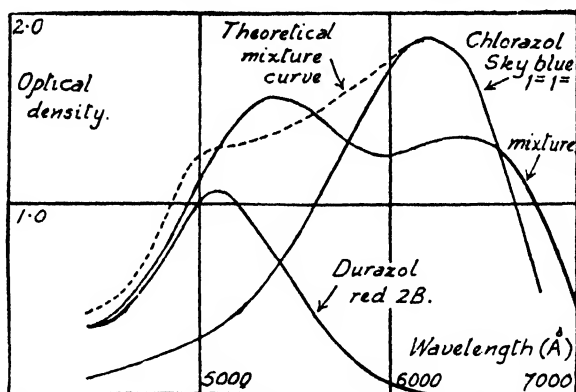


FIG. 1.

of the two dyes in different molecular proportions at a wavelength of 5350 Å., since at this wavelength, equimolecular solutions of the two dyes have similar densities while the deviation from additive behaviour is large. The results are given in Table II.

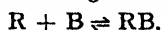
TABLE II.—MIXTURES OF CHLORAZOL SKY BLUE FF AND DURAZOL RED 2B AT ROOM TEMPERATURE. 1 cm. cell.  $\lambda = 5350 \text{ Å.}$

Single Dyes.			
Solution (mol./l.).	Density.	Comparative Density.	
Red ; $2.5 \times 10^{-5}$	0.882	0.882	
Red ; $5.0 \times 10^{-5}$	1.723	0.862	
Red ; $7.5 \times 10^{-5}$	2.531	0.844	
Blue ; $2.5 \times 10^{-5}$	0.660	0.660	
Blue ; $5.0 \times 10^{-5}$	1.303	0.652	
Blue ; $7.5 \times 10^{-5}$	1.907	0.636	

Mixtures.	Observed Density.	Theoretical Density.	Difference.
1 Red + 1 Blue (a)	1.735	1.542	0.193
2 Red + 1 Blue (b)	2.652	2.383	0.269
1 Red + 2 Blue (c)	2.449	2.185	0.264
3 Red + 1 Blue (d)	3.516	3.191	0.325
1 Red + 3 Blue (e)	3.124	2.789	0.335

From the column showing differences between the observed and calculated optical densities of the mixtures, it will be seen that an increase in concentration of one component produces the same change in the difference column (due to the formation of the complex) whether the components be red or blue. This indicates quite clearly that the complex is a bimolecular one formed according to the reaction



In order to use these results to estimate the degree of association of the dyes, it is again necessary to make some simplifying assumption, namely that association proceeds only to the dimeric state and that the association of the individual dyes with themselves is negligible as compared with their association with one another. The validity of the last of these assumptions is open to question. Certainly, however, the change in optical density of either components on doubling its concentration is of much smaller magnitude than the change produced by mixing.

On these assumptions, the observed optical density  $D_0$  at any specific wavelength of a mixture containing  $n$  moles of blue and  $m$  moles of red dye per litre will be

$$D_0 = (m - k)D_R + (n - k)D_B + kD_{RB}$$

where  $k$  is the molecular concentration of dye complex and  $D_R$ ,  $D_B$ ,  $D_{RB}$  are the optical densities of molar solutions of the two components and the complex, at the same wavelength. Hence,

$$k = \frac{D_0 - (mD_R + nD_B)}{D_{RB} - (D_R + D_B)}$$

This expression contains the unknown quantity  $D_{RB}$  but this may be eliminated by the examination of mixtures containing different proportions of the two components. Thus, in a solution molar with respect to each component

$$k_{11} = d_1/x$$

where  $x$  is the unknown denominator and  $d_1$  the observed difference in density due to association. Similarly in a mixture of 2 moles. of red and 1 mole. of blue per l.

$$k_{12} = d_2/x$$

combining these expressions

$$k_{11} = d_1/d_2 k_{12}$$

$k_{11}$  and  $k_{12}$  are also related by means of the equation

$$\frac{k_{11}}{(1 - k_{11})^2} = \frac{k_{12}}{(1 - k_{12})(2 - k_{12})} = K.$$

By substitution for  $k_{11}$  it is then possible to calculate  $k_{11}$  in terms of observed optical densities. In the present case, taking the mean density differences where two results are available, the observed densities can be combined in three ways to give the following values of  $K$  and  $\alpha$  the degree of association.

TABLE III.

Combinations.	$\alpha$ .	$K$ .
$k_{11} + k_{12}$	$\alpha_{11} = 0.58$	$13.1 \times 10^4$
$k_{11} + k_{13}$	$\alpha_{11} = 0.43$	$5.3 \times 10^4$
$k_{12} + k_{13}$	$\alpha_{12} = 0.47$	$5.8 \times 10^4$

where the differences between the theoretical and observed densities is about three times greater and where the density of the red component is almost zero. Solutions containing Chlorazol Sky Blue FF alone and with additions of 1, 2, 4 and 8 times the quantity of Durazol Red 2B were therefore examined at this wavelength. The results obtained are shown in Table IV and the derived values for  $\alpha$  and  $K$  in Table V.

The value of  $K$  is rather higher than that obtained from the measurements at 5350 Å. but is of the same order. Taking the mean value of  $K$ , the theoretical degree of association of the blue in the various mixtures

The large variation in the results is unsatisfactory but the accuracy of the measurements could not be increased with the available apparatus. Some improvements can be obtained, however, by working at a wavelength of 6200 Å.,

may be calculated and hence the theoretical density of the red-blue complex at 6200 Å. and the theoretical density of the mixture.

The results obtained using the mean value of  $K$  of  $1.46 \times 10^5$  and a density of complex 1.038 are given in Table VI.

TABLE IV.

Mixtures of Chlorazol Sky Blue FF and Durazol Red 2B measured at 6200 Å. and room temperature (16° C.). Each solution contained  $2.5 \times 10^{-5}$  moles. of Blue dye/l.

Solution.	Density (1 cm. cell).	Difference due to Association.
Blue alone	1.784	—
Red alone *	0.011	—
Blue + Red (1)	1.342	0.442
Blue + 2 Red (2)	1.149	0.635
Blue + 4 Red (3)	1.080	0.704
Blue + 8 Red (4)	1.054	0.730

\* Value for absorption of red calculated from determination in 10 cm. cell.

In spite of the large variations in  $\alpha$  and  $K$  these results are in excellent agreement with the observed values, the difference nowhere being greater than 2 % on the density figures.

TABLE V.—DERIVED VALUES OF  $\alpha$  AND  $K$  FROM ABOVE RESULTS.

Pair of Differences Used.	$\alpha$ .	$K \times 10^{-4}$ .	Mean $K \times 10^{-4}$ .
1 + 2	$\alpha_{11} = 0.51$	8.48	14.6
1 + 3	$\alpha_{11} = 0.57$	12.32	
1 + 4	$\alpha_{11} = 0.63$	18.40	
2 + 3	$\alpha_{12} = 0.84$	18.08	
2 + 4	$\alpha_{12} = 0.85$	19.68	
3 + 4	$\alpha_{14} = 0.95$	10.80	

Having obtained from these results a value for  $D_{RB}$  it is a relatively simple matter to follow the change in association with change of temperature. A mixture of Chlorazol Sky Blue FF and Durazol Red 2B

TABLE VI.

Mixture.	Degree of Association of Blue Component.	Density Calculated.	Density Observed.
Blue + Red	0.60	1.34	1.34
Blue + 2 Red	0.82	1.17	1.15
Blue + 4 Red	0.92	1.10	1.08
Blue + 8 Red	0.97	1.06	1.05

containing  $2.5 \times 10^{-5}$  mole/l. of each component was examined over the temperature range 15°–80° C. with the results shown in Table VII. A correction has been applied for the increase in volume with increasing temperature.



At this concentration it will be observed that the effect of temperature on the density of the blue component is negligible. The density of the red component is also very small and changes in it have little or no effect on the results. The values of the densities of the red, blue and complex dyes in the mixture which were used in calculating  $k$  and  $K$  were 0.011,

TABLE VII.

Solution.	Temp. ° C.	Density ( $\lambda = 6200 \text{ \AA}$ ).	Association.	$K$ .
Red alone . . . .	16	0.011	—	—
Blue " . . . .	16	1.784	—	—
" " . . . .	20.5	1.787	—	—
" " . . . .	35	1.797	—	—
" " . . . .	59	1.791	—	—
Red + Blue mixture .	16	1.340	0.60	$1.50 \times 10^5$
" " " . . . .	20.5	1.369	0.57	$1.23 \times 10^5$
" " " . . . .	35	1.428	0.49	$7.54 \times 10^4$
" " " . . . .	50	1.509	0.38	$4.08 \times 10^4$
" " " . . . .	60	1.582	0.29	$2.30 \times 10^4$
" " " . . . .	66	1.636	0.22	$1.45 \times 10^4$
" " " . . . .	70	1.680	0.16	$9.08 \times 10^3$
" " " . . . .	79	1.793	0.01	$4.08 \times 10^2$

1.790 and 1.038 respectively. The results show clearly that complex formation is negligible at temperatures above 80° c. but this might not be the case in a normal dyebath containing an electrolyte which will tend to increase aggregation.

If  $\log K$  is plotted against  $1/T$  the resulting graph is linear over the lower range of temperature but deviates at higher temperatures. This is

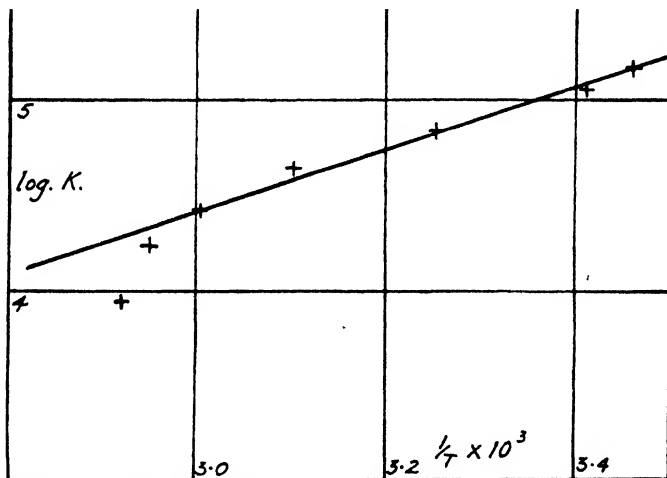


FIG. 2.

shown in Fig. 2. The deviation at higher temperatures is probably due to the increasing experimental error of measurement as the observed density approaches more closely to the density of the blue component. From the graph shown the value of  $-7300 \text{ cal.}$  may be calculated for the heat of reaction, while the free energy changes and entropy changes at 20° c. and 60° c. are  $-6800$ ,  $-6500 \text{ cal.}$  and  $-1.8$  and  $-2.6 \text{ cal/}^\circ \text{ c.}$

respectively. The value obtained for the heat of reaction is of a similar order to the heat of reaction of Chlorazol Sky Blue FF with cotton.

**Methylene Blue.**—The experiments described above show that optical methods may be used to give a very rough estimate of aggregation with some single direct dyes and a rather more accurate estimate in mixtures of dyes which show the phenomenon of non-additive absorption spectra. One of the objects of the present investigation, however, was to try to compare the aggregation of dyes as measured by an optical method with the results obtained with the normal diffusion method and for this purpose the results obtained so far are not sufficiently accurate. It now appears from the work already described and also from references in the literature that Methylene Blue is almost the only dye which shows sufficiently large changes in its absorption spectra on aggregation, to enable the optical

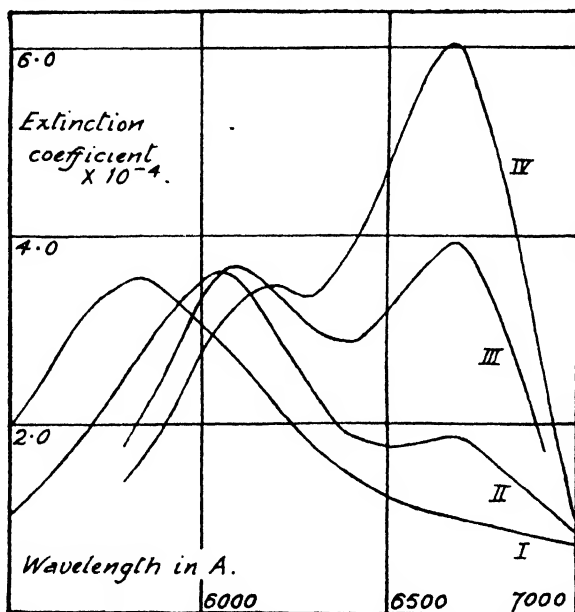


FIG. 3.

I =  $3.13 \times 10^{-3}$  mol./l.      II =  $2.5 \times 10^{-3}$  mol./l.  
 III =  $2.0 \times 10^{-4}$  mol./l.      IV =  $2.0 \times 10^{-3}$  mol./l.

method to yield results of sufficient precision for the comparison. Accordingly measurements on Methylene Blue were carried out in order to confirm the results obtained by Rabinowitch and Epstein and then to apply these results to a comparison between diffusion and optical methods of measuring aggregation. The former workers examined this dyestuff over the concentration range  $2 \times 10^{-3}$  to  $2 \times 10^{-6}$  mol./l. They found that the peak of absorption shifts from 6000 Å. to 6500 Å. on dilution over this range and they associated these bands with dimeric and monomeric forms of the dyestuff respectively. By extrapolating the extinction coefficient at these two wavelengths to infinite and zero concentration respectively, they obtained values which were claimed to be the extinction coefficients of the monomeric and dimeric forms of the dyestuff. Using these extinction coefficients they were able to calculate the extinction coefficients at any concentration and showed that these agreed with the observed values and support the view that aggregation proceeds only to the dimeric stage. This, however, is rather deceptive

as large errors in the degree of association produced only small differences in the extinction coefficients. Further Lange and Herre<sup>6</sup> have reported an activity coefficient of 0.48 for solutions of Methylene Blue which indicates that higher aggregation may occur.

In the present experiments, therefore, absorption spectra for the dye-stuff were determined over the concentration range  $3.13 \times 10^{-3}$  to  $2.5 \times 10^{-6}$  mol./l. and it was found that the peak shifts from 6670 Å. to 6050 Å. on increasing the concentration from  $2.5 \times 10^{-6}$  mol./l. to  $1 \times 10^{-3}$  mol./l., but further increase in concentration to  $3.13 \times 10^{-3}$  mol./l. causes a further shift of the peak to 5850 Å. The curves obtained are shown in Fig. 3. All the evidence indicates that the shift in the peak is not abrupt from one wavelength to another but continuous and proceeds beyond the point indicated by Rabinowitch. This suggests the formation of increasingly complex polymers with increasing concentration and not a simple division into monomer and dimer. If this is the case and higher polymers are formed, then the extinction coefficients of the solution at the dimer wavelength should rise to a maximum value and then begin to decrease as the concentration is further increased and the formation of higher polymers becomes of increasing importance. The figures given

TABLE VIII.—EXTINCTION COEFFICIENTS OF METHYLENE BLUE 2B.

Concentration (mol./l.).	Extinction Coefficients $\times 10^4$	
	at 6050 Å.	at 6670 Å.
$3.13 \times 10^{-3}$	3.32	0.72
$2.5 \times 10^{-3}$	3.92	1.80
$1 \times 10^{-3}$	4.33	2.64
$5 \times 10^{-4}$	4.42	3.00
$2.5 \times 10^{-4}$	4.32	3.82
$1.25 \times 10^{-4}$	4.17	4.62
$5 \times 10^{-5}$	3.68	5.69
$2.5 \times 10^{-6}$	2.90	5.83

in Table VIII show the extinction coefficients obtained at 6050 Å. and 6670 Å. and their variation with concentration.

It will be seen from these figures that at 6670 Å. (the monomer wave-length) the extinction coefficient tends towards a limit with decreasing concentration and decreases steadily with increasing concentration. At 6050 Å., however, the extinction coefficient reaches a maximum value at approximately  $5 \times 10^{-4}$  mol./l. and then decreases with in-

creasing concentration. This effect, together with a further shift of absorption peak to 5850 Å. indicates aggregation beyond the dimeric stage. It must be observed that Rabinowitch and Epstein recorded observations at 4 concentrations only and it would seem dangerous to extrapolate from these results to zero and infinite concentrations respectively. The Methylene Blue used in our experiments was carefully purified and by titanous estimation had a purity of not less than 97 % whereas the sample used by Rabinowitch and Epstein was a commercial product (Merck reagent Methylene Blue). It was also noted that the extinction coefficients obtained in these experiments were considerably higher than those recorded by Rabinowitch and Epstein although both are much lower than those quoted by Lewis *et al.*<sup>7</sup> and by Michaelis and Granick.<sup>8</sup> If the values obtained by Rabinowitch are recalculated on the assumption that their solution is 35 % weaker than our sample, the values are then parallel with the present results. The original and recalculated results together with the results obtained in the present work are plotted in Fig. 4.

Sheppard and Geddes<sup>6</sup> by a similar method have found the aggregation number of 1.57 in the case of Methylene Blue and with other dyestuffs

<sup>6</sup> Lange and Herre, *Z. physik. Chem., A*, 1937, 181, 329.

<sup>7</sup> Sheppard and Geddes, *J. Amer. Chem. Soc.*, 1944, 66, 2003.

<sup>8</sup> Lewis, Goldschmid, Magel and Bigeleisen, *J. Amer. Chem. Soc.*, 1943, 65, 1150.

<sup>9</sup> Michaelis and Granick, *ibid.*, 1945, 67, 1212.

found that the value in all cases was less than 2. On these grounds they concluded that in such solutions, no higher polymers than dimer are formed. They also disagreed with Rabinowitch and Epstein, and Scheibe<sup>9</sup> about the nature of the different bands and ascribed these, not to dimer

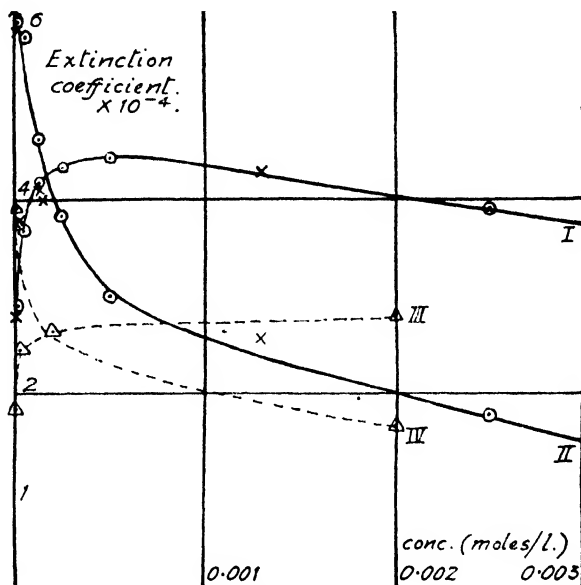


FIG. 4.

- × Rabinowitch figures recalculated on basis of 65 % strength.  
 ○ Present results.      △ Rabinowitch figures.

Curve I—Extinction coefficients at 6050 Å.

Curve II—Extinction coefficients at 6670 Å.

Curve III—Rabinowitch extinction coefficients at 6000 Å.

Curve IV—Rabinowitch extinction coefficients at 6500 Å.

and higher polymers, but to vibrationally coupled transition states of the monomeric ions, which, however, are enhanced in the dimer. It is evident, therefore, that the Methylene Blue system in water is not as simple as might at first appear and its value as a method of investigating the effect on association of the diffusion of dyes is thus greatly reduced.

### Conclusions.\*

From the spectroscopic measurements described in the present paper, it is concluded that many dyes and dye mixtures contain aggregates in aqueous solution at room temperature, but it is difficult to obtain sufficient precision of measurement in most cases to enable a useful estimate of the degree of association to be made. In the case of mixtures of direct dyes, the changes in absorption spectra due to association are much greater than are observed with single dyes, and with a mixture of Durazol Red 2B and Chlorazol Sky Blue FF it has been found possible to establish that the association is bimolecular, one molecule of red dye combining with one molecule of blue dye. In this case the degree of association has been estimated and is found to be greater than 50 % at room temperature in an equimolecular solution of the two dyes. From a study of the effect of concentration and temperature on the system, it is concluded that

\* Scheibe, *Kolloid Z.*, 1938, 82, 1.

association becomes negligible at temperatures above  $80^{\circ}\text{C}$ ., that the free energy change on association at  $20^{\circ}\text{C}$ . is approximately  $-6.8\text{ kcal.}$ , the heat of reaction  $-7.3\text{ kcal.}$  and the entropy change  $-1.8\text{ cal./}^{\circ}\text{C}$ .

A detailed study of the absorption bands of Methylene Blue 2B in aqueous solution over a wide range of concentrations, suggests that aggregates larger than dimer are present in appreciable amounts in strong solution. Deductions based on extrapolation to zero and infinite concentrations are therefore considered unreliable.

### Résumé.

On a utilisé les variations de spectres d'absorption pour étudier l'aggrégation de colorants et de mélanges de colorants en solution aqueuse. En général, les mesures ne sont pas suffisamment précises pour permettre d'estimer le degré d'association, mais, avec les mélanges, les effets sont plus marqués et on a établi qu'il y a association bimoléculaire dans le mélange : Durazol Red 2B et Chlorazol Sky Blue FF. Pour l'association à  $20^{\circ}\text{C}$ .,  $\Delta G = 6.8\text{ kcal.}$ ;  $\Delta H = -7.3\text{ kcal.}$  et  $\Delta S = -1.8\text{ cal.}^{\circ}\text{C}$ . On suggère pour Methylene Blue 2B l'existence d'aggrégats supérieurs au dimère.

### Zusammenfassung.

Veränderungen der Absorptionsspektren sind benützt worden, um die Aggregation von Farbstoffen und Farbstoffgemischen in wässrigen Lösung zu untersuchen. Im allgemeinen sind die Messungen nicht genau genug, als dass aus ihnen der Assoziationsgrad abgeleitet werden könnte, aber mit Gemischen von "Durazol Red 2B" und "Chlorazol Blue FF" ist eine bimolekulare Assoziation bewiesen worden. Für die Assoziation bei  $20^{\circ}\text{C}$ . ist  $\Delta G = 6.8\text{ kcal.}$ ,  $\Delta H = -7.3\text{ kcal.}$  und  $\Delta S = -1.8\text{ cal.}^{\circ}\text{C}$ . In der Assoziation von "Methylene Blue 2B" dürften Aggregate zwischen mehr als zwei Molekülen entstehen.

*Imperial Chemical Industries Limited,  
Dyehouse Laboratories,  
Hexagon House,  
Blakley,  
Manchester, 9.*

## PHYSICO-CHEMICAL MECHANISMS IN PROTEIN SYSTEMS.

### I. THE COMBINATION OF ORANGE II ACID WITH WOOL KERATIN.

By A. B. MEGGY.

*Received 27th March, 1946.*

An equation has been deduced by Rideal and Gilbert<sup>1</sup> for the combination of strong acids with an insoluble protein such as wool, and has been found to fit satisfactorily the experimental data of Steinhardt, Fuggitt and Harris<sup>2</sup> for the combination of wool with HCl in the presence and absence of additional Cl ions. It was of interest to see whether this equation could also be applied in the case of a typical dye acid. For this purpose the dye Orange II, prepared by coupling diazotised sulphanilic acid with  $\beta$ -naphthol, was used. The equation, if applicable, would enable the change in available energy per mol of dye acid transferred from water

<sup>1</sup> Rideal and Gilbert, *Proc. Roy. Soc. A*, 1944, **182**, 335.

to wool to be calculated, thus giving a quantitative measure of the "affinity" of the dye for the wool.

The equation for a monobasic acid has the following form :

$$2RT \ln \frac{\theta}{1-\theta} - RT \ln (H^+) - RT \ln (A^-) + \Delta\mu_H + \Delta\mu_A = 0. \quad (1)$$

( $H^+$ ) and ( $A^-$ ) are the activities of the hydrogen ion and the anion in the aqueous phase;  $\Delta\mu_H$ ,  $\Delta\mu_A$ , are the changes in chemical potential for each ion between the fibre and the solution. Since this is a condensed system,  $\Delta\mu$  is equal to the change in available energy.  $\theta$  is the ratio of the amount of acid bound by the wool at given values of ( $H^+$ ) and ( $A^-$ ), to the maximum amount which can be bound. For wool this has been taken as 0.82 equ. per 1000 g.

The equation agrees quite well with the experimental results of Harris and Steinhardt<sup>2</sup> for the absorption of HCl by wool, both alone and in the presence of NaCl. The addition of NaCl increases ( $A^-$ ) in the above equation, and hence, if ( $H^+$ ) remains constant,  $\frac{\theta}{1-\theta}$  increases, since  $\Delta\mu_H$  and  $\Delta\mu_A$  are constants. Hence  $\theta$  increases, i.e. the addition of NaCl increases the amount of acid bound. This was actually found to be the case.

In the present work, although the pure free acid of Orange II was used, the values of ( $H^+$ ) and ( $A^-$ ) at equilibrium were not in general identical, owing to the liberation of basic substances from the wool which neutralised part of the acid in the solution. Nevertheless, equation (1) should still apply, as it did in the case of the system HCl-NaCl.

### Experimental.

Commercial Orange II was recrystallised once from water; this removed insoluble matter and NaCl. The purified dye was dissolved at 60° c., and enough conc. HCl added (about 1/10 by volume) to precipitate the dye acid. The precipitate was allowed to stand a day, and then filtered with light suction. Heavy suction caused the precipitate to form a slow-filtering gel. The process was repeated twice, and the precipitate dried in a vacuum desiccator over NaOH. The free dye acid was dark red, but became a coppery green when dried in the air oven at 110° c. A specimen of Orange II sodium salt was recrystallised three times from water, and dried at 110°. The Spekker absorptiometer was calibrated with solutions of the dye acid and the sodium salt. Identical readings were obtained at the same molar concentrations. A Spekker reading of 1.00 was equivalent to a solution  $4.8 \times 10^{-5}$  M. Orange II, using a 1 cm. cell, and Ilford Spectrum Filter 603, blue-green. Scoured woollen yarn was washed several times in distilled water, dried, and allowed to condition in the air.

From 0.04 to 0.5 g. of the dye acid was weighed out into a 100 cc. conical flask, and about 30 cc. of distilled water were added to dissolve it. A weighed quantity (about 1 g.) of conditioned wool (moisture content 16 %), was added, and the flask heated to boiling on the hot plate and shaken gently until the wool was completely wetted by the liquor. It was then closed by a cork carrying a glass tube to act as a condenser, and left in a thermostat at 60° c. for two days. A sample of the liquor was pipetted off, and the concentration of dye determined in the Spekker. Another sample was used to determine the pH with the glass electrode. The flask was removed from the thermostat, the wool immediately filtered off with suction, and washed three times with a little cold water to remove adhering liquor. The dyed wool was stripped with 25 % aqueous pyridine,

<sup>2</sup> Steinhardt, Fugitt and Harris, *Bur. Stand. J. Res.*, 1940, **24**, 335.

## 504 PHYSICO-CHEMICAL MECHANISMS IN PROTEIN SYSTEMS

and the amount of dye determined by making up the pyridine solution to a standard volume, and measuring the concentration on the Spekker. The results are given in Table I.

TABLE I.—ABSORPTION OF ORANGE II (FREE ACID) ON WOOL AT 60° C.

No.	Dry Wool.	Conc. Dye (Solution).	Mole. Dye (Wool).	pH.	$\theta$ .
1	0.918	$8.35 \times 10^{-4}$	$12 \times 10^{-5}$	5.20	0.160
2	0.962	$1.29 \times 10^{-3}$	$24 \times 10^{-5}$	4.60	0.304
3	1.131	$1.82 \times 10^{-3}$	$46.6 \times 10^{-5}$	3.98	0.503
4	0.932	$3.97 \times 10^{-3}$	$67.6 \times 10^{-5}$	2.5	0.885
5	1.128	$4.66 \times 10^{-3}$	$81.4 \times 10^{-5}$	2.36	0.880
6	0.982	$5.97 \times 10^{-4}$	$8.5 \times 10^{-5}$	5.36	0.104
7	1.242	$1.17 \times 10^{-3}$	$22.7 \times 10^{-5}$	4.88	0.223
8	1.000	$1.41 \times 10^{-3}$	$34.7 \times 10^{-5}$	4.44	0.424
9	1.086	$1.43 \times 10^{-3}$	$47.3 \times 10^{-5}$	3.82	0.532
10	0.944	$1.84 \times 10^{-3}$	$59.9 \times 10^{-5}$	3.02	0.775

No.	$\log (A^-)$ .	$\log (H^+)$ .	$2 \log \frac{\theta}{1-\theta}$ .	$\frac{[H^+][A^-]}{(\frac{\theta}{1-\theta})^2}$ .	$\Delta\mu_A + \Delta\mu_H$ .
1	-3.08	-5.20	-1.44	$1.45 \times 10^{-7}$	10.36
2	-2.89	-4.60	-0.72	$1.70 \times 10^{-7}$	10.25
3	-2.74	-3.98	0.01	$1.86 \times 10^{-7}$	10.20
4	-2.40	-2.50	1.77	$2.14 \times 10^{-7}$	10.12
5	-2.33	-2.36	1.73	$3.80 \times 10^{-7}$	9.75
6	-3.22	-5.36	-1.87	$1.95 \times 10^{-7}$	10.19
7	-2.93	-4.88	-1.08	$1.86 \times 10^{-7}$	10.20
8	-2.85	-4.44	-0.27	$0.995 \times 10^{-7}$	10.64
9	-2.84	-3.82	0.11	$1.70 \times 10^{-7}$	10.27
10	-2.74	-3.02	1.07	$1.48 \times 10^{-7}$	10.35

The mean value for  $(\Delta\mu_H + \Delta\mu_A)$  is 10.3 kcal./g.mole.

It will be noticed that although the free acid was used,  $[H^+] \neq [A^-]$ , and the relative discrepancy is greatest at low concentration of the dye acid. Obviously some soluble basic material is passing from the wool into the solution. In the case of Expt. 1 and 6, practically the whole of the acid not absorbed by the wool has been neutralised. As there were about 30 cc. of liquid, this is equivalent to 30 cc. of N./1000 acid per g. of wool, on 30 m. equ./kg. No special precautions had been taken to ensure that the wool was in an isoelectric condition. Wool is usually scoured with dilute soap solution, and it is possible that there were sodium ions bound by the wool. These would neutralise an equivalent number of Orange II ions, and the change in pH could be explained in this way. The presence of Orange II as its sodium salt would not interfere with the application of equation (1). However, the following observations show that other factors are involved.

If the solution in which the wool has been lying for several days is cooled to room temperature, a precipitate separates out which, from its colour, is obviously a salt of Orange II. It was at first thought that the basic material liberated by the wool was  $NH_3$ , e.g. from the hydrolysis of aspartamide groups. However, the ammonium salt of Orange II is readily soluble in the cold. Attention was then turned to the individual amino acids. It was found that arginine and histidine gave precipitates with Orange II acid at quite low concentrations (N./1000) but none of

the other acids known to be present in wool did so. However, a comparison of the appearance of the substance obtained from wool with that of the salts of Orange II with arginine and histidine indicated that neither of these amino acids was identical with the base obtained from wool. Moreover the latter substance possessed a remarkable property not shown by the Orange II salts of arginine and histidine. Under the microscope the precipitate had the appearance of orange lumps of no particular shape. On warming a suspension of the precipitate in the liquor, fine hairs radiated from the particles, until they were completely converted into a mass of very fine, long, and quite flexible fibres, about  $2\text{ m}\mu$  thick. The amount of this substance formed was very small. It is intended to make a thorough study of this substance at a later date.

In spite of the apparent hydrolytic effect of the dye acid on the wool, an effect noticed by other workers,<sup>3</sup> it will be seen that the experimental data fit equation (1) reasonably well, and the affinity of Orange II acid for wool is  $10.3\text{ kcal}$ . Part of this is due to the  $\text{H}^+$  ions, and part to the dye anions, and it remains to determine how great is the contribution of each. This question cannot be answered from the data of these experiments, but the following considerations indicate the probable contributions of each ion.

By applying equation (1) to the data of Steinhardt and Harris,<sup>4</sup> for the combination of  $\text{HCl}$  with wool at various temperatures,  $\Delta\mu_{\text{H}} + \Delta\mu_{\text{Cl}} = -6000\text{ cal}$ . approximately, at temperatures from  $0^\circ$  to  $50^\circ\text{C}$ . It is not possible to decide the values of  $\Delta\mu_{\text{H}}$  and  $\Delta\mu_{\text{Cl}}$  separately in practice. It is possible, in principle, from electrokinetic measurements, to obtain values of  $\Delta\mu_{\text{H}} - \Delta\mu_{\text{Cl}}$  by finding under what conditions the electrokinetic potential is zero. However, the values obtained refer only to the surface of the wool fibre. The values for the isoelectric point obtained by these measurements, and by electrophoretic methods<sup>7</sup> are in the neighbourhood of  $\text{pH } 3.5$  and this value differs by 2 or 3  $\text{pH}$  units from the value obtained by titration with acids. Presumably the isoelectric point, and hence the composition, at the surface differs from that of the bulk phase. It is therefore necessary, at present, to assign an arbitrary value to  $\Delta\mu_{\text{Cl}}$ , and to determine the value of  $(\Delta\mu)$  for other ions by reference to  $\text{Cl}$  ion. It is proposed to assume that  $(\Delta\mu_{\text{Cl}}) = 0$ , and hence that  $(\Delta\mu_{\text{H}}) = -6000\text{ cal}$ .

The following considerations show that this assumption is reasonable. If the affinity of the  $\text{H}$  ion for wool is solely due to the tendency of the  $\text{H}$  ion to recombine with the carboxyl ions of the wool to form carboxylic acid groups, then  $\Delta\mu_{\text{H}} = RT \ln K$  where  $K$  is the dissociation constant of the carboxyl group in the wool. These carboxyl groups are those of aspartic and glutamic acids, for which the values of  $\log K$  are  $-3.87$  and  $-4.21$  respectively, in water at  $25^\circ\text{C}$ .<sup>5</sup> If the same values are assigned to the carboxyl groups of the wool, the corresponding values of  $\Delta\mu_{\text{H}}$  are  $-5270$  and  $-5750\text{ cal}$ . respectively. Thus, to a first approximation the whole of the affinity of  $\text{HCl}$  for wool may be considered as due to the  $\text{H}$  ions, so that  $\Delta\mu_{\text{H}} = \Delta\mu_{\text{HCl}} = -6000\text{ cal}$ . Hence  $\Delta\mu_{\text{OII}} = -4300\text{ cal}$ .

I am indebted to Imperial Chemical Industries Ltd. (Dyestuff Group), for permission to publish this paper.

### Summary.

The equation deduced by Rideal and Gilbert for the combination of strong acid with an insoluble protein has been found to hold for the system, Orange II Acid-wool.

<sup>3</sup> Steinhardt and Fugitt, *Bur. Stand. J. Res.*, **29**, 315.

<sup>4</sup> Steinhardt, Fugitt and Harris, *ibid.*, **25**, 519.

<sup>5</sup> Greenstein, *J. Biol. Chem.*, **93**, 491.

<sup>7</sup> Neale, *Trans. Faraday Soc.*, 1945, **42**, 478.

<sup>6</sup> Harris, *ibid.*, **84**, 180.

<sup>6</sup> Harris, *ibid.*, **8**, 779; **9**, 557.



The affinity of Orange II Acid for wool is 10,300 cal. at 60° c. Of this approximately 6000 cal. are due to the H ions, and approximately 4300 cal. are due to the dye anions.

The prolonged action of Orange II Acid on wool at low concentrations causes the liberation of a basic substance from the wool which is neither  $\text{NH}_3$  nor an amino acid.

### Résumé.

L'équation déduite par Rideal et Gilbert pour la combinaison d'acides forts avec une protéine insoluble s'est trouvée valable pour le système laine-Orange II Acid. L'affinité de l'acide pour la laine est de 10,300 cal. à 60° C, quantité qui peut être décomposée approximativement en 6000 cal. dûes aux ions H et 4300 dûes aux anions du colorant. L'action prolongée de Orange II Acid sur la laine à faible concentration libère une substance basique qui n'est ni  $\text{NH}_3$  ni un amino-acide.

### Zusammenfassung.

Es wurde gefunden, dass die Gleichung von Rideal und Gilbert für die Verbindung einer starken Säure mit einem unlöslichen Protein für das System Wolle-Orange II Acid (Diazokupplungsprodukt von Sulfanilsäure mit  $\beta$ -Naphthol) gültig ist.

Die Affinität von Orange II Acid für Wolle beträgt bei 60° c. 10,300 cal., wovon ungefähr 6000 cal. auf die Wasserstoffionen und ungefähr 4300 cal. auf die Farbstoffanionen entfallen.

Die längere Einwirkung von Orange II Acid in geringer Konzentration auf Wolle verursacht die Freisetzung aus der Wolle von einer basischen Substanz, die weder Ammoniak noch eine Aminosäure ist.

*Imperial Chemical Industries Ltd. (Dyestuffs Division),  
Hexagon House, Blackley, Manchester.*

*College of Technology,  
Leicester.*

## THE ADSORPTION OF PARAFFIN-CHAIN SALTS TO PROTEINS.

### PART III. THE FORMATION OF COMPLEXES BETWEEN DODECYL SODIUM SULPHATE AND CHEMICALLY MODIFIED GELATINS.

BY I. I. HARRIS, K. G. A. PANKHURST\* AND R. C. M. SMITH.

*Received 6th January, 1947, as revised 23rd July, 1947.*

In the preceding parts <sup>1, 2</sup> we have studied the formation of insoluble complexes between gelatin and dodecyl sodium sulphate (DSS) under various conditions of salt concentration and pH. It was shown that water-insoluble complexes could be separated at and above the isoelectric point of the gelatin in the presence of certain concentrations of electrolyte, which contained adsorbed dodecyl sulphate anions (DS') equivalent to 93 % of the total nitrogen atoms of the protein. Under acidic conditions, e.g. pH 2.5, in the absence of added electrolyte, complexes containing one adsorbed DS' per approximately 10 nitrogen atoms of the protein were consistently produced. It was suggested that

\* Present address: Brit. Leather Manuf. Res. Ass., London, S.E. 1.

<sup>1</sup> Pankhurst and Smith, *Trans. Faraday Soc.*, 1944, 40, 565.

<sup>2</sup> Pankhurst and Smith, *Trans. Faraday Soc.*, 1945, 41, 630.

where complexes were formed with almost one DS' per nitrogen, adsorption took place (a) at the positively charged groups of the basic side-chains and (b) at the backbone imide nitrogens, the link here being of the ion-dipole type made possible by the resonance of the keto-imide groups. At low pH values, complexes are produced by mechanism (a) only, since the resonance necessary for type (b) adsorption is inhibited by the presence of hydrogen ions.<sup>3</sup> Published figures for the amino acid residues of gelatin<sup>4</sup> support these hypotheses.

In this paper we investigate further the nature of the adsorption of DS' to gelatin, by studying quantitatively the adsorption of DS' to deaminised gelatin, gelatin hydrolysates and to gelatin treated with formaldehyde.

## Experimental.

Deamination was made by the method of Thomas, Kelly and Foster<sup>5</sup> using  $\text{NaNO}_2$  and glacial acetic acid, and afterwards washing with NaCl to reduce swelling. When dried, after washing with water and acetone, the sample was difficultly soluble in water and completely soluble only after prolonged heating. The resulting solution showed no gelling properties on cooling. In a modification of this method, the acetone washing and drying were dispensed with, and the gelatin washed only in running water after the  $\text{HNO}_2$  treatment. The product was again found to be soluble only after prolonged heating. Both of these products were, however, soluble in aqueous alkali. Tests with  $\text{NaNO}_2$  and acetic acid indicated that neither of these methods yielded a fully deaminised gelatin since further nitrogen was evolved. The method finally adopted was to treat a concentrated gelatin sol (ca. 20 %) at 50° C. with  $\text{NaNO}_2$  and glacial acetic acid until on adding further quantities of  $\text{NaNO}_2$  and acid no further nitrogen was evolved. The product (a dark brown solution) was then neutralised with NaOH and then the gelatin was precipitated by the addition of an excess of ethyl alcohol. The neutralisation caused the solution to become even darker in colour. The precipitated dark-brown product was dissolved in the minimum of hot water and re-precipitated with alcohol to ensure as complete removal of electrolyte as possible, and finally left in cold water for several hours, when it completely dissolved to a brown solution which at 3 % strength showed no sign of gelling on cooling. The yield was 90 % of the original weight.

The separation of gelatin-DS' complexes was followed in the manner already described,<sup>1</sup> i.e. by preparing a series of products using constant gelatin (0.5 % w/v), electrolyte concentration, pH, etc., and varying amounts of DSS, allowing any complex formed to separate and then determining the DS' in the supernatant aqueous phase by titration with cetyl trimethylammonium bromide. Two such series were prepared, (a) at pH 5.5 in the presence of  $\text{m. NH}_4\text{NO}_3$ , where adsorption would be expected to take place at the imide nitrogens of the backbone and at the cationic nitrogens of the basic side-chains, and (b) at pH 2.5 in the absence of electrolyte, where adsorption would take place at the cationic side-chain nitrogens only. In each case curves relating initial added DSS concentration to that determined in the supernatant liquor were plotted on a log-log scale.

## Results.

### A. Complexes Formed with Deaminised Gelatin.

Fig. 1 shows the results obtained by titrating the supernatant liquors of the complexes formed with deaminised gelatin at pH 5.5 in the presence of  $\text{m. NH}_4\text{NO}_3$ , where adsorption would be expected at the keto-imide groups, and also at pH 2.5 in the absence of  $\text{NH}_4\text{NO}_3$ , where adsorption would be expected only at those amino groups remaining.

The absence of any well-defined inflection point in the pH 5.5 curve indicates that under these conditions complexes are formed which are more soluble than

<sup>3</sup> Pauling, *The Nature of the Chemical Bond* (Cornell University Press, 1940),

207.

<sup>4</sup> Bowes, *Ann. Rep. Prog. Appl. Chem.*, 1943, 28, 324.

<sup>5</sup> Thomas, Kelly and Foster, *J. Amer. Chem. Soc.*, 1926, 48, 419.

those formed by non-deaminised gelatin. In Part I (Fig. 1) it was shown that a similar lack of definition of inflection point occurred at this pH when complexes were formed with normal gelatin and a low concentration of  $\text{NH}_4\text{NO}_3$ . A fairly well-defined inflection point was, however, obtained at pH 2.5 for the deaminised gelatin, corresponding to an added DSS concentration of 0.00063 N. (for the 0.5 % gelatin concentration used). The corresponding DSS concentration for non-deaminised gelatin, taken from Part II, Fig. 2, was 0.005 N. Thus deamination brought about the elimination of all except 1/8th of the basic side-chain or terminal groups.

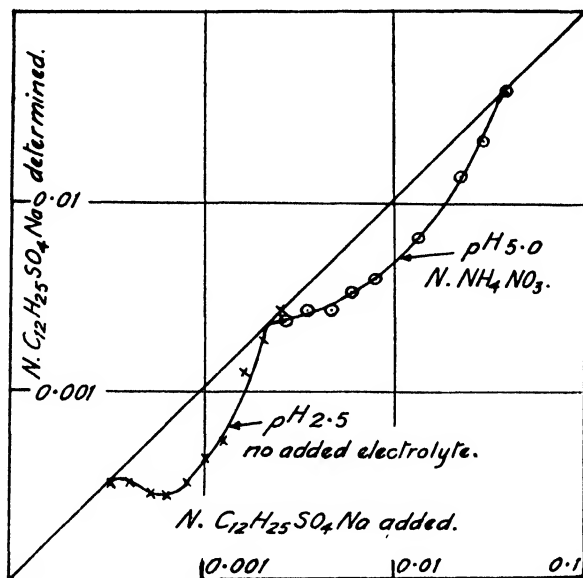


FIG. 1.—Deaminised gelatin complexes.

## B. Complexes Formed with Gelatin Hydrolysates.

Complexes were formed at pH 5.5 in the presence of M.  $\text{NH}_4\text{NO}_3$  and at pH 2.5 without  $\text{NH}_4\text{NO}_3$  using (a) normal gelatin, (b) gelatin partially hydrolysed by boiling for 5 hr. in 10 % solution at its isoelectric point (5.1) and (c) gelatin further hydrolysed by boiling for 24 hr. at the same pH and concentration. The results are shown in Fig. 2.

At the higher pH, the effect of hydrolysis is to produce complexes which are progressively more soluble, without altering the ratio of adsorbed DS' to gelatin to any appreciable extent. The effect is similar to that produced by raising the temperature of complex formation or reducing the concentration of electrolyte in which it is formed.<sup>1</sup>

At pH 2.5, however, the effect is much smaller. As at the higher pH the DS'/gelatin ratio is very little altered, and the curve for the 5 hr. hydrolysate is practically identical with that of the untreated gelatin. The 24 hr. hydrolysate is interesting in that, at concentrations of added DSS between 0.001 and 0.004 N. it forms complexes which are noticeably less soluble than those formed by the less hydrolysed gelatins. In this respect it resembles the curve, shown in the inset to Fig. 1, Part II, for complexes formed by unhydrolysed gelatin at pH 1.0, in the absence of electrolyte.

## C. Complexes Formed with Gelatin in the Presence of Formaldehyde.

Fig. 3 shows the effect of forming complexes at pH 5.5 in the presence of M.  $\text{NH}_4\text{NO}_3$  and at pH 2.5 in the absence of inorganic salt, both in the presence of 1.25 % formaldehyde. At the low pH value the effect is to decrease the solubility of the complexes at all except the lowest DSS concentrations, without altering

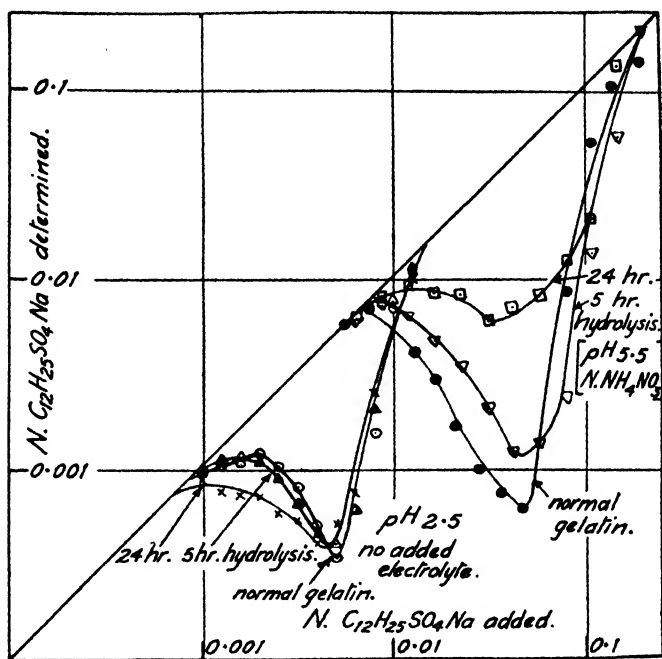


FIG. 2.—Complexes with gelatin hydrolysates.

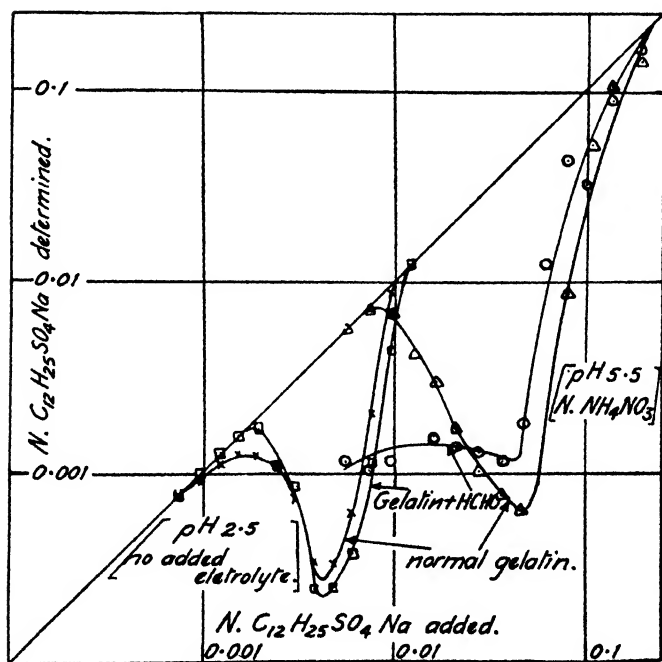


FIG. 3.—Complexes with "formalised" gelatin.

the DS'/gelatin ratio. Even at these lower concentrations of added DSS it is probable that complexes formed in the presence of formaldehyde are less soluble than those formed in its absence, since there remained in the supernatant liquor an opalescence of finely dispersed complex which resisted separation with a hand centrifuge, or by filtration. The DS' of such complexes titrate as free DS', thus giving the slightly higher values recorded. At  $pH$  5.5 the complexes formed in the presence of formaldehyde over the lower range of added DSS concentrations are considerably less soluble than those formed in its absence. Those complexes formed in the presence of formaldehyde were fibrous in appearance even at  $50^{\circ}C$ . in contrast to the oily nature of those formed without formaldehyde.

### Discussion.

The formation of complexes with deaminised gelatin at  $pH$  2.5 in the absence of added inorganic salt provides further evidence that under these conditions adsorption takes place only at the side chain and terminal cationic groups, since the process of deamination reduced the DS'/gelatin ratio by 7/8th. The fact that it is possible to form and separate complexes at all is in accordance with the observations of Atkin<sup>6</sup> that treatment with  $HNO_3$  does not cause the removal of all the amino groups. According to Atkin, it is the arginine residues that resist deamination, unless it is carried out with such violence that disintegration of the protein takes place. Since, however, the arginine residues constitute the lower half of the basic side-chains of the gelatin molecule,<sup>7</sup> it is evident that at least some of these have been deaminated by this treatment. The greater solubility of the complexes formed at the higher  $pH$  values with deaminated gelatin does, indicate that during deamination some degree of hydrolysis may have taken place. At the low  $pH$ , it might be expected that the smaller DS'/gelatin ratio would lead to even greater water solubility. However, the occurrence of hydrolysis produces an increase in carboxyl groups which at  $pH$  2.5 would be less dissociated than at  $pH$  5.5 and would therefore exert a smaller solubilising action than at higher  $pH$  values.

This same effect is seen in the gelatin hydrolysate series, where at low  $pH$  values there is a tendency to greater insolubility of the lower DSS complexes formed with hydrolysed gelatins compared with those formed with unhydrolysed gelatin; whereas at the higher  $pH$  value hydrolysis leads to the formation of considerably more soluble complexes.

As is to be expected, the presence of formaldehyde gives complexes which are less soluble than those with plain gelatin. This greater insolubility, together with the fact that the complexes with formaldehyde are fibrous in character, indicated that the normal reaction between protein and formaldehyde is not greatly influenced by the presence of adsorbed DS', nor does the reaction of the formaldehyde with the protein affect the DS' adsorption to the amino or imino groups of the protein.

We record our thanks to several of our colleagues—especially C. Waller—for helpful discussion, and to the Directors of Ilford, Ltd., for permission to publish this work.

### Summary.

Complexes have been formed between dodecyl sodium sulphate and gelatins which have been (a) deaminised, (b) hydrolysed, and (c) reacted with formaldehyde. At low  $pH$  values in the absence of inorganic salt adsorption takes place only at the side-chain and terminal amino groups of the protein. Hydrolysis produces complexes which are more soluble at high  $pH$  values. The adsorption is quantitatively independent of the presence of formaldehyde at  $pH$  2.5 and 5.5, the effect of the formaldehyde being merely to produce less soluble complexes with a fibrous appearance. A modified method for deaminising gelatin is given.

<sup>6</sup> Atkin, *Stiasny Festschrift*, 1937, 13.

<sup>7</sup> Chibnall, *J. Int. Soc. Leather Trades Chemists*, 1946, 30, 1.

### Résumé.

On a formé des complexes entre le dodécyl sulfate de sodium et des gélatines, qui ont été (1) désaminées, (2) hydrolysées, et (3) mises en réaction avec HCHO. A bas  $pH$  et en l'absence de sels minéraux, l'adsorption a lieu sur les groupes aminés terminaux et sur ceux de la chaîne latérale de la protéine. Elle est indépendante de la présence de HCHO à  $pH$  2.5 et 5.5. On indique aussi une méthode pour désaminer la gélatine.

### Zusammenfassung.

Komplexe zwischen Dodecylnatriumsulfat und Gelatinen, die (a) deaminiert, (b) hydrolysiert und (c) mit HCHO reagiert waren, sind dargestellt worden. Bei niedrigem  $pH$  und in Abwesenheit anorganischer Salze findet die Adsorption an den Aminogruppen in der Seitenkette und am Kettenende des Proteinmoleküls statt. Bei  $pH$  2.5 und 5.5 ist die Adsorption unbeeinflusst von der Gegenwart von HCHO. Es wird eine Methode zur Deaminierung von Gelatine beschrieben.

*The Ilford Research Laboratory,  
Ilford Limited,  
Ilford.*

## THE ADSORPTION OF PARAFFIN-CHAIN SALTS TO PROTEINS.

### PART IV. SOME PHYSICAL AND CHEMICAL PROPERTIES OF GELATIN-DODECYL SULPHATE COMPLEXES.

BY K. G. A. PANKHURST AND R. C. M. SMITH.

*Received 6th January, 1947, as revised 23rd July, 1947.*

When dodecyl sodium sulphate (DSS) is added in increasing quantity to a gelatin solution, complexes are formed which have increasingly hydrophobic character until a minimum water (or aqueous electrolyte) solubility is reached (referred to as the inflexion point).<sup>1,2</sup> Greater proportions of DSS than that corresponding to the inflexion point peptise the complexes, the extent of which increases as the DSS/gelatin ratio is increased. We have shown that the complex formed at the inflexion point corresponds to adsorption of the dodecyl sulphate anions (DS') with their hydrophilic ends attached to the basic sites of the protein molecule and the hydrocarbon chains left free. Complexes formed at DSS/gelatin ratios above the inflexion point, i.e. in the region where peptisation occurs, appear to have a further layer of adsorbed DS' ions, with their hydrophilic ends outermost.

In Part I, some data were given on the water content of such complexes and their refractive indices, and reference was made to their solubility in toluene. In the present paper we examine more fully these properties, together with the acid- and base-combining power of gelatin in the presence of DSS, with and without formaldehyde additions.

### Experimental.

Acid- and base-combining power of the gelatin — DS systems were computed from  $pH$  titration curves, using a glass electrode and valve potentiometer. The

<sup>1</sup> Pankhurst and Smith, *Trans. Faraday Soc.*, 1944, 40, 565.

<sup>2</sup> Pankhurst and Smith, *ibid.*, 1945, 41, 630.

titration liquids were continuously stirred. A fixed quantity of  $N./10$  NaOH was initially added to the liquid to be titrated, and titrations made with  $N./10$  HCl. Throughout, distilled water, DSS and formaldehyde, where used, were adjusted to  $pH$  7.0, the gelatin was isoelectric (5.1). The gelatin solutions were 2 %, and the DSS 5 % (0.16  $N.$ ), i.e. sufficient to give a stoichiometric inflexion point complex at  $pH$  values above the isoelectric pt. (see Fig. 2, Part I). No precipitation of complex occurred during the course of the titration since the quantity of electrolyte formed as the titration progressed was insufficient to cause salting out at  $pH$  values above the isoelectric pt., and at lower  $pH$  values the concentration of DSS was sufficient to cause complete peptisation. Formaldehyde, when present, was in 5 % concentration. Water contents were determined by the Dean and Stark method. Refractive index measurements were made with an Abbé refractometer, using complexes containing amounts of water indicated by the Dean and Stark estimations.

Solubilities were only semi-quantitative. Complexes were prepared from 2.5 % solutions of gelatin, in the presence of  $M. NH_4NO_3$ , at  $pH$  5.3 and  $35^\circ C.$ , using a quantity of DSS corresponding to the inflexion point. After separation, the complex was dried at  $100^\circ C.$  and extracted in a Soxhlet extractor with toluene. An approximately 4 % solution of the complex in toluene was very viscous and gelled on standing at room temperature. The toluene was removed by evaporation and the complex, a waxy solid, used for relative solubility examination.

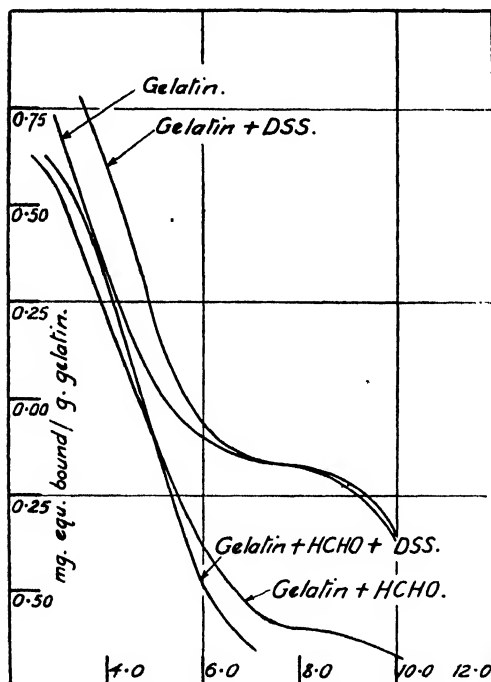


FIG. 1.—Acid- and base-combining power of complexes.

amounting to more than 0.13 mg. eq./g. gelatin. gelatin containing formaldehyde is to restore the  $H^+$ -binding capacity at  $pH$  values below 4.5, i.e. the effect is qualitatively similar, but quantitatively only about one half, that which the DSS exerts in the absence of formaldehyde. At higher  $pH$  values the  $OH^-$ -binding power is increased by a similar small amount, above that exhibited by the gelatin and formaldehyde together.

## Results.

### A. $pH$ Titrations.

Fig. 1 shows the acid- and base-combining power of gelatin, gelatin — DS' complex, gelatin + formaldehyde and gelatin — DS complex + formaldehyde. All curves have been corrected for the effect of DSS alone. The curves show that on the acid side of  $pH$  6.5, the addition of DSS causes gelatin to bind considerably more  $H^+$  ions than normally occurs in its absence. For example, at  $pH$  4, the presence of DSS caused the gelatin to bind 0.65 mg. equivalents per g., compared with 0.35 mg. eq./g. for gelatin alone. Above  $pH$  6.5 the curves are practically identical.

The curve for gelatin and formaldehyde is in agreement with those published elsewhere,<sup>3</sup> and shows that only on the alkaline side of  $pH$  5 is there a very marked difference, the  $OH^-$ -combining capacity being greatly increased. On the acid side, there is a small reduction of  $H^+$ -binding power, never

<sup>3</sup> See Jordan Lloyd and Shore, *Chemistry of the Proteins* (Churchill, 2nd Ed., 1938), 312, etc.

**B. Water Contents.**

The water contents of a number of complexes between gelatin and DSS prepared by various means are shown in Table I.

Section I shows that complexes formed at the inflection point contain less water than those formed on either side, whether the conditions of formation are in the isoelectric region in the presence of electrolyte, or at low *pH* values in the presence or absence of electrolyte. Section II shows that, despite the fact that the

TABLE I.—WATER CONTENTS.

	Gelatin (%).	pH.	Temp. (°C.).	NH <sub>4</sub> NO <sub>3</sub> (M.).	DSS Added (M.).	Water Content (%).
I.	2.5	5.3	35	1.0	0.046	82
					0.099	77
					0.25*	72
					0.45	75
	0.5	2.6	50	—	0.0037	44.3
					0.0052*	43.5
0.0063					50.3	
0.5	2.6	50	1.0 (NaCl)	0.0052	64	
				0.0063*	59	
				0.052	61	
II.	0.2	5.3	35	1.0	0.018*	83
	0.5				0.050*	81
	1.0				0.093†	80
	2.5				0.25*	72
III.	0.5	5.3	35	0.5	0.038*	83
				1.0	0.050*	81
				2.0	0.052†	75
IV.	0.5	5.3	35 50 65	1.0	0.050*	81
					0.040†	73
					0.032†	75
V.	0.5	3.2	35	1.0	0.031†	51
		5.3			0.050*	81
		9.7			0.040*	84
	0.5	2.6	50	1.0 (NaCl) —	0.0063*	59
		5.5			0.052*	70
		2.6			0.0052*	43.5

DSS/gelatin ratio at the inflection point is independent of the concentration of the gelatin from which the complex is formed (cf. Fig. 2, Part I), the water content of inflection point-complexes formed from gelatin solutions of different strengths is higher, the more dilute the original protein solution.

Section III shows that, the higher the concentration of electrolyte (NH<sub>4</sub>NO<sub>3</sub>) from which an inflection point-complex is prepared, the lower is the water content of that complex. This is consistent with the suggestion that the role of the

\* "Inflection point"-complexes, i.e. complexes formed under conditions of maximum separation.

† Complexes formed near the inflection point—inflection point-complexes would have slightly lower water contents—cf. I above.



electrolyte is merely that of a salting-out agent, competing with the complex for the water of the system. Section IV shows that as the temperature of formation is raised, the water content of the inflection point-complex is reduced.

It has been shown in earlier work that the composition and conditions of separation of complexes at and above the isoelectric region are practically independent of  $pH$ , but that at lower  $pH$  values, the DSS/gelatin ratio at the inflection point is considerably reduced, to a final value (in the absence of added electrolyte) of about 1/10th that at the isoelectric point. It is seen in Section V that this reduction of DSS/gelatin ratio, as the  $pH$  is lowered, is accompanied by a reduction in water content of the complex. The reduction is greatest in the case of the complex formed at low  $pH$  in the absence of electrolyte.

### C. Refractive Indices.

A few results showing the variation of refractive index with DSS concentration have been given in Fig. 4, Part I. Table II, below, gives a summary of refractive index measurements carried out on several series of complexes prepared under various conditions of gelatin concentration, DSS concentration,  $pH$ , added electrolyte concentration and temperature.

TABLE II.—REFRACTIVE INDICES.

	Gelatin (%)	$pH$	Temp. (°C.)	( $NH_4NO_3$ ) (M.)	DSS Added (M.)	Refractive Index. ( $n_D^{20}$ )
I.	2.5	5.3	35	1.0	0.046	1.3545
					0.058	1.3605
					0.100	1.366
					0.17	1.370
					0.25*	1.372
					0.33	1.368
					0.46	1.367
	0.5	5.3	35	1.0	0.011	1.3625
					0.016	1.364
					0.050*	1.366
					0.083	1.361
					0.123	1.359
	0.5	5.3	35	1.0	0.021*	1.360
					0.040	1.360
					0.045	1.360
					0.050	1.363
					1.00	1.366
					2.00	1.376
III.	0.5	3.2	35	1.0	0.016†	1.402
		4.3			0.033*	1.400
		5.3			0.050*	1.366
		8.5			0.040*	1.367
		9.7			0.040*	1.357
IV.	0.5	5.3	35	1.0	0.050*	1.366
			50		0.040†	1.372
			65		0.032*	1.374

\* "Inflection point"-complexes, i.e. complexes formed under conditions of maximum separation.

† Complexes formed near the inflection point—inflection point-complexes would have slightly higher refractive indices—cf. I above.

‡ Complex formed under conditions remote from the inflection point—inflection point-complex would be expected to have a much higher refractive index.

Section I reproduces the values already given in Part I, which show that the refractive index of complexes formed at the inflection point is higher than that of complexes formed on either side. It also shows that the refractive index of an inflection point-complex formed from a 2.5 % gelatin solution is higher than that formed from a 0.5 % solution, despite the fact that the DSS/gelatin ratio is the same.

Section II shows the dependence of refractive index on the concentration of  $\text{NH}_4\text{NO}_3$  used for salting out inflection point-complexes in the isoelectric region; the higher the  $\text{NH}_4\text{NO}_3$  concentration the higher the refractive index. Section III shows that inflection point-complexes formed at low pH values have refractive index values considerably higher than those formed at higher pH values. The effect of raising the temperature of formation of an inflection point-complex is to raise its refractive index, see Section IV.

#### D. Solubilities.

Approximately 0.5 g. samples of water-free, electrolyte-free complexes, prepared as already described in the experimental section, were shaken with 10cc. of a variety of solvents, heated and completeness of solubility noted. The results are only semi-quantitative, and for convenience are expressed by arranging the solvents in decreasing order of their solvent power in Table III.

TABLE III.—SOLUBILITIES.

Very soluble	{ Pyridine Chloroform Carbon Tetrachloride Xylene Toluene
Soluble	Benzene Cyclohexanone Glycerin Castor Oil Acetic acid (glacial) Oleic acid
Very slightly soluble	Water Acetone Methyl Alcohol Amyl Acetate
Insoluble*	{ Ethyl Acetate Ethyl Alcohol Amyl Alcohol

It is of some importance that the toluene-extracted, electrolyte-free, water-free complex is very nearly insoluble in water, whereas at the time of preparation, a considerable amount of electrolyte was necessary in order to salt it out from aqueous solution.

#### Discussion.

Examination of Tables I and II indicate that, generally, as the water content of a series of complexes decreases the refractive index increases, the effect being apparently one of dilution. Whilst it is true that, for many of the complexes so compared, the actual composition (i.e. DSS/gelatin ratio) may vary, this seems to be of minor importance compared with the effect of water content. The water-content figures shown in Section II of Table I are interesting in that they show that inflexion point-complexes formed from a range of original gelatin concentrations exhibit a water-combining power which is dependent on the previous history of the gelatin, i.e. complexes formed from dilute solutions of gelatin contain more water than those formed from more concentrated solutions.\*

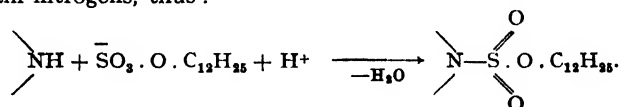
The water content of complexes formed under varying conditions of  $\text{NH}_4\text{NO}_3$  concentration support the hypothesis that the action of the

\* Some decomposition of the complex, some of the DSS of the complex being desorbed by the solvent, the remainder of the "complex" becoming a sticky insoluble mass.

\* Cf. Jordan Lloyd, *Biochem. J.*, 1931, **25**, 1580.

inorganic electrolyte is that of a salting-out agent, since increasing  $\text{NH}_4\text{NO}_3$  results in the formation of a less water-containing complex, the salt competing with the complex for the water of the system.

The solubility of the complexes in organic solvents is of great significance. The fact that, when freed from its original water, by heating in toluene to its boiling point, the inflexion point-complex formed at  $\text{pH } 5.5$ , is insoluble in water yet soluble in such solvents as  $\text{CCl}_4$ ,  $\text{C}_6\text{H}_6$ , etc., suggests that, even if the linkage between the  $\text{DS}'$  anion and the protein was originally of an ionic nature, the dehydration treatment results in the irreversible formation of a link with covalent character. Although it is too early to state with certainty the nature of the changes occurring during this dehydration, it is not unlikely that water is eliminated with the production of an alkoxysulphonamide type of structure at the basic side-chain nitrogens, thus :



This reaction requires the adsorption of an  $\text{H}^+$  ion. In Fig. 1 it is shown that  $\text{H}^+$  ions are in fact adsorbed in the reaction between gelatin and DSS. Such a reaction is analogous to the known formation of sulph-

aminic acids  $\left( \begin{array}{c} \diagup \text{NR}_2 \\ \text{SO}_2 \\ \diagdown \text{OH} \end{array} \right)^{\dagger}$ , esters of which would have compositions similar to that above.

A solution of such a complex in toluene (*ca.* 4 % concentration) exhibits a thermal sol-gel transformation similar to that of gelatin in water, but at a slightly lower temperature. Since adsorption between DSS and gelatin under the conditions of formation used here, took place at cationic side-chain and at backbone nitrogens, the ability of these groups of the protein molecule to form inter-chain salt links and hydrogen-bond short links is prevented, and gelation of the complexes in toluene solution seems likely to be due to secondary forces of the van der Waals type, between the hydrocarbon chains of the adsorbed molecules.

The effect of DSS on the  $\text{pH}$  titration of gelatin is similar to that of inorganic salts which has been fully discussed by other workers.<sup>6</sup> That the effect is similar in the presence of formaldehyde supports the view expressed in Part III<sup>7</sup> that the normal reaction between formaldehyde and gelatin is not greatly influenced by the presence of adsorbed  $\text{DS}'$  ions, nor does reaction of the formaldehyde with the protein affect  $\text{DS}'$  adsorption.

We gratefully acknowledge the assistance in some of this work of I. I. Harris, and the helpful discussion of C. Waller and others on the staff of Ilford Ltd. Our thanks are also due to the directors of that Company for permission to publish this paper.

### Summary.

Some physical and chemical properties of adsorption complexes formed between gelatin and dodecyl sodium sulphate have been studied. A wide range of water contents was obtainable according to the mode of preparation of the complexes. Variations of refractive indices were observed, due mainly to the variation of water content. Complexes which have been dehydrated show a marked solubility in organic solvents such as  $\text{CCl}_4$  and  $\text{C}_6\text{H}_6$ , and are practically

<sup>6</sup> Annalen, 222, 118.

<sup>7</sup> See Cannan, *Symposium on Quantitative Biology* (Cold Springs Harbour, 1938), 1.

<sup>8</sup> Harris, Pankhurst and Smith, *Trans. Faraday Soc.*, preceding paper.

insoluble in water. It is suggested that the original electrovalent link between the DS' anion and the positive sites on the protein nitrogens loses water with the formation of an alkoxysulphonamide type of structure.  $pH$  titration in the presence and absence of formaldehyde indicate that adsorption of DS' ions and the fixation of formaldehyde to the protein, can take place independently of each other.

### Résumé.

On a étudié les propriétés physiques et chimiques des complexes d'adsorption entre la gélatine et le dodécyl-sulfate de sodium. Ceux-ci contiennent une quantité d'eau très variable, selon la méthode de préparation. Les complexes déshydratés ont une solubilité marquée dans  $CCl_4$  et  $C_6H_6$ , phénomène pour lequel on suggère une explication. Des titrages potentiométriques, en présence et en l'absence de  $HCHO$ , montrent que l'adsorption d'ions dodécyl-sulphate et la fixation de  $HCHO$  sur la protéine ont lieu indépendamment l'une de l'autre.

### Zusammenfassung.

Die 'physikalischen und chemischen Eigenschaften von Adsorptionskomplexen zwischen Gelatine und Dodecylnatriumsulfat sind untersucht worden. Je nach der Darstellungsmethode kann der Wassergehalt über ein grosses Zusammensetzungsbereich variieren. Die entwässerten Komplexe zeigen eine deutliche Löslichkeit in  $CCl_4$  und  $C_6H_6$ , wofür eine Erklärung vorgeschlagen wird.  $pH$ -Titrationen in Gegenwart und Abwesenheit von  $HCHO$  zeigen, dass Adsorption von Dodecylsulfationen und Fixierung von  $HCHO$  an das Protein von einander unabhängig eintreten.

*The Ilford Research Laboratory,  
Ilford Limited,  
Ilford.*

---

## THE SWELLING OF CELLULOSE IN AQUEOUS SOLUTIONS OF CERTAIN ACIDS AND SALTS WITH MEASUREMENTS OF THE VAPOUR PRESSURES, DENSITIES AND VISCOSITIES OF THESE SOLUTIONS.

BY G. S. KASBEKAR AND S. M. NEALE.

*Received 23rd December, 1946.*

On account of its great molecular chain length, and of the cross-linking of the chains by numerous resonance bonds between the OH groups, cellulose dissolves only in a small number of highly active solvents, such as cuprammonium hydroxide. Before solution takes place, cellulose swells strongly, and indeed the action of many reagents is limited to swelling of greater or less extent.

The solution of cellulose finds application in the rayon industries and in research work. Slight swelling of cellulose, confined to the inter-crystalline regions where the orientation of the chain molecules is irregular, and the density of the inter-chain hydroxyl bonds is low, occurs in water, and is indispensable in processes such as dyeing. Further swelling, involving the whole structural network and the breaking of the inter-chain hydroxyl bonds in the crystalline regions, is necessary for the completion of nitration, acetylation or methylation, and is also made use of in such processes as mercerisation, in permanent stiffening of cotton fabrics, and the manufacture of "vulcanised fibre". Apart from the swelling in water and in caustic alkalis, however, little is known of the mechanism of the process and quantitative data are lacking.

The present communication sets out the results of a quantitative examination of the swelling of cellulose in a group of reagents, the most active of which are characterised by great affinity for water and by great swelling power for cellulose, namely  $\text{ZnCl}_2$ ,  $\text{Zn}(\text{CNS})_2$ ,  $\text{Ca}(\text{CNS})_2$ ,  $\text{H}_2\text{SO}_4$  and  $\text{H}_3\text{PO}_4$ . The vapour pressures, densities and viscosities of the solutions have also been determined, where these could not be ascertained from the literature, in order to gain some insight into the relative water affinities of the various solutes. The affinity for water affords some indication of the tendency to combine with the OH group, and so to effect the breaking of the transverse inter-chain hydroxyl bonds of cellulose. The outstanding features of the results may be summarised as follows.

1. Cellulose swells only slightly more than in pure water in solutions of  $\text{ZnCl}_2$  up to 9 M.,  $\text{H}_2\text{SO}_4$  up to 11 M.,  $\text{H}_3\text{PO}_4$  up to 24 M., and in all concentrations of  $\text{Ca}(\text{CNS})_2$  and  $\text{Zn}(\text{CNS})_2$ .

2. Higher concentrations of  $\text{ZnCl}_2$ ,  $\text{H}_2\text{SO}_4$  and  $\text{H}_3\text{PO}_4$  cause cellulose to swell greatly and this great swelling is at the optimum concentration followed by solution in less than 5 min. with  $\text{H}_2\text{SO}_4$ , in less than 1 hr. in  $\text{H}_3\text{PO}_4$ , but months are required for solution in  $\text{ZnCl}_2$  at 25° C., and the maximum swelling recorded before solution is much greater.

3. When the swelling is not great there is a slight preferential absorption of the solute, but at high degrees of swelling and high solute concentrations there is a preferential absorption of water.

4. The take-up of solution by cellulose sheet and the shrinkage in length of cotton yarn, which occurs because its chain molecules contract spontaneously when freed from the lateral restraint of the inter-chain hydroxyl bonds, and therefore accompanies swelling, run parallel to each other for different concentrations of each solute. When the various solutes are compared, however, those producing the same shrinkage of yarn do not produce the same swelling of cellulose sheet.

5. Solutions capable of causing great swelling show relative vapour pressures below 0.15, and partial molal contractions of added water (calculated from the variation of density with concentration) greater than 0.8 cc./mole.

6. Solutions of  $\text{Ca}(\text{CNS})_2$  and  $\text{Zn}(\text{CNS})_2$  do not attain the required values and cause relatively slight swelling of cellulose.

### Experimental.

**Cellulose Materials.**—In view of the fact that it is impossible quantitatively to separate the entrained liquid from a mass of textile fibres in any form, most of the measurements were carried out on Cellophane, a sheet cellulose regenerated by the viscose process. Neale<sup>1</sup> has shown that by the simple process of squeezing the swollen sheets with dry filter paper, fairly reproducible values can be obtained for the take-up of sodium hydroxide and water. This procedure was followed in the present work. The length shrinkage of a bleached two-fold Sakellaridis cotton yarn was also used as a convenient index of the swelling of a more coherent form of cellulose. These materials had the following properties, those of the Cellophane indicating the degradation of the cellulose usually caused by oxidation in the viscose process.

	Cellophane.	Yarn.
Mean air dry thickness (cm.) . . .	0.00218	—
Fluidity in cuprammonium . . .	9.0 (2 % soln.)	3.8 (0.5 % soln.)
Copper number (Schwalbe-Braidy) . . .	0.69	0.015
COOH group (milliequiv./100 g.) . . .	5.05	0.4

<sup>1</sup> Neale, *J. Text. Inst.*, 1929, **20**, 373.

**Solutions.**—Solutions of the three salts were prepared by weight dilution from filtered solutions saturated at 25° c. Both the cation and the anion were estimated in each solution, and any in which the respective values differed from equivalence by more than 0.2 % were rejected.

**Swelling.**—Several pieces of Cellophane about 4 cm. square were immersed in about 100 cc. of solution and kept in an air thermostat at 25° c. They were removed by forceps, twice blotted with clean filter paper and weighed. They were then immersed in 200 cc. water, boiled, filtered on to a No. 3 Jena glass filter, and washed with 200 cc. boiling water. For Ca and Zn thiocyanates the residue on the filter was first washed with 25 cc. of cold 0.01 N. HNO<sub>3</sub> and then with 200 cc. boiling water. Material swollen in ZnCl<sub>2</sub> was treated with boiling 0.01 N. HNO<sub>3</sub> at each stage.

The washed cellulose remaining in the funnel was dried at 110° c. and all results are expressed in terms of its final dry weight. The combined extracts were analysed for both cationic and anionic components, using the following methods.

**Analysis.**—Zinc was estimated by titration with K<sub>4</sub>Fe(CN)<sub>6</sub>, using methyl red as an adsorption indicator, after Tananaew and Georgofiani.<sup>2</sup> Calcium was estimated by titration at 60° c. in daylight of a carefully neutralised solution with a standard solution of pure potassium palmitate, made according to Hamer,<sup>3</sup> using phenolphthalein as indicator. The volume of solution taken for titration was adjusted so as to obtain titres not too far from the standard value. This procedure, for which we have to thank our colleague Dr. A. F. H. Ward, proved accurate and convenient. Chloride was estimated by titration with AgNO<sub>3</sub>, using the simple potentiometric nullpoint method of Callan and Horrabin.<sup>4</sup> Thiocyanate was estimated by adding an excess of standard AgNO<sub>3</sub> solution, and then titrating back with standard thiocyanate, using ferric alum indicator, until a pale pink coloration stable to vigorous shaking was obtained. Sulphuric acid was estimated by titration against standard alkali. Phosphoric acid was estimated by titration with standard baryta according to Wilkie's method,<sup>5</sup> which was found to agree with gravimetric estimations as ammonium phospho-molybdate.

**Shrinkage of Yarn.**—The contraction in length of 6 cm. lengths of the cotton yarn, kept taut in the solution at 25° c. by a weight of 0.3 g. of Ni wire, was measured by a travelling microscope.

**Physical Properties of Solutions.**—Certain physical properties of the solutions used, which could not be found in the literature, were determined by experiment, as follows.

Densities: these were determined by the specific gravity bottle method, and are believed to be accurate within 0.01 %.

Viscosities: these were determined in an Ostwald viscometer at 25° c.

Vapour Pressures: these were measured on a mercury manometer of 1 cm. bore,

using 7 cc. of air-free solution, admitted to a highly evacuated vessel in two portions successively. Check results agree well with the data given in the International Critical Tables. The results for zinc chloride were in good agreement with those of Menzies and Boving.<sup>6</sup>

	V.P. (mm. Hg.)	
	I.C.T.	Experimental.
Water 25.0° c. . .	23.50	23.55
Water 26.0° c. . .	24.987	25.10
H <sub>2</sub> SO <sub>4</sub> 38 % . . .	14.50	14.57

<sup>2</sup> Tananaew and Georgofiani, *Z. anal. Chem.*, 1936, **107**, 96-9.

<sup>3</sup> Hamer, *J. Soc. Chem. Ind.*, 1935, **54**, 250T.

<sup>4</sup> Callan and Horrabin, *ibid.*, 1928, **47**, 329T.

<sup>5</sup> Wilkie, *ibid.*, 1909, **28**, 68 : 1910, **29**, 794.

<sup>6</sup> Menzies and Boving, 8th *Int. Cong. Appl. Chem. Reports*, 1912.

## Results.

## Aqueous Solutions of Zinc Chloride. Swelling of Cellophane.

It appears from the results given in Table I that a period of 6 days at 25° C. was sufficient for the establishment of approximate equilibrium

TABLE I.—VARYING PERIODS IN 20.44 M. (73.58 %) SOLUTION AT 25° C.

Time of Swelling (hr.).	Swelling (% Increase on Dry Weight).	G. mol. Absorbed per 162 g. Cellulose.			Ratio Cl/Zn.	g. ZnCl <sub>2</sub> per 100 g. Solution in Gel.
		Zn.	Cl.	H <sub>2</sub> O.		
18	626	5.32	10.56	16.2	1.99	71.2
	601	4.95	10.00	16.4	2.02	69.5
41	9390	81.85	159.5	233	1.95	72.4
	9630	84.9	164.4	234	1.94	73.0
65.5	15150	133.5	257.7	371	1.932	72.8
	13470	117.5	230.3	330	1.956	72.7
89	15030	132.6	259.0	361.4	1.953	73.31
	15160	134.8	263.8	355.8	1.958	73.98
143	13960	122.4	242.4	334	1.980	73.35
	12740	112.1	219.7	305	1.957	73.38

in a highly concentrated solution of ZnCl<sub>2</sub>. The yarn shrinkage experiments showed that the more concentrated solutions were the slower in their action and the period of immersion was therefore standardised at 6 days in a study of the effect of variations of concentration, the results of which are shown in Table II.

TABLE II.—EFFECT OF VARYING CONCENTRATIONS OF ZINC CHLORIDE AT 25° C. (6 DAYS' IMMERSION).

Concentration of Solution.		Swelling (% Increase on Dry Weight.)	G. mol. Absorbed per 162 g. Cellulose.			Ratio Cl/Zn.	g. ZnCl <sub>2</sub> per 100 g. Solution in Gel.
Molality.	%.		Zn.	Cl.	H <sub>2</sub> O.		
0.864	10.53	108.3	0.284	0.520	7.69	1.83	21.1
1.893	20.51	140	0.531	1.000	8.45	1.85	31.5
3.126	29.97	166	0.697	1.407	9.66	2.02	35.4
5.058	40.81	223	1.19	2.33	11.16	1.95	44.4
8.90	54.8	535	3.40	6.66	22.8	1.95	52.7
9.56	55.6	872	5.66	11.1	36.2	1.96	53.9
9.79	57.2	1090	—	14.5	42.5	—	55.2
10.44	58.7	1764	12.4	24.7	65.0	1.99	59.0
11.27	60.6	2430	—	34.8	87	—	60.2
11.77	61.6	5955	—	86.56	208	—	61.1
11.88	61.8	7340	52.7	105.8	256	2.00	61.2
12.51	63.0	9035	—	134.0	306	—	62.4
13.47	64.7	10000	—	158	337	—	64.0
15.17	67.4	13000	—	—	—	—	—
15.81	68.3	12500	—	203	353	—	68.5
16.28	68.9	13000	105	205	395	1.96	66.5
17.99	71.0	12600	—	213	331	—	70.9
20.44	73.6	13000	122	242	334	1.98	73.4

The swelling curve (Fig. 1) rises steeply as the concentration of ZnCl<sub>2</sub> exceeds about 60 % (11 moles/1000 g. H<sub>2</sub>O). At low concentrations

(below 50 %) the salt is absorbed in preference to the water (see last column of Table II) but the results suggest that at the highest concentration there may be a slight preferential absorption of water. This undoubtedly occurs in the earlier stages of swelling with the most concentrated solutions (see Table I). The evidence for a preferential absorption of zinc ion (ratio Cl/Zn less than 2.0) is inconclusive, except perhaps in the two most dilute solutions, and this may be due to reaction with the carboxylic acid groups present in Cellophane.

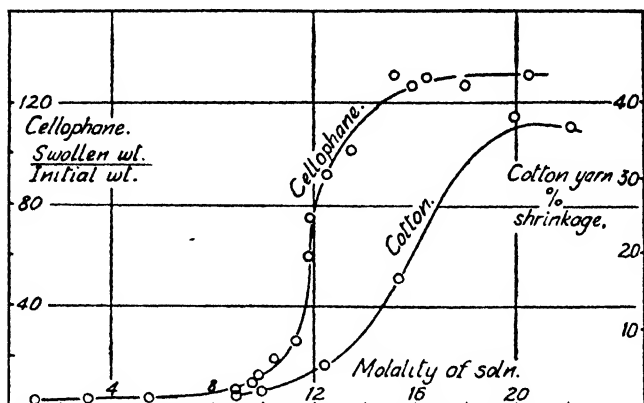


FIG. 1.—Swelling of cellulose in zinc chloride solutions at 25° C.

These results serve to confirm the Cellophane swelling measurements, in showing a sharp increase in swelling as the concentration exceeds 14 M. The effective swelling concentrations are, however, definitely higher for the cotton, no doubt on account of its more coherent structure. The relatively very slow swelling in the most concentrated solutions is also observed with cellulose in NaOH solutions.<sup>1</sup>

TABLE III.—SHRINKAGE OF COTTON YARN IN ZINC CHLORIDE SOLUTIONS AT 25° C.

Concentration of Solution.		Shrinkage in Length.	Time (hr.) for Shrinkage to Attain Maximum.
Molality.	%.	%.	
1.97	21	0.6	—
5.42	42.5	1.1	—
8.97	55.0	1.6	1.0
9.98	57.6	2.3	1.0
12.4	62.8	5.5	15.0
15.3	67.5	16.6	20.0
19.94	73.1	38.1	25.0
22.04	75.0	36.6	45.0

**Physical Properties of  $\text{ZnCl}_2$  Solutions.**—The vapour pressures and viscosities of aqueous solutions of  $\text{ZnCl}_2$ , measured by the methods described, are given in Table IV, and plotted in Fig. 2. The partial molal contraction values were calculated from the density data of International Critical Tables, and signify the contraction in overall volume which occurs when one mole of water is added to an infinitely large amount of solution. Their magnitudes, like that of the vapour pressure lowering, provide an



## 522 SWELLING OF CELLULOSE IN AQUEOUS SOLUTIONS

indication of the affinity of the solution for more water, or, alternatively, for the hydroxyl groups of cellulose. The viscosity probably has a similar significance, high viscosity indicating the existence in the concentrated solution of transient chain-molecules of the type A—B—A—B—A—B

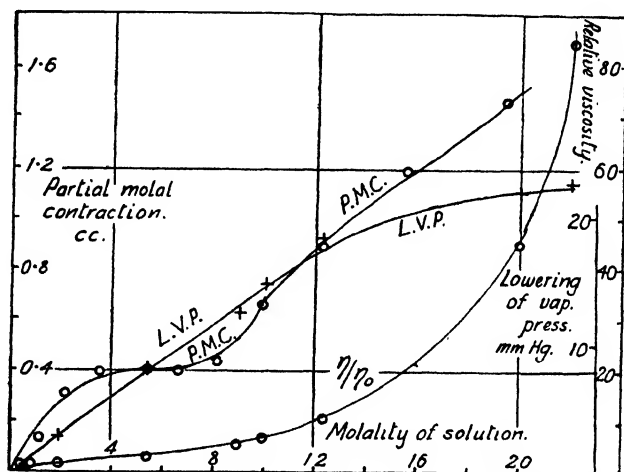


FIG. 2.—Physical properties of zinc chloride solutions at 25° C.

owing to the strong attachment between water molecules and  $\text{ZnCl}_2$ . It is noteworthy that the partial molal contraction remains constant over the concentration range 3.3 to 8 M. (see Fig. 2).

TABLE IV.—ZINC CHLORIDE SOLUTIONS AT 25° C.

Concentration of Solution. Molality.	Partial Molal Contraction of added Water. cc.	Concentration. Molality.	Relative Viscosity. ( $\text{H}_2\text{O} = 1$ ).	Vapour Pressure. mm. Hg.
0.47	0.03	0	1.0	23.5
1.19	0.14	0.863	1.291	—
2.13	0.31	1.960	1.587	20.75
3.53	0.39	5.41	2.81	15.45
4.40	0.40	8.99	5.34	11.00
5.42	0.40	9.98	6.61	9.70
6.63	0.40	12.36	10.29	7.15
8.11	0.43	19.97	44.83	1.3
9.93	0.65	22.04	84.43	0.6
12.23	0.89			
15.24	1.185			
19.34	1.455			

### Swelling of Cellulose in Aqueous $\text{H}_2\text{SO}_4$ .

The swelling of cellulose in concentrated solutions of  $\text{H}_2\text{SO}_4$  is a very rapid process. Solutions stronger than 20 M. dissolve cellulose in less than 2 min. and rapid hydrolysis also occurs. Two minutes was chosen as a standard time of immersion in the study of the effect of  $\text{H}_2\text{SO}_4$ , so as to minimise the effect of hydrolysis.

**Swelling of Cellophane after 2 min. in  $\text{H}_2\text{SO}_4$  Solutions at  $25^\circ\text{C}$ .**

Up to a concentration of 11 M. the swelling increases only slowly, but above that concentration it increases rapidly, reaching a maximum in 16.7 M. solution (62 % by weight) and decreasing slowly thereafter. The last column of Table V shows that there is a marked preferential absorption

TABLE V.—SWELLING OF CELLOPHANE IN SULPHURIC ACID AT  $25^\circ\text{C}$ .

Concentration of Solution.		Swelling % Increased on Dry Weight.	G. moles Absorbed per 162 g. Cellulose.		g. $\text{H}_2\text{SO}_4$ per 100 g. Solution in Gel.
Molality.	%.		$\text{H}_2\text{SO}_4$ .	$\text{H}_2\text{O}$ .	
1.30	11.3	106.6	0.21	8.43	12.0
6.74	39.8	176.2	1.19	9.25	40.7
9.55	48.4	214	1.69	10.0	47.9
11.28	52.5	268	2.32	11.5	51.75
12.90	55.9	496	4.53	19.9	55.3
14.80	59.2	1920	18.74	71.7	58.7
16.44	61.7	2500	25.6	90.0	60.7
18.61	64.6	2200	22.8	72.1	63.2
19.90	66.1	2210	23.4	72.0	64.0
21.90	68.2	1545	17.15	45.6	67.1
23.09	69.4	1540	17.1	45.6	67.1
25.64	71.6	1600	18.15	44.8	66.8

of water from the more concentrated solutions, but as only 2 min. were allowed for swelling this may be simply due to a more rapid take-up of water by the air-dry Cellophane, since water is known to penetrate cellulose with exceptional speed.

TABLE VI.—SHRINKAGE OF COTTON YARN  
IN SULPHURIC ACID AT  $25^\circ\text{C}$ .

Concentration of Solution.		Maximum Shrinkage.	Time for Maximum Shrinkage (min.).
Molality.	%.	%.	
6.74	39.8	0.04	—
11.3	52.5	1.5	1
14.8	59.2	1.5	10
16.4	61.7	17.3	7.5
18.6	64.6	35.0	1.0
19.9	66.1	34.6	0.75
21.9	68.2	16.6	0.5
23.1	69.4	14.2	0.5
25.6	71.55	11.5	0.5

Comparative experiments were also made on the length shrinkage of cotton yarn. The results are summarised in Table VI, and are compared with the cellophane swelling experiments in Fig. 3. The maximum shrinkage is in each case, followed by an extension and finally breakage of the shrunk yarn, on account of the decrease in the cohesive forces which hold the cellulose together.

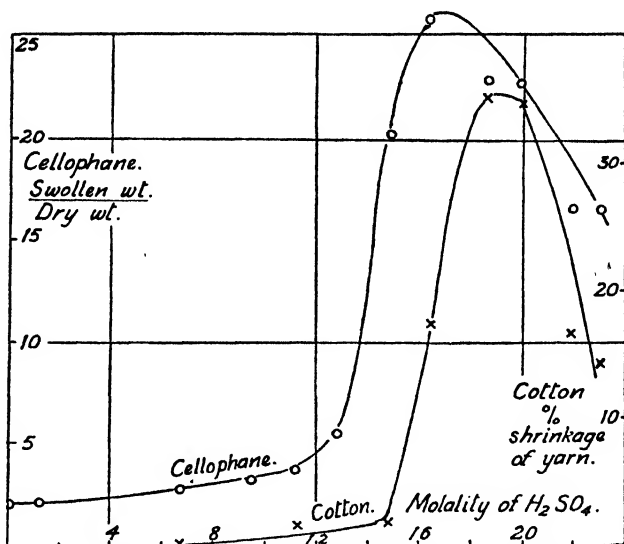


FIG. 3.—Swelling of cellulose in sulphuric acid solutions.

**Physical Properties of Sulphuric Acid Solutions.**—These were obtained from the data of International Critical Tables and are plotted in Fig. 4.

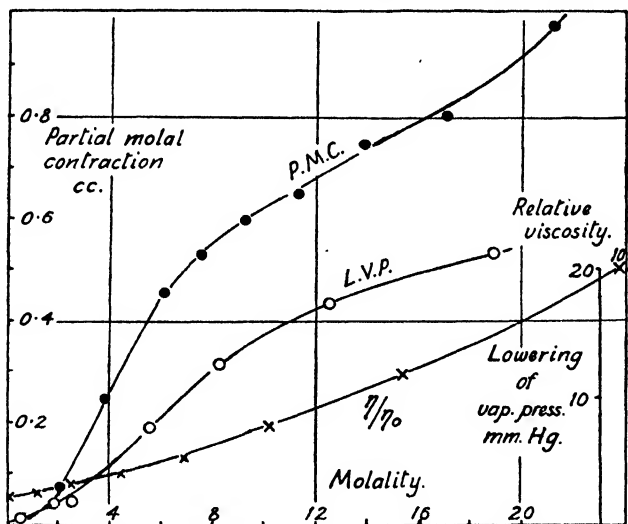


FIG. 4.—Physical properties of sulphuric acid solutions at 25° C.

### Swelling of Cellulose in Phosphoric Acid.

Concentrated solutions of phosphoric acid in water cause cellulose to swell very greatly, and their use as a cellulose solvent for viscosity measurements was suggested by Ekenstam.<sup>7</sup> This possibility was critically

<sup>7</sup> Ekenstam, *Ber.*, 1936, 69, 549.

examined by Neale and Waite,<sup>8</sup> who found that the most effective concentration was 81.5 % (44.8 M.), but that at least 5 hr. were required to dissolve cotton, during which time the cellulose had suffered appreciable breakdown, by hydrolysis, of the glucoside links of the main chain. The

TABLE VII.—SWELLING OF CELLOPHANE IN PHOSPHORIC ACID SOLUTIONS (20 HR. IMMERSION AT 25° C.).

Concentration of Solution.		Swelling % Increased on Dry Weight.	g. Moles Absorbed Per 162 g. Cellulose.		g. $\text{H}_3\text{PO}_4$ Per 100 g. Solution in Gel.
Molality.	%.		$\text{H}_3\text{PO}_4$ .	$\text{H}_2\text{O}$ .	
1.13	10.0	121	0.205	9.77	10.25
2.66	20.7	131	0.450	9.27	20.7
4.64	31.3	146	0.791	8.86	32.7
7.23	41.5	166	1.17	8.60	42.5
11.00	51.9	201	1.75	8.63	52.5
17.83	63.6	237	2.47	8.08	62.4
24.5	70.6	303	3.59	7.71	71.7
29.6	74.4	722	8.91	16.5	74.7
31.9	75.8	Dissolved			
82.5	89.0	Dissolved			

result of the present measurements of swelling of Cellophane in phosphoric acid, are given in Table VII and are plotted in Fig. 5. The extent of swelling increases gradually with the concentration up to 25 M., beyond which point the swelling increases rapidly, so that the Cellophane passes into solution above 30 M.

TABLE VIII.—SHRINKAGE OF COTTON YARN IN  
 $\text{H}_3\text{PO}_4$  SOLUTIONS AT 25° C.

Concentration of Solution.		Maximum Shrinkage.	Time for Maximum Shrinkage (hr.).
Molality.	%.	%.	
13.8	57.5	0.5	—
31.2	75.3	2.3	20
36.0	77.9	2.9	18
43.0	80.8	30.0	6
53.0	83.9	55.0	0.25
67.1	86.8	20.0	1.0
83.77	89.2	20.0	4.0

The swelling of cotton yarn occurs very abruptly above 78 %  $\text{H}_3\text{PO}_4$ , the critical concentration for complete solution being 81.5 %.<sup>8</sup> Cellophane, on the other hand, dissolves in all solutions more concentrated than 75 % if sufficient time is allowed.

**Physical Properties of  $\text{H}_3\text{PO}_4$  Solutions.**—The vapour pressures and viscosities of  $\text{H}_3\text{PO}_4$  solutions were determined and the results of these measurements together with the partial molal contraction of water calculated from the densities given in the literature, are recorded in Table IX and plotted in Fig. 6.

<sup>8</sup> Neale and Waite, *Trans. Faraday Soc.*, 1941, **37**, 261.

Swelling in  $\text{Ca}(\text{CNS})_2$  Solutions.

It has been reported by several workers<sup>9-11</sup> that  $\text{Ca}(\text{CNS})_2$  solutions are capable of acting as powerful swelling agents or as solvents for cellulose. Our measurements showed, however, that whilst their swelling power is

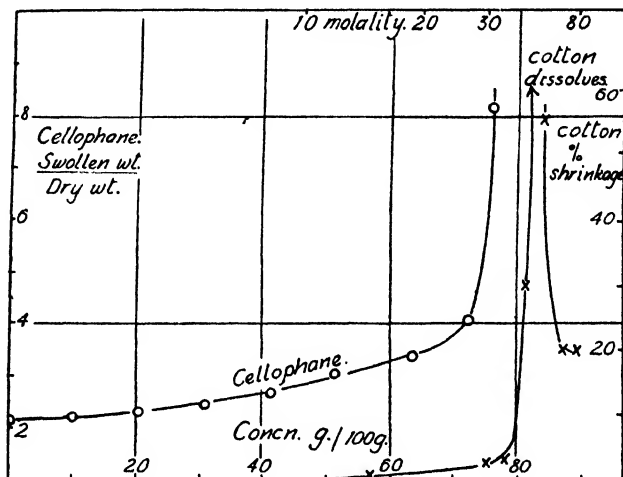


FIG. 5.—Swelling of cellulose in phosphoric acid solutions.

TABLE IX.—PHOSPHORIC ACID SOLUTIONS  
AT 25° C.

Concentration of Solution.		Partial Molal Contraction of added Water. cc.	Relative Viscosity ( $\text{H}_2\text{O}=1$ ).	Vapour Pressure Lowering (mm. Hg.)
Molality.	%.			
1.51	13	0	1.40	1.50
4.04	28.4	0.02	2.33	2.70
6.47	38.8	0.13	3.47	4.50
13.8	57.9	0.39	7.88	10.85
26.4	72.1	0.93	17.86	17.05
32.2	75.9	1.03	22.64	18.20
36.0	77.9	1.10	26.34	19.10
43.0	80.8	1.29	33.19	20.10
53.0	83.85	1.41	39.8	20.8
67.0	86.8	1.57	49.4	21.7
83.8	89.15	1.59	66.7	22.6

greater at 25° c. than that of pure water it is much less than that of the solutions already described in this paper. The results of the Cellophane swelling experiments are given in Table X. The maximum shrinkage of cotton yarn was only 1.1 % (in the 58 % solution).

<sup>9</sup> Dubosc, *Rev. Prod. Chim.*, 1923, **26**, 507.<sup>10</sup> Herzog and Beck, *Z. Physiol. Chem.*, 1920, **111**, 287.<sup>11</sup> Williams, *Manchester Phil. Soc.*, 1921, **65**, No. 12.

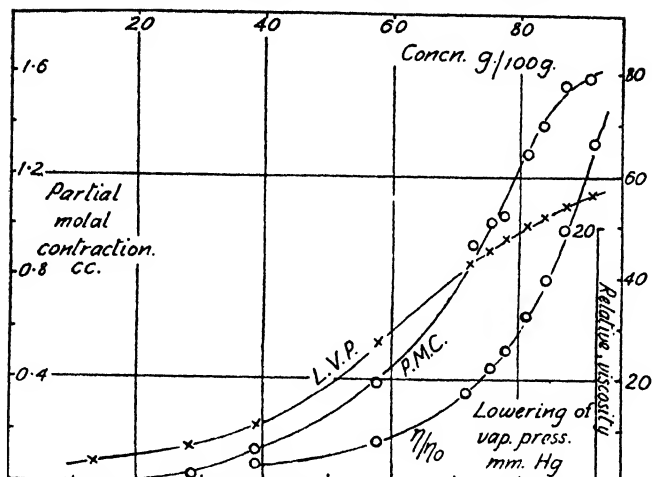


FIG. 6.—Physical properties of phosphoric acid solutions at 25° c.

TABLE X.—SWELLING OF CELLOPHANE IN  $\text{Ca}(\text{CNS})_2$  SOLUTIONS  
(77 DAYS IMMERSION AT 25° C.)

Concentration of Solution.		Swelling % Increase on Dry Weight.	g. mol. Absorbed per 16.2 g. Cellulose.			Ratio CNS/Ca.	g. $\text{Ca}(\text{CNS})_2$ per 100 g. Solution in Gel.
Molality.	%.		Ca.	CNS.	$\text{H}_2\text{O}$ .		
0.61	8.7	121	0.21	0.324	9.3	1.54	14.1
1.55	19.5	148	0.409	0.725	10.0	1.77	24.6
2.92	31.3	181	0.631	1.17	11.1	1.86	31.7
4.36	40.5	525	2.30	4.60	27.3	2.00	42.2
6.70	51.1	630	3.20	6.42	28.8	2.00	49.1
8.64	57.5	671	3.75	7.51	27.8	2.00	53.9
8.84	58.0	688	3.98	7.95	27.4	2.00	55.8

TABLE XI

Concentration of Solution.		Vapour Pressure. mm. Hg.	Density. g./cc.	Partial Molal Contraction. cc.	Relative Viscosity.
Molality.	%.				
0	0	23.50	0.99823	0.0	1.00
0.61	8.69	22.8	1.051	0.01	1.16
1.55	19.52	20.7	1.121	0.27	1.49
2.92	31.3	17.3	1.200	0.59	2.36
0.36	40.5	12.2	1.270	0.62	3.88
6.70	51.1	7.7	1.351	0.66	10.87
8.64	57.4	3.4	1.405		29.8
8.84	58.0				32.00

**Physical Properties of Calcium Thiocyanate Solutions.**—The vapour pressures, densities and viscosities of the solutions used were determined at 25° c. and the results are recorded in Table XI. It appears that

although  $\text{Ca}(\text{CNS})_2$  solutions attain high values for vapour pressure lowering and for relative viscosity, the partial molal contraction does not attain the value ( $> 0.8$  cc.) associated with great swelling power for solutions of  $\text{ZnCl}_2$ ,  $\text{H}_3\text{PO}_4$  and  $\text{H}_2\text{SO}_4$ .

### Swelling of Cellulose in $\text{Zn}(\text{CNS})_2$ Solutions.

In the lyotropic series, zinc is higher than calcium, and thiocyanate is higher than chloride. Very great swelling of cellulose was therefore anticipated in solutions of  $\text{Zn}(\text{CNS})_2$ .

Experiments showed, however, that this was not so. The maximum swelling of Cellophane at  $25^\circ \text{C}$ . was obtained with the saturated solution but was less than 200 % (wt. of soln. absd./wt. of cellulose) and the maximum shrinkage of cotton yarn was only 1.6 %. Zinc thiocyanate is not notably deliquescent, the vapour pressure of the saturated solution was relatively high, and the partial molal contraction of added water is relatively low (see Table XII). Zinc thiocyanate is therefore to be pre-

TABLE XII.—PHYSICAL PROPERTIES OF  $\text{Zn}(\text{CNS})_2$  SOLUTIONS AT  $25^\circ \text{C}$ .

Concentration of Solution.		Vapour Pressure mm. Hg.	Density g./cc.	Partial Molal Contraction cc.	Relative Viscosity.
Molality.	%.				
0	0	23.50	0.99828	(0.053)	1.0
0.53	8.87	22.80	1.0532	0.033	1.20
1.13	17.07	22.20	1.1103	0.13	1.47
1.99	26.56	21.75	1.1805	1.26	2.00
2.89	34.4	20.25	1.2489	0.31	2.76
3.48	38.7	19.45	1.2837	0.33	3.33
4.02	42.2	18.80	1.3143	0.60	3.94
6.92	55.5	14.75	1.4460		5.14

sumed relatively deficient in affinity for water, and also for the hydroxyl groups of cellulose.

### Résumé.

On donne les résultats d'une étude quantitative du "gonflement" de la cellulose par un groupe de réactifs ( $\text{ZnCl}_2$ ,  $\text{Zn}(\text{CNS})_2$ ,  $\text{Ca}(\text{CNS})_2$ ,  $\text{H}_2\text{SO}_4$  et  $\text{H}_3\text{PO}_4$ ), dont les plus actifs sont caractérisés par une grande affinité pour l'eau et par un important pouvoir "gonflant" vis-à-vis de la cellulose. On a déterminé aussi les tensions de vapeur, densités et viscosités de ces solutions pour avoir un aperçu des affinités relatives de ces divers réactifs pour l'eau, puisque cette propriété apporte quelque indication sur la tendance à la combinaison avec le groupe OH et sur la rupture des liaisons hydroxyle transversales entre les chaînes de cellulose.

### Zusammenfassung.

Der Artikel beschreibt die Resultate einer quantitativen Untersuchung der Quellung von Zellulose in einer Serie von Reagenzien ( $\text{ZnCl}_2$ ,  $\text{Zn}(\text{CNS})_2$ ,  $\text{Ca}(\text{CNS})_2$ ,  $\text{H}_2\text{SO}_4$  und  $\text{H}_3\text{PO}_4$ ). Die wirksamsten Reagenzien sind sowohl durch ihre grosse Affinität für Wasser als auch durch ihr Quellungsvermögen gekennzeichnet. Dampfdruck, Dichte und Viskosität dieser Lösungen wurden bestimmt, um einen Einblick in die relative Wasseraffinität der diversen gelösten Stoffe zu gewinnen, da die Affinität für Wasser einen gewissen Hinweis auf ihre Tendenz, sich mit der OH-Gruppe zu verbinden und auf diese Weise die Querhydroxylbindungen zwischen den Ketten von Zellulose zu brechen, darstellt.

## PART II. CRYSTALLINITY IN SOLID COLLOIDS.

### SOLUTION AND DIFFUSION IN HIGH POLYMERS.

BY A. S. CARPENTER.

Received 3rd October, 1946.

High polymeric materials such as natural and synthetic rubbers are solvents for gases and certain other substances and a study of the diffusion of such solutes in them can give results of fundamental significance and practical importance. Mathematically, the problem of the diffusion of a dissolved substance in an immobile solvent medium, resulting from an uneven concentration distribution, is identical with that of the flow of heat in a solid medium resulting from an uneven temperature distribution. This latter problem has received considerable attention,<sup>1-7</sup> while Barrer<sup>8</sup> has made general application to diffusion processes of some of the methods used and the results obtained in the consideration of heat flow. Under certain conditions, mathematical relationships may be deduced defining the absorption of solute by an immobile solvent. The present paper describes a method, based on these relationships, for determining solubility and diffusion coefficients of gases in high polymeric materials. Some experimental results obtained by the use of the method are recorded.

It is assumed that the solvent is isotropic, that diffusion of solute does not depend upon a specific interaction process with the solvent (e.g. the diffusion of water vapour in ordinary natural rubber is specific in this sense, depending as it does upon interaction with the hydrophilic, non-hydrocarbon constituents entrapped in the material during its isolation from the latex) and that solute concentrations are sufficiently low for volume changes to be negligible and for the diffusion coefficient to be independent of concentration. Justification for this latter assumption in the case of most gases in high polymers has been given in a previous publication.<sup>9</sup> We consider the absorption of solute by a block of an immobile solvent when, with an original uniform solute concentration throughout, the concentration in an infinitesimally thin surface layer is instantaneously altered to, and maintained at, a new value. The mathematical relationships defining rate of solute absorption under these conditions depend upon specimen shape and are of the general form

$$\frac{dq}{dt} = \frac{kD(q_{\infty} - q_0)}{X^2} \sum_{l, m, n=1}^{\infty} \phi(l, m, n) e^{-v(l, m, n) \frac{Dt}{X^2}}$$

in which  $D$  is the diffusion coefficient,  $t$  is the time after the change of surface concentration;  $q_0$ ,  $q$  and  $q_{\infty}$  are the total quantities of solute dissolved respectively at zero time, time  $t$  and infinite time,  $X$  is a significant

<sup>1</sup> Byerly, *Elementary Treatise on Fourier Series* (Boston, 1928).

<sup>2</sup> Carslaw, *Mathematical Theory of the Conduction of Heat* (New York, 1921).

<sup>3</sup> Fishenden and Saunders, *The Calculation of Heat Transmission* (H.M. Stationery Office, London, 1932).

<sup>4</sup> Fourier, *Théorie analytique de la chaleur* (Paris, 1822).

<sup>5</sup> Gurney and Lurie, *Ind. Eng. Chem.*, 1923, **15**, 1170.

<sup>6</sup> Ingersoll and Zobel, *Mathematical Theory of Heat Conduction* (Boston, 1913).

<sup>7</sup> Newman, *Trans. Amer. Inst. Chem. Eng.*, 1930, **24**, 44.

<sup>8</sup> Barrer, *Diffusion in and through Solids* (Cambridge, 1941).

<sup>9</sup> Carpenter and Twiss, *Ind. Eng. Chem. (Anal.)*, 1940, **12**, 99.



linear dimension of the specimen;  $\phi(l, m, n)$  and  $\psi(l, m, n)$  are functions of the positive integers  $l, m$ , and  $n$  and  $k$  is a constant. The functions  $\phi(l, m, n)$  and  $\psi(l, m, n)$  are such that the series indicated by the summations are convergent for all values of  $Dt/X^2$  and converge more rapidly the greater the value of  $Dt/X^2$ . In any particular case, as  $t$  increases, the summations become more and more closely approximated by their first terms. Thus the plots of  $dq/dt$  against  $t$  asymptotically approach the curves

$$\frac{dq}{dt} = \frac{kD(q_\infty - q_0)}{X^2} \phi(1) e^{-\psi(1) \frac{Dt}{X^2}}$$

or, plotting semi-logarithmically,  $\log_{10} dq/dt$  against  $t$ , the plots asymptotically approach the straight lines

$$\log_{10} \frac{dq}{dt} = \log_{10} \frac{kD(q_\infty - q_0)}{X^2} \phi(1) - \psi(1) \frac{Dt}{X^2} \log_{10} e.$$

The values of  $k\phi(1)$  and  $\psi(1)$  for solvent specimens in the form of certain geometric shapes are given in Table I.

TABLE I.—VALUES OF  $k\phi(1)$  AND  $\psi(1)$  FOR BLOCKS OF CERTAIN GEOMETRIC SHAPES.

(a) Sheet of "infinite" length and breadth; thickness $X$ . Unidirectional diffusion.	$k\phi(1) = 8$	$\psi(1) = \pi^2$
(b) Rectangular-sectioned rod of "infinite" length; section $X \times Y$ ; $uY = X$ . Diffusion in two directions at right angles.	$k\phi(1) = \frac{64}{\pi^2}(1 + u^2)$	$\psi(1) = (1 + u^2)\pi^2$
(c) Cylindrical rod of "infinite" length; radius $X$ . Radial diffusion in a cylinder	$k\phi(1) = 4$	$\psi(1) = B_1^2$
(d) Brick; $X \times Y \times Z$ ; $vZ = uY = X$ . Diffusion in three directions at right angles.	$k\phi(1) = \frac{512}{\pi^4}(1 + u^2 + v^2)$	$\psi(1) = (1 + u^2 + v^2)\pi^2$
(e) Cylindrical rod; radius $X$ , length $Y$ ; $wX = Y$ . Radial and end-to-end diffusion in a cylinder.	$k\phi(1) = \frac{32}{\pi^2} \left( \frac{\pi^2 + w^2 B_1^2}{B_1^2} \right)$	$\psi(1) = \pi^2 + w^2 B_1^2$
(f) Sphere; radius $X$ . Radial diffusion in a sphere.	$k\phi(1) = 6$	$\psi(1) = \pi^2$

$B_1$  is the first root of Bessel's equation of zero order; its value is 2.4048.

It may be shown that, although absorption rate is dependent upon specimen shape and size for all finite values of  $t$ , for an infinitesimally short initial period, all specimens behave as though semi-infinite in the direction or directions in which diffusion takes place. The absorption rate, under the conditions given above, of a semi-infinite solid is given by

$$\frac{dq}{dt} = \alpha(c_\infty - c_0) \sqrt{\frac{D}{\pi t}}$$

in which  $\alpha$  is the area of the absorbing surface,  $c_0$  is the initial uniform solute concentration and  $c_\infty$  is the solute concentration near the surface after infinite time.

Hence we may write

$$\lim_{t \rightarrow 0} \frac{dq}{dt} \sqrt{t} = \alpha(c_\infty - c_0) \sqrt{\frac{D}{\pi}} \quad (1)$$

for all specimens regardless of shape or size (see Fig. 1).

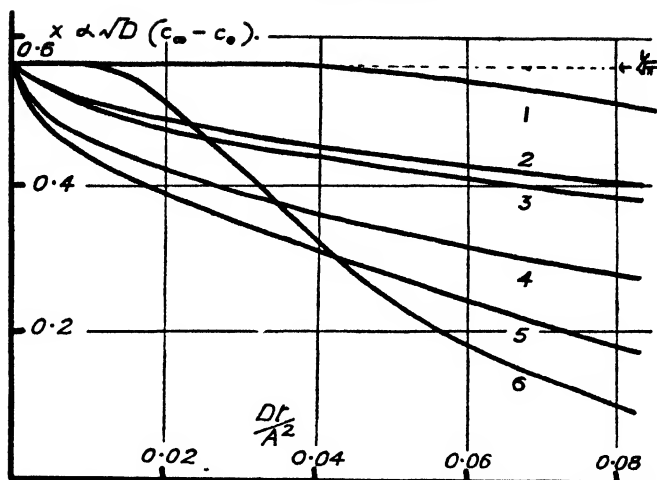


FIG. 1.—Plot of  $\frac{dq}{dt} \sqrt{t}$  against  $\frac{Dt}{A^2}$  for several specimens.

Curve number.	Specimen.
1	"Infinite" sheet, thickness $A$ ,
2	"Infinite" cylinder, radius $A$ .
3	"Infinite", square-sectioned rod, $2A \times 2A$ .
4	Sphere, radius $A$ .
5	"Infinite", square-sectioned rod, $A \times A$ .
6	"Infinite" sheet, thickness $A/2$ .

### Evaluation of Solubility and Diffusion Coefficient from Absorption Rate Data.

Daynes<sup>10</sup> has shown that the permeation of a gas through a rubber membrane consists of the processes of dissolution at one face, diffusion through the body of the membrane, and evaporation from the other face, the rate-determining process being that of diffusion. These conclusions have been shown, either directly or indirectly, to hold also for many other gas-high polymer combinations, e.g.,<sup>11-15</sup>. An infinitesimally thin surface layer of a high polymeric material in contact with a gas may therefore be regarded as being continually in equilibrium with the gas. That is to say, the surface concentration at any instant may be regarded as the saturation concentration which would ultimately be attained throughout a block of the material immersed in the gas maintained at constant pressure equal to the pressure at that instant. (A previous publication<sup>9</sup> compared and related the processes of permeation through a membrane and absorption by a block.) Exposing a block of a high polymer to a gas at one constant pressure for a long time and then quickly altering the pressure to a new constant value brings about the absorption conditions referred to above. The application of the appropriate values from Table I and of eqn. (1) to absorption rate data obtained from experiments

<sup>10</sup> Daynes, *Proc. Roy. Soc. A*, 1920, **97**, 286.

<sup>11</sup> Doty, Aiken and Mark, *Ind. Eng. Chem. (Anal.)*, 1944, **16**, 686.

<sup>12</sup> Reitlinger, *J. Gen. Chem. U.S.S.R.*, 1944, **14**, 420.

<sup>13</sup> Reitlinger and Panjunina, *J. Appl. Chem. Russ.*, 1939, **12**, 886.

<sup>14</sup> Sager, *J. Res. Nat. Bur. Stand.*, 1940, **25**, 309.

<sup>15</sup> Thomas and Gent, *Proc. Physic. Soc.*, 1945, **57**, 324.

in which gas pressure is changed in this way, may be used to evaluate solubility and diffusion coefficients.

If experimental values of  $\log_{10} dq/dt$  are plotted against  $t$ , the curve eventually becomes a straight line the slope and intercept on the  $\log_{10} dq/dt$  axis of which may be estimated. Suppose these are  $\sigma$  and  $i$  respectively. These values, equated to the theoretical values corresponding to the particular shape of the specimen, give two equations yielding values for  $D$  and  $(q_{\infty} - q_0)$ . For example, with a specimen in the form of a slab of uniform thickness having impermeable edges, case (a) of Table I,

$$\sigma = -\pi^2 \frac{D}{X^2} \log_{10} e$$

and

$$i = \log_{10} \frac{8D}{X^2} (q_{\infty} - q_0).$$

If  $V$  is the volume of the specimen,  $p_0$  to  $p$  the pressure change (in cm. mercury) and  $s$  the solubility of the gas per unit volume of specimen, per atmosphere pressure (conformation to Henry's law is assumed, see, e.g. <sup>16-20</sup>).

$$s = \frac{76(q_{\infty} - q_0)}{V(p - p_0)}.$$

An alternative procedure for the determination of solubility is afforded by equation (1). If the same experimental data are used to plot  $\frac{dq}{dt} \sqrt{t}$  against  $t$ , and the graph extrapolated to zero time to give a value,  $\rho$  (say),

$$\rho = \alpha(c_{\infty} - c_0) \sqrt{\frac{D}{\pi}}$$

and hence

$$s = \frac{76(c_{\infty} - c_0)}{(p - p_0)} = \frac{76}{(p - p_0)} \cdot \frac{\rho}{\alpha} \cdot \sqrt{\frac{\pi}{D}}.$$

The value of  $D$  obtained from the slope of the  $\log_{10} dq/dt$  against  $t$  graph may be used in this equation to calculate  $s$ . Values for solubility obtained by these two methods are designated  $s_1$  and  $s_2$  respectively.

### Experimental.

In a previous publication <sup>21</sup> the author described an apparatus designed to measure, at constant oxygen pressure, the rate of disappearance of gaseous oxygen due to chemical combination with a rubber specimen. The apparatus was equally suitable, with minor modifications, for measuring the rate of physical absorption of gases by high polymer specimens, at constant pressure, at any time after a pressure change, i.e. under the conditions considered above. The experimental work to be described was carried out with this apparatus.

The specimens used were made from a natural rubber mixing consisting

of	rubber (smoked sheet)	100.0 parts by weight.
	sulphur	2.5 " " "
	zinc oxide	3.0 " " "
	stearic acid	1.0 " " "
	mercaptobenzthiazole	0.5 " " "
	Agrite white	0.5 " " "

<sup>16</sup> Kayser, *Ann. Physik*, 1891, 43, 544.

<sup>17</sup> Reichler, *J. Chim. physique*, 1910, 8, 617.

<sup>18</sup> Tammann and Bochow, *Z. anorg. Chem.*, 1928, 168, 263.

<sup>19</sup> Venable and Fuwa, *Ind. Eng. Chem.*, 1922, 14, 139.

<sup>20</sup> Wroblewski, *Ann. Physik*, 1879, 8, 29.

<sup>21</sup> Carpenter, *Ind. Eng. Chem.* 1947, 39, 187.

This was vulcanised in the form of cylinders of radius 0.447 cm. (accurately determined from weight, length and specific gravity) and length about 50 cm., by heating in a suitable closed mould for 35 min. at 150° c. These cylinders were cut off squarely into lengths of about 20 cm. and the circular ends rendered impermeable to gas by the application of a layer of tinfoil by means of an adhesive. By this means, end-to-end diffusion of gas was avoided and the values given in Table I for the cylinder of infinite length employed in the calculation of the results. Four of these cylinders, total length 91.5 cm., were separately loosely wrapped in a layer of filter paper and loaded side by side into the specimen tube (see the previous publication, loc. cit. Fig. 1). Light was excluded from the specimen by an opaque covering round the outside of the specimen tube and adjacent glass connection tubing. The relevant details of the apparatus were:

free volume in the specimen tube, 65 cc.; free volume in the large bulb, 1390 cc.; measuring capillary  $8.01 \times 10^{-3}$  cc./cm., graduated in mm. The gases used, nitrogen, hydrogen and oxygen, were pure as supplied by the British Oxygen Company in high pressure cylinders. The gas used for an experiment was passed through an "anhydrene" tube to ensure dryness, and through a copper coil immersed in the thermostat water and connected directly to the inlet tube of the apparatus, to bring it approximately to the required temperature. Volatile substances other than the gas to be used in an experiment were removed from the apparatus and specimen by periodically filling with the gas and evacuating, over a period sufficiently long for the procedure to be effective. Two days was found, by experience, to be adequate in all cases.

To carry out an absorption experiment, the apparatus was first left evacuated to a low pressure, usually 0.1 cm. mercury, until solution equilibrium at this pressure was attained. The gas was then introduced until a pressure of approximately one atmosphere was reached, the time taken for filling being about 30 sec. A stop watch was started 20 sec. after the commencement of the introduction of the gas and this time was taken as zero time. After allowing a period for the attainment of exact temperature uniformity (2 min. was sufficient), the exact pressure was determined and the system closed by turning off tap  $T_1$  (loc. cit. Fig. 1). During the ensuing absorption of the gas by the specimen, the isolating tap  $T_1$  was turned off at intervals as previously described, and the rate of movement of the oil meniscus along the capillary determined using a

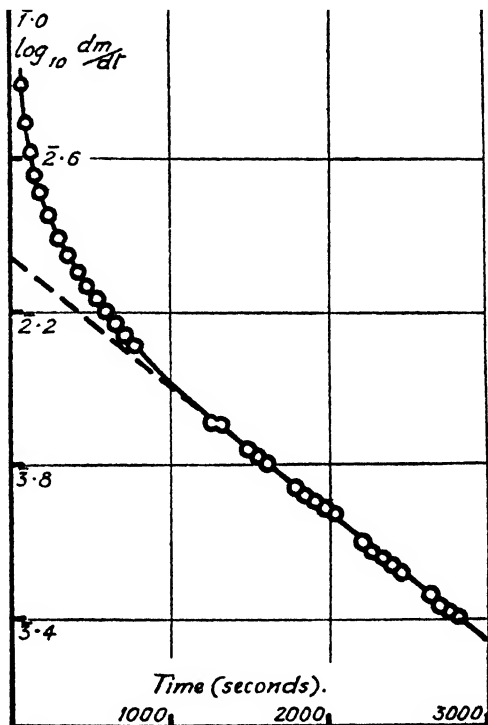


FIG. 2.—The absorption of nitrogen by an "infinite" cylinder of soft-vulcanised rubber at 45° c. Semi-logarithmic plot of  $dm/dt$  against  $t$ .

second stop watch. The results were recorded as (mean) rates of meniscus movement  $dm/dt$  at various (mean) times  $t$  after zero time and graphs were drawn in which  $\log_{10} dm/dt$

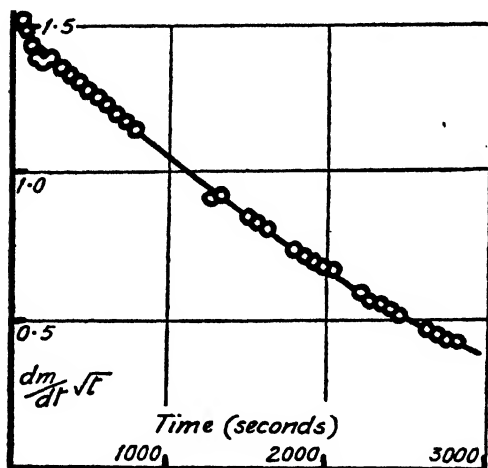


FIG. 3.—The absorption of nitrogen by an "infinite" cylinder of soft-vulcanised rubber at 45° c. Plot of  $\frac{dm}{dt} \sqrt{t}$  against  $t$ .

and  $\frac{dm}{dt} \sqrt{t}$  were plotted

against  $t$ . Fig. 2 and 3 show the graphs obtained for the experiment using nitrogen and a temperature of 45° c. For each experiment the straight line asymptote of the  $\log_{10} dm/dt$  against  $t$  graph was drawn and its slope and intercept on the  $\log_{10} dm/dt$  axis determined:

the  $\frac{dm}{dt} \sqrt{t}$  against  $t$  graph was extrapolated to the  $\frac{dm}{dt} \sqrt{t}$  axis and the value of  $\frac{dm}{dt} \sqrt{t}$  at zero time estimated.

### Calculation of the Results.

Equating the experimental values,  $\sigma$  and  $i$ , to the appropriate values from Table I gives

$$\sigma = -B_1^2 \frac{D}{X^2} \log_{10} e$$

and

$$i = \log_{10} \frac{4D(q_\infty - q_0)}{fX^2}$$

where  $f$  is the factor for converting rate of meniscus movement to rate of gas absorption (expressed in the chosen units) i.e.  $f \frac{dm}{dt} = \frac{dq}{dt}$ . The value

of  $B_1$  is 2.4048 and here the value of  $X$  is 0.447 cm. The units of  $\sigma$  are (time)<sup>-1</sup>, here sec.<sup>-1</sup>. Hence

$$D = 0.07954 \sigma \text{ cm.}^2 \text{ sec.}^{-1}.$$

It will be noted that the conversion factor  $f$  does not appear in the calculation of  $D$ . This is because  $D$  is merely dependent upon the rate at which equilibrium is approached and is uninfluenced by the quantities of gas involved.

If  $s_1$  is the solubility measured as grams of gas per cc. of rubber mixing per atmosphere,

$$s_1 = \frac{(q_\infty - q_0)}{\pi X^2 Y} \cdot \frac{76}{(p - p_0)}$$

where  $Y$  is the total length of the cylindrical specimens,  $p_0$  the original gas pressure,  $p$  the final gas pressure (both in cm. mercury), quantity of gas being measured in grams. Also, with these units,

$$f = \frac{V_1 + V_2}{V_1} \times b \times \frac{p}{76} \times \frac{273}{273 + T} \times \frac{M}{22,400}$$

where  $V_1$  is the free volume of the large bulb,  $V_2$  the free volume of the specimen tube,  $b$  the cross-sectional area of the measuring capillary,  $T$

the temperature of the experiment ( $^{\circ}$  c.) and  $M$  the molecular weight of the gas. Inserting the experimental values,

$$s_1 = \frac{p \cdot M \cdot \text{antilog}_{10} i}{D(p - p_0)(273 + T)} \times 8.888 \times 10^{-8},$$

The alternative procedure for estimating solubility leads to the equation

$$f\rho = 2\pi XY(c_{\infty} - c_0) \sqrt{\frac{D}{\pi}}$$

and hence

$$s = \frac{76}{(p - p_0)} \frac{f\rho}{2\pi XY} \sqrt{\frac{\pi}{D}}$$

which, on substituting the experimental values, gives

$$s = \frac{pM\rho}{(p - p_0)(273 + T)\sqrt{D}} \times 7.050 \times 10^{-7}.$$

Table II gives the results of experiments carried out using nitrogen, hydrogen and oxygen at several temperatures, all on the same specimens without dismantling the apparatus. The experiments with oxygen were carried out last. Table III shows that the results are in reasonable agreement with those obtained by other workers.

TABLE II.—DIFFUSION COEFFICIENT AND SOLUBILITY OF NITROGEN, HYDROGEN AND OXYGEN IN VULCANISED NATURAL RUBBER.

Temp. (°C.).	Gas Pressures (cm. mercury).		Diffusion Coefficient (cm. <sup>2</sup> /sec.).	Solubility. (g. gas/cc./atmosphere).	
	<i>p</i> <sub>0</sub> .	<i>p</i> .		<i>s</i> <sub>1</sub> .	<i>s</i> <sub>2</sub> .
<i>Nitrogen</i>					
25.3	0.9	72.9	$1.21 \times 10^{-8}$	$6.11 \times 10^{-5}$	$5.19 \times 10^{-5}$
30	0.8	73.8	1.41	6.35	5.54
35	0.1	74.0	1.75	6.26	5.58
35	0.1	56.1	1.86	5.92	5.35
35	37.4	74.9	1.72	6.84	6.4
40	1.5	71.5	2.12	6.40	6.29
45	0.1	75.7	2.68	6.58	5.76
50	1.0	72.3	3.02	6.84	6.53
50	0.1	74.9	3.06	6.44	6.01
<i>Hydrogen</i>					
30	0.1	74.9	$1.23 \times 10^{-8}$	$2.70 \times 10^{-6}$	$2.20 \times 10^{-6}$
35	0.1	74.6	1.44	2.73	2.27
40	0.1	76.4	1.70	2.92	2.54
<i>Oxygen</i>					
30	0.5	74.8	$1.88 \times 10^{-8}$	$1.21 \times 10^{-4}$	$1.16 \times 10^{-4}$
35	4.0	74.9	2.07	1.25	1.25
40	4.2	74.2	2.68	1.26	—
45	0.2	74.1	3.09	1.29	—

In a separate experiment, similar to those outlined in a previous publication,<sup>21</sup> it was found that the rate of chemical combination of oxygen

with these specimens was so slow as to be negligible compared with the physical absorption rate over the range required to obtain solubility and diffusion coefficients results. The results for oxygen are therefore unaffected by effects arising from chemical combination with the rubber.

TABLE III.—COMPARISON OF DIFFUSION COEFFICIENT AND SOLUBILITY RESULTS WITH THOSE OF OTHER WORKERS.

Diffusion coefficient at 25 °C. ( $\times 10^{-8}$ cm. <sup>2</sup> /sec.).			Solubility at 21 °C. (cc. at N.T.P./100 cc. rubber/atmos.).		
	This Work. (extrapolated).	Calculated from Data of Daynes <sup>10</sup> and Edwards and Pickering. <sup>32</sup> See Barrer, <sup>8</sup> p. 417.		This Work. (extrapolated).	Venable and Fuwa. <sup>19</sup>
N <sub>2</sub> .	1.2	1.5	N <sub>2</sub> .	4.4	3.5
O <sub>2</sub> .	1.5	2.1	O <sub>2</sub> .	8.3	7.3
H <sub>2</sub> .	10	9	H <sub>2</sub> .	2.4	< 1.0
Solubility at 25 °C. (cc. at N.T.P./100 cc. rubber/atmos.).			Solubility in Rubber Hydrocarbon at 40 °C. ( $\times 10^{-3}$ g./cc./atmos.).		
	This Work. (extrapolated).	Calculated from Data of Daynes <sup>10</sup> and Edwards and Pickering. <sup>32</sup> See Barrer, <sup>8</sup> p. 417.		This Work.	Unpublished Work by the Author Using Direct Methods Involving the Measurement of the Quantity passing into, or recoverable from Solution.
N <sub>2</sub> .	4.6	3.5	N <sub>2</sub> .	6.5	7.5
O <sub>2</sub> .	8.5	7.0	O <sub>2</sub> .	12.8	15.8
H <sub>2</sub> .	2.6	4.0	O <sub>2</sub> .	in G.R.-S.	12.1

It will be noticed from Table II that the first method for calculating solubility from the experimental data gives results somewhat higher than

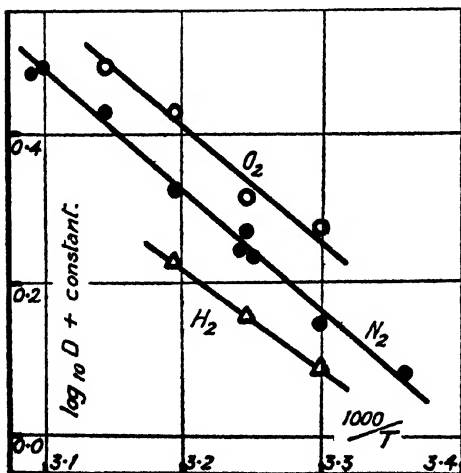


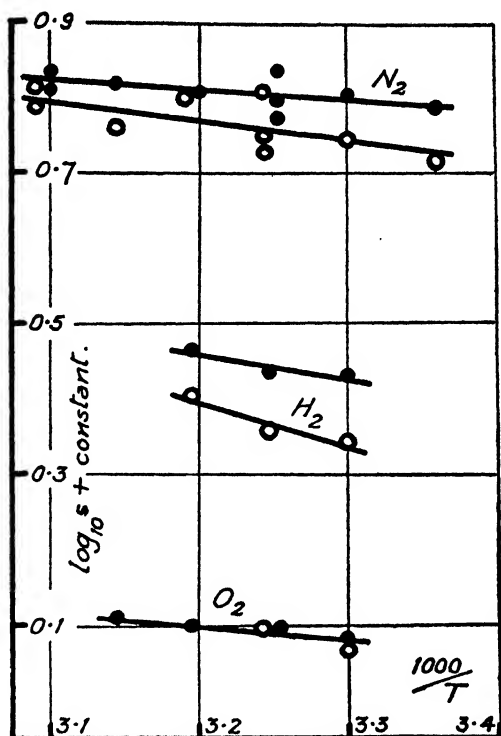
FIG 4.—The diffusion coefficients of nitrogen, hydrogen and oxygen in soft-vulcanised rubber. The constant is introduced into the ordinate in order to condense the graph. Its value for nitrogen and oxygen is 6; for hydrogen, 5.

those obtained by the second method. The reason for this is not clear. It is considered that the first method probably leads to the more accurate results.

In Fig. 4 and 5 the logarithms of diffusion coefficient and solubility are shown plotted against the reciprocal of the absolute temperature.

The linearity of the diffusion coefficient graphs shows that the diffusion

FIG. 5.—The solubilities of nitrogen, hydrogen and oxygen in soft-vulcanised rubber. Closed circles,  $s_1$ , open circles,  $s_2$ . The constant is introduced into the ordinate in order to condense the graph. Its value for nitrogen is 5; for oxygen, 4; for hydrogen, 6.



is in conformity with the relationship

$$D = D_0 e^{-E/RT}$$

in which  $E$  is the activation energy for diffusion.

The solubility graphs also appear to be in agreement with the anticipated relationship

$$s = s_0 e^{-\Delta H/RT}$$

in which  $\Delta H$  is the heat of solution. Table IV gives the calculated values of  $E$  and  $\Delta H$  and of  $E_p$ , the activation energy of permeation through sheet material. The  $\Delta H$  values are subject to a considerable error, probably of the order of 500 cal./mole, that for hydrogen being the least reliable (see Fig. 5).

TABLE IV.—ACTIVATION ENERGIES FOR DIFFUSION AND PERMEATION, AND HEATS OF SOLUTION FOR NITROGEN, OXYGEN AND HYDROGEN IN SOFT-VULCANISED RUBBER.

	$E$ .	$\Delta H$ .	$E_p$ .
	cal./mole.		
$N_2$ . .	7400	1200*	8600
$O_2$ . .	7100	700	7700
$H_2$ . .	6100	2800*	8900

\* Average of the two values given by the two methods for calculating solubility.

lop Rubber Company at Fort Dunlop. The author wishes to thank the Technical Director for permission to publish, Dr. D. F. Twiss for suggestions and criticisms, and Mr. K. G. Burrige for assistance in some of the experimental work.

The experimental work outlined in the above account was carried out in the Chemical Research Laboratories of the Dunlop Rubber Company at Fort Dunlop. The author wishes to thank the Technical Director for permission to publish, Dr. D. F. Twiss for suggestions and criticisms, and Mr. K. G. Burrige for assistance in some of the experimental work.



### Summary.

A method is described for determining the solubility and diffusion coefficient of a gas in a high polymer. It is based upon the mathematical relationships defining the rate of absorption of solute by an immobile solvent specimen of simple shape, consequent upon a change of surface concentration. Experimental results are given for the solubility and diffusion coefficient of nitrogen, oxygen and hydrogen in a soft-vulcanised natural rubber at temperatures between 25° c. and 50° c.

### Résumé.

On décrit une méthode qui permet de déterminer la solubilité et le coefficient de diffusion d'un gaz dans un haut polymère. Elle a pour base les équations qui définissent la vitesse d'absorption d'un soluté—par un échantillon du solvant, immobile et de forme simple—en fonction des changements de la concentration de surface. On indique les résultats expérimentaux pour la solubilité et le coefficient de diffusion de l'azote, de l'oxygène et de l'hydrogène dans un caoutchouc natu rel vulcanisé doux à des températures variant entre 25° et 50° c.

### Zusammenfassung.

Der Artikel beschreibt eine Methode zur Bestimmung der Löslichkeit und des Diffusionskoeffizienten eines Gases in einem Hochpolymeren. Sie hat als Grundlage die mathematischen Beziehungen, die die Geschwindigkeit der durch Änderung der Oberflächenkonzentration bedingten Absorption eines gelösten Stoffs durch einen unbeweglichen lösenden Körper (der eine einfache geometrische Form besitzt) definieren. Versuchsdaten werden für die Löslichkeit und den Diffusionskoeffizienten von Stickstoff, Sauerstoff und Wasserstoff in einem weich-polymerisierten natürlichen Kautschuk zwischen 25° und 50° c. berichtet.

Present Address :

No. 1 Laboratory,  
Messrs. Courtaulds Ltd.,  
Foleshill Road,  
Coventry.

## A MICROSCOPICAL STUDY OF THE SOLUTION OF NITROCOTTON BY NITROGLYCERINE.

By D. FENSOM AND S. FORDHAM.

Received 20th May, 1946.

Although the solution of a single fibre of nitro-cotton in a solvent is of considerable technical and scientific interest, the process has rarely been studied with the microscope, since partially dissolved fibres are difficult to see. The polarising microscope has frequently been employed in the study of nitrocotton fibres mounted in non-gelling media,<sup>1, 2, 3, 4</sup> the interference colours being correlated with the degree of nitration of the cellulose by Ambronn<sup>2</sup> and Tissot,<sup>3</sup> while Phillips<sup>4</sup> emphasises the importance of the degree of dispersion within the fibre. However, if the fibre becomes markedly swollen it becomes invisible under the polarising microscope,

<sup>1</sup> Chardonnet, *Compt. rend.*, 1907, 145, 115.

<sup>2</sup> Ambronn, *Über die Änderung des Optischen Verhaltens der Zellulose bei der Nitrierung. Sammlung wiss. Arbeiten.* Vol. 20 (1914).

<sup>3</sup> Tissot, *Mem. Poudres*, 1926, 22, 31.

<sup>4</sup> Phillips, *J. Physic. Chem.*, 1929, 33, 118.

and although Michel-Levy and Muraour<sup>5</sup> applied the method to the study of double-based powders, their description makes it clear that the nitro-cotton fibres actually observed must have been relatively unaffected by the nitroglycerine during the gelatinising process.

Ambronn<sup>6</sup> studied also the effect of Congo Red and Methylene Blue in alcoholic solution on nitrocotton, but does not appear to have included in his experiments conditions which could have led to swelling or solution. Mangenot and Raison<sup>6</sup> have studied the process of solution of di- and tri-nitrates of cotton and ramie in a number of solvents, using dyes such as Sudan Red and Indophenol Blue to make the process visible. They explained their observations as due to the presence, on the surface of the cotton fibre, of a system of spiral and circular fibrils as suggested by Frey-Wyssling,<sup>7</sup> and postulated that this surface layer contained components incapable of nitration.

In the present work only one solvent was used, namely, a mixture of nitroglycerine with nitroglycol, but a wide range of nitrocottons was studied so that the behaviour on solution could be correlated with the N content and viscosity.

### Experimental.

Preliminary trials indicated that Crystal Violet base was soluble in nitroglycerine and capable of being absorbed on nitrocotton when gelling or swelling commenced. Other dyes which could be used were Methyl Violet base, Rhodamine BS and Rosaniline Red, but these were in general less strongly absorbed or gave variable colours. The solution of 0.02 % Crystal Violet base was made in a filtered base, consisting of 80 % nitroglycerine with 20 % ethylene glycol dinitrate. The samples of nitrocotton were drawn from industrial production and dried at 55-60° C. to constant weight; their properties are detailed in Table I.

TABLE I.

DETAILS OF NITROCOTTON SAMPLES.

Name.	N Content %	Acetone Viscosity.		Remarks.
		Visc. c.g.s.	Conc. % on 95 % Acetone.	
LX . . . . .	10.77	25	40	
LL . . . . .	11.15	35	20	
NH . . . . .	11.69	1	3	
HX . . . . .	11.76	7	40	
HM . . . . .	11.85	6	10	
" S " . . . . .	12.20	59	6	Pulped
" P " . . . . .	12.57	7	6	"
Guncotton . . . . .	13.16	26	6	"
High Nitrogen Guncotton .	13.40	8	6	"

A small amount of nitrocotton was mounted and examined between crossed Nicols; photomicrographs were taken in green unpolarised light after intervals of 5 min., 30 min., 5 days and 30 days at a magnification of 70 diameters.

<sup>5</sup> Michel-Levy and Muraour, *Compt. rend.*, 1929, 189, 1192.

<sup>6</sup> Mangenot and Raison, *Mem. Serv. Chim. de l'Etat*, 1944, 31, 276.

<sup>7</sup> Frey-Wyssling, *Protoplasma*, 1926, 25, 261.



containing more than 12 % N. Fig. 2 shows nitrocotton containing 11.85 % N, and even in this case attack was almost uniform. Fig. 3, showing a guncotton of 13.16 % N, indicates very uniform dyeing and gelatinisation.

The speed of solution also increased as the N content was raised. With fibres containing 11 % N, the first definite signs of gelation appeared only after immersion in nitroglycerine for about 24 hr., whereas with guncottons containing over 13 % N the first effects could be observed after 30 min. However, the speed of solution depended markedly on the physical condition of the nitrocotton, and a badly bruised fibre containing only 11.7 % N might gel as rapidly as one containing 12 or 13 %. It is considered that the observed speed of solution is a reflection of the resistance to penetration of the surface, as much as an intrinsic property of the nitrocotton itself. In the case of soluble nitrocottons, as in the series HX to HH used in the present work, the speed of solution increased as the viscosity decreased. Such dependence of speed of solution on viscosity does not however, imply any variation in affinity of the nitrocellulose for solvent. The work of Jenkins and Bennet<sup>8</sup> and Rubenstein<sup>7</sup> shows in fact, that solvent affinity is not affected by changes in viscosity of the nitrocotton.

Below about 11.4 % N, the nitrocotton and nitroglycerine formed a gel which did not spread rapidly or indefinitely through the liquid, but which retained a sharp outline. Swelling was therefore limited. At N contents between about 11.4 and 12.6 %, a colloidal solution was formed which spread with a diffuse boundary through the entire liquid medium. With high viscosity nitrocottons the diffusion was slow, and the boundaries of the sol at first appeared relatively sharp as in Fig. 4; nevertheless, diffusion continued as the sample aged. At still higher N contents, however, swelling was again limited and a gel instead of a sol was formed. With the two guncottons examined, containing 13.16 % and 13.4 % N, neither diffusion nor swelling was sufficiently great to be observed visually, although the extent of dyeing indicated the progress of gelatinisation. Such limited swelling of nitrocotton with either very high or very low N contents is in accordance with the absorption measurements made by other authors<sup>8, 9</sup>; and in the present work, experiments have shown that guncotton in contact with cold nitroglycerine absorbs its own weight of the liquid in a few days.

With nitrocottons of low viscosity, part of the fibres sometimes dissolved first and produced a sol which spread rapidly through the bulk of the liquid; the other fibres were then unable to swell more than to a limited extent. Such an effect may be seen in Fig. 3.

### Discussion.

The results obtained in this work agree very largely with those of Mangelot and Raison.<sup>6</sup> It has been confirmed that nitrocotton fibres, especially those of low N content, appear to be covered by a relatively insoluble surface skin. Mangelot and Raison observed the same effect and concluded that the skin contained constituents incapable of nitration. We, however, are inclined to the view that the skin is formed by partial de-nitration of the surface of the fibre during the processes of drowning and stabilising, since it affords protection also at the ends of cut fibres. Moreover, the skin is less apparent in nitrocotton of high N content, which are known to be less readily denitrated. The skin naturally has the structure of the outer layer of the cellulose fibre—this may be seen for example, on examination of Fig. 5—but the difficulty of solution should be related rather to other properties.

<sup>8</sup> Jenkins and Bennett, *J. Physic. Chem.*, 1930, 34, 2318.

<sup>9</sup> Rubenstein, *ibid.*, 1930, 34, 2330.

### Summary.

The process of solution of nitrocotton by nitroglycerine has been followed microscopically after addition of Crystal Violet base in a concentration of 0.02 %. The dyestuff was concentrated on the gelatinised nitrocotton and thus made the process of solution visible by ordinary light.

It is considered that the nitrocotton fibres had a surface layer or skin with a N content less than the average value. With nitrocottons containing less than about 11 % N, attack by nitroglycerine took place only through breaks in this skin, but as the N content was raised, attack became more uniform, and was completely so when the N exceeded 13 %. The speed of attack also increased as the skin became less resistant. Outside the limits 11.4-12.6 % N, only limited swelling occurred, but within these limits a sol was formed which could be seen to diffuse at a speed dependent on the viscosity of the nitrocotton. The polarisation colours observed before solution depended on the N content but not on the viscosity of the nitrocotton.

### Résumé.

Le processus de la dissolution du nitrocoton par la nitrocellulose a été suivi au microscope, après addition de violet cristallisé à une concentration de 0.02 %. Le colorant était concentré sur le nitrocoton gélatinisé, rendant ainsi le processus de la dissolution visible à la lumière ordinaire. On considère que les fibres de nitrocoton ont une couche superficielle, ou "peau", dont la teneur en azote est inférieure à la valeur moyenne. Avec des nitrocotons contenant moins d'environ 11 % de N, l'attaque par la nitroglycérine a lieu seulement par des déchirures de la peau, mais devient de plus en plus uniforme à mesure que croît la teneur en azote; elle l'est tout-à-fait, lorsque la teneur dépasse 13 %. La vitesse d'attaque augmente aussi comme la résistance de la peau diminue. En dehors du domaine 11.4-12.6 % de N, il ne se produit qu'un gonflement limité, mais dans ce domaine un sol est formé, que l'on peut voir diffuser à une vitesse dépendant de la viscosité du nitrocoton. Les couleurs de polarisation, observées avant dissolution, dépendent de la teneur en azote, mais pas de la viscosité du nitrocoton.

### Zusammenfassung.

Der Vorgang der Auflösung von Schiessbaumwolle in Nitroglycerin ist nach Hinzufügung von 0.2 % Crystal Violet mikroskopisch untersucht worden. Der Farbstoff war auf der gelatinisierten Schiessbaumwolle konzentriert und der Lösungsvorgang somit in gewöhnlichem Licht sichtbar.

Es wird angenommen, dass die Schiessbaumwollfasern eine Oberflächenschicht oder -haut mit geringerem Stickstoffgehalt als der Durchschnitt besitzen. Bei Schiessbaumwolle mit weniger als *circa* 11 % N fand der Angriff durch das Nitroglycerin nur durch Sprünge in dieser Haut statt, aber bei höherem N-Gehalt wurde dieser Angriff einheitlicher und war völlig gleichmässig bei N-Gehalten > 13 %. Die Angriffsgeschwindigkeit wuchs auch mit abnehmender Widerstandskraft der Haut an. Ausserhalb der Grenzwerte 11.4-12.6 % N trat nur beschränkte Quellung ein, aber innerhalb dieser Werte wurde ein Sol gebildet, dessen Diffusion mit einer von der Viskosität Schiessbaumwolle abhängenden Geschwindigkeit gesehen werden konnte. Die Polarisationsfarben, die vor der Lösung eintreten, hängen vom N-Gehalt aber nicht von der Viskosität der Schiessbaumwolle ab.

*Imperial Chemical Industries Limited,  
Explosives Division,  
Nobel House, Stevenston,  
Ayrshire.*

# THE SWELLING OF NITROCELLULOSE IN BINARY MIXTURES.

By W. R. MOORE.

*Received 18th August, 1946, as amended, 17th December, 1946.*

Reasons for the solubility of nitrocellulose in a particular liquid or mixture of liquids are not entirely clear. The solvation hypothesis does not explain variations in solubility observed between liquids of the same polarity and specific grouping. The use of a precipitant liquid to assess solvent power<sup>1</sup> gives only the volume required to precipitate the least soluble fraction of heterogeneous polymers and the volume varies with different precipitant liquids. Determination of the upper critical temperature of complete miscibility<sup>2</sup> is not always applicable to nitrocellulose, the solubility of which may increase with decreasing temperature. At high concentrations the best solvents give solutions of lowest viscosity; at low concentrations the opposite is generally accepted.<sup>3</sup>

Measurements of the equilibrium swelling of high polymers have been used in measuring the interaction between polymer and liquid.<sup>4, 5, 6</sup> The method usually employed, measurement of the increase in weight or volume of thin films or sheets of the polymer has certain disadvantages when applied to cellulose esters. Equilibrium is reached very slowly and films or sheets may not reproduce conditions occurring when the fibrous polymer interacts with liquids. Nitrocellulose is swelled by relatively few liquids, either a small degree of imbibition occurring or the nitrocellulose is gelled or dispersed.

Microscopic examination showed that nitrocellulose fibres exhibit swelling in mixtures of solvents and liquids such as ethyl alcohol, benzene and hexane. With increasing concentration of solvent the fibres are progressively swollen until at a certain concentration, depending on both constituents of the mixture, solution occurs. Swelling of the fibres appears to occur almost immediately they come in contact with the mixture and increases, for a given mixture, with decreasing nitrogen content of the nitrocellulose. This swelling of nitrocellulose in binary mixtures has been studied as a possible means of assessing nitrocellulose-solvent interaction.

## Experimental.

A nitrocellulose from cotton having a mean N content of 13.2 % was used. Such nitrocellulose is not a homogeneous polymer, but it is probable that the influence of chain length on solubility is small compared with that of N content,<sup>7</sup> which will vary slightly. Before use, the nitrocellulose was dried for 3 hr. at 100° c. and for 7 days at room temperature over sulphuric acid.

To estimate the swelling of the fibres, 0.2 g. of nitrocellulose was weighed into a graduated glass tube and 10 g. of binary mixture added. The mixtures were well stirred, shaken and placed in a thermostat at 25°.

<sup>1</sup> Mardles, *J. Soc. Chem. Ind.*, 1923, **42**, 127.

<sup>2</sup> Frith, *Trans. Faraday Soc.*, 1945, **41**, 17.

<sup>3</sup> Frith, *Trans. Faraday Soc.*, 1945, **41**, 90.

<sup>4</sup> Gee, *Trans. I.R.I.*, 1943, **18**, 226.

<sup>5</sup> Gee and Treloar, *Trans. Faraday Soc.*, 1942, **38**, 148.

<sup>6</sup> Brønsted and Volqvartz, *Trans. Faraday Soc.*, 1939, **35**, 576.

<sup>7</sup> Wadano, *Kolloid. Z.*, 1940, **93**, 324.

The tubes were occasionally shaken during a period of at least 3 hr. and the fibres finally allowed to settle until no further change in volume of the fibres occurred. The volume was estimated, as much as possible of the supernatant liquid decanted off and reserved at 25°, and the tubes centrifuged at a fairly low speed for 3 min. The remaining liquid was carefully sucked up, by filter paper and the tube and fibres weighed. After weighing, some of the previously reserved supernatant liquid was shaken up with the fibres, which were then examined microscopically. Hexane, in excess, was added to the remaining liquid to ascertain whether any dissolved nitrocellulose was present. Errors inherent in this method make it only comparative. While the results obtained by weighing were mutually consistent to about 5 % the accuracy is reduced by temperature changes due to centrifuging and weighing at room temperature, loss of imbibed liquid from the more fully swollen fibres and, in the case of only slight swelling, retention of liquid other than that imbibed by the fibres. Results, however, were reproducible and consistent differences between different binary mixtures were obtained. Qualitative agreement between weight, volume of swollen fibres and microscopic examination was obtained. The degree of swelling appeared to depend only on the composition of the binary mixture, being unaffected by variations, within fairly wide limits, in weight of nitrocellulose or binary mixture. The binary mixtures consisted of mixtures of known solvents for nitrocellulose, or their homologues, with ethyl alcohol, benzene or hexane. The alcohol was dried and redistilled before use. The benzene was redistilled and the hexane obtained as a fraction from petroleum ether. Results given below are the means of at least three determinations.

## Results.

**1. Comparison of Swelling of Fibres and Films.**—Only the swelling of films has any absolute significance and the use of fibres is only justified if comparable results can be obtained. Experiments were first carried out to check this. Films were obtained by evaporating acetone solutions of

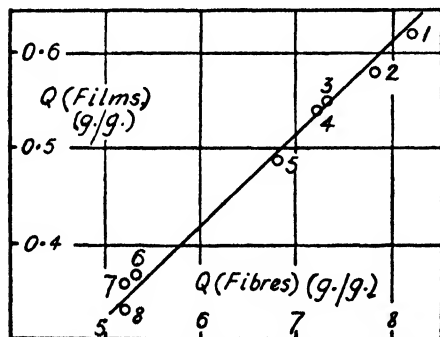


FIG. 1.—Swelling of nitrocellulose in solvent-alcohol mixtures containing 20 % w/w solvent. 1. *n*-Butyl acetate. 2. *n*-Propyl acetate. 3. Amyl acetate. 4. *n*-Butyl *n*-butyrate. 5. Ethyl acetate. 6. Ethyl formate. 7. Acetone. 8. Methyl acetate.

the nitrocellulose over sulphuric acid *in vacuo*. When dry, residual solvent was removed by treatment with water at 90° for 24 hr. and further drying. Thin films, weighing *ca* 0.1 g. were immersed in mixtures containing 20 % w/w of aliphatic solvents in ethyl alcohol and the equilibrium weight compared with that obtained with fibres in mixtures of the same composition. Results are illustrated in Fig. 1 showing a plot of *Q*, the increase in weight per g. for films against that for fibres. While swelling of films is much less than that of fibres, possibly because of difference in structure, the values appear to be

quite comparable. Similar results were obtained with solvent-hexane mixtures containing 40 % w/w of solvent, though swelling of films in mixtures containing amyl acetate and *n*-butyl *n*-butyrate was much less than might have been anticipated from swelling of fibres. Acetone-hexane mixture tended to disperse film but only swelled fibres to a small

extent. Qualitative agreement with mixtures producing a fairly large degree of swelling was obtained and the method involving fibres seems to be a possible comparative one.

## 2. Swelling in Mixtures Containing Equal Weights of Solvents.—

Swelling of fibres in mixtures containing varying concentrations of solvents, or their homologues, in ethyl alcohol, benzene and hexane was examined. Where small concentrations of solvent were used, great differences in swelling power were not observed, possibly because of limitations in the method of estimation. With larger concentrations, while the order of swelling power was the same, considerable differences in degree were observed. Results given in Table I for solvent-alcohol mixtures containing 20 % w/w of solvent, solvent-benzene mixtures containing 30 % w/w and solvent-hexane mixtures containing 40 % w/w illustrate this. Values obtained in pure ethyl alcohol, benzene and hexane are included. These are almost certainly too high for reasons previously stated. The value for hexane may represent an approximate lower limit obtainable by this method of estimation.

TABLE I.—SWELLING OF NITROCELLULOSE IN BINARY MIXTURES OF SOLVENTS.

Solvent.	Values of $Q$ g./g.			$(E/V)^{\dagger}$ (Cal./cc.) <sup>‡</sup>
	20 % w/w Solvent in Alcohol.	30 % w/w Solvent in Benzene.	40 % w/w Solvent in Hexane.	
<i>n</i> -Butyl acetate . . .	8.2	8.6	11.8	8.5
<i>n</i> -Propyl acetate . . .	7.8	12.3	10.0	8.7
Amyl acetate . . .	7.3	5.8	4.3	8.3
<i>n</i> -Butyl <i>n</i> -butyrate . . .	7.2	4.7	3.8	8.0
Dibutyl phthalate . . .	7.0	5.2	gelled	8.4
Ethyl acetate . . .	6.8	gelled	4.4	9.05
Diethyl phthalate . . .	5.7	7.4	6.7	9.4
Ethyl formate . . .	5.3	7.4	4.1	9.4
Acetone . . .	5.2	dispersed	3.4*	9.7
Methyl acetate . . .	5.2	8.0	3.5	9.55
Dimethyl phthalate . . .	5.0	6.1	liquids not miscible	
Nitrobenzene . . .	5.0	5.5	5.3	10.4
Nil . . .	4.1	4.0	2.8	12.7

\* Some loss observed in centrifuging.

The order of swelling power is approximately the same in mixtures containing alcohol and hexane but differs in those involving benzene; 40 % of dibutyl phthalate in hexane produces a gel though its swelling power in alcohol mixtures is less than that of other solvents. In mixtures containing benzene, ethyl acetate produces a gel and acetone dispersion. Following Gee,<sup>4, 5</sup> swelling power was compared with the cohesive energy densities of the solvents. The cohesive energy density is equal to  $(L - RT)/V$ , where  $L$  is the measured latent heat of vaporisation at the absolute temperature  $T$  and  $V$  is the molar volume at this temperature. Values of  $(E/V)^{\dagger}$  at 25° C., where  $E$  equals  $(L - RT)$ , are given in Table I. These values are taken from published data,<sup>4, 5</sup> from heats of vaporisation, from the Hildebrand rule<sup>6</sup> or by estimation from values for homologous compounds. In the last three cases values are only approximate. Some correlation appears to exist. With the solvent-alcohol mixtures maximum swelling is seen at an  $(E/V)^{\dagger}$  value of *ca* 8.5. With solvent-hexane mixtures involving aliphatic solvents the same value for

<sup>6</sup> Hildebrand, *Solubility* (Reinhold, 1936), 103.



maximum swelling is seen but aromatic compounds show greater swelling power. With solvent-benzene mixtures maximum swelling appears at an  $(E/V)^{\frac{1}{2}}$  value of *ca* 9, though the case of acetone is anomalous.

**3. Swelling in Mixtures Containing Equal Molar Fractions of Solvents.**—A relation between swelling power and cohesive energy density

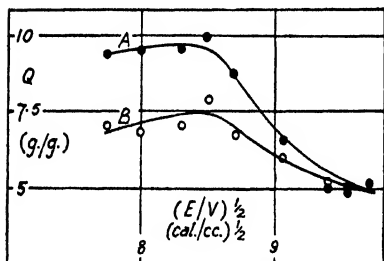


FIG. 2.—Swelling of nitrocellulose in solvent-alcohol mixtures.

A. Molar fraction of solvent 0.1.

B. Molar fraction of solvent 0.075.

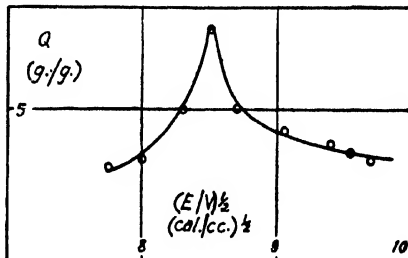


FIG. 3.—Swelling of nitrocellulose in solvent-hexane mixtures. Molar fraction of solvent 0.3.

of solvent is more apparent when equal molar fractions of solvents are compared and if such solvents are of the same chemical type and polarity.

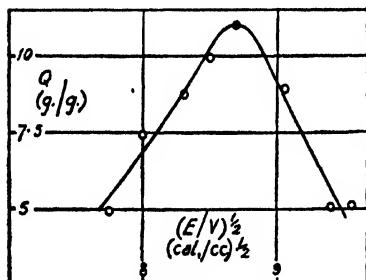


FIG. 4.—Swelling of nitrocellulose in solvent-benzene mixtures. Molar fraction of solvent 0.25.

Using aliphatic solvents, this is shown by solvent-alcohol mixtures containing 0.075 and 0.1 molar fraction, solvent-hexane mixtures containing 0.3 and 0.4 and solvent-benzene mixtures containing 0.25. Results are given in Table II and are shown in Fig. 2-4 as plots of  $Q$  against the solvent  $(E/V)^{\frac{1}{2}}$  values, omitting the results for solvent-hexane mixtures containing 0.4 molar fraction. Swelling is seen to vary with the  $(E/V)^{\frac{1}{2}}$  value and there is a maximum at *ca* 8.5 for mixtures involving alcohol and hexane. With benzene mixtures

the position of the maximum is a little higher. The less clearly defined maxima seen with the alcohol mixtures may be due to solution of nitrocellulose in the case of the solvents showing the greatest swelling power, though another explanation is suggested later. At the higher  $(E/V)^{\frac{1}{2}}$  values the swelling in alcohol mixtures appears to be unaffected by change in molar fraction. The behaviour of acetone in benzene mixtures is still anomalous.

Table III shows results obtained with binary mixtures involving cyclohexanone and aromatic compounds, smaller molar fractions of these giving degrees of swelling similar to those obtained with aliphatic compounds. The same dependence of swelling on cohesive energy density of solvent is seen though cyclohexanone, like acetone, gives anomalous results with benzene.

**4. Determination of Solvent Power by Precipitant Method.**—The variations in swelling seen with the different solvents suggests that some correlation should exist between them and the volume of alcohol, hexane and benzene required to precipitate nitrocellulose from solutions in the solvents. Solutions of 1% were prepared by mechanical shaking, the

solutions being allowed to stand for 12 hr. before use. In some cases solution was not complete and in others the viscosity made determinations impossible. The volume of precipitant liquid required to produce incipient turbidity, when added to 5 cc. of solution at room temperature,

TABLE II.—SWELLING OF NITROCELLULOSE IN BINARY MIXTURES CONTAINING EQUAL MOLAR FRACTIONS OF SOLVENTS.

Non-solvent . . .  Molar Fraction of Solvents . . .	Values of $Q$ g./g.					$(E/V)^{\frac{1}{2}}$ (cal./cc.) $^{\frac{1}{2}}$
	Alcohol.		Hexane.		Benzene.	
	0.075.	0.1.	0.3.	0.4.	0.25.	
Solvent.						
Isobutyl <i>n</i> -butyrate	7.0	9.4	3.1	4.1	4.9	7.75
<i>n</i> -Butyl <i>n</i> -butyrate	6.8	9.5	3.4	6.8	7.4	8.0
Amyl acetate	7.0	9.5	5.0	gelled	8.7	8.3
<i>n</i> -Butyl acetate	7.8	9.9	7.6	gelled	9.9	8.5
<i>n</i> -Propyl acetate	6.7	8.7	5.0	13.4	11.0	8.7
Ethyl acetate	6.0	6.5	4.2	4.7	8.8	9.05
Ethyl formate	5.1	5.0	3.9	4.3	5.0	9.4
Methyl acetate	5.0	4.8	3.6	3.6	5.0	9.55
Acetone	5.0	5.1	3.3	3.5	gelled	9.7

was determined. The end point was not very precise in some cases but consistent differences between different solvents was obtained. Results, with the general character of the solutions and the solvent  $(E/V)^{\frac{1}{2}}$  values at 25° c., are given in Table IV, aliphatic and aromatic solvents being

TABLE III.—SWELLING OF NITROCELLULOSE IN BINARY MIXTURES CONTAINING EQUAL MOLAR FRACTIONS OF SOLVENTS.

Non-solvent . . .  Molar fraction of Solvent . . .	Values of $Q$ g./g.			$(E/V)^{\frac{1}{2}}$ (Cal./cc.) $^{\frac{1}{2}}$
	Alcohol.	Hexane.	Benzene.	
	0.05.	0.2.	0.02.	
Solvent.				
Diethyl phthalate	7.2	3.7	4.3	7.25
Dihexyl phthalate	7.7	4.0	5.9	7.7
Dibutyl phthalate	7.3	gelled	10.1	8.4
Dipropyl phthalate	7.0	13.1	gelled	9.0
Diethyl phthalate	5.1	7.3	13.7	9.4
Cyclohexanone	5.0	3.9	gelled	10.3
Dimethyl phthalate	5.0	liquids not miscible		
Nitrobenzene	5.0	4.6	6.4 5.1	11.4 12.7

separated. Where determinations were possible the volumes of precipitant liquids generally follow the swelling values in mixtures involving the precipitant. The results suggest that complete solubility occurs when the solvent  $(E/V)^{\frac{1}{2}}$  values lies approximately between 8 and 10. Relatively large volumes of benzene were required to precipitate nitrocellulose from its solutions in the ketones.

**5. Viscosity Determinations.**—The relation between swelling and cohesive energy density of solvent is capable of further test. Frith<sup>9, 10</sup> has indicated that the slopes and intercepts of the  $\eta_{sp}/c-c$  curves of dilute

TABLE IV.—VOLUMES OF PRECIPITANT LIQUIDS REQUIRED TO PRODUCE INCIPIENT TURBIDITY WHEN ADDED TO 5 cc. SOLUTION.

Solvent.	Appearance of Solution.	Volume of precipitant cc.			(E/V) <sup>†</sup> (Cal./cc.) <sup>‡</sup>
		Alcohol.	Hexane.	Benzene.	
<i>Isobutyl n</i> -butyrate . . .	not completely dissolved				7.75
<i>n</i> -Butyl <i>n</i> -butyrate . . .	a little cloudy	14.0	5.0		8.0
Amyl acetate . . .	clear	16.0	8.5	4.5	8.3
<i>n</i> -Butyl acetate . . .	clear	20.0	10.0	9.0	8.5
<i>n</i> -Propyl acetate . . .	clear	18.5	8.5	13.5	8.7
Ethyl acetate . . .	clear	18.0	7.0	15.0	9.05
Ethyl formate . . .	a little cloudy	8.5	2.0	1.5	9.4
Methyl acetate . . .	a little cloudy	10.0	4.0	5.0	9.55
Acetone . . .	a little cloudy	15.0	4.5	48.0	9.7
Diethyl phthalate . . .	not completely dissolved				7.25
Dihexyl phthalate . . .	not completely dissolved				7.75
Dibutyl phthalate . . .	very viscous solution				8.4
Dipropyl phthalate . . .	very viscous solution				9.0
Diethyl phthalate . . .	very viscous solution				9.4
Cyclohexanone . . .	clear	12.5	4.0	44.0	10.3
Dimethyl phthalate . . .	not completely dissolved				10.4
Nitrobenzene . . .	a little cloudy	3.0	2.5	3.5	12.7

polymer solutions should vary with the solvent (E/V) values and hence with the equilibrium swelling. Solutions containing 0.05, 0.1 and 0.2 g./1000 cc. of nitrocellulose in alkyl acetates were prepared and the

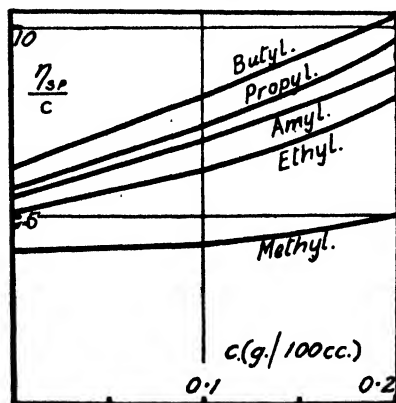


FIG. 5.—Viscosities of dilute solutions of nitrocellulose in alkyl acetates.

viscosity of each measured in a standard Ostwald viscometer at 25° relative to the solvent. Over the concentration range 0.0-0.1 g./100 cc. the increase of  $\eta_{sp}/c$  with  $c$  appeared to be linear. The curves are given in Fig. 5. The limiting intercepts and slopes are given in Table V with the solvent (E/V)<sup>†</sup> values and the corresponding values of  $Q$  for swelling in solvent-hexane mixtures containing 0.3 molar fraction of solvent. Solvent-hexane mixtures were chosen as probably most nearly representing the effect of solvent. Both ethyl alcohol and benzene, under certain conditions, are solvents for nitrocellulose<sup>9, 10, 11</sup> and almost certainly contribute to swelling. General agreement in the order of the solvents is seen.

**6. Temperature Effects.**—The effect of temperature variations on swelling has been examined with solvent-hexane mixtures. Three

<sup>9</sup> Samec, *Colloid Chemistry* (Alexander), 4, 48.

<sup>10</sup> Mason, *Trans. Faraday Soc.*, 1920, 16, 95.

<sup>11</sup> Mardles, *Colloid Chemistry* (Alexander), 4, 94.

temperatures—11°, 25°, and 35°—were used. Results are given in Table VI, aliphatic and aromatic solvents being separated.

TABLE V.—SWELLING AND VISCOSITY RELATIONSHIPS. SWELLING IN SOLVENT-HEXANE MIXTURES CONTAINING 0.3 MOLAR FRACTION SOLVENT.

Solvent.	Intercept.	Slope.	Q g./g.	(E/V) <sup>1/2</sup> (Cal./cc.) <sup>1/2</sup>
Amyl acetate .	5.5	0.58	5.0	8.3
n-Butyl acetate .	6.0	0.73	7.6	8.5
n-Propyl acetate .	5.75	0.61	5.0	8.7
Ethyl acetate .	5.1	0.41	4.2	9.05
Methyl acetate .	4.1	0.07	3.6	9.55

While estimates of temperature coefficients are not possible, in most cases swelling decreases with increasing temperature, suggesting that heat is evolved in swelling. In other cases, variations may be too small to be shown by the method of estimation.

### 7. Swelling in Mixtures of "Non-solvents."

—Nitrocellulose frequently swells or dissolves in mixtures of two liquids which, used singly, have only a very limited solvent action. Gee<sup>18</sup> has recently discussed the solubility of linear polymers in such mixtures. Swelling of nitrocellulose has been examined in the following mixtures: ethyl alcohol-ethyl ether; ethyl alcohol-benzene; benzyl alcohol-anisole; ethyl alcohol-hexane. A range of 0-100 % of each constituent was covered. Results are seen in Fig. 6. An obvious maximum is seen with alcohol-ether, less well defined maxima

being seen with alcohol-benzene and benzyl alcohol-anisole. Swelling in alcohol-hexane appears to depend only on the alcohol content.

TABLE VI.—SWELLING OF NITROCELLULOSE IN SOLVENT-HEXANE MIXTURES. VALUES OF Q g./g.

Solvent.	Aliphatic Compounds, 0.3 Molar Fraction.		
	11°.	25°.	35°.
Isobutyl n-butyrate .	3.1	3.0	2.9
n-Butyl n-butyrate .	3.4	3.2	2.9
Amyl acetate .	6.5	5.0	4.4
n-Butyl acetate .	8.6	7.3	5.6
n-Propyl acetate .	5.5	5.0	4.4
Ethyl acetate .	4.4	4.2	3.9
Ethyl formate .	4.1	3.8	3.3
Methyl acetate .	4.3	3.9	3.6
Acetone .	3.3	3.2	2.8
Solvent.	Aromatic Compounds, 0.2 Molar Fraction.		
	11°.	25°.	35°.
Diethyl phthalate .	3.5	3.5	3.5
Dihexyl phthalate .	4.5	3.9	3.5
Dibutyl phthalate .	gelled	gelled	gelled
Diethyl phthalate .	7.9	7.2	5.1
Cyclohexanone .	4.2	4.2	4.2
Nitrobenzene .	4.7	4.5	3.8

### Discussion.

Within the limited range of solvents studied, swelling and solubility appear to be related to the cohesive energy density of the solvent. With the aliphatic and aromatic esters used, complete solubility occurs when

<sup>18</sup> Gee, *Trans. Faraday Soc.*, 1944, 40, 468.

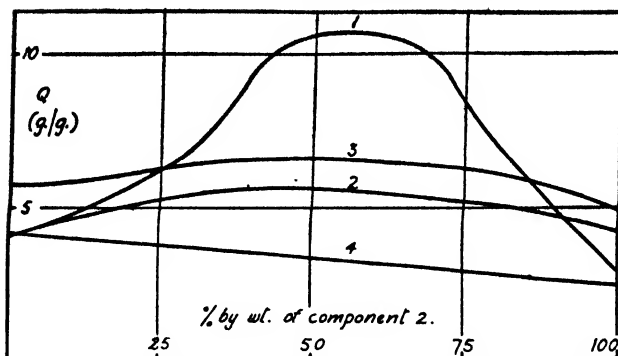


FIG. 6.—Swelling of nitrocellulose in "non-solvent" mixtures. 1. Alcohol-ether. 2. Alcohol-benzene. 3. benzyl alcohol-anisole. 4. Alcohol-hexane.

the cohesive energy density values lie within a certain range. Maxima are seen at particular  $(E/V)^{\frac{1}{2}}$  values in swelling in binary mixtures and there is evidence for similar maxima when solvent power is determined by precipitants. In Gee's treatment the swelling power of a solvent is assumed to be controlled by the heat absorbed in swelling and this is related to the difference of cohesive energy density between polymer and liquid. Clearly this cannot apply directly in the present case since the temperature effect on swelling indicates that heat is evolved. Nevertheless there is experimental evidence that swelling is related to cohesive energy, within a restricted group of liquids. This may provide an explanation for variations in solubility observed when a homologous series of solvents is ascended.<sup>13, 14</sup>

Hexane, compared with ethyl alcohol and benzene, appears to contribute

TABLE VII.— $(E/V)^{\frac{1}{2}}$  VALUES AT 25°.

Liquid.	$(E/V)^{\frac{1}{2}}$
Ethyl alcohol . . .	13.1
Benzyl alcohol . . .	11.7
Anisole . . . . .	9.1
Benzene . . . . .	9.0
Ethyl ether . . . . .	7.6
Hexane . . . . .	7.4

least to swelling and the volume required to precipitate nitrocellulose from its solutions is generally least. The non-polar character of hexane is probably responsible. With solvent-alcohol mixtures the swelling at low solvent values of  $(E/V)^{\frac{1}{2}}$  is greater than might have been anticipated from considerations of cohesive energy density. Gee<sup>13</sup> has suggested a treatment for mixtures of liquids of low solvent power. Swelling and solubility are considered in terms of the heats of mixing of the two liquids with each other and the

polymer. The greater the heat of mixing of the two liquids the greater the swelling or solvent power of the mixture relative to its components. If

$$\alpha \approx [(E_1/V_1)^{\frac{1}{2}} - (E_2/V_2)^{\frac{1}{2}}]^2$$

where 1 and 2 refer to the two liquids and  $\alpha$  is a constant related to their heat of mixing, enhanced swelling and solubility are associated with large values of  $\alpha$ . The value of  $(E/V)^{\frac{1}{2}}$  for ethyl alcohol at 25°, obtained from heat of vaporisation, is 13.1. Enhanced swelling might be anticipated at low solvent  $(E/V)^{\frac{1}{2}}$  values.

The swelling in "non-solvent" mixtures might be interpreted in a similar way. Values for  $(E/V)^{\frac{1}{2}}$  at 25° are given in Table VII.

<sup>13</sup> Davidson and Reid, *Ind. Eng. Chem.*, 1924, 19, 977.

<sup>14</sup> Doolittle, *Ind. Eng. Chem.*, 1944, 36, 239.

Doubt is attached to such values for associated liquids as alcohols and the asymmetry of the heats of mixing of alcohols with hydrocarbons<sup>15</sup> makes estimates of  $\alpha$  doubtful. The figures, however, suggest that the greatest swelling should be seen with alcohol-ether mixtures and that alcohol-benzene should be a little superior in swelling power to anisole-benzyl alcohol. Results are in agreement with these predictions. Swelling in alcohol-hexane emphasises the inert character of hexane.

Maximum swelling in solvent-benzene mixtures occurs at a somewhat higher value of  $(E/V)^{1/2}$  than in mixtures involving alcohol or hexane. The reason for this difference is not clear nor is the reason for the action of ketone-benzene mixtures. In the latter case a tentative suggestion might be advanced. Hess and Trogus have suggested that ketones may act as catalysts in the formation of aromatic hydrocarbon-nitrocellulose compounds.<sup>16</sup>

The approximations inherent in this work should be noted. Association of liquids may introduce discrepancies. Solvent, in binary mixtures, might possibly have been better expressed in terms of activities. This work is being extended to other solvents and binary mixtures and to the distribution of liquids between swollen and liquid phases.

My thanks are due to Dr. G. Gee for suggestions and help in the presentation of this paper. I would like to acknowledge the help of Mr. T. H. M. Chillingworth, who carried out the viscosity determinations. I am indebted to the Director General of Scientific Research (Defence), Ministry of Supply, for permission to publish this paper.

### Summary.

Within a limited range of solvents, swelling of nitrocellulose in certain binary mixtures is related to the cohesive energy density of solvent. Complete solubility in pure solvent appears to occur when the cohesive energy density of solvent lies within a certain range. In most cases, solvent power, as determined by the precipitant method, follows that of swelling in binary mixtures involving the precipitant. Some correlation between swelling power and viscosity of dilute solutions of nitrocellulose has been obtained. In cases studied, the swelling of nitrocellulose in binary "non-solvent" mixtures generally agrees with the treatment of such mixtures by Gee.

### Résumé.

Pour un certain nombre de solvants, le gonflement de la nitrocellulose dans quelques mélanges binaires est relié à la densité d'énergie cohésive du solvant. Lorsque celle-ci se trouve entre certaines limites, une solubilité complète dans le solvant pur apparaît. Dans la plupart des cas, le pouvoir solvant, déterminé au moyen d'un liquide précipitant, suit le pouvoir de gonflement dans des mélanges binaires comportant le précipitant. On a établi quelques relations entre le pouvoir de gonflement et la viscosité de solutions diluées de nitrocellulose. Dans les cas étudiés, le gonflement de la nitrocellulose dans des mélanges binaires "non solvants" s'accorde dans l'ensemble avec le traitement que Gee a donné pour ces mélanges.

### Zusammenfassung.

Innerhalb einer beschränkten Reihe von Lösungsmitteln besteht eine Beziehung zwischen der Quellung von Nitrozellulose in binären Gemischen und der "Kohäsionsenergiedichte" des Lösungsmittels. Völlige Löslichkeit in einem bestimmten Lösungsmittel scheint dann einzutreten, wenn die Kohäsionsenergiedichte in einem gewissen Intervall liegt. In den meisten Fällen verläuft das

<sup>15</sup> Wolf, Pahlke and Wehage, *Z. Physik. Chem.*, 1935, **28**, 1.

<sup>16</sup> Hess and Trogus, *Applications of Electron Beams and X-rays to Problems in Organic Chemistry* (Eggert and Schiebold ed., 1934), 21-68.

Lösungsvermögen—bestimmt durch Hinzufügung einer "Präzipitant"-Flüssigkeit bis die Lösung trüb wird—parallel mit der Quellbarkeit in einem binären Gemisch mit dem Präzipitanten. In verdünnten Nitrozelluloselösungen besteht ein Zusammenhang zwischen Quellbarkeit und Viskosität. In den untersuchten Fällen stimmt die Quellung der Nitrozellulose in binären "Nichtlösungsmitteln" im allgemeinen mit der von Gee ausgearbeiteten Theorie überein.

*The Chemical Laboratories,  
The Technical College,  
Bradford.*

## SORPTION OF LARGE MOLECULES BY KERATIN.

BY G. KING.

*Received 18th September, 1945, as amended 22nd February, 1946.*

The processing and dyeing of wool involves treatment with various compounds of large molecular weight and it is of importance to determine the conditions under which such molecules are sorbed. These conditions have been investigated by Speakman<sup>1, 2</sup> who asserts that "any particular liquid may fail to react with wool for one of two reasons: either the compound is inherently incapable of reaction on chemical grounds, or it is unable to penetrate the fibre capillary structure".

In the case of smaller molecules such as water, which would be unaffected by capillary structure, various quantitative descriptions of the sorption and diffusion processes have been given.<sup>3-7</sup> The results also indicate that similar processes govern the sorption of methyl and ethyl alcohols, but that the molar sorption is greatly restricted and that the diffusion processes are slowed down appreciably.

The present paper extends the investigations of the sorption properties of keratin to cover *n*-propyl alcohol, and acetone, and it is shown that the change in these properties over the whole series shows no abnormalities. An expression for the "minimum" diffusion coefficient is obtained from which the molar heats of sorption are estimated. In the case of methyl and ethyl alcohols the values are shown to compare favourably with those estimated from values of the respective heats of wetting. A qualitative explanation of the restricted molar sorption of the higher alcohols by keratin is also given.

### Experimental.

The experimental work extends previous measurements of the rate of sorption of alcohols by wool<sup>4</sup> at 25° C., to cover *n*-propyl alcohol and acetone, and similar methods were employed. The absorbents were in contact with quick-lime throughout the experiments, and the possible presence of more readily absorbed impurities accounted for by repeating the experiments until constant results were obtained. The resulting rates of sorption and desorption for *n*-propyl alcohol are shown in Fig. 1 and differ from those for the lower alcohols only in the slower rate of diffusion. The value of the minimum diffusion coefficient  $k_0$ ,<sup>4</sup> was determined as  $3.8 \times 10^{-13}$  cm.<sup>2</sup>/sec. Within experimental error, the results for acetone were found to be identical with those in Fig. 1 and are therefore not shown.

<sup>1</sup> Speakman, *Trans. Faraday Soc.*, 1930, **26**, 61.

<sup>2</sup> Speakman, *Proc. Roy. Soc. A*, 1931, **132**, 167.

<sup>3</sup> Cassie, *Trans. Faraday Soc.*, 1945, **41**, 450.

<sup>4</sup> King, *ibid.*, 1945, **41**, 325.

<sup>5</sup> Speakman, *ibid.*, 1944, **40**, 6.

<sup>7</sup> Glückauf, *J. Roy. Met. Soc.*, 1944, **70**, 293.

<sup>6</sup> King, *ibid.*, 1945, **41**, 479.

It is interesting to note that if the wool sample is heated to a temperature of about  $100^{\circ}\text{C}$ . prior to sorption this has the effect of reducing  $k_0$  by a factor of two to three in every case, and normal properties are only restored by washing in water. At normal temperatures, up to at least  $40^{\circ}\text{C}$ ., consistent results are obtained provided evacuation is carried out for at least 24 hr. either by Hyvac or diffusion pump. For all absorbates other than water; the keratin samples must not be used more than once unless they have been thoroughly washed in water.

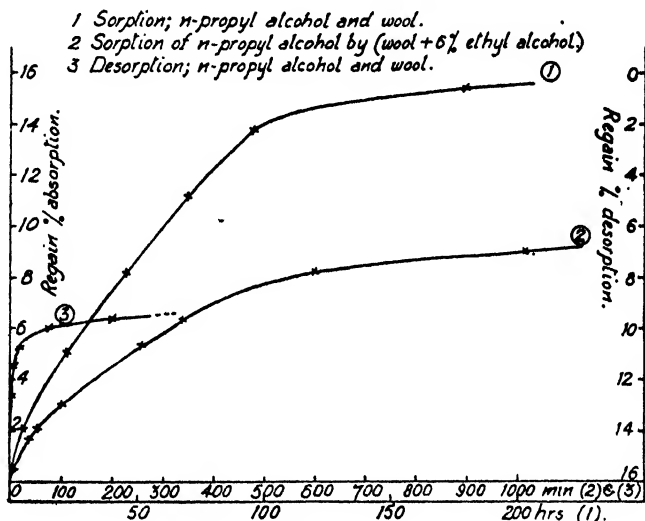


FIG. 1.

**Sorption of *n*-Propyl Alcohol:** It will be seen from Fig. 1 that *n*-propyl alcohol is absorbed up to at least 16 % regain,\* in contradiction with Speakman's results.<sup>1</sup> He found a maximum regain of 3 %, no doubt due to the fact that insufficient time was allowed to elapse for complete sorption. The saturation value must, of course, remain indeterminate to a large extent due to the time factor.

As is well known, the initial presence of an absorbate in keratin greatly facilitates further sorption, either of the same or even of much larger molecules.<sup>1, 2, 4</sup> In the case of ethyl alcohol an increase in the sorption rate of up to six times was obtained by the presence of an initial regain of 6 % ethyl alcohol. Curve (2) of Fig. 1 shows the rate of sorption of *n*-propyl alcohol by wool already containing 6 % ethyl alcohol. It is seen that the rate of absorption ( $1.4 \times 10^{-3}$  regain units per min.) is very nearly six times that for *n*-propyl alcohol in untreated wool ( $2.2 \times 10^{-3}$  regain units/min.).

The increased rate of absorption may be explained along the lines of the theories of diffusion proposed in previous papers.<sup>4, 5</sup> It has been shown that the rate of sorption is controlled by a minimum value of the diffusion coefficient ( $k_0$ ). As the initial regain is increased,  $k_0$  assumes values determined by the relation between  $k$  and regain. Now in the case of water,  $k$  increases from  $10^{-8}$  to  $10^{-7}$  cm.<sup>2</sup>/sec. between 0 % and 23 % regain, so that an increase of six times between 0 % and 7 % regain in the case of ethyl alcohol is quite permissible. The fact that *n*-propyl alcohol is affected in a like manner suggests an identical diffusion mechanism proceeding at a slower rate.

\* Regain is the weight of absorbate per 100 g. of keratin prior to sorption.



**The Sorption Process.**

It is now possible to examine the variation in rate of sorption over the homologous series water-*n*-propyl alcohol. A linear relationship, Fig. 2, exists between  $\ln k_0$  and the molar refraction  $P_0$  defined by:—

$$P_0 = \frac{r^2 - 1}{r^2 + 2} \cdot \frac{M}{\rho} \quad . \quad . \quad . \quad (1)$$

where  $r$  is the refractive index,  $\rho$  is the density, and  $M$  is the mol. weight. The values for  $k_0$  were roughly corrected for the variation in saturation regain, assuming it to be

Water . . . . .	33 %	Ethyl alcohol . . . . .	26 %
Methyl alcohol . . . . .	28 %	<i>n</i> -Propyl alcohol . . . . .	20 %

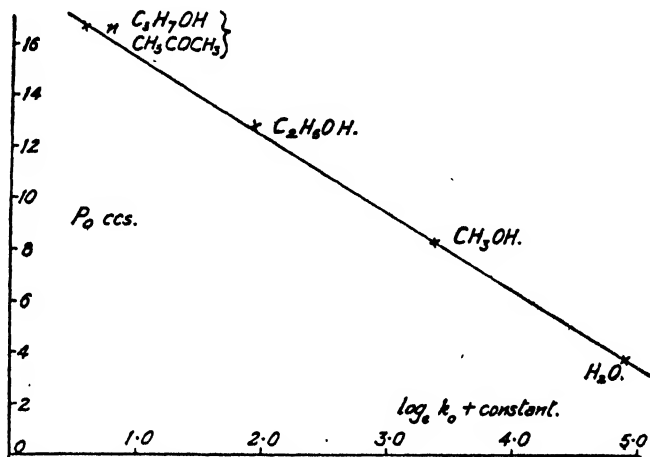


FIG. 2.

The linear relationship, together with the temperature dependence of the diffusion process, suggests that  $k_0$  must be determined by a relation of the form

$$k_0 = k_0' \cdot e^{-E/RT} \quad . \quad . \quad . \quad (2)$$

where  $k_0'$  is some function of the concentration of the absorbate,  $E$  the activation energy of the diffusion process at low concentrations,  $R$  the gas constant per mol.,  $T$  the absolute temperature.

Equation (2) may be derived by use of the diffusion mechanism proposed in a previous paper,<sup>5</sup> which requires Cassie's relation for multimolecular sorption<sup>3</sup>:

$$(A - X)(B - X) = \beta X^2 \quad . \quad . \quad . \quad (3)$$

where  $A$  is the molar sorption per 100 g. of absorbent, of which  $X$  mols. are localised over  $B$  mols. of available low energy sites, and where  $\beta = a \cdot e^{-w/RT}$ , where  $w$  is the heat evolved when one mol. of liquid water is absorbed on to localised sites, and  $a$  is a constant.

Using this relation, the expression for the diffusion coefficient becomes<sup>5</sup>

$$k = \frac{K}{(B - X)^2} \cdot \frac{\partial(A - X)}{\partial A} \cdot e^{-\epsilon/RT} \quad . \quad . \quad . \quad (4)$$

where  $K$  is a constant, and  $\epsilon$  is the energy of activation for diffusion of liquid molecules between the  $X$  mols. of occupied low energy sites. From (3) we have:—

$$(A - X) = \frac{2A(1 - \beta) - A - B + \sqrt{(A + B)^2 - 4AB(1 - \beta)}}{2(1 - \beta)}$$

$$\text{i.e., } \frac{\partial(A - X)}{\partial A} = \frac{1}{2(1 - \beta)} \left[ 2(1 - \beta) - 1 + \frac{A + B - 2B(1 - \beta)}{\sqrt{B^2 - 2A(1 - \beta)}} \right]$$

$$\approx \frac{1}{2(1 - \beta)} \left[ 1 - 2\beta + \frac{A - B(1 - 2\beta)}{B} \cdot \left\{ 1 + \frac{A}{B}(1 - 2\beta) \right\} \right]$$

as  $A \rightarrow 0$

$$\approx \frac{A}{B} \cdot \beta,$$

so that, as  $(B - X) \rightarrow B$  as  $A \rightarrow 0$ , we have

$$k_0 \approx \frac{KA}{B^2} \cdot a \cdot e^{-\frac{(w + \epsilon)}{RT}} \quad (5)$$

The empirical logarithmic relation between  $k_0$  and  $P_0$ , derived experimentally suggests that  $w$  or  $\epsilon$  or both are proportional to  $P_0$ . This result might have been expected, but the further implication that  $\left[ \frac{KAa}{B^2} \right]$  is roughly constant over the homologous series could not be anticipated. Both results are discussed below.

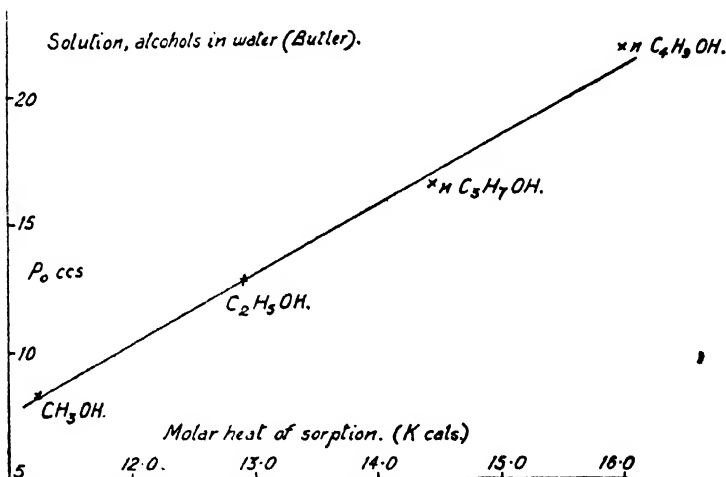


FIG. 3.

If we assume that  $\epsilon$  is determined by the energy of distortion of the lattice of the absorbent, i.e., the energy of hole formation, then Barrer's values for the series, helium, hydrogen, argon and methane<sup>9</sup> indicate that  $\epsilon$  will be proportional to the molar volume of the diffusing molecule and to  $P_0$ .

Then again it is quite possible that  $w$  is determined by London<sup>10</sup> forces. Eley<sup>10</sup> has shown that for the solution of polyatomic gases in organic solvents, the molar energy of sorption is proportional to  $P_0$ , and he also suggests<sup>11</sup> that rubber sorbs organic solvents in a like manner; i.e., the molar heat of sorption will depend mainly on the London forces between the swelling molecule and the neighbouring polyisoprene chains, that it

<sup>9</sup> Barrer, *Trans. Faraday Soc.*, 1939, **35**, 646.

<sup>10</sup> London, *ibid.*, 1937, **33**, 8.

<sup>10</sup> Eley, *ibid.*, 1939, **35**, 1281, 1421.

<sup>11</sup> Eley, *ibid.*, 1942, **38**, 285.

should in fact be a function of the product  $P_0 \times P_0'$  where  $P_0'$  is a parameter dependent on the absorbent.

Both these examples are special cases, in that no permanent dipole interaction will occur during mixing, but Butler's data<sup>12</sup> show a similar relation between molar volume and the molar heat of hydration for the solution of alcohols in water, even in the presence of permanent dipoles (Fig. 3). Now according to London the contribution of permanent dipoles becomes important for dipole moments of the order of that for water, i.e.,  $1.8 \times 10^{-18}$  E.S.U., and it should therefore be an important factor both for Butler's solutions and for the sorption of alcohols by keratin. That such a contribution cannot be detected in either case may be due to the almost constant value of the dipole moment over the series of alcohols used. Such an argument is not applicable, however, to the sorption of acetone by keratin. Acetone has a molar refraction very nearly the same as *n*-propyl alcohol, but has a dipole moment of 2.7 E.S.U. as compared with 1.7 E.S.U. for the alcohol. Despite this their sorption properties are almost identical.

It has been shown for the water-keratin system that the diffusion coefficient is independent of the rigidity of the keratin.<sup>8</sup> This might be due to zeolitic diffusion down so called lattice channels, and sorption discontinuities must then occur as the molar volume of the absorbate is increased.<sup>13</sup> No such discontinuities have been observed as yet, in keratin sorption phenomena, a logarithmic decrease in the sorption rate having been mistaken for the exclusion of the higher alcohols.<sup>1</sup>

If  $\epsilon$  is independent of the lattice constants, and is determined solely by liquid forces in accordance with Brunauer, Emmett and Teller's theory of sorption,<sup>14</sup> then as saturation is attained the low energy sites are almost filled and the diffusion coefficient should approximate to that for self diffusion of the appropriate liquid;  $\epsilon$  should therefore be of the same order of magnitude as the activation energy for self diffusion of the absorbed liquid. In the case of water, this has the value of 5.3 kcal.,<sup>15</sup> half the molar energy of evaporation. If this is true throughout the water alcohol series, then using values for the respective latent heats obtained from the International Critical Tables, the following values for  $\epsilon$  are obtained: water (5.3 kcal., ethyl alcohol (5.0 kcal.), methyl alcohol (4.6 kcal.), *n*-propyl alcohol (5.6 kcal.).

Apart from water the values of  $\epsilon$  increase in a slow but regular manner with increase in molecular weight. The exceptional value for water may be due to its highly associated state.

Rewriting (2) as

$$k_0 = k_0' e^{-\frac{(w + \epsilon)}{RT}} \quad (6)$$

and taking Cassie's<sup>3</sup> value for  $w$  for water as 3.5 kcal.,  $k_0'$  may be determined, and if  $k_0'$  is constant throughout the homologous series, as the experimental results suggest, it is possible to estimate  $w$  for the three alcohols. The results are: methyl alcohol (6.5 kcal.), ethyl alcohol (8.0 kcal.), *n*-propyl alcohol (9.3 kcal.).

Finally, if  $\epsilon$  is constant or zero, then using (6), slightly different values for  $w$  (and  $k_0'$ ) are obtained: methyl alcohol (5.5 kcal.), ethyl alcohol (7.5 kcal.), *n*-propyl alcohol (9.4 kcal.).

### Heat of Wetting of Keratin by Methyl and Ethyl Alcohols.

The slow rate of sorption of the higher alcohols by wool makes it difficult to obtain an accurate value for the heat of wetting even when using

<sup>12</sup> Butler, *Trans. Faraday Soc.*, 1937, 33, 229.

<sup>13</sup> Barrer, *ibid.*, 1944, 40, 555, 206.

<sup>14</sup> Brunauer, Emmett and Teller, *J. Amer. Chem. Soc.*, 1938, 60, 309.

<sup>15</sup> Barrer, *Trans. Faraday Soc.*, 1939, 35, 650.

fine wool. In a preliminary investigation a method similar to that of Hedges<sup>16</sup> has been employed. The wool sample was initially enclosed in a fragile glass bulb and evacuated using a Hyvac pump, prior to breaking in the appropriate liquid when required. The alcohols were in contact with freshly ignited lime throughout the experiments.

Values for the heats of wetting of dry wool determined in this way were: methyl alcohol (26 cal./g.), ethyl alcohol (24 cal./g.).

These values are by no means final, and it is hoped to be able to improve their accuracy by using powdered horn keratin, in order to speed up the sorption rates.

It is interesting, however, to compare the experimental values with those derived by using essentially Cassie's relation<sup>3</sup>:

$$100W = w \cdot X + \int_0^{\Delta V} \Delta P \cdot d(\Delta V) \quad (7)$$

where  $W$  is the heat of wetting per g. of dry wool, and  $\Delta P$  is the increase in hydrostatic pressure for an increase in volume  $\Delta V$  due to swelling.

There is good reason to believe that the absorption isotherms for alcohol-wool systems up to at least *n*-propyl alcohol, are very similar to that for water and wool,<sup>1, 4</sup> but as was pointed out in a previous paper,<sup>4</sup>

TABLE I

$\Delta P$ (Methanol).	$\Delta P$ (Ethanol).	% Diameter Swelling.	Regain %.
$19 = 10^5$ g./cm. <sup>2</sup>	$19 \times 10^5$ g./cm. <sup>2</sup>	2.0	5
$31 \times 10^5$ g./cm. <sup>2</sup>	$32 \times 10^5$ g./cm. <sup>2</sup>	4.4	10
$32 \times 10^5$ g./cm. <sup>2</sup>	$37 \times 10^5$ g./cm. <sup>2</sup>	7.0	15
$32 \times 10^5$ g./cm. <sup>2</sup>	$40 \times 10^5$ g./cm. <sup>2</sup>	10.0	20
$32 \times 10^5$ g./cm. <sup>2</sup>	$42 \times 10^5$ g./cm. <sup>2</sup>	13.0	25

this indicates a marked decrease in the molar sorption with increase in  $M$ . Assuming relation (3) to be applicable to the sorption of alcohols by keratin, it is possible to derive values for  $X$  in each case at saturation regain. If the number of available low energy sites remains the same as that for water, and  $w$  increases for the alcohols in accordance with the previous observations on diffusion, then values for  $X$  are methyl alcohol (0.80 mol.) and ethyl alcohol (0.55 mol.).

According to (7), these low values for  $X$  would produce a decrease in the value for  $W$  provided the term for the swelling energy remained the same as that for water, but there is reason to believe that the term increases substantially in the case of the alcohols. According to Speakman<sup>1</sup> the energies required to stretch wool fibres 30 % in water, methyl, and ethyl alcohols are  $1.43 \times 10^5$ ;  $1.72 \times 10^5$ ; and  $2.44 \times 10^5$  cm. g./cc. respectively. This is quite possible when we remember that Young's modulus for keratin will depend on the molar sorption, i.e., the modulus for an alcohol-keratin system may be obtained from the water-keratin system of equal molar concentration. Also Hirst<sup>17</sup> has found the percentage radial swelling of wool in water, methyl, and ethyl alcohol to be 38, 38, and 33 respectively, so if one assumes  $\Delta V$  to be constant throughout the series at constant regain, then  $\Delta P$  may be estimated in each case. This was done using the values for water; \* the results are shown in Table I.

<sup>16</sup> Hedges, *ibid.*, 1926, 22, 178.

<sup>17</sup> Hirst, *Wool Industries Research Association*, private publication.

\* I am indebted to Mr. F. L. Warburton of these laboratories for more recent values of the elastic constants of horn keratin at different regains. These give smaller values for  $\Delta P$  than those used by Cassie.<sup>3</sup>

The swelling energies  $\left[ \int_0^{\Delta V} \Delta P \cdot d(\Delta V) \right]$  were obtained graphically as methyl alcohol (1650 cal./100 g. wool), ethyl alcohol (2000 cal./100 g. wool). Then assuming values for  $w$  as 5.5 kcal. and 7.5 kcal. for methyl and ethyl alcohols respectively we have:

$$W (\text{methyl alcohol}) = (55 \times 0.8 - 16.5) = 27 \text{ cal./g.}$$

$$W (\text{ethyl alcohol}) = (75 \times 0.55 - 20) = 21 \text{ cal./g.}$$

It is essential, however, that the values for the swelling energies should be verified by an accurate determination of the elastic moduli for keratin as a function of regain in the case of at least methyl and ethyl alcohol, to make these conclusions quantitative.

### Equilibrium Molar Sorption in Keratin for the Homologous Series of Alcohols.

It has been pointed out that there is a marked decrease in the molar sorption by keratin as one proceeds up the homologous series of alcohols.

Now Cassie's relation<sup>3</sup> for unrestricted sorption, free from elastic constraint is:

$$A = \frac{B \cdot p}{(p_0 - p)[\beta + (1 - \beta)p/p_0]} \quad (8)$$

where  $A$ ,  $B$  and  $\beta$  are defined as in (3),  $p$  is the corresponding vapour pressure of the absorbate, and  $p_0$  is the saturation vapour pressure of the absorbate.

According to (8), for a given value of  $(p/p_0)$  the corresponding regain should increase in proportion to the molecular weight of the absorbate provided  $B$  and  $\beta$  remain constant. It has been shown, however, that there is reason to expect a decrease in the value of  $\beta$  with increased molecular weight, which gives rise to a further increase in  $A$  for a given value of  $p/p_0$ .

We have not, however, considered the effect of elastic restraint on the molar sorption, which is determined by the relation<sup>3</sup>:

$$\Delta P = \frac{R \cdot T}{M \cdot V_0} \cdot \ln p'/p \quad (9)$$

where  $\Delta P$  is the increase in hydrostatic pressure of the absorbate defined above,  $M$  is the mol. wt. of the absorbate,  $V_0$  is the specific volume of the

TABLE II

	Regain %.	$A$ .	$\Delta P$ g./cm <sup>2</sup> .	$p'/p$ .	$p'/p_0$ .	$w$ .
Methyl alcohol	7	0.22	$26 \times 10^5$	126	0.28	5.1
	15	0.47	$33 \times 10^5$	200	0.70	5.1
Ethyl alcohol	7	0.15	$28 \times 10^5$	890	0.28	6.0
	15	0.33	$37 \times 10^5$	5100	0.70	7.0

absorbate,  $p$  is the vapour pressure for unrestrained sorption, and  $p'$  is the measured vapour pressure.

For a given regain value,  $(p'/p)$  must increase rapidly with  $M$ , due not only to the increase in  $M$ , but also because of an increase in  $\Delta P$ . In order to test the effectiveness of this expression it is assumed that the absorption isotherms for methyl and ethyl alcohols are the same,<sup>4</sup> and using the values of  $\Delta P$  obtained earlier in the paper, estimate  $w$  in each case, using the relations (8) and (9). The results are shown in Table II.

The agreement with the values of  $w$  suggested in the previous section, is only reasonably good but this is not surprising considering the assumptions made and the nature of the relations (8) and (9). The results do indicate, however, that the increase in elastic constraint with increase in  $M$  may be sufficient to account for the decrease in molar sorption.

I am grateful to Dr. A. B. D. Cassie for discussion of these problems, and to the Director and Council of the Wool Industries Research Association for permission to publish these results.

### Summary.

Observation of sorption rates by keratin indicate that the logarithm of the "minimum" diffusion coefficient increases in a linear manner with the molar refraction of the absorbate  $p$ , throughout the series water- $n$ -propyl alcohol.

The implications of such a relationship are discussed in the light of a diffusion mechanism derived in a previous publication.<sup>5</sup>

A qualitative explanation is given of the decrease in the molar sorption of alcohols by wool keratin, with increasing molecular weight.

### Résumé.

Les vitesses de sorption observées pour la kératine montrent que le coefficient "minimum" de diffusion croît linéairement avec la réfraction molaire  $p$ , du corps adsorbé dans toute la série : eau-alcool  $n$ -propylique. Un mécanisme de diffusion permet d'interpréter ces résultats.

### Zusammenfassung.

Beobachtungen der Sorptionsgeschwindigkeiten durch Keratin für die Reihe Wasser- $n$ -Propylalkohol zeigen, dass der Logarithmus des "Minimum"-Diffusionskoeffizienten eine lineare Funktion der Molrefraktion des Adsorbats ist. Die Bedeutung einer derartigen Relation wird mit Bezug auf den in einer früheren Mitteilung abgeleiteten Diffusionsmechanismus besprochen. Die Abnahme der Molsorption von Alkoholen durch Wollkeratin bei zunehmendem Molekulargewicht wird in qualitativer Weise erklärt.

## THE VISCO-ELASTIC BEHAVIOUR OF CORDITE. PART I. PLASTIC FLOW IN COMPRESSION AT HIGH STRESSES.

BY D. D. ELEY AND D. C. PEPPER.

*Received 5th September, 1946.*

The elastic and flow properties of long chain polymeric materials are of great importance in problems of manufacture and use, and they are characteristically very complicated. There is a great need for the examination of these properties, in specific cases, over wide ranges of stress, temperature and time. This paper, and the succeeding papers, present the results of one such examination for cordite.\* The material throughout has been taken from a single batch of cords of 7 mm. diameter.

In the first instance it is required to separate any deformation into plastic and elastic components, and to formulate expressions for the effects of temperature and stress on the component deformations. The practical utility of such an analysis is clear, and in a later paper a theory of rolling of plastic sheet will be given for the type of flow found in this case.

\* Cordite is necessarily very reproducible in composition and mechanical properties and is therefore very suitable for detailed rheological examination. The methods used and results obtained should have a general significance for the many related plastics in civilian use.

Secondly, an attempt is made to place a molecular interpretation upon the flow properties, but there is a difficulty here. By analogy with other similar materials, cordite may be considered as a network of nitrocellulose chains of length of the order of 2000 Å., in which the nitroglycerine molecules are dissolved. Regions of locally high order (crystallites) alternate with regions of relatively low order (amorphous regions), and since these are supposed to be on the scale of 100 Å., one chain may pass through several such regions. Irreversible flow may be supposed to involve slipping in the network system, and elasticity, by analogy with rubber, the orientation and deformation of chain segments in the amorphous regions. The important effects are *time* effects, viz. rates of flow and development of elastic deformation, and in making a theory for these we require firstly a knowledge of the structure, and secondly a treatment of the rate processes involved in the displacement of chain molecules. With this knowledge, a model may be developed and the time course of its deformation mathematically investigated. At the present stage, however, we are still on uncertain ground in both problems, and this raises what is probably the *major difficulty*. *This is that whenever a discrepancy between observed and calculated behaviour arises, it may do so because of structural considerations, or rate-process considerations.* In discussing a number of details we have frequently been confronted with this dilemma.

In this paper we describe the compression of cylindrical specimens, over the temperature range 17-70° C., and the stress range 6 to 161 kg.cm.<sup>-2</sup>, our particular objective being the unexplored field of plastic flow at high stresses. The cylinders were compressed at constant load, but it was found possible to correct for the decrease in applied stress as the cross-sectional area increased, and to provide data corrected to constant stress, at least for plastic flow. Elastic effects are not discussed in this paper. It will be seen that our experimental results show that *at high stresses* cordite behaves essentially like a thick liquid, and may be characterised by a "differential viscosity constant" independent of stress.

### Experimental.

The apparatus used was a simple compression plastometer, working at constant load to within 0.5 %. The specimen of cordite was compressed between two parallel plates of thermal insulating material. The load was applied by a lever arm, which was operated through a simple quick-release device. The compression of the cordite specimen was followed against time by means of a dial gauge, reading to 0.01 mm. After compressing for a known time the load and lever arm were removed and the elastic recovery curve followed. In all cases the specimen was finally removed from the apparatus and complete elastic recovery obtained by heating to constant length at 100° C. The difference between the initial and final lengths of the cordite specimen, as measured to 0.01 mm. by a micrometer gauge, was taken as the permanent set.

The specimen was thermostatted by a vapour bath, which proved a most convenient method. Three thermocouple junctions were employed to obtain the temperature of the specimen. Two junctions were placed on the lower plate within 1 mm. of the specimen and one on the upper plate. In this way we found that in all cases there was a satisfactory uniformity of temperature within the jacket.

The specimens of cordite were cylinders 16 mm. long × 7 mm. diameter cut from extruded cords. Their ends were filed accurately parallel using a steel former. The cordite was stored in a box in the laboratory (15°-20° C.) and over the period of work the humidity only varied between 40 and 55 %, usually lying between 45 and 50 %. The compression plates had a diameter of 20 mm., i.e. much larger than the cordite specimens. The ends of the specimen were not lubricated, but

in general the cylinder compressed uniformly with little "barrelling". Only at the lowest temperature, viz. 16° c., and even then only at the highest rates of compression, did the cordite specimen show surface cracks.

### Results.

**Reproducibility.**—In Fig. 1 we present a typical set of runs at 16°–17° c. The applied weight used was 25 kg., and since the weight of loading arm plus plunger was 1.47 kg. and the initial cross-sectional area of the specimen was 0.382 cm.<sup>2</sup>, this corresponds to an initial stress of 69.2 kg.cm.<sup>-2</sup>. Fig. 1*a* presents the total compression as a function of time for five separate specimens, compressed respectively for 1, 4, 6, 10 and 20 minutes. The reproducibility is within  $\pm 0.5\%$ . We also show the initial part of the elastic recovery curves. In Fig. 1*b* we plot the permanent

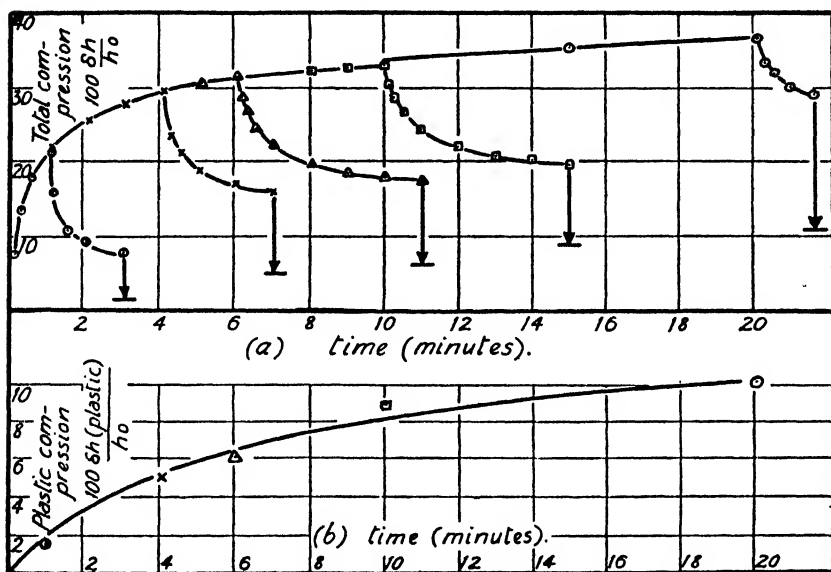


FIG. 1.—Compression at 17° c. and 69.2 kg.cm.<sup>2</sup> initial stress. (a) Total compression; (b) plastic compression.

set for these experiments, determining by relaxing at 100° c., as a function of time of compression. We have found a similar excellent reproducibility in these experiments.

In all cases before compression the cordite specimens were allowed to stand one hour in the plastometer at the temperature of experiment. It is our impression that the plastic flow at these high stresses is not so sensitive to stress or thermal history as in our work at lower stresses, in extension, to be reported later. The humidity in the plastometer was not controlled, but at the higher temperatures a "pine-cone" of cordite was included to minimise loss of volatile matter (which in any case seemed inappreciable).

**Plastic Flow at Constant Stress.**—Our plastic flow-time curves refer to a constant load, i.e. to a continuously decreasing stress as the cross-section of the specimen increases during the course of the compression. If  $h_0$  be the original height of the specimen ( $\sim 16$  mm.) and  $h$  the height at time  $t$  from release of the weight, then the rate of plastic flow is defined as

$$\phi = \frac{1}{h} \frac{dh}{dt} \quad . \quad . \quad . \quad . \quad . \quad . \quad (1)$$





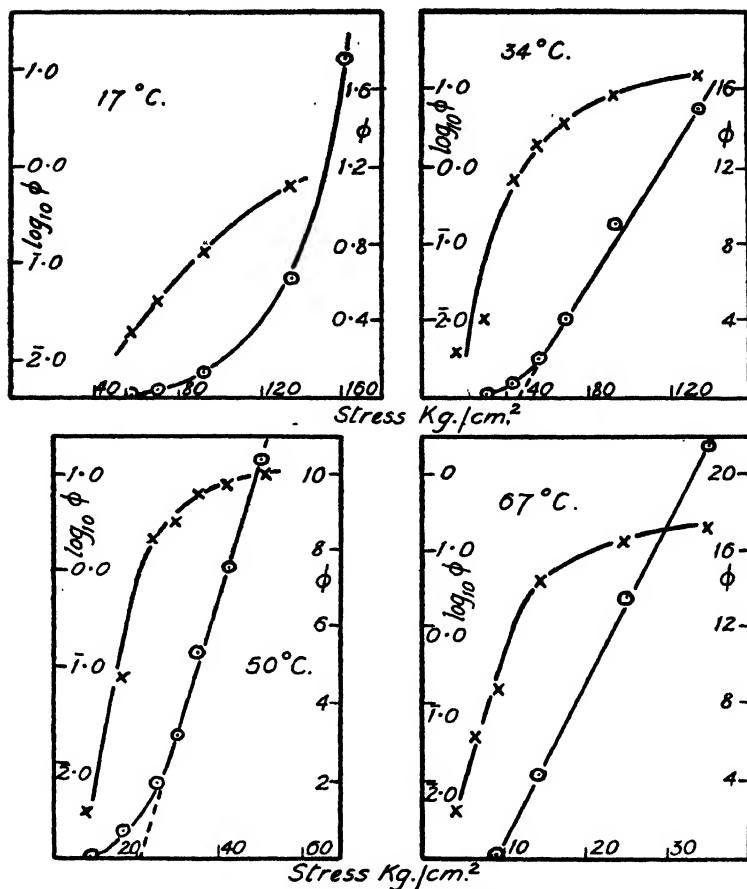


FIG. 3.—Stress-rate of plastic flow relationships.

Circles : stress-rate (% sec.<sup>-1</sup>).  
 Crosses : stress- $\log_{10}$  (rate).

TABLE I.—DATA FOR RATE OF PLASTIC FLOW AT 67° C.

Expt.	Stress kg. cm. <sup>-2</sup>	Time of Compression sec.	$\Delta k/k_0$ (Plastic) %.	$\dot{\phi}$ % sec. <sup>-1</sup>
104	3.8	360	1.74	$4.8 \times 10^{-3}$
105	6.5	120	5.02	$4.2 \times 10^{-3}$
108	14.3	2	8.5	4.25
109	14.3	5	9.8	—
107	14.3	15	14.9	—
112	14.3	60	26.1	—
110	24.8	2	27.2	13.6
111	35.3	2	43.1	21.5

**Effect of Specimen Dimensions.**—It is important that the plastic-flow-time curve, for a given load and temperature, should be independent

TABLE II.

Expt.	$h_0$ mm.	$\Delta h$ (plastic) at 1 min.	100 $\Delta h/h_0$ .
119	5.31	0.83	15.7
114	8.05	1.77	22.0
120	9.34	2.16	23.0
118	8.10	1.67	21.0
49	15.96	3.10	19.4
121	15.80	3.75	23.7

of the initial height of the specimen, if our results on 16 mm. cylinders are to be capable of universal application in problems of flow. This has been tested directly, and it may be noted that the results support the considerations in the next section. Table II presents results in which cordite cylinders of identical initial diameter ( $7 \pm 0.05$  mm.) but different initial height are compressed for 1 min. by an initial stress of 56 kg.

cm.<sup>-2</sup> at 34° C. It will be seen that the plastic flow, expressed as a percentage  $100 \Delta h/h_0$ ,\* is essentially independent of specimen height  $h_0$ , except in the case of very squat cylinders, where  $h_0 < \text{diameter}$ . The % plastic flow at 56 kg.cm.<sup>-2</sup> and 34° C. is also found to be the same at different times for cylinders 8 mm. and 16 mm. high, as shown in Table III. Similar good agreement is found for an experiment at an initial stress of 135 kg.cm.<sup>-2</sup>.

TABLE III.

Time.	6 sec.	20 sec.	1 min.	4 min.
% plastic flow, $h_0 = 8$ mm.	8.4	15.3	22.0 21.0	31.8
% plastic flow, $h_0 = 16$ mm.	8.7	14.0	19.4 23.7	31 (extrap.)

**Course of the Plastic Flow-Time Curve.**—In any one experiment at constant temperature and load, the plastic flow-time curve bends towards the time axis, the rate of plastic flow continually decreasing. In favourable cases it may be shown that this decrease may be accounted for, within a rather large experimental error, by the decrease in stress following upon the increased cross-sectional area of the specimen as it is compressed. We may definitely conclude, for example, that shear-hardening and shear-softening (thixotropic) effects are unimportant, at these high stresses and correspondingly high rates of shear. This is in contrast to the results observed in extension, at very low stresses and with very low deformations ( $\sim 5\%$ ). There we have found shear hardening occurs, lowering the rate of plastic flow  $\phi$  by 20 to 30 times over the initial 2-3 % extension. It may be that even at high stresses the initial 2 % of deformation is "softer," but for the

TABLE IV

Initial Stress kg.cm. <sup>-2</sup>	$h$ , mm.*	$S_0 \frac{h}{h_0}$	Rate.
135	5.1	43	1.2
95	7.27	43	0.9
43	16.0	43	0.7
69	6.95	30	0.15
56	8.55	30	0.11
30	16.0	30	0.12

\*  $h$  is the height of the specimen at the instant of the rate measurement, and  $S_0 \frac{h}{h_0}$  the corresponding stress.

\* For large deformations the amount of plastic flow is more rigidly given by

$$-\int_{h_0}^h \frac{dh}{h} = \ln \frac{h_0}{h}$$

extensive deformations observed in compression this will play a negligible part. On the whole, though, our results favour the explanation that the shear-hardening that occurs at small stresses follows upon the building-up of further internal bonds in the plastic (increased orientation and crystallinity of nitrocellulose molecules). These bonds, however, are not strong enough to resist the high-stresses involved in extensive compression.

The procedure has been to take an experiment, and from the total deformation-time curve to evaluate the cross-sectional area of the specimen through the whole course of compression. So, from the start of the experiment we may list values of the stress for a series of times, for which we may also evaluate  $\dot{\phi}$ 's as the gradients of the corresponding plastic flow-time curves. These values of  $\dot{\phi}$  will possess the usual error associated with the taking of gradients. They may be compared with the values of  $\dot{\phi}$  deduced from the initial rates of flow in independent experiments over a range of stresses (cf. Fig. 2). Table IV shows such a comparison at 34° C. We see that during the course of an experiment in which the plastic flow rate falls 10 to 20-fold, the rate at any instant corresponds very well with that expected from the decrease in stress alone. In other words, shear-hardening effects are unimportant at these high stresses.

### Discussion.

**Plastic Flow Constants.**—It will be seen from Fig. 3*a-3d* that at the three higher temperatures the plot of rate of plastic flow  $\dot{\phi}$  against stress divides into three parts. Until a certain stress is reached, which we may call the "first yield value,"  $\dot{\phi}$  appears to be zero. Actually this is only an apparent yield value, since using more sensitive methods in extension plastic creep has been observed at much lower stresses, e.g. 2.6 kg./cm.<sup>2</sup> Then follows a curved portion in which  $\dot{\phi}$  increases at a rate much greater than the stress  $f$  increases (actually  $\log \dot{\phi}$  is linear with  $f$ ). Finally, in the most interesting part at high stresses,  $\dot{\phi}$  increases linearly with  $f$ . Clearly for a given temperature we may specify the  $\dot{\phi}/f$  line by a slope  $A$ , in units of percentage flow sec.<sup>-1</sup> kg.<sup>-1</sup> cm.<sup>2</sup>, and an intercept,  $f_0$ , in kg.cm.<sup>-2</sup>. This intercept  $f_0$  may be considered as a "second yield-value," but it is no more a true yield value than the "first yield-value," since flow will occur at stresses below it. The appropriate equation is:

$$\dot{\phi} = A(f - f_0). \quad (3)$$

We note that a rather similar behaviour has been found by Dillon and Johnston<sup>1</sup> for the extrusion of rubber stock; their results at the lower stresses (in the curved region of  $\dot{\phi}$  against  $f$ ) cannot be easily compared with ours, however, because of possible complications arising from "plug-flow". Equation (3) was used originally by Bingham<sup>2</sup> to describe flow in solid-liquid paste dispersions.

The constants  $A$  and  $f_0$  for the different temperatures are given in Table V. The value of  $A$  at 17° C. is an estimated value, since we never reached stresses high enough to give a linear  $\dot{\phi}/f$  relation.

Since our results enable us to conclude  $A$  and  $f_0$  are independent of dimensions of the cordite cylinder, it is justifiable to consider the calculations of more general constants than  $A$  and  $f_0$ , i.e. constants relating to a simple shear stress rather than the compressive stress given. This may be done on the assumptions that our material is behaving like a cylinder of Newtonian liquid, with no end-effects. It is difficult at present to assess the probable error on these constants. Provisionally, it is taken as a factor two.

<sup>1</sup> Dillon and Johnston, *Physics*, 1933, 4, 225.

<sup>2</sup> Bingham, *Fluidity and Plasticity* (McGraw Hill, 1922).

With these assumptions,

$$\text{shear stress} = \frac{1}{3} (\text{compressive stress } f),$$

$$\therefore \text{“ yield value ” in shear} = \frac{1}{3} f_0.$$

$$\text{and viscosity } \eta = \frac{(f - f_0)100}{\phi 3} \text{ in sec. kg.cm.}^{-2}$$

$$\eta = \frac{1}{3} \frac{100}{A} \cdot 1000 \times 981 = \frac{3.27 \times 10^7}{A} \text{ poises} \quad (4)$$

TABLE V.—CONSTANTS DESCRIBING THE FLOW OF CORDITE AT HIGH STRESSES.

T° c.	A % sec. <sup>-1</sup> kg. <sup>-1</sup> cm. <sup>3</sup> (Compression Data.)	f <sub>0</sub> kg.cm. <sup>-2</sup> (Compression Data.)	Shear Constant η Poises.	“Yield Value” in Shear kg.cm. <sup>-2</sup>
17	(0.08)	140-150	(41) × 10 <sup>7</sup>	45-50
34	0.17	44	19.3 × 10 <sup>7</sup>	15
50.2	0.33	20	10 × 10 <sup>7</sup>	6.6
67.2	0.85	9	3.85 × 10 <sup>7</sup>	3

**Temperature Coefficient of Plastic Flow.**—The viscosity of simple liquids follows to a high degree of accuracy, in many instances, the

Guzman-Andrade equation

$$\eta = \eta_0 e^{-U_{vis}/RT} \quad (5)$$

This equation has often been applied to data on the flow of plastics, but rarely to data where elastic deformations have been properly separated from plastic deformations. This criticism may be levelled to some extent at the best data available in the literature, viz. that of Mooney<sup>3</sup> on raw rubber and that of Ferry and Parks<sup>4</sup> on polyisobutene.

In Fig. 4 we have plotted log<sub>10</sub> A against 1/T° K. There is a deviation from the straight line which is probably outside the experimental error, and U<sub>vis</sub> in the range 40°-70° C. may be taken as 11 kcal. On the same scale we

FIG. 4.—Temperature dependence of A and f<sub>0</sub>.

plot log<sub>10</sub> f<sub>0</sub> against 1/T. It will be seen that a straight line is obtained of identical slope in the range 40°-70° C. Theoretical justification for such a plot may reside in the fact that f<sub>0</sub> is the stress at which a certain critical rate of flow is reached. At present the plot may be used simply for interpolation purposes.

We may therefore conclude in the first instance that over the range of temperature 40°-70° C.

$$\eta = \eta_0 e^{-11,000/RT} \quad (6)$$

$$f_0 = f_{00} e^{-11,000/RT} \quad (7)$$

<sup>3</sup> Mooney, *Physics*, 1936, 7, 413.

<sup>4</sup> Ferry and Parks, *ibid.*, 1935, 6, 356.

**Theoretical Application of Eyring Theory.**—A preliminary account and discussion of these results has already been published.<sup>5-7</sup> The theory which is probably most relevant to the flow of plastic materials is that due to Eyring.<sup>8, 9</sup> This theory considers flow to involve the passage of flow units, which may be simple molecules or segments of chain molecules, from one position in the material, to a neighbouring position distance  $\lambda$ . If  $U$  be the potential energy barrier to be overcome in the absence of stress and  $f$  the shear stress on the flow unit of area  $\alpha$  (which for simple flow may be taken as the applied shear stress), then the barrier in the direction of stress is  $U - \frac{f\alpha\lambda}{2}$  and opposed to the stress  $U + \frac{f\alpha\lambda}{2}$ .

The rate of flow is then given by,

$$\phi = B \left[ e^{\left( \frac{U - \frac{f\alpha\lambda}{2}}{kT} \right)} - e^{\left( \frac{U + \frac{f\alpha\lambda}{2}}{kT} \right)} \right] \quad (8)$$

For low stresses  $f\alpha\lambda \ll 2kT$ ,  $\phi$  is proportional to  $f$  and Newtonian behaviour is predicted. For high stresses,  $f\alpha\lambda \gg 2kT$ , eqn. (8) predicts

$$\ln \phi = \text{const.} + bf. \quad (9)$$

We have confirmed the application of an equation of the form (9) to our results, but only at moderate stresses below the "second yield-value,"  $f_0$ . Eqn. (3), valid at the higher stresses, is not derivable from eqn. (8). Furthermore, we have confirmed in a general way Eyring's notion that the applied stress decreases the energy barrier to flow. We have no satisfactory values for compression at low stresses, but in Part II we derive a value of  $U = 30$  kcal. for extension at 4.4 kg.cm.<sup>-2</sup>. Increasing the stress to above  $f_0$  has decreased this to 11 kcal., above which stress it remains constant. The departure from Eyring's theory noted above was not predictable in advance, and accordingly considerable caution must be maintained in applying his flow equations to the more complicated behaviour of plastics, e.g. delayed elasticity. Our results would bear out its application at stresses, below  $f_0$ , but an uncertainty arises in connection with the value of  $f_0$ , where this is not experimentally determined, and it will probably depend upon the nature of the flow unit and its cohesive forces. The wider question, as to whether or not the theory is at all applicable to results at high rates of flow cannot be decided. Powell and Eyring<sup>6</sup> have pointed out that the whole stress-flow curve may be reconciled with their theory, if one postulates the operation of two types of flow-process, linked in parallel so that they have the same rate of flow. We have already mentioned some objections to this<sup>7</sup> but we agree that if sufficient assumptions be made about the structure of the plastics, a reconciliation may be possible. There remains, however, the possibility that the place-exchange theory of flow in its present form is restricted to our results at low stresses, or for liquids and solids generally to low rates of flow (since the actual stress required for a definite rate of flow will depend on the potential barrier, a characteristic of the material). At high rates of flow some other mechanism may enter, e.g. the rate of exchange of momentum between parallel layers of molecules may determine the viscosity, as in earlier theories of the viscosities of liquids.<sup>10, 11</sup> It is clearly desirable to test out eqn. (8) over a wide range of stress using

<sup>5</sup> Eley and Pepper, *Nature*, 1944, 154, 52.

<sup>6</sup> Powell and Eyring, *ibid.*, 427.

<sup>7</sup> Eley and Pepper, *ibid.*, 427.

<sup>8</sup> Eyring, *J. Chem. Physics*, 1936, 4, 283.

<sup>9</sup> Eyring and Tobolsky, *The Chemistry of Large Molecules* (Interscience 1943), 125.

<sup>10</sup> van der Waals, *Proc. Acad. Amsterdam*, 1918, 21, 743.

<sup>11</sup> Andrade, *Phil. Mag.*, 1934, 17, 497, 705.

a simple material, for which one may with some certainty assume that only one flow mechanism is involved. The choice of such a material will, however, offer many difficulties.

### Summary.

The rate of plastic flow in compression,  $\phi$ , has been examined over the temperature range 17-70° C., and the stress range 6 to 161 kg.cm.<sup>-2</sup>. At low stresses, i.e. below a certain stress  $f_0$  (which is a function of temperature), the dependence of  $\phi$  upon  $f$  is of the form to be expected from Eyring's theory of flow, viz.,  $\ln \phi = \text{const.} + bf$ , where  $b$  is a constant. At higher stresses,  $f > f_0$ , it is found that  $\phi = A(f - f_0)$  where  $A$  is a constant, independent of stress, and a function of temperature. On certain assumptions a "viscosity coefficient" in poises, may be calculated from  $A$ . This result at high stresses is not easily reconcilable with Eyring's theory. Whether the deficiency lies in the theory of flow, or the model to which the theory is applied, must be left an open question at present.

### Résumé.

La vitesse d'écoulement plastique sous compression,  $\phi$ , a été étudiée dans le domaine de température 17-70° C. et sous des efforts de 6 à 161 kg.cm.<sup>-2</sup>. Pour des efforts faibles,  $f > f_0$  ( $f_0$  est fonction de la température),  $\phi$  dépend de  $f$  de la façon prévue par la théorie de l'écoulement d'Eyring, soit  $\ln \phi = \text{const.} + bf$ , où  $b$  est une constante. Pour des efforts supérieurs,  $f > f_0$ , on trouve que  $\phi = A(f - f_0)$ , où  $A$  est une constante, indépendante de l'effort et une fonction de la température. En faisant certaines hypothèses, on peut calculer, à partir de  $A$ , un "coefficient de viscosité" en poises. Ce résultat, pour les efforts élevés, n'est pas facilement conciliable avec la théorie d'Eyring. Que le défaut se trouve dans la théorie ou dans le modèle auquel elle est appliquée, tel est le débat qui reste ouvert pour l'instant.

### Zusammenfassung.

Die Geschwindigkeit des plastischen Fließens ( $\phi$ ) bei Kompression ist im Temperaturintervall 17-70° C. und für Drucke zwischen 6 und 161 kg.cm.<sup>2</sup> untersucht worden. Bei geringen Drucken, d.h. unterhalb eines bestimmten Drucks  $f_0$  (dessen Wert von der Temperatur abhängt), hat die Beziehung zwischen  $\phi$  und  $f$  die Form, die Eyring's Theorie zufolge zu erwarten ist, nämlich  $\ln \phi = \text{Konstante} + bf$ , wobei  $b$  eine Konstante ist. Bei höheren Drucken ( $f > f_0$ ) wird gefunden, dass  $\phi = A(f - f_0)$ , wo  $A$  eine vom Druck unabhängige aber von der Temperatur abhängende Konstante ist. Unter bestimmten Annahmen kann aus dem Wert von  $A$  ein Viskositätskoeffizient in Poisen berechnet werden. Dieses Resultat bei hohen Drucken ist nicht leicht mit Eyring's Theorie vereinbar. Es muss vorläufig dahingestellt bleiben, ob dies an einem Fehler in der Theorie liegt oder in dem Modell, auf das die Theorie angewendet wird.

## PART II. THE PLASTIC AND ELASTIC EXTENSION OF CORDS AT LOW STRESSES.

In this paper we report results on the extension of cylindrical specimens of cordite at approximately constant stress, over the stress range 2.6-5.2 kg.cm.<sup>-2</sup> and the temperature range 20-78° C. As in Part I we take steps to separate plastic (non-recoverable) flow from elastic (recoverable flow). It has been found possible to present an analysis of elastic behaviour which was not possible in the compression work. The plastic flow results at low stresses in extension are found to be more complex than at high stresses in compression, but to be in agreement with those at low stresses in compression, at least in so far as the effect of stress on flow-rate is concerned. Instrumental difficulties precluded any examination of shear-hardening effects in compression at low stresses, such as we report here for extension. Our objective has been to describe our results in terms of molecular flow-processes, and the probable structure of our material.

### Experimental.

Cords 30 cm. long by 0.7 cm. diameter, were clamped at their upper end, so that they hung vertically down a condenser tube of diameter 1.0 cm., which served as a vapour jacket to thermostat the specimen over a length of 20 cm. Two Indian-ink marks on the cord were observed through a cathetometer so that their separation (originally 12 cm.) could be observed to an accuracy of 0.005 cm. At the lower end of the cord was a brass clamp of weight 70 g. to which at zero time a weight  $W$  could be attached. The first cathetometer reading on the lower mark could be made within 5 sec. of zero time, and by extrapolation a fairly reliable value of the initial rapid extension of the cord obtained, corresponding to a time interval of about 1 sec. from loading. In this fashion the "creep" of cordite was examined from 1 sec. to periods up to 3 weeks, at the lower temperatures, the time of observation being determined by a more or less reproducible "time to rupture" of the cord, itself a function of temperature and stress, to be discussed later.

Observations of length as described above gave the total creep curve. After loading for a certain time the load was removed and in certain cases the recovery of length followed at the temperature of experiment. To secure complete recovery of the cord it was necessary to heat up to 78° c. for 3 hr., giving a final length from which the plastic flow that had occurred could be derived. The efficiency of this treatment was checked by an experiment in which the recovered cord was swollen in acetone vapour, with a negligible further recovery.

In most experiments the cords before extension were given a thermal pretreatment of 3 hr. at 78° c., under the clamp weight only, to secure release of strains from manufacture. Such a treatment is labelled " $p$ " in what follows, and has a "softening effect" on the cord. For this reason it was necessary to hold the cord for a certain time at any lower temperature before it was loaded, to readjust the internal equilibrium of the cord to that characteristic of the temperature of experiment. This readjustment may take days and is discussed later, where experiments immediately following 78° c. pretreatment are distinguished from those in which the cord has been brought to equilibrium before extension.

In securing a plastic flow-time curve the procedure was to stress and relax a single cord alternately four or five times. In each case the above condition for securing equilibrium after heating at 78° c. was observed. Later we shall discuss the basis for this method of analysis, but here merely note that we have established, for the *torsion* of cords, that the plastic flow curve resulting differs by only a small amount from that in which a series of fresh cords are taken and stressed and relaxed, each for a different time of stressing. A similar result has been established, more roughly for extension. The method of analysis will become clearer in the next section.

If  $W$  kg. be the weight used, then the initial stress is  $W + 0.70/0.383$  kg.cm.<sup>-2</sup>, and since the extension is always less than 10 %, this is effectively the tensile stress throughout the experiment. The cords were stored at 15-20° c. and 45-50 % R.H. During the experiment humidity was not controlled, and this factor was probably a minor cause of experimental error, the major cause being variations in the specimens.

### Analysis of an Experiment.

Fig. 1 presents the results of a complete experiment at 4.4 kg.cm.<sup>-2</sup> and 78° c., consisting of two separate extension experiments on two separate cords (both pretreated " $p$ "). Experiment 17 consisted of three alternate extension and recovery experiments  $a$ ,  $b$ ,  $c$  of the type mentioned above. It gives the plastic-flow time curve shown. Experiment 15



consists of a single continuous extension, which to be satisfactory must coincide exactly with experiment 17 over the early part of its course. On relaxation finally it should give a point lying approximately on the plastic flow curve from the interrupted experiment 17. This it usually did to within about  $\pm 20\%$  on the plastic flow observed, and reasons may be advanced for the deviations from an exact agreement when these occurred, due to the different history of temperature and stressing.

We have adopted the following method of analysis into three terms,  $D_e$ ,  $D_1(t)$  and  $D_p(t)$ . Here  $D_e$  is a rapid elastic extension, corresponding to the extrapolation of the total creep curve to zero time;  $D_1(t)$  is a delayed elastic extension, the magnitude of which depends on the time, and  $D_p(t)$  is the plastic, non-recoverable extension. So if the total deformation at time  $t$  is  $D(t)$ , corresponding to a point on the total creep curve, then

$$D(t) = D_e + D_1(t) + D_p(t). \quad (1)$$

There is a certain practical usefulness about this analysis, but it must

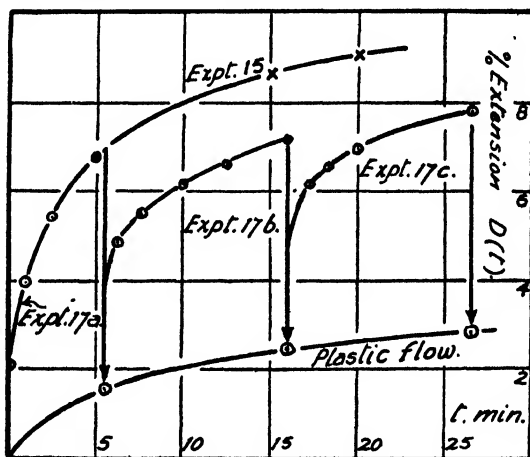


FIG. 1.—To show how two experiments with separate cords are used to analyse the extension into plastic and elastic components. The experiments shown are at  $78^\circ\text{C}$ . to  $4.4\text{ kg.cm.}^{-2}$ .

be emphasised that  $D_e$  cannot be identified with the ordinary elastic deformation  $D_{0E}$  of Alexandrov and Lazurkin.<sup>1</sup> Their analysis of rubber-like bodies identifies  $D_{0E}$  as due to the separation of molecular centres, an instantaneous deformation with a theoretical modulus of  $10^6\text{--}10^8\text{ kg.cm.}^{-2}$ . In their analysis  $D_1(t)$  would be the highly-elastic contribution,  $D_{HE}(t)$ , corresponding to the time-dependent uncoiling of the rubber chains, characterised by a much lower modulus of about  $20\text{ kg.cm.}^{-2}$ , with a total extensibility to break of  $100\text{--}1000\%$ . In our case  $D_e$  corresponds to a time of stressing of about  $1\text{ sec.}$ , and contains  $D_{0E}$  and also a time dependent contribution with a much lower modulus, the latter making the main contribution. Here  $D_1(t)$  may be treated in a similar fashion to the  $D_{HE}(t)$  of Alexandrov and Lazurkin. The moduli, however, are much higher than  $D_{HE}(t)$  for rubbers, and the extensibility much less. This difference may be explained if we attribute to a plasticised nitrocellulose a higher degree of local order and crystallinity than is possessed by a rubber. We may still, however, consider that  $D_1(t)$  arises mainly from the orientation and bending of chains in the locally amorphous regions of the plastic. We may attribute  $D_p(t)$  to the irreversible dis-

<sup>1</sup> Alexandrov and Lazurkin, *Acta Physicochim.*, 1940, 12, 647.

placements of chains, perhaps due to slipping in the regions of local crystallinity or entanglement, which may be regarded as the bonding points of the elastic network. As a further complicating factor we must expect the degree of order of the nitrocellulose plastic to depend upon temperature<sup>2</sup> and extension<sup>3</sup> and adjustments of this order (often re-

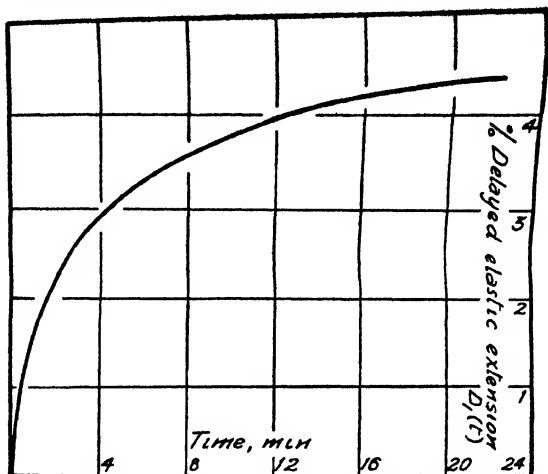


FIG 2—To show the time course at the delayed elastic extension. The experiment shown is at  $78^{\circ}\text{C}$  and  $4.4\text{ kg cm}^{-2}$

ferred to as the crystalline-amorphous ratio) to require time, since such adjustments depend on the 'diffusion' of segments of the long chain molecules. For example after heating to  $78^{\circ}\text{C}$  for 3 hr a subsequent 24 hr at  $38^{\circ}\text{C}$  are required to bring the internal structure of the cord to equilibrium at this temperature as judged by the extension-time curve at a stress of  $4.4\text{ kg cm}^{-2}$

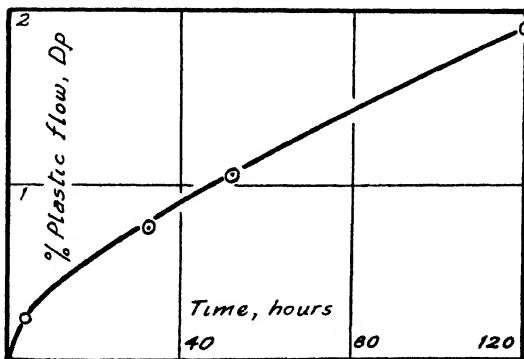


FIG 3—Plastic flow-time curve for an experiment at  $37^{\circ}\text{C}$  and  $4.4\text{ kg cm}^{-2}$

In Fig 2 we show a plot of  $D_1(t)$  against time for the data of Fig 1,  $D_1(t)$  being obtained by subtracting  $D_0 + D_p(t)$  from the total deformation curve  $D(t)$ . It is seen that the delayed elastic extension at first increases rapidly, finally appearing to tend asymptotically to a value  $D_1(\infty)$

<sup>2</sup> Baker, Fuller and Pape *J Amer Chem Soc*, 1942, 64, 776

<sup>3</sup> Hermans, *J. Physic Chem*, 1941, 45, 827

**Plastic Flow.**

Fig. 3 (and also Fig. 1) gives an example of a plastic flow curve, and it is seen that the rate of flow continuously decreases during the course of the experiment. Both time and strain may be supposed to enter as the possible variables determining this hardening effect. It has been found possible to give an equation to the flow curves observed, if in the first instance we assume that strain is the important factor. We start from the Eyring flow equation <sup>4</sup> (see Part I), which gives the rate of flow  $\phi$  as

$$\phi = B \left[ e^{-(U-bf)/RT} - e^{-(U+bf)/RT} \right] = 2B e^{-U/RT} \sinh \frac{bf}{RT} \quad (2)$$

Here  $B$  and  $b$  are constants, ( $b = \alpha\lambda/2$  in Part I),  $f$  the stress on the flow unit, taken as the applied stress in accordance with our method and  $U$  the height of the barrier. For the case  $bf \gg RT$

$$\phi = Be^{-(U-bf)/RT} \quad (3)$$

We now make the additional assumption that the barrier height  $U$  is a linear function of plastic strain  $U = U_0 + \gamma D_p$ ,  $\gamma$  being the constant of proportionality.

$$\frac{\partial D_p}{\partial t} = \phi = Be^{-(U_0-bf+\gamma D_p)/RT} = ke^{-\beta D_p} \quad (4)$$

This equation gives the plastic flow as a function of time, at constant stress and temperature ( $\beta = \gamma/RT$ ). It integrates to

$$D_p = \frac{1}{\beta} \ln (\beta kt + 1) \quad (5)$$

i.e. 
$$D_p = \frac{1}{\beta} \ln t + \text{const.}, \text{ for long times.} \quad (5a)$$

Equations (4) and (5) give a reasonable account of most of our data. Values of  $\beta$  may be derived either from the initial part of the flow, using equation (4), i.e. a plot of  $\ln \phi$  against  $D_p$ , or from the final part of the flow, using equation (5a). Values of  $\beta$ , referred to  $D_p$  as percentage elongation, together with derived values of  $\gamma$ , expressed as cal./per cent. plastic elongation, are listed in Table I. No marked effect of stress or temperature upon

TABLE I.

$T^\circ \text{C.}$	$f$ , kg.cm. <sup>-2</sup>	$\beta$ (eqn. 4).	$\gamma$ (eqn. 4).	$\beta$ (eqn. 5).	$\gamma$ (eqn. 5).
38	4.4	0.74	460	1.1	590
56	4.4	0.53-0.92	330-590	0.96	620
61	4.4	0.74	490	0.92	610
78	4.4	1.24	870	1.29	900
78	3.7	0.7-1.26	490-880	1.25	870
78	2.6	1.26	880	1.29	900

$\gamma$  is apparent in these results, the variation being within the experimental error.

In our opinion the main deficiency in this treatment is that it does not consider time as an additional independent variable determining the hardening effect. The molecular basis for the hardening effect is probably that elongation of the cord induces further crystallisation of segments of the long chains, so effectively increasing the resistance to flow. Such

<sup>4</sup> Tobolsky, Powell and Eyring, *Chemistry of Large Molecules* (Interscience, 1943), 125.

effects are well known in rubber-like materials, and have also been demonstrated by X-ray diffraction for cellulose derivatives.<sup>5</sup> If then the plastic

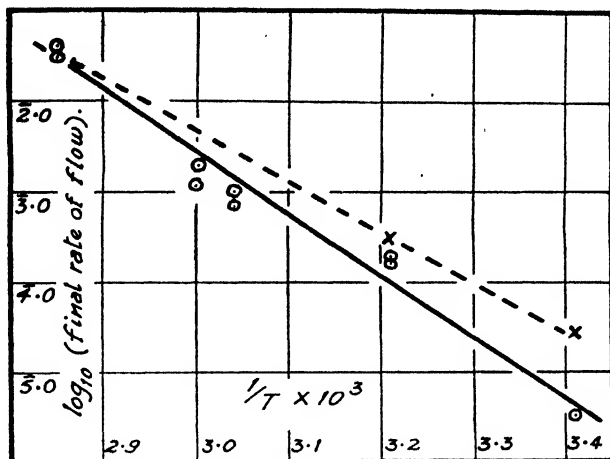


FIG. 4(a).—Effect of temperature on the final rate of plastic flow at a stress of  $4.4 \text{ kg./cm.}^2$ . The circles refer to cords at internal equilibrium at the temperature of experiment. The crosses refer to cords stretched within a short time of a thermal pretreatment at  $78^\circ \text{C}$ .

be subjected to a certain strain, it is reasonable to expect that some time must elapse before the new crystallites are fully developed. In Part III we note some evidence for the specific effects of time on the plastic flow curve.

According to experiment, and to the theory above, no true steady state of flow is ever set up. Therefore, in evaluating the effects of stress or temperature, we should strictly consider either the initial plastic flow, or the flow at some definite strain. However, in practice, since the effect of  $\gamma$  is small compared with the effects of either stress or temperature, it suffices to take the final rate of flow, taken as the tangent to the flow-curve, which may refer to any strain in the range 2 to 5 %, dependent on conditions of stress and temperature. This has been done, the results being shown in Fig. 4a and 4b. The results are qualitatively in accordance with eqn. (3),  $\log_{10} \dot{\phi}$  varying linearly with  $1/T$  at constant  $f$ , and  $f$  at constant  $T$ . The value of the activation energy  $U$  calculated from Fig. 4a is  $30 \pm 10 \text{ kcal. mol.}^{-1}$ .

Referring to Fig. 4a it will be seen that the plastic flow at  $20^\circ \text{C}$ . and  $4.4 \text{ kg./cm.}^2$  is ten times as fast if the specimen be stretched directly after

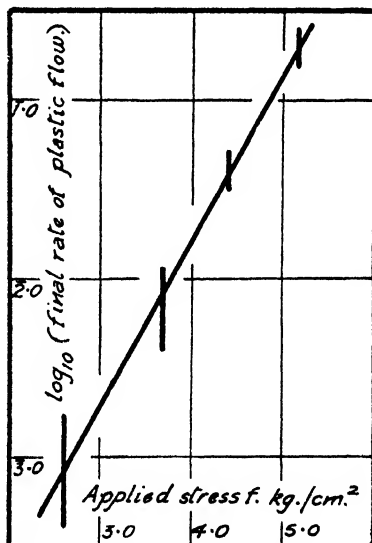


FIG. 4(b).—Effect of applied stress  $f$  upon the final rate of plastic flow at  $78^\circ \text{C}$ .

<sup>5</sup> Baker, *Ind. Eng. Chem.*, 1945, 37, 246.

heating to 78° c. for 3 hr., than if stretched without thermal pretreatment. Such behaviour may be attributed to the "melting" of nitrocellulose chain contacts, which require time to become re-established, and fits in with the X-ray observations of Baker, Fuller and Pape.\*

### Rapid Elastic Extension.

The value of  $D_0$ , obtained by extrapolation from values at 10, 30 and 60 sec., may be considered to correspond roughly to a time of stressing of 1 sec. The following data all support the notion that this deformation is largely made up of relaxation elastic effects, and is not a simple time-independent separation of molecular centres. If we make the usual

TABLE II.  
 $f = 4.4 \text{ kg.cm.}^{-2}$ .

Temp. °c.	Expt.	Value of $E_0$ , kg.cm. <sup>-2</sup> .
20	26	2600
38	L14, L13, L16, 34, 36	910, 1010, 1090, 810, 890
56	37, 38, 41	440, 470, 490
61	L18, L19	400, 430
78	17, L10, L2	210, 230, 210

hypotheses that such a relaxation elasticity is due to orientation of segments of chains in the amorphous regions, and that these regions are increased by increase of temperature, then all the results below may be systematised.

Firstly, thermal pretreatment ( $p$ ) is found markedly to lower  $E_0$ , particularly at 20° c., where the rate of recrystallisation after heating is very slow. For example,  $E_0 > 2600$  \* before heating to 78° c., and 1060 after heating (Expt. 26,  $f = 4.4 \text{ kg.cm.}^2$ ,  $T = 20^\circ \text{ c.}$ ). Secondly, considering the extension of cords at internal equilibrium at the temperature of experiment, and at a constant stress, we find a most marked decrease

TABLE III

Temp. °C.  <i>f</i>	Values of $E_0$ , kg.cm. <sup>-2</sup> at Values of Stress.					
	2.6.	3.7.	4.4.	5.2.	6.5.	13.1.
61	—	—	400	350	280	200?
78	280	250	210	210	—	—

of  $E_0$  with increase of temperature. This decrease may arise both from an increase in the amount of amorphous material, due to a "melting" of chain contacts, and also from an increased rate of orientation of segments. The latter suggestion would mean that a contribution appearing in the delayed elasticity  $D_1$  at low temperatures, would become sufficiently rapid to appear in  $D_0$  at higher temperatures. The constancy of  $E_1(\infty)$ , discussed later, with temperature suggests on the simplest view that this effect is small, and therefore that the main effect of temperature on  $E_0$  is due to an increased equilibrium percentage of amorphous chains, rather than a rate effect.

The experimental results in Table III indicate that  $E_0$  tends to decrease with increasing applied stress  $f$ , but the results are not sufficiently

\* Young's modulus  $E_0 = f/D_0$  is given in kg.cm.<sup>-2</sup>.

reproducible to establish the dependence of  $E_s$  on  $f$  accurately. If  $E_s$  contains time-dependent displacements of chains involving a relaxation mechanism, then eqn. (3) leads us to expect the rate of such displacements to be very sensitive to stress; in fact a kind of yield-value may be associated with each kind of segment. Higher stresses may then cause the orientation of longer segments to contribute to  $E_s$ , which may then be considered as only an apparent modulus.

### Delayed Elastic Extension.

**The Modulus.**—The curve for the delayed elastic extension obtained by the previous method of analysis, tends to an asymptotic value, and from this value a Young's modulus,  $E_1(\infty) = f/D_1(\infty)$ , may be calculated. Within a rather large experimental error, this is found to be constant ( $E_1(\infty) = 120 \pm 30 \text{ kg.cm.}^{-2}$ ), independent of thermal pretreatment, temperature of experiment and applied stress, as Table IV shows.

We should hesitate to extrapolate this result to much higher stresses, since here  $E_1(\infty)$  might decrease if further elastic mechanisms come into play. The exponential dependence of rate of place-exchange on stress, as typified in equation (3) may well introduce what is effectively a yield value for the orientation of longer segments (i.e. those involving a higher value of the potential barrier  $U$ ), as noted for  $E_s$ .

TABLE IV.

T° c. of expt.	Pretreatment.	Stress kg.cm. <sup>-2</sup> .	$E_1(\infty)$ , kg.cm. <sup>-2</sup> .
21	$p$	4.4	170?
38	$p$	4.4	114
38	No $p$	4.4	100
38	$p$ , then 20 hr. at 38° c	4.4	111
50	$p$	4.4	203
56	$p$ , then 15 hr. 56° c.	4.4	147
61	$p$	5.2	104
61	$p$	4.4	103
61	$p$	2.6	108
78	$p$	4.4	94
78	$p$	3.7	103
78	$p$	2.6	124

### The Time-Course of the Elastic Creep Curve.

Unlike the modulus  $E_1(\infty)$ , the time course of the elastic extension is markedly influenced by temperature of experiment, and is also influenced by thermal pretreatment, and applied stress. While some qualitative understanding of these results may be obtained, no quantitatively satis-

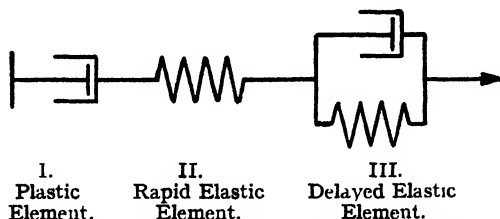


FIG. 5.—A conventional mechanical model, which illustrates the method of analysis used. The applied stress  $f$  falls on all three elements.

factory treatment, based on a molecular model, can be given at present. Our analysis is based on the assumption that the total applied stress falls on plastic, rapid elastic and delayed elastic elements, and this assumption is most briefly illustrated in the mechanical model of Fig. 5, in which component III is relevant to the present discussion.

This type of model for delayed elastic extension has been often considered. The differential equation for component III, in the case of a Hookian spring of modulus  $E_1(\infty)$ , and a Newtonian dashpot of viscosity  $\eta$ ,

$$\text{is} \quad f = E_1(\infty) \cdot D_t + \eta \partial D_1(t) / \partial t \quad . \quad . \quad . \quad (6a)$$

$$\text{i.e.} \quad -dx/dt = \frac{E_1(\infty)}{\eta} \cdot t \quad . \quad . \quad . \quad (6b)$$

$$\text{and its solution is} \quad x = x_0 e^{\frac{E_1(\infty)}{\eta} \cdot t} \quad . \quad . \quad . \quad (7)$$

where

$$x = D_1(\infty) - D_1(t)$$

$$x_0 = D_1(\infty) = f/E_1(\infty).$$

Alternatively, the same equation may be derived if we assume the increase in length obeys a first order equation. In this case the rate constant  $k$  is equivalent to  $E_1(\infty)/\eta$ .<sup>1, 6</sup> Our results all show the characteristic deviation from this equation (7), exemplified by the plot of  $\log_{10} x$  against  $t$  shown in Fig. 6. Taylor has observed a similar kind of deviation

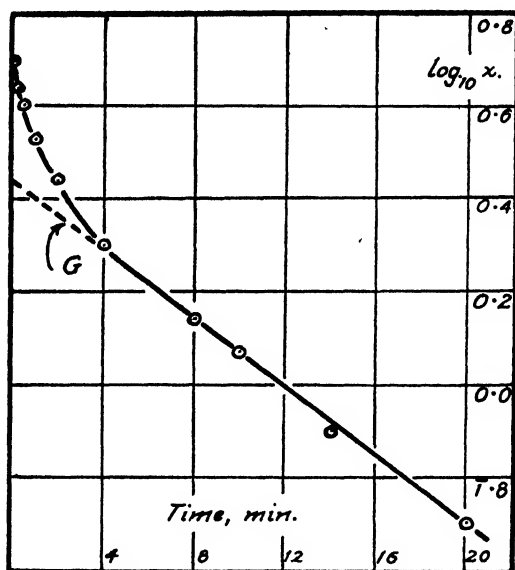


FIG. 6.—The course of the delayed elastic extension with time at 78° and

$$x = D_1(\infty) - D_1(t) \quad \text{in } \% \text{ extension of the cord.}$$

for potash-silica glasses, and Robinson, Ruggy and Slantz<sup>7</sup> for polymethyl methacrylate. These authors have fitted their results by the sum of two or three exponential terms, and this procedure will also describe our own results. There is, however, a certain arbitrariness in the method. While two terms suffice to describe the results above 56° c., at lower temperatures the need for three terms becomes apparent.

Another approach is that due to Tobolski and Eyring,<sup>8</sup> and they effectively substitute their relaxation equation (2) in place of the Newtonian

<sup>1</sup> Taylor, *J. Physic. Chem.*, 1943, 47, 235.

<sup>7</sup> Robinson, Ruggy and Slantz, *J. Appl. Physics*, 1944, 15, 343.

<sup>8</sup> Tobolsky and Eyring, *J. Chem. Physics*, 1943, 11, 126.

expression in equation (6) obtaining a new differential equation

$$f = E_1(\infty) \cdot D + \frac{1}{b} \sinh^{-1} \frac{1}{a} \frac{\partial D}{\partial t} \quad (8)$$

where  $\frac{\partial D}{\partial t} = a \sinh bf$ , defines  $a$  and  $b$ . Full details may be found in the references quoted.<sup>1</sup>

This integrates to

$$\tanh \frac{bE_1(\infty)}{2} \cdot x = \tanh \frac{bE_1(\infty)x_0}{2} \cdot e^{-abE_1(\infty)t} \quad (9)$$

This equation is found to give a good account of the time-course of our individual experiments, but since  $b$  and  $a$  are found to be functions of the applied stress  $f$  ( $b$  decreasing and  $a$  increasing as  $f$  increases, a result also noted by the original authors), it has been concluded that such an elaborate analysis is scarcely justified in our case.

None of the above equations takes into account the possibility of an increased resistance to elastic deformation with increased extension, as the average degree of crystallinity increases following increased orientation of chains. The general X-ray evidence for this effect in cellulosic materials is supported in our particular case by the shear-hardening nature of the plastic-flow. If we assume, as in equation (4) that the slow process in the elastic extension possesses an activation energy that is a linear function of percentage extension,  $U = U_0 + \gamma D_1$ , then equations (6) and (7) are replaced by

$$-\frac{dx}{dt} = k \cdot x = xBe^{\frac{-(U_0 + \gamma D_1)}{RT}} = xZe^{\frac{\gamma x}{RT}} \quad (10)$$

where

$$Z = Be^{\frac{-(U_0 + \gamma D_1(\infty))}{RT}} \quad (11)$$

The integral of (10) is

$$\ln x - \frac{\gamma}{RT} \cdot x = -Zt + \text{const.}, \text{ for } \gamma x \ll RT \quad (12)$$

The particular mechanism postulated as leading to (12), since it involves a "freezing" of the material on extension, will lead to a rate of recovery on unloading which is relatively small. There is evidence in some cases only that this is so, and the data are discussed later in the light of Boltzmann's superposition principle, the logical framework for such

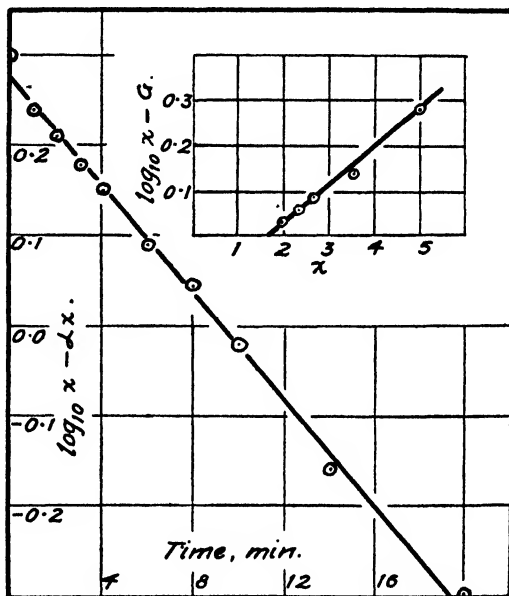


FIG. 7.—To show the course at the delayed elasticity against time. The inset is the plot from which the constant  $\alpha$  is derived. The experiment shown is at 78° c. and 4.4 kg.cm.<sup>2</sup>



considerations. It can, however, be shown that equation (12) will also arise on the basis of a certain non-Newtonian behaviour of the dashpot,

viz. if in equation (6b) we employ the equation  $\eta = \eta_0 e^{\frac{U_0 - \gamma f_s}{RT}}$  where  $f_s = E_1(\infty)\alpha$  is the internal stress on the dashpot.\* In this case the recovery curve should agree with the extension curve, according to the dictates of the

superposition principle. Since it has not been found possible completely to disentangle the two possibilities, the question is left open as to what extent each mechanism leads to the postulated increase of activation energy for elastic flow with strain.

Equation (12) is found to give a good account of the time course of our individual experiments,

Temp. °C.	$f$ , kg.cm. <sup>-2</sup>	$\gamma$ , % Extension.	$Z$ , min. <sup>-1</sup>
38	4.4	160	$6.4 \times 10^{-4}$
56	4.4	230	$3.4 \times 10^{-3}$
61	4.4	260	$3.0 \times 10^{-3}$
78	4.4	130	$7.1 \times 10^{-3}$
78	3.7	180	$1.7 \times 10^{-2}$
78	2.6	300	$1.0 \times 10^{-2}$

an example being shown in Fig. 7. The value for the constant  $\alpha = 0.435\gamma/RT$  is obtained from the inset plot of  $\log_{10} \alpha - G$  against  $\alpha$ . Here  $G$  is the value, at a given time, of the line  $(-0.435Zt + \text{const.})$ , and is indicated by a dotted line in Fig. 6.

In Table V values of  $Z$  (the rate constant of extension at the end of the experiment) and  $\gamma$  are given for a series of experiments, all on cords brought to internal equilibrium at the temperature of experiment. There appears to be a variation of  $\gamma$  with stress and this is clearly a deficiency of the simple formulation. The temperature variation of the "rate constant"  $Z$  corresponds to  $U_0 \sim 26$  kcal.† A similar result is given by the temperature variation of the rate constants in the other formulations referred to previously. Also,  $Z$  is found to be a function of stress. The effect of this is perhaps best shown in the delayed extension curves of Fig. 8, where the fraction of the total extension is plotted as a function of time. In this way all the curves tend to the same asymptotic value, and the accelerating influence of increased stress is clearly seen. This result has been confirmed in torsion. It is an important one for the theory of visco-elasticity, since no formulation so far advanced can account for it. (The effect of stress on  $Z$  is equivalent to its effect on the analogous constant  $a$  in the Eyring-Tobolski theory already noted.)

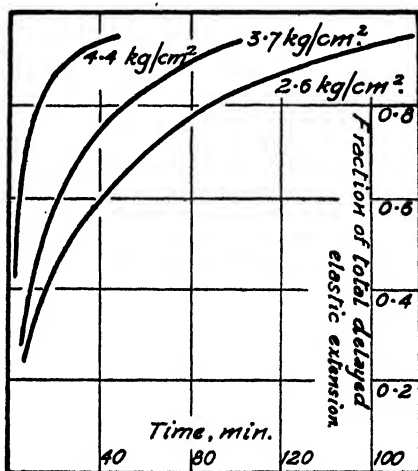


FIG. 8.—To show the effect of stress upon the rate of development of delayed elasticity.

\* This is to be regarded as only an approximate empirical formulation of non-Newtonian flow.

† Strictly this gives  $U_0 + \gamma D_1(\infty)$ .

The values of  $\gamma$  here listed are only about 25 % those previously given for the plastic flow. If, however, in each case the increase in activation energy is referred to the *total* (i.e. elastic plus plastic) extension, then the discrepancy becomes much less. In this case, however, the integral equations (5) and (12) cannot be derived, and values of  $\gamma$  must be obtained from the original differential equations.

### Effect of Thermal Pretreatment.

If a cord be heated to 78° C. for 3 hr., then brought to 21° C. or 38° C. and extended, the elastic flow (as the plastic flow), is found to be much greater than for cords brought to internal equilibrium. At 56° C. and above the difference is hardly noticeable, presumably since the adjustment of internal equilibrium is an activated process accelerated by temperature rise, and at these temperatures the readjustments from the 78° C. equilibrium occurs rapidly. The magnitude of the effect at 21° C. is shown in Fig. 9. In this case it might be thought that the pretreatment increases the modulus  $E_1(\infty)$ , but this is probably not so. By experimenting at 38° C. it is possible to achieve in both cases (pretreated cords and those at internal equilibrium), the full development of elastic extension, and to obtain values of the modulus  $E_1(\infty)$ , the rate  $Z$ , and the hardening constant  $\gamma$ . The results in Table VI show that the main effect of the thermal pretreatment on the delayed elastic extension  $D_1$  is to cause an acceleration of the rate  $Z$  at which the equilibrium is reached, and not seriously to alter the modulus.

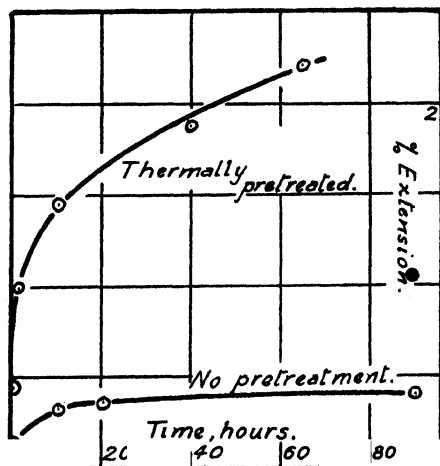


FIG. 9.—To show the large effect of thermal pretreatment (78°, 3 hr.) on the extension of cords at 21° C. and 4.4 kg.cm.<sup>-2</sup>

TABLE VI.—EFFECT OF THERMAL PRETREATMENT ON DELAYED ELASTIC EXTENSION AT 38° C., AND 4.44 kg.cm.<sup>-2</sup> APPLIED STRESS.

Expt.	Pretreatment.	$E_1(\infty)$ kg.cm. <sup>-2</sup>	$\gamma$ cal./% ext.	$Z$ , min. <sup>-1</sup>
19	(p)	114	170	$4.6 \times 10^{-3}$
34, 36	(p), 20 hr. at 38° C.	111	160	$6.4 \times 10^{-4}$
13, 14	None	109	140	$6.2 \times 10^{-4}$

### The Elastic Recovery Curve.

For a material obeying the Boltzmann superposition principle (B.S.P.) the total elastic extension at any time is given by the sum of the extensions due to the separate loading effects. In applying this principle to recovery on unloading, the cord is treated as though it is continuously loaded throughout the whole experiment, but that at the actual time of unloading, an equal and opposite stress is applied. The summation of the effects

of these equal and opposite stresses then gives the observed recovery curve. Reference should be made to Leaderman,<sup>9</sup> for a full discussion of this type of analysis. In Fig. 10 we show a case where the B.S.P. describes our results within the experimental error. In another case we find a slower recovery than that predicted by the principle, which we have taken to mean that a "freezing" of the plastic occurs on extension, the chains in the amorphous sections showing increased crystallisation as they are orientated in the direction of strain. Qualitatively, this kind of behaviour probably underlies the need for thermo-recovery after extension at temperatures of 61° C. or lower, i.e. the need to heat the cord to 78° C. before complete retraction after unloading is obtained. We have not secured a complete analysis of these complex recovery effects. Loading for short times, or at high temperatures, seems to favour the B.S.P. type of recovery, independent of the extension reached (in Fig. 10

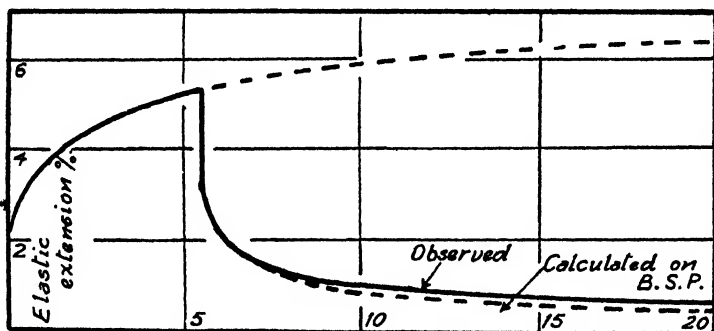


FIG. 10.—To show a case where the observed recovery approximates to that calculated assuming the Boltzmann Superposition Principle. The experiment constant shown is at 78° and 4.4 kg.cm.<sup>2</sup>

the value of 5 % elastic extension is as high as occurs in most experiments). In torsion, under such conditions, recovery may even be faster than predicted by the B.S.P. On the other hand loading for long times seems to favour the reduced rate of recovery. Our preliminary conclusion is that the freezing effects that we postulate as occurring on extension, must require time to be established, i.e. be associated with a definite rate-process. So in spite of the partial success of equation (12) its theoretical basis (i.e. that the increase of activation energy for extension is a function only of extension), is clearly oversimplified. According to the simple theory given, recovery after extension cannot fit the B.S.P. If, however, equation (12) arises on the basis of a non-Newtonian flow mechanism, as we have indicated it might, then recovery would be expected to fit the B.S.P. We can only conclude, then, that both effects are entering into the elastic extension in a way impossible to analyse at present. The usefulness of equation (12) in describing the extension probably arises in that it may, to a first approximation, describe both effects working simultaneously.

### Rupture of Cords under Load.

A cord, loaded with 4.4 kg.cm.<sup>-2</sup>, was found to break after a fairly reproducible time, and this time was markedly influenced by the temperature of experiment, suggesting that breaking of the cord was the result of some activated process. In Fig. 11 we plot the  $\log_{10}$  (breaking time) against the reciprocal of the absolute temperature. A reasonable

<sup>9</sup> Leaderman, *Creep of Filamentous Materials* (Textile Foundation, Washington, U.S.A., 1943).

straight line is obtained corresponding to an activation energy of 37 kcal. For comparison, the dotted line represents a plot of  $\log_{10}$  (reciprocal of final plastic flow rate), for  $f = 4.4 \text{ kg.cm.}^{-2}$ , taken from the line in Fig. 4b. This line corresponds to an activation energy of 30 kcal., but a rather large experimental error is attached to this result, as may be seen by referring to Fig. 4b. Accordingly, within this error, the activation energies for flow and rupture may be considered to be the same, and to involve in each case a similar process of slipping of the nitrocellulose chains. The breaking time was found also to be very sensitive to stress, and probably

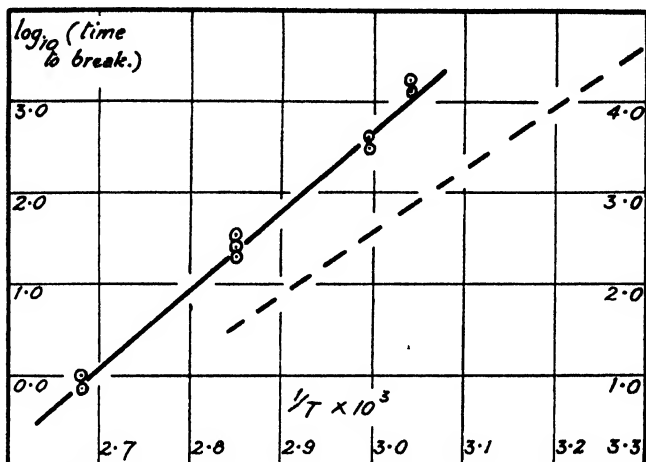


FIG. 11.—Effect of temperature on time to break at an applied stress of  $4.4 \text{ kg.cm.}^{-2}$ . For comparison, the dotted line represents the reciprocal of the final rate of plastic flow plotted in the same way (taken from data of Fig. 4).

depends exponentially on this variable, as does the plastic flow. An activated process of chain-slipping leading to rupture has already been suggested for textile materials by Busse and co-workers.<sup>10</sup>

Some time before actual rupture, numerous blemishes appear on the surface of the cord, suggestive of the formation of internal fissures. These may be expected to arise when internal slipping of chains results in a number of chain heads coming together, a process which will accelerate as an increased internal stress falls on chains neighbouring the region of discontinuity. Eventually breakage occurs, without "necking" of the cord, at one of these blemishes, which may be anywhere in the specimen, and not necessarily near the clamps at either end.

### Discussion.

A general review of the results presented suggests that, over the range of stress and temperature concerned, the activated processes of plastic flow, elastic flow, and rupture possess similar activation energies of about 30 kcal., within an error of  $\pm 10$  kcal., and therefore that they probably involve a similar molecular process. We had previously suggested (on structural grounds) that the plastic flow might be expected to involve slippage at locking points of the network, e.g. "crystallites" of nitrocellulose and points where two chains are entangled, and that elasticity resulted from the orientation and stretching of segments of chains in the locally amorphous regions of the plastic. This distinction may still be

<sup>10</sup> Busse, Lessig, Loughborough and Lavrick, *J. Appl. Physics*, 1942, 13, 715.

real, and the potential barriers be closely similar in the two cases, as found experimentally. An alternative view, however, is that in plastic flow, as in elasticity, the flow process is determined by the motion of chains in the amorphous regions, which in the case of highly plasticised material, may be expected to make up the bulk of the structure. The activation energy observed is too high to be accounted for by the Newtonian flow of plasticiser (nitroglycerine) in the structure.

In an earlier paper dealing with rubber-like materials<sup>11</sup> a distinction was drawn between the flow processes of plastic flow and elasticity, the latter being considered to possess a much higher activation energy. It may well be, however, that when the two processes are compared for the same material, over the same temperature and stress range (as they are here), they will be found to possess similar activation energies. At low temperatures, where elastic flow is most easily measurable since plastic flow is small, a high activation energy may be expected, because of the need for activating the internal rotational degrees of freedom of the chains. On the other hand the plastic flow is usually observed at much higher temperatures, where the internal rotations are all completely excited, and so the activation energy is smaller, since it does not contain a contribution for this factor. On this view, similar flow behaviour underlie both plastic and elastic flow, the difference being attributable, mainly to whether or not the chain segment remains attached to the main network of the plastic. Where the internal rotations of the chains are fully excited we may expect entanglements to be easily released and plastic flow to be the dominant effect.

The Eyring relaxation theory of flow-mechanisms, when modified to take account of shear-hardening effects, gives a broad outline of the behaviour of the plastic, as a function of temperature and stress in the range covered. The main deficiency in our work has been its failure to account for the effect of stress upon the rate of elastic extension. This may be associated with the presence of a whole band of relaxation mechanisms (e.g. associated with the orientation of segments of a whole range of sizes), each with a rate of flow depending exponentially on the internal stress on the mechanism. It is natural to assume such distributions of relaxation-times, and their presence is established for the dielectric behaviour of long chain materials.<sup>12, 13</sup> It would seem, however, premature to introduce such complications into the mathematical treatment at the present stage.

In Part I it has been shown that at high stresses in compression, the rate of plastic flow follows a simple linear stress law, rather than the exponential law found in extension (and compression) at lower stresses. It therefore scarcely seems likely that the results obtained here for elastic flow rates and moduli, can be extrapolated to the behaviour of cordite at high stresses.

### Summary.

A study of the extension of cordite in the stress range 2.6 to 5.2 kg.cm.<sup>-2</sup> and temperature range 20 to 78° C. has demonstrated the following effects.

1. The total extension may be expressed as the sum of rapid elastic, delayed elastic, and plastic components to a reasonable approximation.
2. There is a marked thermal hysteresis effect. It is some time before a cord reaches a true internal (crystalline-amorphous) equilibrium, after lowering the temperature.
3. The value of the Young's modulus for the rapid elastic component, together with effects of thermal pretreatment and temperature of experiment thereon, show that this component probably involves orientation of short chain segments of nitrocellulose.

<sup>11</sup> Eley, *Trans. Faraday Soc.*, 1942, **38**, 299.

<sup>12</sup> Wagner, *Archiv. Elektrotech.*, 1914, **3**, 67.

<sup>13</sup> Kirkwood and Fuoss, *J. Chem. Physics*, 1941, **9**, 329.

4. The delayed elastic modulus involves orientation of chain segments. The modulus of  $120 \text{ kg.cm.}^{-1}$  is little influenced by stress, temperature and thermal pretreatment, but the rate of development of the elastic extension is markedly influenced by these factors, and particularly by strain. An equation is given which takes a satisfactory account of the strain-hardening factor.

5. The plastic flow is markedly influenced by temperature, stress, and strain. The Eyring theory gives an account of the effect of stress, and the strain-hardening factor is satisfactorily accounted for in the same way as for the delayed elasticity.

6. We may conclude that both delayed elasticity and plastic flow are activated processes. The rupture of cords is also shown to involve an activated process. In all three cases the activation energy lies in the range  $30 \pm 10 \text{ kcal.}$  at a stress of  $4.4 \text{ kg.cm.}^{-1}$ ; a similar rate process is therefore probably involved in all cases.

### Résumé.

L'allongement de la cordite, étudié sous des tractions de  $2.6$  à  $5.2 \text{ kg.cm.}^{-1}$  et à des températures variant de  $20$  à  $70^\circ \text{C.}$  a montré que :

(1) l'allongement total est la somme des composantes élastique rapide, élastique retardée et plastique, avec une assez bonne approximation.

(2) il y a un notable effet d'hystérésis thermique.

(3) la composante élastique rapide comporte probablement une orientation de segments courts de chaînes de nitrocellulose.

(4) le module élastique retardé comporte lui aussi une orientation de segments de chaînes.

(5) la théorie d'Eyring rend compte, de façon satisfaisante, des effets de traction sur l'écoulement plastique.

(6) l'élasticité retardée et l'écoulement plastique sont tous deux des processus activés.

### Zusammenfassung.

Messungen der Ausdehnung von Cordit unter Zugkräften im Bereich  $2.6$ - $5.2 \text{ kg.cm.}^{-1}$  und zwischen  $20^\circ$  und  $78^\circ \text{C.}$  haben zu folgenden Ergebnissen geführt.

(1) Es ist eine ziemlich gute Näherung zu sagen, dass die totale Ausdehnung die Summe der raschen elastischen, verzögerten elastischen und plastischen Kontributionen ist.

(2) Es besteht ein ausgeprägter Hystereseeffekt.

(3) Die rasche elastische Kontribution ist wahrscheinlich mit der Orientierung der kurzen Kettensegmente der Nitrozellulose verbunden.

(4) Der verzögerte elastische Modulus ist mit der Orientierung der Kettensegmente verbunden.

(5) Eyring's Theorie stellt die Vorgänge in befriedigender Weise dar.

(6) Sowohl die verzögerte Elastizität als auch das plastische Fließen sind aktivierte Vorgänge.

## PART III. THE PLASTIC AND ELASTIC TORSION OF CORDS AT LOW STRESSES.

In this paper we present results on the torsion of cords, and compare the behaviour observed with the results of Part II of this series. In particular we have been concerned to extend our results on the effect of applied stress on the development of delayed elastic deformation.

### Experimental.

The cord,  $20 \text{ cm.}$  long by  $0.7 \text{ cm.}$  diameter was held vertically, by bakelite clamps at the top and bottom of the cord. A glass vapour jacket, fitting over the whole length of cordite and clamps, served to thermostat the cords, the temperature being determined by thermocouple junctions touching the cordite surface. The lower clamp was fixed to a drum, graduated in degrees, supported in a bearing of small

friction. The torsional stress was applied by two weights attached to strings, which passed over pulleys and were attached to the periphery of the drum. The torsional strain was observed on the graduated scale. In an experiment the upper end of the cordite was clamped and at zero time the lower drum, loaded as described, was released, and readings of the torsional strain taken against time. This simple arrangement was very satisfactory for our purpose, and an ink line ruled down the length of the specimen showed that the strain was uniform over the whole cord.

The shearing stress in the cord varies from zero in the axis to a maximum value at the surface, given by  $16M/\pi d^3$ , where  $M$  is the applied couple and  $d$  the diameter of the cord. The corresponding shear is equal to  $\phi \cdot d/2l$  where  $\phi$  is the angle of twist in radians between the ends of the cord of length  $l$ . The shear modulus is given by

$$G = \frac{32Ml}{\pi d^4 \phi} = 2.43 \times 10^8 \cdot \frac{Ml}{\theta},$$

where  $\theta$  = angle of twist in degrees, and  $d = 0.7$  cm. The deformation at any time is proportional to  $\theta/l$  and may conveniently be expressed as  $1/G$ , the shear per unit stress. The non-recoverable flow may be used to calculate a "viscosity coefficient"  $\eta$ . If  $\theta$  in this case refers to the non-recoverable twist

$$\eta = 2.43 \times 10^8 Ml / \left( \frac{d\theta}{dt} \right).$$

The couple  $M$  was applied by two weights, each of value  $W/2$  g., attached to the lower drum of radius 4.7 cm., and so  $M = 4.7 \times 10^{-3} W$  kg.cm.

### Results.

The general behaviour in torsion was similar to that observed in extension. When a couple was applied to the free end of the rod, an initial rapid twist was observed (complete in 1 sec.), followed by a slower

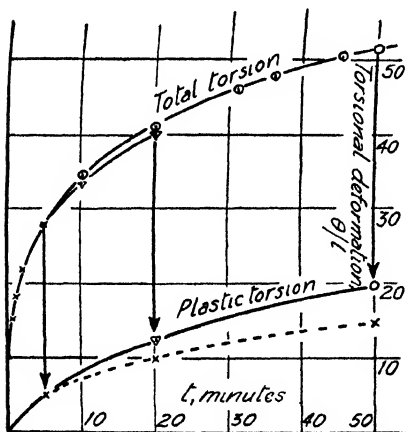


FIG. 1—The total and plastic torsional deformation at  $74^\circ \text{C}$  and  $2.8 \text{ kg cm}^{-2}$ . The dotted curve shows the plastic torsion in a specimen alternately stressed and recovered.

deformation, the rate of which continuously decreased with time. At the lower temperatures the deformations were entirely recoverable, but at high temperatures and stresses a permanent set was observed. As in Part II, the permanent set is defined as the deformation not recoverable after heating the unloaded cord for three hours at  $78^\circ \text{C}$ . The method of analysis of the results into plastic flow, rapid elastic and delayed elastic deformation is the same as that used in Part II. Again, as temperature and applied stress were increased the time to fracture of the cord was markedly diminished, and the data that could be obtained were limited by this effect.

**Plastic Flow.**—This was too small to be observed at room temperature, with stresses up to

$15 \text{ kg.cm}^{-2}$ . Detailed experiments were made at  $74^\circ \text{C}$ ., both by the usual method of repeatedly twisting and relaxing one cord, and also by a new method in which different cords were twisted for different lengths

of time and then relaxed, to give a permanent set-time curve. The strain-hardening effect noted in extension is also present in torsion, i.e. the rate of plastic flow decreases with time (or amount of shear). Fig. 1 shows plastic flow-time curves for 74° C. and a maximum stress of 2.8 kg.cm.<sup>-2</sup>. It can be seen that the rate of flow measured by repeated twisting of a single cord (*T*. 28), falls off more rapidly than when measured by stressing different cords (*T*. 28, 29, 30). This difference was shown to be due to the fact that the repeatedly twisted cord *T*. 28 was maintained at 74° C. for a longer period of time than the other cords (viz. the difference in time required for recovery between periods of stressing).

The behaviour may be described by the equations used in extension (cf. Part II, equation (4)).

$$\ln\left(\frac{\partial D_p}{\partial t}\right) = \ln\left(\frac{\partial D_p}{\partial t}\right)_{\text{initial}} - \frac{\gamma}{RT} \cdot D_p$$

where  $D_p$  is the plastic torsion at time  $t$ .

If we express  $D_p$  in terms of  $\theta/l$  we derive values of  $\gamma$  which are not comparable with those in extension. Such a comparison is indeed difficult, since in torsion the shear varies from a maximum value at the surface of the cord to zero at the middle, and an average shear is difficult to define. We show below a calculated value of  $\gamma$ , expressing  $D_p$  as the maximum shear; it is accordingly a lower limit. The values of  $\eta$  and  $\gamma$  are lower than those obtained in extension, and this is what might be expected on the grounds of the anisotropy of the specimen.

Expt.	T °C.	Stress. kg.cm. <sup>-2</sup>	$\eta$ , Poises (initial).	$\gamma$ , cal./% deformation.*	$\eta$ (final).
Torsion	74	2.8 (max)	$1.9 \times 10^{10}$	210	$2.4 \times 10^{11}$
Extension	78	2.6	$1.3 \times 10^{11}$	600-900	$1.7 \times 10^{12}$

\* In torsion, the deformation is a shear, and in extension, an extension.

It was stated above that, in addition to the strain-hardening, a time-hardening process also occurs at high temperatures. This was demonstrated by preheating a cord for 16 hr. at 74° C., and then twisting with  $W = 40$  g. The plastic flow after 5 min. was much reduced, being only 1.7 units compared with 5 units for a normal experiment (Fig. 1).

The time-hardening is not simply due to loss of volatile constituents, since the same effect was observed when these losses were minimised by surrounding the specimen in the preheating period with chips of cordite. As we have noted in Part II, time, as well as strain, probably plays a part in the process of crystallisation which underlies the observed shear-hardening. Tobolski and Andrews<sup>1</sup> have deduced the presence

of a similar bond forming mechanism in certain rubbers.

**The Rapid Elastic Torsion.**—As soon as the couple was applied (by releasing a clutch on the torsion drum) there occurred a rapid initial

TABLE I.

1 Sec. Modulus.

T° C.	Max Stress kg.cm. <sup>-2</sup>	$\theta/l$ deg. cm. <sup>-1</sup>	$G_0$ kg.cm. <sup>-2</sup>
18	2.8	0.29	1550
18	7.0	1.08	1055
18	14.0	2.16	1055
18	15.4	2.52	995
18	16.8	3.31	825
18	21.0	3.9	876
37	1.4	0.89	256
37	2.8	1.8	254
37	7.0	5.9	193
74	1.4	4.23	53.9
74	2.8	9.75	46.8
74	7.0	32.9	34.6

<sup>1</sup> Tobolski and Andrews, *J. Chem. Physics*, 1945, 13, 3.



deformation which, especially at low temperatures, could be clearly distinguished from the slower deformation which followed it. The following tables record the deformations (expressed as  $\theta/l$ ) after approximately 1 sec., together with the derived values of the shear modulus,  $G_0$ . Measurements on a single cord reproduced to  $\pm 5\%$ . The effect of temperature is marked, as in extension. There seems to be a decrease of  $G_0$  as the applied stress increases, but this has not been accurately established.

In Table II we compare the results of torsion and extension work (these cords differed somewhat from that used above). For comparison purposes, the characteristic stress in torsion has been taken as the

TABLE II.—COMPARISON OF TORSIONAL AND EXTENSION MODULI.

$T^\circ\text{C.}$	Stress $\text{kg.cm.}^{-2}$	Young's Modulus $E_0, \text{kg.cm.}^{-2}$	Shear Modulus $G_0, \text{kg.cm.}^{-2}$	$E_0/G_0$ .
			*	
18	4.4	2600	1200	2.17
18	5.2	2490	1100	2.26
18	26.1	2160	840	2.57
37	4.4	1000	240	4.17
74-78	2.6	280	47	6.0
74-78	3.7	245	—	—
74-78	4.4	200	—	—
74-78	5.2	180	38	4.8

maximum stress. The classical theory of elasticity gives  $E_0/G_0 = 2(1+\mu)$ , where Poisson's ratio  $\mu$  is in the range 0.2 to 0.5. The value obtained for  $E_0/G_0$  at low temperatures is in agreement with expectation, but it becomes larger at higher temperatures. As for  $E_0$ , we conclude that the largest contribution to  $G_0$  arises from very

rapid relaxation mechanisms; viz. those involving orientation and distortion of very small segments of the chain molecules. At higher temperatures the larger segments may be expected to "melt", and contribute to  $G_0$ . The larger the segment involved, the more importantly will the anisotropy of the cord enter into determining  $E_0/G_0$ , causing it to deviate from its classical value.

**The Total Elastic Torsion.**—The time course of the torsion, under various conditions of stress and temperature, is shown in Fig. 2 and 4, in which the total torsion is plotted.\* Fig. 2 shows the strong effect of

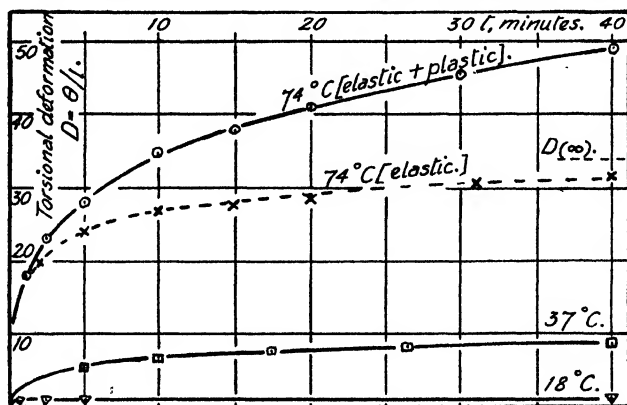


FIG. 2.—The total torsion curves at  $2.8 \text{ kg.cm.}^{-2}$ . At  $18^\circ\text{C.}$  and  $37^\circ\text{C.}$  the plastic flow is negligible, but at  $74^\circ\text{C.}$  is appreciable and must be subtracted to give the elastic curve (shown dotted).  $D(\infty)$  is the asymptotic value of elastic torsion at  $74^\circ\text{C.}$

\* We have neglected to separate the rapid elastic component in the few data considered here. Such a separation is not necessary for deriving the delayed elasticity constants  $Z$  and  $\gamma$ .

temperature at a maximum stress of  $2.8 \text{ kg.cm.}^{-2}$ . At  $18$  and  $37^\circ \text{C}$ . the twist is entirely elastic. At  $74^\circ \text{C}$ . a part of the total twist is plastic, and the dotted curve gives the elastic deformation. The rate of development of the elastic torsion is clearly strongly affected by temperature, but with one exception, we have not been able to determine the asymptotic values of the torsion at long times, and so we cannot say whether  $G(\infty)$  (the modulus corresponding to the full development of elastic torsion) is affected by temperature.

In one case, at  $2.8 \text{ kg.cm.}^{-2}$  and  $74^\circ \text{C}$ ., the complete elastic curve was obtained up to an asymptotic value of  $D(\infty) = 34$ . The data were fitted by equation (12) of Part II, and Fig. 3, shows the relevant plot of  $\log_{10} x$  against time ( $x = 34 - D(t)$ ), together with an inserted plot of  $\log_{10} x - G$  against  $x$  to obtain the constant  $\gamma/2.3 RT$ . We derive values of  $Z = 0.0037 \text{ min.}^{-1}$  and  $\gamma = 59 \text{ cal./per cent. shear}$ , to be compared with

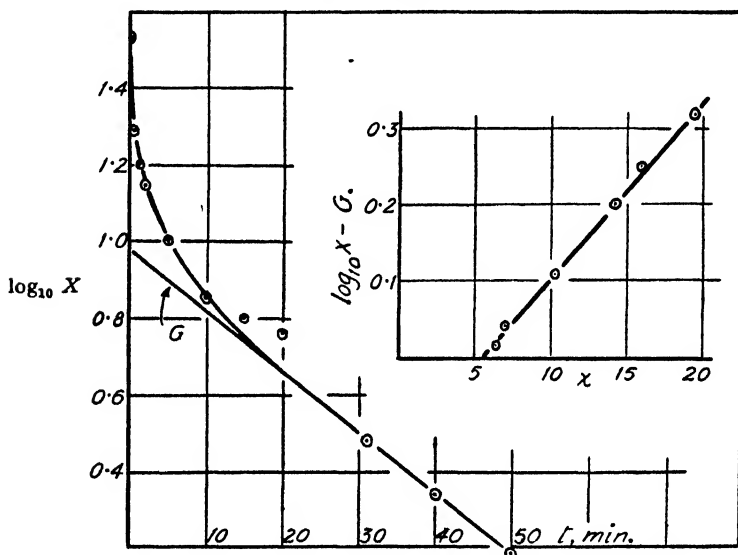


FIG. 3.—Analysis of the elastic deformation  $x = D(\infty) - D(t)$ . Inset is the plot from which the constant  $\gamma/2.3 RT$  is derived.

values of  $Z = 0.01 \text{ min.}^{-1}$  and  $\gamma = 100\text{--}300 \text{ cal./per cent. extension}$ , for extension at  $78^\circ \text{C}$ . and a stress of  $2.6 \text{ kg.cm.}^{-2}$ . The deformation  $D(\infty) = 34$  corresponds to a total elastic shear modulus of  $13.4 \text{ kg.cm.}^{-2}$ . Under these conditions the total elastic Young's modulus is  $E(\infty) = 85 \text{ kg.cm.}^{-2}$ , so that  $E(\infty)/G(\infty) = 6.3$ , a value similar to that obtained for the ratio  $E_0/G_0$ .

In attempting to analyse the effect of stress on the total elastic deformation, we have been limited by the impossibility of securing the complete development of the delayed elasticity under most conditions of stress and temperature. Fig. 4 presents results at  $17^\circ\text{--}19^\circ \text{C}$ . Fig. 4a shows total deformation as a function of time (plastic flow being negligible), and clearly both the rate, and amount of torsion at a given time, increase rapidly with increasing stress. We have tested whether the curves may

be fitted by the conventional equation  $D(t) = \frac{f}{G(\infty)} \cdot \psi(t)$ , where  $\psi(t)$  is a function only of time ( $\psi(t) = 1$  at  $t = \infty$ ,  $\psi(t) = 0$  at  $t = 0$ ,  $f/G(\infty) = D(\infty)$ ). Fig. 4b shows a plot of  $\frac{1}{G}$ , i.e. strain/unit stress,

against time, and if the above equation held, all the results should fall on one curve. Clearly this is not so.

We have not attempted to fit the curves exactly by an empirical equation, but to a rough approximation the data of Fig. 4*b* may be described by

$$\ln(1 + D) = \text{const. } f \psi(t) \quad (1)$$

In discussing these results it must be remembered that they only refer to the early part of the elastic deformation, and that the final equilibrium elastic torsion values were never established. For this reason it has not been possible to obtain the moduli  $G(\infty)$  and to examine whether or not they were affected by stress. Equation (1) above, if it held over the whole course of the deformation, might be taken to imply an exponential dependence of torsion on applied stress, coupled with a creep function  $\psi(t)$  independent of stress. However, the few relevant results obtained in

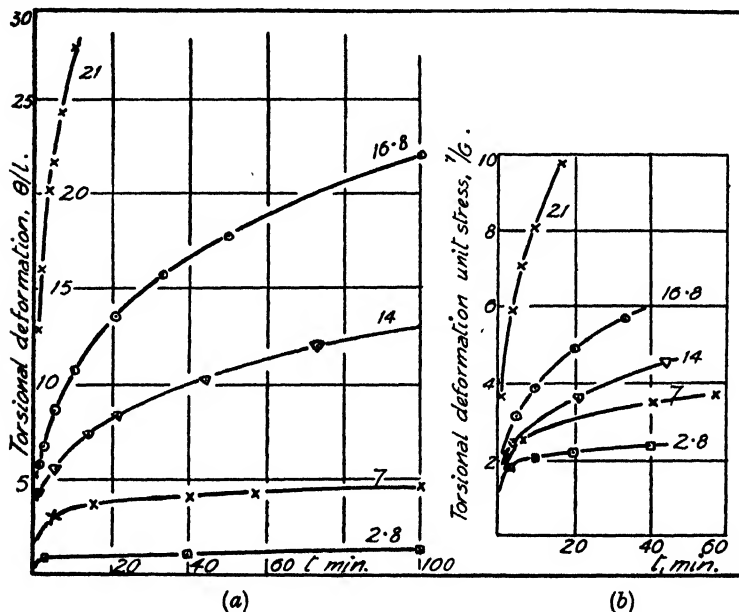


FIG. 4.—The effect of stress on the elastic torsional deformation at 17–19° c.

extension indicated an approximately linear relation between the equilibrium extension and the applied stress, as shown by the approximate constancy of the Young's moduli,  $E_1(\infty)$ . Accordingly, we incline to the view that the formulation (1) is misleading, and that in fact the observed results probably arise from the presence of a stress-dependent creep function—i.e. that over not too wide a range of stress the results would follow

$$D(t) = \frac{f}{G(\infty)} \cdot \psi(t, f).$$

We have not been able to determine the form of  $\psi(t, f)$ .

This effect of stress on the rate of elastic deformation has been observed also in further torsional experiments at 37° c. and 74° c., and in extension at 18° c. at relatively high stresses (10–20 kg.cm.<sup>-2</sup>).

**Elastic Recovery.**—As in Part II, the elastic recovery curves were compared with the elastic torsion curves, in the light of the Boltzmann superposition principle (B.S.P.), and the behaviour found to be complex. In some cases the B.S.P. was obeyed approximately, in other cases the

recovery was faster or slower than predicted. It was observed that when specimens were only twisted for a short time (whatever the magnitude of the twist) the faster type of recovery usually occurred. Specimens twisted for a long time (even if only to small deformations), usually showed the slower type of recovery. The effect is probably related to the time-hardening effect described for plastic flow, having its basis in a time-dependent crystallisation process, involving segments of the nitrocellulose chains.

### Discussion.

The torsion of cords has led to two main results. Firstly, the general elastic and viscous behaviour is the same as that observed in extension. The data are described by the same equations, and in the case where elastic moduli and "viscosity" coefficients have been obtained, these are in reasonable agreement with those obtained in the extension of cords, if allowance be made for the anisotropy of the material. The preferential orientation of nitrocellulose molecules along the axis of the cord might be expected to lead to a relatively large viscous resistance in this direction, and also to relatively large elastic moduli in the case where large segments of chains are involved in the elastic deformation. It has been suggested that the latter condition may hold at the higher temperatures. Secondly, the effect of stress on the rate of development of elastic deformation, first observed in extension, has been confirmed in torsion. Technical difficulties have prevented a confirmation of the observation made in extension, that over small stress ranges the delayed modulus is little affected by stress.

In conclusion, we may review the results of these papers in relation to the main problems, as we see them.

(1) The need to distinguish between rates of deformation and equilibrium deformations, under the action of an applied stress, and to distinguish between reversible and irreversible flow. This has been secured, at least to a good approximation, although the difficulty of obtaining the equilibrium elastic deformation in shear-hardening systems, is always present.

(2) The description of the equilibrium elastic deformations in terms of a molecular model. This has been satisfactorily achieved for vulcanised rubber over ranges of strain where the material remains amorphous (cf. the review by Flory<sup>2</sup>). The pertinent moduli in our work are the total elastic moduli, which, within a rather large experimental error, are all about 100 kg.cm.<sup>-2</sup>, not markedly influenced by temperature, or a two-fold alteration of stress. This modulus is nearly ten times that for a vulcanised rubber, the difference being attributable to the partially crystalline character of plasticised nitrocellulose. The effect of temperature upon partially crystalline polymers has been examined theoretically and their range of melting explained.<sup>3</sup> The quantitative formulation of their stress-strain relationship is a more difficult problem still to be solved. If stress can "melt" randomly oriented crystallites, forming them again along the axis of stress, then we may expect that the modulus will decrease as applied stress increases. In our opinion this problem is best approached, using dilute gels of cross-linked polymer, where plastic flow and time effects are reduced to a minimum.

(3) The general nature of the model employable in problem (2) may be supposed to be that already given, i.e. a network of nitrocellulose chains, partly crystalline, partly amorphous, in which the plasticiser is dissolved. We have seen that our method of analysis of the total strain into plastic and elastic components is relatively successful. As it stands this implies

<sup>2</sup> Flory, *Chem. Rev.*, 1944, **35**, 51.

<sup>3</sup> Frith and Tuckett, *Trans. Faraday Soc.*, 1944, **40**, 251.

that the plastic and elastic elements of the network are linked in series. However, a similar result can arise from other types of model, in which the elements are linked in parallel.

(4) In developing the kinetics of plastic and elastic flow of any particular model we require a treatment of the rate process of molecular flow in plastics. For moderate rates of strain Eyring's equation (modified for the crystalline type of polymer to take account of strain-hardening) seems adequate to account broadly for the results observed. Before it can be used with confidence at high rates of strain, the further work indicated in Part I is necessary. The effect of stress upon delayed elasticity remains an unsolved problem. If, as would appear from our extension results, the effect of stress is solely on the rate and not on the modulus, then we must suspect an inaccuracy in the rate process equations. If, on the other hand, the modulus decreases with increased stress we may suppose that more elastic mechanisms are yielding at the higher stresses. We have not, however, been able definitely to rule out the latter effect (there is some evidence for it in the rapid elastic moduli which we suppose to involve the orientation of relatively short segments of chains).

The authors wish to acknowledge the helpful encouragement of Prof. E. K. Rideal, F.R.S. They are indebted to Mr. A. G. Ward for valuable discussions, in particular on points relating to the effects of thermal history on mechanical properties. These papers are published by the permission of the Chief Scientific Officer, Ministry of Supply.

### Summary.

The torsion of cords of cordite has been analysed into rapid elastic, delayed elastic, and plastic components. The derived elastic moduli at room temperature agree with those obtained in extension. At higher temperatures there is a divergence, probably due to anisotropy. The time course of delayed elastic flow, and plastic flow, is similar to that observed in extension, and the rate constants obtained are in general agreement. The torsional method confirms the effect of applied stress upon the delayed elastic deformation. This is probably primarily an effect on the rate of deformation, but experimental difficulties have prevented an evaluation of moduli at different stresses. It has been shown that the hardening during continued plastic flow is not solely a function of strain, but also involves time. The further problems associated with the field of work have been discussed.

### Résumé.

La torsion de cordes de cordite a été analysée en composantes élastique rapide, élastique retardée et plastique. Les modules élastiques dérivés à la température ordinaire s'accordent avec ceux obtenus en extension. A des températures supérieures il y a une différence probablement due à l'anisotropie. L'écoulement élastique retardé et l'écoulement plastique en fonction du temps sont semblables à ceux observés par allongement et les constantes de vitesse sont généralement en bon accord. La méthode par torsion confirme l'effet de l'effort sur la déformation élastique retardée : l'effet porte principalement sur la vitesse de déformation, mais il a été impossible, à cause des difficultés expérimentales, d'évaluer les modules pour différents efforts. On a montré que le durcissement au cours d'un écoulement plastique continu n'est pas seulement fonction de la charge, mais aussi du temps. On discute également d'autres problèmes, qui appartiennent au même domaine de travail.

### Zusammenfassung.

Die Torsion von Cordit ist in rasche elastische, verzögerte elastische und plastische Komponenten analysiert worden. Für Zimmertemperatur stimmen die daraus abgeleiteten Elastizitätsmoduli gut mit den bei Ausdehnung erhaltenen überein, aber bei höheren Temperaturen besteht ein Unterschied, der wahrscheinlich auf Anisotropie zurückzuführen ist. Der zeitliche Verlauf des verzögerten elastischen und plastischen Fließens ist ähnlich wie bei der Ausdehnung und die Geschwindigkeitskonstanten stimmen im allgemeinen überein.

Die Torsionsmethode bestätigt den Effekt der Spannung auf die verzögerte elastische Deformation. Dies ist wahrscheinlich in erster Linie ein Effekt auf die Deformationsgeschwindigkeit, aber experimentelle Schwierigkeiten haben eine Auswertung der Konstanten bei verschiedenen Spannungen verhindert. Es ist gezeigt worden, dass die Erhärtung bei andauerndem plastischen Fließen nicht nur allein eine Funktion der Deformation ist, sondern auch von der Zeit abhängt. Weitere Probleme in diesem Arbeitsgebiet werden erörtert.

*Dept. of Colloid Science,  
The University,  
Cambridge.*

## DEFORMATION AND SWELLING OF POLYMER NETWORKS CONTAINING COMPARATIVELY LONG CHAINS.\*

By J. J. HERMANS.†

*Received 6th May, 1946.*

### I. The Configurational Entropy of the Network.

The theory of rubber elasticity, first put forward by Kuhn<sup>1</sup> and by Guth and Mark,<sup>2</sup> has been further developed by a number of authors. All these have adopted practically the same model in that they assume a network of randomly-kinked, flexible chains.<sup>3</sup> The degree of flexibility depends on the ease with which successive monomeric units in the chain can rotate with respect to each other. We shall follow a device, introduced by Kuhn, to make ourselves independent of the amount of freedom of rotation between successive monomeric units. This device consists in assuming that each chain on the average behaves as if it were subdivided into a number of "statistical chain-elements" which are completely free to assume any orientation in space whatever, irrespective of the orientations of the other (statistical) chain-elements in the chain. Kramers<sup>4</sup> has shown from kinetic energy considerations that the orientation of adjacent chain-elements in a long-chain molecule are to a certain extent correlated. This correlation, however, is not very pronounced and will be neglected in the present treatment.

Each chain element contains a certain number of monomeric units. Let  $N$  be the average number of chain-elements between two successive junction points in the network, and let  $A$  be the average length of a chain-element. If all chain-fragments were freely dispersed in an indifferent liquid, there would result a certain statistical distribution of chain end-points, which Kuhn showed to be :

$$\psi_0 d\tau = c_0 e^{-\mu^2 \tau^2} d\tau; \mu^2 = \frac{3}{2NA^2}; \tau^2 = x^2 + y^2 + z^2; d\tau = dx dy dz. \quad (1)$$

\* Communication No. 33 from the Laboratory for Cellulose Research of the AKU and Affiliated Companies, Utrecht (Holland).

† Present address: *Inorg. and Phys. Chem. Lab., The University, Gröningen.*

<sup>1</sup> Kuhn, *Kolloid Z.*, 1934, 68, 2; 1936, 76, 258.

<sup>2</sup> Guth and Mark, *Monatsh.*, 1935, 65, 93; see further Pelzer, *Monatsh.*, 1938; 71, 444 and Dostal, *Monatsh. C.*, 1938, 71, 144, 309, 340.

<sup>3</sup> The polymer substance between two successive junction points of the network is called chain-fragment (or chain, for shortness).

<sup>4</sup> Kramers, *Physica*, 1944, 11, 1; *J. Chem. Physics*, 1946, 14, 415.

Here  $\psi_0 d\tau$  represents the probability of finding the one end-point in the volume element  $d\tau$  with co-ordinates  $x, y, z$  with respect to the other end-point.

It is important to note that this formula assumes *large values of  $N$* . It is usually assumed that the distribution (1) also obtains in the solid rubber. If now the material is stretched in the  $x$ -direction, the distribution of end-points becomes different from  $\psi_0$ . The new distribution  $\psi$  determines the structural entropy  $S$  of the stretched polymer, and thus the retractive force

$$P = -T \frac{\partial S}{\partial l}, \quad . \quad . \quad . \quad . \quad . \quad (2)$$

where  $l$  is the length of the material in the direction of strain. The question thus arises how we shall calculate the entropy  $S$  for a given distribution  $\psi$ . In his earlier papers<sup>1</sup> Kuhn assumes that one may assign an entropy  $s = -k\mu^2 r^2$  to a chain fragment with distance  $r$  between the end-points ( $k$  is Boltzmann's constant) and the entropy of an assembly of chains whose distribution of end-points is  $\psi$  becomes

$$S = -k\mu^2 \int d\tau r^2 \psi. \quad . \quad . \quad . \quad . \quad (3)$$

This definition accounts for the change in the probability of the "inner state" of the chains.<sup>5</sup> In later work Kuhn and Gr $\ddot{u}$ n<sup>6</sup> add the entropy of orientation of the vector  $r$ , which involves the assumption that this entropy is simply additive. Finally, in a recent paper,<sup>5</sup> Kuhn and Gr $\ddot{u}$ n give a detailed analysis of various entropy contributions and find that the entropy of orientation of the vectors  $r$  in a stretch at constant volume is cancelled exactly by a smoothing-out of the density distribution. The final conclusion arrived at by Kuhn and Gr $\ddot{u}$ n is simply that used by the present author<sup>7</sup> in 1943, and amounts to the following. The expression  $\psi_{i0} = c_0 \exp(-\mu^2 r_i^2)$  must be considered as the *a priori* probability for the occurrence of a chain-end-point in  $d\tau_i$ . The probability of a distribution  $\nu_i = \psi_{i0} d\tau_i$ ,  $\nu_i = \psi_{i0} d\tau_i \dots$  over the elements  $d\tau_1, d\tau_2 \dots$  is therefore given by<sup>8</sup>

$$W = \frac{\nu!}{\nu_1! \nu_2! \dots} (\psi_{10})^{\nu_1} (\psi_{20})^{\nu_2} \dots$$

This gives  $S/k = \nu \ln \nu - \sum_i \nu_i \ln \nu_i + \sum_i \nu_i \ln \psi_{i0} + \text{const.}$

If the arbitrary constant is so chosen that the entropy  $S_0$  of the undeformed state is zero, we may write:

$$S = S - S_0 = -k \int d\tau \psi \ln (\psi/\psi_0). \quad . \quad . \quad . \quad (4)$$

This result has already been used by the present author.<sup>7</sup> It may also be expressed as follows. The probability of the new distribution is measured by the ratio  $f = \psi/\psi_0$ , and we consider a distribution over elements  $\psi_0 d\tau$  rather than over elements  $d\tau$ . The entropy referred to the undeformed state may therefore be written

$$S - S_0 = -k \int (\psi_0 d\tau) f \ln f = -k \int d\tau \psi \ln f \quad . \quad . \quad (5)$$

which is the result (4). It was also used by Halsey and Eyring.<sup>9</sup> This expression defines in a straightforward and simple manner the entropy change at stretch, and Kuhn and Gr $\ddot{u}$ n's subdivision of this entropy change into a number of different contributions<sup>5</sup> is of a rather artificial nature.

<sup>5</sup> Kuhn and Gr $\ddot{u}$ n, *J. Polymer. Sci.*, 1946, **1**, 183.

<sup>6</sup> Kuhn and Gr $\ddot{u}$ n, *Kolloid Z.*, 1942, **101**, 248.

<sup>7</sup> Hermans, *Kolloid Z.*, 1943, **103**, 210.

<sup>8</sup> Halsey and Eyring, *Text. Res. J.*, 1945, **15**, 451.

<sup>9</sup> Eqn. (10) in ref. 5.

This is also apparent from the complicated formulæ which these authors obtain for some of these contributions, and which exactly cancel.

## II. Distribution of End-points (Stretch of the Dry Polymer Substance).

To find the distribution  $\psi$ , one must make some kind of assumption regarding the mechanism of deformation. The majority of authors have assumed that the components of length of all the chain-fragments are altered in the same ratio as the macroscopic dimensions of the bulk rubber. We will, for shortness, call this "affine deformation"<sup>10</sup> of chain end-points. The volume of the dry gel remains practically constant. If the dimensions along  $x$  are multiplied by a factor  $\alpha$ , those along  $y$  and  $z$  are multiplied by a factor  $\alpha^{-1/2}$ . Consequently, the distribution  $\psi_e$  of end-points is converted into

$$\psi = c_0 e^{-\mu^2(x^2/\alpha^2 + \alpha y^2 + \alpha z^2)} \quad (6)$$

In his earlier work<sup>5, 6</sup> Kuhn considered small degrees of stretch only. If  $\alpha$  is expressed in terms of relative elongation  $\gamma$  (i.e.  $\alpha = 1 + \gamma$ ), this amounts to expanding in powers of  $\gamma$  and retaining only the first non-vanishing term. Later, Wall,<sup>11</sup> Treloar,<sup>12</sup> James and Guth,<sup>13</sup> and recently also Kuhn and Grün<sup>5</sup> have given a complete solution for finite values of  $\gamma$ . For  $G$  chains this solution runs

$$S - S_0 = -\frac{1}{2}kG(\alpha^2 + 2/\alpha - 3) \quad (7)$$

as follows at once from eqn. (4) if the expression (6) for  $\psi$  is inserted. If  $G$  is the number of chains in unit volume, the force per unit cross-section is obtained by differentiation with respect to  $\alpha$

$$P = kTG\left(\alpha - \frac{1}{\alpha^2}\right) \quad (8)$$

A plot of  $P$  against  $\alpha$  is given in Fig. 1. The force-strain diagram of the actual rubber is S-shaped (dotted curve in Fig. 1) and finds its complete explanation<sup>13</sup> in the finite value of  $N$ . The force  $P$  is the stress per unit area of original cross-section. Since the cross-section decreases in the ratio  $\alpha^{-1}$ , the stress per unit cross-section of the stretched polymer is

$$P\alpha = kTG\left(\alpha^2 - \frac{1}{\alpha}\right) \quad (9)$$

As was observed by Kuhn and Grün<sup>5</sup> this expression for  $P\alpha$  conforms to a relation first suggested by Müller,<sup>14</sup> according to which

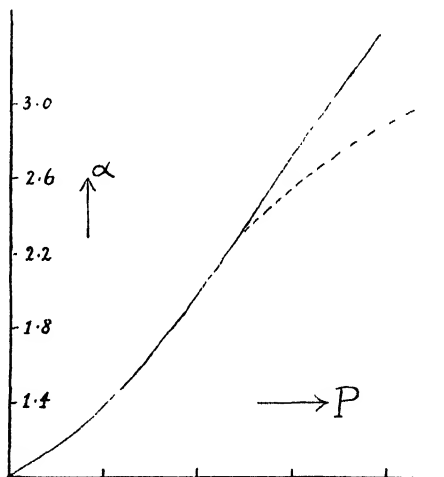


FIG. 1.—Degree of stretch  $\alpha$  plotted against force  $P$  according to eqn. (8) (drawn curve).

<sup>10</sup> The concept affine deformation covers, it is true, a much wider field, but we will none the less retain the present notation which was used in this context by Baule, Kratky and Treer, *Z. physik. Chem. B*, 1941, 50, 255.

<sup>11</sup> Wall, *J. Chem. Physics*, 1942, 10, 485, cited after Flory and Treloar.

<sup>12</sup> Treloar, *Trans. Faraday Soc.*, 1943, 39, 36, 242.

<sup>13</sup> James and Guth, *J. Chem. Physics*, 1943, 11, 455; *J. Appl. Physics*, 1944, 15, 294; Guth, *Amer. Assoc. Adv. Sci.*, No. 21, 103; Hermans, *J. Colloid Sci.*, 1946, 1, 235; Treloar, *Trans. Faraday Soc.*, 42, 1946, 83.

<sup>14</sup> Müller, *Kolloid Z.*, 1941, 95, 172.



the stress  $P\alpha$  per unit cross-section of the stretched polymer is proportional to the double refraction of the stretched material.

So much for the affine deformation of chain end-points. A physical basis to this assumption is lacking. The junction points in the network are not fixed in space and there is no obvious reason why they should follow the macroscopic deformation of the substance. Rather must we expect that when the rubber is stretched, the chain end-points will adjust themselves to some extent to the new situation and will occupy new equilibrium positions which are not necessarily those imposed by the affine deformation.<sup>15</sup> To account for this, the author<sup>7</sup> in 1943 followed another line of attack. The effect of the stretching force is described by assuming that each chain is, on the average, subject to a force  $\bar{p}$  in the direction of stretch. Introducing a potential energy  $-\bar{p}x$ , the new distribution of end-points is given by

$$\psi_0 = c'e^{-\mu^2 r^2 + \bar{p}x/kT}. \quad (10)$$

This distribution leads to a force-strain relation which is very similar to the one laid down in Fig. 1, although it involves a numerical constant which is different from that in eqn. (8). It shows the same dependence on temperature as the force obtained on the basis of affine deformation. Interestingly, it also conforms to Müller's assumption that the tension per unit cross-section of stretched material is proportional to the double refraction. However, there exists an important difference from the theory of affine deformation in that it allows of an immediate extension to *short chains*.<sup>15</sup> A potential energy of the type  $-\bar{p}x$  was also introduced by James and Guth.<sup>15</sup> Their derivation of the complete stress-strain curve is similar to that given by us (cf. ref. 13). Treloar's<sup>15</sup> recent theory is based on an extension of the distribution function  $\psi_0$  to finite values of  $N$ ; his method is not suitable to the treatment of very short chains ( $N$  of the order 2, or 3) which are of importance to the stretch of cellulose.

So far no account has been taken of the fact that the chains are tied together in the junction points of the network. The only quantity in the theory which is representative for the network structure is the number  $N$  of (statistical) chain-elements between two successive junction points, but for the rest the chains might just as well have been freely dispersed in a liquid, since all interaction between different chains is ignored.

An interesting attempt to account for the coherence of the chains in a network structure was made by Flory and Rehner.<sup>16</sup> They calculate the entropy change involved in the formation of the network out of separate molecules, assuming that this network can be replaced by one in which the junctions surrounding a given cross-linkage lie at the corners of a regular tetrahedron. The position of the particular cross-linkage concerned with respect to the four corners of the tetrahedron is not specified and its density distribution in space is calculated. This calculation applies to a special case only, viz. that in which the points on a chain, where cross-linking can occur are specified in advance; it does not apply to network formation in which attachment of the chains to one another may take place at a large number of points along the chains.

The influence of the stretch on the entropy is calculated on the assumption that *the four corners of the regular tetrahedron surrounding a junction point are subject to affine deformation*. Although admittedly the junction point concerned is free to adjust itself to this new situation and is not

<sup>15</sup> James and Guth<sup>15</sup> tried to give a theoretical support to the assumption of affine deformation. In their calculation it is assumed, however, that the probability for given lengths of a number of chains can be found by multiplying the probabilities for the lengths of the individual chains. It was recently shown by Kuhn and Gr $\ddot{u}$ n,<sup>5</sup> that the entropy of an assembly of chains is *not* equal to the sum of the entropies of the individual chains, and this should be accounted for in James and Guth's theory. See also section III of the present article.

<sup>16</sup> Flory and Rehner, *J. Chem. Physics*, 1943, 11, 512.

itself forced to take part in the affine deformation of the tetrahedron, it is not very surprising that this calculation leads again to the formula (7).

### III. Swelling.

If a swelling agent penetrates the network, the whole structure is inflated and a new distribution of chain end-points will result. Here again there are no obvious grounds for assuming that the junction points will follow the changes in the macroscopic dimensions of the material. It can be shown that if the chains are short, i.e., if they contain only a small number of statistical chain-elements, the junction points are even *unable* to follow the changes in macroscopic dimensions. With large values of  $N$ , however, such "affine deformation" of chain end-points probably represents a fair approximation to swelling. On this basis Flory and Rehner<sup>17</sup> give a very interesting analysis of the swelling process. Since our treatment differs from theirs in a number of points, we will consider the matter in some detail.

The authors quoted assume that in the dry gel the "normal" distribution  $\psi_0$  given by eqn. (1) prevailed. Since gels may be formed in the presence of a solvent (in particular the formation of a gel from a solution, by a coagulation process), we shall rather consider a more general case in as far as the degree of swelling at which the "normal" distribution (1) is in existence is left unspecified. Let  $q_0$  be this degree of swelling; i.e. the ratio between the volume of the gel and that of the dry polymer.

If the degree of swelling changes from  $q_0$  to  $q_1$ , the distribution  $\psi$  changes from  $\psi_0$  to

$$\psi_1 = c_1 c^{-\kappa^2 r^2}; \quad c_1 = c_0 \frac{q_0}{q_1}; \quad \kappa^2 = \mu^2 \left( \frac{q_0}{q_1} \right)^{\frac{2}{3}}. \quad (11)$$

The value of  $c_1$  follows at once from the condition that the total number of chains remains constant. Applying eqn. (4) we find the following change in the configurational entropy of  $G$  chains:

$$S_1 - S_0 = kG \ln \frac{q_1}{q_0} - \frac{3}{2} kG \left[ \left( \frac{q_1}{q_0} \right)^{\frac{2}{3}} - 1 \right]. \quad (12)$$

The second term in the right-hand side is the one found by Flory and Rehner. It expresses that the stretch to which the chains must submit at swelling (i.e. if  $q_1 > q_0$ ) brings them in a less probable configuration. The authors note that this term is *approximately* three times the entropy change (7) for *small* deformations if we put  $\alpha = (q_1/q_0)^{\frac{1}{3}}$ . It will be shown below that in reality the formulæ (7) and (12) are two special cases of a general formula.

We find in addition the first term,  $kG \ln q_1/q_0$ , the origin of which may be explained as follows. As shown in an earlier paper,<sup>7</sup> the distribution  $\psi_0$  can be considered as a diffusion equilibrium: the chain end-points tend to acquire a uniform distribution but are prevented from doing so by an elastic force  $2\mu^2 kTr$  which drives the one end-point towards the other. In fact, the equilibrium between this diffusion tendency and the retractive force  $2\mu^3 kTr$  requires that the "diffusion force" is equal to the retractive force:

$$\text{grad } (kT \ln \psi) = -2\mu^3 kTr,$$

the solution of which is given by eqn. (1). This diffusion tendency favours the higher  $q$ -values, and if it were the only effective factor, the configurational entropy would increase by an amount  $kG \ln q_1/q_0$  if the volume increases from  $q_0$  to  $q_1$ , in exactly the same way as the entropy per mole of an ideal gas increases by an amount  $R \ln V_1/V_0$  if the volume increases from  $V_0$  to  $V_1$ . In this latter case the increase in entropy derives from

<sup>17</sup> Flory and Rehner, *J. Chem. Physics*, 1943, 11, 521; Flory, *Chem. Rev.*, 1944, 35, 51.

the fact that we have yielded to the diffusion tendency of the gas molecules, i.e. to their tendency to acquire a more uniform distribution in space. In the assembly of  $G$  chain molecules the term  $kG \ln q_1/q_0$  has exactly the same origin as the term  $R \ln V_1/V_0$  in the entropy change of the gas: we have yielded to the tendency of the chain end-points to attain a uniform distribution in  $xyz$ -space.

We observe further, that by virtue of this logarithmic term the entropy  $S_1(q_1)$  in eqn. (12) has its maximum value at  $q_1 = q_0$ . In other words, both increase and decrease in volume lead to a smaller configurational entropy, as of course it should be. Fig. 2 gives the pressure  $T\partial S_1/\partial q_1$  (force per cm.<sup>2</sup> of swollen gel), resulting from changes in configurational entropy. This pressure is exerted by the network when compressed or inflated.

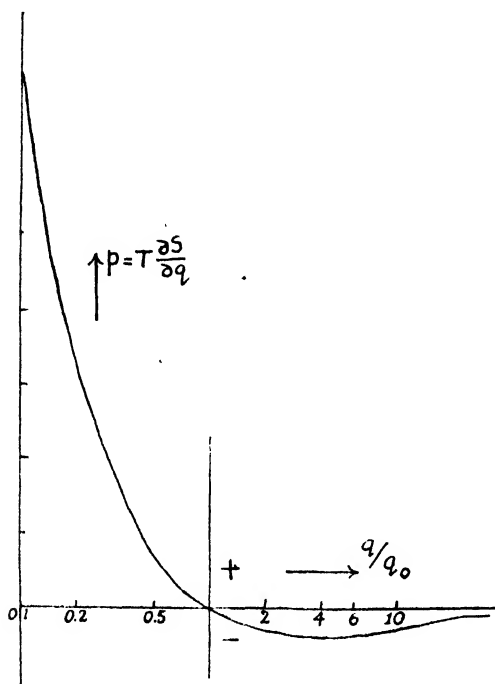


FIG. 2.—Pressure in network resulting from configurational entropy in dependence on degree of swelling  $q_1$  (on logarithmic scale).

equal to the sum of the entropies of the individual chains. As shown by Kuhn and Gr $\ddot{u}$ n<sup>5</sup> this is not correct (cp. <sup>15</sup>).

We obtain the total entropy of the gel if we add the entropy of mixing the polymer with the solvent. Following Flory and Rehner, we will use the simple formula obtained by Huggins<sup>18</sup> and by Flory<sup>19</sup> on the assumption that  $n$  molecules of the solvent are mixed with  $n'$  polymer molecules, each consisting of  $Z$  "segments". A segment is assumed to be of the same size as a solvent molecule and to be able to replace a solvent molecule in the quasi-lattice constituting the liquid. Flory and Rehner

Interestingly, in Flory and Rehner's formula a term  $-kG \ln q_1/q_0$  occurs, because they consider the formation of linkages at specified points of the chain. The probability of the occurrence of such a cross-linkage decreases with increasing volume. We shall see below, however, that a term  $\pm kG \ln q_1/q_0$  is of minor importance in the determination of the swelling equilibrium, provided  $N$  is sufficiently large, and we will therefore forbear from going any further into the matter.

One final observation may be made. In our treatment the configurational entropy of the network is a maximum at the degree of swelling  $q_0$  where coiling is normal. James and Guth<sup>18</sup> argue that this entropy should be a maximum at zero volume, where all chains have zero  $r$ -value. This would only be true, however, if the entropy of the network were

<sup>18</sup> Huggins, *J. Amer. Chem. Soc.*, 1942, 64, 1712.

<sup>19</sup> Flory, *J. Chem. Physics*, 1941, 9, 660; 1944, 12, 425; see further Miller, *Proc. Camb. Phil. Soc.*, 1941, 38, 109; 1942, 39, 54; Orr, *Trans. Faraday Soc.*, 1944, 40, 306; Guggenheim, *Proc. Roy. Soc. A*, 1944, 183, 203; *Trans. Faraday Soc.*, 1945, 41, 107.

put  $Z = N$ , but it seems more appropriate to adopt Huggins' point of view,<sup>30</sup> according to which the polymer in a gel represents a single gigantic molecule:  $Z$  is effectively infinite. The entropy of mixing is then reduced to the simple expression

$$S_{\text{mix}} = kn \ln \frac{n + Zn'}{n} \quad (13)$$

The degree of swelling is obviously determined by

$$q_1 = \frac{1}{v_r} = \frac{n + Zn'}{Zn'} \quad (14)$$

where  $v_r$  represents the volume fraction of polymer in the gel. The partial molecular entropy of the solvent is thus found to be

$$\frac{\partial S}{\partial n} = -k \left[ \ln(1 - v_r) + v_r - \frac{G}{Zn'} v_r + \frac{Gq_0^{-\frac{1}{3}}}{Zn'} v_r^{\frac{1}{3}} \right].$$

Since the size of a segment in Huggins' sense will be of the same order of magnitude as that of a statistical chain-element in Kuhn's sense, the ratio  $G/Zn'$  is of the order  $N^{-1}$ , which shows that the term  $Gv_r/Zn'$  is negligible if  $N$  is large.<sup>31</sup> Since this term originates from the term  $kG \ln q_1$  in (12), it follows that this term is of little consequence. Leaving this term out, and adding a van Laar heat of dilution term<sup>19, 20</sup> proportional to  $v_r^2$ , we finally obtain the partial molecular free energy of the solvent

$$\frac{\partial F}{\partial n} = kT \left[ \frac{1}{2} K v_r^2 + \ln(1 - v_r) + v_r + v_r^{\frac{1}{3}} / N q_0^{\frac{1}{3}} \right] \quad (15)$$

We have for convenience, replaced  $G(Zn')^{-1}$  by  $N^{-1}$ .

Although our treatment differs in some points from Flory and Rehner's, the final result (15) is the same (in their case  $q_0 = 1$ ). As we have seen, this agreement is due to the fact that the number  $N$  of chain-elements between two successive junction points is supposed to be large.

The equilibrium between the gel and the solvent is determined by the condition:  $\partial F / \partial n = 0$ . In the limit of high degrees of swelling (small  $v_r$ ) we may expand  $\ln(1 - v_r)$  and find to a first approximation

$$v_r^{5/3} = \frac{2}{1 - K} \frac{1}{N q_0^{\frac{1}{3}}} \quad (16)$$

For a further discussion we refer to Flory and Rehner, where of course the factor  $q_0^{-\frac{1}{3}}$  does not appear.

#### IV. Stretching of Swollen Gels.

If the swollen gel is stretched, a further change in configurational entropy takes place. Flory and Rehner find

$$-kG \left[ q^{3/2} \left( \frac{\alpha^2}{2} + \frac{1}{\alpha} \right) - \frac{3}{2} \right] \quad (17)$$

where  $\alpha$  is the ratio between the length of the stretched sample and that of the unstretched swollen gel. They conclude from this expression that the gel will de-swell on stretching. In a later paper,<sup>32</sup> however, they observe that when differentiating the expression (17) with respect to the degree of swelling  $q$ , to obtain the molecular free energy of the solvent, the length  $L = \alpha L_0 q^{\frac{1}{2}}$ , instead of  $\alpha$ , must be kept constant,  $L_0$  being the length in the isotropic dry condition. This leads to an increase in the

<sup>30</sup> Huggins, *J. Physic. Chem.*, 1942, 46, 151; *J. Chem. Physics*, 1941, 9, 440; *Ann. N.Y. Acad. Sci.*, 1943, 44, 431; *Ind. Eng. Chem.*, 1943, 35, 216.

<sup>31</sup> If a segment in Huggin's sense is identical with a statistical chain-element in Kuhn's sense, we have, of course,  $Zn' = GN$ .

<sup>32</sup> Flory and Rehner, *J. Chem. Physics*, 1944, 12, 412.

degree of swelling when the sample is stretched. For high degrees of swelling they find to a first approximation:

$$q = q_1 \sqrt{\alpha}. \quad (18)$$

However, the expression (17) for the configurational entropy of the stretched swollen network was derived on the assumption that the volume of the gel remains constant in the deformation process. A general formula can be obtained from eqn. (4) if we insert the distribution of chain end-points in the swollen gel. If the macroscopic dimensions in the direction of  $x$  are increased in the ratio  $\alpha$ , and those along  $y$  and  $z$  in the ratio  $\sigma$ , the assumption of affine deformation leads to a distribution

$$\psi d\tau = \frac{c_1 d\tau}{\alpha \sigma^2} \exp \left[ -\kappa^2 \left( \frac{x^2}{\alpha^2} + \frac{y^2}{\sigma^2} + \frac{z^2}{\sigma^2} \right) \right]. \quad (19)$$

Obviously, if  $q_1$  is the degree of swelling before, and  $q$  that after stretching:

$$\alpha \sigma^2 = q/q_1. \quad (20)$$

The application of the formula (4) gives for the configurational entropy of the network

$$S - S_0 = kG \left[ \ln \frac{q}{q_0} - \left( \frac{q_1}{q_0} \right)^{\frac{1}{2}} \left( \frac{\alpha^2}{2} + \frac{q}{q_1 \alpha} \right) + \frac{3}{2} \right]. \quad (21)$$

We note that the equations (7) and (12) actually represent special cases of the general formula (21). The formula (7) is obtained if we insert  $q = q_1 = q_0$ , and the formula (12) derives from (21) if we take  $\alpha = 1$  and  $q = q_1$ , as it should be. The total entropy and free energy of the system involve, as before, the terms resulting from mixing the polymer with the solvent. These terms, however, play no part in the retractive force  $P$ , because it is assumed that equilibrium with the pure solvent is maintained. If the total free energy  $F$  is considered as a function  $F(q, l)$  of volume  $q$  and length  $l$ , derivation of  $F$  with respect to  $l$  amounts to determining the quantity

$$P = \frac{\partial F}{\partial q} \frac{dq}{dl} + \frac{\partial F}{\partial l}.$$

The swelling equilibrium requires, however, that  $\partial F / \partial q = 0$ . This gives

$$P = kTG \left( \frac{q_1}{q_0} \right)^{\frac{1}{2}} \left( \alpha - \frac{q}{q_1 \alpha^2} \right). \quad (22)$$

We have differentiated with respect to  $\alpha$ . Therefore, if  $P$  is to represent the force per unit cross-section (of unstretched swollen gel),  $G$  must be the number of chains per unit volume of the unstretched swollen gel, which is  $q_1^{-1}$  times that in the dry gel. The slope of the  $P - \alpha$  curve depends on the manner in which  $q$  changes with  $\alpha$  and this is determined by the swelling equilibrium in the stretched state (see below).

The stress per unit cross-section of the stretched gel would be  $P/\sigma^2 = Paq_1/q$ . This quantity, however, is of no particular physical interest, since the force  $P$  acts on the polymer and not on the solvent. The cross-section per unit mass of polymer is decreased in the ratio  $\alpha^{-1}$ , exactly as in the stretch of the dry substance. Therefore  $Pa$  represents the tension in the polymer network, and it is interesting to observe that in this general case too the tension is proportional to the double refraction. We forbear from giving a detailed derivation of the formula concerned. A calculation of the double refraction for a given distribution  $\psi$  can be found in ref. <sup>6</sup> and <sup>7</sup>, and it will suffice to mention that the result obtained by using the expression (19) for  $\psi$  is proportional to  $(q_1/q_0)^{\frac{1}{2}}(\alpha^2 - q/q_1\alpha)$ , i.e. proportional to  $P\alpha$ .

To study the equilibrium of the solvent with the deformed gel, we have to differentiate the entropy  $S$  in (21) with respect to the number  $n$  of solvent molecules. This differentiation must, of course, be carried out

at constant length (constant  $\alpha$ ), since otherwise the force  $P$  would do work on the system.<sup>23</sup> Adding the terms which account for the entropy and heat of mixing, and using the relation  $q = v_r^{-1} = (n + Zn')/Zn'$ , as before, a simple calculation gives:

$$\frac{\partial F}{\partial n} = kT \left[ \frac{1}{2} K v_r^2 + \ln(1 - v_r) + v_r + \frac{G}{Zn'} q_1^{-1} q_0^{-1} \frac{1}{\alpha} \right].$$

We have omitted the term of the order  $v_r/N$  which originates from  $kG \ln q$  in (21). At equilibrium the partial molecular free energy  $\partial F/\partial n$  of the solvent is zero. We observe that the activity of the solvent decreases at stretch, which means that the degree of swelling will increase. If  $q$  is sufficiently high, i.e., if  $v_r$  is small, we find, on expanding  $\ln(1 - v_r)$  and replacing  $G(Zn')^{-1}$  by  $N^{-1}$ :

$$v_r^2 = \frac{2}{1 - K} \frac{q^{-1/2}}{N q_0^{1/2}} \frac{1}{\alpha}, \text{ or } q = q_1 \sqrt{\alpha}. \quad (23)$$

For this particularly simple case the relation (22) between  $P$  and  $\alpha$  becomes

$$P = kTG \left( \frac{q_1}{q_0} \right)^{1/2} (\alpha - \alpha^{-3/2}). \quad (24)$$

Since  $G$  for a given network is proportional to  $q_1^{-1}$ , the modulus of elasticity referred to the initial cross-sectional area of the gel in the swollen condition will be proportional to  $q_1^{-1/2}$ .

The increase in volume of rubber gels in liquids as a result of stretch, and the force-strain behaviour of swollen rubber, was studied experimentally by Gee.<sup>24</sup> It may be mentioned in this connection that according to eqn. (24) we should not expect that the force  $P$  in stretched swollen rubber is proportional to  $\alpha - \alpha^{-3/2}$  as in dry rubber.

An increase in volume on stretching is also observed in swollen cellulose nitrate and cellulose acetate<sup>25</sup> as well as in re-swollen isotropic cellulose model filaments.<sup>26</sup> These gels are obtained if freshly prepared cellulose gels are dried in air and then re-swollen in water. Their volume is about half that of the original freshly prepared gel. It has been shown in earlier papers<sup>27</sup> that a number of properties of cellulose gels can be understood if one assumes a network of short chain-fragments. The average number  $N$  of independent links is close to 1 in the freshly prepared gel, which excludes coiling. The volume of the re-swollen gel, however, is reduced to such an extent that coiling, or folding of chains which is more or less equivalent to coiling, becomes effective.<sup>28</sup> It will be clear, however, that the theory developed so far must fail in these cases, since it assumes explicitly that  $N$  is a large number. This does not only apply to the distribution  $\psi_0$  in eqn. (1), but even more so to the assumption of affine deformation.<sup>27</sup>

To conclude, we want to make a few remarks on the quantities  $q_0$ ,  $N$  and  $G$ , which play a part in the application of the equations in practice. To begin with, it is clear that  $NG$  represents the number of chain-elements per unit of volume and thus is equal to  $Bq_1^{-1}$ , where  $B$  is a constant which

<sup>23</sup> In the formula (21) it is immaterial whether we differentiate with respect to  $q$  at constant  $\alpha$  or at constant length  $L$ , since constant  $\alpha$  means constant length: the relation between  $L$  and  $\alpha$  involves  $q_1$  but not  $q$ .

<sup>24</sup> Gee, *Trans. Faraday Soc.*, 1946, **42**, 585.

<sup>25</sup> Kruyt, Vermaas and Hermans, *Kolloid Z.*, 1942, **100**, 111; Kratky and Platzek, *Kolloid Z.*, 1939, **88**, 78.

<sup>26</sup> Hermans and Platzek, *Kolloid Z.*, 1941, **97**, 329; Hermans, *Cellulosechem.*, 1941, **19**, 122.

<sup>27</sup> Hermans, *Trans. Faraday Soc.* (Swelling and Shrinking Discussion, 1947), *J. Chim. physique* (in press).

<sup>28</sup> That a coiling or folding-up of molecular chains is an inevitable consequence in the contraction of swollen gels has previously been stressed by other authors: Kruyt, *Chim. et Ind.*, 1939, **42**, 1; Hermans, *Kolloid Z.*, 1941, **97**, 231.

depends on the polymer only. The value of  $q_0$  depends on the mechanism of gel-formation, and all statements concerning this value are as yet of a rather speculative nature. In polymers, which are cross-linked in the dry state:  $q_0 = 1$ , provided coiling is "normal" in the dry state. To give an example of quite a different nature, in the formation of cellulose xanthate gels from viscose, where the viscose is brought into sudden contact with a salt solution, it is tempting to assume that the coagulation simply amounts to a *sudden fixation* of the structure prevailing in the viscose, which would mean that the volume of the viscose itself is the volume  $q_0$  at which coiling is normal, provided coiling in the solution is normal. It is further not unreasonable in such cases to assume that the average length  $N$  between two successive junction points is inversely proportional to the concentration  $c$  of the solution,<sup>20</sup> which requires that the number  $G$  of chain-fragments in unit volume would be proportional to  $c^2$ .

Finally, it is perhaps not superfluous to emphasise that the theory assumes that no new junction points are formed on de-swelling. If junction points other than chemical cross-linkages play a part, this is by no means self-evident.

### Summary.

A short summary of the theory of rubber elasticity is given, and attention is drawn to a simple formula for the configurational entropy of an assembly of chains, eqn. (4). Most authors have assumed "affine deformation" of chain end-points; it is emphasised that this assumption is not a necessary one.

Our treatment of swelling phenomena differs from that given by Flory and Rehner, even though it also assumes that the chain end-points follow the macroscopic dimensions of the bulk rubber. A general formula for the configurational entropy of a deformed swollen network is derived (formula 21).

### Résumé.

On résume brièvement la théorie de l'élasticité du caoutchouc et on attire l'attention sur une formule simple pour l'entropie de configuration d'un assemblage de chaînes. La plupart des auteurs ont supposé—hypothèse nullement nécessaire—que les extrémités de chaîne suivent les dimensions macroscopiques du caoutchouc dans son ensemble (ce qu'on appelle déformation "alliée"). Bien qu'il postule, lui aussi, la déformation "alliée", le traitement des phénomènes de gonflement donné ici diffère de celui de Flory et Rehner et conduit à une formule générale pour l'entropie de configuration d'un réseau déformé par le gonflement.

### Zusammenfassung.

Der Artikel gibt eine kurze Zusammenfassung der Theorie der Kautschukelastizität und macht auf eine einfache Formel für die Konfigurationsentropie eines Ensembles von Ketten aufmerksam. Die meisten Autoren haben angenommen, dass die Dimensionen aller Kettenteile bei Deformation im selben Verhältnis wie die makroskopischen Dimensionen des Kautschukstücks verändert werden und es wird hervorgehoben, dass diese Annahme keineswegs notwendig ist.

Die vorliegende Theorie der Quellungserscheinungen ist verschieden von der von Flory und Rehner, obwohl auch angenommen wird, dass die Kettenenden den makroskopischen Dimensionen des Kautschuks folgen. Eine allgemeine Formel für die Konfigurationsentropie eines deformierten gequollenen Gitters wird abgeleitet.

N.V. Onderzoekingsinstituut Research,  
Utrecht, Holland.

<sup>20</sup> Hermans, *Kolloid Z.*, 1944, 106, 95.

# ELECTRIC POLARISATION IN KERATIN-WATER AND KERATIN-METHYL ALCOHOL SYSTEMS

By G. KING.

Received 11th July, 1946.

The total electric polarisation of a dielectric is classified as due to electronic, atomic, or orientation effects, according to the frequency of the applied field. In the case of hydrophilic substances no data appears to be available on atomic polarisation at infra-red frequencies, and very meagre data at frequencies corresponding to visible light. Fox and Finsh<sup>1</sup> have determined the refractive indices of various textile fibres for sodium light obtaining the values:

	$n_y$	$n_x$
Viscose Rayon . . . .	1.547	1.521
Wool . . . . .	1.556	1.547
Silk . . . . .	1.591	1.538

where  $n_y$  denotes the refractive index for the fibre axes parallel to the plane of polarisation of the light (i.e. perpendicular to the electric vector component). For all three substances, the electronic polarisation is slightly greater for fields perpendicular to the fibre axis, but the difference is not significant for the determination of preferential molecular alignments. No indication is given of the water content of the fibres.

More information is available at frequencies below  $10^7$  C.P.S. 2,3,4,5,6,7,8 Errera and Sack<sup>6</sup> have determined the dielectric constant ( $\epsilon$ ) of dry keratin and silk over this range and obtain a value of 4.2 in each case with a certain amount of dispersion at audio-frequencies; the direction of the applied field was perpendicular to the fibre axes. They suggest that it is chiefly the main polypeptide chains which contribute to

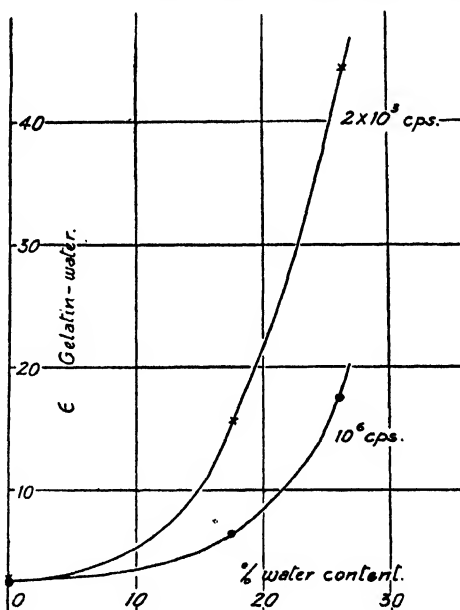


FIG. 1.

$\epsilon$ ; otherwise, different values would have been obtained for wool and silk

<sup>1</sup> Fox and Finsh, *Textile Res.*, 1940, 11, 62.

<sup>2</sup> Garton, *Technical Report A/T 78*, Brit. Electr. Allied Ind. Res. Assoc. (1940).

<sup>3</sup> Stoops, *J. Amer. Chem. Soc.*, 1934, 56, 1481.

<sup>4</sup> Argue and Maass, *Can. J. Res.*, 1935, 13, 3.

<sup>5</sup> Spencer Smith, *J. Text. Inst.*, 1935, 26, 11.

<sup>6</sup> Errera and Sack, *Ind. Eng. Chem.*, 1943, 35, 6, 712.

<sup>7</sup> Dunlap and Makower, *J. Physic. Chem.*, 1945, 49, 6, 601.

<sup>8</sup> Fricke and Parker, *J. Physic. Chem.*, 1940, 44, 716.



which differ from one another only in side-chain structure.<sup>9</sup> Cellulose differs from wool in that it exhibits a pronounced dispersion effect when dry, at radio frequencies,<sup>2,3</sup> while according to Garton,<sup>4</sup> absorbed water promotes a second dispersion band at low frequencies at normal temperatures; his results are restricted to very low water contents. He suggests that the absorbed water has the properties of a polar gas subject to a certain amount of restriction.

No accurate information seems to be available on the variation of  $\epsilon$  with water content, either of cellulose or of keratin due to the fact that investigators have in many instances used dispersed forms of these substances. The protein, gelatin, however, has been investigated over the whole range of concentrations from pure water to dry gelatin by Fricke and others.<sup>8</sup> Using their results Fig. 1 was obtained, which shows the increase in  $\epsilon$  and dispersion for water contents below 30 %; this is the range of water contents which is significant for keratin. Unlike keratin, dry gelatin has  $\epsilon$  very nearly equal to the square of the optical refractive index. The first 10 % or so of strongly bound water has little effect on the dielectric properties, but at about 50 % water content  $\epsilon$  reaches the extremely high maximum of 300. No discontinuities are observed for the gel-sol transition.

Fricke and his collaborators draw attention to the correlation which exists between the polarisability of the gelatin-water system and its mechanical properties. Influences which cause increased swelling, such as a change in  $pH$  from the isoelectric point, increase the polarisability. One explanation proposed is that the sorbed water loosens the forces between the gelatin molecules thus facilitating their rotation together with the combined water. Owing to the dipole ion character of the gelatin molecules, large moments and dielectric constants are possible according to this hypothesis. An alternative suggestion given by the authors is that the increase in  $\epsilon$  is due to the outer molecular layers of the less firmly bound water sorbed on the internal surfaces.

The present work deals with the variation in  $\epsilon$  of horn keratin with water and alcohol content for frequencies of 510 C.P.S.;  $1.1 \times 10^4$  C.P.S., and  $10^6$  C.P.S. The results obtained are similar in character to those outlined above, and are discussed in the light of the theory of multimolecular absorption.<sup>10</sup> Electrical anisotropy in horn keratin has also been investigated.

### Experimental.

A condenser of the parallel plate type was used. The dielectric consisted of two horn films each about 2.5 sq. cm. in area and  $5 \times 10^{-3}$  cm. thick, separating one inner and two outer electrodes, the latter being earthed to serve as a screen. The electrodes were of lead foil, and to ensure good electrical contact, each horn film was coated on either side with colloidal graphite over the area of contact. The assembled condenser was then clamped between two rigid brass plates at a pressure such that any further increase had no effect on the capacity when dry. No correction was made for any increase in pressure due to swelling.

The condenser (A), Fig. 2, was placed in a vacuum system, which in turn was housed in an air thermostat at 25° C. Vapour was introduced from the reservoir (R), and after about 24 hr. in the case of water, and 48 hr. in the case of methyl alcohol, for the attainment of equilibrium conditions indicated by a constant value of the capacity, the amount of vapour absorbed was measured directly by using a second sample of horn film (B), suspended from a spring.

The capacity of the condenser was measured at 510 C.P.S. using a simple form of Wien bridge. In order to cut down stray bridge-capacity effects,

<sup>9</sup> Astbury, *Fundamentals of Fibre Structure* (O.U.P., 1933).

<sup>10</sup> Cassie, *Trans. Faraday Soc.*, 1945, 41, 450.

a substitution method was used in which (A) was replaced by a standard low loss condenser in series with a non-inductive resistance box. At the higher frequencies the well-known resonance method was used employing an oscillator and crystal detector. The audio-frequency oscillator was calibrated using a phonic wheel and oscillograph, while the radio frequency ( $10^6$  c.p.s.) corresponds to the B.B.C. overseas wavelength. Condensers were made using horn films cut parallel and perpendicular to the fibre axis. In the latter case measurements were made at  $10^4$  c.p.s. only.

### Discussion.

Fig. 3 shows the relations obtained between the dielectric constant of the horn and its percentage water content

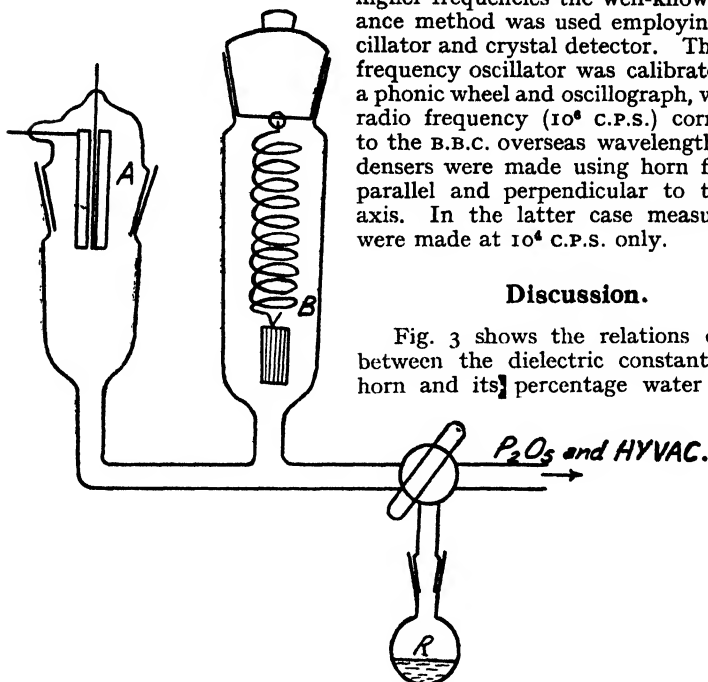


FIG. 2.

for the three frequencies when the films were cut parallel to the fibre axis. The results are similar to those shown in Fig. 1. A small but well-defined dispersion is shown at "zero" water content even when the condenser was evacuated at  $100^\circ\text{C}$ . and must be due to the keratin alone as suggested by Errera and Sack.<sup>6</sup> Fig. 4 shows similar relations for the sorption of methyl alcohol. Much smaller increases in  $\epsilon$  are obtained because of the reduced molar sorption of the alcohol as compared with water.

Accurate estimation of  $\epsilon$  depends largely on accurate measurement of the mean thickness of the horn films, the error in which introduces a constant error of 3-4 % in the results, so that the close agreement with Errera and Sack's results for dry keratin<sup>6</sup> is fortuitous. Increased accuracy could no doubt be achieved in this respect by the use of thicker samples, but this would make it very difficult to ascertain when equilibrium had been reached, due to the slow rate of sorption. Samples cut perpendicular to the fibre axis gave values of 5.4 and 5.6 for  $\epsilon$  of dry horn.

### Molar Polarisation of the Sorbed Water in Horn.

Burton, Turnbull and others<sup>11</sup> have used Debye's relation for the dielectric constant of mixtures to determine the effective polarisation of water of crystallisation for a series of salts. This relation states that :

$$\frac{\epsilon - 1}{\epsilon + 2} \cdot \frac{\sum M_r \cdot f_r}{\rho} = \sum P_r \cdot f_r \quad . \quad . \quad . \quad (1)$$

<sup>11</sup> Burton and Turnbull, *Proc. Roy. Soc., A.*, 1937, 158, 194.

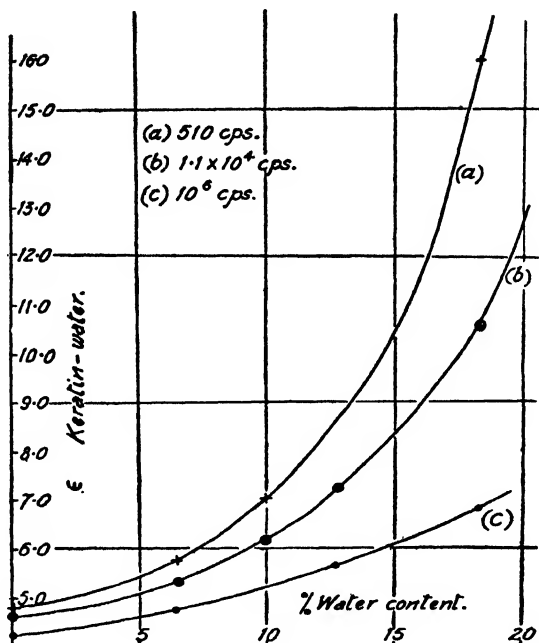


FIG. 3.

where  $\rho$  is the density of the mixture,  $f_r$  is the mol. fraction of component  $r$ ,

$M_r$  is the mol. weight of component  $r$ ,  $P_r$  is the molar polarisation of component  $r$ ,  $\epsilon$  is the dielectric constant of the keratin-absorbate system.

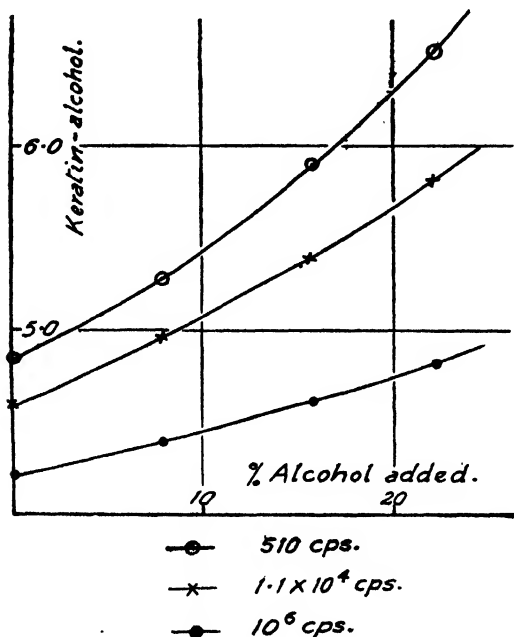


FIG. 4.

It is only true for isotropic mixtures when there is no interaction between the components. This is not strictly true for the compounds used, but the use of (1) is justified in that the molar polarisation of the water of crystallisation has a consistent value of approximately 8 cc. in each case, indicating sufficient restriction to remove orientation effects.

If the increase in  $\epsilon$  of the keratin-water, or -alcohol systems is due to the absorbate alone, it should be possible to apply relation (1) to this system. Cassie<sup>10</sup> has

shown that a certain fraction of the water sorbed by keratin is localised

in low-energy sites, the remainder being mobile with liquid properties, and this suggests that (1) should be expanded in the form

$$\frac{\epsilon - 1}{\epsilon + 2} \cdot \frac{M_K \cdot f_K + M_A \cdot f_A}{\rho} = P_K \cdot f_K + P_X \cdot f_X + P_{(A-X)} \cdot f_{(A-X)} \quad (2)$$

where  $\epsilon$  is the dielectric constant of the keratin-absorbate system,  
 $M_K$  is the average molecular weight of keratin per amino acid residue,  
 $M_A$  is the molecular weight of the absorbate,  
 $\rho$  is the density of the keratin absorbate system,  
 $P_K, f_K$  are the molar polarisation and mol. fraction respectively of the keratin alone,  
 $P_X, f_X$  are the molar polarisation and mol. fraction respectively of the localised water,  
 $P_{(A-X)}, f_{(A-X)}$  are the molar polarisation and mol. fraction respectively of the "mobile" water.  
 $(P_K, P_X, P_{(A-X)})$  are, of course, functions of the frequency of the applied field.)

The use of a relation such as (2) is further justified in that a reasonably linear relationship exists between the dielectric dispersion and  $f_{(A-X)}$ , Fig. 5, implying that orientation effects are due to the mobile fraction of the sorbed water as suggested by Fricke and Parker for gelatin.

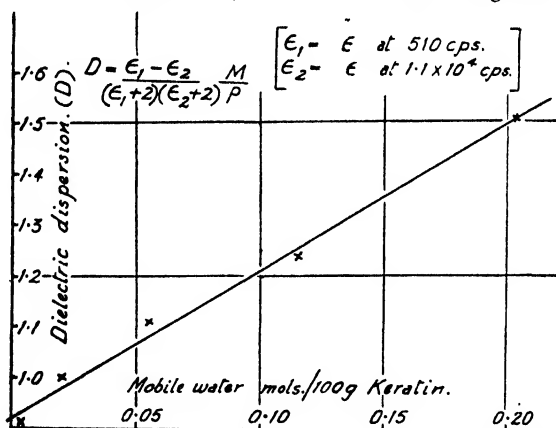


FIG. 5.

Assuming Astbury's value<sup>12</sup> of 118 for the average molecular weight of amino acid residues in keratin,  $P_K$  becomes 51, 50, and 47 cc. at 510, 10<sup>6</sup>, and 10<sup>6</sup> cps. respectively. Values for  $f_X$  and  $f_{(A-X)}$  may be obtained from Cassie's results for water sorption by keratin, when relation (2) may be fitted to curves (a), (b) and (c) of Fig. 3 assuming  $P_X = 8$  cc., and leaving  $P_{(A-X)}$  open to adjustment; the results are shown in Table I.

The calculated values of  $\epsilon$  tend to be low for low water contents, and increasing  $P_{(A-X)}$  to correct for this produces abnormally high values of  $\epsilon$  at higher water contents. The exceedingly high values of  $P_{(A-X)}$  at low frequencies is in accord with Garton's observations that the sorbed water in cellulose has the properties of a polar gas. This is difficult to reconcile with the restricted rotation implied by the audio-frequency dispersion. In the case of cellulose, for instance, Garton's results give an energy of activation for the orientation of the sorbed water,<sup>13</sup> of 12 kcal., and an entropy of activation of 13 E.U., both values being very similar to

<sup>12</sup> Astbury, *J. Chem. Soc.*, 1942, 337.

<sup>13</sup> Kauzmann, *Rev. Mod. Phys.*, 1942, 14, 12.

TABLE I.

Frequency (c.f.s.)	$P_x$ (cc.)	$P_{(\lambda-x)}$ (cc.)	$\epsilon$ (Observed).	$\epsilon$ (Calculated).	% Water Content.
510	8	140	6.0 9.7 15.0	5.5 9.5 17.0	7.2 14.4 18.0
$1.1 \times 10^4$	8	100	5.5 8.0 10.3	5.0 7.4 10.5	7.2 14.4 18.0
$10^6$	8	80	4.8 6.0 6.7	4.5 5.9 7.4	7.2 14.4 18.0

those for molecular rotation in ice, indicating a rotational mechanism of at least equal complexity. The very broad dispersion band, however, suggests a relaxation phenomenon more characteristic of long chain polymers.

In the case of the sorption of methyl alcohol, Fig. 4, one must take into account the reduced molar sorption<sup>14</sup> in calculating the corresponding values of  $\epsilon$ . Cassie's relations for the sorption of water by keratin<sup>10</sup> may be used to determine  $f_x$  and  $f_{(\lambda-x)}$  on the assumption that  $\omega$  the heat of sorption on to the low energy sites is 5.4 kcal. as compared with 3.5 kcal. for water, and assuming the absorption isotherms to be the same.<sup>14</sup> Then assuming a value of 12 cc. for  $P_x$ ,<sup>15</sup> the calculated values of  $\epsilon$  are again low for low alcohol concentrations unless  $P_{(\lambda-x)}$  is abnormally large.

### Rotation in the Keratin Lattice.

As in the case of gelatin, an alternative explanation is that the polar groups in the keratin lattice itself contribute to the observed increases in  $\epsilon$ . The presence of an appreciable amount of dielectric dispersion in dry keratin is attributed by Errera and Sack<sup>6</sup> to the rotation of the CO and NH polar groups, and if we look upon the absorbed water as a plasticiser, then apart from any dipole rotation of the water molecules, there should be increased probability of motion of the polypeptide chains.

Baker and Yager<sup>16</sup> have made a comprehensive study of rotation in polyamides which have a molecular structure resembling  $\alpha$ - and  $\beta$ -keratin<sup>17</sup> in many respects. (Fig. 6(a) and 6(b).) They suggest that oscillation of relatively short sections of the polymer chains is possible, restricted by hydrogen bonding between adjacent CO and NH groups. The sorption of water by these polyamides increases  $\epsilon$  and the dielectric dispersion slightly up to 60 % R.H. followed by a relatively large increase at saturation. The water is considered to have a plasticising action facilitating chain motion of the whole system by breaking inter-molecular polyamide bonds, and combining with the amido groups.

Although the keratin structure is more complicated because of the presence of the various types of side chains, there is every reason to believe that a similar mechanism of chain rotation may be present, causing oscillation of the CO and NH groups or even of the (CONH) group as a whole,

<sup>14</sup> King, *Trans. Faraday Soc.*, (in press).

<sup>15</sup> Hilderbrand, *Solubility* (Reinhold Pub. Corp.).

<sup>16</sup> Baker and Yager, *J. Amer. Chem. Soc.*, 1942, 64, 9, 2176.

<sup>17</sup> Astbury and Bell, *Nature*, 1941, 147, 696, 3736.

which has a dipole moment of 3.8 e.s.u.;<sup>18</sup> the rotation of this group with or without attached water molecules may be sufficient to account for the high observed polarisations.

Inspection of Fig. 6(a) shows that this is a reasonable supposition. Three adjacent coplanar polypeptide chains have been drawn to scale using Neurath's<sup>19</sup> values for atomic dimensions and angles. Atomic radii are indicated by arcs of circles, broken lines indicating groups below the plane of the diagram; the side chain groups are indicated by R and extend alternately above and below the plane of the diagram. If the adsorbed water breaks the hydrogen bonds between adjacent NH and CO groups, then the group ( $N_1C_1O_1H_1$ ), for example, may rotate partially about the axis ( $C_1H_1R_1 - C^1H^1R^1$ ) provided  $O_1$  rises above the plane of the diagram, i.e. away from the group  $R^1$  situated below the plane. If the bound water molecule rotates with the (CONH) group some lattice distortion must occur and this must be linked with the swelling action. Association of the bound water with the CO groups in the main polypeptide chains agrees with Cassie's conclusions on the sorption process.<sup>10</sup>

Increased rotation of groups of atoms in the keratin lattice requires an increase in entropy of the keratin-water system as the water content is increased. Cassie<sup>10</sup> states that such an increase in entropy is required to account for the sorption in excess of the monolayer, associating the entropy increase with the water only. There is no reason, however, why this "mixing entropy" should not be related to the configurational entropy of the loosened polypeptide chains.

### The Plasticising Mechanism.

In the case of polyvinylchloride-plasticiser systems it has been shown that a definite relationship exists between the elastic modulus and the probability of rotation of portions of the polymer chains.<sup>20</sup> A similar condition also appears to be true in the case of keratin-water systems. As the water initially absorbed is ineffective in decreasing the elastic modulus of keratin, the decrease obtained in the later stages of sorption has been associated with the mobile or loosely bound fraction,<sup>21</sup> while according to Fig. 5, this is also true of the dielectric dispersion which in turn must be the result of molecular rotation in one form or another.

Cotton cellulose differs from keratin in that Pierce<sup>22</sup> obtains a linear relationship between the combined fraction of sorbed water and the corresponding reduction in relative rigidity, and he regards this fraction as responsible for changes in the physical properties during sorption. This would appear to be a more plausible explanation of the plasticising action as it is difficult to envisage the mobile fraction of the sorbed water breaking interchain hydrogen bonds in either of these cases without relatively large energy changes taking place.

The two conflicting hypotheses may be reconciled if in the case of the keratin-water system we associate the loosening of the polypeptide chain structure with the bound fraction of the absorbate also, with the restriction that in order to free a length of chain sufficient for reorientation, more than one adjacent intermolecular or, in the case of  $\alpha$ -keratin,<sup>17</sup> interfold bond must be broken. The probability of such an occurrence will be a non-linear function of the concentration of the "bound" water, assuming one bond is broken per water molecule sorbed on to a low energy site. The following very simplified example serves to illustrate this possibility.

Let there be  $N$  adjacent rotatable links in the polypeptide chain system per 100 g. of keratin, and in the dry state suppose each of these is bound

<sup>18</sup> Cohn, *Rev. Biochem.*, 1935, 4, 93.

<sup>19</sup> Neurath, *J. Physic. Chem.*, 1940, 44, 296.

<sup>20</sup> Davies, Miller and Busse, *J. Amer. Chem. Soc.*, 1941, 63, 2, 361.

<sup>21</sup> Speakman, *Trans. Faraday Soc.*, 1944, 40, 6.

<sup>22</sup> Pierce, *J. Text. Inst., T.*, 1929, 20, 133.

by  $K$  interchain bonds. Then if  $p$  is the chance of a single bond being broken, the chance of a link becoming free is  $p^2$ . If  $(Np)$  molecules of the absorbate are distributed throughout, then the number of freed links is  $Np^2$ . But  $N$  represents the number of low energy sites available to

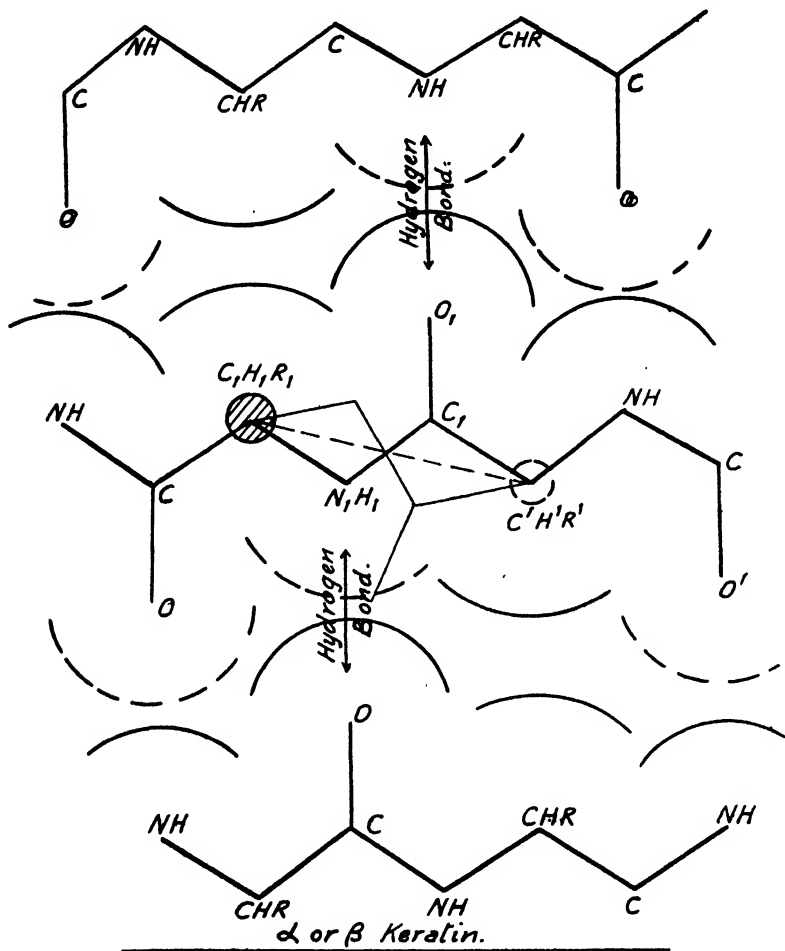


FIG. 6(a)

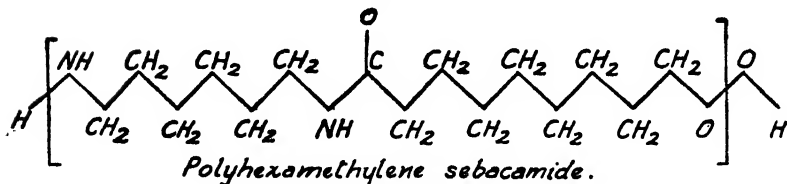


FIG. 6(b)

the absorbate molecules, i.e.  $B$  in Cassie's notation,<sup>10</sup> and  $p$  is the fraction of these filled, i.e.  $(X/B)$  in the same notation. Therefore the number of freed links is  $B \cdot (X/B)^2$ .

If, as previously suggested, it is the  $(\text{NCOH})$  group which rotates as a unit, Fig. 6(a), then two hydrogen bonds must be broken to free the group ;

$K = 2$  and the reduction in elastic modulus with absorption should be roughly proportional to  $X^2$  in the early stages of sorption.

In order to check this experimentally, the reduction in the modulus of rigidity of a wool fibre due to the sorption of water and of methyl alcohol respectively was measured, using essentially the method of Speakman.<sup>22</sup> The apparatus in Fig. 2 was employed, replacing the condenser system by one enclosing a wool fibre capable of undergoing torsional oscillation. The results are shown in Fig. 7. They differ from those of Speakman,<sup>22</sup> in the case of water, in that a different swelling correction was employed,<sup>24</sup> which is more complete at low water contents than Hirst's relation used by Speakman. A proportionately greater swelling was assumed for the methyl alcohol, for Hirst<sup>26</sup> has found that wool fibres swell equally in methyl alcohol and water, for which the amounts sorbed at saturation are 28 % and 33 % respectively. A relation

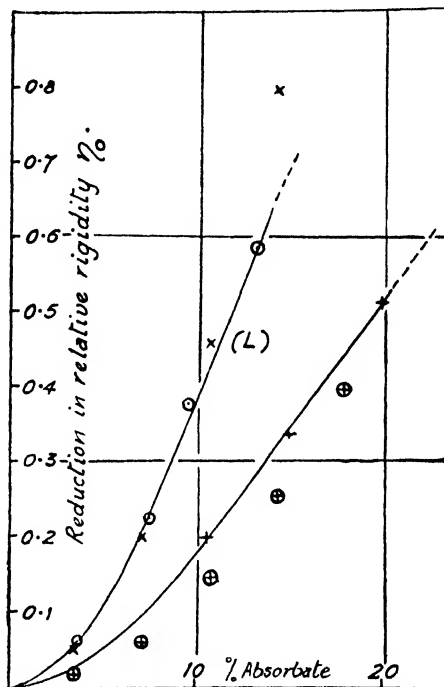
$$\eta = K \cdot X^2 \quad (3)$$

was fitted to the experimental results for a water-wool system at L, Fig. 7, where  $\eta$  is the relative reduction in rigidity,  $K$  is a constant, and Cassie's values for  $X$ <sup>10</sup> have been used. As mentioned earlier in the paper, values for  $X$  in the case of methyl alcohol sorption may be obtained from the corresponding relations for water. Equation (3) can then be applied to the alcohol-keratin system assuming a similar value of  $K$  as for water, and a reasonable fit with the experimental results is obtained.

Such a theory of molecular rotation is also applicable to the estimation of the  $\epsilon$  of keratin-water, or alcohol systems, applying relation (1). For  $X$  mols. of absorbate, sorbed on to low energy sites per 100 g. of keratin,  $1.18 B(X/B)^2$  links are free to rotate with or without attached absorbate molecules, per mol. of amino acid residues. Let these rotating dipoles introduce a molar polarisation  $P_{KX}$ , then as before :

$$\frac{\epsilon - 1}{\epsilon + 1} \cdot \frac{M_K \cdot f_K + M_A f_A}{\rho} = P_K \cdot f_K + 1.18 B(X/B)^2 P_{KX} + f_X \cdot P_X + f_{(A-X)} \cdot P_{(A-X)} \quad (4)$$

where  $P_X$  represents the atomic and electronic contributions of the bound fraction of the absorbate. The dipole moment of the (NHCO) group is



⊗ Water (experiment).

×  $\eta = Kx^2$  fitted at L.

+ Methyl alcohol (experiment).

⊕  $\eta = Kx^2$  [ $K$  as for water].

FIG. 7

<sup>22</sup> Speakman, *Trans. Faraday Soc.*, 1929, **25**, 92.

<sup>23</sup> King, *J. Text. Inst.*, T., 1926, **17**, 53.

<sup>24</sup> Wool Ind. Res. Assoc. (private publication).



## 610 POLARISATION IN KERATIN-WATER AND -METHYL

3.8 E.S.U. as compared with 1.8 for water and 1.7 for methyl alcohol, so without allowing for a dipolar contribution of the bound fraction of the absorbate,  $P_{\text{KX}}$  may be assumed to have values as much as four times those for ice at low frequencies. Table II shows comparative values obtained using relation (4) in the case of water, and it is seen that quite reasonable values of  $P_{\text{KX}}$  give a very close correspondence with the observed values of  $\epsilon$ .

In the case of methyl alcohol  $P_{\text{X}}$  is taken as 12 cc.,<sup>18</sup> while  $P_{(\text{A}-\text{X})}$  is increased by a like amount over and above the corresponding value for water, but this latter factor is not significant in determining the final

TABLE II.

Frequency (c.p.s.)	$P_{\text{X}}$ (cc.)	$P_{(\text{A}-\text{X})}$ (cc.)	$P_{\text{KX}}$ (cc.)	$\epsilon$ Fig. (3).	$\epsilon$ Relation (4).	% Water Content.
510	8	18	40	6.0	6.2	7.2
				9.7	10.5	14.4
				15.0	15.5	18.0
$1.1 \times 10^4$	8	15	30	5.5	5.5	7.2
				8.0	8.0	14.4
				10.3	10.0	18.0
$10^6$	8	10	20	4.8	4.7	7.2
				6.0	5.9	14.4
				6.7	6.6	18.0

result due to the small molar fraction of "mobile" methyl alcohol present in the sorption range considered. The results for methyl alcohol are given in Table III for the frequency of 510 c.p.s. only, the results for the other frequencies are equally consistent. It will be noted that a lower value of  $P_{\text{KX}}$  is required and implies that rotation is further restricted in this case, but it would be unwise to theorise further from such an isolated observation.

Fricke and others<sup>20</sup> have shown that many different suspensions and colloids containing water as the dispersion medium exhibit exceedingly high values of  $\epsilon$  with associated dispersion effects which lead them to conclude that the phenomenon is due to interphase water films. The

TABLE III.

Frequency (c.p.s.)	$P_{\text{X}}$ (cc.)	$P_{(\text{A}-\text{X})}$ (cc.)	$P_{\text{KX}}$ (cc.)	$\epsilon$ Fig. (4).	$\epsilon$ Relation (4).	% Alcohol Content.
510	12	22	25	5.3	5.2	8.0
				5.9	5.7	16.0
				6.3	6.2	20.0

theory requires such films to be as much as 1000 Å. thick, built up of water dipoles in a chain-like structure, "ferro-electric" by nature, and exhibiting high polarisabilities by concerted rotation.

In the case of keratin, at 20 % water content there are, according to Cassie's results, 0.24 mol of "mobile" water and 0.96 mol. of localised water per mol. of amino acid residues, i.e., absorption over and above the monolayer is very incomplete. If then, the high polarisation values obtained are due to the mobile fraction alone, the chance of producing a "dipole chain" of only two such mobile water molecules is still very re-

<sup>20</sup> Fricke and Curtis, *J. Physic. Chem.*, 1937, 41, 729.

mote, so that even allowing for a polarisation factor proportional to the square of the dipole moment no abnormal values are probable.

It is noticeable that all the substances which exhibit high values of  $\epsilon$  when suspended in water are capable of thixotropic or clay gelation and a similar theory of inter-phase water films has been used to explain this effect. Russell and Rideal,<sup>17</sup> however, suggest a more plausible explanation in that a gel forming material must be also present in these systems, partly as a coating on the suspensoid particles and partly as a fine dispersion throughout the liquid medium. They also point out that nearly all thixotropic sols show strong stream double refraction, and therefore consist of particles which are both anisotropic and markedly anisometric. The abnormal dielectric properties of these suspensions may well be a property of this highly dispersed gel forming substance.

Until some more critical test is applied to such hydrophilic systems to determine the relative contributions of absorbate and absorbent to the dielectric increment, no definite conclusions may be drawn. The results with the keratin-water and alcohol systems do suggest that the increased  $\epsilon$  is a property of the absorbent as well as of the absorbate. In this case also, one fact is certain, that there is insufficient mobile water present to build up the chain-like structure required by the hypothesis of Fricke and his collaborators, so that the mobile water fraction alone cannot produce the high observed polarisibilities.

I am grateful to Dr. A. B. D. Cassie, Dr. H. E. Daniels and Mr. R. C. Palmer for discussion of these problems, and to the Director and Council of the Wool Industries Research Association, for permission to publish these results.

### Summary.

The dielectric constant of water-keratin and methyl alcohol-keratin systems has been investigated for increasing concentrations of the absorbate. The results are examined in the light of the multimolecular theory of sorption<sup>10</sup> and it is concluded that the increase in dielectric constant is unlikely to be a function of the absorbate alone. A comparison is drawn between the dielectric dispersion and the elastic properties of keratin-water systems. It is suggested that in both cases the "bound" water fraction breaks hydrogen bonds between the polypeptide chains, allowing increased freedom of rotation of polar groups in these chains.

### Résumé.

La constante diélectrique des systèmes kératine-eau et kératine-alcool méthyl-ique a été étudiée pour des concentrations croissantes de l'absorbat. On examine les résultats d'après la théorie multimoléculaire de sorption et on conclut qu'il est peu probable que l'accroissement de la constante diélectrique soit une fonction de l'absorbat seul. On compare la dispersion diélectrique et les propriétés élastiques des systèmes kératine-eau. Enfin l'on suggère que dans les deux cas la portion d'eau "liée" rompt les liaisons hydrogène entre les chaînes polypeptidiques, accroissant la liberté de rotation des groupes polaires dans ces chaînes.

### Zusammenfassung.

Die Dielektrizitätskonstante der Systeme Wasser-Keratin und Methylalkohol-Keratin ist bei verschiedenen Konzentrationen des Absorbats gemessen worden. Die Ergebnisse werden im Licht der Theorie der multimolekularen Sorption<sup>10</sup> untersucht und es wird geschlossen, dass es unwahrscheinlich ist, dass der Zuwachs in der Dielektrizitätskonstante nur vom Absorbat allein abhängt. Die dielektrische Dispersion und elastischen Eigenschaften des Keratin-Wasser-Systems werden verglichen und es wird vorgeschlagen, dass in beiden Fällen das "gebundene" Wasser Wasserstoffbindungen zwischen Polypeptidketten abbricht und dadurch den polaren Gruppen in diesen Ketten grössere Drehungsfreiheit gibt.

<sup>17</sup> Russell and Rideal, *Proc. Roy. Soc. A.*, 1936, **154**, 548.

## REVIEWS OF BOOKS.

**Modern Advances in Inorganic Chemistry.** By E. B. MAXTED.  
Oxford University Press (Geoffrey Cumberlege, 1947). Pp. 296.  
Price 20s.

The author has attempted to break away from the traditional treatment of inorganic chemistry in terms of the periodic system and to bring into greater prominence the later knowledge of atomic and nuclear structure. The first 80 pages therefore consists of an elementary outline of the physical concepts which are required in the later chapters. A judgment on this introduction would have been easier if the author had identified the class of reader for whom the book was written. Judging from the sections on the chemistry of hafnium, masurium, rhenium and the recent work on the halogen compounds, it is intended for those studying for the Special B.Sc. degree, or its equivalent. With this assumption, then it is thought that much of the elementary material could have been omitted or abbreviated and that such topics as the wave-mechanical atom, hybridisation of bonds, the concept of resonance, etc., could have been treated if not more fully, then at least in a more quantitative manner. We suspect in any case that the greater part of the subject-matter is covered by the undergraduate in his physical chemistry course, and moreover, if this were unfortunately not the case, then he would acquire a very superficial knowledge by reading about them here. Many, however, may argue that this introductory chapter is useful since it brings together a large range of material within the cover of a single book.

Despite the author's attempt to replace the classical systemisation, the subsequent 140 pages, comprising chapters on hydrogen and its isotopes, the recent chemistry of the halogens, hafnium, masurium and rhenium, he follows very closely the traditional lines, and only occasionally remembers his aim, e.g. by the inclusion of details of structure determined by physico-chemical methods. The chapters on hafnium, masurium and rhenium are valuable since much of the data given are widely scattered in the literature or is available only in the German texts of v. Hevesy and of the Noddacks. On the other hand, the chapters on the halogens, hydrogen, and reactions in the discharge tube contribute little more than may be found in the more orthodox, up-to-date treatises on General and Inorganic Chemistry.

The last two sections are concerned with the preparation, properties and uses of artificial radioelements and with the transuranic elements. Attention has been focussed primarily on radio-sodium, -phosphorus, -carbon and -bromine; there is far too much elementary chemistry crowded into the chemical identification of the radioactive products and the greater part of the data presented on disintegration and preparations could have been tabulated. Much space would have been saved and the reader would have been able to get a clearer and more general picture of nuclear reactions. The final chapter on uranium and the transuranic elements is a short recapitulation on what is generally known about these substances together with a short summary of the published knowledge of nuclear fission. It must, of necessity, be a disappointing finale.

An opinion about this book will depend on the reader's views of "omnibus" volumes; if he appreciates a collection of topics, few of which are sufficiently deeply discussed, he will be gratified by the easily readable treatment, the well-written chapter and the meticulous punctuation of the present work. Otherwise he must, like the reviewer, regard it as a luxury in times of short supply of paper—there are quite a few books in the publisher's lists which could have, in preference, been re-printed. A volume on advanced general or inorganic chemistry is needed—we do not think that this is the one.

**Kinetic Theory of Liquids.** By J. FRENKEL. Published by the Oxford University Press and Geoffrey Cumberlege, 1946. Pp. 488. Price 40s. net.

Until quite recently, the gas-like qualities of liquid bodies have been emphasised at the expense of their solid-like properties. This is perhaps to be accounted for by the success of the van der Waals' theory in explaining, although only qualitatively, certain properties characteristic of the liquid state and its relationship to the solid state. As a result it has become common practice to over-estimate the differences of structure in solid and liquid bodies, assuming a crystalline structure in the one case, and an amorphous structure in the other, and to assume a different response to the application of shearing stresses, which are supposed to cause elastic strain in solids, and viscous flow in liquids.

Prof. Frenkel believes that these distinctions are far less drastic and fundamental than hitherto supposed. In this view he is well supported by a good deal of experimental evidence. Under high shearing stresses, solids show a phenomenon of plastic flow, which is somewhat similar to the viscous flow of liquids, while on the other hand, liquid bodies display a shearing elasticity, none the less real, although usually masked by their high fluidity. X-ray diffraction studies of liquids have disclosed the fact, that the arrangement of molecules in the liquid, especially near the crystallisation point, is quite different from the wholly disordered arrangement found in the gaseous state, but for small distances bears a close similarity to the completely regular arrangement into which it is transformed, when the liquid crystallises.

At high temperatures, near the critical point, and at moderate pressures, there is a close similarity between liquids and gases, but at temperatures in the vicinity of the crystallisation point, it is more correct to regard the liquid as a solid, from which the long-range order is missing, but which retains a high degree of local (short-range) order, of the same type as that characteristic of the corresponding solid. This is the basis of Frenkel's thesis, and he accordingly develops his kinetic theory of liquids, as a generalisation and extension of the kinetic theory of solid bodies.

The first two chapters of his book are devoted to the kinetic theory of lattice defects in crystals at high temperatures, to the transport of ions and holes through crystals, and to disturbance of the short- and long-range order in molecular crystals. A general thermodynamic theory of the phenomena associated with variation of the degree of order is developed, and in a subsequent chapter applied to the melting process. It is shown that in the neighbourhood of the crystallisation point, the

character of the heat motion in liquids is the same as that in solids, and two chapters discuss the significance of this fact in relation to the mechanical and electrical properties of liquids. The next two deal with surface phenomena, and with the kinetics of phase transformations, and the book ends with a treatment of the properties of solutions, and of polymeric substances.

If the book is to be criticised in any respect, it may be noted that it contains few references to recent work in this field by scientists in this country, but this is easily understood, if it is remembered that the manuscript was written in 1943, a year of crucial importance to the war effort of the Soviet Union.

Prof. Frenkel has made a stimulating contribution to the literature of this subject, which merits the attention of physical chemists, who might be induced to play a greater part than they have hitherto done, in the development of the theory of liquids.

R. C. S.

**Guide to the Literature of Mathematics and Physics.** By NATHAN GREER PARKE III. McGraw-Hill Book Co., Inc., 1947. Pp. xv + 205. Price 25s.

This book should be in every University library—not necessarily, we believe, because of its main purpose in providing a guide of 1800 references to books covering the field of mathematics and physics, but because of its first four chapters on reading, reference, and library technique. This is not to detract from its value as a guide book to a wide variety of subjects ranging from algebra to nuclear physics; it should prove of use to the industrial scientists who cannot maintain complete awareness of the reference literature; to the student who wishes to know where to find information; and to the librarian who will find much of interest in classification and indexing. It is doubtful whether the average research worker or the University lecturer will find very much in the bibliographic part of the guide about which he is not aware—the average University library together with book reviews such as appear in many scientific journals will have informed them of their existence and their general contents. Moreover, the bibliography is by no means complete, e.g., the first entry, adsorption, makes no mention of the book by McBain or by Freundlich—these are, it is true, somewhat outmoded but few adsorptionists particularly with industrial bias would not find places on their shelves for these informative volumes—one might cite other examples of this kind.

The first part of the book deals with the principles of reading and study and gives many useful hints and much encouragement to the student who embarks upon an entirely new subject; it includes short sections on such topics as the psychology of learning and physical factors in study, on the origin of theory and the convergence of ideas etc. It then deals with self-directed education and the basic principles of literature search; and ends with much detailed information on cataloguing and indexing, much of which will have more direct value in America than in England. Browsing through a guide of this sort is an interesting and useful occupation; one doubts, however, whether the individual would feel that it would justify a personal expenditure of 25s.

## MULTIMOLECULAR ABSORPTION II.

By A. B. D. CASSIE.

Received 29th January, 1946.

### 1. Introductory.

The limited absorption of liquids by gels, such as rubber and keratin, has been described as solution<sup>1, 2</sup> and as multimolecular absorption.<sup>3, 4, 5</sup> The solution theory<sup>2</sup> appears to apply with considerable success to the absorption of organic liquids by rubber, where there are no localised sites of strong exothermic sorption, and where segments of the long rubber molecules are sufficiently free to interchange with the solvent molecules. The sorption of water by wool or keratin, on the other hand, is known to take place in part on to sites with a large evolution of heat, and it is difficult to visualise elements in the keratin structure that could freely interchange places with the water molecules; in short, the sorption of water by keratin provides a much more heterogeneous system than does the sorption of organic liquids by rubber.

An earlier paper<sup>3</sup> applied Branauer, Emmett and Teller's theory<sup>6</sup> of multimolecular absorption on to a free surface to the sorption of water by wool. There are, of course, no free surfaces in the ordinary sense in the bulk of wool or keratin, but the system can be effectively reduced to one of free surfaces by allowing for the energy of swelling of the gel before applying the multimolecular sorption equations. This was the procedure that was followed in the earlier paper.<sup>3</sup> An alternative procedure is to calculate the interfacial energy of water molecules surrounded by keratin, as Langmuir<sup>7</sup> has done for liquids, and after the interfacial energy due to keratin being a bulk material has been allowed for, the equations for sorption on to free surfaces may be applied. In calculating the interfacial energies, the effect of low energy localised sites is ignored, as they are included in the multimolecular sorption isotherms for free surfaces. The difficulty of applying Langmuir's method to keratin is lack of quantitative data, and as the interfacial energy and swelling energy represent different approaches to the same problem, it seems better to use swelling energies where at least semi-quantitative data are available. It is easy to show, however, that interfacial energies will give results of the same order of magnitude and with the same trends as the previous data.<sup>3</sup>

The present paper shows that if the molecules are absorbed as clusters at the localised sites, it may be permissible to count as distinct configurations those that are obtained by interchanging clusters of different size, and the increase in the number of distinguishable configurations given by this method of counting, gives the required increase of entropy.<sup>8</sup>

<sup>1</sup> Katz, *Kolloidchem. Bei.*, 1917-18, 9, 1.

<sup>2</sup> Gee, *Trans. Faraday Soc.*, 1942, 38, 276.

<sup>3</sup> Cassie, *ibid.*, 1945, 41, 458.

<sup>4</sup> Bull, *J. Amer. Chem. Soc.*, 1944, 66, 1499.

<sup>5</sup> Pauling, *ibid.*, 1945, 67, 555.

<sup>6</sup> Brunauer, Emmett and Teller, *ibid.*, 1938, 60, 309. (Referred to as B.E.T.)

<sup>7</sup> Langmuir, *Colloid Symposium Monograph* (The Chemical Catalog Co. Inc., New York, 1925), 3, 48.

<sup>8</sup> Cassie, *Trans. Faraday Soc.*, 1945, 41, 450. (Referred to as Part I.)

## 2. Derivation of the Multimolecular Isotherm.

The absorption is assumed to take place in the form of clusters around the localised sites: molecules will first be absorbed singly on to the sites; each molecule absorbed into this monolayer will have an amount of energy  $w$  less than that of a molecule in the bulk liquid, and its partition function will be different from that for a molecule in the liquid. Clusters begin to form as the number of absorbed molecules increases. A cluster forms around the molecule absorbed on the localised site, and it will be assumed that the molecules in the cluster, apart from the one absorbed on to the site, are identical in energy and partition function with those in the bulk liquid. This conception of a cluster is in accord with the current idea of very short range molecular forces, which led B.E.T.<sup>6</sup> to abandon the polarisation theory of multimolecular absorption.

Let  $B$  be the total number of localised sites, and let  $a_0$  of the sites contain 0 molecules,  $a_1$  contain 1 molecule, and  $a_r$  each contain  $r$  molecules. A cluster of  $r$  molecules on one site is assumed to be distinguishable from a cluster of  $s$  molecules on another site, and when  $r \neq s$  interchange of the two clusters will give rise to a new and distinct configuration of the system.

The number of distinct configurations of  $a_0, a_1, a_2, \dots, a_r, \dots$  clusters on  $B$  sites, the members of each group  $a_r$  being assumed to be identical, is

$$g = \frac{B!}{a_0! a_1! \dots a_r! \dots} \quad (1)$$

We also have

$$\sum_{r=0} a_r = B \quad (2)$$

$$\sum_{r=1} r a_r = A \quad (3)$$

$A$  being the total number of molecules absorbed.

The free energy  $G$  for given values of the  $a_r$ 's is given by

$$\begin{aligned} G/kT = & -B \log B + a_0 \log a_0 + a_1 \log a_1 + \dots + a_r \log a_r + \dots \\ & - (a_1 + \dots + a_r + \dots) \log j_s - (a_1 + \dots + a_r + \dots) w/kT \\ & - \{a_2 + 2a_3 + \dots + (r-1)a_r + \dots\} \log j_L \end{aligned} \quad (4)$$

where  $j_s$  is the partition function for a molecule absorbed on to a localised site,  $j_L$  is the partition function for a molecule in the cluster other than that on the localised site, and  $w$  is the heat evolved when a molecule proceeds from a liquid to a localised site. The zero of energy is taken as that of a molecule in the bulk liquid.

Equation (4) can be written symmetrically as:

$$\begin{aligned} G/kT = & -B \log B + a_0 \log a_0 + a_1 \log a_1 + \dots + a_r \log a_r + \dots \\ & + (a_1 + a_2 + \dots + a_r) \epsilon + \{a_1 + 2a_2 + \dots + r a_r + \dots\} \epsilon' \end{aligned} \quad (5)$$

$$\text{where:} \quad \epsilon = -\log \frac{j_s}{j_L} - \frac{w}{kT} \quad (6)$$

$$\text{and} \quad \epsilon' = -\log j_L \quad (7)$$

The free energy expression (5) has to be minimised by varying the  $a_r$ 's consistently with the equations (2) and (3). Formally this is equivalent to minimising

$$G/kT + \lambda(a_0 + a_1 + \dots - B) + \nu(a_1 + 2a_2 + \dots - A) \quad (8)$$

treating the  $a_r$ 's as completely independent variables while  $A$  is constant and  $\lambda$  and  $\nu$  are the usual undetermined multipliers. Differentiating (7) and equating to zero the coefficients of  $\delta a_0, \delta a_1, \dots$ , gives:

$$a_0 = e^{-(1+\lambda)} \quad (9.0)$$

$$a_1 = e^{-\{1+\lambda+(\nu+\epsilon')+\epsilon\}} \quad (9.1)$$

$$a_2 = e^{-\{1+\lambda+2(\nu+s')+\epsilon\}} \quad . \quad . \quad . \quad (9.2)$$

$$a_r = e^{-\{1+\lambda+r(\nu+s')+\epsilon\}} \quad . \quad . \quad . \quad (9.7)$$

$\lambda$  and  $\nu$  are determined in terms of  $B$  and  $A$  by substituting for  $a_0 \dots$  from equations (9) into equations (2) and (3). The results are:

$$e^{-(1+\lambda)} + e^{-(1+\lambda+s)} \{e^{-(\nu+s')} + e^{-2(\nu+s')} + \dots\} = B \quad (10)$$

$$e^{-(1+\lambda+s)} \{e^{-(\nu+s')} + 2e^{-2(\nu+s')} + \dots\} = A \quad (11)$$

The series in equations (10) and (11) can be summed to infinity when they are convergent to give:

$$e^{-(1+\lambda)} + e^{-(1+\lambda+s)} \cdot \frac{e^{-(\nu+s')}}{1 - e^{-(\nu+s')}} = B \quad . \quad . \quad (12)$$

and 
$$e^{-(1+\lambda+s)} \cdot \frac{e^{-(\nu+s')}}{\{1 - e^{-(\nu+s')}\}^2} = A \quad . \quad . \quad (13)$$

Eliminating  $\lambda$  from (12) and (13) gives the equation for  $\nu$  as:

$$\frac{B e^{-(\nu+s')-\epsilon}}{\{1 + e^{-(\nu+s')-\epsilon} - e^{-(\nu+s')}\} \{1 - e^{-(\nu+s')}\}} = A. \quad . \quad (14)$$

The relation of  $\nu$  to the vapour pressure in equilibrium with the absorbed molecules is obtained from the chemical potential,  $\mu$ , of the absorbed molecules.

$$\begin{aligned} \frac{\mu}{kT} = \frac{1}{kT} \frac{\partial G}{\partial A} &= (\log a_0 + 1) \frac{\partial a_0}{\partial A} + (\log a_1 + 1) \frac{\partial a_1}{\partial A} + \dots + \left( \frac{\partial a_1}{\partial A} + \frac{\partial a_2}{\partial A} + \dots \right) \epsilon \\ &+ \left( \frac{\partial a_1}{\partial A} + 2 \frac{\partial a_2}{\partial A} + \dots \right) \epsilon'. \end{aligned} \quad (15)$$

And from equations (9):

$$a_1 = a_0 e^{-(\nu+s')-\epsilon} \quad . \quad . \quad . \quad (16.1)$$

$$a_2 = a_0 e^{-2(\nu+s')-\epsilon} \quad . \quad . \quad . \quad (16.2)$$

etc. Substituting for  $a_1, a_2, \dots$ , from equations (16) into (15) gives:

$$\frac{\mu}{kT} = (\log a_0 + 1) \left( \frac{\partial a_0}{\partial A} + \frac{\partial a_1}{\partial A} + \frac{\partial a_2}{\partial A} + \dots \right) - \nu \left( \frac{\partial a_1}{\partial A} + 2 \frac{\partial a_2}{\partial A} + \dots \right) \quad (17)$$

which reduces, according to equations (2) and (3), to:

$$\mu/kT = -\nu \quad . \quad . \quad . \quad (18)$$

The chemical potential of the molecules in the gas phase is  $kT(\alpha + \log p)$ , where  $p$  is the pressure of the molecules in this phase, and  $\alpha$  depends on temperature though not on pressure. Equation (18) therefore gives:

$$\mu/kT = -\nu = \alpha + \log p. \quad . \quad . \quad . \quad (19)$$

If the partition function for the molecules in the bulk liquid phase is assumed to be identical with that for the molecules in a cluster, then

$$-\log j_L = \alpha + \log p_0 \quad . \quad . \quad . \quad (20)$$

where  $p_0$  is the saturation vapour pressure of the liquid. Hence:

$$-\nu + \log j_L = \log p/p_0 \quad . \quad . \quad . \quad (21)$$

or from (7):

$$e^{-(\nu+s')} p/p_0 \quad . \quad . \quad . \quad (22)$$

Substitution of  $p/p_0$  for  $e^{-(\nu+s')}$  in equation (14) gives the isotherm equation as:

$$A = \frac{Bp}{(p_0 - p)\{\beta + (1 - \beta)p/p_0\}} \quad . \quad . \quad . \quad (23)$$

where

$$\beta = e^s = \frac{j_L}{j_S} e^{-\omega/kT} \quad . \quad . \quad . \quad (24)$$



Equation (23) is identical with the isotherm deduced<sup>\*</sup> in (1) and it is of the same form as B.E.T.'s equation. The interpretation of absorption data given in (1) in terms of the heat of absorption on to the monolayer, and the liquid and localised partition functions, thus remains unchanged.

### 3. Multimolecular Absorption Relations.

In addition to the isotherm equation, Part I gave two other useful relations which also follow from the present analysis. Let  $X$  denote the number of molecules in the monolayer, i.e.

$$\begin{aligned} X &= a_1 + a_2 + \dots = e^{-(1+\lambda+s)} \{e^{-(\nu+s')} + e^{-2(\nu+s')} + \dots\} \\ &= e^{-(1+\lambda+s)} \frac{e^{-(\nu+s')}}{1 - e^{-(\nu+s')}} \end{aligned} \quad (25)$$

$A$  is given by equation (13), and :

$$(A - X) = e^{-(1+\lambda+s)} \frac{e^{-2(\nu+s')}}{1 - e^{-(\nu+s')}} \quad (26)$$

whence by (22) :

$$\frac{A - X}{A} = e^{-(\nu+s')} = \frac{p}{p_0} \quad (27)$$

$(B - X)$  is, of course, identical with  $a_0$ , and using the value  $e^{-(1+\lambda)}$  given by (9.0) for  $a_0$ , and the expressions (25) and (26) for  $X$  and  $(A - X)$  :

$$(A - X)(B - X) = e^s X^2 = \beta X^2 \quad (28)$$

since according to (24),  $e^s$  is identical with  $\beta$ , (27) and (28) are the two relations previously given in Part I.

### 4. General Remarks.

It may seem surprising that the analysis of Part I and of the present paper should give identical results. The two analyses are not, however, different in their quantitative aspect although their physical hypotheses are different. It was assumed in Part I that there is an entropy of interchange for molecules on the liquid and localised sites, so that the phase volume accessible to a liquid molecule was increased by the ratio  $A/(A - X)$ , and the vapour pressure of these molecules was decreased correspondingly from  $p_0$  to  $(A - X)/A p_0$ . The present analysis assumes that the entropy of the system is increased by the presence of  $X$  clusters of liquid molecules instead of just one continuous volume of liquid molecules. If a liquid molecule transfers from one cluster to another, the two clusters have been effectively interchanged : the phase volume accessible to the liquid molecules is therefore again increased by the ratio  $A/(A - X)$ . The two analyses thus lead to the same increase in phase volume accessible to the liquid molecules, and they must lead to the same quantitative results.

Quantitatively B.E.T.'s isotherm equation will follow if the increase of entropy is assumed, and the physical problem is to decide whether or not the system under consideration can give the necessary number of distinguishable configurations. Condensation of the multilayer molecules as distinct clusters does seem to provide the necessary distinguishable configurations, but condensation as a continuous film on to the monolayer will not provide the necessary distinguishable configurations.

Foster<sup>\*</sup> has recently pointed out that as  $p$  becomes equal to  $p_0$ , B.E.T.'s theory predicts that only one-half of the absorbing space is filled. The same result is evident from the present analysis, for at this limit  $(\nu + s')$  is zero (cf. equation (22)), and equations (9) then show that  $a_1 = a_2 = \dots = a_r = \dots$  : the number of clusters with 1, 2, . . .  $r$  . . . molecules are all equal in number, or each multilayer considered by B.E.T. is only half filled. B.E.T. use this limit to relate  $p$  to  $p_0$ , but

<sup>\*</sup> Foster, *J. Chem. Soc.*, 1945, 769.

it should be noted that the series in equations (10) and (11) are not then convergent, and the solution fails. The statistical analysis avoids this difficulty by assuming at the outset that the non-localised molecules in a cluster have partition functions identical with those of molecules in the bulk liquid, and the relation of  $p$  to  $p_0$  follows from this assumption.

### 5. The Effects of Surface Energies.

The theory ignores surface energies, and these must be considerable for the clusters that it requires. The surface energy will increase the vapour pressure in equilibrium with the clusters, as they must have convex surfaces, and so long as the clusters remain distinct,  $e^{-(\sigma + \sigma')}$  of equation (22) cannot become unity; the absorption at saturation pressure must therefore remain finite as  $p$  approaches  $p_0$  unless the disposition of the clusters is such that they may coalesce to give a large reduction in surface energy. The theory thus offers a mechanism that explains the absorption of a sufficient number of molecules to make possible the phenomena associated with surface energies, such as capillary condensation, but it does not itself explain the approach to an infinite absorption as the saturation pressure is attained.

The absorption of water by keratin provides an example of approach to saturation vapour pressure without the absorption of an infinite amount of liquid. Keratin, in the form of wool or horn, will absorb up to 33 % of its dry weight of water at saturation vapour pressure, but it remains unwettable by liquid water; the advancing contact angle for cut surfaces of horn is, in fact, around  $90^\circ$ . A previous analysis of the keratin-water isotherm<sup>9</sup> has shown that 100 g. of dry keratin contains 1.12 mol. of localised sites, and at saturation pressure, approximately 1 mol. of water is localised and 0.8 mol. is non-localised, whilst because of the swelling energy of the gel,  $p/p_0$  in equation (22) is 0.46. The series in equations (10) and (11) are therefore rapidly convergent, and the average size of a cluster,  $A/X$ , is 1.8 molecules. The clusters, even at saturation pressure, are therefore small, and are unlikely to coalesce.

These conclusions suggest that the surface of keratin at saturation vapour pressure consists of small clusters of water molecules spaced apart in an otherwise water-repellent surface, and it will behave towards liquid water much as the porous, or heterogeneous surfaces discussed by Cassie and Baxter<sup>10</sup> behave towards liquid water. In fact, the observed contact angle,  $\theta$ , for keratin surfaces will be given by:

$$\cos \theta = f_1 \cos \theta_1 + f_2 \cos \theta_2 \quad . \quad . \quad . \quad (29)$$

where  $f_1$  is the fractional area of the surface covered by water clusters and  $\theta_1$  is the contact angle for these clusters, whilst  $f_2$  is the fractional area of the water-repellent surface of contact angle  $\theta_2$ .  $\theta_1$  will be close to zero, and  $f_2$  must be large compared with  $f_1$  to give an observed advancing contact angle,  $\theta$ , as great as  $90^\circ$ . The water-repelling of the surface therefore confirms the deduction from the isotherm analysis that the clusters are always small and are so far apart that they will not coalesce.

I am indebted to Mr. B. H. Wilsdon, Director of Research, for his interest in this work, and to the Council of the Wool Industries Research Association for permission to publish this account.

NOTE: Since this was written, a paper by Hill<sup>11</sup> treats the problem of multi-molecular absorption by essentially the same method. Hill's analysis is more general than that given above, and his results lead directly to the isotherm equations already given for multimolecular absorption on to a mobile monolayer.<sup>9</sup>

<sup>10</sup> Cassie and Baxter, *Trans. Faraday Soc.*, 1944, **40**, 546.

<sup>11</sup> Hill, *J. Chem. Physics*, 1946, **14**, 263.

### Summary.

It is shown that the multimolecular absorption isotherm proposed by Brunauer, Emmett and Teller is only applicable to systems where absorption occurs as distinct clusters of molecules; it is not applicable to multimolecular absorption as continuous layers superposed on a continuous monolayer.

Some effects of surface energies in multimolecular absorption are discussed, and it is shown that the water repellency of keratin is not inconsistent with its absorption of water vapour.

### Résumé.

On montre que l'isotherme d'absorption multimoléculaire, proposée par Brunauer, Emmett et Teller, ne s'applique qu'aux systèmes où les molécules adsorbées forment des grappes distinctes et non pas des couches continues superposées sur une couche monomoléculaire uniforme. On discute quelques effets d'énergie de surface dans l'absorption multimoléculaire et on montre que la répulsion de la kératine pour l'eau n'est pas en désaccord avec l'absorption de la vapeur d'eau par la kératine.

### Zusammenfassung.

Es wird gezeigt, dass die von Brunauer, Emmett und Teller vorgeschlagene multimolekulare Absorptionsisotherme nur für solche Systeme anwendbar ist, bei denen Absorption in separaten Molekülgruppen erfolgt; sie ist nicht anwendbar bei multimolekularer Absorption in zusammenhängenden Schichten, die auf eine zusammenhängende monomolekulare Schichte überlagert sind. Einige Effekte der Oberflächenenergien bei multimolekularer Absorption werden besprochen und es wird gezeigt, dass die Wasserabstossung durch Keratin mit dessen Absorption von Wasserdampf nicht unvereinbar ist.

*Wool Industries Research Association,  
Torridon,  
Headingley,  
Leeds 6.*

---

## THE SEPARATION OF THE OXYGEN ISOTOPES BY THERMAL DIFFUSION.

BY I. LAUDER.

*Received 12th February, 1946, as amended 9th September, 1946.*

In recent years both stable and radioactive isotopes of many elements have found ever increasing application to the study of chemical problems. If a radioactive isotope with a suitable half-life period is available, it is perhaps easier to use as a tracer than a stable isotope of the element. In the case of oxygen, however, the radioactive isotopes<sup>1</sup> have very short half life-periods and, therefore, they are unsuitable for use in tracer experiments. Consequently, the fundamental problem is the separation of its stable isotopes.

Normal oxygen consists of a mixture of  $^{16}\text{O}$ ,  $^{17}\text{O}$  and  $^{18}\text{O}$  in the proportions<sup>2</sup> of 2494 : 1 : 5 respectively. Their separation has been investigated by most of the standard methods, but, prior to the thermal diffusion method, little success has been achieved. Of the two heavy isotopes,  $^{17}\text{O}$  and  $^{18}\text{O}$ , the latter is more easily separated from  $^{16}\text{O}$  due mainly to the greater abundance of  $^{18}\text{O}$  and also to its greater mass. Only small increases above the normal  $^{18}\text{O}/^{16}\text{O}$  ratio have been obtained by gaseous

<sup>1</sup> Seaborg, *Chem. Rev.*, 1940, **27**, 226.

<sup>2</sup> Hahn, Flugge and Matthauch, *Physik Z.*, 1940, **41**, 1.

diffusion,<sup>3</sup> fractional distillation,<sup>4</sup> chemical exchange<sup>5</sup> and electrolytic methods.<sup>6</sup> By the thermal diffusion method, on the other hand, almost complete separation of  $^{18}\text{O}$  from  $^{16}\text{O}$  may be achieved.

The work described here was commenced early in 1940, but was unavoidably held up from time to time. Since that year two communications have been published which deal with the separation of the oxygen isotopes by thermal diffusion. Wells<sup>7</sup> gives a brief description of a six-stage apparatus which produced oxygen containing 14 %  $^{18}\text{O}$  and 0.8 %  $^{17}\text{O}$  after 116 days operation. More recently, Clusius, Dickel and Becker<sup>8</sup> have separated oxygen containing 99 %  $^{18}\text{O}$  and 1 %  $^{17}\text{O}$ . This paper was not available to the author.

The various factors which influence the efficiency of a thermal diffusion-separation column have been investigated experimentally and theoretically by many workers.<sup>9</sup> When the construction of such an apparatus is being considered for the specific purpose of accumulating a supply of some particular isotope, the variable factors such as carrier gas, separation tube diameter, temperature gradient, working pressure, etc., are chosen so as to achieve a maximum separation in a minimum of time. In the present paper, the influence of such factors on the separation of the oxygen isotopes by thermal diffusion is considered.

## Experimental.

### Part I.

Experiments were carried out using a single-stage thermal diffusion unit with the object of determining the optimum working pressure of the apparatus and the maximum degree of separation at this pressure. The results were then applied to a four-stage thermal diffusion unit, described in Part II. The separation column was constructed from galvanised iron water pipes and fittings as shown diagrammatically in Fig. 1. The heating wire, No. 22 gauge Nichrome, was stretched centrally and vertically in a standard  $\frac{1}{2}$  in. diam. pipe which was itself surrounded by a 2 in. diam. pipe. This outer tube, forming the cooling water jacket, was screwed to the inner tube at the lower end only. At the top, a water-tight connection between the cooling water jacket and the separation tube was made by a piece of rubber hose, as in an ordinary Liebig condenser. This connection allowed the two tubes to move relatively to one another, so that any slight expansion of the inner tube produced by heat from the wire, did not cause any undue stress in the system. The greater portion of the cooling water flowed out of the jacket at a level 3 in. from the top of the separation tube. By means of a small subsidiary outlet, screwed into the topmost portion of the cooling jacket, water was caused to flow over the full length of the separation tube.

The heating wire was held by small mica insulators in the form of crosses. These were cemented to small porcelain beads and spaced every 3 in. along the wire. The two ends of the Nichrome wire were compressed into holes in short lengths of brass rods  $\frac{1}{2}$  in. in diameter. Into the other two ends of the brass rods, suitable lengths of heavy gauge copper wire were compressed. This construction of the heating wire was necessary to avoid corrosion troubles caused by the high temperature and the  $\text{O}_2$

<sup>3</sup> Hertz, *Z. Physik*, 1934, **91**, 810.

<sup>4</sup> Huffmann and Urey, *Ind. Eng. Chem.*, 1937, **29**, 531.

<sup>5</sup> Reid and Urey, *J. Chem. Physics*, 1943, **11**, 403.

<sup>6</sup> Tronstad and Brun, *Trans. Faraday Soc.*, 1938, **34**, 766.

<sup>7</sup> Wells, *Physic. Rev.*, 1941, **59**, 679.

<sup>8</sup> Clusius, Dickel and Becker, *Naturwiss.*, 1943, **31**, 210; *Chem. Abstr.*, 1944, **38**, 19.

<sup>9</sup> Clusius and Dickel, *Z. physik. Chem.*, 1939, **B 44**, 397-450; Furry, Clark Jones and Onsager, *Physic. Rev.*, 1939, **55**, 1083; Waldmann, *Naturwiss.*, 1939, **27**, 230; Bardeen, *Physic. Rev.*, 1940, **57**, 35.

atmosphere. A small brass weight on the end of the lower brass rod helped to maintain a slight tension on the wire. Before a heating wire was inserted it was heated to redness and stretched slightly to remove all kinks. The same process was repeated after placing the wire in the tube, to avoid all possibility of contact between the wire and the metal tube.

To allow for the 5.2 cm. expansion which occurred when the wire was fully heated and also to insulate the lower terminal, a glass tube containing mercury was sealed with Apiezon wax to the bottom of the column. The terminal at the top of the column was likewise insulated by a short section of glass tubing. When the wire was fully heated the small brass weight was held in a central position by a brass bush situated just above the

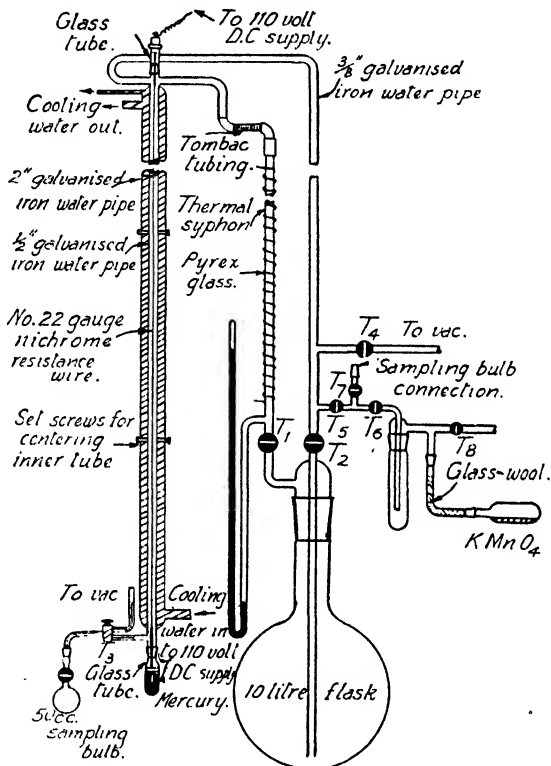


FIG. 1.

mercury in the glass tube at the lower end of the column. The effective length of the heating wire was 13 ft. while the overall length of the column was 14 ft.

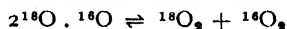
In all experiments 110 v. applied between the two ends of the column caused a D.C. current of 10 amp. to flow and the central wire to reach a temperature of  $810^{\circ}\text{C}$ . This temperature was estimated from the mean coefficient of thermal expansion of the Nichrome wire<sup>10</sup> over this temperature region and its total expansion. Water flowing through the cooling jacket prevented any appreciable rise in temperature of the central tube above room temperature. The inner diameter of a standard  $\frac{1}{8}$  in. diam. pipe is 15 mm. so that the temperature gradient between the hot central wire and the cool wall of the separation tube was  $1080^{\circ}\text{C./cm}$ . The mean temperature in the separation tube was calculated indirectly from the

<sup>10</sup> Hidnert, *Bur. Stand. J. Res.*, 1931, 7, 1031.

pressures in the apparatus before and after the heating current for the central wire was turned on. When the wire was heated to  $810^{\circ}\text{C}$ ., the mean temperature in the separation tube was found to be approximately  $522^{\circ}\text{C}$ ..

The top of the separation tube was connected to the 10 l. flask on ground level by a closed circuit of tubing. By heating 76 cm. of this tubing to  $300^{\circ}\text{C}$ ., adequate circulation of the gas from the flask to the top of the column and back again was produced. At a pressure of 35 cm. Hg. and  $27^{\circ}\text{C}$ ., the calculated time for one complete circulation of gas in the tubing is a little over 2 min. Originally, the thermal syphon was formed by heating a section of the galvanised iron pipe between the top of the column and the flask. It was found, however, that under the action of heat the iron tube gradually became porous, so it was replaced by an equivalent length of Pyrex glass tubing. In order to avoid any stresses caused by the change in length of the thermal syphon as a result of turning on or off the heating current, a short length of Tombac tubing was inserted in the circuit as is shown in Fig. 1.

Oxygen was chosen as the carrier gas on account of ease of preparation in a high state of purity and also because it is thermally stable. In normal oxygen, the heavy molecules are of the type  $^{18}\text{O}$ ,  $^{16}\text{O}$ , and so before a sample of oxygen containing a high proportion of  $^{18}\text{O}$  may be isolated, the equilibrium,



must be established. It is probable that this equilibrium is rapidly catalysed by the film of nickel and chromium oxides<sup>11</sup> on the surface of the hot wire. Furthermore, as mentioned by Clusius, Dickel and Becker,<sup>8</sup> the dissociation of the oxygen molecules at the high temperature of the heating wire leads to the establishment of this equilibrium.

Before each experiment the apparatus was well evacuated and then filled with pure oxygen, produced by the action of heat on pure  $\text{KMnO}_4$ . Particles of  $\text{MnO}_2$  were removed by filtering through glass wool and, after passing through a trap cooled in liquid air, it was fed into the apparatus to the approximate pressure required for the experiment. After turning on the current for the central wire, a few sec. were allowed to elapse in order to establish a steady thermal state and then the pressure was reduced to the desired value. It may be mentioned that a variation in room temperature of  $5^{\circ}\text{C}$ . produced a variation of pressure (0.5 cm. Hg) in the apparatus. Sampling bulb connections were provided for the withdrawal of samples from the bottom and the top of the separation tube. The separation was allowed to continue for the desired length of time and then two separate 50 cc. samples of oxygen gas were withdrawn for isotopic analysis.

These were converted to water by combination with pure electrolytic hydrogen in the presence of a heated Pt filament. After purification of the water samples, as described by Herbert and Lauder,<sup>12</sup> the densities were determined by the micro-pyknometer method of Gilfillan and Polanyi.<sup>13</sup> From such measurements one cannot obtain the true isotopic compositions of the samples because normal oxygen is a mixture of three isotopes.

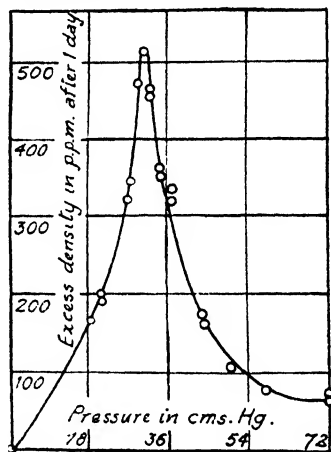


FIG. 2.

<sup>11</sup> Morita, Tanaka and Titani, *Bull. Chem. Soc. Japan*, 1939, 14, 9.

<sup>12</sup> Herbert and Lauder, *Trans. Faraday Soc.*, 1938, 34, 432.

<sup>13</sup> Gilfillan and Polanyi, *Z. physik. Chem.*, 1933, 166, 255.

However, if the degree of separation is small, as is the case here, the  $^{17}\text{O}$  content of a sample will not be much greater than that in normal oxygen. Therefore, one can attribute with little error, all the density excess of any sample to the presence of an increased quantity of  $^{18}\text{O}$ .

The optimum working pressure for the separation column was determined by measuring the isotopic compositions of samples withdrawn from the bottom of the apparatus after 24 hr. operation at various pressures. The results are shown in Fig. 2. It may be seen that the optimum working pressure is fairly sharply defined, the maximum occurring at a pressure 31.25 cm. Hg and at an excess density of the water of 520 p.p.m. The shape of the curve is merely a result of the separation (which is produced by thermal diffusion in a horizontal direction and multiplied by the vertical convection stream) being opposed by the remixing effect of ordinary diffusion. So long as the pressure is not too low, the degree of separation is inversely proportional to the square of the pressure,<sup>9</sup> but at lower pressures the remixing effect of ordinary diffusion becomes more and more important. Therefore, the degree of separation increases as the pressure is lowered, reaches a maximum, and then decreases.

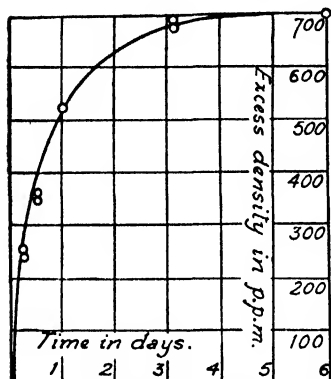


FIG. 3.

reached slightly more than three-quarters of its equilibrium value.

The maximum degree of separation at the optimum working pressure was determined by a procedure similar to that which was used in the former case. The results are shown in Fig. 3. Equilibrium was reached in about 4 days. The maximum excess density at equilibrium, 700 p.p.m., corresponds to about 0.9 %  $^{18}\text{O}$  and as the concentration of the  $^{18}\text{O}$  in the flask was reduced to approximately 0.18 %, the separation factor for the column is about 5. This figure indicates that from the four-stage thermal diffusion unit, oxygen containing about 25 %  $^{18}\text{O}$  may be obtained.

## Part II.

The object of the experiments with the four-stage thermal diffusion unit was the isolation of oxygen containing sufficient  $^{18}\text{O}$  to allow some of the physical properties of heavy oxygen gas and heavy oxygen water to be investigated for use in tracer experiments. Four separation columns, identical with the one described in Part I, were connected in series as is shown diagrammatically in Fig. 4. As the time which is required for the establishment of equilibrium is dependent on the volumes of the various sections in which the concentration of the heavy isotope must be increased, the volumes of the thermal syphons should be kept to a minimum, e.g. the bottom of column No. 1 should be near the top of column No. 2 and so on. Owing to limitations of space this construction could not be adopted.

All the columns were built on the same level. The oxygen was circulated from the bottoms of columns No. 1, 2 and 3 to the tops of columns No. 2, 3 and 4 respectively by thermal syphons.

As the heavy oxygen isotope is present to a very small extent (in normal oxygen  $^{18}\text{O}/^{16}\text{O} = 1/500$ ) a fairly large amount of normal oxygen is required in order to build up relatively high concentrations of  $^{18}\text{O}$  in the various sections before equilibrium is reached. It was decided therefore, to arrange a continuous flow of pure normal oxygen into the system. This was accomplished by electrolysis of dil.  $\text{H}_2\text{SO}_4$  between Pt electrodes in a divided cell and the oxygen was filtered through glass wool and then dried by  $\text{CaCl}_2$ . Traces of hydrogen were removed by passing the gas over heated platinised asbestos and the final drying was performed by  $\text{Mg}(\text{ClO}_4)_2$ .

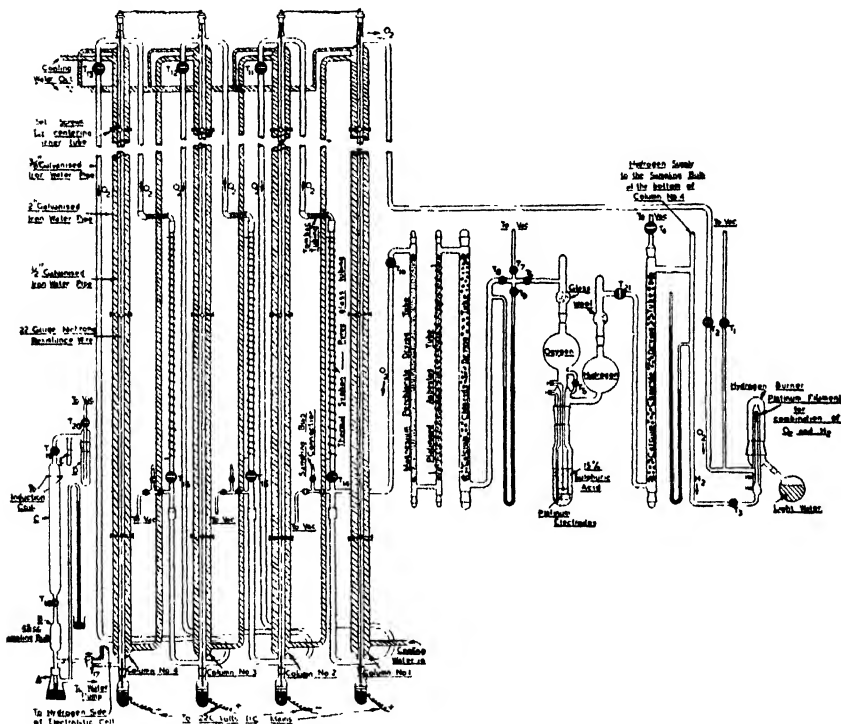


FIG. 4.

This oxygen was fed into the circuit of tubing connecting the bottom of the first column to the top of the second and subsequently it streamed out of the top of column No. 1. Effectively, therefore, column No. 1 was merely acting as a stripper.

The hydrogen generated in the electrolytic cell was filtered through glass wool and dried by  $\text{CaCl}_2$ . It was then combined, in the presence of a hot Pt filament, with the oxygen flowing out of the top of column No. 1. This was carried out by means of the apparatus labelled "hydrogen burner" in Fig. 4. As a partial separation of the hydrogen isotopes occurred in the electrolytic cell, the water which formed in the hydrogen burner was deficient in the heavy hydrogen isotope as well as in the heavy oxygen isotope. This water was consequently lighter than normal water.

The system outlined above for the production of the fresh flow of oxygen into the thermal diffusion unit has proved very effective. The rate of flow can be varied within wide limits and further the system may be



operated at any desired pressure without further modification. The two 1 l. bulbs at the tops of the oxygen and hydrogen sides of the electrolytic cell were introduced as a precautionary measure. If the bulbs were not present any sudden change of pressure, e.g. by the breakage of a tube or by improper evacuation, might cause the liquid in the cell to be blown over into the drying tubes. Taps were provided at appropriate points so that the cell and the drying tubes could be attended to, without interfering with the main thermal diffusion unit.

The central wires in the four columns were constructed as is described in Part I, and by connecting them in pairs to the 220 v. mains, they were heated by a D.C. current of 10 amp. to a temperature of  $810^{\circ}\text{C}$ . The temperature gradient and the mean temperature in each column were therefore the same as in Part I.

After thoroughly outgassing the system, the oxygen side was filled with oxygen generated from  $\text{KMnO}_4$  and the hydrogen side was filled with electrolytic cylinder hydrogen. The pressure in the system was adjusted to the desired value after the heating currents for the central wires had been turned on and the circulation of oxygen through column No. 1 was commenced by starting the electrolysis and by opening the tap  $T_1$ . The

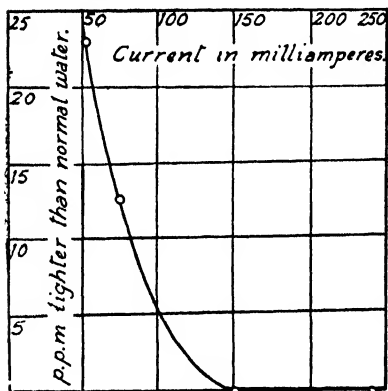


FIG. 5.

rate of flow of fresh oxygen into the thermal diffusion apparatus was controlled by the current flowing through the cell. Experiments were carried out to determine the effect of varying the rate of flow on the isotopic composition of the oxygen in thermal syphon which joined the bottom of column No. 1 to the top of column No. 2. Electrolysis was allowed to occur at definite rates for 24 hr. and, after this period, samples of oxygen were withdrawn for isotopic analysis. The results are shown in Fig. 5. It is seen that the minimum current through the cell necessary for the maintenance of a normal concentration of  $^{18}\text{O}$  (0.2 %) in this thermal syphon, was 0.15 amp. At a pressure 34 cm. Hg and a mean temperature  $522^{\circ}\text{C}$ . in the separation tube, a current of 0.15 amp. produces a flow of 204 cc./hr. The volume of each separation tube was 700 cc. and so the gas in column No. 1 was "replaced" every 3.4 hr. The proportion of the heavy molecules removed from the inflowing stream of normal oxygen during its passage up column No. 1, was determined by measuring the isotopic composition of the water formed in the hydrogen burner. After 17 days at 34 cm. Hg and with a current of 0.15 amp. flowing through the cell, this water was approximately 70 p.p.m. lighter than normal water. In normal water, the heavy oxygen water molecules make a contribution of about 200 p.p.m. to the density, so that under the above experimental conditions, the thermal diffusion apparatus extracted approximately 35 % of the heavy molecules from the inflowing stream of fresh oxygen.

Interest was centred primarily on the isotopic composition of the oxygen at the bottom of column No. 4 and therefore a special sampling apparatus was attached at this point so that a sample of oxygen withdrawn from the apparatus could be combined directly with hydrogen produced from the electrolytic cell. One side of the two-way capillary tap  $T_{17}$  was connected to the bottom of column No. 4 while the other side was connected to the top of the  $\text{CaCl}_2$  tube used for drying the hydrogen from the cell. To avoid a reduction of pressure in the system, as a consequence of the withdrawal of samples of oxygen and hydrogen, the flow of these gases into the

hydrogen burner was temporarily stopped during the sampling procedure by turning off tap  $T_3$ . Electrolysis was continued to generate the necessary volumes of oxygen and hydrogen required for the sample. These were then drawn off by means of the sampling bulb B and passed into the tube C. After sparking the mixture, the water which was formed was pumped into the trap D and was subsequently sublimed into a storage vessel attached to the standard cone E. Although the sampling bulb had a fixed volume (45 cc.) it was not always filled to the working pressure of the apparatus. As the  $^{18}\text{O}$  content of the gas in the plant increased, the volume of the sample withdrawn from the apparatus was decreased. After completing the sampling process tap  $T_3$  was turned on and the normal flow of gases in the system was restored.

Various experiments were carried out to determine the pressure at which the rate of separation or, in other words, the transport of the heavy isotope was a maximum. The experimental results obtained after operation for two weeks at different pressures, are shown in Table I, while the full results are shown in Fig. 6.

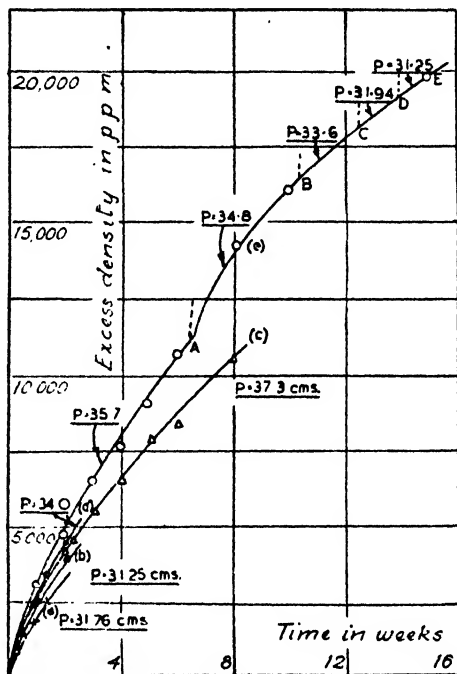


FIG. 6.

In the case of curve (a) Fig. 6, the experimental set-up was slightly different from that which is illustrated in Fig. 4. The stream of pure oxygen was passed directly over the top of column No. 1 and then back to the hydrogen burner. Curves (b), (c), (d) and (e) were obtained with the fresh oxygen flowing into the thermal syphon which joined the bottom of column No. 1 to the top of column No. 2, as is shown in Fig. 4. In these cases, therefore, only three columns were actively used for the separation, while column No. 1 was acting as a stripper of the inflowing gas.

In all experiments except one, the working pressures were maintained constant during the separations. In the one exception the pressure was

gradually diminished to the optimum pressure as the separation progressed. This is represented by the curve (e) Fig. 6, and the pressures for the various portions of this curve, and the corresponding times of operation are given in Table II.

A comparison of curves (a) and (b) shows that the rate of increase of the heavy oxygen concentration at the bottom column No. 4 is slower when

TABLE I.

Curve.	Press. in cm. Hg at 23° C.	Excess Density in p.p.m. after	
		(A) One Week.	(B) Two Weeks.
(a)	31.76	2190	3600
(b)	31.25	2422	3990
(c)	37.3	2650	4100
(d)	34.0	2874	(4270)
(e)	35.7	2910	4630

the fresh oxygen flows over the top of column No. 1 than when it enters the thermal syphon which joins the bottom of column No. 1 to the top of column No. 2. This is because the heavy oxygen isotope had to be transported further than in the second case, and therefore a longer time was required to build up a given concentration in column No. 4.

For a unit consisting of a number of columns in series, the time of operation required for the establishment of equilibrium is much greater than that for a single stage unit. This time may be shortened by increasing the

TABLE II.

Press. in cm. Hg at 23° C.	Time of Operation in Days.
35.7	0-47
34.8	47-74
33.6	74-89
31.9	89-98
31.25	98-105

transport of the heavy isotope through the system. Clusius and Dickel,<sup>14</sup> and Furry, Jones and Onsager<sup>15</sup> have suggested methods by which this may be achieved. The suggestion of Furry, Jones and Onsager, which is a result of their theoretical considerations has not been subjected to any previous experimental verification as far as the author is aware.

It is suggested that the time of operation required for the establishment of a desired concentration difference, may be shortened by starting the separation at a pressure

greater than the optimum working pressure and then, as the separation progresses, by reducing the pressure to the optimum pressure. Thus, if the gas in a separation tube is not too near the equilibrium point, the transport is proportional to the square of the pressure. Therefore, by working at a pressure greater than the optimum pressure, the transport can be increased up to a certain point but, at this higher pressure, the degree of separation at the equilibrium point is not as great as that at the optimum working pressure. However, by gradually decreasing the working pressure

to the optimum pressure as the experiment progresses, the maximum separation may be achieved. The higher rate of transport at the beginning helps considerably to shorten the time required to reach any given concentration. This effect is shown clearly by the portion OA of curve (e). Over this range a better separation was achieved than at any other pressure, although the working pressure, 35.7 cm. Hg was greater than the optimum pressure 31.25 cm. Hg. The large jump over the range A to B which occurred when the pressure was reduced from 35.7 cm. to 34.8 cm. Hg is attributed to the better degree of separation as the working pressure approached the optimum pressure. In the case of curve (c) an unfortunate breakdown of the plant made it impossible to show the effect of reducing the working pressure to the optimum pressure.

A comparison of the slopes of the curves (b), (c), (d) and (e) shows that there must be some pressure, greater than the optimum pressure, at which the rate of separation is a maximum over the early stages of the process. This is shown more clearly by Fig. 7. The point for the pressure 34 cm. Hg curve (B) is rather low. This is probably due to the fact that during the 12th to the 14th day inclusive, the flow was less than that required to

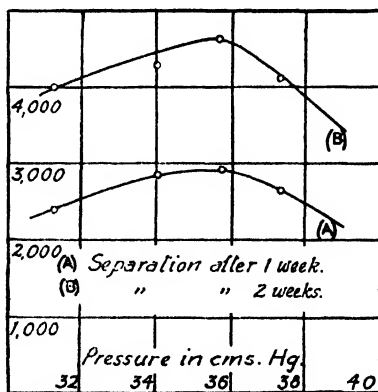


FIG. 7.

<sup>14</sup> Clusius and Dickel, *Z. physik. Chem. B*, 1939, 44, 440.

<sup>15</sup> Furry, Clark Jones and Onsager, *Physic. Rev.*, 1939, 55, 1090.

maintain a normal concentration of  $^{18}\text{O}$  at the top of column No. 2. The maximum of the curve indicates that the best starting pressure for the separation is about 35.25 cm. Hg.

In Part I the value of the separation factor for one column was approximately 5. As the concentration of the heavy oxygen at the top of column No. 2 was maintained at its normal value (0.2 %) by the inflowing stream of fresh oxygen, the maximum concentration of heavy oxygen which could be expected at the bottom of column No. 4 was approximately 25 %. The sample of water obtained after fifteen weeks' operation, corresponding to point E on curve (e) Fig. 6, had an excess density of 20,000 p.p.m. If it is assumed that only the  $^{18}\text{O}$  and the  $^{16}\text{O}$  isotopes are present, this corresponds to the presence of about 20.2 %  $^{18}\text{O}$ . However, some of the excess density must have been due to the presence of  $^{17}\text{O}$  and judging by the results of Wells, it is probable that the sample contained about 19.5 %  $^{18}\text{O}$  and 1 %  $^{17}\text{O}$ . Altogether the equivalent of 94 cc. (N.T.P.) of pure heavy oxygen was obtained during the 24 weeks' operation and so the mean daily transport was 0.56 cc. (N.T.P.). Using this latter figure, it has been calculated that if the volumes of the thermal syphons were negligible and if no samples were withdrawn from the system, oxygen containing 20 %  $^{18}\text{O}$  could be obtained from the system after seven weeks' operation. The total power consumption during the 24 weeks' operation was 17,500 kw.hr.

The author wishes to thank Mr. E. C. M. Grigg for carrying out most of the density determinations and for assisting with much of the other experimental work. It is a pleasure to acknowledge considerable financial assistance from Research Grants given to the University of Queensland by the Commonwealth Council for Scientific and Industrial Research. Without this assistance this work could not have been carried out.

### Summary.

The constructions of a one-stage and a four-stage apparatus for the separation of the oxygen isotopes by thermal diffusion have been described. The most efficient operating conditions have been determined. It has been shown that the time required to reach a given concentration of heavy isotope in the four-stage apparatus may be reduced considerably by starting the separation at a pressure above the optimum working pressure. Subsequently, as the separation progresses, the pressure is gradually decreased to the optimum working pressure.

A simple system for producing a continuous flow of pure oxygen into the thermal diffusion apparatus at any desired rate and pressure has been described. By use of this flow system in combination with the thermal diffusion apparatus, the water which was electrolysed in the cell, was separated into a heavy fraction and a light fraction. The latter fraction contained less heavy oxygen and less heavy hydrogen than normal water. Oxygen containing approximately 20 %  $^{18}\text{O}$  has been isolated by operating the unit under the most suitable conditions for fifteen weeks.

### Résumé.

On décrit ici la construction d'un appareil pour séparer—en une ou quatre étapes—les isotopes de l'oxygène et on indique les conditions pour son fonctionnement le plus efficace. On effectue la séparation plus rapidement en commençant à une pression supérieure à la pression optimum de travail, puis en la réduisant progressivement. On décrit aussi un système capable de produire un courant d'oxygène pur dans l'appareil à une pression et à une vitesse voulues. Enfin, de l'oxygène contenant 20 % de  $^{18}\text{O}$  a été isolé après une opération de 15 semaines.

### Zusammenfassung.

Die Konstruktion eines Einstufen- und Vierstufenapparats zur Trennung der Sauerstoffisotopen durch Thermodiffusion wird beschrieben; die besten Operationsbedingungen sind bestimmt worden. Trennung wird am raschesten

erzielt, wenn bei einem Druck begonnen wird, der etwas höher als der Optimaldruck ist, und der Druck dann langsam reduziert wird. Ein System zur Erzeugung eines ununterbrochenen Stroms von reinem Sauerstoff in den Apparat bei beliebigen Geschwindigkeiten und Drucken wird beschrieben. Nach 15-wöchigem Betrieb wurde Sauerstoff mit 20 %  $^{18}\text{O}$  isoliert.

*Department of Chemistry,  
University of Queensland,  
Brisbane,  
Australia.*

## A METHOD FOR THE DETERMINATION OF VISCOSITY AT LOW RATES OF SHEAR.

BY A. K. HOLLIDAY.

*Received 27th March, 1946.*

For liquids subjected to shear, the shearing stress  $F$  may be related to the rate of shear  $G$  by the equation  $F = \eta G$ . For normal (Newtonian) liquids,  $\eta$  is a constant—the viscosity—of the liquid, but for anomalous (non-Newtonian) liquids, the ratio  $F/G$  is a function of  $G$  and often decreases as  $G$  increases. While for a Newtonian liquid the ratio  $F/G$  is a characteristic property, for a non-Newtonian liquid it is meaningless except in relationship to a specified rate of shear. Therefore we must write

$$\eta_G = \left( \frac{dF}{dG} \right)_G$$

Thus it has been suggested by Conrad<sup>1</sup> that the viscosity of cuprammonium solutions of cellulose should be measured at several different rates of shear and a standard value of  $\eta$  interpolated at a rate of shear of 500 sec.<sup>-1</sup> for each solution. The experimental application of this suggestion is difficult because it is not always possible to compute the rate of shear actually operative in any given viscometer when the liquid used exhibits anomalous behaviour.<sup>2</sup> An alternative method of obtaining a "standard" value of the viscosity is to make measurements at very low rates of shear. It has been shown by Reiner and by Philipoff<sup>3</sup> that some anomalous liquids exhibit "pseudo-Newtonian" behaviour below a certain critical rate of shear, and the constant value of  $\eta$  which characterises the liquid in this range of low shear rates is called the zero or rest viscosity of the liquid.

Measurements at low rates of shear demand either a very refined form of the Couette viscometer or require a capillary viscometer with a long period of flow, and when a large range of rates of shear is to be covered the procedure becomes laborious. The falling sphere type of viscometer has not been used extensively in the study of anomalous liquids because the rate of fall under gravity is not controllable. If, however, a sphere can be moved through a liquid by a force which is readily controllable, then the viscosity at different rates of shear can be obtained by application of Stokes' Law. In the method to be described, a device originally used by Freundlich and Seifriz<sup>4</sup> is adopted in order to move a sphere through a liquid at low velocities. These workers caused microscopic Ni particles

<sup>1</sup> Conrad, *Ind. Eng. Chem. (Anal.)*, 1941, 13, 526.

<sup>2</sup> Lawrence, *Ann. Reports*, 1940, 37, 124.

<sup>3</sup> Reiner, *Kolloid Z.*, 1933, 65, 44; *Physics*, 1934, 5, 321. Philipoff, *Kolloid Z.*, 1936, 75, 142.

<sup>4</sup> Freundlich and Seifriz, *Z. physik. Chem.*, 1923, 104, 233.

to move horizontally in a gel by means of an electromagnet. It will now be shown that the velocity of a ferromagnetic sphere moving in the field of a bar magnet can be calculated in terms of the pole strength of the magnet and the distance of the magnet from the sphere.

Consider a sphere of radius  $r$ , situated at a distance  $d$  from the nearest end of a long bar magnet of pole strength  $P$  and length  $L$ . Then the force  $F'$  on the sphere is given by

$$F' = \frac{2PM}{d^3} \quad (I)$$

where  $M$  is the magnetic moment of the sphere and  $L \gg d \gg r$ ,  $d$  being measured along the axis of the magnet. If  $H$  is the field strength inside the sphere, then

$$H = \frac{3}{2 + \mu} H'$$

where  $H'$  is the field due to the magnet and  $\mu$  is the permeability of the sphere. (The permeability of the medium between sphere and magnet is assumed to be unity.) The intensity of magnetisation  $I$  of the sphere is then given by

$$I = \frac{\mu - 1}{4\pi} H = \frac{3}{4\pi} \cdot \frac{\mu - 1}{\mu + 2} H'$$

and since  $\mu$  is very large for a ferromagnetic sphere, we may put

$$I = \frac{3}{4\pi} H' = \frac{3}{4\pi} \cdot \frac{P}{d^2}, \text{ since } H' = \frac{P}{d^2}.$$

Moreover,

$$M = 4\pi r^3 I/3 \text{ and hence from (I), } F' = \frac{2P^2 r^3}{d^5}. \quad \text{. . . (II)}$$

When the sphere is very close to the magnet, the intensity  $I$  becomes equal to  $I'$ , the saturation intensity, independent of  $H$  and therefore of  $d$ . Hence when  $d$  is very small,  $P/d^3$  in equation (II) is replaced by  $I'$ , so that

$$F' = 2PI'r^3/d^3.$$

If the sphere is moving with velocity  $v$  in a fluid of viscosity  $\eta$ , then  $F' = 6\pi\eta vr$ , and hence

$$v = \frac{PI'r^3}{3\pi\eta d^3}. \quad \cdot \quad \cdot \quad \cdot \quad \cdot \quad (III)$$

By measuring  $v$  for given values of  $\tau$ ,  $d$ , and  $\eta$ , the constants in equation (III) may be obtained, and then the equation can be used to obtain values of  $\eta$  in other liquids, provided that  $d$  is kept sufficiently small for the sphere to be magnetically saturated. The maximum rate of shear  $G_m$  is equal to  $3v/2\tau$ , according to Lamb,<sup>8</sup> and occurs at a point on the surface of the sphere subtending an angle of  $90^\circ$  with the direction of motion.

**Experimental.**—A plan of the apparatus is given in Fig. 1. E is an electromagnet, consisting of a cylindrical iron bar 60 cm. long with one end cut to form a vertical wedge. The coil B is wound with 400 turns of 14 s.w.g. copper wire, and is water-cooled to prevent heating of the bar; the lagging L prevents heating of the surrounding air. The complete electromagnet is mounted horizontally on the pillar of a cathetometer so that it may be moved with precision small distances in a horizontal plane. The wedge end of the magnet projects over the stage of a Zeiss travelling microscope, on which is placed the cell C containing the liquid. The cell has a glass base and brass walls, the latter being soldered to a brass plate to minimise local temperature differences. The whole apparatus is situated in a constant temperature room at  $20 \pm 0.1^\circ \text{C}$ .

<sup>5</sup> Lamb, *Hydrodynamics*, 4th ed., p. 592.

The sphere used is a microscopic iron particle. Ordinary reagent iron filings contain many microscopic particles of regular spherical outline. The filings are sieved and scattered on a slide, and a suitable particle is selected and its

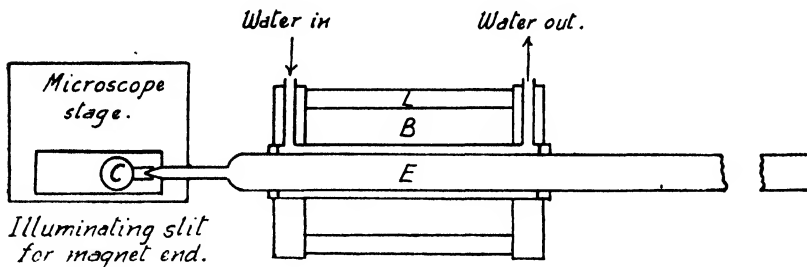


FIG. 1.

diameter measured, using a 6 mm. objective and a  $\times 12$  micrometer ocular. A fine-pointed glass rod, moistened with the liquid under investigation, is used to transfer the particle from the slide to the cell, and the particle is left in the

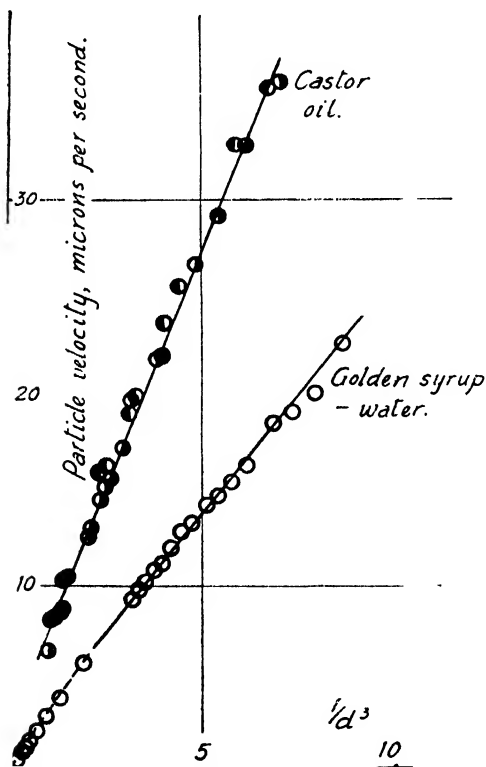


FIG. 2.—Particle velocities in Newtonian liquids.

**Investigations with Newtonian Liquids.**—The first measurements were made with a solution of Golden Syrup in water as a Newtonian liquid. In Fig. 2, values of  $v$ , the particle velocity in microns per second, are plotted against  $1/d^3$  where  $d$  is the distance in cm. from the magnet end to the mid-point of travel of the particle. For values of  $d$  less than about

the liquid in the cell when the rod is withdrawn. A fresh particle must be used for each liquid studied, and it is convenient to keep the diameter the same in every case. For the viscosity range covered in the present investigation (4-300 poise) a particle of diameter  $26 \mu$  has been used. A particle of this size does not fall through the liquid at an inconveniently rapid rate, and yet is large enough to permit of accurate measurement of the diameter. The particle when suspended in the liquid is viewed with a 16 mm. objective and a  $\times 11$  micrometer ocular. The wedge end of the magnet is brought to a suitable distance from the particle, and this distance is measured by means of the travelling microscope. A current of 10.0 amp. is then passed through the coil, and the movement of the particle is timed with a stop watch reading to 0.01 sec. The particle is allowed to travel a short distance before timing commences, and it is usually convenient to time the travel over a distance of about  $100 \mu$  (10 divisions on the scale of the ocular). Measurements of the particle velocity are made over a range of values of  $d$  for each liquid studied.

1 cm., the velocity  $v$  is directly proportional to  $1/d^3$ ; hence the particle is magnetically saturated so that equation (III) holds, and the slope of the straight line drawn through the points is inversely proportional to the viscosity of the liquid. Values of  $v$  are also plotted in Fig. 2 for castor oil as the liquid, and here differently shaded circles represent values for two different particles of equal radius; the degree of reproducibility achieved is to be regarded as satisfactory when the possibility of differences in the magnetic properties of the two particles is considered. Taking the viscosity of the castor oil as 9.86 poise at 20° C., a comparison of the slopes of the two lines gives a value of 20.8 poise for the viscosity of the Golden Syrup-water mixture; the value obtained by measurement in an Ostwald viscometer is 20.4 poise. The method is therefore suitable for the determination of viscosity over a fairly wide range of rates of shear (thus, for example, the maximum rate of shear range covered for castor oil is 0.7 to 4 sec.<sup>-1</sup>).

**Investigations with Non-Newtonian Liquids.**—The method was originally devised in order to study the viscosity characteristics of moderately concentrated solutions of various polymethyl methacrylates in dichlor-diethyl ether as solvent. The examination of these solutions in an Ostwald viscometer showed that they exhibit non-Newtonian behaviour if the molecular weight exceeds 100,000, the apparent viscosity decreasing rapidly with increasing rate of shear. In Fig. 3, data are given for three concentrations of a polymethyl methacrylate in dichlor-diethyl ether, the concentration  $c$  being expressed as g. of solute per 100 ml. of solution.\* Here again two particles were used in each solution, and clearly the rate of shear was sufficiently low to become a linear function of the shearing stress, so that the slopes of the lines are representative of the rest viscosities of the respective solutions. Taking the castor oil line of Fig. 2 as standard, the values for the rest viscosities are: 4.46 poise for  $c = 5.0$ , 26.1 poise for  $c = 8.0$ , and 75.3 poise for  $c = 10.0$ . Corresponding values obtained by measurements in an Ostwald viscometer were always less than these, indicating that the Newtonian behaviour region was never reached. With polymethyl methacrylates of molecular weights up to 400,000, the moving particle method provided

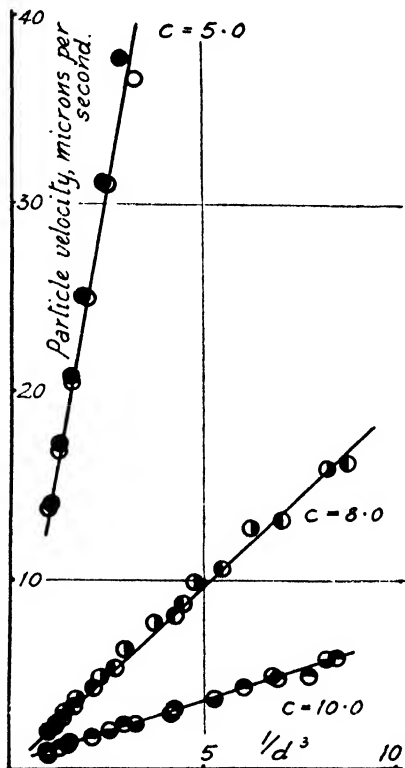


FIG. 3.—Particle velocities in solutions of polymethyl methacrylate of molecular weight 141,000.

\* The molecular weights were obtained by using the expression: molecular weight =  $K[\eta]_0/c$ , where  $\eta_0$  is the specific viscosity and  $K$  the Staudinger constant, taken as  $5.38 \times 10^4$ . Measurements of  $\eta_0$  were made at several low values of  $c$ , using benzene as solvent, and the values were then extrapolated to zero concentration. These measurements were made with an Ostwald viscometer, since at low concentrations the behaviour of the solutions is Newtonian over the range of shear rates operative in the Ostwald instrument.



values of the rest viscosity for every solution examined; values of  $v$  for a solution with  $c = 1.0$  and molecular weight 400,000 are plotted in Fig. 4. In the molecular weight range 300,000-400,000, the apparent viscosity (as measured in an Ostwald viscometer) was very markedly different from the rest viscosity; for example, a solution with  $c = 2.0$  and molecular weight 370,000 gave a rest viscosity value of 7.80 poise, whereas the apparent viscosity was 4.50 poise, the magnitude of this latter quantity depending of course on the rate of shear. Fig. 4 also shows values of the particle velocity in a solution where the molecular weight of the

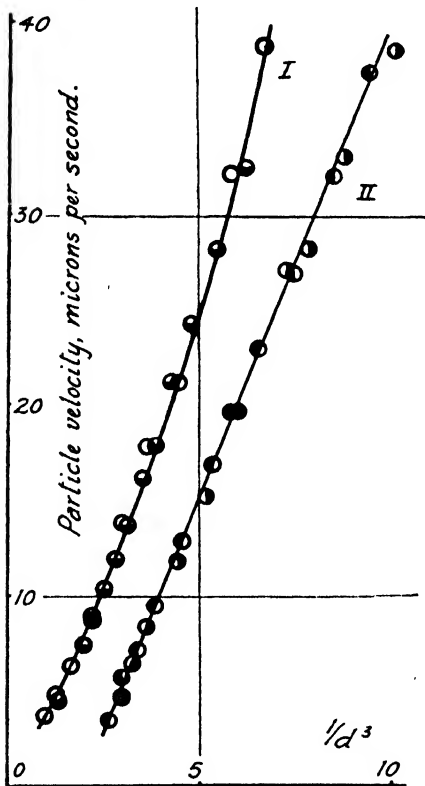


FIG. 4.

- I:  $c = 1.0$ , molecular weight 600,000.  
 II:  $c = 2.0$ , molecular weight 400,000  
 (points displaced 2 units to the right).

polymethyl methacrylate is 600,000, and the concentration equal to 1.0. Here the points no longer lie on a straight line, the flow is non-Newtonian, and the viscosity falls with increasing particle velocity, i.e. with increasing rate of shear. It seems likely, therefore, that the limiting value of the rate of shear below which the latter is a linear function of shearing stress becomes less as the molecular weight of the solute increases, and hence measurements are necessary at very low values of the particle velocity in order to obtain a value of the rest viscosity.

The exigencies of wartime research have prevented a full investigation into the viscosity characteristics of polymethyl methacrylate solutions, and the results obtained are therefore insufficient to merit discussion. Moreover, it is certain that the moving particle method could with advantage be improved in both scope and accuracy: nevertheless, the results achieved by the method are sufficient to justify its usefulness in determining viscosity values over a wide range of rates of shear, and to show that the region of Newtonian flow can readily be surveyed experimentally.

This work was carried out at the University of Leeds as part of an extra-mural investigation for the Ministry of Supply, under the direction of Professor Whytlaw-Gray, F.R.S. To him and his colleagues the author is very grateful for much assistance and advice. Thanks are also due to Professor E. N. daC. Andrade, F.R.S., for some valuable criticism of the theory, and to the Chief Scientific Officer, Ministry of Supply, for permission to publish this paper.

### Summary.

A viscometer is described, in which the velocity of travel of a microscopic iron sphere is measured, the sphere being moved in a horizontal plane through the liquid by means of an electromagnet. An equation relating the velocity to the viscosity of the liquid and the distance  $d$  of the sphere from the magnet

is derived and verified experimentally; by varying  $\dot{\gamma}$ , a wide range of rates of shear can be obtained. The method is applied to the study of solutions of polymethyl methacrylate, which exhibit non-Newtonian behaviour at ordinary rates of shear. Provided that the molecular weight of the polymethyl methacrylate is not greater than 400,000, a range of rates of shear can be obtained sufficiently low to make the shear rate a linear function of the shearing stress, and the viscosity values are then the rest viscosities of the solutions.

### Résumé.

On décrit un viscosimètre, dans lequel la vitesse d'une bille microscopique de fer est mesurée dans un plan horizontal au sein du liquide. On établit pour le système l'équation théorique, qui est vérifiée expérimentalement pour des solutions de méthacrylates de polyméthyle, corps qui se comportent comme des liquides non-newtoniens à des vitesses ordinaires de cisaillement. Si le poids moléculaire du polymère est inférieur à 400.000, la vitesse de cisaillement est une fonction linéaire de l'effort de cisaillement et les viscosités statiques peuvent être mesurées directement.

### Zusammenfassung.

Es wird ein Viskosimeter beschrieben, in dem die Geschwindigkeit einer mikroskopischen Eisenkugel in einer horizontalen Ebene in der Flüssigkeit gemessen wird. Die theoretische Gleichung für das System wird abgeleitet und experimentell für Lösungen von Polymethylmethacrylat bestätigt, das bei gewöhnlichen Schergeschwindigkeiten nicht-Newton'sches Verhalten zeigt. Wenn das Molekulargewicht des Polymeren geringer als 400,000 ist, ist die Schergeschwindigkeit eine lineare Funktion der Scherspannung und die statische Viskosität kann direkt gemessen werden.

*Department of Inorganic and Physical Chemistry,  
The University of Liverpool.*

---

## THE EFFECT OF TURBULENCE ON HETEROGENEOUS REACTION RATES.

BY J. CORNER.

*Received 28th March, 1946.*

### 1. Introduction.

The study of flames in gases is a subject whose technical importance is as great as its scientific interest. One of the more striking features is the effect of turbulence on flames. Damköhler<sup>1</sup> has discussed the effect on Bunsen flames, where at least two types of phenomena can be seen: fluctuations of large linear scale alter the shape of the flame, while at the same time small scale turbulence increases the flame speed. To eliminate the first of these changes it is desirable to discuss flames which are, as far as possible, anchored to some solid surface. Burner flames are supported in this way only at the lip of the burner. A much closer approach to the ideal is a flame produced at the surface of an organic compound decomposing exothermally. We consider the case of a substance undergoing a primary decomposition in the solid, whose products pass out into the vapour phase, there to undergo a reaction which makes itself evident as a flame. Under suitable conditions, the speed of the process is determined by the flame speed in the mixture of intermediate products. The solid plays the role only of a generator of the intermediate products except when there is a turbulent flow parallel to the surface; the solid, receding

<sup>1</sup> Damköhler, *Z. Elektrochem.*, 1940, 46, 601.

at a speed of the order of a cm. per sec., then acts as a constraint on the shape of the flame surface, which would otherwise be distorted. Turbulence can now affect only the speed of the flame. Such systems are in fact known. Here we discuss only the theory of the changes in the flame speed produced by turbulence.

## 2. Experimental.

A set-up which can be realised in practice consists of a large block of the material, with a long cylindrical cavity of circular cross-section. It is necessary to have some device for simultaneous ignition of the surface of the channel, and a valve for controlling the pressure. The simplest form of the latter is a Venturi discharging into the atmosphere. For substances which burn readily the gases produced have a temperature of order  $2500^{\circ}\text{K.}$ , while the pressures which can conveniently be maintained in such a system are of order 50-100 atmos. The velocity of escape of the gases at the throat of the Venturi is the local velocity of sound, which at these temperatures is of order 1000 m./sec. Thus it is possible to produce velocities, down the surface of the cavity, of some hundreds of metres per sec.

The first matter to be considered is the probable value of Reynolds' number. For flow in a cylindrical tube Reynolds' number is usually taken to be

$$R = \frac{\text{velocity} \times \text{radius}}{\text{kinematic viscosity}}.$$

The kinematic viscosity  $\nu$  is equal to  $\mu/\rho$ , where  $\mu$  is the ordinary coefficient of viscosity and  $\rho$  the density. Let us assume that the temperature and pressure of the gases are about  $2500^{\circ}\text{K.}$  and 100 atmos. Taking the kinematic viscosity to be much the same as that of air at this temperature and pressure, its value may be found as follows: the viscosity of many gases varies with temperature according to a law closely represented by Sutherland's formula

$$\mu \propto T^{3/2}/(T + C),$$

where  $C$  is a constant of the order of 100 for light gases such as nitrogen. Viscosity is nearly independent of the pressure  $P$ , for small  $P$ . For example, the viscosity of nitrogen increases only by 15 % as  $P$  increases from 0 to 100 atmos. (at  $75^{\circ}\text{C.}$ ). Hence the kinematic viscosity can be taken to be proportional to

$$T^{3/2}/P(T + C).$$

Its value for air at  $0^{\circ}\text{C.}$  is  $0.132\text{ cm.}^2/\text{sec.}$  (International Critical Tables). Hence the value at  $2500^{\circ}\text{K.}$  and 100 atmos. is about  $5 \times 10^{-2}\text{ cm.}^2/\text{sec.}$  For a radius of 2 cm. and a typical velocity of 250 m./sec., the value of  $R$  proves to be about  $10^6$ . This value of Reynolds' number is proportional to the pressure, but it is substantially independent of the temperature of the gases.

Such a high Reynolds' number is sufficient to set up turbulence not only in the main flow but also in the layer near the boundary. We must consider, however, the distance down the conduit in which the turbulence is developing. For flow in a cylindrical channel with smooth entry, a laminar flow with a large Reynolds' number  $R$  has a transition to turbulence within a distance  $(10^6/R) \times \text{radius of channel}$  (p. 360, *Modern Developments in Fluid Dynamics*, Vol. I and II (ed. Goldstein), Oxford, 1938; subsequently referred to as "*Fluid Dynamics*"). This is of the same order as the radius in our case. After this transition to turbulence has taken place, a further distance is needed before the velocity distribution across the channel cross-section takes up its final form. The distance has been calculated theoretically, assuming fully developed turbulence at the start, and has been measured experimentally (*Fluid Dynamics*, p. 360). The experimental results are larger than the theoretical by a

factor of about two. At  $R = 10^6$ , even the theoretical distance is 30 diameters. It must be concluded that the nature of the flow at any point in the conduit is not likely to be *accurately* described by the final velocity distribution in a long channel in which the flow has the constant Reynolds' number appropriate to this particular point of the cavity. Nevertheless, this approximation seems to be forced on us by the lack of experimental data on turbulence when the velocity varies along the channel. On the other hand, the error in our approximation may not be so large as is suggested by the large value of the "inlet length". The limiting velocity distribution is probably attained at the walls much sooner than at the axis.

Another difficulty arises from the fact that most knowledge of turbulence has been obtained from experiments in which compressibility effects were negligible. At the open end of the conduit the velocity of the gas may be as much as half the local velocity of sound, so that compressibility may considerably modify the nature of the turbulent flow.

Most experiments on turbulence have been carried out in channels with smooth impermeable walls. In the type of experiment we are considering there is an emission of gas from the walls. The velocity normal to the surface is fortunately small, usually of order 1 m./sec., and independent of the pressure. Over the greater part of the length of the channel, this velocity is certainly less than one-tenth of the stream velocity at the relevant distance from the wall. It seems reasonable, therefore, to use the results of experiments on smooth impermeable walls.

### 3. Hydrodynamic Considerations.

There are three current theories of turbulence: Prandtl's momentum transfer theory, Taylor's vorticity transfer theory in its two forms (a) with symmetrical turbulence, (b) with isotropic turbulence and Karman's similarity theory.\* The Prandtl momentum transfer theory is the most convenient to apply to the flow near a solid surface. The vorticity transfer theory does not give satisfactory results for the velocity distribution near a wall (*Fluid Dynamics*, p. 344), which is just the region where the momentum transfer theory seems to work best (for the case of the temperature distribution between rotating cylinders, cf. *Fluid Dynamics*, p. 663). We therefore use the momentum transfer theory, of which descriptions can be found in *Fluid Dynamics* (ch. V, especially § 81).†

The flow near the wall of a tube depends on the Reynolds' number, and for a value of about  $10^6$  it is of the following nature. There is a "laminar sub-layer" next to the wall in which the turbulent velocities, perpendicular to the wall are small. It is obvious that the root-mean-square component of velocity perpendicular to the wall must tend to zero as the wall is approached. Experimental evidence confirms this (Page and Townsend<sup>2</sup>). In the "laminar sub-layer" the Reynolds' stresses (which represent the transport of momentum across a surface due to the velocity fluctuations) are much less than the stresses caused by viscosity.

Outside this sub-layer there is a transition region where the Reynolds' stresses are of the same order as the viscous stresses, both regions together forming the "viscous layer". Further out lies the greater part of the stream, in violent eddying motion with negligible viscous stresses. This forms by far the greater part of the channel cross-section.

Information about the region near the wall can be obtained from the heat transfer from pipes to fluids. This work is summarised in *Fluid*

\* These are fully discussed in *Fluid Dynamics*; cf. also, Dryden, *Aerodynamics of Cooling*, div. T, vol. VI of *Aerodynamic Theory* (ed. Durand), Berlin, 1936, p. 246, where the connection between the Prandtl and Taylor mixing lengths is discussed. This reference will later be abbreviated to "Dryden".

† Cf. also Prandtl, *Mechanics of Viscous Fluids*, div. G, vol. III, of *Aerodynamic Theory* (ed. Durand), Berlin, 1935. This will subsequently be referred to as "Prandtl".

<sup>2</sup> Page and Townsend, *Proc. Roy. Soc. A*, 1932, **135**, 657.



(Prandtl, p. 140). This result, and the constancy of  $V_*$  over the cross-section, can be taken as first approximations to flow with a pressure gradient in a channel. The relation between  $\bar{U}$  and  $V_*$  is

$$\bar{U} = V_*[2.5 \log_e (rV_*/\nu) + 1.75] \quad (4)$$

(equation (22.21), Prandtl, p. 143).

To obtain  $V_*$  as a function of  $\bar{U}$  this equation can be written as

$$r\bar{U}/\nu = [2.5 \log_e (rV_*/\nu)rV_*/\nu + 1.75]$$

so that

$$V_* = (\nu/r) f(r\bar{U}/\nu) \quad (5)$$

where the function  $f(R)$  satisfies the equation

$$R = f(R)[2.5 \log_e (f(R)) + 1.75] \quad (6)$$

We want an explicit form for  $f(R)$  when  $R$  is near  $10^6$ . Typical solutions of (6) are shown in the Table.

These show that  $f(R) \simeq R/30$  for a wide range of  $R$  near  $10^6$ .

Substituting in (5),

$$V_* = \bar{U}/30 \quad (7)$$

It is convenient that the dependence on tube radius  $r$  and kinematic viscosity  $\nu$  has vanished in this region of high Reynolds' numbers

$f$	$R/f$	$R$
$10^4$	24.8	$2.5 \times 10^5$
$10^5$	30	$3.0 \times 10^6$
$10^6$	36.3	$3.6 \times 10^7$

We can now use (7) to obtain the dimensionless distances in our problem in terms of the mean velocity:

$$\eta = V_*x/\nu = \bar{U}x/30\nu \quad (8)$$

Theoretical calculations (Boys and Corner, to be published later) on the structure of flames have shown that for a typical case of decomposition at 100 atmos., the value of  $x$  at the most important region in the flame is about  $10^{-3}$  cm.; if we take  $\bar{U} = 250$  m./sec. and  $\nu = 5 \times 10^{-2}$  cm.<sup>2</sup>/sec., we find that the important region of the flame is in the neighbourhood of  $\eta = 15$ . The "flame thickness" and  $\nu$  are both proportional to  $1/P$ , so this value for  $\eta$  is independent of the pressure.

The point  $\eta = 15$  lies in a region where the heat transfer by conductivity and by turbulent mixing are of the same order of magnitude. As we have mentioned, the heat transfer of fluids in pipes has been studied theoretically, taking into account the layers near the wall where turbulence is not so all-important as in the main stream. A summary of this work can be found in *Fluid Dynamics*, p. 654. The most detailed model is that used by Karman,<sup>3</sup> who distinguished between three regions: (i) "laminar sub-layer" at wall, with negligible turbulence; (ii) transition region with heat transfer by turbulence of same order as transfer by conductivity; (iii) fully turbulent region extending over most of the channel. The division into three regions with changes of the form of velocity distribution at the junctions, is itself only an approximation to the true continuous transition, but it gives good agreement with experimental results, if the boundaries between the three regions occur at  $\eta = 5$  and 30. This shows that part of the flame lies in a region where turbulence can be neglected, and that nowhere in the flame is the heat transfer by turbulent mixing of paramount importance.

The simpler Prandtl-Taylor theory which omits the transition region fits the observations near  $\sigma = 1$ , if the transition occurs where  $U/V_* \simeq 5.6$  (*Fluid Dynamics*, p. 655). The velocity distribution appropriate to the fully turbulent region is

$$U/V_* = 5.8 + 2.5 \log_e \eta \quad (9)$$

(Prandtl, p. 140, eqn. (22.12)), so the transition from laminar to turbulent flow would be placed, by this method, near  $\eta = 1$ . This is, however, no more than a rough confirmation of the more reliable result using a

separate transition region. A similar two-region system has been investigated theoretically by Takahasi,<sup>4</sup> who concluded that the transition lay at  $\eta = 8$ .

We have found the relation between  $x$ , the distance from the wall, and  $\eta$  the hydrodynamical variable. To calculate the heat transfer by turbulence we need also a formula for the mixing length  $l$  near the wall. The result (3), which is of the right form, is valid at high Reynolds' numbers but only for large  $\eta$ , greater than 2500 according to Prandtl (p. 141); below this the ratio  $l/x$  becomes a function of the Reynolds' number. However, (3) is certainly correct in order of magnitude. Karman's treatment leads to

$$U/V_* = -3.05 + 5 \log_e \eta \quad (10)$$

as the velocity distribution in the transition region (*Fluid Dynamics*, p. 657), compared with (9) in the fully turbulent region. The use of (10) instead of (9) means that (3) must be replaced by

$$l = 0.2x \quad (11)$$

in the transition region of Karman's model. We may write, therefore,

$$l = xg(\eta) \quad (12)$$

where  $g$  is a steadily increasing function of  $\eta$ , with  $g(\infty) = 0.4$ ;  $g \simeq 0.2$  for  $\eta$  of order 10, and  $g(\eta)$  probably very small for  $\eta$  near 1. So far as we know, there is at present no other hydrodynamical information about  $g$ . With no more information than this, we can find a great many formulæ to represent  $g(\eta)$ . The simplest appears to be

$$g = 0.47/(10 + \eta). \quad (13)$$

We may note that these results give some support for our approximation of taking the velocity and mixing length distributions to be those appropriate to the Reynolds' number at the cross-section in question and not to the Reynolds' number at some section further upstream. For at these high Reynolds' numbers,  $l/x$  depends only on  $\eta$ , which, at a given  $x$ , does not depend strongly on the cross-section chosen. Also  $V_*/\bar{U}$  is independent of  $R$ .

We have now obtained all the hydrodynamic quantities needed in the calculation of the extra heat conductivity in the flame zone, due to turbulence of the gas flow.

#### 4. Effective Thermal Conductivity in the Flame Zone.

The flame speed depends on the thermal conductivity of the gases in the flame zone. Turbulence enhances this conductivity, and hence increases the flame speed. It is usual to assume that the effective heat conductivity is the sum of the ordinary thermal conductivity together with an "eddy-conductivity," calculated as follows.

Let  $c_p$  be the fluid specific heat at constant pressure, per unit mass. In unit time the heat transferred across unit area normal to the  $x$ -axis, in the direction of  $x$  increasing, is

$$- \rho c_p l^3 \left| \frac{dU}{dx} \right| \frac{\partial T}{\partial x}$$

(Prandtl, p. 163) and the thermal conductivity is therefore  $\rho c_p l^3 \left| \frac{dU}{dx} \right|$ , which, from (2), is equal to

$$\rho c_p^2 V_* = \rho c_p U x g(\eta) / 30 \quad (14)$$

from (7) and (12). Let  $\lambda_0$  be the ordinary thermal conductivity of the gas in the flame. Strictly, this varies through the flame, but only slowly, and an average value can be taken. Near the surface the effective conductivity is therefore

$$\lambda = \lambda_0 + \rho c_p U x g(\eta) / 30 \quad (15)$$

<sup>4</sup> Takahasi, *Proc. Phys.-Math. Soc. Japan*, 1939, 21, 672.

This derivation of the eddy-conductivity is not quite correct in our case, as it has been assumed that a small block of fluid preserves the temperature of its origin until it mixes with its surroundings. This is true in the usual circumstances in which a turbulence conductivity is used (e.g. meteorology). It is also true of a small block of reaction products, passing from outside the flame back into a region of only partly reacted gas, because this block cannot change its temperature by internal reaction. On the other hand a block moving outwards faster than the general stream will rise in temperature as it goes owing to reaction, and only for very high velocities will it traverse its "mixing length" with the temperature at which it started. The conductivity we have derived is therefore somewhat too large.

### 5. Rate of Burning with Turbulence.

In the previous section we have derived a formula, (15), for the conductivity near the decomposing surface. One way of finding the rate of burning associated with such a conductivity would be to integrate the equations of the flame zone with this variable conductivity. Numerical integration would be necessary.

It is possible to use an approximate method which gives an explicit formula for the rate of burning. In this method we replace the constant conductivity  $\lambda_0$  (appropriate to burning with  $\bar{U} = 0$ ) by a different constant value derived from (15) by giving the quantities which vary through the flame their values appropriate to the most important region. This will probably be in the part where the reaction is half-completed. This treatment can be expected to give the right dependence on the pressure, mean velocity, and properties of the reactant, and lead to the right order of magnitude for the various coefficients. The method has been tested by comparison with the results of numerical integration of a number of typical flames, and the agreement is reasonably satisfactory.

Using suffix  $o$  to denote values in the most important region of the flame, we have

$$\lambda = \lambda_o + \rho_o c_{p_o} \frac{\bar{U} x_o}{30} g\left(\frac{\bar{U} x_o}{30 \nu_o}\right) \quad (16)$$

### 6. Formulæ from the Theory of Flames.

In a forthcoming paper by Boys and Corner, the theory of flames maintained by a single chemical reaction will be discussed in some detail. We shall quote certain results from their work.

They show that for a unimolecular reaction,  $x_o \propto \lambda^{\frac{1}{2}} P^{-\frac{1}{2}}$  and the rate of consumption by the flame is proportional to  $\lambda^{\frac{1}{2}} P^{\frac{1}{2}}$ . We write

$$\zeta = (\lambda/\lambda_o)^{\frac{1}{2}} \quad (17)$$

so that as regards pressure and turbulence the dependence of  $x_o$  is  $x_o \propto \zeta P^{-\frac{1}{2}}$  and of the consumption by the flame is  $\propto \zeta P^{\frac{1}{2}}$ . Since  $\rho_o$  is proportional to the pressure and  $\nu_o$  is proportional to  $P^{-1}$ , at pressures of order 50 atmos., we have from (16) and (17)

$$\zeta^2 = 1 + \alpha \theta g(\beta \theta) \quad (18)$$

where

$$\theta = \bar{U} P^{\frac{1}{2}} \zeta \quad (19)$$

and  $\alpha$  and  $\beta$  are independent of pressure and  $\bar{U}$ , depending only on the nature of the substance being burnt. The universal function  $g$  has been discussed in section 3.

For a bimolecular reaction,  $x_o \propto \zeta P^{-1}$  and the rate of burning is proportional to  $\zeta P$ . In this case,

$$\zeta^2 = 1 + \gamma \phi g(\delta \phi) \quad (20)$$

where

$$\phi = \bar{U} \zeta \quad (21)$$

and  $\gamma$  and  $\delta$  depend only on the nature of the substance being burnt.



## 642 TURBULENCE ON HETEROGENEOUS REACTION RATES

Since in this case the equation (20) for  $\xi$  does not contain the pressure, the rate of burning can be written as proportional to (pressure)  $\times$  (a function of  $\bar{U}$ ).

For a typical organic substance decomposing in this manner, yielding a final temperature of 2500° K., it can be shown that  $c_p$  of products  $\approx 0.4$  cal./g.,  $\rho_0 \approx 10^{-4} P$  g./cc.,  $v_0 \approx 5/P$  cm.<sup>2</sup>/sec.,  $\lambda_0 \approx 2 \times 10^{-4}$  cal./cm.<sup>2</sup> sec. (° C./cm.), and  $x_0 \approx 8 \times 10^{-2}/P$  cm. at  $\bar{U} = 0$ . These lead to the orders of magnitude

$$\gamma \sim \delta \sim 5 \times 10^{-4} \quad (22)$$

provided  $U$  is measured in cm./sec.

It has been found important to predict the variation of these parameters from one substance to another. Table I shows our estimates

TABLE I.—VARIATION OF  $\gamma$  AND  $\delta$  WITH SUBSTANCE BEING BURNED.

Substance.	Final Temperature (°K).	Relative Values of $\gamma$ .	Relative Values of $\delta$ .
A	3000	0.77	0.60
B	2500	1	1
C	1800	1.33	1.70

of  $\gamma$  and  $\delta$  for three substances giving very different final temperatures. The quantity  $\delta$  appears to vary as  $\gamma^2$ , roughly. The effect of gas-flow over the surface is seen to be greater the cooler the final products. This agrees with unpublished observations communicated to me

by Dr. S. F. Boys. A similar effect has been noted in experiments with gas mixtures (Kratz and Rosecrans<sup>2</sup>). A fast burning mixture is less affected by whirling of the gas than is a slow burning mixture. The physical explanation is presumably analogous to that of our result.

I am indebted to the Chief Scientific Officer, Ministry of Supply, for permission to publish this paper.

### Summary.

The decomposition of an organic substance by a vapour-phase reaction close to its surface is considered. This process is known to be affected by streaming of the gas parallel to the surface. A theoretical treatment of the effect of turbulence on such a reaction explains the qualitative observations, and shows how the phenomenon is related to the temperature of the products and the gas velocity parallel to the surface.

### Résumé.

On considère la décomposition d'un corps organique dans le voisinage immédiat de sa surface par une réaction en phase gazeuse. On savait que ce processus est affecté par l'écoulement du gaz parallèlement à la surface. L'effet de la turbulence sur une telle réaction, considéré d'un point de vue théorique, permet d'expliquer les observations qualitatives et montre que le phénomène est lié à la température des produits et à la vitesse du gaz parallèlement à la surface.

### Zusammenfassung.

Die Zersetzung einer organischen Substanz durch eine Reaktion in der Dampfphase nahe ihrer Oberfläche wird untersucht. Es ist bekannt, dass dieser Vorgang durch Gasströmungen parallel zur Oberfläche beeinflusst wird. Eine theoretische Ausarbeitung des Effekts der Turbulenz auf eine solche Reaktion erklärt die qualitativ von Beobachtungen und zeigt wie die Erscheinung mit der Temperatur der Produkte und der Gasgeschwindigkeit parallel zur Oberfläche zusammenhängt.

<sup>2</sup> Kratz and Rosecrans, *Univ. Illinois Exp. Stat. Bull.* No. 133, 1922.

# THE ABSORPTION SPECTRA OF SOME MONO-NITRONAPHTHYLAMINES, WITH OBSERVATIONS ON THEIR STRUCTURES. PART II. 3-, 5-, 6-, 7- AND 8-NITRO-2-NAPHTHYLAMINES AND 6-NITRO-1-NAPHTHYLAMINE.

By H. H. HODGSON AND D. E. HATHWAY.

Received 6th May, 1946.

## I.

In a previous communication (Part I),<sup>1</sup> the absorption of 2-, 3-, 4-, 5- and 8-nitro-1-naphthylamines, of 1- and 4-nitro-2-naphthylamines, and of the parent substances, the  $\alpha$ - and  $\beta$ -naphthylamines and  $\alpha$ - and  $\beta$ -nitronaphthalenes, were recorded within the region  $\lambda$  2000-5000 Å. The present investigation extends the study to the rest of the mononitronaphthylamines with the exception of 7-nitro-1-naphthylamine, preparation of which by the procedure of Veselý and Dvůrák<sup>2</sup> has so far been fruitless. Recently,<sup>3</sup> pure 3-nitro-2-naphthylamine has been obtained and is scarlet in colour, while 7-nitro-2-naphthylamine has been isolated<sup>4</sup> and is deep yellow. The earlier statement that all known heteronuclear mononitronaphthylamines were orange-red requires modification in that the 5- and 6-nitro-2-naphthylamines should be styled orange-yellow and golden-yellow respectively.<sup>5-8</sup> (Since this work was completed, Hertel<sup>9</sup> reports that the spectra of 6- and 8-nitro-2-naphthylamines have been recorded, although the paper is unobtainable in this country.)

This further study, while confirming in broad outline the tentative conclusions of Part I, has, however, necessitated a more critical interpretation of the positions of the band-heads of the 5-, 6-, and 7-nitro-2-naphthylamines (Fig. 2) the spectra of which are markedly dissimilar, although this discussion is limited by the absence or inadequacy of data, e.g. the non-existence of unsaturated aliphatic nitro- and nitroamino- compounds exhibiting the desired chromophores prevents analysis of the spectra, while dipole moment data<sup>10, 11</sup> do not apply to any of the isomerides now reviewed.

## Experimental.

Light-absorption measurements were made by means of an Adam Hilger Medium Quartz Spectrometer, the absorption due to 2 cm. paths being compared photographically with a blank cell filled with the solvent used. The tungsten-steel spark-gap, of capacity 0.005 F. gave a 22,000 v. wave-peak. All solutions were in absolute alcohol, and all exposures were taken within 30 minutes of dissolution.  $\epsilon$  is the molecular extinction coefficient defined by:  $\epsilon = (\log_{10} I_0/I)/cl$ , where  $I_0$  and  $I$  are the intensities of the incident and transmitted light respectively,  $c$  = concentration in g.-mol./litre, and  $l$  = cell thickness in cm.

<sup>1</sup> Hodgson and Hathway, *Trans. Faraday Soc.*, 1945, **41**, 115.

<sup>2</sup> Veselý and Dvůrák, *Bull. Soc. Chim.*, 1923, **33**, 319.

<sup>3</sup> Hodgson and Hathway, *J. Chem. Soc.*, 1945, 841.

<sup>4</sup> Hodgson and Ward, *ibid.*, 1945, 590.

<sup>5</sup> Friedländer and Szymanski, *Ber.*, 1892, **25**, 2077.

<sup>6</sup> Morgan and Chazan, *J. Soc. Chem. Ind.*, 1922, **41**, 1.

<sup>7</sup> Hodgson and Crook, *J. Chem. Soc.*, 1936, 1844.

<sup>8</sup> Saunders and Hamilton, *ibid.*, 1932, **54**, 638.

<sup>9</sup> Hertel, *Z. Elektrochem.*, 1941, **47**, 813.

<sup>10</sup> Vassiliev and Sirkin, *J. Physic. Chem. Russ.*, 1938, **12**, 153.

<sup>11</sup> Vassiliev and Sirkin, *Acta Physicochim.*, 1938, **9**, 201.

## Results.

The absorption curves are shown in Fig. 1 and Fig. 2, while Table I records the positions of the band-heads which were found from large-scale

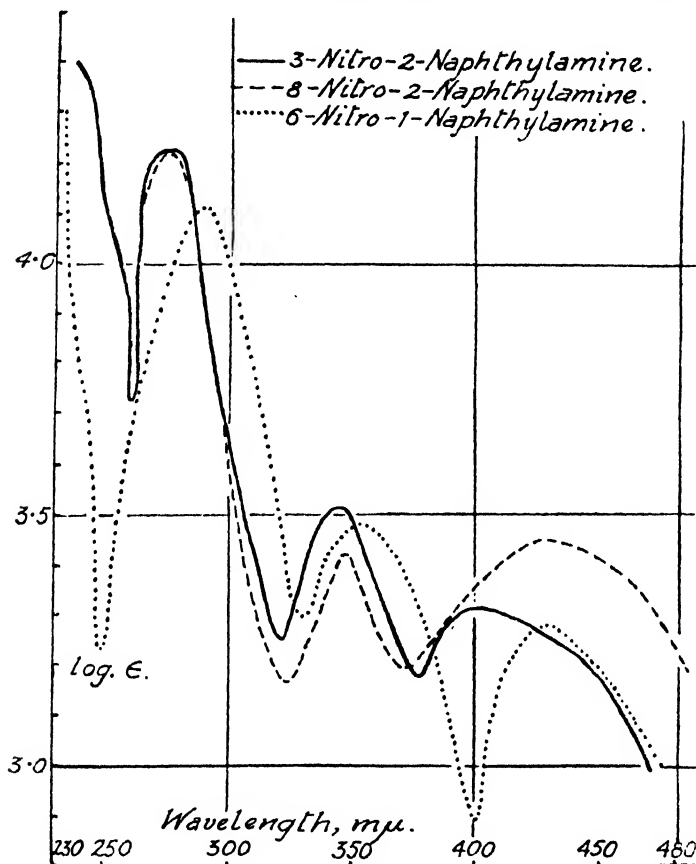


FIG. 1.

drawings. In the region  $\lambda$  2400-3000 Å. the absorption curves of 3- and 8-nitro-2-naphthylamines are almost identical.

TABLE I.—MONONITRONAPHTHYLAMINES.

	$\lambda_{\max}$ (mμ).	$\log_{10} \epsilon_{\max}$ .	$\lambda_{\max}$ (mμ).	$\log_{10} \epsilon_{\max}$ .	$\lambda_{\max}$ (mμ).	$\log_{10} \epsilon_{\max}$ .
<i>Homonuclear.</i>						
3-Nitro-2-naphthylamine	276	4.225	343	3.520	400	3.325
<i>Heteronuclear.</i>						
6-Nitro-1-naphthylamine	290	4.114	353	3.490	429	3.290
5-Nitro-2-naphthylamine	277	4.200	352	3.548	—	—
6-Nitro-2-naphthylamine	292	3.805	—	—	421	4.140
7-Nitro-2-naphthylamine	271	4.260	307	4.185	—	—
8-Nitro-2-naphthylamine	275	4.220	347	3.425	427	3.455

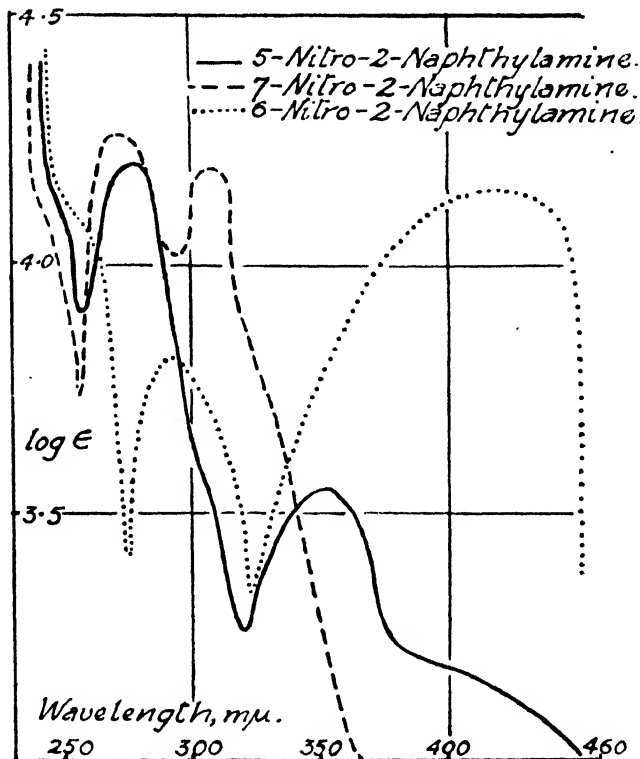
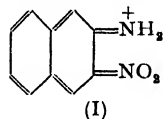


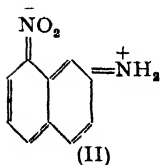
FIG. 2.

### Discussion.

**3-Nitro-2-naphthylamine** exhibits three well-defined bands within the region  $\lambda$  2000-5000 Å. in line with the other previously described red mononitronaphthylamines which also possess three bands. Since the auxochromes (cf. Witt; further defined by Wizinger<sup>12</sup>) are in quinonoid positions, the most probable quinonoid structure (I), would appear to predominate in the resonance hybrid, a view which receives support from the brilliant scarlet colour of the compound.



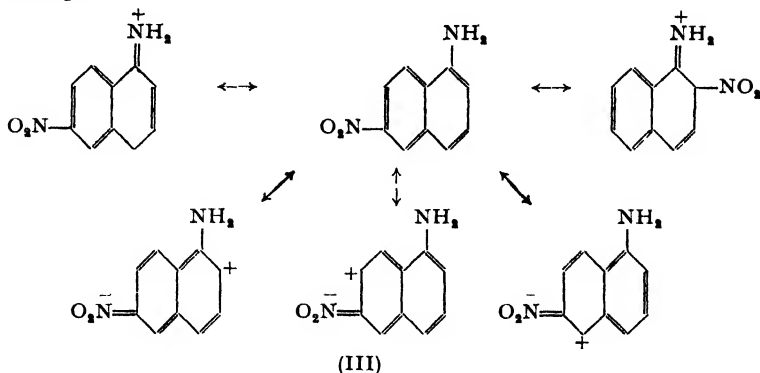
**8-Nitro-2-naphthylamine** also exhibits three bands, in the region where the three bands of the other mononitronaphthalenes appear, and again has its auxochromes in quinonoid positions indicating, together with its red colour, that structure (II), contributes most to the resonance hybrid.



**6-Nitro-1-naphthylamine** differs from the two previous compounds in that the auxochromes must resonate separately into ionic quinonoid structures and, since the resonance hybrid is red and exhibits three bands in its absorption spectrum, it appears reasonable to assume that the central bond in the hybrid is mainly single in character, and that those ionic structures (III) will predominate which possess the single central bond.

<sup>12</sup> Wizinger, *Organische Farbstoffe*, Ferd. Dummlers Verlag (Berlin and Bonn, 1933).

For example :



**6-Nitro-2-naphthylamine** greatly resembles 4-nitro-1-naphthylamine in having the two extreme bands but not the central band in the spectrum and in being golden yellow. In both these molecules, as opposed to the other isomerides, the long wave-length band is of greater area ( $\int \epsilon d\lambda$ ), than the short wave-length band and possesses an ordinate of greater modulus.

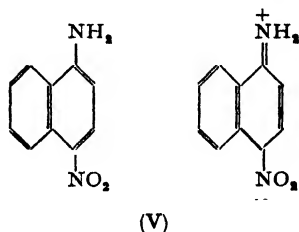
TABLE II.

	$\lambda_{\max}$ (m $\mu$ ).	$\log_{10} \epsilon_{\max}$ .	$\lambda_{\max}$ (m $\mu$ ).	$\log_{10} \epsilon_{\max}$ .
4-Nitro-1-naphthylamine .	269	3.94	443	4.18
6-Nitro-2-naphthylamine .	292	3.805	421	4.14

Here facile resonance into unique quinonoid structures can occur in both cases, and these structures (IV) can be regarded as greatly predominant, if not unique, in the resonance hybrid. The great stability of these para-quinonoid structures is confirmed by the presence of only two bands in the spectrum, i.e. absence of resonance into ionic structures, whereas facile resonance of the red isomerides into other structures is shown by three bands in their spectra.

The parallelism between the spectra of 4-nitroaniline and 4-nitro-1-naphthylamine is of great interest. Lewis and Calvin<sup>13</sup> point out that

4-nitroaniline has a dipole moment considerably greater than the sum of the separate moments of nitrobenzene and aniline, which they regard as illustrative of the principle that a displacement from the ideal molecule renders further displacement easier. Such a displacement is exemplified by the absorption spectrum which exhibits two strong bands of about equal intensity due to an abnormal increase in the mobility of the electrons through the additive effect of the two auxochromes. In the spectrum of 4-nitro-1-naphthylamine as

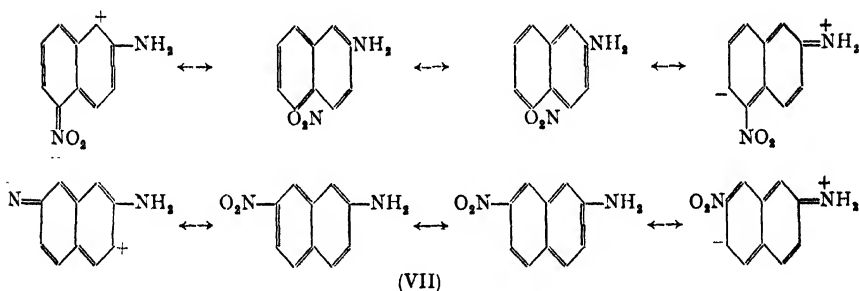
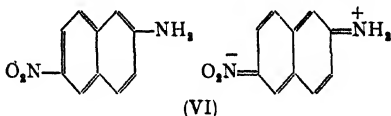


<sup>13</sup> Lewis and Calvin, *Chem. Rev.*, 1939, **25**, 282.

compared with those of the other nitronaphthylamines, the same persistence of two strong bands occurs and the molecule is written as in (V).

It is thus clear that from the close parallelism between the spectra of 4-nitro-1-naphthylamine and 6-nitro-2-naphthylamine, the same principle of displacement from the ideal molecule occurs, and the predominant resonance is (VI). Although no middle band occurs, the resonance of 6-nitro-2-naphthylamine cannot take place without a single central bond, and the yellow colour must indicate stability of the quinonoid form.

**5- and 7-Nitro-2-naphthylamines.** Although the spectra of these compounds exhibit only two bands, it is noteworthy that the extreme long wave-band is absent, causing the second two-band spectra to differ markedly from these of the 2-, 3-, 4-nitro-1-naphthylamines and 6-nitro-2-naphthylamine where the long wave-length band is present and the central band absent. There is also no resemblance between the spectra of the two isomerides themselves other than the fact of two bands of similar wave-lengths. The absence of the long wave-length band might indicate considerable inhibition of electron mobility in the molecule as also does the yellow colour, but the presence of the middle wave-length band is indicative of a central single bond rather than a double bond in the naphthalene structure which may be tentatively assumed for these structures (VII).



While there appears to be resonance mainly between each group and its own ring system, as in the yellow homonuclear nitronaphthylamines where this is exclusive, there will also be limited resonance which is permitted by the central band structure, and evidenced by the middle band between each group and the molecule as a whole. The dominant yellow colour also probably indicates that the homonuclear resonance contributes most to the resonance hybrid in the 5- and 7-nitro-2-naphthylamines.

The authors desire to express their gratitude to Prof. W. Baker, F.R.S., for providing facilities to one of us (D.E.H.) for recording the spectra in his laboratories and for his critical interest in the work. They also thank Imperial Chemical Industries Ltd., Dyestuffs Division, for gifts of chemicals and for a scholarship (to D. E. H.).

### Summary.

1. Yellow and orange-yellow mononitronaphthylamines are 2-, 3-, 4-nitro-1-naphthylamines and 5-, 6-, and 7-nitro-2-naphthylamines; the remaining isomerides are red or orange-red.

2. The spectra of all yellow and orange-yellow mononitronaphthylamines exhibit two absorption bands within the region  $\lambda$  2310-4500 Å., whereas the red and orange-red isomerides have a third band within 3380-3600 Å.

3. The extreme bands are characteristic of both  $\alpha$ - and  $\beta$ -nitro- and  $\alpha$ - and  $\beta$ -amino-naphthalenes, but the middle band is characteristic of  $\beta$ -compounds only.

4. Both of the two extreme bands are characteristic of the yellow and orange-yellow 2-, 3-, and 4-nitro-1-naphthylamines and of 6-nitro-2-naphthylamine, but the extreme long wave-length band is absent from the spectra of the 5- and 7-nitro-2-naphthylamines.

5. Compared with the bands in the  $\alpha$ - and  $\beta$ -nitronaphthalenes and the  $\alpha$ - and  $\beta$ -naphthylamines, the bands of the nitronaphthylamines are shifted towards the longer wave-lengths indicating increased electronic mobility (relief of electronic strain) in the molecule.

6. All the red mononitronaphthylamines which exhibit three bands are thought to possess a single central bond in their structure, and the yellow homonuclear nitronaphthylamines which exhibit two extreme bands to possess a central double bond.

In the cases of 5- and 7-nitro-2-naphthylamines, which possess a central band and one of shorter wave-length, but no extreme long wave-length band, the single central bond for the naphthalene structure is assumed, but the main resonance is confined to the separate nuclei with limited resonance in the molecule as a whole. In the homonuclear nitronaphthylamines, which have two extreme bands, the resonance is restricted to the homonucleus and the naphthalene structure has a central double bond.

### Résumé.

On a enregistré dans la région 2000-5000 Å. les courbes d'absorption des nitro-3, -5, -6, -7, -8  $\beta$ -naphthylamines et de la nitro-6  $\alpha$ -naphthylamine. On donne une interprétation de la position des têtes de bandes pour les nitro-5, -6, -7  $\beta$ -naphthylamines et on montre que les résultats viennent confirmer les conclusions avancées dans la partie I.

### Zusammenfassung.

Die Absorptionskurven der 3-, 5-, 6-, 7- und 8-Nitro-2-naphthylamine im Bereich 2000-5000 Å. werden angegeben. Die Position der Bandkanten der 5-, 6- und 7-Nitro-2-naphthylamine werden erklärt und es wird gezeigt, dass die Ergebnisse im allgemeinen die im I. Teil gezogenen Folgerungen unterstützen.

*Department of Colour Chemistry,  
Technical College, Huddersfield.*

## CONTINUOUS REACTIONS

### PART II. THE KINETICS OF STEADY STATE POLYMERISATION.

BY K. G. DENBIGH.

*Received 2nd July, 1946.*

In an earlier paper<sup>1</sup> (Part I) the general mathematical treatment of continuous reaction processes was discussed and it was shown that differences in the velocity and yield of a reaction may arise, according to whether the reaction is carried out batchwise or continuously. The object of the present paper is to extend the theory to the case of polymerisation processes. Two aspects which are discussed in detail are (a) the effect on molecular weight distribution of a change from a batch to a continuous process, and (b) the possible advantages of using continuous reaction as a laboratory method. Continuous reaction has been used in the laboratory as a means of studying R.D.X. formation,\* and it is certainly a method which is worth applying in a wider field.

<sup>1</sup> Denbigh, *Trans. Faraday Soc.*, 1944, 40, 352.

\* Unpublished work with the Ministry of Supply.

Batch processes and two types of continuous process may be distinguished from each other according to the mode of dependence of the reaction system on the co-ordinates of space and time.

(a) Batch processes, are those in which the system changes with respect to time but is generally uniform throughout its spatial extent, as ensured by good stirring or rapid diffusion. The system is thus temporally variant and spatially invariant. A reaction carried out in a stirred beaker or tank is a familiar example.

(b) A type of continuous process, is that which is carried out by the uniform flow of a fluid through a tubular reaction vessel. Provided that the conditions of flow and temperature remain steady, the system as a whole does not change with respect to time. There is, however, a change of composition along the spatial extent of the reaction vessel and for this reason the process may be conveniently termed *heterocontinuous*. Such a reaction system is spatially variant and temporally invariant.

(c) A second type of continuous process, which may be described as *homocontinuous*, is that in which the composition of the system is uniform throughout its volume. Such a process is that which is commonly carried out in a thoroughly stirred reaction tank, similar to a batch system, but having in addition a continuous feed of new reactant and also a steady outflow of partially reacted material. The properties of this system were discussed in detail.<sup>1</sup> Provided the stirring is good, the composition of the system is the same at all points within the vessel and is equal to the composition of the outflow. Also when the conditions of feed and temperature are steady, the system does not change with respect to time; it is both temporally and spatially invariant and there is a complete stationary state. Although reaction takes place there is no change of the system itself; the reaction is manifest only by a difference in composition between the system and its feed.

The homocontinuous system is thus a reaction entity which maintains itself at a steady state different from that of its environment. In this respect it is similar to a living cell. A second point of resemblance is that it displays an elementary faculty of adaptation, in the form of a change to a new steady state when the external conditions of feed and temperature are changed. It is hoped to develop this view more fully in a later paper.

The rate of a chemical reaction in a batch system is described by a differential equation in which time is the independent variable. The corresponding equation for a heterocontinuous system is one in which the co-ordinate of time is replaced by the co-ordinate of space which is in the direction of flow. In the homocontinuous process, however, there is no change whatsoever in the system when the steady state is attained. The differential equation is then replaced by an algebraic one. For example, consider the simple second order reaction  $A + B \rightarrow C$  and let (A), (B) and (C) be the uniform concentrations in the reaction system and in the outflow. Let  $V$  and  $u$  be the volume of the reaction system and the volume rate of flow respectively. Then  $u(C)$  is the amount of C leaving the reaction system in unit time and  $u(C)/V$  is the amount of C which is formed in unit time in unit volume. Then, by definition of the velocity constant,

$$u(C)/V = k(A)(B) \quad . \quad . \quad . \quad . \quad . \quad (1)$$

It is evident that this is of a simpler form than the corresponding differential equation,

$$\frac{d(C)}{dt} = k(A)(B),$$

for the batchwise reaction. There is thus an intrinsic mathematical simplicity about the homocontinuous reaction process which makes it attractive for the investigation of complex types of reaction for which the integration of the differential equations is often impossible.



The type of reaction for which the mathematical treatment of the batch kinetics is generally most difficult is that in which there are a number of consecutive steps. For each of these steps there is a differential equation containing the concentrations of the species and the specific rate constants. For example, in the case of the hydrolysis of a triglyceride the problem involves the solution of three simultaneous differential equations.

When the number of successive reactions is increased to many thousands, as may be the case for polymerisation, the mathematical difficulties are greatly increased. A completely general solution of the problem of batchwise polymerisation has not been achieved, although solutions have been obtained for certain special cases which depend on the introduction of simplifying assumptions. For example, Dostal and Mark<sup>2</sup> obtained a solution by taking the velocity constants of all the individual propagation reactions as being identical, and neglecting entirely any termination process. The latter is equivalent to making no distinction between a live and dead polymer, as in a polycondensation reaction. The solution was then obtained by a transformation of the time scale, which had the effect of simplifying the integration (*eigenzeit* transformation). Dostal<sup>3</sup> subsequently extended the treatment by making specific allowance for termination processes. Morei<sup>4</sup> and Ginell and Simha<sup>5</sup> adopted a similar procedure. The method of treatment is by no means simple, however, and it remains necessary to retain the assumption of the identity of the velocity constants.

A simplifying treatment of a different kind is that of Gee and Melville,<sup>6</sup> and Herington and Robertson.<sup>7</sup> These authors consider those types of batchwise polymerisation in which the life of the growing polymer is very short compared to the duration of reaction. It is then possible to make the assumption of a stationary state with regard to the concentrations of each of the *active* polymers. A second assumption is that the ratio of the velocity constants of propagation and termination is constant throughout the reaction sequence. It is then possible to obtain a solution of the differential equations for most types of polymerisation reaction which satisfy the above conditions.†

In the section below, the method is described for solving the equations for polymerisation when it is carried out as a homocontinuous process. The treatment is shown to be much simpler than for the corresponding batchwise reaction and can be given in a more general form. This is because the kinetics can be described entirely by means of simple mass balance equations at the stationary state.

### Kinetic Treatment for a Homocontinuous Polymerisation System.

As an example we may consider the case in which there is a first order initiation reaction, followed by bimolecular propagation steps and by a termination process in which two molecules of the active polymer are converted to dead polymer by mutual combination. This is a very suitable example for it is one which is very difficult to deal with in the case of batch

<sup>2</sup> Dostal and Mark, *Z. physik. Chem., B*, 1935, **29**, 299; *Trans. Faraday Soc.*, 1936, **32**, 54.

<sup>3</sup> Dostal, *Monats.*, 1935, **67**, 1, 63, 222; 1937, **70**, 409.

<sup>4</sup> Morei, *Acta Physicochim.*, 1938, **9**, 741.

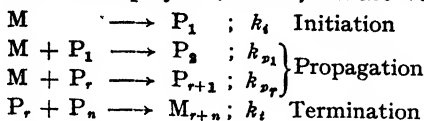
<sup>5</sup> Ginell and Simha, *J. Amer. Chem. Soc.*, 1943, **65**, 706.

<sup>6</sup> Gee and Melville, *Trans. Faraday Soc.*, 1944, **40**, 240.

<sup>7</sup> Herington and Robertson, *Trans. Faraday Soc.*, 1942, **38**, 490; *ibid.*, 1944, **40**, 236. Cf. also Hulbert, Harman, Tobolsky and Eyring, *Ann. N.Y. Acad. Sci.*, 1943, **44**, 371.

† Mention may also be made of the statistical method of Schulz and Flory. This method is not concerned with kinetics but gives the probability of finding in the reaction mixture a polymer of a particular chain length. It is based on an assumption equivalent to that of the identity of the velocity constants.

kinetics. The reaction scheme is as follows, where  $M$  is monomer,  $P_r$  is active polymer,  $M_{r+n}$  is dead polymer, and  $k_i$  etc. are velocity constants.



The notation which is adopted below is based on that of Gee and Melville. With regard to the termination process, these authors point out that any particular dead polymer,  $M_x$ , is formed by a variety of reactions,  $P_1 + P_{x-1}$ ,  $P_2 + P_{x-2}$ , etc. A separate part of the velocity constant,  $k_t$ , must therefore be ascribed to each active polymer, according to the relation  $k_t = k_{m_r} \times k_{m_n}$ .

The basic equations for the steady state system are those which represent the mass balance for each species over a fixed period of time. The amount of any substance which enters the vessel, together with the amount formed internally by reaction, is equated to the amount which passes out together with the amount which is transformed.

It will be supposed that only monomer is present in the feed to the reaction vessel and also that any volume change which takes place is negligible. Then considering the case of  $P_1$ , the amount leaving the vessel in unit time is  $u(P_1)$ , where  $u$  is the volume rate of flow. The amount which is formed in unit time in the reaction vessel, which has a volume  $V$ , is  $Vk_i(M)$ . The amount which is transformed in unit time is determined by the reaction  $P_1 + M$  which converts  $P_1$  into  $P_2$ , and by the series of reactions  $P_1 + P_1$ ,  $P_1 + P_2$ , etc., which convert it into dead polymer. The amount transformed in unit time in the reaction vessel is therefore

$$V k_{p_1}(M)(P_1) + V k_{m_1}(P_1) \sum_1^{\infty} k_{m_r}(P_r).$$

The mass balance for  $P_1$  is therefore

$$V k_i(M) = u(P_1) + V k_{p_1}(M)(P_1) + V k_{m_1}(P_1) \sum_1^{\infty} k_{m_r}(P_r).$$

Dividing through by  $V$  and putting  $V/u = T$ , the time of passage,

$$k_i(M) = T^{-1}(P_1) + k_{p_1}(M)(P_1) + k_{m_1}(P_1) \sum_1^{\infty} k_{m_r}(P_r) \quad (1)$$

Similarly for  $P_2$ , etc.,

$$k_{p_1}(M)(P_1) = T^{-1}(P_2) + k_{p_2}(M)(P_2) + k_{m_2}(P_2) \sum_1^{\infty} k_{m_r}(P_r) \quad (2)$$

The sum of these equations to infinity gives

$$k_i(M) = T^{-1} \sum_1^{\infty} (P_r) + \left\{ \sum_1^{\infty} k_{m_r}(P_r) \right\}^2 \quad (3)$$

and similarly the successive solution of the equations gives

$$(P_r) = \frac{k_i M^r \prod_1^{r-1} k_{p_r}}{\prod_1^r \left\{ T^{-1} + k_{p_r} M + k_{m_r} \sum_1^{\infty} k_{m_r}(P_r) \right\}} \quad (4)$$

where for convenience  $M$  is written in place of  $(M)$  in all the following equations. Considering now the mass balance of any dead polymer,  $M_r$ , the rate of its escape is equal to the rate of its formation:

$$T^{-1}(M_r) = k_{m_1}(P_1) \cdot k_{m_{r-1}}(P_{r-1}) + k_{m_2}(P_2) \cdot k_{m_{r-2}}(P_{r-2}) + \dots$$

## 652 KINETICS OF STEADY STATE POLYMERISATION

In this equation the last term is  $\frac{1}{2}k_m^2 r/2 (P_{r/2})^2$  if  $r$  is even and  $k_{m_{r-1}} \cdot k_{m_{r+1}} \left(\frac{P_{r-1}}{2}\right) \left(\frac{P_{r+1}}{2}\right)$  if  $r$  is odd. The series of terms can be written as:

$$T^{-1}(M_r) = \frac{1}{2} \sum_{x=1}^{x=r-1} k_{m_x}(P_x) \cdot k_{m_{r-x}}(P_{r-x}) \quad (5)$$

By substituting the value of  $(P_r)$ , as given by (4), in equation (5):

$$(M_r) = \frac{T k_i^2 M^r}{2} \sum_{x=1}^{r-1} \frac{k_{m_x} \prod_{y=1}^{x-1} k_{p_y}}{\prod_{y=1}^x \left\{ T^{-1} + k_{p_y} M + k_{m_y} \Sigma k_m(P) \right\}} \times \frac{k_{m_{r-x}} \prod_{y=1}^{r-x-1} k_{p_y}}{\prod_{y=1}^{r-x} \left\{ T^{-1} + k_{p_y} M + k_{m_y} \Sigma k_m(P) \right\}} \quad (6)$$

The weight fraction,  $w_r$ , of the  $r$ 'th polymer is defined by:

$$w_r = \frac{r\{(P_r) + (M_r)\}}{(M_0 - M)} \quad (7)$$

where  $M_0$  is the concentration of monomer in the feed to the reaction vessel. Substituting the values of  $(P_r)$  and  $(M_r)$  as given by equations (4) and (6):

$$w_r = \frac{r M^r}{(M_0 - M)} \left[ \frac{k_i \prod_{x=1}^{r-1} k_{p_x}}{\prod_{x=1}^r \left\{ T^{-1} + k_{p_x} M + k_{m_x} \Sigma k_m(P) \right\}} + \frac{T k_i^2}{2} \sum_{x=1}^{r-1} \frac{k_{m_x} \prod_{y=1}^{x-1} k_{p_y}}{\prod_{y=1}^x \left\{ T^{-1} + k_{p_y} M + k_{m_y} \Sigma k_m(P) \right\}} \cdot \frac{k_{m_{r-x}} \prod_{y=1}^{r-x-1} k_{p_y}}{\prod_{y=1}^{r-x} \left\{ T^{-1} + k_{p_y} M + k_{m_y} \Sigma k_m(P) \right\}} \right] \quad (8)$$

A further equation is obtained by considering the mass balance of monomer:

$$u M_0 = u M + V k_i M + V M \sum_1^{\infty} k_{p_r}(P_r).$$

This equation can be rewritten as

$$T^{-1}(M_0 - M) = k_i M + M \sum_1^{\infty} k_{p_r}(P_r) \quad (9)$$

The quantity on the left hand side of this equation is the quantity of monomer which is converted per unit volume of reaction space per unit time. In part I it was described as the "unit output" and was denoted by the symbol  $\omega$ . It is the measure of the rate of monomer conversion in the continuous reaction vessel and it is thus closely comparable to the differential coefficient,  $d(M)/dt$ , for the corresponding batchwise reaction. The related quantity

$$\omega/M_0 = (M_0 - M)/TM_0$$

is the degree of conversion per unit time of passage.

Equations (8) and (9), which give the weight distribution and the rate of reaction respectively, constitute the solution of the problem in hand. The number and weight average chain lengths,  $\bar{v}_n$  and  $\bar{v}_w$ , may also be obtained by appropriate summation to infinity:

$$\left. \begin{aligned} \bar{v}_n &= \frac{\sum_1^{\infty} r(P_r) + \sum_2^{\infty} r(M_r)}{\sum_1^{\infty} (P_r) + \sum_2^{\infty} (M_r)} \\ \bar{v}_w &= \frac{\sum_1^{\infty} r^2(P_r) + \sum_2^{\infty} r^2(M_r)}{\sum_1^{\infty} r(P_r) + \sum_2^{\infty} r(M_r)} \end{aligned} \right\} \quad \cdot \quad \cdot \quad \cdot \quad (10)$$

The above solution for a homocontinuous polymerisation is one of considerable generality for it is independent of any assumptions with regard to the constancy of the  $k_p$ 's and  $k_t$ 's, or whether or not the chain is of long or short duration compared to the period of reaction. However, in order to make the present equations directly comparable with those for the batch kinetics, the same simplifying assumptions will now be made. This gives rise to two special cases as follows.

(a) It may be supposed that there is no termination process, which is the simplifying assumption adopted by Dostal and Mark. Putting  $k_{tr} = 0$ , equation (8) after rearrangement becomes:

$$w_r = \frac{r}{(M_0 - M)} \cdot \frac{k_t}{k_{pr} \prod_1^r \{1 + (Tk_{pr}M)^{-1}\}} \quad \cdot \quad \cdot \quad (11)$$

If it is further supposed, with Dostal and Mark, that all the  $k_p$ 's are identical the above equation reduces to:

$$w_r = \frac{r\alpha}{(M_0 - M)\{1 + (Tk_pM)^{-1}\}^r} \quad \cdot \quad \cdot \quad (12)$$

where  $\alpha = k_t/k_p$ .

With the same assumptions, equations (3) and (9), when combined to eliminate the sum, give

$$\omega = T^{-1}(M_0 - M) = k_p M(1 + k_p MT) \quad \cdot \quad \cdot \quad (13)$$

A numerical solution of these equations is given later in the paper.

(b) The present equations become comparable with those of Gee and Melville<sup>6</sup> if it is supposed that the chains are of very short duration compared to  $T$ , the time of passage through the reaction vessel. It follows that the probability will be almost zero of active polymer escaping from the reaction vessel before it has suffered a deactivating collision. In equations (1) and (2) the terms in  $T^{-1}(P_r)$  can therefore be eliminated with negligible error. It is further assumed, with Gee and Melville, that the ratio  $\delta = k_{tr}/k_{pr}$  is constant for all lengths of chain. Equation (3) then becomes

$$k_t M = \left\{ \sum_1^{\infty} k_{tr}(P_r) \right\}^2$$

or

$$\delta \sum_1^{\infty} k_{pr}(P_r) = \sqrt{k_t M} \quad \cdot \quad \cdot \quad \cdot \quad (14)$$

Eliminating the sum between equations (9) and (14):

$$\omega = T^{-1}(M_0 - M) = k_p M(1 + M\delta k_t^{-1/2} \delta^{-1}) \quad \cdot \quad \cdot \quad (15)$$

When the chains are of very short duration the concentration of live polymer will be very small compared to the concentration of dead polymer, i.e.  $\{P_r\} \ll (M_r)$ . Hence, from equation (8), and with the above assumptions we have :

$$w_r = \frac{rM^r}{(M_0 - M)} \cdot \frac{Tk_r^2 \delta^2 (r-1)}{2\{M + \delta^2 \Sigma k_{pr}(P_r)\}^r} \quad (16)$$

From this equation the time of passage,  $T$ , and the sum  $\Sigma$ , can be eliminated by use of equations (15) and (14) respectively. After rearranging we have :

$$w_r = \frac{\xi^2 r (r-1)}{2M^{3/2} (1 + \xi M^{-1/2})^{r+1}} \quad (17)$$

where  $\xi$  has been written for  $\delta k_{tr}$ .

A numerical solution of this equation is given in a later section of the paper, together with the solution of the corresponding equation for batch reaction, as obtained by Gee and Melville. This is as follows :

$$w_r = \frac{\xi^2 r^2}{(r-1)(M_0 - M)} [(1 + \xi M_0^{-1/2})^{1-r} - (1 + \xi M^{-1/2})^{1-r}] \quad (18)$$

### Comparison of Batch and Continuous Polymerisation.

The derivation of the equations for homocontinuous polymerisation has been carried through for all the types of initiation and termination considered by Gee and Melville.<sup>6</sup> The treatment is by the same methods as described in the previous section and the same simplifying assumptions have been introduced in order to make the equations comparable with those for the batchwise reaction.

The results are listed in Table I, and may be compared with Gee and Melville's Tables I and II. The expressions for the homocontinuous process are seen to be generally more regular than those for the batch, due to the greater simplicity of the mathematical treatment and also to the constancy of the monomer concentration. Solutions have also been obtained in certain cases where the mathematics were intractable for the batchwise reaction. Table I (no. 13, 14 and 15) also gives the expressions for the cases which correspond to Dostal and Marks' assumptions.

Considering the expressions of Table I as a whole, it is evident that all polymerisation types are kinetically distinguishable, with the exception of types 6 and 9.\* This is the same situation as arises for batchwise reaction.

We give now a detailed comparison of the expressions for the two types of process.

**Reaction Rate.**—As mentioned previously, the quantity

$$\omega = u(M_0 - M)/V$$

is a measure of the reaction rate in the continuous reaction vessel and is exactly comparable to the differential coefficient,  $d(M)/dt$ , for the batchwise reaction. Measurement of the dependence of  $\omega$  on  $(M)$ , in a continuous reaction experiment, can thus be used for the determination of the order of a reaction.

In Gee and Melville's treatment the quantities  $\lambda$  and  $\xi$  are taken to be small compared to unity. If the same assumption is made here the exact expressions for  $\omega$ , as given in Table I, become identical with the expressions for  $d(M)/dt$ , as obtained by Gee and Melville, for all cases where the life of the growing polymer is short.

**Chain Length.**—The expressions for  $\bar{v}_n$  and  $\bar{v}_w$ , the number and weight average chain lengths respectively, are given in Table I. When the approximation of the previous paragraph is made, the expressions become

\* Types 1 and 7 also appear to give similar kinetic expressions, as shown in Table I. For the latter case, however,  $\omega = f(I)(1 + M\xi^{-1}) = f(I)\{1 + M\delta^{-2}f(I)^{-1}\}$ . This is therefore distinguishable from  $\omega = f(I)(1 + M\lambda^{-1})$  of the former case.

very similar to those obtained for batchwise reactions. For the latter, however, there is generally a more complex form of dependence of chain length on the monomer concentration, due to the change in composition

TABLE I.

		Photo-initiation, $f(I)$ .	First Order Initiation, $k_i(M)$ .	Second Order Initiation, $k_i'(M)^2$ .
Spontaneous Termination.	$\omega$	(1) $f(I)(1 + M\lambda^{-1})$	(2) $k_i M(1 + M\lambda^{-1})$	(3) $k_i' M^2(1 + M\lambda^{-1})$
	$\frac{\bar{v}_n}{\bar{v}_t}$	$1 + M\lambda^{-1}$	$1 + M\lambda^{-1}$	$1 + M\lambda^{-1}$
Monomer Termination.	$\omega$	(4) $f(I)(1 + \lambda^{-1})$	(5) $k_i M(1 + \lambda^{-1})$	(6) $k_i' M^2(1 + \lambda^{-1})$
	$\frac{\bar{v}_n}{\bar{v}_t}$	$1 + \lambda^{-1}$	$1 + \lambda^{-1}$	$1 + \lambda^{-1}$
Termination by Disproportionation.	$\omega$	(7) $f(I)(1 + M\xi^{-1})$	(8) $k_i M(1 + M^{\frac{1}{2}}\xi^{-1})$	(9) $k_i' M^2(1 + \xi^{-1})$
	$\frac{\bar{v}_n}{\bar{v}_t}$	$1 + M\xi^{-1}$	$1 + M^{\frac{1}{2}}\xi^{-1}$	$1 + \xi^{-1}$
Termination by Combination.	$\omega$	(10) $f(I)(1 + M\xi^{-1})$	(11) $k_i M(1 + M^{\frac{1}{2}}\xi^{-1})$	(12) $k_i' M^2(1 + \xi^{-1})$
	$\frac{\bar{v}_n}{\bar{v}_t}$	$2(1 + M\xi^{-1})$	$2(1 + M^{\frac{1}{2}}\xi^{-1})$	$2(1 + \xi^{-1})$
No Termination.	$\omega$	(13) $f(I)(1 + M\beta^{-1})$	(14) $k_i M(1 + M\beta^{-1})$	(15) $k_i' M^2(1 + M\beta^{-1})$
	$\frac{\bar{v}_n}{\bar{v}_t}$	$1 + M\beta^{-1}$	$1 + M\beta^{-1}$	$1 + M\beta^{-1}$
	$w_r$	$1 + 2M\lambda^{-1}$	$1 + 2M\lambda^{-1}$	$1 + 2M\lambda^{-1}$
	$w_r$	$\frac{r\lambda^2}{M^2(1 + \lambda M^{-1})^{r+1}}$	$\frac{r\lambda^2}{M^2(1 + \lambda M^{-1})^{r+1}}$	$\frac{r\lambda^2}{M^2(1 + \lambda M^{-1})^{r+1}}$
	$w_r$	$\frac{r\lambda^2}{(1 + \lambda)^{r+1}}$	$\frac{r\lambda^2}{(1 + \lambda)^{r+1}}$	$\frac{r\lambda^2}{(1 + \lambda)^{r+1}}$
	$w_r$	$\frac{r\xi^2}{M^2(1 + \xi M^{-1})^{r+1}}$	$\frac{r\xi^2}{M(1 + \xi M^{-\frac{1}{2}})^{r+1}}$	$\frac{r\xi^2}{(1 + \xi)^{r+1}}$
	$w_r$	$\frac{\xi^2 r(r-1)}{2M^2(1 + \xi M^{-1})^{r+1}}$	$\frac{\xi^2 r(r-1)}{2M^{3/2}(1 + \xi M^{-\frac{1}{2}})^{r+1}}$	$\frac{\xi^2 r(r-1)}{2(1 + \xi)^{r+1}}$
	$w_r$	$\frac{r\alpha}{M(M_0 - M)(1 + \beta M^{-1})^r}$	$\frac{r\alpha}{(M_0 - M)(1 + \beta M^{-1})^r}$	$\frac{r\alpha M}{(M_0 - M)(1 + \beta M^{-1})^r}$

Symbols :

$$\omega = \frac{u}{V}(M_0 - M) ; \quad \lambda = k_{tr}/k_{sp}$$

$$\beta = u/Vk_p \quad ; \quad \delta = k_{mr}/k_{sp}$$

$$\xi = \delta\sqrt{i(I)}, \delta k_i t \text{ or } \delta k_i' t \quad \left. \vphantom{\xi = \delta\sqrt{i(I)}, \delta k_i t \text{ or } \delta k_i' t} \right\} \text{ according to type of initiation.}$$

$$\alpha = f(I)/k_p, k_i/k_p \text{ or } k_i'/k_p$$

of the system as reaction proceeds. For the homocontinuous reaction the weight average chain length is twice the number average for all the types of polymerisation except termination by combination, for which the ratio is 3/2. Herington and Robertson<sup>7</sup> previously obtained the same result for batchwise reaction.

**Weight Distribution.**—The expressions are given in Table I for the fraction  $w_r$  of the  $r$ 'th polymer in the product obtained from the homocontinuous reaction process. The expressions are generally simpler and

more regular than the corresponding expressions for the batchwise reaction, as obtained by Gee and Melville. This is due to the constancy of the monomer concentration.

The expressions of Table I are of two types, according to the manner of dependence of  $w_r$  on  $r$ :

termination by combination,

$$w_r = \frac{ar(r-1)}{b^{r+1}} \quad (19)$$

other termination mechanisms and case of no termination,\*

$$w_r = \frac{ar}{b^{r+1}} \quad (20)$$

In these equations,  $a$  and  $b$  are quantities independent of  $r$ , but which may or may not be dependent on  $(M)$ .

Equation (19) gives a maximum value of  $w_r$  at

$$r = \frac{1 + \frac{1}{2}l_nb + \sqrt{1 + \frac{1}{4}l_n^2b}}{l_nb}$$

which can be approximated to  $r = 2/l_nb$  when  $b$  is not appreciably greater than unity. Equation (20) gives a maximum value of  $w_r$  at  $r = 1/l_nb$ .

For certain types of polymerisation, however, as shown in Table I, the quantity  $b \rightarrow \infty$  as  $(M) \rightarrow 0$ . The maxima in the curves of equations (19) and (20) then fall at a value of  $r$  less than 2, and these maxima therefore do not correspond to physical reality. It follows that there is no maximum in the polymer distribution curve when reaction approaches completion for any case where  $b$  involves  $(M)$ . Thus all types of polymerisation (and this includes also the case of termination by transfer) show a maximum when reaction is far from complete, but only types 4, 5, 6, 9 and 12 continue to show a maximum when the time of passage through the reaction vessel is so large that the monomer concentration is effectively zero.

These conclusions agree entirely with those of Gee and Melville for the corresponding batchwise reaction, except that these authors also obtain a maximum, at complete reaction, for type (11). On the other hand, the conclusions of Herington and Robertson,<sup>7</sup> obtained by an alternative mathematical approach, are considerably different from those of Gee and Melville; they obtain a maximum only in the case of termination by combination, even when reaction is incomplete.

The spread of the distribution curves can be defined statistically by use of the root mean square deviation,  $\sigma$ . Herington and Robertson have shown that this is related to the number and weight average chain lengths as follows:

$$\sigma^2 = \bar{v}_n(\bar{v}_w - \bar{v}_n) \quad (21)$$

By use of this expression the relative spread of the curves for continuous and batch reaction can be compared. It can thus be shown: (a) for types 4, 5, 6, 9 and 12 of Table I the spread is the same for the two kinds of process; (b) for types 1, 2, 3, 7, 8, 10 and 11 the spread is smaller for the continuous process, due to the constancy of the monomer concentration; (c) for types (13), (14) and (15), which refer to slow growing chains, the spread is greater for the continuous process. The latter is due to the fact that some of the growing polymers escape from the reaction vessel within a time which is short compared to the time of passage, while other molecules stay in for a much longer period.

These conclusions may be made clearer by a numerical solution of the distribution equations. This has been carried out for types (11) and (13) of Table I.

\* Where there is no termination, the exponent on  $b$  is  $r$ , but this does not affect the argument since  $b^{r+1} = b \cdot b^r$ .

TYPE II.—The expressions for the weight distribution are equation (17) for the homocontinuous process and (18) for the batch process. Whereas the latter equation contains ( $M_0$ ), the former does not. The distribution obtained in the homocontinuous process thus depends on the stationary concentration of monomer, but not on the degree of conversion. The overall distribution obtained in the batch process, on the other hand, is composite of that obtained at each instantaneous value of the monomer concentration and depends therefore on the degree of conversion.

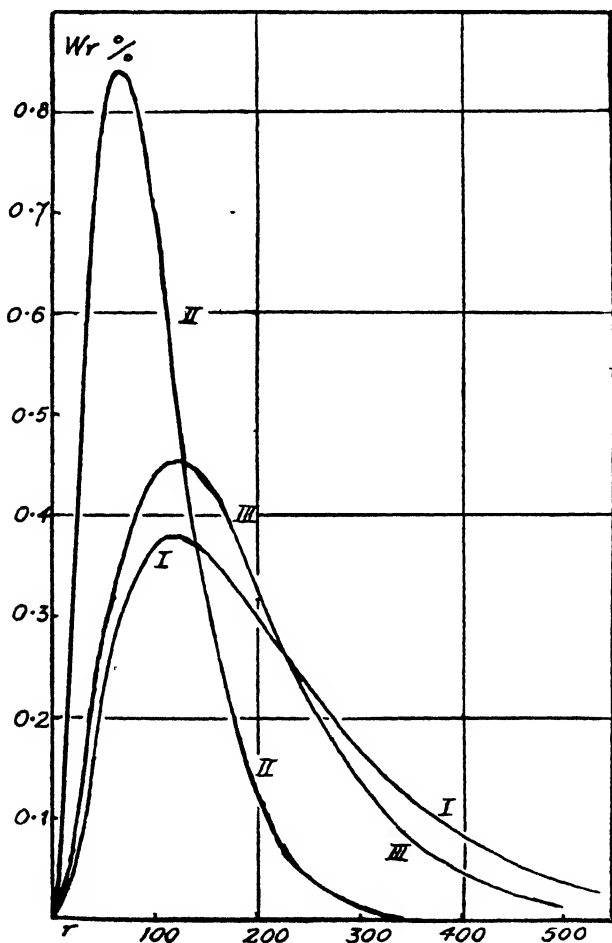


FIG. 1.—Case where life of active polymer is short, compared to duration of reaction. I. Batch reaction. II and III. Continuous reaction.

The extent to which the two types of process give rise to differences of distribution would thus be expected to depend on the amount of change in the batch. When the conversion is small the curves are found to be almost identical, but for 90 % conversion there is considerable difference. This is illustrated in Fig. 1, the curves of which have been worked out for a value of  $\xi$  of  $10^{-3}$ . Curve I refers to the batch process in which the concentration of monomer falls from 1.0 to 0.1. Curves II and III refer to the homocontinuous process operating at steady states of  $M = 0.1$  and  $M = 0.354$  respectively. The latter gives a maximum at the same chain



length as in curve I but its "spread" is appreciably smaller. This is in agreement with the remarks of the previous section.

TYPE 13.—This is the case of slow growth for which Dostal and Mark obtained a solution of the differential equations by use of the *eigenzeit* transformation. The weight percentage of polymer as a function of  $r$  is given as Curve I\* of Fig. 2, for the particular case  $\alpha = k_1/k_p = 10^{-2}$ ,

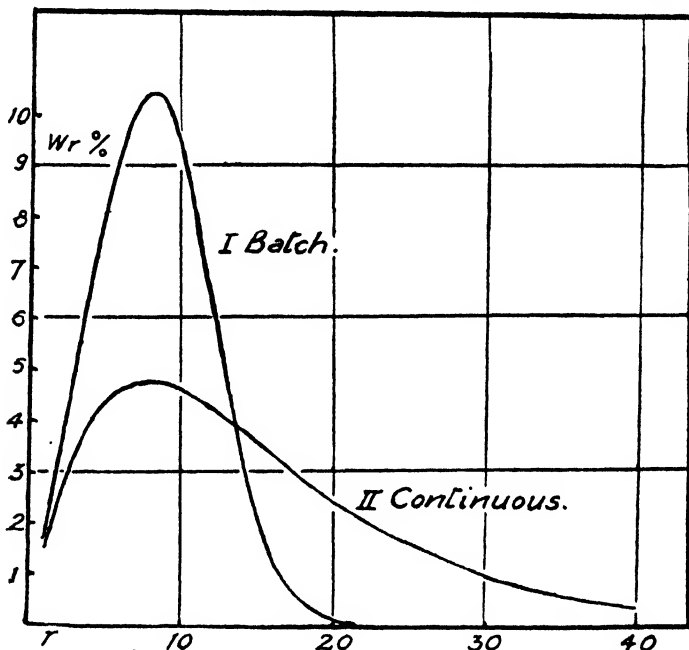


FIG. 2.—Case where life of active polymer is long, or where there is no termination reaction.

( $M_0$ ) = 1.0 and  $z = 10$ , which corresponds to 6 % conversion. The corresponding graph for homocontinuous reaction is shown as curve II in Fig. 2 and was obtained by solution of equations (12) and (13) of the present paper; the same values of  $\alpha$  and ( $M_0$ ) were used and the value of  $Tk_p$  was chosen to give 6 % conversion. It is evident that in this case it is the continuous process which gives the broader distribution.

### Discussion.

The conclusions which have been reached may be summed up briefly by considering them, in the first place, in relation to industrial technique, and secondly, in relation to the investigation of polymer kinetics. Considering first the industrial aspects, it has been shown that a change from a batch to a continuous process, may give rise to either a broader or a narrower distribution of chain lengths. The broader distribution arises when there is a slow growth of chains, as for example, in polycondensation. For such reactions the change from a batch to a homocontinuous process will give rise to a less uniform product. This is due to differences between

\* Curve I has been recalculated from Dostal and Mark's figures as given in ref. 2. The graphs printed in their papers (and also in Mark and Raff, *High Polymers*, Vol. III, Fig. 36, 37 and 40), refer only to the *relative* amounts of polymers, as can be seen from the fact that the areas under the curves are not equal to 100. (Private communication from Prof. Mark, 11th February, 1946.)

individual molecules of their time of passage through the reaction vessel. As shown in Part I, effects of this kind can be reduced by placing a number of homocontinuous reaction vessels in series.

The homocontinuous process gives the more uniform product for many types of polymerisation in which the life of the growing chains is short compared to the time of passage. In such cases the escape from the vessel of the growing polymer is negligible and the statistical factors of the previous paragraph do not operate. The effect in the opposite direction which tends to make the distribution narrower is the constancy of the monomer concentration.

On the other hand, the average chain length tends to be shorter in the continuous process when it operates at a stationary monomer concentration equal to the *final* concentration in the batch. This can be rectified by raising the stationary concentration of monomer; either, (a) by adopting a shorter time of passage, in order to reduce the degree of conversion, or (b) by raising the concentration of monomer in the feed. The latter procedure would have the advantage of giving a rather more uniform product than is obtainable by a batch process, but without sacrifice of either chain length or degree of conversion.

We turn now to a brief consideration of the possibilities of using continuous reaction methods in the study of polymerisation kinetics. It has been shown that the mathematical treatment of complex reactions is greatly simplified by supposing the reaction to be set up as a steady state in a thoroughly stirred continuous reaction vessel. Cases can then be solved which would be intractable when considered as a batch system. For example, for the case of slowly growing chains, equation (11) has been obtained which gives the weight distribution in terms of the velocity constants of each of the separate reaction steps. These individual velocity constants are therefore determinable if a sufficient amount of experimental data can be obtained. For the corresponding batchwise reaction, on the other hand, mathematical treatment of the reaction kinetics can only be carried through by assuming, at the outset, equality of the velocity constants.

For types of polymerisation in which polymer growth is rapid, the mathematical advantages of the homocontinuous process are not so great, for the stationary state method can also be applied for the corresponding batchwise reaction, at least in so far as concentration of *active* polymer is concerned. The expressions which have been obtained for the continuous reaction are in general very similar to those obtained by Gee and Melville for batch reaction, but are rather more regular. Both sets of expressions contain the same velocity constants in the same ratios and the kinetic information which is obtainable is therefore the same for the two methods.

Apart from mathematical simplicity, a further advantage of homocontinuous reaction is that it is possible to adjust the reaction vessel to any desired stationary state. The behaviour can therefore be studied in detail at any desired stationary concentration of catalyst or of monomer. This may be of particular value in cases of very rapid reaction. On the other hand, the difficulty of operating a continuous process in the laboratory is not to be overlooked. The large amount of materials which is required is the greatest difficulty but in cases where this can be overcome, it is thought that the continuous method may prove to be of real value.†

In conclusion, the author wishes to express his thanks to Miss M. J. Hicks for a detailed checking of the derivations.

† The use of the homocontinuous system for experimental work in reaction kinetics has been described in a paper presented to the September meeting of the Faraday Society.

### Summary.

Continuous reaction processes have been classified as homocontinuous and heterocontinuous according to whether or not there is complete mixing of the reaction system. The theory of continuous reaction which was developed in an earlier paper is applied to the case of polymerisation reactions. It is shown that the mathematical treatment of homocontinuous processes is simpler than for batch processes, due to the existence of a complete stationary state. The molecular weight distribution of the polymerised product is discussed and it is shown that the product of the homocontinuous process may be either more or less uniform than is obtainable from a corresponding batch process, according to whether the life of the growing polymer is short or long compared to the duration of reaction. In several types of polymerisation of industrial interest the homocontinuous process can probably be used to obtain a greater uniformity of product. The possible advantages of using continuous reaction as a technique for the study of polymerisation kinetics is also discussed.

### Résumé.

Les processus continus ont été classés en "homocontinus" et "hétérocontinus", selon que le mélange du système est complet ou non. La théorie de la réaction continue, développée dans un article précédent, a été appliquée aux réactions de polymérisation. On a montré que le traitement mathématique des processus homocontinus est plus simple que celui des processus "en fournée" (batch process), grâce à l'existence d'un état stationnaire complet. On discute ici la distribution du poids moléculaire du produit polymérisé et on montre que le processus homocontinu donne un produit soit plus, soit moins uniforme que le processus "en fournée" correspondant, selon que la vie du polymère croissant est courte ou longue par rapport à la durée de la réaction. Le processus homocontinu peut probablement être employé dans plusieurs types de polymérisations d'intérêt industriel, pour donner une plus grande uniformité de produit. On discute aussi les avantages que peut présenter la réaction continue, considérée comme une technique nouvelle pour l'étude cinétique de la polymérisation.

### Zusammenfassung.

Ununterbrochene Reaktionsprozesse sind als "homokontinuierliche" und "heterokontinuierliche" klassifiziert worden, je nachdem ob völlige Mischung des Reaktionssystems eintritt oder nicht. Die in einem früheren Artikel entwickelte Theorie der ununterbrochenen Reaktionen wird auf Polymerisationsreaktionen angewendet. Es wird gezeigt, dass die mathematische Behandlung von homokontinuierlichen Prozessen wegen der Existenz eines völlig stationären Zustands einfacher ist als für die Darstellung in Portionen. Die Molekulargewichtsverteilung des polymerisierten Produkts wird besprochen und es wird gezeigt, dass das Produkt des homokontinuierlichen Prozesses entweder mehr oder weniger einheitlich sein kann als das aus dem entsprechenden portionweisen Prozess, je nachdem ob die Lebensdauer des wachsenden Polymermoleküls kurz oder lang im Vergleich zur Dauer der Reaktion ist. In mehreren Polymerisationen, die industrielle Bedeutung besitzen, kann mit dem homokontinuierlichen Prozess wahrscheinlich eine grössere Einheitlichkeit des Produkts erzielt werden. Die möglichen Vorteile, welche die kontinuierliche Reaktion als Methode für das Studium der Polymerisationskinetik besitzt, werden auch erörtert.

*Imperial Chemical Industries, Ltd.,  
Butterwick Research Laboratories,  
Welwyn, Herts.*

# THE EFFECT OF DIALYSIS ON THE PROPERTIES OF NUCLEAR GOLD SOLS.

BY A. K. HOLLIDAY.

(Communicated by W. C. M. LEWIS.)

Received 5th July, 1946.

In the numerous investigations of the properties of colloidal gold that have been made, it is frequently found that some form of "purification" is adopted before the sol is used for the actual investigation. Usually, dialysis or electro-dialysis is employed, but commonly little attempt is made to standardise the conditions under which dialysis is carried out, because it is assumed that the process removes only foreign electrolytes and does not affect the intrinsic properties of the sol. The extensive researches of Pauli<sup>1</sup> have shown that electro-dialysis does produce quite marked changes in gold sols, although the character of the changes depends very much upon the mode of preparation; in certain cases, electro-dialysis may lead to flocculation and sedimentation of the sol. Other workers, notably Jones and Lewis,<sup>2</sup> Desai and co-workers<sup>3</sup> and Volkov and Rabinowitch<sup>4</sup> have investigated the effects produced by ordinary dialysis, and have found changes in the electrophoretic mobility and the stability of the sol towards electrolytes. There is, however, little information as to the cause of the colour change from red to blue which may ensue during dialysis, although such a change indicates "coagulation" of red (primary) particles to form larger anisotropic particles, which may or may not become large enough to sediment. In some cases the colour change may never be observed, even after prolonged dialysis, but it must be remembered that the use of an organic reducing agent in the preparation of the sol may result in the formation of a partly protected sol which may not be changed in colour by dialysis.<sup>5</sup>

In the present work, an inorganic reducing agent has been used to prepare a nuclear gold sol, and it has been found that dialysis of this sol produces a change of colour in a fairly short period of time. To obtain more information about what is happening during this change, concurrent measurements have been made of (a) the electrophoretic mobility (and therefore of the  $\zeta$ -potential and effective charge also), (b) the degree of "coagulation," i.e. the percentage of primary particles remaining at various time intervals, and (c) the concomitant variation in pH of the system. From a comparison of the results more definite information than heretofore has been obtained regarding the changes produced during the so-called "purification" by dialysis. Thus it has been established that the colour change begins at a value of the mobility or  $\zeta$ -potential higher than that of the original sol, and a completely blue sol is finally formed which possesses an appreciable mobility and which moreover is stable, showing no tendency to flocculate or sediment.

<sup>1</sup> Pauli, *Naturwiss.*, 1932, **20**, 551, 573; *Trans. Faraday Soc.*, 1935, **31**, 11.

<sup>2</sup> Jones and Lewis, *J. Physic. Chem.*, 1931, **35**, 1168.

<sup>3</sup> Desai, Barve and Paranjpe, *Proc. Roy. Soc. Edin.*, 1939, **59**, 22.

<sup>4</sup> Volkov and Rabinowitch, *Acta Physicochim.*, 1942, **17**, 14, 25.

<sup>5</sup> Weiser, *Inorganic Colloid Chemistry*, Vol. I, 33.

### Experimental.

1. **Preparation of the Sol.**—The method employed was that developed by Usher<sup>6</sup> in which phosphine is used as the reducing agent; this method produces a sol with a small and uniform particle size. To 225 ml. of a solution of "gold chloride" ( $\text{HAuCl}_4 \cdot 3\text{H}_2\text{O}$ ) were added 50 ml. of a solution of sodium carbonate containing 2.59 g./l. followed by 225 ml. of an aqueous solution of phosphine. The resulting orange-coloured liquid was then boiled for five minutes, when a clear ruby-red sol resulted, and the last traces of phosphine removed by passage of air through the sol. Sufficient quantities of sol for each experiment were obtained by mixing the requisite number of 500 ml. batches; the gold content was 56 mg./l. in all cases. The water used was redistilled in an all-quartz apparatus and had a specific conductivity of  $1 \times 10^{-6}$  mhos at 25° C.

2. **Dialysis.**—Originally, the sols were dialysed in sets of collodion bags suspended in a stream of distilled water. It was found, however, that there was considerable absorption of water into the bags, to an extent sufficient to affect seriously the rate of the colour change. A single large dialyser was therefore constructed, using Cellophane as the membrane, the latter being stretched over the base of a large bell jar in which the sol was placed; the jar was suspended in the distilled water stream, flowing at the rate of about 1 l./hour, and the sol stirred by bubbling nitrogen through it. Samples of the sol were siphoned out of the jar at intervals during the dialysis. During the first week of a dialysis the sol was in contact with an appreciable area of the bell jar wall, but a sample of sol kept in the jar for the same period of time without dialysis showed no change of colour and no increase of conductivity due to contamination from the glass. After a week of dialysis the volume of sol was so reduced by withdrawal of samples as to make the area of contact between bell jar and sol negligible.

3. **Colour Change.**—The colour of the sol at any time is determined by the proportions of primary (red) and secondary or coagulated particles (blue) present.\* A bicolormeter of the Gillespie type was used to match the colour visually against standard red and blue sols. The undialysed sol was used as the red standard, and the blue standard was obtained by prolonged dialysis until no red particles were detectable. The standards were protected by addition of either sodium alginate or sodium protalbate. The colour is expressed in terms of the percentage of primary particles.

4. **Electrophoretic Mobility.**—Mobilities were determined by the macroscopic moving boundary method, with an apparatus similar to that described by Price and Lewis.<sup>7</sup> The supernatant liquid was obtained either by ultrafiltration of the sol or by ordinary filtration after flocculating by freezing. By either method, a colourless liquid of conductivity nearly equal to that of the sol was obtained, and this on dilution was used as the supernatant liquid. Conductivities were determined by the usual method at 25° C., and mobility measurements were also made at this temperature. *pH* determinations were made with a glass electrode. In all the experimental work, the usual precautions were taken to avoid contamination of the sols by foreign matter.

### Results.

The mobility and colour data for a period of 26 days dialysis are shown in Fig. 1; the mobility values are in units of microns/sec./volt/cm. towards the anode. Over the first 14 days the *pH* of the sol decreased steadily from an initial value of 9.56; thereafter the value remained constant at 6.6. No difference in the mobilities of the red and blue particles could be detected at any stage, the boundaries in the electrophoresis tube being sharp throughout the dialysis. Moreover, there was never any sign of sedimentation, the blue particles forming a sol equally as clear as the original red. The dialysis was actually conducted for a total of 36 days, and at the end of this period the conductivity of the sol approached that

<sup>6</sup> Usher, *Trans. Faraday Soc.*, 1940, **36**, 385, 549.

<sup>7</sup> Price and Lewis, *ibid.*, 1933, **29**, 775.

\* All colloidal gold particles other than primaries (i.e. all particles formed by coagulation) give a blue sol: small aggregations of particles e.g. binary or tertiary particles appear blue because they are not isometric while larger aggregations—which may or may not be isometric—appear blue because of their larger size.

of the distilled water. Repeated freezing of the sol at this stage caused a marked increase in the conductivity of the filtrate, presumably due to liberation of ions from the particle surface, but no trace of either chloride, phosphate or sodium could be detected. It was also noteworthy that the blue sol became extremely susceptible to the effects of light and traces of organic matter at the end of the dialysis; these agents caused rapid and complete sedimentation of the sol, and a loss of mobility.

Qualitatively, the change produced in the mobility in the earlier stages of dialysis is similar to that observed by Desai,<sup>8</sup> but the latter did not observe the final rise in mobility occurring after 18 days dialysis. Emphasis here must be laid on the fact that the colour change begins at a mobility value *higher* than that of the original sol. It follows that

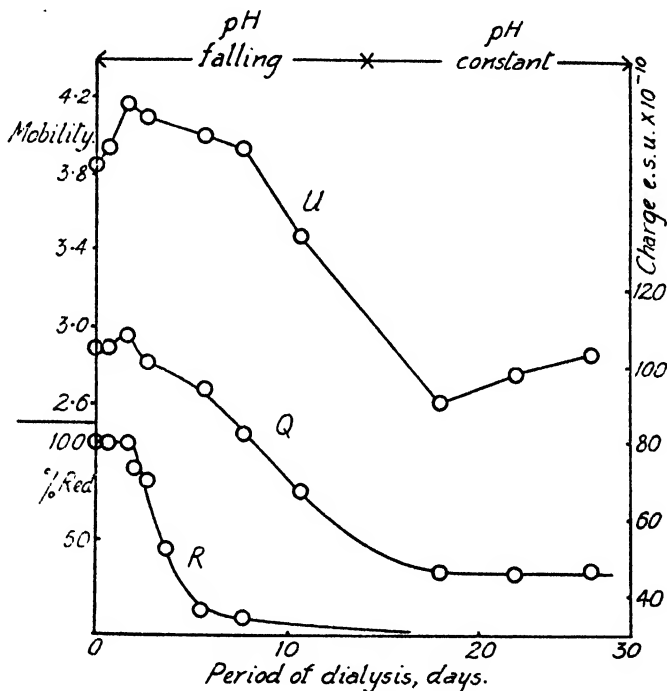


FIG. 1.—Effect of dialysis on electrophoretic mobility ( $u$ ), particle charge ( $Q$ ), and percentage of primary particles ( $R$ ).

the mobility (or the  $\zeta$ -potential) cannot *per se* explain the "coagulation" which is taking place. Now "coagulation" (i.e. union of the primary particles) begins when the force of attraction between the particles is increased sufficiently, either by a contraction of the double layer or by removal of stabilising ions from the particle surface. In the present case, there is no contraction of the double layer; therefore there must be a loss of stabilising ions, i.e. a fall in the effective particle charge  $Q$ . The values of  $Q$  plotted in Fig. 1 have been calculated by means of Henry's equation:

$$Q = 4\pi u \eta (1 + \kappa r) / f(\kappa r)$$

where  $u$  is the electrophoretic mobility,  $r$  is the particle radius,  $\kappa$  is the reciprocal double layer thickness,  $\eta$  is the viscosity of the medium and  $f(\kappa r)$  is Henry's function. The value of  $r$  is taken to be  $3.0 \times 10^{-7}$  cm., from the data of Usher for phosphine sols,<sup>9</sup> and  $\kappa$  is calculated from the ionic strength. To determine the latter for the undialysed sol, the

concentration of phosphate is determined volumetrically and the concentrations of the remaining ions can then be obtained from the stoichiometric equation for the formation of the gold. During dialysis, it is assumed that the normality of each ion or ion group decreases proportionately with the specific conductivity of the sol; the respective concentrations of each ion species may then be calculated at any stage when the conductivity and  $pH$  are known. Since the ionic strength  $\mu$  is small (of the order of  $5 \times 10^{-3}$ ), any error introduced by this assumption will not be large, and the actual error in  $Q$  will be negligible, since  $Q$  is proportional to  $1 + C\sqrt{\mu}$ , where  $C$  is a constant of magnitude 9.81. Although Henry's equation takes no account of effects due to relaxation, surface conductance and the use of unsymmetrical electrolytes, it appears to give values of  $Q$  for proteins which are in good agreement with those obtained by other means,<sup>8</sup> and it will be assumed to give reasonably accurate values in the present instance.

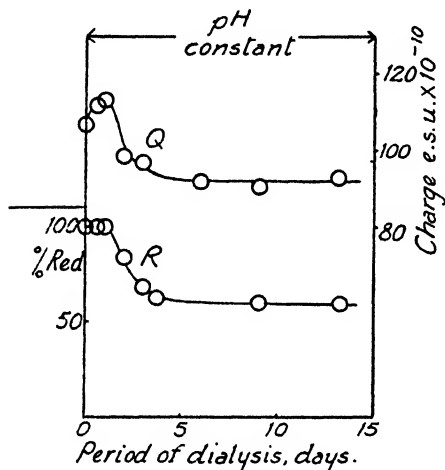


FIG. 2.—Effect of dialysis at constant  $pH$  on particle charge ( $Q$ ), and percentage of primary particles ( $R$ ).

From Fig. 1 it is clear that the sol does begin to change colour at a point where  $Q$  falls just below the value in the original sol.  $Q$  continues to fall as dialysis proceeds, reaching a minimum value only after the  $pH$  has become constant, and then remains constant at this minimum value during the remainder of the dialysis. Hence the rise in mobility occurring in the later stages is not an indication of any increase in the particle charge. The colour change proceeds steadily and almost all the primary particles disappear before  $Q$  reaches its final value. Since the larger particles formed by union of the primaries are found to have the

same mobility as the latter, it follows that the larger particles must have a greater charge. Hence coagulation of these particles will not proceed beyond the point at which their charge becomes sufficient to stabilise them, and so they form a stable blue sol.

The fact that the particle charge and the  $pH$  show similar behaviour during dialysis suggests that the hydrogen ion concentration may be an important charge-determining factor. To investigate this point, a second set of determinations was made in which the  $pH$  of the sol was kept constant throughout dialysis at a value equal to that of the original sol. This was achieved by circulating a solution 0.0004 N. with respect to sodium carbonate through the dialyser, and the rate of flow was adjusted to give a rate of dialysis roughly equal to that obtained with distilled water. The control of  $pH$  by using a weakly-buffered circulating liquid in this way is advantageous in that no electrolyte has to be added to the sol; hence there is no possibility of the effect of  $pH$  on the charge being obscured by a contraction of the double layer due to added cations. The effect of dialysis at constant  $pH$  on the particle charge and colour is shown in Fig. 2; it will be seen that the charge rises fairly sharply to a maximum before falling to a value low enough to permit the colour change to begin. However, in this case,  $Q$  falls to a constant minimum value which is much

<sup>8</sup> Adair and Adair, *ibid.*, 1940, 36, 23; Tiselius and Svensson, *ibid.*, 16.

higher than that observed when the  $pH$  is allowed to fall, and, moreover, this constant value is reached when only about 50 % of the primary particles have disappeared. As soon as  $Q$  reaches its final value, the rate of disappearance of the primaries falls abruptly, and thenceforward remains very small. Now, since the blue particles formed are stable and possess a higher charge than the primaries, the latter will disappear chiefly as a result of primary-primary unions. The rate of colour change measures the rate at which these unions occur, and the rate must depend on both the primary particle charge and the primary particle concentration. A decrease in charge increases the rate, but the simultaneous reduction in the concentration of primaries tends to decrease the rate. In Fig. 2, when the colour change has begun, the charge falls sufficiently rapidly to maintain a fairly rapid rate of colour change, but once the charge becomes constant, the particle concentration—already reduced to half its original value—becomes the rate-determining factor, and the colour change proceeds much less rapidly.

Having established that the particle charge, though dependent on the  $pH$ , does not remain constant during dialysis at constant  $pH$ , it is now necessary to consider the actual nature of the stabilising ion responsible for the charge. According to the theory of Pauli, the charge on the colloidal gold particle is to be attributed to the presence of complex auro-ions; for a sol prepared by reduction with phosphorus, Pauli<sup>9</sup> suggests that the ion concerned is  $AuCl_2'$ , which on dialysis is converted to  $Au(OH)Cl'$ . This hydrolysis of the complex ion reduces the stability of the sol, which may flocculate if dialysis is prolonged. Rabinowitch<sup>4</sup> prefers to regard the stabilising

complex as an auri-ion, but, like Pauli, considers that hydrolysis occurs on dialysis to form a hydroxy-chloro complex. It seems best in the present case to assume that dialysis causes the hydrolysis of a chloro-complex to form a hydroxy-chloro-complex, and not to particularise as to the exact nature of the ions concerned. It follows from the results already obtained that the ion formed on dialysis is a weak acid anion, so that the charge  $Q$  then becomes dependent on the  $pH$ . It is reasonable to suppose further that hydrolysis of the original ion might be prevented if chloride ions (which are a product of the hydrolysis) are not removed during dialysis. To test this idea a third group of determinations was made during dialysis, in which the chloride ion concentration was kept constant by addition of sodium chloride to the water going through the dialyser. Over the first five days the  $pH$  was kept constant as before. The effect on particle charge and colour is shown in Fig. 3. Here again,  $Q$  rises to a maximum and then falls, but rapidly reaches a constant value higher than in the two previous series of determinations. In fact,  $Q$  falls just far enough to allow the colour change to begin, but the rate of

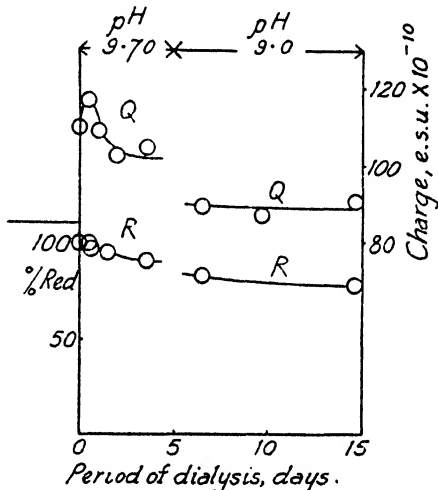


FIG. 3.—Effect of dialysis at constant chloride ion concentration on particle charge ( $Q$ ) and percentage of primary particles ( $R$ ).

<sup>9</sup> Pauli, Russer and Brunner, *Kolloid Z.*, 1935, 72, 26.



colour change remains very slow because of the higher constant value of the charge. After five days, the  $pH$  is allowed to fall somewhat, and there is a corresponding drop in  $Q$  to a lower constant value; the rate of colour change also increases until  $Q$  reaches the new level, and then decreases again. The results shown in Fig. 3 indicate that the constant chloride ion concentration retards, but does not prevent, the fall in  $Q$ ; and the latter still remains sensitive to  $pH$  change. Hence some hydrolysis of the original complex ion probably still occurs.

### Discussion.

The results obtained show that the changes produced by dialysis of a nuclear phosphine sol occur in three stages. In the first stage, the particle charge rises; this may be ascribed to the removal of cations from the inner, fixed part of the double layer, as suggested by I esai,<sup>8</sup> and is a process independent of other changes which may also be occurring. No colour change is observed at this stage. In the second stage, the particle charge falls, and causes a colour change due to union of the primary red particles to form larger blue particles. If the  $pH$  of the sol is allowed to fall far enough, almost all the primary particles disappear, and the third stage is reached where a stable, blue, non-sedimenting sol exists. At the end of this stage, the sol finally becomes sensitive to the effects of light and organic matter, these agents causing flocculation and sedimentation, presumably because they decompose the complex stabilising ion on the particles.

Finally, certain implications of these results require emphasis. Firstly, it is clear that nuclear phosphine sols are extremely sensitive to small changes in the ionic environment of the particles—a characteristic already postulated by Usher<sup>6</sup> from a consideration of the mode of formation of the particles. It follows that any process of "purification" by dialysis must be carefully controlled; if a stable red sol is required, then dialysis must not proceed beyond the point at which the particle charge reaches a maximum. Further dialysis of this type of sol results in the appearance of a special kind of "coagulation," not hitherto investigated, of which the most notable characteristic is that it is governed by the particle charge, not the  $\zeta$ -potential. It is hoped to publish the results of a more detailed investigation of this "coagulation" in a future paper.

### Summary.

1. Dialysis of a nuclear gold sol prepared by reduction with phosphine causes a colour change from red to blue. The colour change is due to union of red primary particles to form larger blue particles.
2. It is shown that the particle charge, rather than the  $\zeta$ -potential, is the critical factor which governs the colour change.
3. When the colour change is complete, a stable, non-sedimenting blue sol is formed, with a constant particle charge.
4. The decrease in particle charge and the velocity of the colour change are both reduced when the dialysis is carried out at constant  $pH$ . It is suggested that the charge decrease is due to hydrolysis of the original stabilising complex ion to form a weak acid anion. When the removal of chloride ions is prevented during dialysis, the hydrolysis is retarded and the charge decrease is smaller.
5. Some implications of the results are mentioned briefly.

### Résumé.

Un sol d'or nucléaire, préparé par réduction au phosphine, passe du rouge au bleu par dialyse. Ce changement est régi par la charge des particules, plutôt que par le potentiel  $\zeta$ , et, quand il est accompli, un sol bleu stable, avec une charge de particules constante, est formé. La diminution de charge, qui accompagne le changement de couleur, est due à l'hydrolyse de l'ion complexe originel stabilisant, pour former un anion acide faible, et est retardée quand la dialyse est conduite à  $pH$  constant.

### Zusammenfassung.

Wenn ein durch Reduktion mit Phosphin dargestelltes Goldsol dialysiert wird, tritt ein Farbwechsel von Rot auf Blau ein. Diese Veränderung wird durch die Teilchenladung eher als das  $\zeta$ -Potential kontrolliert und ergibt als Endprodukt ein stabiles blaues Sol mit konstanter Teilchenladung. Die Abnahme der Ladung, die den Farbwechsel begleitet, wird durch die Hydrolyse des ursprünglichen stabilisierenden Komplexions verursacht, wodurch das Anion einer schwachen Säure gebildet wird, und wird verzögert, wenn die Dialyse bei konstantem pH-Wert durchgeführt wird.

*Department of Inorganic and Physical Chemistry,  
The University of Liverpool.*

---

## THE CATALYTIC OXIDATION OF SULPHUR DICHLORIDE BY OXYGEN.

BY ALWYN G.-EVANS AND G. W. MEADOWS.

*Received 29th July, 1946.*

In this paper we describe experiments which were carried out in order to determine whether sulphur dichloride could be directly oxidised to thionyl chloride by atmospheric oxygen. Dry air, saturated with sulphur dichloride vapour at room temperature was passed over heated charcoal, and the oxidation products, thionyl chloride and sulphuryl chloride, together with the unchanged sulphur dichloride were then condensed out in traps cooled by liquid air.

The products of the oxidation were analysed in two stages. The first stage was the separation of the thionyl and sulphuryl chlorides from the unchanged sulphur dichloride. The second stage was the determination of the individual amounts of thionyl chloride and sulphuryl chloride.

The experiments were carried out at different temperatures, and at each temperature the contact time was increased until equilibrium conditions were obtained.

### Experimental.

The apparatus which was used is shown in Fig. 1. The Pyrex reaction tubes A and B were packed with activated charcoal and electrically heated by means of nichrome ribbon. The temperature of the reaction vessel was measured by a copper-constantan thermocouple contained in a glass sheath passing down the centre of the second reaction vessel. Air, dried over  $P_2O_5$ , and passed through a liquid air cooled trap, C, was saturated with  $SCl_2$  vapour in the bubblers D and E and drawn over the catalyst surface by means of a pump. The temperature at which the air was saturated with  $SCl_2$  vapour was determined by means of a thermometer strapped tightly to bubbler E by asbestos lagging. The rate of flow of the air stream was regulated by valve V. The air was streamed for about two hours to establish steady conditions of temperature and flow before a fraction was collected for analysis in the liquid air traps F and G. At the end of an experiment, tap  $T_1$  was closed, and the catalyst was allowed to adsorb vapour from the  $SCl_2$  saturators as it cooled.

When  $SCl_2$  was first passed over the newly prepared catalyst surface, a large proportion of the reaction products consisted of HCl and  $SO_2$ . This was due, probably, to the reaction of the  $SCl_2$  with the water still present on the catalyst surface. With the continued passage of  $SCl_2$ , however, the production of HCl and  $SO_2$  decreased. In the experiments at  $320^\circ C$ , the sulphur dichloride was passed over the catalyst surface for 50 hours before the products of this hydrolysis reaction were reduced to 18 % of the total reaction products. Because of this difficulty of eliminating the hydrolysis reaction at this temperature, the equilibrium conditions of the oxidation reaction were studied more fully at the lower temperatures of  $238^\circ C$ . and  $193^\circ C$ . where the hydrolysis was only of the order of 4 % of the total reaction.

**Sulphur Dichloride.**—The  $\text{SCl}_2$  was kindly supplied by the Superintendent, Research Establishment, Sutton Oak, St. Helens, and was specified to contain 8 to 10 % of  $\text{S}_2\text{Cl}_2$  and up to 3 % of  $\text{HCl}$  and  $\text{Cl}_2$ . In view of the difference in the boiling points of  $\text{SCl}_2$  and  $\text{S}_2\text{Cl}_2$  ( $59.0^\circ\text{C}$ . and  $135.6^\circ\text{C}$ . respectively), it was considered that the sulphur dichloride could be used directly without purification. A sample of the sulphur dichloride was purified by distillation at  $0^\circ\text{C}$ . and 66 mm. pressure, then resealed by adding  $\text{PCl}_3$ , and used immediately. The results obtained, using this sample, did not deviate from those obtained in experiments on sulphur dichloride which had not been purified. A fresh sample of  $\text{SCl}_2$  was used in the saturators for each experiment.

**Catalyst.**—1300 g. of charcoal were shaken in a solution containing 200 g. of  $\text{CaCl}_2 \cdot 8\text{H}_2\text{O}$  (A.R.) in 2 l. of water. After being allowed to steep for some time the charcoal was filtered, washed with 250 ml. alcohol, followed by 200 ml. ether, and dried at  $100^\circ\text{C}$ . in an oven.\* It was transferred to the reaction tubes while still warm, heated to  $300^\circ\text{C}$ . and pumped out with a liquid air trap in series. Two samples of activated catalyst were used. One had been in contact with the activating solution for 72 hours and was oven-dried at  $100^\circ\text{C}$ . for 5

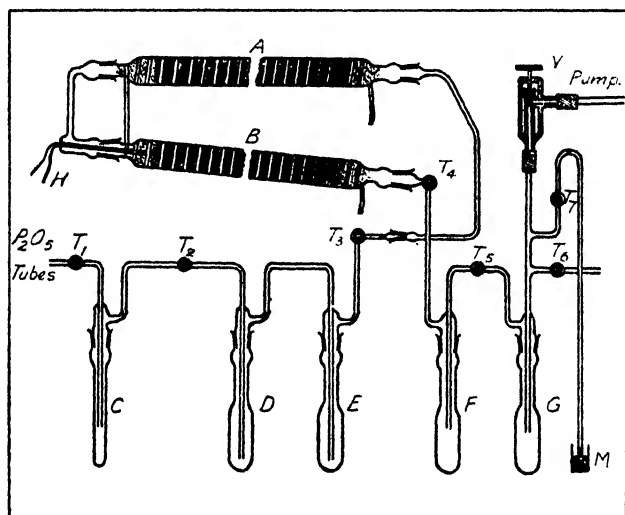


FIG. 1.—Atmospheric oxidation of  $\text{SCl}_2$  over activated charcoal.

hours. The other had been in contact with the activating solution for 115 days and was oven-dried at  $100^\circ\text{C}$ . for 3 days. The latter catalyst was found to be very much more active than the former.

**Analysis of the Products of Oxidation.**—The products of the reaction contained unchanged  $\text{SCl}_2$ , b. p.  $59.0^\circ\text{C}$ .,  $\text{SOCl}_2$ , b. p.  $78.8^\circ\text{C}$ ., and  $\text{SO}_2\text{Cl}_2$ , b. p.  $69.1^\circ\text{C}$ .

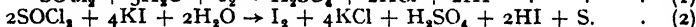
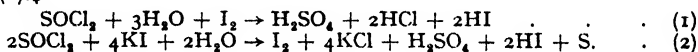
(a) **Determination of the Unchanged  $\text{SCl}_2$ .**—Professor N. K. Adam, F.R.S., informs us that he has found that  $\text{SCl}_2$  can be completely converted into monochloride by refluxing for 30 min. with sulphur, after which the separation of thionyl chloride by fractional distillation with a good column is quite easy. We have adopted this method on his advice, and confirm that it is satisfactory. The product of the reaction was refluxed with excess sulphur for 30 minutes, and then fractionally distilled in a quantitative manner. The fraction distilling between  $60^\circ\text{C}$ . and  $80^\circ\text{C}$ . was collected. This fraction contained the  $\text{SO}_2\text{Cl}_2$  and  $\text{SOCl}_2$  produced in the reaction. The difference between the volume of original product and the volume of the distillate was taken as a measure of the  $\text{SCl}_2$  in the reaction product.

(b) **Determination of  $\text{SOCl}_2$  and  $\text{SO}_2\text{Cl}_2$ .**—The second stage in the analysis was the determination of the  $\text{SOCl}_2$  and  $\text{SO}_2\text{Cl}_2$  content of the fraction which

\* We thank Dr. W. E. Jones, Research Establishment, Sutton Oak, St. Helens, for these details concerning the activation of the charcoal.

had been separated from the  $\text{SOCl}_2$ . This was done by making use of the fact that  $\text{SOCl}_2$  reacts with iodine whereas  $\text{SO}_2\text{Cl}_2$  does not.\*

Experiments on the reaction of  $\text{SOCl}_2$  with solutions containing potassium iodide and iodine were carried out by one of the authors (A. G. E.), in collaboration with E. Warhurst. Kahlbaum's  $\text{SOCl}_2$  was used and taken to be 100 % pure. The method of analysis was that used at the Research Establishment, Sutton Oak, St. Helens.† A small quantity of the  $\text{SOCl}_2$  was drawn into a previously weighed and evacuated glass bulb by breaking a sealed tip beneath the liquid surface. The bulb was then resealed and weighed together with the piece of glass broken from the tip. The weight of the sample taken for analysis was thus known. The sealed bulb, together with a number of glass beads, was placed in a Pyrex conical flask with 100 ml.  $\text{CCl}_4$  and known amounts of aqueous KI (of known strength) and standard iodine (the KI content of which was known). The flask was stoppered and vigorously shaken. The sealed bulb was broken under this treatment, and the shaking was continued for about 5 min. The iodine was then back titrated with standard sodium thiosulphate, and the free acid then determined by titration with standard caustic soda, using brom-cresol purple as indicator. It was found that the amount of iodine absorbed and the quantity of acid liberated corresponded precisely to one fraction of the  $\text{SOCl}_2$  reacting according to equation (1) and the remainder according to equation (2).‡



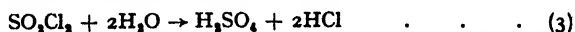
The fraction of the total  $\text{SOCl}_2$ ,  $x$ , which reacts according to equation (1) may be derived both from the iodine titrations and from the acidity titrations. These two values of  $x$  are shown in Table I and it is seen that they are in good agreement. This supports the view that the reaction of  $\text{SOCl}_2$  is accurately described as a competition between the reactions given by equations (1) and (2).

As would be expected, the results show that  $x$  can be increased by increasing the ratio of free iodine to KI. The most favourable  $\text{I}_2/\text{KI}$  ratio possible (using aqueous iodine as a reagent) is when the only KI present is that necessary to keep the iodine in solution. It can also be seen from Table I that an increase in the  $\text{I}_2/\text{SOCl}_2$  ratio causes an increase in  $x$ .

TABLE I.

Moles of $\text{SOCl}_2$ $\times 10^3$ .	Equiv. of Iodine $\times 10^3$ .	Equiv. of Pot. Iodine $\times 10^3$ .	Equiv. of Iodine Absorbed $\times 10^3$ .	Equiv. of Acid Liberated $\times 10^3$ .	$x$ from Iodine Absorption.	$x$ from Acid Liberation.
1.58	0.00	38.1	— 0.17	4.96	0.297	0.283
3.37	0.00	38.1	— 0.54	10.39	0.280	0.273
3.81	3.42	43.64	+ 1.97	15.25	0.506	0.500
3.24	6.84	49.18	+ 3.30	15.20	0.683	0.675
2.45	6.84	49.18	+ 2.78	11.77	0.712	0.700
1.14	6.84	11.08	+ 1.62	5.92	0.807	0.803
4.29	19.53	33.50	+ 5.23	21.25	0.740	0.740
1.21	19.53	33.50	+ 2.05	6.78	0.897	0.898
2.40	39.05	67.00	+ 3.73	12.96	0.852	0.850
4.32	9.76	16.75	+ 5.22	21.27	0.736	0.730

Sulphuryl chloride does not react with the iodine or potassium iodide, but under the same conditions as used above, it undergoes hydrolysis according to the equation: †



that is, 1 mole. of  $\text{SO}_2\text{Cl}_2$  liberates four equivalents of acid. Two samples of

\* Private communication.

† Reports to Ministry of Supply from the Research Establishment, Sutton Oak, St. Helens, 25th April, 1942, and 11th October, 1941.

‡ The fact that  $\text{SOCl}_2$  can react in these two ways was shown by earlier work at the Research Establishment, Sutton Oak, St. Helens. (Report to Ministry of Supply, 11th October, 1941.)

freshly distilled sulphuryl chloride treated with iodine in the same way as for the thionyl chloride analysis, were found to liberate 4.00 and 4.04 equivalents of acid per mole of sulphuryl chloride respectively. Only a very slight absorption of iodine occurred, 0.01 equivalent and 0.05 equivalent per mole of sulphuryl chloride respectively, compared with the 1.40 equivalents absorbed per mole of thionyl chloride. Thus equation (3) represents the behaviour of sulphuryl chloride under these conditions fairly accurately.

The  $\text{SOCl}_2$ — $\text{SO}_2\text{Cl}_2$  mixture obtained from the reaction product after removal of the  $\text{SCl}_2$ , was therefore analysed by the addition of standard iodine, back titration of the iodine with thiosulphate, and then determination of the free acid by titration with caustic soda. These two titrations give values for the total iodine absorbed and the total acid liberated according to equations (1), (2) and (3). Both these titration figures are dependent on the value of  $x$  (the percentage of  $\text{SOCl}_2$ , which reacts according to equation (1)). From these values, and the knowledge of the weight of the thionyl chloride-sulphuryl chloride sample taken for analysis, we can eliminate  $x$  and thus calculate the composition of the mixture.

To test this method, a mixture of  $\text{SOCl}_2$  and  $\text{SO}_2\text{Cl}_2$  containing 47.8 %  $\text{SOCl}_2$ , by weight was made up and analysed by the above procedure. This analysis gave the percentage of  $\text{SOCl}_2$  as 49.5, which is in fairly good agreement with the actual figure.

### Results.

The composition of the products of the oxidation reaction were dependent in the main upon two factors, (a) the temperature of the reaction, and (b) the time of contact of the reacting gases with the catalyst surface. Experiments were carried out at three temperatures, 193° c.,

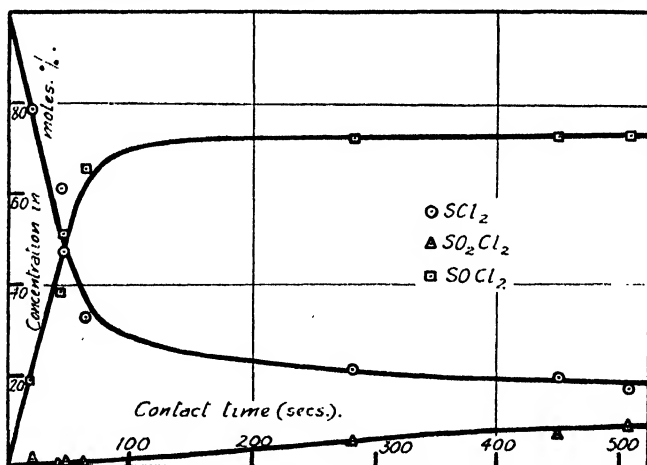


FIG. 2.—Variation in the concentration of  $\text{SCl}_2$ ,  $\text{SOCl}_2$  and  $\text{SO}_2\text{Cl}_2$  with contact time over the catalyst at 193° c.

TABLE II.

Temp. °C.	Time of Contact sec.	% $\text{SCl}_2$ moles.	% $\text{SOCl}_2$ moles.	% $\text{SO}_2\text{Cl}_2$ moles.
320	518	41.2	26.0	32.8
320	164	36.0	23.2	40.8

238° c., and 320° c. The results for the experiments at 193° c. and 238° c. are given in Fig. 2 and 3. Two experiments were done at the temperature of 320° c. and the results are given in Table II.

Although there was a temperature difference of 45° c. between the experiments at 193° c. and 238° c., the rates of the overall oxidation processes at these two temperatures were very similar. We attribute this to the fact that in the experiments at the lower temperature the more highly activated catalyst was used.

In the experiments at 193° c. and 238° c. (Fig. 2 and 3) the concentrations of the three components in the reaction products approached equilibrium values at high contact times. At 193° c. these equilibrium values were 73 %  $\text{SOCl}_2$ , 9 %  $\text{SO}_2\text{Cl}_2$ , and 18 %  $\text{SCl}_2$  (expressed in molar percentages of the initial  $\text{SCl}_2$ ). The amount of oxygen which has been used is, therefore  $(73/2 + 9) = 46$  moles for every 100 moles. of  $\text{SCl}_2$ . The initial gas mixture was air saturated with  $\text{SCl}_2$  at 27° c. Since this initial gas mixture contains 46 moles of oxygen for every 100 moles of  $\text{SCl}_2$ , practically all the oxygen is used up in irreversible oxidation.

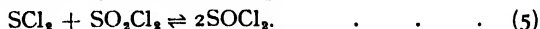
At 238° c. the equilibrium values were 48 %  $\text{SOCl}_2$ , 36 %  $\text{SO}_2\text{Cl}_2$ , and 16 %  $\text{SCl}_2$ . The amount of oxygen which has been used is, therefore  $(48/2 + 36) = 60$  moles for every 100 moles of  $\text{SCl}_2$ . The initial gas mixture was air saturated with  $\text{SCl}_2$  at 21° c. This initial gas mixture contains 65 moles of oxygen for every 100 moles of  $\text{SCl}_2$ . These results

also show that practically all the oxygen is used up in irreversible oxidation.

The oxidation of  $\text{SCl}_2$  may go by the simple bimolecular addition :



thionyl chloride being produced by the further equilibrium reaction :



The possibility of equilibration according to reaction (5) was investigated by passing  $\text{SCl}_2$  and  $\text{SO}_2\text{Cl}_2$  vapour over the catalyst in a stream of nitrogen. It was found that after a contact time of 200 sec. at a temperature of 239° c., the reaction product was 33.0 %  $\text{SOCl}_2$ , 4.9 %  $\text{SO}_2\text{Cl}_2$ , and 62.1 %  $\text{SCl}_2$ . The equilibrium constant for reaction (5),

$$K = (\text{SOCl}_2)^2 / (\text{SCl}_2)(\text{SO}_2\text{Cl}_2),$$

obtained from these results is  $K = 3.6$ . This constant has also been evaluated, using the equilibrium concentrations obtained from the asymptotic values of the curves in Fig. 3 (temp. 238° c.). The value of  $K$  obtained in this way is 4.0. The agreement between these two values of  $K$  shows that in the oxidation of  $\text{SCl}_2$  under the conditions described, the reversible reaction (5) occurs, and reaches equilibrium in the contact time of 200 sec.

**The  $\text{SCl}_2/\text{O}_2$  Ratio.**—For a  $\text{SCl}_2 - \text{O}_2$  mixture of any  $\text{SCl}_2/\text{O}_2$  ratio passed over activated charcoal at a rate slow enough for equilibrium to be attained, the concentrations of  $\text{SCl}_2$ ,  $\text{SOCl}_2$ , and  $\text{SO}_2\text{Cl}_2$  in the reaction

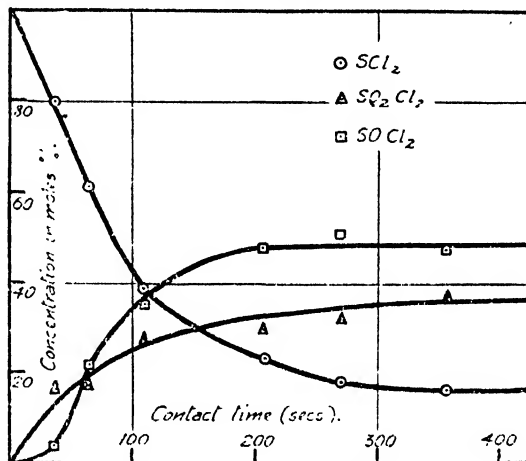


FIG. 3.—Variation in the concentration of  $\text{SCl}_2$ ,  $\text{SO}_2\text{Cl}_2$ , and  $\text{SOCl}_2$  with contact time on the catalyst at 238° c.

## 672 OXIDATION OF SULPHUR DICHLORIDE BY OXYGEN

products can be calculated in the following way. If the initial gas mixture contains  $a$  moles of  $O_2$  and  $b$  moles of  $SCl_2$ , it is equivalent to a mixture of  $(b - a)$  moles of  $SCl_2$  and  $a$  moles of  $SO_2Cl_2$ , since the oxygen reacts

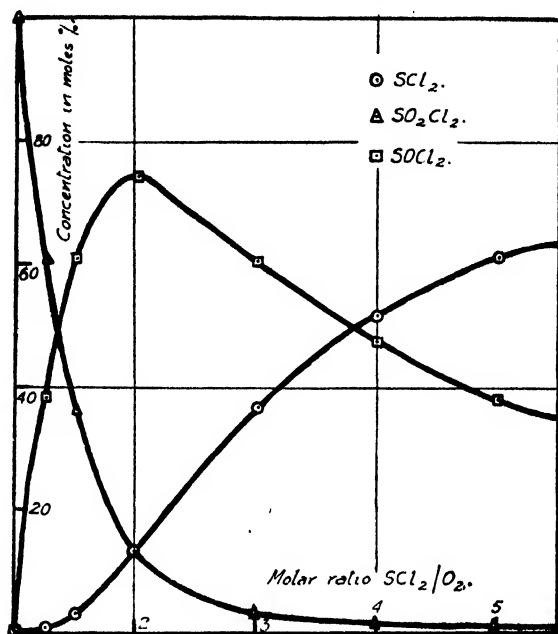


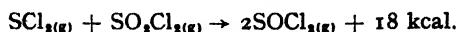
FIG. 4.—Variation in the equilibrium concentration of  $SCl_2$ ,  $SO_2Cl_2$  and  $SOCl_2$  with  $SCl_2/O_2$  ratio at  $193^\circ C$ .

practically irreversibly. (If  $a$  is greater than  $b$ , then there will be  $b$  moles of  $SO_2Cl_2$ ,  $(a - b)$  moles of excess  $O_2$  and no  $SCl_2$ ). The  $a$  moles of  $SO_2Cl_2$  and the  $(b - a)$  moles of  $SCl_2$  will equilibrate according to reaction (5), and the equilibrium concentrations of  $SCl_2$ ,  $SOCl_2$ , and  $SO_2Cl_2$  will be determined by the equilibrium constant of reaction (5) at the appropriate temperature. The equilibrium concentrations have been calculated for various  $SCl_2/O_2$  molar ratios at a temperature of  $193^\circ C$ . ( $K = 33$ ), and the results are given in Fig. 4. It can be seen from the figure that the maximum percentage of  $SOCl_2$  will be obtained by using a  $SCl_2/O_2$  ratio of 2.

TABLE III.

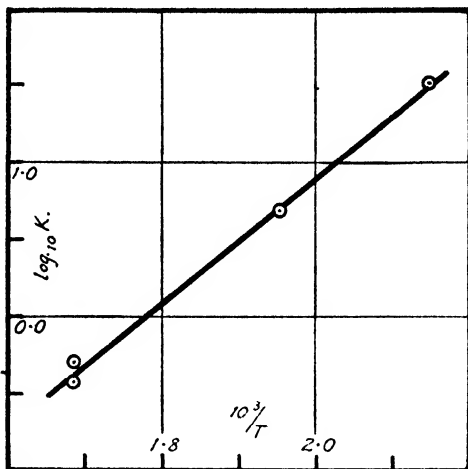
Temp.	Equilibration Constant.
$^\circ C$	$K$
320	0.5
320	0.37
238	4.0
193	33

**Determination of  $\Delta H$  for the Equilibration Reaction.**—The equilibrium constant for reaction (5) has been calculated at the temperatures  $193^\circ C$ .,  $238^\circ C$ . and  $320^\circ C$ . These values are given in Table III. The plot of  $\log_{10} K$  against  $1/T$  is given in Fig. 5. The points lie on a straight line, from the slope of which  $\Delta H$  for reaction (5) is found to be  $-18$  kcal. That is:



This means that if two atoms of oxygen are added in succession to a  $SCl_2$  molecule to give first  $SOCl_2$  and then  $SO_2Cl_2$ , the addition of the first oxygen atom liberates 18 kcal. more energy than does the addition of the second.

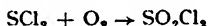
The heat of formation of gaseous  $\text{SOCl}_2$  is 42.7 kcal.,<sup>1</sup> of gaseous  $\text{SO}_2\text{Cl}_2$  is 86.2 kcal.,<sup>1</sup> and of liquid  $\text{SOCl}_2$  is 12.05 kcal.<sup>1</sup> Recent measurements of the vapour pressure of  $\text{SOCl}_2$ \* give a value of 7.6 kcal. for its latent heat. From these values reaction (5) is found to be endothermic to the extent of about 6 kcal. This calculated value thus differs from our experimental value by about 24 kcal. In spite of this disagreement with the limited heat data available, there is some general support for the exothermicity of the equilibration reaction. Practically all the existing  $\text{SOCl}_2$  processes are worked at low temperatures, and an increase in the temperature has been observed to give rise to increased amounts of sulphur halides and some sulphuryl chloride.<sup>2</sup>

FIG. 5.—Plot of  $\log_{10} K$  against  $T^{-1}$ .

The authors wish to express their best thanks to Professor A. R. Todd, F.R.S., and Professor M. Polanyi, F.R.S., for their interest and encouragement in this research, and to the Director General of Scientific Research (Defence), Ministry of Supply, for permission to publish this work.

### Summary.

The oxidation of  $\text{SOCl}_2$  by atmospheric oxygen has been investigated using activated charcoal as a catalyst. The reaction has been discussed in terms of two reactions. Firstly, the irreversible oxidation of  $\text{SOCl}_2$  to  $\text{SO}_2\text{Cl}_2$ :



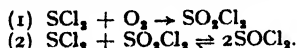
and secondly, the reversible reaction between the  $\text{SOCl}_2$  and the  $\text{SO}_2\text{Cl}_2$  to form  $\text{SOCl}_2$ :



This oxidation has been investigated at the temperatures 193°, 238°, and 320° C., and the equilibrium constant of the reversible equilibrium reaction has been determined for each temperature. From the temperature dependence of this equilibrium constant it is found that the reaction is exothermic to the extent of 18 kcal.

### Résumé.

L'oxydation de  $\text{SOCl}_2$  par l'air, avec le charbon actif comme catalyseur, a été étudiée à trois températures, selon les deux équations suivantes :



On a déterminé la constante d'équilibre de (2) et on a trouvé que la réaction—exothermique—peut dégager 18 kcal.

### Zusammenfassung.

Die Oxydation von  $\text{SOCl}_2$  durch Luft mit Kohle als Katalysator wurde bei drei Temperaturen mit Bezug auf die Reaktionen

<sup>1</sup> Bichowsky and Rossini, *Thermochemistry of Chemical Substances* (Reinhold Publishing Corporation, 1936).

<sup>2</sup> Chem. Fabrik. Buchau, D.R.P. 284,935 (1914).

\* Sutton Oak Report to Ministry of Supply, 3rd July, 1941.





untersucht und die Gleichgewichtskonstante von (2) bestimmt. Die Reaktion ist exothermisch (18 kcal.).

*Chemistry Department,  
University,  
Manchester.*

## THE HYDRATION OF IONS.

BY J. Y. MACDONALD.

*Received 2nd August, 1946.*

Washburn,<sup>1</sup> in a well-known investigation, determined the degree of hydration of certain ions from transference number experiments, by adding a non-electrolyte to the solution as a reference substance. This type of experiment measures the difference in the amount of water transported to the anode and to the cathode, and if the degree of hydration of any one ion is known or assumed, that of the others can be calculated. Washburn drew up a table of the degrees of hydration,  $n$ , of the  $\text{H}^+$ ,  $\text{Li}^+$ ,  $\text{Na}^+$ , and  $\text{K}^+$  ions calculated by assuming for the chloride ion all values of  $n$  from 0 to 12. From this table, the majority of text books quote the values obtained by putting  $n_{\text{Cl}^-} = 4$  or 9 (first two lines of table below), since these give  $n_{\text{H}^+} = 1$  or 2 respectively. The argument is that the proton must be associated with at least one water molecule, forming the oxonium ion  $\text{H}_3\text{O}^+$ .

Bernal and Fowler<sup>2</sup> showed that the exceptionally high conductivity of the hydrogen ion could be explained by a modified "Grotthus"

		Cl <sup>-</sup>	H <sup>+</sup>	K <sup>+</sup>	Na <sup>+</sup>	Li <sup>+</sup>
Washburn	{	4	1.02	5.4	8.4	13.9
		9	2.0	10.5	16.6	25.3
		0	0.28	1.3	2.0	4.7
		1	0.46	2.3	3.6	7.0
Ulich	.	2	(4)	2	3.5	2
Darmois	.	*	(0.3)	*	1	5

(The hydration of ions marked \* works out at a negative value by Darmois' method, which seems to give results which are too low. The values for  $\text{H}^+$  obtained by Ulich and by Darmois are not comparable with Washburn's values, for the proton-jump mechanism can only affect results based on electrical conductivity.)

mechanism, in which the charge jumped from one water molecule to another. Such a mechanism would entail no transport of water, and the ion would act in transference number experiments as if it were not hydrated at all. In actual fact, however, each molecule of water, while it is the temporary home of a proton, will move towards the cathode, so that part of the current will be carried by the normal bodily migration of the  $\text{H}_3\text{O}^+$ , and part by the proton-jump mechanism. If we assume that the mobility of the  $\text{H}_3\text{O}^+$  ion at 18° is about 65 (a value possessed

<sup>1</sup> *J. Amer. Chem. Soc.*, 1909, 31, 322.

<sup>2</sup> *J. Chem. Physics*, 1933, 1, 515.

by a number of simple ions such as  $K^+$ ,  $Cl^-$ , and  $NH_4^+$ , then  $65/315 = 0.22$  of the hydrogen ions' contribution to the current will be associated with the transport of at least one molecule of water, and  $n_{H^+}$  (in transference number experiments) may appear to be as low as 0.22. This is close to the value (0.28) obtained by Washburn on the assumption that  $n_{Cl^-} = 0$  (third line of table). This set of values agrees moderately well with those of Ulich,<sup>3</sup> obtained from entropies, and those of Darmonis,<sup>4</sup> from specific volumes. Even better agreement with Ulich's figures is obtained by taking  $n_{Cl^-} = 1$  (corresponding to a true value of  $n_{H^+}$  of 2, and an apparent value of 0.44), but too much stress should not be laid on this in view of the different results obtained by other workers.<sup>5</sup>

### Résumé.

On considère ici les valeurs données habituellement pour le degré d'hydratation des ions  $H^+$ ,  $Li^+$ ,  $Na^+$  et  $K^+$  à la lumière du mécanisme du saut de proton, employé par Bernal et Fowler pour expliquer la haute conductivité de l'ion  $H^+$ .

### Zusammenfassung.

Die gewöhnlich angegebenen Werte für den Hydratationsgrad von  $H^+$ ,  $Li^+$ ,  $Na^+$ , und  $K^+$  werden unter Annahme des "Protonsprungmechanismus", durch den Bernal und Fowler die hohe Ionenleitfähigkeit des  $H^+$ -Ions erklären, revidiert.

*The Chemistry Department,  
United College,  
St. Andrews.*

<sup>3</sup> Z. Elektrochem. 1930, **36**, 477.

<sup>4</sup> J. Physique Radium, 1941, **8**, (2), 2.

<sup>5</sup> E.g. Babrovsky, Z. physik. Chem., 1927, **129**, 129; and Remy, Trans. Faraday Soc., 1927, **23**, 381.

### ADDENDUM.

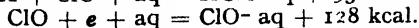
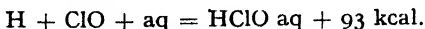
## THE ELECTRON AFFINITY OF ClO.

By JOSEPH WEISS.

*Received 30th September, 1947.*

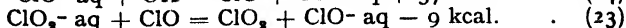
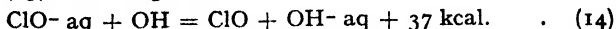
In a paper published in the April issue<sup>1</sup> the value of the Cl—O bond energy used was based on the work of Goodeve and Wallace.<sup>2</sup> I am indebted to Dr. H. A. Skinner for drawing my attention to the more recent value of Goodeve and Marsh<sup>3</sup> which I had previously overlooked. The latter value—67 kcal.—seems more probable according to Skinner<sup>4</sup> who has discussed this point in some detail.

With the new value the figures concerning ClO, given in my previous paper, are diminished by the difference between these two determinations which is  $\sim 37$  kcal. One now obtains:



which, with the previously assumed value of  $S_{ClO^-} \sim 60$  kcal., leads to a value for the electron affinity of  $E_{ClO} \sim 68$  kcal.

Eqn. (14) and (23) are changed to:



<sup>1</sup> Weiss, Trans. Faraday Soc., 1947, **43**, 173.

<sup>2</sup> Goodeve and Wallace, *ibid.*, 1930, **26**, 255.

<sup>3</sup> Goodeve and Marsh, J. Chem. Soc., 1939, 1332.

<sup>4</sup> Skinner, Nature (in press).

## CORRIGENDA.

Volume XLIII :

Page 240: Equation " $\xi = \sqrt{2}OP$ " should read " $\xi = \sqrt{2}OP$ ".

Pages 325-331, 332-337, 338-342. For cellophane, read Cellophane throughout, including French and German summaries.

Page 463. For "Hartree" read "D. R. Hartree".

## REVIEWS OF BOOKS.

**The Metallization of Plastics.** By J. R. I. HEPBURN. Cleaver-Hume Press, Ltd. Pp. 71. Price 6s.

This short monograph deals with four processes for the coating of plastics with metallic films: coating from solution, by spraying, by cathode sputtering, and by evaporation in a high vacuum. Each method is described simply and adequately for any technician wishing to start for himself on the laboratory scale. There is a useful final chapter on the characteristics and testing of metallic films on plastics.

The introductory chapter is marred by the table on page 15 on "Types of plastics and physical characteristics" which appears to be inadequate even for the limited purpose of the monograph. In particular the figures given for maximum temperatures of operation are misleading.

The author hints at large-scale production in the near future and it is to be hoped that, with the accumulation of experience on the industrial scale, this monograph will be suitably expanded.

A. C.

**A Text Book of Physical Chemistry.** By N. C. SEN GUPTA and K. C. SEN. Moudal Bros. & Co., Ltd., Calcutta. Pp. 525. Price Rs. 10.

This is a disappointing book. It is a text-book written specifically for B.Sc. students, both pass and honours, of Indian universities; its purpose is to cover the various syllabuses and a perusal of the examination papers given at the end of each chapter shows that this has been accomplished. The teaching of chemistry is subordinated therefore to the immediate requirements of the student to answer the requisite number of questions up to a certain standard. Most examination syllabuses, one may argue, are bad; the authors have been ill-advised in allowing them to guide them. There are no original references because 'they do not seem to be generally consulted by B.Sc. students of Indian Universities'; in their place is a long list of other text-books for further study, together with some numerical examples. The arrangement of the subject matter is throughout along classical, orthodox lines.

Disappointing, too, are the efforts of the publisher; the typescript, particularly of Greek symbols, is often poor, and the binding for a volume which is intended to have hard wear is exceptionally bad.

However, the appearance of this book written by Indians for their needs and produced in India is a welcome and encouraging sign for the future. One would urge however that the subject of chemistry is more important than the syllabuses of Universities and that later authors should be encouraged to lead and guide the University teachers rather than be dictated to by examination bogeys!

**Physical Chemistry.** By E. D. EASTMAN and G. K. ROLLEFSON.  
McGraw-Hill Book Co. Inc., New York and London, 1947. Pp.  
viii. 504. \$4.50 or 22s.

This book is an addition to the International Chemical Series and is based on the introductory course in physical chemistry given to third and fourth year students at the University of California. The emphasis throughout is on the general nature of the principles involved; an understanding of the physical significance of equations involving differential and integration processes is quite rightly assumed but the space assigned to straightforward algebraic deductions is reduced to an absolute minimum. This is to be commended. The book covers a wide range within a reasonable size largely because of two features; the neglect of historical background and growth of the many aspects treated and an absence of detailed description of instruments, apparatus and techniques. If this means a slight loss, it is more than compensated by the compactness of the contents and the presentation of the subject as it is to-day. The order of treatment of the various branches and the amount of space devoted to these cannot be expected to find favour with all teachers of physical chemistry; atomic structure is not considered until page 171 and electrochemistry is left until page 416; phase rule discussions on one-, two- and three-component systems occupy practically the same space as the whole of electrochemistry; molecular spectra is completed in four pages and surface phenomena in a matter of twelve pages. These however are slight criticisms, e.g. the interdependence of the chapters is somewhat loose, allowing a large flexibility of presentation. The most admirable feature lies in the selective viewpoint of the authors. They have set out to write an introduction to physical chemistry to those people who have some passing acquaintance with the rudiments of the subject; it is not a book on chemical physics but at least forms an excellent groundwork for further study along those lines. There are no complex derivations—the reader will not be able to write down a formula representing a rotational partition function but he will have been introduced to the concept and value of such functions; viscosity is not treated from the transition state theory but there are radial distribution curves to illustrate the molecular structure of liquids. In all, the authors have set out to give a compact, logical presentation of the principles and scope of physical chemistry—they have accomplished their aim in an excellent manner.

**An Introduction to Electrochemistry.** By SAMUEL GLASSTONE. D. van Nostrand Co. Inc., New York; Macmillan & Co. Ltd., London. Pp. 557. Price 31s. 6d. First published 1942, reprinted 1946.

The author states in his preface that the object of this book is to provide an introduction to electrochemistry in its present state of development and to explain the fundamentals of the subject free from obsolete and discarded ideas. In this aim Dr. Glasstone succeeds admirably, and in the space of some 545 pages provides a lucid and reliable account of the main facts and modern theories of the electrochemistry of solutions. The main topics dealt with are electrolytic conductance and related phenomena; the activity concept and theories of electrolytes; reversible cells and electrodes of various types and their physico-chemical applications; ionic

equilibria in acids, bases and amphoteric electrolytes; phenomena at working electrodes including polarisation, metal deposition, and electrolytic oxidation and reduction; and finally electrokinetic phenomena are briefly considered. The treatment given is clear and rigorous throughout, and in dealing with controversial subjects Dr. Glasstone, while in some cases indicating his own preferences, has very impartially summarised alternative views. The author does not deal with phenomena in fused electrolytes, nor are technical electrochemical applications discussed except incidentally.

The book should be especially useful to university students and in this connection two features are particularly valuable: to each chapter is appended a lavish list of numerical problems extracted from recent original papers, and selected references are given throughout the text for further reading. The American convention as regards the sign of electrode potentials is used throughout the work and may possibly cause some confusion amongst students here, although it is only fair to say that the convention is fully discussed in the text. The book has a good subject-index and proof-reading appears to have been done very thoroughly. The printing, paper and binding are excellent and make the book a pleasure to use.

A. H.

**Fatty Acids. Their Chemistry and their Properties.** By KLAIRE S. MARKLEY. Interscience Publishers, New York, 1947. Pp. x + 668. Price 60s.

This treatise provides a very valuable survey of the knowledge available on the fatty acids. The information is drawn from data widely scattered throughout the literature, and since it is often obtained incidentally and not as a result of systematic investigation, there are many gaps that remain to be filled. Therefore the treatise will be very useful in drawing the attention of investigators to fields of work which have not been adequately surveyed.

A brief history is given of the early knowledge on the fatty acids and fats, and this is followed by a discussion of their classification and structure. A good deal of space is devoted to their physical properties, crystal structure, absorption spectra, thermal and other properties. The chemical reactions of the acids and their compounds are reported in considerable detail, special attention being paid to the formation of esters and glycerides, pyrolysis, halogenation, hydrogenation and oxidation. An account of the nitrogen and sulphur derivatives of the acids is included. The methods of synthesis *in vitro* and in the living cell, and the isolation and identification of the acids are also dealt with. The soaps are only very briefly discussed.

The author has succeeded in bringing together a large number of facts in an account which is very readable. It is very largely a statement of the views of others, but is not uncritical in its presentation. Some care has been exercised in the choice of information, without rigidly excluding information that may not be of first-class quality. The author indicates where the information is scanty and uncertain, and makes stimulating comments as to the present state of our knowledge.

It is an excellent summary of the field, and should be read by all interested in the fats and their biological significance.

W. E. G.

# IRREVERSIBLE ELECTRODE POTENTIALS OF METALS AND THEIR SOLID SOLUTIONS.

## PART I. IRREVERSIBLE ELECTRODE POTENTIALS OF METALS.

BY G. W. AKIMOV AND G. B. CLARK.

*Received 29th April, 1946.*

(1) Irreversible electrode potentials (I.E.P.) are important in the field of metallic corrosion, since their determination is involved in any investigation of the electrochemical mechanism of a corrosion process. The data on irreversible potentials given in various studies on corrosion have been obtained under various conditions and by various methods, and therefore cannot be compared with one another; moreover, systematic studies on this subject are few in number.<sup>1-6</sup> There is still less reliable information on electrode potentials of solid solutions, which often form the basis of corrosion resistant alloys. The old data, summarised in a book by Kremann<sup>6</sup> are very valuable but insufficient for any theoretical conclusions. Since 1919, when Tamman's excellent work—in which the existence of "parting limits" had been realised—appeared, there have been practically no publications on the electrochemistry of solid solutions except those in which the only purpose was to provide new experimental data.

The electrochemical behaviour of both pure metals and alloys is determined not only by their electrode potentials, but also by such important properties as their anodic and cathodic polarisation. Nobody will deny, however, that a knowledge of the electrode potentials of pure metals and solid solutions is very important in studying the numerous cases of corrosion, which are of practical significance.

The purpose of the first part of this work was a systematic and comparative study of the electrode potentials of various pure metals in typical electrolyte solution. The potentials of the following 22 metals [Be, Mg, Al, Si, Nb, Cr, Mo, Mn, Fe, Co, Ni, Cu, Ag, Au, Zn, Cd, Hg, Tl, Sn, Pb, Bi, Sb] were determined in solutions of 0.1 N. HCl, 0.1 N. HNO<sub>3</sub>, 0.1 N. NaOH and 3 % NaCl.

In this study we decided not to plot potential-time curves, since these, abstracted from the particular corrosion problem, are generally complicated and of little use. However, it was important to take account of the specific behaviour of various metals as regards the formation of their protective films in air and during the first moments of reaction between the metal and the solution. Therefore it was necessary to determine the electrode potential of the metal *without its protective film* and after it had been in the solution for some time.

<sup>1</sup> Akimov, *Trans. Zani*, 1931, 70. First Comm. New Intern. Assoc. Testing Materials, D, 1930, 127.

<sup>2</sup> French and Kahlenberg, *Trans. Electrochem. Soc.*, 1928, 54, 149.

<sup>3</sup> Krueger and Kahlenberg, *ibid.*, 1930, 58, 107.

<sup>4</sup> Akimov, *Trans. Wiam*, 1938, 56, 27.

<sup>5</sup> Gatty and Spooner, *Electrode potential Behaviour of Corroding Metals in Aqueous Solutions*, 1938.

<sup>6</sup> Kremann in Guwrtler's *Metallographie II. Die Eigenschaften der Metalle und ihre Legierungen*, 1921, 1.

(2) Many methods of measuring the potential after rubbing the metal surface under a solution have been reported in the literature.<sup>7-11</sup> The apparatus shown in Fig. 1 makes it possible to use test-pieces of various shapes. The test-piece is fastened to the bottom of a wide glass vessel through an opening by a rubber washer R and Mendelëeff's wax. The outer end of the test-piece is clamped in a vice. It is thus held fast, and can be mechanically cleaned while retaining good electrical contact. The surfaces of the test-pieces are rubbed under the solution by means of a small carborundum disc A, fastened to the pin T, made of "textolite", which is a good insulator and is stable in all media. The carborundum disc is driven by an ordinary dentist's drill. The test-pieces were preliminarily polished, degreased by means of acetone and alcohol and kept in a desiccator for 24-48 hr. The potentials were measured after 1 and 5 min., firstly, when the solution was agitated by the carborundum disc,\* and secondly while rubbing the surface under solution.

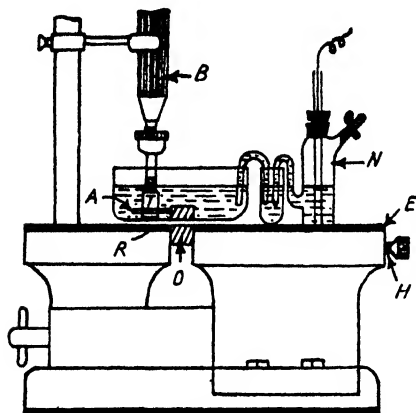


FIG. 1.—Apparatus for measuring the potential while rubbing the surface of the samples under solution.

A—Carborundum disc; T—textolite pin; B—tag of dentist's drill; O—test-piece; R—rubber washer; N—calomel half-cell; E—ebonite plate; H—terminal.

Corrections for liquid junction potential were not made, since the data available suggested that the error so introduced could not possibly exceed 10-15 mv.

(3) By the I.E.P. of metals we mean potentials such as those at a metal-electrolyte interface, when there is no direct indication of the nature of the reversible reaction determining the potential. The electrode potentials of metal in solutions of foreign ions, or in the presence of considerable quantities of such ions, as well as those of solid alloys and of complex electrodes, all belong, according to this definition, to this group. We suggest the following classification.

Various kinds of Irreversible Electrode Potentials.	Example.
1. Those which can be reduced to reversible potentials of the 1st type (great solubility of the products of reaction).	Zinc in a solution of KCl.
2. Those which can be reduced to reversible potentials of the 2nd type (small solubility of the products of reaction).	Copper in a solution of NaOH.
3. True potentials of the protective films.	Oxides of lead.
4. Complex electrodes of the film-pore type.	Aluminium in a solution of NaCl.
5. Potentials of solid solutions.	Potentials of Cu—Ni in a solution of NaCl.
6. Potentials of heterogeneous alloys.	Potential of the Zn—Fe electrode in a solution of NaCl.

<sup>7</sup> Bennwitz and Schultz, *Z. physik. Chem.*, 1926, **124**, 115.

<sup>8</sup> Lange and Berger, *Z. Elektrochem.*, 1930, **36**, 980.

<sup>9</sup> Bennewitz and Bigalke, *Z. physik. Chem.*, 1931, **154**, 113.

<sup>10</sup> Sven Bodfors, *ibid.* A, 1932, **160** 141, <sup>11</sup> May, *J. Inst. Metals*, 1928, **40**, 141.

\* Since the solution is also agitated while the test-piece is being rubbed, preliminary measurement with agitation makes the action of these two factors qualitatively separable.

Potentials of the fourth type, i.e. of metals coated with a protective film, play an important role in corrosion. The behaviour of these electrodes depend greatly upon (1) the ratio of the area coated with film to that occupied by pores, (2) the electrical resistance of the film-pore micro-element, and (3) the polarisation characteristics of the film (cathodic) and of the metal in the pores (anodic). If the pore area is great compared with the film area, the electrode approximates to type 1 or 2. If, however, the pore area is very small or equal to zero, the potential of the electrode should be close to that of an inert electrode except in those cases where the film acts as a true electrode.<sup>3</sup>

With regard to the resistance of the pore-film micro-elements, two extreme cases can be distinguished: (a) if the resistance of the micro-element is high, the measured potential will be related to the potential drop in the anode and cathode parts of the micro-element,<sup>12, 13</sup> (b) if, on the other hand, the resistance of the micro-element is low, the value depends on the polarisation at the anode and cathode areas.<sup>14-18</sup>

The properties of the protective film are of great importance. At temperatures of the order of 0-100° C. a great majority of films, even the thinnest, are probably impermeable to ions (providing there are no pores), and therefore the film-coated area cannot act as anode. However, many compounds, including oxides, are known to have marked electronic conductivity even at comparatively low temperatures.<sup>19</sup> Since the protective films are thin, it may be assumed that conductive films on metals may act as cathodes. The cathode reactions can take place on the areas of protective films, because these reactions only require a supply of excess electrons (flowing from the anode).

In the case of "non-conductive" films, such as  $\text{Al}_2\text{O}_3$ ,  $\text{MgO}$ , the electrons can be transmitted by means of the so-called "tunnel effect," provided that the thickness of the film does not exceed a certain value, probably of the order of 50-100 Å.<sup>20</sup> It may be assumed that cathodic polarisation will be greater in films of low conductivity than in comparatively conductive ones. However, the question is complicated by the fact that low conductivity of the film increases the electrical resistance of the micro-elements, which decreases the role of polarisation phenomena.

Electrodes of the second type are probably capable of high polarisation (anodically), if a considerable part of the slightly soluble corrosion products remains in the form of a protective film on the surface of the metal. The behaviour of electrodes of both the first and second type in corrosion processes is connected to a great extent with the properties of such films.

(4) The adsorption of oxygen and oxidising agents by the surface of a metal is liable to cause saturation of its valences<sup>21</sup> and to increase the electrode potential. The transfer of an electron is rendered more difficult by the adsorption of oxygen by the metal and is facilitated by the adsorption of hydrogen on the surface.<sup>22</sup> The measurements made in our laboratory showed an increase of 0.8-1.0 v. due to the presence of a natural film on aluminium, while further increase in thickness of the film (by means of anodic polarisation) does not result in any further significant increase. The sharp change in the potential and in the rate of platinum solubility effected by adsorption of oxygen were also observed

<sup>13</sup> Akimov and Tomashev, *J. Physic. Chem. (Russ.)*, 1936, 8, 623; *Korros. and Metallsch.*, 1937, 12, 114.

<sup>13</sup> Müller, *ibid.*, 1937, 12, 144.

<sup>14</sup> Evans, *J. Franklin Inst.*, 1929, 208, 45.

<sup>15</sup> Evans and Hoar, *Trans. Faraday Soc.*, 1934, 424.

<sup>16</sup> Brown and Mears, *Trans. Electrochem. Soc.*, 1938, 74, 425.

<sup>17</sup> Akimov, *Ed. Acad. of Science of U.S.S.R.*, 1946 (in Russian).

<sup>18</sup> Akimov, *State Metallurgical Boox Comp.* (1945).

<sup>19</sup> Flechsig, *Hand- und Jahrbuch der Chemischen Physik*, 1933, B. 6 Abschn. II.

<sup>20</sup> Mott, *Trans. Faraday Soc.*, 1939, 35, 1175; 1940, 36, 472.

<sup>21</sup> Tammann, *Lehrbuch der Metallkunde* (1932), 80.

<sup>22</sup> De Boer, *Electron Emission and Adsorption Phenomena*, (1936).



in investigations on platinum passivity.<sup>23</sup> Thus, in considering the I.E.P. of metals, the homogeneous effect of the lower layer (the adsorbed atoms) of the film must be taken into account as well as the heterogeneous effect (pore-films).

(5) In studying the influence of rubbing a section of the metal surface under solution upon its electrode potential, Evans' polarisation diagrams<sup>14-18</sup> may be applied. Theoretically, a number of cases are possible. Here we shall only note that rubbing causes a large negative increase

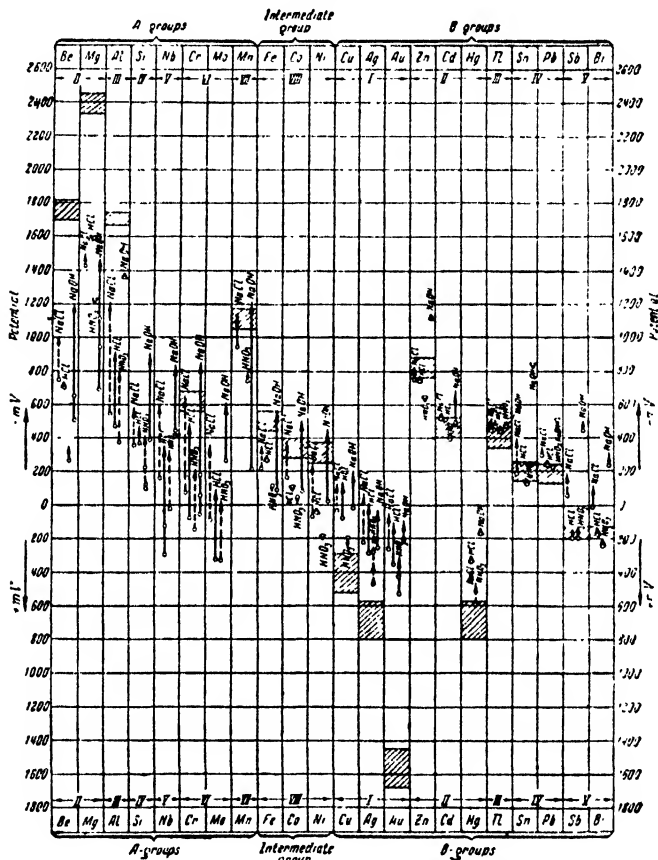


FIG. 2.—Irreversible electrode potentials of metals in various solutions. Base of arrow—potential before rubbing. End of arrow—potential while rubbing. The region of reversible potentials is shaded. All potentials against  $H_2$  electrode.

in the potentials of those metals, which have micro-couples of the film (cathode)-pore (anode) type on their surface, and on which the micro-anodes become greatly polarised due to the small area of the anode.

A significant decrease of the potential must also occur in rubbing a surface, on which there is a layer of adsorbed oxygen, which has a large passivating effect. Rubbing should not cause any change in the potentials of pure metals, whose surfaces do not become "film-coated" (true reversible electrodes of the first and second type), since polarisation does not take place in this case. Thus, the change of potential after rubbing is, to

<sup>23</sup> Ershler, *J. Physic. Chem. (Russ.)*, 1940, 14, 357.

TABLE I.—IRREVERSIBLE ELECTRODE POTENTIALS OF METALS IN TYPICAL ELECTROLYTES (mv.).

Metal.	3% NaCl.				0.1 N. HCl.				0.1 N. HNO <sub>3</sub> .				0.1 N. NaOH.			
	1 Min.	5 Min.	Stirring.	Rubbing.	1 Min.	5 Min.	Stirring.	Rubbing.	1 Min.	5 Min.	Stirring.	Rubbing.	1 Min.	5 Min.	Stirring.	Rubbing.
Be	—	760	—	733	—	724	—	710	—	717	—	712	—	710	—	712
Mg	—	1418	—	1432	—	1622	—	1575	—	1590	—	1595	—	1575	—	1595
Al	—	577	—	551	—	493	—	497	—	916	—	478	—	493	—	478
Si	—	301	—	358	—	378	—	391	—	466	—	371	—	400	—	393
Nb	—	202	—	166	—	176	—	117	—	348	—	115	—	477	—	452
Cr	—	32	—	82	—	39	—	56	—	482	—	74	—	72	—	54
Mo	—	125	—	83	—	351	—	330	—	92	—	324	—	412	—	182
Mn	—	995	—	948	—	908	—	888	—	857	—	865	—	330	—	270
Fe	—	255	—	255	—	328	—	319	—	283	—	276	—	1000	—	386
Co	—	146	—	106	—	147	—	166	—	108	—	110	—	101	—	94
Ni	—	23	—	66	—	31	—	58	—	22	—	44	—	147	—	82
Cu	—	70	—	34	—	154	—	146	—	135	—	70	—	128	—	27
Ag	—	227	—	216	—	277	—	285	—	4	—	281	—	27	—	33
Au	—	250	—	238	—	348	—	330	—	117	—	350	—	300	—	253
Zn	—	772	—	750	—	769	—	750	—	752	—	747	—	245	—	200
Cd	—	530	—	520	—	510	—	515	—	510	—	510	—	1126	—	1123
Hg	—	302	—	286	—	330	—	330	—	331	—	332	—	505	—	487
Tl	—	443	—	450	—	410	—	457	—	487	—	474	—	174	—	163
Sn	—	205	—	192	—	248	—	256	—	251	—	251	—	425	—	474
Pb	—	288	—	298	—	233	—	235	—	237	—	236	—	801	—	841
Sb	—	59	—	62	—	195	—	197	—	161	—	193	—	511	—	506
Bi	—	40	—	8	—	168	—	165	—	176	—	178	—	403	—	448
	—		—	+	—	109	—	+	—	+	—	+	—	251	—	244

## 684 IRREVERSIBLE ELECTRODE POTENTIALS OF METALS

some extent, evidence of the presence of a protective film (or of an adsorbed oxygen layer).

(6) The results for 22 metals in 4 media are given in Table I and Fig. 2. The points correspond to potentials measured 5 min. after the metals had been immersed in the solution, which was stirred constantly. The arrows show the magnitude and direction of the change by rubbing under the solution. Besides this, the region of normal reversible potentials in 0.001-1 N. concentration of its own ions of the lowest valency is shaded for each metal.

From Fig. 2 it follows that the ability to form strong protective films decreases in general from the left side of the Mendelèeff's table to the right side.\* Thus, the most protective films form on metals of the A groups, where rubbing changes the potential of the metal by 300 to 1000 mv. In the case of the transition metals, rubbing only decreases the potential by 200-500 mv., i.e. the film-forming ability of this group is lower. Metals of the group B form films, but the change of potential in this case is much smaller, i.e. 100-200 mv. The rest of the metals of the B groups (2-5) form weak protective films in nearly every case, and seldom show negative potential jumps exceeding 100 mv. Of course, the films will remain intact on the metals (or will form in the electrolyte) only if the electrolyte is of the proper kind. Thus, a good protective film on Al remains intact in solutions of NaCl, HCl and  $\text{HNO}_3$ , but dissolves in NaOH. Good protective films will form on Mg and Mn only in NaOH, but not in other solutions, etc. The difference in chemical behaviour between A group (or transition group), and B group metals was especially emphasised by Evans<sup>24</sup> on the basis of qualitative data; thus, his idea has been confirmed quantitatively in this study.

The potentials clearly depend on the  $pH$  of the solution only in the case of Sb and Bi. The metals of each group respond similarly to rubbing in spite of the difference in the absolute values of their electrode potentials (cp. e.g. Be and Mg, Cr and Mo, Zn, Cd, Hg). The initial electrode potentials (before rubbing) of the A group and transition metals are more positive, while those of the B group metals are more negative than the equilibrium values.

The potentials of a number of metals of A group and intermediate metals remain unchanged, or are even somewhat "ennobled" upon rubbing, especially in  $\text{HNO}_3$  solutions. This anomalous behaviour may be due to the following reasons: (a) the film forms so rapidly that we cannot prepare a surface free of film even for a short time; (b) the corrosion process is controlled completely, or almost completely, by the cathode reaction; (c) stirring, during rubbing, greatly reduces cathodic polarisation when the process is controlled both by the anode and cathode reactions.

The following assumption can be made as to the nature of the electrode potentials of the metals investigated. Metals of A groups and intermediate metals in most of the typical solutions form complex electrodes of the film-pore type, where the pore may act as an electrode of the first or the second type, in accordance with the solubility product of the compounds formed by the reaction of the metal and the solution.

The metals of group IB, in most cases, form a complex electrode of the film-pore type (electrode of the second type). The rest of the metals of the B group preferentially form simple electrodes of the first or second type. Films on these metals have been detected (by rubbing) only in a few cases and their effect is small.

\* The form of the Mendelèeff's table used in our discussion was proposed by Evans.<sup>24</sup>

<sup>24</sup> Evans, *Metallic Corrosion, Passivity and Protection* (1937), 352.

## PART II. ELECTRODE POTENTIALS OF SOLID SOLUTIONS.

(7) About 10 years ago we began our investigations on the electrode potentials of solid solutions. This work has proved extremely laborious and complicated. Before it was possible to co-ordinate the results into a theoretical scheme, as yet rather imperfect, it was necessary to pursue theoretical researches, which often had no direct connection with this work. At present, it is impossible to publish all our results, and we have decided to give only a short summary, together with the preliminary theoretical treatment of electrode potentials of solid solutions.

(8) Electrode potentials are mainly connected with the properties of metallic atoms and depend to a much less extent on the lattice. For instance, the potentials of solid zinc and fluid amalgams of zinc are known to be similar, although the amalgam has no definite lattice. Numerous metals are capable of forming solid solutions, at least up to a limiting solubility. Only the uniform distribution of atoms of a component among atoms of another one is of importance to us, and details of the crystallographic structure of solid solutions have no significance. The energy of formation of solid solutions is, however, of great importance. In this process more or less stable chemical bonds arise between different atoms, and thus the separation of atoms of a solid solution requires some additional energy. The rate of diffusion of metals in solid solutions is small at room temperatures. The composition in the surface layer, changing under the influence of an electrolyte, cannot quickly restore itself on account of the slow diffusion of atoms from the body of the alloy and therefore the electrode potentials of solid solutions belong to the group of irreversible potentials.

(9) In considering the problem of electrode potentials and its dependence on composition, it is important to know what part of the surface of an alloy is occupied by each kind of atom entering into solid solution. Therefore the composition must be expressed in % by volume. Knowing the composition as % by weight it is possible to express it by means of the following approximate formula :

$$V_A = \frac{100 P_A \delta_B}{\delta_B P_A + \delta_A (100 - P_A)}$$

where

$V_A$  is % by volume of the component A,  
 $P_A$  is % by weight of the component A,  
 $\delta_A$  is density of the component A,  
 $\delta_B$  is density of the component B.

In studying the electrode potential-composition diagram of a solid solution, it is essential to isolate the individual factors. It has been impossible as yet to separate all the factors; but the role of such a significant one, as a protective film, can be made clear, if electrode potentials

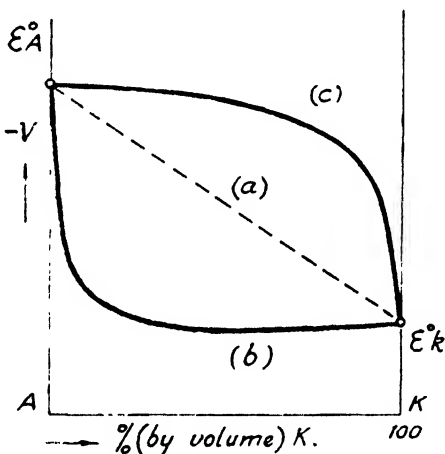


FIG. 3.—Potential change of a solid solution on account of polarisation.

are measured, not only by the usual method, but also during continuous rubbing of the metal surface by a carborundum pin immersed in the solution, when the protective film effect is minimised. The comparison of electrode potentials measured with and without rubbing gives data concerning the role of the protective film.

(10) If the role of impurities is not significant, it is natural to suppose that the anodic processes take place mainly upon the atoms of the anodic component of the solid solution, and the cathodic processes upon the atoms of the cathodic component. Neglecting numerous complicating factors, the potentials of solid solutions would be expressed on the composition-diagrams by a straight line (*a*) connecting the potentials of the pure components (Fig. 3).

Let  $\epsilon_u$  be the potential of a solid solution, then

$$\epsilon_u = \frac{\epsilon_A F_A + \epsilon_K F_K}{F_A + F_K}$$

where

$\epsilon_A$  is the potential of the anodic component and

$F_A$  is its area;

$\epsilon_K$  is the potential of the cathodic component and

$F_K$  is its area.

In an alloy,  $F_A + F_K = I$

$$\epsilon_u = \epsilon_A F_A + \epsilon_K (I - F_A) = \epsilon_K - (\epsilon_K - \epsilon_A) F_A.$$

(11) In studying the potentials of solid solutions, however, it is necessary to consider the influence of a series of complicating circumstances, which can entirely change the expected relations. Let us consider briefly the influence of the most important of these.

**Polarisation.**—In formation of a solid solution, the properties of each component will be changed because of the deformation of atoms due to interaction between atoms of different kinds. Therefore, the polarisation characteristics (both anodic and cathodic) of each component can be changed. This can also be brought about by the presence of ions of one or both components of the solid solution in the electrolyte. No matter what the true polarisation characteristics of components in the solid solution are,

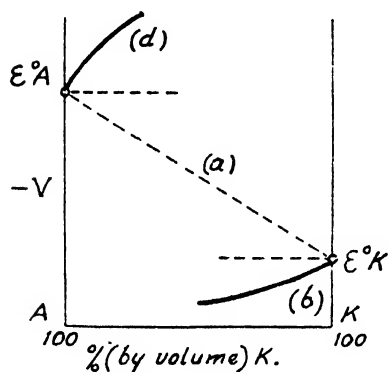


FIG. 4 —An abnormal potential change of a solid solution with conversion of electrochemical properties of components.

the polarisation of one of the components of the solid solution can be far more important than that of the other. If the anodic polarisation predominates for a given series of solid solutions, then the potentials of the solid solutions will be displaced from the straight line (*a*) to the positive region of curve (*b*), Fig. 3; but if the cathodic polarisation predominates, then on the contrary, the potentials will be more electro-negative (curve (*c*), Fig. 3). Clearly the polarisation cannot bring the potential of the solid solution beyond the limits of potentials of its components.

The potentials of the components can also be altered by the *deformation of atoms* in a solid solution, since this may be considered to be another expression of the energy change involved in solid solution formation. Such extreme cases are also possible when an alteration of the electrode potentials leads to the "inversion" of the electrochemical properties of the components of a solid solution, i.e. the cathodic component, introduced into the solid solution, will really behave itself as an anodic one

## THE FARADAY SOCIETY

The following papers have been accepted for publication. (This list does not include papers presented at General Discussions.)

<i>Author(s).</i>	<i>Title.</i>	<i>Date Received.</i>
1. Schwab, G. M.	Crystallite Orientation in Coating Films. Parts III and IV.	18 6 46
2. Strickland-Constable, R. F.	The Interaction of Carbon Filaments at High Temperatures with Nitrous Oxide, Carbon Dioxide and Water Vapour.	4 9 46
3. Booth, A. D.	Distribution Functions and Crystalline Materials.	12 8 46
4. Gilbert, G. A., and Marriott, J. V. R.	Starch-Iodine Complexes. Part I.	23 10 46
5. Richards, R. E.	The Force Constants of some OH and NH Links.	12 8 46
6. Clark, N. O., and Blackman, M.	The Degree of Dispersion of the Gas Phase in Foam.	28 3 46
7. Clark, N. O., and Blackman, M.	The Transmission of Light through Foam.	28 3 46
8. Clark, N. O.	The Electrical Conductivity of Foam.	28 3 46
9. Ogston, A. G., Holiday, E. R., Philpot, J. St. L., and Stocken, L. A.	The Replacement Reactions of $\beta$ - $\beta'$ -dichlorodiethyl Sulphide and of some Analogues in Aqueous Solution: the isolation of $\beta$ -chloro- $\beta'$ -hydroxy diethyl sulphide.	20 9 46
10. Raynor, G. V., and Hume- Rothery, W.	Primary Solid Solution in the System Aluminium Magnesium-Zinc.	7 8 46
11. Raynor, G. V.	The Constitution of the Magnesium Indium Alloys in the Region 20 to 50 atomic % of Indium.	7 8 46
12. Cowley, J. M.	Electron Diffraction by Fatty Acid Layers on Metal Surfaces.	3 10 46
13. Cowley, J. M., and Symonds, J. L.	Electron Diffraction and Rectification from Silicon and Pyrite Surfaces.	3 10 46
14. Stokes, R. H.	A Thermodynamic Study of Bivalent Metal Halides in Aqueous Solution. Part XVI.	11 11 46
15. Abel, E., and Fanto, J. M.	Thermodynamics of the Conversion $KCl \rightarrow K_2SO_4$ with the aid of $CaSO_4$	4 3 46
16. Moffitt, W. E., and Coulson, C. A.	The Free Radicals $CH_2(CH)_n-1CH_3$	21 10 46
17. Bockris, J. O'M., and Egan, H.	The Salting-Out Effect and Dielectric Constant.	9 10 46
18. Lauder, I. M.	Some Notes on the Gilfillan-Polanyi Micropyknometer.	7 10 46
19. Gregg, S. J., and Maggs, F. A. P.	Detection of Changes of State in Films Adsorbed at the Gas-Solid Interface.	9 9 46

<i>Author(s).</i>	<i>Title.</i>	<i>Date Received.</i>
20. Evans, A. G., and Warhurst, E.	An investigation of the Chemical Equilibria involving the Molecules Arsenic Trichloride, Monophenyl-chlorarsine, Diphenyl-chlorarsine and Triphenylarsine.	19 8 46
21. Price, W. C., and Sugden, T. M.	The Ionisation Potentials of Poly-atomic Molecules. I.	23 7 46
22. Sugden, T. M., and Price, W. C.	The Ionisation Potentials of H <sub>2</sub> O and H <sub>2</sub> S. II.	23 7 46
23. Melville, H. W., and Watson, W. H.	A Refractometric Method for following Reactions in Closed Systems.	3 10 46
24. Whittingham, G.	The Oxidation of Sulphur Dioxide in Slow Combustion Processes.	5 12 46
25. Gordon, M.	Reaction Kinetics of Adiabatic Systems.	15 11 46
26. Aten, A. H. W., Jnr., and van Drever, J.	A simple Apparatus for the Measurement of Diffusion Rates.	27 11 46
27. Tompkins, F. C.	The Thermal Decomposition of Silver Oxalate.	14 1 47
28. Weber, G.	Quenching of Fluorescence by Complex Formation. Estimation of the Mean Life of the Complex.	8 7 46
29. Blackman, M.	On the transformation of "solid" Foam to a "fluid" Foam under Shear.	31 12 46
30. Mackenzie, H. A. E., and Winter, E. R. S.	Kinetic Studies in the Solvent Acetic Acid and Acetic Anhydride. Parts I, II, III.	4 3 47
31. Eley, D. D.	The Absolute Rate of Conversion of Parahydrogen by Metallic Catalysts.	28 1 47
32. Epton, S. R.	A new Method for the Rapid Titrimetric Analysis of Sodium Alkyl Sulphates and Related Compounds.	29 1 47
33. Bosworth, R. C. L.	An Interpretation of the Viscosity of Liquids.	14 3 47
34. Fröhlich, H.	General Theory of the Static Dielectric Constant.	14 2 47
35. Stokes, R. H.	A Thermodynamic Study of Bivalent Metal Halides in Aqueous Solution. Part XVII: Revision of data for all 2 : 1 and 1 : 2 Electrolytes at 25°, and Discussion of Results.	11 3 47
36. Hirshberg, Y.	The Absorption Spectra of Phenylated Anthracene.	19 2 47
37. Wood, A. M., Crank, J., and Twigg, G. H.	The Application of the Differential Analyser to a Problem in Chemical Kinetics.	4 3 47
38. Birse, E. A. B., and Roberts, J. K.	The Action and Design of Mechanical Filters for Dust and Smoke.	12 11 46
39. Ramsay, D. A.	Infra-Red Absorption Spectrum and Structure.	5 3 47
40. Gage, J. C.	A Cell for the Measurement of Diffusion in Aqueous Solutions.	18 4 47
41. Randles, J. E. B.	A Cathode Ray Polarograph. Parts I and II.	12 11 46
42. Bremner, J. G. M., and Thomas, G. D.	The Free Energies of Formation of Gaseous Organic Compounds.	7 2 47

<i>Author(s).</i>	<i>Title.</i>	<i>Date. Received.</i>
43. Lloyd, D. Jordan- (the late), and Garrod, M.	A Contribution to the Theory of the Structure of Protein Fibres, with special reference to the so-called "Thermal Shrinkage" of the Collagen Fibre.	6 1 47
44. Balson, E. W., and Adam, N. K.	Studies in Vapour Pressure Measurement. Part IV: The total Vapour Pressure of a Mixture of Sulphur Trioxide and Chlor-sulphonic Acid.	11 4 47
45. Birch, A. J., and MacDonald, D. K. C.	Some Physical Properties of Solidified Sodium-Ammonia Solutions.	10 3 47
46. Makinson, K. R.	On the Cause of the Frictional Difference of the Wool Fibre.	16 12 46
47. Winsor, P. A.	Solubilisation and Related Emulsification Processes. Parts I-VIII.	13 1 47 12 5 47
48. Booth, A. D.	A new "averaging" method for the location of Atomic Positions from X-ray data.	11 2 47
49. Buchanan, A. S., and Heymann, E.	Notes on the Electrokinetic Potential of Cellulose and on Electrokinetic Equations.	10 3 47
50. Hirst, W.	The Mechanical Interaction between Mobile Insoluble Adsorbed Films, Capillary Condensed Liquid, and Fine Structured Solids.	19 3 47
51. Barrer, R. M.	Rate Constants of "Unimolecular" Reactions.	25 3 47
52. Frost, W. E., and Linnett, J. W.	The Mechanism of Spark Ignition. Parts II and III.	21 4 47
53. Hickling, A., and Taylor, D.	The Anodic Behaviour of Metals. Part V—Copper.	28 5 47
54. Bremner, J. G. M., and Thomas, G. D.	The Calculation of Resonance Energies from Thermal Data.	13 6 47
55. Andrew, E. R., Axford, D. W. E., and Sugden, T. M.	The Measurement of Ionisation in a Transient Flame.	12 6 47
56. Prigogine, I.	Surface Tension of a Regular Solution.	11 7 47
57. Jellinek, H. H.	On the Degradation of Long-Chain Molecules. Part II.	28 11 44
58. MacEwan, D. M. C.	Complexes of Clays with Organic Compounds. Part I. Complex Formation between Montmorillonite and Halloysite and Certain Organic Liquids.	14 11 46
59. Mackenzie, R. C.	Complexes of Clays with Organic Compounds. Part II. Investigation of the Ethylene Glycol-Water-Montmorillonite System using the Karl Fischer Reagent.	14 11 46
60. Denbigh, K. G., Hicks, Margaret, and Page, F. M.	The Kinetics of Open Reaction Systems.	13 3 47
61. Bennett, J. G., and Griffith, R. O.	The Photo-Reaction between Iodine and Hydrogen Peroxide in Aqueous Solution.	11 3 47*
62. Baughan, E. C.	The Absorption of Organic Vapours by thin Films of Polystyrene. as amended	28 3 47 1 6 47



## THE FARADAY SOCIETY

<i>Author(s).</i>	<i>Title.</i>	<i>Date Received.</i>
63. Stokland, K.	The Thermal Decomposition of Disilane and Trisilane.	2 4 47
64. Gold, V.	The Hydrolysis of Acetic Anhydride.	19 6 47
65. Bockris, J. O'M. and Ignatowicz, S.	Studies in Electrolytic Polarisation. Part IV.	2 7 47
66. Gregg, S. J., and Jacobs, J.	An Examination of the Adsorption Theory of Brunauer, Emmett, and Teller, and Brunauer, Deming, as revised	19 2 47
	Deming and Teller.	9 7 47
67. Carman, P. C.	Molecular Distillation and Sublimation.	24 1 47
68. Heath, D. F., and Linnett, J. W.	Molecular Force Fields. Part I: The Structure of the Water Molecule. Part II: The Force Field of the Tetrahalides of the Group IV Elements.	11 4 47
69. Sherratt, S., and Linnett, J. W.	The Determination of Flame Speeds in Gaseous Mixtures.	21 8 47
70. Powles, J. G., and Jackson, Willis.	Measurement of Absorption in Liquids at 1.2 cm. and 0.8 cm. wavelength using a waveguide absorption cell operating in the $H_{01}$ Mode.	27 3 47
71. Morton, C.	A Feedback Potentiometer for the Measurement of $pH$ values and oxidation-reduction potentials.	18 8 47
72. Jackson, S., and Hinshelwood, C. N.	Penetration of Proflavine into Bacterial Cells.	25 6 47
73. Jackson, S., and Hinshelwood, C. N.	The Training of Bacteria to New Carbon Sources <i>Bact. Lactis Aerogenes</i> and <i>d</i> -Arabinose.	18 6 47
74. Ives, D. J. G., and Pittman, R. W.	An amplifier for use with Conductance Bridges.	23 7 47

and *vice versa*. Then the curves, expressing the relationship between the electrode potential and composition of a solid solution, will have an abnormal slope as shown in Fig. 4. The addition of the cathodic component will result in some displacement of the potential in a negative direction (*d*), and the addition of the anodic component will cause, on the contrary, some displacement of the potential in the positive direction (*b*).

**Change of Protective Film Properties.**—The introduction of atoms of one of the components into a solid solution can change the properties of the film. Thus, the protective properties of the film of a solid solution can be higher or lower than those of the films which exist upon the metals themselves, and electrode potentials can be more positive or negative respectively. These changes can, in the extreme cases, bring the potential of the solid solution beyond the limits of the potentials of its components.

**Removal of the anodic component atoms** from the surface of a solid solution, leading to excess of the cathodic component, can occur even in the first stages of reaction with the electrolyte. If the anodic com-

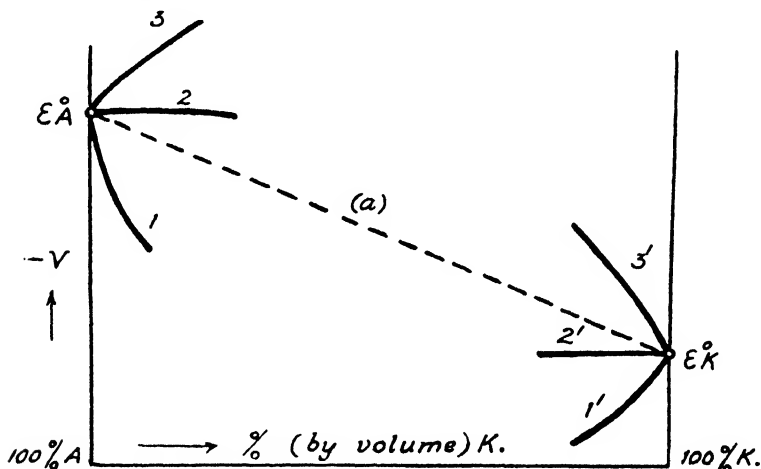


FIG. 5.—The principal types of relationship between the electrode potential of a solid solution and its composition, and principal factors defining the character of the curve.

ponent atoms have been *completely* removed, even from a very thin surface layer, and if the rate of diffusion is insufficient to move a considerable quantity of atoms of the anodic component to the surface of metal, then the electrode potential of the alloy will be equal to that of the cathodic component.

Thus, this factor can bring the potential of a solid solution to that of the cathodic component.

**Secondary Precipitation of the Cathodic Component.**—In the decomposition of a solid solution with a high content of anodic component, both components can pass into solution since the passage of the anodic component atoms into the solution results in the destruction of all the elementary crystallographic units of the solid solution. In this case, if the atoms of the anodic component pass into the solution electrochemically, then the atoms of the cathodic component will pass into the electrolyte mechanically, i.e. as fragments of lattice of the alloy. However, the ions of the cathodic component can reprecipitate from the solution on the cathodic areas (at the minimum value of overvoltage for deposition of the metal in question) forming a deposit. In this case, an increase of the cathodic component surface will shift the potential of a

## 688 IRREVERSIBLE ELECTRODE POTENTIALS OF METALS

solid solution in the direction of positive values. This factor, in an extreme case—which is hardly possible in practice—can also bring the potential of a solid solution to the potential of its cathodic component.

Thus, the potential of a solid solution is defined by many factors, which are interrelated in a complex manner and it is impossible at present to predict the value of its potential from that of its components.

THE TABLE TO FIG. 5.

No.	The most Probable Factors, Defining the Character of the Curve; Potential of a Solid Solution-composition.	Type of Curve.					
		1.	2.	3.	1'.	2'.	3'.
1	Prevailing polarisation of the anodic component of a solid solution . (+)	●			●	●	
2	Prevailing polarisation of the cathodic component of a solid solution . (—)		●	●			●
3	Improvement of the protective properties of a film by introducing atoms of another component into solid solution . (+)	●			●	●	
4	Deterioration of the protective properties of a film by introducing atoms of another component into the solid solution (—)		●	●			●
5	Conversion of the electrochemical properties of the anodic component (+)				●		
6	Conversion of the electrochemical properties of the cathodic component (—)		●	●			
7	Removal of the anodic component atoms from the surface by the action of an electrolyte . . . (+)					●	
8	The secondary precipitation of the cathodic component . . (+)	●					
9	The energy of formation of the solid formation . . . (+)	●			●	●	

NOTE.—The sign (+) means that the factor makes the potential value higher and the sign (—), lower.

Possible cases of the changes of potential of a solid solution with composition are shown in Fig. 5. In the Table accompanying the diagram, the factors which define separately or severally the character of the curve, are shown for each type. All the factors, designated by the sign (+) might, it would seem, be significant for any more positive curve, and those designated by the sign (—) for more negative one as compared with the middle straight line (*a*). This, however, is not so. For the curve of the first type, the factor (5), i.e. a conversion of the electrochemical properties, and the factor (7), i.e. the removal of the anodic component atoms from the surface of an alloy, cannot play any significant role if the curve of this type refers to solid solutions with an excess of the anodic component. The curve of the second type can be related to all factors depressing the potential of a solid solution. For the curve of the third type, all three factors can be significant, but the factor (2) will be certainly of a minor importance, as it is not capable of bringing the potential of a solid solution beyond

the value  $\epsilon_A^\circ$ . Similarly, for the curve of the type 1', the polarisation, i.e. the first factor, cannot be of a paramount importance as it cannot make the potential of a solid solution more positive than that of the cathodic component  $\epsilon_K^\circ$ . The influence of the factors 7 and 8 is also doubtful, since the removal of the anodic component atoms and the secondary precipitation of the cathodic component can bring the potential only to the value  $\epsilon_K^\circ$ . The type 2' is defined by two principal factors—namely, the removal of the atoms of the anodic component (factor (7)) and the excess polarisation of the anodic component (factor (1)).

The other factors, making the potentials of a solid solution higher, are apparently of minor importance. It is obvious that the factor (6), i.e. the "inversion" of the electrochemical properties, cannot be important in the "normal" type 3'.

(12) In all these considerations, we have supposed that the impurities (both in the anodic and in the cathodic components) which pass into the solid solution, do not influence materially the potential. In some instances, however, we have to take this influence into account as well. The polarisation diagram for the initial component A is shown in Fig. 6 (continuous line), where it is clear that the cathodic impurities cause a significant anodic polarisation of the component A, and the potential is displaced from the point  $\epsilon_A^\circ$  to the point  $\epsilon_A'$  in the more positive region. Let us now suppose that the addition of the cathodic component causes a sharp weakening of the effect of the cathodic impurities, e.g. by the formation of intermetallic compounds with these impurities and thereby causing a much increased overvoltage. This weakening will cause a decrease of anodic polarisation. If, at the same time, the cathodic component K of a solid solution is strongly polarised in the solid solution then the potential can become more negative. ( $\epsilon_A'$ : dotted lines.) Thus, the addition of the cathodic component will make the solid solution less noble with a simultaneous decrease of the rate of corrosion (displacement from  $J'' \text{ max.}$  to  $J'' \text{ max.}$ ).

This is thus another explanation of the abnormal character of the curve of the third type, in addition to that deduced from the behaviour of anodic and cathodic components of the solid solution. Similarly, the introduction of the component A into the solid solution can produce the abnormal curve (type  $J''$ ), if the added component largely increases the anodic polarisation of the component K or decreases the cathodic polarisation of the impurities. It must be noted that the first of these abnormal displacements of the potential of a solid solution to the negative region by the addition of the cathodic component (type 3), may be also explained by a decrease of the anodic polarisation, provided, however, that an increase of the corrosion rate (i.e. an increase of corrosion current  $J'' \text{ max.}$ ) takes place. Such cases can be treated more rigorously by using the theory of *poly-electrode systems*.<sup>25</sup>

(13) In our laboratory, the electrode potentials of the following solid solutions were examined: (a) Al with Cu, Zn, Mg, Li, Si; (b) Zn with Al,

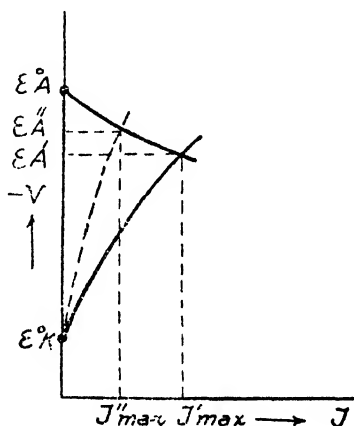


FIG. 6.—The explanation of the abnormal type of the potential-composition curve (3) on the ground of the polarising action of impurities.

<sup>25</sup> Akimov, *Advances in Chemistry* (in Russ.), 1943, 12, 374.

## 690 IRREVERSIBLE ELECTRODE POTENTIALS OF METALS

Cu, Ag, Au; (c) Mg with Al, Zn, Cd, Tl, Sn, Pb; (d) Cu with Al, Zn, Ni, Mn, Ag, Be, Cd, Sn.

The measurements were performed in 3 % NaCl, 0.1 N. HCl, 0.1 N. HNO<sub>3</sub>, 0.1 N. NaOH, and sometimes in N. solutions of the electronegative component of the alloy in question. The solid solutions were prepared from pure metals where available. To obtain a homogeneous solution, every alloy was heated for 240 hr. in sealed glass tubes, which were evacuated or filled with argon at temperatures below the solidus curve, and quenched in water. The degree of homogeneity of the solid solution was

TABLE II.—PRINCIPAL TYPES SHOWING RELATIONSHIP BETWEEN THE ELECTRODE POTENTIAL AND COMPOSITION (FIG. 7).

The systems measured with rubbing are parenthesised.

The Electrolyte in which the Measurements were made.				
3 % NaCl.	0.1 N. HCl.	0.1 N. HNO <sub>3</sub> .	0.1 N. NaOH.	Others.
<b>Type 1.</b>				
(Al—Zn)	(Al—Zn)	(Al—Si) <sup>1</sup>	(Al—Zn)	(Mg—Sn) in the N. Mg—Sn MgSO <sub>4</sub> sol.
(Al—Cu)	(Al—Cu)	(Al—Zn) <sup>2</sup>	(Al—Zn)	
Al—Cu	(Al—Si)	(Al—Cu)	Al—Mg	
			(Al—Cu)	
(Mg—Sn)	Al—Si	Al—Cu	Al—Cu	Ni—Cu in the NiSO <sub>4</sub> solution
(Mg—Al)	Al—Cu	(Mg—Tl)	(Mg—Sn) <sup>3</sup>	
Mg—Sn <sup>2</sup>	(Mg—Cd)	Mg—Tl	Mg—Al	Cu—Au in the CuSO <sub>4</sub> solution
	Mg—Cd	(Mg—Sn) <sup>4</sup>	(Zn—Au)	Al—Cu in the Cu(OH) <sub>2</sub> solution
	(Mg—Zn)	Mg—Sn <sup>3</sup>	Zn—Au <sup>2</sup>	Mn—Fe in the 0.1 M. MnSO <sub>4</sub> solution
	Mg—Zn	(Mg—Zn)		
	Mg—Sn	Mg—Zn		
	(Zn—Au)			
	Zn—Au <sup>3</sup>	(Mg—Cd)		
	(Zn—Cu) <sup>3</sup>	Mg—Cd		
	Zn—Cu <sup>3</sup>	(Zn—Au) <sup>4</sup>		
	(Cu—Ni)	Zn—Au <sup>4</sup>		
		(Zn—Ag)		
		Zn—Ag		
		(Zn—Cu)		
		Zn—Cu		
<b>Type 2.</b>				
Al—Si	Zn—Al	Zn—Al	(Mg—Tl)	Zn—Au in the M. ZnSO <sub>4</sub> solution
Mg—Cd	(Zn—Ag)	(Cu—Ag)	(Mg—Cd)	Mg—Sn in the M. MgSO <sub>4</sub> solution
Mg—Al <sup>5</sup>	Zn—Ag	Cu—Ag	(Zn—Cu)	Pb—Bi in the PbCl <sub>2</sub> solution
Zn—Al	Cu—Ag		Zn—Cu	Mg—Cd <sup>6</sup> in the MgSO <sub>4</sub> solution
Zn—Cu	(Cu—Ag)		(Zn—Ag)	Sn—Sb in the N. H <sub>2</sub> SO <sub>4</sub> solution
(Zn—Cu)			Zn—Ag	
Zn—Ag			(Cu—Ag)	
(Zn—Ag)			Cu—Ag	
Zn—Au				
(Zn—Au)				
(Cu—Ag)				
Cu—Ag				
<b>Type 3.</b>				
(Mg—Tl)	(Mg—Tl)	(Mg—Al)	(Mg—Zn)	Mg—Tl in the N. MgSO <sub>4</sub> solution
Mg—Tl	Mg—Tl	Mg—Al		
(Mg—Cd)	(Mg—Al) <sup>7</sup>			
(Mg—Zn)	Mg—Al <sup>7</sup>			

TABLE II.—PRINCIPAL TYPES SHOWING RELATIONSHIP BETWEEN THE ELECTRODE POTENTIAL AND COMPOSITION (FIG. 7).—(continued).

The systems measured with rubbing are parenthesised.

The Electrolyte in which the Measurements were made.				
3 % NaCl.	0.1 N. HCl.	0.1 N. HNO <sub>3</sub> .	0.1 N. NaOH.	Others.
<b>Type 1'.</b>				
(Al—Mg)	(Al—Li) (Al—Mg) (Cu—Sn) Cu—Ni	(Al—Li) (Al—Mg) Cu—Cd	(Al—Mg) (Cu—Al) (Cu—Mn)	
<b>Type 2'.</b>				
(Al—Li) (Zn—Al) (Cu—Zn) <sup>o</sup> (Cu—Mn) <sup>o</sup> (Cu—Al) Cu—Ni <sup>1</sup> (Cu—Ni) <sup>1</sup> (Cu—Be) Cu—Be (Cu—Sn) Cu—Mn  Cu—Al Cu—Zn Cu—Sn  Cu—Cd	Al—Mg <sup>o</sup> Al—Li (Zn—Al) (Cu—Zn) (Cu—Mn) <sup>o</sup> (Cu—Al) <sup>o</sup> Cu—Al <sup>o</sup> Cu—Zn Cu—Sn  Cu—Cd Cu—Be <sup>o</sup> Cu—Mn <sup>o</sup>  Cu—Be <sup>o</sup> (Cu—Cd) <sup>o</sup> Cu—Mn <sup>o</sup>  Cu—Cd Cu—Be <sup>o</sup> Cu—Mn <sup>o</sup>  Cu—Cd	Al—Li <sup>o</sup> Al—Zn (Zn—Al) (Cu—Al) (Cu—Zn) (Cu—Ni) (Cu—Mn)  (Cu—Sn) Cu—Cd Cu—Be  (Cu—Be) <sup>o</sup> Cu—Zn Cu—Mn  Cu—Ni Cu—Sn  Cu—Ni Cu—Sn	(Al—Li) Al—Li (Zn—Al) Zn—Al (Cu—Be) (Cu—Ni) <sup>o</sup> (Cu—Sn)  (Cu—Cd) Cu—Be  Cu—Ni <sup>o</sup> Cu—Al <sup>o</sup> Cu—Mn Cu—Zn (Cu—Zn) Cu—Cd	Ag—Zn in the 0.1 N. ZnSO <sub>4</sub> solution Fe—Zn in the 0.05 N. ZnSO <sub>4</sub> solution Ag—Al in the Cu(OH) <sub>2</sub> solution Pd—Cu in the CuSO <sub>4</sub> solution Pd—Ag in the Ag—NO <sub>3</sub> solution  Cu—Ni in the NiSO <sub>4</sub> solution Au—Cu in the CuSO <sub>4</sub> ; Cu(NO <sub>3</sub> ) <sub>2</sub> solutions  Pb—Pb in the Pb(NO <sub>3</sub> ) <sub>2</sub> solution Pb—Sn in the N. KOH solution Cu—Al in the Cu(OH) <sub>2</sub> solution Cu—Sn in the M. H <sub>2</sub> SO <sub>4</sub> solution
<b>Type 3'.</b>				
Al—Zn Al—Mg Al—Li <sup>o</sup>	Al—Zn (Cu—Be) <sup>o</sup> (Cu—Cd)	Al—Mg <sup>2</sup>	Cu—Sn	Au—Zn in the M. ZnSO <sub>4</sub> solution Cd—Mg in the MgSO <sub>4</sub> solution Ag—Cd in the M. CdSO <sub>4</sub> solution Fe—Mn in the M. MnSO <sub>4</sub> solution

followed by microscopic and sometimes X-ray examinations. The potentials were measured both during rubbing of the test-pieces under the solution and without rubbing. The turbulence of the solution, which is produced near the test-piece during rubbing, was taken into account and

Approximately follows the middle straight line (a).

Close to the straight line (a).

<sup>o</sup>Maximum at the beginning.

<sup>1</sup>Not sharply marked minimum.

<sup>2</sup>The curve with maximum.

<sup>3</sup>The curve intersects the straight line (a).

<sup>o</sup>The curve with minimum.

<sup>1</sup>Slight slope downwards.

<sup>2</sup>The curve with slight slope.

special experiments were made in order to differentiate between these two factors (rubbing and turbulence).

Systems measured during rubbing are enclosed in brackets. The measurements were repeated from 3 to 10 times for every alloy. Since all the alloys were prepared in the same laboratory and were tested under similar conditions and by similar methods, comparable data can be expected. These can be compared with the few reliable data of previous investigations.<sup>6</sup>

All the experimental data obtained by us cannot be given here. Therefore we shall restrict ourselves to the summarised results and certain characteristic examples. In Table II, all the systems investigated are classified according to the principal types shown in Fig. 5. From these data it is possible to draw a number of important conclusions. Firstly, all six principal types appear to occur, though the frequency of occurrence

of each is quite different. For solid solutions with excess of anodic component, the first type (where there is the normal increase of potential) occurs most frequently, i.e. in more than 60 % of all systems investigated. The second type (where there is an insignificant change of potential on addition of the cathodic component to the anodic base of solid solution) occurs in only about 25 % of all cases. Lastly, the third type (the abnormal increase of the potential value on addition of the cathodic component) occurs in only about 12 %. It must be noted that the third type is confined to a series of magnesium base solid solutions. For solid solutions with excess cathodic component, the type 2' (retaining the potential of the cathodic component) seems to occur most frequently, i.e. in about 80 % of all the cases investigated. This indicates the significance of one factor in this group of solid solutions, namely, the removal of the anodic component atoms from the surface by an electrolyte. The normal type 3' (the potential drop with addition of the anodic component) occurs in this group relatively seldom (viz. about 10 %). The type 1' (abnormal increase of potential with addition of anodic component to the solid solution) occurs also in about 10 %. It is interesting to note, that contrary

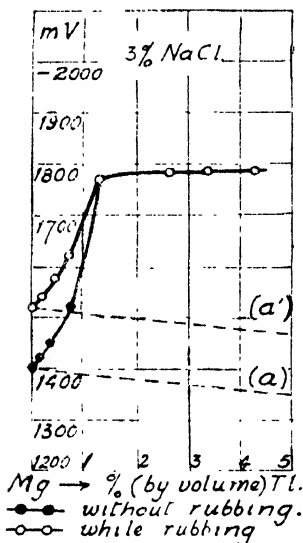


FIG. 7. Electrode potentials of solid solutions Mg—Tl in the 3 % NaCl solution.  $\epsilon_{\text{Tl}}$  without rubbing—440 mv.;  $\epsilon_{\text{Tl}}$  while rubbing—500 mv.

to expectation, only the potentials measured while rubbing (when the role of the protective film is minimised) belong to this type. The experimental data also show in many cases a more complicated relationship, e.g. curves with maximum and minimum, and curves intersecting the middle line (a). In very few the curve (potential-composition) coincides or closely approaches the middle curve (a).

(14) The examination of Table II shows that in general the type of a curve is defined by the solid solution. However, there are instances showing the importance of the electrolyte; in these, the type to which a system of solid solutions belongs, can be altered by change of electrolyte, e.g. the system Mg—Tl in 3 % NaCl, 0.1 N. HCl and 1 N.  $\text{MgSO}_4$  solutions is of the third type (Fig. 7), in 0.1 N. NaOH solution, of the second type and in the 0.1 N.  $\text{NH}_4\text{NO}_3$  solution of the first type. The system (Cu—Sn) belongs to type 2' when rubbed in 3 % NaCl, 0.1 N.  $\text{HNO}_3$  and 0.1 N. NaOH solutions and to the type 1' in the 0.1 N. HCl solution.

Another example of the effect of the electrolyte composition is shown in Fig. 8. Here the results of the measurements of the potentials of the

solid solutions of the system Mg—Cd (with rubbing and without it) are plotted. In the 3 % NaCl solution, either an almost horizontal curve (without rubbing) is observed, or a curve with a maximum (abnormal type, 3); in the 0.1 N. HCl solution, the presence of 4.5 % by volume of Cd in solid solution leads to an increase of potential by 300-400 mv. (whether with rubbing or without it). An unusually sharp and large increase of potential of 700-800 mv. is observed in the 0.1 N.  $\text{HNO}_3$  solution. The system does not show any noticeable alteration of potential (while rubbing) with increase of Cd content in 0.1 N. NaOH solution.

The role of a protective film often appears to be significant, e.g. the system Al—Mg in 3 % NaCl, 0.1 N. HCl and 0.1 N.  $\text{HNO}_3$  solutions belongs

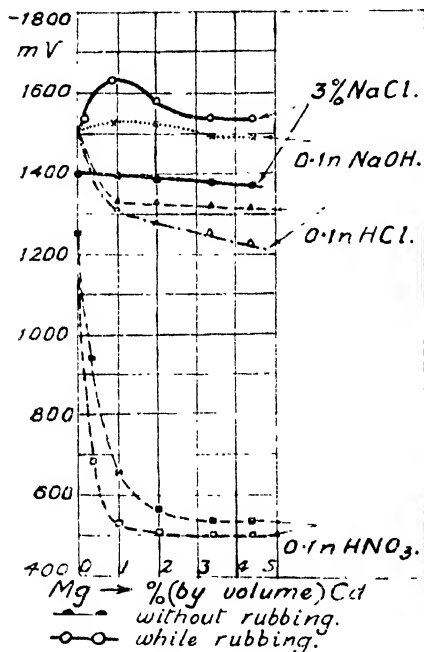


FIG. 8.—Electrode potentials of the Mg—Cd solid solutions in different media.

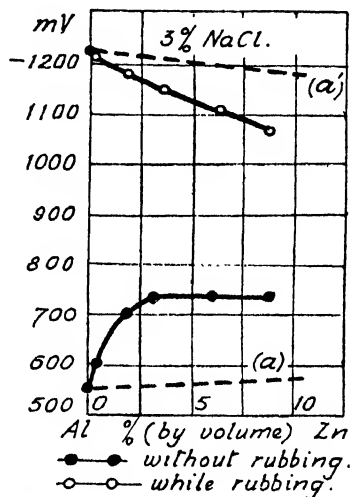


FIG. 9.—Electrode potentials of the solid solutions Al—Zn in 3 % NaCl solution.  $\epsilon_{\text{Zn}}^{\circ}$  without rubbing—760 mv.;  $\epsilon_{\text{Zn}}^{\circ}$  while rubbing—820 mv.

to the type 2' or 3', while the same system with rubbing belongs to the type 1'.

Rubbing materially changes the electrode potentials of the components themselves, and with metals belonging to group A and transition metals (Fig. 2), the measurements with rubbing and without it are, as a matter of fact, of quite different systems. Fig. 9 shows the results of the potential measurements of the Al—Zn solid solutions in 3 % NaCl. When measurements are made without rubbing,  $\epsilon_{\text{Al}}^{\circ} = -550$  mv. and  $\epsilon_{\text{Zn}}^{\circ} = -760$  mv., i.e.  $\epsilon_{\text{Al}}^{\circ} > \epsilon_{\text{Zn}}^{\circ}$ , and these solid solutions belong to the group with excess cathodic component. The experimental data show that the curve for the alloy Al—Zn (without rubbing) sharply differs from the straight line (a) connecting  $\epsilon_{\text{Al}}^{\circ}$  and  $\epsilon_{\text{Zn}}^{\circ}$  and rises from the beginning rather abruptly to the negative side. Thus this system belongs to the normal type 3'. The measurements with rubbing show that the potential of aluminium is more negative (= 1220 mv.) but that of zinc drops much less, namely to -820 mv. Thus here ( $\epsilon_{\text{Zn}}^{\circ}$ ) > ( $\epsilon_{\text{Al}}^{\circ}$ ), and



# 694 IRREVERSIBLE ELECTRODE POTENTIALS OF METALS

the system now belongs to the group of solid solutions with excess anodic component. The curve for (Al—Zn) belongs to the normal type 1.

The system Cu—Sn in 0.1 N. NaOH solution belongs to type 3' (Fig.

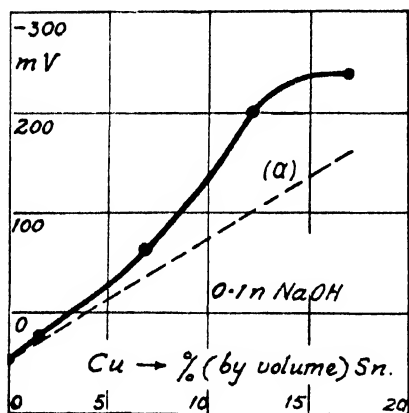


FIG. 10.—Electrode potentials of the Cu—Sn solid solutions in 0.1 N. NaOH solution (without rubbing).

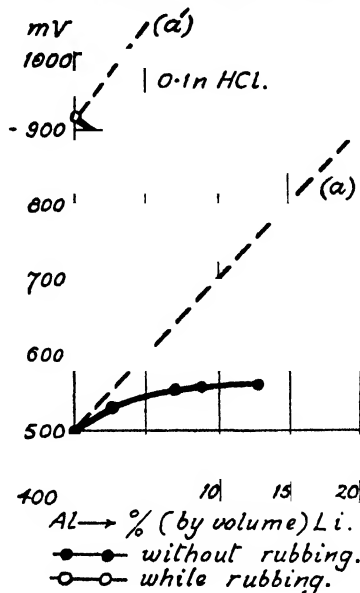


FIG. 11.—Electrode potentials of the Al—Li solid solutions in the 0.1 N. HCl solution.

10), but, during rubbing, to type 2'. The role of a film is less significant for solid solutions of Mg and Zn since rubbing does not influence materially the potential of pure Mg and Zn themselves in most electrolytes.

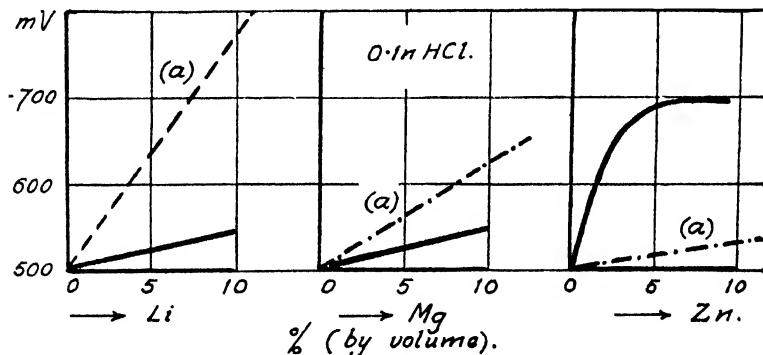


FIG. 12.—Electrode potentials of the solid solutions Al—Li, Al—Mg and Al—Zn (without rubbing).

1 per cent. (by volume) of Li.  
2 per cent. (by volume) of Mg.  
3 per cent. (by volume) of Zn.

A remarkable case of the system Al—Li is shown in Fig. 11. In spite of the exceedingly negative potential of lithium (— 3000 mv.) and of the absence of films on it—owing to the easy solubility of LiOH in water—the entrance of Li into solid solution with Al either makes the electrode

potential less noble (without rubbing) or increases the potential value (with rubbing). These data show that the abnormal behaviour of Al—Li alloys cannot be explained by changes in properties of the protective film. Alteration of the electrochemical properties of lithium in the solid solution with aluminium probably takes place here.

When comparing the influence of different components upon the potential of solid solution, even in the same, or closely related types, no *correspondence* between the potential of the component and the effect produced by it is observed. The influence (without rubbing) of the three components, Li, Mg and Zn, upon the potential of the corresponding solid solution with aluminium is shown in Fig. 12. It will be seen that the greatest displacement of potential to the negative region is caused by Zn and the least by Li, i.e. in the opposite direction of the electrode potentials of these metals. We have much less data concerning those systems where a

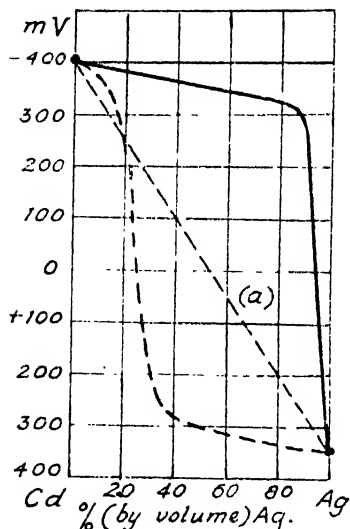


FIG. 13.—Electrode potentials of the Cd—Ag solid solutions in the N.  $\text{CdSO}_4$  solution.

— initial values.  
 --- final values.

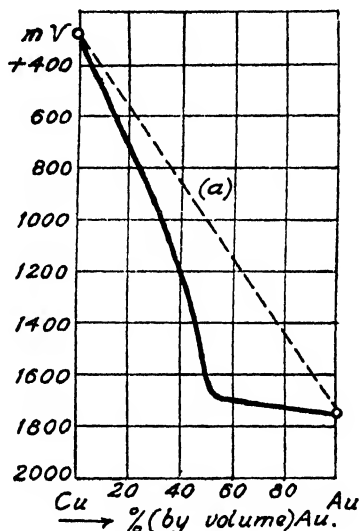


FIG. 14.—Electrode potentials of the Cu—Au solid solutions in the N.  $\text{CuSO}_4$  solution.

continuous series of uniform solid solutions is formed. The electrode potentials of solid solutions of Cd—Ag in N.  $\text{CdSO}_4$  are illustrated in Fig. 13. The continuous curve, corresponding to initial values, shows that the addition of silver to cadmium gradually shifts the potential to the positive region. The addition of cadmium to silver, on the contrary, rapidly diminishes the potential of the alloy. Such a curve may be explained by the excess polarisation of the cathodic component of the solid solution. Later, however, the curve is sharply displaced to the region of the positive value and its character is considerably changed. This is shown in the diagram by the dotted line. The removal of the anodic component atoms from the surface of the alloys by the solution, seems to be the most probable explanation of the phenomenon.

The electrode potential curve for the system Cu—Au is illustrated in Fig. 14. The whole curve is much more positive than the straight line (a) and, moreover, it has a sharp inflection. The shape of the curve again corresponds to excessive polarisation of the anodic component or to removal of the atoms of anodic component. Similar curves are observed

## 696 IRREVERSIBLE ELECTRODE POTENTIALS OF METALS

for a series of other continuous solid solutions of electropositive metals. It must be noted that the inflection of the curve is often (but not always) situated in the neighbourhood of 50 % (by volume), e.g. for the system Cu—Pd in  $\text{CuSO}_4$  53-58 % (by volume); for the system Ag—Pd in  $\text{AgNO}_3$  49 % (by volume); for the system Cu—Au in  $\text{CuSO}_4$  50 % (by volume); for the system Cd—Ag in  $\text{CdSO}_4$  45 % (by volume).

### Summary.

(1) A method of measurement of electrode potential of metals and alloys during the rubbing of the surface of a test-piece under a solution was developed. The comparison of the potentials obtained, without rubbing and while rubbing, permits conclusions to be made about the tendency of a metal to form a protective film.

(2) The electrode potentials of 22 metals—Be, Mg, Al, Si, Nb, Cr, Mo, Mn, Fe, Co, Ni, Cu, Ag, Au, Zn, Cd, Hg, Tl, Sn, Pb, Sb, Bi—were measured in the 0.1 N. HCl, 0.1 N.  $\text{HNO}_3$ , 0.1 N. NaOH and 3 % NaCl solutions. The measurements were performed both while rubbing the surface of test-pieces under the solution, and without rubbing.

(3) From the results for pure metals it is concluded that :

(a) the greatest tendency to form a protective film is observed in metals belonging to group A, less in metals of the transition group and least, but appreciable, in metals of IB-group. The metals of other B groups show little tendency.

(b) the behaviour of metals of the same group of Mendelëff's table as regards alteration in electrode potential caused by rubbing of the surface under solution (mechanical activation) is similar, being independent of the electrode potential value.

(4) Some suggestions are made about the nature of irreversible potentials of pure metals and solid solutions.

(5) The electrode potentials of the following 23 systems : Al with Cu, Zn, Mg, Li, Si ; Zn with Al, Cu, Ag, Au ; Mg with Al, Zn, Cd, Tl, Sn, Pb ; Cu with Al, Zn, Ni, Mn, Ag, Be, Cd, Sn were measured. The measurements were performed in the 0.1 N. HCl, 0.1 N.  $\text{HNO}_3$ , 0.1 N. NaOH and 3 % NaCl solutions by the usual and by newly developed methods.

(6) The results of the electrode potentials of solid solutions have been classified into groups according to the relationship between the potential of a solid solution and its composition.

Beside the normal relationship between the electrode potential and the composition of the solid solution (decrease of the potential with introduction of the anodic component and increase with introduction of the cathodic component, both anomalous cases occur, namely, potential drop with the addition of the cathodic component (the type 3) and increase of potential with the addition of the anodic component (type 1'). The anomalous case (1') cannot be explained solely in terms of the protective film, since it was also observed when the metal surface was rubbed under the solution, i.e. when the role of a film was minimised.

(7) There is no correspondence between the potential of the component and its effect on the potential of the solid solution.

(8) The typical group—relating potential and composition—to which a given system of alloys belongs is defined principally by the nature of (a) the components and their interaction, (b) the solution and (c) the protective film.

### Résumé.

Pour étudier la tendance d'une électrode à former un film protecteur, on a développé une méthode de mesure des potentiels d'électrodes, avec frottement de la surface d'essai sous des solutions. Des mesures ont été faites pour 22 métaux et 23 alliages avec des solutions décimales de HCl,  $\text{HNO}_3$  et NaOH et une solution à 3 % de NaCl. La tendance à former un film protecteur décroît lorsqu'on passe du groupe A au groupe de transition et enfin aux groupes B des métaux de la classification périodique. Les potentiels d'électrodes de solutions solides de métaux ont été classés d'après la relation entre potentiel et composition de l'alliage ; le groups type est défini principalement par (1) les composants et leur interaction, (2) la solution et (3) le film protecteur.

### Zusammenfassung.

Eine Methode für die Messung der Elektrodenpotentiale von 22 Metallen und 23 Legierungen während das untersuchte Stück unter Lösungen von 0.1 norm.

HCl, 0.1 norm. HNO<sub>3</sub>, 0.1 norm. NaOH und 3 % NaCl gerieben wird, ist entwickelt worden, um die Neigung der Elektrode, einen Schutzfilm zu bilden, zu untersuchen. Diese Tendenz fällt, wenn man von den Metallen der A-Gruppe des Periodischen Systems zu den Übergangsmetallen und dann zu den B-Gruppen-Metallen geht. Die Elektrodenpotentiale von festen Lösungen sind in Gruppen geordnet worden, je nach der Beziehung zwischen den Potential und der Zusammensetzung der Legierung. Die typische Gruppe, der ein Legierungssystem angehört, wird hauptsächlich durch (a) die Komponenten und ihre Aufeinanderwirkung, (b) die Lösung und (c) den Schutzfilm bestimmt.

*Laboratory of Physics of Metals,  
All Union Institute for Aircraft Materials,  
U.S.S.R.,  
Moscow, U.S.S.R.*

## THE DECOMPOSITION OF HYDROGEN AND DEUTERIUM IODIDES.

BY N. F. H. BRIGHT AND R. P. HAGERTY.

(Communicated by Prof. W. E. GARNER.)

Received 27th May, 1946.

The absolute rates of reaction of hydrogen and deuterium with halogens have been calculated by Wheeler, Topley and Eyring<sup>1</sup> by the statistical mechanical method, and assuming 20 % coulomb energy for the chemical bond, they obtain activation energies in approximate agreement with the experimental values where these are available. On the basis of their model for the transition state, they have calculated that the zero-point energies for the transition states of HI and DI are higher than for the initial states, being 7.8 cal. for HI and 5.56 cal. for DI as compared with 6.5 and 4.7 cal. respectively for the initial states. Assuming these data and that the activation energy at the absolute zero for HI and DI is  $E_0 = 35,500$ , they find that the velocity of combination for  $D_2 + I_2$  should be slower than for  $H_2 + I_2$  by the ratio 2.6, 2.34, 2.26 at the three temperatures 575, 700, 781° K. respectively.

The classical researches of Bodenstein<sup>2</sup> provide experimental data for  $H_2 + I_2$  over a wide range of temperatures, which have been confirmed by other workers, but until recently there were very incomplete data for  $D_2 + I_2$ . The present research was therefore undertaken in 1935 in order to fill this gap, with a view to deriving the zero-point energies for the transition state.

Since the commencement of the research, a number of papers have been published on this problem. Rittenberg and Urey<sup>3</sup> have determined the velocities of decomposition and equilibrium constants for HI and mixtures of HI and DI, and their values for HI are in agreement with those of Bodenstein and those for the mixed iodides are in agreement with those calculated from spectroscopic data. Blagg and Murphy<sup>4</sup> have also derived the equilibrium constants from spectroscopic data using a value for the energy at the absolute zero from Bodenstein's and Rittenberg and Urey's results. The theoretical curve obtained when  $\log K$  is plotted against  $1/T$  possesses a slight curvature and fits the experimental values fairly well over the middle range of temperatures, but Bodenstein's,

<sup>1</sup> Wheeler, Topley and Eyring, *J. Chem. Physics*, 1936, 4, 178.

<sup>2</sup> Bodenstein, *Z. physik. Chem.*, 1899, 29, 295.

<sup>3</sup> Rittenberg and Urey, *J. Chem. Physics*, 1933, 1, 137; *J. Amer. Chem. Soc.*, 1934, 56, 1885.

<sup>4</sup> Blagg and Murphy, *J. Chem. Physics*, 1936, 4, 631.

and Rittenberg and Urey's values at the lower and the highest temperatures lie somewhat below this curve. Blagg and Murphy, and Taylor and Crist<sup>5</sup> have investigated experimentally the velocity and equilibrium constants for both iodides. The equilibrium constants are in agreement with the theoretical calculations of Murphy after adjustment of the energy at the absolute zero, but are in marked disagreement with those of Bodenstein for the decomposition of HI, especially at the highest temperatures. The velocity constants are similar to those of earlier workers.

Taylor and Crist's experimental ratio for the velocity of combination of hydrogen and deuterium with iodine is 1.97 at 700° K., which is considerably lower than the theoretical calculations of Wheeler, Topley and Eyring at this temperature.

The velocity of the decomposition of HI and DI has usually been followed by analysis of the products after chilling the reaction. Geib and Lendle,<sup>6</sup> however, measured the velocities by an absorption-photometric method which has been applied successfully in other cases. They used white light, which was open to the objection that for wavelengths shorter than 5,000 Å., there are changes in the mean extinction coefficient due to broadening of the lines by pressure effects, and also to the disadvantage that photochemical reactions are possible under the action of such wavelengths. A continuous method of measurement of the reaction rates, which obviates errors due to chilling of the reaction and is most sensitive in the initial stages of the reaction has, however, many advantages and it was considered to be worth while repeating Geib and Lendle's method, using light from the red end of the spectrum. A method of recording the rate of production of iodine from HI and DI has therefore been developed, using light of wavelengths greater than 5,800 Å.

### Experimental.

An absorption-photometric method, similar in principle to that used by Geib and Lendle, has been developed, and shown to give satisfactory results at gas pressures in the neighbourhood of 10-20 cm. This method consists in following the rate of production of iodine, in a silica cell with optically flat windows, by measuring the absorption of light of wavelengths greater than 5,800 Å. Since there was the possibility that the absorption spectrum of iodine was affected by foreign molecules, the method was checked by chemical analyses of the gaseous products at equilibrium, where the quantities of iodine produced were sufficiently great for the application of the usual analytical methods.

**Preparation of Gases.**—Deuterium was obtained by the electrolysis of heavy water of purity 99.6 to 99.95 % by the electrolytic method of Norling,<sup>7</sup> and as a matter of convenience, hydrogen was also prepared by the same method using low conductivity water free from gases. The iodides were prepared in dark chambers by passing the hydrogen or deuterium, together with iodine, over red-hot platinum filaments and through a trap surrounded by CO<sub>2</sub>-methylated spirits to remove excess of iodine and then into a vessel at liquid air temperature to condense the iodide (see Fig. 1 for outline of apparatus). The hydrogen or deuterium was re-circulated by means of an automatic Sprengel pump. The iodides were stored in a large bulb attached to a U-tube which could be cooled to liquid air temperatures when required. The iodides were pure white in colour and on analysis showed a negligible content of iodine.

**Reaction Vessel and Standard Tube.**—This consisted of a silica tube 20 cm. long, with an internal diameter of 1.5 cm. and with walls 1 mm. thick; the end plates were of optically-true clear silica and a side tube

<sup>5</sup> Taylor and Crist, *J. Amer. Chem. Soc.*, 1941, **65**, 1377.

<sup>6</sup> Geib and Lendle, *Z. physik. Chem. B*, 1936, **32**, 463.

<sup>7</sup> Norling, *Physik. Z.*, 1935, **36**, 711.

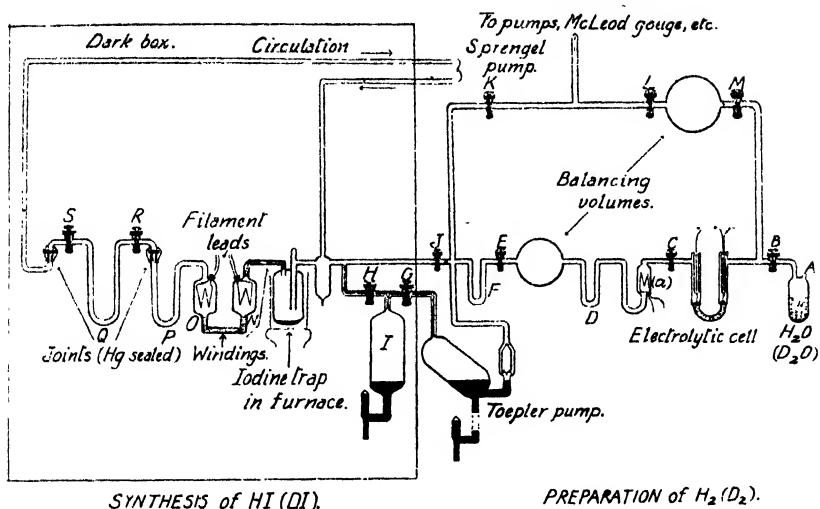


FIG. 1.

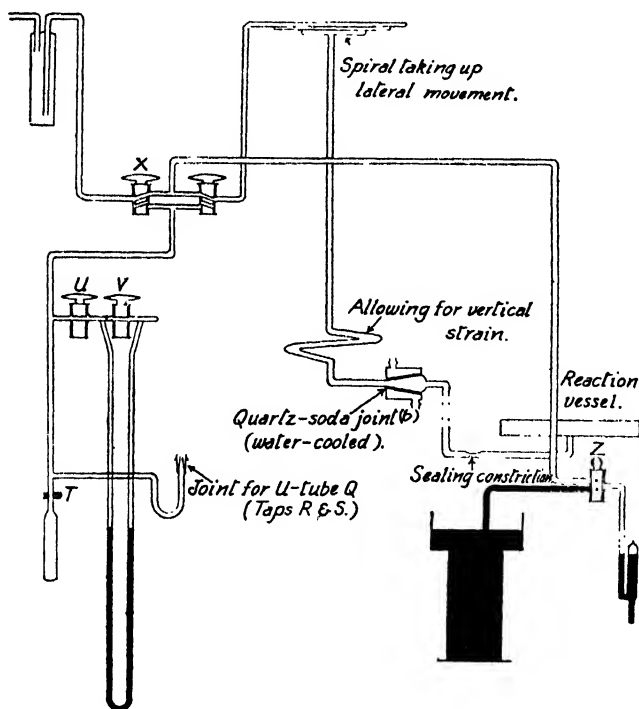


FIG. 2.

of a few mm. bore served to introduce the gases (see Fig. 2). The reaction vessel was mounted in a cradle of Hadfield's special heat-resisting steel in an electric furnace. Just outside the furnace the side tube was constricted to a capillary. The quartz tube was connected with the reservoir of iodide and to a manometer through a water-cooled quartz-glass ground

joint. Two flat glass tube spirals were included in the gas line to facilitate movement of the reaction tube and furnace during the measurements of absorption of light. An evacuated standard silica tube with similar dimensions to that of the reaction tube was arranged parallel to the reaction vessel in the furnace. A bulb containing resublimed iodine was attached to the standard tube and any desired pressure of iodine could be obtained by immersing the bulb in a constant temperature bath.

**Furnace and Thermocouple.**—A cylindrical steel furnace, of 5 cm. internal diameter and of the same steel as the cradle was used. It had three separate windings of Nichrome wire, two of which were designed to warm the ends of the furnace. It was possible to adjust the current in the three coils so as to obtain a temperature constant to  $\pm 0.5^\circ \text{C.}$  along the length of the furnace in which the reaction tube lay. The temperature was measured by a thermocouple which was calibrated against the boiling point of water and the setting points of tin, zinc and cadmium. These were repeated on a number of occasions during the research. The furnace was mounted on a rigid steel table on two lateral benches which

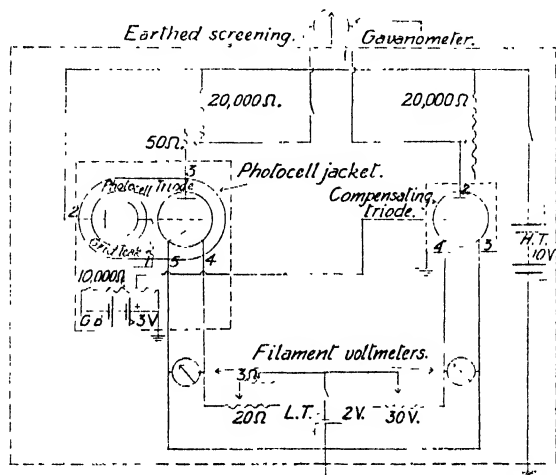


FIG. 3.

permitted a travel of some 3 cm. between fixed stops at right angles to the light beam. This enabled the reaction vessel or the standard iodine tube to be brought into position in the light beam at will.

**Optical System.**—The optical system and furnace were housed in a dark box and the reaction vessel was filled from the storage bulb placed in another dark box. The light from a 500 w. projection lamp, with its planar filament normal to the line of the optical bench, was passed through a pinhole and through Wratten No. 23A orange-coloured filter. The lamp was run on an accumulator battery and the lamp housing was water cooled and blacked on the inside. The light then passed through an iris diaphragm and collimating lens and a parallel beam passed down the reaction tube without grazing the sides, on to a photocell.

The photocell was an Osram K.M.V. 6, which had good sensitivity for the red end of the spectrum and the E.M.F. from it was amplified with a triode electrometer valve, using a Moll galvanometer for measurement of change in the radiation falling on the photocell. The maximum deflection of the Moll galvanometer on illuminating the photocell was adjusted to 35-40 cm. by modifying the size of the iris, which was then left unchanged throughout the research. The ratio of the transmissions through the evacuated reaction vessel and standard cell was measured

and also the ratio  $I/I_0$  was obtained for various pressures of iodine in the standard tube, the furnace being heated to a selected temperature. In the course of the measurements, readings were taken alternately through the standard tube and the clean dry reaction vessel, in order to note any change in the transmission of light or in the sensitivity of the photocell. This procedure was also followed during the measurement of the rates of reaction. The sensitivity of the photocell varied only 1-2 % over long intervals of time. The circuit used with the photocell is shown in Fig. 3. The values of  $I/I_0$  for four temperatures are given in Fig. 4.

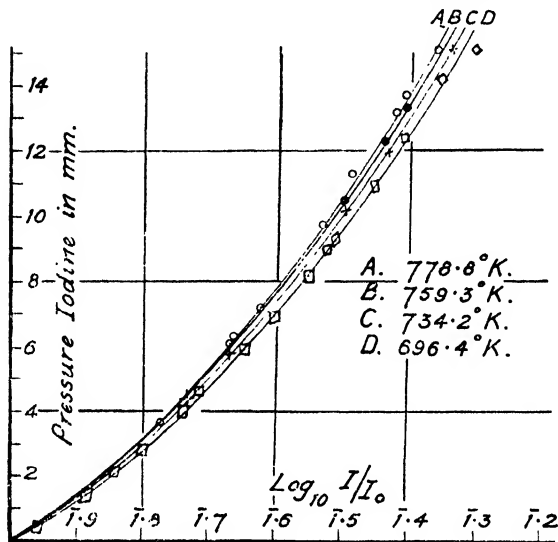


FIG. 4.

### Measurement of Reaction Velocity.

The reaction tube and standard tube were set up in the furnace and the former fused on to the line leading to the iodide supply (Fig. 2). The reaction tube, heated to the temperature selected for an experiment, was continuously evacuated overnight. This method of degassing the tube was found to give similar results to pretreatment with hydrogen at 780°, or higher. Unless one of these processes was used, abnormally rapid initial rates of reaction were obtained, which were possibly due to adsorbed oxygen. Before admitting the HI or DI, the zero ratio of the transmission of the two tubes was read on the photocell circuit. The gas was admitted from a U-tube cooled to about  $-70^{\circ}\text{C.}$ , the temperature of which was read with a pentane thermometer, and its vapour pressure in the reaction vessel was measured on a mercury manometer opened to the gas for as short a time as possible. A period of from 4-6 min. was allowed for the gas to stream through the constriction in the silica tube leading into the reaction vessel. The constriction was then sealed off with a fine oxyacetylene blowpipe. The amount of decomposition occurring during sealing off could be reduced by practice to small dimensions. A correction for the duration of the filling process and for the small amount of decomposition during sealing off was made in the calculation of reaction rate (see later).

During the decomposition, readings of  $I$  and  $I_0$  were taken at appropriate intervals of time and when  $I/I_0$  became constant, the reaction vessel was removed from its cradle and quenched in cold water, an operation which took 5 sec. to complete. A typical curve is shown in Fig. 5, which shows the method of correcting for zero errors.



**Analytical Estimation.**—The free and total iodine were estimated. The constriction of the silica tube was broken under gas-free distilled water and the gases being under less than atmospheric pressure the water entered the tube and the iodide and some iodine dissolved. A nipple on the reaction tube was then broken and the contents of the reaction tube blown out into a 50 cc. flask. Some iodine crystals remained in the tube, which was washed out with water and finally with aqueous KI solution, the latter being kept and titrated separately. The free iodine was titrated with N./100 thiosulphate, freshly prepared and standardised against dichromate. The iodate method for the estimation of HI was found to be inaccurate at the concentrations available, since the iodate-iodide reaction was too slow. A method was worked out based on the oxidation of the iodide with  $\text{H}_2\text{O}_2$ , and the extraction of iodine from the aqueous layer with  $\text{CCl}_4$ . The aqueous solution of iodine and HI in the 50 cc. flask was divided into two equal portions and to one portion was added

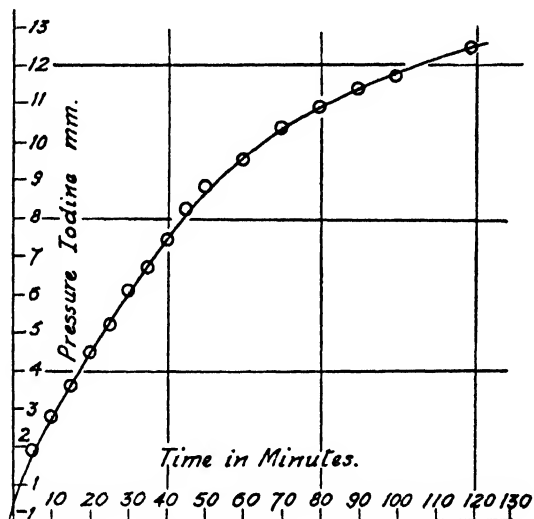


Fig. 5.

3 cc.  $\text{H}_2\text{O}_2$  (20 vol.) and 25 cc.  $\text{CCl}_4$ . The latter was shaken violently in a stoppered bottle and left to stand for a few hours. Three titrations were carried out. The KI washings of the reaction tube were estimated with thiosulphate, using fresh starch, and the untouched portion of the aqueous washings titrated similarly. 20 cc. of the  $\text{CCl}_4$  layer were removed from the second aqueous portion and titrated with thiosulphate after adding some KI to facilitate extraction of iodine from the  $\text{CCl}_4$ . The distribution coefficient of the iodine between the aqueous solution and the  $\text{CCl}_4$  layer was determined. The volume of the reaction vessel was measured by weighing empty and full of water. These analyses were carried out as a check on the iodine at equilibrium as measured by the absorption method and on the total iodine introduced into the reaction vessel. The results are given in Tables I to IV.

## Results.

### Hydrogen Iodide.

The furnace temperature was kept within  $\pm 0.5^\circ$  during a run and results were obtained for the average temperatures  $696.4$  and  $778.8^\circ \text{K}$ . The initial pressure of the iodide was measured in three ways: (a) from the

vapour pressure curves of HI quoted in the International Critical Tables (b) by manometric measurement, and (c) by analysis of the total iodine in the reaction vessel at the end of the experiment. They usually agreed within 1-2 %. The iodine pressure at the end of the run was derived from the photometric curve and was also obtained by direct analysis. The photometer reading was used in the calculations of the rates of reaction and equilibrium constants, and a typical run is given in Fig. 5.

The values for the velocity constants were calculated from the Bodenstein equation,

$$k = \frac{X}{0.8686(1 - X)at} \log_{10} \frac{X - x(2X - 1)}{X - x},$$

where  $X$  is the fractional decomposition at equilibrium,  $x$  is the fractional decomposition at a time  $t$  and  $a$  is the initial iodide concentration in g. mol./cc. The values of  $k$  were calculated from the pressure-time curves over equal decomposition intervals and were constant within  $\pm 2$  % over about 4/5 of the curve for any individual run and the variation was usually considerably less. Individual values estimated near equilibrium were, however, ignored.

TABLE I.

No. of Exptl. Run.	Temp. of Decomposition °K.	Initial Pressure of HI mm. of Hg.			Equilibrium Press. of I <sub>2</sub> mm. of Hg.	
		V.P. Data.*	Manometer.	Analysis.	Photometer.	Analysis.
1	694.0	415.0	350†	‡	§	‡
2	698.4	92.5	92	‡	9.48	‡
3	699.5	96.0	96	‡	10.69	‡
4	693.0	126.5	127.5	125.1	13.40	12.96
5	693.7	118.4	118	116.8	12.64	--
6	698.2	135.6	134	130.6	14.60	13.37
7	779.8	127.4	125	127.3	15.22	15.85
8	774.3	123.0	129	124.9	15.22	15.40
9	774.5	110.4	112	110.5	12.90	13.18

\* The pressures in this column were calculated from the vapour pressure-temperature relations for HI quoted in the International Critical Tables: -

$$\text{Solid HI } (-97^{\circ} \text{ to } -51^{\circ} \text{ C.): } \log_{10} p = \frac{-0.05223 \times 24,160}{T} + 8.259.$$

$$\text{Liquid HI } (-50^{\circ} \text{ to } -34^{\circ} \text{ C.): } \log_{10} p = \frac{-0.05223 \times 21,580}{T} + 7.630.$$

† There was insufficient HI in the storage bulb to set up the equilibrium vapour pressure, corresponding to the bath temperature, throughout the filling system and reaction vessel.

‡ In this experimental run, the equilibrium pressure of iodine was outside the range of measurement of the photometer unit.

§ In some of the earlier runs, the analytical figures were regarded as unreliable, the analytical technique not having been satisfactorily worked out. Also on occasions, no analysis was done, owing to the reaction vessel having been broken upon removal from the furnace.

The agreement between the various values of the pressures of the iodide and iodine is regarded as satisfactory in view of errors in the temperature of the bath containing the solid iodide, the vapour pressure data, attack on the mercury of the manometer by the iodide, and errors in the method of analysis.

TABLE II.

No.	Mean Temp. °K.	$\log_{10} k$ .	$k$ (cc. mol. <sup>-1</sup> sec. <sup>-1</sup> ).	Mean $k$ ( $\log_{10} k$ ).	Bodenstein $k$ ( $\log_{10} k$ ).	X.		Mean X.	Bodenstein X.	HI $\log_{10} K$ .	Taylor and Crist $\log_{10} K$ .
						Photo- meter.	Anal- ysis.				
1	696.4	0.0311	1.07	1.05	0.976*	—	—	0.2126	0.2144	2.2606	2.2570 (inter- polated)
2	—	1.9960	0.99	(0.0224)	(1.9894)	0.2054	—	—	—	—	—
3	—	0.0298	1.07	—	—	0.2217	—	—	—	—	—
4	—	0.0231	1.05	—	—	0.2154	0.2083	—	—	—	—
5	—	0.0160	1.04	—	—	0.2152	—	—	—	—	—
6	—	0.0370	1.09	—	—	0.2173	0.2044	—	—	—	—
7	778.8	1.6019	40.0	37.2	36.1	0.2388	0.2487	0.2426	0.2400	2.4092	2.34 (extra- polated)
8	—	1.5430	34.9	(1.5706)	(1.5575)†	0.2452	0.2481	—	—	—	—
9	—	1.5657	36.8	—	—	0.2350	0.2401	—	—	—	—

† Taylor and Crist, 1.545—extrapolated value.

\* Taylor and Crist, 1.05.

The individual values of  $k$  and  $X$  given in Table II have been corrected from the experimental results

given in Table I to bring them to a common temperature. The corrections are small and have been deduced from the temperature coefficients of  $\log k$  and  $\log X$ . Good agreement is found with Bodenstein's values calculated from Kassel's equation,

$$\log_{10} k_{HI} = -\frac{5196}{T} + 16 \log_{10} T - 38.032$$

and the empirical expression of Bodenstein's results,

$$X = 0.13762 + 7.221 \times 10^{-5}T + 2.5764 \times 10^{-7}T^2. \quad (T \text{ in } ^\circ\text{C.})$$

Bodenstein's results for  $X$  have been confirmed by Rittenberg and Urey at 671° and 741° K. There is also good agreement with Taylor and Crist's data for the velocity of decomposition of hydrogen iodide (see Fig. 6) and with their data for the equilibrium constant for the lower

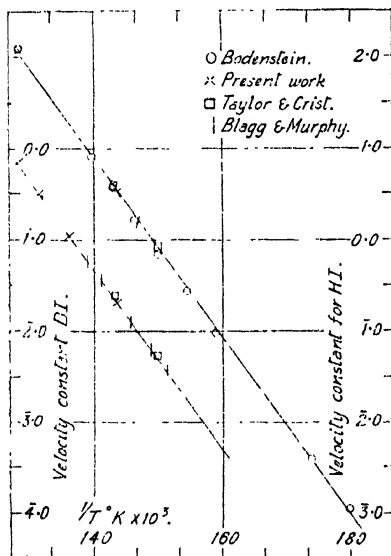


FIG. 6.

temperatures, but there is a serious discrepancy between the results for the higher temperatures as calculated from Blagg and Murphy's equation.

#### Deuterium Iodide.

The thermal decomposition was studied for the average temperatures 696.4, 734.2, 759.3 and 778.8° K. (see Tables III and IV).

The velocity and equilibrium constants are given in Table IV and compared with Blagg and Murphy's data for  $k_{DI}$  over their experimental range and with the data of Taylor and Crist for the equilibrium constant.

TABLE III.

No. of Exptl. Run.	Temp. of Decomposition °K.	Initial Pressure of DI mm. of Hg.			Equilibrium Press. of I <sub>2</sub> mm. of Hg.	
		V.P. Data.*	Manometer.	Analysis.	Photometer.	Analysis.
1	695.0	116.4	120	116.0	13.52	12.57
2	696.4	124.8	127	125.2	14.60	14.44
3	696.6	304.2	307	305.0	—	35.34
4	731.0	124.8	124	124.3	15.04	15.23
5	735.0	124.8	126	123.8	15.28	14.82
6	734.2	94.2	91	93.0	11.36	11.61
7	759.5	116.4	111	109.2	13.72	13.96
8	760.7	116.4	114	115.1	14.68	15.16
9	759.3	108.6	106	104.4	13.36	13.06
10	774.3	60.4	60	†	7.82	†
11	778.8	120.6	123	120.2	15.44	15.85
12	778.8	108.6	110	110.5	14.08	14.16
13	779.6	101.2	101	102.6	13.32	14.17

\* Calculated from the vapour pressure relations given by Bates, Halford and Anderson (*J. Chem. Physics*, 1935, 3, 419).

Solid deuterium iodide,  $\log_{10} p = 10.505 - 0.003107T - 0.377 \log_{10} T - 1406/T$ .

† Tube broken during removal from furnace.

There is a reasonable agreement between the present values for the rate of decomposition of deuterium iodide and those obtained by Blagg and Murphy and Taylor and Crist over the common range of temperature and all of the values for  $\log_{10} k$  against  $1/T$  fall on a reasonably straight line (Fig. 6). There are, however, more serious divergencies for the equilibrium constant in the higher temperature range.

TABLE IV

No.	Mean Temp. °K.	$\log_{10} k$ .	$k$ (cc. mol. <sup>-1</sup> sec. <sup>-1</sup> ).	Mean and ( $\log_{10} k$ ).	Blagg & Murphy $k$ ( $\log_{10} k$ ), Interpolated.	X.		Mean X.	DI $\log_{10} K$ .	Taylor and Crist $\log_{10} K$ .*
						Photo-meter.	Analysis.			
1	696.4	1.7964	0.626	0.639	0.657	0.2338	0.2173	0.2294	2.3456	2.3460
2	—	1.7988	0.629	(1.8056)	(1.8174)	0.2333	0.2307	—	—	—
3	—	1.8214	0.663	—	—	—	0.2317	—	—	—
4	734.2	0.5287	3.38	3.47	3.31	0.2432	0.2462	0.2450	2.4206	2.3935
5	—	0.5415	3.48	(0.5403)	(0.5194)	0.2467	0.2393	—	—	—
6	—	0.5505	3.55	—	—	0.2444	0.2490	—	—	—
7	759.3	1.0209	10.5	10.1	—	0.2513	0.2558	0.2551	—	2.4215
8	—	0.9860	9.7	(1.0045)	—	0.2547	0.2627	—	2.4672	—
9	—	1.0060	10.1	—	—	0.2561	0.2503	—	—	—
10	778.8	1.3477	22.3	22.9	—	0.2620	—	0.2611	2.4944	2.4435 (extrapolated)
11	—	1.3496	22.4	(1.3600)	—	0.2569	0.2630	—	—	—
12	—	1.3792	23.9	—	—	0.2548	0.2563	—	—	—
13	—	1.3629	23.1	—	—	0.2594	0.2760	—	—	—

\* By extrapolation and interpolation from experimental results.

### Discussion.

**Equilibrium Constants.**—The experimental values for the equilibrium constants for HI and DI fall into two groups. On the one hand there is

good agreement between the results of Bodenstein, Rittenberg and Urey and the present investigators, but these values are not in accord with those of Blagg and Murphy and Taylor and Crist, especially in the higher temperature range (cf. Tables II and IV). Bodenstein's values for the equilibrium constant for HI cover a wider range of temperatures than those of any other investigator, and the plot of  $\log K_{HI}$  against  $T$  shows a distinct curvature, which cannot be accounted for completely in terms of spectroscopic data. Attempts have been made to re-calculate his temperatures by Murphy,<sup>8</sup> in the hope of improving the situation, but without success. The theoretical curve of Blagg and Murphy can be fitted to Bodenstein's results within experimental error if some of the latter's measurements at low and high temperatures are ignored.

A wide variety of techniques has been used for following the reactions and for the analysis of the products and the agreement between the velocity constants obtained by the various investigators is an indication that the methods of analysis must be reasonably sound. The measurements of velocities of reaction have been obtained after relatively short reaction times and it may be that the discrepancies which have arisen are due to experimental errors which creep in when the times of measurement, as will happen with the attainment of equilibrium, are relatively long. These errors may be due to the diffusion of hydrogen and deuterium through the containing vessel or to reaction with oxygen or other contaminant on the walls. Taylor and Crist have evaluated those due to the diffusion of hydrogen and deuterium through quartz and shown them to be small. It has been customary to bake out the apparatus in high vacuum before an experimental run and hence water and oxygen might be regarded as completely removed. Kistiakowsky,<sup>9</sup> who carried out measurements with HI at pressures considerably higher than atmospheric, refers to the bursting of quartz tubes during his experiments, which indicates that some change is occurring in the quartz with time, and this may involve increase in porosity. If the discrepancies between different investigations at high temperatures are due to wall effects, then surrounding the reaction tube with hydrogen or deuterium may be an effective means of control. The present investigation was completed in 1939 before the results of Taylor and Crist were published, and there has been no opportunity to look into this matter further.

**Rate of Decomposition.**—The rate constants for the hydrogen iodide decomposition in the present investigation may be satisfactorily represented by the equation,

$$\log_{10} k_{HI} = -\frac{10030}{T} + 0.5 \log_{10} T + 13.001$$

which is also in agreement with Bodenstein's results. This gives an activation energy of 45.9 kcal./g. mol. A plot of  $\log_{10} k_{HI}$  is shown in Fig. 6, giving the present results, together with those by other workers.

The rate constants for deuterium iodide may be represented by the equation

$$\log_{10} k_{DI} = -\frac{10130}{T} + 0.5 \log_{10} T + 12.914.$$

This gives an activation energy of 46.4 kcal./g. mol.; the plot of  $\log_{10} k_{DI}$  is given in Fig. 6.

In view of the agreement between the experimental values of the velocity constants for the decomposition of HI and DI, it is not surprising that the ratio of the velocity constants is concordant, as is seen in Table V. The values of Geib and Lendle should perhaps be left out of account since their experimental method may be subject to experimental errors due to the use of white light for absorption measurements.

<sup>8</sup> Murphy, *J. Chem. Physics.*, 1936, 4, 344.

<sup>9</sup> Kistiakowsky, *J. Amer. Chem. Soc.*, 1928, 50, 2315.

TABLE V.

Author.	$\frac{k_{\text{HI}}}{k_{\text{DI}}}$		$\frac{k'_{\text{HI}}}{k'_{\text{DI}}}$	
	700° K.	781° K.	700° K.	781° K.
Wheeler, Topley and Eyring . . . . .	—	—	2.34	2.26
Geib and Lendle . . . . .	—	—	2.45	2.15
Blagg and Murphy . . . . .	1.53	—	1.88	—
Bright and Hagerty . . . . .	1.70	1.64	2.09	2.02
Taylor and Crist . . . . .	1.60	—	1.96	—
" " " . . . . .	—	—	1.93	—

It will be seen, therefore, that the theoretical calculations of Wheeler, Topley and Eyring give too high a ratio. The differences between the activation energy can be derived from

$$\frac{k_{\text{HI}}}{k_{\text{DI}}} = \sqrt{\frac{M_{\text{DI}}}{M_{\text{HI}}}} \cdot e^{-\frac{(E_{\text{HI}} - E_{\text{DI}})}{RT}}$$

assuming that the rates can be represented by the simple kinetic theory,  $E_{\text{DI}} - E_{\text{HI}} = 0.5$  kcal./g. mol. at 700° K. This difference is, however, of the same order as the errors in the estimation of the activation energies. The zero point energies (Z.P.E.) for the initial states of the reactions are  $2\text{HI} = 6.5$  kcal./g. mol. and  $2\text{DI} = 4.62$  kcal./g. mol. ( $\Delta = 1.88$  kcal.) and employing the above value of  $E_{\text{DI}} - E_{\text{HI}} = 0.50$  kcal./g. mol., Z.P.E. for  $(\text{H}_2\text{I}_2 - \text{D}_2\text{I}_2) = 1.40$ , which is considerably less than the calculated value, 2.22, of Wheeler, Topley and Eyring. In fact, the experimental data can be accounted for without assuming any differences between the Z.P.E.'s of HI and DI in the transition state, as was tacitly assumed in Urey and Rittenberg's calculation.

The authors wish to express their thanks to Professor W. E. Garner for his interest in this work.

### Summary.

(1) The rates of decomposition of HI and DI have been determined by an absorption-photometric method over the range of temperatures 696-779° K. The velocity constants are given by the equations

$$\log_{10} k_{\text{HI}} = -\frac{10030}{T} + 0.5 \log_{10} T + 13.001.$$

$$\log_{10} k_{\text{DI}} = -\frac{10150}{T} + 0.5 \log_{10} T + 12.914.$$

The experimental results for the velocity of reaction are in good agreement with Bodenstein's data for HI and those of later observers.

(2) The equilibrium constants have been measured over the same range of temperatures and agree with those of Bodenstein, and Rittenberg and Urey, but not with those of Taylor and Crist.

(3)  $\frac{k'_{\text{HI}}}{k'_{\text{DI}}}$  at 700° = 2.09, as compared with 2.34 predicted by Wheeler, Topley and Eyring from statistical mechanical considerations.

### Résumé.

(1) La décomposition de HI et DI a été étudiée par une méthode d'absorption photométrique dans le domaine de température 696-779° K. Les constantes de vitesse sont données par les équations :

$$\log_{10} k_{\text{HI}} = -\frac{10030}{T} + 0.5 \log_{10} T + 13.001$$

$$\log_{10} k_{DI} = -\frac{10150}{T} + 0.5 \log_{10} T + 12.914$$

Les résultats expérimentaux pour la vitesse de réaction sont en bon accord avec les valeurs de Bodenstein et celles des chercheurs ultérieurs pour HI.

(2) Les constantes d'équilibre ont été mesurées dans le même domaine de température et s'accordent avec celles de Bodenstein et celles de Rittenberg et Urey, mais pas avec celles de Taylor et Crist.

(3)  $k'_{HI}/k'_{DI}$  à  $700^\circ = 2.09$ , ce qu'on peut comparer à 2,34, chiffre déterminé par Wheeler, Topley et Eyring d'après des considérations de mécanique statistique.

### Zusammenfassung.

(1) Die Zerfallsgeschwindigkeiten von HJ und DJ sind mit Hilfe einer absorptionsphotometrischen Methode im Temperaturbereich  $696^\circ$ - $779^\circ$  K. gemessen worden. Die Geschwindigkeitskonstanten werden durch die Gleichungen

$$\log_{10} k_{HJ} = -\frac{10030}{T} + 0.5 \log_{10} T + 13.001$$

$$\log_{10} k_{DJ} = -\frac{10150}{T} + 0.5 \log_{10} T + 12.914$$

ausgedrückt. Die Versuchsergebnisse stimmen gut mit den Daten von Bodenstein für HJ und denen späterer Forscher überein.

(2) Die Gleichgewichtskonstanten sind im selben Temperaturbereich gemessen worden und stimmen mit denen von Bodenstein und von Rittenberg und Urey, aber nicht mit denen von Taylor und Crist überein.

(3) Bei  $700^\circ$ :  $k'_{HJ}/k'_{DJ} = 2.09$ ; der Wert 2.34 wurde von Wheeler, Topley und Eyring auf Grund statistisch-mechanischer Erwägungen vorausgesagt.

Department of Chemistry,  
The University,  
Bristol.

## THE THEORY OF RATE PROCESSES AND THE VISCOSITY OF LONG-CHAIN COMPOUNDS.

BY WILLIAM C. WAKE.

Received 3rd April, 1946.

### (1) Introduction.

The theory of viscous flow developed by Eyring *et al.*,<sup>1</sup> treats flow as the passage of the flow-unit from one equilibrium position to another, the vacant equilibrium positions being identified with holes in the liquid. This requires energy which can either be assumed to activate the flow-unit or to produce a hole of requisite size for the translation to occur. The formation of the hole, or of this intermediate activated state, then becomes the rate-determining process which can be treated by the theory of rate processes giving equation (1) for viscosity in which  $\Delta G^*$  is the Gibbs free energy of activation.

$$\eta = \frac{hN}{V} e^{-\frac{\Delta G^*}{RT}} \quad . \quad . \quad . \quad (1)$$

The molar volume ( $V$ ) is the only term with marked temperature dependence and this is negligible. It is, therefore, possible to obtain the heat of activation of the process ( $\Delta H_{vis}$ ) from the slope of the graph ( $\log \eta$  against  $1/T$ ),  $\Delta H_{vis}$  being related to  $\Delta G_{vis}$  by the Gibbs equation.

Eyring and his collaborators have considered several alternatives. If an unoccupied equilibrium position is identified with a hole in the mass

<sup>1</sup> Glasstone, Laidler and Eyring, *The Theory of Rate Processes* (New York, 1941), Ch. IX; Kauzmann and Eyring, *J. Amer. Chem. Soc.*, 1940, **62**, 313.

of the liquid, then it may be expected that fluidity will be related to the number of holes already available, and/or the energy required to form a hole of sufficient size. That fluidity is related to the number of holes available is shown by these authors to be in accord with Batschinsky's equation,<sup>2</sup> but the influence of these holes on the energetics of flow does not seem to have been considered. If holes exist in the structure of a stationary fluid, then these must be available for the flow process either directly or indirectly in the form of a reduction in the energy requirement. An attempt is made in this paper to allow for the effect of pre-existent holes on the energetics of the system proposed, and to calculate the sizes of the flow-units concerned.

## (2) Energy Required for the Formation of Holes.

It is assumed that the volume of holes in a g.mol. of liquid is given by the difference of molar volume of solid and liquid, the solid being regarded as a perfect solid. The molar volume of a solid normal hydrocarbon chain is given by Mark<sup>3</sup> as

$$V = 18.5 (1.27n + 1.83) \text{ \AA}^3. \quad (2)$$

where  $n$  is the number of carbon atoms in the chain, which becomes

$$V = 11.2 (1.27n + 1.83) \text{ cc./mol.} \quad (3)$$

TABLE I.— $\Delta E_{fus}$  calculated from  $\Delta E_{vap}$  and volume increase.

	Density of Solid at M. Pt.	M. Pt.	Density of Liquid at M. Pt.	$\Delta E_{vap}$ kcal.	$\frac{V_L - V_S}{V_S}$	$\frac{V_L - V_S}{V_S} \Delta E_{vap}$ kcal.	$\Delta H_{fus}$ Observed. kcal.
<i>Metals.</i>							
Na . . .	0.952	97.6° C.	0.929	24.0	0.0236	0.57	0.58
K . . .	0.851	63.5	0.83	19.6	0.025	0.49	0.57
Rb . . .	1.52	35.7	1.475	17.5	0.0320	0.56	0.52
Cs . . .	1.90 (at 20° C.)	28.5	1.84	16.0	0.0314	0.53	0.50
Hg . . .	14.2	-38.7	13.7	13.5	0.0376	0.51	0.56
<i>Hydrocarbons</i>							
C <sub>10</sub> H <sub>22</sub> . . .	0.870*	-32	0.767	9.5	0.133	1.26	6.6
C <sub>15</sub> H <sub>32</sub> . . .	0.910*	+10	0.776	14.2	0.172	2.44	11.6

\* In view of the discrepancies which exist in the literature for the values of  $\Delta E_{vap}$  and  $\Delta E_{fus}$  (or, more strictly, the latent heats) for paraffin hydrocarbons, it is necessary to emphasise that the lack of agreement does not arise from the use of wrong values for these constants. It is assumed by Eyring and Kauzmann that straight line extrapolation from lower hydrocarbons, for the purposes mentioned above, is necessary, because the graph of  $\Delta E_{vap}$  plotted against the number of carbons in the compound falls away considerably from a straight line. The figures given by Doss<sup>4</sup> and quoted elsewhere, for the latent heat of vaporisation for normal paraffins above C<sub>8</sub> are based on an extrapolation formula given by Schultz.<sup>5</sup> These are obviously wrong when compared with the values given by branched-chain compounds shown in the legend to Fig. 1, which will be somewhat low compared with the  $n$ -paraffins having the same number of carbon atoms. They disagree also with the experimental values obtained by Ubbelohde<sup>6</sup> for C<sub>14</sub>, C<sub>15</sub>, C<sub>16</sub>, C<sub>17</sub> and C<sub>18</sub>, and consequently a smooth curve (Fig. 1) has been drawn through these values. There is, in fact, no reason for assuming the curve to be other than linear, an assumption which, as is shown in section (4), is fully consistent with other ideas.

<sup>2</sup> Ref. 1, p. 487.

<sup>3</sup> Mark, *The Physical Chemistry of High Polymeric Systems* (New York, 1940), p. 141.

<sup>4</sup> Doss, *The Physical Constants of the Hydrocarbons*, 4th Ed. (Texas Oil Company, Texas, 1944).

<sup>5</sup> Schultz, *Ind. Eng. Chem.*, 1930, **22**, 785.

<sup>6</sup> Ubbelohde, *Trans. Faraday Soc.*, 1938, **34**, 282.



If the assumptions are true, then the energy required to mix the number of holes with molecules of the liquid is given by

$$\frac{V_L - V_S}{V_S} \Delta E_{\text{vap.}} \quad . \quad . \quad . \quad . \quad . \quad (4)$$

where  $V_S$  is given by equation (3) and  $V_L$  is the molar volume, calculated from the density of the liquid. It would seem reasonable that equation (4) should be used in calculating the energy of fusion and Table I shows that this is so for the metals but not for the hydrocarbons.

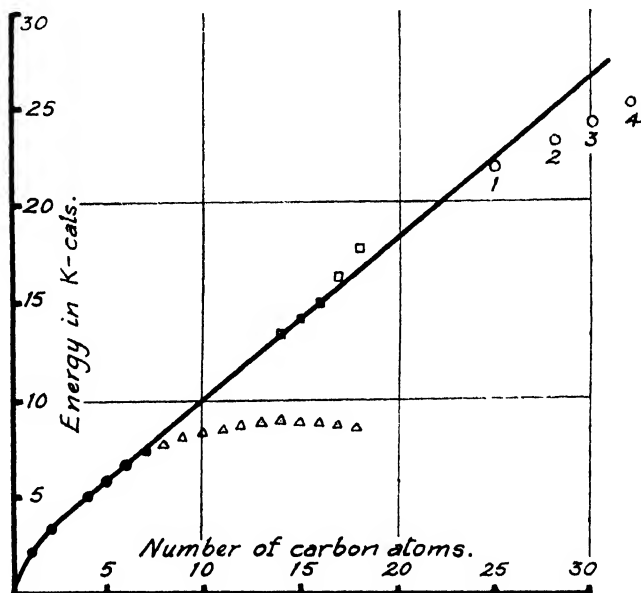


FIG. 1.—Energies of evaporation given by  $\Delta E_{\text{vap.}} = L - RT$ ,  $L$  being taken as follows:

- |                             |                        |          |
|-----------------------------|------------------------|----------|
| ● Quoted in ref. 8.         | 1. 9-octyl heptadecane | } ref. 8 |
| △ Schultz (ref. 9).         | 2. 7-hexyl docosane    |          |
| □ Ubbelohde (ref. 10).      | 3. 9-octyl docosane    |          |
| ○ Branched chain compounds. | 4. decyl docosane.     |          |

An alternative way of picturing fusion is to assume a loosening, or general spacing out of the molecules, and this can be checked by a calculation of the ratio  $\Delta E_{\text{fus}}/\Delta E_{\text{vap}}$  from the intramolecular forces. This is abnormally high for the  $n$ -paraffins, a peculiarity which would be presumably common to all long chain compounds. We may seek to connect these differences with the classification suggested by Bernal<sup>7</sup> for liquids, i.e., the dependence of the structure on the type of the intramolecular force between the molecules. With metals, the particles are spherical with an isotropic intermolecular force falling off slowly with distance, whereas the  $n$ -hydrocarbons have intermolecular forces falling off perpendicular to the chain axis as the sixth power of the distance. The potential energy between two molecules may be considered as given approximately by eqn. (5),

$$U_r = \frac{ma}{r^m} - \frac{nb}{r^n} \quad . \quad . \quad . \quad . \quad . \quad (5)$$

where  $U_r$  is the potential energy at distance  $r$ , and  $a$ ,  $b$ ,  $m$ , and  $n$  are constants.

<sup>7</sup> Bernal, *Trans. Faraday Soc.*, 1937, **33**, 27.

In the cases considered here, the second or repulsion term may be ignored, and we can write  $U_r = \frac{a^1}{r^6}$  for the paraffins compared with  $U_r = \frac{a^{11}}{r^8}$  for the metals. From this simplified law it can be shown that

$$\Delta E_{fus} = \frac{(r_{liquid}^6 - r_{solid}^6)}{r_{solid}^6} \Delta E_{vap} \quad . \quad . \quad . \quad (6)$$

into which can be inserted  $r_{solid} = 4.3 \text{ \AA}$  (i.e.  $18.5$ , the area occupied by a single chain according to Müller<sup>8</sup>) and Warren's figure of  $5.0 \text{ \AA}$ . as the best available for the liquid state.<sup>9</sup> This gives  $\Delta E_{fus} = 1.5 \Delta E_{vap}$  which is too high, and  $5.0 \text{ \AA}$ . as the average of a normal distribution gives too great a volume increase on melting. Given, however, that general loosening does occur, thermal fluctuations would provide the means of variable separation between chains, the larger separations obtained by this means in the loosened environment being, for all intents and purposes, holes of molecular size into which a molecule on moving, could be said to evaporate. The representation of melting as a general loosening does not exclude the existence of holes and may be, in part, formally equivalent to their formation. If a distribution of separations of molecules in the liquid is imagined such that say,  $\frac{1}{3}$  of the liquid exists with this loosened spacing and the other  $\frac{2}{3}$  with a spacing more nearly that of the solid but more irregularly so that there are holes of molecular size, we should have by combining eqn. (4) and (6) as an approximation,

$$\begin{aligned} \Delta E_{fus} &= \Delta E_{vap} \left[ \frac{2}{3} \cdot \frac{(V_L - V_S)}{V_S} + \frac{1}{3} \times 1.5 \right] \quad . \quad . \quad (7) \\ &= 0.63 \Delta E_{vap} \end{aligned}$$

Good agreement with the observed ratio can be obtained in this way.

Thus with a loosening of the molecules with respect to each other and with thermal vibration, there will be a distribution of distances between the chains which, because the forces between them fall away by a sixth power law, can be regarded as being made up of two components. In the first (i.e. at short distances), allowances must be made for the power law, but in the second, where  $1/r^6$  is negligible, the distances are such as to be designated holes. Thus, although the ratio  $\Delta E_{fus}/\Delta E_{vap}$  is adequately explained by the formation of holes, in the case of the metals this is only so for the hydrocarbons if it is assumed that holes account for only part (about  $\frac{2}{3}$ ) of the volume increase, the remainder being due to a general loosening of the molecular structure. If holes are present, then during the existence of a particular hole, the molecules, or parts of molecules forming the boundary to that hole, are already free from the cohesive forces of each other—this is the basic requirement for a hole to exist—and energy is not required for this purpose. It is reasonable, therefore, to consider existent holes as an energy saving, the equivalent of which should be reckoned in assessing the energetics of the flow-process and, further, since loosening provides potentially for the existence of holes, an approximation can be made by assuming that all the volume increase is given by holes, although it has been shown that this does not give an accurate physical picture of the structure of the liquid. Therefore, in section (4), this assumption has been made and the energy equivalent of the holes present taken as that given by eqn. (4).

### (3) Estimate of Size of Flow-Unit.

It may be considered that the energy of activation of viscous flow of a normal paraffin is proportional to the number of carbon atoms, if the

<sup>8</sup> Müller, *Proc. Roy. Soc., A*, 1936, **154**, 624.

<sup>9</sup> Warren, *Physic. Rev.*, 1933, **44**, 969.

chain moves rigidly as a whole, since the volume of a hole to receive it and any work function involved in entering the hole will vary directly as the number of carbon atoms. Departure from linearity must involve some assumption such as Eyring and Kauzmann have made, namely, that only part of the molecule moves.\*

To estimate this flow-unit, the energies of activation of flow for the homologous series of normal paraffins are considered. Fig. 2 includes  $\Delta H_{\text{visc}}^*$  for the normal paraffins<sup>4</sup> plotted against  $n$ , and Fig. 3 shows  $\Delta H_{\text{visc}}^*$  against  $\log n$ .† Calculations from this graph gives

$$n = 2.585 e^{\frac{\Delta H_{\text{visc}}^*}{3.23RT}} \quad (8)$$

No data are available for hydrocarbons above  $C_{32}$ .

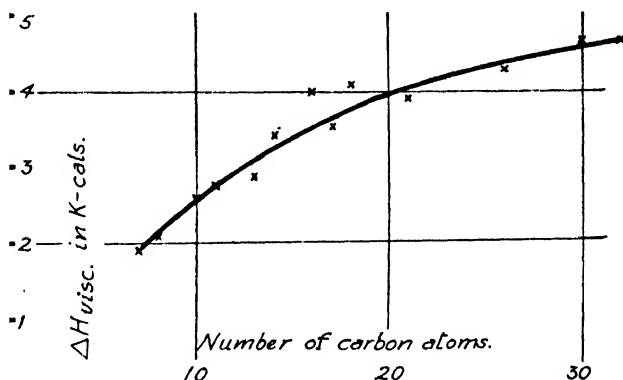


FIG. 2.

As stated above, if all the molecule required activation at the same time we should expect :

$$\Delta H_{\text{total}}^* = kn \quad (9)$$

If we distinguish the observed energy of activation, from that of eqn. (9) by the subscript "total" for the latter, and if  $p$  is the static equivalent of the number of carbon atoms in the chain activated at one and the same time then

$$\Delta H^* / \Delta H_{\text{total}} = p/n \quad (10)$$

Substituting for eqn. (8) and (9), we have :

$$p = 3.23k (\ln n - \ln 2.585) \text{ when } n > 7$$

Thus,  $p$ , the equivalent segment size, varies linearly with the logarithm of the total number of carbon atoms in the compound and the equation defining it (11) contains three empirically determined quantities. Eqn. (8)

\* The suggested segment should not be regarded as rigid since to postulate movement only about C—C bonds at the ends of segments suggests either that there is something inherently different about those bonds, or a discreet partitioning of the available energy at certain widely scattered points. It seems more probable that the energy would be available in a particular zone, the distribution being such as to diminish effectively to zero on either side of it, the flow-unit or segment being that portion of the molecular chain over which the energy is distributed. In estimating the size of the flow-unit the figures quoted in terms of numbers of carbon atoms are, therefore, the average static equivalent of the activated zones.

† The lower members of the series have been ignored because the flow-unit will be the molecule, and  $\Delta H_{\text{visc}}^*$  will be proportional to  $n$ , the number of carbon atoms.

written in log. form shows that the constant 2.585 is associated with the size of a molecule after the number of carbon atoms over which the energy is distributed has become smaller than the number in the molecule. The value of  $K$  determined from Fig. 2 as 258 cal./g.mol. for  $-\text{CH}_2-$  groups, is equivalent to the  $\Delta E_{\text{vap}}/4$  used by Eyring and Kauzmann since for eqn. (9)

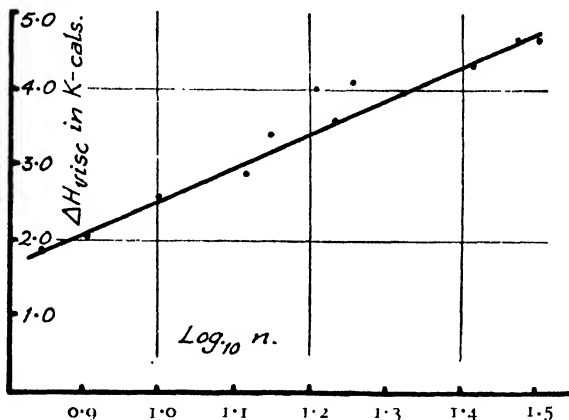


FIG. 3.

to be dimensionally sound,  $K$  must be in cal. and if, as has been stated (cf. ref. 1)  $\Delta H_{\text{visc}}$  can be equated to a linear extrapolation of  $\Delta E_{\text{vap}}/4$  against  $n$ , then eqn. (9) could be rewritten with this factor inserted instead of  $\Delta H_{\text{visc}}$ . Furthermore, the van der Waals' potential for  $-\text{CH}_2-$  groups in liquids (say 1.0 kcal.) inserted instead of  $\Delta E_{\text{vap}}$ , gives  $K$  equal to 250. The values of equivalent flow-unit size ( $p$ ) obtained from eqn. (11) are given in Table II for various hydrocarbons for which data are available.

#### (4) The Molecular Cohesion of the Activated Flow-Unit.

The cohesive forces uniting a long polymethylene chain with its neighbours have been calculated by Mark<sup>10</sup> using London's<sup>11</sup> procedure. The molar cohesion of polyethylene is given by Mark as 1.00 kcal. per mole per 5 Å. length of chain, a co-ordination of 4 being assumed (i.e. each chain is surrounded by 4 others and the figures quoted refer to the cohesive forces between any two chains). The van der Waals' cohesion per g.mol. where the chain length is 1.25 ( $n - 1$ ) Å. is therefore, 250 ( $n - 1$ ) cal./mol., where  $n$  is the number of methylene groups. Given the size of the flow-unit or segment, it is possible to calculate the cohesive energy required to separate it from its environment. If a single molecule is removed from the mass, then the total cohesive energy required is four times that quoted above from Mark, but if the mass of the molecules is "loosened" so as to permit relative movement then, since in separating molecule A from molecule B, molecule B is thereby separated from molecule A, only one half of the total energy is required and the cohesive energy required for  $n$  methylene groups is 500 ( $n - 1$ ) cal./mol. Calculating on this basis, Table II gives the molar cohesive force required to be overcome in releasing the segments for flow. Where holes exist in the liquid, the molecules are already free to move and if from the cohesive energy required the energy already consumed in hole formation (col. 4, Table II) is subtracted there is left in col. 5 the amount of energy required to render the flow-units free from their mutual attractions. It must be clearly pointed out that there is no immediately available justification for splitting

<sup>10</sup> Mark, *The Chemistry of Large Molecules* (New York, 1943), p. 66.

<sup>11</sup> London, *J. Physic. Chem.*, 1942, 46, 305.

the energy parameter of the rate process in this way but it seems reasonable that if  $\Delta H_{\text{visc}}$  energy is that required to overcome cohesion then an amount can be subtracted from it to represent regions where cohesive forces are reduced.

To allow for the fact that the molar volume of a g.mol. of flow-units is related to the true molar volume of the compound by ratio  $p/n$ , eqn. (4) has been multiplied by this ratio to give the energy allowance for holes given in col. 4 of Table II. The necessary values of  $\Delta E_{\text{vap}}$  have been read off from Fig. 1.

TABLE II.—Size of flow-unit and its energy requirement compared with  $\Delta H_{\text{visc}}^*$ .

<i>n.</i>	<i>p.</i>	Energy Required to Overcome Molar Cohesion of $p$ $-\text{CH}_2$ -Groups. kcal.	Energy Allowance for Existent Holes. kcal.	Energy Required after Allowance for Holes. kcal.	$\Delta H_{\text{visc}}^*$ kcal.
10	9.9	4.45	1.9	2.55	2.6
11	10.6	4.8	1.9	2.9	2.8
12	11.2	5.1	2.05	3.05	3.0
13	11.8	5.4	2.1	3.3	3.1
14	12.3	5.65	2.1	3.5	3.3
15	12.8	5.9	2.2	3.6	3.4
16	13.3	6.15	2.25	3.9	3.5
17	13.8	6.4	2.3	4.1	3.6
18	14.2	6.6	2.4	4.2	3.7
19	14.6	6.8	2.4	4.4	3.8
20	14.9	6.95	2.4	4.55	3.85
21	15.3	7.15	2.5	4.65	3.9
26	16.8	7.9	2.65	5.15	4.3
30	17.9	8.45	2.8	5.65	4.7

As mentioned above, col. 5, Table II, shows the remaining energy required to render the flow-units free from their mutual attractions. Comparison of this figure with the observed  $\Delta H_{\text{visc}}^*$  (col. 6) shows good agreement supporting the suggestion that  $\Delta H_{\text{visc}}^*$  may be equated to the van der Waals' potential of the activated flow-unit when once allowance has been made for the holes in the liquid. Until more data are available, further discussion is undesirable, except that it would seem useful to apply these ideas to a high polymer, natural rubber, not to expect agreement because several extrapolations are involved, but to see the order of the results obtained and to compare them with experiment.

Using eqn. (10) and (11) with the observed  $\Delta H_{\text{visc}}^*$  of 10.5 kcal. for a natural rubber<sup>12</sup> of molar weight 175,000, a flow-unit of 41 chain carbon atoms is obtained. The energy required to overcome the molar cohesion of this flow-unit is 21 kcal., using Mark's calculations.<sup>10</sup> To calculate the energy allowance for existent holes it is first necessary to decide on a hypothetical figure for the energy of evaporation of rubber. If linear extrapolation of Fig. 1 for a hydrocarbon of 10,300 chain atoms is made and the result multiplied by 1.30, i.e. by the figure given by Mark for the ratio of the cohesions of rubber and polyethylene, then  $\Delta E_{\text{vap}}$  for rubber becomes 11,260 kcal./mol. (this may be compared with the value of 11,500 which can be derived from the cohesive energy density for rubber<sup>13</sup> assuming a molar volume of 175,000). Further  $\frac{V_L - V_S}{V_S}$  can be estimated

<sup>12</sup> Piper, private communication, 1945. I am indebted to Dr. G. H. Piper for the use of this data from an unpublished paper.

<sup>13</sup> Gee, *Trans. Faraday Soc.*, 1942, 38, 418.

as 0.2 and hence, the energetic equivalent of holes,  $\frac{V_L - V_S}{V_S} \cdot \Delta E_{\text{vap}} \cdot p/n$  becomes 9 kcal. The remaining energy needed to be supplied for a viscous flow is, therefore, 12 kcal, compared with the observed  $\Delta H_{\text{visc}}^*$  of 10.5 kcal.

A fuller development of these ideas will, it is hoped, be ready for publication in the Journal of Rubber Research shortly.

The author's thanks are due to Dr. D. D. Eley of Bristol University for valuable criticism and to the Research Association of British Rubber Manufacturers for allowing publication of this paper.

### Summary.

1. Eyring's theory of rate processes as applied to the viscosity of paraffin hydrocarbons is outlined and the holes in a liquid are held to be equivalent to a contribution to the flow process by reducing the energy required for it. An alternative method of estimating segmental size is described and the evaluation of the energetic equivalent of the holes, together with the cohesive forces of the paraffin chains, is shown to account reasonably well for the observed  $\Delta H_{\text{visc}}^*$ . In this way a better picture of the process is obtained.

2. Attention is drawn to the inadequacy of existing data on latent heats of evaporation of hydrocarbons and the dependence of the relation of the heat of fusion to the heat of evaporation on the nature of the liquid is discussed.

### Résumé.

On applique la théorie d'Eyring, concernant la vitesse des processus moléculaires, à la viscosité des hydrocarbures saturés et on considère que les "trous" dans le liquide contribuent au processus d'écoulement par réduction de l'énergie nécessaire. On décrit une autre méthode pour évaluer la taille des segments et on montre que l'énergie équivalant aux "trous," ajoutée aux forces de cohésion dans les chaînes des paraffines, rend assez bien compte du  $\Delta H_{\text{visc}}^*$  observé. On discute aussi la façon dont la relation entre les chaleurs de fusion et d'évaporation dépend de la nature du liquide.

### Zusammenfassung.

Die Anwendung von Eyring's Theorie der "Geschwindigkeitsvorgänge" auf die Viskosität von Paraffin kohlenwasserstoffen wird beschrieben. Es wird angenommen, dass die Löcher in einer Flüssigkeit als eine Kontribution zum Fliessvorgang betrachtet werden können, da sie die für diesen nötige Energie verringern. Eine alternative Methode für die Bestimmung der Segmentgrösse wird beschrieben und es wird gezeigt, dass die Auswertung des Energieäquivalents der Löcher zusammen mit den Kohäsionskräften der Paraffinketten ziemlich gut mit den beobachteten  $\Delta H_{\text{visc}}^*$ -Werten übereinstimmen. Es wird erörtert wie die Relation zwischen der latenten Wärme des Schmelzens und der des Verdampfens von der untersuchten Flüssigkeit abhängt.

## CRYSTALLITE ORIENTATION IN COATING FILMS.

### PART III.—ORIENTATION OF SILVER IODIDE UPON SILVER BROMIDE.

BY GEORGE-MARIA SCHWAB.

Received 18th June, 1946.

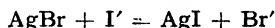
Layers formed on a solid surface by a chemical reaction of the surface with its environment, e.g. AgBr films formed by reaction of (a) silver surfaces with bromine or (b) AgCl surfaces with KBr solutions will be designated "Coating films". It has been shown by us and by other

workers<sup>2</sup> that such films often show a certain orientation of their crystal lattices relative to that of the underlying solid. This only occurs if both lattices contain planes in which corresponding atoms fit on each other periodically, and if the difference of corresponding atom distances does not exceed 5 %, the coating lattice being the larger one. In the case of isomorphy, all the planes fit in this manner, and full parallelity of both lattices is found (isomorphous coating). From this point of view it is surprising<sup>3</sup> that on regular silver bromide, exposed to potassium iodide solutions, hexagonal AgI is formed in an orientated arrangement. The purpose of the present investigation was to examine this phenomenon in detail, i.e. to find what is the exact orientation of the iodide lattice relative to the bromide lattice, which planes of the two lattices are parallel, and which relations they show in respect of the arrangement of the atoms.

### Polymorphism of Free and Grown Silver Iodide.

Silver Iodide shows a cubic modification, stable at high pressures only,<sup>4</sup> corresponding to a zinc blende lattice,<sup>5</sup> but not identical with any of the other cubic modifications.<sup>6</sup> At ordinary pressure, from the melting point down to 146° C., the "hot cubic" modification is stable, the iodine ions forming a face-centred cubic lattice and the silver ions being distributed statistically over the gaps.<sup>7</sup> Between 146° and 137° C., the hexagonal  $\beta$ -silver iodide, crystallising in the Wurtzite type,<sup>8</sup> is stable, and below 137° the "cold cubic"  $\gamma$ -form, belonging to the zinc blende type exists. The transition of the "hot cubic" into the hexagonal, or into the "cold cubic" form, or into a mixture of both, is rapid, but the transition between the "cold cubic" and hexagonal modifications at 137° is strongly retarded, mixtures of both frequently being encountered<sup>9</sup> (cf. later).

If silver iodide is formed on the surface of silver bromide at room temperature according to



the iodide formed is mostly of the hexagonal  $\beta$ -form, on monocrystals orientated but irregularly arranged on precipitated powder. In some cases, when the crystals have been formed very rapidly at high I' concentrations, or have remained a long time (> 24 hr.) in contact with the solution, some cubic  $\gamma$ -crystals are additionally formed, but mostly without orientation. Also, an orientated, hexagonal coating film, on heating up to the "hot cubic" temperature region and cooling to room temperature,<sup>8</sup> gives a non-orientated mixture of the  $\beta$ - and  $\gamma$ -forms. Likewise a strongly orientated  $\beta$ -film after a fortnight at room temperature partly changed into disordered  $\gamma$ -iodide, and the remaining  $\beta$ -iodide lost most of its orientation. However, the  $\gamma$ -form, the only stable one under the experimental conditions, never grows alone on silver bromide, exemplifying the validity of Ostwald's rule.

### Theoretical Possibilities of Orientation.

Hexagonal silver iodide always grows in the coating process, but since its transition into the  $\gamma$ -form destroys the orientation, the hexagonal lattice has therefore a special relation to the lattice of the basic crystal. Theoretical considerations about this kind of relation give the following aspects.

<sup>1</sup> Schwab, *Z. physik. Chem. B*, 1942, **51**, 245; *Koll. Z.*, 1942, **101**, 204; *Naturwiss.*, 1943, **31**, No. 27/28 (Preliminary Note).

<sup>2</sup> Cf. ref. <sup>1</sup> and the literature cited there.

<sup>3</sup> See 1, Fig. 19. Note that the indices given in that figure ought to be (110), (201) and (300), instead of (111), (201) and (301).

<sup>4</sup> Tammann, *Z. physik. Chem.*, 1910, **75**, 733.

<sup>5</sup> Landolt-Börnstein, Suppl. vol. 2.

<sup>6</sup> *Ibid.*, Suppl. vol. 3.

<sup>7</sup> Strock, *Z. physik. Chem. B*, 1934, **25**, 441; 1935, **31**, 132.

<sup>8</sup> Wilsey, *Phil. Mag.* 1921, **42**, 262; 1923, **46**, 487.

<sup>9</sup> Bloch and Möller, *Z. physik. Chem. A*, 1930, **152**, 245.

In the cubic face-centred silver bromide lattice the distance of nearest neighbours Ag—Br is  $a/2 = 2.88$  A.; Goldschmidt's radius of the iodine ion (2.20) is 0.24 A. greater than that of the bromine ion (1.96). Thus, at equal deformation, the distance Ag—I ought to be 3.12 A. Now, it is known that, because of the greater deformability of the iodine ion, the whole lattice goes over to the zinc blende or the Wurtzite type, and, because of the decrease of ionic radius when the co-ordination number changes from 6 to 4,<sup>10</sup> the distance Ag—I becomes as short as 2.81 A. Thus it differs from the distance in silver bromide by 2.6 % only. This is within the tolerance limits found for orientated coating, whereas the calculated distance of 3.12 A. differs by 10 % and thus would not allow an orientated coating. Hence the greater deformability of the iodine ion sufficiently compensates for its greater radius so that the two ion pairs fit on each other.

But this fitting of ion pairs does not warrant the necessary fitting ("affinity") of whole lattice planes, as the two lattices are of entirely different symmetry. Precluding accidental coincidences (see p. 718) only one *a priori* possibility can be foreseen. If the ion distance in the silver iodide lattice occurs in a direction parallel to the *c*-axis (perpendicular to the basis), and if the identity period in any

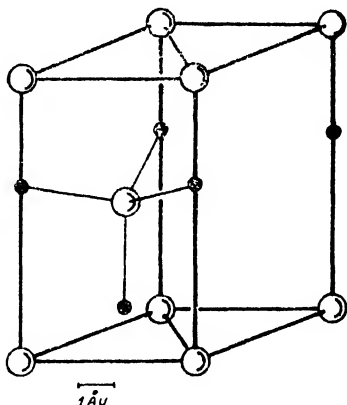


FIG. 1.—Elementary parallelepiped of  $\beta$ -AgI.

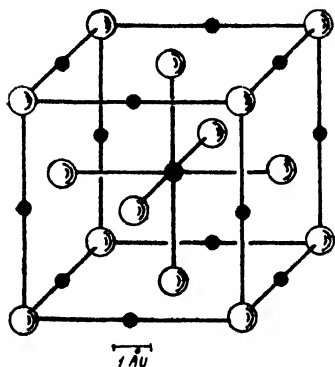


FIG. 2.—Elementary parallelepiped of AgBr.

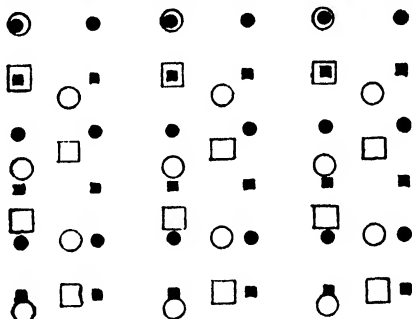


FIG. 3.—Theoretical "fitting" arrangement of AgI (110) upon AgBr (110).

● ■ AgBr. □ ○ AgI.

direction parallel to the basis, coincides with one  $[hk0]$  of silver bromide then, in this direction at least, the whole series of ion pairs will fit. In fact the respective ion distance does occur in the *c*-direction (Fig. 1), and an (accidental) relation of the postulated kind does exist in the perpendicular direction: the great basis diagonal of the elementary parallelepiped of silver iodide is of a length of  $a\sqrt{3} = 4.593 \sqrt{3} = 7.96$  A., and the face diagonal of the elementary cube of silver bromide (Fig. 2) of  $a\sqrt{2} = 5.76 \sqrt{2} = 8.14$  A. The difference of 2.3 % lies within the tolerance limit, so that

<sup>10</sup> Hassel, *Kristallchemie* (Dresden-Leipzig, 1934), p. 30.



in the hexagonal  $[110]$  direction, whole series of ion pairs can coincide. It is true that in the perpendicular  $c$ -direction only every tenth ion pair of the iodide meets one of the bromide. The planes, AgI  $(110)$  and AgBr  $(110)$ , superposed in this way, are shown in Fig. 3, the upper series of ion pairs having been brought to coincidence.

Another "fitting" arrangement of a more accidental nature is shown in Fig. 4. Here the plane AgI  $(110)$  has been superimposed on the AgBr

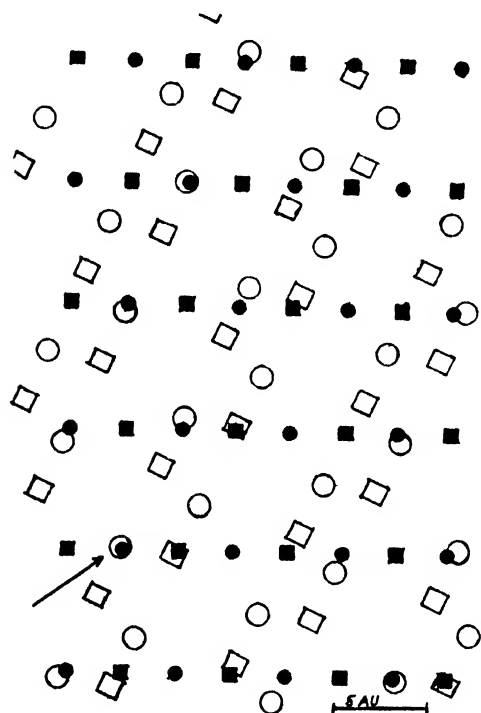


FIG. 4.—Theoretical "fitting" arrangement of AgI  $(110)$  upon AgBr  $(102)$ .

● ■ AgBr    □ ○ AgI.

In that case, the orientated arrangement was unstable compared with another orientation. Later on, we shall point out the principal difference of both cases.

### Experimental.

Monocrystals of silver bromide were prepared according to Pohl's method (cf. Part I); they were annealed at  $300^\circ$ , etched with  $\text{Na}_2\text{S}_2\text{O}_3$  or KCN and then exposed to the action of potassium iodide solutions of definite concentrations over measured time intervals. Sometimes the same crystal was used several times, the previous silver iodide film having been removed by bromine and etching until glass-clear. Before and after the iodide treatment, X-ray rotation diagrams were taken, the cylinder axis being the axis of rotation. After coating, the diagram showed the pattern of silver iodide only, because the basic crystal was covered by this strongly absorbing substance.

As mentioned above, orientated films are not always formed, and the orientation is not always perfect. If the basic crystal has a highly indexed rotation axis, i.e. giving a diagram with narrow layer lines, the coating film usually gives numerous layer lines too. Where there is imperfect orientation, it is not possible to attribute the spots, which are diffuse in height, to the layer lines. (This diffuseness is to be observed e.g. in Fig. 19 of Part I.) In isolated circumstances,

of the bromide coincide with those of the iodide *not* lying in the  $c$ -axis. Starting from the point indicated by the arrow, a whole series of coincidences progresses from left below to right above. In this direction, the identity period in the bromide lattice is  $a\sqrt{3}/2 = 7.06$  Å, and  $c = 7.50$  Å, in the iodide lattice, a difference of 6%. At the right margin of the figure, the second coincidence series of this kind begins; the distance between the two is  $a\sqrt{15}/2 = 15.78$  Å, from the bromide lattice and  $2a\sqrt{3} = 15.91$  Å, from the iodide lattice, the difference being 0.8% only. The angle, at which the axes of both lattices had to be inclined to each other, is calculated from the bromide as  $24^\circ$ , from the iodide as  $19.5^\circ$ .

Both the above theoretical arrangements are comparable to that found in Part I for silver bromide on the dodecahedron planes of silver, in that only certain rows of atoms coincide.

unorientated films are found; as a rule, the orientation is worse the more intensive the interferences of the cold cubic iodide appear beside those of the hexagonal one.

From visual observation, when illuminated on one side, and rotated about the cylinder axis, the coating films show a strong monocrystal gleam in several azimuths, and the orientated (gleaming) parts of the film often appeared not to be distributed uniformly over the whole length of the drawn, and therefore notched, monocrystal, but to have grown in the form of spots on surfaces at a certain inclination to the axis. This shows that the orientation of the film occurs only on certain crystallographic planes of the basic crystal. With highly symmetrical silver bromide, the set numbers are high, and on the undulated surface of drawn monocrystals, faces of equal indices may occur in many different positions; this results in the simultaneous occurrence of different orientations of silver iodide in the same preparation. This fact too does not facilitate the interpretation of the diagrams.

To obtain conclusive results the method had to be changed. Firstly, silver bromide monocrystals with smooth cylindrical surfaces were prepared; silver bromide was melted in a bromine vapour atmosphere, and sucked into glass capillaries of about 0.5 mm. inner diameter, slowly solidified and annealed at 350°; the glass mantle was then dissolved in conc. hydrofluoric acid. After coating, these monocrystals showed the gleam in the same azimuths throughout their length. Secondly the crystals were not dismantled between the X-ray photographs, but treated with the solutions *in situ* in the camera cover. Thirdly, it proved useful not to effect the coating at high concentration of potassium iodide, and thus at high supersaturation for silver iodide, but to develop the film slowly (in presence of N. KBr, which greatly lowers the Ag<sup>+</sup> concentration) by adding N./10 KI solution in single drops. After completion of the reaction, the film shows a distinct gleam. By this method, especially in one case on which we shall base most of the following conclusions, a very definite layer line diagram was obtained.

Before giving the outlines of the calculations, we shall show that the orientation of the coating film is really determined by the lattice orientation of the basic crystal, and not by its surface orientation. For this purpose a polycrystalline silver bromide cylinder with a smooth surface was prepared by rapid crystallisation in a capillary without annealing. Its Debye-Scherrer lines still showed spots, but with a random distribution. The silver iodide grown upon this cylinder was purely hexagonal, but entirely disorientated. Hence the film orientation observed on monocrystals is caused by their lattice.

## Evaluation.

The basic crystal of the diagram to be evaluated showed the axis orientation (3 8 12) in the photograph taken before coating. The table summarises the results.

TABLE I.—INTERFERENCE ON THE LAYER LINE  $n/2$ .

	3	8	12
200			
220	4	5	9
222	1	7	11, 15, 20
400		6	17, 23
420	2	4	16, 24
422	1 2	7	13, 14, 16, 18, 19, 21, 27, 28, 32
			10, 13, 14, 19, 25, 26, 29, 31, 35

The observed spots are printed in *heavy type*. Up to the 9th layer line (properly the 18th, if we count the odd ones, not occurring in this lattice), and the last in our photograph, the expectance is fulfilled well in all details. Likewise the layer line distances agree with the calculated within a small error:

$n/2$	1	2	3	4	5	6	7	8	9
$e_n$ calc.	1.31	2.61	3.95	5.32	6.70	8.14	9.65	11.25	12.9
$e_n$ obs.	1.3	2.7	4.4	6.0	7.0	8.6	10	11.5	13.2

Hence the orientation is absolutely definite.

The silver iodide coating gives a rotation diagram belonging to a purely hexagonal iodide, represented in Table II.

TABLE II.—ROTATION DIAGRAM OF A COATING FILM OF SILVER IODIDE.

Diameter of Rings, cm.	$\sin^2 \theta$ Obs. Uncorr.	$\sin^2 \theta$ calc.	$hkl$ .	On the Layer Lines $n$ .
3.18	0.075	0.075	101	0 1 2 3 ?
5.17	0.188	0.177	110	1 2
6.08	0.256	0.253	201	1 2 3
8.25	0.431	0.430	121	not to be separated
9.51	0.548	0.532	300	0 3

Layer line distances : mm.

 $n =$   
 $e_n =$ 

1

4.5

2

~9

3

~15

(By accident, the basic crystal was orientated such that the diagram of its coating layer was simpler than its own ; it is to this fact that the good evaluation of the experimental data is to be ascribed.)

From the distance of the first layer line, according to  $\tan \mu = 2e/A$  ( $A$ , the camera diameter, 57.3 mm.), and  $\sin \mu = \lambda/J$ , with  $\lambda = 1.032$  Å. for  $\text{FeK}\alpha$ , we calculate the identity period in the rotation axis  $J = 12.5$  Å. If now  $[uvw]$  is the required triple index of the rotation axis, the equation

$$J = a\sqrt{u^2 + v^2} \quad uv + w^2(c/a)^2 = a\sqrt{R} \quad \text{is valid}^{11}$$

From this, with  $a = 4.593$  Å. and  $c/a = 1.633$ † we may calculate which index triples are compatible with the observed value of  $J = a\sqrt{7.4}$ .

With an allowed error of  $\pm 2$  for the radicand  $R$  (i.e.  $\pm 1.3$  mm. for  $e_1$ , which is more than the broadness of the respective interference spots), only the triples given in Table III are possible.

TABLE III.—SELECTION OF THE ROTATION AXIS ON GROUND OF  $J$ .

$[uvw]$ .	$R$ .
021	6.7
121	5.7
130	7.0
221	6.7
230	7.0

Of these orientations, the  $[121]$  is discarded because it would require a reflex(110) or, more accurately,  $(\bar{2}10)$  on the equator, in accordance with the layer line relation,  $n = hu + kv + lw$ . This reflex is definitely absent. Of the other four orientations,  $[021] \equiv [2\bar{2}1]$  and  $[130] \equiv [230]$ , (because of the relation derived for the hexagonal system :

$$[uvw] \equiv [(u-v), (-v), w].$$

In Table IV the interferences expected for the orientations  $[021]$  and  $[221]$  are printed in heavy type, and that for  $[130]$  and  $[230]$  are marked with an asterisk (\*).

The dotted line marks the margin of the photograph. We see, by comparing Table IV with Table II, that the diagram found cannot be represented by either of the two possible orientations, but can be completely by a combination of both.

Thus, in one part of the silver iodide crystals, the direction  $[021]$  and in the other,  $[130]$ , coincide with the rotation (cylinder) axis. The first axis is the diagonal of the face of the double elementary prism, and the second is a line situated in the basis plane and inclined at  $19.1^\circ$  to the second-

TABLE IV

CALCULATED LAYER LINE DIAGRAM

$hkl$ .	On Layer Line, $n$ .							
101	0	1*	2*	3*	4			
110		1*	2		4*	5*		
201		1	2*	3	4*	5	6*	
300	0			3*			6*	9*

<sup>11</sup> Glocker, *Materialprüfung mit Röntgenstrahlen*, 2nd ed. (Berlin, 1936), p. 348.

† Ref. <sup>11</sup>, p. 246.

ary axis. Apparently, even on our smooth cylindrical monocrystal, the lattice plane for orientated coating still occurs in at least *two different positions*.

For a determination of this plane and the type of orientation, it is necessary to know which planes of the two lattices can be parallel in any azimuth on free rotation about their axis, and then to find how they fit on each other in this position. Every lattice plane describes a cone mantle having the rotation axis as cone axis, and only planes with equal cone angle can coincide. Thus we must calculate these angles for all the lattice planes of AgBr [3 8 12], AgI [021] and AgI [130].

We have used the formulæ given in the literature<sup>12</sup> for the angle between the planes (*hkl*) and (*h'k'l'*). Putting (*h'k'l'*) for the indices of the plane normal to the axis (*uvw*), we thus obtain the complements  $\phi$  of the cone angles.

In the cubic silver bromide, the indices of this normal plane are simply  $h' : k' : l' = u : v : w$ . For the hexagonal silver iodide, the geometrically derivable equation :

$$h' : k' : l' = \left(u - \frac{v}{2}\right) : \left(v - \frac{u}{2}\right) : w(c/a)^2 \quad \text{holds.}$$

Thus for the axis [221] we have to use the plane (338) and for the axis [230] the normal plane (140).

The next step is to put together all the pairs of planes having the same angle of inclination in the bromide and in the iodide lattice and, taking into account the direction of the axis projections in the planes, to examine the fit of the atomic arrangement. Because generally every plane exists in as many angles of inclination as it occupies layer lines in the rotation diagrams, it is easily seen that the highly symmetrical bromide, in particular, gives such a rich angle spectrum that, even with a strict angle tolerance, a great number of angle coincidences is bound to occur. Therefore we refrain from reproducing all the comparisons and only give the final result found by trial and error.

The basis (001) of AgI is inclined to the equator of the axis [021] by the angle  $\phi_\alpha = 50.6^\circ$  and to the equator of the axis [130] by  $\phi_\beta = 90^\circ$ . The octahedral plane (111) of AgBr is inclined to the equator of the axis [3 8 12] by the angles  $\phi_1 = 25.4^\circ$ ;  $\phi_2 = 48.2^\circ$ ;  $\phi_3 = 74.1^\circ$  and  $\phi_4 = 87.7^\circ$ . We see that  $\phi_\alpha \approx \phi_2$  and  $\phi_\beta \approx \phi_4$  and that

$$\phi_\alpha - \phi_2 = \phi_\beta - \phi_4 = 2.3^\circ.$$

Thus, except for this small deviation, easily accounted for by an elastic hysteresis of the wax at winter temperatures, the basis planes of *both* sorts of iodide crystals coincide with two octahedral planes of the *same* bromide lattice in certain azimuths.

Now, we see that if the "fitting planes" being in these azimuths, fit to each other, then this is also true with respect to their atom distribution. Both of them (cp. the elementary parallelepipeds in Fig. 1 and 2) contain *one* sort of atoms only, and in both it is in the arrangement of equilateral triangles, being the basis planes of close sphere packings. The only question is whether, the planes being parallel, the triangles contained in them are parallel too, i.e. whether the projection of the rotation axis in the "fitting plane" has the same inclination to the sides of the triangle in both lattices.

Let us consider first the coating  $\phi_\alpha - \phi_2$ . In the iodide, the projection of the axis [021] on the plane (001) falls on the side of the triangle. Let the angle between this projection and the side be  $\delta$ ; then here,  $\delta = 0$ . The projection of the axis [3 8 12] of the bromide on the octahedral plane forming an angle  $\phi_2 = 48.2^\circ$  with the equator, is inclined to the side of the triangle (except for a second-order correction) by  $\arctan \left( \frac{1}{36} \sqrt{3} \right) = \delta = 2.75^\circ$ . Thus the deviation is of the same magnitude as that of the inclination of the planes.

For the other coating,  $\phi_\beta - \phi_4$ , we find that the axis [230] of the iodide is itself situated in the plane (001), and there it encloses an angle,  $\arctan \left( \frac{1}{9} \sqrt{3} \right) = \delta = 10.9^\circ$  with the *height* of the triangle [120]. The projection of the axis [3 8 12] of the bromide on the octahedral plane (111) that nearly contains it, encloses the angle  $\arctan \left( \frac{5}{36} \left( \sqrt{3} \right) \right) = \delta = 13.5^\circ$  with the height of the triangle [112]. Here the deviation between the two lattices is  $\Delta\delta = 2.6^\circ$ ; again, about the same as for

<sup>12</sup> *Ibid.*, p. 347; the  $h_1 k_1 l_1$  and  $h_2 k_2 l_2$  given there correspond to our *hkl* and *h'k'l'*.

the plane parallelity. Thus, but for a small adjustment of the rotation axis between the two photographs, both orientations signify parallelity of the sides and heights of the triangle in a common plane. (The deviation would be zero, if the orientation of the bromide, instead of [3 8 12], were [3 9 12] resp. [134].) The absolute length of the sides of the triangle will be discussed later.

Both orientations follow from the same principle, viz., the coincidence in the position of the planes as well as of their atoms of the iodide basis plane with the bromide octahedral plane. Two only out of four possible positions of the octahedral plane act as orientating planes; one is contained in the cylinder surface, the other can occur as a microplane only. The fact that the remaining two positions, for which the same is true, did not act as orientating planes, is probably due to accidental influences. (It may be remarked here that our earlier photographs with drawn monocrystals showed parallelity of the same planes, within much greater errors, due to inaccurate adjustments.)

It is remarkable that the orientation found here in the exchange coating of silver bromide in iodide solutions, is identical with a natural case of "epitaxy" of silver chloride on silver iodide, found by Royer<sup>13</sup> in a mineral. He likewise states that (111) of the chloride coincides with (001) of the iodide and that the octahedral edges of the chloride are parallel to the edges between (001) and (100) of the iodide.

## Conclusions.

Our type of coating differs from the types found previously in exchange coating. In the formation of silver bromide on silver chloride<sup>1</sup> or, under certain circumstances, vice versa<sup>2</sup> we had an isomorphy relation which caused, on each plane of the basic crystal, the formation of the corresponding plane of the coating lattice. The decisive point is the small difference of the ionic distances Ag—Cl and Ag—Br, which may be called a chemical relation. Now, we have seen (p. 717) that in spite, or even because of, its different lattice type, silver iodide participates in this chemical relation as for the ionic distance, and it was for this reason that, in Fig. 3 and 4, we searched for "fitting" arrangements based on this approximate coincidence of distances. Because of the different symmetry of the two lattices, these arrangements must be such that only rows of pairs of ions coincided, separated by relatively large interstitial distances. In fact, in the formation of silver bromide on dodecahedral planes (110) of metallic silver, we had shown<sup>1</sup> that such a bad "fitting" arrangement can result, at least in a transitory orientation.

But with silver iodide on silver bromide those arrangements are not found for the following reason. On the almost non-polar silver surface a row of "fitting" ion pairs, formed at first preferably, may act as a unidimensional germ of a whole lattice plane in the sense of the Kossel-Volmer-Stranski concept, and it does not matter that other parts of this plane have no further relation to the underlying lattice. But on the strongly polar silver bromide surface, as is evident from Fig. 3 and 4, numerous positions of repulsion between the ions are encountered between the "fitting" rows. These would require a strongly endothermic addition process which would stop the whole growth of the plane.

Therefore, the orientation takes place on planes occupied by only one kind of ion, and thus perturbations of the kind described are precluded. At the same time, these planes, AgBr (111) and AgI (001), are the only ones that coincide in their atom distribution. It is true, however, that the agreement of the *absolute dimensions* of the lattices is not exactly satisfactory. The sides of the equilateral triangles are, in the bromide

lattice,  $\frac{a}{2} \sqrt{2} = 4.07 \text{ \AA.}$ , in the iodide  $a = 4.59 \text{ \AA.}$  Although the sign of

the deviation, producing an enlargement in the coating, is the normal one observed in coating phenomena,<sup>1</sup> its magnitude of 13 % must be considered as extremely high in view of the other results on orientated coatings.

This great tolerance may be due in part to the non-polarity of the coating planes. It appears, however, that in our case the good agreement

of the ion distances, Ag—Br and Ag—I, plays a part too. In general,<sup>13, 14</sup> distances not lying in the coating plane, have no influence on the mutual orientation of two lattices. But our case is such that an influence of this kind is imaginable and even probable. In the silver bromide lattice (Fig. 2) every silver ion is surrounded by six nearest bromine ions at the corners of an octahedron. This octahedron is cut in two halves by the (111) plane so that the silver ions of this plane retain three bromine neighbours on the bromide side. If now the iodide lattice grows upon this plane with the *c*-axis as normal, either (1) an iodide ion may be added as a fourth neighbour in the *c*-direction (see the ion pairs lying in the *c*-direction in Fig. 1), thus completing the three bromine ions to a co-ordination complex of four, characteristic of silver iodide, or (2) three iodine ions (in the position of the three black spheres above the central white one in Fig. 1) can grow, again in the silver iodide arrangement, in a way that they complete the three bromine ions to a complex of six, thus continuing the bromide co-ordination once more in the transition layer. Thus, the transition layer contains (oblique) tetrahedra [AgBr<sub>3</sub>I] or octahedra [AgBr<sub>3</sub>I<sub>3</sub>]. It is to be expected that these mixed complexes can be formed only if both ion distances agree approximately, a condition fulfilled here within 2.6 %. This possibility of mixed co-ordination apparently stabilizes the coating in the (111) plane, and sufficiently compensates the energetic hindrance caused by the 13 % deviation of the distances within the planes themselves. Thus, finally, it is the deformability of the iodine ion and the "levelling" of the distances caused by it, that makes possible the orientated coating of the two halides.

### Summary.

Silver iodide films formed by exchange coating of silver bromide in iodide solutions are examined by X-rays to obtain their lattice orientation. As long as they do not undergo recrystallisation or polymorphous change, they belong to the hexagonal modification and grow upon the lattice of the basic bromide crystal such that the hexagonal basis (001) coincides with the octahedral plane (111) of the bromide. Both planes have the same closest hexagonal arrangement of atom and contain ions of one sign only. Because of this, the phenomenon differs from the formation of the other silver halides on each other or on silver. In the coating plane the distances of nearest neighbours differ by as much as 13 %. This probably is allowed for because of the lack of polarity in the plane and of the similarity of the ion distances Ag - Br and Ag—I. This, caused by the deformability of the iodine ion, makes the formation of mixed complexes possible, having the co-ordination number of one of the lattices, in the transition layer.

### Résumé.

On a examiné aux rayons X l'orientation du réseau dans les films de AgI, formés sur AgBr à partir de solutions d'iodure. Le film présente une modification hexagonale, telle que son plan 001, coïncide avec le plan 111 du bromure. Ceci s'explique par la similarité des distances ioniques de AgBr et AgI.

### Zusammenfassung.

Die Gitterorientierung von aus Jodidlösungen auf AgBr gebildeten AgJ—Filmen wurde mit Röntgenstrahlen untersucht. Der Film bildet eine hexagonale Modifikation, deren 001-Ebene mit der 111-Ebene des Bromids zusammenfällt. Dies wird durch die Ähnlichkeit der Jonenabstände Ag—Br und Ag—I erklärt.

<sup>13</sup> Royer, *Bull. Soc. Fran. Miner.*, 1928, **51**, 7, and esp. 137.

<sup>14</sup> Neuhaus, *Angew. Chem.*, 1941, **54**, 527; *Z. physik. Chem.*, 1943, **192**, 309.

# CRYSTALLITE ORIENTATION IN COATING FILMS.

## PART IV.—ORIENTATED COATING FILMS ON THALLOUS HALIDES.

BY GEORGE-MARIA SCHWAB.

Received 18th June, 1946.

In the first communication of this series,<sup>1</sup> we examined the conditions under which a coating film is formed in orientated crystallites on a crystallised material. These were: (1) increase of molecular volume; (2) fitting of the atoms in a pair of lattice planes; (3) coincidence of the corresponding lattice distances within 5-6 %. The condition (2) is fulfilled best by the equality of lattice types of the basic crystal and the coating film (isomorphous coating; e.g. AgBr on AgCl), but it may be fulfilled by any pair of lattice planes accidentally "affined".<sup>1, 2, 4</sup> Later, it was found, that condition (1) is unnecessary if a continuous series of mixed crystals enables a smooth transition to the narrower lattice (e.g. AgCl on AgBr (Part II)). Further, we showed that the tolerance limit in condition (3) may be considerably exceeded if, in spite of the stress, the coating is energetically stabilised by a favourable arrangement of chemical co-ordination (AgI on AgBr).<sup>4</sup>

In the present paper<sup>2</sup> the conditions above, proposed originally on the basis of few data, are confirmed by a new series of orientated coating. These will be of interest, especially in view of the relations they have to the orientated building up of foreign material, lately studied by different workers.<sup>3, 4, 6</sup> In particular we shall show that with an insoluble coating of product formed by reaction of the basic crystal itself, conditions and mechanisms of building up that cannot occur in the crystallisation from solutions on cleavage faces may be verified.

### Experimental.

The starting material was metallic thallium ("*purissimum* for commerce") from the mine Oker (Harz mountains), obtained by the kind mediation of Prof. Hönigschmid and Dr. Büttner. It was dissolved in dilute sulphuric acid (and proved thereby to be free of lead), and the halides were precipitated from this solution by the respective halogen acids, washed and dried. To prepare *monocrystals*, they were melted in a stream of air (a stream of chlorine or bromine, as described in Part I for the silver halides, is not practicable here as it would cause oxidation to thallic salts). The liquid was sucked into thin glass capillaries, solidified therein and freed from the glass coat by hydrofluoric acid<sup>4</sup> ("*cast*" crystals), or, according to Pohl's method, thin monocrystal rods were drawn slowly from the liquid on a glass rod ("*drawn*" crystals—Part I).

Then the orientation of the cylinder axis (rotation axis) of these crystals with respect to the lattice was examined by an X-ray photograph (for technique, cf. Part I), the coating reaction performed *in situ* and a second rotation photograph taken, which now showed the interferences of the coating film and gave its orientation with respect to the same rotation axis.

Before coating, the crystals must be etched by a suitable reagent in order to develop fresh crystal faces, for the thalious halides, conc. sulphuric acid proved to be suitable. After removing the coating film by a suitable solvent and repeated etching, the same basic crystal may be used repeatedly.

<sup>1</sup> Part I: Schwab, *Z. physik. Chem. B*, 1942, **51**, 245; Part II: *Koll. Z.*, 1942, **101**, 204; Part III: (preceding paper).

<sup>2</sup> Schwab, *Naturwiss.*, 1944, **32**, 32; preliminary note.

<sup>3</sup> Neuhaus, *Angew. Chem.*, 1941, **54**, 527; *Z. physik. Chem.*, 1943, **192**, 309. *Naturwiss.*, 1943, **31**, No. 27/28 (preliminary note).

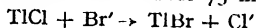
<sup>4</sup> Neuhaus, ref. <sup>3</sup> and *Z. physik. Chem. A*, 1943, **191**, 359.

<sup>6</sup> Willems, *Naturwiss.*, 1943, **31**, 146, 208, 232.

## (1) Films on Thallous Chloride.

Thallous chloride has been used in "cast" crystals only. Fig. 1, 2 and 3 show that their orientation is not very uniform. Annealing at 350° (m.pt. 427°) for 5 hr. does not improve the crystals appreciably. In this respect thallous chloride largely differs from the silver halides, where the best diagrams are obtained with annealed "cast" crystals.<sup>4</sup> In spite of this, the following facts about these crystals could be stated.

(a) **Thallous Bromide on Thallous Chloride.**—When a thallous chloride crystal remains in a N. KBr solution for over 75 min., the bromide formation,



is not detectable by X-rays nor by any visible surface opacity. In the case of silver chloride the corresponding silver bromide formation (Part II) was already noticed after 20 sec. and was complete in 10 min. The respective solubility products are shown in table opposite. Apparently the coating is favoured by the lack of solubility of the reaction product rather than by the solubility of the reactant, as found in reprecipitation.<sup>7</sup>

Salt.	Solubility Product.	Ratio.
TlCl . . .	$1.5 \times 10^{-4}$	75
TlBr . . .	$2 \times 10^{-6}$	
AgCl . . .	$1.1 \times 10^{-10}$	275
AgBr . . .	$4 \times 10^{-13}$	

After 24 hr. exposure to N. KBr the same crystal, however, became opaque and distinctly showed (Fig. 2) the phenomenon of isomorphous coating (I), every interference spot of the mother crystal being accompanied by one of equal shape of the daughter film, thus indicating two parallel isomorphous lattices. In fact, thallous chloride and bromide both crystallise in the caesium chloride type, as is shown by the indices in Fig. 2.

Using the "distance method", described in Part II for analysis of mixed crystals, we compare the distance  $\Delta_1$  of the mother and daughter spots in the equator for different lattice planes with half the difference  $\Delta_0$  of the diameters of the Debye-Scherrer rings of pure chloride and bromide, taken from powder photographs. In this way, we obtain Table I, showing that  $\Delta_1$  is only about one half of  $\Delta_0$ .

TABLE I

<i>hkl.</i>	$\Delta_1$ (mm).	$\Delta_0$ (mm).	$C_1$ (%).	$\Delta_2$ (mm).	$C_2$ (%).
110	(0.5)	0.9	(55.6)	(0.75)	(83)
112	0.8	1.65	48.5	1.65	100
220	1.0	2.10	47.5	2.0	95.2
321	2.5	5.02	49.8	5.0	99.6
			48.6		98.3

This means that no pure thallous bromide has been built up here, but a 50 % mixed crystal. This exactly corresponds to the phenomena observed in the formation of silver bromide from chloride (Part II) except for the much greater velocity in the latter case. Probably too, with the thallous halides, a mixed crystal in equilibrium with a solution containing a great excess of  $\text{Cl}'$  ion, is formed in a solution containing excess bromide, because a local  $\text{Cl}'$  excess exists in the diffusion zone near the surface.

But, as in the silver case, the mixed crystal is bound to be an unstable intermediate state. In fact, Fig. 3, taken from the same crystal after another two days' exposure to the same solution, shows an increase of the interference distances  $\Delta_2$ , corresponding to the final formation of pure thallous bromide as shown in column  $C_2$  in Table I.

It may be added that the lattice constant of thallous chloride is 3.834 Å., and of the bromide 3.980 Å., so that the difference of 3.7 % is within the tolerance limits given above. (An inversion of this coating process, i.e. formation

<sup>7</sup> Schwab and Schwab-Agallidis, *Koll. Z.*, 1943, 104, 67.



of the chloride from the bromide, as has been performed with the silver salts, is unfortunately impossible here because of oxidation to thallic salts.)

(b) **Thallous Iodide on Thallous Chloride.**—It is not possible, even by a 48 hr. exposure to a 20 % KI solution, to obtain an orientated coating of thallous iodide on the chloride. The thallous iodide is precipitated mostly in the solution; the yellow layer finally deposited on the crystal is dense, as shown by the strong absorption of the chloride interferences, but is entirely without texture and nearly amorphous (giving broad lines of low intensity).

At ordinary temperatures, thallous iodide crystallises in the rhombic system but it is possible that the cubic modification, stable above 165°, might be metastable due to its isomorphy relation with the basic crystal, in a manner similar to the hexagonal silver iodide, which, stable above 136°, coats silver bromide due to a "fitting" of the lattice planes (III). That this is not happening here is due to the orientation conditions given in the introduction. The lattice constant of cubic thallous iodide is 4.198 Å. and thus 9.6 % greater than that of thallous chloride, and this difference exceeds our tolerance limit.

This gap cannot be closed by formation of mixed crystals, for the cubic thallous iodide is not miscible in all proportions with the chloride, as is the bromide, but in the solid state a mixture gap exists between 18 and 99 % mole. TlCl. Hence the two saturated solid solutions have lattice constants of 3.838 and 4.132 Å. respectively (Vegard's rule); these differ by 8 %, which precludes orientated coating.

(c) **Silver Chloride on Thallous Chloride.**—The bad "cast" monocrystal of thallous chloride, represented in Fig. 1, was exposed to a 10 % silver nitrate solution for 5 min. It became white and opaque. The diagram of the coating film is one of silver chloride (Fig. 4) showing a distinct texture. As more than three reflexes are to be found on the ring (200), several orientations co-exist. Furthermore, as the basic crystal (Fig. 1) is not a clear monocrystal, and as the relatively large solubility of thallous chloride makes the reproducible preparation of the coating films difficult, the determination of the mutual orientation is postponed until the analogous case of the bromides (p. 727) has been treated. Of course, this coating is not an isomorphous one, the thallous halides belonging to the caesium chloride type and the silver halides to the sodium chloride type.

## (2) Films on Thallous Bromide.

Because of the poor results obtained with the "cast" thallous chloride crystals, thallous bromide was prepared in the form of "drawn" crystals. These show a uniform orientation, although the deviation of single crystallites from the average orientation can be considerable at first (Fig. 5). In this case annealing effects an appreciable improvement. The crystal of Fig. 5 was annealed at 350° (m.pt. 459°) for three days, and then gave the diagram in Fig. 6. Sometimes excellent monocrystals were obtained without annealing, as is shown by Fig. 7.

(a) **Thallous Iodide on Thallous Bromide.**—The crystal (cp. Fig. 5) after an exposure of 10 min. in a 20 % KI solution does not show any signs of coating except for a faint yellow coloration. Hence the reaction is slow like that between

TABLE II

<i>hkl.</i>	$\Delta_0$ (mm.)	$\Delta_2$ (mm.)	$C_2$ (%).
110	1.16	0.8	69.0
112	2.34	1.6	68.4
220	2.99	2.15	72.0
321	6.84	4.4	64.4
			68.5

TlCl and Br' ions. But after 48 hr. the crystal became intensely yellow and gave the diagram (Fig. 5), characteristic of an isomorphous coating. We calculate the line distance  $\Delta_0$  of pure thallous bromide and pure cubic thallous iodide ( $a = 4.189$  Å.) from the formula (Part II) :

$$da \cot \theta d\theta$$



FIG. 1.—“Cast” monocrystal of  $\text{TlCl}$ .

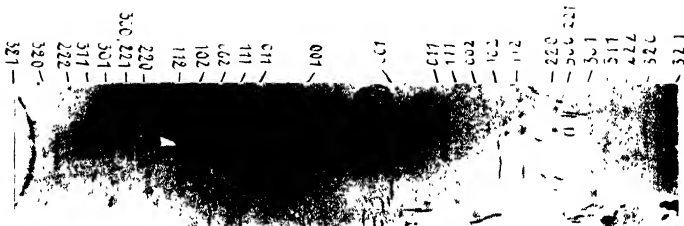


FIG. 2.—TlBr on TlCl, isomorphous coating, early stage.



FIG. 3.—TlBr on TlCl, isomorphous coating, late stage.

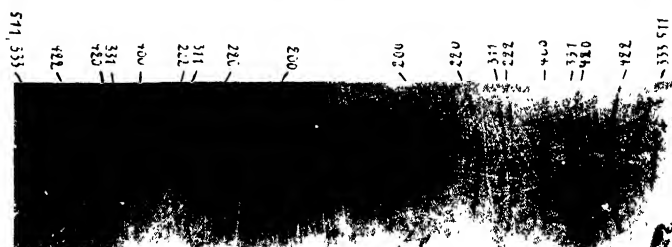


FIG. 4.—AgCl orientated upon TlCl of Fig. 1.

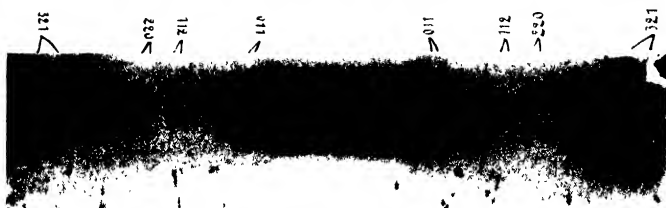


FIG. 5. TlI [111] upon a drawn monocrystal of TlBr [111], isomorphous coating

[To face page 726.

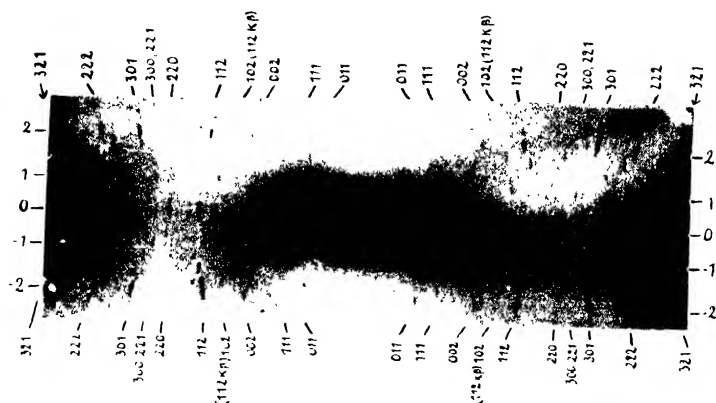


FIG. 6.—TlBr, monocrystal  $[111]$ , annealed.



FIG. 7.—TlBr, drawn monocrystal  $[1\ 3\ 10]$ .



FIG. 8.—AgBr orientated on TlBr  $[1\ 3\ 10]$  of Fig. 7.



FIG. 9.—AgBr  $[112]$  and  $[0\ 1\ 5.8]$  on TlBr  $[111]$  of Fig. 6

[To face page 727.

( $a$  = lattice constant,  $\theta$  = diffraction angle,  $A$  = camera diameter = 57.3 mm.). In Table II,  $\Delta_0$  is compared with the  $\Delta_3$  measured in Fig. 5, and  $C_3$ , the thallous iodide content of the film was calculated therefrom according to Vegard's rule.

We see that a mixed crystal TlBr—TlI of about 70 % has been built up, for reasons similar to those which caused a mixed thallous chloride-bromide crystal to grow at first upon the chloride. The present mixed crystal has a lattice constant of 4.141 Å. It differs from the basic lattice by 4.1 % and thus is lying within the tolerance limit. It appears questionable that the same is also true for pure cubic thallous iodide, having a difference of 5.5 % (i.e. the mixed crystal changes into pure metastable iodide on prolonged iodination) for the reaction was probably finished after 48 hr. because the ratio of the solubility products is 71 and therefore of the same order as in the case of the chloride-bromide.

A summary of the isomorphy relations of the three thallous halides is given below.

Salt Pair.	Difference of Lattice Constants (%)	Solid Solubility.	Isomorphous Coating.
TlCl—TlBr	3.7	complete	up to 100 % TlBr
TlCl—TlI	9.6	gap 18-99 % TlCl	none
TlBr—TlI	5.5	complete	up to 70 % TlI

Thus the greater isomorphous affinity of the iodide for the bromide is perceptible most distinctly in the isomorphous coating.

### (b) Silver Bromide on Thallous Bromide.

(a) **Determination of the Mutual Orientation.**—As shown above, silver chloride coats thallous chloride with an orientated film. The mechanism of the orientation will be made clear with the more easily handled bromides. With these, the phenomenon was absolutely reproducible, e.g. on the crystal in Fig. 7, identical coating film photographs like Fig. 8 could be obtained on three successive occasions by etching off the films with  $S_2O_3^{2-}$  or  $CN^-$  and treating with 10 % silver nitrate solutions for 1-5 min.

In contrast to the anion exchange reactions previously described, this cation exchange is rather rapid, probably because the ratio of the solubility products is as high as  $5 \times 10^6$ . Formerly<sup>4</sup> we were able to regulate the rapid transition of silver bromide into iodide (solubility product ratio  $4 \times 10^3$ ) by addition of  $Br^-$  ions to the iodide solution. In an analogous way, we attempted to retard the present reaction by the presence of thallous sulphate in the silver nitrate solution. But an undesirable side-reaction was obtained: a compound of silver bromide and thallous bromide of low symmetry is formed. It has no orientation relations to the basic crystal and hence is mostly formed in the solution and not on the crystal. The complicated diagram of this compound (some of its lines are slightly perceptible on Fig. 6) could also be obtained by precipitation of silver-thallium-solutions with bromide in the ratio  $(Tl^+) : (Ag^+) > 1.5$ . Probably it corresponds to the incongruent melting compound  $2 AgCl \cdot 3 TlCl$  detected by thermal analysis by Sandonnini and Aureggi.<sup>8</sup> Nevertheless, even without using this retardation method, reproducible photographs like Fig. 8 could be obtained.

As for this particular diagram, the following remarks must be made. According to the layer line relation<sup>9</sup>

$$hu + kv + lw = n$$

( $hkl$ ) a lattice plane,  $[uvw]$  the rotation axis,  $n$  the number of the layer line), the sinuses of the equator distances of the three most intensive reflexes on (200) in Fig. 8 ought to be proportional to the values  $2u$ ,  $2v$ ,  $2w$ , and from them the

<sup>8</sup> Sandonnini and Aureggi, *Atti Linc.* 1911, (5), 20, 11, 588; Landolt-Börnstein erroneously gives  $TlCl \cdot 2 AgCl$ .

<sup>9</sup> Glocker, *Materialprüfung mit Röntgenstrahlen*, 2nd ed. (Berlin, 1936), p. 200; Bijvoet, Kolkmeijer, McGillavry, *Röntgenanalyse von Krystallen* (Berlin, 1940), p. 23.

sinuses of the equator distances of the six most intensive reflexes on (220) can be calculated to be proportional to  $2(u+v)$ ,  $2(u+w)$ ,  $2(v+w)$ .

However, it is easily seen that this is far from true; this unmistakably shows that the three former reflexes do not belong to the same crystal position, but to more than one, and that the apparently simple diagram is in fact complex. This effect, often encountered in this sort of work, is due to the occurrence of the coating plane in several positions on the same basic crystal (especially if, as in our case, it is highly symmetrical). For the first determination of the mutual orientation such a case is unsuitable. Therefore we shall pass on to another example and come back to this one later (p. 730); then it will offer an extraordinarily sensitive confirmation of the accepted orientation.

The same treatment of the ("cast", annealed, see p. 724) basic crystal in Fig. 6 produced a coating film giving the diagram Fig. 9. Its relative "plainness" is due to the simple orientation of the crystal in Fig. 6. Its rotation axis has the indices  $[uvw] = [111]$ , i.e. it is the space diagonal of the elementary cube.

In this case we have:

- on the equator: (110), (112), (220), (321);
- on the 1st layer line: (100), (111), (102), (221);
- on the 2nd layer line: (110), (200), (112), (301), (222), (321).

The distance of the second layer line should be 19.2 mm. (observed  $18 \pm 2$ ). In Fig. 6 the layer lines are marked on both sides, and it is seen that all the criteria are fulfilled and the orientation is correctly determined.

As mentioned above, the coating film gives the diagram Fig. 9. (Some single reflexes, not indexed in Fig. 9, belong to the underlying thallous bromide, as can easily be verified by comparison with Fig. 6). Unfortunately the reproduction does not show all the reflexes on the higher layer lines. The evaluation of the original film gave the following results. Intensity maxima occur on all the rings which belong to the group of equator distances, 7.6 mm., 17.7 mm. and 33.5 mm. The corresponding  $\sin \mu$  ( $\mu$  being the layer line angle) are in the proportion 1 : 2.05 : 2.97. Hence the numbers of the layer lines (the face-centred cubic lattice giving even numbers only) are 2, 4, 6. From the layer line distances, the identity period in the rotation axis is calculated as being  $J = 15 \text{ \AA}$ . Since

$$J = a\sqrt{u^2 + v^2 + w^2} \text{ and } a = 5.76 \text{ \AA},$$

this value is compatible only with the index triple  $[uvw] = [112]$ .

In this case we have:

- in the equator: (220), (222), (420);
- on the 2nd layer line: (200), (220), (420), (422);
- on the 4th layer line: (200), (220), (222), (400), (422);
- on the 6th layer line: (220), (420), (422).

A comparison of the reflexes with the numeration of the layer lines given on the inner margins of Fig. 9 proves that all these reflexes exist. Thus, the orientation is really  $[uvw] = [112]$ .

But it will be seen that besides these, still other reflexes exist. In particular,

a reflex on (220) near the equator is manifest, evidently belonging to another system of layer lines. This system, however, is not sufficiently clear for an evaluation in the same manner. This, however, was attempted but the several possibilities could not be distinguished on the basis of the diagram, but, as we found afterwards, they contained the right solution. It appears more opportune to determine the second orientation theoretically from the first and to confirm it by the diagram. In this way we can arrive at the same time at an explanation of the more complicated diagram of Fig. 8.

**(b) Geometrical Explanation of the Orientation.**—What is the meaning of an orientation giving

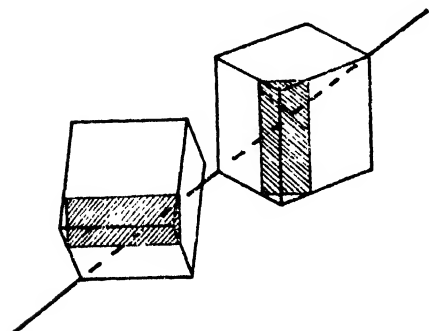


FIG. 10.— Mutual orientation of the elementary cubes of AgBr [112] (left) and TlBr [111] (right).

the indices [111] to the cylinder axis for the basic crystal and [112] for the built up crystal? Fig. 10 is drawn in perspective, the right cube being the

elementary cube of the basic crystal, and the left one that of the coating crystal. The full line, dotted in its covered parts, is the rotation axis. The question is, what planes of the two lattices are parallel in this arrangement and thus coincide?

For many planes this can be seen directly from the figure: e.g. the two shaded (110) planes are parallel, and so is the (110) plane (not indicated) situated "at the top" in the left cube with the "above" (100) plane of the right one, the right (100) plane of the left cube with the left (not shown) (110) plane of the right cube, etc. The calculation for the general case of free rotation of both cubes about the axis (see (III)), gives coincidences at the inclination angles  $\phi$  to the axis equator plane, shown in Table III for the most closely occupied lattice planes.

TABLE III

cos $\phi$ .	(hkl) AgBr.	(hkl) TlBr.
0	110	110*
0	111	112
0	102	123
0.333	112	111
0.472	111	112
0.578	110	100
0.578	110	122
0.723	102	103
0.816	100	110
0.044	111	112
1.000	112	111

As will be shown below, out of all these coincidences only one, marked by the asterisk in the table, and by shading in Fig. 10, satisfies the other postulate that the atoms of both lattice planes must fit on each other periodically when the projections of the rotation axis on both planes have the same position. It is plausible that this pair of coating planes will give the most intense layer line system of Fig. 9, as these planes with  $\cos \phi = 0$  are tangents of the cylinder surface and hence occur in great extension in the surface.

(c) **Other Proofs of the Orientation.**—Consideration of Fig. 10 and Table III shows that besides the orientating dodecahedral plane (110) of TlBr parallel to the axis, another sort exists cutting it at an angle  $\cos \phi = 0.816$ . If this also occurs in the outer surface of our preparation, say in form of scale steps, it will cause a second orientation of silver bromide crystallites by the same coating mechanism.

Let us treat the general case, independent of the accidentally high symmetry of the rotation axis of the crystal (Fig. 6). The position of the left cube of Fig. 10 is derived from that of the right one by turning the latter first about one edge through  $45^\circ$  and then about an edge perpendicular to the first again through  $45^\circ$ . If the original indices of a direction invariant to this operation (as is the cylinder axis) are  $[uvw]$ , a simple co-ordinate transformation shows that these become:

$$[(u + v + w\sqrt{2}), (u + v - w\sqrt{2}), (u - v)\sqrt{2}],$$

or

$$[(u - v + w\sqrt{2}), (u - v - w\sqrt{2}), (u + v)\sqrt{2}].$$

(The two triples differ according to which of the two initially unused cube edges is used as axis of the second rotation of the cube).

If the set  $[uvw] = [111]$  (crystal of Fig. 6), then the second index triple is  $[\sqrt{2}, \sqrt{2}, 2\sqrt{2}]$  or  $[112]$ . This is the orientation caused by coincidence of the shaded planes in Fig. 10. But the first index triple gives:  $[(2 + \sqrt{2}), (2 - \sqrt{2}), 0]$  or  $[0, 1, 5.83]$ . Hence, this must be the second orientation of silver bromide in Fig. 9, traces of which we anticipated. It postulates an identity period in the rotation axis of  $J = 34$  Å. and thus the layer line system given at the outer margin of Fig. 9. Calculating approximately with  $[uvw] = [016]$  we expect:

- on the equator: (200), (400);
- on the 2nd layer line: (200), (220), (420);
- on the 4th layer line: (400), (420);
- on the 6th layer line: —;
- on the 8th layer line: (420), (422).

Of these reflexes, those given in *heavy type* occur in as far as the superposition of the more intensive first orientation reflexes allows one to judge. (Only the two equator reflexes are doubtful.) Thus the second orientation may be explained unambiguously by the same coating mechanism acting on the same kind of planes in a second position.

And now we come back to the other coating preparation of Fig. 7 and 8, postponed previously (p. 728). Our results, if correct, are bound to apply to Fig. 8 too, and if they do, they will receive greater confirmation.

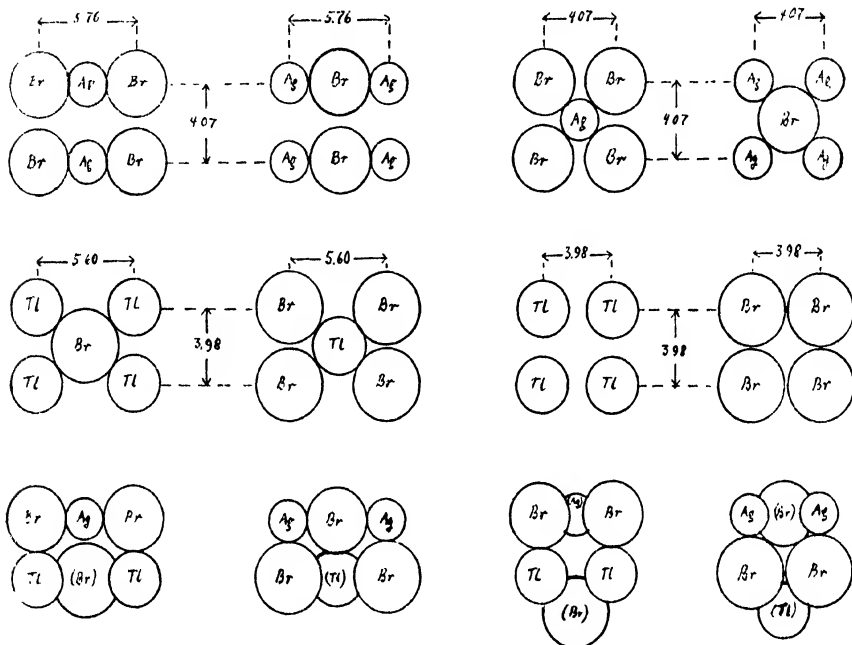


FIG. 11.—1st line: elementary quadrangle of AgBr; 2nd line: elementary quadrangle of TlBr; 3rd line: side-view of the coating zones; 1st and 2nd columns: coating (110) on (110); 3rd and 4th columns: coating (100) on (100).

The axis of the basic thallous bromide crystal of Fig. 7 has the indices (1 3 10).

On this assumption we must find:

- on the equator: (301);
- on the 1st layer line: (100), (102), (301), (321);
- on the 2nd layer line: (110), (200), (221);
- on the 3rd layer line: (100), (112), (300), (321);
- on the 4th layer line: (110), (102), (220);
- on the 5th layer line: (102), (112);
- on the 6th layer line: (111), (200), (221), (301);
- on the 7th layer line: (110), (102), (301), (321);
- on the 8th layer line: (111), (102), (220), (301);
- on the 9th layer line: (110), (112), (300);
- on the 10th layer line: (100), (301), (321);
- on the 11th layer line: (110), (112);
- on the 12th layer line: (111), (102), (222), (321);
- on the 13th layer line: (110), (221), (301), (321).

The equator distance of the 9th layer line is calculated to be 15 mm., the same value is found. Originally the orientation was determined on the basis of the three reflexes printed in *heavy type*; on checking, it correctly

gave the other 42 reflexes, a beautiful example of the reliability of the method of Graf<sup>9</sup> for layer line diagrams.

This highly indexed rotation axis implies six different positions of the dodecahedral plane instead of two, this being the general case. Corresponding to this, not only two, but six different orientations of the silver bromide coating are to be expected, dependent on which of the three indices are named  $u$ ,  $v$  or  $w$  in the co-ordinate transformation described above. From the formulæ given above, the following six index triples are found for the rotation axis with respect to the silver bromide lattice.

None of them can be expressed by small rational indices. The absolute values given are chosen such that they be long to the layer line system indicated in Fig. 8, having  $J = 41.7$  Å. (it coincides with that of the basic crystal and of Fig. 7). By this measure, the blackenings do not fall on whole numbered layer lines. We must now superpose theoretically the six calculated systems of interference spots and examine, at what points (equator distances) blackening maxima have to occur on the Debye-Scherrer rings. Of necessity we ascribe equal intensity to all spots of the same ring. In this manner, for the four rings which can be evaluated in Fig. 8, we calculate the following blackening statistics (Table IV). The maxima are given in *heavy print*. A comparison with Fig. 8 shows that they coincide well with the experimental blackening maxima. We showed above (p. 728) that Fig. 8, although giving the impression of a uniform layer line diagram, cannot be evaluated as such. The reason is now known. It does not

$u$ .	$v$ .	$w$ .
6.4	1	3.6
5.1	3.5	4.1
5.4	4.5	2.4
2.0	4.3	5.7
6.5	2.0	3.0
5.5	4.7	1.7

TABLE IV.—NUMBER OF INTERFERENCE SPOTS ON THE LINE  $hkl$  BETWEEN THE LAYER-LINES  $n - (n + 1)$

$n =$	0-1.	1-2.	2-3.	3-4.	4-5.	5-6.	6-7.	7-8.	8-9.	9-10.	10-11.	11-12.	12-13.
$hkl$													
200	0	<b>1</b>	0	<b>3</b>	<b>1</b>	<b>1</b>	<b>1</b>	<b>1</b>	<b>3</b>	<b>1</b>	<b>3</b>	<b>1</b>	<b>1</b>
220	0	<b>6</b>	0	<b>1</b>	<b>2</b>	<b>3</b>	<b>3</b>	<b>2</b>	<b>1</b>	<b>2</b>	<b>1</b>		
222	0	<b>3</b>	<b>1</b>	<b>1</b>	<b>2</b>	<b>1</b>	<b>0</b>	<b>1</b>	<b>1</b>	<b>0</b>	<b>1</b>	<b>2</b>	
420	<b>3</b>	<b>3</b>	<b>1</b>	<b>3</b>	<b>2</b>	<b>2</b>	<b>1</b>	<b>2</b>	<b>2</b>	<b>1</b>	<b>0</b>	<b>1</b>	<b>4</b>

contain interference spots, but accumulations caused by superposition of six different interference systems. But each of these is again a result of the same coating mechanism found in the simpler example. The elucidation of this complicated example makes this mechanism absolutely certain.

(d) *Atomistic Explanation of the Orientation.*—According to Fig. 10 the coating proceeds such that the dodecahedral planes of the two crystals touch each other, but the cube edges obtunded by them are perpendicular to each other.

These conditions are shown in Fig. 11 by the model. For the radius ratios of the ion spheres we used Goldschmidt's ion radii:

Ag <sup>+</sup>	. 1.12 Å.
Tl <sup>+</sup>	. 1.50 Å.
Br <sup>-</sup>	. 1.95 Å.

In silver bromide the deforming influence of the small silver ion is remarkable in so far as here, according to the ion distances, the radius of the bromine ion is only 1.75 Å.



Fig. 11 contains three rows and four columns. In the first column is represented the elementary quadrangle of the silver bromide dodecahedral plane, and below this, that of thallous bromide. The dimensions are in the case of silver bromide:  $a \times \frac{a}{2}\sqrt{2} = 5.76 \times 4.07 \text{ \AA.}^2$ , in the case of thallous bromide:  $a\sqrt{2} \times a = 5.60 \times 3.98 \text{ \AA.}^2$ . The difference of the linear dimensions is 2.5 % in favour of the silver bromide. Thus, the coating is found in agreement with the rule (1) and with rule (2), mentioned in the introduction. In the first column below, the fitting of the above quadrangles is shown in side-view. In the second column, the same drawings are repeated with the positions of cations and anions interchanged. This results in a slight change of the distance of the planes, due to the different size ratios. In both cases, it is seen that a *very close packing* is formed in the coating zone. Not only the ions fitting immediately on each other, but also the intermediate ones (in the silver bromide lattice on the long edges of the quadrangle, in thallous bromide in its centre) come very close to each other. (In the second column the packing is still somewhat closer because of the small radius of the silver ion.) From these considerations it is easily understood why this mode of crystallisation is preferred in the coating. (We made sure that none of the other pairs of parallel planes (Table III) shows a fitting arrangement admitting such considerations).

The only essential condition for this arrangement is a sodium chloride lattice, of lattice constant  $\sqrt{2}$  times greater than that of a caesium chloride lattice. Other salt pairs are known, which satisfy this condition. The best known is PbS (NaCl lattice,  $a = 5.93 \text{ \AA.}$ ) and  $\text{NH}_4\text{Br}$  (CsCl lattice,  $a = 4.05 \text{ \AA.}$ ). Of course, in this case of hetero-ionic salts, no orientated coating exists, but an orientated building-up is possible (as cp. Neuhaus<sup>3</sup>). But in this case the cube plane (100) of ammonium bromide grows upon fresh cleavage faces (100) of lead sulphide, the crystal axes forming an angle of  $45^\circ$ . In this manner a "fitting" arrangement of the same tolerance as ours is achieved; it has been represented in columns 3 and 4 of Fig. 11 as applied to our salt pair. We are absolutely sure, that in our case, this orientation does *not* occur; according to Table III, (100) and (100) are never parallel, and we made sure that our diagrams cannot be explained on this assumption. In fact, the two lower figures of columns 3 and 4 in Fig. 11 show that this building-up of the cube planes gives a *much looser structure* of the coating zone; the non-fitting ions (situated a little behind the plane of the paper) do not approach each other, but leave large empty spaces. (Of course the same can be shown for  $\text{PbS}-\text{NH}_4\text{Br}$ ). There is therefore no doubt that the building-up of the dodecahedral planes is energetically more favoured.

In spite of this, the observation that this orientation is not verified and remained unknown in the building-up of dissolved salts is due apparently to the fact that under these conditions the respective plane does not exist in the free state. Orientated growing up from solution is known to happen on fresh cleavage faces only. However, galenite cleaves exclusively and distinctly along the (100) plane and therefore the dodecahedral plane (110) is never exposed to the ammonium bromide, and this is bound to be satisfied with a possible second-order orientation. It is true that (110) occasionally occurs on natural galenite crystals as a grown surface,<sup>10</sup> but, as we expected and found, it has no orientating power because it is not fresh. In contrast, the coating experiment offers two advantages. Firstly the basic lattice is not of the NaCl type, but of the CsCl type, and secondly, perpetually fresh etching surfaces are formed and offered by the reaction itself. In CsCl lattices, (110) occurs as outer surface, and thus the orientation on it is preferred for energetic reasons.

<sup>10</sup> I am much indebted to Mr. Papastamatiou of the Mineral. Inst. of the Athens University for a fine specimen of this kind.

### Summary.

The crystalline orientation in films formed by chemical reactions on the surface of thallous halide monocrystals is examined by X-rays. On  $\text{TlCl}$ , films of  $\text{TlBr}$  grow up in a isomorphously orientated arrangement, forming intermediate mixed crystals;  $\text{TlI}$  does not do so, and  $\text{AgCl}$  is orientated.

On  $\text{TlBr}$ , an isomorphous orientated mixed crystal, rich in  $\text{TlI}$ , is formed;  $\text{AgBr}$  is orientated too. On  $(110)$  of  $\text{TlBr}$ , the  $(110)$  of  $\text{AgBr}$  builds up, the crystallographic axes within these planes being perpendicular to each other. This orientation of a  $\text{NaCl}$  lattice on a  $\text{CsCl}$  lattice is energetically much more favoured than the  $(100)$  on  $(100)$ . In the usual microscopic technique it cannot be detected because  $(110)$  is not a cleavage face of the  $\text{NaCl}$  lattice.

All the orientated coatings described agree with the rules stated previously by the author.

### Résumé.

On a examiné par les méthodes décrites dans la partie III, des films d'halogénures de thallium et d'argent, formés par réaction chimique à la surface de cristaux d'halogénure thalleux. Les orientations cristallines observées s'accordent avec les règles précédemment établies par l'auteur.

### Zusammenfassung.

Filme von Silber- und Thalliumhalogeniden, die durch chemische Reaktionen auf Thallohalogenidkristallen gebildet wurden, sind mit Hilfe der im III. Teil beschriebenen Methoden untersucht worden. Die so gefundenen Kristallorientierungen stimmen mit den früher vom Autor angegebenen Regeln überein.

*Department of Inorganic, Physical and Catalytic Chemistry of the  
Institute of Chemistry and Agriculture,  
"Nicolaos Canellopoulos,"  
Piraeus, Greece.*

## THE ADAPTATION OF *BACT. LACTIS AEROGENES* TO GLYCEROL AND TO VARIOUS CARBOHYDRATES.

By E. G. COOKE AND C. N. HINSHELWOOD.

*Received 16th July, 1946.*

When *Bact. lactis aerogenes* has become adapted to the use of glucose in growth, transfer to a medium containing another carbon source usually results in a slower rate of proliferation. On further serial subculture in the new medium, however, the strain exhibits an increasing growth rate, which eventually reaches a limit—not infrequently the same as the value ordinarily found for growth in glucose. This adaptation has been shown to occur when glycerol is used as the new carbon source. The training was found to be complete after a few subcultures.<sup>1</sup> Loss of the adaptation to glycerol was observed to occur when the trained cells were grown several times in the original glucose medium. The reversibility of the training was assumed to depend upon a normal characteristic of the enzyme systems involved.

Later studies on the adaptation of *Bact. lactis aerogenes* to lactose revealed a much more complex behaviour.<sup>2</sup> It was found that on training the optimum growth rate was attained after two or three passages in the new medium, the trained cells having a generation time approximately the same as that in glucose. Cells trained in this way lost their adaptation readily. The ease with which reversion could be brought about was now

<sup>1</sup> Lodge and Hinshelwood, *Trans. Faraday Soc.*, 1944, **40**, 571.

<sup>2</sup> Postgate and Hinshelwood, *ibid.*, 1946, **42**, 45.

found to depend in a very important way on the number of training passages the cells had experienced. Thus with increasing numbers of subcultures in lactose three stages of training were observed—training which reversed easily, training which showed delayed reversion, and training which was stable to reversion.

These results re-opened the whole question of adaptation to glycerol. Although in the previous experiments the cells had been completely trained in the sense that the maximum growth rate was reached, the serial subculture in glycerol had not been extended over more than 8 passages. It now seemed possible that the reversibility of the adaptation might depend upon the length of the training, and it was of interest to see whether the effects observed with lactose adaptation applied to that one example only, or whether, in fact, they could be reproduced with a completely different source of carbon, namely glycerol. In the present work, experiments have been made which show that the phenomena are very probably general and that the adaptation-reversion relationships conform to a single pattern. In the interpretation of these results the questions of the part played by natural selection arises, and it becomes relevant to inquire into the changes in proportions which a mixture of cells of different degrees of glycerol-adaptation would show on subculture in glucose. Experiments have therefore been made on the behaviour of a population made artificially by mixing cells both trained and untrained to glycerol.

In the previous studies,<sup>1,2</sup> the sole criterion of adaptation has been growth rate. In the present work, an investigation has also been made into the connection between adaptation and ability of the trained or reverted cells to oxidise glycerol. The adaptation of *Bact. lactis aerogenes* to various pentoses has also been investigated.

### Method.

For most of the following experiments a fresh strain of *Bact. lactis aerogenes*, obtained from the National Collection of Type Cultures, was used. This was necessary since older strains, which had been subcultured monthly in bouillon in the laboratory, had acquired some considerable degree of adaptation to glycerol.

For all culturing and measurement of growth rates artificial media are made up as follows: 1 cc. of  $\text{MgSO}_4$ , 1 g./l.; 10 cc.  $\text{KH}_2\text{PO}_4$ , 9 g./l., to which NaOH is added to adjust the  $pH$  to 7.12; 10 cc. of carbohydrate, 20 g./l., except in the case of glucose, where a 50 g./l. solution is used; 5 cc. of  $(\text{NH}_4)_2\text{SO}_4$ , 5 g./l. The course of adaptation to a new medium is followed by determining growth curves for a series of successive subcultures ("training series"). Any given subculture involves 6-8 bacterial generations. Reversion is studied by further successive subculture of these trained cells in glucose medium ("reversion series"). Its extent at any particular stage is measured by a test in the medium to which the cells were originally trained. Growth occurs in tubes kept at  $40 \pm 0.02^\circ \text{C}$ . and aerated with a slow stream of sterile air. A growth curve is obtained by sampling a growing culture at intervals, killing with formaldehyde and counting in a haemocytometer.

### Experiments on Adaptation to Glycerol and its Reversal.

The form of growth curve shown by an untrained strain in the glycerol medium has already been described. It is of a composite character, that is, a slow rate of increase is replaced after a certain time by a more rapid one. This behaviour is shown in Fig. 1. As the cells become more trained, the transition occurs earlier, until eventually it appears too early to be detected. Because of the form of the curves, a single mean generation time cannot be used as a criterion of training. The progress of adaptation is followed by observing the decrease in the quantity  $T_{1:4}^{1:8}$  which is the

time taken for the logarithm of the hæmocytometer count to increase from 1.4 to 2.8. Normally the transition point occurs between these two values and is thereby taken into account.<sup>1</sup>

The progress of adaptation to glycerol with serial number of subcultures is shown in Fig. 2. It is seen that growth is very slow (*high* value of  $T_{1.4}^{2.8}$ ) at the first subculture of cells into glycerol, but improves rapidly until the fifth subculture, when a steady value of  $T_{1.4}^{2.8}$  is reached. This value is retained at least until the 25th subculture. Later in the training series, namely at the 60th, 62nd and 93rd subcultures, the value has fallen somewhat further to about 170 min., which corresponds to a mean generation time only slightly higher than that of normal cells growing in a glucose medium.

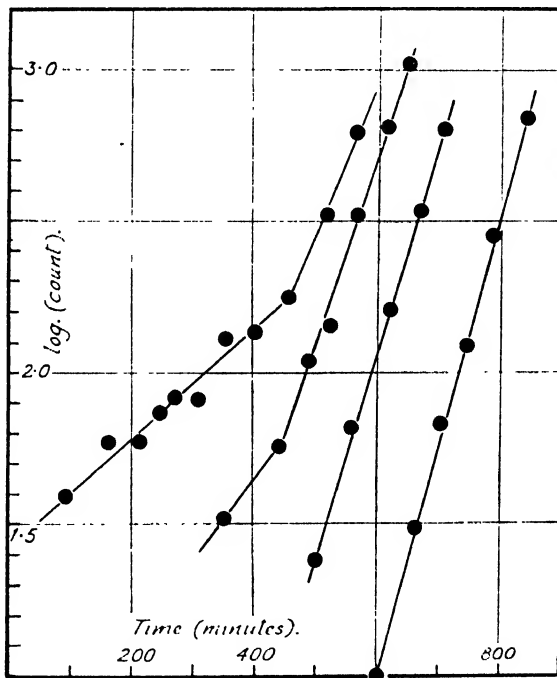


FIG. 1.—Successive growth curves in the glycerol medium, showing change in form as adaptation occurs. (Horizontal scale shifted to avoid overlapping.)

The number of passages through glucose required to cause reversion of a strain trained to glycerol depended on the extent to which the training process had been carried out. The following stages of reversion were observed. (a) Immediate Reversion. Cells which had been subcultured into glycerol 5 times, and were thus just trained, lost their adaptation rapidly. After 6 passages in glucose, the limit of reversion had been attained (Fig. 3). (b) Delayed Reversion. After 12 subcultures in the new medium, the training was lost more slowly, and did not reach a constant limit until the cells had been passed through glucose 17 times (Fig. 3). In both the above cases, reversion is only partial and tends to the same limit. (c) Stable training. Strains which had been trained by 49 and 71 passages respectively could not be caused to revert at all.

The above results are completely parallel with those obtained in lactose training; it thus appears that the sequence of immediate reversion, delayed reversion, and stable adaptation is probably general.

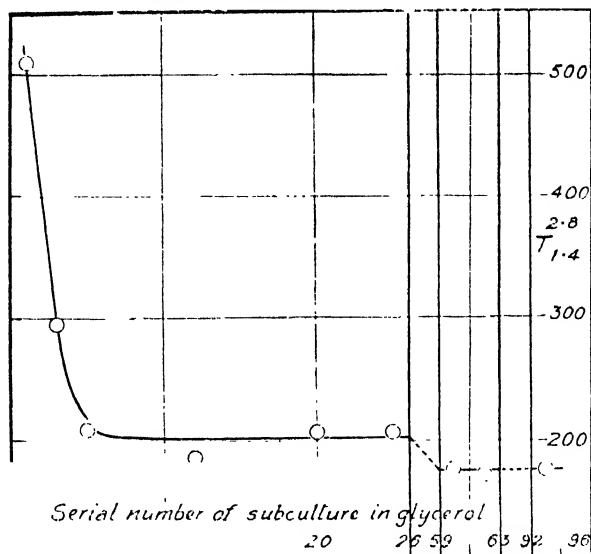


FIG. 2.—Progress of adaptation to glycerol. (Falling values correspond to increasing adaptation.) Note discontinuities in horizontal scale.

Various attempts to induce reversion were made. (1) By passage through a maltose medium. (Maltose has been found in some circumstances to cause loss of adaptation in lactose-trained cells which were

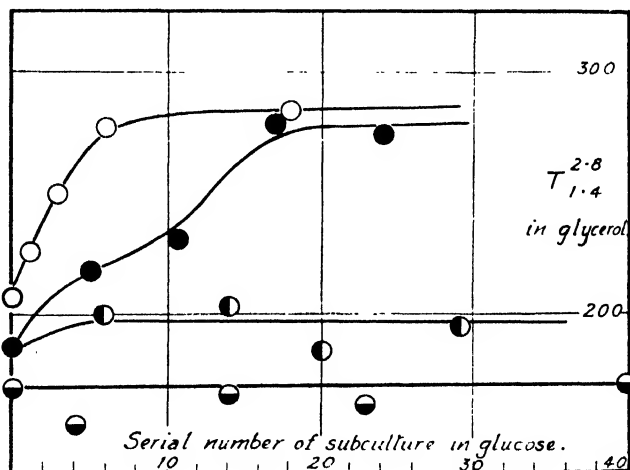


FIG. 3.—Loss or retention of glycerol adaptation.

The curves in descending vertical order correspond respectively to 5, 12, 49 and 71 training passages in glycerol.

stable in the glucose medium.<sup>3</sup>) Strains which had respectively experienced 63 and 96 passages in glycerol were used and re-tested in glycerol after 9 passages in maltose medium. (2) By passage through media containing partially inhibitory concentrations of Crystal Violet. Three strains which had been passed respectively 11, 54 and 87 times through the glycerol media were used. The two latter were grown in successively

increasing concentrations of Crystal Violet until the concentration reached a value of 5.7 mg./l. The cells were then tested in glycerol, after the Crystal Violet had been removed from the culture by one passage through glucose medium. All the attempts to induce reversion proved negative.

### Behaviour of Mixed Cell Populations.

One obvious interpretation of the facts about adaptation and reversion described above is that training consists in the selection of certain cells specially endowed with the power of utilising glycerol, and present in the original inoculum. According to this selection theory, the final stabilisation of the adaptation on long continued training would be due simply to the complete elimination of the sub-strain which uses glycerol less efficiently. Reversion, where it occurs, would be due to a restoration of

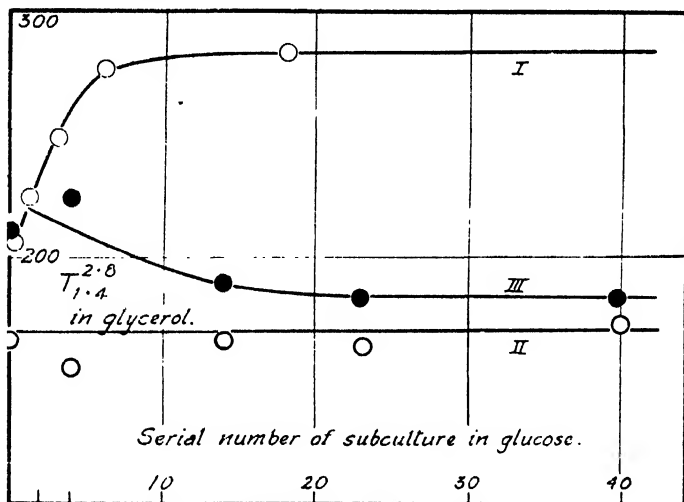


FIG. 4.—Behaviour of mixed population on subculture in absence of glycerol. Comparison with unstable and stable strains.

Curve I. Unstable strain which reverts.

Curve II. Stably trained strain showing no reversion.

Curve III. Artificial mixture of stably trained and untrained cells, which is shown, in contrast with Curve I, to undergo no reversion.

the preponderance of these cells, which would have to be brought about by subculture in glucose.

As a matter of fact, the completely trained strain appears to grow as fast in glucose as the untrained strain, so that this interpretation is not very likely. To test it more thoroughly, however, an artificial mixture of stably trained and completely untrained cells was prepared and its behaviour tested. The proportions of each type were so chosen that the mixture, when used as an inoculum, would behave initially as almost completely trained to glycerol. If this mixture is subcultured repeatedly into the glucose medium, the hypothetical selective process should ultimately result in a predominance of the untrained portion of the mixed strain. The latter should eventually be selected out and the culture as a whole should behave as untrained to glycerol.

A mixture containing one part of trained cells and one part of untrained cells was found to behave as though trained to grow in glycerol. Both parents were mixed when they were at the age of minimum lag, to ensure that no preferential early growth by one or other strain would occur. The count of the stationary population of the trained glycerol

strain in glucose medium was found to differ little from that of normal cells in the glucose medium. (This offset any tendency for the proportions of the strains to change for secondary reasons on subculturing.) A control series of experiments were made in parallel on the trained glycerol strain alone to ensure that it did not itself revert on passage through the glucose medium.

Both the mixture and control were now passed through the glucose medium exactly the same number of times and their growth rates in glycerol were tested at various identical stages in the series. The results are shown graphically in Fig. 4, where  $T_{1.4}^{2.4}$  (for the growth in glycerol) is plotted against the serial number of subcultures in the glucose medium. The diagram shows that the mixed strain shows no tendency whatever to change its character and behave as unadapted, that is, the proportion of trained to untrained cells has not appreciably altered during the series of experiments. The only interpretation that can reasonably be placed on these results is that no selection of the untrained cells is brought about by prolonged subcultures in a glycerol-free medium. Thus it appears that when reversion does occur, it must be due to some other cause than a change in the population balance. The natural conclusion is that adaptation and reversion depend upon changes in the individual cells and not upon selection.

### Correlation between Growth Rate and Dehydrogenase Activity of *Bact. lactis aerogenes*.

There is some evidence of a close connection between growth rate of cells in a given carbon source and the rate of oxidation of that source by the cells when they are in a resting condition.<sup>3</sup> The present work was

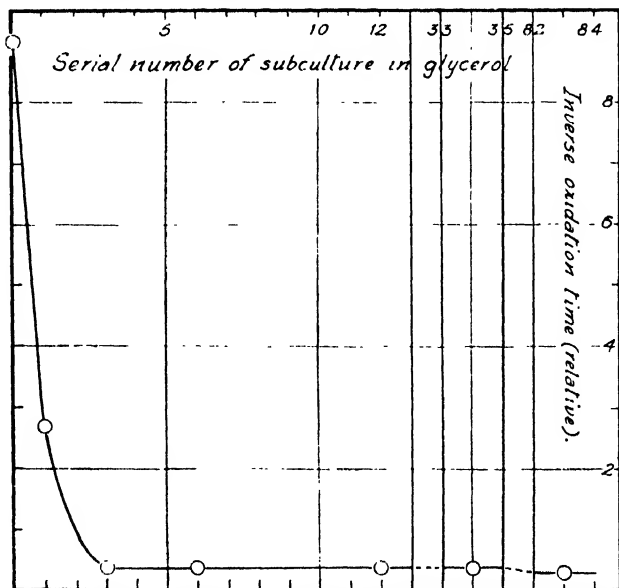


FIG. 5.—Development of glycerol dehydrogenase activity (falling curve) on serial subculture in glycerol. (Note discontinuities in horizontal scale.)

made in order to test the use of the oxidation rate as a criterion of adaptation, and thereby to ascertain further how close a connection exists between growth rate and oxidation rate. The rate of oxidation of the

<sup>3</sup> Davis and Hinshelwood, *Trans. Faraday Soc.*, 1947, **43**, 257.

glycerol by enzymatic activity was measured by the Thunberg Methylene Blue technique, in a way which has been described previously.<sup>8</sup> In order to make the results comparable and to eliminate effects, such as age of cells, which alter the absolute rate, the relative oxidation rate of glucose and glycerol was measured. This is possible because the absolute rate of oxidation of glucose does not alter appreciably on training to other carbon sources. Thus the glucose is used as a standard in each measurement. The rate is expressed as the reciprocal of the time ( $t$ ) taken for the colour of the Methylene Blue to disappear. The results are recorded as ratios of  $t$  for glycerol to  $t$  for glucose: i.e. a lower value represents increased glycerol oxidation.

For cells which, by the criterion of growth rate, were completely untrained to glycerol, the values of the above ratio, found in two sets of experiments, were 8.9 and 9.0. After the cells had grown in glycerol once

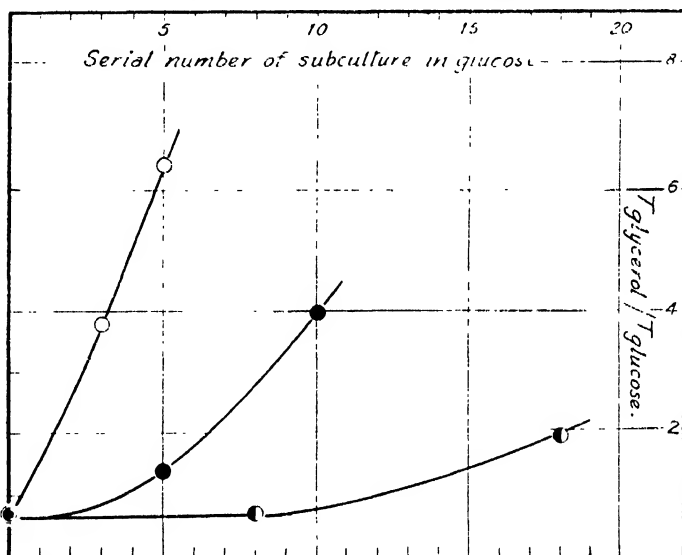


FIG. 6.—Loss (rising curve) or retention (horizontal line) of glycerol dehydrogenase activity after subculture in absence of glycerol.

From left to right the curves correspond to strains which had previously received 5, 12 and 26 training passages respectively in glycerol.

the ratio fell to 2.7, and after 3 passages in glycerol it had fallen to 0.67. Further tests on cells after different numbers of serial subcultures all gave ratios between 0.66 and 0.77, and a test on a very highly trained glycerol strain, at the 83rd subculture, showed the slightly lower value of 0.57. These results are plotted in Fig. 5, and it is seen that the curve follows very much the same course as that in Fig. 2 which shows the change in growth rate. It appears then that growth rate and oxidation rate are equally suitable as criteria of the adaptation of cells to the new carbon source.

Reversion was studied as before by growing cells the desired number of times in glycerol and then serially subculturing in glucose, the Thunberg activity towards glycerol being tested at intervals. Cells which had experienced 5, 12 and 26 passages in glycerol were investigated in this way. The results are shown in Fig. 6, where the ratio  $t_{\text{glycerol}}/t_{\text{glucose}}$  is plotted against serial number of subculture in the glucose medium.

With only 5 training passages, reversion is rapid: after 12 it is slower, and after 26 passages, the number of subcultures in glucose required to



produce any effect is considerable. It must be stated that tests done at still later stages in these reversion series showed a somewhat erratic behaviour, but the initial values are sufficiently well defined to reveal the same pattern as that appearing in the study of growth rate, namely the sequence: immediate reversion, delayed reversion, non-reversion. As a quantitative measure of the loss of adaptation, however, the growth rate is probably the more reliable.

### Experiments on Adaptation to Various Pentoses.

(a) *d*-xylose and *l*-arabinose.—The initial mean generation times in *d*-xylose and *l*-arabinose are 47 min. and 45 min. respectively, compared with 33 min. in glucose. Further subculture in presence of the appropriate sugars does not increase the growth rate rapidly: at the 3rd subculture the mean generation time for both is 45 min. and at the 8th, 41 and 37 min. respectively. The value for *d*-xylose had fallen to the same value as for glucose by the 20th subculture. Neither in *d*-xylose nor in *l*-arabinose is there any appreciable lag even at the first subculture, provided that the cells are of the appropriate age. The lag-age curve<sup>4</sup> of normal cells for the first subculture into *d*-xylose is much flatter than the curve for normal cells in glucose, early and minimum lag being almost zero. Training to *d*-xylose by 7 passages does not alter the shape of the curve, except that the lag of older cells is somewhat decreased.

Untrained cells in *l*-arabinose showed appreciably early lag, zero minimum lag, and quite considerable late lag. For cells trained by 7 subcultures in *l*-arabinose, the lag-age curve was almost identical with that observed for cells trained to *d*-xylose. Cells which had previously been cultured only in the glucose medium were tested for their ability to oxidise the two pentoses. For *d*-xylose, the ratio  $t_{\text{pentose}}/t_{\text{glucose}}$  was 1.6, whereas for *l*-arabinose it had the high value of 20. On training by 31 passages, both ratios fell, that for *d*-xylose to 1.03, and that for *l*-arabinose to 0.90. It appears that the oxidation rate of *l*-arabinose, though low for untrained cells, increases very substantially on training. Cells fully trained to *d*-xylose and *l*-arabinose oxidise these substrates and glucose equally well.

(b) *d*-arabinose.—When normal cells are inoculated into a medium whose sole source of carbon is *d*-arabinose, they exhibit a behaviour remarkably different from that in *l*-arabinose. Growth will occur only if the parent cells are just at the age of minimum lag, and therefore in their most active state. Even under these optimum conditions, the lag phase is extremely long and has been observed with various values between 36 and 72 hours, and certainly nothing below 36 hours. When growth does set in, it is fairly rapid. The mean generation time could not be determined accurately, however, as the clustering which occurred in the cultures vitiated the counting of samples.

Cells which had been grown in *d*-arabinose once grew with a minimum lag of about 2 hours on subculture into a fresh *d*-arabinose medium. It appears then, that one passage is sufficient to train the lag from an initially very great value to little more than that ordinarily found for growth in glucose. These observations are paralleled in the case of initial growth of *Bact. coli mutabile* in lactose,<sup>5</sup> where an extremely long lag for the first subculture is fully trained after one further subculture.

The question now arises whether the training of *Bact. lactis aerogenes* to *d*-arabinose is stable or whether reversion occurs. To test this, cells which had grown once in *d*-arabinose were passed through glucose media 6 times and then re-tested in *d*-arabinose. The lag was very short, which shows that the training had not been lost. Attempts were made to induce reversion by growth in presence of various drugs—proflavine, 2:7—

<sup>4</sup> Lodge and Hinshelwood, *J. Chem. Soc.*, 1943, 213.

diaminoacridine, Crystal Violet, sulphanilamide, propamidine, and *meta*-cresol. All gave negative results. Cells which had been stably trained to glycerol did not grow with shorter lag in *d*-arabinose than normal cells.

Massini,<sup>5</sup> working with *Bact. coli mutabile*, demonstrated that if this bacterium was grown on a special agar medium containing lactose, this sugar was not at first fermented. After a few days, however, secondary colonies, which were capable of fermenting lactose, appeared on the original ones. Massini ascribed this effect to a mutation of non-lactose fermenting cells. The analogy between growth of *Bact. lactis aerogenes* in *d*-arabinose and *Bact. coli mutabile* in lactose referred to earlier, leads one to suspect that, if *Bact. lactis aerogenes* is grown on agar-*d*-arabinose medium, secondary colonies, capable of fermenting *d*-arabinose, would appear. Accordingly this was subjected to experimental test. The agar medium used contained sodium taurocholate, peptone, sodium chloride, agar, *d*-arabinose and a drop of neutral red, whose presence serves to indicate the occurrence of fermentation. This medium was sterilised by autoclaving and introduced into sterile Petri dishes. Normal glucose-trained cells were plated out on the agar in the usual way and the plates incubated at 37° C. The cultures were examined periodically and it was found that after several days small reddish colonies had appeared upon the existing large yellow colonies. Thus the growth of *Bact. lactis aerogenes* in *d*-arabinose seems in every way parallel to the growth of *Bact. coli mutabile* in lactose.

Koser and Vaughan<sup>6</sup> have studied the delayed fermentation of *d*-arabinose by *Bact. lactis aerogenes*, which attacks *l*-arabinose quite promptly, and the results obtained are closely analogous with the ones obtained in the present work. There was an initial delay in the onset of fermentation for normal cells and serial transfer into *d*-arabinose progressively shortened the interval required for fermentation to begin. On *d*-arabinose-agar plates, daughter colonies containing rapidly fermenting variants appeared within the original non-fermenting colonies.

A Thunberg test on normal cells in *d*-arabinose and glucose in parallel revealed that the oxidation rate of *d*-arabinose was too low to be capable of measurement by the technique employed. Cells which had been trained by 20 passages in *d*-arabinose gave the ratio of  $t_{d\text{-arabinose}}/t_{\text{glucose}}$  as 0.77 when their dehydrogenase activity was measured. This ratio corresponds to a fully trained strain (compare the value for cells trained to glycerol).

### Summary.

When *Bact. lactis aerogenes* is adapted by serial subculture to utilise glycerol as a carbon source, three stages are passed through successively: adaptation complete (in the sense that the optimum growth rate is attained) but unstable, being lost rapidly on cultivation in absence of glycerol ("reversion"): adaptation from which delayed reversion occurs: adaptation stable to prolonged subculture in absence of glycerol.

The same general pattern of adaptation-reversion relations is revealed whether the criterion adopted is growth-rate in the glycerol medium, or the glycerol-dehydrogenase activity (Thunberg test).

Artificial mixed populations of stably adapted and unadapted cells do *not* behave like an unstably adapted strain: the reversion of the latter, therefore, probably depends upon changes in individual cells, rather than on selective changes in proportions of different types.

Minor adaptive changes are observed on training to xylose and *l*-arabinose. With *d*-arabinose a major change occurs. The first growth cycle shows an extraordinarily long lag (several days), subsequent ones practically none. The acquired adaptation appears to be very difficultly reversible. The behaviour of *Bact. lactis aerogenes* with *d*-arabinose closely parallels that of *Bact. coli mutabile* with lactose.

<sup>5</sup> Massini, *Arch. Hyg.*, 1907, **61**, 250.

<sup>6</sup> Koser and Vaughan, *J. Bact.*, 1937, **33**, 587.

## Résumé.

Lorsque le *Bact. lactis aerogenes* est adapté par une série de repiquages à utiliser le glycérol comme source de carbone, il passe par trois stades successifs : adaptation complète, mais instable et rapidement perdue par culture sans glycérol (réversion) ; adaptation présentant une réversion tardive ; enfin adaptation stable, même après repiquage prolongé en l'absence de glycérol.

On observe de façon générale cette même succession lorsqu'on prend comme critère l'activité de deshydrogénase.

Si l'on mélange artificiellement des cellules adaptées de façon stable avec d'autres inadaptées, elles ne se comportent pas comme une variété adaptée de façon instable ; il est probable, par conséquent, que la réversion de cette dernière dépend de changements dans les cellules individuelles plutôt que de changements sélectifs dans les proportions des divers types.

On observe avec le xylose et le *l*-arabinose de faibles variations d'adaptation, tandis qu'elles sont importantes avec le *d*-arabinose. Avec celui-ci, le comportement du *Bact. lactis aerogenes* est tout-à-fait semblable à celui du *Bact. coli mutabile* avec le lactose.

## Zusammenfassung.

Wenn *Bact. lactis aerogenes* durch fortlaufende Umpflanzungen in Tochterkulturen daran gewöhnt wird, Glycerin als Kohlenstoffquelle zu verwerten, sind drei aufeinanderfolgende Stadien wahrzunehmen : (1) Anpassung ist komplett aber nicht stabil und geht rasch verloren, wenn die Zellen in Abwesenheit von Glycerin gezogen werden ("Rückschlag"); (2) der Rückschlag ist verzögert und (3) die Anpassung ist stabil nach fortgesetzten Tochterkulturen in Abwesenheit von Glycerin.

Dasselbe allgemeine Schema der Anpassung-Rückschlag-Beziehungen zeigt sich auch, wenn "Glycerin-Dehydrogenaseaktivität" als Masstab gewählt wird.

Künstliche Mischungen von stabil-adaptierten und nicht-adaptierten Zellen verhalten sich nicht wie eine unstabil-adaptierte Zucht. Der Rückschlag der letzteren hängt daher eher von Veränderungen in den einzelnen Zellen als von selektiven Veränderungen in den Proportionen der verschiedenen Typen ab.

Kleinere Anpassungsveränderungen werden beobachtet, wenn Zellen an Xylose und *l*-Arabinose gewöhnt werden. Mit *d*-Arabinose tritt eine grössere Veränderung auf und das Verhalten ist hier ähnlich wie das von *Bact. coli mutabile* mit Laktose.

*Physical Chemistry Laboratory,  
Oxford University.*

## THE ADAPTATION OF *BACT. LACTIS AEROGENES* TO VARIOUS INHIBITORS.

BY J. M. PRYCE AND C. N. HINSHELWOOD.

*Received 22nd July, 1946.*

The phenomenon of adaptation, whereby bacterial cells acquire resistance to an inhibitor, has been discussed in previous papers.<sup>1</sup> The process of training, which leads to the adaptation, consists in growing the cells in the presence of an incompletely inhibitory concentration of the substance. Simple quantitative relations are found to exist between the degree of resistance of a bacterial strain and the training concentration of the inhibitor. Studies on these relations have been made with *Bact. lactis aerogenes* adapted to proflavine, Methylene Blue, Crystal Violet and *p*-aminobenzene sulphonamide. Since the behaviour with proflavine is especially simple it has been used as a standard of comparison for studies with further drugs.

The experimental procedure in testing a strain is as follows : a series of tubes are prepared containing a standard synthetic medium of pH 7.12

<sup>1</sup> Davies, Hinshelwood and Pryce, *Trans. Faraday Soc.*, 1944, **40**, 397 ; 1945, **41**, 163, 778 ; Pryce, Davies and Hinshelwood, *ibid.*, 1945, **41**, 465.

(glucose, potassium phosphate-NaOH buffer, magnesium and ammonium sulphates) and about 10 appropriate concentrations of drug from zero upward. These are placed in a thermostat at 40.0° c., and given identical 0.1 cc. inocula taken from the parent culture of the strain when its logarithmic growth phase has just ended. The culture medium is gently aerated. Under these conditions the daughter cultures show a minimum of lag (delay in the onset of multiplication). The lag, which with zero drug concentration is usually small, is determined for each culture. The results of the tests are usually expressed in two ways: (1) as a lag-concentration curve, where the increase in lag, ( $\Delta L$ ), due to the drug is plotted against the drug concentration,  $m$ ; (2) as the drug concentration,  $m_*$ , required to cause a given increase in lag (usually 1000 min.) over that for a normal culture (usually about 50 min.).

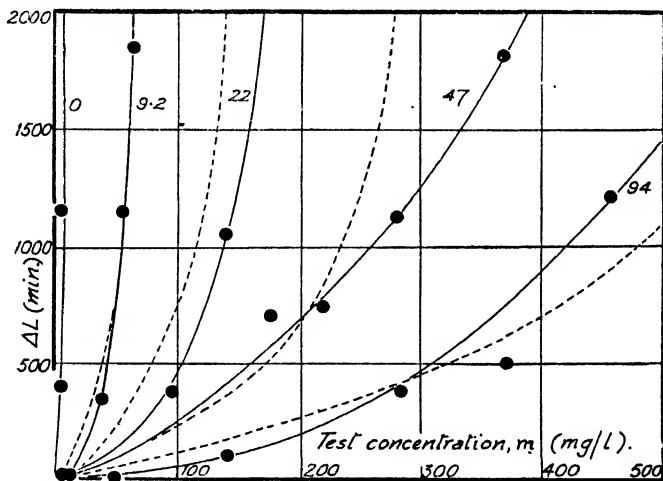


FIG. 1.—Lag-concentration curves for *Bact. lactis aerogenes* trained in potassium tellurite.

Numbers on curves indicate concentration of drug during training. In this figure, numerical values in both legends should be  $\times 2$ .

Strains trained to a concentration  $\bar{m}$  of drug are obtained by repeated subculture in the presence of that concentration—if necessary starting with cells trained at drug concentrations increasing progressively up to the one required. Usually 10 subcultures are enough but, particularly in higher drug concentrations, about 30 subcultures may be necessary to take the adaptation to its limit.

### Adaptation to Proflavine.

The family of lag-concentration curves, obtained with proflavine (2:8-diaminoacridine sulphate) has already been given in Fig. 2 of the previous paper by Davies, Hinshelwood and Pryce.<sup>2</sup> The characteristics of this family are:

(1) The slope of each curve increases as the drug concentration increases and very large or infinite values of the lag are rapidly reached. The curves obey equations of type,  $1/\Delta L = a/m + b$ .

(2) The form is such that cells trained at a concentration  $\bar{m}$  of proflavine possess almost complete immunity up to that concentration but not beyond.

(3) The horizontal spacing of any two curves—measured, for example, on the line  $\Delta L = 1000$  min.—is equal to the differences in the corresponding values of  $\bar{m}$ .  $m_*$  (the drug concentration necessary to raise  $\Delta L$  to 1000)

<sup>2</sup> *Trans. Faraday Soc.*, 1945, 41, 163.

is given by the simple expression  $m_s = \bar{m} + 33$ . This relation is obeyed by all but very highly trained strains and certain reverted strains (which will be dealt with in a later paper).

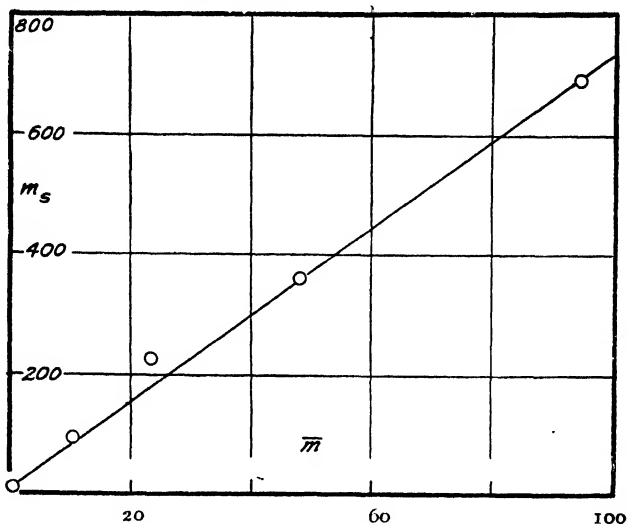


FIG. 2.—Relation of  $\bar{m}$  and  $m_s$  for potassium tellurite.

(4) Each member of the family of curves intersects a given horizontal line,  $\Delta L = 1000$ , for example, at the same angle.  $d(\Delta L)/dm = \text{constant}$  for  $m = m_s$ .

The behaviour of cells when grown in very high concentrations of proflavine (150 mg./l. and above) shows certain special characteristics which have been previously discussed and will not be further commented on here.

### Adaptation to Potassium Tellurite.

Fig. 1 shows the family of lag-concentration curves obtained when

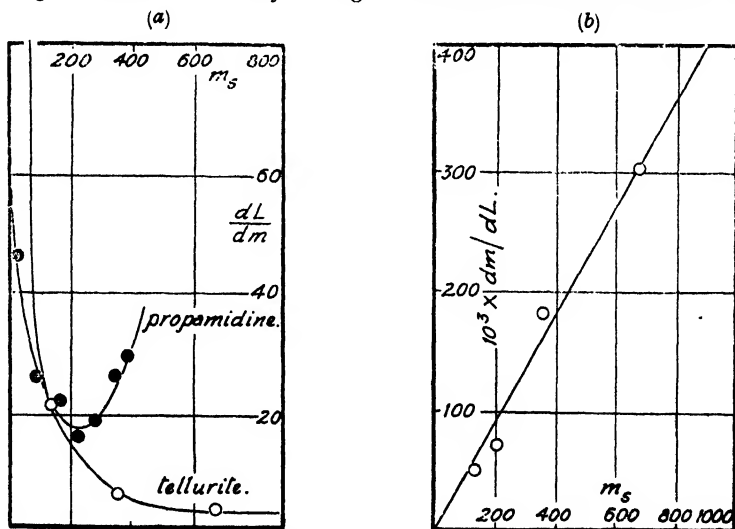


FIG. 3.—Relation between slopes and  $m_s$ .

*Bact. lactis aerogenes* is trained in potassium tellurite. The separate

curves resemble those obtained with proflavine in that they slope sharply upwards towards an infinite value of the lag, except for the highest values of  $\bar{m}$ . Once again there is almost complete immunity to any test concentration of drug up to  $\bar{m}$ . The spacing relationships are, however, different from those shown by the proflavine family, and if  $m_s$  is plotted against the training concentration  $\bar{m}$ , Fig. 2 is obtained, which is expressed by the relation  $m_s = 7.1 \bar{m} + 6$ . Moreover, the slopes of the curves where they cut the line  $\Delta L = 1000$  min., gradually decrease as  $m$  increases. Fig. 3a shows the value of  $d(\Delta L)/dm$  at  $\Delta L = 1000$  plotted against  $m_s$ , and Fig. 3b shows that  $dm/d(\Delta L)$  plotted against  $m_s$  gives approximately a straight line.

### Adaptation to Propamidine.

Propamidine was used in the form of its dihydrochloride. The family of lag-concentration curves obtained is shown in Fig. 4. The individual

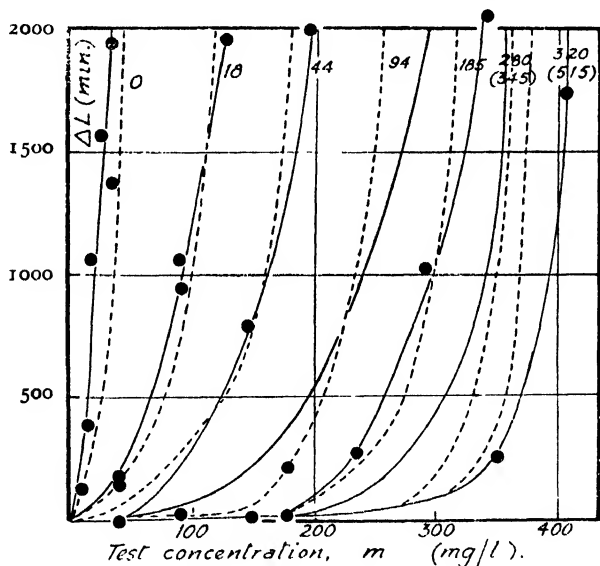
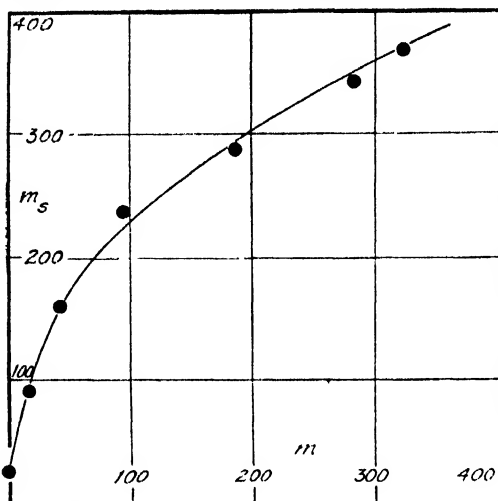


FIG. 4.—Lag-concentration curves for *Bact. lactis aerogenes* trained in propamidine.

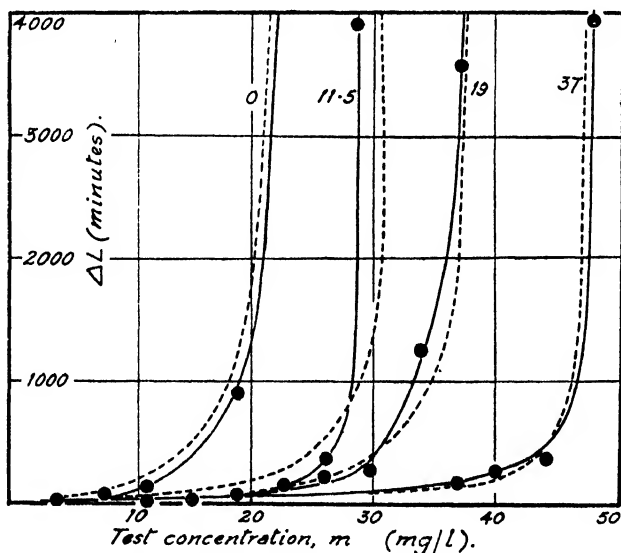
Numbers on curves indicate concentration of drug during training. (For the two highest concentrations the numbers in brackets indicate the experimental concentrations while the first numbers given are the concentrations to which immunity was in fact achieved in the time of training.)

curves are similar in shape to those for proflavine and potassium tellurite and almost complete immunity to any test concentration up to  $\bar{m}$  is observed except for the two most highly trained strains. With these, adaptation had occurred extremely slowly and it is very likely that the limiting degree of adaptive response had not been obtained. The spacing between the curves is at first large for small increments of  $\bar{m}$  but as the latter increases the curves gradually close up on each other till, apparently at least, a limit to the possible degree of adaptation is reached. This is shown more clearly by the curve relating  $m_s$  and the training concentration  $\bar{m}$  (Fig. 5). The slopes at  $m = m_s$  at first decrease as  $m_s$  increases, pass through a minimum when  $m_s$  is about 200 mg./l. and then increase once more (Fig. 3a).

FIG. 5.—Relation of  $\bar{m}$  and  $m_s$  for propamidine.

### Adaptation to 5-Aminoacridine.

Fig. 6 shows the family of curves obtained in experiments with 5-aminoacridine hydrochloride—which bears a close structural resemblance

FIG. 6.—Lag-concentration curves for *Bact. lactis aerogenes* trained in 5-aminoacridine.

Numbers on curves indicate concentration of drug during training.

to proflavine. The usual form of lag-concentration curve is found but complete adaptation to concentrations higher than 45-50 mg./l. appears to be impossible. Training at lower concentrations than this does, however, lead to a strain showing little or no lag at that particular concentration.

The spacing of the curves is initially similar to the spacing observed with proflavine; i.e. the  $m_s - \bar{m}$  curve is initially a straight line of unit slope.

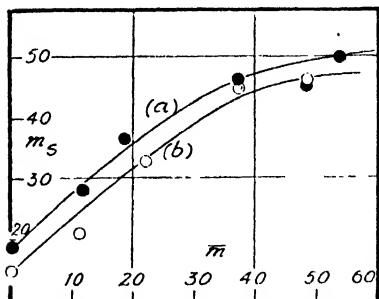


FIG. 7.—Relation of  $\bar{m}$  and  $m_s$  for 5-aminoacridine (a), and 2:7-diaminoacridine (b).

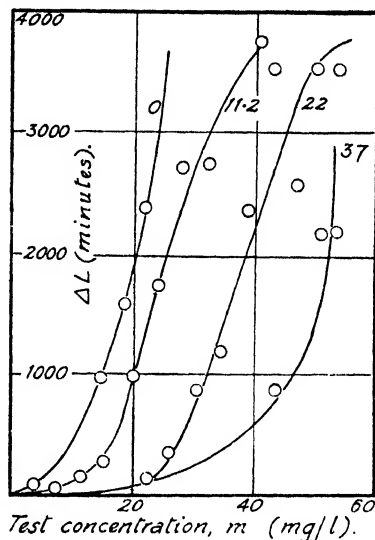


FIG. 8.—Lag-concentration curves for *Bact. lactis aerogenes* trained to 2:7-aminoacridine.

However, as the drug concentration increases the curves gradually crowd together so that  $m_s$  reaches an upper limit (Fig. 7a). There is no significant trend in the slopes of the curves at the points where  $\Delta L = 1000$  min.

### Adaptation to 2:7-Diaminoacridine.

Fig. 8 and 7b show that the lag-concentration curves obtained by training to 2:7-diaminoacridine hydrochloride bear a close qualitative resemblance to those obtained with 5-aminoacridine.

### Discussion.

#### An Enzyme Model to Account for Adaptation.

A hypothesis to account for adaptation to proflavine and Methylene Blue has been put forward in previous papers. It is based on the fact that training to these inhibitors ultimately leads to a strain which has a constant activity in their presence. Cells acquire biochemical properties (nature and proportions of enzymes) characteristic of the environment to which they have been adapted. If the latter is altered the biochemical properties often tend towards a new stable state characteristic of the new conditions. Further, it has been found that, in general, the stable state, reached in the presence of an inhibitor, has the same apparent enzyme activity (as measured by the overall growth rate) as the original stable state in the absence of the drug. Calculations can be made based upon kinetic equations which are assumed for a sequence of processes in the cell and including the inhibited process. These equations relate the rate of expansion of the enzymes with their own concentrations and those of the corresponding substrates. The ratios of the enzyme masses can be shown to tend to stable values—in fact to the state where their specific rates of increase are equal. If now an inhibitor slows down the synthesis of a part of the enzyme system on which division depends, the relatively greater activity and expansion of the non-inhibited parts will compensate



for the inhibition by increasing the concentrations of substrates supplied to one or several of the inhibited processes. The uninhibited parts of the cell substance increase in relative amount till all the processes once more show the same specific growth rate—i.e. the enzymes double in amount in the same interval of time. With a new stable ratio of enzymes now set up, the growth rate and lag are the same in the presence of the drug as for the original cells in a drug-free medium.

### The Relation between Lag and Enzyme Activities.

It is a convenient working hypothesis to assume the lag to be inversely proportional to the rate of synthesis of an inhibited enzyme. We can temporarily avoid choosing any more specific hypothesis by defining an enzyme activity  $R$  by means of the expression,  $\text{lag } L = A/R$ , where  $A$  is a constant. It is an experimental fact that adaptation restores the lag to its normal value  $L_0$  corresponding to an activity  $R_0$ . Now  $R$  is a function of the amount of enzyme  $x$ , the concentrations of substrate, and the concentration  $m$  of the inhibitor. We write

$$R = G \cdot x \cdot \{f(s) - \phi(m)\} \quad (1)$$

where  $G$  is a constant and  $f(s)$  and  $\phi(m)$  are the appropriate functions of substrate and drug concentrations respectively. These functions are assumed independent. For untrained cells with no drug,  $R = R_0$  and  $\phi(m) = 0$ .

$$R_0 = G \cdot x \cdot f(s_0) \quad (2)$$

where  $s_0$  is the normal stationary concentration of substrate. When the drug concentration is  $m$ ,  $R$  has, with untrained cells, the lower initial value

$$R = G \cdot x \cdot \{f(s_0) - \phi(m)\} \quad (3)$$

but is restored to the value  $R_0$  by adaptation involving a rise in  $s$  to  $s_m$ . We now have

$$R_0 = G \cdot x \cdot \{f(s_m) - \phi(m)\} \quad (4)$$

From equations (2) and (4) we have

$$f(s_0) = f(s_m) - \phi(m)$$

or

$$f(\bar{m}) = f(s_0) + \phi(m) \quad (5)$$

where  $\bar{m}$  is now the symbol for the training concentration. We may now consider a standard activity  $R'$  which corresponds to a lag of 1000 min.—i.e. to  $m_s$  values. In general, from (3) and (4)

$$R' = G \cdot x \cdot \{f(s_0) + \phi(\bar{m}) - \phi(m_s)\} \quad (6)$$

where  $m_s$  is the test concentration causing a lag of 1000 min. for a strain trained to a concentration of  $\bar{m}$ .

From a family of lag-concentration curves we can derive a curve relating  $m_s$  and  $\bar{m}$  (Fig. 2, 5, 7). From equation (6) we have

$$\phi(\bar{m}) - \phi(m_s) = R'/Gx - f(s_0).$$

For a given drug, the right-hand side should be a constant, since  $R'$  and  $x$  have standard values ( $x$  has a constant average over a large number of cells). Hence

$$\phi(m_s) - \phi(\bar{m}) = B \quad (7)$$

where  $B$  is a constant.

Since we know the relation between  $m$  and  $\bar{m}$ , the relation between  $\phi(m)$  and  $m$  can be expressed, either in the form of an empirical expression or, failing that, graphically. The  $\phi(m)$ - $m$  relations provide a basis for the calculation of lag-concentration curves—comparison of which with experimental curves will provide certain tests of the theory. The method of calculating lag-concentration curves from the  $\phi(m)$ - $m$  curves is as follows:

$L = A/R$ , and in the absence of drug  $L_0 = A/R_0$ , so that we have  $\Delta L = L - L_0 = A \left[ \frac{1}{R} - \frac{1}{R_0} \right]$  and with the values of  $R$  and  $R_0$  given by equations (1), (2) and (5) we find

$$\Delta L = \frac{A}{Gx} \left[ \frac{1}{\{f(s_0) + \phi(\bar{m}) - \phi(m)\}} - \frac{1}{\{f(s_0) + \phi(\bar{m})\}} \right] \quad (8)$$

In equation (8) the two constants  $A/Gx$  and  $f(s_0)$  can be found from the experimental curve for the *untrained* strain itself. Then, with the aid of the  $\phi(m)$ - $m$  relation, the whole family of lag-concentration-curves can be calculated.

Fig. 9 shows the  $\phi(m)$ - $m$  curves for proflavine (a)—a straight line,

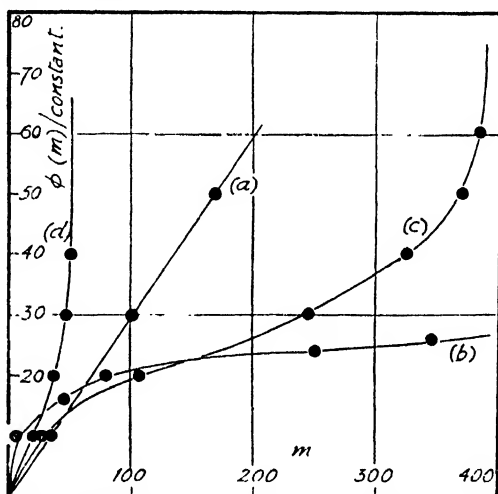


FIG. 9.— $\phi(m)$ - $m$  relations for proflavine (a), potassium tellurite (b), propamidine (c) and 5-aminoacridine (d).

potassium tellurite (b), propamidine (c), 5-aminoacridine (d). By use of these in conjunction with equation (8), the families of lag-concentration curves shown as dotted lines in the figures were calculated.

### Comparison of Experiment and Theory.

The constants of equation (8) are chosen to fit one single curve of a lag-concentration family and the derivation of  $\phi(m)$  depends upon the experimentally observed relation of  $m_s$  to  $\bar{m}$ . Thus the calculated lag-concentration curve for untrained cells should follow the experimental one, and the rest of the curves must intersect the line  $\Delta L = 1000$  at the correct points. There is nothing in this choice of constants or of  $\phi(m)$ , however, which necessarily imposes the right shape on these remaining curves. In particular, the slopes of the curves at the points where  $m = m_s$  depend on the hypothetical expressions used in deriving equation (8). That, in fact, there is a reasonable fit between the calculated and observed curves is not automatic and provides some measure of support for the theoretical treatment.

### Slopes $dL/dm$ at $m_s$ .

In expressing the slope it is simpler to use the expression for actual lag  $L$  rather than for the increase in lag,  $\Delta L$ . This causes little error as  $L_0$  is insignificant.

$$L = \frac{A}{Gx} \frac{1}{\{f(s_0) + \phi(\bar{m}) - \phi(m)\}}$$

so that

$$\frac{dL}{dm} = \frac{GxL^2}{A} \cdot \frac{d\{\phi(m)\}}{dm} \quad (9)$$

When  $m = m_0$ ,  $L = 1000$  and  $\frac{GxL^2}{A}$  is thus constant. Equation (9) can be used to correlate the experimentally observed slopes with predictions from  $\phi(m)$ - $m$  curves.

(1) Proflavine. The  $\phi(m)$ - $m$  curve is linear so that  $d\{\phi(m)\}/dm$  is constant. This means (eqn. (9)) that  $(dL/dm)_0$  is constant—as is indeed found.

(2) Potassium tellurite. The  $\phi(m)$ - $m$  curve can be described empirically by the equation  $\phi(m) = a \log (1 + bm)$  where  $a$  and  $b$  are constants—a consequence of the relation  $m_0 = 7.1 \bar{m} + 6$ . Hence,  $\frac{d\{\phi(m)\}}{dm} = \frac{ab}{1 + bm}$ . From equation (9) we have

$$\left(\frac{dL}{dm}\right)_0 = \text{constant} \cdot \frac{d\{\phi(m)\}}{dm} = \frac{\text{constant } ab}{1 + bm_0}.$$

This means that  $(dm/dL)_0$ , plotted against  $m_0$ , should give a straight line—as is actually observed (Fig. 3b).

(3) Propamidine. The  $\phi(m)$ - $m$  curve has a point of inflection where  $m$  is about 200. At this point, therefore,  $\frac{d^2\{\phi(m)\}}{dm^2} = 0$  and this should, by equation (9), correspond to a minimum value of the slope in agreement with Fig. 3a. The experimental data are, however, not accurate enough to define the position of the minimum with certainty.

(4) 5-Aminoacridine and 2:7-diaminoacridine.  $d\{\phi(m)\}/dm$  is constant over part of the range and then rapidly increases. Corresponding to this  $dL/dm$  at the  $m_0$  point is constant over a large range. The increase at higher values of  $m$  was not detected but the results for this region are incomplete.

### Conclusion.

The behaviour of *Bact. lactis aerogenes* on training to these various inhibitors is consistent with the enzyme expansion hypothesis earlier suggested to explain adaptation to proflavine and Methylene Blue. Such differences in behaviour as exist with various drugs appear to reside in the differing forms of curve relating inhibitor concentration to the activity of the inhibited process. While this curve is, it seems, linear in the case of proflavine, with the other drugs studied departure from linearity is observed. The effect of this depends on the particular strain of cells. Referring, for example, to the  $\phi(m)$ - $m$  curve obtained with potassium tellurite, we see that a concentration  $m_1$  might completely inhibit an untrained strain, the curve up to this point being approximately linear. A strain that has undergone some training will need a higher concentration  $m_0$  of drug for complete inhibition, and at  $m_0$  the curve may show considerable departure from linearity.

The relation, activity  $R = G \cdot x \cdot \{f(s) - \phi(m)\}$ , corresponds best to a drug action depending on adsorptive blocking of an enzyme, but other mechanisms might also give such a relation.

The various forms of curve might, alternatively, result from the simultaneous action of individual drugs on more than one cell process. In such cases adaptation by relative enzyme expansion would still be probable, but the relations would tend to be more complex than in the simple proflavine case.

The fact that a whole series of strains can be obtained with properties which are quantitatively characteristic of a particular drug and a particular concentration suggests strongly that adaptation to these inhibitors consists fundamentally in the modification of individual cells. The alternative hypothesis of the selection of resistant types present in the original culture, or of resistant mutants arising independently of the drug, could not, without arbitrary auxiliary assumptions, explain the formation of the continuous range of strains which, individually, show immunity up to the training concentration but not beyond. A selection process would tend to increase the proportion of *all* cells immune to the drug, without any quantitative relation to  $\bar{m}$ .

The following paper of this series will show how this view is supported by results on the rate of training and on the reversion of adaptation.

### Summary.

*Bact. lactis aerogenes* has been trained by growth in presence of potassium tellurite, propanidinc, 5-aminoacridine and 2:7-diaminoacridine, and subjected to a quantitative study similar to that previously made with proflavine. Cells trained at a concentration  $\bar{m}$  have been tested over a whole range of concentrations of drug. Lag-concentration relations have been determined for a series of values of  $\bar{m}$ , thus giving families of curves, the shape and spacing of which is characteristic of the various drugs. By a theoretical treatment it is possible to correlate the spacing of the curves in the family with the shapes of the individual curves. The results as a whole are regarded as consistent with the hypothesis that adaptation occurs by change in the enzyme balance of individual cells rather than by selection of resistant types.

### Résumé.

Le *Bact. lactis aerogenes* a été adapté par culture en présence de tellurite de potassium, de propanidine, d' amino-5-acridine et de diamino-2-7-acridine; il a été soumis à une étude quantitative, semblable à celle faite précédemment avec la proflavine. Les cellules, adaptées à la concentration  $\bar{m}$ , ont été éprouvées dans un vaste domaine de concentration en drogue. Des relations: concentration—retard à la multiplication ont été déterminées pour une série de valeurs de  $\bar{m}$ , donnant ainsi des familles de courbes, dont la forme et l'écartement sont caractéristiques des différentes drogues employées. Un traitement théorique permet d'établir l'allure des courbes individuelles et l'écartement des courbes dans une même famille. Les résultats dans l'ensemble s'accordent avec l'hypothèse selon laquelle l'adaptation est due à une variation de l'équilibre enzymatique des cellules individuelles, plutôt qu'à une sélection des types résistants.

### Zusammensetzung.

*Bact. lactis aerogenes* ist durch Züchtung in der Gegenwart von Kaliumtellurit, Propamidin, 5-Aminoakridin und 2:7-Diaminoakridin an diese Substanzen gewöhnt worden und auf ähnliche Weise wie mit Proflavin quantitativen Beobachtungen unterworfen worden. Zellen, die bei einer Konzentration  $\bar{m}$  gezüchtet worden waren, wurden für ein ganzes Bereich von Konzentrationswerten untersucht. Die Beziehung zwischen dem Zeitintervall vor Einsetzen der Vermehrung und der Konzentration ist für eine Reihe von  $\bar{m}$ -Werten bestimmt worden, sodass Gruppen solcher Kurven erhalten wurden, deren Formen und Abstände für die verschiedenen Drogen charakteristisch sind. Die Theorie gestattet, die Abstände der Kurven innerhalb einer Kurvengruppe mit den Formen der einzelnen Kurven in Zusammenhang zu bringen. Es wird die Meinung vertreten, dass Anpassung durch Veränderung der Enzymzusammensetzung der einzelnen Zellen eher als durch Züchtung widerstandsfähiger Typen erfolgt.

*Physical Chemistry Laboratory,  
Oxford University.*

# THE STABILITY OF THE ADAPTATION OF *BACT. LACTIS AEROGENES* TO PROFLAVINE.

BY J. M. PRYCE AND C. N. HINSELWOOD.

Received 22nd July, 1946.

## Adaptation to Lower Concentration.

Previous work has shown that *Bact. lactis aerogenes* trained by several subcultures in low concentrations of proflavine retains the acquired immunity during repeated subculture in the absence of the drug.<sup>1</sup> It has also been shown that after as few as 1-3 cell divisions with the drug present, the immunity to proflavine (at the concentration in question)

TABLE I.

SERIES I.—(Medium of parent culture contained 50 mg./l. proflavine : initial count 32 units.)

Reference Letter of Sub-strain.	Time from Inoculation of Parent. Minutes.	Count of Parent.	Lag in Norml Medium.	Lag in 43 mg./l. Proflavine.	ΔL.	No. of Cell Divisions of Parent.
<i>H</i> <sub>1</sub>	915	32	<900	4000	+c. 3500	0
<i>H</i> <sub>2</sub>	1010	29	<800	2445	+c. 2500	0
<i>H</i> <sub>3</sub>	1240	44	300	<700	<370	0.4
<i>H</i> <sub>4</sub>	1280	88	200	<700	<450	1.5
<i>H</i> <sub>5</sub>	1345	176	100	280	180	2.4
<i>H</i> <sub>6</sub>	1410	175	70	210	140	2.4
<i>H</i> <sub>7</sub>	1600	308	110	460	350	3.3
<i>H</i> <sub>8</sub>	2410	505	210	410	170	4.0

SERIES II.—(Medium of parent culture contained 48 mg./l. proflavine : initial count 32 units.)

<i>F</i> <sub>1</sub>	910	81	165	415	250	1.3
<i>F</i> <sub>2</sub>	1010	148	100	330	230	2.2
<i>F</i> <sub>3</sub>	1140	180	90	245	155	2.5
<i>F</i> <sub>4</sub>	1235	182	5	150	145	2.5
<i>F</i> <sub>5</sub>	1345	262	110	130	20	3.0
<i>F</i> <sub>6</sub>	1655	280	<390	<390	<390	3.2
<i>F</i> <sub>7</sub>	2410	310	655	<1100	<445	3.3
<i>F</i> <sub>8</sub>	4440	520	950	1150	200	4.1

NOTE.—Growth in Series II was accompanied by the formation of numerous filamentous cells instead of the short rod forms observed in Series I.

is considerable. The stability of this very rapidly attained adaptation has now been studied, the experimental methods being as described in previous papers.<sup>2</sup>

A tube of the usual synthetic medium with addition of 48-50 mg./l. proflavine received a large inoculum of untrained *Bact. lactis aerogenes* : for several hours no multiplication occurred, but later rapid growth set in. At intervals during the growth cycle cell counts were made and standard

<sup>1</sup> Davies, Hinshelwood and Pryce, *Trans. Faraday Soc.*, 1944, 40, 397.

<sup>2</sup> See <sup>1</sup>; Davies Hinshelwood and Pryce, *ibid.*, 1945, 41, 163, 778; Postgate and Hinshelwood, *ibid.*, 1946, 42, 45.

0.1 cc. inocula were transferred in parallel into (a) the normal medium and (b) similar medium with 43 mg./l. proflavine. The lags were measured, the comparison of those in (a) and those in (b) affording an estimate of the degree of adaptation to the drug. Table I shows the results of two such experiments.

The lag of a normal inoculum (0.1 cc. with a count of 400 units) into 43 mg./l. proflavine is from 1500-2000 min.: inspection of Table I shows therefore that adaptation, as far as lag is concerned, is almost complete as soon as the population of cells has undergone a moderate increase in presence of the drug. This extremely rapid adaptation is not halted by the formation of filaments as in Series II. Moreover, ageing of the cells in the presence of the drug for 4000 min. causes no loss of the immunity acquired earlier in growth (compare strains  $F_8$  and  $F_6$  or  $F_4$ ). The immunity acquired after so little growth in the presence of the drug proves, however, to be unstable. Table II records the minimum lags shown in

TABLE II.

Sub-strain.	$\Delta L$ before Growth in Normal Medium Minutes.	$\Delta L$ after Growth in Normal Medium Minutes.
$H_1$	c. 3500	800
$H_3$	< 370	740
$H_6$	140	720
$H_8$	170	720
$F_1$	250	720
$F_3$	155	790
$F_6$	20	770
$F_7$	< 445	{ 130*
$F_8$	200	{ 710
		{ 710

\* 130 after 2 subcultures, 710 after 10 subcultures.

43 mg./l. proflavine by the various sub-strains derived from the above experiments after they have been subcultured 2 or 3 times in a drug-free medium.

A large part of the immunity is seen to be lost:  $\Delta L$  for all the "reverted" strains is about 750 min. (Completely untrained cells give  $\Delta L$  of 1500-2000 min.) With sub-strain  $F_7$ , the immunity survived 2 subcultures in normal medium but not 5 subcultures. Sub-strain  $H_1$ , although removed from the parent culture near the end of the lag phase for an unexplained reason behaved like the other sub-strains. (The partial immunity acquired by  $H_1$  may be connected with increase in cell size during the lag, or the early division of a small proportion of the cells. Why this immunity is "developed" by passage through the normal medium is not known.)

The behaviour of more thoroughly trained cultures was next studied further. Normal cells were adapted to 43 mg./l. proflavine by 15 subcultures. The resulting strain was tested in 43 mg./l. proflavine both at this stage and after various numbers of subcultures in a drug-free medium. Fig. 1 shows the minimum lags in proflavine (43 mg./l.) plotted against the number of "de-training" subcultures in the normal medium. The first 4 or 5 subcultures caused little reversion, the full extent of which appeared almost entirely in the 6 subsequent subcultures. The resulting strain still retains a certain degree of immunity to proflavine: for completely untrained cells the lag is 1500-2000 min. A similar result was obtained with another strain which only reverted after 10 subcultures in the normal medium.



training to the stage of stability. On subculture in the normal medium, partial reversion to the required state occurred, but no further loss of the residual proflavine immunity took place during many subsequent subcultures. This strain gives an unusual type of lag-concentration curve in proflavine: <sup>8</sup> with increasing drug concentration the lag first shows a progressive increase, and then settles down to a fairly high value showing little systematic change over a wide range of high concentrations.

It seemed likely that the "equilibrium" strain might consist of a mixture of strain-types each characterised by a particular level of proflavine-adaptation. This was subjected to experimental test, by isolation of strains from single colonies derived from the parent equilibrium strain. A dilute culture of the latter was inoculated on to agar-glucose solid media in Petri dishes where, after 24 hours, colonies appeared, each probably derived from a single parent cell. Eight such colonies were transferred to separate tubes of sterile bouillon and the resulting cultures were again plated in 8 more Petri dishes. One colony was again transferred from each plate and, in this way 8 pure strains were isolated from the original equilibrium strain. They were grown in the usual synthetic medium, then submitted to test for their proflavine resistance, and the lag-concentration curves determined.

TABLE III.

Strain.	$m_{3000}$ .
1	61
2	126
3	47
4	43
5	47
6	158
7	105
8	47

NOTE.— $m_{3000}$  is the concentration (mg./l.) of proflavine required to cause a lag of 3000 min.

Fig. 2 shows the curves, obtained for the strains (numbered 1-8) and Table III gives a numerical indication of the departure from homogeneity.

It is clear that either the "equilibrium" strain is in fact a mixture of sub-strains with differing degrees of proflavine adaptation, or that the process of cultivation on the solid medium has induced, in varying degrees, a further reversion. To test this latter possibility several of the derived strains were again plated out and shown respectively to give colonies of unaltered proflavine resistance. Thus the plating process itself is not responsible for the differences, and the equilibrium strain is proved to have been a mixture of types, each stably trained to a given level of resistance. Some of the individual components behaved as untrained strains.

### Discussion.

#### (a) General Pattern of Adaptation-reversion Relationships.

It now appears that in training cells to proflavine, whether at lower or at higher concentrations, the following stages are passed through successively: (1) instability—immediate reversion in drug-free medium, (2) instability—delayed reversion, (3) stability—no reversion. This same picture has recently been found in other examples, namely the adaptation of *Bact. lactis aerogenes* to utilise lactose,<sup>4</sup> or glycerol,<sup>5</sup> and is probably a general one. Reversion when it occurs need not be complete: but a stable lower level of immunity may be reached.

#### (b) Selective Changes in the Population Balance.

If it could be shown that proflavine-trained cells were at a disadvantage in the drug-free medium compared with untrained cells, many of the facts

<sup>4</sup> Postgate and Hinshelwood, *Trans. Faraday Soc.*, 1946, **42**, 45.

<sup>5</sup> Unpublished experiments of E. G. Cooke.



of reversion would receive a convenient explanation. But there is already some evidence against this supposition to the extent that the actual growth rate in the synthetic medium is the same for all types of cell, adapted and unadapted.

Even if other factors such as possible viability changes are thought to make this argument inconclusive, the experiments on the "equilibrium" strain provide good evidence that the trained and untrained cells behave similarly in the ordinary medium. This strain is proved to be highly heterogeneous. Yet its lag-concentration relations in proflavine remain constant during repeated subcultures. Therefore the proportions of the different types are not changing during growth in the normal medium. The loss of adaptation which occurs during the reversion to the equilibrium strain from the fully adapted strain must therefore have been due to changes in the individual cells and not to a shift in the proportions of different sub-strains. The conditions of unstable or stable adaptation must therefore be characteristics of the cells themselves, and not reflections of the impurity or purity of the trained strains.

In the very highly trained, but incompletely stabilised strain, therefore, it appears that some cells have progressed further in their training than others. Different cells suffer varying degrees of reversion on return to the ordinary medium. The general level of stable adaptation rises during training, but lags behind that of the unstable adaptation.

### (c) Characteristics of the Trained Strains Obtained by Partial Reversion.

It is clear from Fig. 2 that several of the curves are different in actual form from those given by strains directly trained to proflavine.<sup>6</sup> With the isolated "reverted" strains, the lag rises gradually and only reaches very high values at concentrations of 100-200 mg./l. With the directly trained strains there is virtually no lag up to a certain concentration  $\bar{m}$ , after which the curve turns up sharply towards infinite lag at about  $\bar{m} + 50$ .

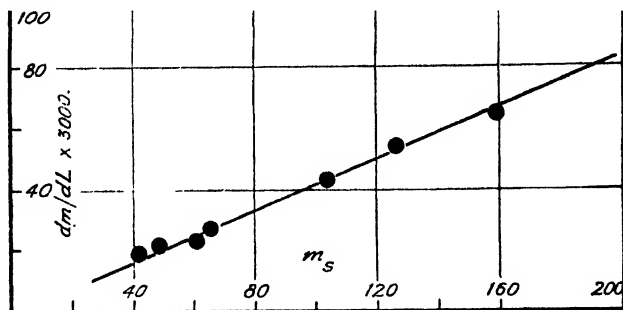


FIG. 3.

The difference in form of the curves is most clearly shown as follows. With directly trained cells the slopes of the curves,  $dm/dL$ , measured at a given value of  $L$ , are the same for all strains.<sup>7</sup> With the reverted strains, however, the slopes vary. In Fig. 3,  $dm/dL$  for  $L = 3000$ , is plotted against  $m_{3000}$  for the strains isolated from the "equilibrium" strain. The line has a strong positive slope (compare the results with potassium tellurite),<sup>7</sup> whereas for a family of curves derived from directly trained cells it would be horizontal.

<sup>6</sup> Davies, Hinshelwood and Pryce, *Trans. Faraday Soc.*, 1945, 41, 163  
 Pryce, Davies and Hinshelwood, *ibid.*, 1945, 41, 465.

<sup>7</sup> See previous paper.

Since we are dealing with isolated homogeneous strains the conclusion must be drawn that the reversion is not merely a symmetrical reversal of the adaptation. The enzyme constitution of the reverted strains—in a quantitative or qualitative sense—does not exactly correspond to that of any of the intermediate strains obtained when normal cells are progressively trained. These facts indicate that the complete explanation of reversion is not to be found in terms of the simple enzyme model alone but that secondary adjustments of the kind discussed in a previous paper<sup>3</sup> must also be taken into account.

### Summary.

Resistance of *Bact. lactis aerogenes* to low concentrations of proflavine develops rapidly during growth in presence of the drug, being almost complete by the time the bacterial mass has increased a few times. This rapidly attained adaptation is unstable and is lost on one subculture in the drug-free medium. Further subcultures in the presence of the proflavine lead, however, to a stably adapted strain. There is an intermediate stage from which reversion to the unadapted state only sets in after a delay corresponding to several consecutive subcultures in the normal drug-free medium.

The same sequence of events occurs on training to high concentrations: but much longer is required for the adaptation to become complete. Return to the ordinary medium before stability is reached gives partial reversion, not to the unadapted state but to an "equilibrium" condition in which a certain lower degree of drug-resistance is stably retained. Comparison with other investigations suggests that the sequence: immediate reversion: delayed reversion: stable adaptation, is a general one.

Certain quantitative results found with the "reverted" strains of cells suggest that loss of adaptation may not follow a path which is strictly the reverse of that followed during adaptation.

The phenomena of reversion cannot be explained in terms of a shift in population balance, since mixed strains with different levels of drug resistance are shown not to change their proportions on subculture in the ordinary medium.

### Résumé.

Le *Bact. lactis aerogenes* devient rapidement résistant à de faibles concentrations de proflavine au cours de la culture en présence de ce produit. Cette adaptation est instable et est perdue par un repiquage dans un milieu sans proflavine. Des repiquages successifs en présence de cette dernière donnent une variété stablement adaptée. Il existe aussi un stade intermédiaire, où il y a réversion retardée. On rencontre le même ordre dans l'adaptation à fortes concentrations et la comparaison avec d'autres recherches suggère que la suite: réversion immédiate, réversion retardée, et adaptation, est générale. Les résultats obtenus avec des variétés revenues au type primitif font penser que la perte d'adaptation peut ne pas suivre exactement le chemin inverse de l'adaptation. Le phénomène de réversion ne peut pas être expliqué par un changement de l'équilibre de population.

### Zusammenfassung.

Die Widerstandsfähigkeit von *Bact. lactis aerogenes* gegen niedrige Konzentrationen von Proflavin entwickelt sich äusserst rasch im Verlauf des Wachstums in Gegenwart der Droge. Die Anpassung ist instabil und geht nach einer Überpflanzung in eine drogenfreie Nährlösung verloren. Weitere Überpflanzungen in Tochterkulturen in der Gegenwart von Proflavin führen zu einer stabil adaptierten Zucht. Es besteht auch eine Übergangsstufe mit verzögerter Rückveränderung. Die gleiche Folge wird bei Züchtung in höheren Konzentrationen gefunden und ein Vergleich mit anderen Untersuchungen deutet darauf hin, dass diese Aufeinanderfolge (sofortiger Rückschlag, verzögerter Rückschlag, stabile Anpassung) eine allgemeine ist. Ergebnisse mit rückveränderten Zuchten weisen darauf hin, dass der Verlauf des Anpassungsverlusts nicht genau die Umkehrung des Anpassungsverlaufs ist. Die Erscheinung der Rückveränderung kann nicht durch eine Verschiebung in der Zuchtzusammensetzung erklärt werden.

# SOME FURTHER STUDIES ON THE MORPHOLOGY OF *BACT. LACTIS AEROGENES*.

BY A. M. JAMES AND C. N. HINSHELWOOD.

Received 30th July, 1946.

When *Bact. lactis aerogenes* which has been cultivated in bouillon is transferred to an artificial medium consisting of glucose, ammonium sulphate, magnesium sulphate and phosphate buffer, long snake-like cells or filaments are formed if the glucose concentration lies below a certain limit.<sup>1, 2</sup> A similar abnormality is observed to accompany growth of the bacterium in presence of *m*-cresol<sup>3</sup> or of proflavine.<sup>4</sup> The present work is a study of (1) the effect on abnormal growth of the temperature at which the cells are grown and tested; (2) the effect of additions of salt on the induced filament formation in presence of drugs.

As a convenient measure of the abnormality of the size distribution the coefficient,  $\sigma$ , defined previously by the relation

$$\sigma = \sum_{l=3}^{l=\infty} l\nu_l$$

is adopted, where  $\nu_l$  is the number of cells in unit range in the neighbourhood of  $l$  ( $l$  being the length measured in arbitrary units).  $\sigma$  gives a good representation of the abnormality values greater than about 10 corresponding to recognisable, and values of 100 to very marked, degrees.

## Experimental.

The artificial medium consisted, as before, of ammonium sulphate (0.96 g./l.) potassium dihydrogen phosphate (3.46 g./l.) brought to  $pH$  7.1 with sodium hydroxide, magnesium sulphate (0.04 g./l.) and glucose. The normal concentration of the latter was 40 g./l. When first inoculated from bouillon into media containing 2 g./l. instead of the customary 40, the cells grew into the filamentous forms referred to above. For the desired comparisons, it was essential to grow several cultures from identical inocula. The following method was therefore adopted. Ten loops of a culture in bouillon were transferred into the artificial medium: this was aerated for a short time and 5 ml. portions were then added to each of 5 dilute glucose media of 20 ml. volume. These latter were then subjected to observation under the required conditions. From the time when slight turbidity appeared, samples were removed at intervals and examined, and  $\sigma$  was plotted against  $n$ , the total count. The resulting curve shows a maximum as in Fig. 1.

For the experiments with proflavine and *m*-cresol, the standard synthetic medium (40 g./l. glucose) was used throughout, and to it was added the requisite amount of more concentrated solutions of the drugs to give 700-1000 mg./l. *m*-cresol or 40-55 mg./l. proflavine respectively. The inocula were 0.2 ml. of a normal culture at its stage of minimal lag.

<sup>1</sup> Hinshelwood and Lodge, *Proc. Roy. Soc. B*, 1944, **132**, 47.

<sup>2</sup> Lodge and Hinshelwood, *Trans. Faraday Soc.*, 1943, **39**, 420.

<sup>3</sup> Spray and Lodge, *ibid.*, 1943, **39**, 425.

<sup>4</sup> Davies, Hinshelwood and Pryce, *ibid.*, 1944, **40**, 397.

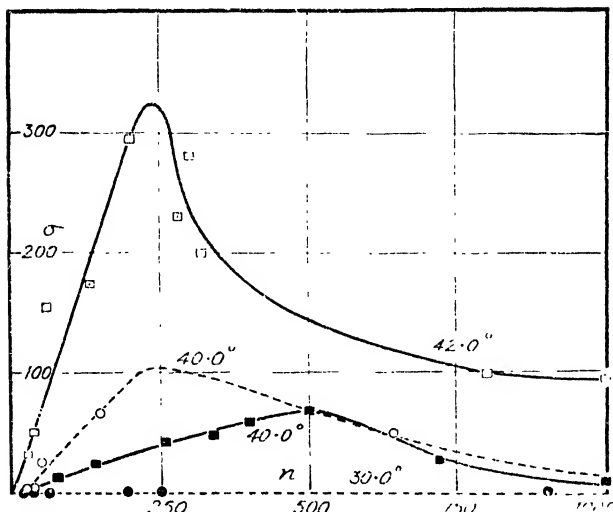


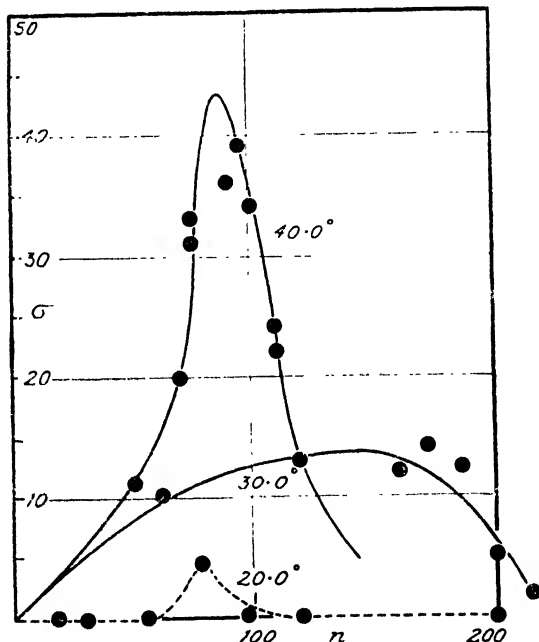
FIG. 1. Influence of temperature on filament formation in dilute glucose artificial medium.

$\sigma$  = coefficient of abnormal size distribution;  $n$  = total count;  
dotted lines: culture 1; continuous lines: culture 2.

### Temperature Effects.

By the method described, a series of dilute glucose media were inoculated from bouillon and the cultures grown at 30°, 40.0° and 42.0° C.

FIG. 2.—Influence of temperature on filament formation induced by *m*-cresol (780 mg./l.).



respectively. From Fig. 1 it can be seen that increase in temperature enhances the abnormal growth. Furthermore, it was observed that at

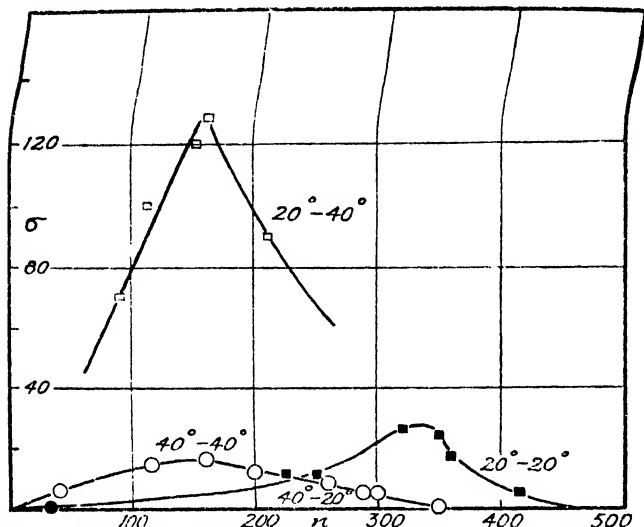


FIG. 3.—Influence of training temperature and test temperature on the formation of filaments induced by proflavine. The first mentioned temperature is the training temperature, the second that of the test.

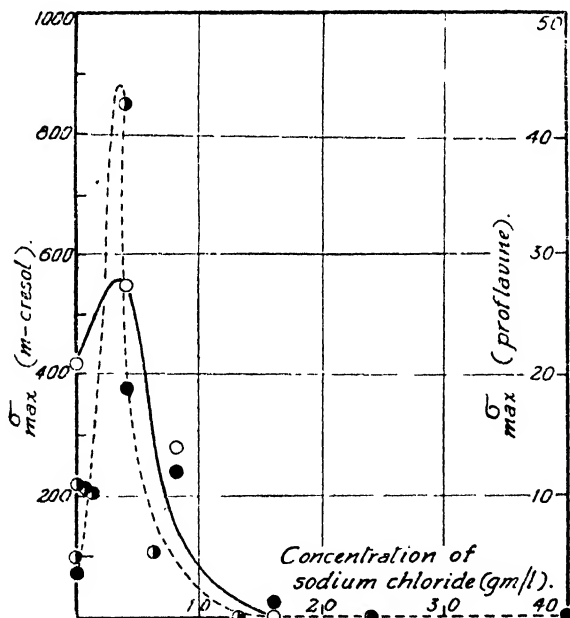


FIG. 4.—Influence of NaCl additions on filament formation induced by  $m$ -cresol (709 mg./l.) and by proflavine (43 mg./l.). The dotted line refers to two sets of observations with cresol, the continuous line to those with proflavine. Note different scales, left and right.

$42^{\circ}$  c. the exceptionally long cells, instead of dividing towards the end of the logarithmic phase, persisted. In the next series of experiment, identical inocula from a culture which had been adapted by repeated growth at  $40.0^{\circ}$  c. were made into media containing appropriate amounts

of *m*-cresol or proflavine: and tests were made at 20°, 30°, 40° and 42° C. Once again it appeared that abnormal growth was greatly favoured by increased temperature (Fig. 2).

One sub-strain of the *Bact. lactis aerogenes* was subcultured daily at 20.0° C. for some months in the normal medium. Inocula from this were transferred to media containing *m*-cresol or proflavine at 20.0° and 40.0° C. respectively. The results are shown in Fig. 3 (where the first recorded temperature is that at which the cells were trained and the second that at which they were grown in the test). The filament formation at 20° C. is seen to be much greater with cells that have been trained at this temperature than with those trained at 40° C. The most marked abnormality appears with strains which have become adapted to growth at 20° C. and are then grown at the higher temperature 40° C. (It was also found that cells grown repeatedly in the medium with 2 g./l. glucose gave fewer filaments when inoculated into *m*-cresol media of the same glucose concentration than those which had been previously grown in 40 g./l. glucose.)

### The Effect of Salt Additions on Filamentation Induced by Drugs.

The addition of excess ammonium sulphate or sodium chloride to the dilute glucose medium is known to cause a marked reduction in the value of  $\sigma$ . It was considered of interest, therefore, to study the effect of the addition of varying amounts of sodium chloride on the abnormal growth induced by *m*-cresol or proflavine. The experimental method was to inoculate with normal cells, at the stage of minimal lag, a series of media containing *m*-cresol or proflavine together with sodium chloride at concentrations up to a maximum of about 10%. Fig. 4 shows how the value of  $\sigma_{\max}$ , representing the abnormal growth induced by the drug varies with the salt concentration. The formation of filaments is known in appropriate circumstances to be correlated with change in the lag of the culture.<sup>1</sup> It was therefore relevant to determine the lags corresponding to the measurements of Fig. 4. Fig. 5 shows that as the salt concentration increases in the *m*-cresol medium, the value of the lag passes through a minimum while the value of  $\sigma_{\max}$  passes through a maximum at the same salt concentration.

### Discussion and Summary.

Whether a strain of *Bact. lactis aerogenes* is transferred from bouillon into a dilute glucose artificial medium, or whether a normal strain is subcultured into a medium containing proflavine or *m*-cresol, increase of temperature always favours filamentation. The whole phenomenon shows a marked adaptive effect in that cells, trained by repeated growth at a lower temperature than the test temperature, produce a much more

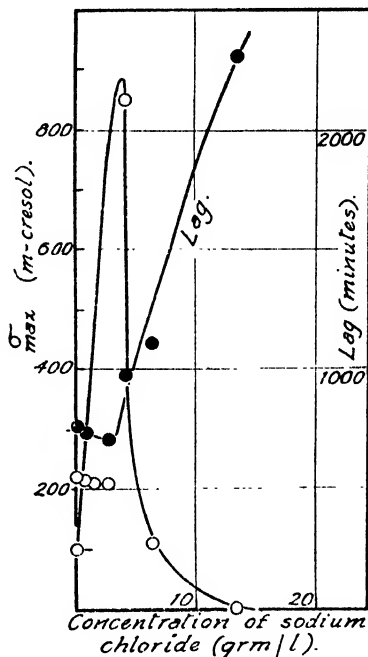


FIG. 5.—Influence of NaCl upon size coefficient and upon lag (right-hand scale). 709 mg./l. *m*-cresol. Open circles = size coefficient; blacked-in circles = lag.

abnormal size distribution than those trained at a higher temperature and tested at an equal or lower temperature.

It had previously been observed that with the dilute glucose medium, increase of osmotic pressure by the addition of salt caused complete elimination of the abnormal growth. It was interesting therefore to observe the effect of salt additions on the abnormal growth caused by proflavine or *m*-cresol. Very small additions actually caused quite definite increases in filamentous growth, while higher concentrations, as might have been expected from the earlier results, completely inhibited the appearance of any filaments.

The initial increase in filamentation was accompanied by a reduction of the lag. There is a clear correlation between the two effects. The cells grow to abnormal lengths when the processes of mass increase and of division are out of balance. When the lag is shorter the process of division, already delayed, is even more unable to keep pace with the mass increase, and filament formation is enhanced. When the lag, on the other hand, lengthens, the division has time to overtake the mass increase, so that the cells divide normally.

### Résumé.

Le *Bact. lactis aerogenes*, en présence de *m*-crésol ou de proflavine, présente une croissance anormale. On a étudié l'effet de la température de culture sur cette croissance anormale et l'effet de sels ajoutés sur la formation provoquée de filaments en présence des deux produits cités.

### Zusammenfassung.

Das Wachstum von *Bact. lactis aerogenes* weist in der Gegenwart von *m*-Kresol oder von Proflavin abnormales Verhalten auf. Der Effekt der Temperatur, bei der die Zellen gezüchtet werden, auf das abnormale Wachstum sowie der Effekt der Hinzufügung von Salz auf die Fadenbildung der Zellen in der Gegenwart von Drogen sind untersucht worden.

*Physical Chemistry Laboratory,  
Oxford University.*

## THE ANODIC BEHAVIOUR OF METALS. PART III.—NICKEL.

BY A. HICKLING AND J. E. SPICE.

*Received 16th August, 1946.*

In Parts I and II,<sup>1</sup> the anodic polarisation of the noble metals platinum and gold was investigated by an oscillographic method which records the variation of potential with quantity of electricity passed prior to oxygen evolution. The method has now been applied to nickel which was selected as a metal which readily becomes passive. No previous work on nickel from the present standpoint has been published, but a certain amount of information on the anodic behaviour of the metal is available from other methods of investigation. The general conclusion reached from numerous passivity studies<sup>2</sup> is that nickel in the passive state is covered with a

<sup>1</sup> Hickling, *Trans. Faraday Soc.*, 1945, **41**, 333; 1946, **42**, 518.

<sup>2</sup> Evans and Stockdale, *J. Chem. Soc.*, 1929, 2651; Tronstad, *Z. physik. Chem.*, 1929, **142**, 272; Müller, *Monatsh.*, 1927, **48**, 559; Müller, Cameron and Machu, *ibid.*, 1932, **59**, 73; Georgi, *Z. Elektrochem.*, 1932, **38**, 681, 714; 1933, **39**, 736.

protective film, probably of nickelic oxide  $\text{Ni}_2\text{O}_3$  or hydroxide  $\text{Ni}(\text{OH})_2$ . Observations on the behaviour of the nickel electrode in the Edison accumulator<sup>3</sup> suggests that on charging, nickelous oxide  $\text{NiO}$  is oxidised to  $\text{Ni}_2\text{O}_3$ , and a certain amount of the dioxide  $\text{NiO}_2$  also is formed<sup>4</sup>; some doubt appears to exist as to whether  $\text{Ni}_2\text{O}_3$  is primarily formed or arises from  $\text{NiO}_2$  initially produced.<sup>5</sup>

### Experimental.

The electrical circuit and the electrolytic cell employed were as previously described.<sup>1</sup> Nickel wire anodes of 0.1 sq. cm. area were used throughout the investigation; they were made from nickel wire of diameter 0.019 cm., sealed into glass tubes with sealing wax, and mounted vertically. It was found that relatively gentle cleaning of the metal gave the most reproducible results, and before each experiment the anode to be used was washed with warm dil. HCl and water, and rubbed with filter paper. Observations have been made mainly with N. NaOH as electrolyte; additional observations have been carried out in a variety of buffer solutions. Dissolved oxygen was expelled from the electrolyte initially by boiling and all subsequent operations were carried out in an atmosphere of nitrogen. Except where otherwise stated, all experiments were made at 20° C.

The results are shown as photographed oscillograms in which the ordinates represent potentials and the abscissae are proportional to quantities of electricity passed. Suitable horizontal reference lines at intervals of 0.25 v. were photographed immediately after recording the polarisation tracks, so that significant potentials can be read directly from the oscillograms. All potentials quoted are on the hydrogen scale. The quantity of electricity passed at any stage in the polarisation is computed from the known capacity of the condenser used in series with the electrolytic cell and the horizontal displacement which is governed by the voltage to which the condenser is charged (on the original photographs, before reduction, 1 v. on the condenser corresponds to an average horizontal displacement of 1.0 mm.). Except where otherwise stated, a 10.6  $\mu\text{F}$ . condenser was used in series with the cell as this was found to be a convenient value for the exhibition of the full polarisation track.

### Results.

**Behaviour in Alkaline Solution.**—In Plate I, A, is shown the characteristic oscillogram in N. NaOH for the anodic polarisation of nickel at 20° C. with a polarising c.d. of 0.01 amp./sq. cm. The spots on the extreme left of the photograph indicate the steady hydrogen and oxygen evolution potentials at the same c.d. It may be noted that a very rapid initial build-up of potential is followed by a horizontal step from which the potential rises more gradually to the oxygen evolution value. The oscillogram was found to change slightly if the pulsating electrolysis were prolonged, the change corresponding to an increase in the area of the electrode probably due to alternate oxidation and reduction of the metal surface. Provided, however, that the oscillogram was recorded in the first few minutes of electrolysis with a clean electrode it was found to be satisfactorily reproducible, and different nickel electrodes under the same conditions gave very similar tracks. Change of c.d. had very little influence on the oscillogram, which is illustrated in Plate I, B; tracks 1 and 2 were obtained with c.d.'s of 0.025 and 0.005 amp./sq. cm. respectively. Increase of temperature had likewise only a slight effect, increasing slightly the length of the horizontal step and decreasing somewhat the oxygen

<sup>3</sup> Zedner, *J. Chem. Soc.*, 1905, 11, 809; 1906, 12, 463; 1907, 13, 572; Foerster, *ibid.*, 1907, 13, 414; 1908, 14, 385; 1910, 16, 461.

<sup>4</sup> See also, Grube and Vogt, *ibid.*, 1938, 44, 353.

<sup>5</sup> Foerster, *loc. cit.*<sup>3</sup>



evolution potential; this is illustrated in Plate I, C, in which tracks at  $20^\circ$  and  $65^\circ$  C. are shown, a polarising c.d. of 0.01 amp./sq. cm. being used. Anodic prepolarisation had no significant effect on the oscillogram provided the potential of the working electrode was taken well below the value corresponding to the horizontal step in each cathodic pulse; if, however, the quantity of electricity was insufficient for this to be achieved, then anodic prepolarisation tended to shorten the step. In Plate I, D, are shown the anodic and cathodic polarisation tracks at a c.d. of 0.01 amp./sq. cm. photographed together; it is to be noted that the cathodic track shows a single arrest of identical length and at almost the same potential as that found in the anodic track.

The influence of various anions in alkaline solution was ascertained by using N. NaOH electrolytes which had been made 0.1 M. with respect to  $\text{Na}_2\text{PO}_4$ ,  $\text{Na}_2\text{B}_4\text{O}_7$ ,  $\text{KNO}_3$ ,  $\text{K}_2\text{SO}_4$ , and  $\text{KCl}$  severally; in no case was any appreciable effect manifested. The presence of 0.1 M.  $\text{NH}_4\text{OH}$ , which dissolves nickelous hydroxide, was likewise without effect.

**Behaviour in Buffer Solutions.**—The effect of decrease of pH value on the anodic behaviour of nickel was investigated using a variety of buffer solutions as electrolytes, but it soon became apparent that here the anions present might exert specific effects. Except where otherwise stated, a c.d. of 0.01 amp./sq. cm. was used throughout these experiments. In Plate I, E, is shown the anodic track in N.  $\text{Na}_2\text{CO}_3$  (approx. pH 12); the oscillogram is fundamentally similar to that in N. NaOH with a step of approximately the same extent but displaced to a somewhat higher positive potential. In 0.1 N.  $\text{Na}_2\text{B}_4\text{O}_7$  (approx. pH 9.2), however, as shown in Plate I, F, the step was considerably reduced in extent, while in a mixture of 0.2 M.  $\text{KH}_2\text{PO}_4$  + 0.2 M.  $\text{Na}_2\text{HPO}_4$  (approx. pH 6.8), as shown in Plate II, G, the step had practically disappeared; this was also the case with the cathodic tracks, and is illustrated in the latter example. That the effect was not solely one due to hydrogen ion concentration was shown by using a dilute mixture of  $\text{KH}_2\text{PO}_4$  and  $\text{Na}_2\text{B}_4\text{O}_7$  (approx. pH 6.6). Here, under the same conditions as before, the anodic and cathodic tracks obtained were those in Plate II, H, and a poorly defined step is apparent. From numerous experiments it appeared that whenever phosphate was present in quantity in the electrolyte, the step tended to disappear.

In all the preceding experiments the nickel appeared passive, the oscillograms giving no indication of nickel dissolution. In 0.1 N.  $\text{H}_3\text{PO}_4$  (approx. pH 1.8), however, the normal anodic track was 1 in Plate II, I, indicating continuous passage of metal into solution; by short pulses of anodic polarisation at very high c.d.'s the electrode could be made passive and then gave track 2; 3 is the corresponding cathodic polarisation track. In N.  $\text{H}_2\text{SO}_4$  the electrode was continually active and the anodic and cathodic tracks appeared to correspond merely to dissolution and deposition of the metal; they are shown in Plate II, J.

Since in solutions rich in phosphate the potential of the electrode in the passive state could apparently go from the hydrogen to the oxygen evolution value, and vice versa, without any arrests indicating oxidation or reduction of the metal, it was deemed of great interest to ascertain whether or not any protective film was in fact present on the surface in these circumstances. For such a film to be present, it must be of such a nature that (unlike an oxide film) it is not continually reduced and reformed in the pulsating electrolysis, as otherwise these processes would inevitably appear on the oscillogram; this might be the case with an insoluble salt coating, initially formed in the electrolysis and which is subsequently reasonably stable towards cathodic hydrogen. To test this, the 0.2 M.  $\text{KH}_2\text{PO}_4$  + 0.2 M.  $\text{Na}_2\text{HPO}_4$  electrolyte (approx. pH 6.8) was used with a clean nickel electrode which was first polarised cathodically at 0.01 amp./sq. cm. for 3 min. to free the surface from any existing film. The pulsating current (at the same c.d.) was then switched on, and the

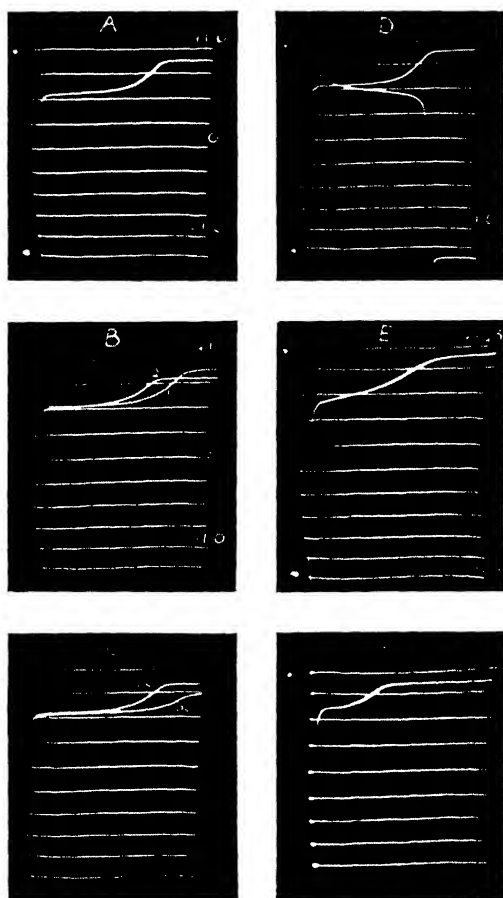


Plate I.

[To face page 764.

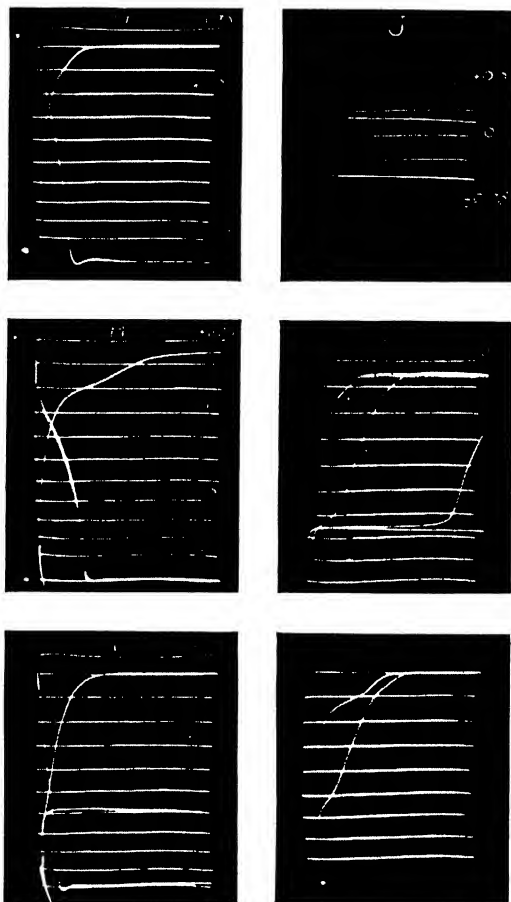


Plate II.

*To face page 705.*

anodic tracks photographed *from the beginning* of the electrolysis; the result is shown in Plate II, K, the successive tracks being labelled 1, 2, 3 and 4. From this photograph it is clearly seen that in 1 a process occurs at a potential of *ca.*  $-0.1$  v.; it continues during most of 2, the potential beginning to rise at the end of the pulse; in 3 the potential rises towards the oxygen evolution value, and in 4 the track has assumed its normal form and thereafter remains unchanged. The conclusion which seems to be unmistakably indicated is that on being made anodic, the nickel initially dissolves forming an insoluble phosphate which coats the electrode, forming a protective and conducting film, which subsequently remains stable; it can, however, be removed by continuous cathodic polarisation for after such treatment the sequence of tracks could again be observed. It seems likely that a somewhat similar process takes place in the  $0.1$  N.  $\text{Na}_2\text{B}_4\text{O}_7$  electrolyte, and some evidence of this was obtained by carrying out a similar experiment with the borax buffer using a c.d. of  $0.005$  amp./sq. cm.; the result is shown in Plate II, L, successive tracks being labelled 1 and 2. The process here is not so clearly defined as in the phosphate case, but there is an indication of an initial reaction commencing at about  $-0.1$  v., the oscillogram then reverting rapidly to its usual form suggesting that any salt film formed is of an only partially stable or protective character.

**Measurement of the  $\text{Ni-Ni}_2\text{O}_3$  Potential.**—Previous workers have reported difficulties in measuring the  $\text{Ni-Ni}_2\text{O}_3$  potential using chemically prepared nickelic oxide,<sup>6</sup> and the values given have usually been obtained with electrolytically formed oxide. In the present work to avoid any possible ambiguity, the chemically prepared oxide has been used, and with the technique adopted, no difficulty was experienced in obtaining satisfactory potential measurements. Hydrated nickelic oxide was prepared by slow addition of a solution of bromine in potassium hydroxide with mechanical stirring to an aqueous solution of nickelous nitrate. The black precipitate obtained was thoroughly washed and filtered, and mixed with finely powdered metallic nickel. A portion of the mixture was then shaken up with the chosen electrolyte, a short platinum wire electrode wholly immersed in the sludge formed, and the potential measured against a saturated calomel electrode using a valve potentiometer. Under these conditions, very steady and reproducible readings were obtained, the values on the hydrogen scale being as below.

Electrolyte	.	.	N. NaOH	N. $\text{Na}_2\text{CO}_3$	$0.1$ N. $\text{Na}_2\text{B}_4\text{O}_7$
Potential	.	.	$+0.56$	$+0.68$	$+0.85$ v.

The potential in N. NaOH is in good agreement with the early measurements<sup>3</sup> on the electrolytically formed oxide, shown by analysis to be  $\text{Ni}_2\text{O}_3$ , which lead to a value of approx.  $+0.55$  v. for N. alkali. It may be noted that although the potential measured above was set up by the system nickel-nickelic oxide, and has hence been referred to as the  $\text{Ni-Ni}_2\text{O}_3$  potential, it probably represents the oxidation-reduction potential for the system  $\text{Ni}(\text{OH})_2\text{-Ni}_2\text{O}_3$ .

**Measurement of the True Area of the Nickel Electrode.**—The measurement of the ratio, accessible area/apparent area, of a metal surface is a matter of considerable difficulty, and indeed the value obtained will depend to some extent on the means adopted for exploring the surface. In the present work, the method of Bowden and Rideal<sup>7</sup> was employed in which the double layer capacity of the metal, when used as a cathode in acid solution, is measured and compared with that of mercury for which the accessible area may be assumed to be the same as the apparent area. Since the effective agent involved in exploring the surface is here the hydrogen ion, it is probable that this method gives maximum values for the ratio. The present oscillographic method was used for the measurements,

<sup>6</sup> Cf. Zedner, *Z. Elektrochem.*, 1905, 11, 809.

<sup>7</sup> Bowden and Rideal, *Proc. Roy. Soc., A*, 1928, 120, 80.

and the electrolyte was  $N. H_2SO_4$ . Mercury electrodes of known area were made by depositing mercury electrolytically either directly on platinum, or upon platinum which had previously been copper-plated; the nickel electrodes were of the wire used in the investigation of anodic polarisation and were subjected to the usual treatment. In each case the electrode was made continuously cathodic for a short time, so that hydrogen was freely evolved, and the pulsating electrolysis was started, the series condenser being chosen so that the build-up of cathode potential from about 0 v. to the hydrogen evolution value extended across the whole of the oscillograph screen. By measurement of the linear sections of the photographed tracks, the quantity of electricity required for a given change of cathode potential was found, and hence the double layer capacity per apparent sq. cm. of electrode surface was evaluated. The results are summarised in Table I.

TABLE I.

Electrode.	Apparent Area in sq. cm.	Series Condenser $\mu F$ .	Voltage (v.) of Condenser for 0.25 v. Change in Cathode Potential.	Capacity of Cathode per Apparent sq. cm. $\mu F$ .
Mercury (on Pt)	0.098	0.0360	7.7	11.3
(on Cu)	0.098	0.0134	18.7	10.2
(on Cu)	0.098	0.0360	7.5	10.2
(on Cu)	0.199	0.0360	15.3	11.1
				—
				Mean 10.9
Nickel	0.100	0.0575	19.0	43.7
	0.100	0.0360	25.0	36.0
	0.197	0.1150	16.0	37.4
	0.097	0.0935	21.0	39.9
				—
				Mean 39.3

It is seen that for mercury under different conditions the capacity is fairly constant and has a mean value of 10.9  $\mu F$ ,<sup>8</sup> while for nickel the average value is 39.3  $\mu F$ . It would thus appear that for the nickel wire used the accessible area is about 3.6 times the apparent area. In the most nearly comparable case studied by Bowden and Rideal,<sup>7</sup> that of rolled nickel, it was found that the accessible area varied between 5.8 and 3.5 times the apparent area according to the age of the specimen.

### Discussion.

The oscillograms show that nickel in alkaline solution gives a characteristic anodic polarisation track which is not very markedly dependent upon experimental variables such as c.d. and temperature. Two general stages in the anodic polarisation can be detected:

- (1) a rapid, probably linear, rise of potential constituting the initial section of the track,

<sup>8</sup> The accepted value for the capacity of the double layer at mercury in acid solution is *ca.* 20  $\mu F$ . per sq. cm. (Bowden and Agar, *Ann. Report*, 1938, **35**, 94). Appreciably lower values have frequently been reported and it has been suggested that these are due to the presence of adsorbed impurities (Proskurnin and Frumkin, *Trans. Faraday Soc.*, 1935, **31**, 110). It seems doubtful, however, if the discrepancy can be so readily dismissed. Measurements made in this laboratory over a number of years by both direct and a.c. methods using mercury and amalgamated electrodes prepared under widely different conditions have given consistently a value of *ca.* 11  $\mu F$ . (See also Grahame, *J. Amer. Chem. Soc.*, 1941, **63**, 1207).

- (2) a stage of almost constant potential passing non-linearly into oxygen evolution.

By analogy with the previous metals studied,<sup>1</sup> it appears probable that stage (1) corresponds to the charging of a double layer. It was not possible in the present instance to obtain a very precise measure of this double layer capacity, since the initial sections of the oscillograms were very steep and not very clearly defined, but measurements on a large number of oscillograms suggest that the value is in the region 200 to 400  $\mu\text{F./apparent sq. cm. of nickel surface}$ .

Stage (2) is very clearly defined in the oscillograms and commences in N. NaOH at a potential of +0.55 v., and in N.  $\text{Na}_2\text{CO}_3$  at +0.65 v.; in 0.1 N.  $\text{Na}_2\text{B}_4\text{O}_7$ , the potential was found to vary with the current used, suggesting the presence of some resistance at the surface of the electrode, but by working at different currents and extrapolating to zero, the value of +0.85 v. (free from ohmic voltage drop) was obtained. As discussed in the experimental section, the static reversible potentials of nickel against nickelic oxide in these three solutions are +0.56, +0.68, and +0.85 v. severally. The very close agreement between these two sets of values strongly suggests that the onset of stage (2) corresponds to the commencement of the formation of nickelic oxide (or hydroxide) on the nickel surface. The quantity of electricity passed from the beginning of stage (2) to the point at which the potential approaches the oxygen evolution value can be estimated approximately from the oscillograms and is found to be about 4500 microcoulombs/apparent sq. cm. of nickel surface in N. NaOH and N.  $\text{Na}_2\text{CO}_3$  electrolytes; this is sufficient to liberate approximately  $14 \times 10^{16}$  atoms of oxygen. Taking the specific gravity of nickel as 8.8, the diameter of the nickel atom may be calculated to be approximately  $2.2 \times 10^{-8}$  cm., and hence there would be about  $2.0 \times 10^{16}$  atoms of metal/true sq. cm., or  $7.2 \times 10^{15}$  atoms of metal/apparent sq. cm. at a nickel surface, assuming the measured value of 3.6 for the ratio accessible area/true area to be substantially correct. Hence it would seem that the quantity of electricity passed in stage (2) is sufficient to provide approximately 3.9 atoms of oxygen for every 2 nickel atoms in the electrode surface, and is thus slightly larger than would correspond to the formation of a unimolecular layer of nickelic oxide. The general conclusion arrived at, therefore, is that in the anodic polarisation of nickel in alkaline solution, nickelic oxide is primarily formed, the process occurring at its reversible potential, and resulting in a protective film 1-2 molecules thick<sup>9</sup> on the electrode, the potential of which then rises to the oxygen evolution value. Cathodic polarisation serves to reduce this oxide, again at its reversible potential, and the quantity of electricity required is identical with that involved in the formation of the oxide.

In the  $\text{Na}_2\text{CO}_3$  and NaOH electrolytes the nickel becomes anodically passive, as demonstrated above, by the formation of a highly protective film of nickelic oxide or hydroxide.<sup>10</sup> In the phosphate buffer, however, there is practically no indication of the arrest corresponding to this process, but as shown in the experimental section, nickel initially dissolves, and the only conclusion to be drawn seems to be that there is formed a stable and protective film of an insoluble phosphate which can persist indefinitely during the pulsating electrolysis. It is probable that this film is relatively thick since in its initial formation more than 10,000 microcoulombs of

<sup>9</sup> This thickness is, of course, the *initial* thickness of the film prior to oxygen evolution. It is very likely that further oxide formation may accompany oxygen evolution, and in continuous anodic polarisation the *ultimate* thickness of the film may be much greater.

<sup>10</sup> An interesting question here arises as to whether the oxide or hydroxide is formed by the nickel going into solution and immediately reacting with hydroxyl ions, or whether it is formed by direct discharge of hydroxyl ions on the metal surface. It does not seem possible at present to distinguish between these two mechanisms.

electricity/apparent sq. cm. are used (Plate II, K) ; this is equivalent to the dissolution of about  $30 \times 10^{16}$  nickel atoms in the bivalent state, or rather more than 4 atomic layers from the electrode surface. In the borax solution it appears that some metal dissolution initially occurs but any film formed confers only partial protection since a certain amount of oxide formation subsequently occurs. This corresponds, however, only to about 2600 microcoulombs/apparent sq. cm., which suggest that the surface is already partially protected ; the existence of a surface resistance at the electrode (vide supra) is in conformity with this view.

In the more acid electrolytes investigated, the behaviour of the nickel anode appears to be conditioned entirely by the presence or absence of a protective film which usually seems to be of a sparingly soluble salt type. If the pretreatment is such that a film of this kind is formed, then the potential can rise to the oxygen evolution value, while in the absence of the film or after its removal (e.g. by continuous cathodic polarisation) then the nickel goes into solution indefinitely.

The authors' thanks are due to Mr. D. Taylor for making the measurements of the ratio of the accessible to the apparent area of nickel.

### Summary.

1. The initial build-up of anodic polarisation at a nickel anode over a wide range of conditions has been investigated, using the cathode ray oscillograph.

2. In alkaline solutions ( $pH$  12-14), two main stages in the polarisation have been distinguished corresponding to the charging of a double layer and the deposition of oxygen at the electrode ; from measurements of potentials and quantities of electricity passed it is concluded that the latter process corresponds to the formation of a layer of nickelic oxide rather greater than one molecule in thickness. Further thickening of the film may occur on prolonged anodic treatment.

3. In buffer solutions ( $pH$  5-10), a nickel anode may become passive by the primary formation of a sparingly soluble salt film ; this may be followed by oxide formation if the film is porous. In more acid solutions, the behaviour is conditioned by the presence or absence of a protective film dependent on the pretreatment of the electrode.

4. All the observations made are in conformity with the film theory of passivity.

### Résumé.

On a étudié au moyen d'un oscillographe cathodique la formation initiale de la polarisation à une anode de nickel dans des conditions opératoires très variées.

Dans des solutions alcalines ( $pH$  12-14), on observe deux stades principaux : l'un étant la charge de la double couche et l'autre, le dépôt d'oxygène ; en fait, ce dernier correspond à la formation d'une couche d'oxyde nickellique, dont l'épaisseur est légèrement supérieure à une molécule.

Dans des solutions tampons ( $pH$  5-10), une anode de nickel peut devenir passive par formation initiale d'un film de sel à peine soluble ; ceci peut être suivi d'une formation d'oxyde, si le film est poreux. Dans des solutions plus acides, le comportement est déterminé par la présence ou l'absence d'un film protecteur, qui dépend du traitement préalable de l'électrode.

Toutes ces observations s'accordent avec la théorie de la passivité, basée sur l'existence d'un film.

### Zusammenfassung.

Das anfängliche Anwachsen der anodischen Polarisation an einer Nickelkathode ist bei diversen Bedingungen unter Benützung eines Kathodenstrahloszillographen untersucht worden. In alkalischen Lösungen ( $pH$  12-14) bestehen zwei Hauptstadien, die der Aufladung der Doppelschicht und der Abscheidung von Sauerstoff an der Elektrode entsprechen ; der letztere Vorgang ist die Bildung einer Nickeloxidschichte, die wesentlich dicker als ein Molekül ist. In Pufferlösungen ( $pH$  5-10) kann die Nickelanode durch die primäre Bildung eines wenig löslichen Salzfilms passiv werden, worauf Oxydbildung folgen kann, wenn der Film porös ist. In saureren Lösungen hängt das Verhalten von der

Gegenwart oder Abwesenheit eines Schutzfilms—je nach der Vorbehandlung der Elektrode—ab. Alle diese Beobachtungen stehen mit der Filmtheorie der Passivität im Einklang.

*Department of Inorganic and Physical Chemistry,  
University of Liverpool.*

## THE INTERACTION OF CARBON FILAMENTS AT HIGH TEMPERATURES WITH NITROUS OXIDE, CARBON DIOXIDE AND WATER VAPOUR.

BY R. F. STRICKLAND-CONSTABLE.

*Received 4th September, 1946.*

Meyer<sup>1,2,3</sup> has described experiments on the interaction of carbon filaments with  $O_2$ , with  $CO_2$  and with  $H_2O$ . The author<sup>4</sup> has also described experiments with filaments in  $O_2$ , the results of which were very different from those of Meyer. In the present work the results with  $CO_2$  and  $H_2O$  are found to differ from those of Meyer in the same way as did those with  $O_2$ . The reaction between  $N_2O$  and filaments has not, as far as is known, been previously studied.

### Experimental.

The apparatus was the same as that described previously<sup>4</sup> except for the Macleod gauge, which was modified to enable water vapour pressures to be measured<sup>5</sup> by encasing the compression stem in a water jacket at  $100^\circ C$ . The  $N_2O$  was taken from a cylinder, redistilled, using liquid

TABLE I.

	Taken %.	Found %.
$N_2O$ . .	33	29
$CO$ . .	$19\frac{1}{2}$	$18\frac{1}{2}$
$CO_2$ . .	$11\frac{1}{2}$	13
$O_2$ . .	36	$37\frac{1}{2}$
$N_2$ . .	0	2

air, and dried over  $P_2O_5$ ; the  $CO_2$  was prepared by the combustion of  $CO$  with  $O_2$  on the platinum filament in the analysis bulb, the resulting  $CO_2$  being separated by means of liquid air, and dried over  $P_2O_5$ . The methods of analysis of mixtures of  $O_2$ ,  $CO_2$  and  $CO$ , as well as of  $H_2$ ,  $CO_2$  and  $CO$ , have already been described.<sup>4,5</sup> With  $N_2O$  as the reacting gas, the product could contain  $N_2O$ ,  $CO_2$ ,  $CO$  and  $N_2$  (and possibly  $O_2$ ). The  $CO_2$  was determined by absorption in Sofnolite, the  $N_2O$  by condensation with liquid air, the  $CO$  was burned to  $CO_2$  with added  $O_2$  on the platinum filament, and the  $N_2$  determined by difference. Oxygen, if present, could be determined in a separate sample of gas by burning on the platinum filament with  $CO$ . An analysis on a known mixture is given in Table I.

Further experimental details will be found in the papers already mentioned. All the necessary precautions described there were taken to avoid interference in the reactions by electrons thermionically emitted by the filament.

<sup>1</sup> Meyer, *Z. physik. Chem.*, B, 1932, 17, 385.

<sup>2</sup> Martin and Meyer, *Z. Elektrochem.*, 1935, 41, 136.

<sup>3</sup> Meyer, *Trans. Faraday Soc.*, 1938, 34, 1056.

<sup>4</sup> Strickland-Constable, *ibid.*, 1944, 40, 333.



## Results.

## Nitrous Oxide.

All pressures are given in mm.  $\times 10^{-3}$  Hg, unless otherwise stated. The product of the reaction of  $N_2O$  with carbon filaments contained virtually no  $CO_2$  throughout the temperature range of  $900^\circ$  to  $2000^\circ$  C. investigated, as shown by the analyses in Table II.

The yields of nitrogen and oxygen given in the last two columns refer to the amounts accounted for in the products, expressed as a percentage

TABLE II.—ANALYSIS OF PRODUCT.

Temp. °C.	Initial Pressure. (mm. $\times 10^{-3}$ )	Analysis %.				Yields %.	
		$CO_2$ .	CO.	$N_2O$ .	$N_2$ .	N.	O.
950	14	1½	19½	56	23	99.7	102
1200	139	1	17½	63	18½	99.4	100.3
1600	10½	1½	29	37½	32	96.5	96.5
1800	15	0	19½	62	18½	99.5	100.5
1800	53½	1½	29½	37½	31½	97.8	99.7

of the amounts present as  $N_2O$  in the reacting gas. The fact that these figures are very near 100 % in every case shows that the experiments have been correctly carried out, and that no appreciable quantities of surface oxides have been formed.

The order of reaction at  $1800^\circ$  C. was investigated in a series of runs given in Table III. The experimental method will be described using the figures for the first run in the table.  $N_2O$  was admitted to the reaction

TABLE III.—ORDER OF REACTION.  $1800^\circ$  C.

Initial Pressure. (mm. $\times 10^{-2}$ ).	$CO + N_2$ formed (mm. $\times 10^{-3}$ ).	Time (min.)	$k$ (min $^{-1}$ ).
460	14.8	0.75	0.021
460	47	2	0.026
460	9.7	0.5	0.021
460	12.2	0.5	0.027
48	7.4	2	0.039
48	6.2	2	0.032
48	6.6	2	0.034
11	1.85	2	0.042
11	1.95	2	0.044
534	22	0.5	0.041
534	107	2	0.050
3520	114	0.25	0.065

bulb, the pressure measured on the Macleod being  $460 \times 10^{-3}$  mm. The filament was heated at  $1800^\circ$  C. for 0.75 min. and liquid air was then applied to the appendix of the reaction bulb to condense all unchanged  $N_2O$ . The pressure of the uncondensed gases ( $CO + N_2$ ) was found to be 14.8, so that the amount of  $N_2O$  decomposed was 7.4. From this and the time of reaction (in min.) the value of  $k$ , the first order reaction constant was calculated. All the results will be quoted in terms of  $k$ , determined as above, even when the reaction was found not to be of the first order. This method of experiment, using liquid air, had the great advantage that small

reaction percentages could be measured with considerable accuracy, and with a resulting small consumption of the filament.

TABLE IV.—ORDER OF REACTION. 900° C. AND 1100° C.

Initial Pressure (mm. $\times 10^{-3}$ ).	$k$ (min. <sup>-1</sup> ).	Initial Pressure (mm. $\times 10^{-3}$ ).	$k$ (min. <sup>-1</sup> ).
1510	0.00105	9270	0.00024
1510	0.00075	9270	0.00028
1510	0.00075	9270	0.00026
141	0.00125	952	0.00040
141	0.00100	1000	0.00034
27	0.00087	1000	0.00049
27	0.00104	1000	0.00048
672	0.00106	123	0.00071
		123	0.00079
		123	0.00081
		8950	0.00026

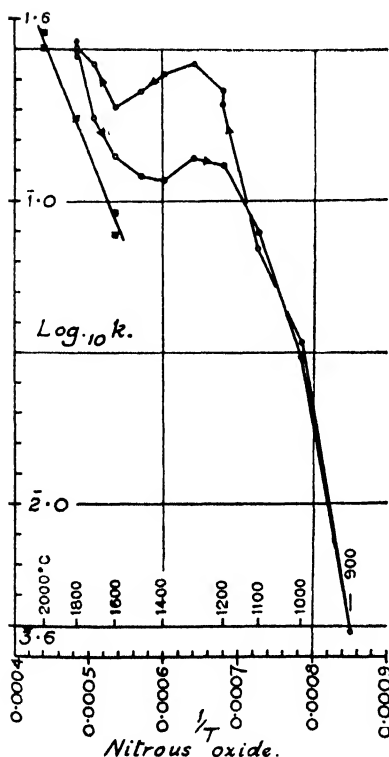


FIG. 1.

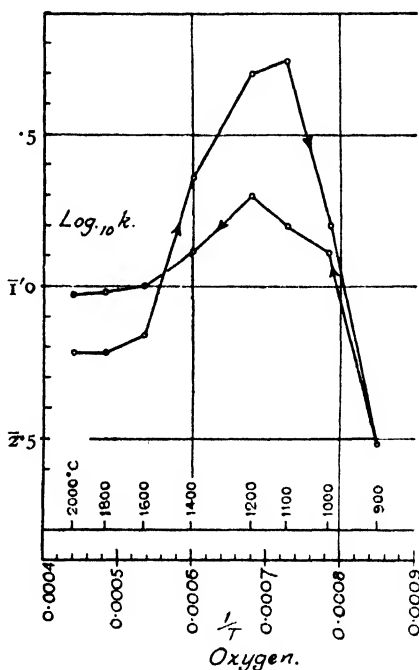


FIG. 2.

The values of  $k$  show a small steady increase throughout the series, due to change in the state of the surface of the filament, but they are virtually independent of the initial pressures which vary through a range of

320 to 1. The reaction is therefore of the first order. The order of reaction at 900° c. and at 1100° c. was examined as shown in Table IV. At 1100° the reaction is of the first order since a variation of 50 to 1 in the initial pressure corresponds to a change in  $k$  of less than 2 to 1. At 900° c. the reaction, which is extremely slow, is no longer of the first order, since  $k$  increases for low initial pressures. The figures may be expressed by taking the rate as proportional to the 0.7 power of the initial pressure.

The variation of rate with temperature is shown in Fig. 1. Runs were carried out at 100° intervals, starting at 1800°, going down to 900° and rising again to 1800°. A separate curve from 1600° to 2000°, obtained with a different filament, is also shown. The initial pressure in all runs was approximately 100. In the figure,  $\log_{10} k$  is plotted against  $1/T$ , and a scale in °C. is also given. The rate rises steeply from 900° to 1200° and again from 1600° to 2000°, but is roughly constant in the middle section from 1200° to 1600°, and here the "up" and "down" curves follow a widely different course. This peculiarity is common to  $O_2$ ,  $N_2O$  and  $H_2O$ , and is referred to as the hysteresis effect. (It was not investigated in the case of  $CO_2$ .) In the case of  $N_2O$  and  $H_2O$  it is explained by saying that if a filament is made to react at a low temperature it becomes activated for reactions at a higher temperature. Conversely, reaction at a high temperature (as well as simply heating *in vacuo* at a high temperature) reduces the activity of the filament for reactions at a lower temperature. These effects will be illustrated later for  $H_2O$ .

It is recalled that with  $O_2$  the effect worked in the opposite sense, as shown in Fig. 2, on which are plotted complete temperature curves for  $O_2$ , obtained during the previous work on this gas.<sup>4</sup> The "down" curve is here above the "up" curve in the middle section: reaction at a high temperature appeared to increase the reactivity for reaction at lower temperatures and vice versa. The effect is very pronounced.

It will be seen that the rates given in Tables III and IV do not agree with those in Fig. 1. A layer of graphite was deposited on the filaments before use by heating them in  $CH_4$ . The freshly coated filament was of a silver white appearance and reacted extremely slowly with  $N_2O$ ,  $CO_2$  and  $H_2O$ . The rate of reaction rose slowly with use, and it was convenient to determine the temperature coefficient curves with an old and therefore very reactive filament.

$N_2O$  differs from all the other gases in that the temperature coefficient of reaction rate is positive above 1600° c. It appeared possible that this might be due to some electronic reaction not completely eliminated such as was encountered in the  $O_2$  experiments. Accordingly, runs were performed with the filament entirely surrounded by a solenoid of copper wire of about 2 cm. diameter, maintained at 100 v. negative with respect to the filament. Such a cage will entirely repress such thermionic emission as might cause electronic reactions. The results obtained were identical with those obtained with the normal set-up, thereby confirming the reliability of the general results.

## Carbon Dioxide.

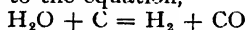
This gas reacts with a carbon filament according to the equation,  $CO_2 + C = 2CO$ . The order of reaction was examined at 1800° c. and 1100° c. as shown in Table V. At 1800° c. the reaction is of the first order; but at 1100° c. the order was calculated to be 0.7. The effect of temperature on rate is shown in Fig. 3. This is an "up" curve: the "down" curve was not determined. The curve is of the same general form as the  $N_2O$  curve except that the rate remains constant in the upper section above 1600°, in contrast to the steep increase obtained with  $N_2O$ .

TABLE V.—ORDER OF REACTION.

1800° c.		1100° c.	
Initial Pressure. (mm. $\times 10^{-3}$ ).	$k$ (min. $^{-1}$ )	Initial Pressure. (mm. $\times 10^{-3}$ ).	$k$ (min. $^{-1}$ ).
860	0.012	855	0.00080
860	0.010	855	0.00090
111	0.014	87	0.0026
111	0.013	144	0.0018
8.74	0.022	144	0.0021
16.7	0.016	8250	0.00046
16.7	0.016	8250	0.00035
16.7	0.017	263	0.0015
6.5	0.024	263	0.0013
6.5	0.025	622	0.00092
		622	0.00086

**Water.**

This reacted according to the equation,



as shown by the analyses in Table VI. The amounts of  $\text{CO}_2$  recorded do not exceed the experimental error in the method of analysis. The order of reaction was examined as shown in Table VII.

TABLE VI.—ANALYSIS OF PRODUCT OF REACTION.

Temp. °c.	% Reaction.	Analysis of Dry Gases.		
		$\text{CO}_2$ %	CO %.	$\text{H}_2$ %.
1000	38	0	54.5	45.5
1400	80	2	51	47
1800	75	2	45	50

TABLE VII.—ORDER OF REACTION.

1000° c.			
Initial Pressure. (mm. $\times 10^{-3}$ ).	$k$ (min. $^{-1}$ ).	Initial Pressure. (mm. $\times 10^{-3}$ ).	$k$ (min. $^{-1}$ ).
2600	0.0041	1316	0.00048
2600	0.0045	1316	0.00041
145	0.0044	178	0.0010
145	0.0038	217	0.0010
30	0.0048	210	0.0010
31.4	0.0043	622	0.00067
		975	0.00053
		1013	0.00054

At 1800° c. the order is clearly 1, whereas at 1000° it was calculated to be 0.6. The relation between rate and temperature is shown on the curves, Fig. 4. There is a pronounced "hysteresis" effect as for  $\text{N}_2\text{O}$ . Water differs

from  $N_2O$  and resembles  $CO_2$  in that the rate does not rise above  $1600^\circ C$ . The hysteresis effect was further examined in a series of runs shown in Table VIII.

It will be seen that the runs at  $1200^\circ$  are slowed down when preceded by either a reaction at  $1800^\circ C$ . or by heating *in vacuo* at  $1800^\circ$ . The runs at  $1800^\circ$  are accelerated if preceded by a run at  $1200^\circ$ , but not by heating alone at  $1200^\circ$ . It should be noted that run 1 was preceded by a number at  $1800^\circ$ , and its rate can therefore be contrasted with the faster

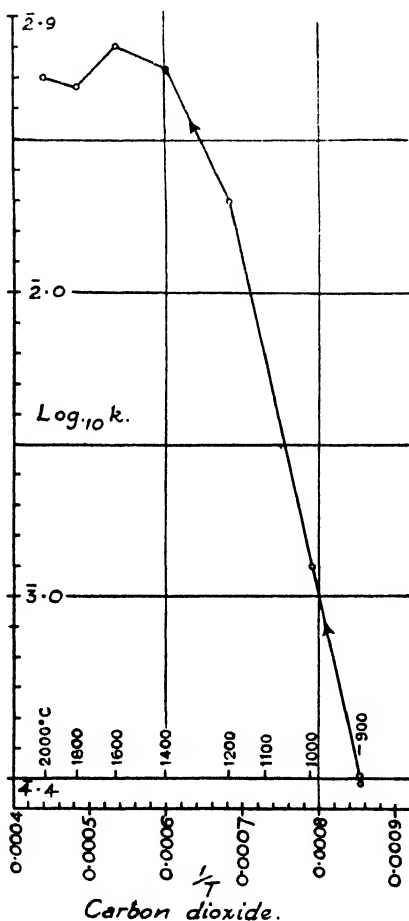


FIG. 3.

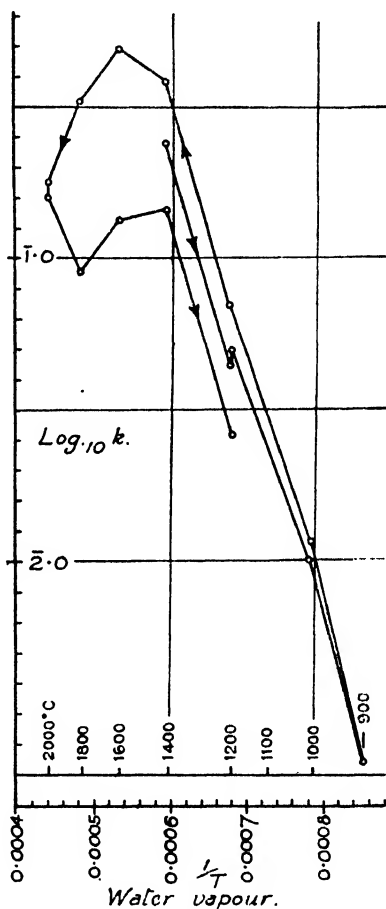


FIG. 4.

rate of run 13, which was preceded by a number of runs at  $1200^\circ$ . The rate of run 5, on the other hand, is the same as that of run 4, and has not been affected by the preceding heating *in vacuo* at  $1200^\circ$ .

For purposes of discussion it is useful to obtain a comparison of the absolute rates obtained with the different gases. The following table gives a rough comparison of  $N_2O$  and  $O_2$  for a filament of 1 sq. cm. area. The figures are not based on experiments with any one filament, but on a survey of a number of results. The reactivity with  $N_2O$  was very dependent on the age of the filament especially at low temperatures; with  $O_2$ , the rate was largely independent of the state of the filament.

TABLE VIII.—RATE OF REACTION AFTER ABRUPT CHANGES OF TEMPERATURE.

Initial Pressure in all runs approx. $400 \times 10^{-3}$ mm.				
Run.	Temp. °c.	Reaction Time (sec.).	% Reaction.	k (min. <sup>-1</sup> )
1	1800	10	2.2	0.13
2	1200	240	7.7	0.019
3	1800	10	3.9	0.244
4	1800	10	3.0	0.180
	1200	300	Heating filament <i>in vacuo</i>	
5	1800	10	2.8	0.17
6	1200	140	5.4	0.023
7	1200	120	6.6	0.033
	1800	30	Heating filament <i>in vacuo</i>	
8	1200	60	2.0	0.020
9	1200	30	1.9	0.037
10	1200	30	2.0	0.044
	1800	75	Heating filament <i>in vacuo</i>	
11	1200	30	0.66	0.013
12	1200	240	15.0	0.042
13	1800	11	5.7	0.31

TABLE IX.—RATES OF REACTION COMPARED. (k.)

		900° c.	1400° c.	1800° c.
N <sub>2</sub> O	Fresh filament	0.00006	0.0035	0.027
N <sub>2</sub> O	Much used filament	0.004	0.1 to 0.25	0.3
O <sub>2</sub>	Any filament	0.04	0.2 to 0.5	0.2

So far as H<sub>2</sub>O and CO<sub>2</sub> are concerned, complete comparison figures with N<sub>2</sub>O are not available, but it appeared on the whole that the rates with all three gases were of the same order at all temperatures investigated and that the relative rates were also independent of the state and age of the filament. This is also confirmed by one direct comparison made on the same filament at 1400° c.: the filament happened to be a very old one, and therefore very fast.

$$\text{N}_2\text{O} \quad k = 0.26$$

$$\text{CO}_2 \quad k = 0.10$$

$$\text{H}_2\text{O} \quad k = 0.30.$$

The rates are seen to be very nearly the same.

### Discussion.

A comparison of the kinetics of the reactions of the four gases N<sub>2</sub>O, CO<sub>2</sub>, H<sub>2</sub>O and O<sub>2</sub> with carbon filaments reveals striking similarities. The curves relating rate of reaction with temperature have the same general shape, the rate rising from 900° c. to about 1200° c. and then remaining roughly constant above this, with the exception of the N<sub>2</sub>O curve which rises again above 1600° c. All the gases show a hysteresis effect in the middle section, where the rate appears to depend to a considerable extent on the temperature at which the immediately previous reactions have been carried out. The absolute rates with N<sub>2</sub>O, CO<sub>2</sub> and H<sub>2</sub>O appeared to be very similar under all conditions; the rate with oxygen was rather faster, but is sufficiently close to the others to enable the reactions of all

four gases to be studied over the same temperature range of no less than  $1100^{\circ}\text{C}$ . (an unusual state of affairs in kinetic work). All the reactions are of the first order above  $1200^{\circ}\text{C}$ ., but  $\text{N}_2\text{O}$ ,  $\text{CO}_2$  and  $\text{H}_2\text{O}$  all tend to fractional order at lower temperatures.

These great similarities are considered to be due more to the nature and behaviour of the common reactant carbon, than to any special similarity between the gases, whose structures are markedly different. The following theory is tentatively advanced to account for the observed facts.

The graphite crystal consists of planes of carbon atoms held together in a chemically stable configuration, each plane being loosely bound to the next. The  $\text{N}_2\text{O}$ ,  $\text{CO}_2$  and  $\text{H}_2\text{O}$  are assumed only to react with the carbon atoms on the edges of the planes. The reaction has a positive temperature coefficient, which causes the rate to rise steadily up to  $1200^{\circ}\text{C}$ . It is also assumed that above  $1200^{\circ}\text{C}$ . a further process begins to take place, by which the atoms on the edges of the carbon planes tend continually to take up a more stable configuration in which they are much less reactive. This process may be thought of as involving a straightening of the edge of the plane: any atoms that are left protruding can move along the edge and fill up gaps, which may exist at other points. This "healing" action will continuously reduce the reactivity of the edges, and this will account for the fact that the reaction rate ceases to rise above  $1200^{\circ}\text{C}$ .

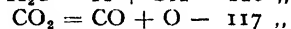
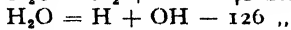
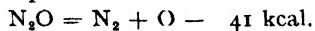
The hysteresis effect with  $\text{N}_2\text{O}$ , and  $\text{H}_2\text{O}$  can be accounted for in the following way: a reaction at a low temperature, by allowing fresh unhealed edges to be formed, will temporarily increase the reactivity at higher temperatures, it being assumed that the healing is an activated process requiring time for its completion. Conversely, heating the filament at a high temperature will cause healing to take place and reduce the reactivity of the edges at lower temperatures. The extreme slowness of a freshly coated filament will be due to the perfection of the graphite crystal structure, and the absence of edges.

The behaviour of  $\text{N}_2\text{O}$ ,  $\text{CO}_2$  and  $\text{H}_2\text{O}$  can thus be accounted for in a fairly simple manner, but with  $\text{O}_2$  it is necessary to make further assumptions to account among other things for the fact that the hysteresis effect works in the opposite sense to that of the other gases. As with the other gases,  $\text{O}_2$  is assumed to react at low temperatures principally with the edges, but it can also react by direct attack on the crystal faces, in a reaction which is assumed to have a rather low temperature coefficient. This will account for the fact that  $\text{O}_2$  reacts with a freshly coated filament not much more slowly than with an old one: the face reaction can make breaches in the crystal faces and thereby create edges on which the more rapid edge reaction can then occur. As with the other gases the healing effect reduces the rate of the edge reaction as the temperature is raised progressively above  $1200^{\circ}\text{C}$ ., and in consequence the rate ceases to rise above this temperature. At high temperatures such as  $1800^{\circ}\text{C}$ ., the  $\text{O}_2$  reacts principally by the face reaction. The faces of the crystals are thereby broken up in such a way as to produce a very large number of edges. If the temperature is now lowered the edge reaction will again take place at a greatly increased rate, owing to the great number of edges, which more than compensates for the fact that the edges are healed. In this way the hysteresis effect with  $\text{O}_2$  is accounted for.

The theory will also account for a further independent observation, namely that the filament burned sooty-black in  $\text{O}_2$  at high temperatures, but recovered its silvery appearance when allowed to react again at a low temperature. With  $\text{N}_2\text{O}$  the filament retained its silvery appearance at all temperatures. If the silvery appearance of a filament is due to the crystal faces being largely parallel to the surface, the face reaction of  $\text{O}_2$  at high temperatures will cause blackening by breaking up the crystal

faces. The edge reaction which takes place with  $O_2$  at low temperatures and with all the other gases at all temperatures, will tend to peel off the crystal layers one after another, leaving the reflecting surfaces intact.

$N_2O$  differs from the other gases in giving a rising rate of reaction above  $1600^\circ C$ . If any of these gases is heated to a sufficiently high temperature it can be expected to dissociate, and the heats of dissociation, which are given for instance by Sponer <sup>6</sup> are as follows:



If the activation energy for a dissociation process can be considered to be roughly related to the heat of dissociation then  $N_2O$  will be expected to dissociate at a far lower temperature than either of the other gases. The rising rate of reaction of  $N_2O$  above  $1600^\circ$  may therefore be associated with incipient dissociation on the filament. With the other gases a similar rise in rate may be expected to occur at some considerably higher temperature.

The reaction of  $H_2O$  and charcoal at  $700^\circ C$ . has been studied by the

TABLE X. RATES WITH  $O_2$  AND  $CO_2$  COMPARED.  $1900^\circ C$ .

Reactant.	Initial Pressure (mm. $\times 10^{-3}$ ).	Composition of Product.			
		% $CO_2$ .	% CO.	% $O_2$ .	$k$ (min $^{-1}$ ).
$O_2$ . . .	621	0.15	8.65	91.2	0.20
$O_2$ . . .	19	2.75	35.8	61.4	0.19
$O_2$ . . .	191	0	3.4	96.6	0.10
$O_2$ . . .	20	5.2	37.5	57.3	0.09
$CO_2$ . . .	31	—	—	—	0.003
$CO_2$ . . .	24	—	—	—	0.001
$CO_2$ . . .	24	—	—	—	0.0025
$CO_2$ . . .	34	—	—	—	0.0025

writer.<sup>5</sup> The  $H_2O$ , after being strongly adsorbed on the charcoal, reacted with it in the adsorbed condition to form  $H_2$  and CO. The CO was, however, only desorbed very slowly. At the higher temperatures used in the present work, the separate stages of the reaction will occur much more rapidly and cannot therefore be distinguished, although the fact that  $H_2O$ ,  $CO_2$  and  $N_2O$  all showed a tendency towards zero order reaction at temperatures around  $1000^\circ C$ ., can be explained as due to the slow desorption of the CO produced in all the reactions. Since the gases all react at approximately the same rate, the reactions will all tend to zero order at about the same temperature, owing to the slow desorption of a common product.

The present results provide direct evidence that the primary product of the reaction of  $O_2$  with carbon above  $1000^\circ C$ . is principally CO and not  $CO_2$ . The results in Table X were obtained in a consecutive series of runs with the same filament.

The rates of reduction of  $CO_2$  are so low as to preclude the possibility that the high percentages of CO formed in the  $O_2$  runs were the result of secondary reduction of the primary product,  $CO_2$ . To account in such a way for the observed CO/ $CO_2$  ratios it would be necessary for the reaction constant for the reduction of  $CO_2$  to be substantially greater than that for the  $O_2$  reaction, rather than about 50 times less as it was found to be.

<sup>5</sup> Strickland-Constable, *Proc. Roy. Soc. A*, 1947, 189, 1.

<sup>6</sup> Sponer, *Molekülspektren*, Vol. I, part 4.



The small amounts of  $\text{CO}_2$  formed are, on the contrary, probably the result of the secondary oxidation of  $\text{CO}$ .

Meyer<sup>3</sup> has found that the reactions of  $\text{CO}_2$  and  $\text{H}_2\text{O}$  with carbon filaments at temperatures above  $1800^\circ\text{C}$ . are both of zero order, with a strong positive temperature coefficient represented by an activation energy of 90,000 cal. These results differ from the present ones in the same way as Meyer's results with  $\text{O}_2$  differed from the writer's, and presumably the differences must have the same explanation.

Meyer, when discussing the differences between his own results and those of other workers, has laid stress on the purity of the materials, and in particular of the graphite surface. Since the present writer has always attempted to prepare the graphite in the same manner as Meyer, and has paid considerable attention to the purity of the gases, he finds it difficult to believe that the differences are attributable to such causes.

In the case of  $\text{O}_2$  the possibility that the discrepancies were due to glow discharge has been discussed in detail,<sup>4</sup> and what was said for  $\text{O}_2$  would also apply to the gases discussed here. The present investigation has moreover disclosed no fresh clue as to the cause of the differences, so that although the glow discharge explanation may be open to some objection, no other at present can be advanced.

The writer wishes to express his special thanks to Prof. C. N. Hinshelwood for his advice and help throughout the work described in this paper. The work was carried out as part of the programme of the Fuel Research Board of the Department of Scientific and Industrial Research, and is published by permission of the Director of Fuel Research. The illustrations are Crown copyright and are reproduced by permission of the Controller of His Majesty's Stationery Office.

### Summary.

1. A study has been made of the reactions of  $\text{N}_2\text{O}$ ,  $\text{H}_2\text{O}$  and  $\text{CO}_2$  with carbon filaments at temperatures of from  $900^\circ\text{C}$ . to  $2000^\circ\text{C}$ . and at pressures of less than 1 mm.
2. All the reactions are of the first order above  $1200^\circ\text{C}$ . but tend to fractional order below this.
3. The rates of reaction of all three gases rise from 900 to  $1200^\circ\text{C}$ ., and then remain approximately constant up to  $2000^\circ\text{C}$ ., except in the case of  $\text{N}_2\text{O}$ , whose rate increases again above  $1600^\circ\text{C}$ .
4. The rates of reaction depend to a certain extent on the immediate past history of the filament, especially in the middle temperature region from  $1200^\circ$  to  $1600^\circ\text{C}$ . Heating the filament at a high temperature reduces the rate of reaction at low temperatures. Reactions at low temperatures increase the rate of subsequent reactions at higher temperatures.
5. In the reactions of  $\text{N}_2\text{O}$  and  $\text{H}_2\text{O}$  the principal oxygen containing product is  $\text{CO}$ ; very little  $\text{CO}_2$  is formed.

### Résumé.

On a étudié les réactions de  $\text{N}_2\text{O}$ ,  $\text{H}_2\text{O}$  et  $\text{CO}_2$  avec des filaments de carbone à des températures variant de 900 à  $2000^\circ\text{C}$ . et à des pressions inférieures à 1 mm. Toutes les réactions sont du premier ordre au-dessus de  $1200^\circ\text{C}$ ., mais leur ordre devient fractionnaire au-dessous de cette température. Les vitesses de réaction des trois gaz présentent une variation anormale au-dessus de  $1200^\circ\text{C}$ . et dépendent en partie du passé récent du filament.

### Zusammenfassung.

Die Reaktionen von  $\text{N}_2\text{O}$ ,  $\text{H}_2\text{O}$  und  $\text{CO}_2$  mit Kohlenfäden sind bei Temperaturen zwischen  $900^\circ$  und  $2000^\circ\text{C}$ . und Drucken geringer als 1 mm. untersucht worden. Oberhalb  $1200^\circ$  sind diese Reaktionen von der ersten Ordnung aber zeigen unterhalb  $1200^\circ$  Bruchordnungen. Für alle drei Gase ist die Temperaturabhängigkeit oberhalb  $1200^\circ$  abnormal und ist zu einem gewissen Grad von der Vorgeschichte des Kohlenfadens abhängig.

*Physical Chemistry Laboratory,  
Oxford University.*

# THE EXTENSION OF THERMODYNAMIC VALUES FROM THE ALIPHATIC TO THE AROMATIC SERIES.

BY J. G. M. BREMNER AND G. D. THOMAS.

Communicated by DR. M. P. APPLEBEY.

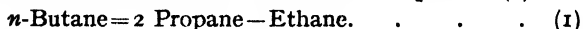
Received 13th September, 1946.

The heat of formation of an organic compound, in the absence of effects due to resonance, may be derived with fair accuracy by summing the individual contributions assigned to each valence bond. Tables of such bond values have been prepared by Pauling<sup>1</sup> and others.<sup>2, 3</sup>

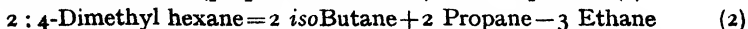
In this paper it will be briefly demonstrated that the free energies of formation and consequently entropies of aliphatic hydrocarbons may also be regarded as additive properties. Entropy values derived from the aliphatic series cannot, however, be applied directly to cyclic compounds since the process of ring closure will itself be shown to involve a considerable entropy change. It is the main object of this paper to distinguish the various entropy changes which accompany the referring of benzene to the aliphatic hydrocarbons and, in particular, to assess the magnitude of the entropy change associated with the resonance effect.

## I. The Additivity of Thermodynamic Properties and their Estimation by Group Equations.

In showing the free energies of formation and consequently entropies to be additive properties, the aliphatic molecule is broken down into characteristic groups. For the paraffin hydrocarbons the main groups considered are  $-\text{CH}_3$ ,  $=\text{CH}_2$ ,  $-\text{CH}-$  and  $=\text{C}-$ , while for the olefin series we include groups such as  $\text{CH}_2=\text{CH}-$  and  $-\text{CH}=\text{CH}-$ . In this way an attempt has been made to take into account the known differences between isomers which valence bond<sup>4</sup> methods ignore. Free energy values have been assigned to the characteristic groups, but a full account of this method awaits subsequent publication. Instead of summing individual group contributions, our present purpose is served by estimating the thermodynamic properties of an organic compound, in equivalent fashion by referring it to other compounds containing the same number and type of groups. Thus *n*-butane may be regarded as being formed from two propane molecules minus one ethane molecule as in equation (1):



Similarly, 2 : 4-dimethyl hexane may be represented as being formed by the de-ethanation of (propane + isobutane), as in equation (2).



Equations such as (1) and (2) in which there is an identity of groups on either side are termed "group" equations. They clearly ignore the question of "best" values.

<sup>1</sup> Pauling, *The Nature of the Chemical Bond* (1939), Chap. 2 and 4.

<sup>2</sup> Sidgwick, *The Covalent Link in Chemistry* (1933).

<sup>3</sup> Rice, *Electronic Structure and Chemical Binding* (1940).

<sup>4</sup> Bruins and Czarnecki, *Ind. Eng. Chem.*, 1941, 33, 201.

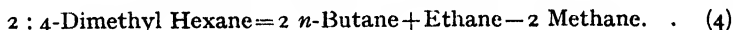
Both the free energy and heat change associated with the right-hand side of equations (1) and (2) are given in Table I, together with the known

TABLE I.—THE FREE ENERGY AND HEAT OF FORMATION OF *N*-BUTANE AND 2 : 4-DIMETHYL HEXANE DERIVED FROM GROUP EQUATIONS (1) AND (2).

Thermodynamic Property (kcal.) \ Temperature (°K.)	300.	600.	800.	1000.
$\Delta G(2C_3H_8 - C_4H_{10})$ . . . . .	- 3.3	25	45	65.2
$\Delta G_{n}C_4H_{10}$ . . . . .	- 3.6	24.6	44.5	64.7
Deviation . . . . .	+ 0.3	+ 0.4	+ 0.5	+ 0.5
$\Delta H(2C_3H_8 - C_4H_{10})$ . . . . .	29.4	-34.0	-35.7	-36.5
$\Delta H_{n}C_4H_{10}$ . . . . .	-29.85	-34.3	-36.0	-36.88
Deviation . . . . .	+ 0.5	+ 0.3	+ 0.3	+ 0.4
$\Delta G(2 \text{ iso}C_4H_{10} + 2C_3H_8 - 3C_2H_6)$ . . . . .	4	63.5	104.8	146.6
$\Delta G_{2:4 \text{ D.M.H.}}$ * . . . . .	3.14	61.9	102.8	144.1
Deviation . . . . .	+ 0.8	+ 1.6	+ 2.0	+ 2.5
$\Delta H(2 \text{ iso}C_4H_{10} + 2C_3H_8 - 3C_2H_6)$ . . . . .	-51.9	-59.4	-61.9	-62.8
$\Delta H_{2:4 \text{ D.M.H.}}$ * . . . . .	-52.5	-59.7	-62.1	-63.2
Deviation . . . . .	+ 0.6	+ 0.3	+ 0.2	+ 0.4

\* Dimethyl hexane.

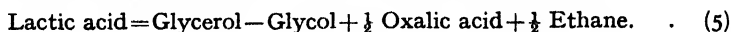
values<sup>5</sup> for *n*-butane and 2 : 4-dimethyl hexane respectively. The deviation is of the 1 kcal. order and is smaller than that given by the bond equations (3) and (4) in which there are no restrictions as to identity of groups.



At 300° K. the deviation in the free energy and heat of formation is + 4.4 and + 4.8 respectively for *n*-butane and + 6.1 and + 8.3 respectively for 2 : 4-dimethyl hexane, as given by equations (3) and (4).

With regard to the olefinic hydrocarbons it is interesting to note that Thacker, Folkins and Miller<sup>6</sup> gave the same free energy of formation for more than one olefin in five cases.\* On splitting their formulæ down it is evident that where this is the case, the groups comprising the molecules are the same. This additivity of free energies and therefore of entropies is clearly related to the approximately constant vibration frequencies which are associated with a given group in different compounds.<sup>7</sup>

As a final illustration of the group method lactic acid, comprising CH<sub>3</sub>, CHOH and COOH groups, may be represented as in equation (5).



The data of Parks and Huffman<sup>8</sup> applied to the right-hand side of equation (5) give -119 kcal. for the free energy of formation of gaseous lactic acid at 298° K. as against the known value of around -121 kcal.

<sup>5</sup> Rossini, *Bur. Stand. J. Res.*, 1945, **34**, 403.

<sup>6</sup> Thacker, Folkins and Miller, *Ind. Eng. Chem.*, 1941, **33**, 584.

<sup>7</sup> Thompson, *J. Chem. Soc.*, 1944, 183.

<sup>8</sup> Parks and Huffman, *Free Energies of Some Organic Compounds* (1932).

\* 2 Methyl-penten-1 and 2-ethyl buten-1; 3-methyl penten-1 and 4-methyl penten-1; *trans*-hexen-2 and *trans*-hexen-3; 2-methyl buten-2 and 3-methyl buten-2; 2 methyl penten-2 and 3 methyl penten-2.

## II. The Extension of the Group Method to the Alicyclic Series.

Group equations (6) to (10) are given in Table II to represent the formation of cyclohexane and cyclohexene from aliphatic hydrocarbons. Instead of using these equations to derive the thermodynamic properties of cyclohexane and cyclohexene we have given the thermodynamic changes accompanying these reactions.

The individual thermodynamic values used are those of Rossini<sup>8</sup> for the paraffins and of Aston<sup>9</sup> *et al.* for *cis*-buten-2. Values for both the entropy<sup>10</sup> of gaseous cyclohexane and its heat of formation<sup>11</sup> in the liquid state have recently been given. Taking 8.0 kcal. as the heat of vaporisation<sup>10</sup> gives  $\Delta H_f^\circ 298 = -29.7$  kcal. for gaseous cyclohexane.

TABLE II.—THE THERMODYNAMIC CHANGES ACCOMPANYING THE FORMATION OF CYCLOHEXANE AND CYCLOHEXENE FROM ALIPHATIC HYDROCARBONS AT 298° K.

Reaction.	Free Energy. (kcal.)	Reaction Heat. (kcal.)	Entropy Change (cal./degr.)
<i>Cyclohexane</i> —			
$3\text{CH}_3\text{CH}_2\text{CH}_2\text{CH}_3 = \text{Cyclohexane} + 3\text{C}_2\text{H}_6 \quad (6)$	-5.0	-0.9	+14.2
$2\text{CH}_3(\text{CH}_2)_3\text{CH}_3 = \text{Cyclohexane} + 2\text{C}_2\text{H}_6 \quad (7)$	-4.4	-0.1	+14.7
$2\text{CH}_3(\text{CH}_2)_4\text{CH}_3 = \text{Cyclohexane} + 2\text{C}_3\text{H}_8 \quad (8)$	-4.0	+0.6	+15.0
$2\text{CH}_3(\text{CH}_2)_5\text{CH}_3 = \text{Cyclohexane} + 2\text{C}_4\text{H}_{10} \quad (9)$	-4.4	+0.5	+15.9
<i>Cyclohexene</i> —			
$\text{CH}_3\text{CH}=\text{CH} \cdot \text{CH}_3 + 2\text{CH}_3(\text{CH}_2)_2\text{CH}_3 = \text{Cyclohexene} + 3\text{C}_2\text{H}_6 \quad (10)$	-5.9	-0.7	+17.3

Recent data for cyclohexene are not available. The heat of formation is, however, given with some accuracy by combining its heat of hydrogenation,<sup>12</sup> 28.6 kcal. with the heat of formation of cyclohexane to give  $\Delta H_f^\circ 298 = -1.1$  kcal.\* The known difference between the entropy of liquid cyclohexane and cyclohexene<sup>13</sup> has been used to give the entropy of gaseous cyclohexene by reference to gaseous cyclohexane. From this  $S^\circ_{298}$  of 72.3 units we obtain  $\Delta G_f^\circ 298 = 26.3$  kcal.

In Table II the formation of cyclohexane is represented by four equations (6-9) as the hydrocarbon series is ascended. Owing to the lack of reliable<sup>6</sup> data for the higher *cis*-2 olefins only one equation (10) is given

<sup>8</sup> Aston, Szasz, Woolley and Brickwedde, *J. Chem. Physics*, 1946, **14**, 67.

<sup>10</sup> Aston, Szasz and Fink, *J. Amer. Chem. Soc.*, 1943, **65**, 1138, and Ruehrwein and Huffman, *ibid.*, 1943, **65**, 1620.

<sup>11</sup> Moore, Renquist and Parks, *ibid.*, 1940, **62**, 1507.

<sup>12</sup> Conant and Kistiakowsky, *Chem. Rev.*, 1937, **20**, 182.

<sup>13</sup> Parks and Huffman, *J. Amer. Chem. Soc.*, 1930, **52**, 4388.

\* The value of -6 kcal. given by Parks and Huffman, *loc. cit.*<sup>8</sup>, p. 90, is evidently too low.

for the formation of cyclohexene. For all five reactions the entropy change is very similar, falling in the range 14-17 units. By contrast, the reaction heats are only  $\pm 1$  kcal., showing the heat of formation to be additive even when ring closure occurs. Somewhat surprisingly the entropy change is positive in sign. However, equations (6-10) differ from those, (1-5), treated previously in the paraffinic field in that they are of the general type.

$$N \text{ molecules} = N \text{ molecules} + 1 * \quad (11)$$

Otherwise the referring of the alicyclic to the aliphatic series by a group equation represents a reaction in which there is an increase in the entropy of translation. The same conclusion holds for bond equations of types (3) and (4), such a one for cyclohexane being for example



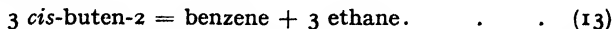
The Sackur-Tetrode<sup>14</sup> equation gives a measure of the increase in translation entropy accompanying reactions (6-10). The value calculated in this way is around 35 entropy units. As the entropy increase given in Table II for these reactions is around 15 units only, we infer the process of cyclisation to be accompanied by a decrease of about 20 entropy units. Such a decrease may be accounted for by considering the decrease in internal rotations<sup>15, 16</sup> and the increase in symmetry<sup>16</sup> accompanying reactions (6-10).

The symmetry numbers of butane, cyclohexane (chair form)<sup>17</sup> and ethane are 2, 6 and 6 respectively. Consequently, the changes in the external rotations in reaction (6) account for an entropy decrease of  $R(\log_e 6 + 3 \log_e 6 - 3 \log_e 2) = 10$  units, leaving a decrease of 10 units to be accounted for by a change in the number of internal rotations. For butane and ethane the number of internal rotations per molecule is 3 and 1 respectively giving the change in their number for reaction (6) as 6. If we ignore the small contribution of vibration to the entropy change, this gives 1.5 cal./degree as the entropy contribution of each degree of internal rotation. Such a contribution to entropy corresponds to the internal rotation of an ethane-like molecule with a barrier of some 3 kcal. hindering rotation.<sup>18</sup>

Reaction (10) depicting the group equation for cyclohexene formation may be treated in a similar manner. In this case the entropy decrease, allowing for the translational effect, is about 17 cal./degree. The symmetry number is 2 for both cyclohexene and *cis*-buten-2 giving  $R(\log_e 2 + 3 \log_e 6 - 3 \log_e 2) = 8$  units for the entropy change due to increased symmetry. The remaining 9 units may be accounted for by the decrease of 5 internal rotations which accompanies reaction (10).

### III. The Extension of the Group Method to Benzene.

As a typical group equation we may write the de-ethanation of *cis*-buten-2 to give benzene.



In deriving the thermodynamic changes accompanying this reaction we have used the entropy value of 64.4 units given by Pitzer and Scott<sup>19</sup> for benzene vapour at 298° K. Rossini<sup>20</sup> has recently determined the

<sup>14</sup> Wenner, *Thermochemical Calculations* (1941), p. 116.

<sup>15</sup> Wenner, *loc. cit.*<sup>14</sup>, Chap. 7.

<sup>16</sup> Herzberg, *Infra-red and Raman Spectra* (1945), Chap. 3, 4 and 5.

<sup>17</sup> Aston, Szasz and Fink, *J. Amer. Chem. Soc.*, 1943, **65**, 1138. Rasmussen, *J. Chem. Physics*, 1943, **11**, 249. Herzberg, *loc. cit.*<sup>16</sup>, p. 369.

<sup>18</sup> Herzberg, *loc. cit.*<sup>16</sup>, p. 525.

<sup>19</sup> Pitzer and Scott, *J. Amer. Chem. Soc.*, 1943, **65**, 810.

<sup>20</sup> Rossini, *Bur. Stand. J. Res.*, 1945, **34**, 65.

\* For bicyclic molecules, e.g. naphthalene, this equation becomes  $N \text{ molecules} = N \text{ molecules} + 2$ .

combustion heat of liquid benzene from which we derive  $\Delta H_{f,298}^\circ = 19.9$  kcal. for the vapour. Combining these values gives  $\Delta G_{f,298}^\circ = 31.0$  kcal. which differs by 1 kcal. from that given by Pitzer and Scott owing to their use of the earlier value of 782 kcal. as the combustion heat of benzene. The heat capacity data given by Pitzer and Scott enable these thermodynamic quantities to be calculated for the range 298-1000° K. Combining these data with those of Aston<sup>9</sup> and Rossini<sup>5</sup> for *cis*-buten-2 and ethane respectively gives the values presented in Table III.

TABLE III.—THE FREE ENERGY, HEAT AND ENTROPY CHANGE FOR THE DE-ETHANATION OF *cis*-BUTEN-2 TO BENZENE.

Temperature (°K.)	Free Energy (kcal.)	Reaction Heat (kcal.)	Entropy Change (cal./degr.)
0	-36.5	-36.5	—
298.1	-40.6	-36.6	13.4
400	-42.1	-36.7	13.5
500	-43.4	-36.7	13.4
600	-44.8	-36.6	13.7
700	-46.1	-36.7	13.4
800	-47.5	-36.7	13.5
900	-49.0	-36.8	13.6
1000	-50.3	-36.9	13.4

The heat change for reaction (13) is substantially constant at -36.5 kcal. over the temperature range examined. This quantity is equivalent to the resonance "energy" or resonance heat of benzene which is normally arrived at by the use of bond energies. The bond energies given by Pauling<sup>1</sup> are derived from the aliphatic series. Their sum represents the heat change at 18° C. for the formation of gaseous molecules from gaseous atoms. The difference between the value obtained by summation and that determined experimentally,  $E_{\text{benzene}}$ , for an aromatic compound is termed the resonance energy ( $\Delta H_{291}^R$ ).

$$3E_{C=C} + 3E_{C-C} + 6E_{C-H} = E_{\text{benzene}} - \Delta H_{\text{Benzene}}^R \quad (14)$$

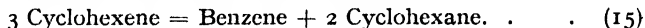
In equation (14) the use of the Pauling bond energy values with 17.2 kcal.\* as the heat of formation of benzene gives a resonance heat,  $\Delta H^R = 39.2$  kcal. Equations as (14) represent not only a bond but also an atom balance since a C=C bond, by the method of calculation, corresponds to one carbon atom, a C—C bond to a half and a C—H bond to a quarter of a carbon atom. Consequently the magnitude of  $\Delta H^R$  is independent of the sublimation heat of carbon and the dissociation heat of hydrogen. So far as the calculation of resonance heat, equations (13) and (14) are identical but that (13) deals with specific hydrocarbons while (14) is concerned with best values. Unlike equation (14), however, equation (13) enables the resonance heat to be calculated at other than room temperatures. The values given in Table III show it to be temperature independent up to 1000° K.

While the heat change of reaction (13) is customarily termed the resonance heat, it is evident from the previous treatment of alicyclic compounds that the entropy and free energy changes cannot be regarded likewise as resonance values. As with the alicyclic compounds, reactions such as (13) and, by implication, (14) involve an increase in the entropy of translation. In magnitude this increase amounts to 33.4 entropy units.

\* Calculated on a diamond basis from the 19.9 kcal. value given earlier in the paper which is for a graphite basis.

As the calculated entropy increase for reaction (13) is only 13.4 units, a decrease of 20 units is involved during the formation of benzene. As with reactions (6) and (10), we may account for this decrease partly by a change in the number of internal rotations and partly by an increase in symmetry. The effect of the latter in reaction (13) accounts for an entropy decrease of  $R(\log_e 12 + 3 \log_e 6 - 3 \log_e 2) = 11.5$  units. The remaining 8 units may be associated in part, at least, with the decrease of 3 internal rotations.

An alternative method of presentation is to combine equations (6), (10) and (13) in the form of the group equation (15).



Such an equation represents a reaction which is free from any effects due to increase in translational entropy or variation in internal rotations. From the previously derived data for benzene, cyclohexene and cyclohexane the thermodynamic changes accompanying this reaction may be written :

$$\begin{aligned}\Delta H^\circ_{298} &= -36.2 \text{ kcal.} \\ \Delta G^\circ_{298} &= -33.3 \text{ kcal.} \\ \Delta S^\circ_{298} &= -9.7 \text{ cal./degree.}\end{aligned}$$

With the appropriate change in sign the heat change represents the resonance energy of benzene. This calculation is, in fact, equivalent to that already carried out using the heats of hydrogenation of benzene and cyclohexene to derive the resonance energy.<sup>21</sup>

If in equation (15) we replace benzene by cyclohexatriene, the reaction involves no change in the number of rings or in the nature of the groups and linkage involved. Under these conditions the entropy change will be determined essentially by the symmetry numbers, and would be  $-R(\log_e 6 + 2 \log_e 6 - 3 \log_e 2) = -6$  cal./degree. The observed decrease is greater than this figure by 3.7 units, which may be termed the "resonance entropy" of benzene. Of this 3.7 units, 1.4 ( $R \log_e 2$ ) is accounted for by the fact that benzene has a higher symmetry than cyclohexatriene. The remaining 2.3 units is of the same order of magnitude as some of the discrepancies in Table I : however, if real, it can be related to the fact that the change from cyclohexatriene to benzene will involve a change in the characteristic vibration frequencies associated with singly and doubly bound carbon.

The authors wish to express their gratitude to Mr. R. P. Bell for his many helpful suggestions throughout the work.

### Summary and Conclusion.

The free energy of formation of the aliphatic hydrocarbons may be expressed as the sum of contributions characteristic of individual groups. The Pauling method of deriving the resonance energy of aromatic compounds by reference to the aliphatic series cannot be simply applied to the calculation of resonance free energy. The referring of bond or group values derived from the aliphatic to the aromatic series implies a reaction which is accompanied by an increase in the entropy of translation. The entropy decrease which remains when this effect is allowed for may, in the main, be attributed to a decrease in the number of internal rotations and an increase in symmetry. The additional small decrease due to resonance effects is estimated to be about 4 cal./degree for benzene.

### Résumé.

L'énergie libre de formation des hydrocarbures aliphatiques peut être exprimée comme la somme des contributions caractéristiques des divers groupes. La méthode de Pauling pour calculer l'énergie de résonance des composés aromatiques à partir de la série aliphatique, ne peut être appliquée simplement au calcul de l'énergie libre de résonance. En effet, le passage pour un groupe ou une liaison de la série aliphatique à la série aromatique implique une réaction qui s'accompagne d'un accroissement de l'entropie de translation. On peut

<sup>21</sup> Pauling, *loc. cit.*<sup>1</sup>, p. 126.

attribuer la diminution d'entropie, qui subsiste lorsque l'on tient compte de cet effet, principalement à la diminution du nombre des rotations internes et à l'accroissement de la symétrie. La faible diminution supplémentaire, due aux effets de résonance, est d'environ 4 cal./degré pour le benzène.

### Zusammenfassung.

Die Freie Energie der Bildung von aliphatischen organischen Verbindungen wird als Summe der Kontributionen, die verschiedenen charakteristischen Gruppen zugeteilt werden, ausgedrückt. Eine ähnliche Summierung ist für Ringverbindungen nicht gültig wegen der grossen Entropieveränderungen, die deren Bildung aus aliphatischen Verbindungen begleiten. Eine einfache Prozedur wird befolgt, um diese zu bestimmen.

#### *Note added in Proof.*

The reason for the 3 kcal. difference between the group and the Pauling resonance heats is the subject of a subsequent paper: the former is, naturally, similar to that given by the Kistiakowsky treatment.

*Imperial Chemical Industries Ltd.,  
Billingham Division,  
Billingham,  
Co. Durham.*

---

## ELECTRODE REACTIONS IN ALTERNATING FIELDS.

### III. THE DYNAMIC CAPACITANCE.

BY B. BREYER AND F. GUTMANN.

*Received 23rd September, 1946.*

In a paper entitled "Properties of the Electrical Double Layer at a Mercury Surface,"<sup>1</sup> Grahame studied several kinds of capacity which may be encountered in a study of the properties of the electrical double-layer by using a similar experimental arrangement as described by the present authors. When investigating the reversible electro-reduction Grahame noticed "phenomena which simulate the behaviour of a condenser of very large capacity," and which he termed "pseudo-capacity." This "pseudo-capacity" enters Grahame's work only incidentally. The present paper is devoted to the theoretical treatment and computation of this capacity, which it is proposed to call "dynamic capacitance" by analogy to the "dynamic resistance" treated in the previous papers of this series.

It has been shown in Part I<sup>2</sup> that alternating current maxima occur at the standard potential of an electrode, which, when the applied direct potential is increased, passes from a polarised state through a reversible stage into a state of concentration polarisation, while at the same time a small alternating voltage is superimposed on the direct potential governing the electrode process. These maxima have been shown to be due to changes in the "dynamic resistance" of the system, as a consequence of the non-linear relationship between current and voltage as expressed in the reversible electrode equation. Over a limited range of concentrations the observed values were shown (see Paper II) to be in close agreement with the values calculated on the basis of the theory of dynamic resistance.

It has been shown too (cf. Paper I.) that electrically, the system can be represented by an equivalent network (Fig. 1) where  $R_D$  represents

<sup>1</sup> *J. Amer. Chem. Soc.*, 1941, **63**, 1207.    <sup>2</sup> *Trans. Faraday Soc.*, 1946, **42**, 645.



the dynamic resistance,  $r$  the series resistance of the solution and  $C$  the capacitance.

In complex vector notation the impedance of such a network is given by  $Z = r + \frac{X_C R}{X_C + R}$ , where  $X_C = j/\omega C$  is the capacitive reactance of the system.

The theoretical treatment given in Part I assumed that the equivalent capacitance  $C$  of the electrode remains unaffected by the discharge processes. It has been pointed out (*loc. cit.*), however, that this is not quite the case, since the non-linearity between voltage and current, as expressed in the Nernst equation, gives rise to capacity changes as well.

It is convenient to regard  $C$  as the sum of two capacity terms,  $C_H$  and  $C_N$ . The former is the capacity of the Helmholtz double layer due to the presence of a supporting electrolyte, while the latter is a variable capacity due to the reversible electrochemical process.  $C_N$  will be referred to as "dynamic capacitance" and it is the purport of the present paper to

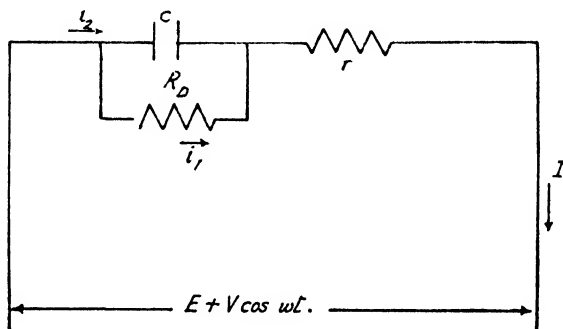


FIG. 1.

derive a quantitative expression for this varying capacity. This will permit the theoretical prediction of the total current through the cell over a wide range of concentrations.

The static capacitance of a system of conductors charged to a potential  $E$  by a charge  $Q$  is given by

$$C = Q/E \quad (1)$$

In the present case the law connecting voltage and current is non-linear and the "dynamic capacitance" is defined by:

$$C_N = dQ/de \quad (2)$$

i.e. by the rate of change of charge with the total applied potential (direct and alternating). The total instantaneous voltage  $e$  across the cell is the sum of the direct voltage  $E$  governing the electrode process and of the small superimposed alternating component  $V \cos \omega \tau$ . Therefore it follows that

$$e = E + V \cos \omega \tau \quad (3)$$

$$\text{Hence from (2) and (3)} \quad C_N = \frac{dQ}{d(E + V \cos \omega \tau)} \quad (4)$$

$$\text{or} \quad 1/C_N = \frac{dE - \omega V \sin \omega \tau d\tau}{dQ} = dE/dQ - \omega V \sin \omega \tau \frac{d\tau}{dQ} \quad (5)$$

Since  $d\tau/dQ = 1/i$ , it follows that

$$1/C_N = dE/dQ - \frac{\omega V \sin \omega \tau}{i} \quad (6)$$

From the reversible electrode equation

$$e = E_0 + A \log e^{\frac{i_d - i}{i}} \quad (7)$$

Where  $E_0$  is the standard potential of the electrode,  $i_s$  the saturation current and  $A$  stands for  $RT/nF$ , it follows that

$$i = \frac{i_s}{1 + e^{(E-E_0)/A}} \quad (8)$$

Inserting  $E + V \cos \omega \tau$  for  $E$  and then substituting (7) into (6) yields:

$$1/C_N = dE/dQ - \frac{\omega V \sin \omega \tau}{i_s} \cdot e^{(E+V \cos \omega \tau - E_0)/A} \quad (9)$$

To evaluate  $dE/dQ$ , i.e. the rate of change of charge with applied direct potential, the reversible electrode equation (7) is expressed in terms of concentrations, thus

$$e = E_0 + A \log \frac{C_{ox}^{el}}{C_{red}^{el}} \quad (10)$$

where  $C_{ox}^{el}$  and  $C_{red}^{el}$  stand for the concentrations of the oxidised and reduced component respectively *at the electrode*.

Solving (10) for  $C_{red}^{el}$ :

$$C_{red}^{el} = C_{ox}^{el} \cdot e^{-(E-E_0)/A} \quad (11)$$

The net free charge residing within a space of small thickness,  $d$  around an electrode of total area  $s$  is given by

$$Q_f = nFsd (C_{ox}^{el} - C_{red}^{el}) \quad (12)$$

or, substituting from (11):

$$Q_f = nFsd C_{ox}^{el} (1 - e^{-(E-E_0)/A}) \quad (13)$$

In the case of a dropping mercury electrode of drop time  $t$  and a mass of  $Hg(m)$  flowing per sec. from the capillary, the surface  $s$  can be expressed in terms of the capillary characteristics thus:

$$s = bm^{2/3}t^{2/3} \quad (14)$$

where  $b = 8.5 \times 10^{-1}$ , having dimensions  $M^{-2/3} L^2$  and involving the specific gravity of mercury.

The concentration of the oxidised component at the electrode can be deduced as follows: the flux of diffusing substance, i.e. the number of moles of solute diffusing per sec. through  $1 \text{ cm}^2$ , is given by

$$\text{Flux} = D \, dC/dx \quad (15)$$

where  $D$  is the diffusion coefficient and  $C$  the concentration at a point distant  $x$  from the electrode. Assuming a linear concentration gradient

$$dC/dx = \frac{C_{ox} - C_{ox}^{el}}{x} \quad (16)$$

The current is given by

$$i = nFs (\text{flux}) \quad (17)$$

Equating (8) and (17) and combining with (14), (15) and (16), it follows that the concentration of the oxidised component at the electrode is given by

$$C_{ox}^{el} = C_{ox} - \frac{x i_s}{DnFb(m t)^{2/3} [1 + e^{(E-E_0)/A}]} \quad (18)$$

Substituting the Ilkovič equation,<sup>3</sup> for  $i_s$

$$i_s = 0.732 \, nFD^{1/2} m^{1/2} t^{1/2} C_{ox} \quad (19)$$

which is the proper expression for the diffusion current at a dropping mercury electrode, and recalling that the thickness of the diffusion layer  $x$  is related to the diffusion current by

$$x = \frac{DnFs}{i_s} C_{ox} \quad (20)$$

it follows from (13) that the free space-charge  $Q_f$  equals

$$Q_f = \frac{nFb m^{1/2} t^{1/2} d [e^{(E-E_0)/A} - 1]}{1 + e^{(E-E_0)/A}} C_{ox} \quad (21)$$

<sup>3</sup> Ilkovič, *Coll. Czech. Chem. Comm.*, 1934, 6, 498.

Differentiating (21) yields for  $dQ/dE$ :

$$dQ/dE - C_{ox} \cdot \frac{2 n F b m^{2/3} l^{2/3} d}{A} \cdot \frac{e(E + V \cos \omega \tau - E_0)/A}{[1 + e(E + V \cos \omega \tau - E_0)/A]^2} \quad (22)$$

Combining (6) and (22), again substituting the Ilkovič equation for  $i_d$ , resubstituting for  $A$  and  $b$  and combining the numerical constants yields:

$$C_N = \frac{c(E - E_0 + V \cos \omega \tau)/A}{1 + e(E - E_0 + V \cos \omega \tau)/A} \cdot \frac{1 \cdot 245 m^{2/3} l^{2/3} d n F D^{1/2}}{n F D^{1/2} [1 + e(E - E_0 + V \cos \omega \tau)/A] - 3 \cdot 4 d \omega V l^{1/2} \sin \omega \tau} \quad (23)$$

Equation (23) can be written in the form

$$C_N = \frac{e\phi}{1 + e\phi} \cdot \frac{P}{M(1 + e\phi) - N} \quad P : M \neq 0 \quad (24)$$

Differentiating with respect to  $E$  and equating to zero:

$$dC_N/dE = 0 = \frac{e\phi}{1 + e\phi} \cdot \frac{-PM d\phi/dE}{(M(1 + e\phi) - N)^2} + \frac{P d\phi/dE}{M(1 + e\phi) - N} \cdot \frac{(1 + e\phi) e\phi - e^2\phi}{(1 + e\phi)^2} \quad (25)$$

This reduces to

$$0 = \frac{d\phi}{dE} \left[ \frac{1}{1 + e\phi} - \frac{Mc\phi}{M(1 + e\phi) - N} \right] - (d\phi/dE)[M(1 + e^2\phi) - N] \quad (26)$$

Equation (26) is true for all values of  $M$  only if

$$d\phi/dE = 0 \quad (27)$$

or, since

$$\phi = \frac{E - E_0 + V \cos \omega \tau}{A}$$

$$\phi = \text{Const.} \quad (28)$$

The condition (28) is valid for all ions, i.e. for all values of  $E_0$  only if

$$\phi = 0 : \text{hence } E + V \cos \omega \tau = E_0 \quad (29)$$

Since  $V \ll E$ , the dynamic capacitance will attain its maximum at the standard potential  $E_0$ , at which point its instantaneous value is given by

$$C_N(E_0) = \frac{2 \cdot 40 m^{2/3} l^{2/3} d n F D^{1/2}}{4 R T D^{1/2} - 6 \cdot 8 l^{1/2} d \omega V \sin \omega \tau} C_{ox} \quad (30)$$

The dynamic capacitance is thus seen to oscillate around a mean value. At  $E_0$  and at the instant when  $\sin \omega \tau = \pm 1$ ,

$$C_N(E_0) = \frac{n F b m^{2/3} l^{2/3} d D^{1/2} \cdot 3 \cdot 66 \cdot 10^{-1}}{(7 \cdot 32 \cdot 10^{-1} D^{1/2} R T \mp \omega V b l^{1/2} d)} C_{ox} \quad (31)$$

which is the maximum value of the dynamic capacitance, as registered by an instrument reading peak values of alternating current.

The quantity  $d$  in equation (31) is of dimension (length) and is a measure of the thickness of the ionic space-charge surrounding the electrode. It should be clearly understood, however, that while the direct current passing through the cell is due exclusively to the transport of electric charges by the ions across the double layer and their discharge at the electrode, the flow of the alternating component is due to a different mechanism. Only part of the A.C. is due to actual transport of charges, whereas the greater part is caused by charge *transfers*, i.e. changes in the instantaneous electrical state and spatial composition of the ionic atmosphere around the electrode. The alternating current resistance, or dynamic resistance (see Paper I) is equivalent to the rate of change of resistance encountered by the ions during discharge. This resistive component represents energy irreversibly expended in the discharge process.

The dynamic capacitance, on the other hand, is essentially reversible and represents changes in the energy stored in and released from the electric field between the ions during subsequent halfcycles. These changes are

a function of the sum of the applied direct potential and the instantaneous value of the superimposed alternating voltage. In the proximity of a reversibly depolarised electrode there exists at every instant an equilibrium between the oxidised and reduced components, the relative concentrations of which depend on the total instantaneous potential. So the dynamic capacitance is a consequence of the *changes* in the ion-atmosphere participating in the electrochemical reaction. Due to the absence of an electrochemical process the dynamic capacitance is zero before the beginning of the discharge. It vanishes again, when the diffusion current region has been reached, because of the virtual disappearance of the oxidised component from the ion-atmosphere. The dynamic capacitance becomes a maximum at the standard potential, when the rate of change of the current as well as of the reaction becomes a maximum.

In addition there is energy stored in the electric field between the ion-sheath *as a whole* and the electrode, giving rise to the capacity of the electric double layer. This capacity is independent of the discharge and primarily governed by the supporting electrolyte. As far as is known, the nature of the supporting electrolyte also determines the thickness of the double layer itself. In contradistinction,  $d$  is the thickness of an ion-sheath, consisting of ions actually undergoing electrochemical reduction, as distinct from the ions of the supporting electrolyte, which remain unaffected by the discharge process.

### Experimental.

In the preceding mathematical discussion the alternating voltage has been assumed to be small compared with the direct voltage applied simultaneously. It has been found that values of approx. 45 mv. yield good and consistent results for concentrations above M./20,000.

In order to facilitate the numerical calculation, a schedule based upon the equivalent circuit in Fig. 1 has been developed. The following quantities enter therein and have to be evaluated or measured beforehand:

$C_H$ : the capacity of the Helmholtz-Gouy double layer at the electrode.

$r$ : the series resistance of the electrolyte, leads, voltage-dropping resistor in the circuit, etc.

$C_N$ : the dynamic capacitance as previously defined in equation (31) for  $E_0$ .

$d$ : already discussed, is a constant for any one ion species and depends neither on the capillary characteristics, nor on the concentration of the substance participating in the discharge process.  $d$  has to be evaluated from experimental data for every ion species investigated. Values for Cd, Zn, and Tl are shown in Table I, and  $R_D$  is the dynamic resistance as defined in Part I.

The series resistance  $r$  can be measured by determining the alternating current flowing through the cell under application of a superimposed potential of such a value as to render  $r$  constant, i.e. sufficient to discharge the ions of the supporting electrolyte (2.4 v. for potassium ions).

$C_H$  can be calculated from a knowledge of  $r$  and determination of the alternating current  $i_1$  through the cell at the lowest point immediately preceding the rise in current due to the ion-discharge. At this point, the total cell-impedance is  $Z = \sqrt{r^2 + X_{C_H}^2}$ , and since  $|X_{C_H}| = 1/\omega C_H$ ,

$$C_H = \frac{i_1}{[V_{(rms)}^2 - r^2 i_1^2]^{1/2}} \quad . \quad . \quad . \quad (32)$$

$C_N$  can be computed from equation (32)

$R_D$  represents the dynamic resistance and can be calculated from

$$R_D = \frac{4RT}{nF i_d} \quad . \quad . \quad . \quad (33)$$

TABLE I.\*

Compound.	Concentration (mol.)	$t$ (sec.).	$d$ , A.	$i$ in $\mu$ s.	
				Calculated.	Observed.
CdCl <sub>2</sub>	$2 \times 10^{-3}$	2.06	72.3	15.75	16.9
CdCl <sub>2</sub>	$2 \times 10^{-3}$	4.03		22.5	22.4
CdCl <sub>2</sub>	$1 \times 10^{-3}$	3.96		21.15	21.0
CdCl <sub>2</sub>	$5 \times 10^{-4}$	4.4		19.25	19.6
CdCl <sub>2</sub>	$2.5 \times 10^{-4}$	4.5		16.5	18.9
CdCl <sub>2</sub>	$1.25 \times 10^{-4}$	6.57		15.5	16.0
CdCl <sub>2</sub>	$5 \times 10^{-5}$	2.06		8.5	8.9
CdCl <sub>2</sub>	$5 \times 10^{-5}$	4.5		11.2	11.15
TiNO <sub>3</sub>	$2 \times 10^{-3}$	3.9	216	22.0	21.8
TiNO <sub>3</sub>	$1 \times 10^{-3}$	4.1		18.3	18.0
TiNO <sub>3</sub>	$5 \times 10^{-4}$	4.2		16.3	16.4
TiNO <sub>3</sub>	$1.25 \times 10^{-4}$	4.2		12.9	13.4
TiNO <sub>3</sub>	$5 \times 10^{-5}$	4.3		11.4	11.9
ZnSO <sub>4</sub>	$1 \times 10^{-3}$	3.4	72.3	16.95	15.75

\* N./10 KCl served as supporting electrolyte for CdCl<sub>2</sub> and ZnSO<sub>4</sub>, whilst TiNO<sub>3</sub> was dissolved in N./10 KNO<sub>3</sub>.

The authors are induced to think that the quantity  $d$  is connected with the diffusion coefficient  $D$  of the ion undergoing discharge.

which expression is identical with equation 29 in paper I. The diffusion current  $i_d$  can be calculated from the Ilkovič Equation.

The equivalent circuit given in Fig. 1 can be first simplified by introducing

$$C = C_H + C_N \quad (34)$$

since these capacities are in parallel. Next, it is convenient to convert the parallel arrangement  $C - R_D$  into an equivalent series circuit. For this, the well-known relationships

$$C_s = C \left[ 1 + \frac{1}{\omega^2 C^2 R_D^2} \right] \quad \text{and} \quad R_s = \frac{R_D}{1 + \omega^2 C^2 R_D^2} \quad (35)$$

are employed. These transformations result in the equivalent network shown in Fig. 2, which can be further simplified by adding the resistances.

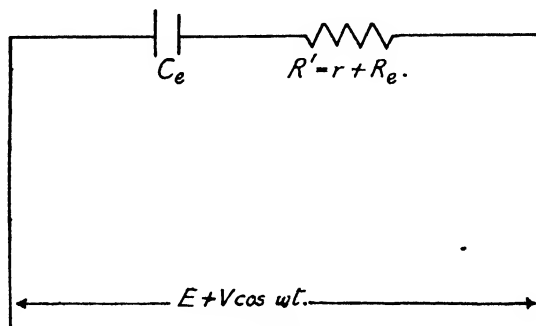


FIG. 2.

$$r + R_s = R' \quad (36)$$

The impedance of the whole network can then be written

$$Z = [R'^2 + X_{C_e}^2]^{1/2} \quad \text{where} \quad X_{C_e} = 1/\omega C_e \quad (37)$$

Finally, the total current passing through the cell can be calculated from

$$i_{\text{total}} = \frac{V_{\text{rms}}}{Z} \cdot \cdot \cdot \cdot \cdot \quad (38)$$

It is seen that for high concentrations of the electro-reducible ion the total current will tend to be limited by the series resistance, so that higher concentrations lead to hardly any further increase in  $i$ , whereas at very low concentrations the shunt capacitance  $C_H$  will become the current determining factor.

The experimental results summarised in Table I were obtained with the experimental arrangement described in Part II. The calibration of the amplifier-valve-voltmeter was checked before every measurement, but was found to keep constant within 1 % over a period of months. A.C. of mains frequency (50 cycles/sec.) was employed. It is obvious from the equivalent circuit in Fig. 1, that a lower frequency would permit somewhat better results at higher concentrations, since it would tend to increase the capacitive component of the total impedance.

The authors' thanks are due to Prof. E. C. Earl for his constant encouragement, to Dr. G. Larri for most helpful advice and constructive criticism, and to the University of Sydney for a Commonwealth Research Grant which made this work possible.

### Summary.

The capacity changes at a reversibly depolarised electrode in an alternating field have been investigated theoretically and experimentally. Quantitative expressions have been derived for the "dynamic capacitance" due to the non-linear current-voltage relationship at such an electrode and it has been shown that the capacitance reaches a maximum at the standard potential. Its origin is to be found in charge-transfers within the ion atmosphere participating in the electrochemical process.

### Résumé.

On a étudié d'un point de vue théorique et d'un point de vue expérimental les variations de capacité à une électrode réversiblement dépolarisée dans un champ alternatif. On a déduit des expressions quantitatives pour la "capacité dynamique," due à ce que la relation entre intensité et voltage n'est pas linéaire à une telle électrode et on a montré que la "capacitance" atteint au potentiel standard un maximum, qui a pour origine les transferts de charge dans l'atmosphère ionique, participant au processus électrochimique.

### Zusammenfassung.

Die Kapazitätsveränderungen an einer reversibel-depolarisierten Elektrode in einem wechselnden Feld sind theoretisch und experimentell untersucht worden. Quantitative Formeln sind für die "dynamische Kapazität," die von der nicht-linearen Beziehung zwischen Stromstärke und Spannung hervorgerufen wird, abgeleitet worden und es wird gezeigt, dass die Kapazität beim Normalpotential einen Maximalwert hat. Die Kapazität hat ihren Ursprung in den Ladungsübertragungen innerhalb der Ionenatmosphäre, die am elektrochemischen Vorgang teilnimmt.

*Physico-Chemical Laboratory,  
Faculty of Agriculture,  
The University of Sydney,  
Australia.*

# SOME PHYSICAL PROPERTIES OF SOLIDIFIED SODIUM-AMMONIA SOLUTIONS.

BY ARTHUR J. BIRCH AND D. K. C. MACDONALD.

*Received 10th March, 1947.*

Sodium-ammonia solutions have recently come into fresh prominence as a result of reports that superconductivity had been observed in the solidified state in the temperature range— $183^{\circ}$  to  $-95^{\circ}$  c. R. A. Ogg (Jr.)<sup>1, 2, 3</sup> observed a considerable drop in resistance to a low value on cooling a N. solution in liquid oxygen. He also reported the observation of a magnetic moment indicative of a persistent current in a ring specimen frozen in a magnetic field. A number of workers<sup>4, 5</sup> have failed to confirm this observation; Hodgins,<sup>6</sup> however, reported the same phenomenon in a much weaker degree. In view of these reports and because of the intrinsically interesting nature of the solutions their physical properties have been examined over the temperature range  $-33^{\circ}$  to  $-183^{\circ}$  c. A short note on the significance of this work has been published elsewhere.<sup>7</sup>

## Experimental.

**Thermometry.**—A variation of the standard Beckmann procedure was used. The appropriate amount of sodium in 50 cc. of ammonia was placed in a thin-walled test tube and supported in a somewhat larger tube with plugs of cotton-wool. For the melting-point measurements the specimen was first frozen in liquid oxygen and then transferred to the outer vessel and left to warm in the atmosphere, measurement being started as soon as a steady rate of warming had been achieved. For the freezing-point measurements the whole system was immersed in liquid oxygen.

Temperature measurements were taken by means of a bi-thermocouple system (copper-constantan-copper), one junction being permanently immersed in liquid oxygen, the other in the specimen. Since the substance is an electrical conductor and chemically very active, the wires leaving the junction were encased in glass tubes with rubber plugs. If this precaution was not observed irregular results were obtained because of the formation of a pseudo-junction through liquid formed on the surface at higher temperatures. The definition of the curves (Fig. 1 and 2) bears witness to the efficacy of the method (cp. those of Ruff and Zedner).

**Conductivity. A.**—A search-coil of some 3000 turns was immersed in a Dewar vessel filled with liquid oxygen, in turn fitted into a solenoid providing fields up to the order of 1000 gauss. The specimen was frozen—in some cases in the field, in others the field was switched on after freezing—the field was then switched off and the galvanometer placed in circuit before withdrawing the specimen a second or so later.

**B.**—A T-piece of glass tubing about 8 mm. diam. was constructed, the cross-piece being 45 mm. long with its ends sealed. Four platinum leads were sealed externally and passed round the head of the T, the outer (current) electrodes being 36 mm. apart and the inner (potential) electrodes 30 mm. apart. A bare copper-constantan junction was attached to the apparatus so as to lie parallel and close to the cross-piece. The heat capacity of this system was very low. The

<sup>1</sup> Ogg, Jr., *Physic. Rev.*, 1946, **69**, 243, *ibid.*, **69**, 544, *ibid.*, **70**, 93.

<sup>4</sup> Boorse, Cook, Pontius and Zemansky, *Physic. Rev.*, 1946, **70**, 92.

<sup>5</sup> Daunt, Desirant, Mendelssohn, and Birch, *Physic. Rev.*, 1946, **70**, 219.

<sup>6</sup> Hodgins, *Physic. Rev.*, 1946, **70**, 568.

<sup>7</sup> MacDonald, Mendelssohn and Birch, *Physic. Rev.*, 1947, **71**, 563.

specimen was prepared by immersing the T-piece for about a minute in the solution and then transferring rapidly to a bath of petrol (b.p. 40-60°) pre-cooled to the desired temperature by means of liquid oxygen. This bath solidified at about  $-130^{\circ}$  but could usually be super-cooled to about  $-160^{\circ}$  when required. A measuring current of  $\sim 0.7$  ma. was usually employed: the potential leads were taken via a resistance of  $10^6 \Omega$  to a sensitive galvanometer system. Where necessary with the highly-concentrated solutions the arrangement was modified to enable the very low resistivities to be measured. Warming of the bath was carried out by leaving it in air.

**Magnetic Susceptibility.**—These measurements were carried out using a ballistic method incorporating a compensating secondary coil to minimise random fluctuations arising in the primary field. The two secondary coils, each of some 4000 turns, suitably spaced apart, were oppositely wound on a brass cylinder provided with a hard-soldered base impervious to liquid oxygen. The apparatus was immersed in liquid oxygen and the whole placed in the primary solenoid. The system was carefully balanced with no specimen present so as to give minimum random deflection of the galvanometer connected across the coils. The apparatus was then rigidly clamped to ensure avoidance of vibration during observations. The required specimen—normally 39 cc.—in a test-tube, was placed inside the cylinder and raised from one coil to the other. Approximate calibrations were effected using the same volume of liquid oxygen and  $\text{CuSO}_4 \cdot 5\text{H}_2\text{O}$ .

## Discussion and Results.

### Thermometry.

Ruff and Zedner<sup>8</sup> have constructed an approximate diagram of state for the system sodium-ammonia using cooling curves. A further examination of both cooling and warming curves on concentrations between 0.88 % ( $\sim 0.5$  N.) and 13 %\* ( $\sim 7$  N.) has now shown more clearly even than the results of these workers that a eutectic of concentration somewhat greater than 13 % is formed, with a melting point of about  $-114^{\circ}$ † (see Fig. 1 and 2). It is of particular importance to note (see curve B, Fig. 2) that supercooling of this eutectic can occur even with comparatively slow cooling. This phenomenon specifically indicates the formation of a new crystalline phase which is probably metallic sodium, since the evidence<sup>10</sup> is against the formation of a definite compound of sodium and ammonia. From an examination of the slope of the curve for the super-cooled solution it is evident that the specific heat is higher than that of the crystallised solution, as would be expected for a liquid. There is evidence of formation of the eutectic with even a 0.88 % ( $\sim 0.5$  N.) concentration, since the curve (C, Fig. 1) has an inflection at about  $-110^{\circ}$  C.

It is well known<sup>8,9</sup> that solutions of sodium in liquid ammonia exhibit liquid-liquid phase separation with an upper consolute temperature of

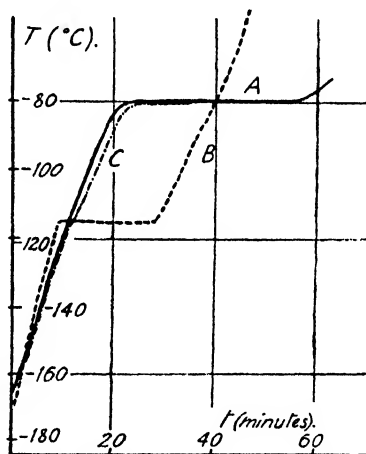


FIG. 1.—Heating curves for various concentrations.

<sup>8</sup> Ruff and Zedner, *Ber.*, 1908, 41, 1948.

<sup>9</sup> Krauss, *J. Amer. Chem. Soc.*, 1907, 29, 1557; 1908, 30, 1197; 1922, 44, 1949.

<sup>10</sup> Kraus, *J. Amer. Chem. Soc.*, 1908, 30, 653.

\* Concentrations are expressed as the % ratio of Na atoms to the total number of Na atoms and  $\text{NH}_3$  molecules.

† More accurate temperature-calibration has shown the eutectic temperature to be more closely  $-110^{\circ}$  C.



—  $41.6^{\circ}$  C. The theoretical basis for super-conductivity as predicted by Ogg<sup>1</sup> is founded on the assumption that this phase separation can be prevented by sufficiently rapid freezing. In order to examine this point small samples of various concentrations including 2.1 % (approx. N.) were dropped into a bath of petrol pre-cooled in liquid oxygen to about  $-150^{\circ}$  C. In every case phase separation was observed, drops of the bronze-coloured concentrated phase separating on the surface. In this connection it is also interesting to note a statement by Kraus and Lucasse (1922)<sup>2</sup>—"Judging by the reproducibility of the results, the system has little tendency to pass into the metastable regions. The second phase appears to separate immediately when the composition along the solubility curve is reached."

As a model experiment, examination of the phenol-water system, which shows a similar separation, proved that it was impossible to inhibit it even by the most rapid cooling of small samples to somewhat below the upper consolute temperature ( $68.3^{\circ}$  C.) using liquid oxygen as the cooling agent.

### Conductivity.

A. A further attempt was made to reproduce the persistent currents observed by Ogg<sup>3</sup> and later in much weaker degree by Hodgins.<sup>4</sup> The exact experimental procedure adopted by Ogg for the detection of persistent currents in his specimens is not completely clear. Our method (see experimental procedure) ensured that the high paramagnetic susceptibility of liquid oxygen did not interfere with the experiment. In a number of preliminary experiments transient magnetic moments of the order reported by Hodgins<sup>4</sup> were indeed observed. Careful investigation showed that these arose as a result of minute vibration of the search coil, or of iron objects in the laboratory. It is significant that the largest persistent current observed by Hodgins was equivalent to a field of only 0.01 gauss, which only amounts to about 1/50th of the vertical component of the earth's magnetic field. Having eliminated all disturbances of this type, 85 experiments were carried out with specimens prepared in the manner described by Ogg<sup>3</sup> but in no one of these was any indication of any persistent current obtained.

It should also be noted that in the course of a total of some 75 experiments on the conductivity of specimens carried out by the current-potential method no case of a resistance too low to be measured was encountered. An approximate calculation of the surface magnetic fields resulting from the measuring currents employed showed these to be much smaller than the earth's field. Consequently no effect on the incidence of superconductivity is to be expected from this source.

B. A systematic investigation of the variation of conductivity between  $-183^{\circ}$  and  $-33^{\circ}$  C. was undertaken using solutions of concentration varying between 0.88 % ( $\sim 0.5$  N.) and 13.0 % ( $\sim 7$  N.) with slow and rapid freezing. With rapidly frozen specimens reasonably reproducible results were obtained below  $-110^{\circ}$  C.; in all cases the results were reproducible above  $-110^{\circ}$  C. Some typical conductivity-temperature curves are shown in Fig. 3, 4, and 5. Slow freezing and rapid freezing give practically the same results for solutions of concentration greater than  $\sim 3.5$  % but for solutions of 2.1 % ( $\sim$  N.) a striking difference appears, since with slow freezing there is an initial rise to a very high resistance varying in an irregular manner with warming until there is a rapid drop around  $-110^{\circ}$  C.; while with rapid freezing the initial value is very low, rising in a regular manner with warming until there is again a rapid drop at  $-110^{\circ}$  C. This fall was present in a varying degree with different concentrations, becoming less marked with increasing concentration (cf. Fig. 5). The drop in resistance is readily explained by the melting

of the eutectic to give a highly conducting mobile liquid<sup>11</sup> which flows rapidly and fills up cracks in the specimen. During the thermometric experiments this flow could be visually observed quite clearly. In one instance of a slowly cooled 2.1 % ( $\sim$  N.) solution a current reading of

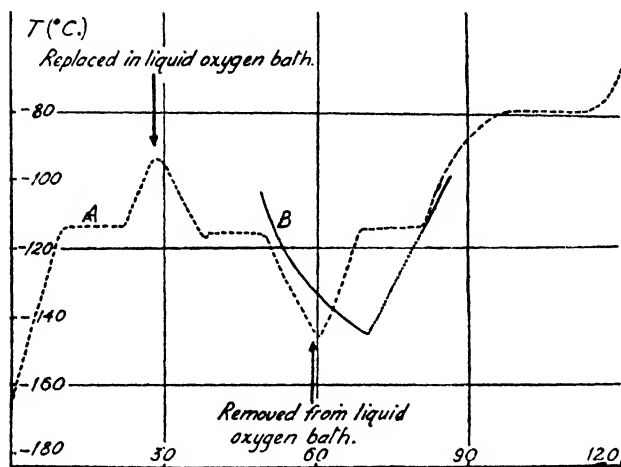


FIG. 2.

zero and no galvanometer deflection clearly indicated the presence of a complete break between the current and the potential lead. At the eutectic point the full value of the current was established over a tem-

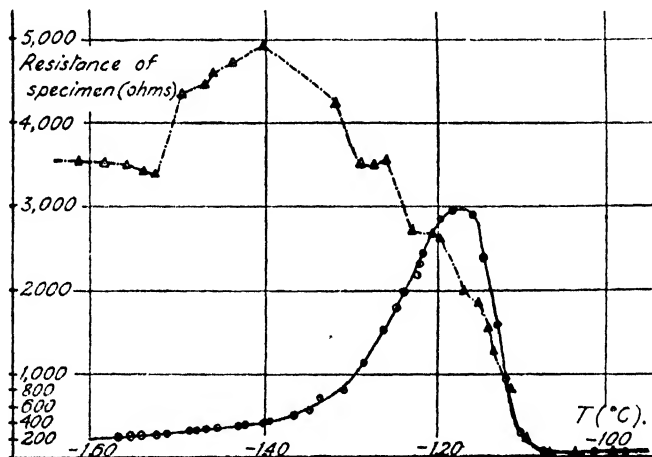


FIG. 3.—Resistance variation of 2.1 % specimen after rapid and slow freezing. perature range of less than  $1^{\circ}$  C. and the normal galvanometer potential reading was restored.

The low resistance initially obtained on rapid freezing of the 2.1 % ( $\sim$  N.) specimens can be explained by the persistence of a liquid phase due to super-cooling of the eutectic—already observed—and the consequent filling of cracks with a highly conducting solution. The rapid

<sup>11</sup> Kraus, *J. Amer. Chem. Soc.*, 1922, 44, 1949; Johnson and Meyer, *Chem. Rev.*, 1931, 8, 273; Farkas, *Z. physik. Chem.*, 1932, 161, 355.

rise on warming might at first sight appear to be anomalous temperature-dependent variation, but is almost certainly due to crystallisation of the eutectic, which becomes more rapid at higher temperatures. This was confirmed by the observation that a specimen rapidly cooled to  $-132^{\circ}$  and kept at that temperature in a petrol bath in a Dewar flask showed a rise in resistance by a factor 3.3 in 5 min.

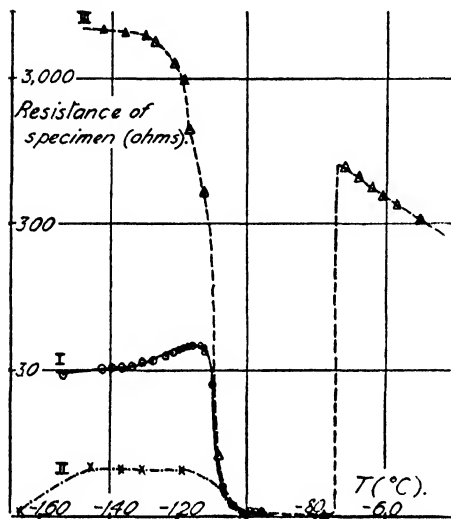


FIG. 4.—Resistance variation of 2.7 % specimen under differing conditions.

occasion, even with specimens warmed to  $-33^{\circ}\text{C.}$ , and must therefore be ascribed to some chemical deterioration of the sample. With a somewhat higher concentration (2.7 %) a series of 3 results on the same specimen yielded further confirmation of this theory (see Fig. 4). Curve I exhibits qualitatively similar behaviour to the initially rapidly frozen 2.1 % solution; curve II, obtained by slow cooling taking particular care to avoid vibration of the specimen can only be explained by persistence of the supercooled liquid during the warming to  $\sim -110^{\circ}\text{C.}$ ; curve III, which was obtained by slow freezing with very gentle tapping of the end of the glass former, shows clearly that complete crystallisation of the eutectic, probably accompanied by cracking, had occurred.

The reason for the smaller rise in resistance with the more concentrated solutions (cf. Fig. 5) is probably the larger amount of eutectic present, containing a considerable amount of sodium, which thus has the opportunity to separate in well-connected chains of crystals. The failure of the solutions of less than 2.1 % concentration to show the low resistance on rapid freezing may be due to the presence of an insufficient quantity of the super-cooled liquid to provide a continuous conductive path. In the case of the 2.1 % solution initial cooling to below the consolute temperature where phase separation has occurred, made no difference to the results obtained on subsequent freezing.

The rise was also found to be irreversible, re-cooling producing a further rise. Confirmation that the crystallisation proceeded more slowly at lower temperatures was obtained when a specimen was held at  $-183^{\circ}\text{C.}$  where its resistance was initially very low, and rose very slowly over a period of 2 hr. It is well known that if a liquid mixture can be sufficiently supercooled its rate of crystallisation becomes increasingly slow.

It would be expected on the basis of this hypothesis that if the same specimen were rapidly re-frozen after raising the temperature above that of the eutectic melting point, the above results would be reproduced. For a 2.1 % ( $\sim \text{N.}$ ) solution, however, this was observed on only one

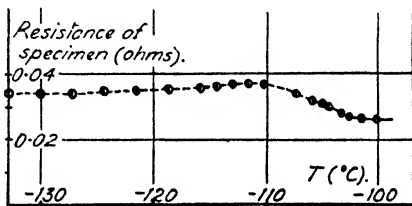


FIG. 5.—Resistance variation of 13 % specimen.

The changes in resistivity accompanying warming to  $-33^{\circ}\text{C.}$  are also of interest. There is a rapid rise at about the melting point of ammonia which clearly occurs as the result of the production of a large proportion of the immiscible dilute phase of much lower conductivity.<sup>11</sup> As the two phases approach one another in concentration with increasing temperature the resistance falls steadily to a value at  $-33^{\circ}\text{C.}$  agreeing satisfactorily with that originally observed before freezing.

Three specimens were frozen to liquid hydrogen temperature ( $\sim 20^{\circ}\text{K.}$ ). Out of two experiments where the sample was directly frozen in liquid hydrogen from  $-33^{\circ}\text{C.}$ , one gave a low resistance, indicating that the eutectic may be super-cooled even to this temperature.

A 4.2 % solution of potassium in ammonia was frozen to  $\sim -157^{\circ}\text{C.}$  where it showed a very low resistance which rose very slightly without anomaly until the melting point of ammonia was reached. This is in accordance with the known fact<sup>8</sup> that the eutectic point of potassium and ammonia lies below  $-183^{\circ}\text{C.}$ \* It is hoped at a later date to investigate both potassium and lithium solutions in more detail.

### Magnetic Susceptibility.

In view of the fact that magnetic anomalies might possibly account for Ogg's results (e.g. <sup>5</sup>) measurements of the magnetic susceptibility,  $\chi$ , were undertaken. Pure ammonia at  $-183^{\circ}\text{C.}$  gave a value of  $\chi \doteq -1.6 \times 10^{-6}$ ; a 2.1 % solution of sodium in ammonia gave the same value; a 6.9 % solution gave a slightly lower figure in agreement with the fact that sodium is weakly paramagnetic. Freezing the solution "rapidly" by adding the liquid drop by drop into the vessel cooled in liquid oxygen yielded identical results. "Spot" readings of the susceptibility as the temperature was raised showed no apparent anomaly.

**Conclusion.** The formation of the highly conducting eutectic and its ability to super-cool afford a complete explanation of all the anomalous conductivity phenomena so far reported by workers on sodium-ammonia solutions; the same explanation appears most probable for qualitatively similar results on potassium-methylamine solutions reported by Weissman;<sup>12</sup> these solutions are also known to exhibit liquid-liquid phase separation.<sup>13</sup> No direct explanation of the reported magnetic measurements can be given, but in view of the large number of possible sources of error, some of which have been indicated above, it is strongly felt that the hypothesis of superconductivity can be dismissed.

The authors wish to express their warm appreciation of the valuable advice and kindly criticism of Dr. K. Mendelssohn whose earlier work in the field encouraged them to undertake this investigation. This work was carried out during the tenure of a Nuffield Fellowship (D. K. C. M.) and an I.C.I. Research Fellowship (A. J. B.).

### Summary.

Thermometric, resistance and magnetic susceptibility measurements have been carried out on solidified solutions of sodium in liquid ammonia. The formation of a concentrated, highly conducting eutectic which can be supercooled below its m.p. ( $-110^{\circ}\text{C.}$ ) explains apparent anomalies in electrical resistance. No evidence of superconductivity or of anomalous magnetic properties was obtained.

<sup>12</sup> Weissman, *Physic. Rev.*, 1946, **70**, 571.

<sup>13</sup> Gibson and Phipps, *J. Amer. Chem. Soc.*, 1926, **48**, 312.

<sup>14</sup> Birch and MacDonald, *Nature*, 1947, **159**, 811.

\* More recent work by the writers<sup>14</sup> has shown that the m.p. of the eutectic of K and  $\text{NH}_3$  is  $\sim -157^{\circ}\text{C.}$ , i.e. fortuitously almost identical with the lowest temperature used by us in this experiment.

## Résumé.

Des analyse thermiques, et des mesures de résistance et de susceptibilité magnétique ont été faites pour des solutions solidifiées de sodium dans l'ammoniac liquide. La formation d'un eutectique concentré, hautement conducteur et qui peut être surfondu (point de fusion:  $-110^{\circ}\text{C.}$ ), explique les anomalies apparentes de la résistance électrique. Mais aucune superconductivité et aucune propriété magnétique anormale n'ont été mises en évidence.

## Zusammenfassung.

Thermometrische Messungen, sowie Messungen des elektrischen Widerstands und der magnetischen Suszeptibilität wurden an gefrorenen Lösungen von Natrium in flüssigem Ammoniak durchgeführt. Die Bildung eines konzentrierten, äusserst gut leitenden Eutektikums, das unter seinen Schmelzpunkt ( $-110^{\circ}\text{C.}$ ) unterkühlt werden kann, erklärt die scheinbaren Anomalien des elektrischen Widerstands. Es konnte kein Beweis für Supraleitfähigkeit oder anomale magnetische Eigenschaften gefunden werden.

*The Dyson Perrins Laboratory ;  
The Clarendon Laboratory,  
Oxford University.*

THE REACTIONS OF ORGANIC HALIDES  
IN SOLUTION.

By E. D. HUGHES AND C. K. INGOLD.

*Received 28th November, 1947.*

A short time ago A. G. Evans published some preliminary notes<sup>1</sup> dealing with the subject of substitution at a saturated carbon atom, and particularly with the role of steric hindrance. These notes represented our position in ways which seemed to us so far from the facts as to necessitate our issuing corrections.<sup>2</sup> Evans has now published two closely corresponding papers covering the same field.<sup>3</sup> In them, mistakes generally similar to those which we hoped we had corrected are again made. One of these can be dealt with simply at this time. The others, already partly covered, may suitably be left for further explicit treatment in association with later reports of new experimental work.

Contrary to implications by Evans, steric hindrance in nucleophilic bimolecular substitutions of alkyl compounds was recognised by Hughes and Ingold<sup>4</sup> in 1935. Calculations directed to its quantitative assessment were first reported by Hughes<sup>5</sup> in 1941; his account referred to a study of such substitutions in methyl, ethyl, *n*-propyl, isobutyl and neopentyl halides. The work has since been described in detail.<sup>6</sup> It has been shown, theoretically and practically, that steric hindrance appreciably affects the bimolecular nucleophilic substitutions of the compounds of all alkyl radicals except methyl, and that it plays a quite outstanding part in the case of the radical neopentyl.

<sup>1</sup> (a) Evans, *Nature*, 1946, **157**, 438; (b) *idem, ibid.*, **158**, 586; (c) *idem, ibid.*, 1947, **159**, 166.

<sup>2</sup> Hughes and Ingold, *Nature*, 1946, **158**, 94; (b) *idem, ibid.*, 1947, **159**, 166.

<sup>3</sup> (a) Evans, *Trans. Faraday Soc.*, 1946, **42**, 719; (b) *idem*, "Reactions of Organic Halides in Solution," *Mem. Proc. Manchester Lit. Phil. Soc.*, vol. 87.

<sup>4</sup> Hughes and Ingold, *J. Chem. Soc.*, 1935, 244.

<sup>5</sup> Hughes, *Trans. Faraday Soc.*, 1941, **37**, 603.

<sup>6</sup> Dostrovsky and Hughes, *J. Chem. Soc.*, 1946, pp. 157, 161, 164, 166, 169, 171; (b) Dostrovsky, Hughes and Ingold, *ibid.*, p. 173.

In the second of his preliminary notes,<sup>1b</sup> Evans dealt with the earlier history by stating that, whereas Hughes in 1941 had estimated steric compressions in the series methyl, ethyl, *n*-propyl, *isobutyl* and *neopentyl*,<sup>5</sup> Polanyi and he, in 1942, were the first similarly to consider *isopropyl* and *tert*-butyl.<sup>7</sup> We commented<sup>2b</sup> that, in the approximation to which we have hitherto worked, the case of ethyl covers that of *isopropyl* and *tert*-butyl, in which the steric compressions of ethyl are merely duplicated and triplicated. We may add that the five examples specified similarly cover all alkyl groups with only  $\alpha$ -  $\beta$ - and  $\gamma$ -carbon atoms (up to  $C_{13}H_{27}$ ), and therefore cover alkyl groups in general, since only in rare cases could  $\delta$ - or more distant carbon atoms be sterically important. This, of course, was why that particular set of five groups was selected for detailed study. We should make it clear that the additive relations indicated are expected to hold only in first approximation, and that, on the experimental side, our work was confined to the five key cases (though it has since been extended).

It would have been unnecessary to submit this note for publication but for the circumstance that Evans's historical comments in his latest papers<sup>3</sup> are still unsatisfactory, implying, as they plainly do, that we failed to recognise the steric effect in the substitutions of any alkyl group except *neopentyl*.<sup>8</sup>

### Summary.

The accounts which have been given by A. G. Evans of the recognition and estimation of steric hindrance in bimolecular nucleophilic substitution are supplemented and corrected.

### Résumé.

On a complété et corrigé l'exposé de A. G. Evans concernant l'identification et de l'évaluation de l'empêchement stérique dans la substitution bimoléculaire nucléophile.

### Zusammenfassung.

Der von A. G. Evans gegebene Bericht über die Feststellung und Auswertung der sterischen Hinderung bei der bimolekularen nucleophilen Substitution werden ergänzt und berichtet.

*University College, Bangor.*

*University College, London.*

<sup>1</sup> Evans and Polanyi, *Nature*, 1942, **149**, 608; (b) *ibid.*, p. 655.

<sup>8</sup> We may refer, but in illustration only, to Evans's page 728 of ref. 3 (a). One reads there that Evans and Polanyi estimated steric hindrance, by mathematical methods which are explained at some length, but (in a footnote) that Hughes only discussed the possibility of steric hindrance, without drawing any significant conclusion except for *neopentyl* substitutions. The facts are that Hughes in 1941 reported mutually confirmatory calculations and experiments pointing to significant steric effects in alkyl groups (ref. 5, cp. especially pp. 621-625), consistently with Hughes and Ingold's qualitative conclusion of 1935 (ref. 4, p. 246); and that Evans and Polanyi in 1942 reported parallel calculations without experiments (ref. 7 (a)), and subsequently referred to Hughes's previous paper (ref. 7 (b)).

## REVIEWS OF BOOKS.

**Conduction of Heat in Solids.** By E. L. S. CARSLAW and J. C. JAEGER. Oxford, at the Clarendon Press, 1947. Pp. vi + 386. Price 30s. net.

Physical chemists will welcome a re-written and modernised edition of what was Carslaw's standard text "The Mathematical Theory of the Conduction of Heat" published in 1921. Those who are familiar with the latter will realise on inspecting the new book how greatly the subject has advanced in the interim years. One sees much that is familiar in the old edition, especially in Chapters I to IX and in Chapter XIII, but throughout these chapters there is a steady enrichment in the number and variety of the chosen examples of heat flow problems used to illustrate the general methods. These examples are valuable to physicist, chemist, or engineer, and must greatly facilitate the study of diffusion kinetics in all its complexities. A new sequence of chapters has been devoted to the Laplace transformation method, which proves to be a very powerful method of approach to complex diffusion problems.

The number of heat transfer problems successfully solved is a tribute to the painstaking work of pioneer mathematicians, not least among whom are the authors themselves. The chemist may perhaps be rather bewildered when called upon to relate his own boundary conditions for flow of matter to those for one of the diverse solutions for heat flow, but the effort will repay handsomely any time thus spent since a considerable proportion of these heat flow problems has chemical analogues. In some of these analogues the simple isothermal transport of solutes by diffusion is under consideration; in another important group the flow of heat generated by chemical reaction within the diffusion medium is to be considered. A third group of problems involves transport of heat across boundaries where a heat resistant layer, regarded as infinitely thin, exists, so that discontinuities arise at the boundaries. The well-known phenomenon of rate-controlling phase-boundary processes in the transport of gases through metals provides an analogue which is at least partial, and may under special conditions be complete. The reader will find numerous other analogues throughout the book.

From the viewpoint of the chemist there are still gaps in the mathematical technique. He so often has to deal with problems where the diffusion coefficient is a function of the concentration of the diffusing species, and while there are graphical procedures for handling this problem, and at least one *approximate* mathematical procedure, a *precise* general method awaits evolution. To this extent the present book does not cover all the requirements of the chemist, and while on page 330 the authors make the briefest reference to the problem, it is not otherwise discussed. The other problem requiring a generalised diffusion equation, in which the diffusion coefficient is a function of the positional co-ordinates in the medium has also been only briefly reviewed. For the latter problem, however, the mathematical techniques given will be found adequate to obtain explicit solutions of the diffusion equation at least in a number of cases.

The format of the book is excellent and the Oxford University Press have maintained their usual high standards in the printing. The book should form a most useful addition to physico-chemical libraries.

R. M. B.

**The Photographic Recording of Cathode Ray Tube Traces.** By R. J. HERCOCK. Ilford Ltd., Ilford, London, 1947. Pp. iv + 60. Price 5s.

Slight in bulk, but well produced and clearly written, this little monograph deserves a warm welcome. For one thing, it is the first of a series of technical publications planned by Ilford's, and therefore—like *Oliver Twist*—one may reasonably ask for more. The various forms of focussing and electron reflection are briefly described, and after an account of the advantages to be gained by recording, we come to the nature of the traces, and the two methods of registering them, namely, oscillograms and cyclograms. The photographic part then begins in earnest, and deals with the formation of the latent image, by direct electronic action or by fluorescence. The remainder of the booklet is largely a collection of useful hints and data. As far as the reviewer has been able to check, the information is accurate and adequate. Indeed, both beginners and more experienced folk will be well rewarded by studying these pages carefully. They provide yet another instance of how rapidly photography is becoming the handmaid of other sciences, and (as has so often happened in other branches of knowledge before) in thus doing is tending to deepen and expand its own territory.

F. I. G. R.

**Symposium on Plasticisers:** Paper presented at the Centennial Celebrations of the University of Buffalo, June, 1946. Reprinted from *J. Polymer Sci.*, Vol. II, No. 2. Interscience Publishers, Inc., New York, and Elsevier Publishing Company, Inc., New York, 1947. Pp. 208. Price \$1.75.

During the war, the need for the production of plasticised vinyl chloride polymer and copolymer compositions, capable of enduring severe conditions in service uses, occasioned a great deal of work on plasticisers for these polymers both in this country and in the U.S.A. This occurred while the chemistry and physics of polymers themselves were in a phase of particularly rapid development; as a result much progress has been made in the interpretation of the available data on plasticised polymers in physico-chemical terms.

Apart from a paper by M. C. Reed, which outlines the technological requirements and main classes of plasticiser for vinyl polymers, most of the others are concerned with the two problems of the compatibility of the plasticiser and polymer, and the effect of the plasticiser on the mechanical properties of the polymer. A paper by V. L. Simril, however, discusses the bearing of the constitution of the polymer itself, showing how structural variations (such as *N*-substitution in the polyamides, or interpolymerisation of vinyl acetate with vinyl chloride) produce effects which may be termed internal plasticisation.



R. F. Boyer and R. S. Spencer discuss the effect of plasticiser on the so-called "second-order transition point," showing how this correlates with various empirical tests of brittleness, etc. A relationship is exhibited between these essentially kinetic properties, and the thermodynamic property specified by the Huggins'  $\mu$  constant. The least efficient plasticisers are those which are just solvents; very good solvents or just non-solvents are better.

W. Aiken, T. Alfrey, A. Janssen and H. Mark present some interesting data on the delayed elasticity of plasticised "Vinylite" and show that the shape of the creep curve differs according to the plasticiser. Their discussion of the molecular mechanism of plasticisation is enlightening; as they remark, the role of the plasticiser is not simple.

Though much progress has been made, much remains to be done; this symposium is an admirable summary of present views, although it also indicates their incompleteness.

P. A. S.

## MINUTES OF THE 41ST ANNUAL GENERAL MEETING

Held on WEDNESDAY, 24th September, 1947, at 9.45 a.m. in the Physical Chemistry Laboratory, South Parks Road, Oxford.

The President, Prof. W. E. Garner, C.B.E., D.Sc., F.R.S., was in the Chair.

1. The Minutes of the 40th Annual General Meeting were taken as read and confirmed.
2. The Annual Report and Statement of Accounts, together with the Report of the Auditors for the year 1946, were presented by the Honorary Treasurer, who said that although there had been an excess of income over expenditure for the year, next year the position might be reversed. This would merely mean, however, that the Society was spending money which had accumulated during the war years. He was glad to be able to report that the recent allowance of extra paper for printing the General Discussion Reports would release more paper for printing the monthly *Transactions*. Within two years it was hoped to catch up with arrears and be back to normal printing conditions. The Report was unanimously adopted and a vote of thanks was accorded to Dr. Slade for his very successful trusteeship of the Society's affairs.
3. The President mentioned that as Professor Allmand had accepted nomination for election to the Presidency he would be unable to continue as Chairman of the Publications Committee, an office he had held for ten years, and Professor E. A. Guggenheim, F.R.S., had consented to serve in this office.
4. A vote of thanks was then proposed by Sir John Lennard-Jones to Professor Garner for the very successful way in which he had controlled the activities of the Society during the past two years. The General Discussions had during that time got back to their pre-war strength, and had even exceeded it, and the continued success of the Society seemed assured.
5. The Officers and Ordinary Members of Council were elected to take office on the 1st of October as follows :—

### *President.*

PROF. A. J. ALLMAND, D.Sc., F.R.S.

### *Vice-Presidents who have held the Office of President.*

PROF. C. H. DESCH, D.Sc., F.R.S.

PROF. N. V. SIDGWICK, Sc.D., D.Sc., F.R.S.

PROF. M. W. TRAVERS, D.Sc., F.R.S.

PROF. E. K. RIDEAL, M.B.E., D.Sc., F.R.S.

PROF. W. E. GARNER, C.B.E., D.Sc., F.R.S.

### *Vice-Presidents.*

SIR CHARLES H. GOODEVE, D.Sc., F.R.S.     R. LESSING, Ph.D.

R. O. GRIFFITH, M.Sc.

PROF. H. W. MELVILLE, Ph.D., F.R.S.

PROF. C. N. HINSHELWOOD, F.R.S.

PROF. M. POLANYI, F.R.S.

SIR JOHN LENNARD-JONES, K.B.E.,  
D.Sc., F.R.S.

### *Honorary Treasurer.*

R. E. SLADE, D.Sc.

## 804 MINUTES OF THE ANNUAL GENERAL MEETING

*Chairman of the Publications Committee.*

PROF. E. A. GUGGENHEIM, M.A., Sc.D., F.R.S.

*Ordinary Members of Council.*

A. E. ALEXANDER, M.A., Ph.D.

G. S. HARTLEY, D.Sc.

R. P. BELL, M.A., F.R.S.

W. G. PENNEY, O.B.E., D.Sc., F.R.S.

PROF. G. M. BENNETT, M.A., Sc.D.

F. I. G. RAWLINS, M.Sc., F.R.S.E.,

C. W. DAVIES, M.Sc.

F.INST.P.

J. FERGUSON, Ph.D.

SIR ROBERT ROBERTSON, K.B.E.,

G. GEE, Sc.D.

D.Sc., F.R.S.

6. The thanks of the Society were accorded with acclamation to the retiring Officers and Members of Council.

This concluded the business of the Meeting.

# Transactions of the Faraday Society.

## AUTHOR INDEX—VOLUME XLIII, 1947.

	PAGE
<b>Adam, N. K.</b> See <i>Balson, E. W., Denbigh, K. G., and</i>	
<b>Akimov, G. W., and Clark, G. B.</b> Irreversible Electrode Potentials of Metals and their Solid Solutions. Part I: Irreversible Electrode Potentials of Metals . . . . .	679
Part II: Electrode Potentials of Solid Solutions . . . . .	685
<b>Anderson, J. S., and Morton, Mrs. M. C.</b> Semiconducting Properties of Stannous Sulphide. Part II: Thermoelectric Effect . . . . .	185
<b>Angus, W. R., and (the late) Tilston, D. V.</b> Magnetochemical Investigations. Part V: The Diamagnetism of Binary Liquid Mixtures. . . . .	221
Part VI: Additional Notes on Standardisation and Technique . . . . .	235
<b>Balson, E. W., Denbigh, K. G., and Adam, N. K.</b> Studies in Vapour Pressure Measurement, Part I: The Vapour Pressure of $\beta\beta^1$ -Dichloroethyl Sulphide (Mustard Gas) . . . . .	42
<b>Balson, E. W.</b> Studies in Vapour Pressure Measurement. Part II: A New All-Glass Manometer Sensitive to 0.001 mm. . . . .	48
— Part III: An Effusion Manometer Sensitive to $5 \times 10^{-6}$ Millimetres of Mercury: Vapour Pressure of D.D.T. and Other Slightly Volatile Substances . . . . .	54
<b>Barnes, A. W.</b> See <i>Bowen, E. J., Barnes, A. W., and Holliday, P.</i>	
<b>Barrer, R. M.</b> The Solubility of Gases in Elastomers . . . . .	3
<b>Baxendale, J. H., and Evans, M. G.</b> Velocity Constants of the Propagation and Termination Steps in Polymerisation Reactions . . . . .	210
<b>Besseling, J. L. N.</b> See <i>Guelke, R., Besseling, J. L. N., Newbery, E., and Semmelink, A.</i>	
<b>Birch, A. J., and Macdonald, D. K. C.</b> Some Physical Properties of Solidified Sodium-Ammonia Solutions . . . . .	792
<b>Bockris, J. O'M.</b> Electrolytic Polarisation. Part I: The Overpotential of Hydrogen on some Less Common Metals at High Current Densities. Influence of Current Density and Time. . . . .	417
<b>Bolland, J. L., and ten Have, P.</b> Kinetic Studies in the Chemistry of Rubber and Related Materials. Part IV: The Inhibitory Effect of Hydroquinone on the Thermal Oxidation of Ethyl Linoleate . . . . .	201
<b>Bosworth, R. C. L.</b> Chemical Similarity in Heterogeneous Catalysis . . . . .	399
<b>Bowen, E. J., Barnes, A. W., and Holliday, P.</b> Bimolecular Quenching Processes in Solution . . . . .	27
<b>Bremner, J. G. M., and Thomas, G. D.</b> The Extension of Thermodynamic Values from the Aliphatic to the Aromatic Series . . . . .	779
<b>Breyer, B., and Gutmann, F.</b> Electrode Reactions in Alternating Fields. Part III: The Dynamic Capacitance . . . . .	785
<b>Bright, N. F. H., and Hagerty, R. P.</b> The Decomposition of Hydrogen and Deuterium Iodides . . . . .	697
<b>Brodersen, R.</b> Inactivation of Penicillin G by Acids. A Reaction-Kinetic Investigation . . . . .	351
<b>Carpenter, A. S.</b> Solution and Diffusion in High Polymers . . . . .	529
<b>Cassie, A. B. D.</b> Multi-molecular Absorption II. . . . .	615
<b>Clark, G. B.</b> See <i>Akimov, G. W., and</i>	
<b>Cole, E. C., and Hinshelwood, C. N.</b> The Catalase Activity of <i>Bact. Lactis Aerogenes</i> . . . . .	266
<b>Cooke, E. G., and Hinshelwood, C. N.</b> The Adaptation of <i>Bact. Lactis Aerogenes</i> to Glycerol and to Various Carbohydrates . . . . .	733
<b>Cooke, P. W., and Haresnape, J. N.</b> The Effect of Steam on some Alumina Transitions . . . . .	395
<b>Corner, J.</b> The Effect of Turbulence on Heterogeneous Reaction Rates. . . . .	635
<b>Coulson, C. A.</b> See <i>Longuet-Higgins, H. C., and</i>	
<b>Dainton, F. S.</b> X—X and X—O Bond Energies of Phosphorus, Arsenic and Antimony and their Importance in the Kinetics of the Oxidation of these Elements . . . . .	244
— The Inhibition of the Photochemical Formation of Phosgene by Nitrosyl Chloride—I . . . . .	365
— See <i>Ivin, K. J., and</i>	

- Davies, D. S.**, and **Hinshelwood, C. N.** The Effect of Adaptation on the Activity of the Dehydrogenases of *Bact. Lactis Aerogenes* . . . 257
- **Hinshelwood, C. N.**, and **James, A. M.** The Adaptation of *Bact. Lactis Aerogenes* to Crystal Violet and to Sulphanilamide . . . 138
- Denbigh, K. G.** Continuous Reactions. Part II: The Kinetics of Steady State Polymerisation . . . 648
- See *Balson, E. W.*, *Denbigh, K. G.*, and *Adam, N. K.*
- De Smet, M.** See *Rutgers, A. J.*, and
- Dickinson, H. O.** The Aggregation of Cyanine Dyes in Aqueous Solution . . . 486
- Eley, D. D.**, and **Pepper, D. C.** The Catalytic Polymerisation of *N*-Butyl Vinyl Ether . . . 112
- The Visco-Elastic Behaviour of Cordite. Part I: Plastic Flow in Compression at High Stresses . . . 559
- Part II: The Plastic and Elastic Extension of Cords at Low Stresses . . . 568
- Part III: The Plastic and Elastic Torsion of Cords at Low Stresses . . . 583
- Evans, Alwyn G.**, and **Meadows, G. W.** The Catalytic Oxidation of Sulphur Dichloride by Oxygen . . . 667
- Evans, M. G.** See *Barendale, J. H.*, and
- Fensom, D.**, and **Fordham, S.** A Microscopical Study of the Solution of Nitrocotton by Nitroglycerine . . . 538
- Fishwick, C. E. F.**, and **Neale, S. M.** The Absorption of Dyes by Cellulose. Part IX: Measurements of the Absorption of Sky Blue FF by Cotton . . . 332
- Fordham, S.** See *Fensom, D.*, and
- French, C. M.** The Diamagnetic Susceptibility of some Aliphatic Acids and Esters . . . 356
- Gaydon, A. G.** The Emission Spectrum of Glyoxal . . . 36
- Guelke, R.**, **Besseling, J. L. N.**, **Newbery, E.**, and **Semmelink, A.** A Cathode Ray Oscillograph for Detection of Low Voltage D.C. Signals . . . 123
- Gutmann, F.** See *Breyer, B.*, and
- Hagerty, R. P.** See *Bright, N. F. H.*, and
- Haresnape, J. N.** See *Cooke, P. W.*, and
- Harris, I. I.**, **Pankhurst, K. G. A.**, and **Smith, R. C. M.** Adsorption of Paraffin-chain Salts to Proteins. Part III: The Formation of Complexes between Dodecyl Sodium Sulphate and Chemically Modified Gelatins . . . 506
- Hathway, D. E.** See *Hodgson, H. H.*, and
- Hermans, J. J.** Deformation and Swelling of Polymer Networks containing Comparative Long Chains . . . 591
- Hickling, A.**, and **Spice, J. E.** The Anodic Behaviour of Metals. Part III: Nickel . . . 762
- Hill, C. G. A.**, **Lovering, P. E.**, and **Rees, A. L. G.** Electrophoretic Deposition of Powdered Materials from Non-aqueous Suspensions . . . 407
- Hinshelwood, C. N.** See *Cole, E. C.*, and
- See *Cooke, E. G.*, and
- See *Davies, D. S.*, and
- See *Davies, D. S.*, *Hinshelwood, C. N.*, and *James, A. M.*
- See *James, A. M.*, and
- See *Pryce, J. M.*, and
- Hodgson, H. H.**, and **Hathway, D. E.** Absorption Spectra of some Mononitronaphthylamines, with Observations on their Structures. Part II: 3-, 5-, 6-, 7- and 8-Nitro-2-Naphthylamines and 6-Nitro-1-Naphthylamine . . . 643
- Holliday, A. K.** A Method for the Determination of Viscosity at Low Rates of Shear . . . 630
- Holliday, A. K.** The Effect of Dialysis on the Properties of Nuclear Gold Sols . . . 661
- Holliday, P.** See *Bowen, E. J.*, *Barnes, A. W.*, and
- Hughes, E. D.**, and **Ingold, C. K.** The Reactions of Organic Halides in Solution . . . 798
- Hutchinson, E.** On Adsorption and Lubrication at Crystal Surfaces. Part II: On the Adsorption of Paraffin Chain Compounds on Sodium Nitrate . . . 439
- Part III: On Heats of Wetting and Adsorption on Ionic Crystals . . . 443
- and **Rideal, E. K.** Part I: On the Boundary Lubrication of Sodium Nitrate . . . 435
- Ingold, C. K.** See *Hughes, E. D.*, and

- Ivin, K. J., and Dainton, F. S.** The Vapour Pressures, Latent Heats of Sublimation and Transition Points of Solid Hexachloroethane. . . . . 32
- James, A. M., and Hinshelwood, C. N.** Loss of Sulphanilamide Adaptation Induced by Growth of *Bact. Lactis Aerogenes* in Presence of Proflavine . . . . . 274
- Some Further Studies on the Morphology of *Bact. Lactis Aerogenes*. . . . . 758
- See *Davies, D. S., Hinshelwood, C. N., and*
- Kasbekar, G. S., and Neale, S. M.** The Swelling of Cellulose in Aqueous Solutions of certain Acids and Salts with Measurements of the Vapour Pressures, Densities and Viscosities of these Solutions . . . . . 517
- King, G.** Sorption of Large Molecules by Keratin . . . . . 552
- Electric Polarisation in Keratin-Water and Keratin Methyl-Alcohol Systems . . . . . 601
- Kirkwood, J. G.** See *Westheimer, F. H., and*
- Le Fèvre, R. J. W., and Russell, P.** The Dependence on State of the Apparent Dipole Moments of Ammonia, Methylamine, Dimethylamine and Trimethylamine . . . . . 374
- Lauder, I.** The Separation of the Oxygen Isotopes by Thermal Diffusion . . . . . 62c
- Lemin, D. R., and Vickerstaff, T.** The Aggregation of Direct Dyes and of Methylene Blue 2B in Aqueous Solution . . . . . 491
- Long, L. H., and Walsh, A. D.** Remarks on the Structure of Carbon Monoxide . . . . . 342
- Longuet-Higgins, H. C., and Coulson, C. A.** A Theoretical Investigation of the Distribution of Electrons in some Heterocyclic Molecules containing Nitrogen . . . . . 87
- Lovering, P. E.** See *Hill, C. G. A., Lovering, P. E., and Rees, A. L. G.*
- Macdonald, D. K. C.** See *Birch, A. J., and*
- Macdonald, J. Y.** The Hydration of Ions . . . . . 674
- Macleod, D. B.** The Calculations of the Latent Heat of Vaporisation and the Viscosity of CO<sub>2</sub> under Pressure on the Basis of a Revised Equation of State . . . . . 169
- Mark, H.** The Mechanical Properties of High Polymers . . . . . 447
- Matalon, R., and Schulman, J. H.** Penetration of Sodium Cetyl Sulphate into Cetyl Alcohol. Effect of Salt on the Time-Penetration Curves . . . . . 479
- Meadows, G. W.** See *Evans, A. G., and*
- Meggy, A. B.** Physico-Chemical Mechanisms in Protein Systems. Part I: The Combination of Orange II Acid with Wool Keratin . . . . . 502
- Mokrushin, S. G.** The Surface Layer of Colloidal Solutions and the Size of Colloidal Particles . . . . . 1
- Moore, W. R.** The Swelling of Nitrocellulose in Binary Mixtures . . . . . 543
- Morton, Mrs. M. C.** Semiconducting Properties of Lead Sulphide . . . . . 194
- See *Anderson, J. S., and*
- Mott, N. F.** The Theory of the Formation of Protective Oxide Films on Metals. Part III . . . . . 429
- Neale, S. M.** The Absorption of Dyestuffs by Cellulose. Part VIII: The Analysis of Ionic Distribution by Means of Diffusion Potentials . . . . . 325
- Part X: The Absorption of Cationic Dyes . . . . . 338
- See *Fishwick, C. E. F., and*
- See *Kasbekar, G. S., and*
- Newbery, E.** Reversible Overvoltage . . . . . 127
- See *Guelke, R., Besseling, J. L. N., Newbery, E., and Semmelink, A.*
- Orr, (the late) W. J. C.** Statistical Treatment of Polymer Solutions at Infinite Dilution . . . . . 12
- Pankhurst, K. G. A., and Smith, R. C. M.** The Adsorption of Paraffin-Chain Salts to Proteins. Part IV: Some Physical and Chemical Properties of Gelatin-Dodecyl Sulphate Complexes . . . . . 511
- See *Harris, I. I., Pankhurst, K. G. A., and Smith, R. C. M.*
- Pepper, D. C.** See *Elev, D. D., and*
- Prout, E. G., and Tompkins, F. C.** The Thermal Decomposition of Mercuric Oxalate . . . . . 148
- Pryce, J. M., and Hinshelwood, C. N.** The Adaptation of *Bact. Lactis Aerogenes* to Various Inhibitors . . . . . 742
- The Stability of the Adaptation of *Bact. Lactis Aerogenes* to Proflavine . . . . . 752
- Rees, A. L. G.** See *Hill, C. G. A., Lovering, P. E., and*
- Reichenberg, D.** Apparent Anomalies in the Surface- and Interfacial Tension-Concentration Curves of Aqueous Solutions of Paraffin-Chain Salts . . . . . 467
- Rideal, E. K.** See *Hutchinson, E., and*
- Russell, P.** See *Le Fèvre, R. J. W., and*

<b>Rutgers, A. J., and De Smet, M.</b> Electrosmosis, Streaming Potentials and Surface Conductance . . . . .	102
<b>Schulman, J. H.</b> See <i>Matalon, R.</i> , and	
<b>Schwab, G. M.</b> Crystallite Orientation in Coating Films. Part III: Orientation of Silver Iodide upon Silver Bromide . . . . .	715
— Part IV: Orientated Coating Films on Thallous Halides . . . . .	724
<b>Semmelink, A.</b> See <i>Guelke, R.</i> , <i>Besseling, J. L. N.</i> , <i>Newbery, E.</i> , and	
<b>Smith, R. C. M.</b> See <i>Harris, I. I.</i> , <i>Pankhurst, K. G. A.</i> , and	
<b>Spice, J. E.</b> See <i>Hickling, A.</i> , and	
<b>Springall, H. D.</b> The Bond Energy, Bond Length and Dissociation Energy Data for Cyanogen and their Relation to the Heats of Atomisation of Carbon and Nitrogen . . . . .	177
<b>Strickland-Constable, R. F.</b> The Interaction of Carbon Filaments at High Temperatures with Nitrous Oxide, Carbon Dioxide and Water Vapour . . . . .	769
<b>ten Have, P.</b> See <i>Bolland, J. L.</i> , and	
<b>Thomas, G. D.</b> See <i>Bremner, J. G. M.</i> , and	
<b>Tilston, (the late) D. V.</b> Magnetochemical Investigations. Part VII: Calculations on the Magnetic Field . . . . .	238
— See <i>Angus, W. R.</i> , and	
<b>Tompkins, F. C.</b> See <i>Prout, E. G.</i> , and	
<b>Treloar, L. R. G.</b> The Photo-Elastic Properties of Rubber. Part I: Theory of the Optical Properties of Strained Rubber . . . . .	277
Part II: Double Refraction and Crystallisation in stretched Vulcanised Rubber . . . . .	284
<b>Vickerstaff, T.</b> See <i>Lemin, D. R.</i> , and	
<b>Wake, W. C.</b> The Theory of Rate Processes and the Viscosity of Long-Chain Compounds . . . . .	708
<b>Walsh, A. D.</b> Remarks on the Strengths of Bonds . . . . .	60
— The Dependence of the Properties of Carbonyl Compounds upon Polarity . . . . .	158
— Processes in the Oxidation of Hydrocarbon Fuels. Part II . . . . .	297
Part III . . . . .	305
— See <i>Long, L. H.</i> , and	
<b>Weiss, J.</b> The Electron Affinity and Some Reactions of the Azide Ion in Solution . . . . .	119
— Some Reactions of Hypochlorites in Solution. Part I: The Electron Affinity of the $\text{ClO}^-$ and $\text{ClO}_2^-$ ions . . . . .	173
— Some Aspects of the Chemical and Biological Action of Radiations . . . . .	314
— The Electron Affinity of $\text{ClO}$ . . . . .	675
<b>Westheimer, F. H., and Kirkwood, J. G.</b> The Electrostatic Influence of Substituents on the Dissociation Constants of Organic Acids. A Reply to Wynne-Jones and Rushbrooke . . . . .	77
<b>Willis, J. B.</b> The Heats of Combustion of some Organic Bases and their Salts. The Resonance Energies of Acridine and Phenazine . . . . .	97

## INDEX TO REVIEWS—VOLUME XLIII, 1947.

<b>Akimov, G. V.</b> The Theory and Methods of Investigation of Metallic Corrosion . . . . .	296
<b>Bailey, Alton E.</b> Industrial Oil and Fat Products . . . . .	95
<b>Berry, A. J.</b> Modern Chemistry . . . . .	96
<b>Bouwers, A.</b> Achievements in Optics . . . . .	464
<b>Cady, W. G.</b> Piezoelectricity . . . . .	465
<b>Carlsaw, H. S., and Jaeger, J. C.</b> Conduction of Heat in Solids . . . . .	800
<b>Clark, W.</b> Photography by Infra Red . . . . .	218
<b>Dyatkina, M. E.</b> See <i>Syrkin, Y. K.</i> , and	
<b>Eastman, E. D., and Rollefson, G. K.</b> Physical Chemistry . . . . .	677
<b>Fletcher, A., Miller, J. C. P., and Rosenhead, L.</b> An Index of Mathematical Tables . . . . .	167
<b>Frenkel, J.</b> Kinetic Theory of Liquids . . . . .	613
<b>Glasstone, S.</b> An Introduction to Electrochemistry . . . . .	677
<b>Glasstone, S.</b> Thermodynamics for Chemists . . . . .	466
<b>Griffith, R. H.</b> The Mechanism of Contact Catalysis . . . . .	296

Gupta, N. C. Sen, and Sen, K. C. A Text Book of Physical Chemistry . . . . .	676
Hartree, D. R. Calculating Machines . . . . .	643
Hepburn, J. R. I. The Metallisation of Plastics . . . . .	676
Herccock, R. J. The Photographic Recording of Cathode Ray Tube Traces . . . . .	801
Hinshelwood, C. N. The Chemical Kinetics of the Bacterial Cell . . . . .	394
Hume-Rothery, W. Atomic Theory for Students of Metallurgy . . . . .	217
Jaeger, J. C. See <i>Carlsaw, H. S.</i> , and . . . . .	
Lea, D. E. Actions of Radiations on Living Cells . . . . .	94
Luder, W. F., and Zuffanti, S. Electronic Theory of Acids and Bases . . . . .	295
Mark, H., and Whitby, G. S. Advances in Colloid Science. Vol. II: Scientific Progress in the Field of Rubber and Synthetic Elastomers . . . . .	164
Markley, K. S. Fatty Acids . . . . .	678
Maxted, E. B. Modern Advances in Inorganic Chemistry . . . . .	612
Miller, J. C. P. See <i>Fletcher, A.</i> , <i>Miller, J. C. P.</i> , and <i>Rosenhead, L.</i> . . . .	
Parke, Nathan Greer, III. Guide to the Literature of Mathematics and Physics . . . . .	614
Pirene, M. H. The Diffraction of X-Rays and Electrons by Free Molecules . . . . .	396
Price, C. C. Mechanism of Reactions of Carbon-Carbon Double Bonds . . . . .	396
Richter, Victor von. The Chemistry of the Carbon Compounds. Vol. III: The Aromatic Compounds . . . . .	168
Rollefson, G. K. See <i>Eastman, E. D.</i> , and . . . . .	
Rosenhead, L. See <i>Fletcher, A.</i> , <i>Miller, J. C. P.</i> , and <i>Rosenhead, L.</i> . . . .	
Sen, K. C. See <i>Sen Gupta, N. C.</i> , and . . . . .	
Symposium on Plasticizers. Journal of Polymer Science, Vol. II, No. 2 . . . . .	801
Syrkin, Y. K., and Dyatkina, M. E. The Chemical Link and the Structure of Molecules . . . . .	393
Weatherburn, C. E. A First Course in Mathematical Statistics . . . . .	463
Weissberger, Arnold. Physical Methods of Organic Chemistry . . . . .	219
Weygand, Conrad. Organic Preparations . . . . .	293
Whitby, G. S. See <i>Mark, H.</i> and . . . . .	
Wild, F. Characterisation of Organic Compounds . . . . .	395
Williams, Trevor L. An Introduction to Chromatography . . . . .	219
Wright, W. D. The Measurement of Colour . . . . .	294
Zuffanti, S. See <i>Luder, W. F.</i> , and . . . . .	295

# CORRIGENDA.

Volume XLIII :

Page 7. Paper of R. M. Barrer. Curve 1 in Fig. 1 (a) is not, as stated, that for  $s = \infty$ . The latter curve lies between curves 1 and 2 in this figure and close to curve 2.

Page 240. Equation " $\zeta = \sqrt{2OP}$ " should read " $\xi = \sqrt{2OP}$ ".

Pages 325-331, 332-337, 338-342. For cellophane, read Cellophane throughout, including French and German summaries.

Page 463. For "Hartree" read "D. R. Hartree".

Page 601. For "Finsh" read "Finch".





# DISCUSSION ON COLLOIDAL CRYSTALLITES AND MICELLES.

REPORT of the one-day meeting held in the Chemistry Department, University College, London, W.C. 1 (by kind permission of Prof. C. K. Ingold, F.R.S.) on Friday, 19th December, 1947, under the chairmanship of Sir Robert Robertson, K.B.E., D.Sc., F.R.S. The papers discussed were published in the August-September Number of the *Trans. Faraday Soc.*, 1947, 43, 467-611, and were therefore taken as read.

## GENERAL INTRODUCTION.

BY DR. D. D. ELEY (*Bristol*).

In calling this meeting, the Faraday Society had in mind that a number of papers were in press on a variety of colloidal topics, and it was decided that these papers might form the basis of a one-day meeting. In an attempt to give some form to the discussion, a title was chosen which was made sufficiently broad so as to include within its scope all the papers concerned. Shortage of paper has indeed led us to put the cart before the horse in this fashion, and prevented us from inviting further papers beyond those already accepted for publication in the usual way. It is hoped, however, that this meeting, in spite of its departure from tradition, will help to satisfy the need for more frequent meetings of the Society.

How far can our discussion provide a further insight into the nature and behaviour of the colloidal micelle? It might be helpful if we briefly reminded ourselves of the history of this term.

In the first place the term micelle was applied by Nägeli to the micro-crystalline regions of substances such as starch and cellulose, as revealed by double refraction. He viewed the microcrystals as more-or-less discrete units, and his picture was applied in recent times by Meyer and Mark to cellulose. When it became clear that often the micelles are several times shorter than the long-chain molecules which build up the structure, the fringed-micelle picture was put forward by Hermann, Gerngross, and Abitz. In this model, one chain molecule may pass alternately through crystalline and amorphous regions. The model has been applied to cellulose by Frey-Wissling and the whole subject, in relation to this polymer, reviewed by Mark. In the nature of things this type of micelle is crystalline, and in my view it is preferable to refer to it as a crystallite, and thus distinguish it from the micelle in solution. This is not to say that one cannot visualise an amorphous micelle in a solid, that is, an amorphous sub-microscopic structure distinguishable from its surroundings. Such a term might possibly be applicable to the amorphous patches of material dispersed through otherwise highly crystalline structures such as polyethylene.

In solution, the term is classically applied, by Duclaux, to the colloidal particle plus adsorbed molecules and ions. The term is perhaps most familiar in its application by McBain to aggregated soap molecules

Now micelles in solution may differ as to the crystallinity of the core of the micelle. Thus, Hartley's spherical soap micelles are amorphous, while soap micelles in more concentrated solutions have been shown by Hess *et al.* to possess a laminar structure, and many inorganic oxides and salt particles are highly crystalline. In all cases, however, we have to consider the additional adsorbed components, so the term crystallite would be inappropriate.

Under the pressure of surface chemistry and polymer chemistry, colloid science grows apace. Some of the classical terms of colloid chemistry may well drop out of use, as the phenomena to which they are applied receive explanations in terms of physical chemistry. I believe that "micelle" is not one of these, but has a further period of useful life before it.

## PART I.—THE MICELLE IN SOLUTION.

Mr. D. Reichenberg (*London*) said, in introducing his paper: The thermodynamical argument shows that to account for the minima found experimentally, we must assume either experimental error or impurities in the materials. The wide range of methods employed by various workers would seem to eliminate the former possibility. I have suggested in my paper that the impurity may be either polyvalent ions of opposite charge to the long-chain ion of the soap (these will presumably be present in the water) or organic compounds (present in the soap).

Mr. C. R. Bury (*Billingham*) said: I wish to congratulate Mr. Reichenberg on his explanation of one of the puzzling features of colloid chemistry. In support of his explanation, I bring forward the fact that with non-ionic "soaps" there is no minimum in the surface tension-log concentration curves, as can be predicted from Mr. Reichenberg's paper, for neither salt ion will be attracted to the surface by the non-ionic surface layer of "soap" and  $\Gamma_{\text{salt}}$  of eqn. (2) will therefore be zero. Thus, Mr. J. Browning and I have measured, but not yet published, surface tensions of octyl glucoside solutions; there are also measurements for solutions of butyric acid,<sup>1</sup> which is a "soap" as defined by Mr. Reichenberg: in neither case is there a minimum.

Mr. Browning and I have, however, found a minimum in the surface tension-log concentration curve for aqueous solutions of octyl pyridinium bromide. This should be due to a polyvalent negative ion. What polyvalent negative ions are likely to be present as impurities in reasonably pure distilled water?

Mr. D. Reichenberg (*London*) (*communicated*): I agree with Dr. Crisp's simple interpretation of my treatment in terms of a molecular "picture" (p. 815). I would point out, however, that my treatment depends on the fact that when aggregation commences  $d\mu_{p++}/d \ln c_{\text{soap}}$  decreases sharply before  $\Gamma_{p++}$  has greatly decreased. This point might not be brought out sufficiently by the "picture" taken by itself.

The results quoted by Mr. Bury on non-electrolytic detergents are interesting and appear to support the theory. It must not be overlooked, however, that these compounds when aggregated will almost certainly have a solubilising action on organic compounds similar to the soaps, so that organic impurities in the detergent might still cause a minimum. As regards the minima shown by cationic soaps, I agree with Dr. Alexander in attributing this to organic impurities. The possibility of polyvalent anions, while unlikely, cannot wholly be ruled out, e.g. silicate or polysilicate ions. In the latter case, the high charge on the ions may cause the merest trace of polysilicate ions to have an appreciable effect.

Dr. J. B. Matthews (*Thornton*) said: Several years ago, in an experimental investigation of the phenomenon discussed by Mr. Reichenberg, I found that minima and maxima in the interfacial tension-concentration

<sup>1</sup> *Phil. Mag.*, 1927, 4, 980.

curve for methylcellulose at the cyclohexane-water interface could be artificially produced, not necessarily by introducing salts or other impurities into the system, but by juggling with the time factor.<sup>3</sup> In general, the interfacial tension decreases rapidly with increasing interfacial age, passes through a minimum and then through a maximum, before reaching its equilibrium value. More recently, in conjunction with Mr. E. J. Clayfield, I have observed the same phenomenon for the case of an alkyl-substituted succinic acid at a hydrocarbon oil-water interface,<sup>3</sup> and Hauser and co-workers<sup>4</sup> have published data showing the same effect. This remarkable phenomenon, for which I can offer no complete explanation, is very important from the experimental point of view. For, unless care is taken to plot the equilibrium values in constructing the interfacial tension-concentration curve, a variety of curves can be obtained exhibiting maxima and minima, which are very similar in shape to the curves published in the literature. On the other hand, the indications are that the curve constructed from the true equilibrium values does not contain a maximum or minimum. The time taken for equilibrium to be reached depends on the solute concentration. It was about 15 min. for the lowest methylcellulose concentration investigated, and fell to about 3-4 min. for higher concentrations. In the case of soap solutions a period of about 1 min. is required for equilibrium to be established,<sup>5</sup> but the data of Powney and Addison used by Mr. Reichenberg to support his thermodynamical arguments were obtained from measurements on interfaces which were only 10-15 sec. old. Hence there is some doubt attached to their use in verifying his theory. In stating this I do not want to suggest that the theory is wrong, but merely desire to point out that there appears to be a need for more convincing experimental data than at present exist. Furthermore, the correct explanation for the change of interfacial tension with time may throw additional light on the processes which occur at the interfaces of solutions. Diffusion undoubtedly plays a part, and is probably responsible for the initial rapid fall in the interfacial tension value, and, if one can legitimately regard the lowering of the interfacial tension to be due to the surface pressure of the film of adsorbed solute molecules, perhaps the subsequent changes in interfacial tension are connected with the type of penetration phenomena described by Matalon and Schulman.<sup>6</sup>

Mr. A. Couper and Dr. D. D. Eley (*Bristol*) said: While we have no experience with soap solutions, our recent results on the lowering of surface tension by linear polymers causes us to support the query of Dr. Matthews as to how far equilibrium tensions were established. We examined polyoxy ethylene glycols in the range of M.W. 1000-6000<sup>7</sup> and a polyvinyl alcohol (partly acetylated) of M.W. 40,000. In general, the time to reach equilibrium increases with (a) increase in M.W., (b) decreasing concentration, e.g., for polyoxy ethylene glycol 6000 we obtained

$$\begin{array}{ll} C = 0.01 \text{ g./l.} & t = 20 \text{ min.} \\ C = 0.0025 \text{ g./l.} & t = 60 \text{ min.} \end{array}$$

The higher M.W. solvar took times as long as 1000 min. Of course, the fatty acids have much lower molecular weights and so will diffuse much more quickly, but Adam and Shute and others have reported on a similar behaviour for dilute soap solutions. We hope to publish the  $\gamma$ -time curves for the polyvinyl alcohols in the future. Their shape is such that the form of the  $\gamma$ -log<sub>10</sub>  $C$  curve varies widely according to the arbitrary time chosen.

<sup>3</sup> Matthews, *Nature*, 1946, **157**, 407.

<sup>3</sup> Unpublished work.

<sup>4</sup> Andreas, Hauser and Tucker, *J. Physic. Chem.*, 1938, **42**, 1001.

<sup>5</sup> Lottermoser and Baumgurtel, *Trans. Faraday Soc.*, 1935, **31**, 200.

<sup>6</sup> Matalon and Schulman, *ibid.*, 1947, **43**, 479.

<sup>7</sup> *J. Polymer Sci.* (in press).

Again we would ask how far is the  $\gamma$ -log<sub>10</sub> *C* curve truly horizontal, or very slightly sloping, at the higher concentrations? The latter case might be ascribed to adsorption of a component of large molecular area, viz., a plate-like micelle that might have been broken off from a micelle of the laminar-type.

We would congratulate Mr. Reichenberg on his excellent paper. Our query is simply how far the actual experimental conditions and results accord with those assumed by him in his theory.

**Mr. D. Reichenberg** (*London*) (*communicated*): Dr. Matthews<sup>8</sup> finds that with methylcellulose, the minimum in the interfacial tension-concentration curves is manifested with fresh surfaces and tends to disappear with time. Precisely the opposite effect is found by most workers on soap solutions.<sup>9</sup> Indeed, I suspect strongly that the time-effect in the case of electrolyte soaps is due, at least partly, to the slow adsorption of polyvalent ions. Owing to the minute concentrations involved and the fact that the electric potential due to the long-chain ions decreases rapidly with distance from the interface, diffusion will be very slow. Owing to the adsorption of polyvalent ions on the micelles, adsorption at the macroscopic surface will be very slightly above the critical concentration. Hence this accounts both for the extreme slowness with which equilibrium is attained and for the fact that the time-effect is not manifested above the critical concentration. It does not appear to account readily for the observations of Alexander on the variation of surface potential with time unless these can be explained as the effect of adsorption of polyvalent ions on the zeta-potential. Unfortunately, I have not so far been able to find the published account of Mr. Couper's work but, as Dr. Alexander has pointed out in this discussion, methylcellulose is not a homogeneous product and a similar remark would apply to long-chain polymers.

**Mr. H. E. Garrett** (*Liverpool*) said: Data<sup>10-12</sup> for rigorously purified detergents suggest that, for non-hydrolysing compounds, the general surface tension-log concentration curve has the form shown in Fig. 1, the sharp change of direction of the curve occurring at the critical concentration for micelle formation. The horizontal portion of the curve has usually been felt to be anomalous since the application of Gibbs' equation has been interpreted as implying zero surface-adsorption. The alternative interpretation, that the activity of the paraffin-chain salt is constant in this region is compatible with the view that micelle formation corresponds with the formation of a second phase, equilibrium between micelle and intermicellar liquid being closely analogous to the equilibrium between a crystal and the corresponding saturated solution. If, in fact, the lamellar crystals which are shown by X-ray methods to occur

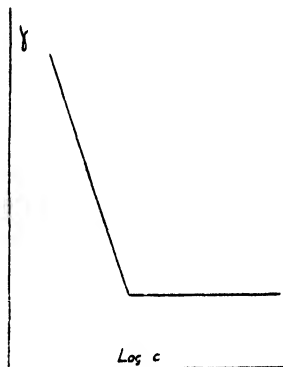


FIG. 1.

in solutions of detergents of concentrations above 10 % persist fragmentally in the very dilute solutions, the micelle would correctly be regarded as a crystalline form and constant activity over a range of concentration of micelles would be expected.

I must also protest against the proposal to extend the meaning of the

<sup>8</sup> Matthews, *Nature*, 1946, **157**, 407.

<sup>9</sup> McBain and Wood, *Proc. Roy. Soc., A*, 1940, **174**, 286.

<sup>10</sup> Robinson, *Wetting and Detergency* (Harvey 1937), 137.

<sup>11</sup> Powney and Addison, *Trans. Faraday Soc.*, 1938, **34**, 372.

<sup>12</sup> Miles and Shedlovsky, *J. Physic. Chem.*, 1944, **48**, 57.

<sup>13</sup> Miles, *ibid.*, 1945, **49**, 70.

word "soap". We already have an adequate generic term in "detergent", hence the proposed extension of the meaning of "soap" is unnecessary. It is also very undesirable as being likely to lead to confusion, particularly among industrial users, of surface-active agents.

**Dr. D. J. Crisp** (*Cambridge*) said: A physical picture embodying the principles of Mr. Reichenberg's more rigorous approach might be described in the following manner.

When the soap (A) is present in low concentration, it is molecularly dispersed in solution, and a second molecular species (B), able to cause a further lowering of surface energy, would be adsorbed only at the air-water interface. But when the critical concentration of the soap is exceeded a relatively large internal surface arises, namely that of the micelles, and in consequence the species B must be partitioned between the bulk phase and a now much larger surface phase. This will result in a lowering of the concentration of B in the bulk-phase and a withdrawal of B from the external surface. At the same time the concentration and surface activity of the soap will have increased, so that the net result might be either an increase, or a decrease, in surface tension according to the magnitude of the two effects.

It follows that (a) any second substance, ionic or otherwise, capable of adsorbing on, or dissolving in the micelle (as suggested by Dr. Alexander), might lead to such an anomaly; and (b) the true surface tension-concentration curve of the species A lies at all points above the observed curve, though approaching it more closely at higher concentrations. It would be interesting to know whether these conclusions can be verified by Mr. Reichenberg.

**Mr. D. Reichenberg** (*London*) (*communicated*): Dr. Schulman, in introducing his paper, raised the interesting question of whether complexes analogous to those discovered by him and his co-workers in monolayers might be shown to exist in bulk. In this connection, I would like to refer to some experiments of my own. Unfortunately, the work had to be left in an incomplete state and the materials used were admittedly impure, which is why the work has not hitherto been published. On the other hand, similar results were found for a variety of substances and it seems unlikely that a more careful investigation will overthrow the main results.

If to a 0.305 M. aqueous solution of sodium oleate is added mixed xlenols (obtained by vacuum distillation of "semi-refined xlenols 98-100 %" from P.R. Chemicals) in the molecular ratio 2.16 xlenol: 1 soap, the whole sets to a semi-solid opaque mass. On raising the temperature, the mixture clears sharply at 33.5° C. On increasing the ratio, moles xlenol/moles soap, to 2.70, the clearing temperature is raised to 50.0° C. By taking a series of such points, a curve is obtained showing a maximum at 79° C. corresponding to 6 moles xlenol: 1 soap. Above about 8 moles, the clearing temperature rises again but this is merely the normal consolute curve of the sodium oleate-xlenol-water liquid mixture. If the curve is repeated with a 0.153 M. Na oleate solution, a curve is obtained lower on the temperature scale with a maximum at 58° C. but with the same molecular ratio 6/1. Using varying soap concentrations, a family of curves may be obtained, all exhibiting the maximum at a mole ratio of 6/1.

Using Na stearate solutions, two new features are exhibited: (1) the initial effect of the xlenol is to reduce the solution temperature of the soap. This effect was discovered by Lawrence<sup>14</sup> and was termed by him "peptisation." (2) A symmetrical maximum is only shown by soap solutions more concentrated than 0.25 M. The molecular ratio at the maximum is still 6/1.

With sodium oleate and *n*-amyl alcohol, symmetrical maxima are obtained. The molecular ratio appeared to vary from *ca.* 6-8 but this

<sup>14</sup> Lawrence, *Trans. Faraday Soc.*, 1937, 33, 325.

may have been due to impurity in the alcohol. With Na dodecyl sulphate and xylenol, symmetrical maxima were obtained with solutions above 0.2 M. and mol ratio 6/1. With Na oleate and mixed cresols (obtained by vacuum-distillation of "pale cresylic acid 99-100 %" from P. R. Chemicals) a symmetrical maximum was found with a molality of 1.6 at 75° C. corresponding to 2 moles cresol/1 soap. With Na oleate and *m*-toluidine, a symmetrical maximum was found with a molality of 1.1 at a temp. of 56° C. corresponding to 1 mole *m*-toluidine/1 soap.

Examination of the 6/1 xyleneol-sodium oleate complex through crossed-Nicols showed a typical smectic pattern over a limited temperature range. Neither xyleneol nor sodium oleate solution in this concentration is birefringent. It seems reasonable to suppose that complexes of composition corresponding to the maxima in the curves are precipitated from solution.

**Dr. D. J. Crisp** (*Cambridge*) said: The term "complex" as applied to two-component surface films has been used in different senses which should be carefully distinguished.

Firstly there is the possibility of mere association between the components; for instance if one is soluble the association is indicated by "penetration". When complete two-dimensional miscibility exists equilibrium is defined by

$$d\pi = \Gamma_1 d\mu_1 + \Gamma_2 d\mu_2 \quad . \quad . \quad . \quad (1)$$

where the symbols have their usual meanings, the surface excesses of the soluble and insoluble components,  $\Gamma_2, \Gamma_1$ , being referred to the convention,  $\Gamma_{\text{water}} = 0$ . Clearly the surface pressure depends both on  $\mu_1$  and  $\mu_2$ , the system is bivalent with a distinct  $\pi - A_1$  curve for every concentration ( $c_2$ ) of the penetrant. The system described here appears to be of this type, though the authors postulate second-order phase changes related to stoichiometric complexes when the film is rapidly compressed in a metastable condition.

Quite different phase relations exist if the associated molecules form a new surface phase not miscible with the original film.<sup>15</sup> Denoting the phase containing the greater surface excess of component 1 by  $\alpha$ , we may define equilibrium by two equations:

$$\begin{aligned} d\pi &= \Gamma_1^\alpha d\mu_1 + \Gamma_2^\alpha d\mu_2 \\ d\pi &= \Gamma_1^\beta d\mu_1 + \Gamma_2^\beta d\mu_2 \end{aligned}$$

Hence

$$d\pi = \left[ \frac{\Gamma_1^\alpha \Gamma_2^\beta - \Gamma_2^\alpha \Gamma_1^\beta}{\Gamma_1^\alpha - \Gamma_1^\beta} \right] d\mu_2 \quad . \quad . \quad . \quad (2)$$

and  $\pi$  is now dependent only on  $\mu_2$ , the  $\pi - A_1$  curve being parallel to the area axis, and component 2 being ejected at this pressure. This kind of behaviour was described by Schulman and Stenhagen<sup>16</sup> for the system cholesterol (1)—sodium cetyl sulphate (2), where they found that  $d\mu_2/d\pi$  gave an area of 20 Å<sup>2</sup>, equal to that probably occupied by the ejected component ( $\bar{A}_2$ ). Supposing a 1:1 complex to exist as a distinct phase and to dissociate at the ejection pressure, we have  $\Gamma_1^\beta = \Gamma_2^\beta$  and  $\Gamma_2^\alpha = 0$ ; hence  $\frac{d\mu_2}{d\pi} = \frac{1}{\Gamma_1^\beta} - \frac{1}{\Gamma_1^\alpha} = A_1^\beta - A_1^\alpha = \bar{A}_2$ , where  $A_1^\beta$  and  $A_1^\alpha$  are the areas occupied by one molecule of the species 1 in the states  $\beta$  and  $\alpha$ , at a given surface pressure  $\pi$ .

It should be observed that eqn. (2) is general and applies whenever a phase separation accompanies penetration, and does not depend on the presence of a stoichiometric complex.

**Dr. H. A. Standing** (*Manchester*) (*communicated*): At the Shirley Institute, we have studied the absorption spectra of aqueous solutions of direct dyes to which sodium chloride had been added. When the dye

<sup>15</sup> Crisp, *Trans. Faraday Soc.* (Bordeaux Meeting, 1947), (in press).

<sup>16</sup> Schulman and Stenhagen, *Proc. Roy. Soc., B*, 1938, **126**, 356.

concentration is maintained constant, the absorption spectra of some direct dyes in aqueous solution depend upon the concentration of sodium chloride also present in the solution. Thus for Benzopurpurine 4B, and also for its isomer *meta*-Benzopurpurine 4B, the maximum extinction coefficient is progressively decreased as the concentration of sodium chloride in solution is increased. The spectral peak is also progressively displaced towards the shorter wavelengths as the sodium chloride concentration increases.

Both these dyes are considerably aggregated in aqueous solutions containing sodium chloride, and the dependence of the absorption spectrum on the sodium chloride concentration is probably due to aggregation. The absorption spectrum of a freshly prepared Benzopurpurine 4B solution containing sodium chloride also changes with time during the first 24 hr. after the preparation of the solution. This may be due to a slow attainment of the final state of aggregation.

The absorption spectrum of an aqueous Benzopurpurine 4B solution containing 25 % pyridine is almost independent of the concentration of sodium chloride also present in the solution. Similar effects occur when polyethylene oxide condensates are used instead of pyridine.\* It is possible that the dye forms a complex with either pyridine or the polyethylene oxide condensate and that aggregation of the dye is therefore prevented.

The absorption spectra of aqueous solutions of either Chrysophenine G or Naphthalene Orange G are not appreciably changed when sodium chloride is added to the solution. Both these dyes are not appreciably aggregated in aqueous solutions containing sodium chloride.

Dr. Mansel Davies (*Aberystwyth*) said: In the paper by H. O. Dickinson it is implied that the three absorption peaks for dye A are ascribable to a monomeric (5250 Å.), a dimeric, or low, aggregate (4850 Å.), and a much higher aggregate (5730 Å.). If this interpretation were correct, it is surely remarkable that the second and third features lie on opposite sides of the "monomeric" absorption: presumably indicating that the high aggregation involves forces, or structural considerations, quite different from that of the dimerisation. The band ascribed to the latter stage clearly shifts its peak with varying concentration and this, as in Lemin and Vickerstaff's paper, certainly suggests that this feature is not to be coupled with a single-stage aggregation. Some quite different explanation of the 5730 Å. peak apart from a continuation of the process causing the 4850 Å. absorption is desirable. Might it be due to the separation of a distinct phase (solid particles?) of the dye?

The conductivity results (Fig. 6) in the region  $c = 25 \times 10^{-4}$  are taken to correspond to that of the micellar solutions. Reference to Fig. 1 shows no sign of an absorption due to the "micelle" at this concentration.

Lemin and Vickerstaff emphasise the qualitative nature of the explanation of the absorption curves in terms of "monomer" and "dimer" peaks. This will remain a reasonable but speculative picture until the intensities can either be used to provide sensible association constants or be correlated with other determinations of the association equilibrium. The deduction of a series of equilibrium constants for the successive stages of an association process can readily be based on measurements of the monomer concentration (absorption) only. This has been done, for instance, with the alcohols and phenols.<sup>17</sup>

<sup>17</sup> See, *inter alia*, *Z. physik. Chem. B*, 1940, 46, 229; 1941, 49, 309; 1943, 53, 185.

\* Cp. Taylor and Simon, *Amer. Dyestuff Rep.*, 1945, 34, 319.



**PART II.—CRYSTALLINITY IN SOLID COLLOIDS.****Introduction.**

By DR. D. D. ELEY (*Bristol*).

In considering this group of papers it is convenient to distinguish between equilibrium and kinetic properties, and to consider equilibrium properties first, since, in general, they are simpler. The statistical theory of rubber has undergone great developments since it was first initiated by the efforts of Wohlsch, Kuhn, Meyer and Mark. The early authors gave an account of the modulus of rubber in terms of the configurations of a single rubber molecule, and the recent workers, Wall, Flory and Rehner, Guth and James and Treloar have put the theory on a more logical basis by treating a network of rubber molecules. Dr Herman's paper goes over some of this ground, using a modified mathematical method. Similarly, the statistical theory of the swelling and solution of amorphous polymers in solvents is in a fairly satisfactory state, at least where heats of mixing are small. The theoretical work of Rushbrooke, Flory, Huggins, Guggenheim and others has been borne out in large measure by the careful studies on rubber-benzene by Gee and Treloar. These studies of elasticity and solubility, however, are limited to amorphous polymers, and, in general, nitrocellulose-solvent interactions fall into a different category. This polymer possesses some degree of crystallinity, and its solutions are usually formed exothermically. Its solubility phenomena, such as its solubility in ether-alcohol when it is insoluble in either solvent alone, have aroused interest for many years.

Early studies such as that of Highfield have been followed in recent years by a number of papers from various countries, stimulated, no doubt, by its military importance. One may mention papers by Schulz, Desmaroux, Mathieu, Calvet and Petipas, and Kargin and Papkov. Dr. Moore's paper is of some considerable interest in that he shows that Gee's cohesive energy density method will give an account of the behaviour of nitrocellulose in mixed solvents. However, as he says, the theory is really only applicable to endothermic solutions, and the position is by no means as clear as it would seem at first sight. One would imagine that any account of nitrocellulose solutions must take account of solvation of the polymer. Indeed, when one considers the remarkable "gelatinising" action of camphor and the substituted ureas on nitrocellulose (and the X-ray evidence of Derksen, Hess, Katz and Trogus), it seems likely that some of these effects are quite specific. Experimentation with nitrocellulose is not made easier by its many possibilities for heterogeneity. Besides a distribution of chain lengths, there are possible differences in arrangements of nitrate groups along chains and between chains, and the presence of foreign groups such as sulphate and carboxyl. Thus, Fensom and Fordham consider that the rate of solution of a nitrocellulose fibre in nitroglycerine is limited by an insoluble skin of low nitrogen content.

Coming now to kinetic phenomena, we can make the quite general observation that a great deal of work is needed on amorphous polymeric systems. In applying theories of rate processes to partly crystalline polymeric systems, we always have to make two groups of assumptions, first about the structure of the polymer, and secondly, about the rate process and the equations governing it. Logically, therefore, we should test out our rate equations on completely amorphous systems and thus papers like that of Carpenter, which deals with the diffusion of gases through rubber, start at the right end of the scale. It is, however, tempting to enquire how the diffusion process changes with the introduction of crystallites, by cooling or stretching. Certainly, this reservation applies to investigation of processes of elastic and plastic flow. There are very few data on simple amorphous polymers, and logically there is

much more work to do on dilute gels of nitrocellulose, along the line initiated twenty years ago by Poole. Practical considerations, however, were responsible for the work on cordite by Pepper and myself, which I fancy brings out a number of interesting points (such as the increase in viscous resistance with tensile strain), but which also raises as many questions as it settles. The whole question of checking on rate-process equations in the simplest amorphous cases is also complicated by the presence even here of a range of sizes of kinetic units leading to a distribution of relaxation times.

Finally, we must refer to Dr. King's two papers on keratin. Previous work from the Wool Industries Research Association by Cassie has accounted for the sorption of water by wool in terms of multimolecular adsorption. Such a picture might be expected to be valid for a predominantly micellar or microcrystalline material, and to be complementary to the Flory-Huggins treatment of amorphous polymers as liquids. The picture, in fact, seems to me to be quite general; one has a monolayer of water held on low-energy sites, and the rest of the water presumably distributed through the amorphous parts of the structure. King considers the diffusion of alcohols in keratin and the dielectric polarisation in keratin-water systems. It is interesting that Cassie's picture can give an account of these kinetic phenomena, the dielectric dispersion bearing out quite clearly the presence of the two kinds of water.

**Dr. H. J. Poole** (*Waltham Abbey*) (*communicated*): The Chairman has asked me to write a short account of the work which led up to the researches on cordite that have been described in the papers read here to-day.

It was in 1920 that I first became interested in this subject. At that time I was concerned with the development of local spots of decomposition in the cordite of that period. These "corrosion spots", as they were termed, were a matter of great importance then because they marked the onset of a dangerous condition that had resulted in the destruction of quite a number of ships in various navies. It seemed to me that in order to gain some knowledge of the diffusion mechanisms that governed their growth it was very necessary to know just what was the physical structure of the gel in which they occurred.

At that time there were several different theories of the structure of gels and I felt that something more definite was needed. Since the characteristic property of gels is rigidity it seemed to me that a study of the elastic properties of gels and of cordite in particular should provide facts from which sound deductions might be drawn as to their structure.

The laboratory in which I was working was not officially concerned with research and it contained practically no physical apparatus. I therefore made from materials, such as old cartridge cases that were available, an extensometer based in principle upon Searle's apparatus for determination of Young's modulus of wires, and with this I started to measure the elastic moduli and Poisson's ratio of cordite M.D. The latter quantity involved the use of another piece of home-made apparatus for measuring the lateral contraction of the test piece. It consisted of two fingers supported on torsion wires; each finger pressed upon the cordite stick at opposite ends of a diameter and each carried a small mirror. By means of a telescope and scale the relative movement of the mirrors could be measured. Despite the crudeness of the gear, consistent values of 0.47 were obtained.

During the first experiments it became obvious that cordite was not a truly elastic substance and that a time-factor was involved. This suggested to me that a viscous effect was present and I set up a simple equation in which the stress at any instant was balanced by the growing elastic distortion and by the diminishing viscous flow in the material, and the early stages of the distortion were found to agree with this equation.

Cordite is a very concentrated system and at that time I was not able to alter the nitrocellulose content in order to study the effects of such variation and it seemed to me that a similar study of gels of gelatin or of cellulose acetate would provide information that would be useful for comparison with cordite. To this end I converted an attic room at home into a small laboratory. I had no grant or any financial assistance and so I had to construct all my own apparatus, even the balance. The thermostat extensometer was made from scrap forged in the kitchen fire, the travelling microscope embodied a carefully lapped Mecanno lead screw and the microscope itself was an old toy one of about 100 magnifications. A reluctant spider provided the cross-wires after a lot of persuasion. I mention all this because I often feel that present-day workers with all sorts of up-to-date gear must miss the tremendous fun that is to be got from starting absolutely from scratch.

Shortly after this I joined the Research Department at Woolwich and I took there my assortment of home-made apparatus with which

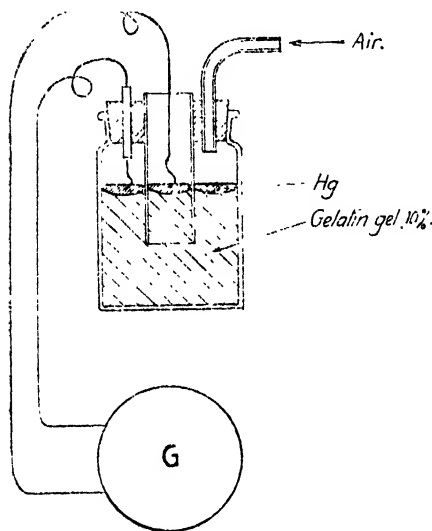


FIG. 1.

much useful work was done while professionally-made gear was being designed and made. The apparatus was used on cordite during official hours and on gelatin and cellulose acetate at other times. The work on these two latter was reported in the *Transactions* of this Society in 1925 and 1926.\* The structure of gels of these materials was shown to consist of a felt of interconnected ultramicroscopic fibrils. The elasticity of such a structure was calculated and found to be of the right order and the variation with concentration was also in agreement with that calculated. The increase in the elastic moduli as the strain increases was predicted and demonstrated experimentally.

At about this time I devised an experiment that has never been formally reported

because I had wished to be able to investigate the effect thoroughly. As it seems unlikely that I shall ever be able to spare the time to do this, I mention it here. It occurred to me that if in fact the structure of dilute gels is fibrillar and that if the elastic fore- and after-effects are due to the flow of the interstitial liquid, it should be possible to demonstrate streaming potentials in the gel when it was of an ionic type, such as gelatin. The apparatus for this is very simple (Fig. 1). It consists of a wide-mouthed bottle whose stopper is fitted with a very wide tube which reaches down to within about one diameter from the bottom. The stopper is also provided with a side-tube and a copper wire sealed in to make an airtight fit. A 10-15 % gelatin solution is poured in till it reaches up the wide tube about one diameter from the bottom of the tube. After the gel has set a thin layer of mercury is run on top of the gel both within the wide tube and in the annulus around it. Contact is made with these two mercury pools by the wire mentioned above and another passing down inside the wide tube. These leads are connected to a D'Arsonval

\* *Trans. Faraday Soc.*, 1925, **21**, 114; *ibid.*, 1926, **22**, 82; *ibid.*, 1933, **29**, 1305.

galvanometer of about 50 ohms resistance. The apparatus is allowed to stand for several minutes and air pressure is applied by blowing down the side tube. A vigorous kick of the galvanometer is immediately observed. If, instead of blowing, connection is made to a constant-pressure source so that the pressure is maintained, it will be seen that the galvanometer deflection dies away as the creep of the gel diminishes, and on releasing the pressure an opposite deflection is obtained which dies away gradually in the same way. The apparatus may be varied in many ways provided that the source of creep fluid is separated electrically from its sink. I think that this experiment can be made into a useful tool for the investigation of the ionic equilibria within gels.

To revert now to the work that was done on cordite in the period up to 1925, it was found that there was a marked delay in the attainment of steady physical properties after any change in temperature. The lag in reaching equilibrium was, however, very much greater when the temperature was lowered than when it was raised. Absorption of moisture by the cordite was found to reduce the elastic moduli very considerably. The elastic moduli were found to increase with increasing strain and in the case of one special composition in which the incorporation had been done with hot alcohol, the load-strain diagram was curvilinear leading to an asymptote at a strain of 0.7, resembling closely that obtained with cellulose acetate gels, and indicating clearly a fibrillar or reticulated structure since fibrils are in general more easily bent than stretched and so the resistance increases as the elements of the structure become more nearly parallel. Most of this work was done with solvent cordites of the type of Cordite M.D. in which the gelatinisation of the nitrocellulose was generally more complete than is the case with the solventless types dealt with in the papers read to-day. This, together with the fact that the solvent is nearly completely removed during drying renders this type of composition a better research material than solventless cordite. A very interesting set of experiments was done on the variation in creep with varying temperature. In order to explain this, I must first set down the equations that I referred to earlier in this note. If a load  $L$  is applied to the ends of unit length of a right prism of gel of unit cross-sectional area and the resultant extension is  $E$  at any instant, the following expression should be true if fluid viscosity contributes to the resistance to motion. This expression does not include any terms describing irreversible flow due to linkage breaking, etc., but it has been found to describe the initial part of the extension fairly well.

$$L = K_1 E + K_2 \eta \frac{dE}{dt}.$$

In this,  $K_1$  is the modulus of elasticity of the relaxed material,  $K_2$  is a factor determined by the size and deviousness of the internal flow-paths and  $\eta$  is the coefficient of viscosity of the fluid.

Since  $L$  is constant,

$$\frac{dE}{dt} = \frac{L - K_1 E}{K_2 \eta}$$

and 
$$\frac{d\left(\frac{dE}{dt}\right)}{dE} = -\frac{K_1}{K_2 \eta}.$$

Hence, if the time-rate of strain at any instant is plotted against the total strain at that instant, a straight line should result whose slope is negative and is directly proportional to the elastic modulus and inversely proportional to the viscosity of the fluid phase.

In this series of experiments, a single stick of Cordite M.D. about 1 cm. diam. and 10 cm. long was stored at constant humidity in a constant-temperature extensometer and creep curves obtained in the way described in the 1926 paper referred to earlier. The temperature was then

raised and, after constant elastic properties had been attained, the experiment was repeated and so on for a number of different temperatures. These creep curves were then differentiated and the plots of  $\frac{dE}{dt}/E$  shown

in Fig. 2 were obtained. From these  $\frac{d\left(\frac{dE}{dt}\right)}{dE}$  was evaluated and plotted against temperature. At the same time, the viscosity of liquid nitroglycerine was measured over the same range of temperature and the resultant curve is also shown in Fig. 2. It is seen that the two curves are of very similar character and this result supports the view that there is a fluid-phase of nitroglycerine in Cordite M.D. It may be mentioned here that guncotton is not gelatinised by nitroglycerine but requires an additional solvent so that when the solvent is removed, the resulting structure is fixed and its flow-paths will remain constant.

The work on the physical structure and properties of cordite was

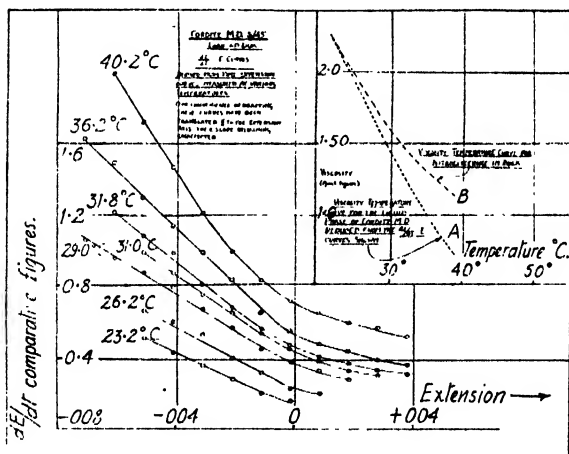


Fig. 2.

discontinued in 1926, and except for an attempt to measure the flow-path dimensions in collaboration with the late Dr. J. Brittain in 1933, nothing more was done until 1940 when a laboratory was set up under Mr. A. G. Ward to study the physical properties of the solventless types of cordite then coming into use as rocket propellants and extra-mural researches were started under Prof. E. Rideal. These led to the results now reported by Dr. Eley, Pepper and Tuckett.

This note is published by permission of the Chief Scientist, Ministry of Supply.

Dr. A. S. Carpenter (Coventry) said: Since submitting the manuscript of my paper for publication, a paper has appeared in the literature<sup>1</sup> recording the results of experiments designed to measure, by the method of Daynes,<sup>2</sup> the diffusion coefficient and solubility of several gases in several rubbers at temperatures between 17°C. and 50°C. The comparison of results with those of other workers given in Table III in my paper, is amplified by Table V, which covers Van Amerongen's work.

In making these comparisons, however, it must be borne in mind that the method involving the measurement of gas permeation rate through

<sup>1</sup> Van Amerongen, *J. Appl. Physics*, 1946, **17**, 972.

<sup>2</sup> Ref. <sup>10</sup> in my paper.

a membrane under a pressure difference, the method used by all the workers quoted in Tables III and V, introduces difficulties<sup>3</sup> the most fundamental of which arises out of the need for supporting the membrane. Distortion, and the restriction of the free surface (and hence the rate of evaporation of gas) on the low-pressure side, owing to contact with the supporting grid, must be factors appreciably affecting results. The absorption method of the present paper, and that of a previous publication,<sup>3</sup> were specifically designed to avoid this difficulty.

The absorption method of determining diffusion coefficient has to-day been said to be less satisfactory than the permeation method. It was stated (Dr. R. F. Tuckett) that the absorption method measures the mean diffusion coefficient over a range of concentrations whereas the permeation method measures the coefficient at one concentration. This latter statement is, of course, untrue and indeed all methods of determining diffusion coefficients, depending upon the movement of solute resulting from an initial non-uniform concentration distribution, must give a mean value for the finite range of concentrations used. In the

TABLE V.

	This work.			Van Amerongen.		
	N <sub>2</sub> .	O <sub>2</sub> .	H <sub>2</sub> .	N <sub>2</sub> .	O <sub>2</sub> .	H <sub>2</sub> .
Diffusion coefficient at 35° C. ( $\times 10^{-6}$ cm. <sup>2</sup> /sec.). $D$	1.78	2.17	14.4	2.05	2.75	14.0
Solubility at 35° C. (cc. at N.T.P./100 cc. rubber-atmos.). $s_1$	5.07	8.75	3.03	5.55	10.2	4.05
Activation energy for diffusion (cal./mole). $E$	7400	7100	6100	8650	7550	6000
Heat of solution (cal./mole). $\Delta H$	1200	700	2800	1250	750	1500

absorption method, the range is from the initial to the final saturation concentration, while in the permeation method the range is from the concentration corresponding with the lower gas pressure to that corresponding with the higher. Working between the same pressures therefore, the two methods give the same result.

In the experimental results quoted in the paper, however, the highest concentration of gas is so low that the dependence of diffusion coefficient upon concentration must be very slight. Concentrations of  $6.5 \times 10^{-5}$  g./cc. N<sub>2</sub>,  $2.8 \times 10^{-6}$  g./cc. H<sub>2</sub> and  $1.3 \times 10^{-4}$  g./cc. O<sub>2</sub> (see Table II, p. 535) are only  $2.3 \times 10^{-3}$ ,  $1.4 \times 10^{-3}$  and  $3.9 \times 10^{-3}$  M. respectively. Expressed differently, at these concentrations, the ratios of the numbers of gas molecules to C<sub>6</sub>H<sub>8</sub>-units of the rubber are approximately 1 : 6000, 1 : 10,000 and 1 : 3500 respectively. Mutual interaction between the dissolved molecules can hardly be appreciable at these concentrations.

**Dr. S. Fordham** (Stevenson) said in introducing the paper: The slides of nitrocottons which have been immersed in nitroglycerine containing Crystal Violet base show that as the nitrogen content is reduced from 13.40 % the swelling is increased and complete solution occurs at values between 12.5 and 11.5 %. With the lower nitrogen content the attack becomes less uniform and much of the surface of the fibres including their ends is covered by a protective layer of partially denitrated material. Nitrocottons of high viscosity diffuse slowly through the liquid but those of low viscosity spread very rapidly. It was frequently observed with

<sup>3</sup> Ref. <sup>3</sup> in my paper.

nitrocottons of low viscosity that a fibre could become surrounded by a gel and thus be prevented from dissolving in the usual manner.

**Mr. W. R. Moore** (*Bradford*) said: Possibly the chief point meriting discussion in my paper is the relation between interaction of the nitrocellulose and solvent—as measured by swelling, precipitation with non-solvent or viscosity—and the cohesive energy density of the solvent. Such a relation is well known for non-polar polymers and, in Gee's treatment, swelling or solubility is controlled by the heat absorbed in mixing which is related to the difference between the cohesive energy densities of polymer and solvent. In the case of nitrocellulose heat is evolved and Gee's treatment cannot be applied directly. A tentative suggestion may be put forward as a basis for discussion. It is known that in the swelling or solution of nitrocellulose a process of solvation occurs. There is evidence from the work of Nakashima and Saito,<sup>4</sup> and of Kargin and Papkov,<sup>5</sup> that heat is evolved in solvation and that swelling or dispersion of the solvated polymer may occur with absorption of heat. There may therefore be a relation between swelling or solubility of the solvated polymer and the cohesive energy density of the solvent which would be related to the heat absorbed in swelling or solution of the solvated polymer.

Two further points may be noted. Essentially the same result has been obtained by the three methods of assessing nitrocellulose-solvent interaction. Swelling of nitrocellulose in non-solvent mixtures agrees, in the few cases studied, with the treatment of such mixtures by Gee.

**Dr. A. Lovecy** (*London*) said: I do not see why the cohesive energy-density (C.E.D.) of the pure "solvent" should be regarded as the dominant factor in swelling by solvent-non-solvent mixtures. It would seem better to consider each binary mixture as a whole for the purpose of comparing C.E.D. with swelling action. This is, of course, the approach adopted, when considering the related problem of polymer solubility, to explain the variation of solvent power when diluent is added to solvent in a fractionation experiment.

The point may be illustrated by reference to Fig. 6 in Moore's paper, where alcohol-ether mixtures show a decided hump in the swelling curve, in contrast to alcohol-hexane mixtures, although hexane and ether individually have quite similar  $(E/V)^{\frac{1}{2}}$  values. If C.E.D. is the significant property, one must conclude that its relationship to composition of the mixture is very different in the two systems. Doubtless alcohol-ether is a special case—but it is a special case of the general proposition that the effect of a binary mixture cannot be inferred from the C.E.D. of one component alone.

There is, however, reason to doubt whether the C.E.D. of the liquid is the dominant factor in the dispersion of polymers, particularly the heterochemical types such as cellulose esters. In the case of cellulose acetates, for example, an average degree of substitution of 2.2 to 2.4 ester groups per glucose unit confers solubility in acetone but not in chloroform, whilst products with over 2.7 substitution dissolve in chloroform but not in acetone, although the C.E.D.'s of the two liquids are probably not widely dissimilar. At an intermediate degree of substitution, 2.5 to 2.6, solubility in both solvents is obtained. An explanation in terms of C.E.D. involves postulating significant changes in the structure-energy of the solid polymer as the degree of substitution is varied. General experience indicates, however, that a degree of substitution close to 2.5 is favourable to swelling and dispersion in quite a wide range of organic liquids for which a similarity of C.E.D. values would not be expected.

As swelling is a limited condition of dispersion, it is not permissible to ignore the heterogeneity of the sample, as suggested by Dr. Eley. Individual molecules of a heterogeneous specimen will differ in their

<sup>4</sup> Nakashima and Saito, *J.C.S.I. Japan, B*, 1935, **38**, 232.

<sup>5</sup> Kargin and Papkov, *J. Physic Chem. (U.S.S.R.)*, 1936, **7**, 483.

tendency to disperse in a given liquid environment, and this circumstance may well be reflected in the swelling. Guncotton, as employed by Mr. Moore, is demonstrably heterogeneous and the response elicited by liquids of differing C.E.D. should presumably arise from different component fractions.

**Dr. D. D. Eley** (*Bristol*) said: Surely there is no conflict in the view advanced by Moore and Lovecy? In comparing a series of cellulose polymers of different average nitrate- or acetate-content in a single solvent, the variations in solubility are to be explained in terms of a variation in lattice energy, which, as Lovecy remarks, is bound to play an important role in semicrystalline polymers. In comparing one polymer sample (neglecting effects due to heterogeneity in chemical substitution and molecular weight) in a series of solvents, Moore's view seems a distinct advance in this field.

**Dr. R. R. Smith** has asked about the entropy effects in the swelling of nitrocellulose. The properties of nitrocellulose-acetone over the concentration range 0.1 to 70 % nitrocellulose by weight have been discussed by Schulz.<sup>†</sup> In the concentrated range (20 to 75 % nitrocellulose) the entropy term is relatively small compared to the heat term. Schulz gives an interesting calculation of the heat of solvation of the fibre in terms of intermolecular forces.

**Mr. W. R. Moore** (*Bradford*) said: Some nitrocellulose dissolves in the liquid phase at higher degrees of swelling. The difference between swelling in alcohol-hexane and alcohol-ether mixtures can be explained by assuming that in the former case only alcohol takes part in solvation. Swelling in alcohol-ether mixtures has been interpreted by Highfield<sup>6</sup> in terms of solvation of different groups on the nitrocellulose chains by alcohol and ether. Further work on sorption of solvent from solvent-hexane mixtures by nitrocellulose suggests that the relation between swelling and cohesive energy density of solvent only becomes apparent after a certain amount of solvent has been taken up by the nitrocellulose. The work is being extended to cellulose acetate.

**Dr. Fordham** (*Stevenson*) said: It was not strictly justified to compare results obtained in swelling experiments and the solubility characteristics of the polymer. Available evidence suggested that the two problems were different in character. This is presumably because swelling depends on breaking the weakest contacts between the chains whereas solution involves breaking the strongest.

With reference to Dr. Moore's results, the compositions of the liquids after swelling had occurred would be appreciably different from the values given owing to preferential absorption. The results, therefore, were equivalent to measuring the absorptive powers of the nitrocotton for the various solvents. Viewed in this way it was satisfactory to note that they agreed in relative magnitudes with those previously found by workers such as Rubenstein.

**Mr. A. G. Ward** (*Hemel Hempstead*) said: In their papers<sup>7, 8, 9</sup> Eley and Pepper have discussed the application of a theory of the structure of cordite to their mechanical measurements. Although this theory was developed<sup>10</sup> in the first instance to explain the mechanical behaviour, the most important evidence in its favour is derived from X-ray studies.<sup>11</sup> The nitrocellulose from which cordite is made is obtained by nitrating specially prepared paper to a mean nitrogen content of 12.2 %. In the

<sup>†</sup> *Z. physik. Chem.*, A, 1939 184, 1; B, 1943, 52, 253.

<sup>6</sup> Highfield, *Trans. Faraday Soc.*, 1926, 21, 57.

<sup>7</sup> Eley and Pepper, *ibid.*, 1947, 43, 559.

<sup>8</sup> Eley and Pepper, *ibid.*, 1947, 43, 568.

<sup>9</sup> Eley and Pepper, *ibid.*, 1947, 43, 583.

<sup>10</sup> Ward and Nicholson (unpublished work, 1942).

<sup>11</sup> Parry and Ward (unpublished work, 1945).



preparation of cordite, the nitrated paper is pulped, mixed with nitroglycerine and stabiliser, and the mixture dried in sheet form. The sheet is then hot-rolled to give a gelatinised material which is extruded through a die to give the finished product. X-ray diffraction photographs were taken<sup>11</sup> at all stages of the manufacturing process, in order to examine the effect of the nitroglycerine on the nitrocellulose structure. Crystal monochromatised (pentaerythritol)  $\text{CuK}_\alpha$  radiation was used throughout, owing to the danger of spurious effects resulting from the lower absorption of the white radiation component. The original nitrocellulose gave a poor X-ray diffraction picture, consisting of a fairly well-defined inner ring (at about 7 Å. spacing) together with an outer broad band in which some traces of detailed ring-structure could be observed. It is evident that with this initial picture, considerable care is necessary in drawing any conclusions from changes observed. The general appearance of the X-ray photographs for specimens at the various stages of manufacture was unchanged. There was no significant change in the 7 Å. spacing and no additional rings appeared. This is of importance since substances known to penetrate the nitrocellulose lattice—e.g. acetone—have been shown by Mathieu and others to affect this particular spacing. The only significant change was a decrease in the intensity of the ring corresponding to the 7 Å. spacing compared with the broad band.

It would therefore appear that a number of nitrocellulose crystallites remain unmodified in the final structure, while the nitroglycerine has swollen amorphous regions in the structure and effected some swelling of crystalline regions which has rendered them amorphous. It is not suggested that there are two distinct structures, "crystalline" and "amorphous" but rather a wide range of degrees of order.

It had previously been thought that the nitroglycerine existed largely in liquid form in the structure. If this was so, however, it would be expected that the damping coefficient for mechanical vibrations would be a function of frequency. It has been shown<sup>12</sup> that, within experimental error, the damping coefficient is independent of the frequency.

If a sample of normal production cordite is taken and thin sections cut, these can be examined with the polarising microscope between crossed Nicol prisms. Sections parallel to the extrusion direction show, against an isotropic background, birefringent fibres which are incompletely gelatinised. It is possible, by continued rolling, to produce a cordite in which these fibres are completely eliminated. Such cordite differs in no essential respect from normal production material, although there are small changes in the various constants describing the mechanical behaviour. In formulating a theory on the lines of that of Eley and Pepper it would appear not to be necessary to consider the ungelatinised fibres as a structural component in the first instance. The main elastic element, and source of the strength of the material, resides in the crystalline component on the colloidal scale, together with the fact that a single nitrocellulose molecule probably runs through a number of crystalline and amorphous regions.

It should be mentioned that the extruded cordite charge and the rolled sheet are both markedly anisotropic.<sup>13</sup> This is shown in measurements of elastic properties and thermal expansion. A further development of Eley and Pepper's theory would be needed to cover this point.

If a tensile test is performed on cordite, rupture will occur after a relatively small extension (10-15 %). In rolling or extrusion, however, very large shears occur without rupture. The difference is almost certainly due to the presence of hydrostatic pressure in both these instances. The effect can be illustrated for cordite (and for other plastics) by taking a small disc of the material at an appropriate temperature and

<sup>11</sup> Rainbird and Ward (unpublished work, 1944).

<sup>12</sup> Ward (unpublished work, 1942).

compressing it to a fraction of its original thickness. It will be found that, at the centre of the disc, where the frictional forces between disc and the compressing surfaces give rise to a considerable hydrostatic pressure, the material is still coherent, but at the periphery there are cracks and the whitening and opacity which precede rupture. It is not evident whether frictional forces in Eley and Pepper's parallel-plate plastometer are of importance. Since little barrelling was observed it is possible that they can be neglected, but it is also true that future work in this field will have to take account of the influence of hydrostatic pressure.

**Dr. R. N. Haward** (*Manchester*) said : Dr. Eley and Pepper have given an extremely interesting series of experimental papers in a field where this type of work is badly needed. Perhaps it would be of interest to say something about two aspects of these results which appear to be of special interest, namely the effect of stress on the development of delayed elasticity and the question of fracture times.

With regard to delayed elasticity, it has been found here that when the stress is increased both the final deformation and the rate at which this deformation is reached, are raised. This sort of behaviour can be regarded as transitional between two extreme cases. In the first class there are materials where the highly elastic deformation depends on the stress and the rate at which it is reached does not. The theoretical aspects of this behaviour have been widely discussed in the literature. In the second class come those materials, of which certain plasticised cellulose derivatives appear to be typical,<sup>14, 15</sup> where the final value of  $D_{HE}$  is approximately independent of the load, but where the rate at which it is approached is strongly dependent on the stress. In the case of the latter materials it appears possible to envisage a treatment of deformation at constant stress analogous to the kinetics of a first-order reaction. Thus the deformation approaches the limit of extensibility at a decreasing rate, the overall rate-constant for the process being logarithmically dependent on the stress as required by the theory of Eyring.<sup>16</sup> Unfortunately my results do not allow of a possibility of testing this hypothesis owing to the use of a constant load instead of a constant stress. However, the existence of linear log load-log rate of deformation relations over small ranges of load is suggestive of an Eyring mechanism.

Considerable interest attaches to the measurement of breaking times. It would be very desirable to extend this type of work particularly with soft materials giving good reproducible results. I would particularly like to ask Dr. Eley and Pepper whether they were able to confirm (or otherwise) my experiments in which fracture appeared to be independent of the highly elastic deformation process. In the case of plasticised cellulose acetate it was found that if a sample was stretched for a time  $t_1$ , nearly to the point of fracture, a large highly elastic deformation took place. On warming, the deformation is reversed but when the stress is applied again under the same conditions as before the material breaks in time  $t_2$ , where  $t_1 + t_2 = T$ , the time taken for fracture in a continuous test. Thus the damage done by the stress is not repaired when the deformation is reversed. This cellulose acetate also showed a similarity to the cordite described in to-day's papers in that visible changes could be observed as fracture approached. This took the form of a whitening of the acetate film.

With regard to the question of activation energies derived from fracture times these were not measured in my early papers. However, it is a simple matter to derive the breaking times at constant stress and variable temperature from a series of breaking time-stress curves at different

<sup>14</sup> Haward, *Trans. Faraday Soc.*, 1942, **38**, 394.

<sup>15</sup> *idem.*, *ibid.*, 1943, **39**, 267.

<sup>16</sup> Tobolsky, Powell and Eyring, *Chemistry of Large Molecules*, (Interscience 1943), 125.

temperatures and these may be plotted to yield activation energies as shown in Fig. 1. It will be seen that the activation energy is apparently independent of stress and corresponds to a value of 15-16,000 cal./g. mol. This value is notably less than that found by Dr. Eley and Pepper with a much softer material but falls within the range of 8,000-20,000 cal./g. mol. recorded by Busse *et al.*<sup>17</sup>

Dr. Fordham (Stevenston) said: I can confirm that cordite has a heterogeneous structure. In the case of blasting gelatine the viscosity at high stresses is of the order of  $10^7$  poises and this suggests that the lowest viscosity nitrocellulose present in the guncotton used for cordite might conceivably give on solution a viscosity of the order of  $10^6$  poises. This was the figure required to explain Eley and Pepper's results on the

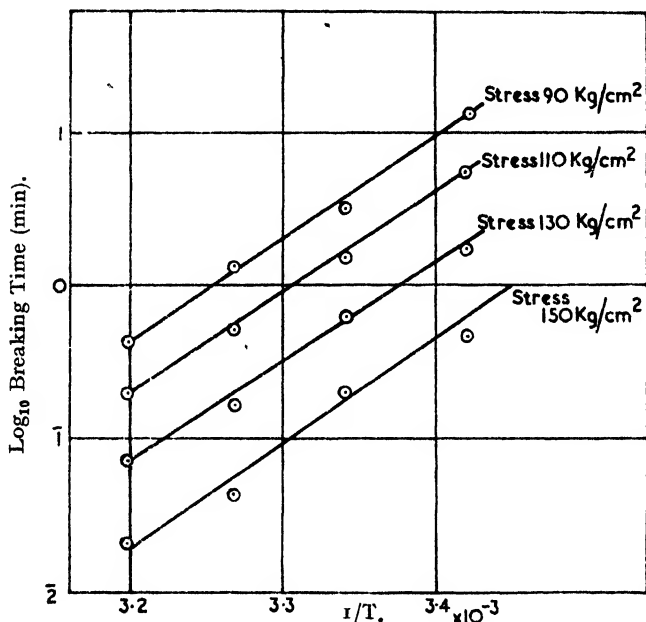


FIG. 1.—The Logarithm of the Breaking Time of Plasticized Cellulose Acetate Film against the Reciprocal of the Absolute Temperature.

basis of two independent phases and I suggest that the results could be explained on this basis although on a scale higher than molecular.

In a compression plastometer the stress distribution would affect the calculated results and I would ask if the authors have found a method of correcting for or estimating the effect.

Dr. A. Lovecy (London) said: In connection with the adoption of a mixed crystalline-amorphous structure as the model for cordite, it appears of interest to mention the implications of the manufacturing process. Essentially, nitrocellulose in the form of fibre-fragments is admixed with nitroglycerine and stabiliser; further treatment, hot-rolling in particular, converts the aggregate of particles into a coherent, translucent mass. There is evidence, both optical and X-ray, that homogeneous distribution on the molecular scale is not attained and, indeed, as the proportion of nitroglycerine to nitrocellulose is approximately one molecule per glucose unit, complete uniformity of distribution is hardly to be expected. The

<sup>17</sup> Busse, Lessig, Loughborough and Larrick, *J. Appl. Physics*, 1942, 13, 715.

picture presented is the progressive penetration of nitroglycerine inwards from the surfaces of the nitrocellulose particles, disrupting the organised structure and decreasing the proportion of polymer-polymer contacts. Because of irregularities in the shape and composition of the nitrocellulose particles, *inter alia*, the extent of penetration at any moment will vary from point to point in the mass (cf. Fordham and Fensom). We can therefore visualise regions of unaffected nitrocellulose surrounded by the softer "gelatinised" material into which the plasticiser has diffused. Under the compressive and shearing stresses applied in rolling, etc., the boundaries of the original fragments are obliterated and cohesive forces brought into play. The result is a composite structure comprising residua of nitrocellulose shading off into a gelatinous matrix of nitroglycerine, nitrocellulose, and stabiliser, molecularly admixed. Such a structure is in accordance with visual, microscopic, birefringency, and X-ray observations on the material at various stages of manufacture and with its complex visco-elastic properties and response to temperature changes. It is of the same essential character as the model adopted by Eley and Pepper, differing only in placing less emphasis on crystallinity as a factor in the survival of the residua of nitrocellulose, and more upon the chemical heterogeneity of this ingredient and the circumstances under which the plasticiser obtains access.

Dr. D. D. Eley (*Bristol*) said: Sir Robert Robertson's question on the degree of orientation of cordite having been answered by Mr. A. G. Ward, I will limit myself to saying that an examination of the mechanical properties of the more highly crystalline cordites would be of great interest. In conjunction with work on completely amorphous cordite, one might expect to bracket, as it were, the properties of the modern cordites.

Dr. R. N. Haward's results are indeed of great interest, bearing out, as they do, the effect of stress on the rate of delayed elastic creep in cellulose derivatives. My own very tentative view on the rupture of chain polymers is that the limiting dynamical process is the slipping or diffusion of chain segments. There is, however, an important probability factor relating to the chance of producing the necessary discontinuity of structure, at which stress may be concentrated, leading to ruptures. Initially these discontinuities may be simply the conjunction of a certain critical number of chain-ends, soon enlarging to the visible spots at one of which rupture eventually occurs. The presence of this probability factor would mean that a material with relatively high activation energy might yet have a relatively low tensile strength. Dr. Haward's views on a limiting tensile stress for zero time is interesting. Our own work was over a relatively small stress range and we found no such effect. Incidentally this view of the rupture process would lead one to expect that rupture would be independent of elastic deformation as Haward found. While in each case we are concerned with the same activation energy and the diffusion of chain-segments, in the one case we have an irreversible diffusion, in the second case we are concerned with segments tied at each end by cross-links which must inevitably return on release of stress.

The suggestion of Dr. Fordham, as supported by the X-ray observations of Mr. Ward, seems to offer a rather nice explanation of the results on the flow of cordite at high stresses, but I should hesitate to offer a definite opinion on its validity at such a short acquaintance.

Our specimens were relatively tall and narrow cylinders as compared with those used by Dr. Scott and Mr. Ward. Barrelling of the cylinders was small. In reply to Dr. Fordham, I cannot say how far our results might be due to a decrease in hydrostatic pressure across the radius of the cylinder. This remains a matter for experimental investigation, e.g. with piezo crystals distributed across the diameter of the compression plate.

Dr. S. M. Neale (*Manchester*) said: In Dr. King's paper the figures for double refraction of fibres should be transposed since the higher re-

fractive index is observed when the electric vector of the light is *parallel* to the fibre axis and not perpendicular, as stated.

**Dr. J. M. Preston** (*Manchester*) (*communicated*): I would call attention to some errors of fact in the paper by King (*Trans. Faraday Soc.*, 1943, 43) on p. 601. In l. 11 "parallel" should read "perpendicular," and in l. 13 and 18 "perpendicular" should read "parallel"; the word "not" should be deleted in l. 20; furthermore (cp. l. 23 and 24), data on the refractive indices of fibres of known moisture content are available.

**Mr G. King** (*Leeds*) (*communicated*): I should like to thank Dr. Preston for pointing out my error in quoting Fox and Finch's results. In the absence of any contrary evidence I assumed their "plane of polarisation" to be defined on the original and not the modern version.

With regard to Dr. Preston's concluding remarks I should like to say that since writing this paper Dr. Herman's comprehensive work on the refractive indices of fibres has become available.





L.A.R.I. 75

INDIAN AGRICULTURAL RESEARCH  
INSTITUTE LIBRARY, NEW DELHI.

[illegible]